STRUCTURES MANUAL

ISSUED TO: 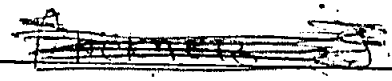

GRUMMAN'S STRUCTURES MANUAL
TABLE OF CONTENTS

Instructions for changes to:

Revision No. 0 , JUNE 1980

Remove Superseded Pages	Insert New Pages (dated JUNE 1980)	Insert Pages Reprinted w/o Change
-	A1-4	-
-		-
B1-1	B1-1	-
-	B1.50.4-2	-
B1.60-1 & B1.60-2	B1.60-1 & B1.60-2	-
B1.60-3	B1.60-3	-
B2-1	B2-1	-
B2.50-3 & B2.50-4	B2.50-3	B2.50-4
B2.50-7	B2.50-8	B2.50-7
B3.42.10-1	B3.42.10-1	-
B4-1	B4-1	-
B4.12-1 & B4.12-2	B4.12-2	B4.12-1
B4.20-1 & B4.21.10-1	B4.20-1 & B4.21.10-2	-
B4.30-1 & B4.30-2	B4.30-1 & B4.30-2	-
B4.30-3	B4.30-3	-
B4.31.10-1 & B4.31.10-2	B4.31.10-1 & B4.31.10-2	-
B4.40-1 & B4.40-2	B4.40-1	B4.40-2
B5.11.13-1 & B5.11.13-2	B5.11.13-2	B5.11.13-1
~~B5.11.13-3~~	~~B5.11.13-3~~	-
B6-1	B6-1	-
B6.11.1-1 & B6.11.1-2	B6.11.1-1 & B6.11.1-2	-
B6.11.1-3	B6.11.1-3 & B6.11.1-4	-
-	B6.11.1-5 & B6.11.1-6	-
B6.11.2-1 & B6.11.2-2	B6.11.2-1 & B6.11.2-2	-
B6.11.2-3 & B6.11.2-4	B6.11.2-3 & B6.11.2-4	-
B6.11.2-5 & B6.11.2-6	B6.11.2-5 & B6.11.2-6	-
B6.11.2-7	B6.11.2-7	-
B6.11.3-1 & B6.11.3-2	B6.11.3-1	-
B6.11.3-3 & B6.11.3-4	-	-
B6.11.4-1	B6.11.4-1 & B6.11.4-1.1	-
B6.11.5-1	B6.11.5-1 & B6.11.5-2	-
-	B6.11.5-3 & B6.11.5-4	-
-	B6.11.5-5 & B6.11.5-6	-
-	B6.11.5-7 & B6.11.5-8	-
-	B6.11.5-9 & B6.11.5-10	-
B6.11.6-1 & B6.11.6-2	B6.11.6-1 & B6.11.6-2	-
B6.11.6-3 & B6.11.6-4	B6.11.6-3 & B6.11.6-4	-
B6.11.6-5 & B6.11.6-6	B6.11.6-5 & B6.11.6-6	-
-	B6.11.6-7 & B6.11.6-7	-
-	B6.11.6-9 & B6.11.6-10	-

GAC 6410
2-74

Instructions for changes to:

Revision No. 0 , JUNE 1980 (Cont.)

Remove Superseded Pages	Insert New Pages (dated JUNE 1980)	Insert Pages Reprinted w/o Change
-	B6.11.6-11 & B6.11.6-12	-
-	B6.11.6-13 & B6.11.6-14	-
-	B6.11.6-15 & B6.11.6-16	-
-	B6.11.6-17	-
B6.11.7-1 & B6.11.7-2	B6.11.7-1 & B6.11.7-2	-
B6.11.7-3 & B6.11.7-4	-	-
B6.11.7-5 & B6.11.7-6	-	-
B6.11.7-7 & B6.11.7-8	-	-
B6.11.7-9 & B6.11.7-10	-	-
B6.11.7-11 & B6.11.7-12	-	-
B6.11.7-13 & B6.11.7-14	-	-
B6.12.1-1 & B6.12.1-2	B6.12.1-1 & B6.12.1-2	-
B6.12.1-3 & B6.12.1-4	B6.12.1-3 & B6.12.1-4	-
B6.12.1-5 & B6.12.1-6	B6.12.1-5	B6.12.1-6
B6.12.1-7 & B6.12.1-8	B6.12.1-7 & B6.12.1-8	-
B6.12.1-9 & B6.12.1-10	B6.12.1-9 & B6.12.1-10	-
B6.12.1-11 & B6.12.1-12	B6.12.1-11 & B6.12.1-12	-
B6.12.1-13 & B6.12.1-14	B6.12.1-14	B6.12.1-13
B6.12.1-15 & B6.12.1-16	B6.12.1-15 & B6.12.1-16	-
B6.12.2-1 & B6.12.2-2	B6.12.2-1 & B6.12.2-2	-
B6.12.2-3 & B6.12.2-4	B6.12.2-3	B6.12.2-4
B6.12.2-5 & B6.12.2-6	B6.12.2-6	B6.12.2-5
B6.12.3-1 & B6.12.3-2	B6.12.3-1 & B6.12.3-2	-
B6.12.3-3 & B6.12.3-4	B6.12.3-3 & B6.12.3-4	-
B6.12.3-5 & B6.12.3-6	B6.12.3-5 & B6.12.3-6	-
B6.12.3-7 & B6.12.3-8	B6.12.3-7 & B6.12.3-8	-
B6.12.4-3 & B6.12.4-4	B6.12.4-4	B6.12.4-3
B6.12.4-5 & B6.12.4-6	B6.12.4-6	B6.12.4-5
B6.12.4-7 & B6.12.4-8	B6.12.4-7 & B6.12.4-8	-

Section A1 - Log of Revisions

Rev. No./Date	
A/ 5/67	Pages Revised: A2-1, A6.00-1, A6.01-1,-2,-3,-4,-5,-6 A6.06-1 B1.031-7, B3.11-2, B3.11-3,-4, B3.32-1, B3.42.10-1, B3.44.31-1, B3.81-1,-2,-3, B4-1, B4.11.09-1, B4.13.10-1, B4.40.10-1, B5.11.11-2,-3, B5.11.12-2, B6.12.20-6,-7,-12,-15, B6.31-1, C2.06-2 Pages Added: A1-1, B4.40-5,-6
B/ 7/67	Pages Revised: A1-1, B3.11-3, B3.81-1, -3.
C/ 8/68	Pages Revised: A1-1, A2-2. Pages Added: B3.11-9.1 Section Added: Section F - Statistics.
D/ 12/68	Pages Revised: A1-1, A2-1, B0-1, B1-1, B2-1, B3-1, B3.42.10-1. Pages Added: B2.22-11, B3.20-1, B3.40-1, B7-1, B7.030-1 thru-26, B7.031-1 thru-26, B7.040-1,-2, B7.040.1-1 thru-18, B7.040.2-1 thru-10, B7.040.3-1,-2, B7.040.4-1, B7.040.7-1,-2. *Pages Deleted: B1.030-1 thru-26, B1.031-1 thru-12, B3.11-1 thru-15, B3.26-1 thru-7.
E/ 12/68	Pages Revised: A1-1. Pages Added: B6.11.1-1,-2,-3, B6.11.2-1 thru -7; B6.11.3-1,-2,-3,-4, B6.11.4-1, B6.11.5-1, B611.6-1 thru -6, B6.11.7-1 thru -14, B6.11.8-1,-2,-3. Pages Deleted: B6.11.21-1,-2

* NOTE: Deleted sections are now incorporated in new section B7 Fatigue.

Section A1 - Log of Revisions

Rev. No./Date	
F/ 1/69	Pages Revised: B1-1, B6-1 Pages added: A1-2, B1.10-1,-2,-3, B1.20.0-1, -2, B1.20.1-1 thru -9, B1.20.2-1,-2,-3, B1.20.3-1, B1.30-1,-2, B1.40-1,-2,-3, B1.50.0-1, -2,-3, B1.50.1-1,-2, B1.50.2-1, B1.50.3-1, B1.50.4-1, B1.60-1,-2,-3, B1.70-1, -2,-3, B6.12.1-1,-2,-3,-4, B6.12.2-1, B6.12.3-1, B6.12.4-1 thru 7, B6.12.5-1 thru 7, B6.12.6-1 thru-18. Pages Deleted: B1.22-1,-2, B1.23-1, B6.12.20-1 thru -22; B7.040.1-4 (Please mark this page "do not use" until next revision is printed)
G/ 5/69	Pages Revised: A1-2, B3-1, B3.32-1, -2, C3.02-2, C3.05.5-2. Pages Added: B3.32-3 thru -9, B3.51.40-1 thru -10. Pages Reprinted: B7.040.1-1, -2, -3, -6, -7, -8, -15, -16, -17, -18.
H/ 12/69	Pages Revised: A1-2, A2-1, B1.50.0-2, B3.13-31, B3.51.30-1, B5.21-1, B6.31-1, B7.030-18 Pages Added: B5.11.13-1, B8-1, B8.11-1, -2, B8.13-1 thru -8, B8.14-1 thru -4, B8.15-1 thru -13, B8.16-1, -2, -3, B8.17-1, B8.61-1, -2
I/ 2/74	Pages Revised: A1-2, A2-2, and B3-1 Pages Added: B3.44.32-1 thru -4, C4.00-1, C4.02-1 thru -9, C4.03-1 thru -16, C5.00-1, C5.02-1 thru -10, C11.00-1, C11.02-1 thru -5
J 6/74	Pages Revised: B2-1, B6.12.5-1 thru -3, B8.15-4 thru -5, B8.15.13, B8.61-2, C4.03-16, C5.02-1 thru -3, C5.02-8 Pages Added: B2.50-1 thru -7, B8.15-14

Section A1 - Log of Revisions

Rev. No./Date	
K 4/75	Pages Revised: A1-2, B2.50-2,-3, B3.13-5, -20,-21,-28,-31, C4.03-16, C5.02-3,-6,-7, -8,-9,-10 Pages Added: A1-3, B7.030.1-1,-2,-3,-4,-5, B7.040-3.3, B7.32-1,-2,-3,-4,-5,-6,-7,-8,-9, -10,-11,-12,-13,-14,-15,-16, C0-1
L 6/76	Pages Revised:A1-3, B7-1, B7.030-1, -4, B7.032-3,-5,-9 Pages Added: B7.030-27 thru -44
M 1/77	Pages Revised: A1-3, B3-1, B3.40-1, B3.44.32-2 thru -4, B6.1, B7.030-30, B7.030-37, B7.032-1 thru -3, C4.03-16,C11.02-3 Pages Added: B3.40-2, B3.44.10-4 thru -7, B3.44.32-5,-6 B.6.13-1
N 7/78	Pages Revised: A1-3, B6.12.1-1 thru B6.12.1-4, B6.12.2-1, B6.12.3-1, B6.12.4-1 thru B6.12.4-7, B7.030-27, B7.030-28, B7.030-30, B7.030-31, B7.030-32, B7.030-33, B7.030-35, B7.030-36, B7.030-37, C5.02-6. Pages Added: B5.11.13-2, B5.11.13-3, B6.12.1-5 thru B6.12.1-18, B6.12.2-2 thru B6.12.2-6, B6.12-3.2 thru B6.12.3-8, B6.12-4-8 thru B6.12.4-10. Pages Deleted: B6.12.5-1 thru B6.12.5-7, B6.12.6-1 thru B6.12.6-18.

Section A1 - Log of Revisions

Rev. No./Date	
0 6/80	Pages Revised: B1-1, B1.60-1 thru B1.60-3, B2-1 B2.50-3, B3.42.10-1, B4-1, B4.12-2, B4.20-1, B4.21.10-1, B4.30-1, B4.30-2, B4.31.10-1, B4.31.10-2, B4.40-1, B5.11.13-2, B5.11.13-3, B6-1, B6.11.1-1 thru B6.11.1-3, B6.11.2-1 thru B6.11.2-7, B6.11.3-1, B6.11.4-1, B6.11.5-1, B6.11.6-1 thru B6.11.6-6, B6.11.7-1, B6.11.7-2, B6.12.1-1 thru B6.12.1-5, B6.12.1-7 thru B6.12.1-12, B6.12.1-14 thru B6.12.1-16, B6.12.2-1 thru B6.12.2-3, B6.12.2-6, B6.12.3-1 thru B6.12.3-8, B6.12.4-4, B6.12.4-6 thru B6.12.4-8. Pages Added: A1-4, B1.50.4-2, B2.50-8, B4.30-3, B6.11.1-4 thru B6.11.1-6, B6.11.4-1.1, B6.11.5-2 thru B6.11.5-10, B6.11.6-7 thru B6.11.6-17. Pages Deleted: B6.11.3-2 thru B6.11.3-4, B6.11.7-3 thru B6.11.7-14, B6.11.8-1 thru B6.11.8-3.
P 3/82	Pages Revised: A1-4, B1.60-1, B4.30-2, B4.30-3, B5.11.13-2, B6.11.2-2, B6.11.5-3, B6.11.5-8, B6.11.6-4, B6.11.6-7, B6.11.6-9 thru B6.11.6-11, B6.12.1-3, B6.12.1-8, B6.12.1-11, B6.12.1-13 thru B6.12.1-18, B6.12.2-4 thru B6.12.2-6, B6.12.3-3 thru B6.12.3-8. Pages Added: B3.23.10-5 thru B3.23.10-7, B6.12.4-11.
Q 12/82	Pages Revised: A1-4, B1.60-1, B3-1, B6.11.2-1, B6.11.2-2, B6.11.2-3, B6.11.5-9, B6.11.5-10, B6.11.6-4, B6.11.6-5, B6.11.6-7, B6.11.6-11, B6.12.1-3, B6.12.1-4, B6.12.1-14, B6.12.1-15, B6.12.1-16, B6.12.2-4, B6.12.3-3, B6.12.3-5, B6.12.3-7, B7-1. Pages Added: B3.23.10-8 thru B3.23.10-20, B6.11.2-2.1, B7.050-1 thru B7.050-13. Pages Deleted: B7.030.1-1 thru B7.030.1-5.

Section A1 - Log of Revisions

Rev. No./Date

R 11/86

Pages Revised: B3.23.10-5, B3.23.10-6, B3.23.10-7, B5.11.13-2, B5.11.3-3, B6.11.1-1, B6.11.2-2, B6.11.3-1, B6.12.1-11, B6.12.1-15, B6.12.2-1, B6.12.2-2, B6.12.2-3, B6.12.2-4, B6.12.2-5, B6.12.2-6, B6.12.3-3, B6.12.3-4, B6.12.3-5, B6.12.3-6, B6.12.3-7, B6.12.3-8, B6.12.4-11

Pages Added: A1-5, B3.44.10-8, B3.44.10-9, B3.44.10-10, B3.44.10-11, B3.44.10-12

Pages Re-issued (With Old Date): B1.60-2, B3.23.10-11, B3.44.23-1, B6.11.2-2.1, B7.040.3-3

SECTION A - GENERAL

The Structures Manual is issued in three volumes. Volume I contains Section A and subsections B1 and B5 of Section B - Allowable Stresses. Volume II contains the remainder of Section B. Volume III contains all the other sections.

The Table of Contents shown below indicates the topics treated in each of the sections and major subsections of the Structures Manual. Within each section, or where necessary, within a major subsection, a more detailed Table of Contents will be found.

Structures Manual Table of Contents

SECTION A6 - PUBLICATIONS FROM THE STRUCTURAL MECHANICS SECTION

A listing of the publications issued by the Structural Mechanics Section is presented on the following pages. The listing is in chronological order within the subject topics;

Where a digital computer program is associated with the publication, the program number is shown. Additional information concerning some of these computer programs can be found in Section G.

These publications do not have a formal distribution list so that every copy of a particular report may not have the latest revisions. It is important to make sure that one's copy contains the latest revisions. This can be done by checking with the author or the Administrator of the Structural Mechanics Section.

PUBLICATIONS FROM THE STRUCTURAL MECHANICS SECTION

Stress Distribution

Title	Ref. & Date	Author(s)	Digital Computer Program No.
A Method for Reducing The Analysis of Complex Redundant Structures to A Routine Procedure	J.A.S. 10/52	L. B. Wehle, Jr. W. Lansing	
Comprehensive IBM Fuselage Analysis	SMM 3 1/18/57	W. Mueller J. Sposito T. Taglarine M. Guss	
Comprehensive IBM Fuselage Analysis (II)	SMM 6 3/14/57	W. Mueller W. R. Jensen P. Ratner	
IBM Redundant Structures Analysis	SMM 8 6/4/57	W. Mueller	
Comprehensive IBM Fuselage Analysis (III)	SMM 9 8/15/57	W. Mueller J. Malakoff P. Ratner	
Wing Cover Shear Lag	SMM 10 10/4/57	P. Ratner	
Fail Safe Wing Cover Analysis Design 159	SMM 11	P. Ratner I. Jones I. Villalba	
On Simplified Fuselage - Structure Stress Distributions	J.A.S. Vol. 25 No. 10 10/58	W. R. Jensen	
Eagle Missile - Bending Moments In Shell Reinforcement At Booster Fin Tie Down	SMM 16 9/60	P. Ratner J. Malakoff	
Redundant Structure Analysis: Examples & Comments	GE 191 5/61 Rev. 6/62	E. Lerner	

PUBLICATIONS FROM THE STRUCTURAL MECHANICS SECTION

Stress Distribution

Title	Ref. & Date	Author(s)	Digital Computer Program No.
A Matrix Force Method For Analyzing Heated Wings, Including Large Deflections	ADR 02-11-61.1 * 5/61	W. Lansing P. Ratner I. W. Jones	
Analysis of Redundant Structures With Thermal Strains	ADR 02-12-61.2 6/61	I. W. Jones	
Some Refinements To Wing Redundant Structure Analysis Methods	ADR 02-12-61.3 6/61	I. W. Jones	
Heated Wing Analysis Method - Formulas and Details	ADR 02-12-61.4 7/61	I. W. Jones	
Bending Moments For The Design of Pressurized Shell Reinforcing Rings At Concentrated Loads	ADR 02-11-61.2	W. R. Jensen	45099
Section Properties and Stress Program For IBM 1620	Str. Section Memo No. 62-5-25 1/62	W. Elkins	1620 Program
Redundant Analysis of A2F-1 Wing	GE 194 2/62	W. R. Jensen	
Non-Linear Analysis of Heated, Cambered Wings By The Matrix Force Method	AIAA Journal Vol. 1, No. 7 7/63 ADR 02-12-62.1 7/63	W. Lansing I. W. Jones P. Ratner	
Flexibility Influence Coefficients	GE 180 6/62	P. Ratner	
A Simple Check on Structural Flexibilities	SMM 19 6/15/62	W. R. Jensen E. Lerner	

* Also Symposium Proceedings, Structural Dynamics of High Speed Flight, April 1961, Office of Naval Res. ACR-62, Vol. 1, pp. 533-566 (1962).

PUBLICATIONS FROM THE STRUCTURAL MECHANICS SECTION

Stress Distribution

Title	Ref. & Date	Author(s)	Digital Computer Program No.
Digital Computer Instructions For a Symmetrical Wing Redundant Structure Analysis	GE 196 7/62 Rev. 6/64	W. R. Jensen P. Ratner	45051 45091
Non-Linear Analysis of Shallow Shells By The Matrix Force Method	ADR 02-11-62.1 7/62 NASA TN D-1510, 1962	I. W. Jones W. Lansing P. Ratner	45131
Finite Element Solution For a Type of Non-Linear Shell Buckling	ADR 02-11-62.2 8/62	I. W. Jones	
Digital Computer Instructions For Obtaining-Wing Flexibility Influence Coefficients	GE 197 (prelim.) 8/62 (not rel.)	P. Ratner	45035 A & B
Small Scale Elastic Analysis On 1620	Str. Section Memo (63-5-8) 7/63	W. Elkins	1620 Program
Fatigue Damage Caused By Loading Distribution	GE 200 (Prelim.) 1/64 (not rel.)	A. Kelsey	
Comparison of Matrix Methods For Inelastic Structural Analysis	Jnl. of Spacecraft & Rockets, Vol. 3 No. 4, pg 449-457 4/66 AIAA J. 3, pg 1307 - 1313 (1965) ADR 02-11-64.1 2/64	T. J. Mentel	45153

PUBLICATIONS FROM THE STRUCTURAL MECHANICS SECTION

Stress Distribution

Title	Ref. & Date	Author(s)	Digital Computer Program No.
Non-Linear Numerical Analysis of Axisymmetrically Loaded Arbitrary Shells of Revolution	AIAA Jrl. 3, No. 7 ADR 02-11-64.3 7/64	P. Mason R. Rung J. Rosenbaum R. Ebrus	45156
Non-Linear Analysis of a Shallow Arch	SMM 25 4/15/64	J. Rosenbaum	45156
Barrel Roof Shell Analysis	GE 209 11/64	J. Rosenbaum	45164
On Evaluation of Matrix Methods For Non-Linear Biaxial Stress Analysis	ADR 02-11-64.2 6/64	T. J. Mentel	
Analysis Methods for Barrel Shells	ADR 02-11-64.4 8/64	T. J. Mentel	
Non-Linear, Axi-Symmetric Analysis of Spherical Caps by the Matrix Force Method	ADR 02-11-64.5	J. Rosenbaum	
Comparison of Matrix Force And Direct Stiffness Methods of Redundant Structure Analysis	ADR 02-11-65.1 1/65	W. E. Falby J. Zalesak	
Matrix Analysis Methods For Inelastic Structures Part I Elastic - Plastic Solution of Shear Lag Problem	ADR 02-11-65.2 2/65	W. R. Jensen J. Zalesak W. E. Falby	45128
A User's Manual for the ASTRAL (Automated Structural Analysis) System	ADN 02-11-65.1 3/65	P. Mason	

PUBLICATIONS FROM THE STRUCTURAL MECHANICS SECTION

Stress Distribution

Title	Ref. & Date	Author(s)	Digital Computer Program No.
Structural Synthesis of an Integrally Stiffened Panel Subjected to Compressive Load	ADR 02-21-65.1 3/65	J. Rosenbaum A. Kelsey H. Pardo	45175
An Introduction to Automated Structural Analysis Methods	ADR 02-11-65.7 6/65	P. Mason	
Matrix Analysis Methods For Isotropic Inelastic Structures	ADR 02-11-65.4* 11/65	W. Lansing W. R. Jensen W. Falby	45128
The ASTRAL Tri-Diagonal Stiffness Program	ADR 02-11-65.6 11/65	P. Mason S. Iaccarino	45174
Unsymmetric Analysis of Shells of Revolution	ADR 02-11-65.3 12/65	R. Rung P. Mason J. Rosenbaum	45156
Matrix Analysis Methods for Anisotropic Inelastic Structures	Air Force Report AFFDL-TR-65-220 ADR 02-11-65.5 2/66	W. Jensen W. Falby N. Prince	45128
Unsymmetric Non-Linear 2nd Order Analysis of Orthotropic Shells of Revolution	ADR 02-11-66.1 4/66	V. Svalbonas	
Modif. of Hill's Theory for Anisotropic Plastic Materials	000-SM-004 4/66	N. Morris	
Structural Analysis of the Lunar Excursion Module (Flexibilities and Internal Load Distribution)	000-SM-005 5/66	P. Mason	

* Presented at conference on "Matrix Methods in Structural Mechanics," October 26-28, 1965 at Air Force Inst. of Technology, Wright-Patterson Air Force Base, Ohio.

PUBLICATIONS FROM THE STRUCTURAL MECHANIC SECTION

Stress Distribution

Title	Ref. & Date	Author(s)	Digital Computer Program No.
Unsymmetric Non-Linear First Order Analysis of Layered Orthotropic Shells of Revolution	ADR 02-11-66.2 5/66	N. Prince R. Rung V. Svalbonas	
Analysis of Beams Subjected To Combined Bending and Axial Loads in the Plastic Range	ADR 02-21-66.1 8/66	L. Brown	45171
Bending & Stretching of Plates By Shot Forming	ADR 08-03-66.1 8/66	H. Switzky	
Unsymmetric Non-Linear Analysis of Thick Orthotropic Sandwich Shells of Revolution	ADR 02-11-67.1 1/67	V. Svalbonas	

PUBLICATION FROM THE STRUCTURAL MECHANICS SECTION

Dynamic Loads Under Transient Conditions

Title	Ref. & Date	Author(s)	Digital Computer Program No.
Shock Load Criteria For the Design of Electronic Equipment For the WF-2 Airplane	IOM 7/10/57	R. Harris A. Kelsey	45041
Dynamic Response of a Linear Single Degree of Freedom System	GE 90A 10/58 Rev. 12/59	S. Kaplan A. Kelsey	45151
Hydrofoil Boat Hull-Wave Impact Loads	GE 173 8/59	W. R. Jensen	45069
Effect on Airframe Response of Variable Coefficient of Group Friction	GE 174 12/59	W. H. Mueller S. M. Kaplan A. S. Kelsey	
A Physical Interpretation of Generalized Harmonic Analysis	SMM 14 12/3/59	A. Kelsey	
Mechanical Reliability of Electronic Equipment	IOM 4/60	A. Kelsey	
Tail Bumper Loads During Braked Rearward Roll	3803.3 6/60	M. Mantus	45043
Analysis of Symmetric Landing Conditions	GE 176 6/60	E. Lerner J. Malakoff W. H. Mueller	45036
Transient Wing Loads Due To Landing and Catapulting	GE 172 6/60	M. Mantus W. H. Mueller J. Malakoff A. Kelsey	45122 A,B 45123 A,B, C,D
Dynamic Loads During Nose Tow Catapulting	ASME Paper 60-AV-49 Aviation Conf., Dallas, Texas 6/5-9/60	W. Lansing W. H. Mueller J. Malakoff M. Mantus	

PUBLICATION FROM THE STRUCTURAL MECHANICS SECTION

Dynamic Loads Under Transient Conditions

Title	Ref. & Date	Author(s)	Digital Computer Program No.
Eagle Ejection - Test and Analysis	SMM 17 10/60	A. Kelsey M. Mantus	
Dynamics of the Arresting Hook Due to Impact with the Deck	GE 184 11/60	M. Mantus A. Kelsey	45023
Dynamic Acceleration at Eagle Attachment Point to A3D, 2P Ult. Landing Loads	Grumman Eagle Project Memo No. 61-022 1/23/61	A. Kelsey M. Mantus	
An Introduction to Mechanical Transfer Functions	Structural Methods Note 5/61	A. Kelsey	45087 45087 TF
Dynamics of a Lunar Roving Vehicle	ADR 06-04b-61.1 6/61	M. Mantus J. Malakoff	45103
Dynamics of a Soft Lunar Landing Vehicle	ADR 06-04c-61.1 7/61	J. Malakoff M. Mantus	
Dynamics of a Re-Entry Vehicle During Earth Landing Impact	ADR 02-10-61.2 9/61	W. Mueller M. Mantus J. Malakoff A. Kelsey	
Water Impact of Manned Spacecraft	ARS Journal 12/61 ADR 02-10-61.1 4/61	W. Mueller J. Malakoff	45067 M
W2F Transient Response Comparison of Drop Test and Analysis	SMM 18 3/23/62	A. Kelsey M. Mantus	
Water Impact of the Mercury Capsule Correlation of Analysis With NASA Tests	AIAA Journal Vol. 1, No. 5 9/62 ADN 02-08-62.1 12/62	J. D. Rosenbaum W. R. Jensen	

PUBLICATION FROM THE STRUCTURAL MECHANICS SECTION

Dynamic Loads Under Transient Conditions

Title	Ref. & Date	Author(s)	Digital Computer Program No.
LEM Landing Investigation	SMM 20 9/7/62	M. Mantus E. Lerner	45126
LEM Docking Investigation	SMM 21 9/7/62	E. Lerner M. Mantus W. Elkins	45127
Dynamics of Unsymmetric Landing	ADR 02-10-62.1 1/63	E. Lerner	45130
E-2A Engine Interference Problem Analytical Evaluation	SMM 23 10/30/63	E. Lerner M. Simonian	45152
Docking: Extendible Probe Concept Cable Reel-In Status Report No. 1	LEM Engr. Memo LMO 520-95A 11/8/63	E. Lerner R. Portnoy	45510
A2F-1 Nose Gear Shimmy Damper Malfunction	SMM 22 SMM 22R 11/12/63	A. Kelsey	
E-2A Nose Gear Shimmy Damper Malfunction	SMM 24 12/4/63	M. Simonian	
Landing Dynamics of the Lunar Excursion Module (Method of Analysis)	LED 520-6 3/6/64	M. Mantus E. Lerner W. Elkins	45500 45501 45505
LEM Docking - Center Probe and Drogue Analysis	SMM 26 4/20/64	E. Lerner	45511
Analysis of the Effect that Engine Flexibility and Gyroscopically Induced Moments Have on E-2A Engine Response Under Landing Conditions	GE 205 5/64	M. Simonian E. Lerner	45152

PUBLICATION FROM THE STRUCTURAL MECHANICS SECTION

Dynamic Loads Under Transient Conditions

Title	Ref. & Date	Author(s)	Digital Computer Program No.
A Method For Predicting The Dynamic Behavior of a Particular Type of Articulating Landing Gear	ADN 02-10-65.1 6/65	E. Lerner H. Pardo	45182
Handbook for Application of Unsymmetric Landing Analysis Computer Program	GE-212 8/65	H. Pardo	45130
A Method for Predicting Dynamic Loads During Nose Tow Catapulting	ADR 02-10-65.1 10/65	E. Lerner	45145
An Introduction to Structural Dynamics	000-SM-1 2/66	E. Lerner A. Kelsey	
Extension of 'A Method for Predicting Dynamic Loads During Nose Tow Catapulting' To Include Airframe Flexibility	ADR 02-10-66.1 4/66	E. Lerner	45145
Inertia Load Distr. Progr.	000-SM-009 10/66	M. Mantus W. Elkins	45508
Landing Dynamics of the Lunar Excursion Module	JNL. of Spacecraft & Rockets, Vol. 3, 10/66 (pg. 1484)	W. Mueller R. Hilderman M. Mantus	
Nose Tow Catapulting, Off-Center Spotting	ADR 02-10-66.2 11/66	H. Pardo	45142

PUBLICATIONS FROM THE STRUCTURAL MECHANICS SECTION

Temperature Distribution

Title	Ref. & Date	Author(s)	Digital Computer Program No.
Aerodynamic Heating of Canopies Comparison of Calculated and Flight Test Recorded Temperatures	SMM 1 1/57	E. Diamant	
Calculation of Transient Temperature Distribution in Sandwich Panel of F11F-1F Main Fuel-Cell Duct-Wall	SMM 2 1/57	E. Diamant G. Myers	
Temperature Distribution in a Proposed Liquid Cooled Wing Skin	SMM 7 4/57	E. Diamant W. Wolter	
Heat Transfer in Welding Analysis	ADR 02-07-62.1 5/62	M. C. Daley	
Heat Transfer and Residual Stress Analysis in Quenching a Hollow Cylinder	ADR 02-12-62.2 11/62	M. B. Reiber M. C. Daley W. A. Wolter	45065
General Computer Programs for the Determination of Radiation Configuration Factors in the Presence of Shadowing Surfaces	ADR 02-20-64.1 10/64	M. B. Reiber	45113
Surface Temperatures During Re-Entry of Design 359A Obtained with "Thermopaint" Technique	SDM 2 10/64	A. D'Ammassa	
Determination of Radiation Config. uration Factors in the Presence of Shadowing Surfaces	000-SM-2 2/66	M. B. Reiber	45113

PUBLICATIONS FROM THE STRUCTURAL MECHANICS SECTION

Allowable Stresses

Title	Ref. & Date	Author(s)	Digital Computer Program No.
Method for Calculating Shear Lag Type Load Distributions in Multiple Fastener Joints	GE 145 6/56	I. Villalba W. Lee	
Fatigue Allowables for Mechanically Fastened and Spot Welded Joints	GE 150 7/56	I. Villalba L. Fischer	
Evaluation of Magnesium Sheet for Use in Aircraft Structures	GE 163 4/57	L. S. Perkins A. Gomza R. Micich	
Canopy Glazing Materials	SDM 1 4/57	W. Wolter	
Fatigue Curves for 2014, 2024 and 7075 Aluminum Alloys and 4340 Steel Alloy	GE 144 2/58	D. O. Eisele A. Gomza	
Calculation of Fatigue Life by Grumman Method and Comparison with Test Data	GE 168 2/59 Rev. 3/59	F. Ripp	45006
Low Temperature Properties of Welded and Unwelded 2014-T6 Clad Aluminum Alloy	GE 177 3/60	A. Gomza W. Lee I. Villalba	
Fatigue Tests of Welded and Unwelded 4130, 4330 V Modified and Hy80 Steels	GE 182 3/61	R. Heitzmann F. Ripp	
Investigation of Strength and Fabricability of Welded Stainless Steel Corrugated Core Sandwich Panels	ADR 02-02-62.2 12/62	I. Villalba	

PUBLICATIONS FROM THE STRUCTURAL MECHANICS SECTION

Allowable Stresses (Cont'd)

Title	Ref. & Date	Author(s)	Digital Computer Program No.
Theoretical Increase in Stress Concentration Factor in Bending for Thin Sheets, due to Chem-Milling Process	GE 198 1/63	I. Villalba	
Strength of Fiberglass Laminates Under Combined Stress	ADN 02-13-64.1 10/64	M. B. Reiber	45132
Stress Analysis of Multi-Layer Laminates Subjected to In-Plane Loads	GE 181 11/64	L. Fischer	
Strength and Deflection Characteristics of Mechanically Fastened Joints	GE 148 (Not Rel.)	I. Villalba W. Lee	
Theoretical and Experimental Investigation of Lugs Loaded by a Transferve or Oblique Load	ADR 02-12-65.2 1/66	I. Villalba	

PUBLICATIONS FROM THE STRUCTURAL MECHANICS SECTION

Aeroelasticity

Title	Ref. & Date	Author(s)	Digital Computer Program No.
An Engineering Evaluation of Airplane Gust Load Analysis Methods		D. George J. Smedfjeld G. Schriro	45745 6 7
Vol. I - Theoretical Devel.	ADR 06-14-63.1 10/63		8
Vol. II - Calculation Proced.	ADR 06-14-63.2 11/63		9
Theory and Digital Computer Programs for Application of Power-Spectral Gust-Response Analysis Methods	ADR 06-14-66.1 10/66	D. George J. Smedfjeld	45710
Gust Effects Due to Special Weapons Delivery, A-6A Airplane. (c)	DA 128-495.1	D. George G. Schriro	45741 2
Vol. I - Theoretical Devel.			3
Vol. II - Calculation Proced.			4
Vol. III - Results			

PUBLICATION FROM THE STRUCTURAL MECHANICS SECTION

General

Title	Ref. & Date	Author(s)	Digital Computer Program No.
Introduction to Statistical Techniques Pertinent to Structural Analysis	ADR 02-12-64.1 9/64	A. Kelsey	

SECTION B - ALLOWABLE STRESSES

Table of Contents

SECTION B1 - MATERIAL PROPERTIES

TABLE OF CONTENTS

NOTE: The Section on Structural Design for Fatigue may be found in Section B7

B1.10 INTRODUCTION

Compressive Stress-Strain Relations in the Yield Range

Stress-strain curves are of fundamental importance in the computation of inelastic instability and failure stresses. The number of design charts required for the many available structural materials and the various allowable stresses for these materials at room and elevated temperatures can be greatly reduced by use of a non-dimensional mathematical description of stress-strain relations.

Symbols

E_c	Design elastic modulus (figure B1.10-1), psi
E_S	Secant modulus of elasticity, psi
E_T	Tangent modulus of elasticity, psi
E'	Typical elastic modulus (figure B1.10-1), psi
F	Stress, psi
F_{crel}	Elastic buckling stress, psi
F_{cr}	Plastic buckling stress, psi
F_{cy}	Design compressive yield stress (figure B1.10-1), psi
$F_{0.7}$	Reference stress, stress at secant modulus $.7E_c$ (figure B1.10-1), psi
$f_{.05}$	.05% offset stress, typical stress-strain curve (figure B1.10-1), psi
$f_{0.2}$	0.2% offset stress, typical stress-strain curve (figure B1.10-1), psi
n	Shape factor of stress-strain curve
ϵ	Strain
η	Plasticity correction factor
ν	Instantaneous Poisson's ratio
ν_e	Elastic Poisson's ratio
ν_p	Fully plastic Poisson's ratio, = 0.5 for isotropic materials.

The stress-strain relation of a material can be represented by the modified Ramberg-Osgood equation:

$$\frac{E_c \epsilon}{F_{0.7}} = \frac{F}{F_{0.7}} + \frac{3}{7}\left(\frac{F}{F_{0.7}}\right)^n \qquad \text{B1-1}$$

which is plotted in non-dimensional form on page B1.30-2

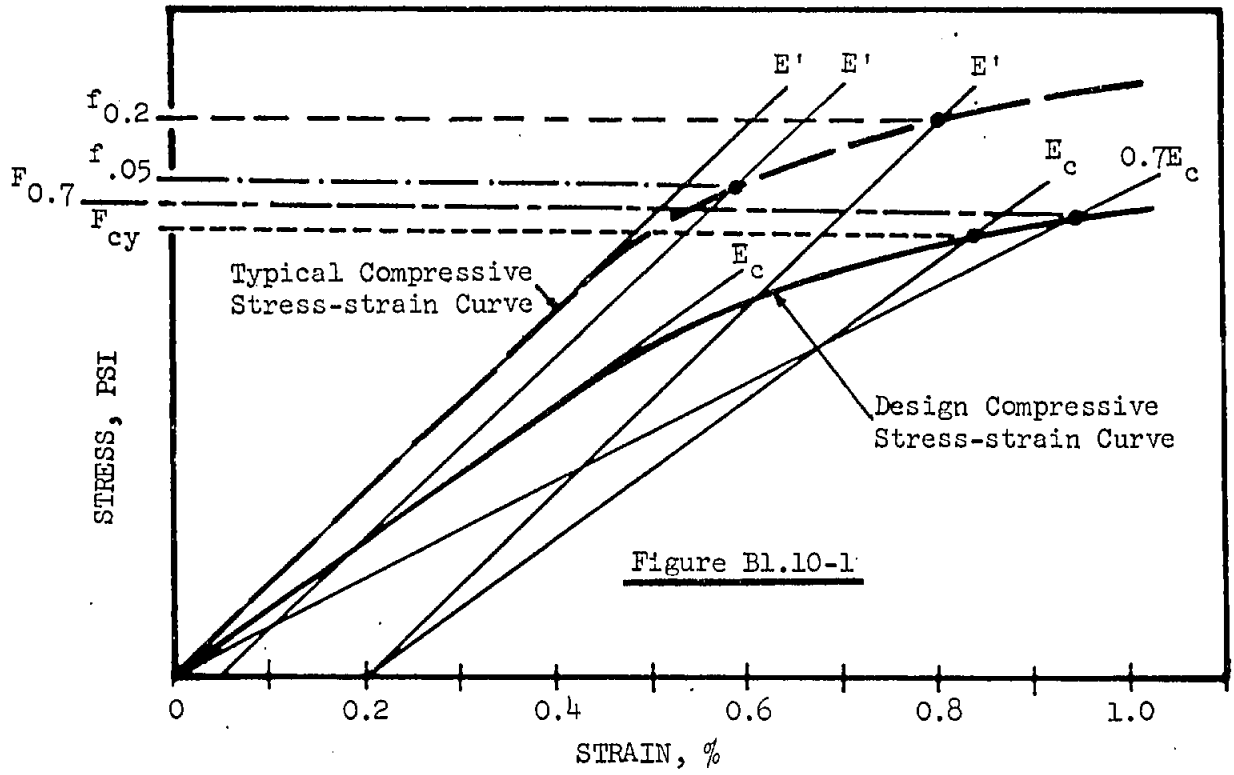

Figure B1.10-1

The parameter n describes the shape of the stress-strain curve in the yield region. It can be found from a typical stress-strain curve by scaling two stresses and their corresponding offset strains. The .05% and 0.2% offsets have been used here as shown in figure B1.10-1. Hence

$$n = \frac{\text{Log}_e\ (.2/.05)}{\text{Log}_e\ (f_{.2}/f_{.05})} \qquad \text{B1-2}$$

Equation B1-2 is plotted for convenience in figure B1.10-2.

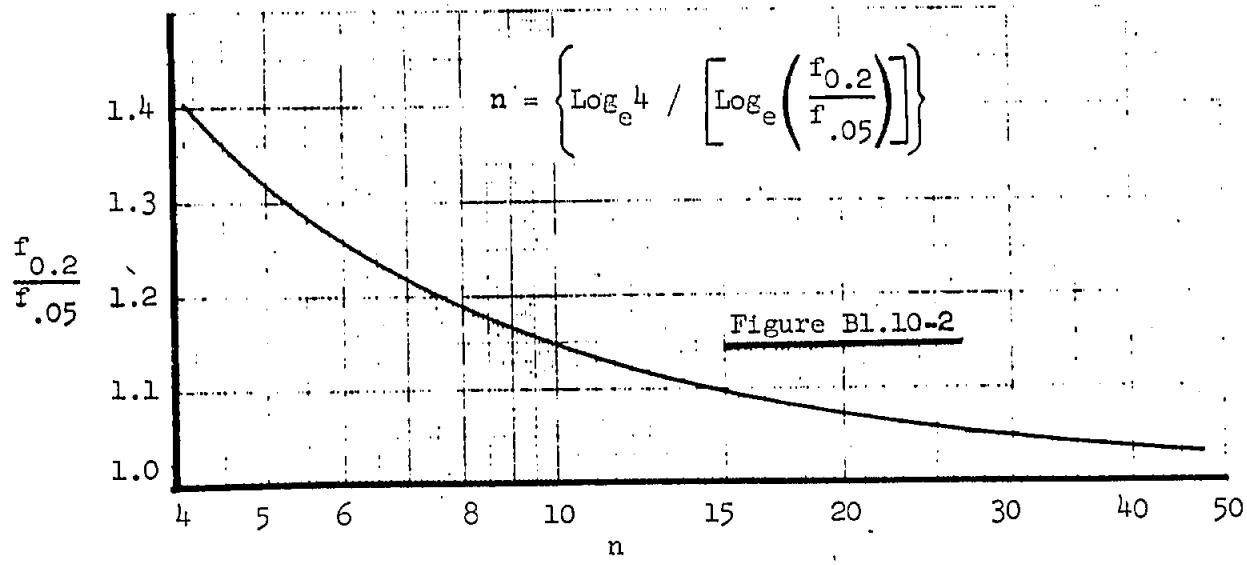

Figure B1.10-2

Grumman

The reference stress $F_{0.7}$, is chosen so that a stress-strain curve, having the same curvature (described by n) as the typical stress-strain curve, will pass through a specified value of the yield stress. Then

$$F_{0.7} = F_{cy}\left(214.3\,\frac{F_{cy}}{E_c}\right)^{1/(n-1)} \qquad \text{B1-3}$$

is the reference stress corresponding to the design compressive stress-strain curve. In equation B1-3, F_{cy} and E_c are <u>design</u> values and n describes the curvature of a <u>typical</u> compressive stress-strain curve.

Design values of $F_{0.7}$, E_c, and n for a large number of materials are tabulated in Section B1.20. From these values and the curves of B1.30-2, appropriate compressive stress-strain relations are easily found.

To determine the design stress-strain relation of a material not included in the tables of Section B1.20 (but whose design yield stress and design elastic modulus are known, and for which a typical stress-strain curve is available), the following procedure should be followed:

1) From the typical stress-strain curve determine $f_{.05}$ and $f_{0.2}$.
2) From figure B1.10-2 determine n
3) From equation B1-3 determine $F_{0.7}$

For inelastic buckling problems the modulus ratios E_c/E_S and E_c/E_T appear. These ratios have been computed as follows and have been plotted in non-dimensional form on pages B1.40-2,-3:

$$\frac{E_c}{E_S} = 1 + \frac{3}{7}\left(\frac{F}{F_{0.7}}\right)^{n-1} \qquad \text{B1-4}$$

$$\frac{E_c}{E_T} = 1 + \frac{3n}{7}\left(\frac{F}{F_{0.7}}\right)^{n-1} \qquad \text{B1-5}$$

The non-dimensional approach has been applied to determining the effect of exceeding the proportional limit of material on its buckling stress. This is discussed in paragraph B1.50.0.

B1.20 MATERIAL PROPERTIES

The following pages present basic data and material properties for a large number of flight vehicle materials. The following information is listed:

(1) MATERIAL - The alloy, temper and/or heat treatment designation is listed under this heading. For definitions of the various tempers and heat treatments see MIL-HDBK-5A.

(2) FORM - as indicated. Note that the designation "plate" refers to material greater than 0.249 inch thick.

(3) THICKNESS - The thickness of the material. Note that in the case of extrusions, a cross-sectional area exceeding 20 in^2 can influence material properties; see MIL-HDBK-5A.

(4) DIRECTION OF LOADING - The direction in which the material is loaded is referred to the three material axes shown below.

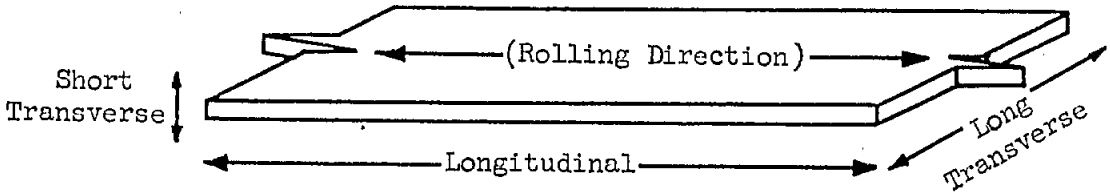

(5) TEMPERATURE - Temperature of material in degrees Fahrenheit Exposure time is $\frac{1}{2}$ hour unless otherwise indicated.

(6) ELONGATION (e) - A measure of the ductility of the material measured generally in accordance with Federal Test Method Standard 151. Values given in tables are A-values unless otherwise indicated.

(7) ULTIMATE TENSILE STRESS (F_{tu}) - The stress at maximum tensile load. Stresses are based on the original cross-section area of the section. Values given in the tables are A-values unless otherwise indicated.

(8) COMPRESSIVE YIELD STRESS (F_{cy}) - the compressive stress corresponding to a permanent strain of .2% as shown in figure B1.10-1. A and B-Values of F_{cy} are listed in the tables, unless otherwise indicated.

(9) COMPRESSIVE MODULUS OF ELASTICITY (E_c) - the ratio of stress to strain below the proportional limit of the material. Values of the modulus of elasticity in the tables are average values unless otherwise indicated. For clad materials, only secondary modulii are given in the tables.

(10) REFERENCE STRESS ($F_{0.7}$) - As discussed earlier in section B1.10. Given with the design yield stress on which it is based.

(11) SHAPE PARAMETER (n) - as discussed earlier in section B1.10.

BASIS - Primary strength properties appearing in the tables are identified by a letter indicating the basis on which they were established:

B-Value is the value above which at least 90 percent of the population of values is expected to fall with a confidence of 95 percent.

A-Value is the value above which at least 99 percent of the population of values is expected to fall with a confidence of 95 percent.

S-Value the specified minimum value of the governing Military Spec. or SAE Aerospace Material Spec. of the material.

REFERENCES

1. MIL-HDBK-5A
2. Section B1.70
3. BRUHN, Analysis and Design of Flight Vehicle Structures, 1965
4. Mechanical Properties of Stress-Relieved Stretched Aluminum Alloy Plate. ML-TDR-64-105. Air Force Materials Laboratory, Wright Patterson A.F. Base, Ohio, May 1964.
5. GAEC IN-PLANT TESTS
6. GRUMMAN TITANIUM DESIGN GUIDE
7. TIMET Bulletin #1; February, 1965
8. BATTELLE MEMORIAL INSTITUTE AFML-TR-67-142; March,1967
9. TIMET Case Study M515; November, 1968
10. TIMET Eng'g Bulletin #10. September, 1967

B1.20.1 Aluminum Alloys

MATERIAL	FORM	THICKNESS (IN.)	LOADING DIRECTION	TEMP. (F^o)	e (%)	F_{TU} (ksi)	E_c (10^3ksi)	n	A-VALUE F_{cy} (ksi)	A-VALUE $F_{0.7}$ (ksi)	OTHER* F_{cy} (ksi)	OTHER* $F_{0.7}$ (ksi)	REFERENCE
2024-T3	Bare Sheet	0.020-0.249	L. Transv.	R.T.	15[a]	64[a]	10.7	10.5	---	---	45[a]	44.5[a]	1
		0.020-0.249	Longit.	R.T.	12[b]	65[b]	10.7	10.5	----	---	42[b]	41.2[b]	2,3
		0.020-0.249	Longit.	300	12[b]	63[b]	10.2	8.5	---	---	37[b]	35.8[b]	3
	Clad Sheet	0.020-0.062	Longit.	R.T.	15	60	9.7[c]	13.5	37	36.4	39	38.5	1
		0.063-0.249			15	63	10.2[c]	13.5	38	37.3	40	39.4	
		0.020-0.062	L. Transv.		15	59	9.7[c]	18	42	41.8	44	43.9	
		0.063-0.249			15	62	10.2[c]	18	43	42.7	45	44.8	
		0.020-0.062	Longit.	212	15	54.9	9.46[c]	6[d]	35.5	34.0[e]	37.4	36.2[e]	
		0.063-0.249			15	57.6	9.95[c]	6[d]	36.4	34.7[e]	38.4	37.0[e]	
		0.020-0.062	L. Transv.		15	54.0	9.46[c]	8	40.3	39.8	42.2	41.9	
		0.063-0.249			15	56.8	9.95[c]	8	41.2	40.5	43.2	42.8	
		0.020-0.062	Longit.	300	15	49.8	9.24[c]	7.5[d]	34.1	32.9[e]	35.9	34.9[e]	
		0.063-0.249			15	52.4	9.70	7.5[d]	35.0	33.6[e]	36.8	35.6[e]	
		0.020-0.062	L. Transv.		15	49.0	9.24[c]	10	38.7	38.2	40.5	40.2	
(cont'd)	(cont'd)	0.063-0.249			15	51.5	9.70[c]	10	39.6	39.0	41.4	41.0	

* - B-Value unless otherwise indicated

a - S. Value or Based on S-Value

b - Statistical basis not known

c - Secondary Modulus - See Ref. for Primary Modulus

d - Estimated Value

e - Based upon estimated value of n

Grumman

B1.20.1 Aluminum Alloys (cont'd)

MATERIAL	FORM	THICKNESS (IN.)	LOADING DIRECTION	TEMP. (°F)	e (%)	F_{TU} (ksi)	E_c (10^3ksi)	n	A-VALUE F_{cy} (ksi)	A-VALUE $F_{0.7}$ (ksi)	OTHER* F_{cy} (ksi)	OTHER* $F_{0.7}$ (ksi)	REFERENCE
2024-T3 (cont'd)	Clad Sheet (cont'd)	0.020-0.062	Longit.	400	15	44.3	8.67[c]	10.5[d]	31.6	30.8[e]	33.3	32.6	1
		0.063-0.249			15	46.5	9.12[c]	10.5[d]	32.5	31.6[e]	34.2	33.4[e]	
		0.020-0.062	L. Transv.		15	43.5	8.67[c]	14	35.9	35.6	37.6	37.4	
		0.063-0.249			15	46.7	9.12[c]	14	36.7	36.3	38.5	38.2	
2024-T351	Bare Plate	0.250-0.499	Longit.	R.T.	--	65	10.7	8.5	38	36.6	41	40.0	1,4
		0.500-1.000			--	62	10.7	8.5	38	36.6	41	40.0	
		1.001-1.500			--	62	10.7	8.5	38	36.6	40	38.8	
		1.501-2.000			--	61	10.7	8.5	38	36.6	39	37.8	
		0.250-0.499	L. Transv.		12	64	10.7	12	43	42.4	46	45.7	
		0.500-1.000			8	62	10.7	12	44	43.5	47	46.7	
		1.001-1.500			7	62	10.7	12	44	43.5	46	45.7	
		1.501-2.000			6	61	10.7	12	43	42.4	45	44.6	

* - B-Value unless otherwise indicated

c - Secondary Modulus - See Reference for primary modulus

d - Estimated Value

e -based on estimated value of n

Grumman

B1.20.1 Aluminum Alloys (cont'd)

MATERIAL	FORM	THICKNESS (IN.)	LOADING DIRECTION	TEMP. (^{o}F)	e (%)	F_{TU} (ksi)	E_c (10^3ksi)	n	A-VALUE F_{cy} (ksi)	A-VALUE $F_{0.7}$ (ksi)	OTHER* F_{cy} (ksi)	OTHER* $F_{0.7}$ (ksi)	REFERENCE
2024-T4	Extrusion	0.050-0.249	Longit.	R.T.	12	57	10.7	16.5	38	36.3	41	40.5	1,2
		0.250-0.499			12	60	10.7	10.5	39	38.0	42	41.2	
		0.500-0.749			12	60	10.7	10.5	39	38.0	42	41.2	
		0.750-1.499			10	65	10.7	10.5	44	43.4	52	52.2	
2024-T81	Clad Sheet	0.010-0.062	Longit.	R.T.	--	64[a]	9.7[c]	19	--	---	55[a]	55.6[a]	1
		0.063-0.249			--	67[a]	9.7[c]	19	--	---	57[a]	57.7[a]	
		0.010-0.062	L. Transv.		--	62[a]	9.7[c]	19[d]	--	---	55[a]	55.6[f]	
		0.063-0.249			--	65[a]	9.7[c]	19[d]	--	---	57[a]	57.7[f]	
		0.010-0.062	Longit.	200^{o}	--	61.4[a]	9.5[c]	19[d]	--	---	51.8[a]	52.3[f]	
		0.063-0.249			--	64.2[a]	9.5[c]	19[d]	--	---	53.7[a]	54.3[f]	
		0.010-0.062	L. Transv		--	59.5[a]	9.5[c]	19	--	---	51.8[a]	52.3[a]	
		0.063-0.249			--	62.4[a]	9.5[c]	19	--	---	53.7[a]	54.3[a]	
		0.010-0.062	Longit.	300	--	55.2[a]	9.24[c]	17.5[d]	--	---	47.3[a]	47.6[f]	
		0.063-0.249			--	57.7[a]	9.24[c]	17.5[d]	--	---	49[a]	49.4[f]	
		0.010-0.062	L. Transv		--	53.3[a]	9.24[c]	17.5	--	---	47.3[a]	47.6[a]	
(cont'd)	(cont'd)	0.063-0.249			--	56.0[a]	9.24[c]	17.5	--	---	49[a]	49.4[a]	

* - B-Value unless otherwise indicated

a - S-Value or based on S-Value

c - Secondary Modulus - See reference for primary modulus

d - Estimated value

f - based on estimated value of n and S-Value of F_{cy}

Grumman

B1.20.1 Aluminum Alloys (cont'd)

MATERIAL	FORM	THICKNESS (IN.)	LOADING DIRECTION	TEMP. (°F)	e (%)	F_{TU} (ksi)	E_c (10^3ksi)	n	A-VALUE F_{cy} (ksi)	A-VALUE $F_{0.7}$ (ksi)	OTHER* F_{cy} (ksi)	OTHER* $F_{0.7}$ (ksi)	REFERENCE
2024-T81 (cont'd)	Clad Sheet (cont'd)	0.010-0.062	Longit.	400	--	44.5[a]	8.67[c]	11[d]	--	--	41.3[a]	41.4[f]	1
		0.063-0.249			--	46.6[a]	8.67[c]	11[d]	--	--	42.8[a]	43.0[f]	
		0.010-0.062	L. Transv.		--	43.2[a]	8.67[c]	11	--	--	41.3[a]	41.4[a]	
		0.063-0.249			--	45.2[a]	8.67[c]	11	--	--	42.8[a]	43.0[a]	
	Bare Sheet	0.010-0.249	Longit.	R.T.	--	67	10.7	16	59	59.7	61	61.8	1,4,5
		0.010-0.249	L. Transv.		5	67	10.7	25	58	58.4	60	60.5	
2024-T851	Bare Plate	0.250-0.499	Longit.	R.T.	--	67	10.7	17.5	59	59.6	61	61.7	1,4,5
		0.500-1.000			--	66[a]	10.7	17.5	--	--	58[a]	58.5[a]	
		0.250-0.499	L. Transv.		5	67	10.7	21	59	59.5	61	61.6	
		0.500-1.000			5[a]	66[a]	10.7	21	--	--	59[a]	59.5[a]	
2219-T62	Sheet and Plate	0.125-2.000	Longit.	R.T.	-	54	10.8	15.5	38	37.3	39	38.3	1
		0.125-2.000	L. Transv.		6	54	10.8	15.5	38	37.3	39	38.3	
2219-T81	Sheet	0.040-0.249	Longit.	R.T.	-	60	10.8	21.5	46	45.8	47	46.8	1
		0.040-0.249	L. Transv.		6	61	10.8	21.5	47	46.8	48	47.9	

* - B-Value unless otherwise indicated

a - S -Value or based on S-Value

c - Secondary Modulus - See reference for primary modulus

d - Estimated value

f - Based on estimated value of n and S-Value of F_{cy}

Grumman

B1.20.1 Aluminum Alloys (cont'd)

MATERIAL	FORM	THICKNESS (IN.)	LOADING DIRECTION	TEMP. (^{o}F)	e (%)	F_{TU} (ksi)	E_c (10^3ksi)	n	A-VALUE F_{cy} (ksi)	A-VALUE $F_{0.7}$ (ksi)	OTHER* F_{cy} (ksi)	OTHER* $F_{0.7}$ (ksi)	REFERENCE
2219-T851	Plate	0.250-2.000	Longit.	R.T.	-	60	10.8	21.5	46	45.8	47	46.8	1
		0.250-2.000	L. Transv.		6	61	10.8	21.5	47	46.8	48	47.9	
2219-T87	Sheet and	0.040-1.000	Longit.	R.T.	-	62	10.8	13	50	50.1	51	51.1	1
	Plate	0.040.1.000	L. Transv.		5	63	10.8	16.5	53	53.2	54	54.2	
6061-T6	Sheet and	0.010-2.000	Longit.	R.T.	-	42	10.1	20.5	35	34.5	37	36.5	1
(T651)	Plate	0.010-2.000	L. Transv.		8-10	42	10.1	25.0	36	35.6	38	37.7	
	Extrusion	≤3.000	Longit.	R.T.	10	38	10.1	16.5	34	33.3	--	----	
7075-T6	Clad	0.012-0.039	Longit.	R.T.	7	70	9.7[c]	13	62	64.1	65	67.1	1,2
	Sheet	0.040-0.062			8	72	9.7[c]	13	64	66.1	66	68.1	
		0.063-0.187			8	73	10.0[c]	13	65	67.1	67	69.1	
		0.188-0.249			8	75	10.2[c]	13	66	68.1	68	70.1	
		0.012-0.039	L.Transv.		7	70	9.7[c]	11.5	64	66.6	67	69.6	
		0.040-0.062			8	72	9.7[c]	11.5	66	68.6	68	70.7	
		0.063-0.187			8	73	10.0[c]	11.5	67	69.6	69	71.6	
(cont'd)	(cont'd)	0.188-0.249			8	75	10.2[c]	11.5	68	70.7	70	72.6	

* - B-Value unless otherwise indicated

c - Secondary modulus - See Reference for primary values

B1.20.1 Aluminum Alloys (cont'd)

MATERIAL	FORM	THICKNESS (IN.)	LOADING DIRECTION	TEMP. (°F)	e (%)	F_{TU} (ksi)	E_c (10^3ksi)	n	A-VALUE F_{cy} (ksi)	A-VALUE $F_{0.7}$ (ksi)	OTHER* F_{cy} (ksi)	OTHER* $F_{0.7}$ (ksi)	REFERENCE
7075-T6 (cont'd)	Clad Sheet (cont'd)	0.012-0.039	Longit.	200	-	61.7	9.2[c]	18[d]	58.2	59.2[e]	61	62.3[e]	1,2
		0.040-0.062			-	63.5	9.2[c]	18[d]	60	61.2[e]	62	63.4[e]	
		0.063-0.187			-	64.4	9.5[c]	18[d]	61	62.2[e]	62.9	64.2[e]	
		0.187-0.249			-	66.1	9.7[c]	18[d]	62	63.2[e]	63.8	65.1[e]	
		0.012-0.039	L. Transv.		-	61.7	9.2[c]	16	60	61.4	62.9	64.5	
		0.040-0.062			-	63.5	9.2[c]	16	61.9	63.6	63.8	65.6	
		0.063-0.187			-	64.4	9.5[c]	16	62.8	64.4	64.8	66.5	
		0.188-0.249			-	66.1	9.7[c]	16	63.7	65.3	65.7	67.4	
		0.012-0.039	Longit.	300	-	51.8	8.6[c]	18[d]	51.5	52.3[e]	54.0	55.0	
		0.040-0.062			-	53.3	8.6[c]	18[d]	53.2	54.1[e]	54.9	55.9[e]	
		0.063-0.187			-	54.0	8.9[c]	18[d]	54.0	54.8[e]	55.7	56.7[e]	
		0.188-0.249			-	55.5	9.1[c]	18[d]	54.8	55.6[e]	56.5	57.4[e]	
		0.012-0.039	L. Transv.		-	51.8	8.6[c]	16	53.2	54.3	55.6	56.8	
		0.040-0.062			-	53.3	8.6[c]	16	54.8	56.1	56.5	57.8	
		0.063-0.187			-	54.0	8.9	16	55.7	56.9	57.2	58.4	
(cont'd)		0.188-0.249			-	55.5	9.1[c]	16	56.5	57.7	58.1	59.3	

* - B-Value unless otherwise indicated

c - Secondary modulus - See reference for primary values

d - Estimated value

e - Based on estimated value of n

Grumman

B1.20.1 Aluminum Alloys (cont'd)

MATERIAL	FORM	THICKNESS (IN.)	LOADING DIRECTION	TEMP. (^{o}F)	e (%)	F_{TU} (ksi)	E_c (10^3ksi)	n	A-VALUE F_{cy} (ksi)	A-VALUE $F_{0.7}$ (ksi)	OTHER* F_{cy} (ksi)	OTHER* $F_{0.7}$ (ksi)	REFERENCE
7075-T6 (cont'd)	Bare Sheet And Plate	0.015-0.039	Longit.	R.T.	7	76	10.5	14.5	67	68.7	70	71.8	1,2,4
		0.040-0.249			8	77	10.5	14.5	68	69.8	71	72.9	
		0.250-0.499			8	77	10.5	21	69	70.2	71	72.3	
		0.500-1.000			6	79	10.5	21	69	70.2	72	73.4	
		1.001-2.000			5	78	10.5	21	68	69.1	71	72.3	
		0.015-0.039	L. Transv.		7	76	10.5	14.5	70	72.1	73	75.2	
		0.040-0.249			8	77	10.5	14.5	71	73.2	74	76.3	
		0.250-0.499			8	77	10.5	21	69	70.2	71	72.3	
		0.500-1.000			6	77	10.5	21	69	70.2	72	73.4	
		1.001-2.000			4	77	10.5	21	68	69.1	71	72.3	
	Extrusion	≤0.249	Longit.	R.T.	7	78	10.5	27.5	71	72.0	75	76.2	1,2
		0.250-0.499			7	81	10.5	27.5	74	75.1	78	79.4	
		0.500-0.749			7	81	10.5	27.5	73	74.0	77	78.3	
		0.750-1.499			7	81	10.5	27.5	72	73.0	76	77.3	
		1.500-2.999			7	81	10.5	27.5	72	73.0	75	76.2	

* - B-Value unless otherwise indicated

Grumman

B1.20.1 Aluminum Alloys (cont'd)

MATERIAL	FORM	THICKNESS (IN.)	LOADING DIRECTION	TEMP. (°F)	e (%)	F_{TU} (ksi)	E_c (10^3ksi)	n	A-VALUE F_{cy} (ksi)	A-VALUE $F_{0.7}$ (ksi)	OTHER* F_{cy} (ksi)	OTHER* $F_{0.7}$ (ksi)	REFERENCE
7075-T651	Clad Plate	0.250-0.499	Longit.	R.T.	8	74	10.2[c]	13	65	66.8	67	69.0	1,4
		0.500-1.000			6	74	10.2[c]	13	64	65.7	66	67.9	
		1.001-2.000			5	74	10.2[c]	13	63	64.5	65	66.7	
		0.250-0.499	L. Transv.		8	75	10.2[c]	15	68	69.8	70	72.0	
		0.500-1.000			6	75	10.2[c]	15	68	69.8	70	72.0	
		1.001-2.000			4	75	10.2[c]	15	68	69.8	70	72.0	
	Bare Plate	0.250-0.499	Longit.	R.T.	8	76	10.5	12.5	67	68.8	69	71.1	1,4
		0.500-1.000			6	76	10.5	12.5	66	67.9	68	70.0	
		1.001-2.000			5	76	10.5	12.5	65	66.6	67	68.8	
		0.250-0.499	L. Transv.		8	77	10.5	15	70	71.8	72	74.0	
		0.500-1.000			6	77	10.5	15	70	71.8	72	74.0	
		1.001-2.000			4	77	10.5	15	70	71.8	72	74.0	
7075-T73, -T7351	All	Available data is insufficient for adequate presentation. See Reference 1 for available S-Values of e, F_{TU}, and F_{cy} and Average values of E_c.											

* - B-Value unless otherwise indicated

c - Secondary modulus - See reference for primary modulus

Grumman

Bl.20.1 Aluminum Alloys (cont'd)

MATERIAL	FORM	THICKNESS (IN.)	LOADING DIRECTION	TEMP. (^{o}F)	e (%)	F_{TU} (ksi)	E_c (10^3ksi)	n	A-VALUE F_{cr} (ksi)	A-VALUE $F_{0.7}$ (ksi)	OTHER* F_{cy} (ksi)	OTHER* $F_{0.7}$ (ksi)	REFERENCE
7079-T6	Bare Plate	0.250-1.500	Longit.	R.T.	-	73	10.5	23	63	63.8	65	65.8	1,4
		1.501-2.000			-	73	10.5	23	63	63.8	65	65.8	
		0.250-1.500	L. Transv		8	73	10.5	23	66	67.0	68	69.0	
		1.501-2.000			7	73	10.5	23	66	67.0	68	69.0	
7079-T651	Bare Plate	0.250-1.500	Longit.	R.T.	-	71	10.5	14.5	63	64.3	64	65.3	1,4
		1.501-2.000			-	71	10.5	14.5	62	63.2	63	64.2	
		0.250-1.500	L. Transv		8	73	10.5	17	66	67.3	67	68.3	
		1.501-2.000			7	73	10.5	17	63	64.2	67	68.3	

* - B-Value unless otherwise indicated

B1.20.2 Titanium Alloys

MATERIAL	FORM	THICKNESS (IN.)	LOADING DIRECTION	TEMP. (°F)	e (%)	F_{TU} (ksi)	E_c (10^3ksi)	n	A-VALUE F_{cy} (ksi)	A-VALUE $F_{0.7}$ (ksi)	OTHER* F_{cy} (ksi)	OTHER* $F_{0.7}$ (ksi)	REFERENCE
Ti-4Al-3Mo 1V (STA)	Sheet	≤0.250	Longit. and L. Transv.	RT	3-5	175	16.0	19	154	160	161	168	1
				200		161	15.4	18	139	144	145	151	
				400		143	14.5	15	118	123	123	128	
				600		131	13.7	15	105	109	110	114	
Ti-6Al-4V annealed TENTATIVE	Sheet	≤0.250	Longit. and L. Transv	RT	8-10	134	16.4	30	132	134	138	141	1,6,7
				200		121	15.6	28	118	120	124	126	
				400		107	14.6	26	101	103	105	107	
				600		100	13.4	24	90	91	94	96	
Ti-6Al-4V (STA)	Sheet	≤0.250	Longit.	RT	3-5	157	16.4	20	152	158	157	163	1,6
				200	---	143	15.5	28	137	140	142	146	
				400	---	127	14.8	22	116	119	120	123	
				600	---	118	14.0	13	102	106	105	109	
			L. Transv.	RT	3-5	157	16.4	22	160	167	165	171	
				200	---	143	15.5	27	142	146	147	151	
				400	---	127	14.8	26	119	122	123	126	
				600	---	118	14.0	9	104	110	107	114	

* - B-Value unless otherwise indicated

B1.20.2 Titanium Alloys (cont'd)

MATERIAL	FORM	THICKNESS (IN.)	LOADING DIRECTION	TEMP. (°F)	e (%)	F_{TU} (ksi)	E_c (10^3ksi)	n	A-VALUE F_{cy} (ksi)	A-VALUE $F_{0.7}$ (ksi)	OTHER* F_{cy} (ksi)	OTHER* $F_{0.7}$ (ksi)	REFERENCE
Ti-6Al-6V-2Sn annealed TENTATIVE	Sheet	≤0.187	Longit.	RT	10	155	16.0[b]	40	148	151[b]	152	155[b]	5,6,8,9
		≤0.187		200	--	---	15.2[b]	28	134[b]	137[b]	137[b]	141[b]	
		≤0.187		400	--	---	14.8[b]	38	115[b]	117[b]	118[b]	120[b]	
		≤0.187		600	--	---	14.0[b]	34	101[b]	102[b]	104[b]	105[b]	
	Sheet and Plate	0.188-2.000	Longit.	RT	10[a]	150[a]	16.0[b]	45	---	---	142[a]	144[b]	5,8,9
		0.188-2.000		250	--	136[b]	15.1[b]	40	---	---	123[b]	125[b]	
		0.188-2.000		425	--	124[b]	14.7[b]	45	---	---	109[b]	110[b]	
		0.188-2.000		500	--	120[b]	14.4[b]	45	---	---	98[b]	99[b]	
Ti-6Al-6V-2Sn STA TENTATIVE	Sheet and Plate	0.188-1.500	Longit.	RT	8[a]	170[a]	16.5	48	---	---	163[a]	166[a]	5,6,8,10
		0.188-1.500		250	--	160[a]	16.0[b]	43	---	---	150[b]	152[b]	
		0.188-1.500		425	--	150[a]	15.3[b]	30	---	---	137[b]	140[b]	
		0.188-1.500		500	--	144[a]	15.0[b]	30	---	---	131[b]	134[b]	

* - B-Values unless otherwise indicated

a - S-Value or based on S-Value

b - Statistical Basis not known

Grumman

B1.20.2 Titanium Alloys (cont'd)

MATERIAL	FORM	THICKNESS (IN.)	LOADING DIRECTION	TEMP. (^{o}F)	e (%)	F_{TU} (ksi)	E_c (10^3ksi)	n	A-VALUE F_{cy} (ksi)	A-VALUE $F_{0.7}$ (ksi)	OTHER* F_{cy} (ksi)	OTHER* $F_{0.7}$ (ksi)	REFERENCE
Ti-8Al-1Mo-1V Duplex annealed	Sheet	0.025-0.187	Longit.	RT	10	133	18.0	64	128	129	131	132	1,8
		0.187-0.250			10[a]	130[a]	18.0	64	---	---	127[a]	128[a]	
		0.025--.187	L. Transv.		10	130	18.0	64	127	128	130	131	
		0.187-0.250			10[a]	130[a]	18.0	64	---	---	127[a]	128[a]	
TENTATIVE		0.025-0.187	Longit.	200	--	123	17.1	54[d]	112	113	115	116[e]	
		0.187-0.250			--	120[a]	17.1	54[d]	---	---	111[a]	112[f]	
		0.025-0.187	L. Transv.		--	120	17.1	58[d]	111	112	114	115[e]	
		0.187-0.250			--	120[a]	17.1	58[d]	---	---	111[a]	112[f]	
		0.025-0.187	Longit.	400	--	109	16.2	38[d]	92	92.5	94	94.5[e]	
		0.187-0.250			--	107[a]	16.2	38[d]	---	---	91.5[a]	92.0[f]	
		0.025-0.187	L. Transv.		--	107	16.2	47[d]	91.5	91.9	93.5	93.9[e]	
		0.187-0.250			--	107[a]	16.2	47[d]	---	---	91.5[a]	91.9[f]	
		0.025-0.187	Longit.	550	--	102	13.7	25	84.5	85.5	86.5	87.6	
		0.187-0.250			--	100[a]	13.7	25	---	---	84[a]	85[a]	
		0.025-0.187	L. Transv.		--	100	13.7	39	84	84.6	86	86.7	
		0.187-0.250			--	100[a]	13.7	39	---	---	84[a]	84.6[a]	

* - B-Value unless otherwise indicated

a - S-Value or based on S-Value

d - Estimated value

e - based on estimated value of n

f - based on estimated value of n and S-Value of F_{cy}

B1.20.3 Steel Alloys

MATERIAL	FORM	THICKNESS (IN.)	LOADING DIRECTION	TEMP. (^{o}F)	e (%)	F_{TU} (ksi)	E_c (10^3ksi)	n	A-VALUE F_{cy} (ksi)	A-VALUE $F_{0.7}$ (ksi)	OTHER* F_{cy} (ksi)	OTHER* $F_{0.7}$ (ksi)	REFERENCE
17-7 PH TH 1050 (Material has not been cold-worked prior to final heat treatment	Plate, Sheet, and Strip	0.005-0.500	ALL	RT	3-7	177	30.0	11	158	160	178	182	1
				200	---	173	29.4	9.5	151	153	170	175	
				400	---	164	28.4	10.0	139	140	157	160	
				600	---	151	26.8	8.5	126	126	143	146	

DESIGN DATA FOR OTHER STEEL ALLOYS WILL BE SUPPLIED AT A LATER DATE. AVAILABLE DATA (see Ref.1) IS INSUFFICIENT FOR ADEQUATE PRESENTATION.

Grumman

B1.30 NON-DIMENSIONAL STRESS STRAIN CURVES

Non-dimensional stress strain curves are given on the following page and are used as follows:

General Procedure

1. Determine values of n, E_c, and $F_{0.7}$ from the tables of Section B1.20
2. To determine the stress F corresponding to a given strain ϵ:
   a) Compute the ratio of $(E_c \times \epsilon)/F_{0.7}$
   b) Enter the appropriate curve of page B1.30-2 and determine the ratio $(F/F_{0.7})$
   c) The stress at strain ϵ is then computed to be $F=(F/F_{0.7}) \times F_{0.7}$
3. To determine the strain ϵ corresponding to a given stress F:
   a) Compute the ratio of $(E_c \times \epsilon)/F_{0.7}$
   b) Enter the appropriate curve of page B1.30-2 and determine the ratio $(E_c \times \epsilon/F_{0.7})$
   c) The strain at stress F is then computed to be $\epsilon = \{(E_c \times \epsilon)/F_{0.7}\} \times (F_{0.7}/E_c)$

Note: The non-dimensional stress-strain relations of page B1.30-2 are most accurate at stress levels below $F_{0.7}$; beyond this stress they may not adequately define the true stress-strain curve of the material.

NON-DIMENSIONAL STRESS-STRAIN CURVES

Obtain values of n, E_c and $F_{0.7}$ from Section B1.20

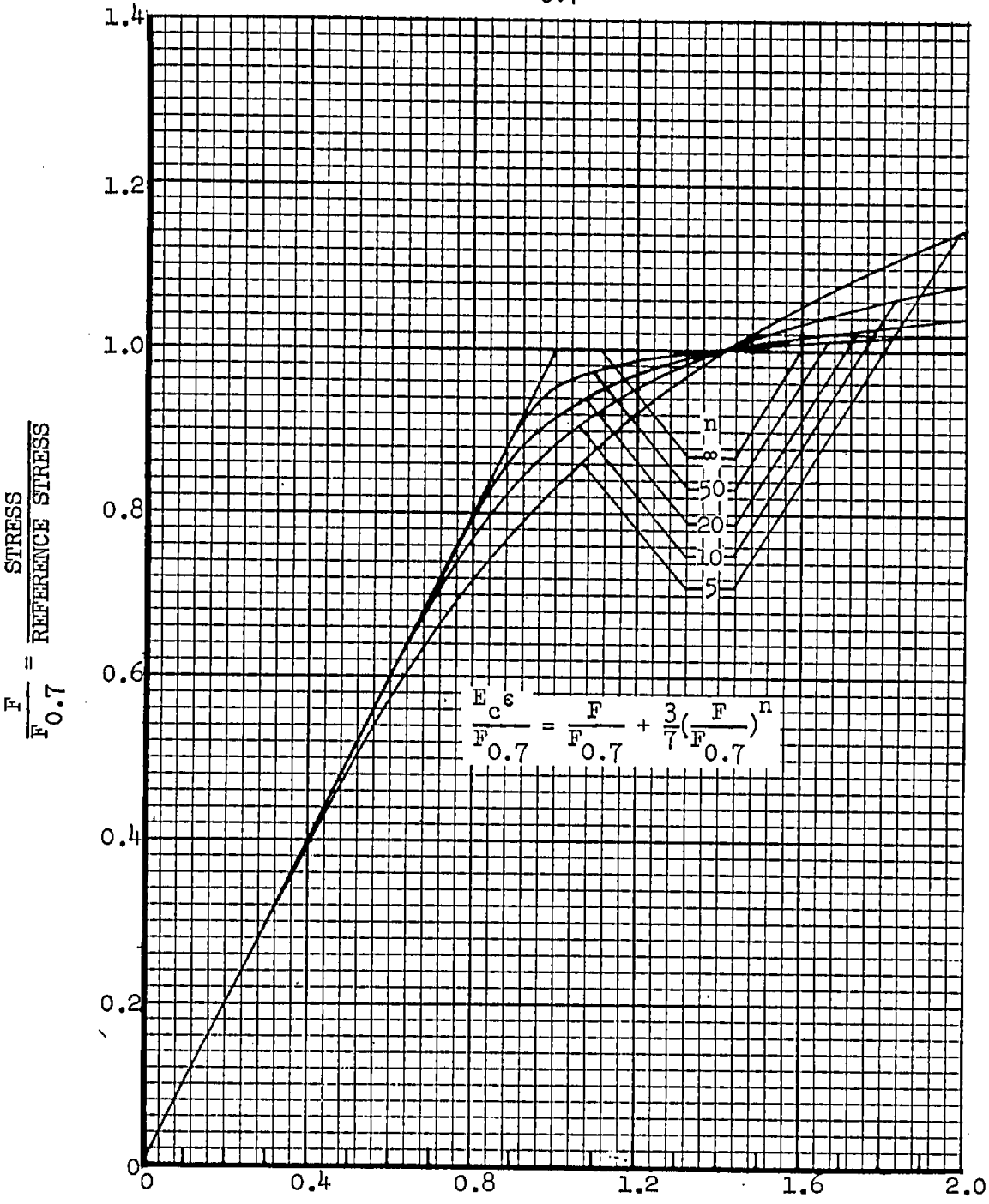

Grumman

B1.40 NON-DIMENSIONAL MODULUS CURVES

Non-dimensional secant- and tangent-modulus curves are given on the following two pages and are used as follows:

General Procedure

(1.) Determine values of n, E_c, and $F_{0.7}$ from the tables of Section B1.20

(2.) To determine the secant modulus E_S at a stress F. determine the ratio of $(F/F_{0.7})$. Enter the appropriate curve on page B1.40-2 and determine the ratio (E_S/E_c). The secant modulus at stress F is calculated to be $E_S = (E_S/E_c) \times E_c$.

(3.) To determine the tangent modulus E_T at a stress F, the same procedure as used in (2) above is followed using the curves of page B1.40-3 instead of those of page B1.40-2.

NON-DIMENSIONAL SECANT MODULUS CURVES

Obtain values of n, E_c and $F_{0.7}$ from Section B1.20

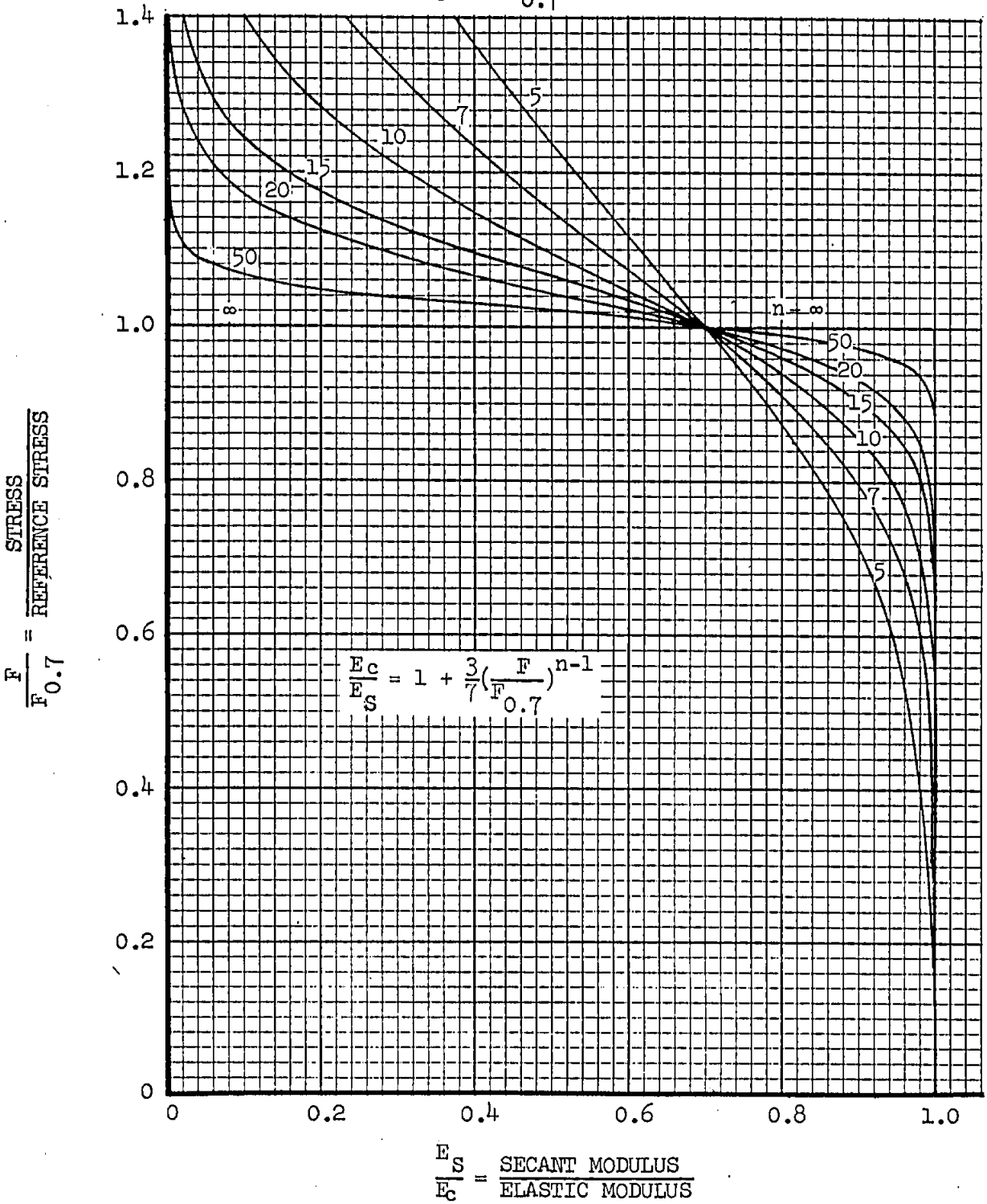

NON-DIMENSIONAL TANGENT MODULUS CURVES

Obtain values of n, E_c and $F_{0.7}$ from Section B1.20

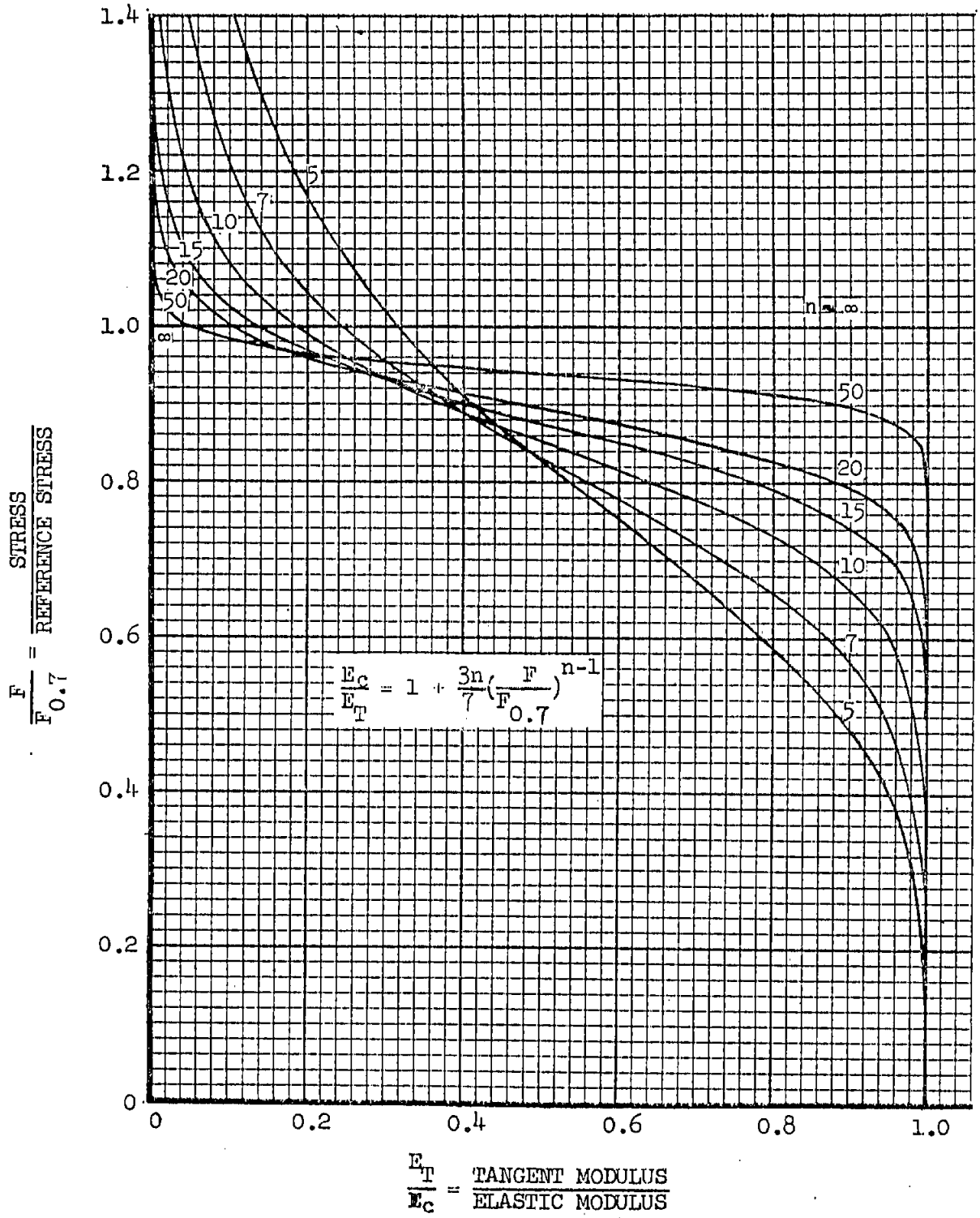

Grumman

B1.50 NON-DIMENSIONAL PLASTIC BUCKLING CURVES

When the theoretical elastic buckling stress of a structure exceeds the proportional limit of the material, there is a reduction in bending stiffness which allows the structure to buckle at a stress below the theoretical elastic value. The effects of exceeding the proportional limit are incorporated into a plasticity correction (reduction) factor η which, when multiplied by the theoretical elastic buckling stress gives the stress at which the section will actually buckle (plastic buckling stress).

Recommended values of the plasticity correction factor for various cases are given below.

TABLE B1.50 (Ref. NACA TN 3781)

LOADING	STRUCTURE	η	CHART ON PAGE
COMPR.	LONG PLATE, BOTH UNLOADED EDGES SIMPLY SUPPORTED	$\frac{E_S}{E_c}\left\{\frac{1}{2}+\frac{1}{4}\left[1+\left(\frac{3E_T}{E_S}\right)\right]^{\frac{1}{2}}\right\} \times j$	B1.50.1-1
COMPR.	LONG FLANGE, ONE UNLOADED EDGE SIMPLY SUPPORTED	$\frac{E_S}{E_c} \times j$	B1.50.1-2
COMPR.	SHORT PLATE COLUMN -ALSO INTERRIVET BUCKLING	$\left\{\frac{E_S}{4E_c}+\frac{3E_T}{4E_c}\right\} \times j$	B1.50.2-1
SHEAR	RECTANGULAR PLATE, ALL EDGES ELASTICALLY RESTRAINED	$\left\{\frac{.83E_S}{E_c}+\frac{.17E_T}{E_c}\right\} j$	B1.50.3-1
COMPR.	LONG COLUMNS	E_T/E_c	B1.50.4-1
where	$j = (1-\nu_e^2)/(1-\nu^2)$	(see Equation B1-6)	

The value j in the above table is the correction to account for the instantaneous value of Poisson's ratio ν, which is determined from the equation:

$$\nu = \nu_p - \left\{[E_S/E_c] \times [\nu_p - \nu_e]\right\} \qquad \text{B1-6}$$

In plotting the curves of this section a value of 0.5 was assumed for the fully plastic Poisson's ratio, ν_p; a value of 0.3 was assumed for the elastic Poisson's ratio, ν_e. These values may be used without appreciable error for aluminum, titanium, and steel alloys.

The non-dimensional buckling stress charts of pages B1.50.1 through B1.50.4 were constructed from the basic stress strain and modulii equations of section B1.10 and the plasticity correction factors of table B1.50. Since there is little difference among the numerical values of the plasticity correction factors applicable to a long clamped flange, to a long plate with any amount of edge rotational restraint, and to a thin walled section, these cases are grouped into one curve (B1.50.1-1) employing the correction factor of the simply supported plate.

A general procedure is given for determining the plastic buckling stress of a section whose elastic buckling stress, F_{crel} is known.

GENERAL PROCEDURE

(1) From section B1.20 determine the appropriate material properties n, E_c, $F_{0.7}$

(2) Using the values of the ratio $(F_{crel}/F_{0.7})$ and the exponent n, determine the value of the ratio $(F_{cr}/F_{0.7})$ from the appropriate curve of section B1.50.
The plastic buckling stress is then found as $F_{cr}=(F_{cr}/F_{0.7})x F_{0.7}$

EXAMPLE

Determine the local plastic compressive buckling stress of a simply supported, bare 7075-T6 sheet loaded in compression along the short edges. The sheet dimensions are 6.0" x 1.4" x 0.064".

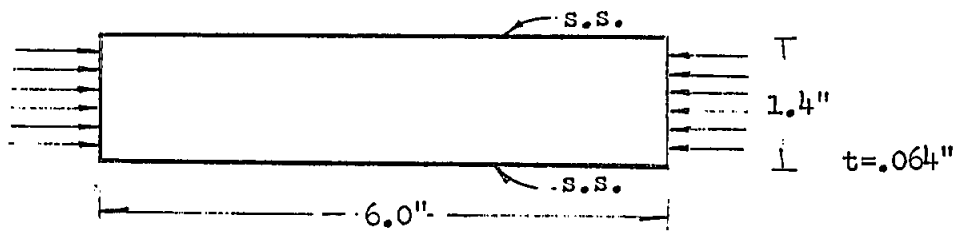

From Section B1.20.1, $n = 14.5$

$E_c = 10.5 \times 10^6$ psi

$F_{0.7} = 72900$ psi (B-value)

(cont'd)

EXAMPLE (Cont'd)

From page B5.11.11-1, $F_{crel} = 3.62 \times 10.5 \times 10^6 \times (.064/1.4)^2 =$ 79,100 psi

$(F_{crel}/F_{0.7}) = (79,100/72,900) = 1.087$

For long plates with simply supported edges, the curves of page B1.50.1-1 apply: from them $(F_{cr}/F_{0.7}) = 0.89$

The stress at which the sheet buckles is :
$F_{cr} = 0.89 \times 72,900 = 64,800$ psi.

January 1969

NON-DIMENSIONAL PLASTIC BUCKLING OF PLATES IN COMPRESSION

Curves are for long plates with both unloaded edges simply supported but may be applied to long flanges with one unloaded edge clamped and to long plates with both unloaded edges clamped.

$$F_{cr\ el} = F_{cr}/\eta = KE_c(t/b)^2$$

where η = plasticity correction factor (see below)
E_c = elastic modulus
t = plate thickness
b = plate width
K = the appropriate buckling stress coefficient from Section B5.11

Obtain values of n, E_c and $F_{0.7}$ from Section B1.20

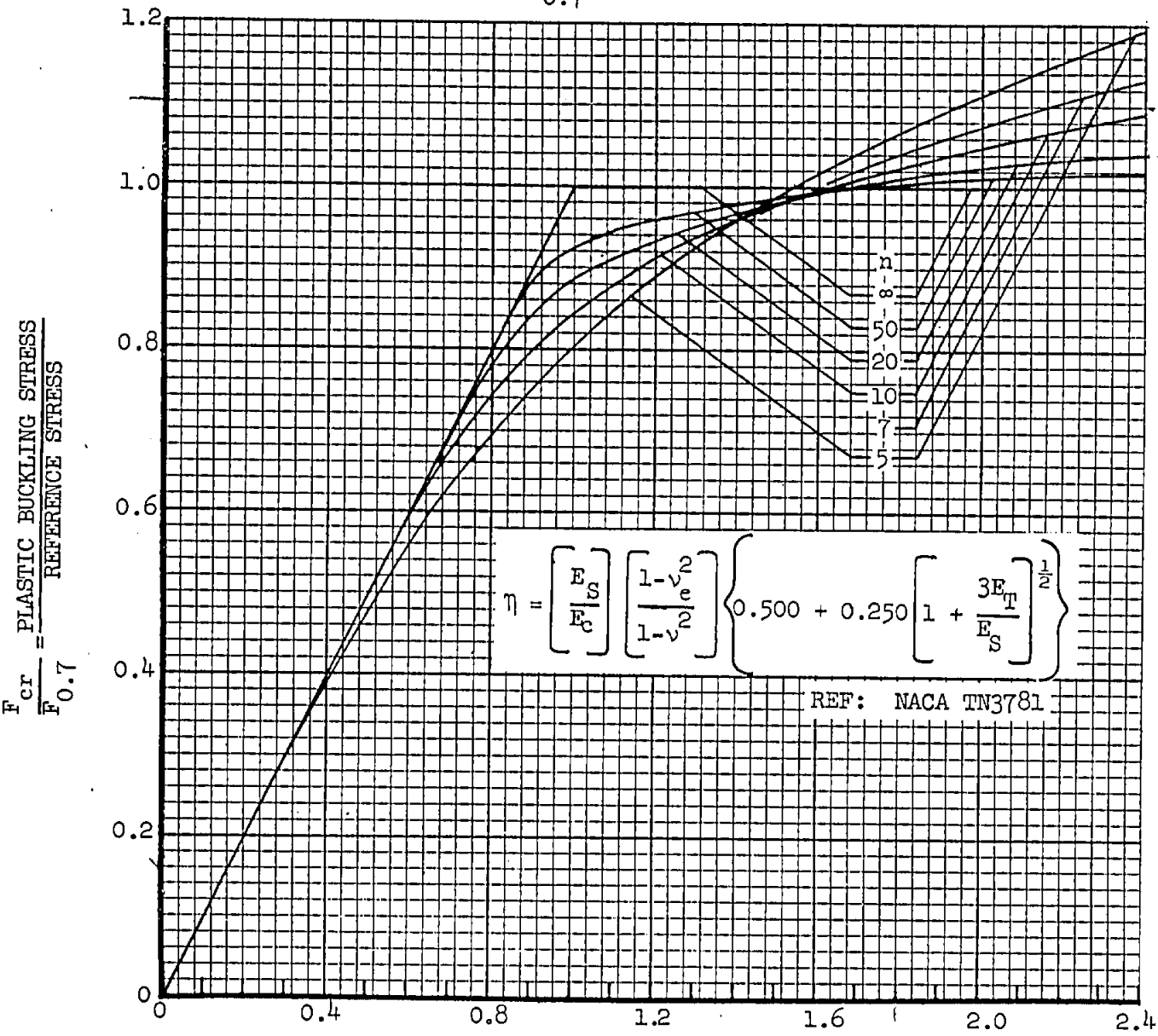

Grumman

NON-DIMENSIONAL PLASTIC BUCKLING OF A LONG FLANGE, IN COMPRESSION, ONE UNLOADED EDGE SIMPLE SUPPORTED

$$F_{cr\ el} = F_{cr}/\eta = KE_c(t/b)^2$$

where η = plasticity correction factor (see below)
E_c = elastic modulus
t = flange thickness
b = flange width
K = buckling stress coefficient (see page B5.11.11-1)

Obtain values of n, E_c and $F_{0.7}$ from Section B1.20

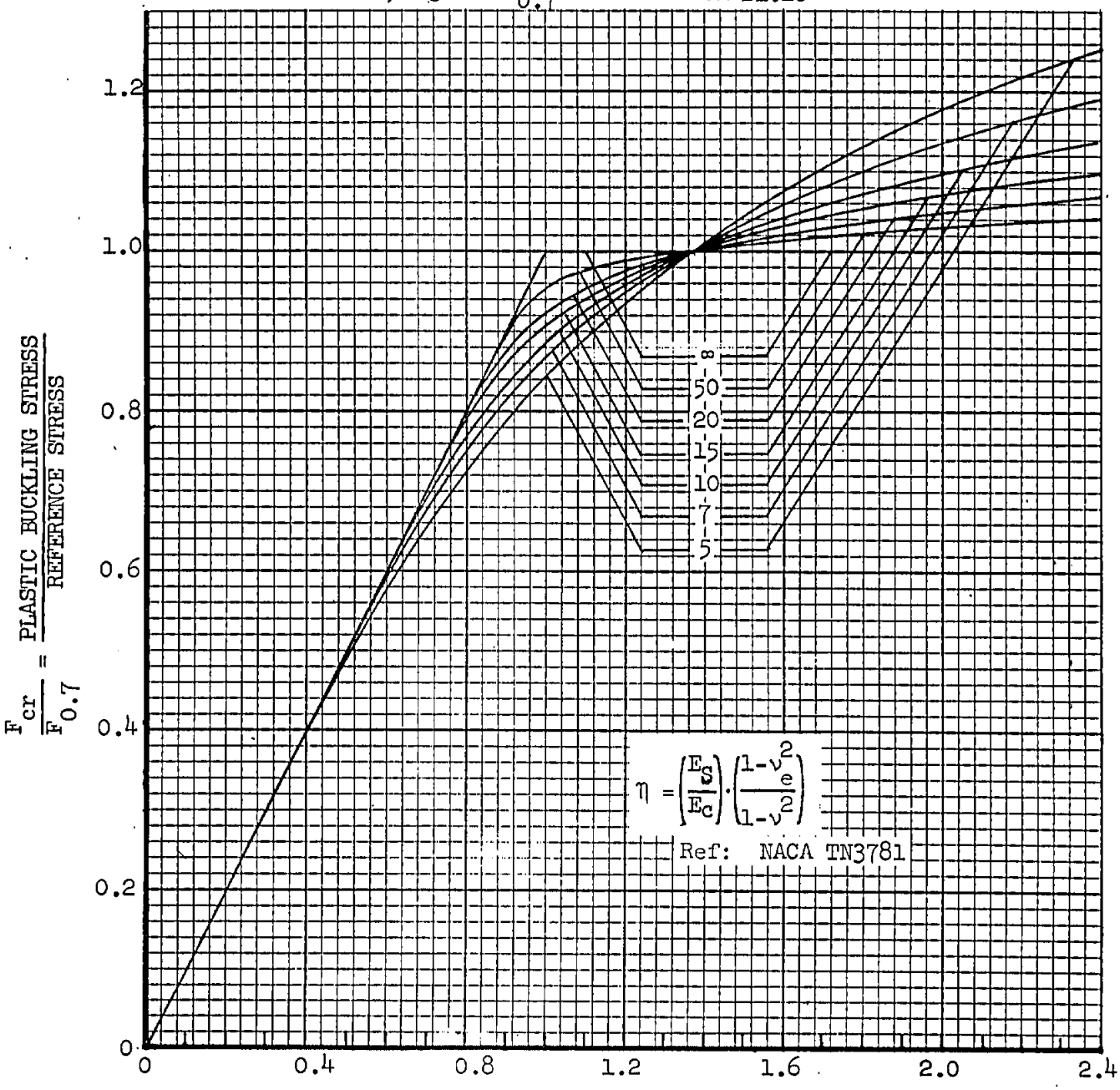

Grumman

January 1969

NON-DIMENSIONAL PLASTIC BUCKLING OF SHORT PLATE COLUMNS, INTERRIVET BUCKLING OF PLATE-STRINGER COMBINATIONS

$$F_{cr\ el} = F_{cr}/\eta = \frac{e\pi^2 E_c}{12(1-\nu^2)} \left(\frac{t}{p}\right)^2$$

where η = plasticity correction factor (see below)
E_c = elastic modulus
t = plate thickness
p = rivet pitch
e = rivet end fixity coefficient (see page B6.11.4)
ν = Poisson's ratio

Obtain values of n, E_c and $F_{0.7}$ from Section B1.20

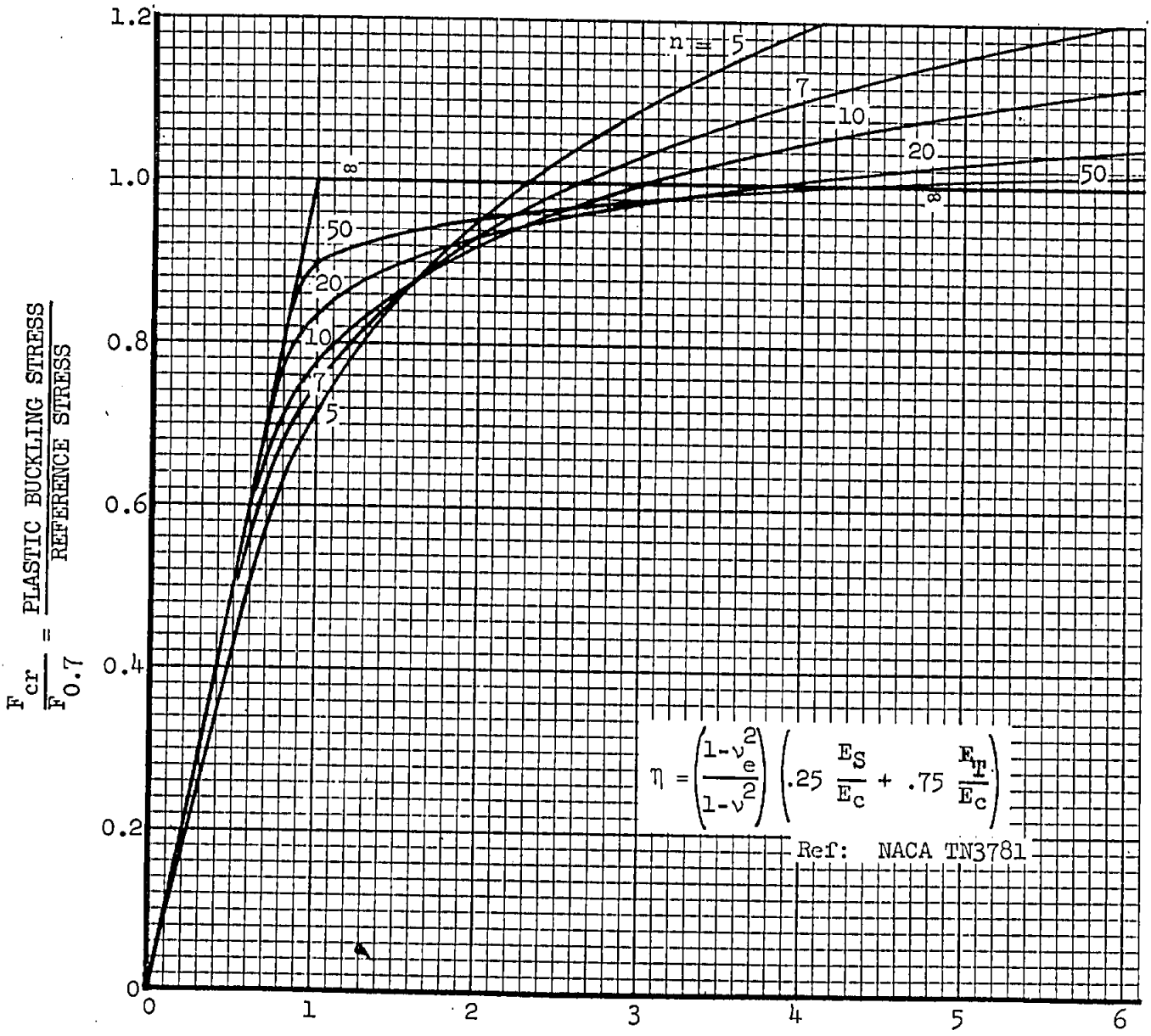

Grumman

NON-DIMENSIONAL PLASTIC BUCKLING OF PLATE IN SHEAR

$F_{cr\ el} = F_{cr}/\eta = KE_c(t/b)^2$

where η = plasticity correction factor (see below)

E_c = elastic modulus

t = plate thickness

b = plate width

K = buckling stress coefficient (see page B5.11.12-1).

Obtain values of n, E_c and $F_{0.7}$ from Section B1.20

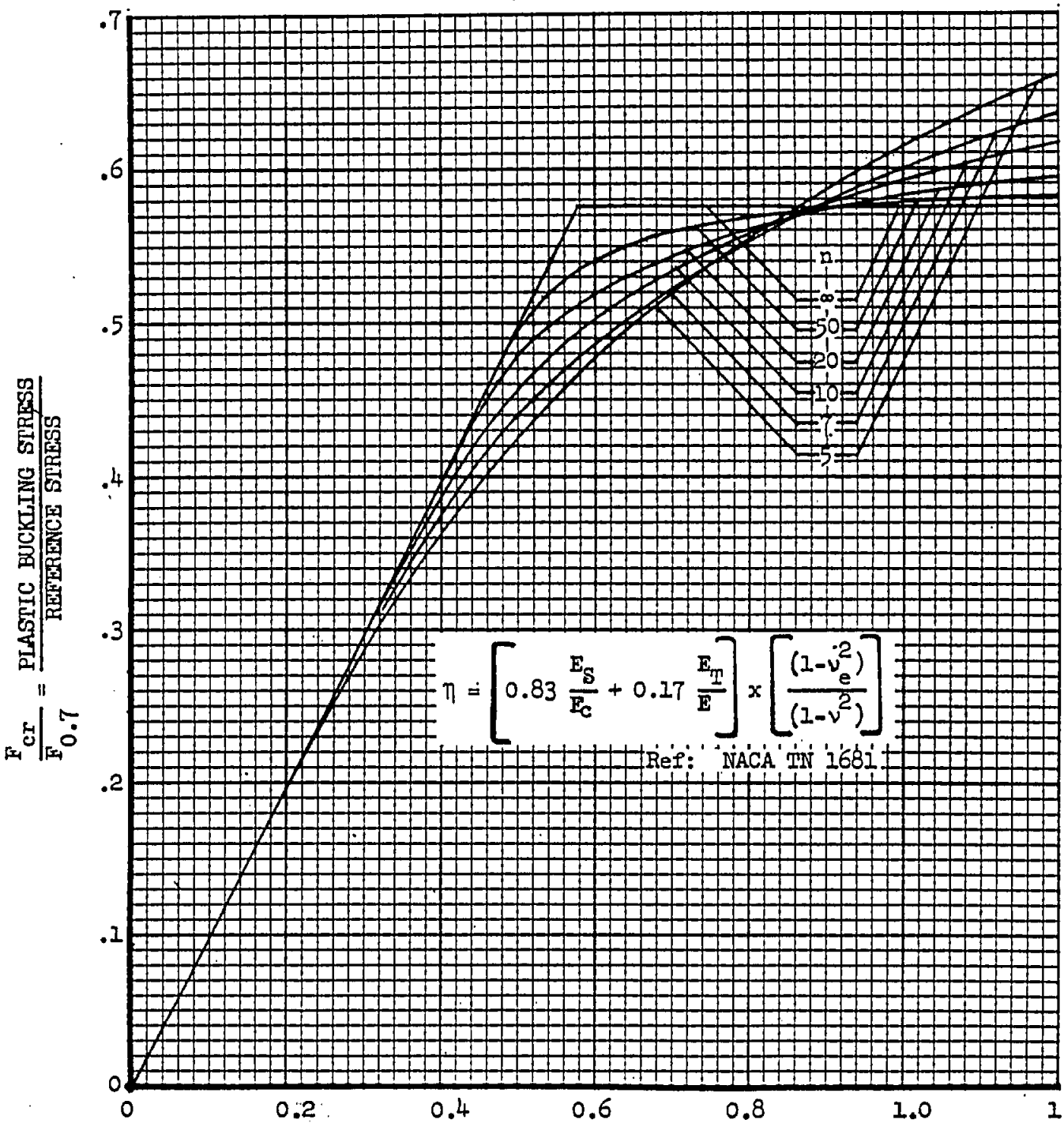

Grumman

NON-DIMENSIONAL COLUMN CURVES (BASED ON TANGENT MODULUS)

$$F_{cr\ el} = \frac{F_{cr}}{\eta} = \frac{C\pi^2 E_c}{(L/\rho)^2} = \frac{\pi^2 E_c}{(L'/\rho)^2}$$

where η = plasticity correction factor = E_T/E_c
C = end fixity factor (see page B3.40-1)
L = column length
L' = equivalent pinned-end length = $L/\sqrt{C}$
ρ = section radius of gyration

Obtain values of n, E_c and $F_{0.7}$ from Section B1.20

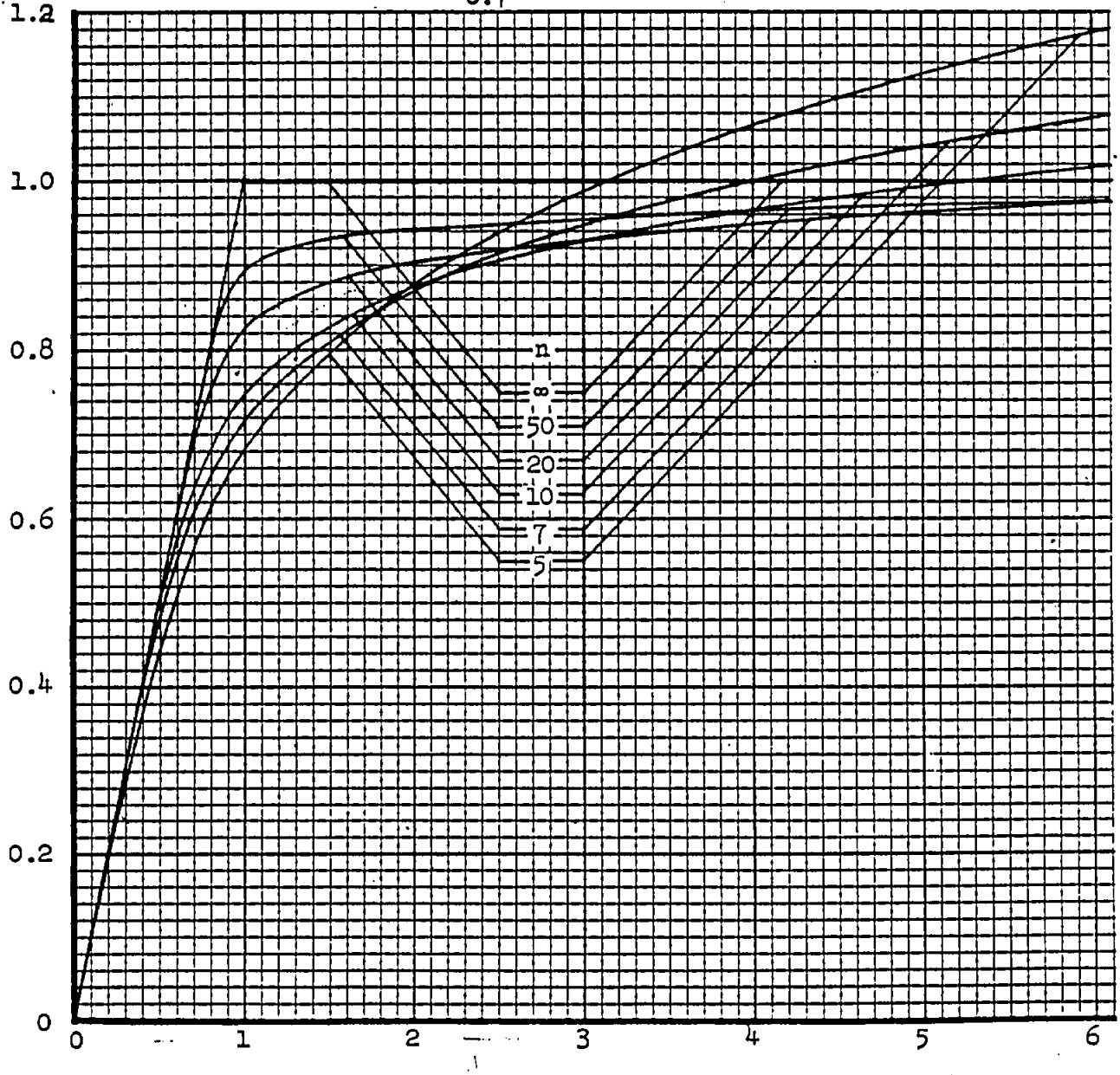

$\frac{F_{cr}}{F_{0.7}} = \frac{\text{PLASTIC BUCKLING STRESS}}{\text{REFERENCE STRESS}}$

$\frac{F_{cr\ el}}{F_{0.7}} = \frac{\text{ELASTIC BUCKLING STRESS}}{\text{REFERENCE STRESS}}$

NON-DIMENSIONAL PLASTIC BUCKLING OF A COLUMN ON AN ELASTIC FOUNDATION

$$F_{crel} = \frac{F_{cr}}{\eta} = 2\sqrt{\frac{E_c \rho^2 \psi}{A}}$$

η = plasticity correction factor = $\sqrt{E_T/E_c}$

ρ = section radius of gyration

ψ = foundation modulus

A = section area

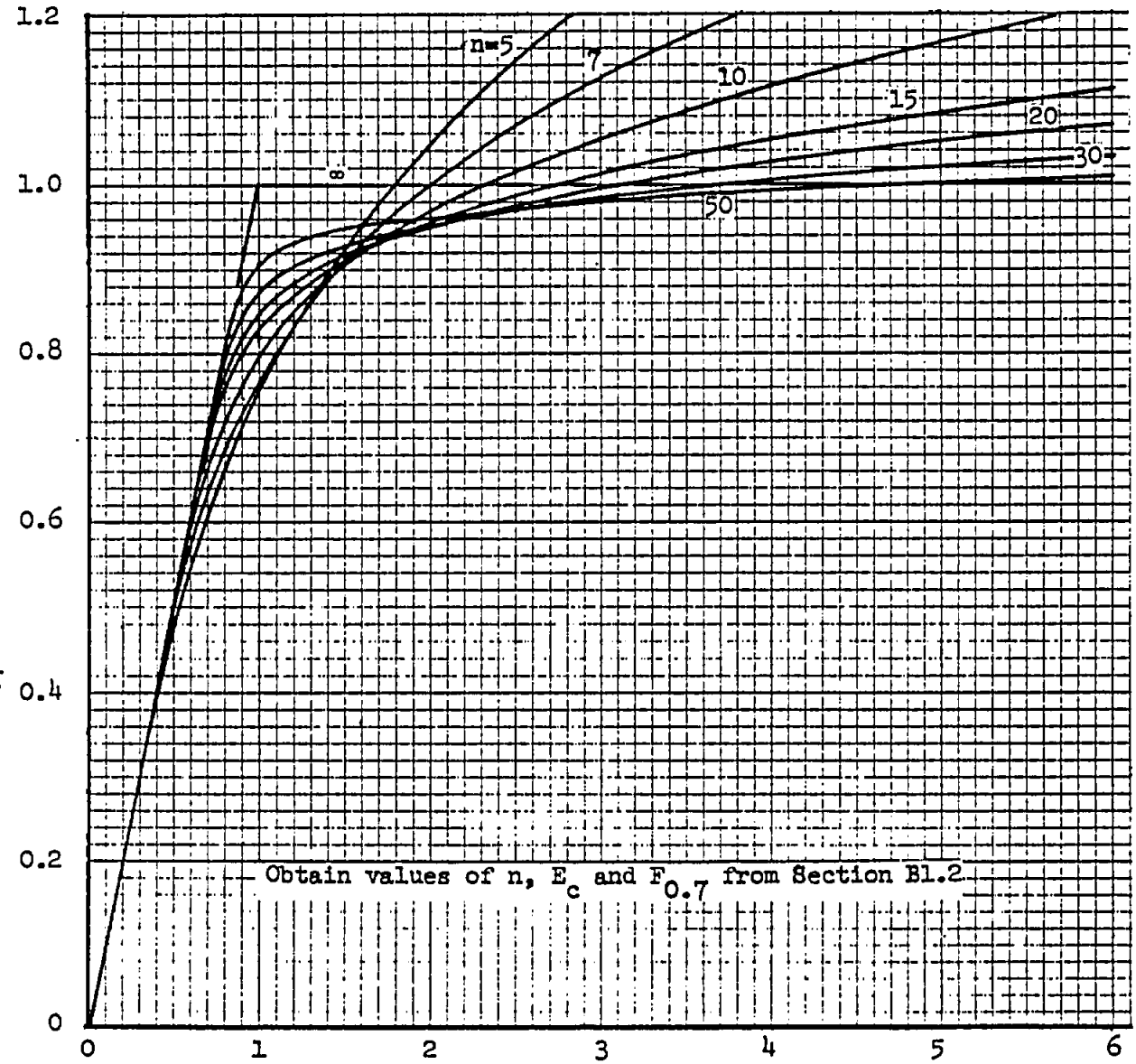

B1.60 CRIPPLING OF THIN-WALLED SECTIONS

A physical description of the crippling of thin-walled sections is given in Section B4.30. The crippling stress of a thin-walled section can be determined using the non-dimensional crippling curve of page B1.60-2 in conjunction with the tables of Section B1.20. The crippling curve is specifically for "formed-type" sections. Crippling strength of extruded thin-walled sections is determined from B1.60.2 plus a correction term that adds in the strength due to the corner area present in the extruded sections that does not exist in formed sections. The calculation required for an extruded section is shown in the following equation.

Crippling for Extruded Thin-Walled Sections:

$$(F_{cc}/F_{0.7})_{Extrusion} = (F_{cc}/F_{0.7})_{Frmd}\ (A - \sum A_{corner})/A + F_e/F_{0.7} \cdot \sum A_{corner}/A$$

$(F_{cc}/F_{0.7})_{Frmd}$ is from B1.60-2. Calculate $F_{crel}/F_{0.7}$ in accordance with instructions of page B4.11-2.

F_e is the maximum stress on the section and is the stress acting on each of the individual corner areas. This stress is obtained from page B1.60-3.

$\sum A_{corner}$ is the area of all corner material common to the intersecting elements of the section. The area of the fillets may be included in this item.

A is the total section area <u>including all</u> corner area that is included in the $\sum A_{corner}$ calculation.

The areas required are shown for the following typical section.

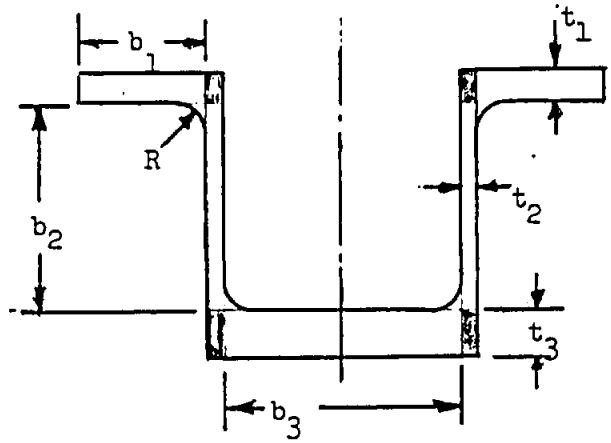

$$\sum A_{corner} = 2t_1t_2 + 2t_2t_3 + (4 - \Pi)R^2$$
$$A = 2b_1t_1 + 2b_2t_2 + b_3t_3 + \sum A_{corner}$$

Application of this section on crippling is included in the numerical examples of Section B4.30.

NON DIMENSIONAL CURVES FOR THE CRIPPLING OF "FORMED-TYPE" THIN-WALLED SECTIONS IN COMPRESSION

For "Extruded Sections" See Page B1.60-1

Obtain values of n, E_c and $F_{0.7}$ from Section B1.20

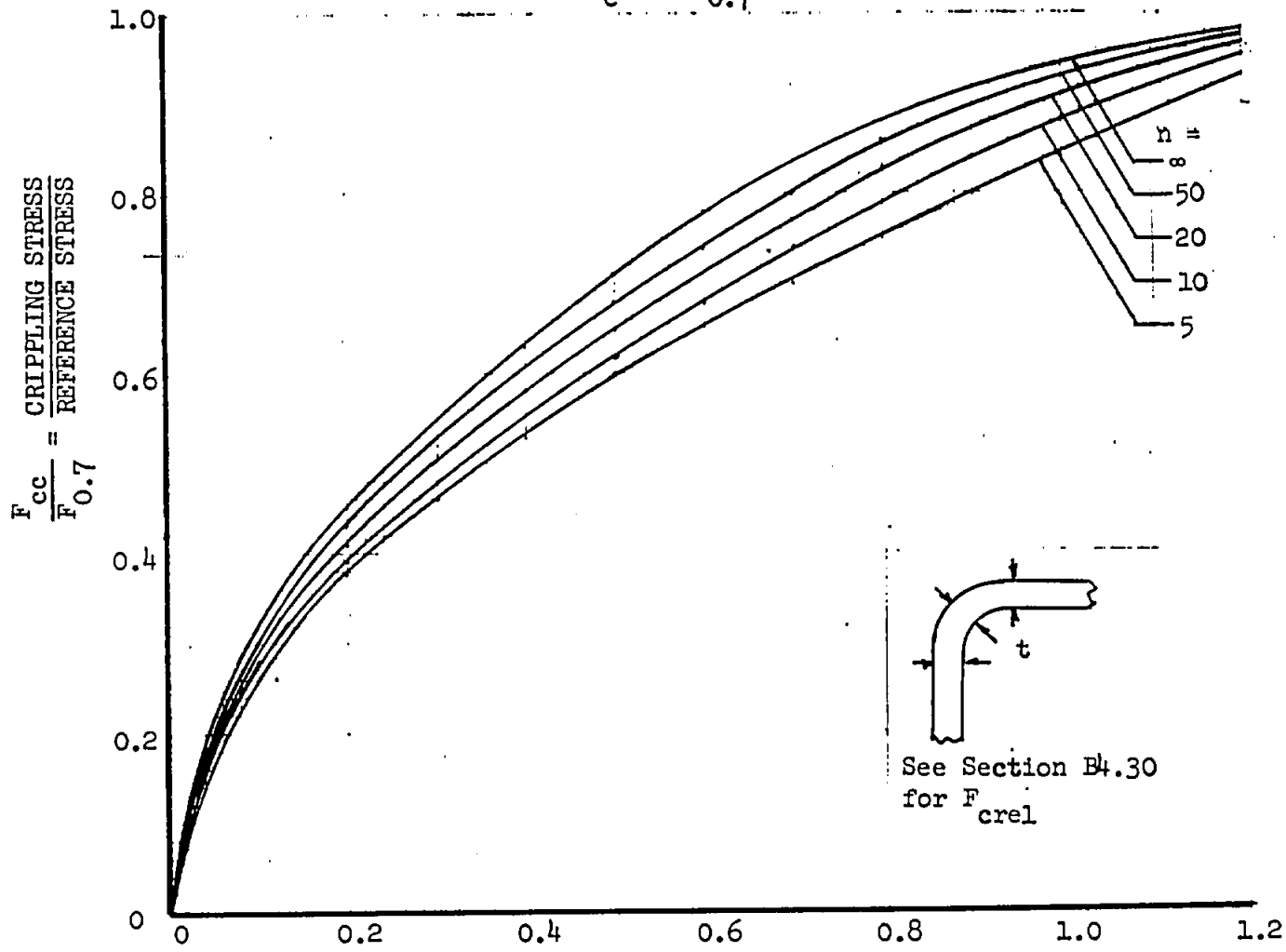

$$\frac{F_{crel}}{F_{0.7}} = \frac{\text{ELASTIC BUCKLING STRESS}}{\text{REFERENCE STRESS}}$$

MAXIMUM SECTION STRESS FOR COMPRESSION CRIPPLING
OF THIN-WALLED SECTIONS

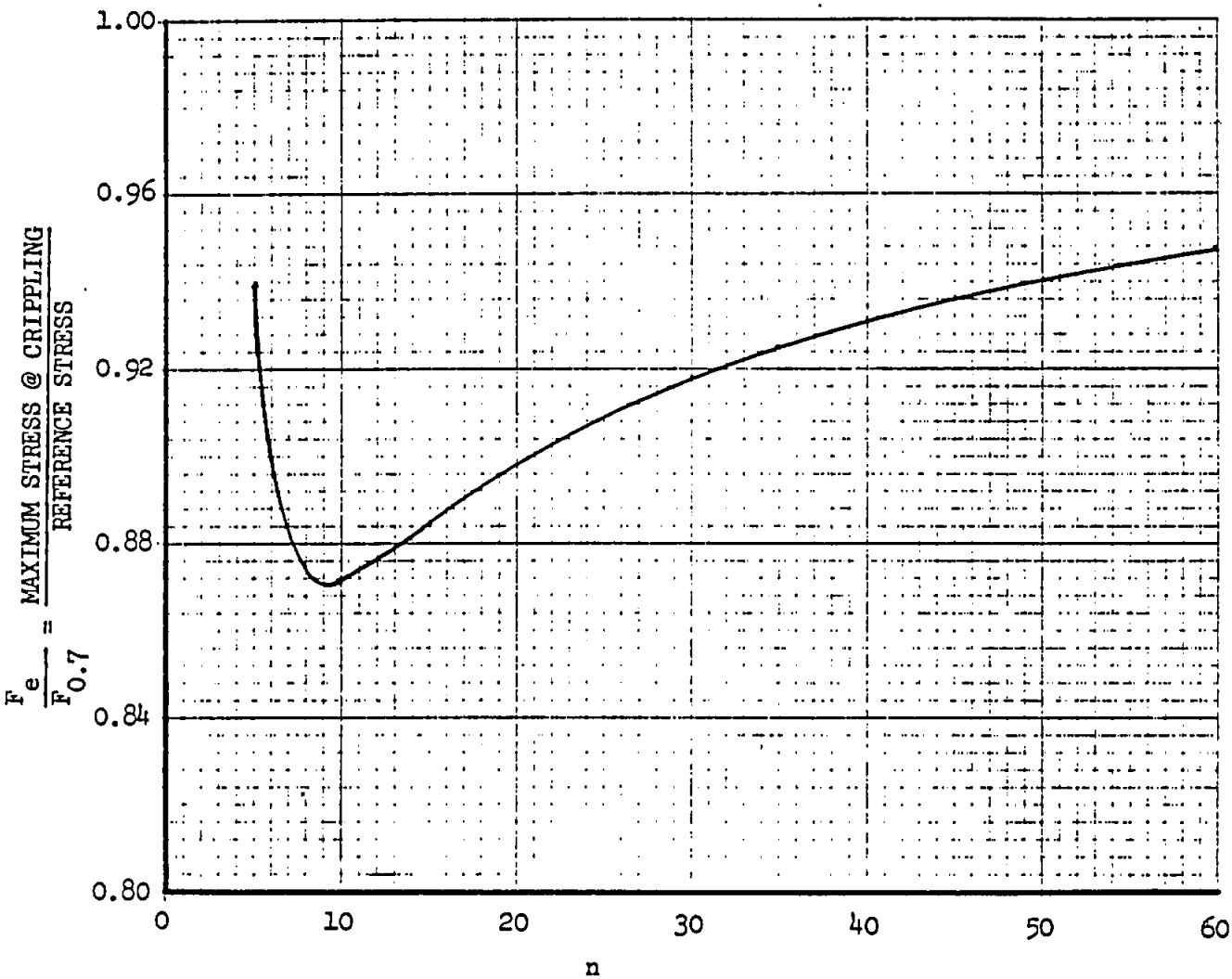

Stress-Strain Curve Shape Factor
Values from Section B1.20

STRESS - STRAIN CURVES FOR ALUMINUM ALLOYS IN LONGITUDINAL TENSION

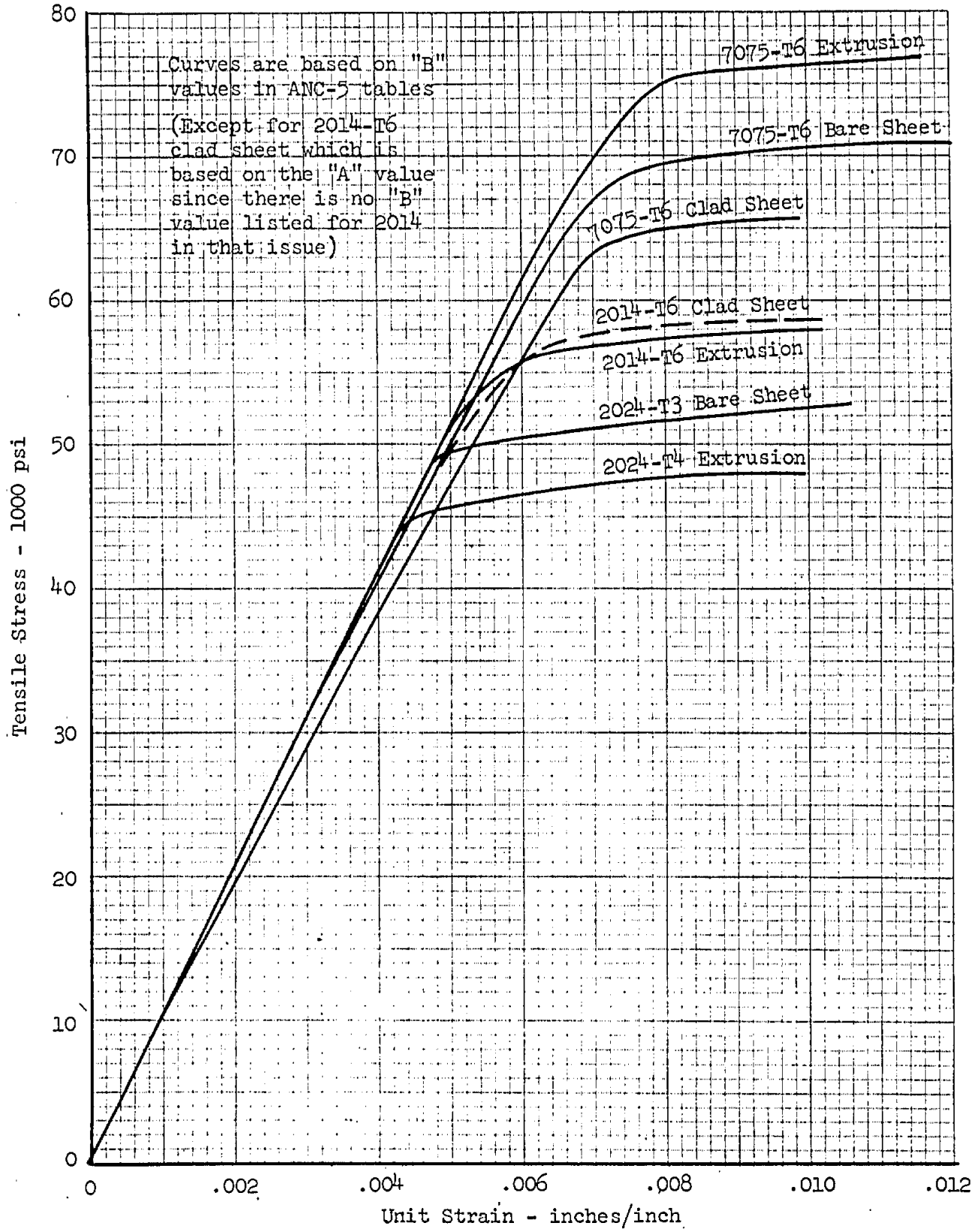

Ref ANC-5 June 1951
TN 1010, 1385, 2085

Grumman

STRESS STRAIN CURVES FOR ALUMINUM ALLOYS IN LONGITUDINAL COMPRESSION

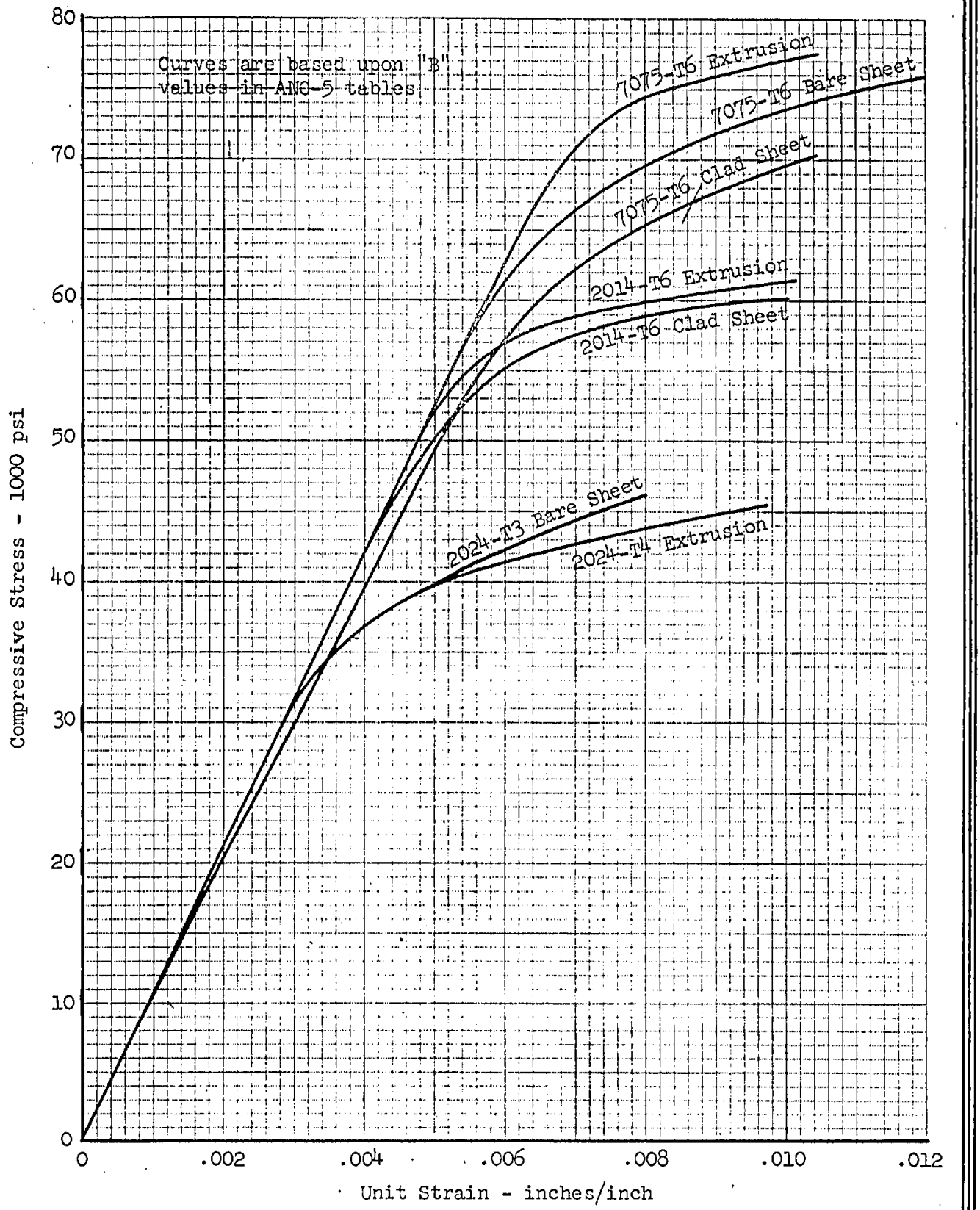

Ref: ANC-5 June 1951
TN 1010 1385, 2085

TANGENT MODULUS CURVES FOR ALUMINUM ALLOYS IN COMPRESSION

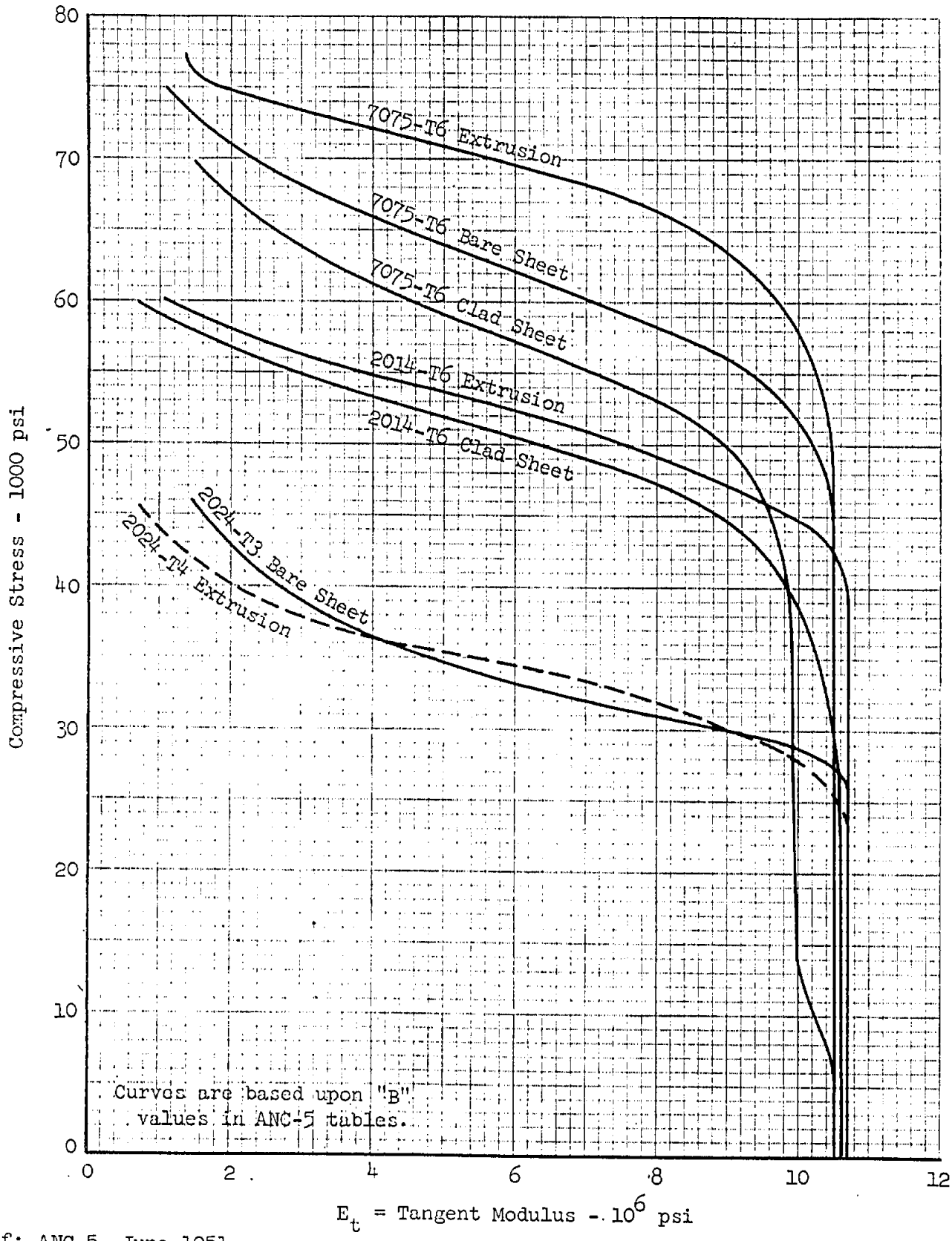

Ref: ANC-5, June 1951
& TN 1010, 1385, 2085

SECTION B2 - FITTINGS, FASTENERS, BUSHINGS, AND BEARINGS

Table of Contents

FITTING DESIGN REQUIREMENTS

Introduction

A large proportion of structural failures in aircraft occur in, or because of, improperly designed fittings, and a large percentage of airplane cost is absorbed in fitting manufacture. The purpose of this discussion is to aid in reducing both the number of failures associated with fittings, and the high cost of making them.

Definition

Fittings are defined as those parts which connect one primary member to another. Structurally, they shall also include that part of the primary member adjacent to the fitting. Riveted and bolted connections between members are considered as fittings. Riveted seams between large sheets, wherein there is no stress concentration, are not considered fittings.

General Design

Fittings in general should be cheap, simple, and rugged. A fitting must be stronger and less critical than the main member it connects. Because negligible additional weight will make a questionable fitting satisfactory, weight saving should not be a primary consideration in fitting design.

Fatigue

Small fittings with complex sections subjected to frequent stress reversals are particularly sensitive to fatigue, because of the resulting stress concentrations. In designing fittings, stress concentrations should be kept to a minimum, and critical fittings should be checked for fatigue, using the methods of Sect. B1.03.

Distortion Due to Heat Treat

Heat treating frequently causes the length of a part when ready for drilling end holes to be different from its length before heat treatment. Thus, centering limits of holes shall be large enough to allow for this variation, and such tolerance shall be specifically noted on the drawing of the part.

Provision for Reaming Oversize

A diameter of at least 1/16 inch over minimum allowable edge distance shall be allowed on unbushed holes to provide for subsequent reaming oversize. Drawings shall note either that this provision has been made or that the hole may not be reamed oversize.

FITTING DESIGN REQUIREMENTS (cont.)

Tapped Holes

In parts subject to frequent field disassembly, tapping should be avoided because of high initial cost and difficulty of replacement if threads are damaged.

Bolts

Only steel bolts 1/4 diameter and larger and aluminum alloy bolts 5/16 diameter and larger shall be used in primary structures. Shear loads are taken only on the unthreaded portion of a bolt. Special bolts, stressed otherwise than in shear, shall have between head and body a fillet equal to 1/4 the body diameter.

Rotation on Aluminum Alloy Parts

Rotation must be taken by bushings or appended bearing surfaces other than the aluminum alloy part itself.

Fitting Factors

In general, it is desirable that any failure in an airplane structural assembly take place in a long structural member, rather than in a fitting. A long member will fail more gradually and with more warning, will absorb more energy in failing, and can sustain more damage without complete disintegration; for example, a wing test specimen which has failed properly at ultimate load somewhere in the compression material will usually sustain at least 1.5g after failure.

On the other hand, failure in a fitting will occur suddenly with no warning and little absorption of energy, and with no possibility of sustaining load after failure. These probabilities are all aggravated by the susceptability of fittings to stress concentrations because of their small size and usual complication and because of the uncertainty as to the actual stress distribution in the fitting.

Therefore, in order to insure that failure will not take place in the fitting, it is standard practice to design fittings for a higher load than the structural members which they connect; the standard factor of increase is 1.15 (SB-73A). If the strength of a fitting is to be demonstrated by static test, the fitting factor may be reduced to 1.0 (SB-73A). However, in the early stages of design when the applied loads may not be in final form, a factor of 1.15 should be applied to all fittings.

FITTING DESIGN REQUIREMENTS (cont.)

In certain special cases, different fitting factors are specified in the following references:

Plain Journal Bearings: ANC-5 (June 1951) Tables 2.6112-2 (a) and (b).

Castings: SR-111a, superseded by MIL-C-6021 on late contracts.

TYPICAL RELATIVE FATIGUE STRENGTHS OF RIVETED AND SPOTWELDED JOINTS IN ALUMINUM ALLOY

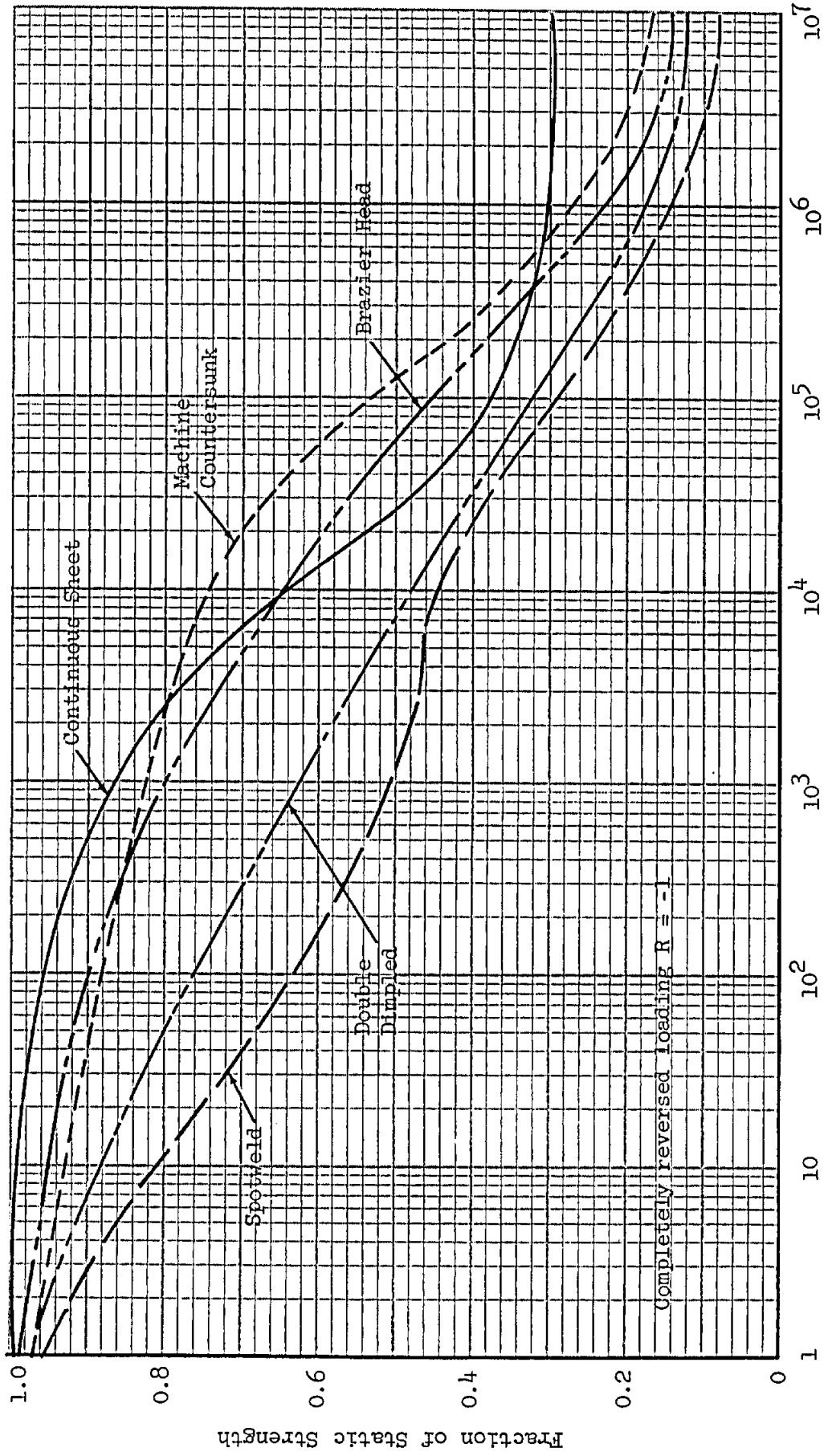

Ref: Holt & Hartman, Welding Res. Sup. Apr. 1952
and NACA TN 2012

ALLOWABLE ULTIMATE STATIC SHEAR STRENGTH FOR HS-48 HI-SHEAR RIVETS - PROTRUDING HEAD - IN 4130 STEEL SHEET(1)

e/D = 2.0 (Sheet H.T. = 150 ksi) W/D = 6.0

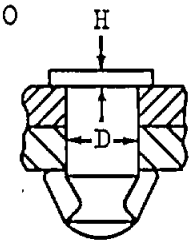

H/D ~ .246

Sheet Thickness	Strength in Lbs.(2), (3) Rivet Diameter			
	3/16	1/4	5/16	3/8
.025	1135			
.028	1365	1395		
.032	1625	1860		
.036	1850	2290	2320	
.040	2040	2670	2910	
.045	2230	3075	3780	3665
.050	2385	3420	4170	4530
.063	2600	4095	5380	6380
.071	2620	4385	5955	7295
.080		4580	6475	8150
.090		4650	6890	8915
.095			7040	9255
.100			7155	9535
.125			7300	10405
.160				10500

(1) All test specimens were single shear, single rivet lap joints. Reference Grumman Report GE-148.

(2) In cases where the lower sheet is thinner than the upper sheet, the shear bearing allowable for the lower sheet-rivet combination should be computed.

(3) Yield strength is not critical (1.304 x yield load exceeds design ultimate load for all cases listed).

ALLOWABLE ULTIMATE STATIC SHEAR STRENGTH FOR HS-48 HI-SHEAR RIVETS - PROTRUDING HEAD - In 4130 STEEL SHEET(1)

e/D = 2.0 (Sheet H.T. = 180 ksi) W/D = 6.0

Strength in Lbs.(2), (3)				
Sheet Thickness	Rivet Diameter			
	3/16	1/4	5/16	3/8
.025	1270			
.028	1470	1630		
.032	1850	2105		
.036	2100	2555	2700	
.040	2325	3000	3290	
.045	2465	3520	3990	4210
.050	2550	3930	4690	5070
.063	2620	4470	6185	7230
.071		4575	6690	8395
.080		4650	7005	9290
.090			7175	9880
.095			7250	10065
.100			7300	10195
.125				10500

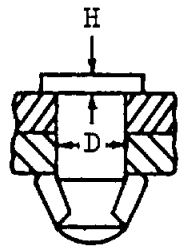

H/D ~ .246

(1) All test specimens were single shear, single rivet lap joints. Reference Grumman Report GE-148.

(2) In cases where the lower sheet is thinner than the upper sheet, the shear bearing allowable for the lower sheet - rivet combination should be computed.

(3) Yield strength is not critical (1.304 x yield load exceeds design ultimate load for all cases).

ALLOWABLE ULTIMATE STATIC SINGLE SHEAR STRENGTH FOR HS-48 HI-SHEAR AND SALP HUCK FASTENERS- PROTRUDING HEAD - IN 7075-T6 BARE SHEET (1)

e/D = 2.0 W/D = 6.0

Strength in lbs. (2), (3)				
Sheet Thickness	Rivet Diameter			
	3/16	1/4	5/16	3/8
.040	985			
.045	1140			
.050	1290	1600		
.056	1405	1855		
.063	1650	2140	2530	
.071	1850	2460	2950	
.080	2070	2790	3410	3930
.090	2190	3140	3905	4550
.100	2300	3490	4360	5150
.125	2505	3960	5450	6550
.160	2620	4380	6230	8240
.190		4590	6675	8975
.250		4650	7300	10000
.3125				10500

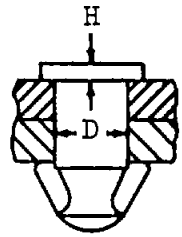

HS-48, H/D ~ .246
SALP, H/D ~ .312

(1) All test specimens were single shear lap joints, (1 or 2 rivets). --Ref. Grumman Report GE-148 and 123MT520.

(2) In cases where the lower sheet is thinner than the upper sheet, the shear-bearing allowable for the lower sheet-rivet combination should be computed.

(3) Yield strength is not critical (1.304 x yield load exceeds design ultimate load for all cases listed).

ALLOWABLE ULTIMATE STATIC SINGLE SHEAR STRENGTH FOR HS-48 HI-SHEAR AND SALP HUCK FASTENERS- PROTRUDING HEAD-IN 2014-T6 CLAD SHEET (1)

e/D = 2.0 W/D = 6.0

Sheet Thickness	Strength in lbs. (2), (3) Rivet Diameter			
	3/16	1/4	5/16	3/8
.032	715			
.036	805			
.040	900			
.045	1025	1340		
.050	1135	1495		
.056	1275	1695	2085	
.063	1405	1915	2355	2810
.071	1535	2155	2685	3170
.080	1680	2400	3040	3600
.090	1840	2630	3420	4100
.100	1990	2850	3750	4555
.125	2350	3370	4450	5575
.160	2620	4060	5355	6720
.190		4650	6105	7650
.250			7300	9420
.3125				10500

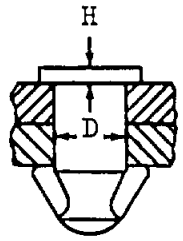

HS-48, H/D ~ .246
SALP, H/D ~ .312

(1) All test specimens were single shear single rivet lap joints Ref. Grumman Report GE-148 and 123MT520.

(2) In cases where the lower sheet is thinner than the upper sheet, the shear-bearing allowable for the lower sheet-rivet combination should be computed.

(3) Yield strength is not critical (1.304 x yield load exceeds design ultimate load for all cases listed).

ALLOWABLE ULTIMATE STATIC SHEAR STRENGTH FOR HS-47 HI-SHEAR RIVETS - COUNTERSUNK HEAD - IN 4130 STEEL SHEET(1)

e/D = 2.0 (Sheet H.T. = 150 ksi) W/D = 6.0

Strength in Lbs.(2), (3)				
Sheet Thickness	Rivet Diameter			
	3/16	1/4	5/16	3/8
.025	795			
.028	925	1100		
.032	1100	1335		
.036	1275	1570	1790	
.040	1450	1805	2090	
.045	1675	2095	2455	2735
.050	1875	2380	2820	3190
.063	2210	3150	3760	4320
.071	2310	3530	4350	5005
.080	2415	3820	5000	5805
.090	2500	4030	5570	6690
.095	2545	4110	5795	7125
.100	2570	4190	5970	7505
.125	2620	4500	6545	8790
.160		4650	7100	9660
.190			7300	10500

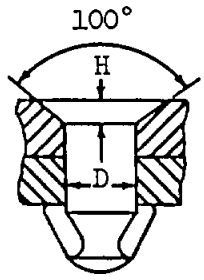

H/D ~ .228

(1) All test specimens were single shear, single rivet lap joints. Reference Grumman Report GE-148.

(2) In cases where the lower sheet is thinner than the upper sheet, the shear bearing allowable for the lower sheet - rivet combination should be computed.

(3) Yield strength is not critical (1.304 x yield load exceeds design ultimate load for all cases listed).

ALLOWABLE ULTIMATE STATIC SHEAR STRENGTH FOR HS-47 HI-SHEAR RIVETS - COUNTERSUNK HEAD - IN 4130 STEEL SHEET(1)

e/D = 2.0 (Sheet H.T. = 180 ksi) W/D = 6.0

Strength in Lbs.(2), (3)				
Sheet Thickness	Rivet Diameter			
	3/16	1/4	5/16	3/8
.025	910			
.028	1060	1270		
.032	1260	1535		
.036	1455	1800	2070	
.040	1660	2060	2400	
.045	1910	2390	2810	3160
.050	2140	2725	3225	3650
.063	2540	3590	4300	4935
.071	2620	4045	4975	5725
.080		4410	5705	6630
.090		4635	6395	7640
.095		4650	6665	8125
.100			6890	8560
.125			7300	10125
.160				10500

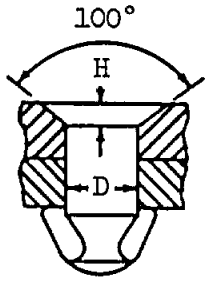

H/D ~ .228

(1) All test specimens were single shear, single rivet lap joints. Reference Grumman Report GE-148.

(2) In cases where the lower sheet is thinner than the upper sheet, the shear bearing allowable for the lower sheet - rivet combination should be computed.

(3) Yield strength is not critical (1.304 x yield load exceeds design ultimate load for all cases listed).

ALLOWABLE ULTIMATE STATIC SINGLE SHEAR STRENGTH FOR

HS-47 HI-SHEAR AND SAL100 HUCK FASTENERS-

FLUSH HEAD - IN MACHINE COUNTERSUNK 7075-T6 BARE SHEET(1)

e/D = 2.0 W/D = 6.0

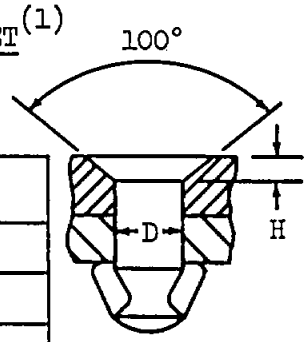

HS-47, H/D ~ .228
SAL100, H/D ~ .240

Strength in lbs.(2)					
Sheet Thickness	Rivet Diameter				
	5/32	3/16	1/4	5/16	3/8
.032	525				
.036	635	675			
.040	740	820			
.045	860	980			
.050	975	1130	1300		
.056	1100	1300	1570		
.063	1245	1490	1860	2060	
.071	1405	1695	2175	2505	2640
.080	*1540	1915	2510	2975	3265
.090	*1665	*2155	2860	3460	3920
.100	1820	*2305	3195	3920	4520
.125		2620	*3935	4990	5925
.160			*4605	*6230	7670
.190			4650	*6965	*8905
.250				7300	10500

(1) All test specimens were single shear, single rivet lap joints. Ref. Grumman Report GE-148, 123MT520, and Chance Vought "Structural Design Data" Pocket Handbook, Dec. 1955.

(2) In cases where the lower sheet is thinner than the upper sheet the shear-bearing allowable for the lower sheet-rivet combination should be computed.

* Yield is critical ($1.304 \times \text{yield load} < \text{test ultimate load}/_{1.15}$)

ALLOWABLE ULTIMATE STATIC SINGLE SHEAR STRENGTH FOR HS-47 HI-SHEAR AND SAL100 HUCK FASTENERS- FLUSH HEAD-IN MACHINE COUNTERSUNK 2014-T6 CLAD SHEET(1)

e/D = 2.0 W/D = 6.0

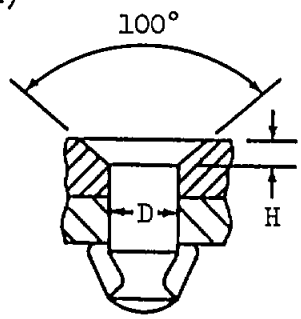

HS-47, H/D~.228
SAL100, H/D~.240

Strength in lbs.(2), (3)				
Sheet Thickness	Rivet Diameter			
	3/16	1/4	5/16	3/16
.040	765			
.045	895			
.050	1010			
.056	1155	1455		
.063	1315	1685	1970	
.071	1485	1945	2310	
.080	1665	2220	2685	3060
.090	1860	2510	3085	3570
.100	2040	2785	3465	4055
.125	2410	3430	4355	5230
.160	2620	4185	5475	6665
.190		4575	6295	7810
.250		4620	7300	9660
.3125				10500

(1) All test specimens were single shear lap joints, (1 or 2 rivets). Ref. Grumman Report GE-148 and 123MT520.

(2) In cases where the lower sheet is thinner than the upper sheet, the shear-bearing allowable for the lower sheet-rivet combination should be computed.

(3) Yield strength is not critical (1.304 x yield load exceeds design ultimate load for all cases listed).

ALLOWABLE ULTIMATE STATIC SHEAR STRENGTH FOR HS-67-5 HI-SHEAR RIVET-COUNTERSUNK HEAD-IN 17-7PH(TH1050) STAINLESS STEEL SHEET(1)

e/D = 1.5 W/D = 6.0

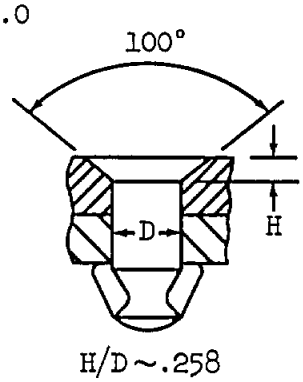

H/D ~ .258

Strength in Lbs. (2), (3)	
Sheet Thickness	Rivet Diameter 5/32
.025	765
.028	1080
.032	1300
.036	1450
.040	1575
.045	1720
.050	1835
.063	2115
.071	2270
.080	2350

(1) All test specimens were single shear, single rivet lap joints. Reference Grumman Report GE-148.

(2) In cases where the lower sheet is thinner than the upper sheet, the shear-bearing allowable for lower sheet - rivet combination should be computed.

(3) Yield strength is not critical (1.304 x yield load exceeds design ultimate load for all cases).

NOTE: Minimum guaranteed values of 17-7PH(TH1050) stainless steel sheet: F_{tu} = 180,000 psi; F_{ty} = 150,000 psi; F_{bru} = 305,000 psi (e/D = 1.5).

TENSION ALLOWABLE ULTIMATE STATIC STRENGTH FOR

HS-67-5 HI-SHEAR RIVETS-COUNTERSUNK HEAD-IN 17-7PH(TH1050) STAINLESS STEEL(1)

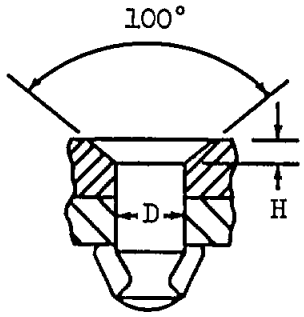

H/D ~ .258

Strength in Lbs.	
Sheet Thickness	Rivet Diameter 5/32
.025	420
.028	535
.032	670
.036	785
.040	875
.045	915
.050	935
.063	965
.071	995
.080	1025
.090	1060
.095	1080
.100	1095
.125	1170

(1) Reference Grumman Report GE-148.

NOTE: Minimum guaranteed value of 17-7PH(TH1050) stainless steel sheet: F_{tu} = 180,000 psi; F_{ty} = 150,000 psi.

ALLOWABLE ULTIMATE STATIC SHEAR STRENGTH FOR NAS1097 DD5 AND DD6 RIVETS-COUNTERSUNK HEAD-IN 7075 CLAD SHEET(1)

e/D = 2.0 W/D = 6.0

Strength in Lbs. (2), (3)		
Sheet Thickness	Rivet Diameter	
	5/32	3/16
.032	395	
.036	495	
.040	550	620
.045	590	755
.050	620	825
.056	640	870
.063	655	910
.071	675	940
.080	685	960
.090	695	980
.100	700	995
.125	720	1010
.160	765	1060
.190	815	1095
.250		1180

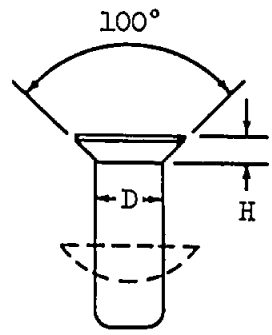

H/D ~ .242

(1) All test specimens were single shear, single rivet lap joints. Reference Grumman Report GE-148.

(2) In cases where the lower sheet is thinner than the upper sheet, the shear bearing allowable for the lower sheet-rivet combination should be computed.

(3) Yield strength is not critical (1.304 x yield load exceeds design ultimate load for all cases listed).

ALLOWABLE ULTIMATE STATIC SINGLE SHEAR STRENGTH FOR NA1097-AD RIVETS - FLUSH HEAD COLD DIMPLED - MACHINE COUNTERSUNK 2024-T3 CLAD SHEET (1)

W/D = 6.0

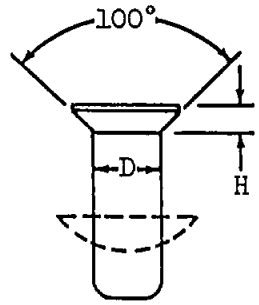

H/D ~ .238

Sheet (2) Thickness	Strength in Lbs. (3)					
	e/D = 1.5			e/D = 2.0		
	Rivet Diameter					
	1/8	5/32	3/16	1/8	5/32	3/16
.016	165			165		
.020	195	260		195	295	
.024	215	315	375	215	345	425
.028	255	365	440	255	380	500
.032	285	415	500	285	415	570
.036	320	445	560	320	445	640
.040	350	475	625	350	475	675
.045	388	515	700	388	515	705
.050		550	740		550	740
.056		596	775		596	775
.063			820			820
.071			862			862

(1) All test specimens were single shear, single rivet lap joints. Ref. Grumman Report GE-148 and 128MT509.

(2) The thickness of the machine-countersunk lower sheet must be at least one tabulated gauge thicker than the dimpled sheet; and the minimum gauge of the lower sheets are .032, .040 and .050 for the 1/8, 5/32 and 3/16 diameter rivets respectively. Ref. Engineering Manual, Section D.

(3) Yield strength is not critical (1.304 x yield load exceeds design ultimate load for all cases listed).

ALLOWABLE ULTIMATE STATIC SHEAR STRENGTH FOR AN427 MONEL RIVETS - COUNTERSUNK HEAD - IN 7075-T6 CLAD SHEET(1)

e/D = 2.0 W/D = 6.0

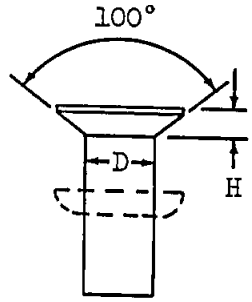

H/D ~ .395

Strength in Lbs. (2), (3)			
Sheet Thickness	Rivet Diameter		
	1/8	5/32	3/16
.032	380		
.040	520	595	
.050	610	810	920
.063	665	955	1215
.071	675(4)	1020	1320
.080		1040	1425
.090		1055(4)	1520(4)

(1) All test specimens were single shear, single rivet lap joints. Reference Grumman Report GE-148.

(2) In cases where the lower sheet is thinner than the upper sheet, the shear bearing allowable for the lower sheet - rivet combination should be computed.

(3) Yield strength is not critical (1.304 x yield load exceeds design ultimate load for all cases listed).

(4) Shear values based on annealed rivet material (F_{su} = 55 ksi).

TENSION ALLOWABLE ULTIMATE STATIC STRENGTH FOR AN427 MONEL RIVETS - COUNTERSUNK HEAD - IN 7075-T6 CLAD SHEET(1)

Strength in lbs.			
Sheet Thickness	Rivet Diameter		
	1/8	5/32	3/16
.040	310		
.050	420	485	560
.063	565	660	745
.071	650	780	875
.080	675	900	1025
.090		1025	1200
.100		1155	1360
.125		1250	1735
.160			1995

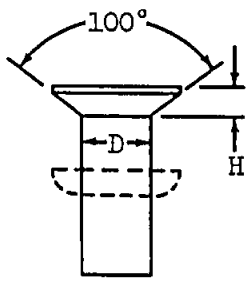

H/D .395

(1) Reference Grumman Report GE-148.

Allowable Ultimate Static Shear Strength for Hi-Lok GB510A and GB510B Fasteners - Countersunk Head

(In Ti-6Al-4V STA and Ti-6Al-6V-2Sn Annealed Titanium Sheet) (1) (2)

e/D = 2.0 W/D = 6.0

Room Temperature Strength in lbs. (3) (4) (5) (6)				
Sheet Thickness	Fastener Diameter			
	3/16	1/4	5/16	3/8
.063	1890	—	—	—
.071	2080	2820	—	—
.080	2235	3220	3850	—
.090	2380	3555	4470	5030
.100	2475	3825	5030	5850
.125	2600	4280	5975	7500
.160	2610	4600	6750	8940
.190	2630	4650	7240	9700
.250			7265	10410
.3125				10490
.375				
Fastener Shear Strength	2690	4650	7290	10490

(1) All tests were of single shear, single fastener joints at room temperature.

(2) All tests were of GB510A fasteners in Ti-6Al-4V STA sheet.

(3) For effects of elevated temperature, see Grumman Titanium Design Guide, Fig. 450.4.4-13.

(4) 5/16" diameter fasteners were not tested. The values listed are based upon the design static shear envelope obtained from tests of fasteners of the other three sizes.

(5) In cases where the lower sheet is thinner than the upper sheet, the shear-bearing allowable for the lower sheet-fastener combination should be computed.

(6) Yield strength is not critical (1.304 x yield load exceeds design ultimate load for all cases tested).

ULTIMATE STRENGTH OF BLIND RIVETS

(in 2024-T3, Clad 2024-T3, 2014-T6, 7075-T6, and Clad 7075-T6 sheets)

Rivet Type		Protruding Head(1)				100° Dimpled(2)				100° Machine Countersunk(2)			
Diameter		1/8	5/32	3/16	1/4	1/8	5/32	3/16	1/4	1/8	5/32	3/16	1/4
Sheet Thickness(3)	.012	142				110							
	.016	161	234			151	185						
	.020	197	251	341		183	237	281					
	.025	247	309	373	586	216	287	354	463				
	.032	303	395	474	643	252	343	433	606	100			
	.040	355	474	587	789	283	393	508	733	129	156		
	.051	399	561	714	1006	313	446	585	873	215	206	240	
	.064	406	617	828	1213		490	658	1006	334	343	316	400
	.072		635	878	1319			689	1076	381	439	413	454
	.081			911	1430			721	1136	407	530	546	521
	.091			914	1524				1199		603	691	644
	.102				1594				1252		635	812	861
	.125				1626							914	1288
Rivet Shear Strength		406	635	914	1626					406	635	914	1626

(1) Huck "P", Huck "9SP-B-A", Rocket "SB-A", Cherry "CR163", du Pont DR, MS 20600 AD

(2) Huck "100V", Huck "9SP-100-A", Rocket "SC-A", Cherry "CR162", du Pont DR, MS 20601 AD

(3) Sheet gage is that of the thinnest sheet for protruding head and for dimpled applications.

Sheet gage is that of the upper sheet for machine countersunk applications, except that where the lower sheet is thinner than the upper, the shear-bearing allowable for the lower sheet-rivet combination should be computed from MIL-HDBK-5

ALLOWABLE ULTIMATE STATIC SHEAR STRENGTH FOR MLS100-M4 AND -M5 (HUCK) BLIND RIVETS COUNTERSUNK HEAD - IN 7075-T6 CLAD MATERIAL(1), (4)

e/D = 2.0 W/D = 6.0

Strength in Lbs.(2)		
Sheet Thickness	Rivet Diameter Ultimate(3)	
	1/8	5/32
.032	415	
.036	470	
.040	515	645
.045	570	730
.050	610	795
.056	670	880
.063	725	960
.071	790	1045
.080	870	1140
.090	950	1235
.100	970(5)	1345
.125		1490(5)

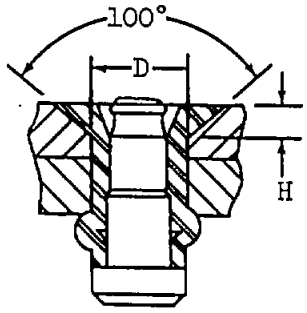

H/D ~ .342

(1) All test specimens were single shear, single rivet lap joints. (Ref. Grumman Report GE-148) and 123MT514.

(2) In cases where the lower sheet is thinner than the upper sheet, the shear-bearing allowable for the lower sheet fastener combination should be computed.

(3) Ultimate load = Test Ultimate Load Average Curve/1.15.

(4) When used in conjunction with other fasteners, the deflection characteristics of the MLS100-M Blind Rivets should be taken into account.

(5) Shear values based on Huck Manufacturing Company data sheet.

ALLOWABLE ULTIMATE STATIC SINGLE SHEAR STRENGTH FOR MLS100-EU (A286) HUCK BLIND RIVETS-FLUSH HEAD-IN MACHINE COUNTERSUNK 7075-T6 CLAD SHEET(1), (2)

e/D = 2.0 W/D = 6.0

Strength in lbs.(3)			
Sheet Thickness	Rivet Diameter		
	1/8	5/32	3/16
.036	*405		
.040	*435		
.045	*485	*630	
.050	*540	*675	*875
.056	*620	*750	*925
.063	675	*850	*1010
.071	735	*980	*1140
.080	800	*1120	*1310
.090	875	*1275	*1500
.100	945	*1425	*1685
.125	970(4)	1490(4)	*2130
.160			2150(4)

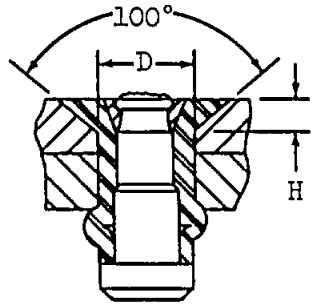

H/D ~ .342

(1) All test specimens were single shear, single rivet lap joints. Ref. Grumman Report GE-148 and 128MT508.

(2) When used in conjunction with other fasteners, the deflection characteristics of the MLS100-EU rivets should be taken into account.

(3) In cases where the lower sheet is thinner than the upper sheet, the shear-bearing allowable for the lower sheet-fastener combination should be computed.

(4) Shear values based on Huck Manufacturing Co. data sheet.

* Yield is critical (1.304 x yield load test ultimate load/1.15)

ALLOWABLE ULTIMATE STATIC SHEAR STRENGTH FOR AN509 SCREWS-COUNTERSUNK HEAD-IN 17-7PH(TH1050) STAINLESS STEEL(1)

e/D = 1.5 W/D = 6.0

Strength in lbs. (2)		
Sheet Thickness	Screw Diameter	
	10 (.190)	416 (.2475)
.040	*1255	
.045	*1360	
.050	*1460	*1900
.063	*1690	*2180
.071	*1820	*2300
.080	1945	*2435
.090	1980	*2560
.095	1990	*2615
.100	2005	*2675
.125	2090	2795
.160	2126	2870
.190		2985
.224		3215
.250		3340
.3125		3680

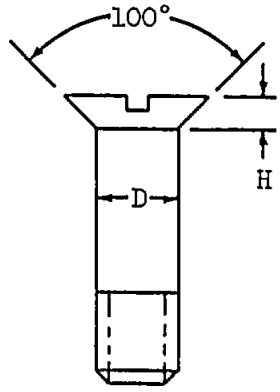

H/D ~ 0.427

(1) All test specimens were single shear, single fastener lap joints. Reference Grumman Report GE-148.

(2) In cases where the lower sheet is thinner than the upper sheet, the shear bearing allowable for the lower sheet-fastener combination should be computed.

NOTE: Minimum guaranteed values of 17-7PH(TH1050) stainless steel sheet: F_{tu} = 180,000 psi; F_{ty} = 150,000 psi, F_{bru} = 305,000 psi (e/D = 1.5)

* Allowable ultimate load equals 1.304 X yield load.

ALLOWABLE ULTIMATE STATIC SINGLE SHEAR STRENGTH FOR AN509 SCREWS - FLUSH HEAD - IN DIMPLED-MACHINE COUNTERSUNK 7075-T6 CLAD SHEET(1)

e/D = 2.0

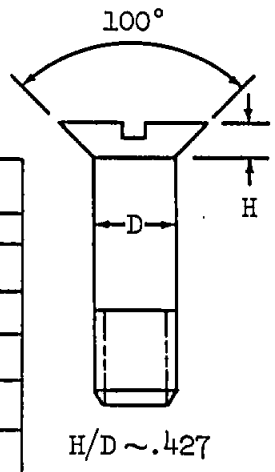

H/D ~.427

Sheet Thickness	Strength in lbs.(2) Screw Diameter			
	#8(.164)	#10(.190)	1/4	5/16
.024	430			
.028	520	585		
.032	605	685		
.036	685	785	975	
.040	765	880	1115	
.045	855	995	1285	1525
.050	* 925	1095	1445	1745
.056	* 970	*1225	1630	1995
.063	*1015	*1285	1835	2275
.071	*1065	*1350	2030	2550
.080	*1120	*1415	2190	2910
.090	*1180	*1485	*2300	3260
.100	*1220	*1555	*2395	*3430
.125	*1335	*1690	*2625	*3745
.160	*1555	*1875	*2900	*4150
.190	1584	*2020	*3090	*4430
.250		2126	*3500	*4960
.3125			3680	*5465
.375				5750

(1) Ref. (a) A.I.A. Report on Flush Screw Joint Strength, January 22, 1952.
(b) Grumman Report GE-148.

(2) The thickness of the machine-countersunk lower sheet must be at least one tabulated gauge thicker than the dimpled sheet; and the minimum gauge of the lower sheets are .071, .080, .125 and .160 for the #8, #10, 1/4 and 5/16 screws respectively. Ref. Engineering Manual, Section D.

* Yield strength is critical (1.304 x yield load < test ultimate load/1.15)

ALLOWABLE ULTIMATE STATIC SINGLE SHEAR STRENGTH FOR AN509 SCREWS - FLUSH HEAD - IN DIMPLED-MACHINE COUNTERSUNK 2014-T6 CLAD AND 2024-T3 CLAD SHEET(1)

e/D = 2.0

Sheet Thickness	Strength in lbs.(2) Screw Diameter			
	#8(.164	#10(.190)	1/4	5/16
.024	385			
.028	465	525		
.032	545	615		
.036	615	705	875	
.040	685	790	1000	
.045	770	890	1150	1370
.050	855	990	1295	1565
.056	* 920	1110	1455	1790
.063	* 970	*1210	1645	2050
.071	*1025	*1285	1825	2280
.080	*1075	*1355	*2060	2610
.090	*1135	*1425	*2185	2930
.100	*1185	*1495	*2300	*3220
.125	*1310	*1640	*2530	*3600
.160	*1470	*1835	*2800	*4000
.190	1584	*2000	*3040	*4290
.250		2126	*3440	*4840
.3125			3680	*5365
.375				5750

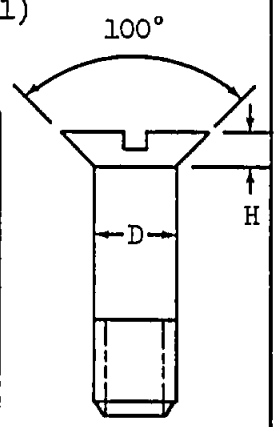

(1) Ref. (a) A.I.A. Report on Flush Screw Joint Strength, January 22, 1952.
(b) Grumman Report GE-148.
(c) Grumman Report 134MT515.

(2) The thickness of the machine-countersunk lower sheet must be at least one tabulated gauge thicker than the dimpled sheet; and the minimum gauge of the lower sheets are .041, .080, .125 and .160 for the #8, #10, 1/4 and 5/16 screws respectively. Ref. Engineering Manual, Section D.

* Yield strength is critical (1.304 x yield load < test ultimate load/115)

ALLOWABLE ULTIMATE STATIC SINGLE SHEAR STRENGTH FOR AN509 SCREWS - FLUSH HEAD - DOUBLE DIMPLED 2014-T6 CLAD AND 2024-T3 CLAD SHEET(1)

e/D = 2.0 W/D = 6.0

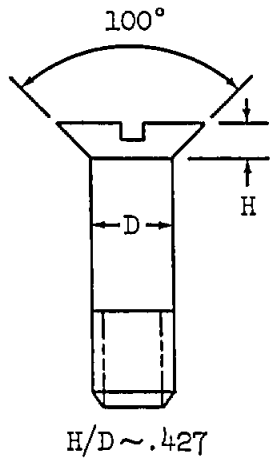

Sheet(2) Thickness	Strength in lbs. Screw Diameter		
	#8(.164)	#10(.190)	1/4
.016	180	* 190	
.020	* 230	* 265	
.024	* 275	* 320	410
.028	* 325	* 375	* 490
.032	* 370	* 430	* 560
.036	* 420	* 480	* 630
.040	* 470	* 540	* 705
.045	* 540	* 615	* 790
.050	* 610	* 690	* 885
.056	* 695	* 785	* 995
.063	* 805	* 905	*1130
.071	* 930	*1040	*1300
.080	*1075	*1205	*1490
.090	*1235	*1390	*1720
.100	*1395	*1580	*1955
.125	1584	*2045	*2560
.160		2126	*3430
.190			3680

(1) All test specimens were single shear, single rivet lap joints. Ref. Grumman Report GE-148, 134MT507 and 134MT516.

(2) Sheet gauge is that of the thinnest sheet for a double dimpled joint.

* Yield strength is critical (1.304 x yield load < test ultimate load/1.15)

ALLOWABLE ULTIMATE STATIC SHEAR STRENGTH

NAS1200 SCREWS-COUNTERSUNK HEAD-IN 17-7PH(TH1050) STAINLESS STEEL(1)

e/D = 1.5 W/D = 6.0.

Strength in lbs.(2)		
Sheet Thickness	Screw Diameter	
	1203 (.189)	1204 (.249)
.040	1640	
.045	1815	
.050	1980	2455
.063	2290	*2605
.071	2400	*2625
.080	2500	*2640
.090	2550	*2820
.095	2590	*2900
.100	2605	*2995
.125	2620	*3590
.160		4145
.190		4335
.224		4650

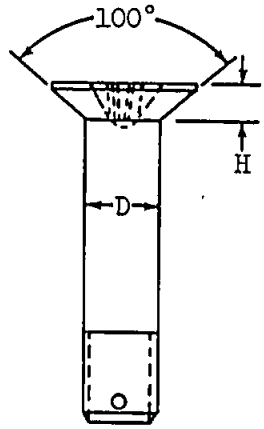

H/D ~ .425

(1) All test specimens were single shear, single fastener lap joints. Ref. Grumman Report GE-148.

(2) In cases where the lower sheet is thinner than the upper sheet, the shear bearing allowable for the lower sheet-fastener combination should be computed.

NOTE: Minimum guaranteed values of 17-7PH(TH1050) stainless steel sheet: F_{tu} = 180,000 psi; F_{ty} = 150,000 psi; F_{bru} = 305,000 psi. (e/D = 1.5)

* Allowable ultimate load equals 1.304 x yield load.

STIFFNESS OF MECHANICALLY ATTACHED SINGLE SHEAR JOINTS

Introduction

The data on the following pages provide the stiffness of single shear, single fastener, mechanically attached lap joints. Stiffness is the slope of the load-deflection curve from test specimens of this configuration. The data is presented for some of the common combinations of fasteners and plate materials that are encountered in aircraft and spacecraft design.

Discussion

Stiffness data are a necessary part of any analysis which treats the problem of fastener load distribution in a joint with multiple connections. The load distribution problem is usually most important when fatigue is a design factor, since the stress concentration due to the loaded fastener is a significant part of the total stress concentration factor. Because the magnitude of the predicted load concentration within a fastener group is a direct function of fastener stiffness, it is necessary to make this prediction on the basis of a linear elastic analysis. (i.e. the stiffness value for the fasteners should be the maximum reasonable value of the slope of the straight line portion of the load deflection curve.)

It should also be noted that fasteners contribute a significant amount to the flexibility of a shear panel when it is attached to its framing members with discrete mechanical fasteners (Reference a, page 431) as well as to the flexibility of a structural assembly of axial load members joined by a group of mechanical fasteners.

Derivation

The presented data was obtained by fairing curves through plotted values of available test data. These data were modified from the raw data in order to remove the increment of flexibility due to the axial strain of the test specimen. Faired test data was then curve fit in order to extrapolate it to the range of fastener sizes and plate thicknesses included in the presented data. The test data was obtained from References (b), (c), and (d).

Materials

The data presented is applicable to plate materials of the common structural aluminum alloys in the heat treated condition, 6Al-4V or 6Al-6V-2Sn titanium alloys in the annealed condition, and steel of moderate heat treat (say 160 ksi to 180 ksi F_{tu}). The pin materials are steel or titanium in the 160 ksi F_{tu} heat treat range. Until test data becomes available it is recommended that data for steel fasteners

Materials (Continued)

in aluminum plate can be used for the case of titanium fasteners in aluminum plate.

Geometry and Material Variations

The data presented in this section is for the case of equal plate thicknesses and like materials in each plate. When plates of significantly different thicknesses and/or dissimilar materials are joined, a reasonable adjustment of the available data must be made. The following adjustment is suggested, referring to the figure.

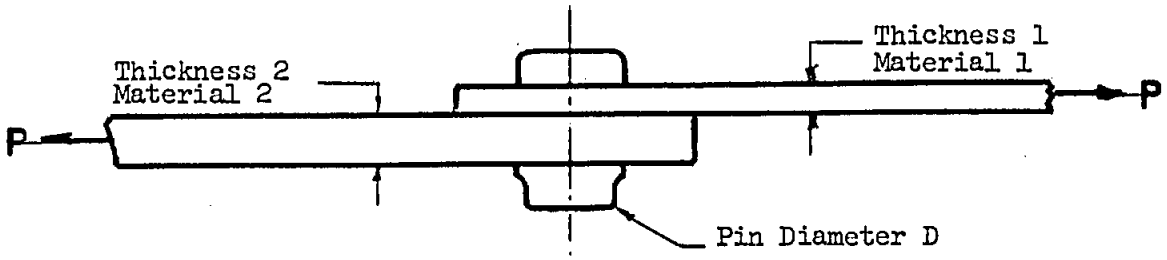

Let k_1 be the stiffness value for two plates of thickness 1, material 1
Let k_2 be the stiffness value for two plates of thickness 2, material 2
where k_1 and k_2 are obtained from the appropriate figure of page B2.50-4 thru B2.50-7 for consistant values of D and T/D.

The value of k for the multi-thickness or mixed material joint is then:

$$k = \frac{2\ (k_1 \cdot k_2)}{k_1 + k_2}$$

This approach has been checked favorably with a few test points for one thickness configuration with plates of like material. No test data exists for mixed material configurations.

Double Shear Joints

No attempt has been made to extrapolate test data for double shear joints primarily because of a paucity of test data. However, there are 18 usable test data points in the reference that can be used to establish the value of a simple multiplying factor to apply to single shear data in order to obtain double shear data. This factor ranges in value from 2.5 to 3.4 as determined from the test data mentioned above. Again, since conservative fastener loads are usually

Double Shear Joints (Continued)

desired, the higher factor is recommended. The factor is applied as shown, referring to the following figure.

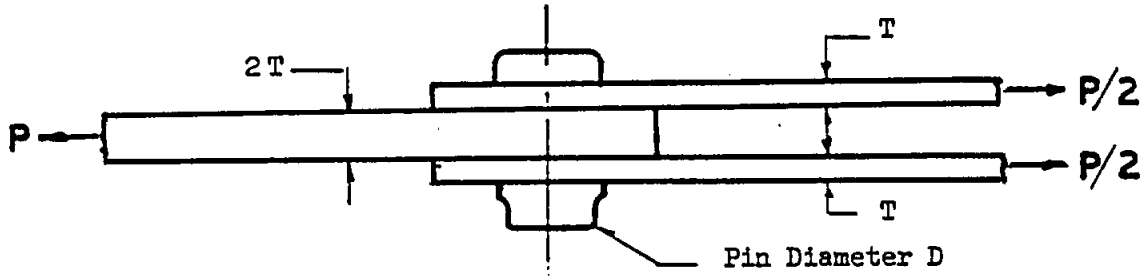

Determine the stiffness for a plate and fastener configuration of D and T (NOT 2T) from pages B2.50-4 thru B2.50-7. The stiffness of the double shear joint shown above is then this stiffness increased by the factor 2.5 → 3.40 .

If the center member is not 2x the thickness of the outer strap, the joint stiffness is calculated as shown for the following case.

The actual joint is structurally equal to the idealized joint.

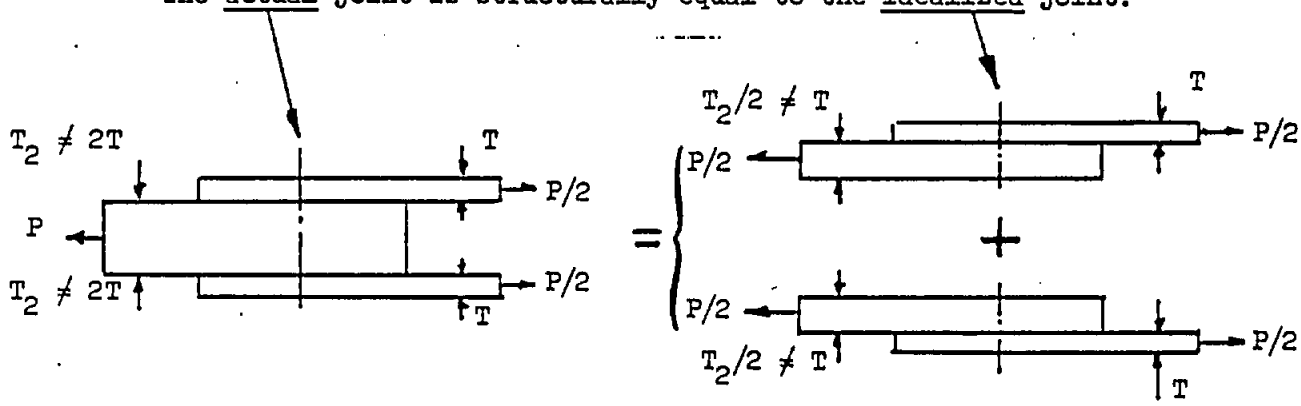

Then follow the proceedure for single shear joint of unequal plate thickness from the previous page to obtain the joint stiffness k for each idealized member. The double shear joint stiffness is then:

$$k\ (\text{double}) = (2.5 \longrightarrow 3.4) \times k$$

for the two shear faces. If the stiffness of a single shear face is desired, it is

$$k\ (\text{single}) = (1.25 \longrightarrow 1.7) \times k$$

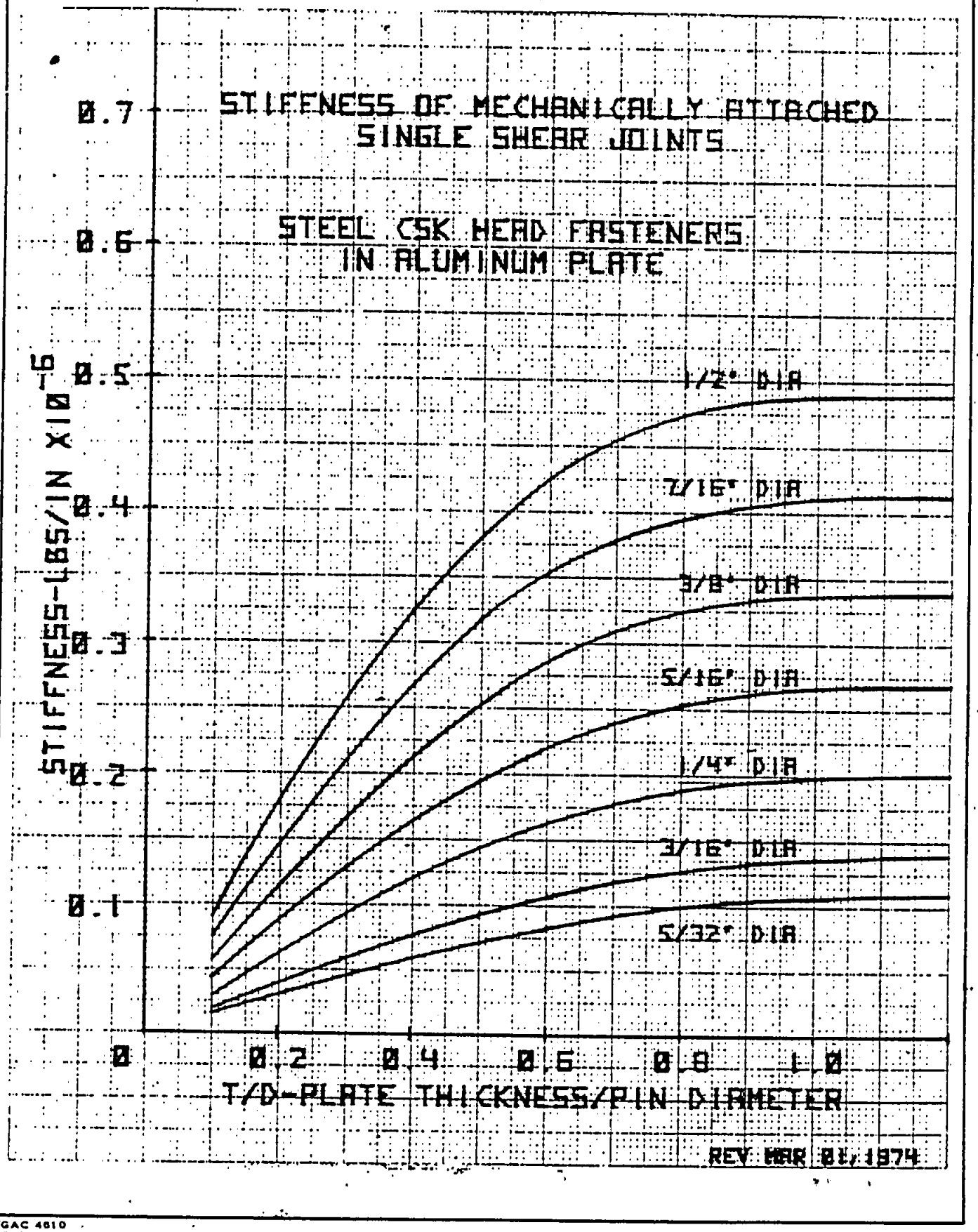
STIFFNESS OF MECHANICALLY ATTACHED SINGLE SHEAR JOINTS
STEEL CSK HEAD FASTENERS IN ALUMINUM PLATE
STIFFNESS-LBS/IN X10⁻⁶
0.7
0.6
0.5
0.4
0.3
0.2
0.1
0
0.2
0.4
0.6
0.8
1.0
T/D-PLATE THICKNESS/PIN DIAMETER
1/2" DIA
7/16" DIA
3/8" DIA
5/16" DIA
1/4" DIA
3/16" DIA
5/32" DIA
REV MAR 8I, 1974

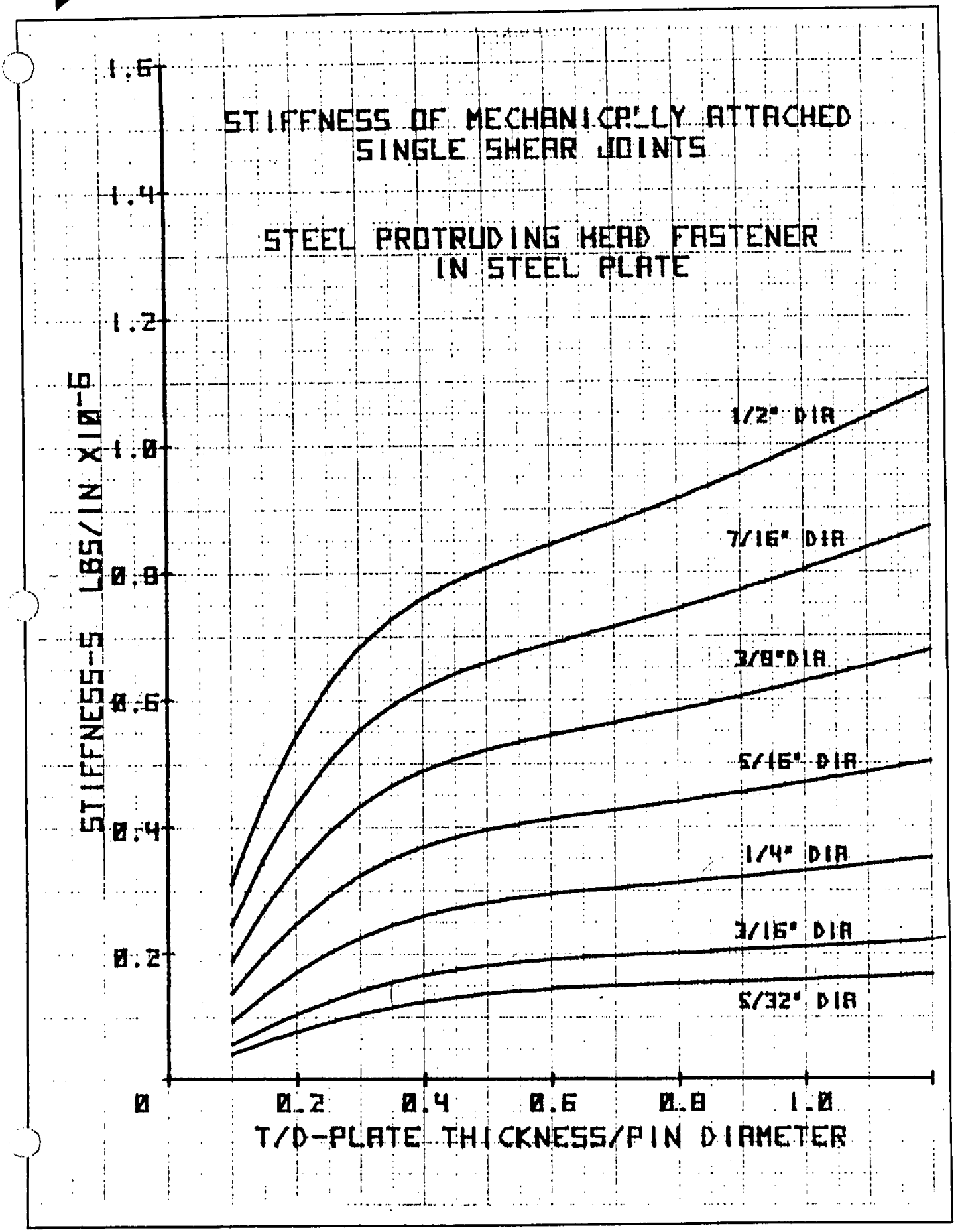
STIFFNESS OF MECHANICALLY ATTACHED SINGLE SHEAR JOINTS
STEEL PROTRUDING HEAD FASTENER IN STEEL PLATE
STIFFNESS-S LBS/IN X10-6
1.6
1.4
1.2
1.0
0.8
0.6
0.4
0.2
0
0.2
0.4
0.6
0.8
1.0
T/D-PLATE THICKNESS/PIN DIAMETER
1/2" DIA
7/16" DIA
3/8"DIA
5/16" DIA
1/4" DIA
3/16" DIA
5/32" DIA

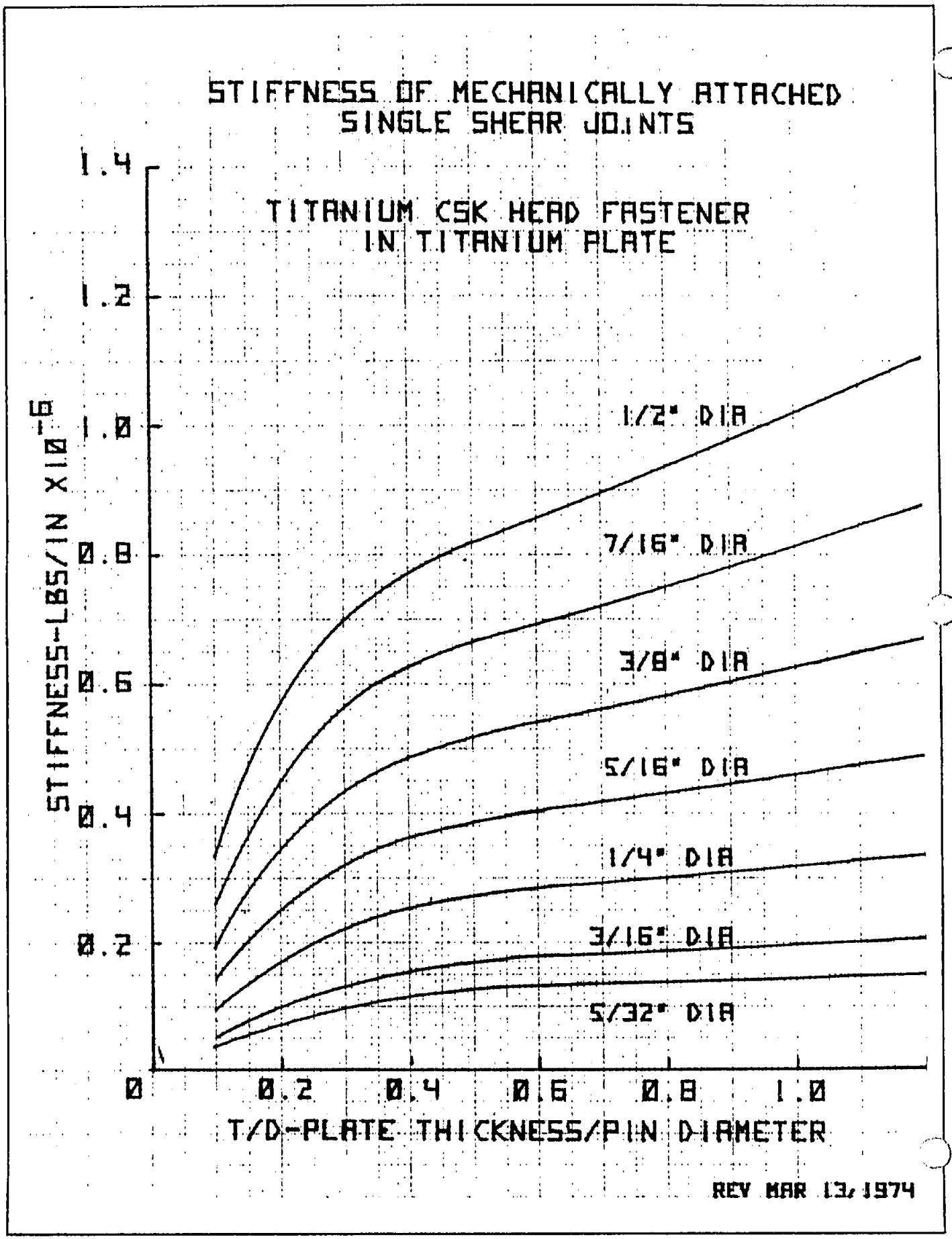
STIFFNESS OF MECHANICALLY ATTACHED
SINGLE SHEAR JOINTS
TITANIUM CSK HEAD FASTENER
IN TITANIUM PLATE
STIFFNESS-LBS/IN X10⁻⁶
1.4
1.2
1.0
0.8
0.6
0.4
0.2
0
1/2" DIA
7/16" DIA
3/8" DIA
5/16" DIA
1/4" DIA
3/16" DIA
5/32" DIA
0.2
0.4
0.6
0.8
1.0
T/D-PLATE THICKNESS/PIN DIAMETER
REV MAR 13, 1974

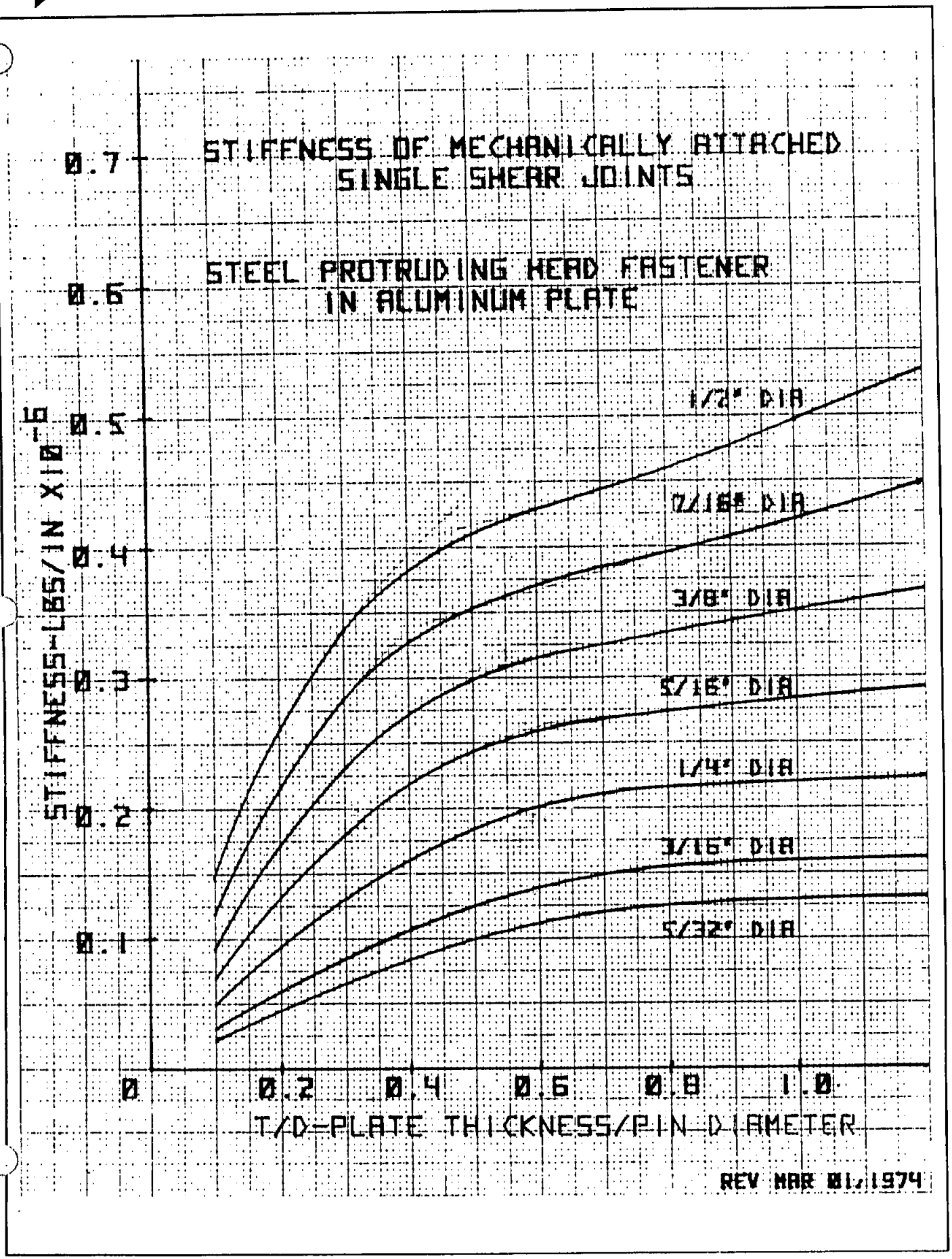
STIFFNESS OF MECHANICALLY ATTACHED
SINGLE SHEAR JOINTS
STEEL PROTRUDING HEAD FASTENER
IN ALUMINUM PLATE
1/2" DIA
7/16" DIA
3/8" DIA
5/16" DIA
1/4" DIA
3/16" DIA
5/32" DIA
STIFFNESS-LBS/IN X10⁻⁵
0.7
0.6
0.5
0.4
0.3
0.2
0.1
0
0.2
0.4
0.6
0.8
1.0
T/D-PLATE THICKNESS/PIN DIAMETER
REV MAR 01, 1974

MINIMUM HOUSING RADII FOR STANDARD BUSHINGS BASED UPON PRESS FIT

Steel Bushings in Aluminum Alloy Housings
(Reference Grumman Standard Part G B10A)

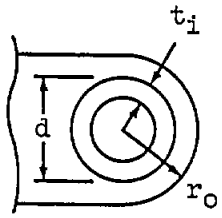

d = Bushing Nominal Outer Diameter
t_i = Bushing Wall Thickness
r_o = Housing Wall Radius

For $d \leq 7/8"$, $t_i = 3/32"$
$d > 7/8"$, $t_i = 1/8"$

F_{ty} = Transverse tensile yield stress of housing material.

Item G B10A	Bushing I.D. (Nominal)	Bushing O.D. (Nominal)	Maximum Interference δ	r_o - Housing Wall Radius			
				F_{ty}=48,000 psi	F_{ty} = 56,000 psi (14S-T6 Extruded Bar)	F_{ty} = 60,000 psi (14S-T6 Plate 75S-T6 Extr Bar)	F_{ty} = 68,000 psi (75S-T6 Plate)
-4-	1/4	7/16	.0015			29/32	1/2
-5-	5/16	1/2	.0015		19/32	17/32	13/32
-6-	3/8	9/16	.0017	1-1/16	5/8	17/32	7/16
-7-	7/16	5/8	.0019	31/32	5/8	9/16	15/32
-8-	1/2	11/16	.0021	15/16	21/32	19/32	1/2
-9-	9/16	3/4	.0023	29/32	11/16	5/8	17/32
-10-	5/8	13/16	.0023	27/32	21/32	5/8	17/32
-11-	11/16	15/16	.0025	29/32	23/32	11/16	19/32
-12-	3/4	1	.0027	15/16	3/4	23/32	5/8
-13-	13/16	1-1/16	.0028	29/32	3/4	23/32	21/32
-14-	7/8	1-1/8	.0028	7/8	3/4	23/32	11/16
-16-	1	1-1/4	.0030	15/16	13/16	25/32	3/4
-20-	1-1/4	1-1/2	.0035	1	29/32	7/8	7/8

Notes:

1. These standard bushing housings are designed for press fit stresses only following the method of B3.50 and are based upon the maximum interferences of the Grumman Standard Part G B10A. Each housing must also be checked for applied load (B3.13) and fatigue life.
2. If short transverse grain direction in housing is not parallel to bushing, double the housing wall thickness.
3. For non-standard bushings, see B3.50.
4. Below the dotted line of the table, the housing wall radius is based on a 1/8" minimum housing wall thickness.

MINIMUM HOUSING RADII FOR STANDARD BUSHINGS BASED UPON PRESS FIT

Bronze Bushings in Aluminum Alloy Housings
(Reference Grumman Standard Part G B10B)

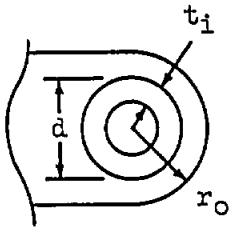

d = Bushing Nominal Outer Diameter

t_i = Bushing Wall Thickness

r_o = Housing Wall Radius

For $d \leq 7/8"$, $t_i = 3/32"$

$d > 7/8"$, $t_i = 1/8"$

F_{ty} = Transverse tensile yield stress of housing material.

Item G B10B	Bushing I.D. (Nominal)	Bushing O.D. (Nominal)	Maximum Interference δ	r_o - Housing Wall Radius			
				F_{ty}=48,000 psi	F_{ty} = 56,000 psi (14S-T6 Extruded Bar)	F_{ty} = 60,000 psi (14S-T6 Plate 75S-T6 Extr Bar)	F_{ty} = 68,000 psi (75S-T6 Plate)
-4-	1/4	7/16	.0015	23/32	15/32	7/16	3/8
-5-	5/16	1/2	.0015	1/2	13/32	13/32	3/8
-6-	3/8	9/16	.0017	17/32	7/16	7/16	13/32
-7-	7/16	5/8	.0019	9/16	15/32	15/32	7/16
-8-	1/2	11/16	.0021	9/16	1/2	1/2	15/32
-9-	9/16	3/4	.0023	19/32	17/32	17/32	1/2
-10-	5/8	13/16	.0023	5/8	9/16	17/32	17/32
-11-	11/16	15/16	.0025	11/16	5/8	19/32	19/32
-12-	3/4	1	.0027	23/32	21/32	5/8	5/8
-13-	13/16	1-1/16	.0028	23/32	11/16	21/32	21/32
-14-	7/8	1-1/8	.0028	3/4	11/16	11/16	11/16
-16-	1	1-1/4	.0030	13/16	3/4	3/4	3/4
-20-	1-1/4	1-1/2	.0035	29/32	7/8	7/8	7/8

NOTES:

1. These standard bushing housings are designed for press fit stresses only following the method of B3.50, and are based upon the maximum interferences of the Grumman Standard Part G B10B. Each housing must also be checked for applied load (B3.13) and fatigue life.
2. If short transverse grain direction in housing is not parallel to bushing, double the housing wall thickness.
3. For non-standard bushings, see B3.50.
4. Below the dotted line of the table, the housing wall radius is based on a 1/8" minimum housing wall thickness.

MINIMUM HOUSING RADII FOR STANDARD BUSHINGS BASED UPON PRESS FIT

Steel Shoulder Bushings in Aluminum Alloy Housings

(Reference Grumman Standard Part G B10C)

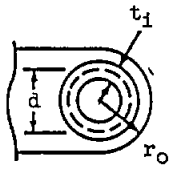

d = Bushing Nominal Outer Diameter

t_i = Bushing Wall Thickness

r_o = Housing Wall Radius

For $d \leq 3/4"$, $t_i = 1/16"$

$d > 3/4"$, $t_i = 3/32"$

F_{ty} = Transverse tensile yield stress of housing material.

Item G B10C	Bushing I.D. (Nominal)	Bushing O.D. (Nominal)	Maximum Interference δ	r_o - Housing Wall Radius			
				F_{ty}=48,000psi	F_{ty} = 56,000 psi (14S-T6 Extruded Bar)	F_{ty} = 60,000 psi (14S-T6 Plate 75S-T6 Extr Bar)	F_{ty} = 68,000 psi (75S-T6 Plate)
-4-	1/4	3/8	.0015			29/32	1/2
-5-	5/16	7/16	.0015		19/32	17/32	13/32
-6-	3/8	1/2	.0015	1-1/16	5/8	17/32	7/16
-7-	7/16	9/16	.0017	31/32	5/8	9/16	15/32
-8-	1/2	5/8	.0019	15/16	21/32	19/32	1/2
-9-	9/16	11/16	.0021	29/32	11/16	5/8	17/32
-10-	5/8	3/4	.0023	27/32	21/32	5/8	17/32
-11-	11/16	13/16	.0023	29/32	23/32	11/16	9/16
-12-	3/4	7/8	.0025	15/16	3/4	23/32	19/32
-13-	13/16	1	.0027	29/32	3/4	23/32	21/32
-14-	7/8	1-1/16	.0028	7/8	3/4	23/32	11/16
-15-	15/16	1-1/8	.0028	29/32	25/32	3/4	23/32
-16-	1	1-3/16	.0030	15/16	13/16	25/32	3/4
-18-	1-1/8	1-5/16	.0030	1	7/8	27/32	13/16
-20-	1-1/4	1-7/16	.0035	1	29/32	7/8	7/8
-22-	1-3/8	1-9/16	.0035	1	15/16	15/16	15/16
-24-	1-1/2	1-11/16	.0035	1-1/32	1	1	1
-26-	1-5/8	1-13/16	.0035	1-1/16	1-1/16	1-1/16	1-1/16
-28-	1-3/4	1-15/16	.0035	1-1/8	1-1/8	1-1/8	1-1/8
-30-	1-7/8	2-1/16	.0035	1-3/16	1-3/16	1-3/16	1-3/16
-32-	2	2-3/16	.0035	1-1/4	1-1/4	1-1/4	1-1/4

NOTES:

1. These standard bushing housings are designed for press fit stresses only following the method of B3.50 (modified to account for the stiffening effect of the bushing shoulder) and are based upon the maximum interferences of the Grumman Standard Part G B10C. Each housing must also be checked for applied load (B3.13) and fatigue life.
2. If short transverse grain direction in housing is not parallel to bushing, double the housing wall thickness.
3. Below the dotted line of the table, the housing wall radius is based on a 5/32" minimum housing wall thickness.

STANDARD HOUSING RADII

STANDARD HOUSING RADII FOR HEAVY DUTY, SINGLE ROW BALL BEARINGS

(TYPE KS IS SELF-ALIGNING)

(1)					(2)		
		Limit Load Rating			Required Housing Radius, in.		
Bearing Number	AN Bolt Size	Radial, lb.	Thrust, lb.	Moment, in. lb.	14S-T	75S-T	150 ksi Steel
AN200K3L	AN3	1560	700	58	1/2	15/32	7/16
KP3	3	1880	900	88.7	17/32	17/32	1/2
KP4	4	2680	1200	136	5/8	19/32	9/16
KP5	5	5620	2500	370	15/16	29/32	3/4
KP6	6	7910	3500	644	1-1/16	1	7/8
KP8	8	11800	5200	1170	1-5/16	1-1/4	1-1/32
KP10	10	14100	6200	1520	1-17/32	1-7/16	1-3/16
AN200KS3L	AN3	550	100		7/16	7/16	7/16
KS3	3	900	200		1/2	1/2	1/2
KS4	4	1410	300		19/32	9/16	9/16
KS4A	4	900	200		1/2	1/2	1/2
KS5	5	2190	300		25/32	3/4	3/4
KS6	6	2980	400		7/8	27/32	27/32
KS6A	6	1120	200		9/16	9/16	9/16
KS8	8	3670	500		1	1	31/32
KS10	10	5320	600		1-5/32	1-1/8	1-3/32

(1) From manufacturer's catalog, "Fafnir Aircraft Type Ball Bearings, " revised Nov.'53.

(2) Housing radius required to carry a radial load equal to 1.2 x 1.5 x Radial Limit Load Rating, based upon an F_{tu} of 55 ksi for 2014-T, and 66 ksi for 7075-T (press fit stresses are less critical) ref. tables 4.1 and 6.1, E12-A.

NOTES:

1. For combined radial, thrust & moment loading, the bearing M.S.

$$= \frac{1}{R/R_a + T/T_a + M/Ma} - 1.$$

2. If short transverse grain direction in dural housing is not parallel to bolt, double housing wall thickness.

3. A fitting factor of 1.2 is incorporated in the above Required Housing Radii.

4. The above housing radii are based upon static strength criteria alone. Each housing should be checked separately for fatigue life.

STANDARD HOUSING RADII

STANDARD HOUSING RADII FOR INTERMEDIATE DUTY (AN201-), FOR EXTRA LIGHT DUTY (AN202-), AND FOR EXTERNAL SELF-ALIGNING, SINGLE ROW BALL BEARINGS

(1)					(2)		
Bearing Number	AN Bolt Size	Limit Load Rating			Required Housing Radius, in.		
		Radial, lb.	Thrust, lb.	Moment, in. lb.	14S-T	75S-T	150 ksi Steel
AN201KP3A	AN3	1560	700	49.6	15/32	15/32	7/16
4	4	1880	900	85	9/16	9/16	1/2
5	5	2190	1000	114	5/8	19/32	17/32
6	6	2500	1100	143	21/32	5/8	9/16
8	8	3910	1700	277	27/32	25/32	11/16
10	10	6700	3000	598	1-3/32	1-1/32	27/32
12	12	8790	3900	945	1-9/32	1-7/32	1
16	16	11900	5200	1600	1-9/16	1-15/32	1-7/32
20	20	13800	6100	2170	1-3/4	1-21/32	1-3/8
AN202KP21B		9840	4400	1480	1-9/16	1-15/32	1-1/4
23		10500	4700	1700	1-21/32	1-9/16	1-5/16
25		11300	5000	1930	1-3/4	1-21/32	1-13/32
29		12700	5600	2420	1-15/16	1-27/32	1-17/32
33		14400	6400	3150	2-5/32	2-1/32	1-11/16
37		15800	7000	3780	2-11/32	2-7/32	1-27/32
47		24700	10900	6880	2-31/32	2-25/32	2-5/16
49		27500	12100	8520	3-1/8	2-15/16	2-13/32
KP21BS		9840	2000		1-21/32	1-9/16	1-11/32
23		10500	2200		1-3/4	1-21/32	1-13/32
25		11300	2300		1-27/32	1-3/4	1-15/32
29		12700	2600		2-1/32	1-15/16	1-5/8
33		14400	2900		2-1/4	2-1/8	1-25/32
37		15800	3200		2-7/16	2-5/16	1-15/16
47		24700	5000		3-1/16	2-29/32	2-7/16
49		27500	5500		3-1/4	3-1/16	2-17/32

(1) From manufacturer's catalog, "Fafnir Aircraft Type Ball Bearings," revised Nov. '53.

(2) Housing radius required to carry a radial load equal to 1.2 x 1.5 x Radial Limit Load Rating, based upon an F_{tu} of 55 ksi for 2014-T, and 66 ksi for 7075-T (press fit stresses are less critical) ref. tables 4.2 and 6.2, E12-A.

NOTES:

1. For combined radial, thrust and moment loading, the bearing M.S. $= \frac{1}{R/R_a + T/T_a + M/M_a} - 1.$
2. If short transverse grain direction in dural housing is not parallel to bolt, double housing wall thickness.
3. A fitting factor of 1.2 is incorporated in the above Required Housing Radii.
4. The above housing radii are based upon static strength criteria alone. Each housing should be checked separately for fatigue life.

Ref: E12-A

STANDARD HOUSING RADII

STANDARD HOUSING RADII FOR HEAVY DUTY, DOUBLE ROW BALL BEARINGS (TYPE DS IS SELF-ALIGNING)

(1)					(2)		
Bearing Number	AN Bolt Size	Limit Load Rating			Required Housing Radius, in.		
		Radial, lb.	Thrust, lb.	Moment, in. lb.	14S-T	75S-T	150 ksi Steel
AN206DSP3	AN3	1420	200		1/2	1/2	1/2
DSP4	4	1780	300		9/16	9/16	9/16
DSP5	5	3740	600		25/32	3/4	3/4
DSP6	6	5100	800		7/8	7/8	27/32
DSP8	8	7120	1000		1-1/32	1	31/32
DSP10	10	9000	1300		1-3/16	1-5/32	1-3/32
AN207DPP3	AN3	2950	1700	38.3	17/32	1/2	1/2
4	4	5370	1800	90.9	11/16	21/32	9/16
5	5	11000	4000	56.3	31/32	29/32	25/32
6	6	15760	5300	278	1-1/8	1-1/16	7/8
8	8	23600	7800	590	1-13/32	1-5/16	1-1/16
10	10	28400	9400	1600	1-19/32	1-1/2	1-7/32

(1) From manufacturer's catalog, "Fafnir Aircraft Type Ball Bearings," revised Nov. '53.

(2) Housing radius required to carry a radial load equal to 1.2 x 1.5 x Radial Limit Load Rating, based upon an F_{tu} of 55 ksi for 2014-T, and 66 ksi for 7075-T (press fit stresses are less critical) ref. tables 4.3 and 6.3, E-12A.

NOTES:

1. For combined radial, thrust and moment loading, the bearing M.S. $= \frac{1}{R/R_a + T/T_a + M/M_a} - 1.$

2. If short transverse grain direction in dural housing is not parallel to bolt, double housing wall thickness.

3. A fitting factor of 1.2 is incorporated in the above Required Housing Radii.

4. The above housing radii are based upon static strength criteria alone. Each housing should be checked separately for fatigue life.

Ref: E12-A

STANDARD HOUSING RADII

STANDARD HOUSING RADII FOR BELLCRANK BALL BEARINGS (DW SERIES) AND AIRFRAME CONTROL BEARINGS (DSRP SERIES)

(1)					(2)		
Bearing Number	AN Bolt Size	Limit Load Rating			Required Housing Radius, in.		
		Radial, lb.	Thrust, lb.	Moment, in. lb.	14S-T	75S-T	150 ksi Steel
DW4K2	AN4	1400	500	129	7/16	7/16	7/16
DW4K	4	2770	900	392	1/2	1/2	1/2
DW5	5	5140	1600	882	19/32	9/16	9/16
DW6	6	8440	2600	2010	23/32	11/16	21/32
DW8	8	13520	4700	4860	15/16	29/32	27/32
DSRP4	4	3025	908		5/8	19/32	19/32
DSRP5	5	7350	2200		7/8	27/32	3/4
DSRP6	6	9600	2880		1	15/16	27/32
DSRP8	8	12500	3750		1-5/32	1-1/8	1
DSRP10	10	17700	5310		1-11/32	1-9/32	1-1/8
DSRP12	12	26900	8070		1-21/32	1-19/32	1-3/8

(1) From manufacturer's catalog, "Fafnir Aircraft Type Ball Bearings," revised Nov. '53.

(2) Housing radius required to carry a radial load equal to 1.2 x 1.5 x Radial Limit Loads Rating, based upon an F_{tu} of 55 ksi for 2014-T, and 66 ksi for 7075-T (press fit stresses are less critical) ref. tables 4.4 and 6.4, E-12A.

NOTES:

1. For combined radial, thrust and moment loading, the bearing M.S. $= \frac{1}{R/R_a + T/T_a + M/M_a} - 1.$

2. If short transverse grain direction in dural housing is not parallel to bolt, double housing wall thickness.

3. A fitting factor of 1.2 is incorporated in the above Required Housing Radii.

4. The above housing radii are based upon static strength criteria alone. Each housing should be checked separately for fatigue life.

Ref: E12-A

STANDARD HOUSING RADII

STANDARD HOUSING RADII FOR HEAVY DUTY, TRACK-ROLLER, SINGLE ROW (NAS502 SERIES) AND DOUBLE ROW (NAS503 SERIES) NEEDLE BEARINGS

(1)			(2)		
Bearing Number	AN Bolt Size	Manufacturer's Yield Rating, Radial, lb.	Required Housing Radius, in. 14S-T	75S-T	150 ksi Steel
NAS502-3	AN3	2700	5/8	19/32	1/2
4	4	4300	23/32	11/16	9/16
6	6	8100	15/16	7/8	11/16
8	8	13000	1-1/8	1-1/16	27/32
10	10	19200	1-5/16	1-7/32	31/32
12	12	32000	1-17/32	1-13/32	1-1/8
14	14	41200	1-3/4	1-19/32	1-9/32
NAS503-6	6	16100	29/32	27/32	23/32
8	8	28100	1-5/32	1-1/16	7/8
10	10	44900	1-13/32	1-5/16	1-1/32
12	12	64100	1-21/32	1-17/32	1-3/16
14	14	86600	1-7/8	1-3/4	1-3/8

(1) From manufacturer's catalog, "Torrington Needle Bearings," Ed. 32-B, 1952.

(2) Housing radius required to carry a radial load equal to 1.2 x 1.305 x Manufacturer's Yield Rating, based upon an F_{tu} of 55 ksi for 2014-T and 66 ksi for 7075-T (press fit stresses are less critical) ref. tables 4.5 and 6.5, E12-A.

NOTES:

1. If short transverse grain direction in dural housing is not parallel to bolt, double housing wall thickness.

2. A fitting factor of 1.2 is incorporated in the above Required Housing radii.

3. The above housing radii are based upon static strength criteria alone. Each housing should be checked separately for fatigue life.

Ref: E12-A

STANDARD HOUSING RADII

STANDARD HOUSING RADII FOR HEAVY DUTY, SELF-ALIGNING, NON-SEPARABLE (NAS504 SERIES); HEAVY DUTY, NON-SEPARABLE, SINGLE ROW (NAS505 SERIES); AND THIN SHELL, NON-SEPARABLE. SINGLE ROW (NAS506 SERIES) NEEDLE BEARINGS

(1)			(2)		
Bearing Number	AN Bolt Size	Manufacturer's Yield Rating, Radial, lb.	Required Housing Radius, in. 14S-T	75S-T	150 ksi Steel
NAS504-3	AN3	2700	11/16	21/32	9/16
4	4	4300	3/4	23/32	19/32
5	5	6100	7/8	13/16	21/32
6	6	6800	7/8	13/16	23/32
7	7	8800	31/32	29/32	25/32
8	8	13000	1-3/32	1-1/16	29/32
9	9	17700	1-1/4	1-3/16	1
NAS505-3	AN3	2700	19/32	9/16	15/32
4	4	4300	11/16	5/8	1/2
5	5	6100	3/4	11/16	9/16
6	6	9500	27/32	3/4	19/32
7	7	12000	29/32	27/32	21/32
8	8	17400	1-1/16	31/32	3/4
9	9	22500	1-1/8	1-1/32	13/16
NAS506-3	AN3	2050	1/2*	15/32*	7/16
4	4	2600	1/2*	15/32*	7/16
5	5	2920	1/2*	15/32	15/32
6	6	5720	17/32	17/32	1/2
7	7	6290	19/32	9/16	17/32
8	8	6880	11/16	21/32	5/8
10	10	7870	25/32	3/4	11/16
12	12	13200	7/8	27/32	3/4
14	14	14700	31/32	29/32	13/16
16	16	16200	1-1/32	1	7/8

(1) From manufacturer's catalog, "Torrington Needle Bearings," Ed. 32-B, 1952.

(2) Housing radius required to carry a radial load equal to 1.2 x 1.305 x Manufacturer's Yield Rating, based upon an F_{tu} of 55 ksi for 2014-T and 66 ksi for 7075-T (except for those housings marked with an asterisk; for them press fit stresses are critical) ref. tables 4.6 and 6.6, E12-A.

NOTES:

1. If short transverse grain direction in dural housing is not parallel to bolt, double housing wall thickness.
2. A fitting factor of 1.2 is incorporated in the above Required Housing Radii.
3. The above housing radii are based upon static strength criteria alone. Each housing should be checked separately for fatigue life.

Ref: E12-A

STANDARD HOUSING RADII

STANDARD HOUSING RADII FOR SCHAFER ROLLER BEARINGS

Bearing Number (Schafer)	(1) AN Bolt Size	(1) Mfgr.'s Yield Rating Radial, lb.	(1) Mfgr.'s Yield Rating Thrust, lb.	(2) Required Housing Radius, in. 14S-T	(2) Required Housing Radius, in. 75S-T	(2) Required Housing Radius, in. 150 ksi Steel
A-4, AB-4A	AN4	6100	4400	25/32	25/32	3/4
A-5, AB-5	5	10600	7000	1-1/32	31/32	29/32
A-6, AB-6	6	10600	7000	1-1/32	31/32	29/32
A-7, AB-7	7	16400	10800	1-9/32	1-1/4	1-1/8
A-8, AB-8	8	16400	10800	1-9/32	1-1/4	1-1/8
A-9, AB-9	9	24600	14750	1-9/16	1-1/2	1-11/32
A-10, AB-10	10	24600	14750	1-9/16	1-1/2	1-11/32
A-12, AB-12	12	34500	20700	1-25/32	1-23/32	1-1/2
C-4, AD-4	AN4	6100	4400	25/32	25/32	3/4
C-6, AD-6	6	10600	7000	1-1/32	31/32	29/32
C-7, AD-7	7	10600	7000	1-1/32	31/32	29/32
C-8, AD-8	8	16400	10800	1-9/32	1-1/4	1-1/8
C-10, AD-10	10	16400	10800	1-9/32	1-1/4	1-1/8
C-12, AD-12	12	24600	14750	1-9/16	1-1/2	1-11/32
C-14	14	34500	20700	1-25/32	1-23/32	1-1/2

(1) From manufacturer's catalog, "Schafer Aircraft Bearings, " catalog No. 50, 1950.

(2) Housing radius required to carry a radial load equal to 1.2 x 1.305 x Manufacturer's Yield Rating, based upon an F_{tu} of 55 ksi for 2014-T, and 66 ksi for 7075-T (press fit stresses are less critical) ref. tables 4.7 and 6.7, E12-A.

NOTES:

1. For combined radial and thrust loading, the bearing M.S.

$$= \frac{1}{R/R_a + T/T_a} - 1.$$

2. If short transverse grain direction in dural housing is not parallel to bolt, double housing wall thickness.

3. A fitting factor of 1.2 is incorporated in the above Required Housing Radii.

4. The above housing radii are based upon static strength criteria alone. Each housing should be checked separately for fatigue life.

Ref: E12-A

SECTION B3 - THICK SECTIONS

Table of Contents

LUGS

This section presents static strength analysis procedures for uniformly loaded lugs and bushings, for double-shear joints, and for single-shear joints, subjected to either axial, transverse or oblique loading. The procedures on pages B3.13-3 through B3.13-33 apply to lugs made from materials having ultimate elongations in the plane of the lug of at least 5% in any direction. Modifications for lugs with less than 5% elongation are presented on pages B3.13-34 through B3.13-35.

In addition, a procedure is presented for the optimum design of an axially loaded, symmetrical, double-shear joint. Some parts of this procedure may be useful in obtaining efficient designs for other joints.

Examples are given to illustrate the analysis and design procedures.

Since lugs are especially critical in fatigue, the fatigue strength must always be checked. For lugs in which motion is possible see Reference 7.

TABLE OF CONTENTS

REFERENCES

1) I.P. Villalba, "Theoretical and Experimental Investigation of Lugs Loaded by a Transverse or Oblique Load", ADR 02-12-65.2.

2) F.P. Cozzone, M.A. Melcon, F.M. Hoblit, "Analysis of Lugs and Shear Pins Made of Aluminum or Steel Alloys", Product Engineering, May 1950.

3) M.A. Melcon, F.M. Hoblit, "Development in the Analysis of Lugs and Shear Pins", Product Engineering, June 1953.

4) Convair, Fort Worth, Structures Manual, Vol. 1, "Methods of Analysis", Section 10.6.

5) GAEC Structures Section Memo 63-S-9 (Rev.), July 31, 1964, "Allowable Design Yield Bearing Stress for Highly Loaded Bushings Under Stationary (Static) Load Condition."

6) GAEC unpublished calculations.

7) W.D. Craig, Jr., "Bearing Design Manual", GAEC Report No. MD-100010-M1, Feb. 1958.

SYMBOLS

A	area, in.^{2}
a	distance from edge of hole to edge of lug, inches
B	ductility factor for lugs with less than 5% elongation
b	effective bearing width, inches
C	$\dfrac{P_{uLB①}\ P_{uLB②}}{P_{uLB①}\ t_{L①} + P_{uLB②}\ t_{L②}}$
D	hole diameter or pin diameter, inches
E	modulus of elasticity, psi
e	edge distance, inches
F	allowable stress, psi
F_{tux}	cross grain tensile ultimate stress of lug material
F_{tyx}	cross grain tensile yield stress of lug material
f	stress, psi
g	gap between lugs, inches
$h_1,..h_4$	edge distances in transversely loaded lug, inches
h_{av}	effective edge distance in transversely loaded lug, inches = $\dfrac{6}{3/h_1 + 1/h_2 + 1/h_3 + 1/h_4}$
K	allowable stress (or load) coefficient

k_{bL}	lug or lug tang plastic bending coefficient (k_{bL} is approximately 1.4 for rectangular cross-section lugs made from reasonably ductile materials)
k_{bP}	pin plastic bending coefficient (k_{bP} is approximately 1.56 for solid pins made from reasonably ductile materials)
M	bending moment, in. lbs.
P	load, lbs.
R	dimensionless ratio indicating whether pin is critical in shear or bending (eq. 32)
t_B	bushing wall thickness, inches
t	lug thickness, inches
w	lug width, inches
α	angle of load to axial direction, degrees
ϵ	strain, inches/inch
ρ	density, lbs/in.^{3}

SUBSCRIPTS

all	allowable	opt	optimum
ax	axial	P	Pin
B	bushing	s	shear
b	bending	T	tang
br	bearing	t	tensile
c	compression	tr	transverse
L	lug	u	ultimate
max.	maximum	x	cross grain
n	net tensile	y	yield
o	oblique	①, ②	female and male lugs

AXIALLY LOADED LUG ANALYSIS

LUG AND BUSHING STRENGTH (UNIFORM BEARING)

Axially loaded lugs in tension must be checked for bearing strength and for net-section strength. The bearing strength of a lug loaded in tension, as shown in the figure below, depends largely on the interaction between bearing, shear-out, and hoop-tension stresses in the part of the lug ahead of the pin. The net section of the lug through the pin must be checked against net-tension failure. In addition, the lug and bushing must be checked to ensure that the deformations at design yield load are not excessive.

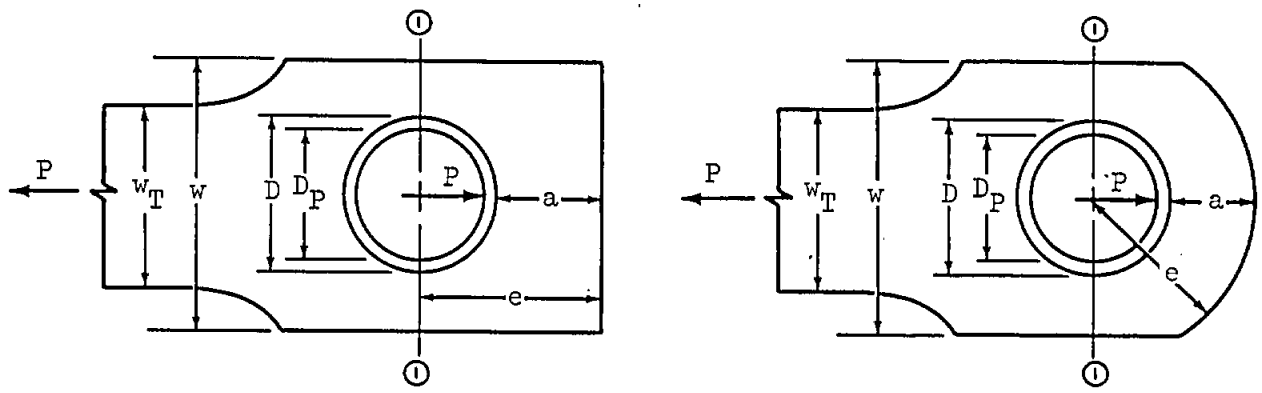

1 - Lug Bearing Strength

(a) The bearing stresses and loads for lug failure involving bearing, shear-tearout or hoop tension in the region forward of the net-section ① -① are determined from the equations below, with an allowable load coefficient (K) determined from the graph on page B3.13-27. For values of e/D less than 1.5 lug failures are likely to involve shear-out or hoop-tension, while for values of e/D greater than 1.5 bearing is likely to be critical. Actual lug failures may involve more than one failure mode, but such interaction effects are accounted for in the values of K.

The lug ultimate bearing stress (F_{brL}) is

$$F_{brL} = K \frac{a}{D} F_{tux}, \ (e/D < 1.5), \quad \text{.....(1a)}$$

$$F_{brL} = K F_{tux}, \ (e/D \geq 1.5), \quad \text{.....(1b)}$$

The graph on page B3.13-27 applies only to cases where D/t is 5 or less. This covers the majority of cases. If D/t is greater than 5, there is a reduction in strength which can be approximated by the curves in Figure 13 of Reference 3.

(b) The lug yield bearing stress (F_{bryL}) is:

$$F_{bryL} = K \frac{a}{D} F_{tyx}, \ (e/D < 1.5), \quad \text{.....(2a)}$$

$$F_{bryL} = K F_{tyx}, \ (e/D \geq 1.5), \quad \text{.....(2b)}$$

(c) The allowable lug ultimate bearing load (P_{brL}) for lug failure in bearing, shear-out or hoop tension is:

$$P_{brL} = F_{brL} Dt, \ (\text{if } F_{tux} \leq 1.304 F_{tyx}) \quad \text{.....(3a)}$$

$$P_{brL} = 1.304 F_{bryL} Dt, \ (\text{if } F_{tux} > 1.304 F_{tyx}) \quad \text{.....(3b)}$$

P_{brL}/Dt should not exceed either F_{bru} or 1.304 F_{bry}, where F_{bru} and F_{bry} are the allowable bearing stresses for the lug material for e/D = 2.0, as given in MIL-HDBK-5 or other applicable specification.

Equations (3a, b) apply, however, only if the load is uniformly distributed across the lug thickness. If the pin is too flexible and bends excessively, the load on the lug will tend to peak up near the shear faces and possibly cause premature failure of the lug.

A procedure to check the pin bending strength in order to prevent premature lug failure is given below in the section, "Double Shear Joint Strength."

2. Lug Net-Section Strength

(a) The allowable lug net-section tensile ultimate stress (F_{tL}) on section ① - ① is affected by the ability of the lug material to yield and thereby relieve the stress concentration at the edge of the hole.

$$F_{nL} = K_L F_{tu} \quad \text{..... (4)}$$

K_L, the net-tension stress coefficient, is obtained from the graphs on page B3.13-28 as a function of the ultimate and yield stress and strains of the lug material in the direction of the applied load. The ultimate strain (ϵ_u) can be obtained from MIL-HDBK-5 or the Grumman Structural Design Data pocket manual.

(b) The lug net-section tensile yield stress (F_{nyL}) is

$$F_{nyL} = K_L F_{ty} \quad \text{..... (5)}$$

(c) The allowable lug net-section ultimate load (P_{nL}) is

$$P_{nL} = F_{nL} (w-D)t, \text{ (if } F_{tu} \leq 1.304 F_{ty}) \quad \text{..... (6a)}$$

$$P_{nL} = 1.304 F_{nyL} (w-D)t, \text{ (if } F_{tu} > 1.304 F_{ty}) \quad \text{..... (6b)}$$

3. Lug Design Strength

The allowable design ultimate load for the lug (P_L) is the lower of the values obtained from eqs. 3 and 6.

$$P_L \leq P_{brL} \text{ (eqs. 3a, b), or } P_{nL} \text{ (eqs. 6a, b)} \quad \text{..... (7)}$$

4. Bushing Bearing Strength

(a) The allowable bearing yield stress for bushings (F_{bryB}) is restricted to the compressive yield stress (F_{cyB}) of the bushing material, unless higher values are substantiated by tests.

(b) The allowable bearing ultimate stress for bushings (F_{brB}) is

$$F_{brB} = 1.304 F_{cyB} \quad \text{..... (8)}$$

4. Bushing Bearing Strength (Cont'd)

(c) The allowable bushing ultimate load (P_B) is

$$P_B = 1.304\ F_{cyB}\ D_p\ t \quad \text{.....(9)}$$

This assumes that the bushing extends through the full thickness of the lug.

5. Combined Lug-Bushing Design Strength

The allowable lug-bushing ultimate load (P_{LB}) is the lower of the loads obtained from equations (7) and (9).

$$P_{LB} \leq P_L \text{ (eq. 7), or } P_B \text{ (eq. 9)} \quad \text{.....(10)}$$

DOUBLE-SHEAR JOINT STRENGTH

The strength of a joint such as the one shown below depends on the lug-bushing ultimate strength (P_{LB}) and on the pin shear and pin bending strengths.

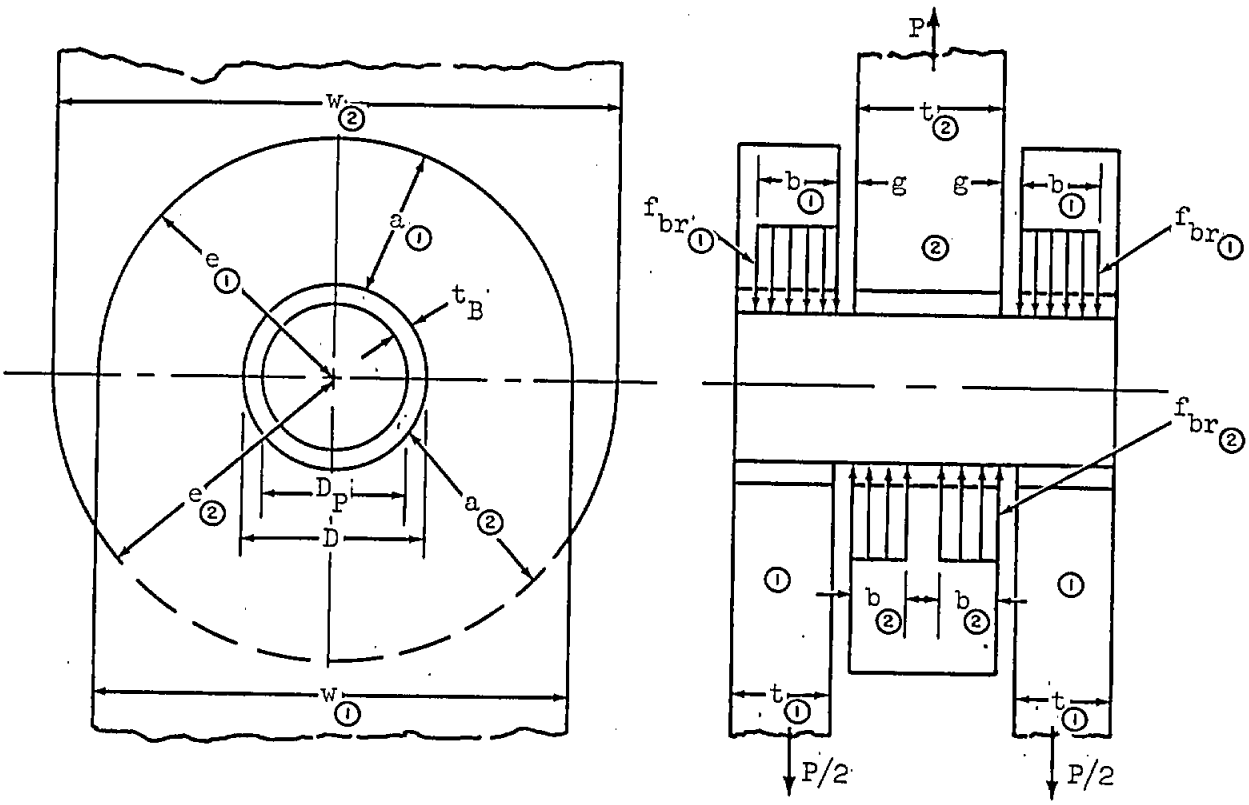

1 - Lug - Bushing Design Strength

The allowable lug-bushing ultimate load (P_{LB}) for the joint is computed, using eq. 10. For the symmetrical joint shown in the figure, eq. 10 is used to calculate the ultimate load for the two outer lugs and bushings ($2P_{LB\,①}$) and the ultimate load for the inner lug and

1 - Lug - Bushing Design Strength (Cont'd)

bushing ($P_{LB\ ②}$). The allowable value of P_{LB} for the joint is the lower of these two values.

$$P_{LB} \leq 2P_{LB\ ①} \text{ (eq. 10), or } P_{LB\ ②} \text{ (eq. 10)} \quad \ldots\ldots\ldots\ldots\ldots\ldots (11)$$

2 - Pin Shear Strength

The pin ultimate shear load (P_{sP}) for the symmetrical joint shown above is the double shear strength of the pin.

$$P_{sP} = 1.571\ D_P^{\,2}\ F_{suP} \quad \ldots\ldots\ldots\ldots\ldots\ldots\ldots\ldots\ldots\ldots\ldots\ldots\ldots\ldots (12)$$

Where F_{suP} is the ultimate shear stress of the pin material.

3 - Pin Bending Strength

Although actual pin bending failures are infrequent , excessive pin deflections can cause the load in the lugs to peak up near the shear planes instead of being uniformly distributed across the lug thickness, thereby leading to premature lug or bushing failures at loads less than predicted by eq. 11. At the same time, however, the concentration of load near the lug shear planes reduces the bending arm and, therefore, the bending moment in the pin, making the pin less critical in bending. The following procedure is used in determining the pin ultimate bending load.

(a) Assume that the load in each lug is uniformly distributed across the lug thickness ($b_{①} = t_{①}$, and $2b_{②} = t_{②}$). For the symmetrical joint shown in the figure, the resulting maximum pin bending moment is

$$M_{maxP} = \frac{P}{2}\left(\frac{t_{①}}{2} + \frac{t_{②}}{4} + g\right) \quad \ldots\ldots\ldots\ldots\ldots\ldots\ldots\ldots\ldots\ldots (13)$$

The ultimate failing moment for the pin is

$$M_{uP} = 0.0982\ k_{bP}\ D_P^{\,3}\ F_{tuP} \quad \ldots\ldots\ldots\ldots\ldots\ldots\ldots\ldots\ldots\ldots\ldots\ldots (14)$$

where k_{bP} is the plastic bending coefficient for the pin. The value of k_{bP} varies from 1.0 for a perfectly elastic pin to 1.7 for a perfectly plastic pin, with a value of 1.56 for pins made from reasonably ductile materials (more than 5% elongation).

The pin ultimate bending load (P_{bP}) is, therefore,

$$P_{bP} = \frac{0.1963\ k_{bP}\ D_P^{\,3} F_{tuP}}{\left(\frac{t_{①}}{2} + \frac{t_{②}}{4} + g\right)} \quad \ldots\ldots\ldots\ldots\ldots\ldots\ldots\ldots\ldots\ldots\ldots\ldots (15)$$

If P_{bP} is equal to or greater than either P_{LB} (eq. 11) or P_{sP} (eq. 12), then the pin is a relatively strong pin that is not critical

3 - Pin Bending Strength (Cont'd)

in bending, and no further pin bending calculations are required. The allowable load for the joint (P_{all}) can be determined by going directly to (eq. 19a).

(b) If P_{bP} (eq. 15) is less than both P_{LB} (eq. 11) and P_{sP} (eq. 12), the pin is considered a relatively weak pin, critical in bending. However, such a pin may deflect sufficiently under load to shift the c.g. of the bearing loads towards the shear faces of the lugs, resulting in a decreased pin bending moment and an increased value of P_{bP}. These shifted loads are assumed to be uniformly distributed over widths $b_{①}$ and $2b_{②}$, which are less than $t_{①}$ and $t_{②}$, respectively, as shown in the figure. The portions of the lugs and bushings not included in $b_{①}$ and $2b_{②}$ are considered ineffective. The new increased value of pin ultimate bending load is

$$P_{bP} = \frac{0.1963\ k_{bP}\ D_p^3\ F_{tuP}}{\left(\frac{b_{①}}{2} + \frac{b_{②}}{2} + g\right)} \qquad \text{.....(15a)}$$

The maximum allowable value of P_{bP} is reached when $b_{①}$ and $b_{②}$ are sufficiently reduced so that P_{bP} (eq. 15a) is equal to P_{LB} (eq. 11), provided that $b_{①}$ and $2b_{②}$ are substituted for $t_{①}$ and $t_{②}$, respectively. At this point we have a balanced design where the joint is equally critical in pin-bending failure or lug-bushing failure.

The following equations give the "balanced design" pin ultimate bending load (P_{bPmax}) and effective bearing widths ($b_{①\,min}$ and $2b_{②\,min}$)

$$P_{bPmax} = 2C\sqrt{\frac{P_{bP}}{C}\left(\frac{t_{①}}{2} + \frac{t_{②}}{4} + g\right) + g^2} - 2Cg \qquad \text{.....(16)}$$

$$\text{where } C = \frac{P_{LB①}\ P_{LB②}}{P_{LB①}\ t_{②} + P_{LB②}\ t_{①}}$$

The value of P_{bP} on the right hand side of eq. 16 and the values of $P_{LB①}$ and $P_{LB②}$ in the expression for C are based on the full thickness of the lugs being assumed effective, and have already been calculated. (eq's. 10 and 15)

If the inner lug strength is equal to the total strength of the two outer lugs ($P_{LB②} = 2\,P_{LB①}$), and if $g = 0$, then

$$P_{bPmax} = \sqrt{P_{bP}\ P_{LB②}} \qquad \text{.....(17)}$$

The "balanced design" effective bearing widths are

$$b_{①\,min} = \frac{P_{bP\,max}\ t_{①}}{2P_{LB①}} \qquad \text{.....(18a)}$$

3 - Pin Bending Strength (Cont'd)

$$2b_{②\,min} = \frac{P_{bPmax}\, t_②}{P_{LB\ ②}} \quad \text{.....(18b)}$$

where P_{bPmax} is obtained from eq. 16 and $P_{LB\ ①}$ and $P_{LB\ ②}$ are the previously calculated values based on the full thicknesses of the lugs. Since any lug thicknesses greater than $b_{①\,min}$ or $b_{②\,min}$ are not considered effective, an efficient static strength design would have $t_① = b_{①\,min}$ and $t_② = 2b_{②\,min}$.

4 - Double-Shear Joint Strength

The allowable joint ultimate load (P_{all}) for the double-shear joint is obtained as follows:

(a) If P_{bP} (eq. 15) is greater than either P_{LB} (eq. 11) or P_{sP} (eq. 12), then P_{all} is the lower of the values of P_{LB} or P_{sP}.

$$P_{all} \leq P_{LB} \text{ (eq. 11) or } P_{sP} \text{ (eq. 12)} \quad \text{.....(19a)}$$

(b) If P_{bP} (eq. 15) is less than both P_{LB} and P_{sP}, then P_{all} is the lower of the values of P_{sP} and P_{bPmax}.

$$P_{all} \leq P_{sP} \text{ (eq. 12), or } P_{bPmax} \text{ (eq. 16)} \quad \text{.....(19b)}$$

5 - Lug Tang Strength

(a) If equation (19a) was used to determine the joint allowable load, then we have a condition where the load in the lugs and tangs is assumed uniformly distributed. The allowable stress in the tangs is F_{tu}. The lug tang strength (P_T) is the lower of the following values.

$$P_T = 2F_{tu\ ①} w_{T\ ①} t_{①} \quad \text{.....(20a)}$$

$$P_T = F_{tu\ ②} w_{T\ ②} t_{②} \quad \text{.....(20b)}$$

(b) If equation (19b) was used to determine the joint allowable load, the tangs of the outer lugs should be checked for the combined axial and bending stresses resulting from the eccentric application of the bearing loads. Assuming that the lug thickness remains constant beyond the pin, a load (P/2), applied over the width $b_①$ in each outer lug will produce the following bending moment in the tangs.

$$M_① = \frac{P}{2}\left(\frac{t_① - b_①}{2}\right)$$

5 - Lug Tang Strength (Cont'd)

The strength of the tang under combined tension and bending can be checked with the method given on pages B3.21.24.0-1 and B3.21.24.1-1. A simple, but generally conservative approximation to the maximum combined stress in the outer lug tangs is

$$f_{tT①} = \frac{P}{2w_{T①}\ t_{①}} + \frac{6M_{①}}{k_{bL}\ w_{T①}\ t_{①}^2} \qquad \text{.....(21)}$$

where k_{bL}, the plastic bending coefficient for a lug tang of rectangular cross-section, varies from 1.0 for a perfectly elastic tang to 1.5 for a perfectly plastic tang, with a value of 1.4 representative of rectangular cross-sections with materials of reasonable ductility (more than 5% elongation). The allowable value of $f_{tT①}$ is $F_{tu①}$. The lug tang strength is the lower of the following values:

$$P_T = \frac{2\ F_{tu①}\ w_{T①}\ t_{①}}{1 + \frac{3}{k_{bL}}\left(1 - \frac{b_{① min}}{t_{①}}\right)} \qquad \text{.....(22a)}$$

$$P_T = F_{tu②}\ w_{T②}\ t_{②} \qquad \text{.....(22b)}$$

where $b_{① min}$ is given by eq. 18a.

SINGLE-SHEAR JOINT STRENGTH

In single-shear joints, lug and pin bending are more critical than in double shear joints. The amount of bending can be significantly affected by bolt clamping. In the cases considered below, no bolt clamping is assumed, and the bending moment in the pin is resisted by socket action in the lugs.

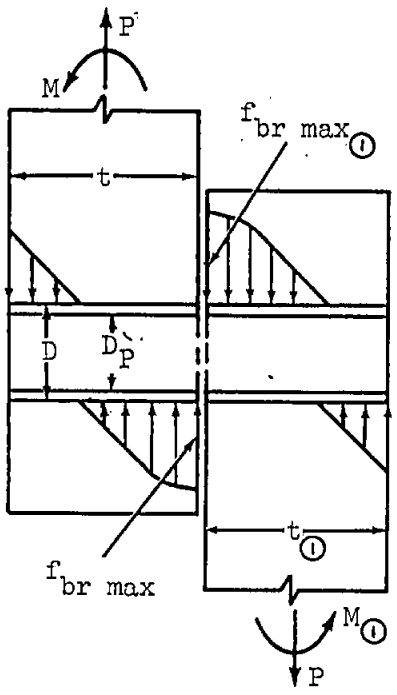

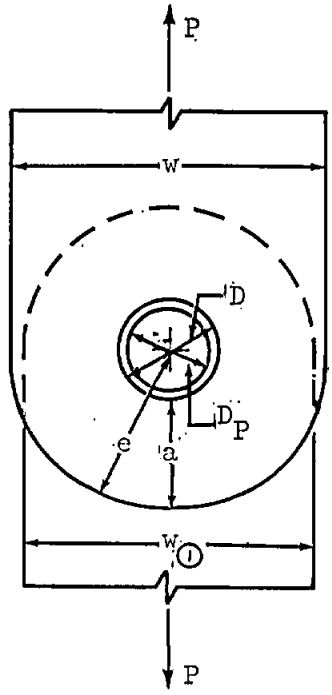

In the figure above a representative single-shear joint is shown, with centrally applied loads (P) in each lug, and bending moments (M and $M_{①}$) that keep the system in equilibrium. (Assuming that there is no gap between the lugs, $M + M_{①} = P(t + t_{①})/2$). The individual values of M and $M_{①}$ depend on the relative stiffness of the two lugs and are assumed to be known.

The strength analysis procedure outlined below applies to either lug. The joint strength is determined by the lowest of the margins of safety calculated for the different failure modes defined by eqs. (23) through (27), below

1 - Lug Bearing Strength

The bearing stress distribution between lug and bushing is assumed to be similar to the stress distribution that would be obtained in a rectangular cross-section of width (D) and depth (t), subjected to a load (P) and moment (M). At ultimate load the maximum lug bearing stress ($f_{br\ max\ L}$) is approximated by

$$f_{br\ max\ L} = \frac{P}{Dt} + \frac{6M}{k_{brL} Dt^2} \quad \text{.....(23)}$$

where k_{brL} is a plastic bearing coefficient for the lug material, and is assumed to be the same as the plastic bending coefficient (k_{bL}) for a rectangular section.

The allowable ultimate value of $f_{br\ max\ L}$ is either F_{brL} (eqs. 1a, 1b) or 1.304 F_{bryL} (eqs. 2a, 2b), whichever is lower.

2 - Lug Net-Section Strength

At ultimate load the nominal value of the outer fiber tensile stress in the lug net-section is approximated by

$$f_{t\ max} = \frac{P}{(w-D)t} + \frac{6M}{k_{bL} (w-D)t^2} \quad \text{.....(24)}$$

where k_{bL} is the plastic bending coefficient for the lug net-section.

The allowable ultimate value of $f_{t\ max}$ is F_{nL} (eq. 4) or 1.304 F_{nyL} (eq. 5), whichever is lower.

3 - Bushing Strength

The bearing stress distribution between bushing and pin is assumed to be similar to that between the lug and bushing. At ultimate bushing load the maximum bushing bearing stress is approximated by

$$f_{br\ max\ B} = \frac{P}{D_P t} + \frac{6M}{k_{brL} D_P t^2} \quad \text{.....(25)}$$

where k_{brL}, the plastic bearing coefficient, is assumed the same as the plastic bending coefficient (k_{bL}) for a rectangular section.

The allowable ultimate value of $f_{br\ max\ B}$ is $1.304\ F_{cyB}$, where F_{cyB} is the bushing material compressive yield strength.

4 - Pin Shear Strength

The maximum value of pin shear can occur either within the lug or at the common shear face of the two lugs, depending upon the value of M/Pt. At the lug ultimate load the maximum pin shear stress ($f_{s\ max}$) is approximated by

$$f_{s\ max} = \frac{1.273\ P}{D_P^2}, \quad (\text{if } \frac{M}{Pt} \leq 2/3) \quad \ldots\ldots\ldots\ldots\ldots\ldots\ldots\ldots (26a)$$

$$f_{s\ max} = \frac{1.273\ P}{D_P^2} \cdot \frac{\left(\sqrt{\left(\frac{2M}{Pt}\right)^2 + 1} - 1\right)}{\left(\frac{2M}{Pt} + 1 - \sqrt{\left(\frac{2M}{Pt}\right)^2 + 1}\right)}, \quad (\text{if } \frac{M}{Pt} > \frac{2}{3} \quad \ldots (26b)$$

Equation (26a) defines the case where the maximum pin shear is obtained at the common shear face of the lugs, and eq. (26b) defines the case where the maximum pin shear occurs away from the shear face.

The allowable ultimate value of $f_{b\ max}$ is F_{suP}, the ultimate shear stress of the pin material.

5 - Pin Bending Strength

The maximum pin bending moment can occur within the lug or at the common shear faces of the two lugs, depending on the value of M/Pt. At the lug ultimate load the maximum pin bending stress ($f_{b\ max}$) is approximated by

$$f_{b\ max} = \frac{10.19M}{k_{bP} D_P^3} \left(\frac{Pt}{2M} - 1\right), \quad (\text{if } \frac{M}{Pt} \leq 3/8) \quad \ldots\ldots\ldots\ldots\ldots\ldots (27a)$$

$$f_{b\ max} = \frac{10.19M}{k_{bP} D_P^3} \cdot \frac{\left(\sqrt{\left(\frac{2M}{Pt}\right)^2 + 1} - 1\right)}{\frac{2M}{Pt}}, \quad (\text{if } \frac{M}{Pt} > 3/8) \quad \ldots\ldots\ldots (27b)$$

where k_{bP} is the plastic bending coefficient for the pin.

Equation (27a) defines the case where the maximum pin bending moment is obtained at the common shear face of the lugs, and eq. (27b) defines the case where the maximum pin bending moment occurs away from the shear face, where the pin shear is zero.

The allowable ultimate value of $f_{b\ max}$ is F_{tuP}, the ultimate tensile stress of the pin material.

TRANSVERSELY LOADED LUG ANALYSIS

LUG AND BUSHING STRENGTH (UNIFORM BEARING)

Transversely loaded lugs and bushings are checked in the same general manner as axially loaded lugs. The transversely loaded lug, however, is a more redundant structure than an axially loaded lug, and it has a more complicated failure mode. The figures below illustrate the different lug dimensions that are critical in determining the lug strength.

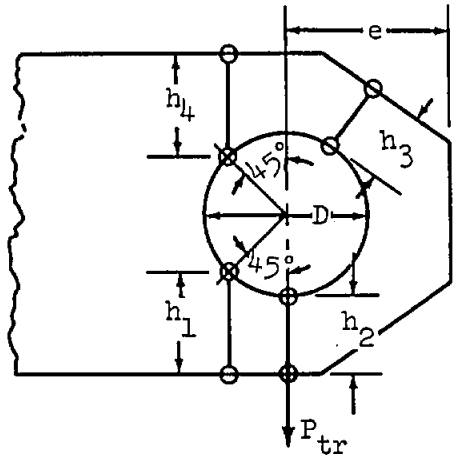

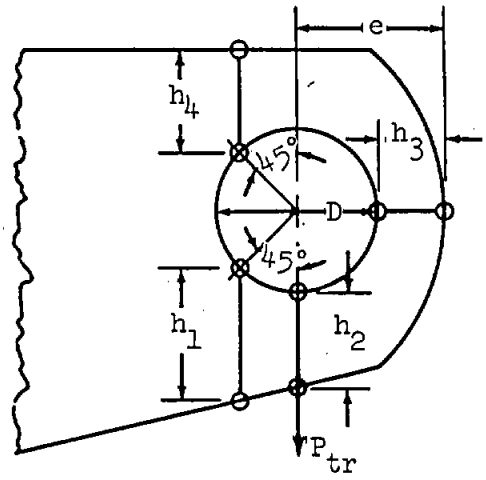

1 - Lug Strength

(a) The lug ultimate bearing stress (F_{brL}) is

$$F_{brL} = K_{tru} F_{tux} \quad \text{.....(28)}$$

where K_{tru}, the transverse ultimate load coefficient, is obtained from the graph on page B3.13-29, as a function of the "effective" edge distance (h_{av}).

$$h_{av} = \frac{6}{3/h_1 + 1/h_2 + 1/h_3 + 1/h_4}$$

The different edge distances (h_1, h_2, h_3, h_4) indicate different critical regions in the lug, h_1 being the most critical. If the lug is a concentric lug with parallel sides h_{av}/D can be obtained directly from the graph on page B3.13-30, for any value of e/D.

(b) The lug yield bearing stress (F_{bryL}) is

$$F_{bryL} = K_{try} F_{tyx} \quad \text{.....(29)}$$

where K_{try}, the transverse yield load coefficient, is obtained from the graph on page B3.13-29.

1 - Lug Strength (Cont'd)

(c) The allowable lug transverse ultimate load (P_{trL}) is

$$P_{trL} = F_{brL}\, Dt \text{ (if } F_{tux} \leq 1.304\, F_{tyx}) \quad \text{.....(30a)}$$

$$P_{trL} = 1.304\, F_{bryL}\, Dt \text{ (if } F_{tux} > 1.304\, F_{tyx}) \quad \text{.....(30b)}$$

where F_{brL} and F_{bryL} are obtained from eqs. (28) and (29).

(d) If the lug is not of constant thickness then A_{av}/A_{br} is substituted for h_{av}/D on the horizontal scale of the graph on page B3.13-29, where A_{br} is the lug bearing area, and $A_{av} = \dfrac{6}{3/A_1 + 1/A_2 + 1/A_3 + 1/A_4}$.

A_1, A_2, A_3 and A_4 are the areas of the sections defined by h_1, h_2, h_3 and h_4, respectively.

The values of K_{tru} and K_{try} corresponding to A_{av}/A_{br} are then obtained from the graph on page B3.13-29, and the allowable bearing stresses are obtained as before from eqs. (28) and (29).

2 - Bushing Strength

The allowable bearing stress on the bushing is the same as for the bushing in an axially loaded lug and is given by equation 8. The allowable bushing ultimate load (P_{trB}) is equal to P_B (eq. 9).

DOUBLE-SHEAR AND SINGLE-SHEAR JOINT STRENGTHS

The strength calculations are basically the same as for an axially loaded joint (eqs. 11 through 19 for a double shear joint, and eqs. 23 through 27 for a single shear joint) except that the maximum lug bearing stresses at ultimate and yield loads must not exceed those given by eqs. 28 and 29.

OBLIQUELY LOADED LUG ANALYSIS

The analysis procedures used to check the strength of axially loaded lugs and of transversely loaded lugs are combined to analyze obliquely loaded lugs such as the one shown on the right. These procedures apply only if α does not exceed 90°.

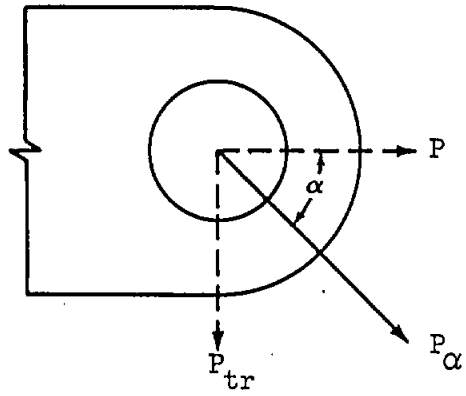

LUG AND BUSHING STRENGTH (UNIFORM BEARING)

1 - Lug Strength

The obliquely applied load (P_α) is resolved into an axial component ($P = P_\alpha \cos\alpha$) and a transverse component ($P_{tr} = P_\alpha \sin\alpha$). The allowable ultimate value of P_α is $P_{\alpha L}$ and its axial and transverse components satisfy the following equation

$$\left(\frac{P}{P_L}\right)^{1.6} + \left(\frac{P_{tr}}{P_{trL}}\right)^{1.6} = 1 \quad \text{.....(31)}$$

where P_L is the strength of an axially loaded lug (eq. 7) and P_{trL} is the strength of a transversely loaded lug (eqs. 30a, b). The allowable load curve defined by equation 31 is plotted on the graph on page B3.13-31.

For any given value of α the allowable load ($P_{\alpha L}$) for a lug can be determined from the graph on page B3.13-31 by drawing a line from the origin with a slope equal to ($P_L \tan\alpha / P_{trL}$). The intersection of this line with the allowable load curve (point ① on the graph) indicates the allowable values of P/P_L and P_{tr}/P_{trL}, from which the axial and transverse components, P and P_{tr}, of the allowable load can be readily obtained.

2 - Bushing Strength

The bushing strength calculations are identical to those for axial loading (eqs. 8 and 9).

DOUBLE-SHEAR AND SINGLE-SHEAR JOINT STRENGTHS

The strength calculations are basically the same as for an axially loaded joint (eqs. 11 through 19 for a double shear joint, and eqs. 23 through 27 for a single shear joint) except that the maximum lug bearing stress at ultimate load must not exceed $P_{\alpha L}/Dt$, where $P_{\alpha L}$ is defined by eq. 31.

AXIALLY LOADED LUG DESIGN

This section presents procedures for the optimized design of lugs, bushings and pin in a symmetrical, double-shear joint, such as shown on page B3.13-6 subjected to a static axial load (P). One design procedure applies to the case where the pin is critical in shear, the other to the case where the pin is critical in bending. A method is given to help determine which mode of pin failure is more likely, so that the appropriate design procedure will be used.

Portions of the design procedures may be useful in obtaining efficient designs for joints other than symmetrical, double-shear joints.

MANNER OF PIN FAILURE

An indication of whether the pin in an optimized joint design is more likely to fail in shear or in bending can be obtained from the value of R (eq. 32) below. If R is less than 1.0 the pin is likely to fail in shear and the design procedure for joints with pins critical in shear should be used to get an optimized design. If R is greater than 1.0 the pin is likely to be critical in bending and the design procedure for joints with pins critical in bending should be used.

$$R = \frac{\pi F_{suP}}{k_{bP} F_{tup}} \left(\frac{F_{suP}}{F_{br\ all①}} + \frac{F_{suP}}{F_{br\ all②}} \right) \quad \text{.....(32)}$$

where F_{suP} and F_{tuP} are the ultimate shear and ultimate tension stresses for the pin material, k_{bP} is the plastic bending coefficient for the pin, and $F_{br\ all①}$ and $F_{br\ all②}$ are allowable bearing stresses in the female and male lugs. The value of $F_{br\ all①}$ can be approximated by the lowest of the following three values:

$$K\ F_{tux①}\ \frac{D}{D_P}\ ; \qquad 1.304\ K\ F_{tyx①}\ \frac{D}{D_P}\ ; \qquad 1.304\ F_{cyB①}$$

where $F_{tux①}$ and $F_{tyx①}$ are the cross grain tensile ultimate and tensile yield stress for female lugs, $F_{cyB①}$ is the compressive yield stress of the bushings in the female lugs, and K is obtained from the graph on the next page. Assume $D = D_P$ if a better estimate cannot be made.

$F_{br\ all②}$ is approximated in a similar manner.

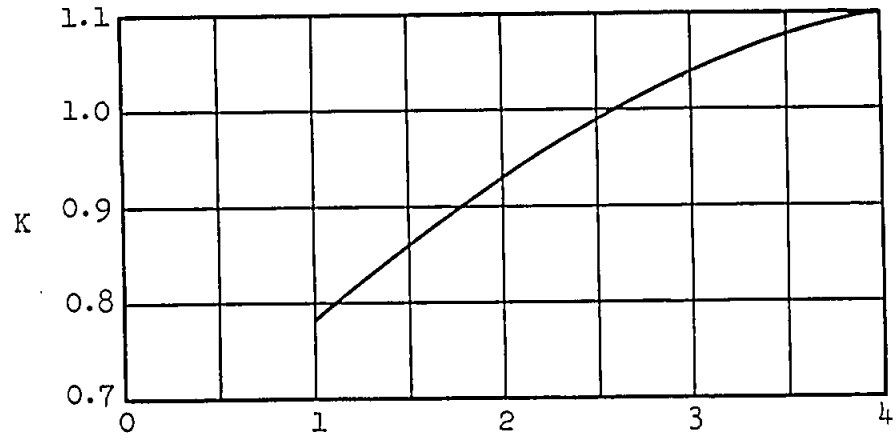

$$\frac{\rho_P}{\rho_L} = \frac{\text{Pin Material Density}}{\text{Lug Material Density}}$$

DESIGN PROCEDURE WHEN THE PIN FAILS IN SHEAR (R < 1.0)

1 - Pin and Bushing Diameters

The minimum allowable diameter for a pin in double shear is

$$D_P = 0.798\sqrt{\frac{P}{F_{suP}}} \quad \text{.....(33)}$$

The outside diameter of the bushing is $D = D_P + 2t_B$, where t_B is the bushing wall thickness.

2 - Edge Distance Ratio (e/D)

The value of e/D that will minimize the combined lug and pin weight is obtained from the upper graph on page B3.13-32 for the case where lug bearing failure and pin shear failure occur simultaneously. The lug is assumed not critical in net tension, and the bushing is assumed not critical in bearing.

The curves on page B3.13-32 apply specifically to concentric lugs ($a = e - D/2$, and $w = 2e$) but they can be used for reasonably similar lugs.

3 - Allowable Loads

The allowable loads for the different failure modes (lug bearing failure, lug net-tension failure, and bushing failure) are determined from eqs. 3, 6, and 9 in terms of the (unknown) lug thickness. The lowest of these loads is critical.

4 - Lug Thicknesses

The required male and female lug thicknesses are determined by equating the applied load in each lug to the critical failure load for the lug.

b) Pin Shear Strength (eq. 12)

$$P_{sP} = 1.571 \times (0.75)^2 \times 82000 = \underline{72400} \text{ lbs.}$$

c) Pin Bending Strength (eq. 15)

The pin ultimate bending load, assuming uniform bearing across the lugs, is

$$P_{bP} = \frac{0.1963 \times 1.56 \times (0.75)^3 \times 125000}{0.25 + 0.1875 + 0.10} = \underline{30100} \text{ lbs.}$$

Since P_{bP} is less than both P_{LB} and P_{sP}, the pin is a relatively weak pin which deflects sufficiently under load to shift the bearing loads towards the shear faces of the lugs. The new value of pin bending strength is, then

$$P_{bPmax} = 2C \times \left(\sqrt{\frac{30100}{C} \times (0.25 + 0.1875 + 0.10) + (0.10)^2} - 0.10 \right),$$

(from eq. 16) where $C = \frac{28600 \times 44000}{28600 \times 0.75 + 44000 \times 0.50} = 29000$ lbs/in.

$\therefore P_{bPmax} = 2 \times 29000 \times (0.754 - 0.10) = \underline{37900}$ lbs.

The "balanced design" effective bearing widths are

$$b_{①\,min} = \frac{37900 \times 0.50}{2 \times 28600} = \underline{0.331} \text{ in. (from eq. 18a)}$$

$$2b_{②\,min} = \frac{37900 \times 0.75}{44000} = \underline{0.646} \text{ in. (from eq. 18b)}$$

Therefore, the same value of P_{bPmax} would be obtained if the thickness of each female lug was reduced to 0.331 inches and the thickness of the male lug reduced to 0.646 inches.

d) Joint Strength (eq. 19b)

The final allowable load for the joint, exclusive of the lug tangs is

$$P_{all} = P_{bPmax} = \underline{37900} \text{ lbs.}$$

4. Lug Tang Analysis

$$P_T = \frac{2 \times 64000 \times 2.50 \times 0.50}{1 + \frac{3}{1.4} \times \left(1 - \frac{0.331}{0.500}\right)} = 92700 \text{ lbs. (from eq. 22a)}$$

or, $P_T = 77000 \times 3.00 \times 0.75 = 173300$ lbs. (from eq. 22b)

Therefore, the lug tangs are not critical and the allowable joint load remains at 37900 pounds.

AXIALLY LOADED LUG DESIGN (Example)

Using the same materials for the lug, bushing and pin as in the above example, and assuming the same allowable static load of 37900 pounds, a symmetrical double-shear joint will be designed to carry this load, using the procedure described in the section "AXIALLY LOADED LUG DESIGN ". A 0.10 inch gap is again assumed between the lugs. The bushing wall thickness is assumed to be 1/8 inch.

The lug will first be assumed to be concentric ($a = e - D/2$, and $w = 2e$) but the final minimum weight design will not necessarily be concentric.

1. Pin Failure Mode (eq. 32)

The pin is first checked to determine whether it will be critical in shear or bending, using eq. 32. Assuming $D = D_P$ as a first approximation, determine $F_{br\ all\ ①}$ and $F_{br\ all\ ②}$, using the graph on page B3.13-17 to determine K.

$KF_{tux\ ①} = 1.02 \times 64000 = 65300$ psi; $1.304\ KF_{tyx\ ①} = 1.304 \times 1.02 \times 40000 = 53100$ psi;

$1.304\ F_{cyB\ ①} = 1.304 \times 60000 = 78200$ psi; $\therefore F_{br\ all\ ①} = \underline{\underline{53100}}$ psi

$KF_{tux\ ②} = 1.02 \times 77000 = 78500$ psi; $1.304\ KF_{tyx\ ②} = 1.304 \times 1.02 \times 66000 = 87900$ psi

$1.304\ F_{cyB\ ②} = 1.304 \times 60000 = 78200$ psi; $\therefore F_{br\ all\ ②} = \underline{\underline{78200}}$ psi

$$\therefore R = \frac{\pi \times 82000}{1.56 \times 125000} \times \left(\frac{82000}{53100} + \frac{82000}{78200}\right) = \underline{\underline{3.4}} \text{ (eq. 32)}$$

Therefore the design procedure for pins critical in bending applies.

2. Pin and Bushing Diameters - First Approximation (eq. 35)

$$D_P = \sqrt[4]{\frac{1.273}{1.56} \times \left(\frac{37900}{125000}\right)^2 \times \left(\frac{125000}{52160} + \frac{125000}{77000}\right)} = \underline{\underline{0.741}} \text{ in.}$$

$D = 0.741 + 2 \times 0.125 = \underline{\underline{0.991}}$ in.

3. Edge Distance Ratio (e/D)

The optimum value of e/D for both male and female lugs is 1.24 (from the lower graph on page B3.13-32). Therefore a/D is 0.74 and w/D is 2.48 for a concentric lug ($\therefore w = 2.46$ in.).

4. Allowable Loads - Female Lugs and Bushings (First Approximation)

a) Lug Bearing Strength (eqs. 2a, 3b)

$P_{brL①} = 1.304 \times 1.46 \times 0.74 \times 40000 \times 0.991\ t_{①} = \underline{\underline{55900}}\ t_{①}$ lbs.

where K = 1.46 is obtained from page B3.13-27 for e/D = 1.24

b) Lug Net-Section Tension Strength (eqs. 5, 6b)

$K_{n①} = 0.74$ (obtained by interpolation from the graphs on page B3.13-28 for:

$\frac{D}{w_{①}} = 0.403$; $\frac{F_{ty}}{F_{tu}} = 0.625$; $\frac{F_{tu}}{E\epsilon_{u}} = 0.051$)

$P_{nL①} = 1.304 \times 0.74 \times 40000 \times (2.46 - 0.991)\ t_{①} = 56600\ t_{①}$ lbs.

c) Bushing Bearing Strength (eq. 9)

$P_{B①} = 1.304 \times 60000 \times 0.741\ t_{①} = \underline{\underline{58000}}\ t_{①}$ lbs.

5. Allowable Loads - Male Lug and Bushing (First Approximation)

a) Lug Bearing Strength (eqs. 1a, 3a)

$P_{brL②} = 1.46 \times 0.74 \times 77000 \times 0.991\ t_{②} = \underline{\underline{82500}}\ t_{②}$ lbs.

b) Lug Net-Section Tension Strength (eqs. 4,6a)

$K_{n②} = 0.88$ (obtained by interpolation from graphs on page B3.13-28 for:

$\frac{D}{w_{②}} = 0.403$; $\frac{F_{ty}}{F_{tu}} = 0.857$; $\frac{F_{tu}}{E\epsilon_{u}} = 0.125$)

$P_{nL②} = 0.88 \times 77000 \times (2.46 - 0.991)\ t_{②} = \underline{\underline{99500}}\ t_{②}$ lbs.

c) Bushing Bearing Strength (eq. 9)

$P_{B②} = 1.304 \times 60000 \times 0.741\ t_{②} = \underline{\underline{58000}}\ t_{②}$ lbs.

6. Lug Thicknesses (First Approximation)

$t_{①} = \frac{37900}{2 \times 55900} = \underline{\underline{0.339}}$ in.; $t_{②} = \frac{37900}{58000} = \underline{\underline{0.654}}$ in.

7. Pin Diameter - Second Approximation (eq. 34)

$$D_P = \sqrt[3]{\frac{2.55 \times 37900}{1.56 \times 125000}} (0.339 + 0.327 + 0.200) = \underline{0.755} \text{ in.}$$

$$D = 0.755 + 2 \times 0.125 = \underline{1.005} \text{ in.}$$

8. Final Pin and Bushing Diameter (eq. 36)

$$D_{Popt} = \frac{0.741}{2} + \frac{0.755}{2} = 0.748 \text{ in. (Use 0.750 inch pin)}$$

$$D = 0.750 + 2 \times 0.125 = \underline{1.000} \text{ in.}$$

9. Pin Shear (eq. 33)

$$D_P = 0.798 \sqrt{\frac{37900}{82000}} = \underline{0.541} \text{ in.}$$ Therefore, the pin is not critical in shear.

10. Final Lug Thicknesses

$$t_{①} = 0.339 \times \frac{0.991}{1.000} = \underline{0.336} \text{ in.}$$

$$t_{②} = 0.654 \times \frac{0.741}{0.750} = \underline{0.646} \text{ in.}$$

11. Reduced Edge Distance

The lug tension strength (eq. 3) exceeds the bushing strength (eq. 9) for the male lug. Therefore, a reduced e/D can be obtained for the male lug from graph on page B3.13-33.

$$\frac{D_P}{D} \frac{F_{br\ B}}{F_{tux}} = \frac{0.750}{1.000} \times \frac{1.304 \times 60000}{77000} = 0.762$$

$\therefore$ e/D = 0.97 (male lug)

12. Reduced Lug Width

The lug net-section tension strength (eq. 6) exceeds the bearing strength (eq. 3) for both the male and female lugs. Therefore the widths can be reduced as follows:

$$w_{①} = 1.00 + (2.48 - 1.00)\left(\frac{55900\ t_{①}}{56600\ t_{①}}\right) = \underline{2.46} \text{ in.}$$

$$w_{②} = 1.00 + (2.48 - 1.00)\left(\frac{82500\ t_{②}}{99500\ t_{②}}\right) = \underline{2.23} \text{ in.}$$

13. Final Dimensions

D_P = 0.750 in.; D = 1.000 in.

$t_{①}$ = 0.336 in.; $e_{①}$ = 1.24 in.; $w_{①}$ = 2.46 in.

$t_{②}$ = 0.646 in.; $e_{②}$ = 0.97 in.; $w_{②}$ = 2.23 in.

Since $w_{②}$ is larger than 2 $e_{②}$, the final male lug is not concentric.

ULTIMATE & YIELD STRENGTH OF AXIALLY LOADED LUGS

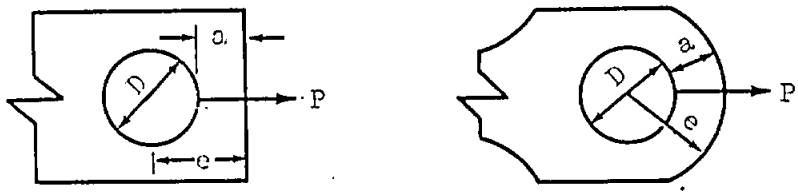

The lug ultimate load, for lug failures involving bearing, shear-out or hoop tension is:

$$P_{brL} = K F_{tux} at, \quad (\text{if } e/D < 1.5),$$

$$P_{brL} = K F_{tux} Dt, \quad (\text{if } e/D \geq 1.5),$$

where t is the lug thickness, and F_{tux} is the cross-grain ultimate tensile stress of the lug material. (P_{brL}/Dt should not exceed F_{bru} or 1.304 F_{bry}, where F_{bru} and F_{bry} are the allowable bearing stresses for the lug material for e/D = 2.0).

The lug yield load is obtained by substituting F_{tyx} for F_{tux} in the above equations.

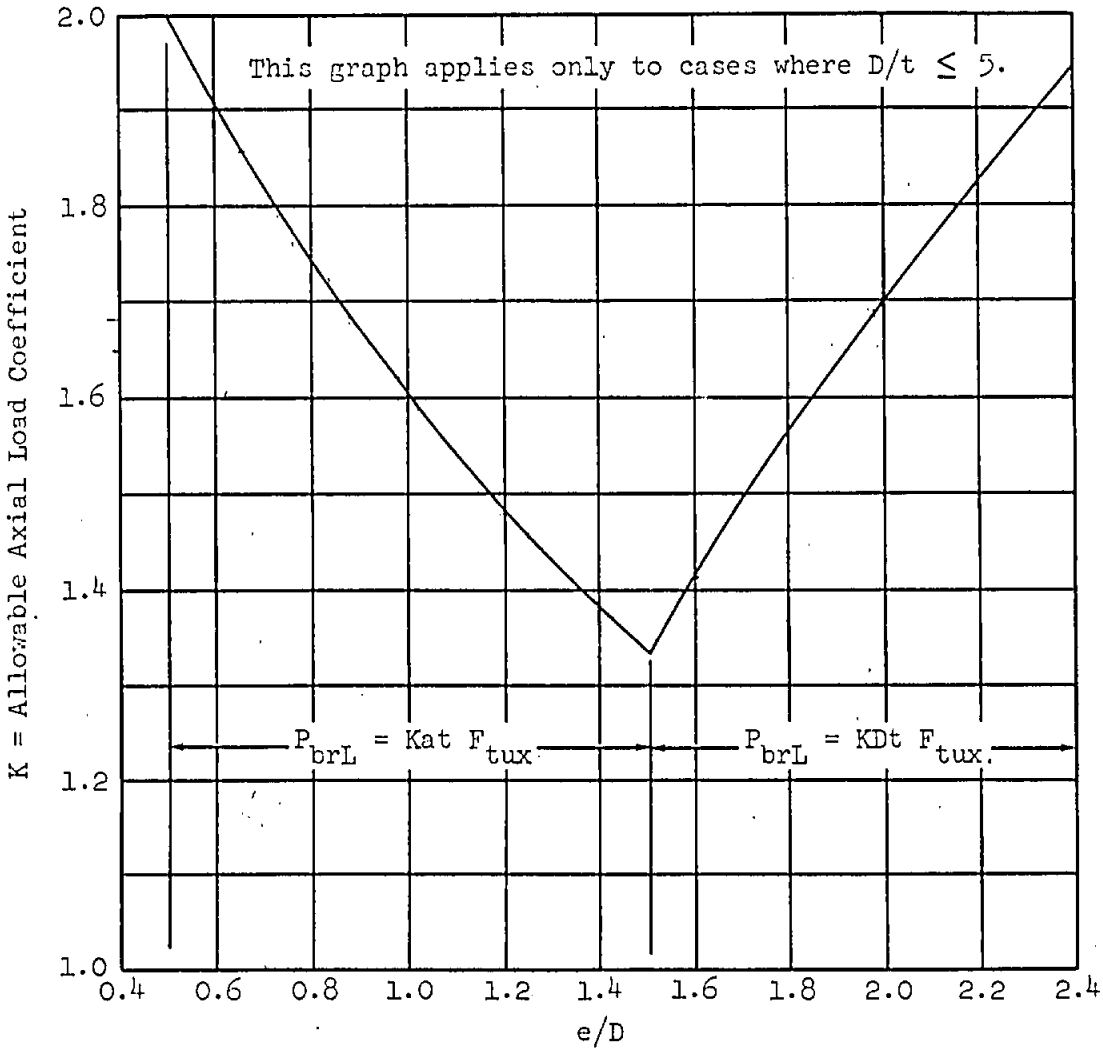

ULTIMATE AND YIELD STRENGTH IN NET TENSION OF AXIALLY LOADED CONCENTRIC LUGS

Allowable net-tension ultimate stress on section ① - ① is $F_{nL} = K_L F_{tu}$

Allowable net-tension yield stress on section ① - ① is $F_{nyL} = K_L F_{ty}$

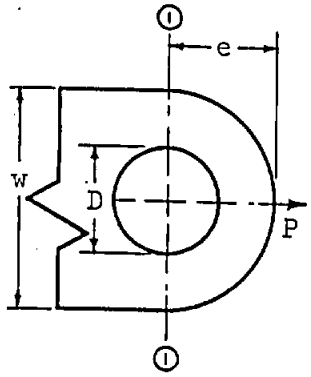

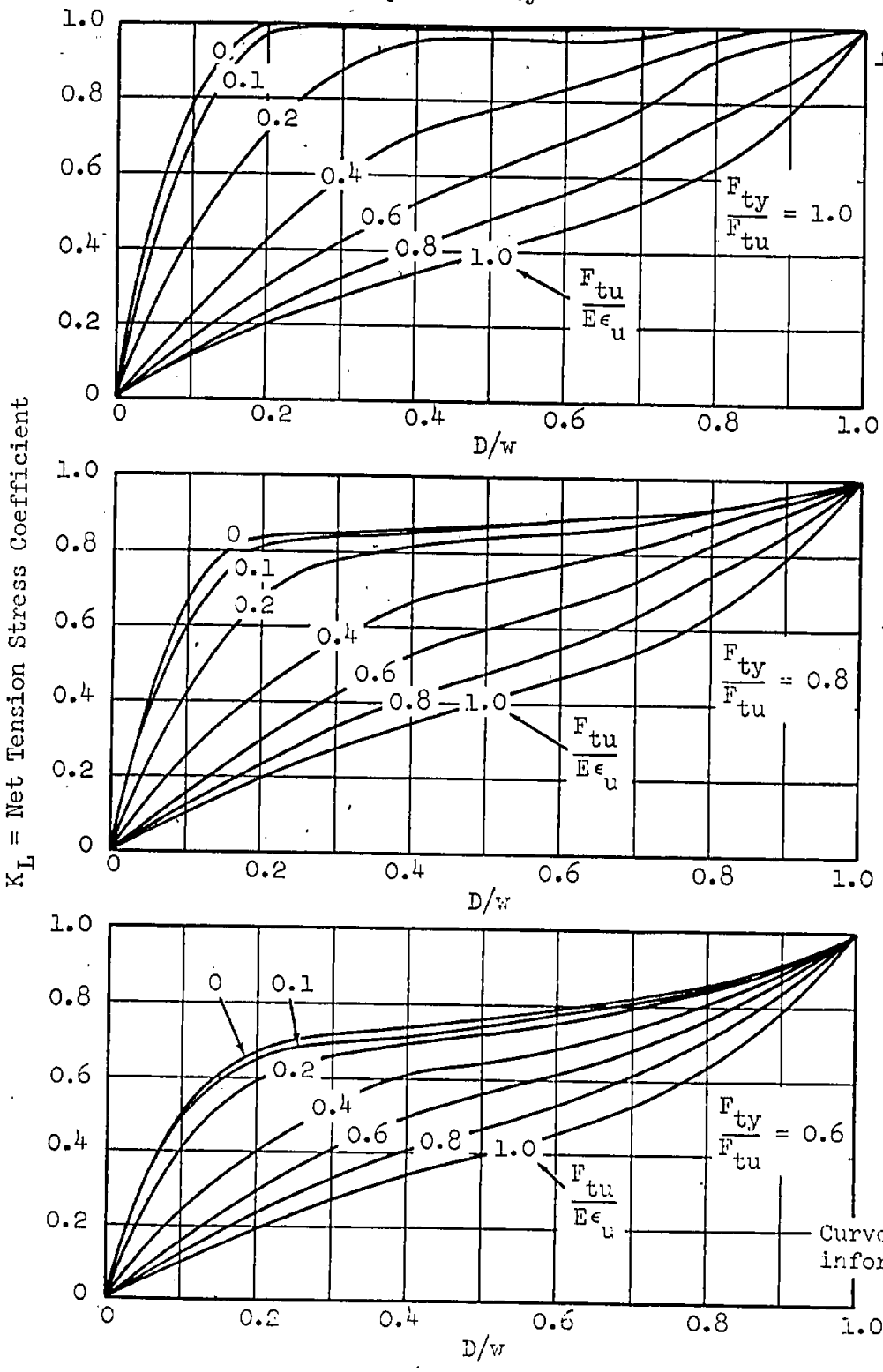

Curves are based on information in Ref. 4

ULTIMATE AND YIELD STRENGTH OF TRANSVERSELY LOADED LUGS

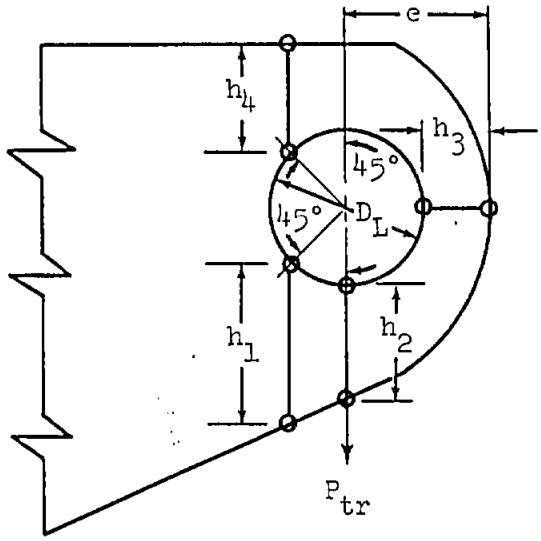

Lug ultimate load, $P_{tru} = K_{tru} F_{tux} Dt$

Lug yield load, $P_{try} = K_{try} F_{tyx} Dt$

where t = lug thickness

F_{tux}, F_{tyx} = cross-grain ultimate and yield strengths of the lug material

$$h_{av} = \frac{6}{3/h_1 + 1/h_2 + 1/h_3 + 1/h_4}$$

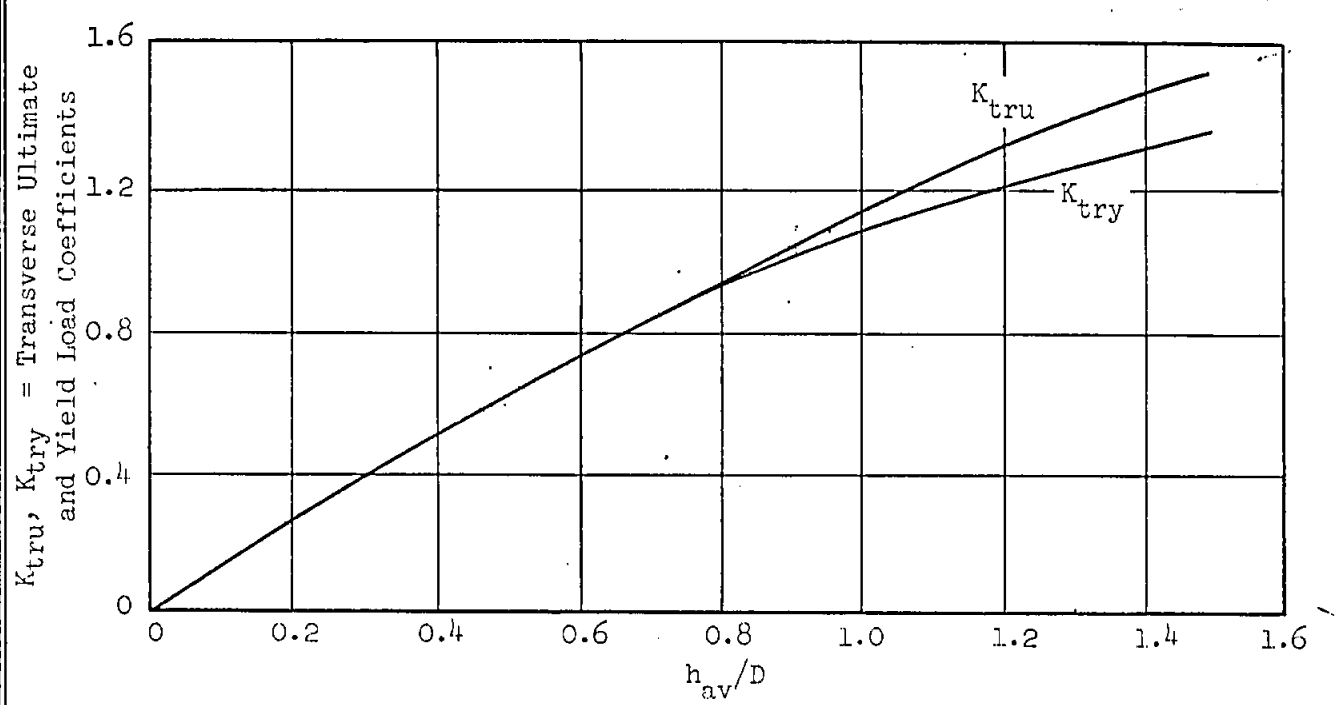

CURVE RELATING c/D & h_{av}/D FOR CONCENTRIC, CONSTANT THICKNESS LUGS WITH PARALLEL SIDES

$$h_{av} = \frac{6}{3/h_1 + 1/h_2 + 1/h_3 + 1/h_4}$$

In concentric lugs $h_1=h_4$, and $h_2=h_3$

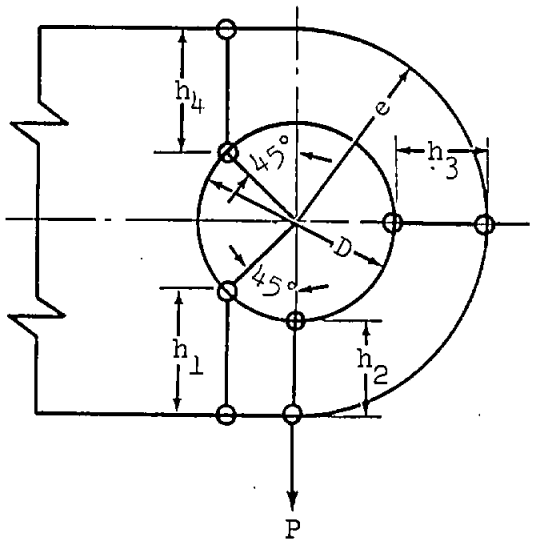

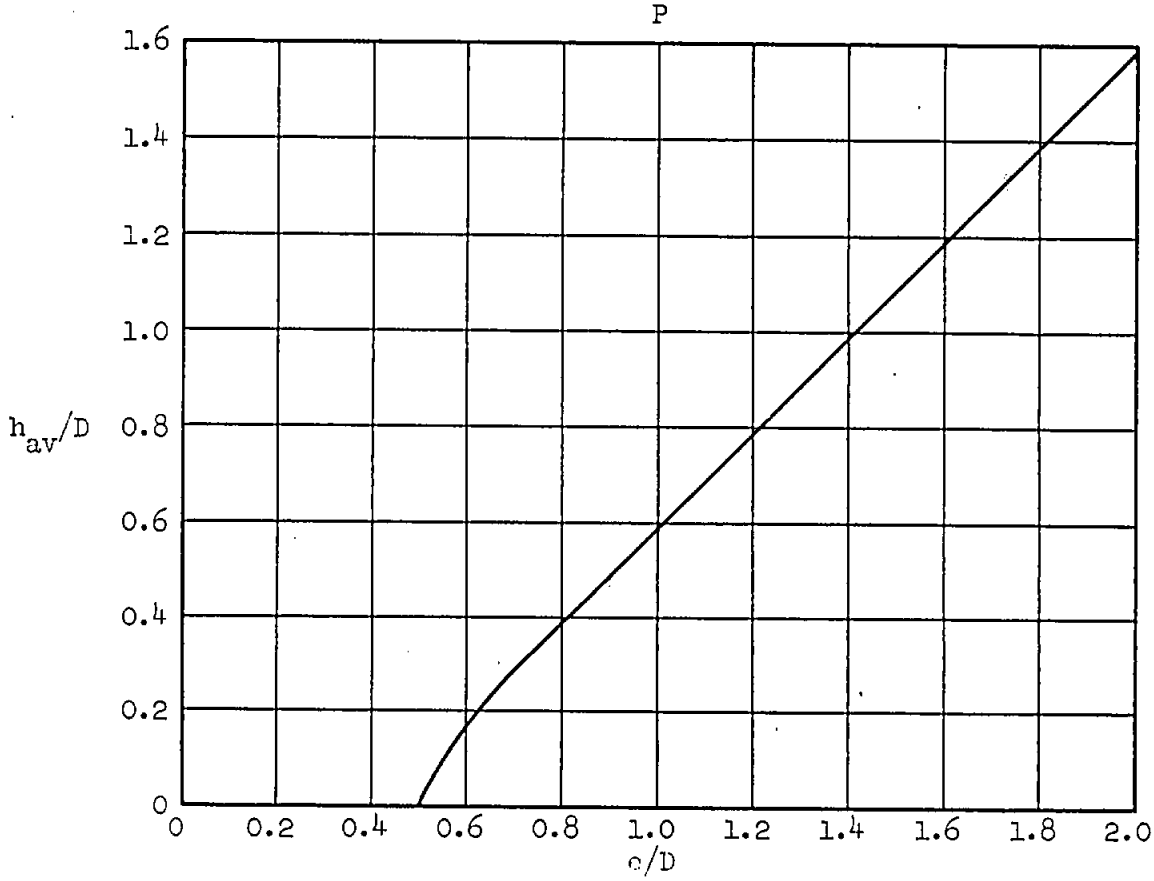

INTERACTION CURVE FOR OBLIQUELY LOADED LUGS

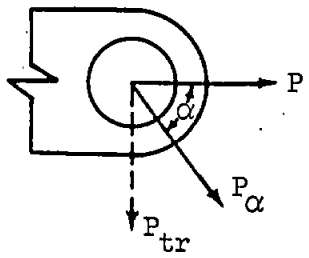

P and P_{tr} are the axial and transverse components of the applied load, P_α. P_L and P_{trL} are the respective allowables for axially loaded lugs and transversely loaded lugs.

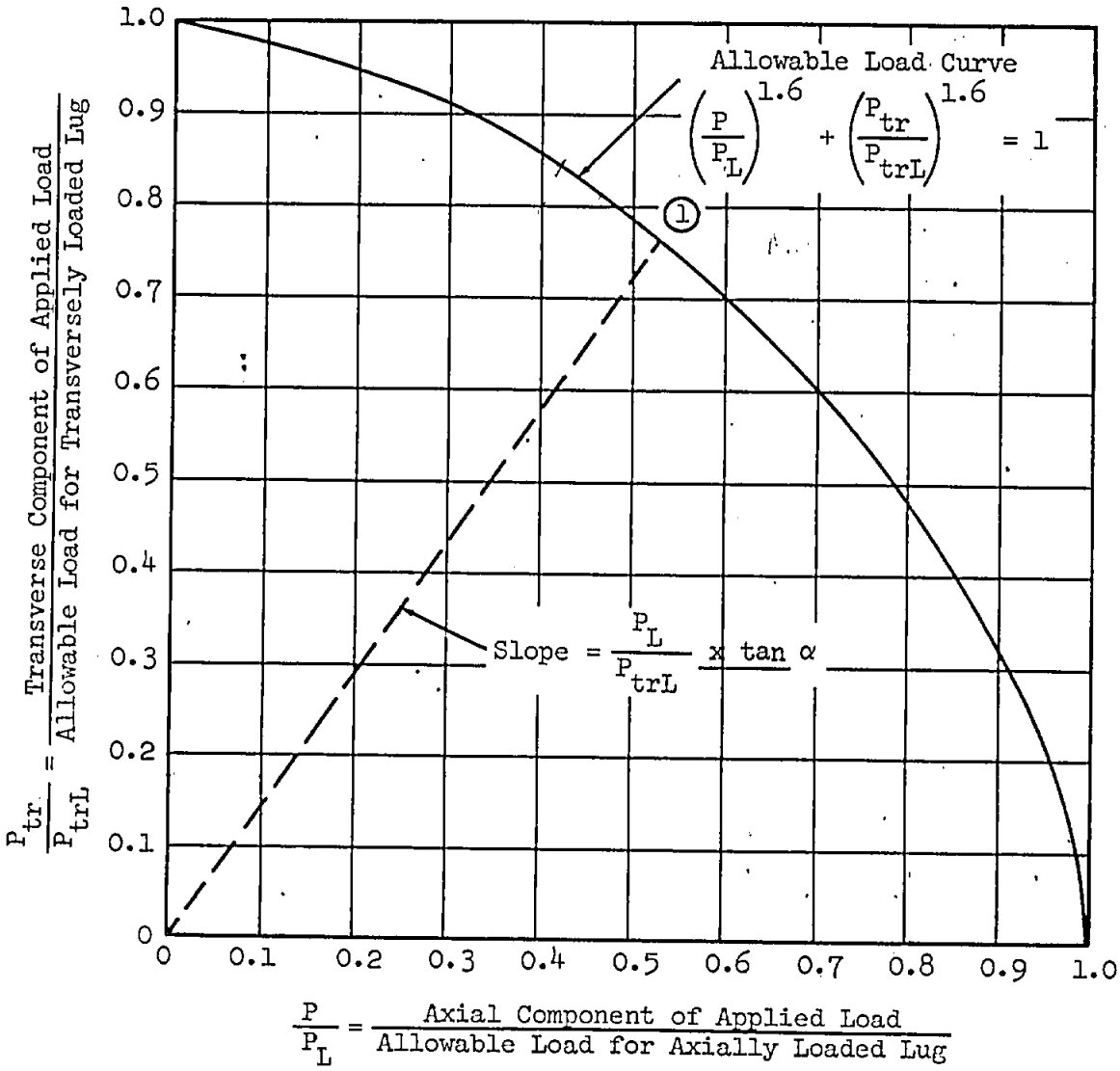

Grumman

OPTIMUM VALUES OF e/D FOR AXIALLY LOADED CONCENTRIC LUGS
(Lugs Not Critical in Net Tension and Bushings Not Critical in Yield)

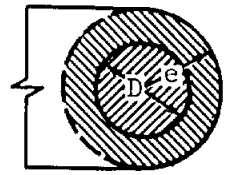

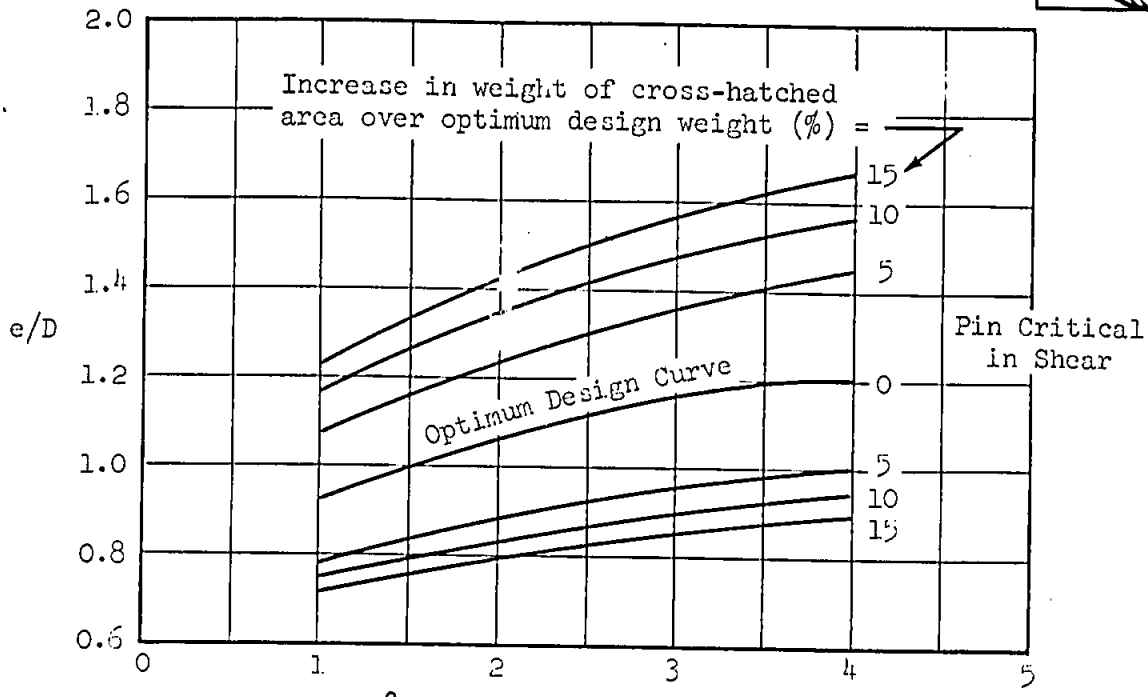

$$\frac{\rho_P}{\rho_L} = \frac{\text{Pin Material Density}}{\text{Lug Material Density}}$$

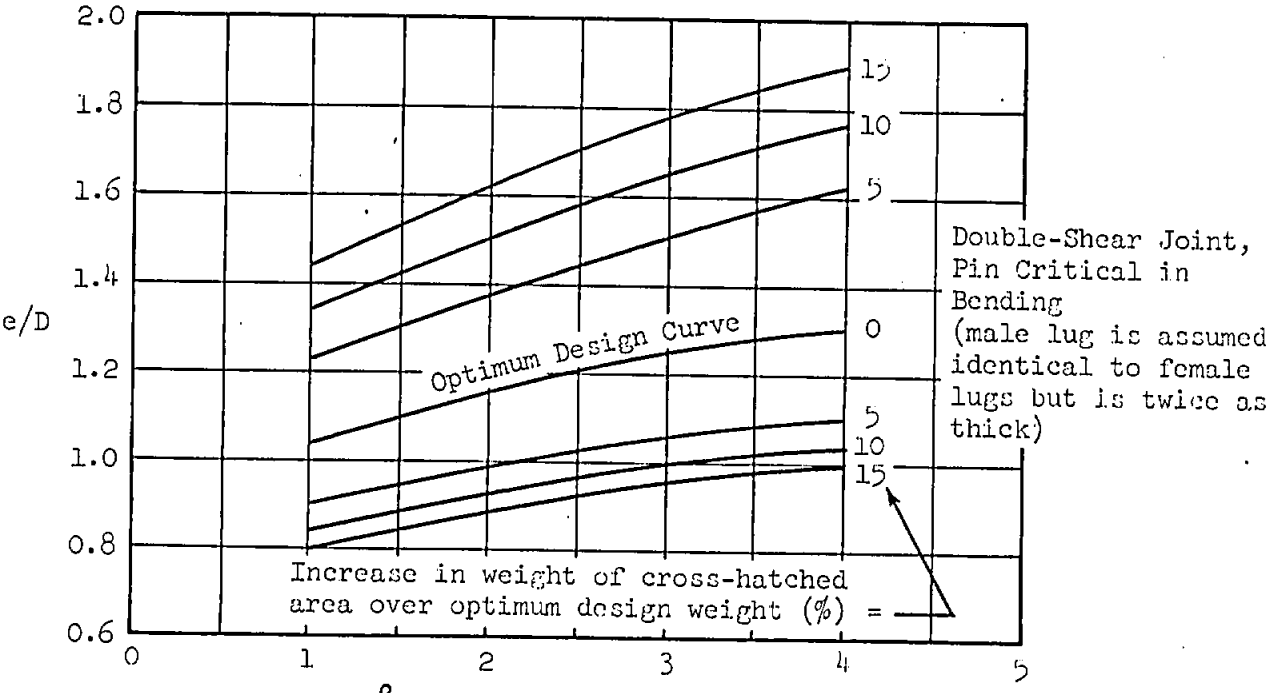

$$\frac{\rho_P}{\rho_L} = \frac{\text{Pin Material Density}}{\text{Lug Material Density}}$$

OPTIMUM VALUES OF e/D FOR AXIALLY LOADED CONCENTRIC LUGS WHERE BUSHING YIELD IS CRITICAL

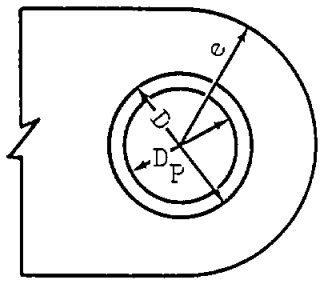

F_{brB} = Allowable bushing ultimate bearing stress

F_{tux} = Lug material cross-grain ultimate tensile stress

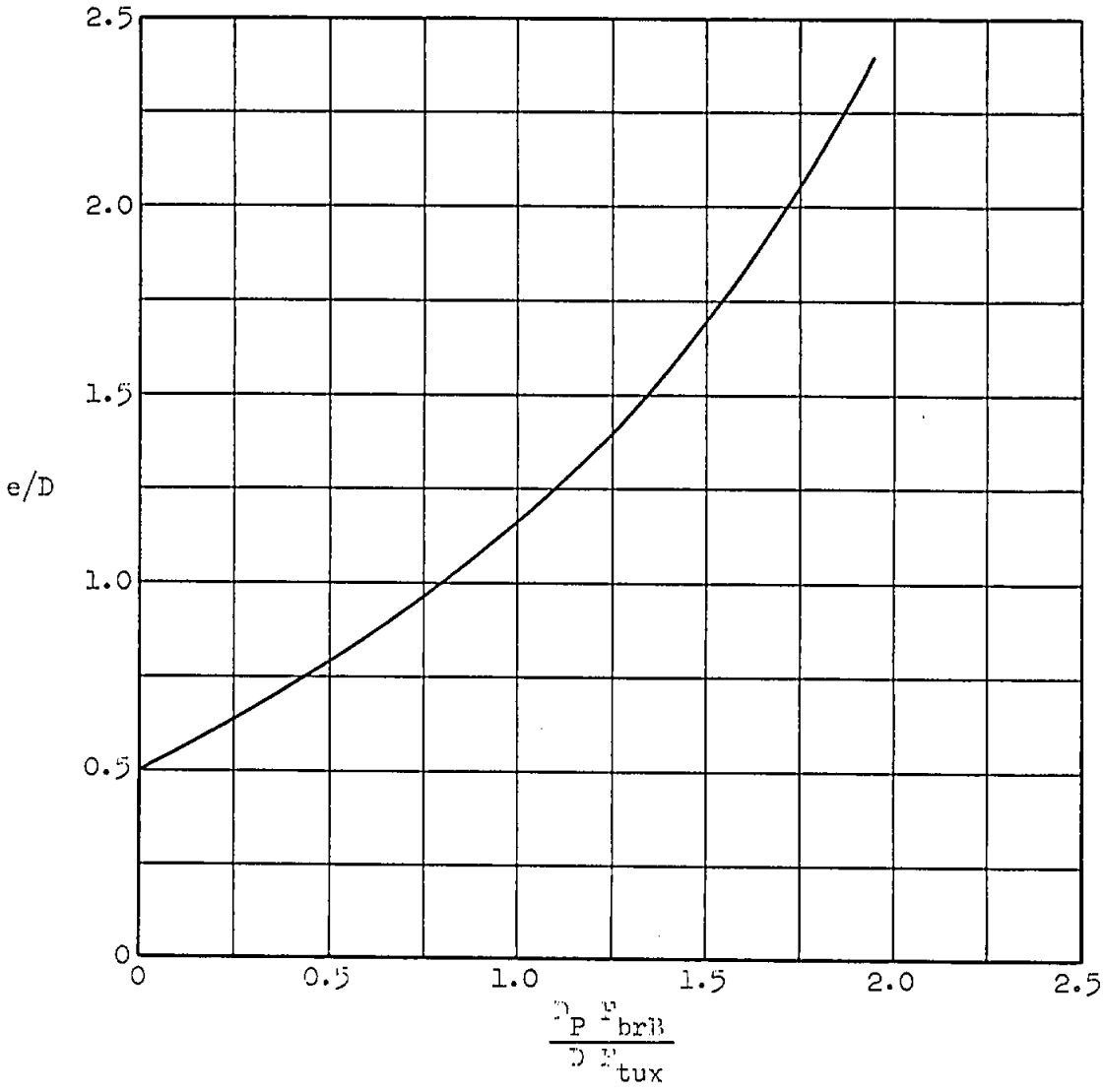

BE SURE TO CHECK FATIGUE

LUGS WITH LESS THAN 5 ELONGATION

The procedures given on pages B3.13-3 through B3.13-33 for determining the static strength of lugs apply to lugs made from materials which have ultimate elongations, ϵ_u, of at least 5% in all directions in the plane of the lug. This section describes procedures for calculating reductions in strength for lugs made from materials which do not meet this elongation requirement. In addition to using these procedures, special consideration must be given to possible further loss in strength resulting from material defects when the short transverse gain direction of the lug material is in the plane of the lug.

The analysis procedures for lugs made from materials without defects but with less than 5% elongation are as follows:

BEARING STRENGTH OF AXIALLY LOADED LUGS (eqs. 1a through 3b on page B3.13-4).

1). Determine F_{ty}/F_{tu} and ϵ_y/ϵ_u, using values of F_{ty}, F_{tu}, ϵ_y and ϵ_u that correspond to the minimum value of ϵ_u in the plane of the lug.

2). Determine the value of B, the ductility factor, from the graph below

3). Determine a second value of B (denoted by $B_{.05}$), for the same values of F_{ty}, F_{tu} and ϵ_y as before, but with $\epsilon_u = 0.05$.

4). Multiply the bearing stress and bearing load allowables given by eqs. 1a through 3b by $B/B_{.05}$ to obtain the corrected allowables.

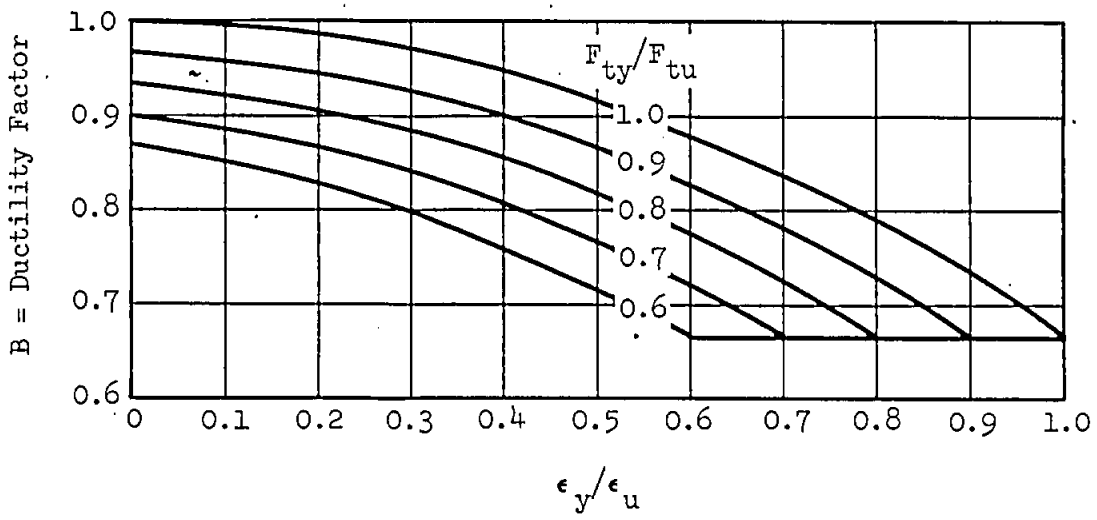

NET-SECTION STRENGTH OF AXIALLY LOADED LUGS (eqs. 4 through 6b on page B3.13-5)

The procedure for determining net-section allowables is the same for all values of ϵ_u. The graphs on page B3.13-28 are used to obtain a value of K_n which is substituted in eqs. 4 and 5. If the grain direction of the material is known, the values of F_{ty}, F_{tu} and ϵ_u used in entering the graphs should correspond to the grain direction parallel to the load. Otherwise, use values corresponding to the minimum value of ϵ_u in the plane of the lug.

STRENGTH OF LUG TANGS IN AXIALLY-LOADED JOINTS (eqs. 21 and 22a on page B3.13-10)

The plastic bending coefficient for a rectangular cross-section can be approximated by $k_{bL} = 1.5B$, where B is obtained from the graph above, in which $_y$ and $_u$ are the yield and ultimate strains of the lug tang material in the direction of loading. The maximum allowable value of k_{bL} for a rectangle is 1.4.

LUG AND BUSHING STRENGTHS IN AXIALLY LOADED SINGLE-SHEAR JOINTS (eqs. 23, 24, 25 on page B3.13-11)

The values of k_{brL} and k_{bL} for rectangular cross-sections are approximated by 1.5B, where B is determined from the graph as described above. The maximum allowable values of k_{brL} and k_{bL} are 1.4.

BEARING STRENGTH OF TRANSVERSELY LOADED LUGS (eqs. 28 thru 30b on pages B3.13-13, -14)

The same procedure is used as for the bearing strength of axially loaded lugs.

1). Determine B and $B_{.05}$ as described for axially loaded lugs, where B corresponds to the minimum value of ϵ_u in the plane of the lug.

2). Multiply the bearing stress and bearing load allowables given by eqs. 28 through 30b by $B/B_{.05}$ to obtain the corrected allowables.

BENDING MOMENTS AND DEFLECTIONS IN BEAMS OF UNIFORM SECTION

TYPE & LOADING		δ_{max}	M_{max}
Simple Beam, Single Concentrated Load at Midspan		$\frac{WL^3}{48EI}$	$\frac{WL}{4}$
Simple Beam, Uniformly Distributed Load	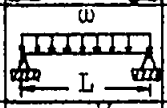	$\frac{5\omega L^4}{384EI}$	$\frac{\omega L^2}{8}$
Simple Beam, Single Concentrated Load at Distance a From Support a > b	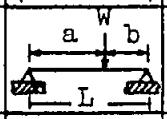	$\frac{Wb(L^2-b^2)^{3/2}}{15.6\ EIL}$	$\frac{Wab}{L}$
Simple Beam, Two Concentrated Loads W, at Equal Distances, a, from Supports	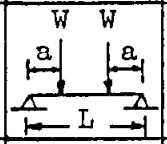	$\frac{Wa(3L^2-4a^2)}{24\ EI}$	Wa
Simple Beam, Subjected to Uniform Bending	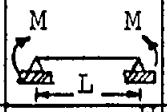	$\frac{ML^2}{8EI}$	M
Cantilever Beam, Single Concentrated Load at Free End	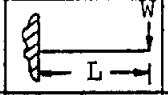	$\frac{WL^3}{3EI}$	WL
Cantilever Beam, Uniformly Distributed Load	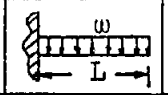	$\frac{\omega L^4}{8EI}$	$\frac{\omega L^2}{2}$
Cantilever Beam, Uniform Bending Moment, M	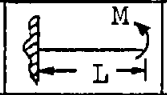	$\frac{ML^2}{2EI}$	M
Beam Fixed at One End, Simply Supported at Other, Uniformly Distributed Load	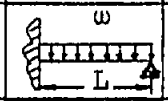	$\frac{\omega L^4}{185EI}$	$\frac{\omega L^2}{8}$
Beam Fixed at One End, Simply Supported at Other, Concentrated Load at Midspan	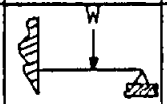	$\frac{.009317\ WL^3}{EI}$	$\frac{3WL}{16}$
Beam, Fixed at Ends, Single Concentrated Load at Center	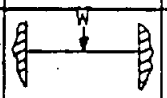	$\frac{WL^3}{192EI}$	$\frac{WL}{8}$
Beam Fixed at the Ends, Uniformly Distributed Load		$\frac{\omega L^4}{384EI}$	$\frac{\omega L^2}{12}$
Beam Fixed at the Ends. Two Concentrated Loads, W, at Equal Distances, a, from Supports	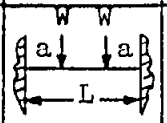	$\frac{Wa^2(3L-4a)}{24EI}$	$\frac{Wa(L-a)}{L}$

MAXIMUM BENDING STRESSES IN CURVED BEAMS

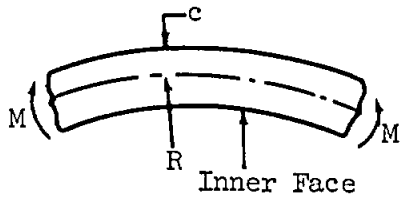

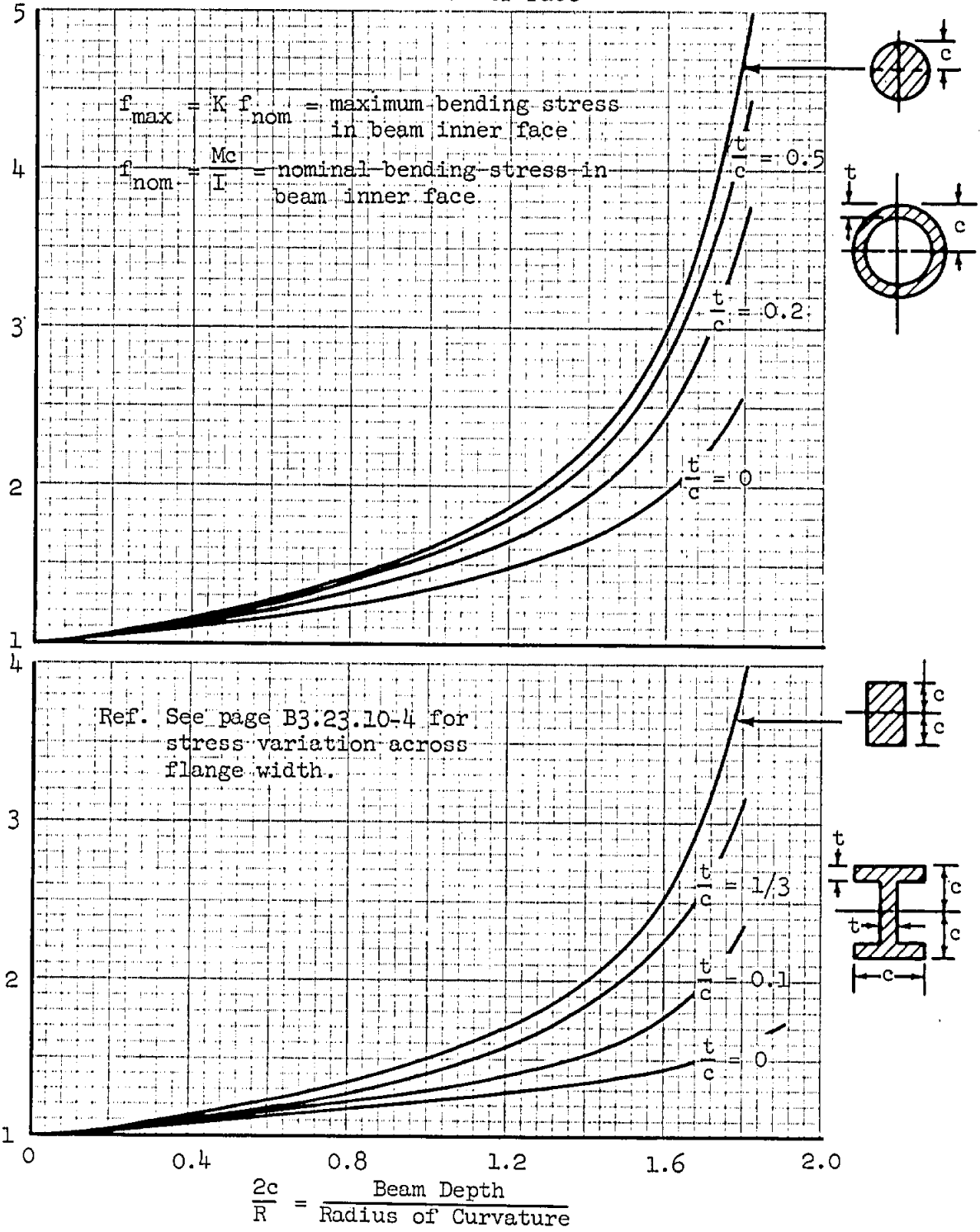

Ref: R. E. Peterson, "Stress Concentration Design Factors," Fig. 109 & GAEC Data

EFFECTIVE WIDTH OF CURVED BEAM IN BENDING

NOTE: This effective width effect is due to curling of the flanges and has nothing to do with compressive buckling

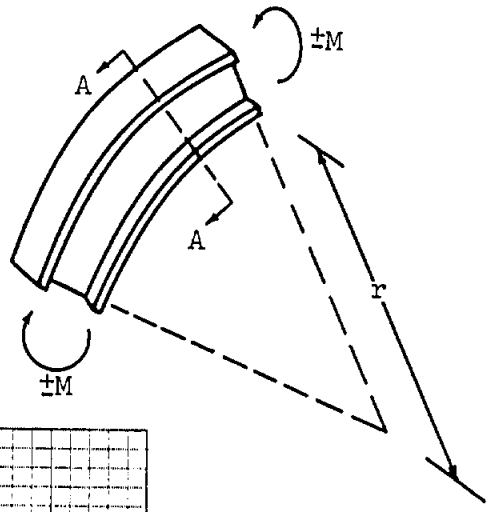

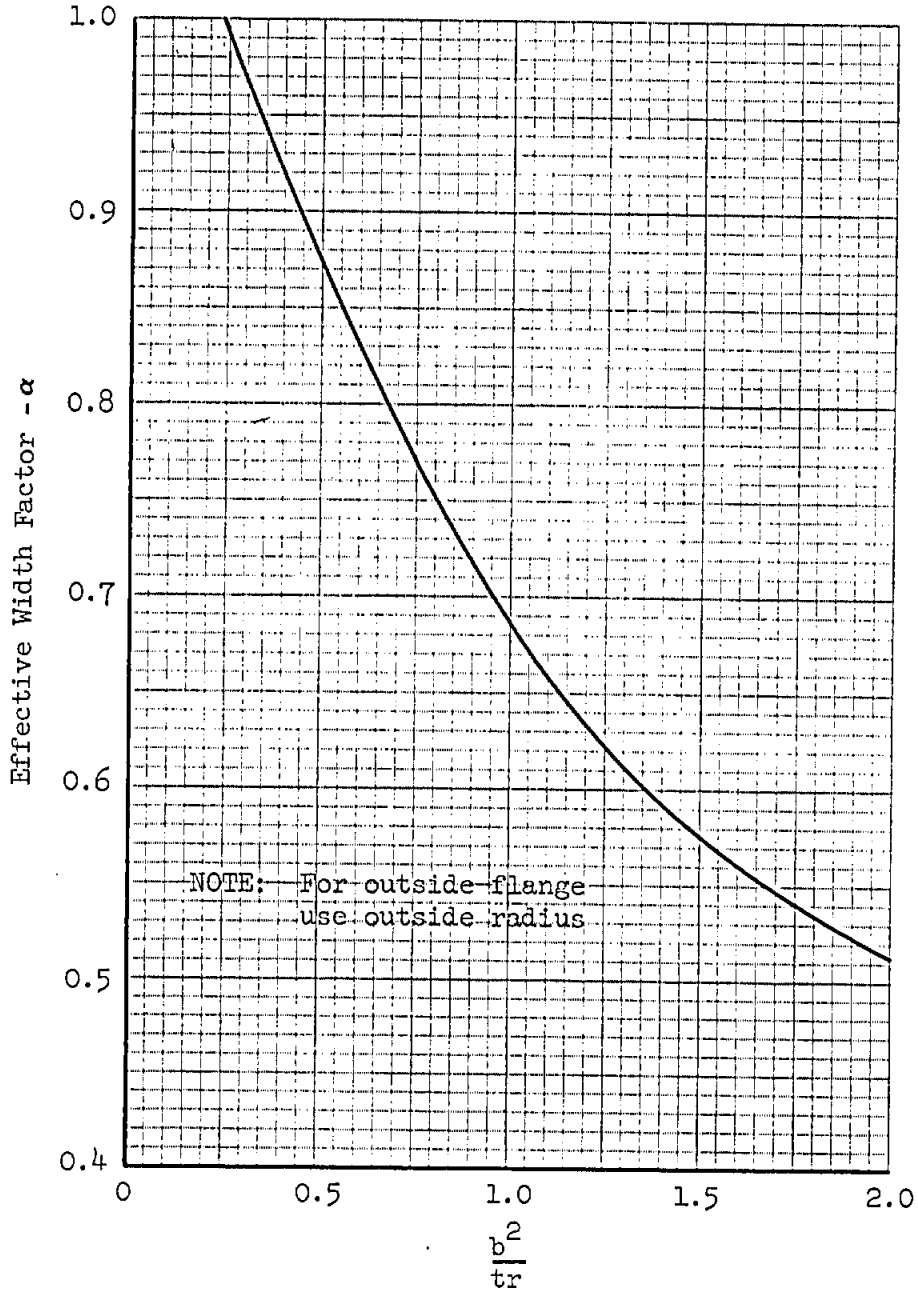

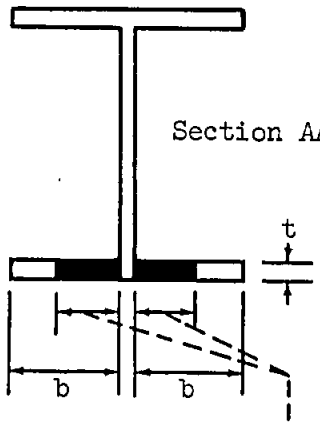

Effective Width - αb

Ref: Timoshenko, "Strength of Materials", Vol. 2. page 112

MAXIMUM TRANSVERSE STRESS IN FLANGE
OF CURVED BEAM IN BENDING

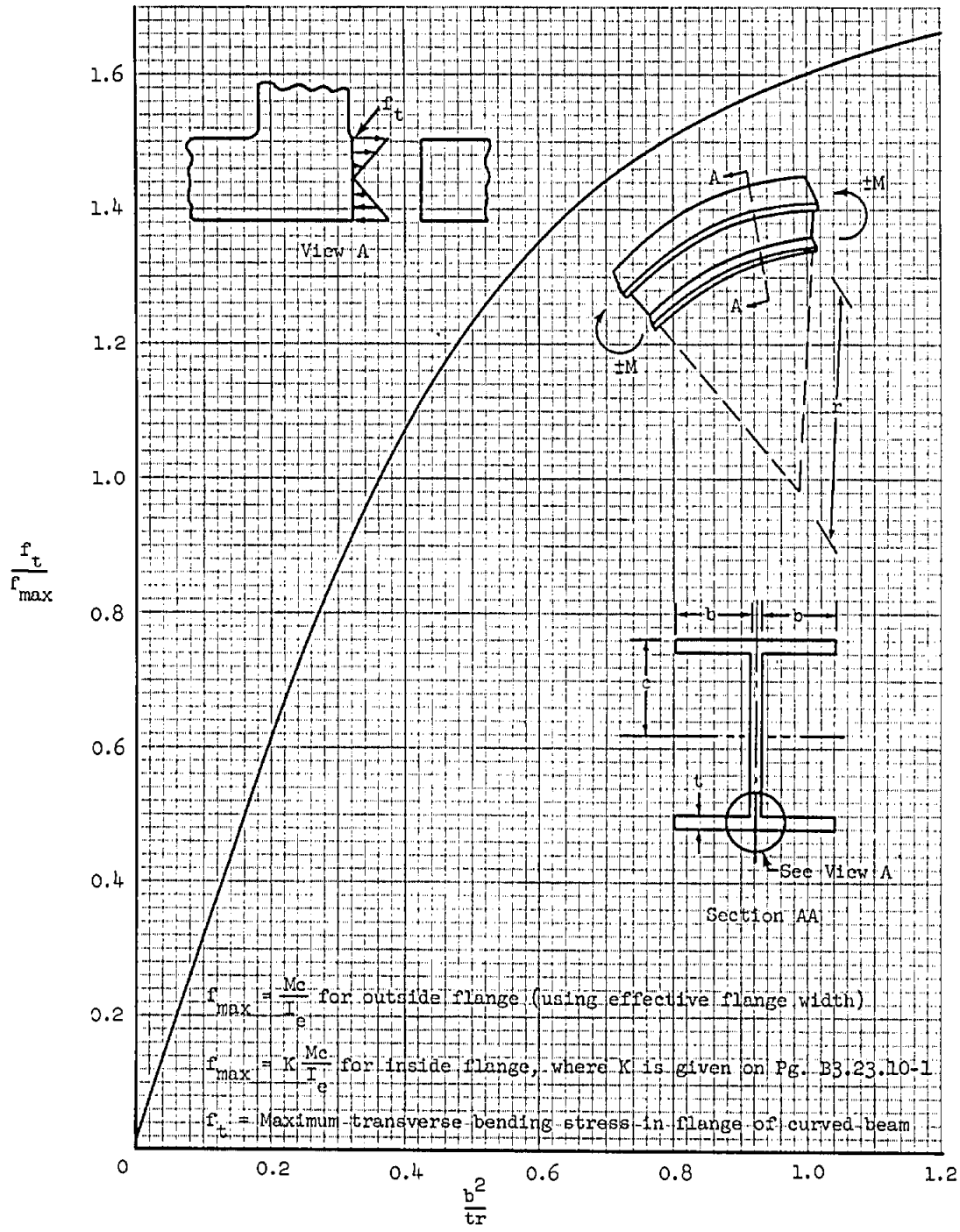

Ref: Timoshenko, "Strength of Materials", Vol.2, page 112

LONGITUDINAL STRESS VARIATION ACROSS
FLANGE OF CURVED BEAM IN BENDING

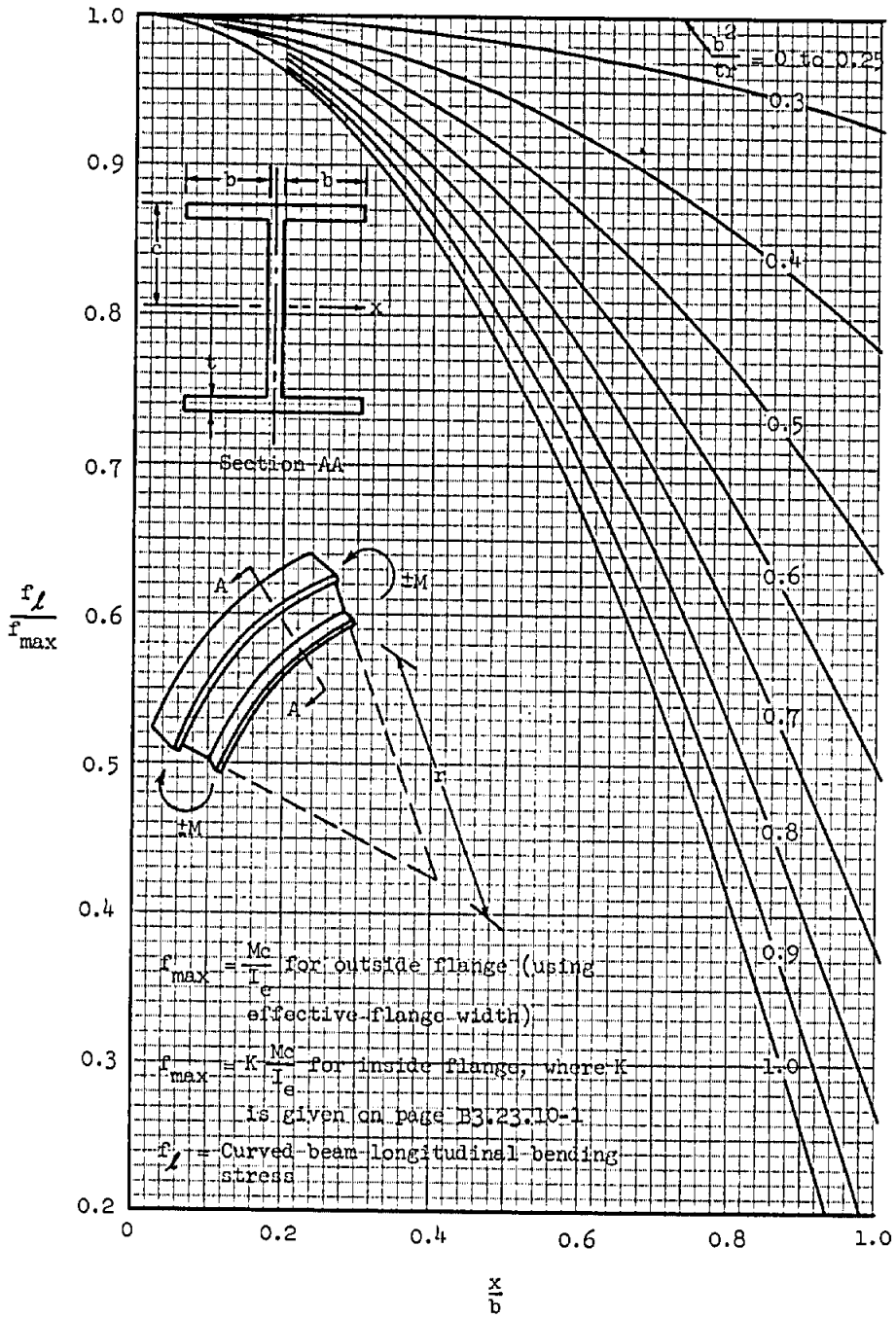

Ref: Timoshenko, "Strength of Materials", Vol. 2, page 112

EFFECTIVE WIDTH OF CURVED BEAMS IN BENDING

UNLIPPED FLANGES

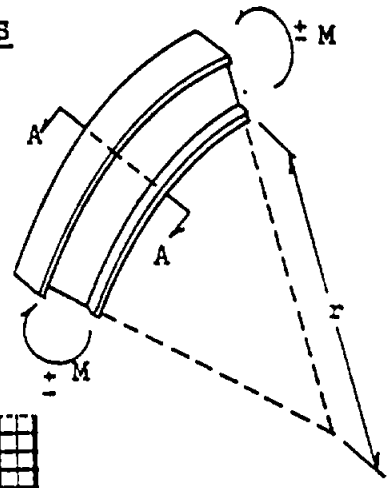

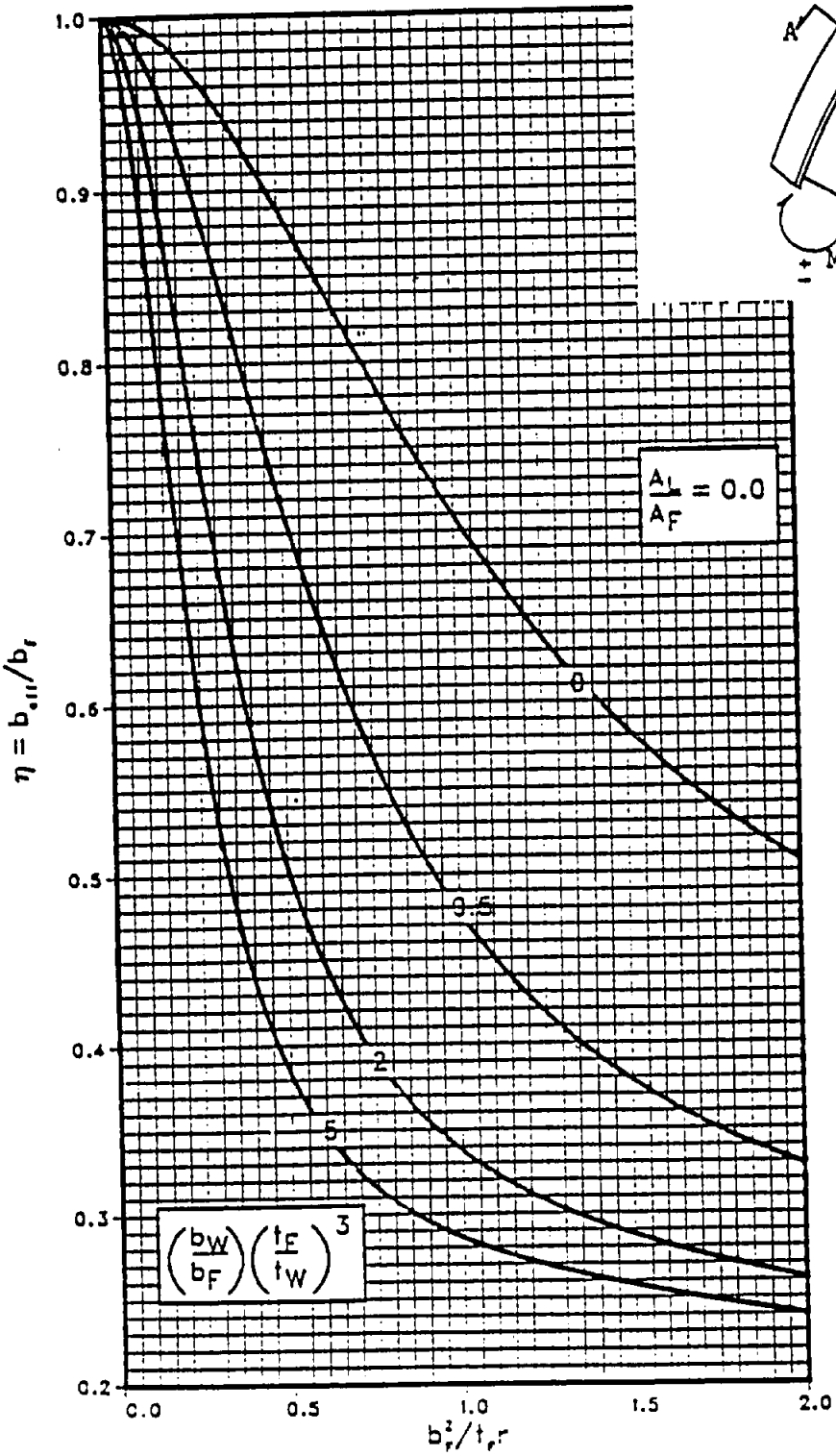

Note: This effective width is due to curling of the flanges and has nothing to do with compressive buckling

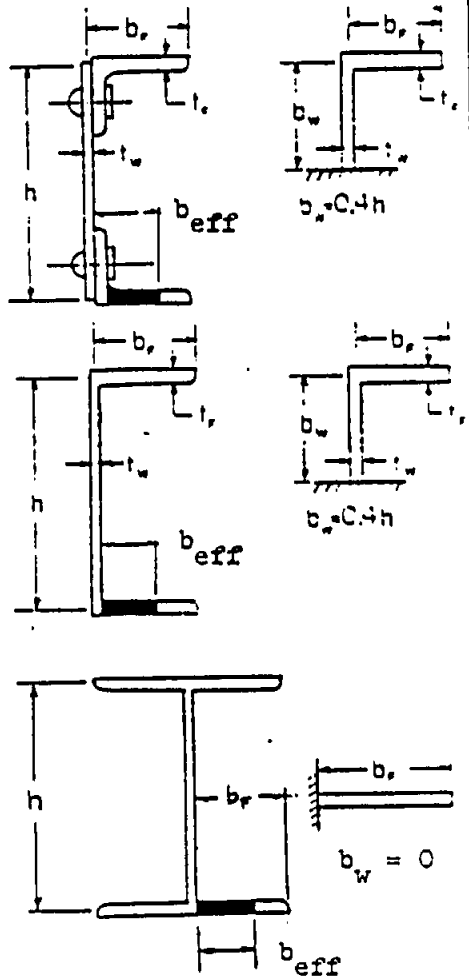

Ref. Journal of the Aero/Space Sciences-Sept.1958, Pg.570

EFFECTIVE WIDTH OF CURVED BEAMS IN BENDING

LIPPED FLANGES

Note: This effective width effect is due to curling of the flanges and has nothing to do with compressive buckling

Note: For outside flanges use outside radius

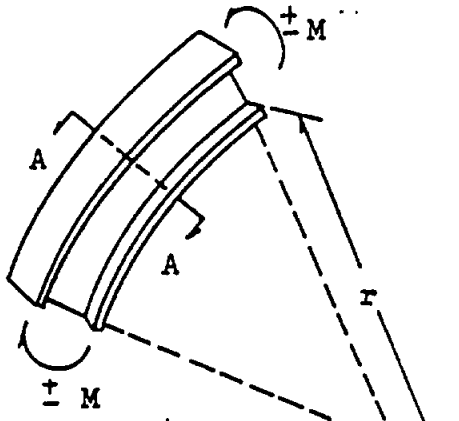

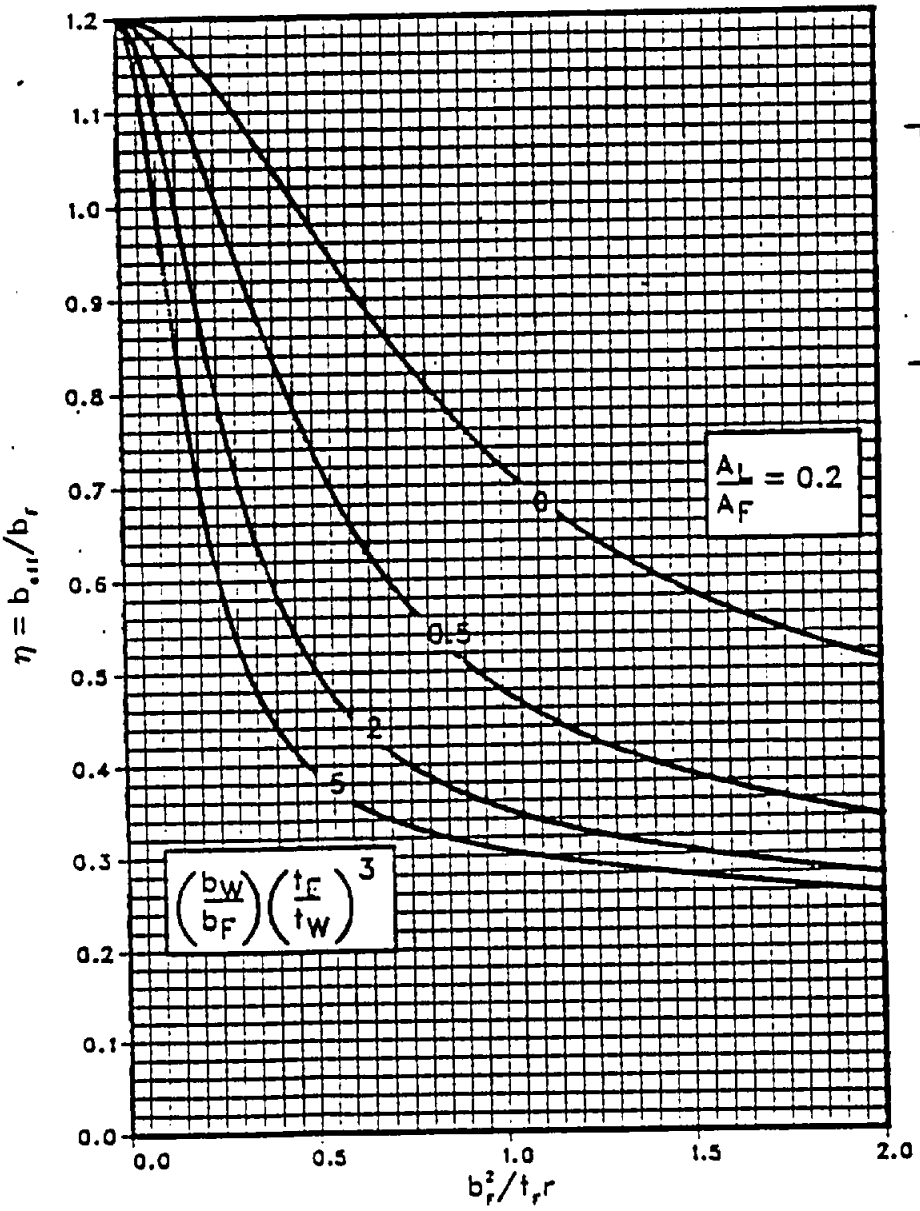

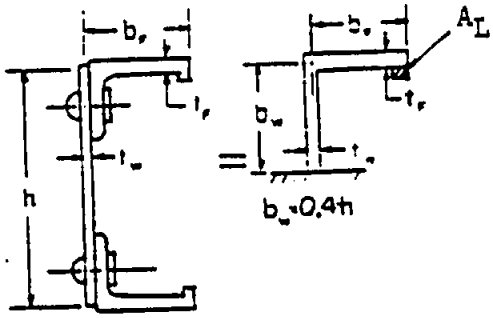

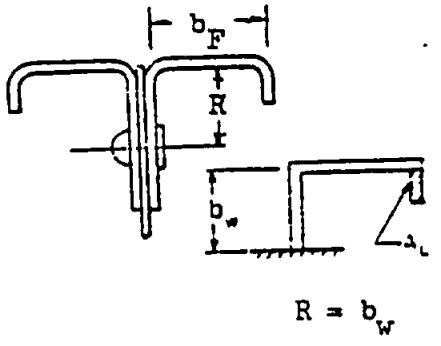

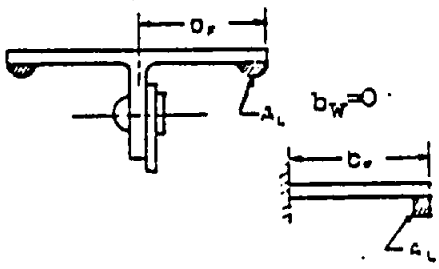

Ref. Journal of the Aero/Space Sciences-Sept. 1958, page 570

EFFECTIVE WIDTH OF CURVED BEAMS IN BENDING

LIPPED FLANGES

Note: This effective width effect is due to curling of the flanges and has nothing to do with compressive buckling

Note: For outside flange use outside radius

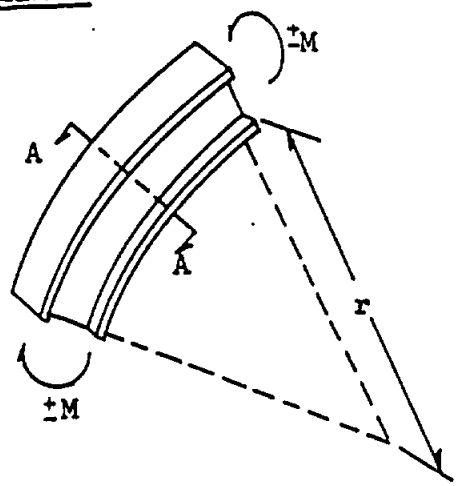

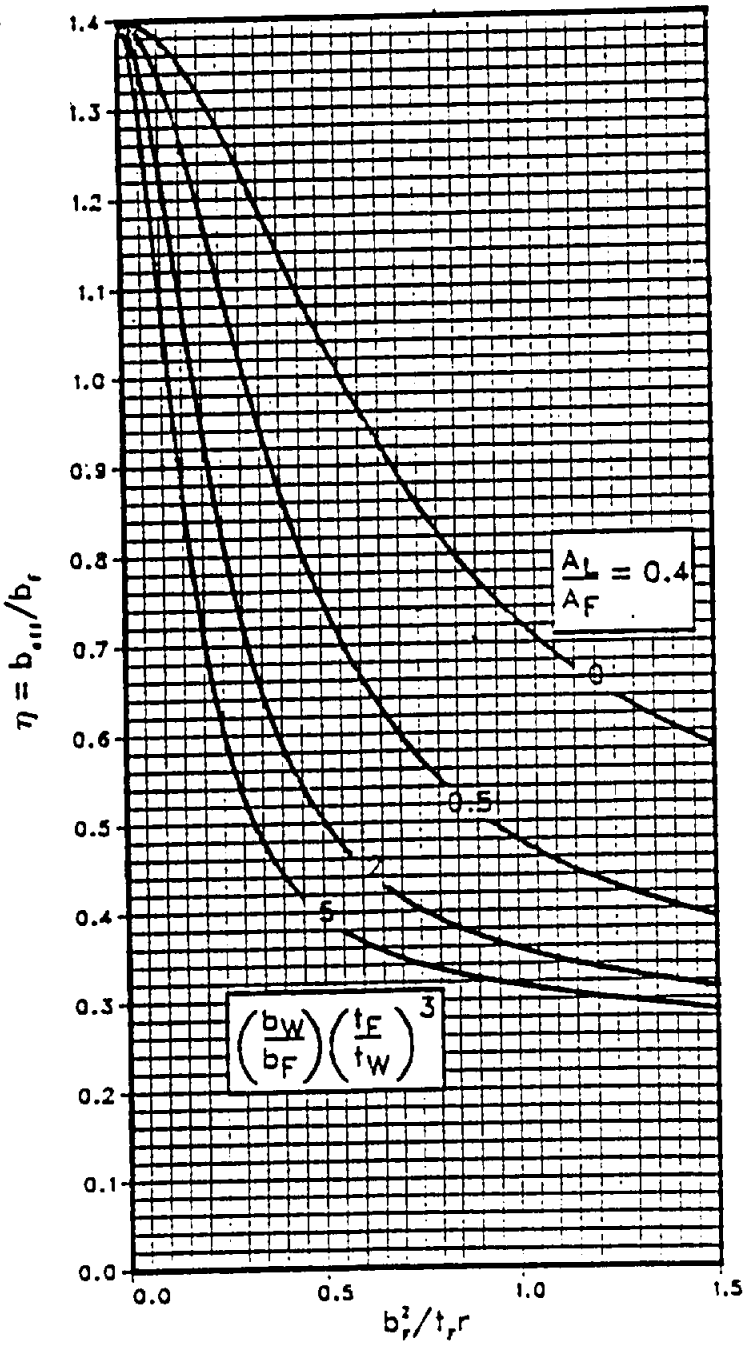

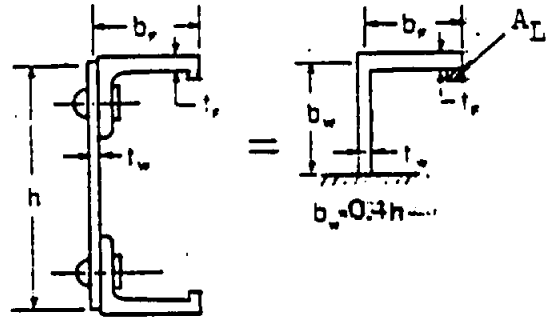

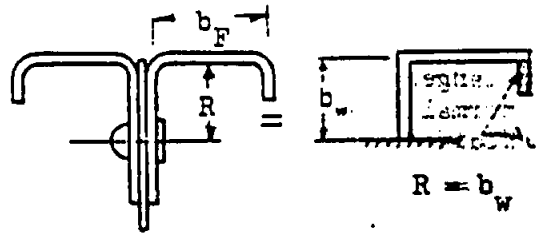

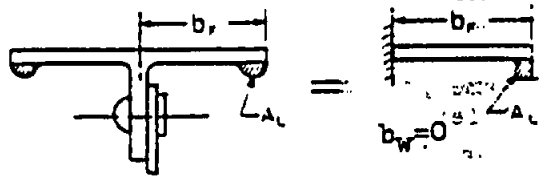

Ref. Journal of the Aero/Space Sciences-Sept. 1958, page 570

THE EFFECTIVENESS OF CURVED SHEET FOR CIRCUMFERENTIAL AXIAL LOAD

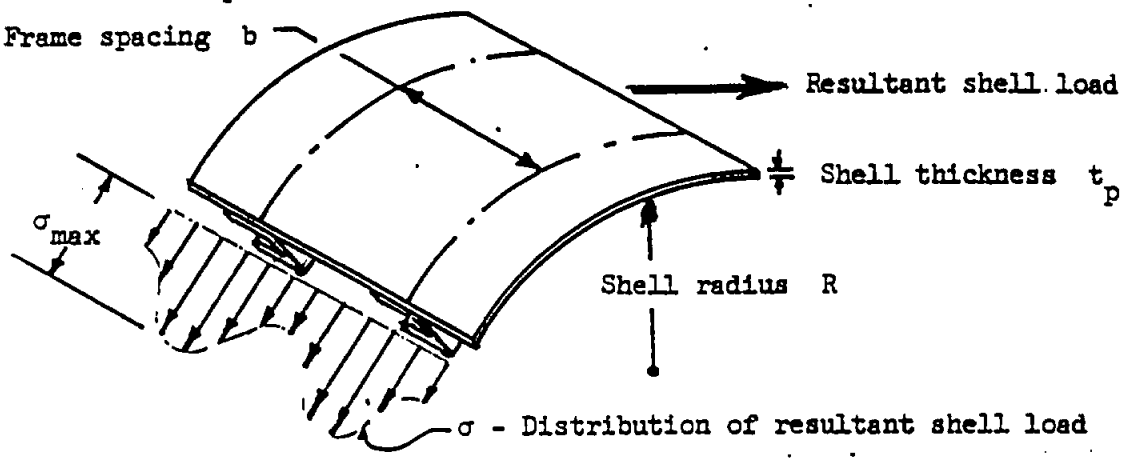

The effective width of a cylindrical shell that will carry circumferential axial load can be determined from the figure on B3.23.10-11. The fixed edge case is used when the shell is continuous over the supporting frames. The hinged edge case applies when the skin is discontinuous at the frames, such as an end bay. The effective width equations are taken from Reference 1, and are for the case where the frame attachment flange is rigid in a direction normal to the shell generators. The effective width is determined from equilibrium of the shell resultant load so that:

$$\sigma_{max}\, b_{eff}\, t_p = \int_0^b \sigma t_p\, dx = \text{Resultant shell load}$$

The effective width ratio, $(b_{eff}/b)_{sh}$, and the equations for its calculation are shown on B3.23.10-11.

The more general case encountered in aerospace structures is for the frame flanges to have significant flexibility due to flange bending in the direction normal to the shell generators. In this case the shell effective width ratio is modified to account for this added flexibility in the following manner:

$$b_{eff}/b = (b_{eff}/b)_{sh} \times \psi_i/(\psi_i + \psi_{sh}) \qquad (1)$$

where ψ_i is the frame stiffness and ψ_{sh} is the shell stiffness. For single frame members such as channels, zees, angles, etc., ψ_i is determined from B6.11.2-2, where ψ_1 is used when the shell moves towards the frame and ψ_2 is used when the shell moves away from the frame.

The frame stiffness for other configurations may be determined from the same proceedures used for the channel sections. This derivation is shown in Reference 2. The stiffness for back to back channel sections is given on page 24.1 of Reference 2.

Computer aid for the calculation of frame stiffness for single or double sections is available on the Structures Section B-DISK. The EXEC name is EFFEC and is fully interactive with computer supplied clues to guide the user in supplying the required input data.

THE EFFECTIVENESS OF CURVED SHEET FOR CIRCUMFERENTIAL AXIAL LOAD (CONT)

The shell stiffness, ψ_{sh}, is calculated from the following equations.

For continuous shell skin at the frame:

$$\psi_{sh} = 1.556\ E\ (t/R)^{3/2} \left\{ \frac{\text{Cosh } \beta b - \text{Cos } \beta b}{\text{Sinh } \beta b + \text{Sin } \beta b} \right\} \qquad (2a)$$

For discontinuous shell skin at frame:

$$\psi_{sh} = 0.389\ E\ (t/R)^{3/2} \left\{ \frac{\text{Sinh } \beta b + \text{Sin } \beta b}{\text{Cosh } \beta b + \text{Cos } \beta b} \right\} \qquad (2b)$$

The shell stiffness equations are from Reference 3, Equation (289) for the discontinuous case and Equation (291) for the continuous case. These equations are derived for a cylinder of arbitrary length and therefore may be used in any calculation of stress distribution in a circumferentially loaded shell.

The stress distribution in a shell supported by flexible frames is shown on page B3.23.10-12. Application of the shell effective width and the frame flange efficiency is indicated. The qualitative example shown is for the structure loaded by a constant circumferential bending moment which is similar to problems typically encountered in the analysis of inlet duct structure. The principles illustrated by this example also apply when the structure is loaded by axial load or combination of axial load and bending moment.

The shell effective width on page B3.23.10-11 and discussed in this section applies for both tension or compression stress. If the shell stress is compression, the effective width due to compression buckling of the shell skin must also be determined and the minimum value used in the subsequent stress calculation. The compression effective width may be obtained by application of B6.11.5-3. The most significant difference between the two effective widths is that the effective width due to curvature is not load dependent (only geometry) and the effective width due to buckling is load dependent. In the first case, the stress variation with load is linear, whereas in the second case the stress variation is non-linear, compounding the stress distribution calculation problem.

As the external load is applied to the structure, the resulting stresses will cause it to move to a deflected position as indicated on the sketch on page B3.23.10-12. It is evident from the sketch that there are transverse bending moments present in the elements of the frame (as well as the skin). Fatigue testing of full scale aircraft indicates the critical section to be in the frame attachment flange either at the rivet line or at the intersection with the frame web. These bending moments result in stresses that caused fatigue failures in the cases mentioned above.

It is possible to determine the moments and stresses and the static strength allowable from analyses currently available. The fatigue problem is another story since it presents a case of fatigue in a biaxial stress field for which GAC has no established analysis procedure at the present time.

In order to determine the bending moments in the frame flange, use is made of the moment equation from B6.11.6-4 for single channel, zee, or angle section frames. This equation gives the bending moment at the rivet attachment line. The moment at the flange/web intersection can then be determined from equilibrium of the attached flange. If the frame configuration is back to back channel or angle

THE EFFECTIVENESS OF CURVED SHEET FOR CIRCUMFERENTIAL AXIAL LOAD (CONT)

sections, the bending moments are available from Ref 2, pg 24.2. For other frame section configurations, the bending moments will be a part of the frame stiffness calculation.

The case of primary interest is when the shell skin tries to pull away from the frame (i.e. up-spring direction). The moment equation of B6.11.6-4 is only true for this case. The load on the flange and resulting bending moments are determined as follows. Calculate the maximum section stress, σ_w, on the shell skin side. Using the nomenclature of B3.23.10-12

$$\sigma_w = M z_a / I \tag{3}$$

The flange load is then calculated from:

$$P_{fl} = [\psi_{sh} R \sigma_w] \Big/ [E (\psi_{sh}/\psi_2 + 1.0)] \tag{4}$$

The flange load P_{fl} is then used for P_a of Equation 14, B6.11.6-4 and the bending moment at the rivet line calculated from:

$$m_a = P_{fl} \left[\frac{c (1.5 c + h (t_a/t_{we})^3)}{2c + d_a + h (t_a/t_{we})^3} \right] \tag{5}$$

The bending moment at the frame flange/web intersection is next calculated from the following equation.

$$m_{f/w} = m_a - P_{fl} \cdot c \tag{6}$$

For static strength evaluation, the plastic bending strength of the frame elements can be used provided the plastic bending strength used reflects the presence of the longitudinal stress acting orthogonally to the bending stress. This interaction is accounted for in Figure 5, page B6.12.4-6. This figure is used by substituting the longitudinal stress for $f_{ST\ max}$ of the figure. Because the allowable bending stress is a function of the longitudinal stress, it is necessary to perform the bending strength check at both the rivet line and the frame flange/web intersection. The critical section may not be at the section with the maximum bending moment. This strength evaluation is shown in the following numerical example.

References:

1. Westrup, R. W. and Silver, P.: Some Effects of Curvature on Frames, Journal of the Aero/Space Sciences, Vol. 25, No., 9, pp 567-572, September 1958.

2. Ranalli, E. R. and Bunce, F. E.: The Analaysis of Stiffened Compression Panels That Fail in the Forced Crippling Mode, Grumman Aerospace Corporation Report SAR-71-1, June 1977.

3. Timoshenko, S. and Woinowsky-Krieger, S.: Theory of Plates and Shells, Second Edition, McGraw-Hill Book Co., Inc., 1959.

THE EFFECTIVENESS OF CURVED SHEET FOR CIRCUMFERENTIAL AXIAL LOAD (CONT)

EFFECTIVE WIDTH OF CIRCUMFERENTIALLY LOADED CURVED SHEET

$$\beta b = 1.285\sqrt{b^3/tR} \quad (7)$$

$$(b_{eff}/b)_{sh} = C_5/\beta b \quad (8)$$

Edges fixed:

$$C_5 = 2(\text{Cosh } \beta b - \text{Cos } \beta b)/(\text{Sinh } \beta b + \text{Sin } \beta b) \quad (9a)$$

Edges hinged:

$$C_5 = \frac{(\text{Sinh } \beta b + \text{Sin } \beta b)(\text{Cosh } \beta b - \text{Cos } \beta b)}{(\text{Sinh}^2 \beta b + \text{Sin}^2 \beta b)} \quad (9b)$$

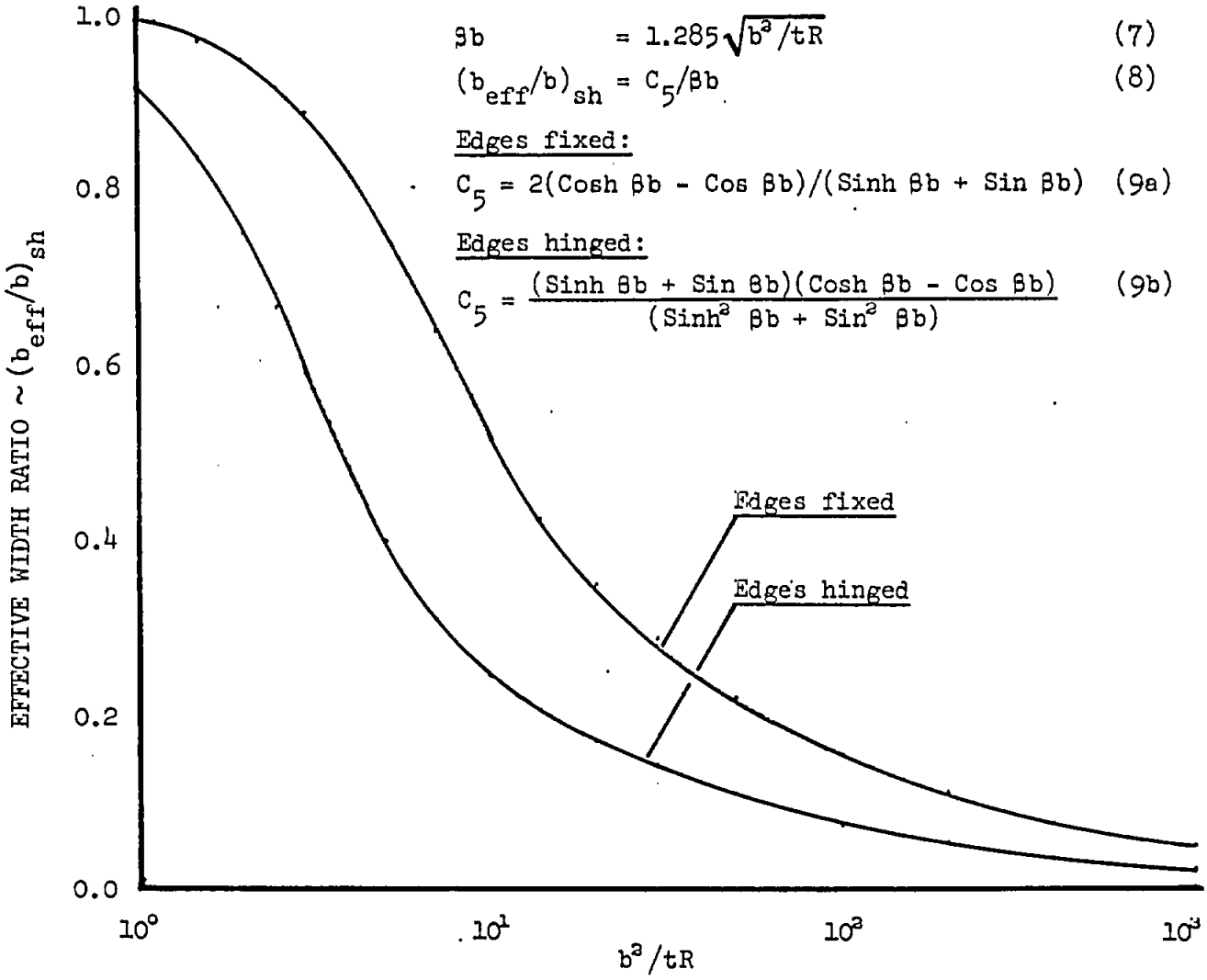

THE EFFECTIVENESS OF CURVED SHEET FOR CIRCUMFERENTIAL AXIAL LOAD (CONT)

Stress in Shell and Supporting Frame

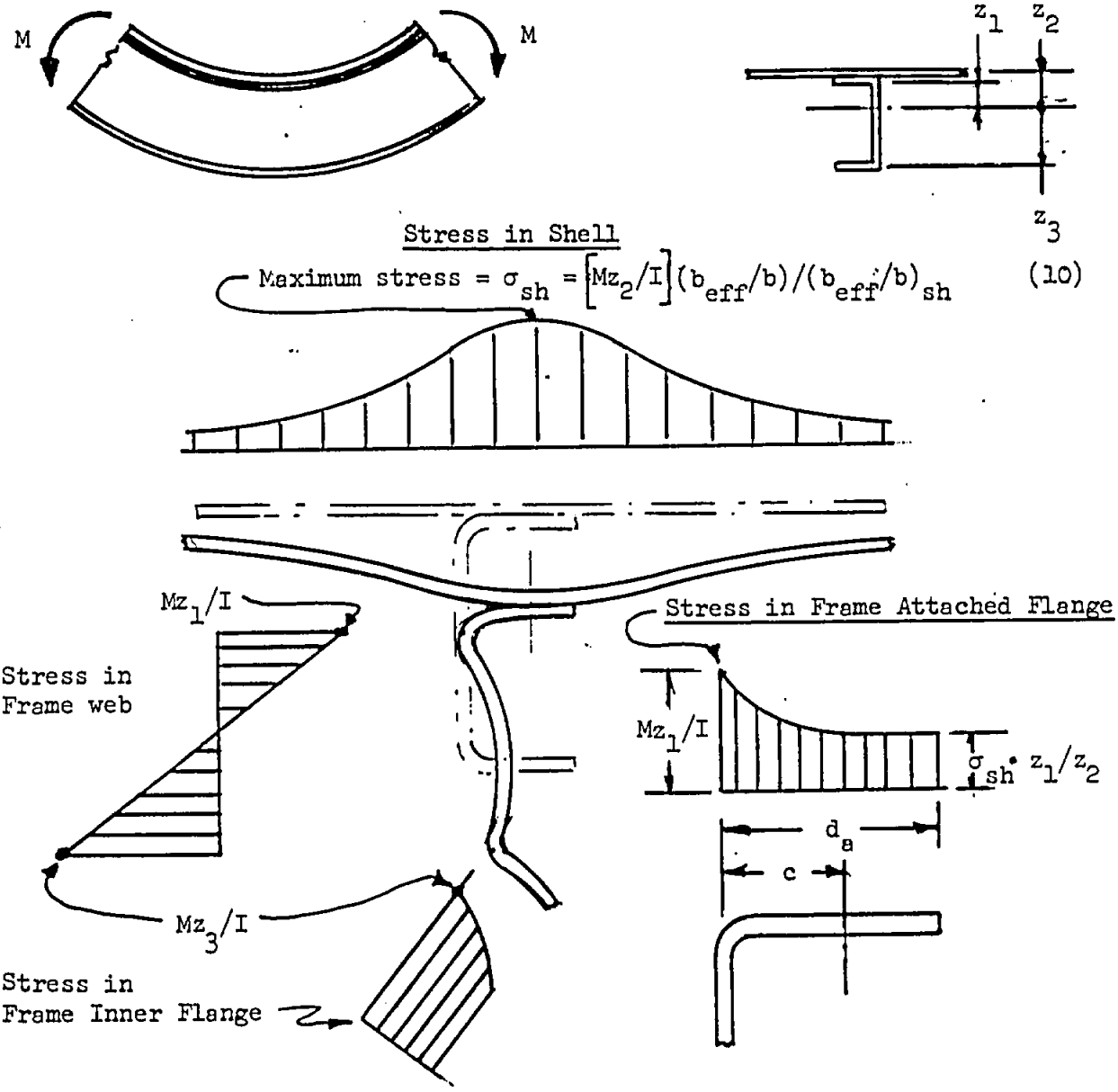

Frame inner flange efficiency when not attached to shell structure is from pages B3.23.10-5 thru -7.

The attached flange efficiency is based on the stress distribution shown on above sketch and is equal to:

$$\bar{\eta}_{fl} = (b_{eff}/b)/(b_{eff}/b)_{sh} \cdot [1.0 - c/(3d_a)] + c/(3d_a) \qquad (11)$$

THE EFFECTIVENESS OF CURVED SHEET FOR CIRCUMFERENTIAL AXIAL LOAD (CONT)

Illustrative example of frame supported shell

For the structure sketched on the previous page, assign the following dimensions to shell and frame. Let the shell skin be continuous over the frame and all material be 7075-T6 Aluminum alloy.

Shell:

Frame spacing	b	6.00 in
Shell thickness	t_p	0.10 in
Shell radius	R^p	14.00 in

Frame:

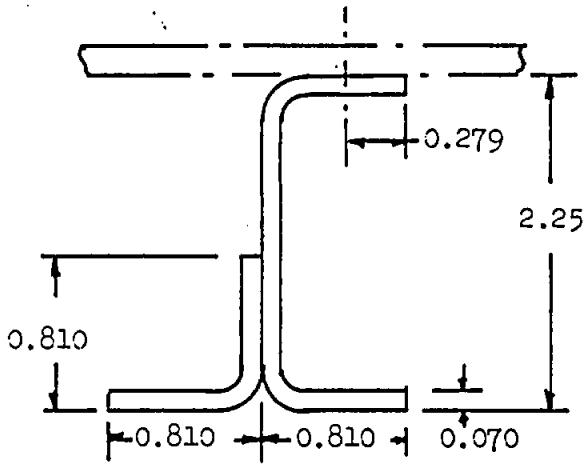

d_a = 0.775 in

c = 0.496 in

Frame stiffness:

With the bending moment, M, as indicated, the shell skin is in tension and will try to pull away from the frame. Therefore, the upspring or ψ_2 is required. From B6.11.2-2:

$$\psi_2 = \frac{E}{(1.0 - \nu^3)} \left[\frac{0.070}{0.496}\right]^3 \left[\frac{2.0 \times 0.496 + 0.810 + 2.18}{4.0 \times 0.810 - 0.496 + 4.0 \times 2.18 \times 0.810/0.496}\right]$$

$$= 7600 \text{ lb/in}^2 \quad \text{for an aluminum frame}$$

Shell stiffness from Equation 2a:

$$\psi_{sh} \text{ (for continuous skin)} = 1.556\ E\ (0.10/14.0)^{3/2}$$

$$= 9862 \text{ lb/in}^2$$

Determine the shell effective width, $(b_{eff}/b)_{sh}$ from Equation 8:

$$\beta b = 1.285\sqrt{36.0^2/(0.10 \times 14.0)}$$

$$= 6.516$$

THE EFFECTIVENESS OF CURVED SHEET FOR CIRCUMFERENTIAL AXIAL LOAD (CONT)

Illustrative example (Cont)

Shell effective width (Cont)

$C_5 = 2\ (\text{Cosh } 6.516 - \text{Cos } 6.516)/(\text{Sinh } 6.516 + \text{Sin } 6.516)$, from Equation 9a

$= 1.993$

$(b_{eff}/b)_{sh} = 1.993/6.516$

$= 0.306$

Determine shell effective width corrected for frame stiffness effect, Equation 1

$b_{eff}/b = 0.306 \times 7600/(7600 + 9862)$

$= 0.133$

Frame attached flange efficiency from Equation 7

$$\eta_{fl} = \frac{0.133}{0.306} \cdot [1.0 - 0.496/(3.0 \times 0.775)] + 0.496/(3.0 \times 0.775)$$

$= 0.555$

Frame inner flange efficiency

For page B3.23.10-6:

$b_w = 0.513, \quad b_f = 0.810$

$b_w/b_f = 0.633, \quad b^2/tR = 0.81^2/(0.07 \times (14.0 + 2.25)) = 0.58$

Flange efficiency = 0.60 (from B3.23.10-6)

Determine section properties of effective material

Dimensions	η b_{eff}/b	z Reference	η A	η A z	η A z^2	z Centroid
0.070 x 0.740	0.555	.035	0.0287	0.00101	0.00004	1.0312
2.110 x 0.070	1.000	1.125	0.1477	0.16616	0.18693	
0.070 x 0.740	0.600	2.215	0.0311	0.06889	0.15258	1.1488
0.740 x 0.070	1.000	1.810	0.0518	0.09376	0.16970	
0.070 x 0.740	0.600	2.215	0.0311	0.06889	0.15258	1.1488
0.100 x 6.000	0.133	-0.050	0.0798	-0.00399	0.00020	1.1162
Σ			0.3702	0.39472	0.66203	

$\bar{z} = 0.39472/0.3702 = 1.0662$ in

$I = 1/12 \times 2.110^3 \times 0.070 + 0.66203 - 0.39472^2/0.3702 = 0.29596$ in^4

THE EFFECTIVENESS OF CURVED SHEET FOR CIRCUMFERENTIAL AXIAL LOAD (CONT)

Illustrative example (Cont)

Determine stresses for M = 15000 in lb

Tension stresses

Max shell stress = (15000 x 1.1162/0.29596) x (0.133/0.306) = 24558 psi

Frame attached flange stress at rivet line

= (15000 x 1.0312/0.25956) x (0.133/0.306) = 22715 psi

Frame attached flange stress at frame web

= 15000 x 1.0312/0.25056 = 52264 psi

Compression stresses

Frame inner flange stress at frame web

= 15000 x 1.1488/0.29596 = 58224 psi

Frame inner flange stress (average)

= 15000 x 1.1488 x 0.60/0.29596 = 34934 psi

Strength analysis, tension:

F_{tu} = 77000 psi

MS = 77000/52264 - 1.0 = 0.47

Strength analysis, compression:

Flange strength

Inner flange buckling stress = 0.384 x E x $(0.070/0.810)^2$ = 30100 psi

$F_{0.7}$ = 70000 psi, $F_{crel}/F_{0.7}$ = 30100/70000 = 0.43

From B1.60-2, $F_{cc}/F_{0.7}$ = 0.61, F_{cc} = 42700 psi

and from B1.60-3, $F_e/F_{0.7}$ = 0.884, F_e = 61900 psi

MS = 61900/58224 - 1.0 = 0.063

MS = 42700/34934 - 1.0 = 0.220

Web strength

For B5.11.13-2, α = (58224 + 52264)/58224 = 1.897, K = 20.40

F_{crel} = 20.40 x E x $(0.070/2.21)^2$ = 215900 psi obviously not critical

THE EFFECTIVENESS OF CURVED SHEET FOR CIRCUMFERENTIAL AXIAL LOAD (CONT)

Illustrative example (Cont)

Strength analysis, frame flange transverse bending

Determine flange bending moments

σ_w = 15000 x 1.1162/0.29596 from Equation 3

= 56751 psi

P_{fl} = [9862 x 14.0 x 56751] / [10.5 x 10^6 x (9862/7600 + 1.0)] Equation 4

= 324 lb/in

$m_a = 324 \cdot \frac{0.496\ (1.5 \times 0.496 + 2.18)}{2.0 \times 0.496 + 0.775 + 2.18}$ Equation 14, B6.11.6-4

= 119 in lb/in

$m_{f/w}$ = 119 - 324 x 0.496 from Equation 5

= -42 in lb/in

Determine allowable flange bending moment

At the rivet line, for Figure 5, B6.12.4-6

$f_{ST\ max}/F_{cy}$ = 22715/70000 = 0.324, H = 0.88

M_{all} = 0.88/4 x 0.070^2 x 70000

= 75.5 in lb/in

MS = 75.5/119 -1.0 = -0.366

At flange/web intersection for Figure 5, B6.12.4-6,

$f_{ST\ max}/F_{cy}$ = 52264/70000 = 0.750, H = 0.56

M_{all} = 0.56/4 x 0.070^2 x 70000

= 48.0 in lb/in

MS = 48/42 - 1.0 = 0.143

THE EFFECTIVENESS OF CURVED SHEET FOR CIRCUMFERENTIAL AXIAL LOAD (CONT)

Illustrative example (Cont)

Determine stresses for M = 10000 in lb and an axial load P =7000 lb

Tension stresses

Max shell stress =

= (10000 x 1.1162/0.29596 + 7000/0.3702) x (0.133/0.306) = 24610 psi

Frame attached flange stress at rivet line

= (10000 x 1.0312/0.25956 + 7000/0.3702) x (0.133/0.306) = 25486 psi

Frame attached flange stress at frame web

= 10000 x 1.0312/0.25956 + 7000/0.3702 = 58637 psi

Compression stresses

Frame inner flange stress at frame web

= 10000 x 1.1488/0.25956 - 7000/0.3702 = 19907 psi

Frame inner flange stress (average)

= (10000 x 1.1488/0.25956 - 7000/0.3702) x 0.60 = 11944 psi

Strength analysis, frame flange transverse bending

Determine flange bending moments

σ_w = 10000 x 1.1162/0.25956 + 7000/0.3702

= 56622 psi

P_{fl} = 9862 x 14.0 x 56622 / 10.5 x 10^6 x (9862/7600 + 1.0)

= 324 lb/in

This load is the same as case with M = 15000 in lb and P = 0.0. The flange strength calculations are therefore identical from this point onward and are not repeated.

THE EFFECTIVENESS OF CURVED SHEET FOR CIRCUMFERENTIAL AXIAL LOAD (CONT)

Illustrative example (Cont)

In order to demonstrate the stress sensitivity to the assumptions and some of the physical parameters of this problem, let us change the reinforcing angle section to a full channel, thereby increasing the frame stiffness. This change will not only add area and inertia directly, but will also increase the efficiency of the shell skin and the frame attached flange. The effects of this change are illustrated by the following calculations.

Determine the frame up-spring ψ_a

For page B6.11.2-2.1:

$b_{ref}/t_a = 0.810/0.070 = 11.60, \qquad t_p/t_a = 0.10/0.070 - 1.429$

From page B6.11.2-2.1:

$\psi_a/E = 0.00308, \qquad \psi_a = 32340$ psi

Shell effective width corrected for frame stiffness, from Equation 1

$$b_{eff}/b = 0.306 \times 32340/(32240 + 9862)$$
$$= 0.234$$

Frame attached flange efficiency, from Equation 11

$$\eta_{fl} = \frac{0.234}{0.306} \cdot \left[1.0 - 0.496/(3.0 \times 0.775)\right] + 0.496/(3.0 \times 0.775)$$
$$= 0.815$$

Determine section properties of effective material

Dimensions	η b_{eff}/b	z Reference	η A	η A z	η A z^2	z Centroid
0.070 x 0.740	0.815	0.035	0.0422	0.00148	0.00005	0.7652
0.070 x 0.740	0.815	0.035	0.0422	0.00148	0.00005	
2.110 x 0.070	1.000	1.125	0.1477	0.16616	0.18693	
2.110 x 0.070	1.000	1.125	0.1477	0.16616	0.18693	
0.070 x 0.740	0.600	2.215	0.0311	0.06889	0.15258	1.4148
0.070 x 0.740	0.600	2.215	0.0311	0.06889	0.15258	
0.100 x 6.000	0.234	-0.050	0.1404	-0.00702	0.00035	0.8502
Σ			0.5824	0.46604	0.67947	

$\bar{z} = 0.46604/0.5824 = 0.80021$ in

$I = 2/12 \times 2.110^3 \times 0.070 + 0.67947 - 0.46604^2/0.5824 = 0.4164$ in^4

THE EFFECTIVENESS OF CURVED SHEET FOR CIRCUMFERENTIAL AXIAL LOAD (CONT)

Illustrative example (Cont)

Determine stresses for M = 15000 in lb

Tension stresses

Max shell stress = (15000 x 0.8502/0.41614) x (0.234/0.306) = 23435 psi

Frame attached flange stress at rivet line
= (15000 x 0.7652/0.41614) x (0.234/0.306) = 21092 psi

Frame attached flange stress at frame web
= 15000 x 0.7652/0.41614 = 27582 psi

Compression stresses

Frame inner flange stress at frame web
= 15000 x 1.4148/0.41614 = 50998 psi

Frame inner flange stress (average)
= 15000 x 1.4148 x 0.60/0.41614 = 30600 psi

Margins of safety for the reinforced configuration

Tension, frame attached flange at frame web

MS = 77000/27582 - 1.0 = 1.792

Compression, inner flange at frame web

MS = 61900/50998 - 1.0 = 0.214

Strength analysis, frame flange transverse bending

Determine flange bending moments

σ_w = 15000 x 0.852/0.4164 from Equation 3
= 30691 psi

$P_{fl} = [9862 \times 14 \times 30691]/[10.5 \times 10^6 \times (9862/32340 + 1.0)]$ Equation 4
= 309 lb/in

For B6.11.2-2.2, b_{ref}/t_a = 0.810/0.070 = 11.6

and from B6.11.2-2.2

$m_a/(t_a P) = 1.46$ and $m_{f/w}/(t_a P) = -1.285$

$m_a = 1.46 \times 0.07 \times 309 = 31.6$

$m_{f/w} = 1.285 \times 0.07 \times 309 = 27.8$

THE EFFECTIVENESS OF CURVED SHEET FOR CIRCUMFERENTIAL AXIAL LOAD (CONT)

Illustrative example (Cont)

Strength analysis, frame flange transverse bending (Cont)

Determine allowable flange bending moment

At the rivet line, for Figure 5, B6.12.4-6

$f_{ST\ max}/F_{cy} = 21092/70000 = 0.301, \quad H = 0.90$

$M_{all} = 0.90/4 \times 0.070^2 \times 70000$

$= 77.1$ in lb/in

MS = = 77.1/31.6 - 1.0 = 1.44

At the flange/web intersection, for Figure 5, B6.12.4-6

$f_{ST\ max}/F_{cy} = 27582/70000 = 0.394, \quad H = 0.860$

$M_{all} = 0.86/4 \times 0.070^2 \times 70000$

$= 73.7$ in lb/in

MS = 73.7/27.8 - 1.0 = 1.65

Strength improvement due to reinforcement

The addition of the full channel reinforcement to the frame represents a weight increase of 15% on the entire section. The compression stress decrease is 14% or about one to one. The tension stress decrease is 189% for the same weight increase. This large stress change on the tension side is due to the favorable placement of the reinforcement relative to the tension side of the structure. The reinforcement not only added area to the section but additionally improved the section efficiency. The most critical static strength point on the single channel configuration is the frame flange transverse bending strength with a negative margin of -0.366. By adding the reinforcing channel, a margin improvement of 384% is realized so that this item is no longer the critical strength item.

THE BENDING OF A THIN RING WITH INTERNAL PRESSURE AND APPLIED RADIAL LOAD

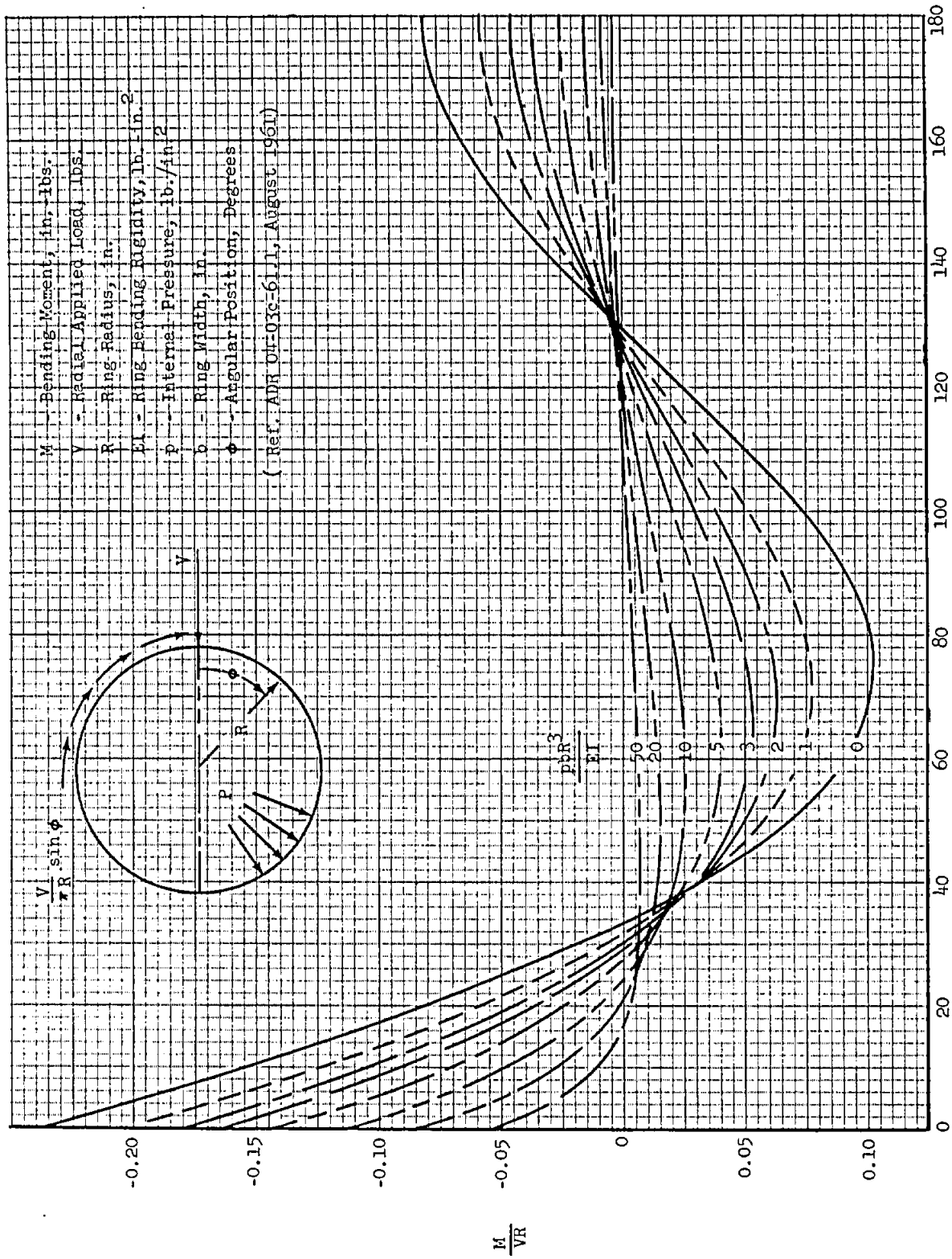

THE BENDING OF A THIN RING WITH INTERNAL PRESSURE AND APPLIED COUPLE LOAD

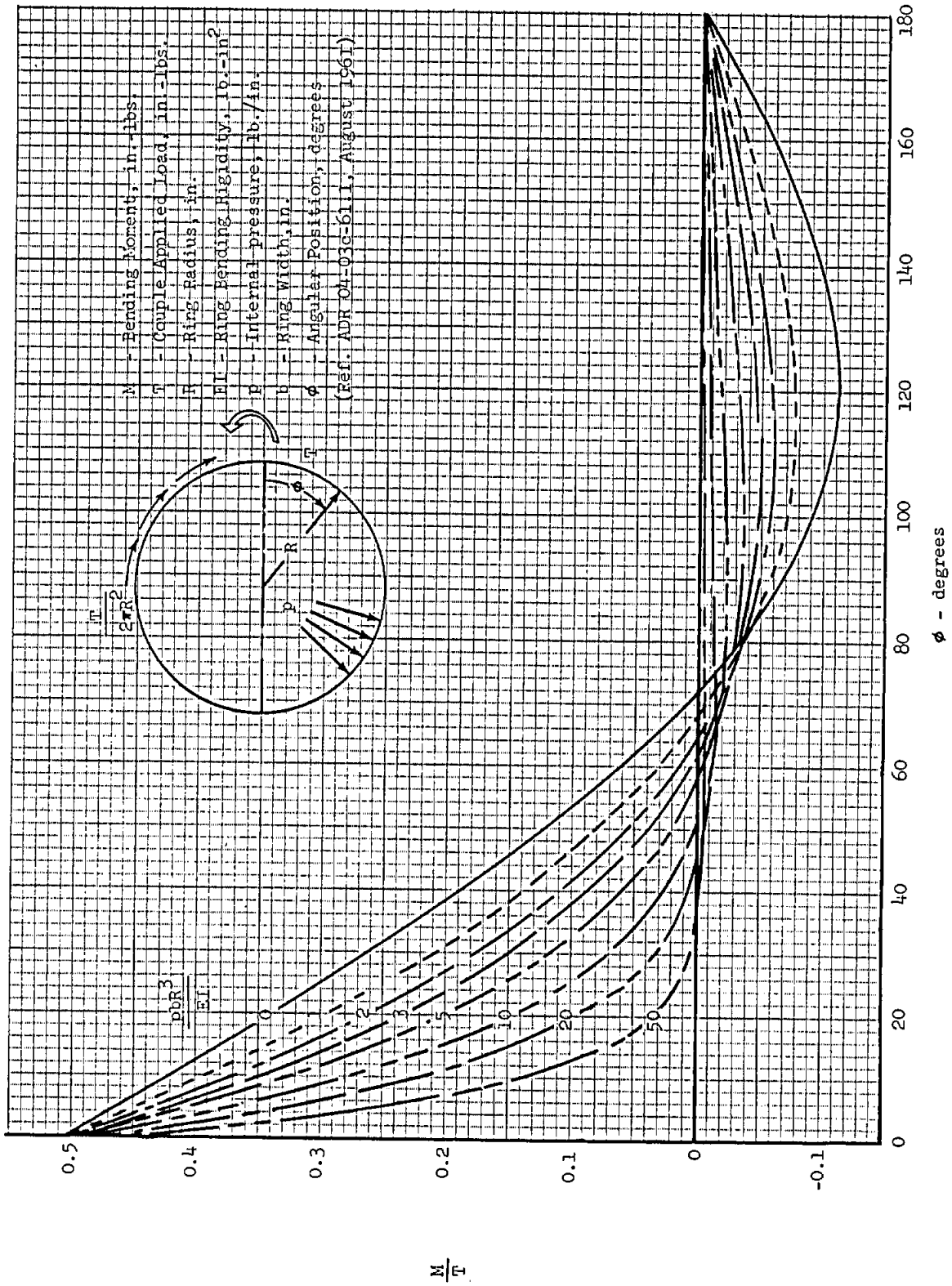

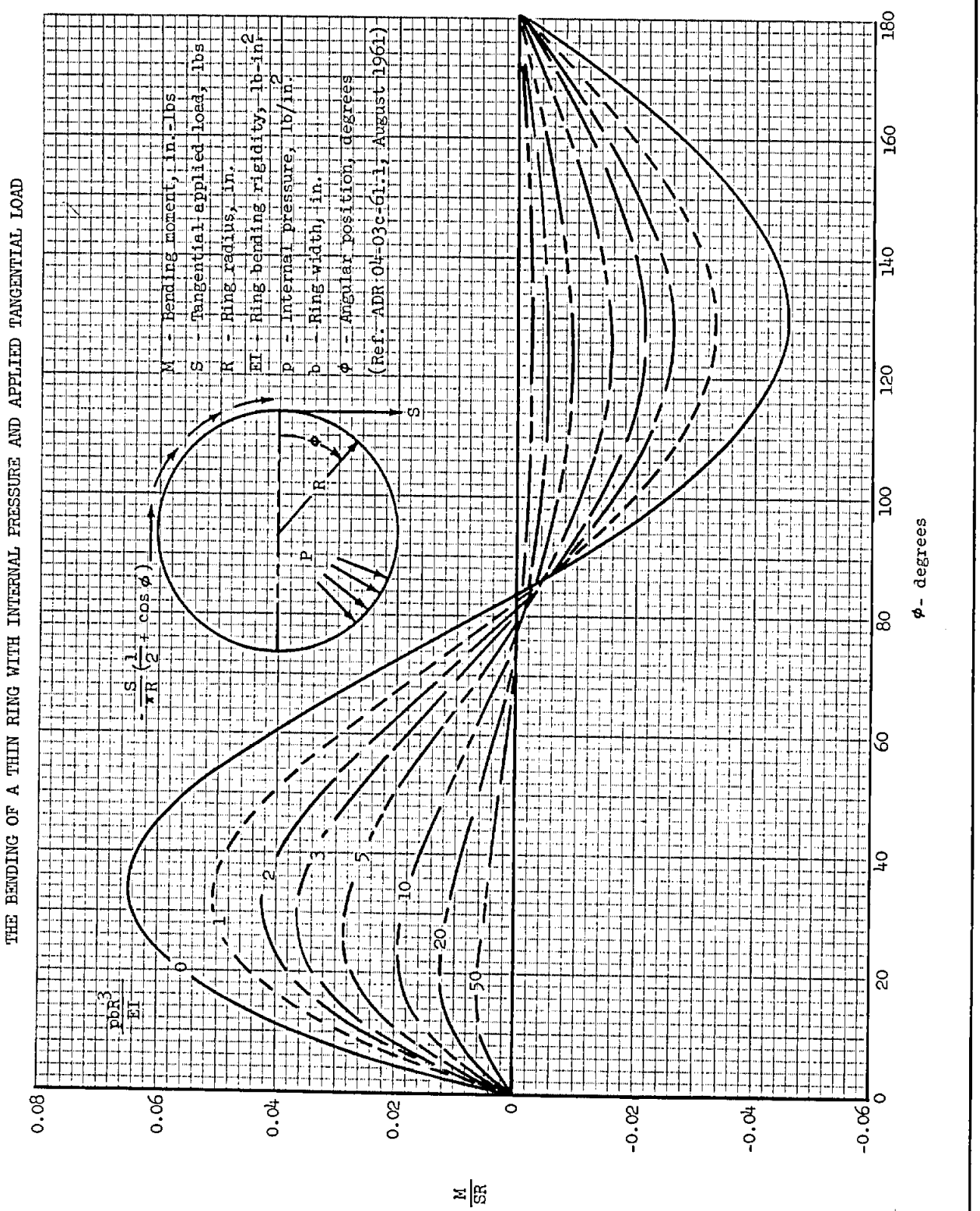
THE BENDING OF A THIN RING WITH INTERNAL PRESSURE AND APPLIED TANGENTIAL LOAD
$-\frac{S}{\pi R}\left(\frac{1}{2}+\cos\phi\right)$
M = Bending moment, in.-lbs
S = Tangential applied load, lbs
R = Ring radius, in.
EI = Ring bending rigidity, lb-in.^{2}
p = Internal pressure, lb/in.^{2}
b = Ring width, in.
ϕ = Angular position, degrees
(Ref. ADR-04-03c-61.1, August 1961)
$\frac{pbR^3}{EI}$
0
1
2
3
5
10
20
50
$\frac{M}{SR}$
0.08
0.06
0.04
0.02
0
-0.02
-0.04
-0.06
0
20
40
60
80
100
120
140
160
180
ϕ- degrees

COMBINED BENDING AND AXIAL LOAD IN THE INELASTIC RANGE

Discussion

The bending strengths of beams loaded in the inelastic range by bending moments or by a combination of bending moments and axial load are presented in this section.

The method is applicable to beams with cross-sections that have one or more axes of symmetry. The axis of the bending moment is normal to an axis of symmetry.

The method assumes that large plastic strains (up to 3%) can be developed linearly in the cross-section considered. This implies that the beam is sufficiently long to develop such strains, and that there are no stress concentrations near the section considered.

Fatigue, creep, buckling and crippling are not considered in this section. These items must be checked independently from this analysis.

The data presented in this section does not supersede the bending strength data for steel and aluminum tubing given in MIL-HDBK-5A.

Bending strength is given in terms of a stress commonly referred to as the bending modulus. This stress is used in the conventional bending stress equation as follows:

$$M_{max} = F_B \cdot I/c$$

where M_{max} is the maximum permissible bending moment
F_B is the bending modulus
I/c is the minimum section modulus

F_B is presented as a function of the shape factor, k, and the tensile yield stress, F_{ty}, if a yield criterion is critical, or the ultimate tensile stress, F_{tu}, if the ultimate strength criterion is critical.

REFERENCE: Brown, Lawrence D., "Analysis of Beams Subjected to Combined Bending and Axial Loads in the Plastic Range," GAEC Report No. ADR 02-21-66.1, August 1966.

Discussion (Cont'd)

The bending modulus is also a function of the shape of the stress-strain curve of the material of the beam. This relationship is investigated in the Reference source of this section.

The values of F_B presented in this section are the minimum determined for a realistic range of aircraft structural materials.

The shape factor, k, is given in B3.32-5 for the several common structural shapes. For other doubly symmetric shapes, k is equal to $2 \cdot Qc/I$ (see list of symbols for definitions).

The presence of axial loading in addition to bending reduces the maximum bending capability of any doubly symmetric section. For a section with one axis of symmetry, such as a Tee, the maximum bending capability is reduced due to axial load when that load acts so as to cause failure of the outstanding leg. The strength reduction due to axial load is shown on the interaction curve of B3.32-7 .

SYMBOLS

A	Cross-section area	in^2
c	Distance from neutral axis to extreme fiber	in
D/t	Diameter-wall thickness ratio for tubular section	
F_{bu}	Allowable ultimate bending modulus	lb/in^2
F_{by}	Allowable yield bending modulus	lb/in^2
F_{tu}	Ultimate tensile stress	lb/in^2
F_{ty}	Tensile yield stress	lb/in^2
I	moment of inertia	in^4
k	shape factor, $2 \cdot Q \cdot (c/I)$	
M	applied bending moment	in - lb.
m	exponent, pageB3.32-7	
n	exponent, page B3.32-7	
P	Applied axial tension load	lb
Q	Static moment about the neutral axis in pure bending of the area between the extreme fiber and the neutral axis	in^3

ASSUMPTIONS AND RESTRICTIONS

1. It is assumed that the tensile and compressive stress-strain curves for bending are identical and correspond to the stress-strain curve in uniaxial tension.

2. Cross-sections which are plane and normal to the neutral axis before bending remain plane and normal to that axis after bending.

3. The D/t of tubular sections should not exceed 12 unless crippling of the cross-section is also checked.

4. The maximum value of k (shape factor) should not exceed 2.0 when determining the ultimate bending factor, and 1.5 when determining the yield bending factor.

5. Material properties:
   ultimate elongation ≥ 3%
   tensile yield stress ≥ 75% ultimate tensile stress
   The strength properties of the materials analyzed in the preparation of this section were within the following limits:

$$10 \text{ ksi} \leq F_{ty} \leq 250 \text{ ksi}$$

$$20 \text{ ksi} \leq F_{tu} \leq 300 \text{ ksi}$$

Method

Pure Bending

1. Determine shape factor k
   a. Values for common cross-sections with two axes of symmetry are given on B3.32-5.
   b. For other cross-sections with two axes of symmetry use $k = 2Qc/I$ (See B3.32-3 Item 4).
   c. For Tee sections use B3.32-5.
2. Find F_{by} and/or F_{bu} from B3.32-6.
3. The applied moment which would cause yielding of the extreme fiber is $M_y = \frac{F_{by} I}{c}$. The ultimate moment which can be carried by the cross-section is $M_u = F_{bu} I/c$.

Combined Bending and Axial Load

The allowable strength under combined loading can be determined from the interaction curves of B3.32-7.

1. Determine shape factor, k, as in 1 (a), (b) or (c) above.
2. Determine the bending modulus, F_B, which is allowable without the presence of axial load from B3.32-6.
3. Determine the bending moment which is allowable without the presence of axial load: $M_y = \frac{F_{by} I}{c}$ when the yield criterion is critical; $M_u = \frac{F_{bu} I}{c}$ when the ultimate strength criterion is critical.
4. Determine the allowable axial load (without the presence of bending) P_y or P_u from $P_y = A \cdot F_{ty}$ or $P_u = A \cdot F_{tu}$.
5. The value of n for use in B3.32-7 is obtained from B3.32-7 through B3.32-9.

SHAPE FACTOR, k, FOR SOME COMMON CROSS-SECTIONS

(For Moment About Axis x-x)

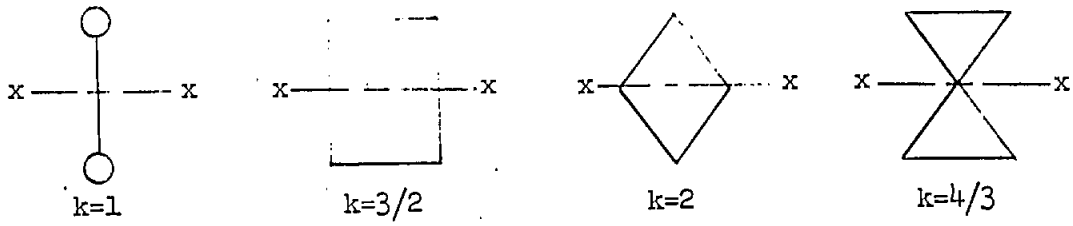

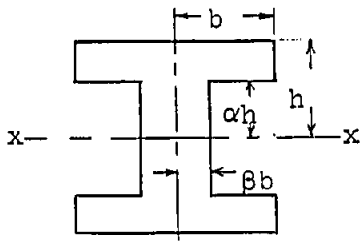

$$k = \frac{3}{2}\,\frac{1-(1-\beta)\,\alpha^2}{1-(1-\beta)\,\alpha^3}$$

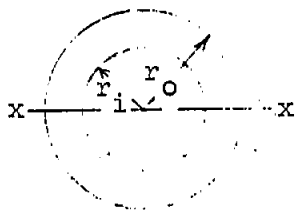

$$k = \frac{16}{3\pi}\,\frac{1-\bar{r}^3}{1-\bar{r}^4}$$

$$\bar{r} = \frac{r_i}{r_o}$$

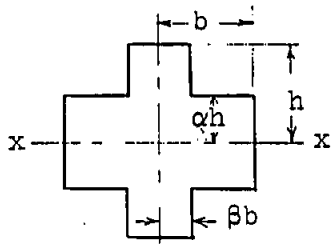

$$k = \frac{3}{2}\,\frac{\beta+(1-\beta)\,\alpha^2}{\beta+(1-\beta)\,\alpha^3}$$

— Ultimate Use k = 1.5 for Yield

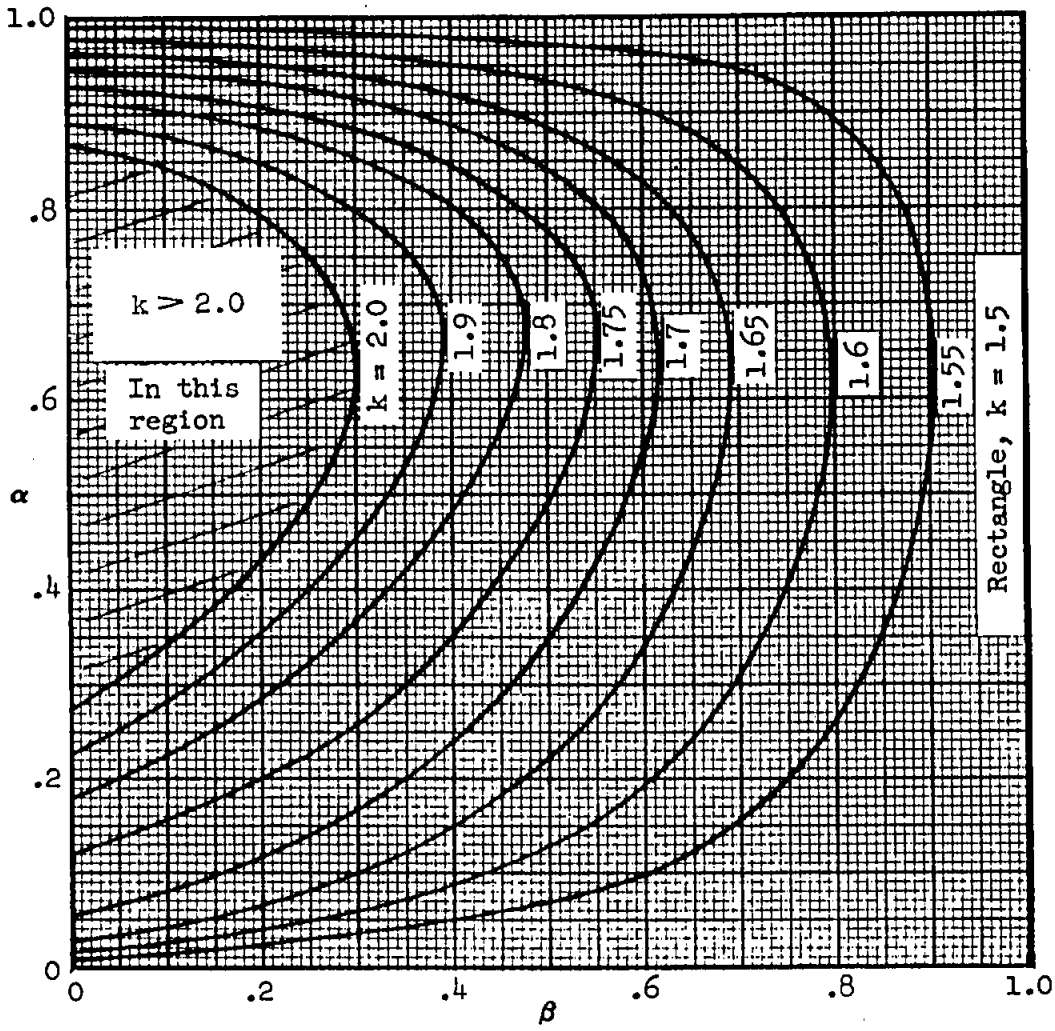

TEE SECTION*

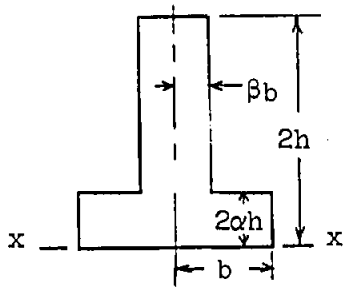

* For moment about axis parallel to x - x

Grumman

Ultimate

$$F_{bu} = \frac{1 + 4k}{5} F_{tu}$$

F_{bu} = Ultimate Bending Modulus

F_{tu} = Ultimate Stress

Yield

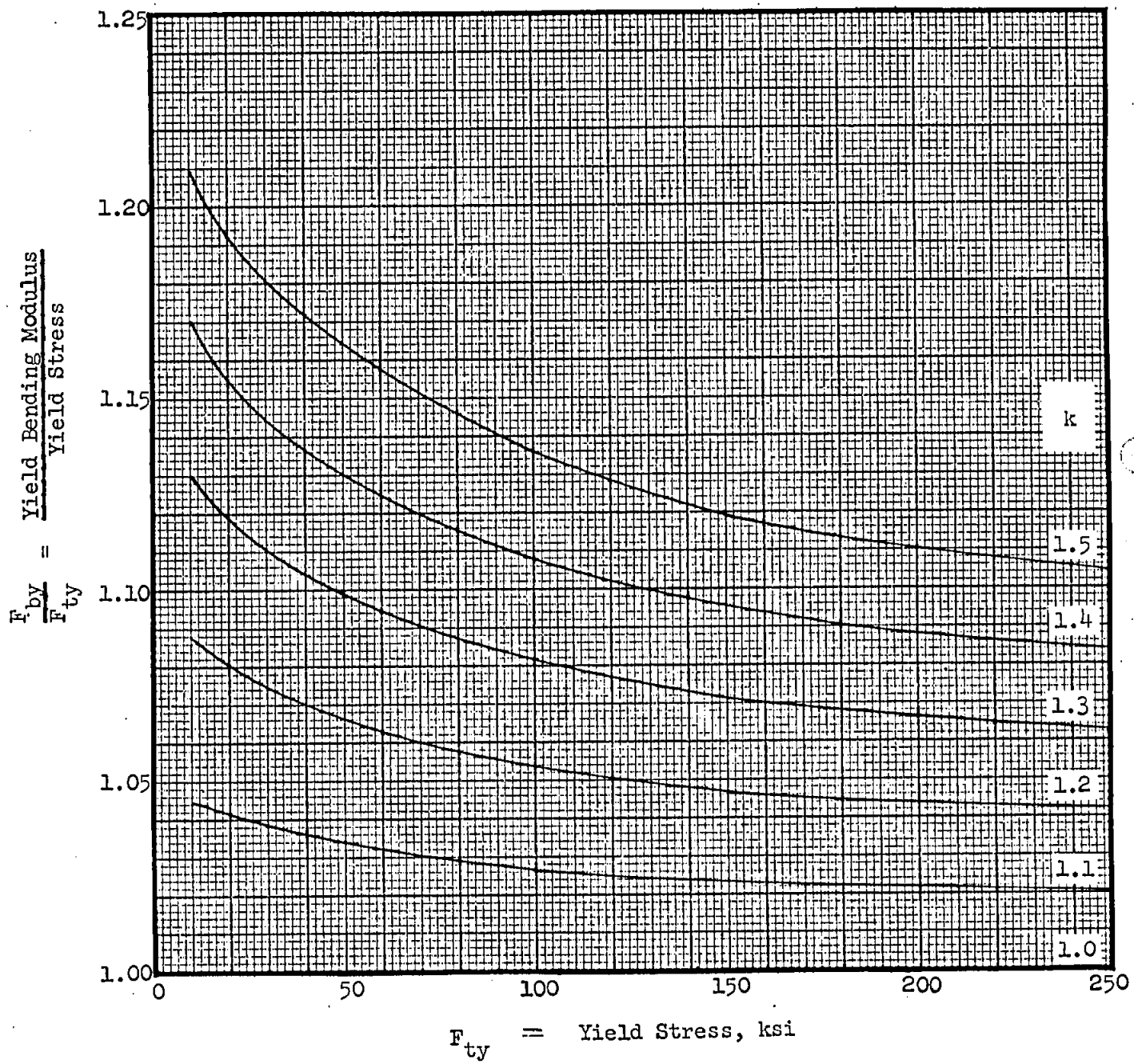

Grumman

VALUES OF EXPONENT, n, FOR USE IN INTERACTION CURVES

Shape	n yield	n ultimate
	1.5	2.4
	1.3	1.9
	1.2	1.6
	1.0	1.0
	see B3.32-8	
	see B3.32-8	
	see B3.32-9.	
	see B3.32-9	

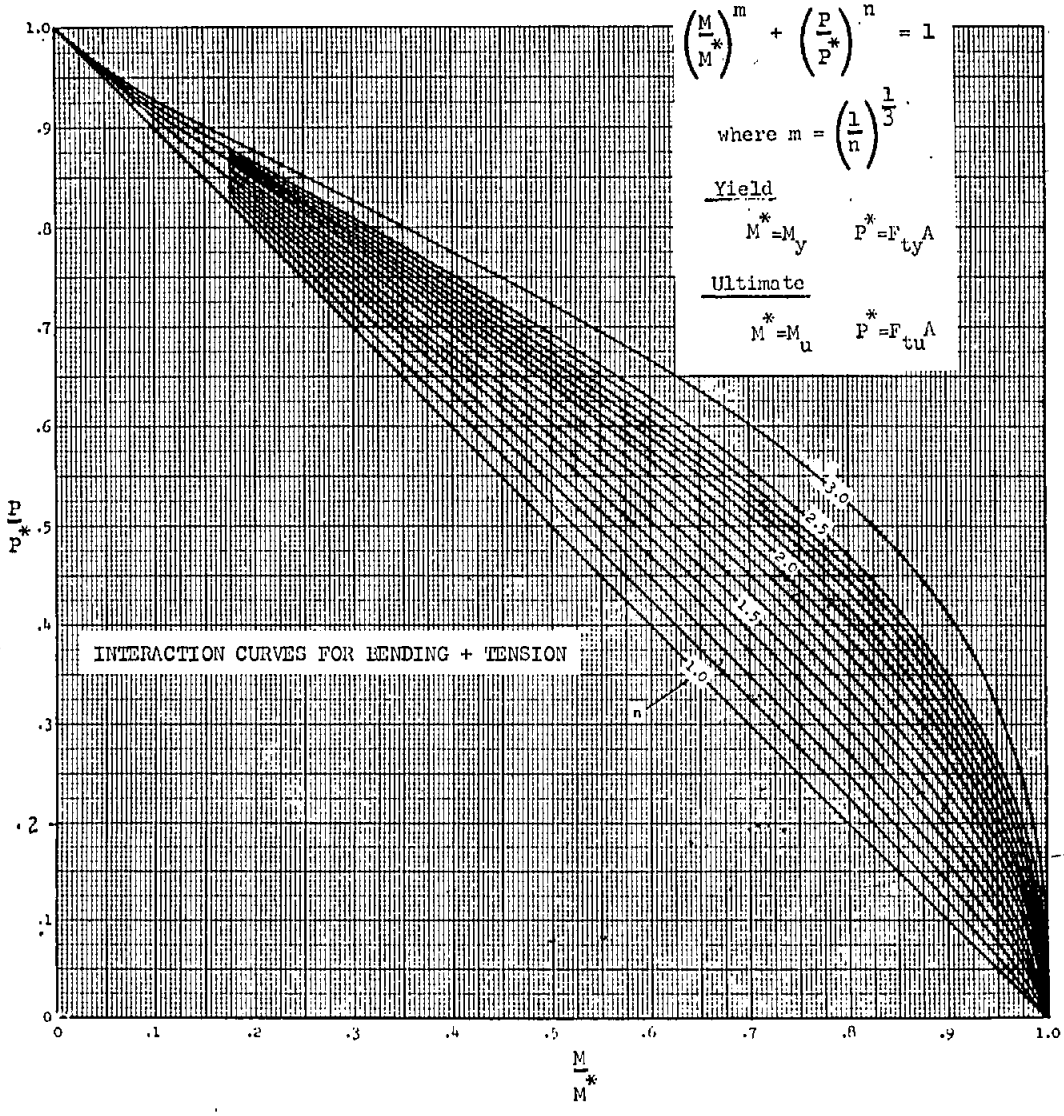

Grumman

VALUES OF EXPONENT, n, FOR USE IN INTERACTION CURVES OF B.3.32-7

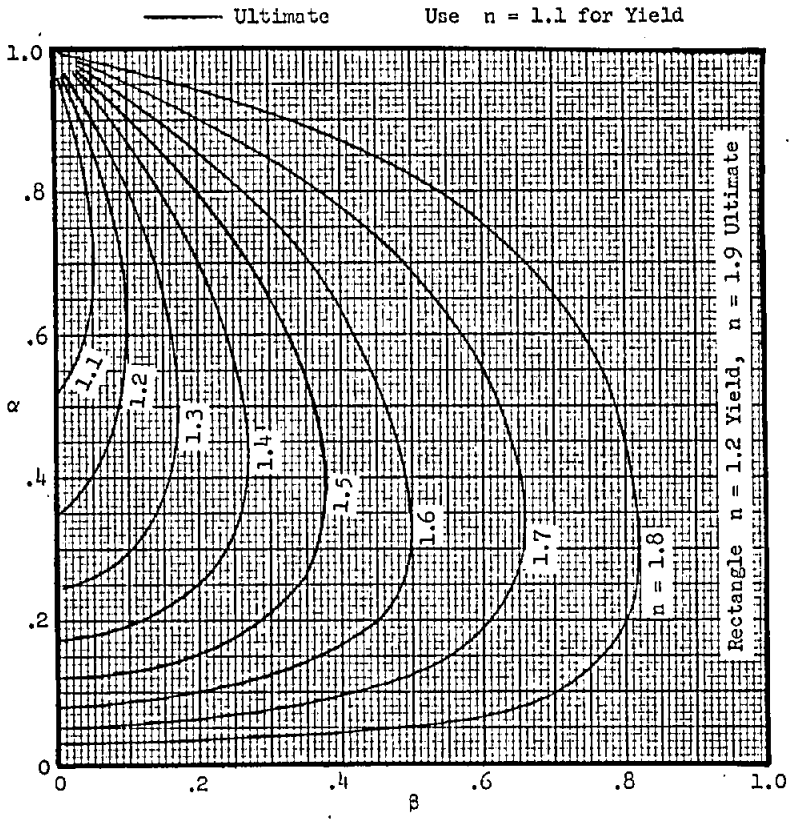

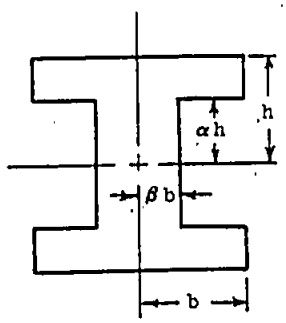

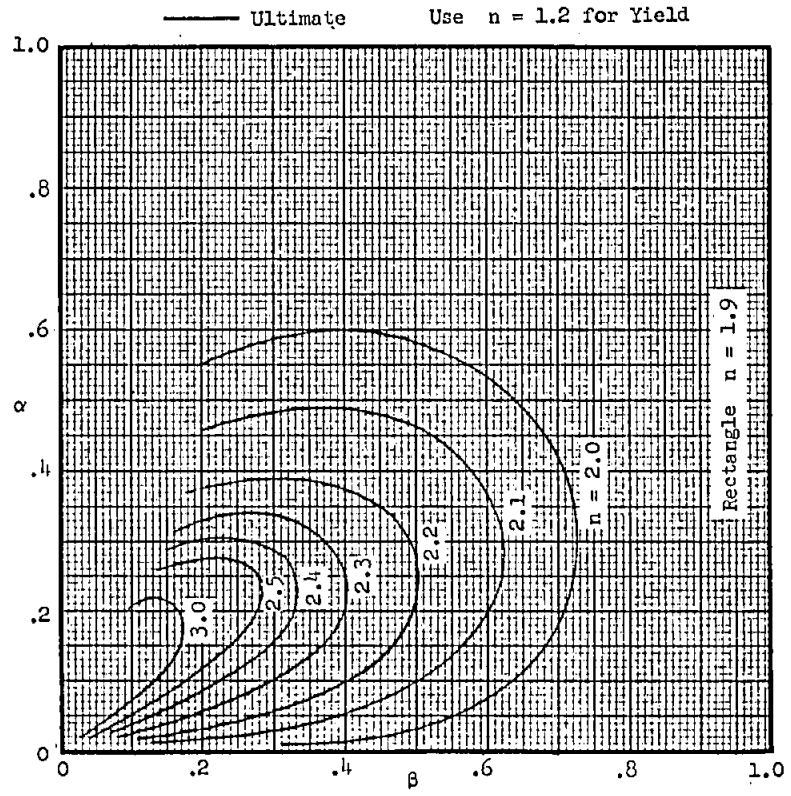

For moment about x - x axis

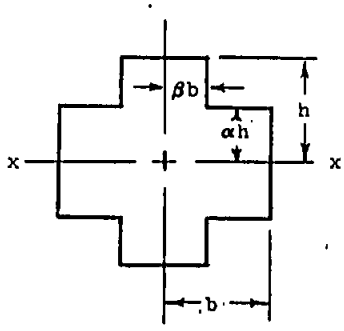

Grumman

VALUES OF EXPONENT, n, FOR USE IN INTERACTION CURVES OF B.3.32-7

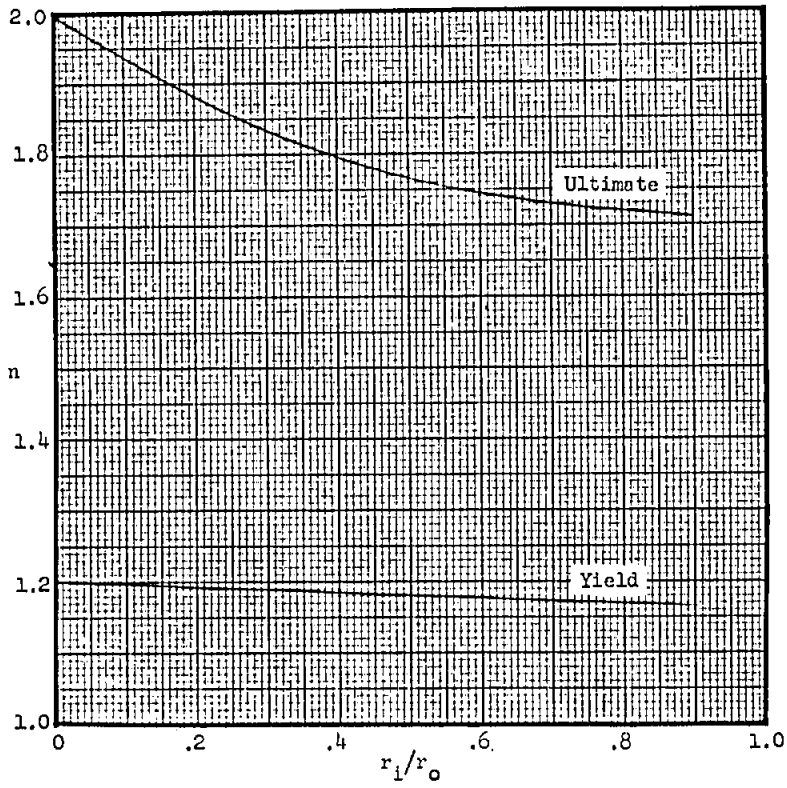

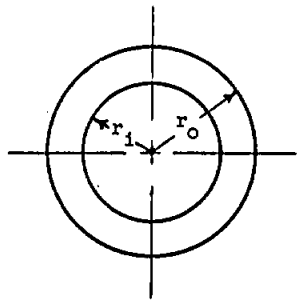

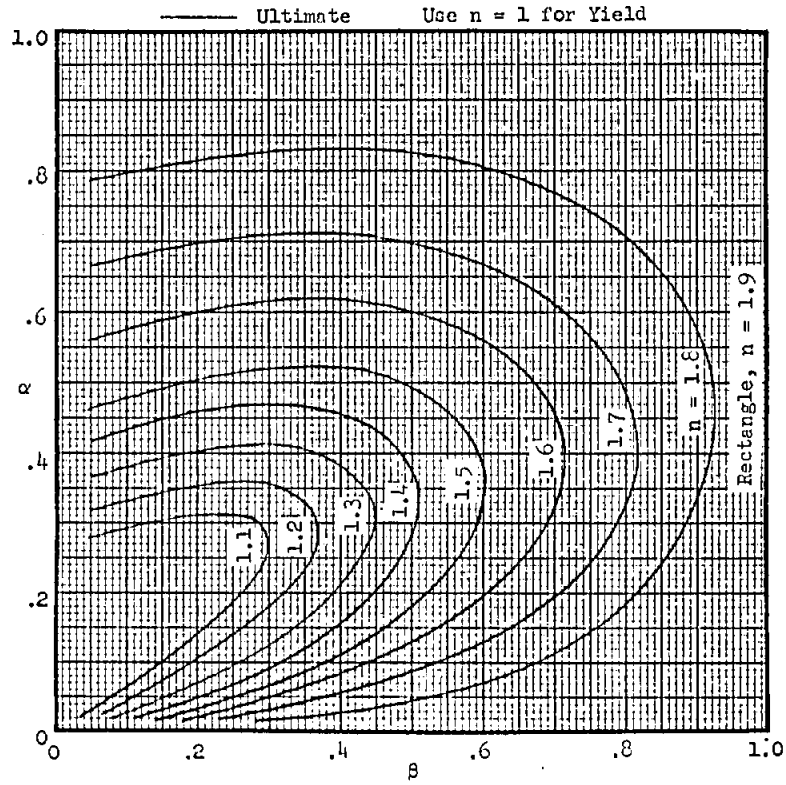

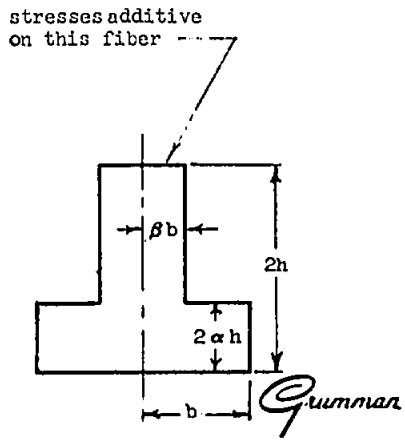

Grumman

COLUMN BUCKLING COEFFICIENTS FOR VARIOUS LOADING AND END CONDITIONS

$$P_{cr} = \frac{C\ \Pi^2\ E_T\ I}{L^2}$$

E_T = Tangent Modulus of Elasticity
I = Column Moment of Inertia
L = Column Length

COLUMN LOAD AND END CONDITION	C	COLUMN LOAD AND END CONDITION	C
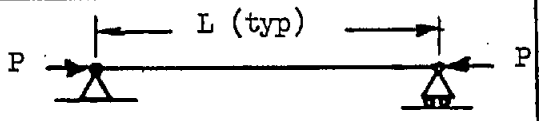	1.00	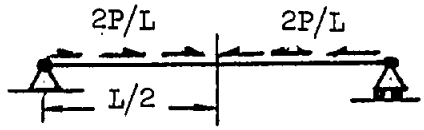	3.19
	2.05	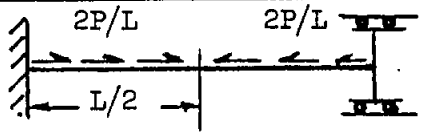	7.68
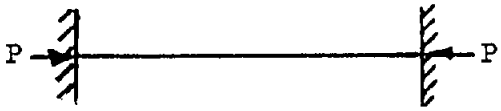	4.00	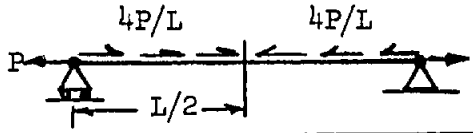	16.66
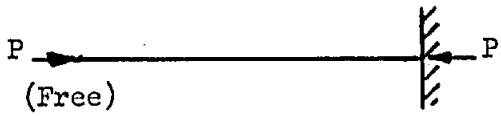	0.25	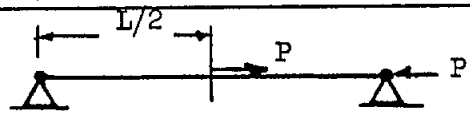	1.89
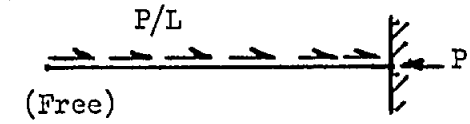	0.79	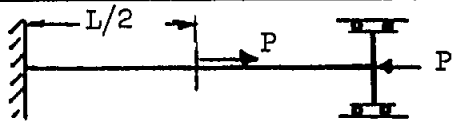	7.54
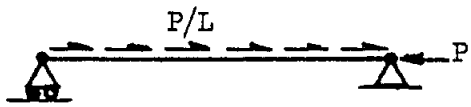	1.90	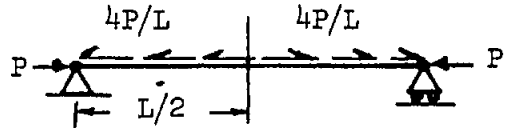	2.27
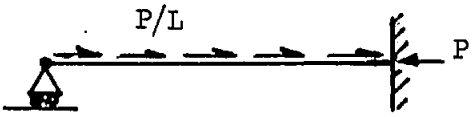	5.32	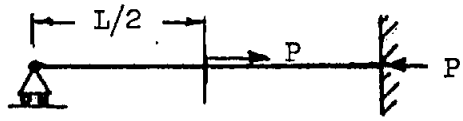	4.80
	3.05	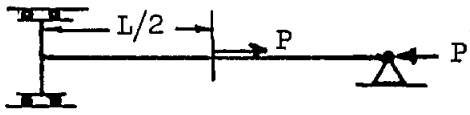	3.13
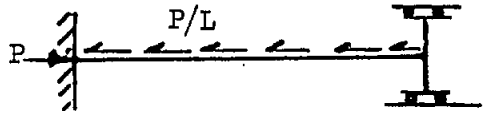	7.57	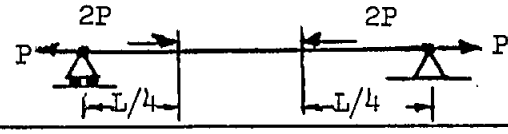	8.93

Note: All loads are applied concentrically.
The buckling load is the maximum compression load in the column.

COLUMN BUCKLING COEFFICIENTS FOR VARIOUS LOADING AND END CONDITIONS

$$P_{cr} = \frac{C \quad \Pi^2 \quad E_T \quad I}{L^2}$$

E_T = Tangent Modulus of Elasticity
I = Column Moment of Inertia
L = Column Length

COLUMN LOAD AND END CONDITION	C	COLUMN LOAD AND END CONDITION	C
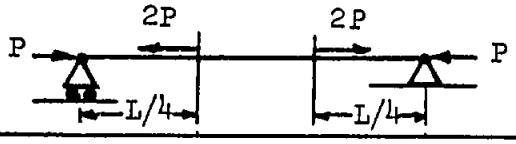	1.43		

Note: All loads are applied concentrically.
The buckling load is the maximum compression load in the column.

COLUMN CURVES FOR ALUMINUM ALLOYS

The material previously contained on this page may now be found in Section B1.

BUCKLING OF STEPPED, PIN-ENDED COLUMNS

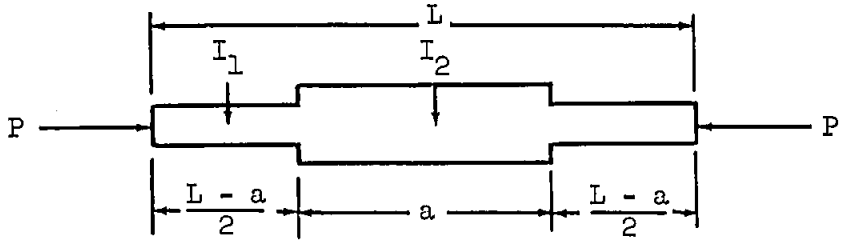

$$P_{cr} = m \frac{\pi^2}{L^2} (E_t I)_1$$ where E_t is the tangent modulus

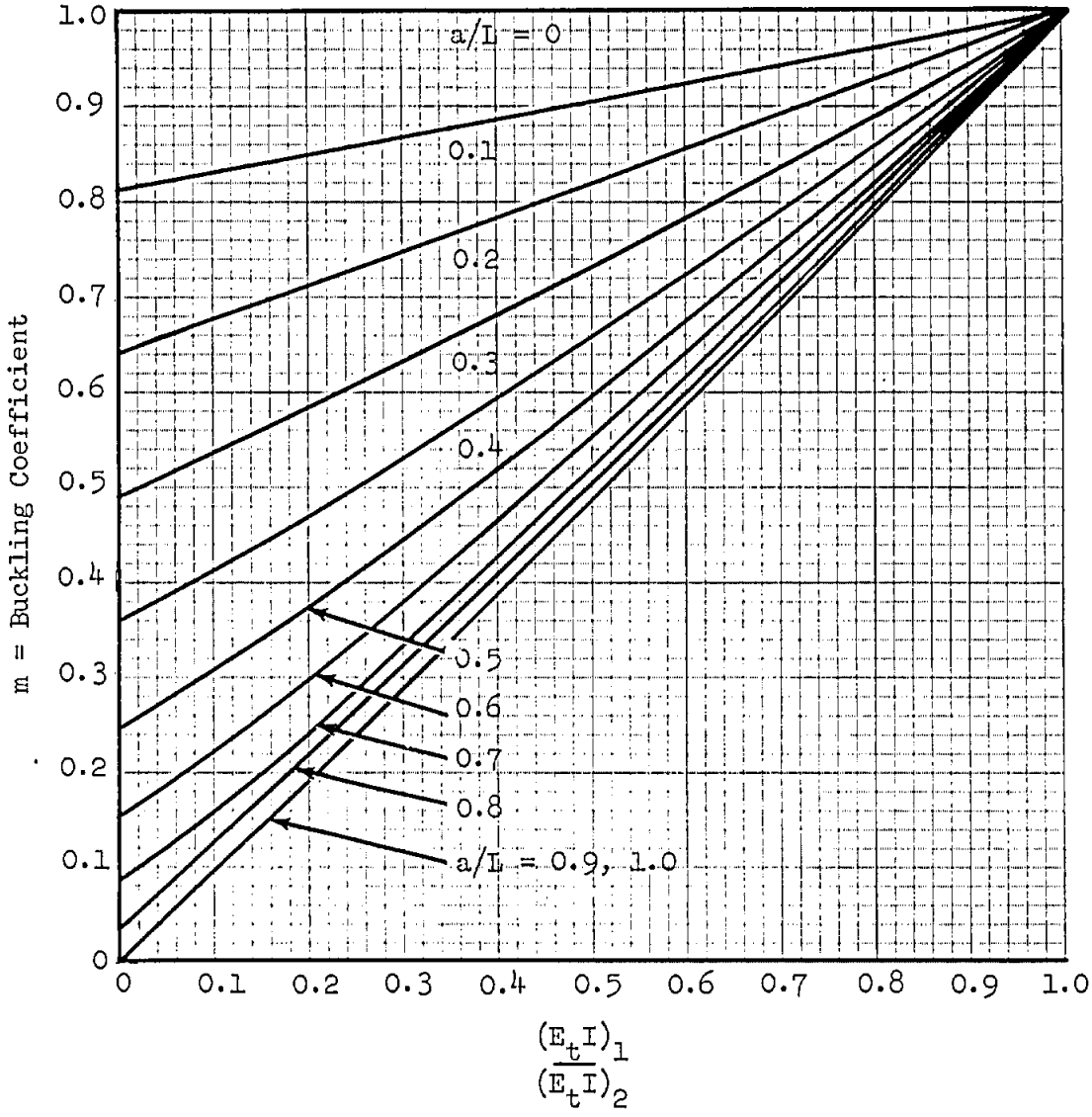

Ref: Timoshenko, "Theory of Elastic Stability"

BUCKLING OF STEPPED, PIN-ENDED COLUMNS

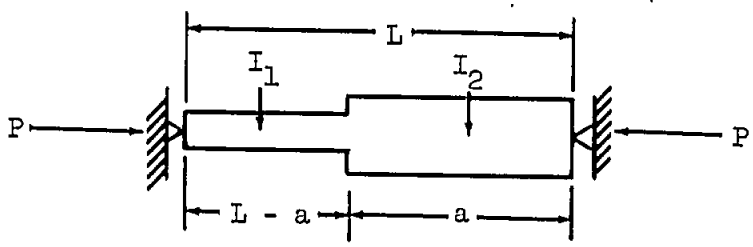

$$P_{cr} = \frac{\pi^2}{m} \frac{(E_t I)_1}{L^2}$$

where E_t is the tangent modulus

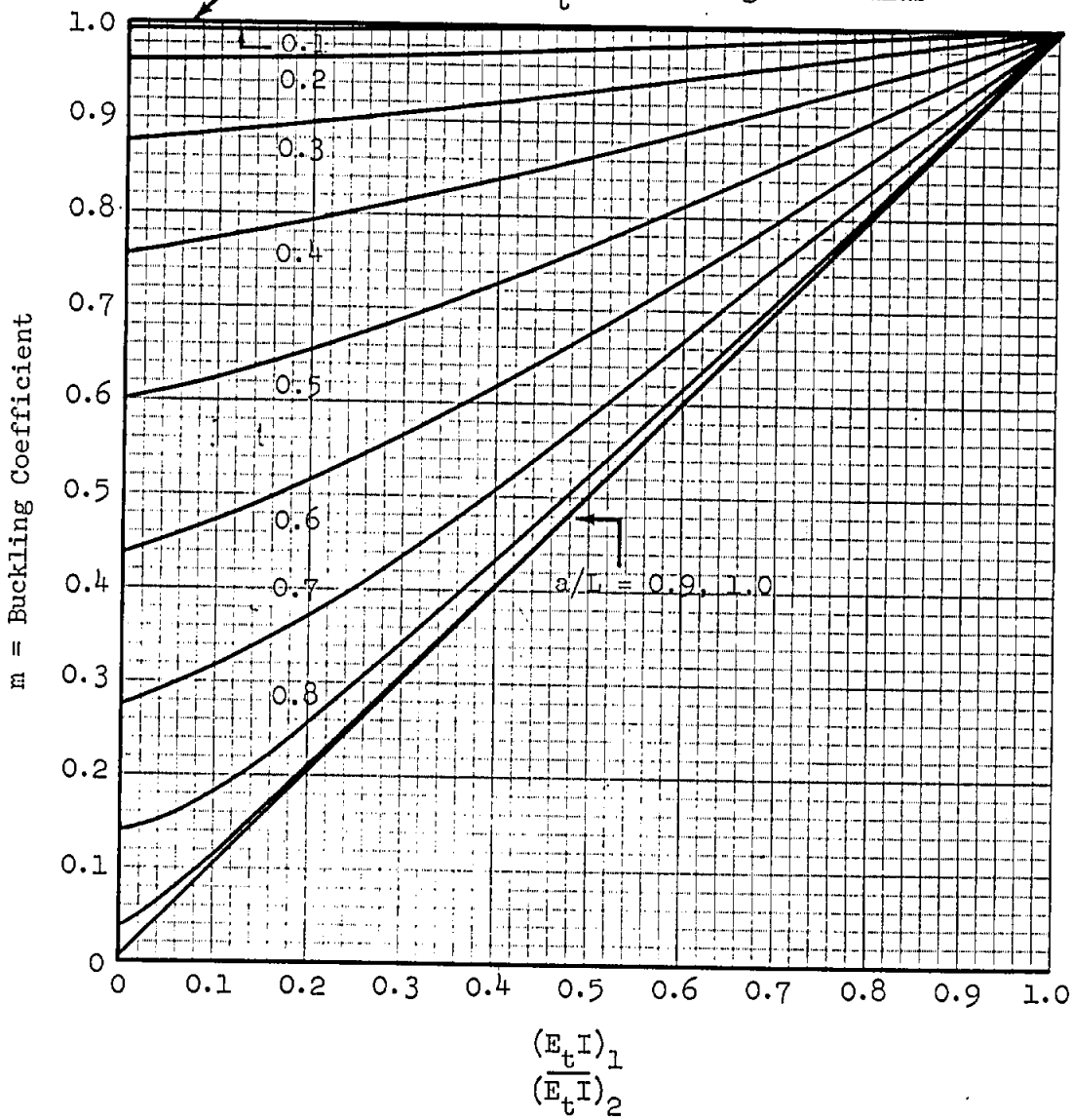

Ref: Timoshenko, "Theory of Elastic Stability"

BUCKLING OF STEPPED, PIN-ENDED COLUMNS

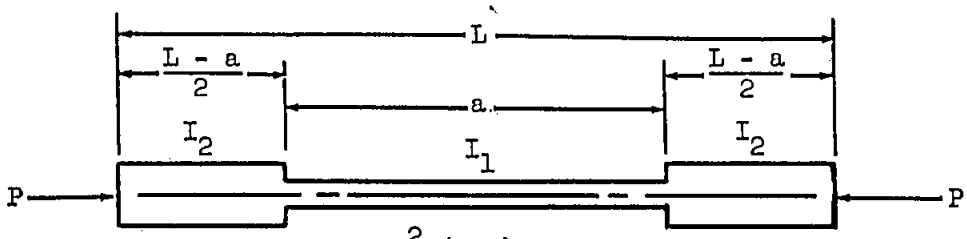

$$P_{cr} = \frac{\pi^2}{m} \frac{(E_t I)_1}{L^2}$$ where E_t is the tangent modulus

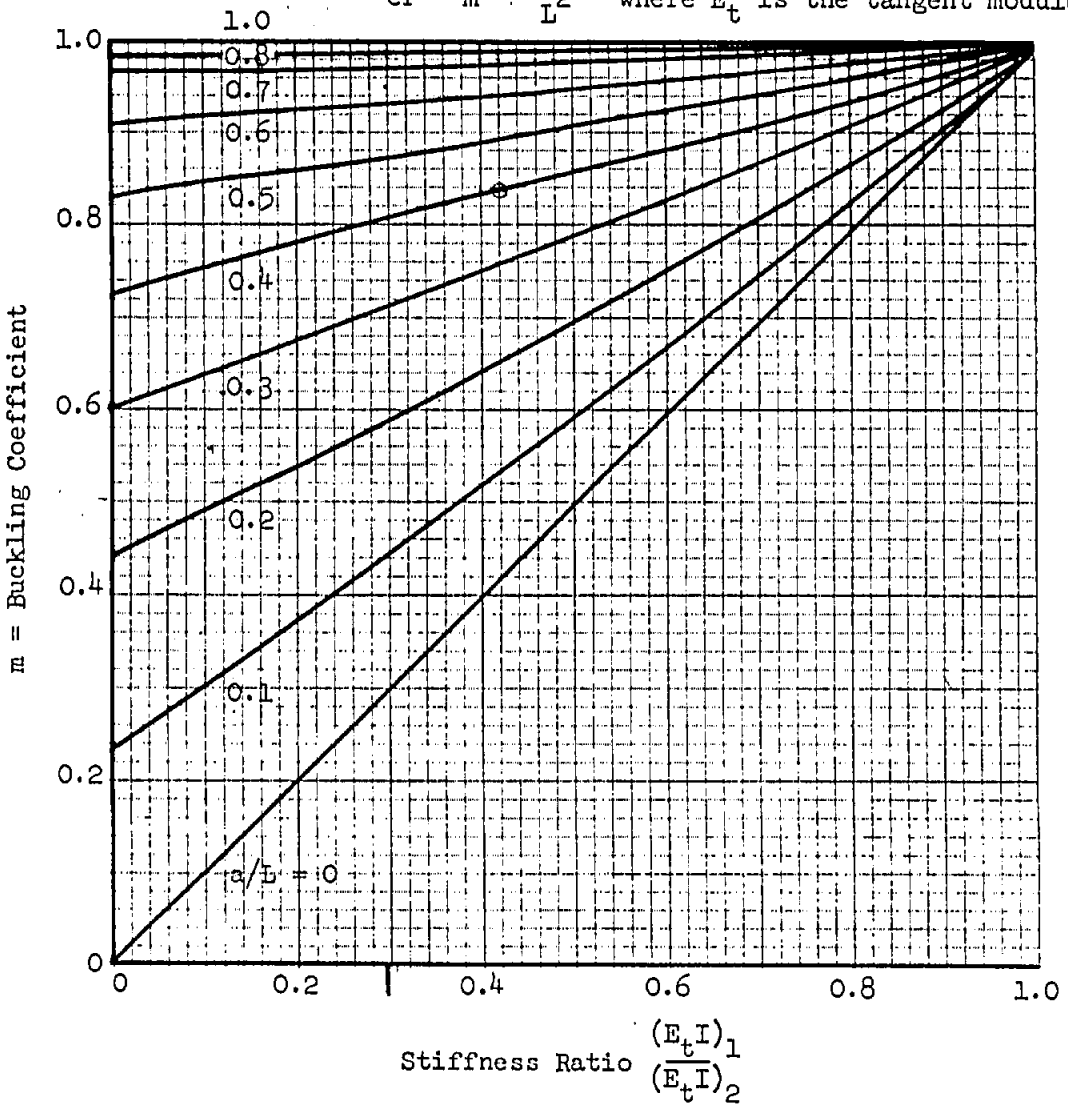

Ref: Timoshenko, Theory of Elastic Stability

Grumman

BUCKLING OF TAPERED PIN-ENDED COLUMNS
END PORTIONS TAPERED IN WIDTH AND HEIGHT

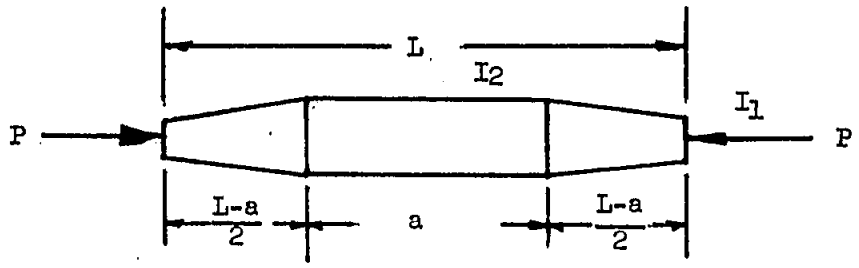

$$P_{cr} = \frac{C\,\Pi^2\,E_t\,I_2}{L^2} \qquad (E_t = \text{Tangent Modulus})$$

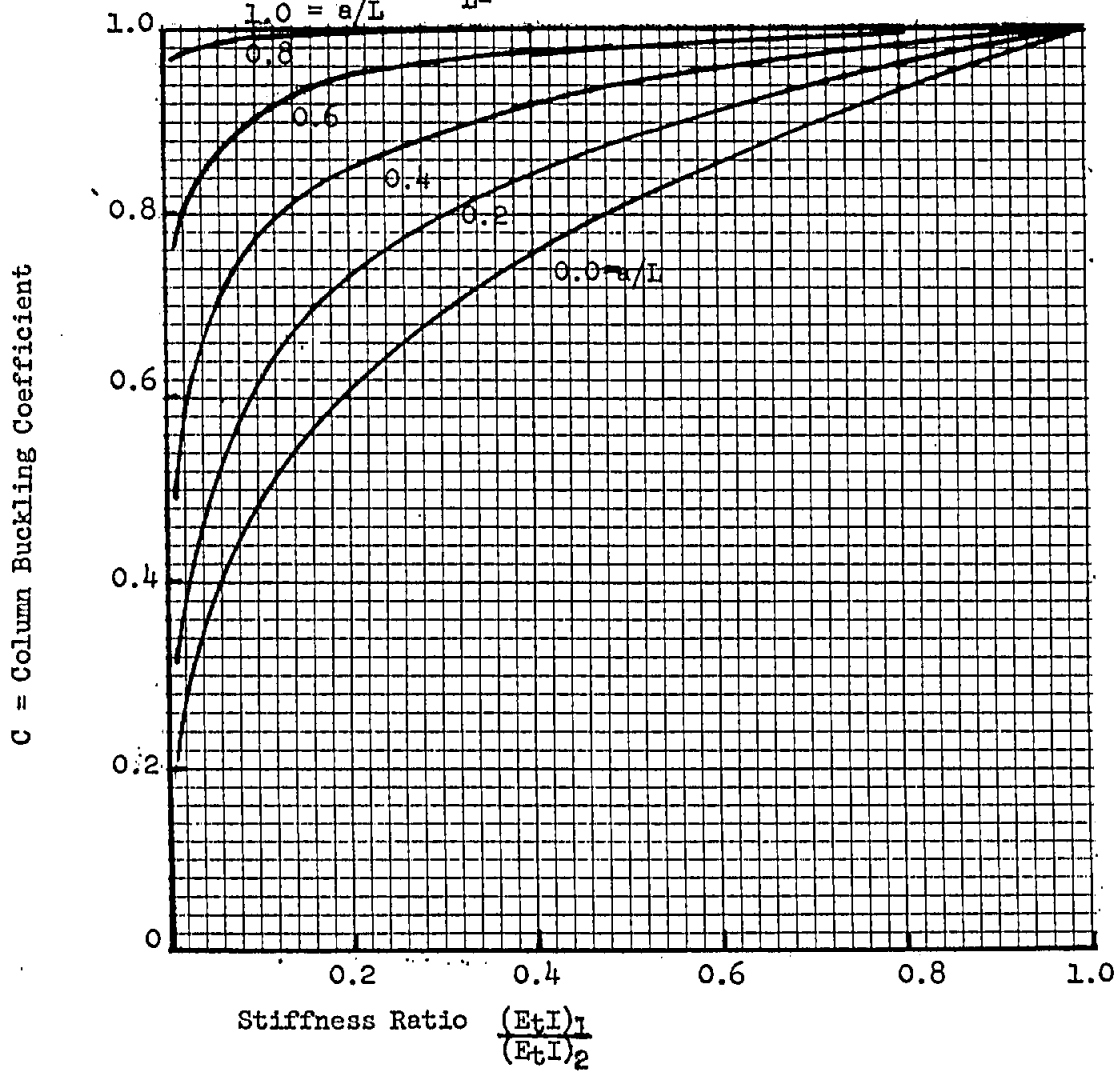

Ref: Roark, Table XV Case 24

BUCKLING OF TAPERED PIN-ENDED COLUMNS
END PROTIONS TAPERED IN WIDTH ONLY

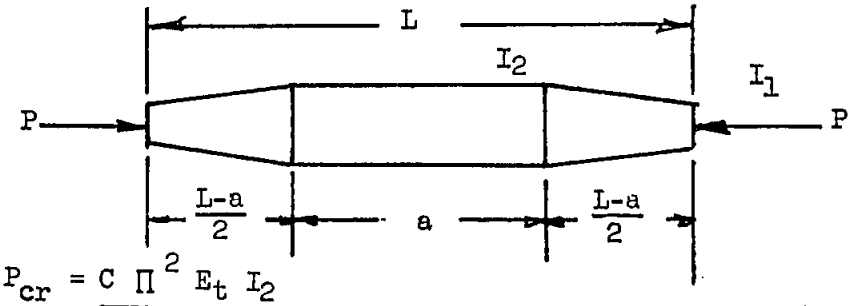

$$P_{cr} = \frac{C \Pi^2 E_t I_2}{L^2}$$

(E_t = Tangent Modulus)

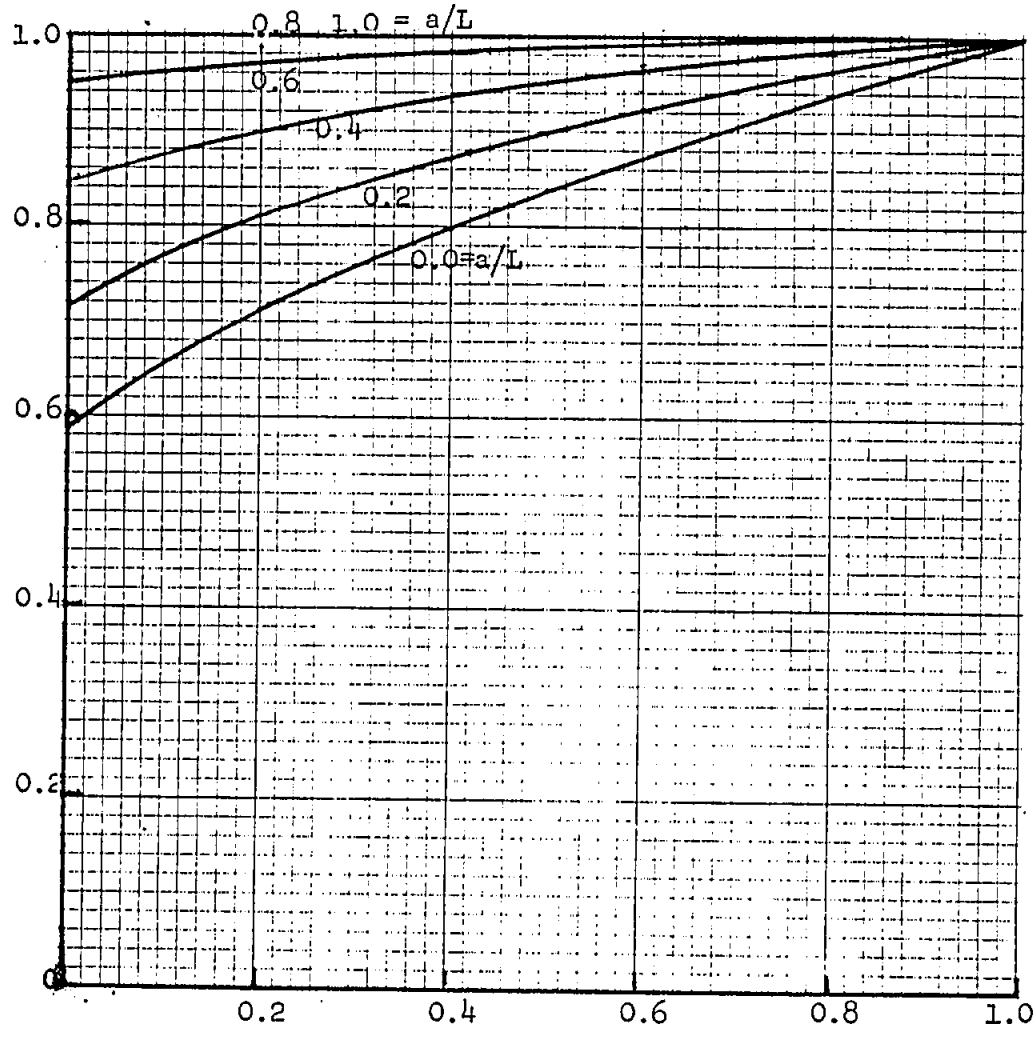

Ref: Roark, Table XV, Case 21

BUCKLING OF TAPERED FIXED-END COLUMNS
END PORTIONS TAPERED IN WIDTH AND HEIGHT

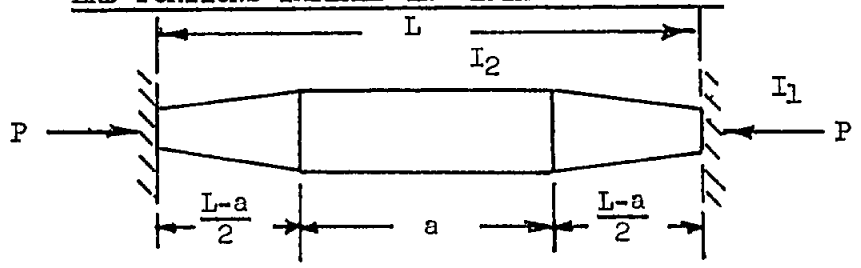

$$P_{cr} = \frac{C \Pi^2 E_t I_2}{L^2} \qquad (E_t = \text{Tangent Modulus})$$

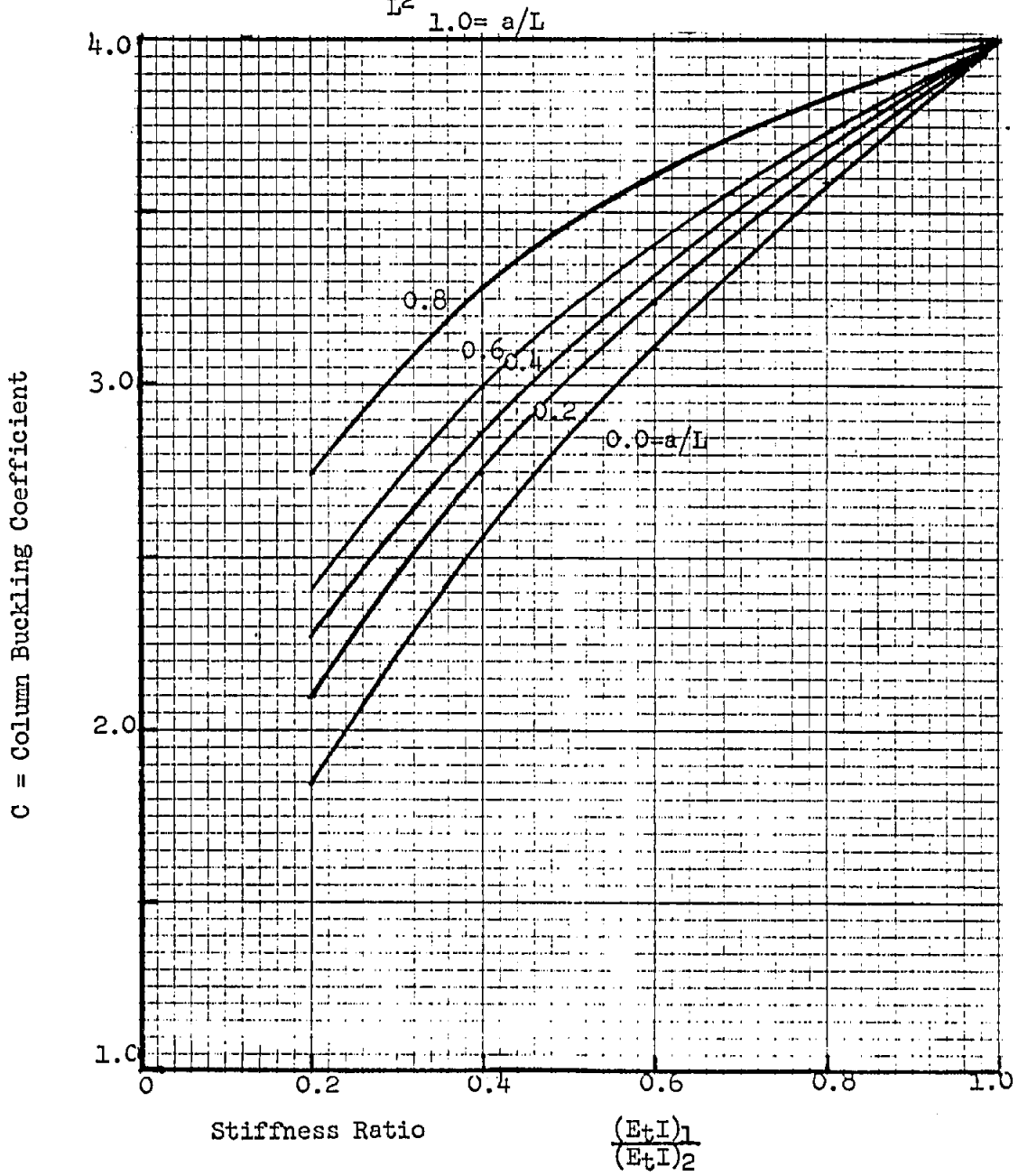

BUCKLING OF TAPERED FIXED-END COLUMNS
END PORTIONS TAPERED IN WIDTH ONLY

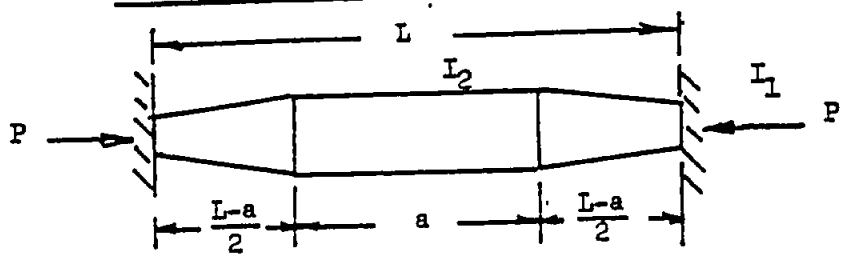

$$P_a = \frac{C\,\Pi^2\,E_t\,I_2}{L^2}$$

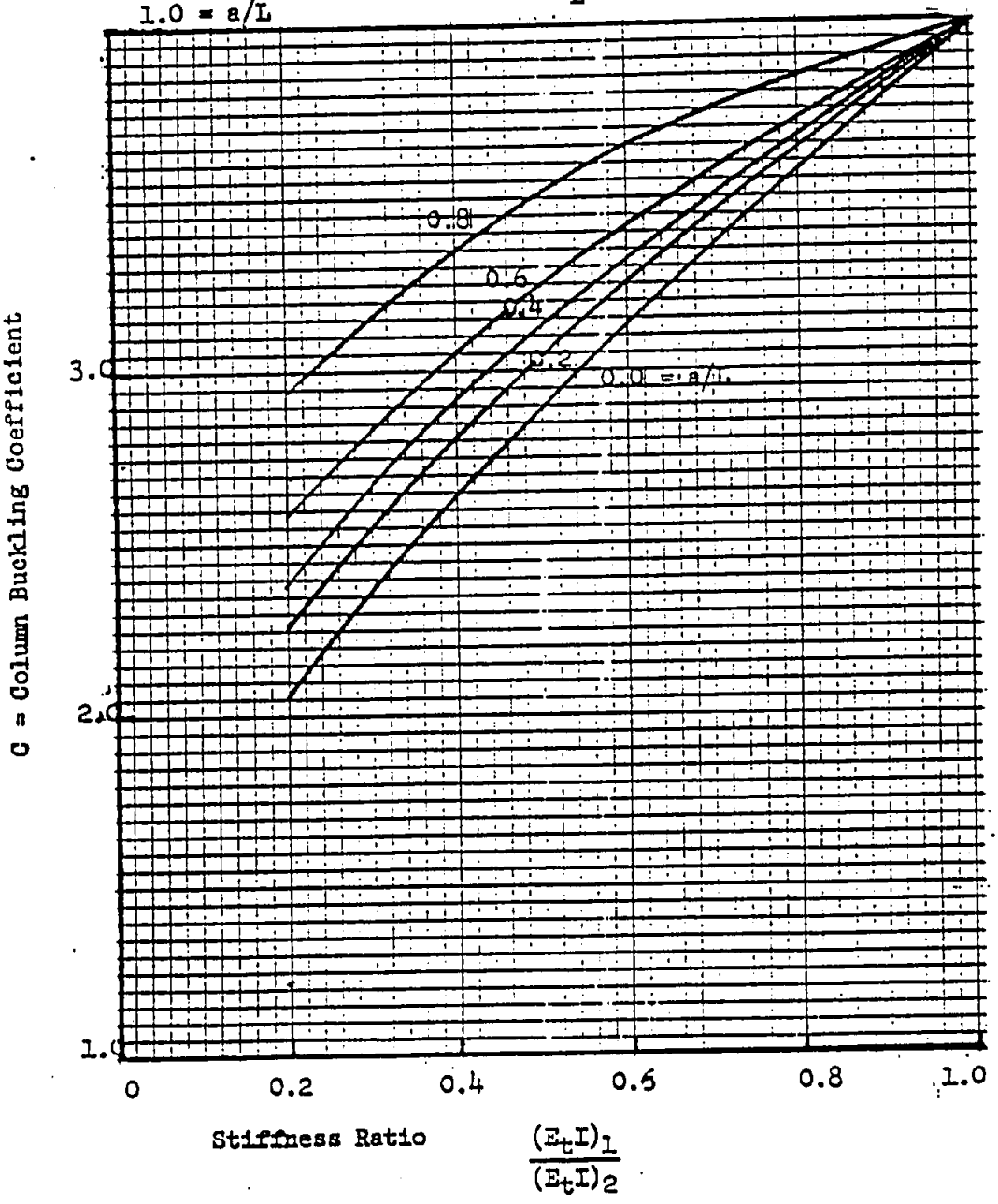

BUCKLING OF STEPPED, FIXED-ENDED COLUMNS

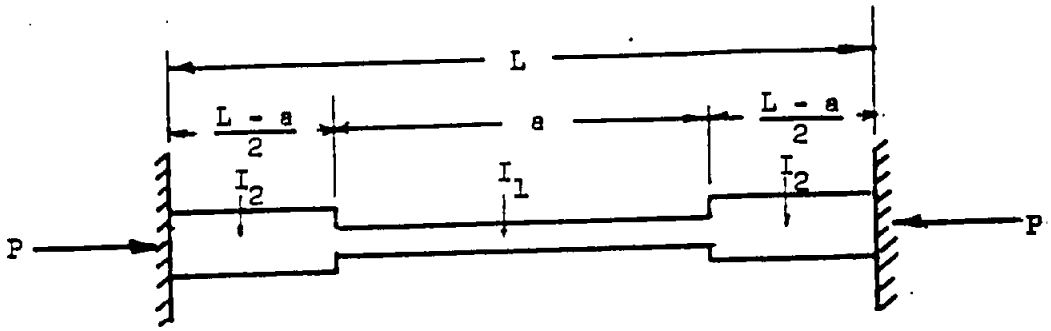

$$P_{cr} = \frac{4\pi^2 EI_1}{mL^2}$$

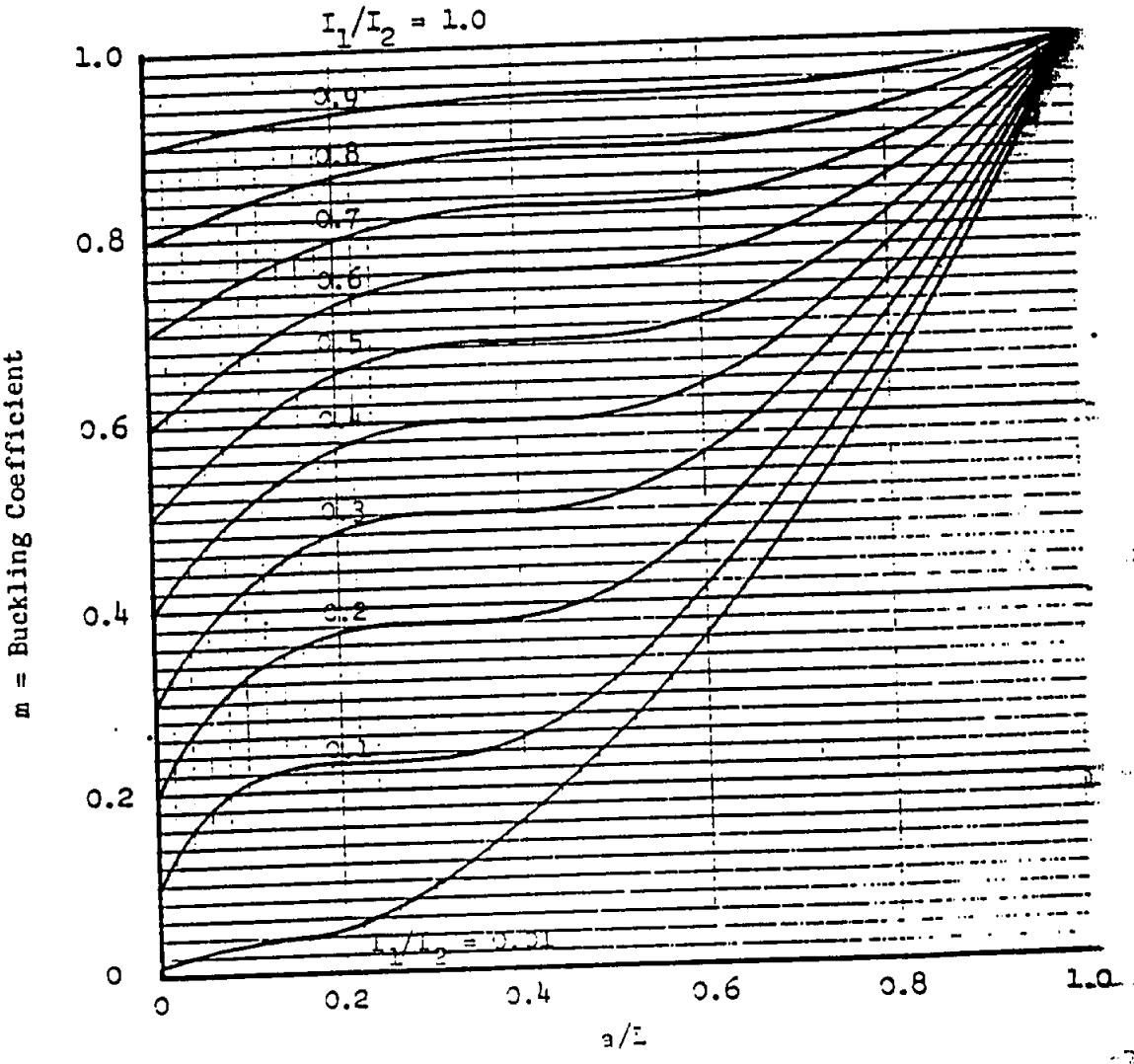

BUCKLING OF STEPPED, FIXED-ENDED COLUMNS

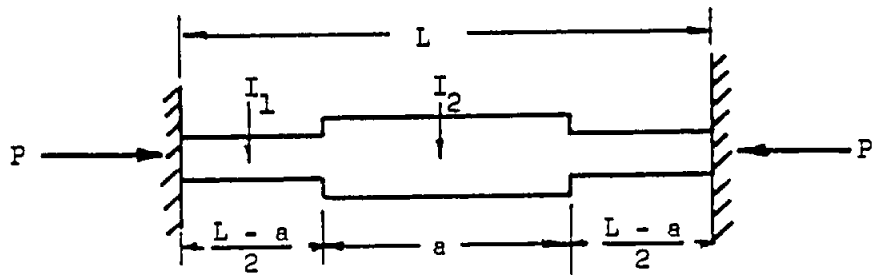

$$P_{cr} = \frac{4\pi^2 EI_1}{mL^2}$$

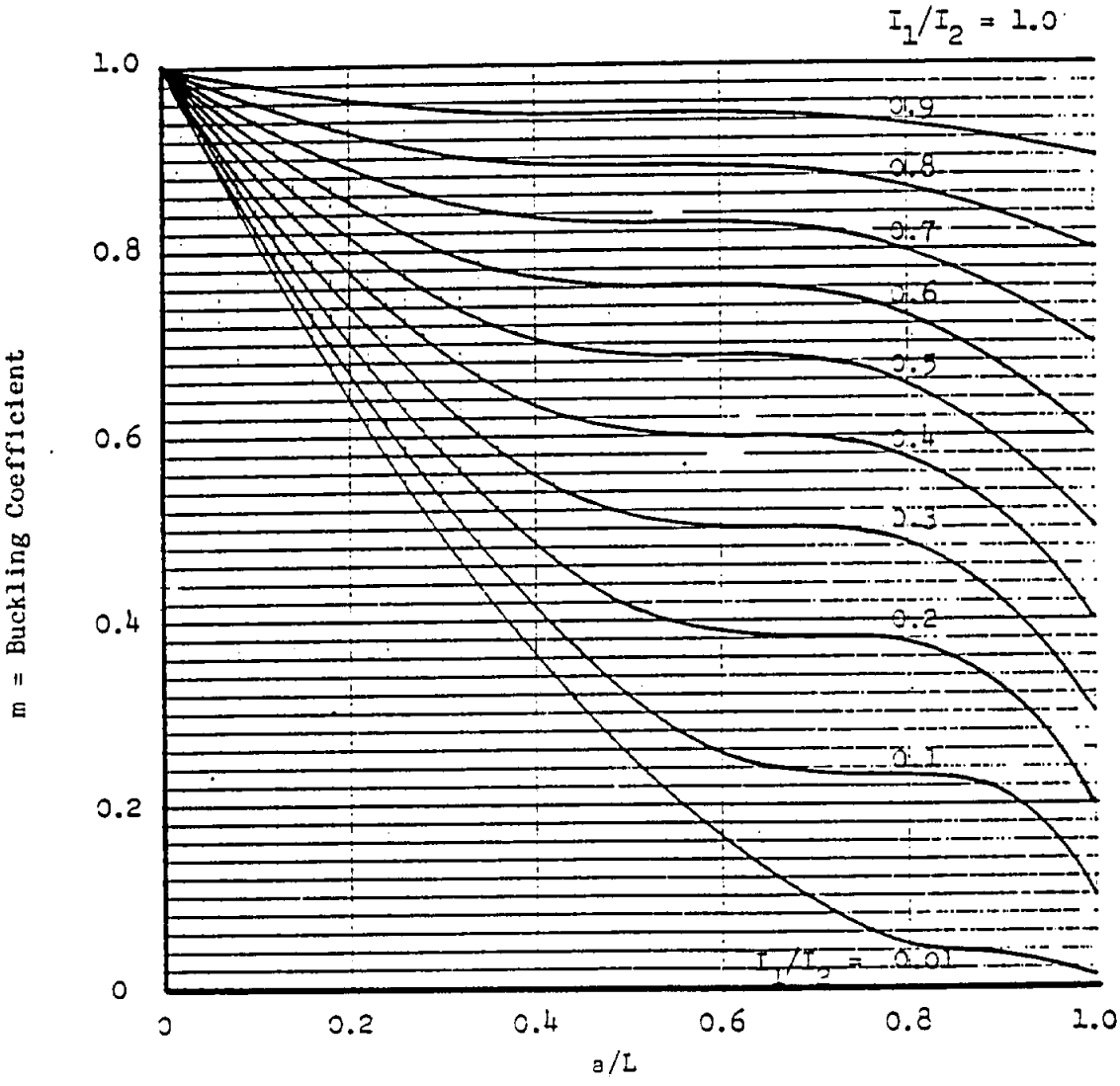

BUCKLING OF STEPPED, PIN-FIXED-ENDED COLUMNS

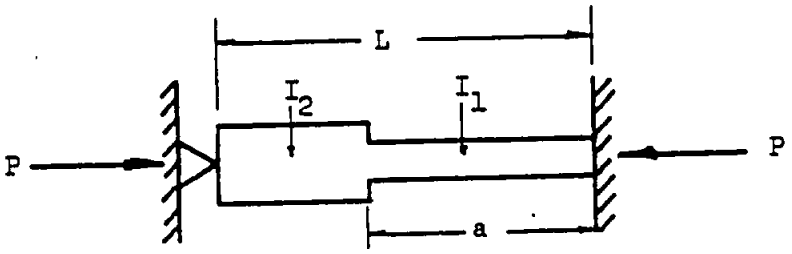

$$P_{cr} = \frac{2.0454\pi^2 EI_1}{mL^2}$$

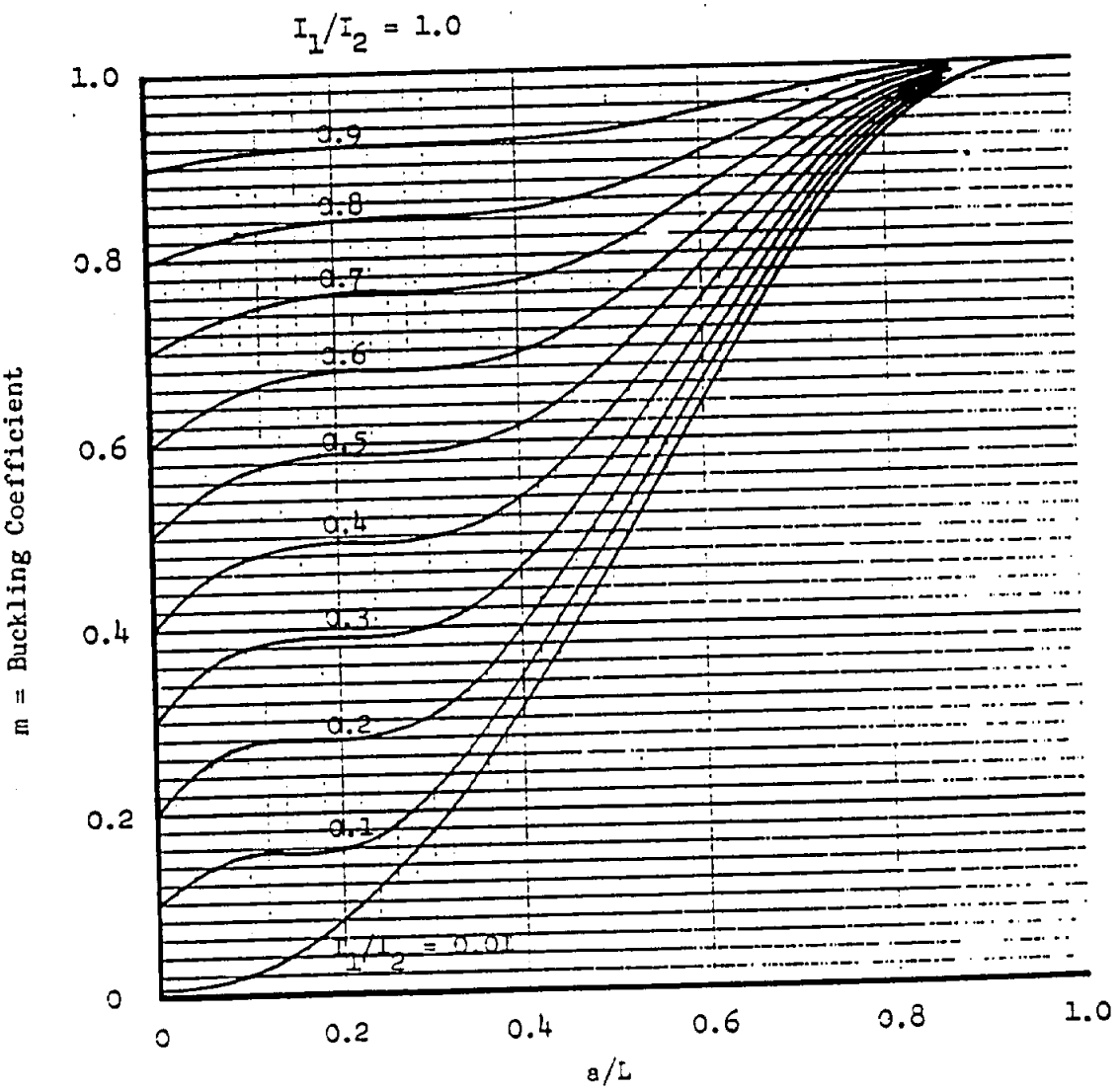

BUCKLING OF STEPPED, PIN-FIXED-ENDED COLUMNS

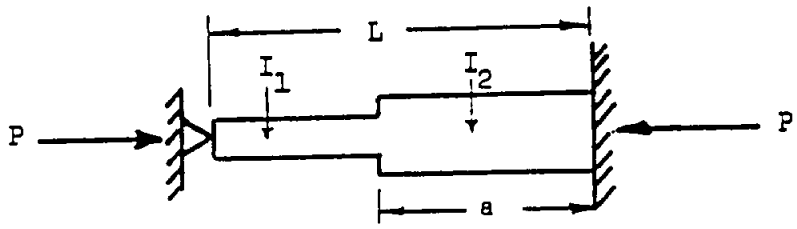

$$P_{cr} = \frac{2.0454\pi^2 EI_1}{mL^2}$$

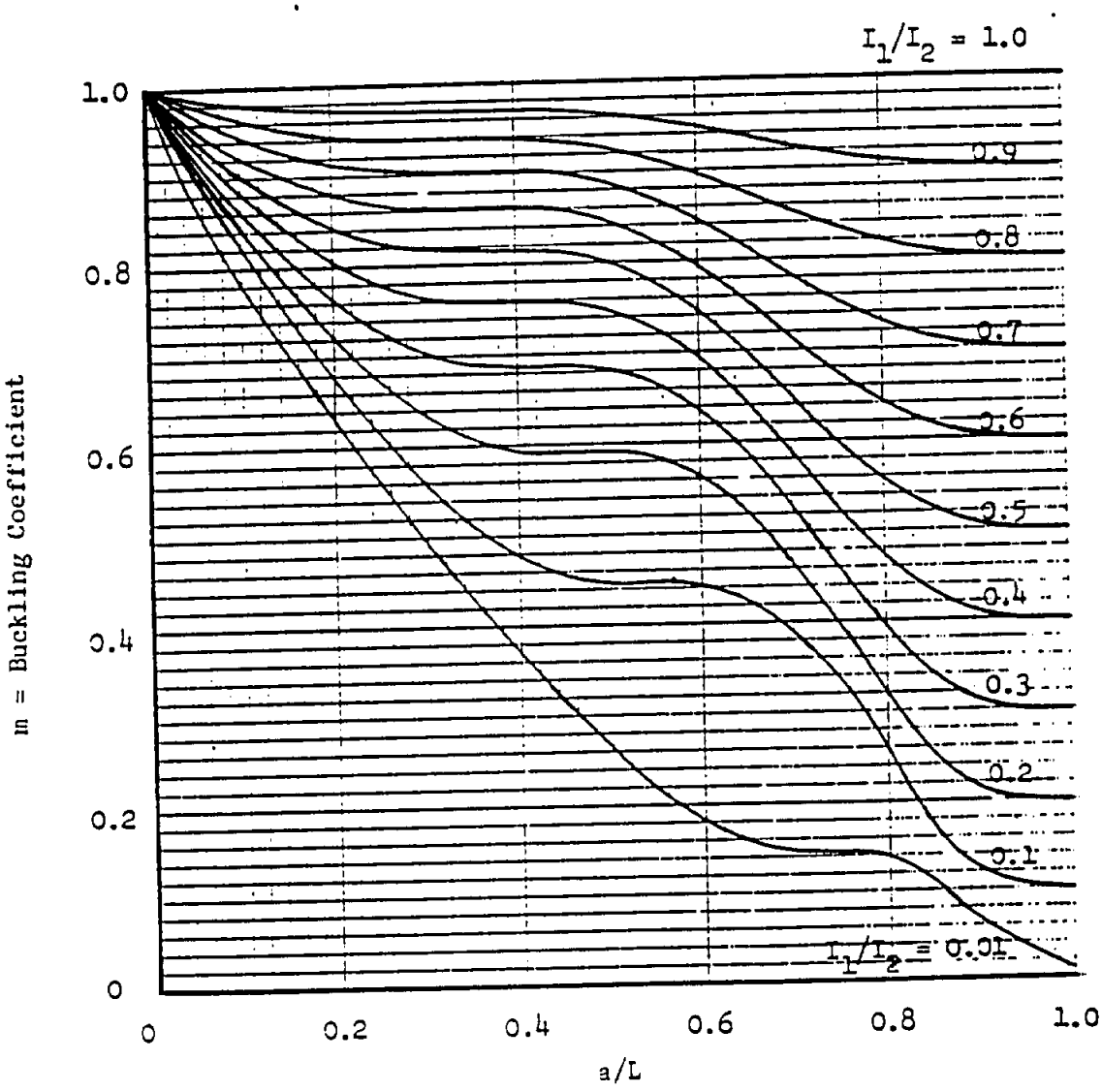

BUCKLING OF STEPPED, FIXED-ENDED COLUMNS

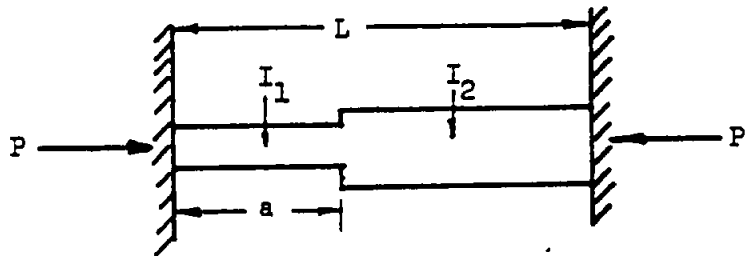

$$P_{cr} = \frac{4\pi^2 E I_1}{mL^2}$$

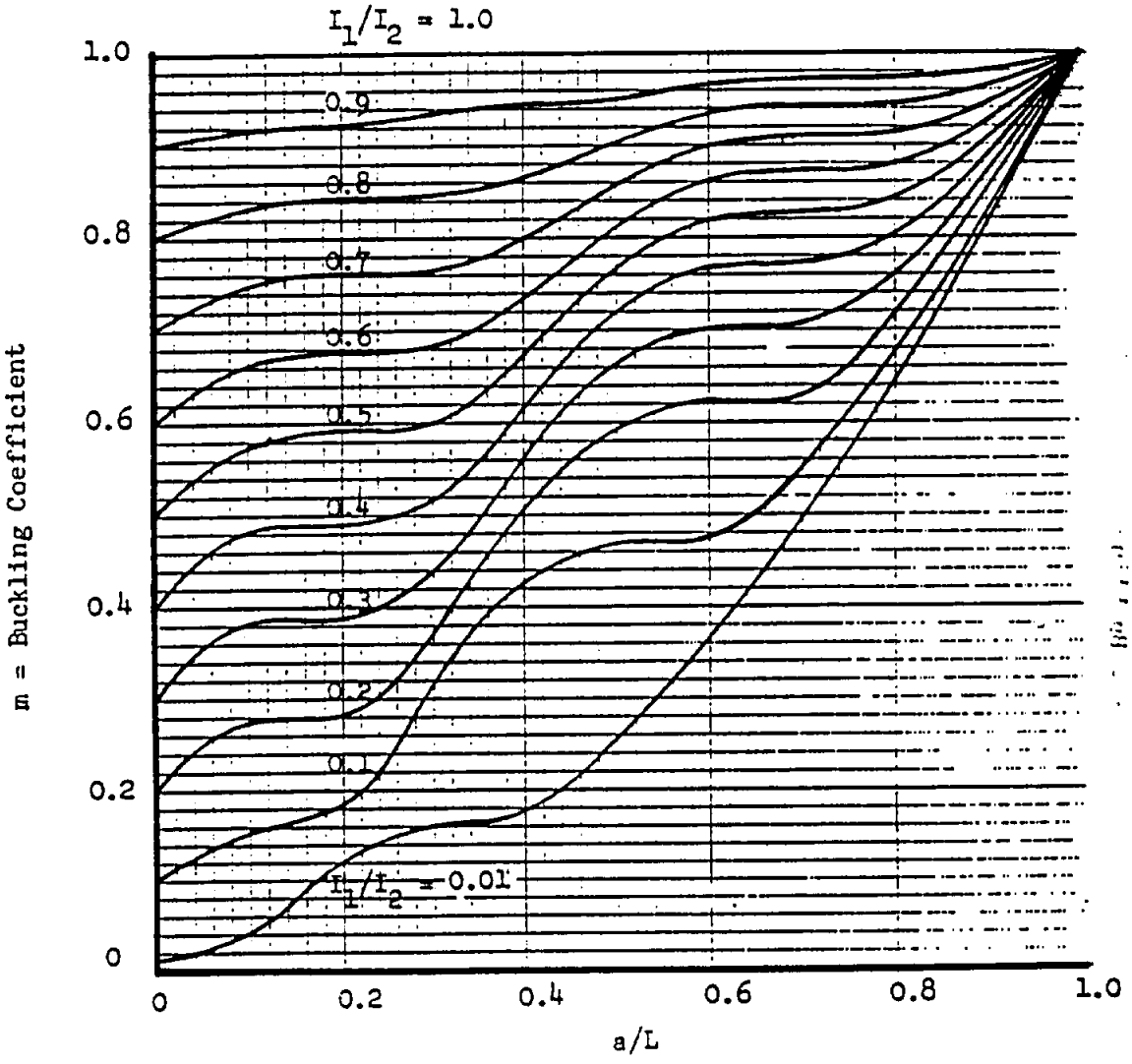

COLUMN ON AN ELASTIC FOUNDATION

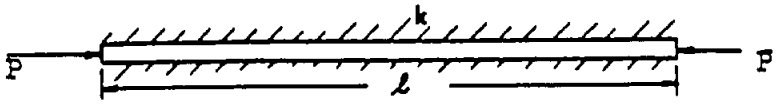

ℓ = Length of column (in)
k = Modulus of elastic foundation (lbs/in^2)
EI = Flexural rigidity (lbs-in^2)
P_{Eu} = Euler buckling load, π^2 EI/ℓ^2 (lbs)
P_{cr} = Buckling load (lbs)
n = number of waves into which column buckles (n = 1,2,3...)

For columns with discrete spring supports a minimum of 3n equally spaced is required.

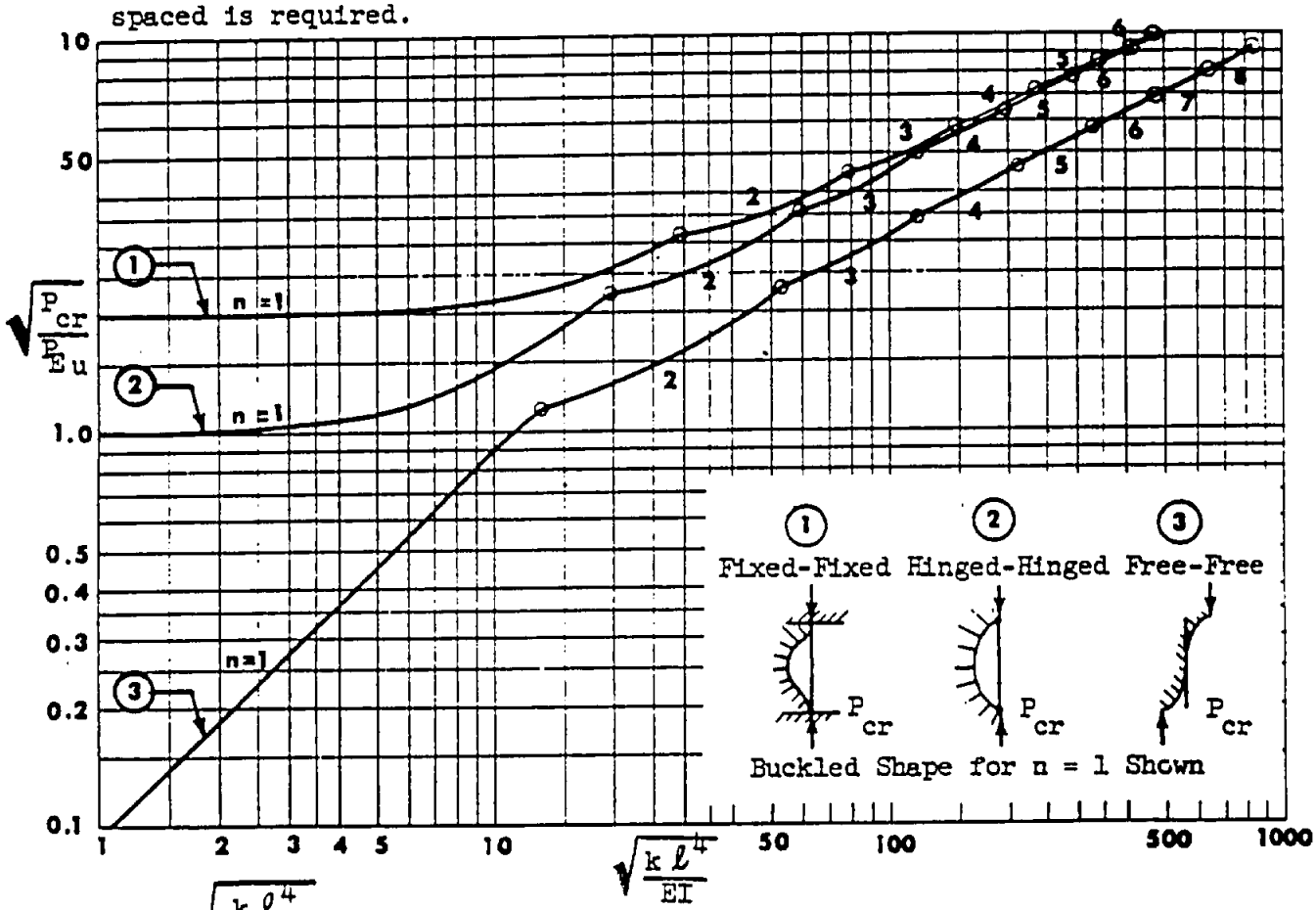

NOTE: For $\sqrt{\frac{k\ell^4}{EI}} > 500$, use the following approximations:

End Conditions	P_{cr}	n
(1) Fixed-Fixed	$2\sqrt{kEI}$	$\sqrt{1 + \frac{1}{\pi^2}\sqrt{\frac{k\ell^4}{EI}}}$
(2) Hinged-Hinged	$2\sqrt{kEI}$	$-\frac{1}{2} + \sqrt{\frac{1}{4} + \frac{1}{\pi^2}\sqrt{\frac{k\ell^4}{EI}}}$
(3) Free-Free	$\sqrt{kEI}$	$\sqrt{\frac{3}{4\pi^2}\sqrt{\frac{k\ell^4}{EI}}}$

Reference:
Hetenyi, M.: "Beams on Elastic Foundation", pages 141-150.

BUCKLING OF UNIFORM COLUMNS WITH COMPRESSIVE OR TENSILE END LOADS & APPLIED SHEAR LOAD - PIN-ENDED

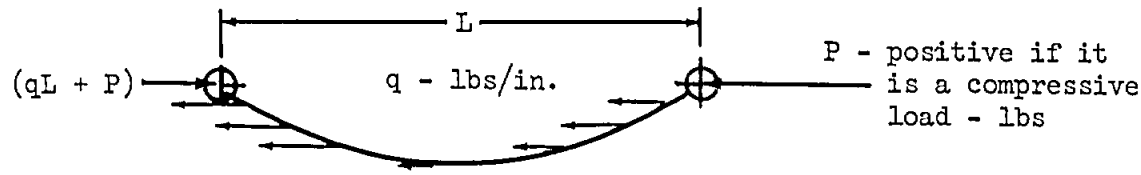

$$(qL + P)_{cr} = \frac{\pi^2 EI}{mL^2}$$ EI is constant

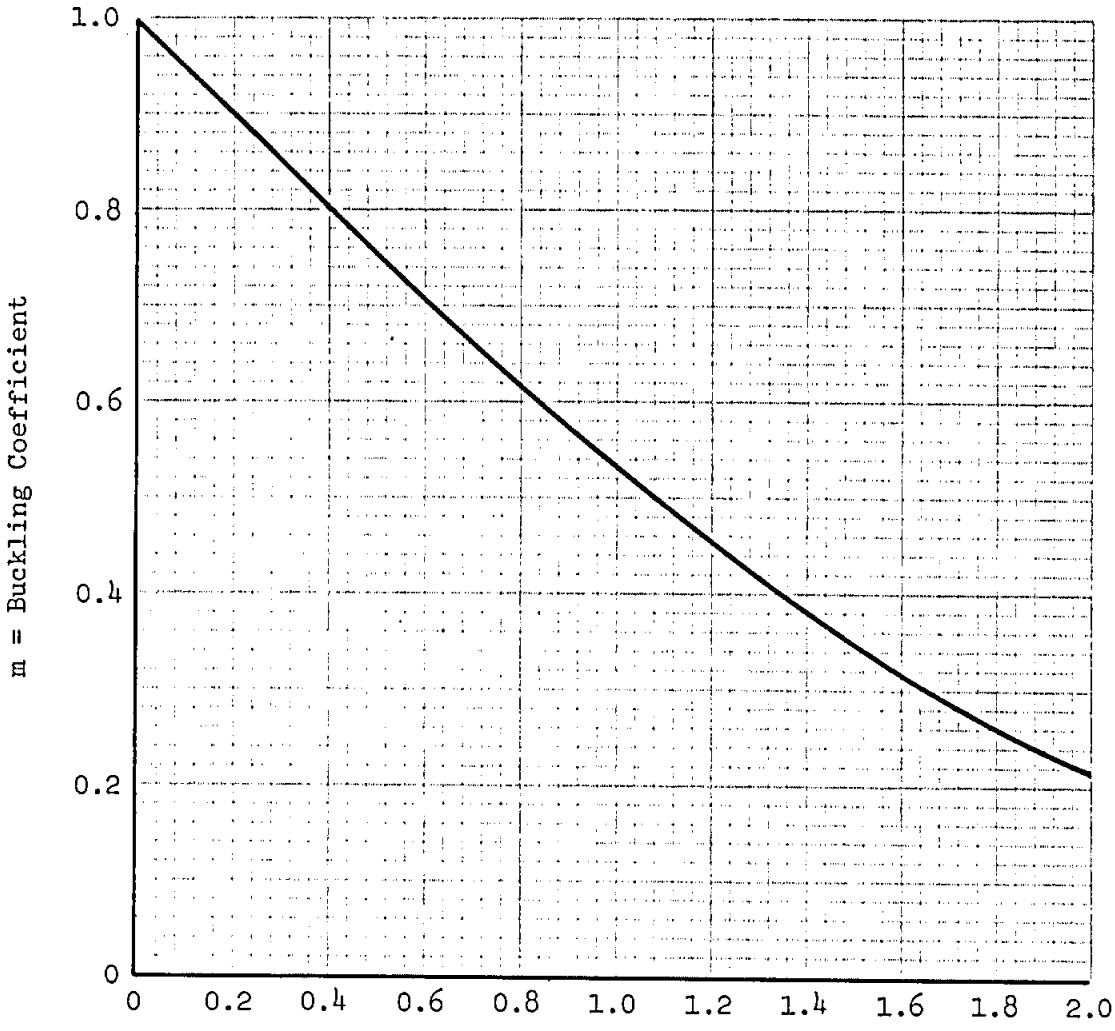

$$\frac{\text{Shear Load}}{\text{Largest Comp. Load}} = \frac{qL}{(qL + P)}$$

ELASTIC BUCKLING LOAD FOR COLUMNS WITH VARYING AXIAL LOAD

Introduction

The problem of column buckling for the case of varying axial load is frequently encountered in such structures as beam or bulkhead capstrips, longerons, stiffeners, etc. This type of column loading has also been used for the determination of the allowable compressive stress at the edge of access holes in shear webs. Certain assumptions, of course, are required in order to idealize the shear web with access holes to a straight pin-ended column.

Discussion

The buckling load is given on pages B3.44.32-2, 3, and -4 for several combinations of axial load variations. The buckling load is presented as a fixity coefficient, C, to multiply the conventional pin-ended column buckling load equation.

The buckling loads were determined by the use of the numerical analysis procedure commonly refered to as the "Newmark Method". This procedure is described in References a and b. Because the analysis is based on an iterative scheme, the exact answer as given by a closed form solution cannot always be obtained. The factors presented are the result of a reasonable and practical number of iterations and are slightly conservative when compared to the results from available closed form solutions.

The use of the coefficients is adequately described in the figures and requires no added description here except to point out that P_{cr} is the maximum value of compression load at any point in the column at buckling.

Reference:

(a) Newmark, N. M., "Numerical Procedure for Computing Deflections, Moments and Buckling Loads", Trans. ASCE, vol. 108, p 1161, 1943.

(b) SACP-16, Page G1.01-1 and-2 of this manual.

FIXITY COEFFICIENTS FOR COLUMNS UNDER CONCENTRATED AXIAL & DISTRIBUTED SHEAR LOADS

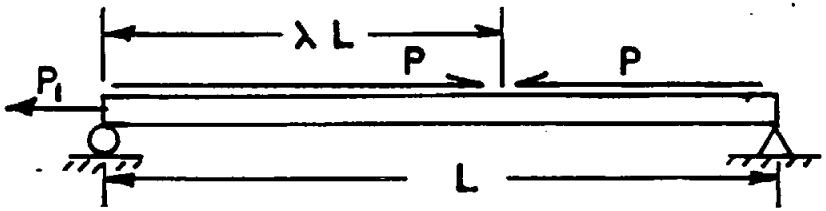

Basic Assumptions

- Column is pinned at each end
- EI is constant
- Applied loads are positive as shown in sketch
  - P_1 is a concentrated load and is reversible
  - Loads indicated by ⟶ ⟵ are applied by uniform shear flows and always act as shown

Procedure for Using Curves

- Determine K = P/(MAX COMPRESSION LOAD IN COLUMN)
- Determine C from curves or cross-plots thereof
- Determine critical buckling load

$$P_{CR} = C \frac{\Pi^2 EI}{L^2}$$

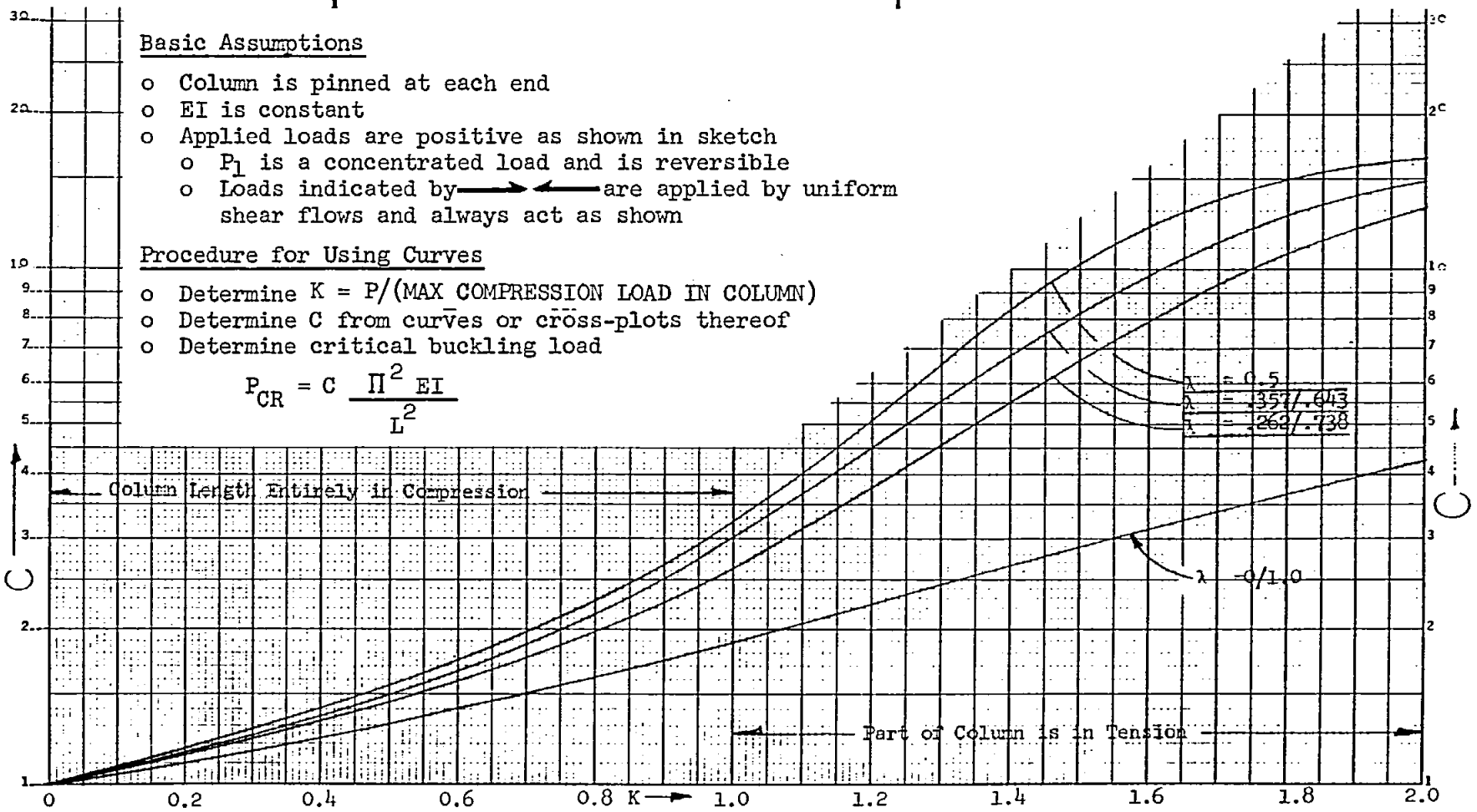

FIXITY COEFFICIENTS FOR COLUMNS UNDER CONCENTRATED AXIAL & DISTRIBUTED SHEAR LOADS

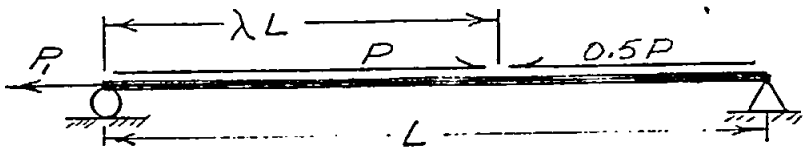

Basic Assumptions

- Column is pinned at each end
- EI is constant
- Applied loads are positive as shown in sketch
  - P_1 is a concentrated load and is reversible
  - Loads indicated by ⟶ ⟵ are applied by uniform shear flows and always act as shown

Procedure for Using Curves

- Determine K = P/(MAX COMPRESSION LOAD IN COLUMN)
- Determine C from curves or cross-plots thereof
- Determine critical buckling load

$$P_{cr} = C\frac{\pi^2 EI}{L^2}$$

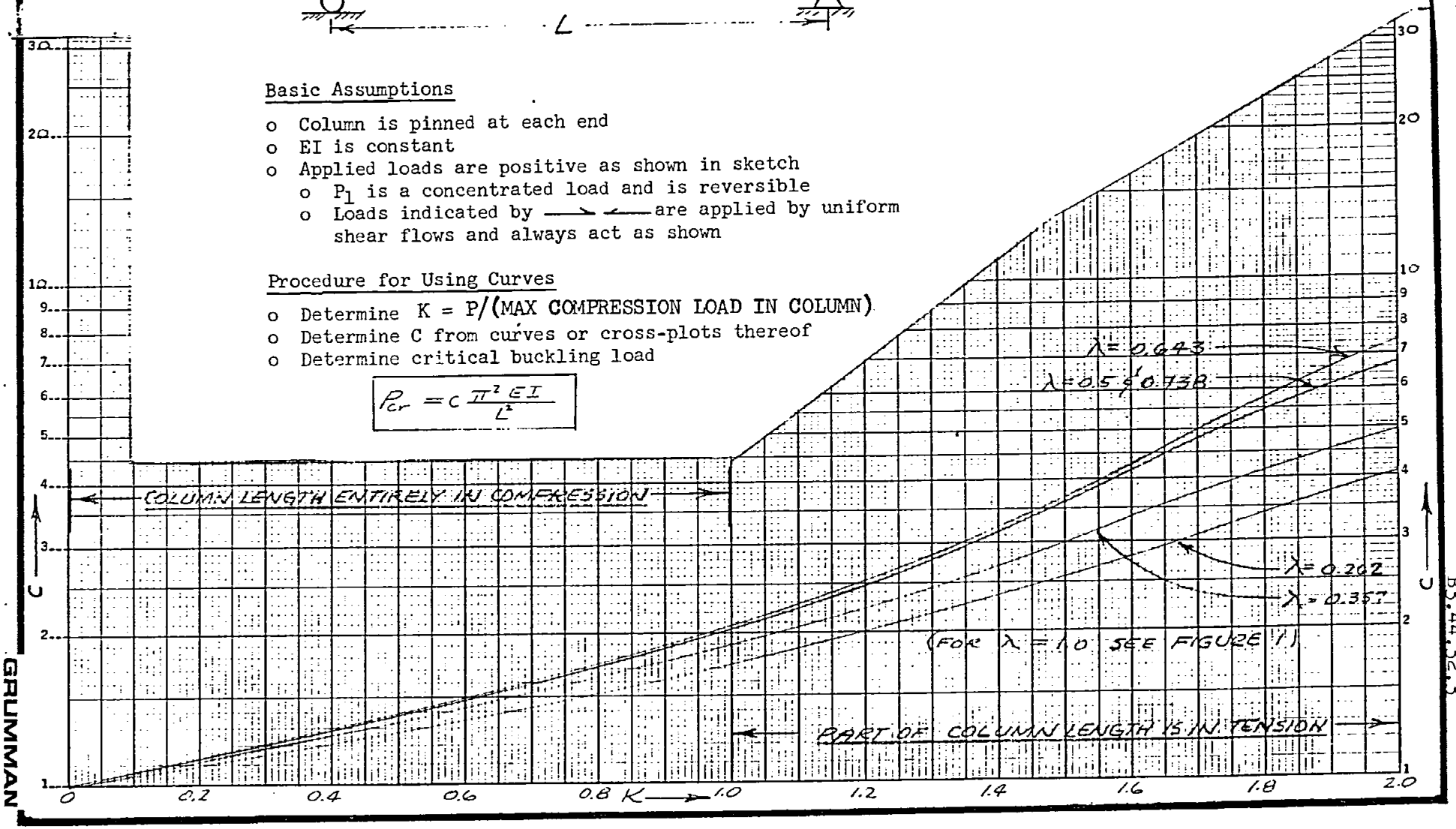

FIXITY COEFFICIENTS FOR COLUMNS UNDER CONCENTRATED AXIAL & DISTRIBUTED SHEAR LOADS

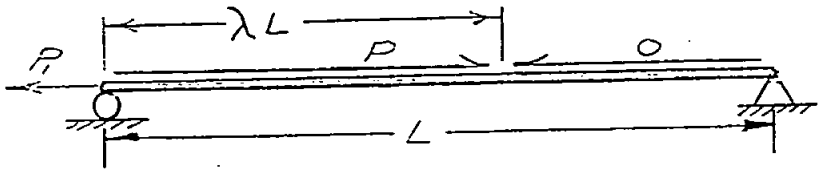

Basic Assumptions

- Column is pinned at each end
- EI is constant
- Applied loads are positive as shown in sketch
  - P_1 is a concentrated load and is reversible
  - Loads indicated by → ← are applied by uniform shear flows and always act as shown

Procedure for Using Curves

- Determine K = P/(MAX COMPRESSION LOAD IN COLUMN)
- Determine C from curves or cross-plots thereof
- Determine critical buckling load

$$P_{cr} = C\frac{\pi^2 EI}{L^2}$$

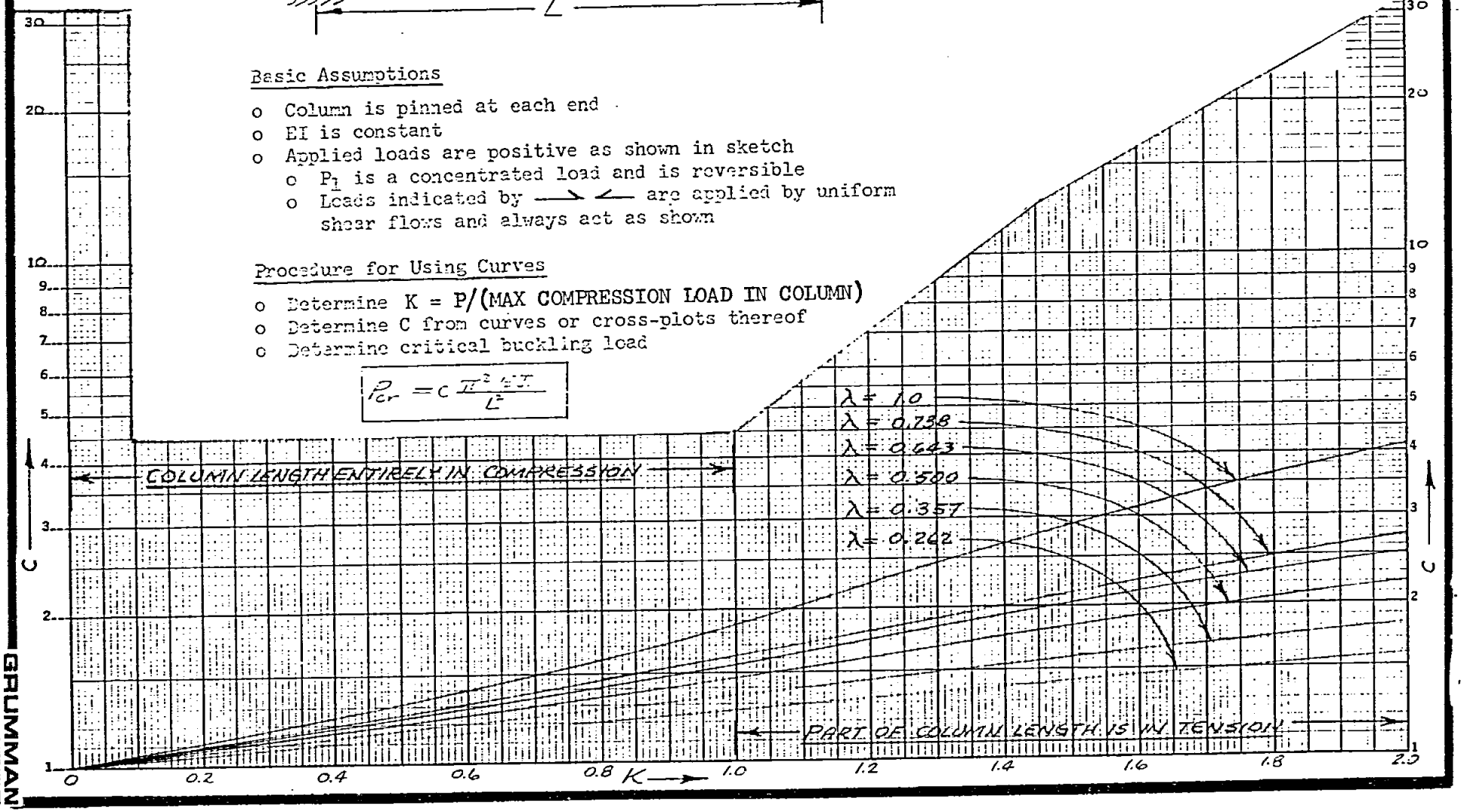

BUCKLING COEFFICIENTS FOR PIN-ENDED COLUMNS SUBJECT TO CONCENTRATED AXIAL & DISTRIBUTED SHEAR LOADS

Basic Assumptions

- Column pinned at both ends
- EI is constant
- Applied loads act only in direction shown in sketch

Procedure for Using Curves

- Determine ratio of end load to the distributed shear load, P_1/P
- Determine C from curves
- Determine critical value of end load from $P_{cr} = \frac{C \pi^2 EI}{L^2}$

P_{cr} is then the critical value of P_1

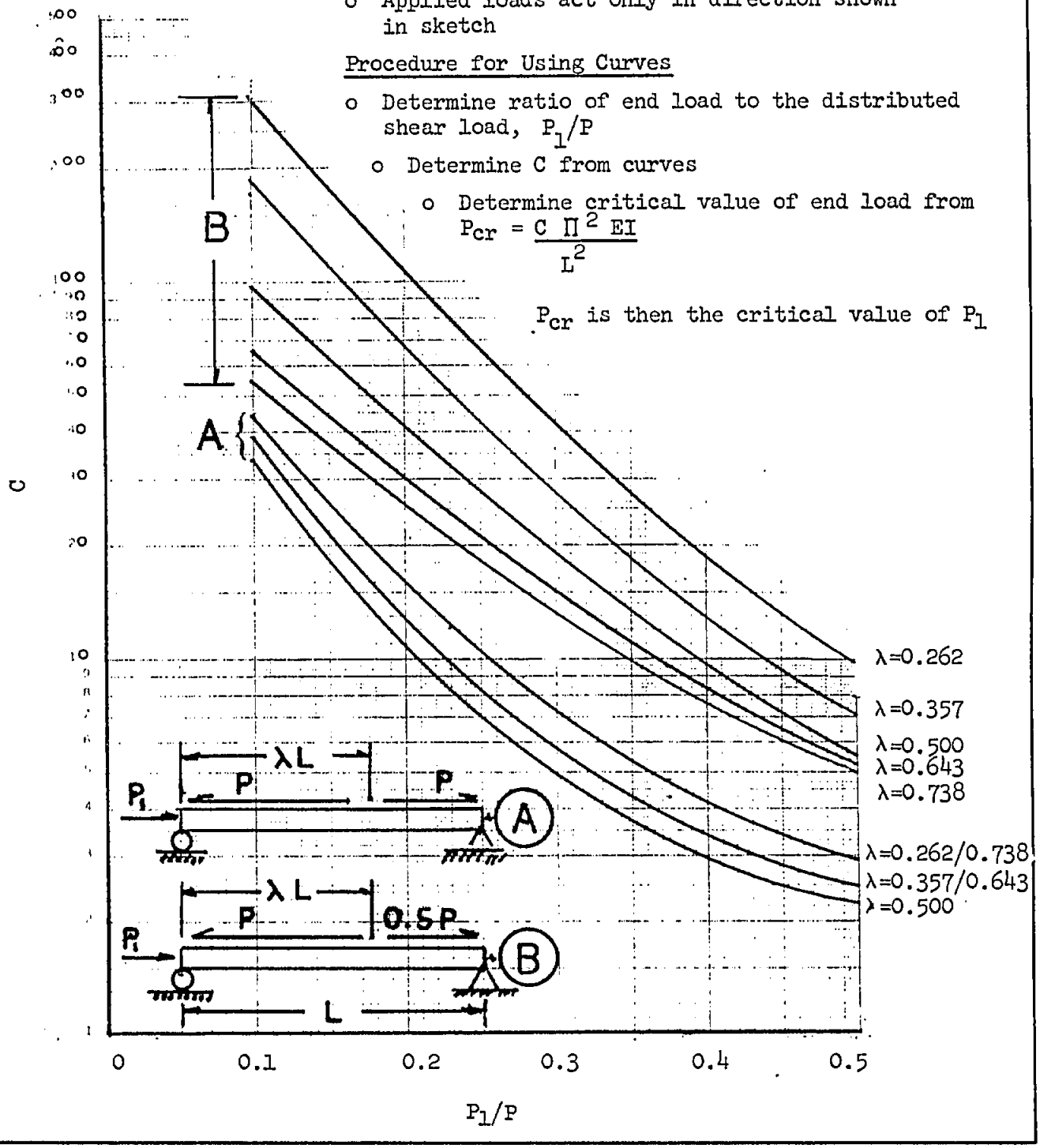

BUCKLING COEFFICIENTS FOR PIN-ENDED COLUMNS SUBJECTED TO CONCENTRATED AXIAL & DISTRIBUTED SHEAR LOADS

Basic Assumptions

- Column pinned at both ends
- EI is constant
- Applied loads act only in direction shown in sketch

Procedure for Using Curves

- Determine ratio of end load to the distributed shear load, P_1/P
- Determine C from curves.
- Determine critical value of end load from $P_{cr} = \frac{C \Pi^2 EI}{L^2}$.
- P_{cr} is then the critical value of P_1

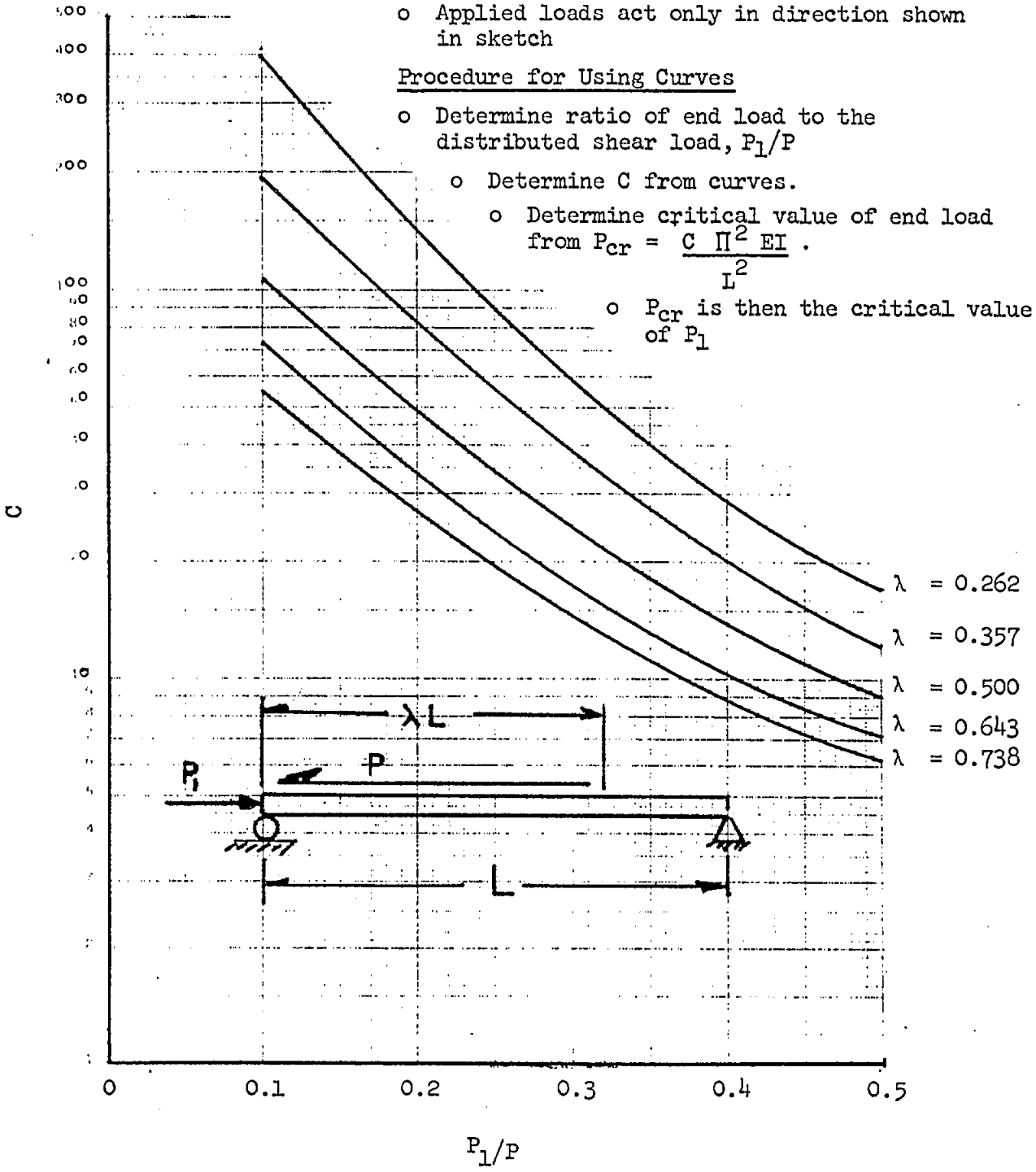

B3.51.10 ECCENTRIC COLUMNS

Use of Eccentric Column Curves

The eccentric column curves of pages B3.51.11, B3.51.12-1,-2,-3 are for use in designing or analyzing eccentrically loaded columns of all slenderness ratios where the load line is parallel to the elastic axis. The curves take into account both the direct stress and the primary plus secondary bending stresses.

The method for obtaining an allowable average compressive stress will depend upon whether or not the cross section is subject to local buckling. If doubt exists upon this point, the calculation should be made both ways, and the lower of the two allowables obtained should be used.

If the cross section is not subject to local buckling, the allowable average compressive stress may be read directly from the curves on pages B3.51.12-1, -2, -3.

If the cross section is subject to local buckling, the curves on page B3.51.11 give the allowable average compressive stress in the following way:

1. Compute the local compressive buckling stress, $F_{c_{cr}}$ (Ref. B4.20).
2. Assume a value for the allowable average compressive stress F_{ce}.
3. From the stress strain curve for the column material, read off the strains $\epsilon_{c_{cr}}$ and ϵ_{ce} corresponding to the stresses $F_{c_{cr}}$ and F_{ce}, respectively.
4. Calculate a "chordal" modulus E_{ch} according to the formula

$$E_{ch} = (F_{c_{cr}} - F_{ce})/(\epsilon_{c_{cr}} - \epsilon_{ce}) .$$

5. Compute an effective column buckling stress F_c for buckling in the direction of the eccentricity by the formula

$$F_c = \pi^2 E_{ch}/(\ell/\rho)^2,$$

in which ℓ is the column length and ρ is the radius of gyration.

6. Evaluate the extreme fiber stress ratio F_c/F_{fiber}, using for F_{fiber} the local compressive buckling stress $F_{c_{cr}}$ from step 1.

B3.51.10 ECCENTRIC COLUMNS (Cont.)

Use of Eccentric Column Curves (Cont.)

7. Evaluate the eccentricity ratio ec/ρ^2, in which e is the initial eccentricity of the load, c is the distance from the center of gravity to the extreme fiber, and ρ is the radius of gyration.

8. Using the ratios of steps 6 and 7 enter the curves of page B3.51.11 to obtain the factor F_{ce}/F_c. This factor, when multiplied by F_c from step 5, yields a value for the allowable average compressive stress F_{ce}. If F_{ce} so obtained is substantially different from the assumed F_{ce} of step 2, the procedure must be repeated using the new value of F_{ce}.

9. In cases where F_c/F_{fiber} is greater than 6, the allowable average compressive stress is given directly by the formula

$$F_{ce} = \frac{F_{fiber}}{1 + \frac{ec}{\rho^2}}$$

STRENGTH OF ECCENTRICALLY LOADED COLUMNS - SECANT FORMULA

F_{ce} = Allowable Average Compressive Stress over Section

F_{fiber} = Allowable Extreme Fiber Stress

F_c = Column Buckling Stress with no Eccentricity

e = Initial Eccentricity of Load

c = Arm from c.g. to Extreme Fiber

ρ = Radius of Gyration

Curves Based on Secant Formula
See B3.51.10 for Explanation

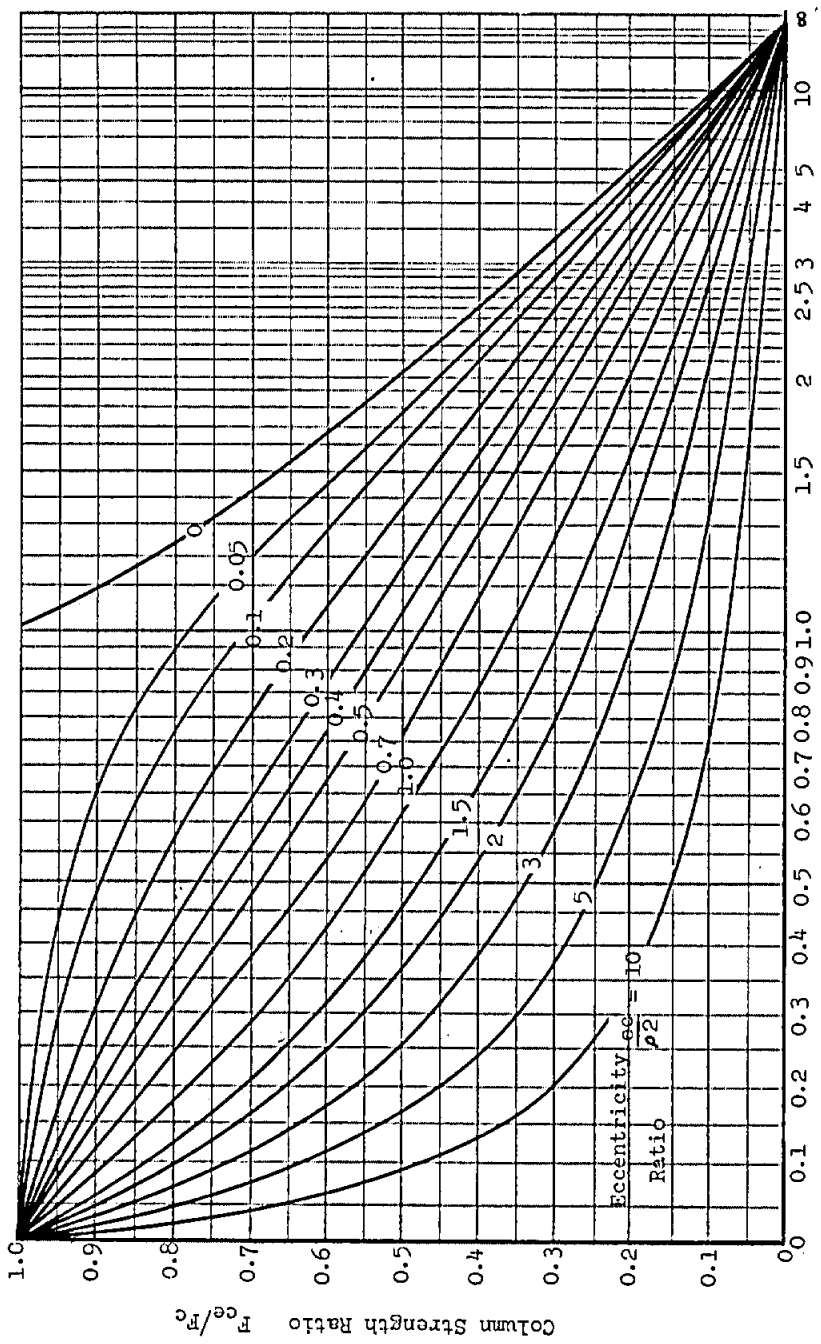

STRENGTH OF ECCENTRIC COLUMNS
2014-T6 CLAD SHEET

Load Line Parallel to Elastic Axis
Column Not Subject to Local Instability
e = Initial Eccentricity of
Load From Centroidal Axis.
c = Arm From Centroidal Axis to Extreme Fiber

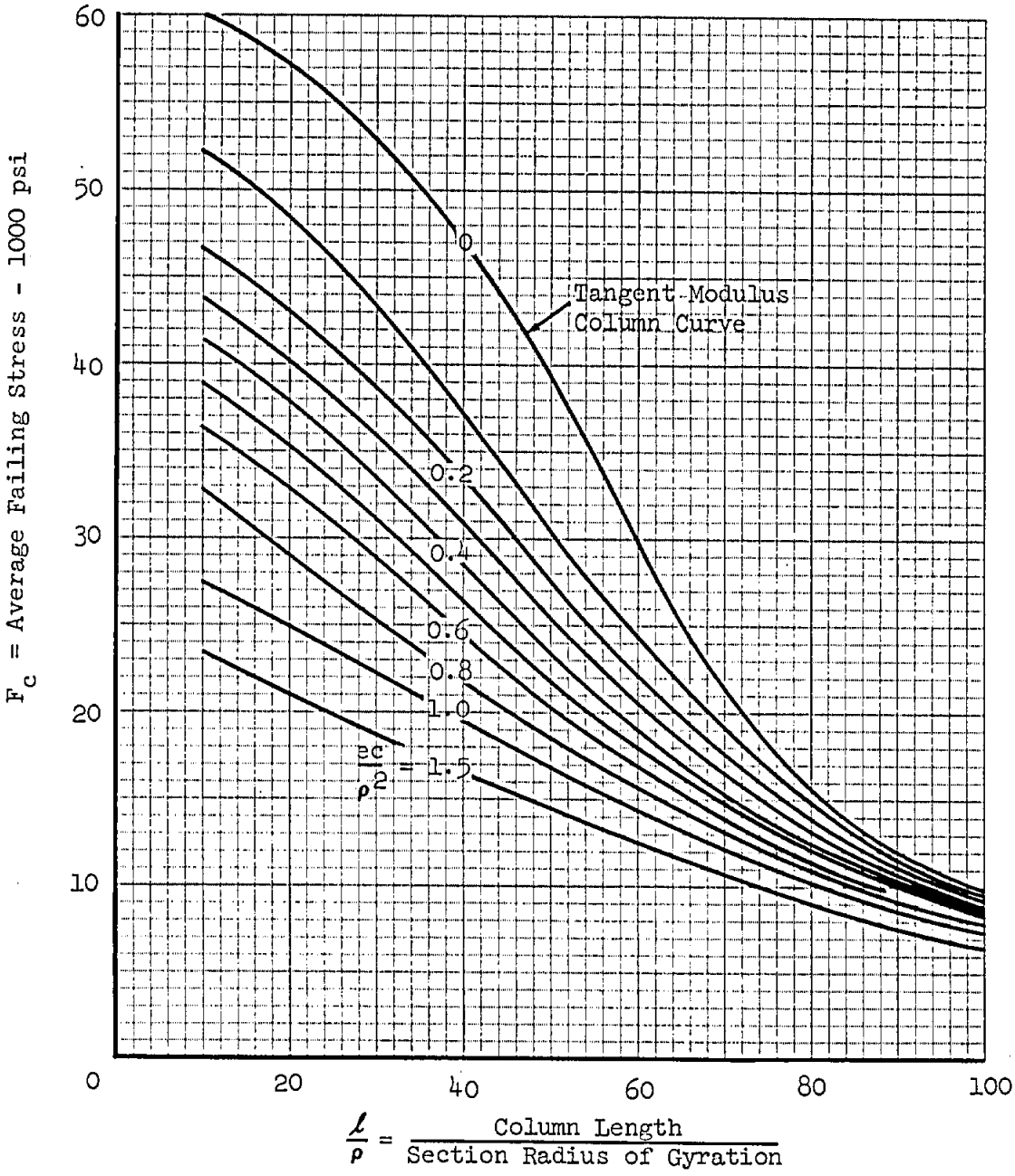

Ref: "Buckling of Aluminum Columns in the Inelastic Range of the Material", A. Chajes, M.C.E. Thesis, Polytechnic Institute of Brooklyn, May 1955

STRENGTH OF ECCENTRIC COLUMNS
7075-T6 BARE SHEET

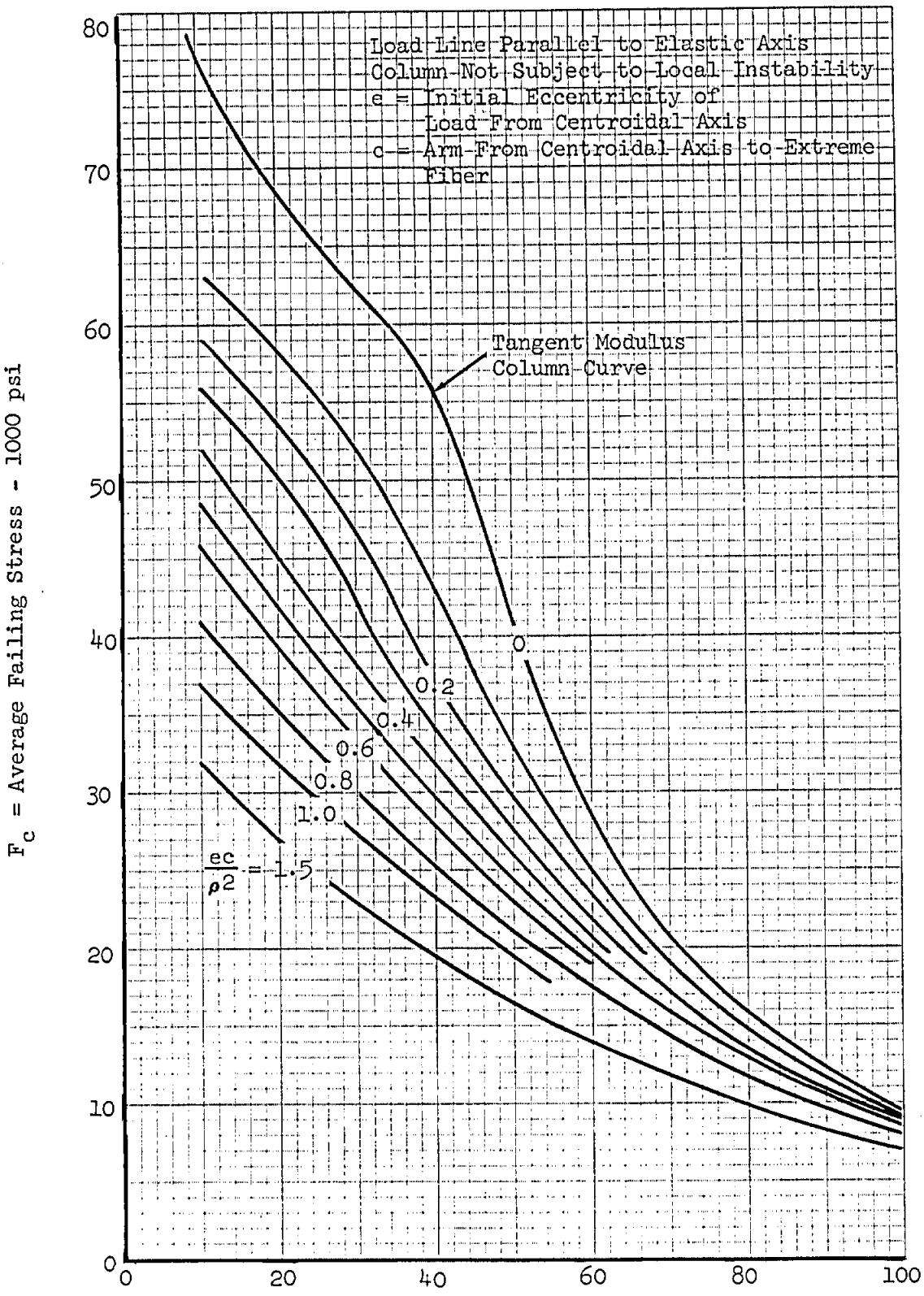

Ref: See Page B3.51.12-1

STRENGTH OF ECCENTRIC COLUMNS
7075-T6 EXTRUSION

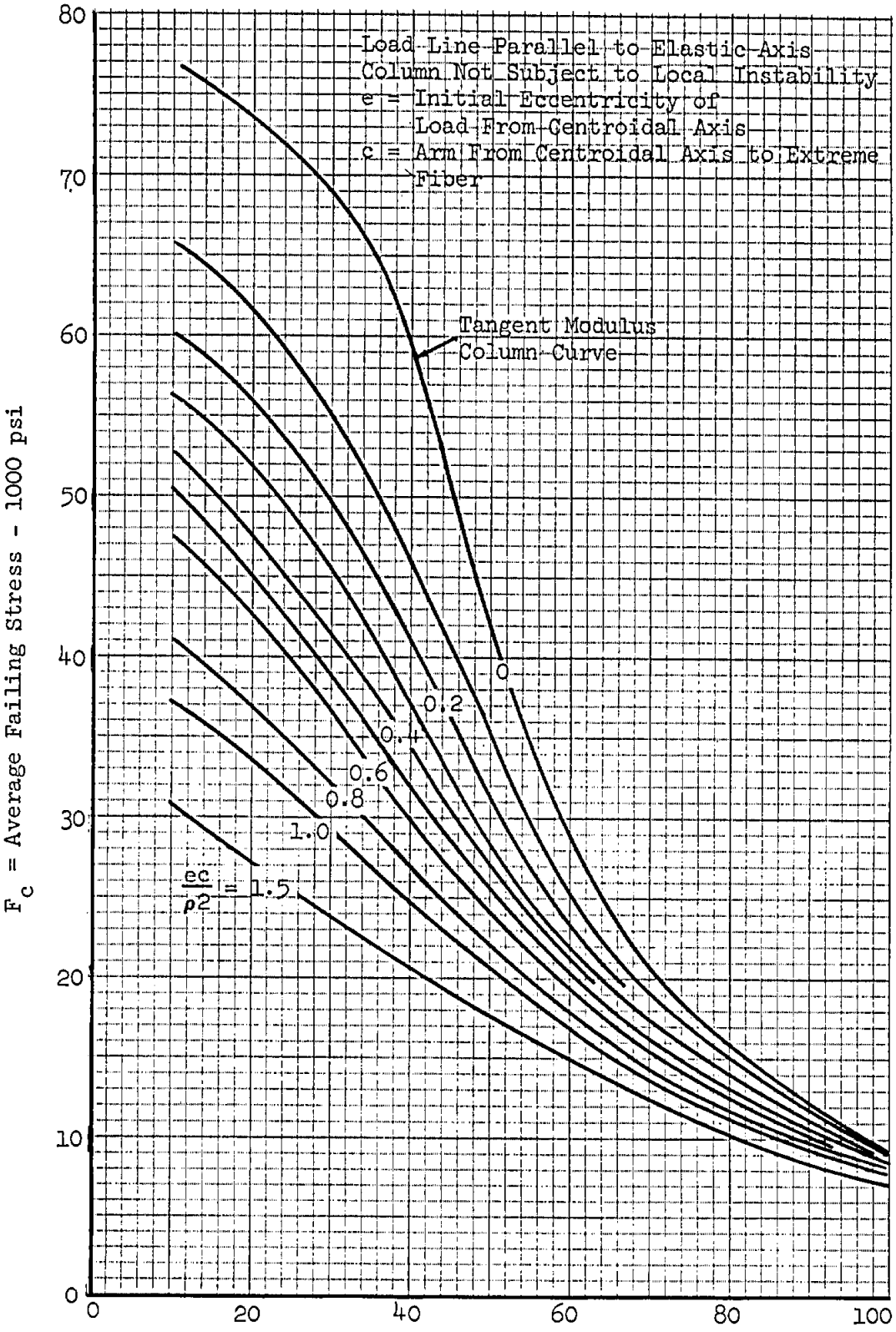

Ref: See Page B3.51.12-1

BEAM - COLUMN CURVES
CENTRALLY LOADED COLUMNS WITH END COUPLES

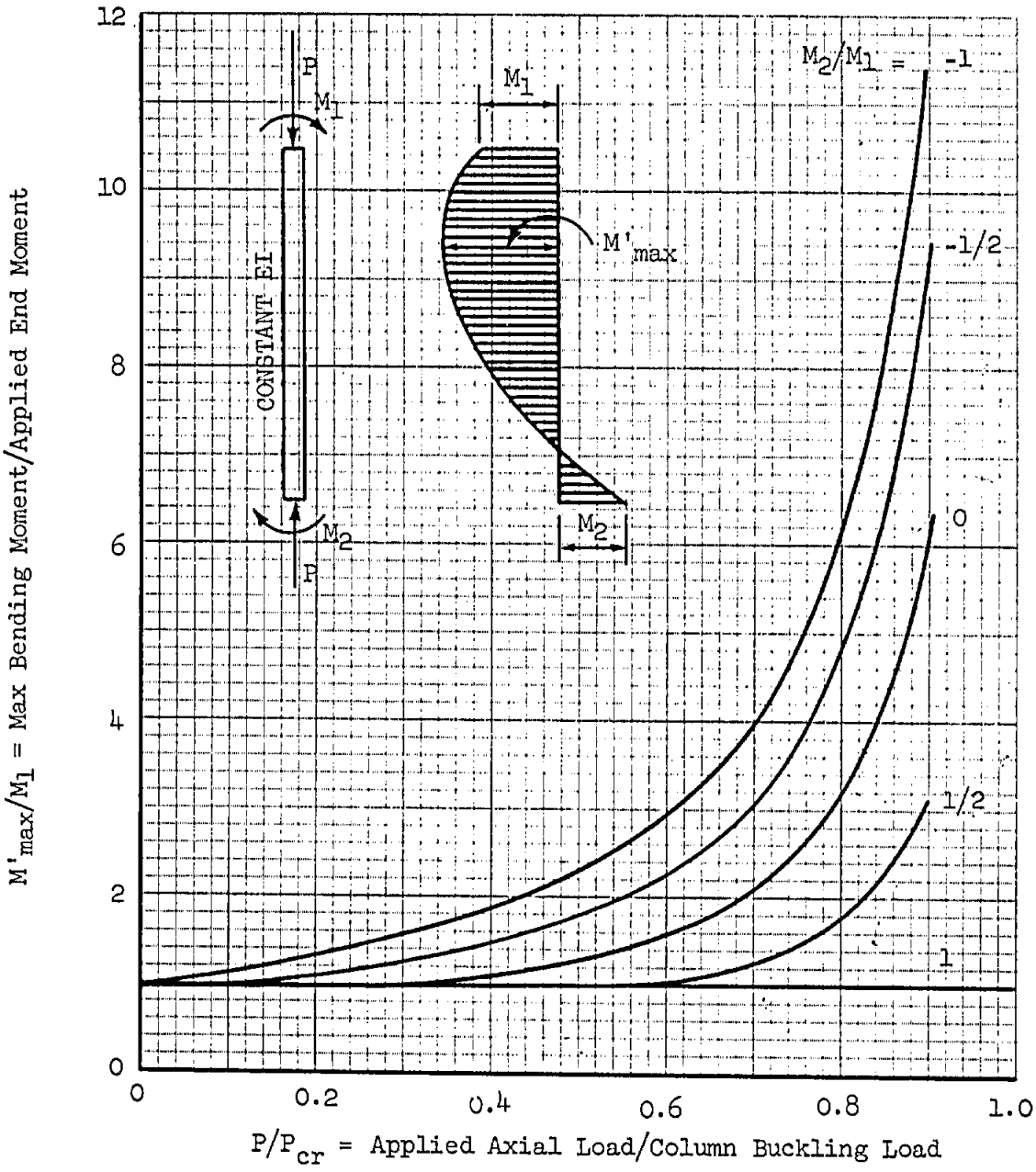

P = Applied Axial Load
$P_{cr} = F_c \times A$ = Column Buckling Load
F_c = Column Buckling Stress from B3.42.10
M_1, M_2 = Applied End Moment
M'max = Max. Total Bending Moment Including Secondaries

Ref: "Buckling of Elastic Structure", H.M. Westergaard, Trans. ASCE 1922, p594

Grumman

Approximate Beam - Column Equations

Use for straight columns with constant EI where stresses are in elastic range.

P = Applied Axial Load

$P_{cr} = F_c \times A$ = Column Buckling Load

F_c = Column Buckling Stress from B3.42.10

M_c, M_e = Total Bending Moment at Center or End, Respectively.

Hinged Ends

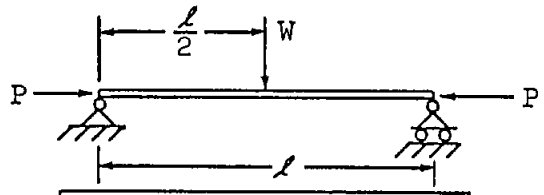

$$M_c = \frac{W\ell}{4}\left(1 + 0.8\,\frac{P}{P_{cr}-P}\right)$$

Error Less Than 1.4%

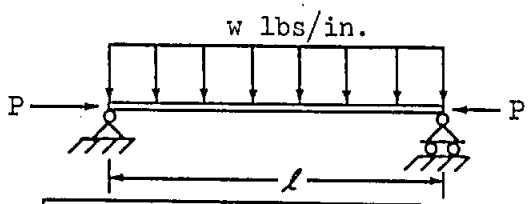

$$M_c = \frac{w\ell^2}{8}\left(1 + 1.03\,\frac{P}{P_{cr}-P}\right)$$

Error Less Than 0.2%

Fixed End Columns

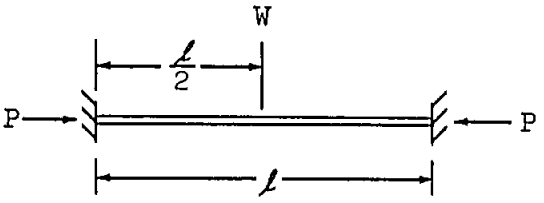

Mom. at Center

$$M_c = \frac{W\ell}{8}\left(1 + 0.8\,\frac{P}{P_{cr}-P}\right)$$

Mom. at Ends

$$M_e = -\frac{W\ell}{8}\left(1 + 0.8\,\frac{P}{P_{cr}-P}\right)$$

Error Less Than 1.4%

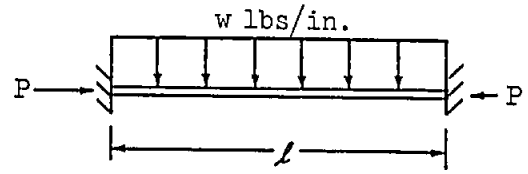

Mom. at Center

$$M_c = \frac{w\ell^2}{24}\left(1 + 1.2\,\frac{P}{P_{cr}-P}\right)$$

Mom. at Ends

$$M_e = -\frac{w\ell^2}{12}\left(1 + 0.65\,\frac{P}{P_{cr}-P}\right)$$

Error Less Than 6.5% and on Conservative Side. For $\frac{P}{P_{cr}} \leqq 0.5$ Error Less Than 1%

Ref: "Buckling of Elastic Structures," H.M. Westergaard, Trans ASCE 1922, P. 576

BEAM-COLUMNS: GENERAL METHOD OF ANALYSIS

This method of analysis is applicable to the general case of a beam-column under a system of applied loads consisting of concentrated lateral loads $W_1, W_2, \ldots, W_m$, uniformly distributed lateral loads $q_1, q_2, \ldots, q_{mm}$, couples $m_1, m_2, \ldots, m_n$, and axial loads $\Delta p_1, \Delta p_2, \ldots, \Delta p_{nn}$ applied along the length of the beam, in addition to the end loads P_A and P_B and end moments M_A and M_B (Figure 3.51.40-1). The beam-column may have initial curvature and may be of uniform or varying cross-section.

The method is an extension of that developed by W. Gittleman in Reference 1. Use of the method involves dividing the beam-column into segments and calculating the rotations and bending moments at the ends of each section due to the applied loads. Two trial solutions are required, from which the final solution is obtained.

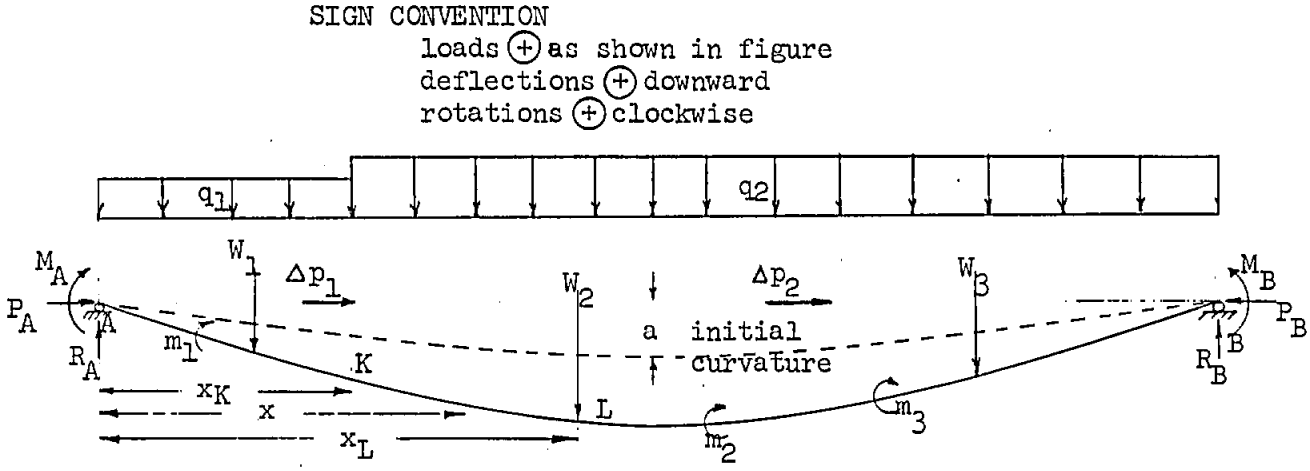

Figure 3.51.40-1: Beam-Column With General Loading

References:

1. Gittleman, W., "Laterally Loaded Non-Uniform Struts," "Aircraft Engineering," Feb. 1953, p. 56.

2. Torczyner, R.D., "Beam-Columns: General Method of Analysis," Structural Mechanics Note No. 18, 1969.

SYMBOLS

Symbol	Units	Description
a	inches	initial midspan deflection of the beam with the initial deflected shape assumed to be $y = a \sin \pi \frac{x}{L}$
i_x	radians	slope at x
L	inches	total length of beam column
m	in.-lb.	applied couple
M_x	in.-lb.	bending moment at x
P	lbs.	axial end load
Δp	lbs.	incremental axial loads applied along the span
q	lbs./in.	distributed lateral load
R_A	lbs.	reaction at A due to all the loads -- W,m,q,M_A,M_B
W	lbs.	concentrated lateral load
y	inches	deflection
For a segment $\overline{KL}$ having ordinates x_K and x_L, the following properties apply		
E	psi	Young's modulus
I	inches^4	moment of inertia of cross-section
ℓ	inches	length of segment = $x_L - x_K$
P^*	lbs.	$P_A + \sum \Delta p$
$\sum \Delta p$	lbs.	sum of all incremental axial loads, Δp, to the left of K including any axial load at K
$\sum \bar{q}$	lbs.	total lateral force due to all of the distributed lateral loads to the left of K
$\sum W$	lbs.	sum of all concentrated applied lateral loads to the left of K, including any load at K
μ^2	in.^{-2}	P^*/EI

Subscripts

Single letters refer to points on beam-column; M_K = moment at point K

Pairs of letters refer to segments; $I_{\overline{AC}}$ = moment of inertia of segment $\overline{AC}$

METHOD

For a segment $\overline{KL}$ of the beam column (see Figure 3.51.40-1) equations (1) and (2) relate the slope and bending moment at L to the slope and bending moment at K.

$$i_L = - M_k \mu \frac{\sin \mu\ell}{P^*} + i_k \cos \mu\ell + \alpha \qquad (1)$$

$$M_L = M_k \cos \mu\ell + i_k P^* \frac{\sin \mu\ell}{\mu} + \beta \qquad (2)$$

where

$$\alpha = \frac{(1 - \cos \mu\ell)}{P^*} \cdot (\sum W + \sum \bar{q} - R_A) - (\frac{\sin \mu\ell}{\mu} - \ell) \cdot q/P^*$$

$$- \frac{a\,\pi}{L} \cos \frac{\pi x_k}{L} \cos \mu\ell \left[\frac{1}{\left(\frac{\pi}{\mu L}\right)^2 - 1} + 1 \right] + \frac{a(\pi/L)^2}{\left[\left(\frac{\pi}{\mu L}\right)^2 - 1\right]\mu} \cdot \sin \frac{\pi x_k}{L} \sin \mu\ell$$

$$+ \frac{a\,\pi}{L} \cos \frac{\pi x_L}{L} \left[\frac{1}{\left(\frac{\pi}{\mu L}\right)^2 - 1} + 1 \right]$$

$$\beta = - \frac{\sin \mu\ell}{\mu} \cdot (\sum W + \sum \bar{q} - R_A) - (1 - \cos \mu\ell) \cdot q/\mu^2$$

$$- \frac{P^* a\,\pi}{\mu L} \cdot \cos \frac{\pi x_k}{L} \sin \mu\ell \left[\frac{1}{\left(\frac{\pi}{\mu L}\right)^2 - 1} + 1 \right]$$

$$- \frac{P^* a\,\pi^2/L^2}{\left[\left(\frac{\pi}{\mu L}\right)^2 - 1\right]\mu^2} \left[\sin \frac{\pi x_k}{L} \cos \mu\ell - \sin \frac{\pi x_L}{L} \right]$$

Note: α and β depend solely upon the loading and beam geometry.

Procedure

1. Divide the beam-column into a convenient number of segments following these guidelines:
   a. Segments must be of constant cross-section.
   b. Distributed lateral load cannot vary along the length of a segment.
   c. No point loads-- W, m, Δp -- may be applied within the length of a segment.

d. Moments and rotations are determined at the ends of segments only; segments must be chosen which have ends at points where values of the moment and rotation are required.

2. First trial solution

a. Assume the slope at A equal to zero. Equations (1) and (2) can be solved for the slope and moment at C. Here, K corresponds to A, and L to C.

$$i_k = 0;\ M_k = M_A = \text{applied moment at A}$$

b. Consider next the segment $\overline{CD}$. The slope and moment at C were found from segment $\overline{AC}$ to be $i_{L_{\overline{AC}}}$ and $M_{L_{\overline{AC}}}$. To apply equations (1) and (2) to segment $\overline{CD}$ let $i_{K_{\overline{CD}}} = i_{L_{\overline{AC}}}$ and $M_{K_{\overline{CD}}} = M_{L_{\overline{AC}}}$ + the applied moment at C (if there is one).

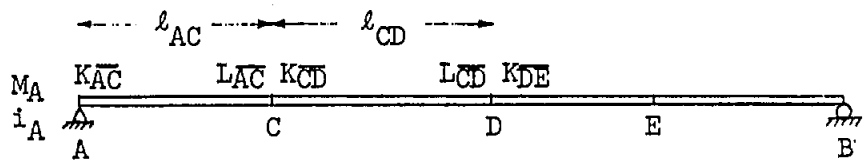

Figure 3.51.40-2 - Illustration of Beam Segment Designations

c. Continue the process for each segment until values for all segments have been determined. The values of slope and moment at the right end of the beam are i_{B_1} and M_{B_1} (the subscript "1" refers to trial solution 1).

3. Since addition of and multiplication by known numerical quantities are the only arithmetic operations performed in order to obtain M_B from i_A and M_A,

$$M_B = C_1\, i_A + C_2 \qquad (3)$$

where C_1 and C_2 are constants.

Then,

$$M_{B_1} = C_1\,(0) + C_2$$

$$C_2 = M_{B_1}$$

4. Second Trial Solution

Repeat the calculations of slope and moment for each segment, starting with an assumed slope at A of 0.1. The resulting slope and moment at B are i_{B_2} and M_{B_2}.

5. From Equation (3)

$$M_{B_2} = C_1 (.1) + C_2$$

but, $C_2 = M_{B_1}$ (from step 3)

$$C_1 = \frac{M_{B_2} - M_{B_1}}{.1} \qquad (4)$$

6. Solve Equation (3) for the actual slope at A.

$$i_A = \frac{M_B - C_2}{C_1}$$

where M_B is the applied moment at B.

7. Actual moments and slopes are obtained by repeating the calculations, this time with the actual slope i_A.

NUMERICAL EXAMPLE

An initially curved beam-column under a complex system of loads is analyzed. Figure 3.51.40-3 shows the dimensions of the beam (not to scale), (b) shows the initial curvature, (c) shows the loading and (d) shows the division of the beam-column into segments. $E = 30 \times 10^6$ psi.

1. Calculate the value of the reaction at A, R_A.

Summing moments about B,

$$R_A x40-300-1000x30+700+400x16-15x14x33-25x26x13+\frac{(1000-1600)}{40} = 0$$

$$R_A = 979.5 \text{ lbs}$$

2. To demonstrate the step-by-step calculations, the significant computations are illustrated in the following tables. It is suggested that this method be used with the aid of a small computer such as that available with the G.E. Time Sharing System. For an example see Reference 2.

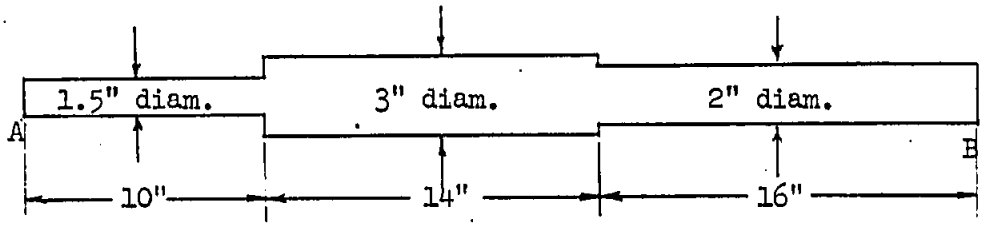

(a) Dimensions of Beam-Column (not to scale)

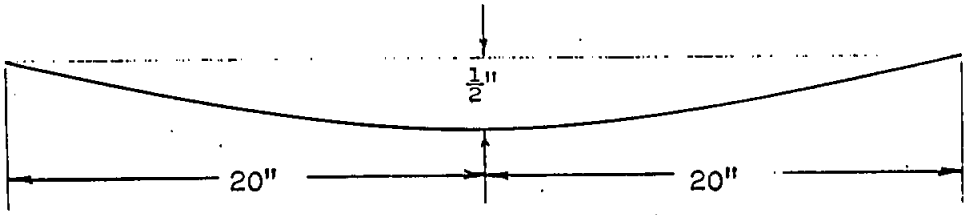

(b) Initial Curvature (not to scale)

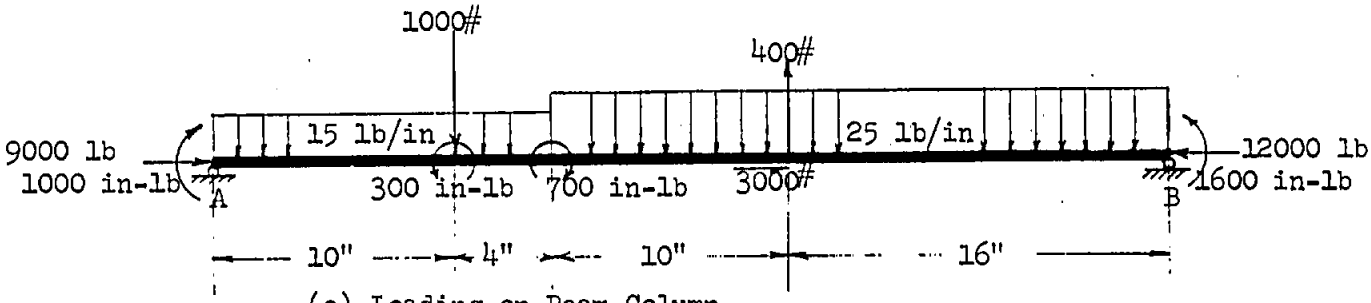

(c) Loading on Beam-Column

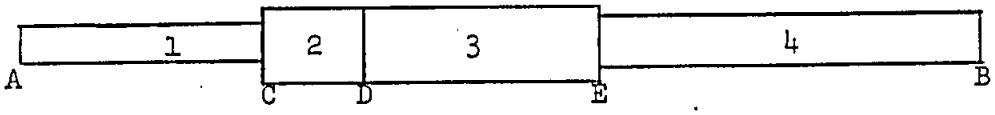

(d) Division of Beam-Column into Segments

FIGURE 3.51.40-3

For each segment, calculate the values in Table 3.51.40-1 and then α (Table 3.51.40-2) and β (Table 3.51.40-3). These values will remain constant throughout the remaining calculations of the problem.

3. The first trial solution is shown in Table 3.51.40-5. It is found that M_B for this trial solution $(M_{B_1}) = -18005.2$

From Equation (3)

$$M_{B_1} = C_1 (0) + C_2$$

then

$$C_2 = -18005.2$$

4. The second trial solution is shown in Table 3.51.40-6. It is found that $M_{B_2} = +18827.7$

From Equation (4)

$$C_1 = \frac{+18827.7 - (-18005.2)}{.1}$$

$$C_1 = 368,329$$

5. The actual value of i_A is calculated with Equation (5).

$$i_A = \frac{1600 - (-18005.2)}{368,329}$$

$$i_A = +.053227$$

6. Final Solution

The final solution gives the actual moments and rotations at the ends of each segment. These values are tabulated in Table 3.51.40-7. Note that the calculated moment at B = 1600.9 $\approx$ 1600 = M_B applied. This is a check of the correctness of the solution.

Table 3.51.40-1

	Segment	1	2	3	4
	x_K	0	10	14	24
	x_L	10	14	24	40
	$\ell = x_L - x_K$	10	4	10	16
	Moment of Inertia I	.2845	3.9761	3.9761	.7854
	$P^* = P_A + \Sigma\Delta p$	9000	9000	9000	12000
	$\mu = \sqrt{P^*/EI}$	.032473	.0086862	.0086862	.022568
ⓐ	sin $\mu\ell$ ($\mu\ell$ in radians)	.31905	.034738	.086753	.35329
ⓑ	cos $\mu\ell$ ($\mu\ell$ in radians)	.94774	.99940	.99623	.93551
	$\sum W$	0	1000	1000	600
	$(\sum W - R_A)$	- 979.5	+ 20.5	+ 20.5	- 379.5
	q	15	15	25	25
	$\Sigma \bar{q}$	0	150	210	460
ⓒ	a π/L	.039270	.039270	.039270	.039270
ⓓ	$\left(\frac{\pi}{\mu L}\right)^2 - 1$	4.8497	80.756	80.756	11.111
ⓔ	sin $\frac{\pi x_K}{L}$ $\left(\frac{\pi x_K}{L}$ in radians$\right)$	0	.70711	.891008	.95106
ⓕ	cos $\frac{\pi x_K}{L}$ $\left(\frac{\pi x_K}{L}$ in radians$\right)$	1	.70711	.45399	-.309015

Table 3.51.40-2 For Calculating α

ⓖ	$\frac{(\sum W - R_A)}{P^*}(1 - \cos \mu\ell)$	- .0056875	+ .0000113667	+ .000096554	+ .0004326
ⓗ	$\left(\frac{\sin \mu\ell}{\mu} - \ell\right) q/P^*$	- .00029152	- .0000013048	- .000034857	- .00071986
ⓙ	$\alpha' = ⓖ - ⓗ$	- .0053961	+ .000012672	+ .00013141	+ .0011525
	note: for initially straight beam-columns $\alpha = \alpha'$				
ⓚ	ⓕ x ⓑ $\left(\frac{1}{ⓓ} + 1\right)$	+ 1.14316	+ .71544	+ .45788	- .31510
ⓛ	$\left(ⓔ \times ⓐ / ⓓ\right)$ $\pi/\mu\ell$	0	+ .0027503	+ .0086547	+ .10524
ⓜ	$\left(1/ⓓ + 1\right)$ cos $\frac{\pi x_L}{L}$	+ .85291	+ .45961	- .31284	- 1.0900
ⓝ	$\alpha = ⓙ + \left[ⓒ \times (-ⓚ + ⓛ + ⓜ)\right]$	- .016794	- .0099258	- .029795	- .025145

Table 3.51.40-3 For Calculating β

ⓟ	$\frac{\sin \mu\ell}{\mu}(\sum W - R_A)$	- 9623.67	+ 681.867	+ 2302.102	- 1260.18
ⓠ	$q/\mu^2 (1 - \cos \mu\ell)$	+ 743.39	+ 119.284	+ 1249.17	+ 3165.53
ⓢ	$\beta' = -ⓟ - ⓠ$	+ 8880.28	- 801.151	- 3551.27	- 4425.71
	note: for initially straight beam-columns $\beta = \beta'$				
ⓣ	ⓐ x ⓒ x ⓕ x $\frac{P^*}{\mu}\left(\frac{1}{ⓓ} + 1\right)$	+ 4188.50	+ 1011.84	+ 1622.37	- 2484.77
ⓤ	ⓔ x ⓑ - sin $\frac{\pi x_L}{L}$	- .70711	- .184322	- .063411	+ .889726
ⓥ	$\frac{ⓒ}{ⓓ} \times \frac{P^*\pi}{\mu^2 L} \times ⓤ$	- 3838.13	- 839.72	- 288.88	+ 5819.00
ⓦ	$\beta = ⓢ - ⓣ - ⓥ$	+ 8529.91	- 973.27	- 4884.76	- 7759.94

Table 3.51.40-4

	1	2	3	4
$\mu/P^* \sin \mu\ell$	1.1512×10^{-6}	$.0335268 \times 10^{-6}$	$.0837282 \times 10^{-6}$	$.664421 \times 10^{-6}$
$\cos \mu\ell$	.94774	.99940	.99623	.93551
$\left(P^*/\mu\right)\sin \mu\ell$	88425.8	35993.0	89887.1	187854
m	0	-300	+700	0

Table 3.51.40-5 - First Trial Solution

M_K	+ 1000	+ 9177.65	+ 8252.98	+ 805.17
i_K	0	- .017945	- .028168	- .058548
$-M_K\ \mu/P^* \sin \mu\ell$	$- 1.1512 \times 10^{-3}$	$- .307697 \times 10^{-3}$	$- .691007 \times 10^{-3}$	$- .534972 \times 10^{-3}$
$i_K \cos \mu\ell$	0	- .0179342	- .0280618	- .0547722
α	- .016794	- .0099258	- .029795	- .025145
i_L	- .017945	- .028168	- .058548	- .080452
$M_K \cos \mu\ell$	+ 947.74	+ 9172.14	+ 8221.87	+ 753.24
$i_K\left(P^*/\mu\right)\sin \mu\ell$	0	- 645.89	- 2531.94	- 10998.48
β	+ 8529.91	- 973.27	- 4884.76	- 7759.94
M_L	+ 9477.65	+ 7552.98	805.17	- 18005.2

NOTE:

When transferring M_L from segment $\overline{AC}$ to M_K at segment $\overline{CD}$, it is necessary to add the couple at C, -300 in-lb.

Similarly, when transferring M_L from segment $\overline{CD}$ to M_K at segment $\overline{DE}$ it is necessary to add the couple at D, +700 in-lb.

Table 3.51.40-6 - Second Trial Solution

M_K	+ 1000	+ 18020.2	+ 20501.4	+ 21494.6
i_K	.1	+ .076829	+ .066253	+ .034491
$-M_K\ \mu/P^* \sin \mu\ell$	$- 1.1512 \times 10^{-3}$	$- .604160 \times 10^{-3}$	$- 1.71655 \times 10^{-3}$	$- 14.2815 \times 10^{-3}$
$i_K \cos \mu\ell$	+ .094774	+ .076783	+ .066003	+ .0322667
α	- .016794	- .0099258	- .029795	- .025145
i_L	+ .076829	+ .066253	+ .034491	- .007160
$M_K \cos \mu\ell$	+ 947.74	+ 18009.4	+ 20424.1	+ 20108.4
$i_K\left(P^*/\mu\right)\sin \mu\ell$	+ 8842.58	+ 2765.31	+ 5955.29	+ 6479.27
β	+ 8529.91	- 973.27	-4884.76	- 7759.94
M_L	+ 18320.2	+ 19801.4	+ 21494.6	+ 18827.7

Table 3.51.40-7 Final Solution

M_K	+ 1000	+ 13884.3	+ 14772.5	+ 11818.6
i_K	+ .053227	+ .032500	+ .022089	- .009026
$-M_K\left(\mu/F^*\right) \sin \mu\ell$	$- 1.1512 \times 10^{-3}$	$- .465496 \times 10^{-3}$	$- 1.23687 \times 10^{-3}$	$- 7.85253 \times 10^{-3}$
$i_K \cos \mu\ell$	+ .050445	+ .0324805	+ .022006	- .008444
α	- .016794	- .0099258	- .029795	- .025145
i_L	+ .032500	+ .022089	- .009026	- .041442
$M_K \cos \mu\ell$	+ 947.74	+ 13876.0	+ 14716.8	+ 11056.4
$i_K\left(P^*/\mu\right)\sin \mu\ell$	+ 4706.64	+ 1169.77	+ 1985.52	- 1695.57
β	+ 8529.91	- 973.27	- 4884.76	- 7759.94
M_L	+ 14184.3	+ 14072.5	+ 11818.6	+ 1600.9

TAPERED BEAM-COLUMNS

When analyzing tapered beam-columns, the segments into which the beam is divided are assumed to be of uniform cross-section. It is suggested that the moment of inertia of each segment be based on the dimensions of the midspan of that segment.

The tapered beam-column in Figure 3.51.40-4 can be segmented as shown in that Figure and Table 3.51.40-8.

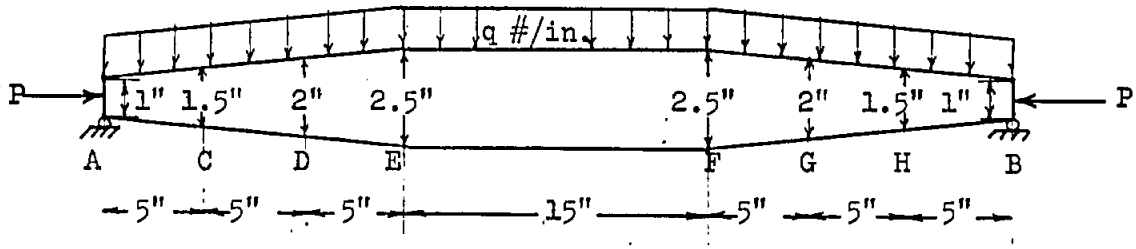

Figure 3.51.40-4 - Tapered Beam Column

TABLE 3.51.40-8

SEGMENT	AC	CD	DE	EF	FG	GH	HB
length, ℓ	5"	5"	5"	15"	5"	5"	5"
diameter	1.25"	1.75"	2.25"	2.5"	2.25"	1.75"	1.25"

Note that the accuracy of the solution depends upon the number of segments used in the tapered portions.

STABILITY

The results obtained using this method do not indicate whether or not the beam-column is stable under the applied loads. The computer program in Reference 2, however, does check stability by incrementally increasing all axial loads until the lateral deflection of the beam approaches infinity. The factor by which the axial loads of a given problem are above or below this "critical load" is printed as output by the computer program.

AXIAL POINT LOADS

The line of action of the axial point loads is assumed to be the straight line from A to B.

PRESS FIT STRESSES

Design of Housing For Press Fit

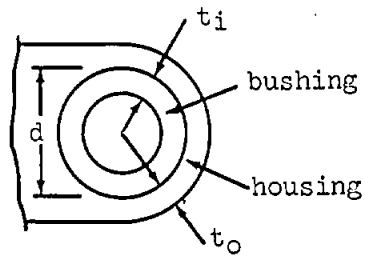

The press fit stress curves of pages B3.81-1,-2,-3 are for use in designing or analyzing housings into which bushings or bearings are pressed. The curves take into account only those stresses produced by press fit.

The figure above represents a typical busing and housing design. The curves of pages B3.81-1,-2,-3 are used to obtain the minimum housing wall thickness (t_o) required to resist press fit stresses. The method is as follows:

1. For a given bushing, find d, t_i and δ . δ , the maximum interference, is the maximum difference between the outer diameter of the busing and the inner diameter of the housing.

2. Compute t_i/d.

3. Evaluate $\frac{f_o\, d}{KE_o\, \delta}$, where

   f_o = the maximum press fit stress in the housing (a tangential stress at the inner surface of the housing).

   E_o = Young's modulus for the housing material.

   K = a stress concentration factor.

In order to prevent stress corrosion, the maximum press fit stress in the housing must not exceed 0.50 F_{ty}, where F_{ty} is the transverse tensile yield stress of the housing material (Ref. SD24-F, 2 April 1947). Therefore, the maximum allowable value of f_o is 0.50 F_{ty}.

A value of 1.5 is chosen for the stress concentration factor K to account for the stiffening action of the thicker portion of the housing wall. Therefore, the minimum allowable wall thickness is obtained when

$$\frac{f_o\, d}{KE_o\, \delta} \geq \frac{1}{1.5}\left(\frac{F_{ty}}{2}\right)\frac{d}{E_o\, \delta}$$

PRESS FIT STRESSES

Design of Housing For Press Fit (Cont.)

In Cases where $\frac{f_o\ d}{KE_o\delta}$ is greater than unity, the press fit is not a critical condition in the design of the housing. In such cases, the housing can only be critical for applied static load or for fatigue. If $\frac{f_o\ d}{KE_o\delta}$ is less than unity, proceed as follows:

4. Using the values computed in steps 2 and 3, enter the curves of pages B3.81-1,-2,-3 to obtain the factor t_o/t_i .

5. The factor t_o/t_i , where multiplied by t_i from step 1, yields the minimum housing wall thickness, t_o .

6. Add 1/32" to t_o for possible variation in position of reamed hole in housing due to production techniques.

   If short transverse grain direction in dural housing is not parallel to busing, double the housing wall thickness.

   Each housing must also be checked for applied static load (B3.13), and for fatigue.

Example - Determine the minimum housing wall thickness due to the press fit of the bushing pictured below. The housing material is 7075-T6 plate and the bushing material is heat treated 4130 steel. The short transverse grain direction is parallel to the bushing.

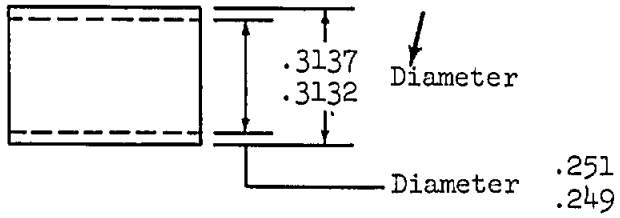

Step 1. d = .3125 = nominal diameter of reamed hole

t_i = .03125 = nominal thickness of bushing

Reamed hole = .3125 ± .0005

Bushing O.D. = .3137 + .0000
- .0005

Max. Interference, = (.3137 + .0000) - (.3125 - .0005)
= .0017

PRESS FIT STRESSES

Design of Housing For Press Fit (Cont.)

Step 2. $t_i/d = \frac{.03125}{.3125} = .100$

Step 3. $F_{ty} = 66000$ psi (Ref. MIL-HDBK-5, "A" value)

$$\frac{f_o\, d}{KE_o\delta} = \left(\frac{1}{1.5}\right) \frac{(66000/2)(.3125)}{(10.3)(10)^6(.0017)} = .393$$

Step 4. $T_o/t_i = 12$

Step 5. $(t_o/t_i)t_i = 12\ (.03125)$

$t_o = 3/8"$

Step 6. Minimum Housing Wall Thickness $= t_o + 1/32"$

$= 13/32"$

Strength checks for applied static load and for fatigue are made separately.

STRESS IN HOUSING PRODUCED BY PRESS FIT

Inner Cylinder of Steel - Housing of Dural

f_o = Tangential stress at inner surface of housing, in psi. In no case should f_o exceed 1/2 F_{ty}, where F_{ty} is the transverse tensile yield stress of the housing material.

K = Stress concentration factor:
K = 1 for the case of one cylinder pressed into another, as shown by the dotted line in the figure.
K = 1.5 for the case of a cylinder pressed into a housing such as shown in the figure.

E_o = Young's modulus for the housing material (10.3×10^6 psi).

δ = Interference (difference between outside diameter of inner cylinder and inside diameter of housing, in inches.)

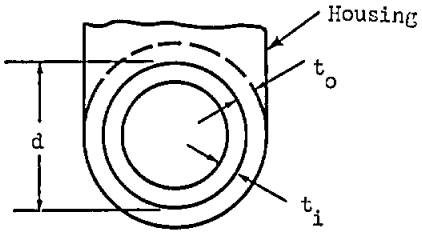

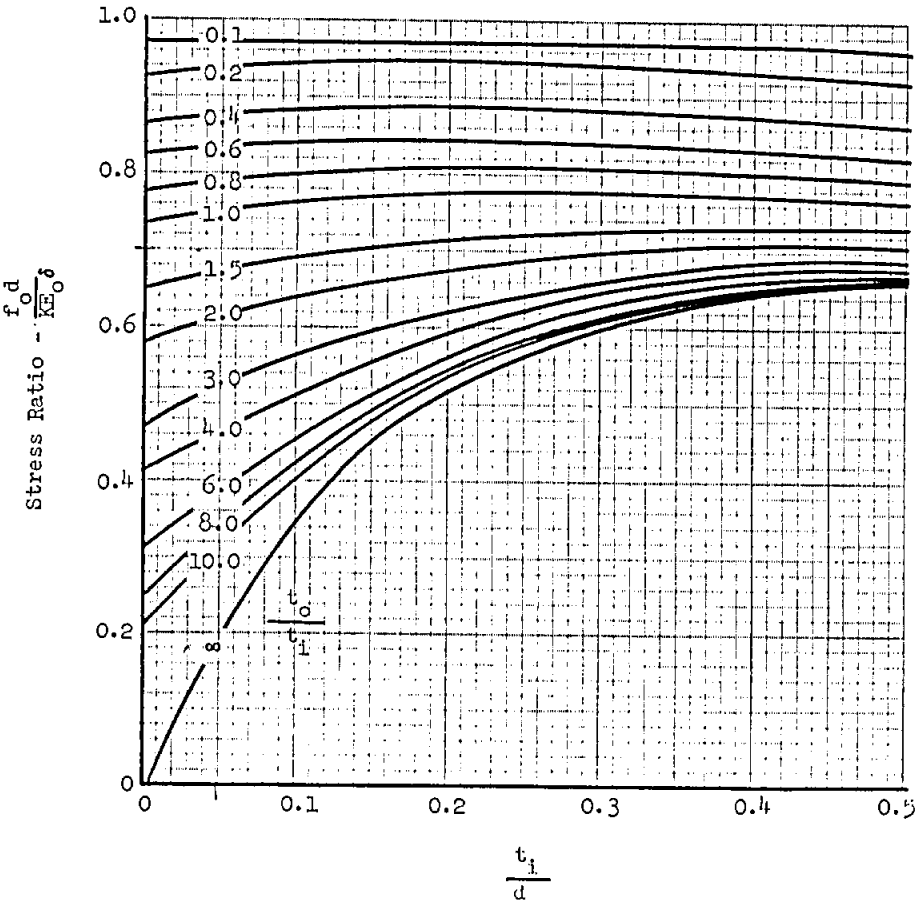

Ref: E12-A

STRESS IN HOUSING PRODUCED BY PRESS FIT

Inner Cylinder of Steel - Housing of Steel

f_o = Tangential stress at inner surface of housing, in psi. In no case should f_o exceed 1/2 F_{ty}, where F_{ty} is the transverse tensile yield stress of the housing material.

K = Stress concentration factor:
K = 1 for the case of one cylinder pressed into another, as shown by the dotted line in the figure.
K = 1.5 for the case of a cylinder pressed into a housing such as shown in the figure.

E_o = Young's modulus for the housing material (30×10^6 psi).

δ = Interference (difference between outside diameter of inner cylinder and inside diameter of housing, in inches.)

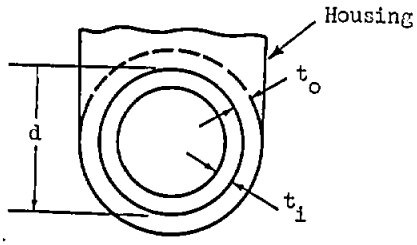

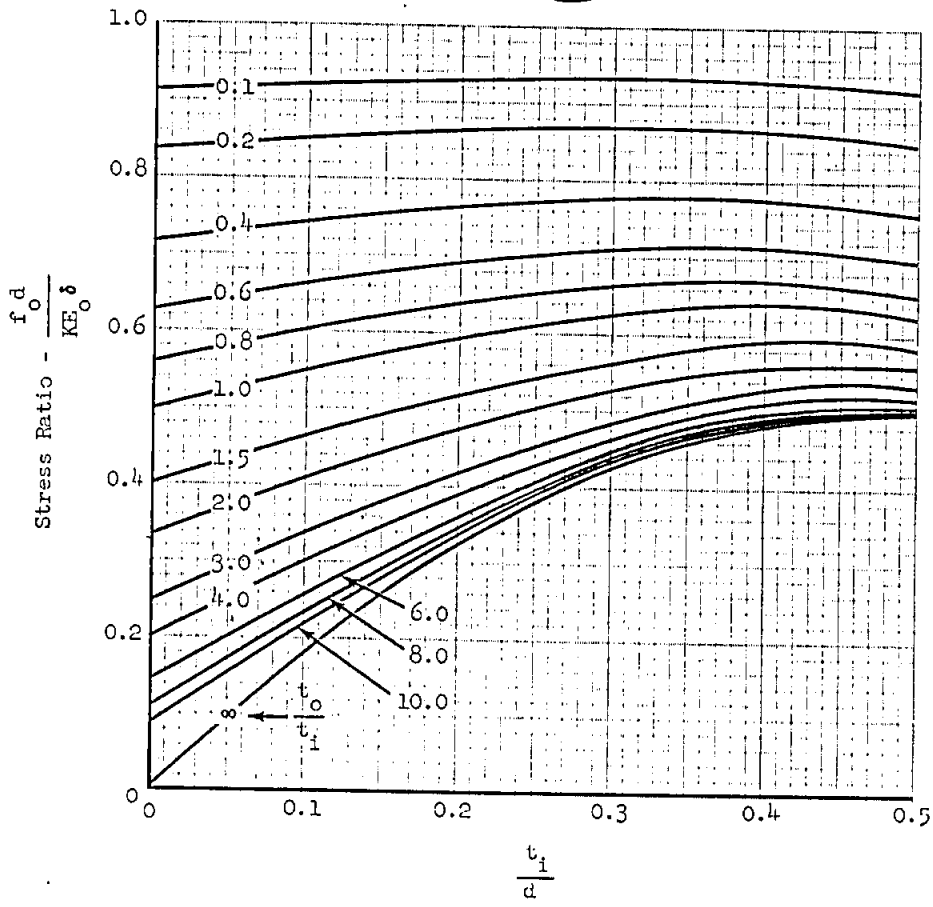

Ref: E12-A

STRESS ON HOUSING PRODUCED BY PRESS FIT

Inner cylinder of Bronze - Housing of Dural

f_o = Tangential stress at inner surface of housing, in psi. In no case should f_o exceed 1/2 F_{ty}, where F_{ty} is the transverse tensile yeild stress of the housing material.

K = Stress concentration factor:
K = 1 for the case of one cylinder pressed into another, as shown by the dotted line in the figure.
K = 1.5 for the case of a cylinder pressed into a housing such as shown in the figure.

E_o = Young's modulus for the housing material (10.3×10^6 psi).

δ = Interference (difference between outside diameter of inner cylinder and inside diameter of housing, in inches)

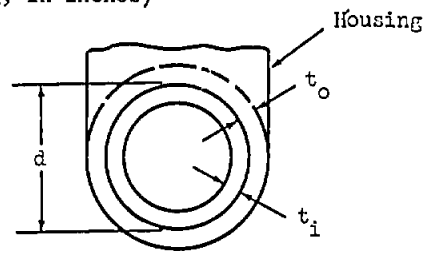

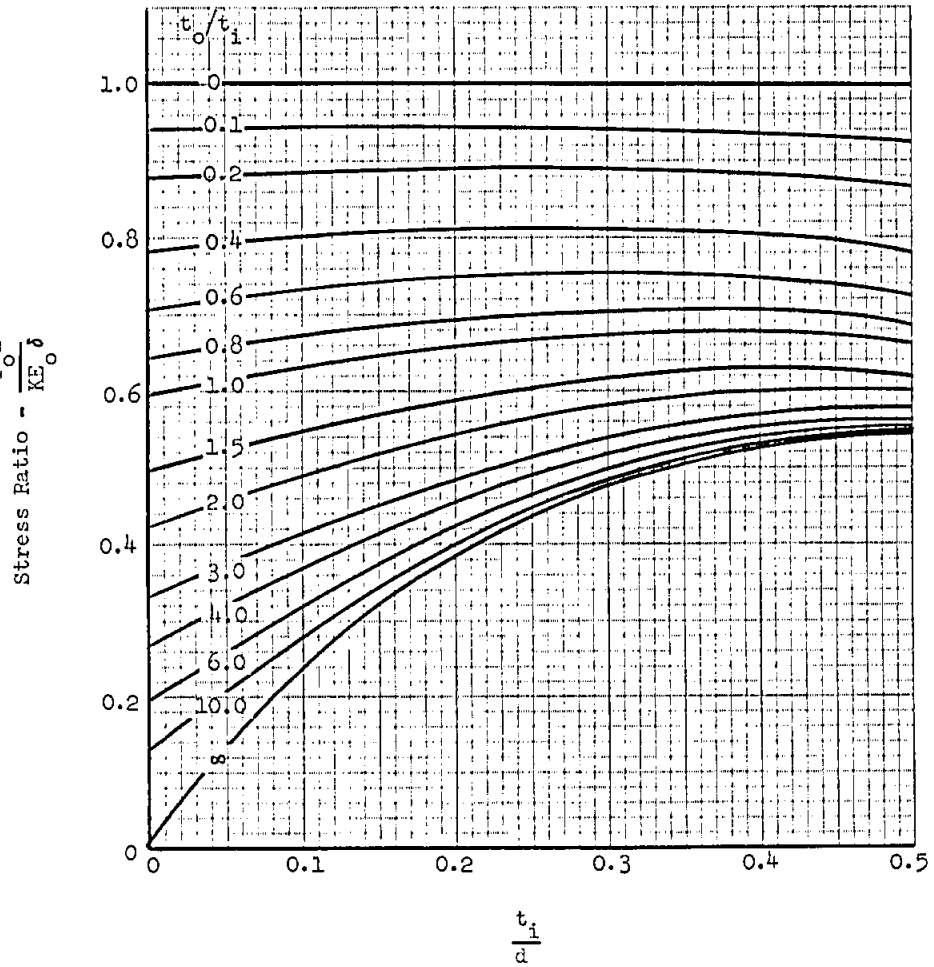

Ref: E12-A

NEUTRAL AXIS LOCATIONS FOR
EXTRUDED CHANNELS AND ANGLES

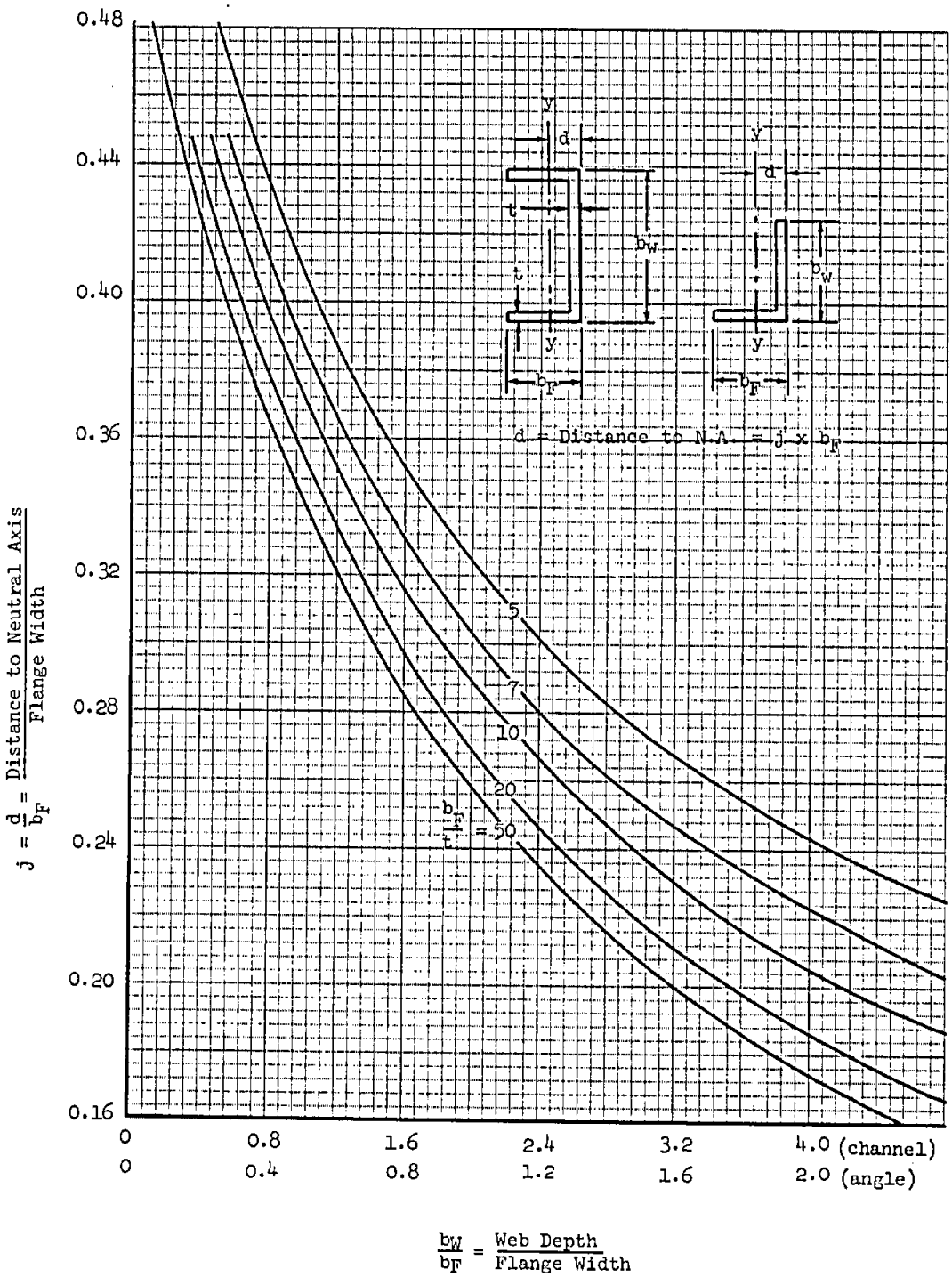

RADII OF GYRATION OF EXTRUDED CHANNELS AND ANGLES

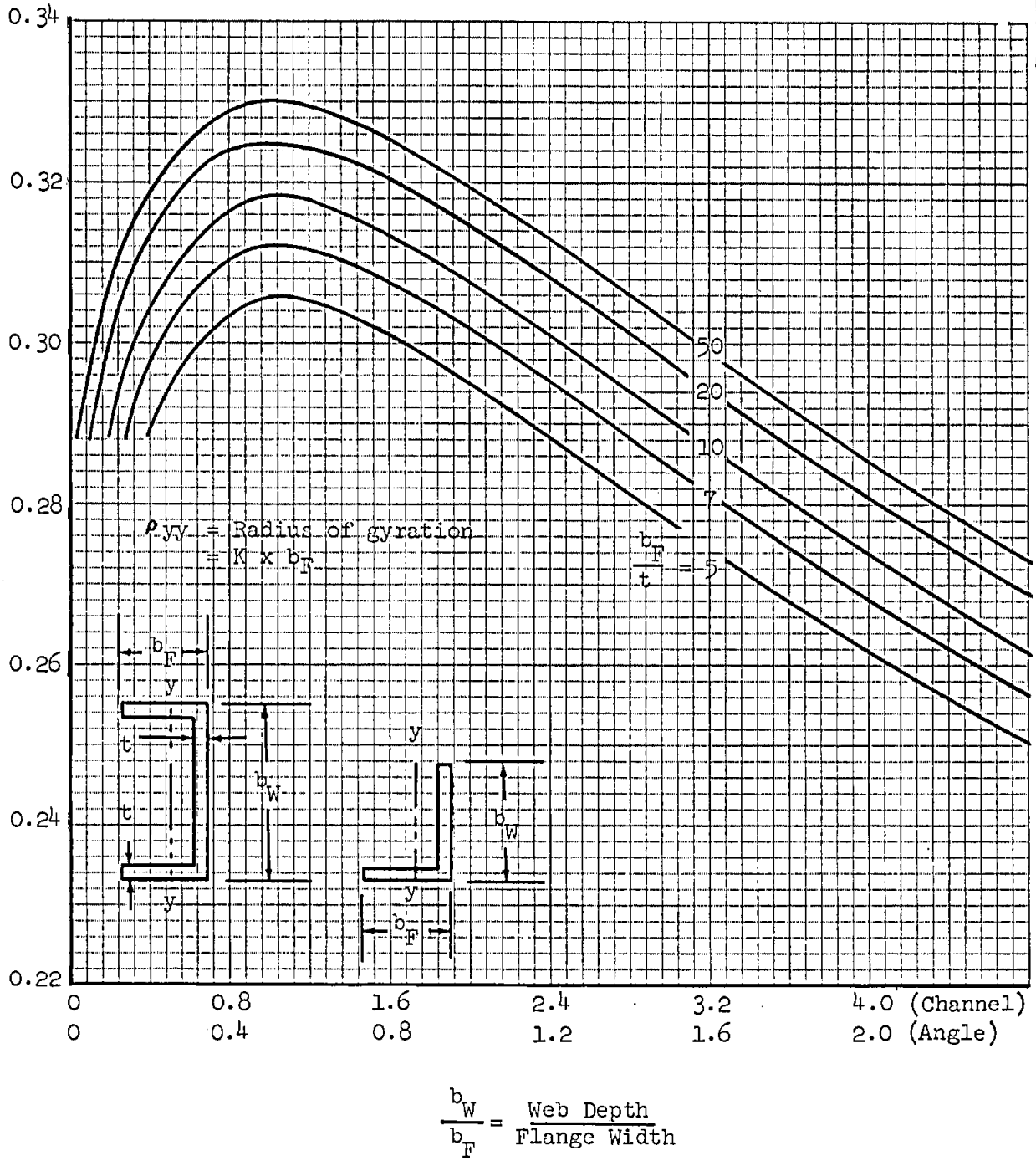

RADII OF GYRATION OF EXTRUDED
CHANNELS AND ZEES

ρ_{xx} = Radius of Gyration = K x b_w

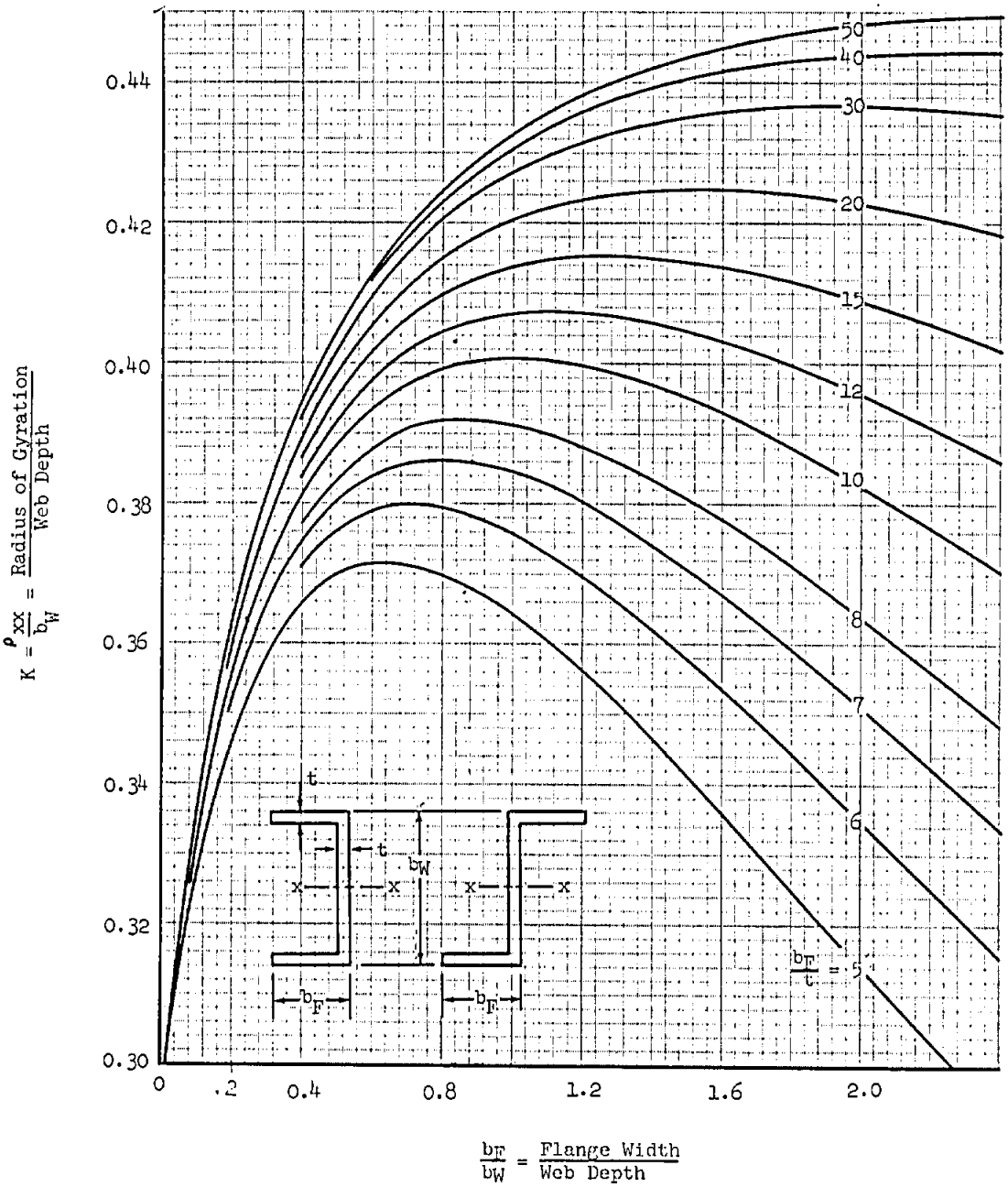

$K = \frac{\rho_{xx}}{b_w} = \frac{\text{Radius of Gyration}}{\text{Web Depth}}$

$\frac{b_F}{b_w} = \frac{\text{Flange Width}}{\text{Web Depth}}$

NEUTRAL AXIS LOCATIONS FOR FORMED CHANNELS AND ANGLES

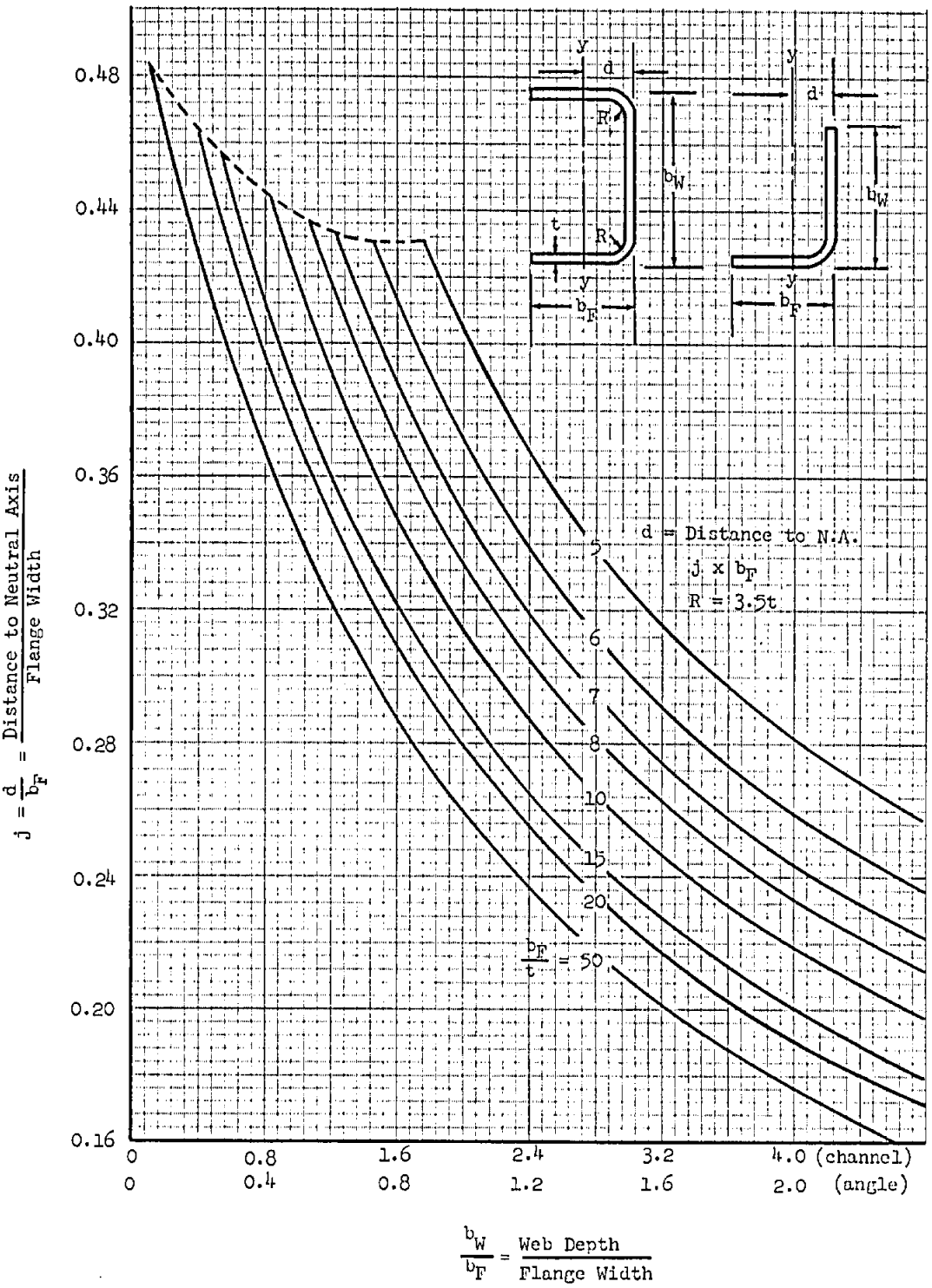

RADII OF GYRATION OF FORMED CHANNELS AND ANGLES

ρ_{yy} = Radius of gyration
= K x b_F

R assumed to be 3.5t

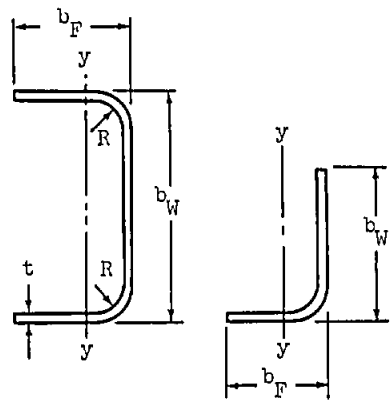

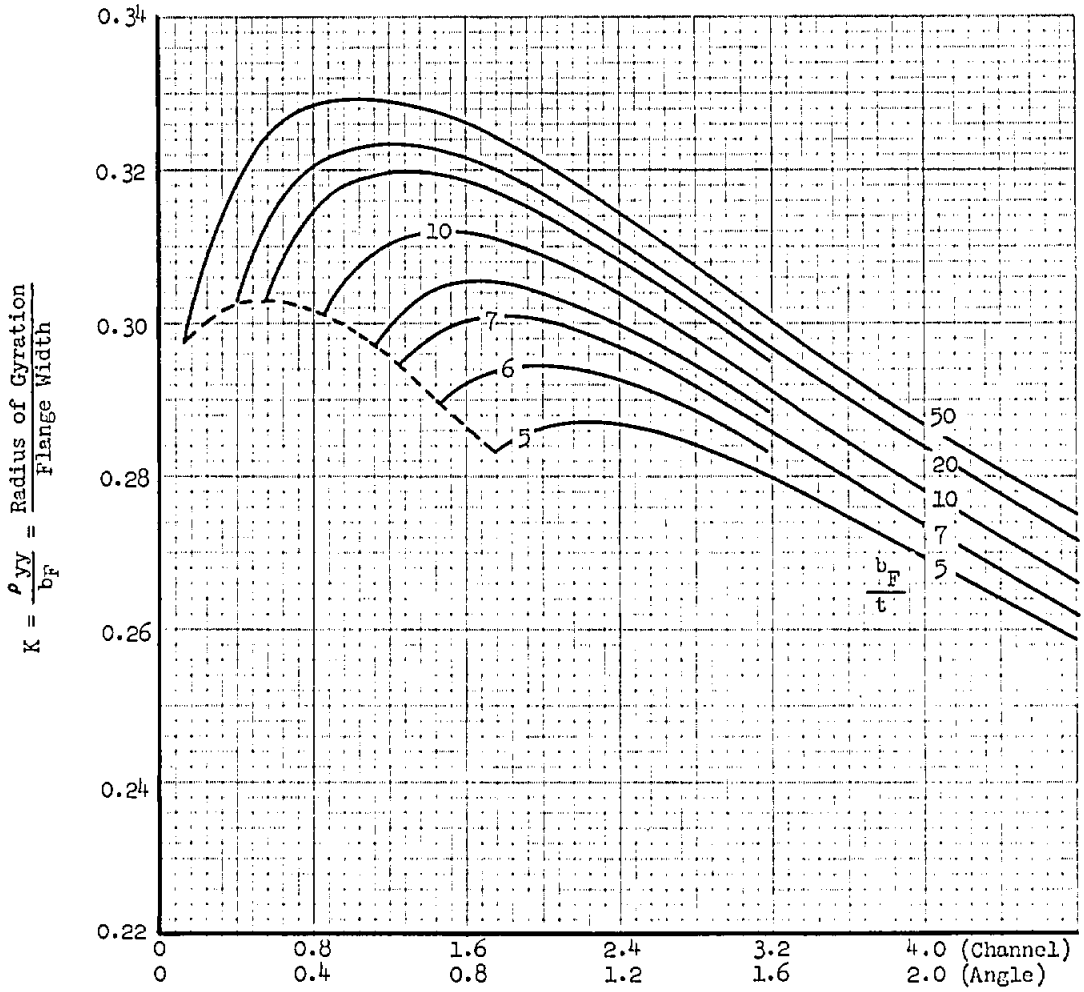

Grumman

RADII OF GYRATION OF FORMED CHANNELS AND ZEES

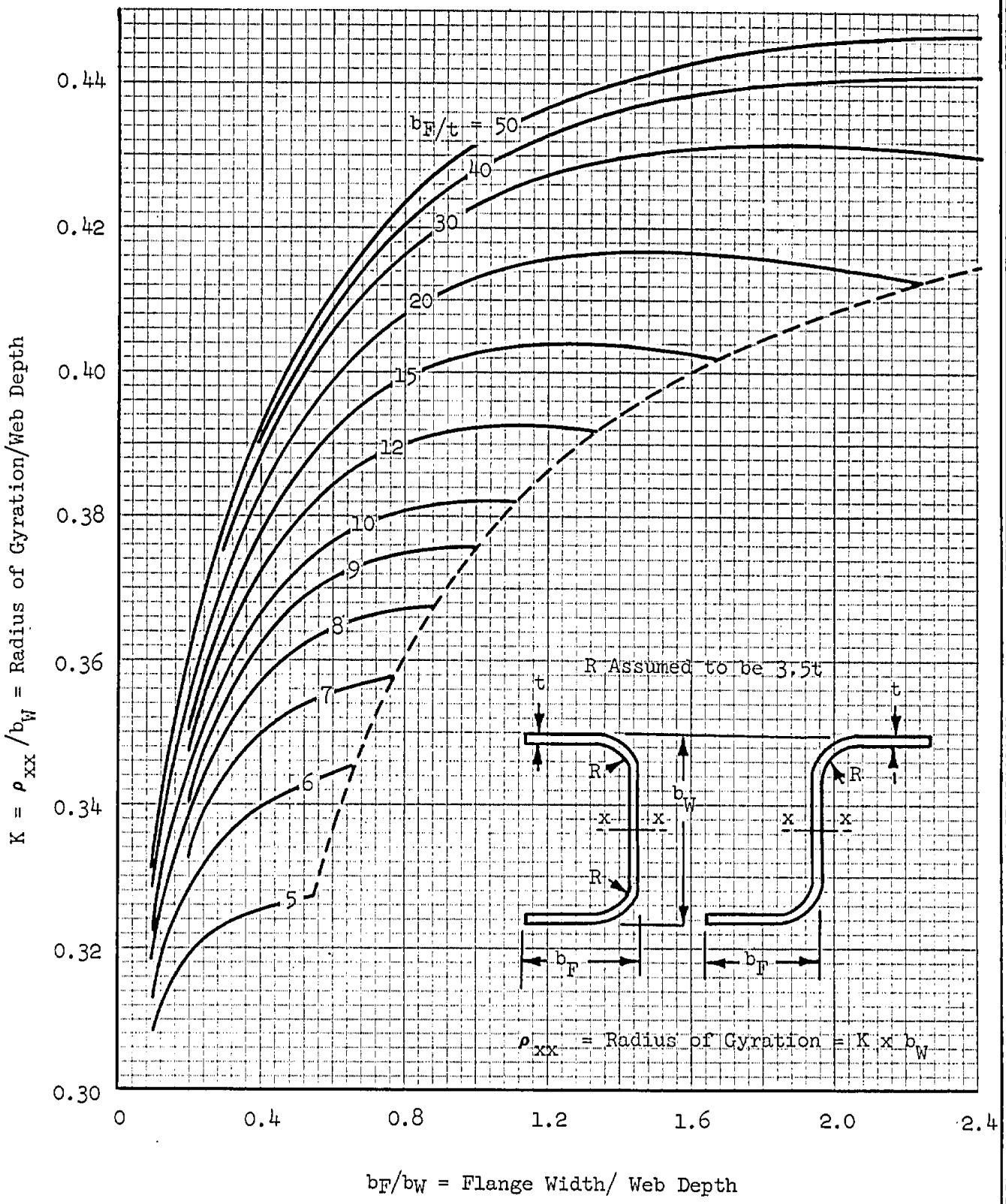

SECTION B4 - THIN WALLED SECTIONS

Table of Contents

B4.00 STRENGTH OF SHORT, THIN-WALLED SECTIONS

4.00 Introduction

This part deals with the local strength of the cross-section of a thin-walled compression member, such as a channel, zee, or I-section. By definition, the local strength of a column depends only upon the properties of the cross-section and is independent of column length effects. The local strength of the section is important in the design of thin-walled columns because it serves as a cut-off or upper limit to the column-curves in the short column range (see B4.40).

The local strength of a cross-section is best described in terms of its local buckling stress $F_{c_{cr}}$ and its crippling stress F_{cc}. The local buckling stress defines the point at which the cross-section of a short column will first begin to distort (see B4.10 and B4.20). The crippling stress is defined as the ultimate compressive stress a very short, thin-walled column can support (see B4.30). In both cases the column is assumed to be so short or so restrained that there is no possibility of any interaction between local failure and a primary column failure. This assumption is maintained in the following pages dealing with local buckling and crippling.

It is intended that the strength of the section obtained in the following pages be only the first part of the calculation of the strength of a column. The second part of the calculation is found in B4.40, entitled, "Interaction of Column Failure with Local Failure".

B4.10 ELASTIC LOCAL BUCKLING OF THIN-WALLED SECTIONS

4.10 Explanation

The various elements in a short, thin-walled column act like compressed plates supported at the corners of the cross-section. When the compressive stress reaches the local buckling stress, the cross-section begins to distort as buckles appear throughout the section, the length of the buckles being approximately equal to the width of the web (see Figure a). The local buckling stress of the section depends upon the buckling strengths of the individual plate elements which make up the section, and on the interaction between the elements. In general, when local buckling occurs, the corners of the cross-section are assumed to be restrained against any lateral movement. An exception to this arises in the case where a lip is inadequate to support its corner. This case is treated in B4.13.02, under Sections With Unstable Lips.

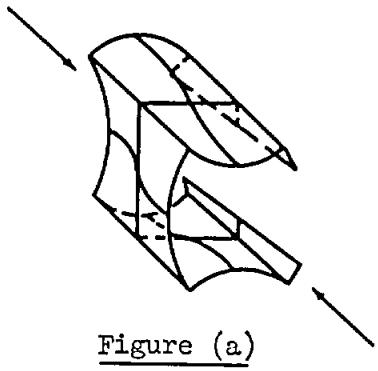

Figure (a)

Methods for determining $F_{cr_{el}}$, the elastic value of the local buckling stress, are given below for various types of sections loaded in compression and for a few sections in bending. Procedures for correcting the elastic buckling stress to take into account plastic effects are given in B4.20 under Plastic Local Buckling of Thin-Walled Sections.

It should be realized, however, that, in general, a very short thin-walled column can be loaded beyond its local buckling stress. Procedures for determining the ultimate stress a thin-walled section can support are given in B4.30 under Crippling of Thin-Walled Sections.

B4.11 ELASTIC LOCAL BUCKLING OF STANDARD SECTIONS

4.11 Standard Sections

4.11.01 Standard Sections in Compression

The local elastic buckling stresses of plain zee, channel, and I-sections have been determined by the NACA, and are given in coefficient form on pages B4.11.10-1, -2. These graphs apply to both formed sections and extrusions.

Example: Find the local elastic buckling stress in compression for the channel shown at the right. The material is 7075-T6 bare aluminum alloy sheet. Since this is a formed section, centerline dimensions are used.

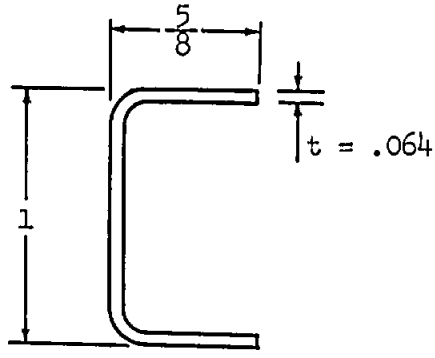

$t_F = .064$ $b_F = .625-.032 = .593$

$t_W = .064$ $b_W = 1.00-.064 = .936$

$t_W/t_F = 1$ $b_W/b_F = .936/.593 = 1.58$ $t_F/b_F = .064/.593 = .108$

Refer to page B4.11.10-1.

$K_F = .73$ (from graph)

$F_{cr_e\ell} = K_F E (t_F/b_F)^2 = (.73)(10.5)(10)^6(.108)^2 = 89300$ psi(*)

This theoretical buckling stress is higher than the proportional limit for the material, and obviously has to be corrected for plastic effects according to the method of B4.20.

4.11.02 Standard Sections in Bending

The local elastic buckling stress $F_{cr_e\ell}$ of plain zee or channel sections in symmetrical bending can be calculated with the use of the curves for the local instability coefficient on page B4.11.20-1. The top and bottom flanges of the zees or channels need not be identical, but the curves apply directly only to the particular case where the neutral axis is at the center of the web. When the stress in the compression flange reaches $F_{cr_e\ell}$, the section becomes unstable and begins to distort. The corners, however, are assumed to be restrained against any lateral movement, and remain straight.

(*) or See B4.11.09-1

B4.11 ELASTIC LOCAL BUCKLING OF STANDARD SECTIONS (Cont.)

4.11.02 Standard Sections in Bending (Cont.)

The most pronounced buckles will occur in the compression flange and in the part of the web near the compression flange, but will die out towards the tension flange.

Example: The channel at the right is in symmetrical bending about axis x-x. Find the elastic stress in the compression flange at which the section will buckle locally. The material is 7075-T6 aluminum alloy extrusion. Since this is an extruded section, use inside dimensions.

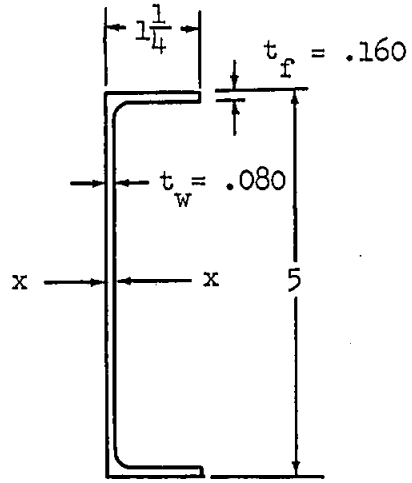

$t_F = .160$ $b_F = 1.25-.080 = 1.17$

$t_W = .080$ $b_W = 5.0-(2)(.160) = 4.68$

$t_W/t_F = .50$ $b_W/b_F = 4.68/1.17 = 4.0$

$t_F/b_F = .160/1.17 = .137$

Refer to page B4.11.20-1

$K_F = .405$ from graph.

$$F_{cr_\ell} = K_F E (t_F/b_F)^2 = (.405)(10.5)(10)^6(.137)^2 = 79800 \text{ psi } (*)$$

This stress is higher than the proportional limit for the material, so a plastic correction must be made (see B4.20).

(*) or See B4.11.09-1

ELASTIC LOCAL BUCKLING STRESSES FOR
THIN ALUMINUM ALLOY FLANGES

NOTE: (1) The dashed horizontal lines on the graph separate the elastic region (below the dashed lines) from the plastic region (above the lines) for the various alloys

(2) In the elastic region the buckling stress is obtained directly from the graph

(3) In the plastic region the buckling stress = $F_{c_{cr}}$ and is determined as follows: (a) obtain $F_{cr_{e\ell}}$ from this graph;

(b) enter the appropriate curve on page B4.21.10-1 with $F_{cr_{e\ell}}$ and determine $F_{c_{cr}}$

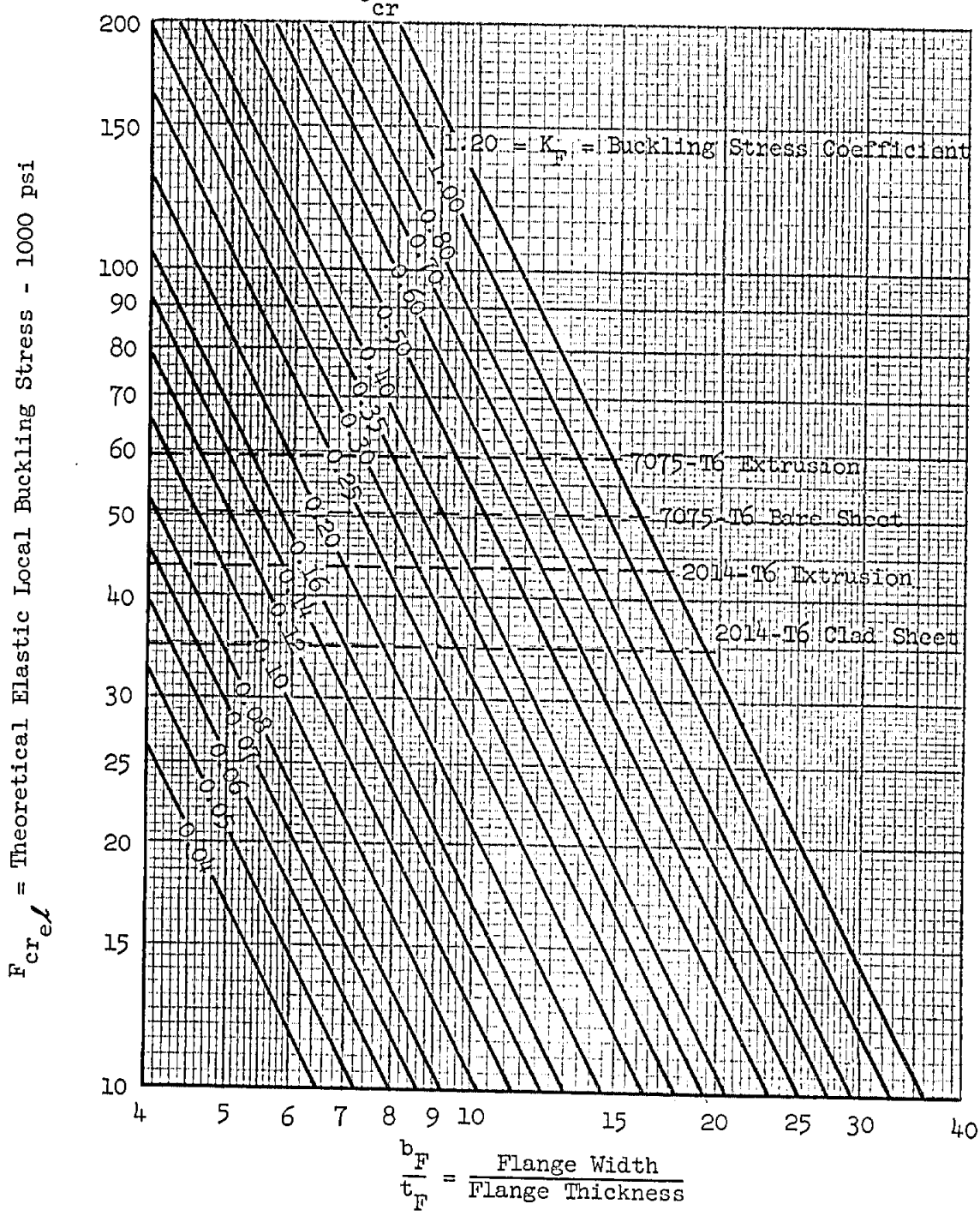

LOCAL INSTABILITY COEFFICIENT FOR ZEE AND CHANNEL SECTION COLUMNS

Theoretical elastic buckling stress - $F_{cr_{e\ell}} = K_F E (t_F/b_F)^2$

Refer to B4.21.10-1 for plastic buckling stress
Refer to B4.31.10-1, -2 for crippling stress

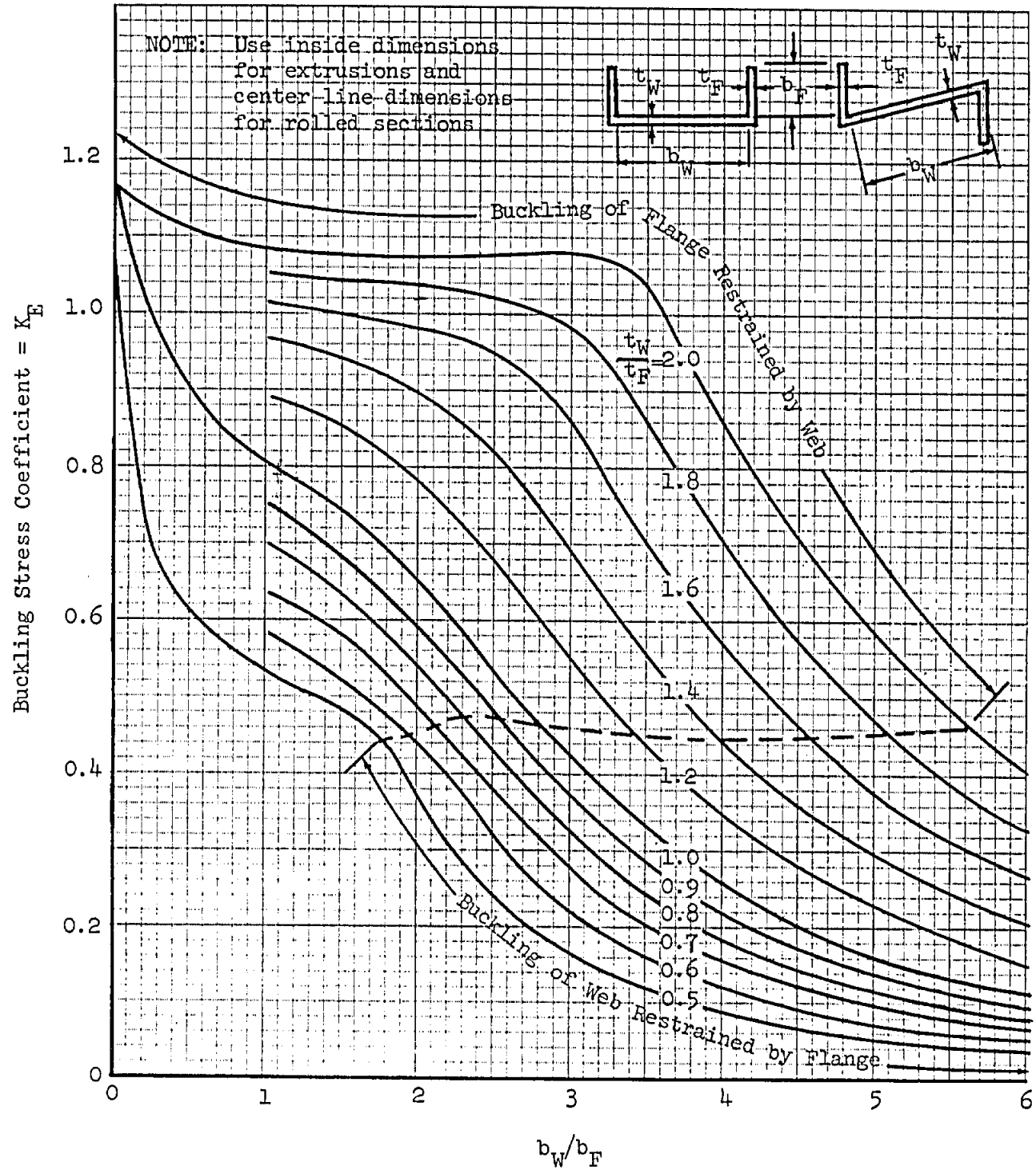

Ref: ARR No. 3K04

LOCAL INSTABILITY COEFFICIENT FOR I-SECTION COLUMNS

Theoretical elastic buckling stress = $F_{cr_{el}} = K_F E (t_F/b_F)^2$

Refer to B4.21.10-1 for plastic buckling stress
Refer to B4.31.10-1, -2 for crippling stress

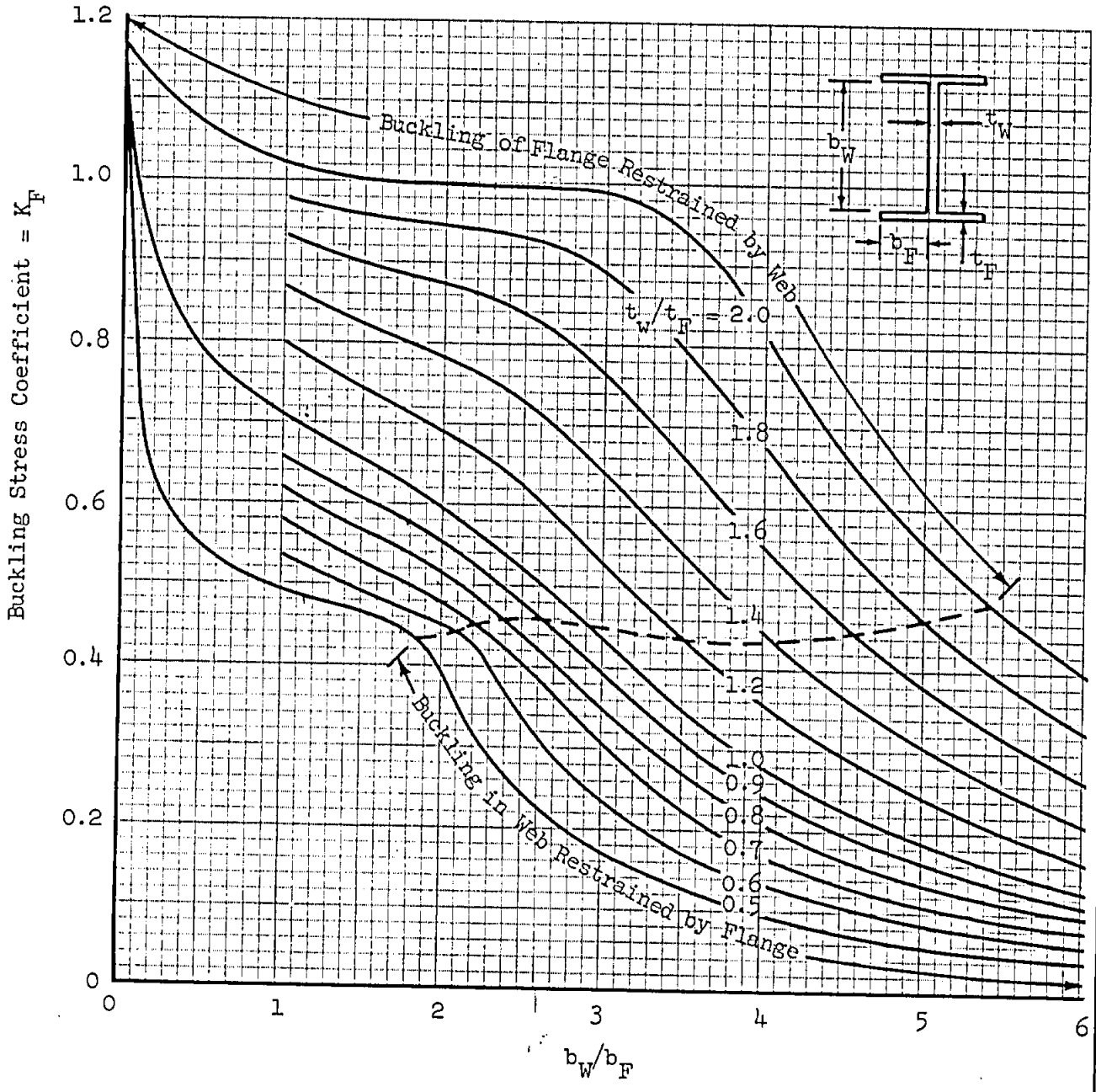

Ref: ARR No. 3K04

LOCAL INSTABILITY COEFFICIENT FOR ZEE AND CHANNEL SECTION IN PURE BENDING

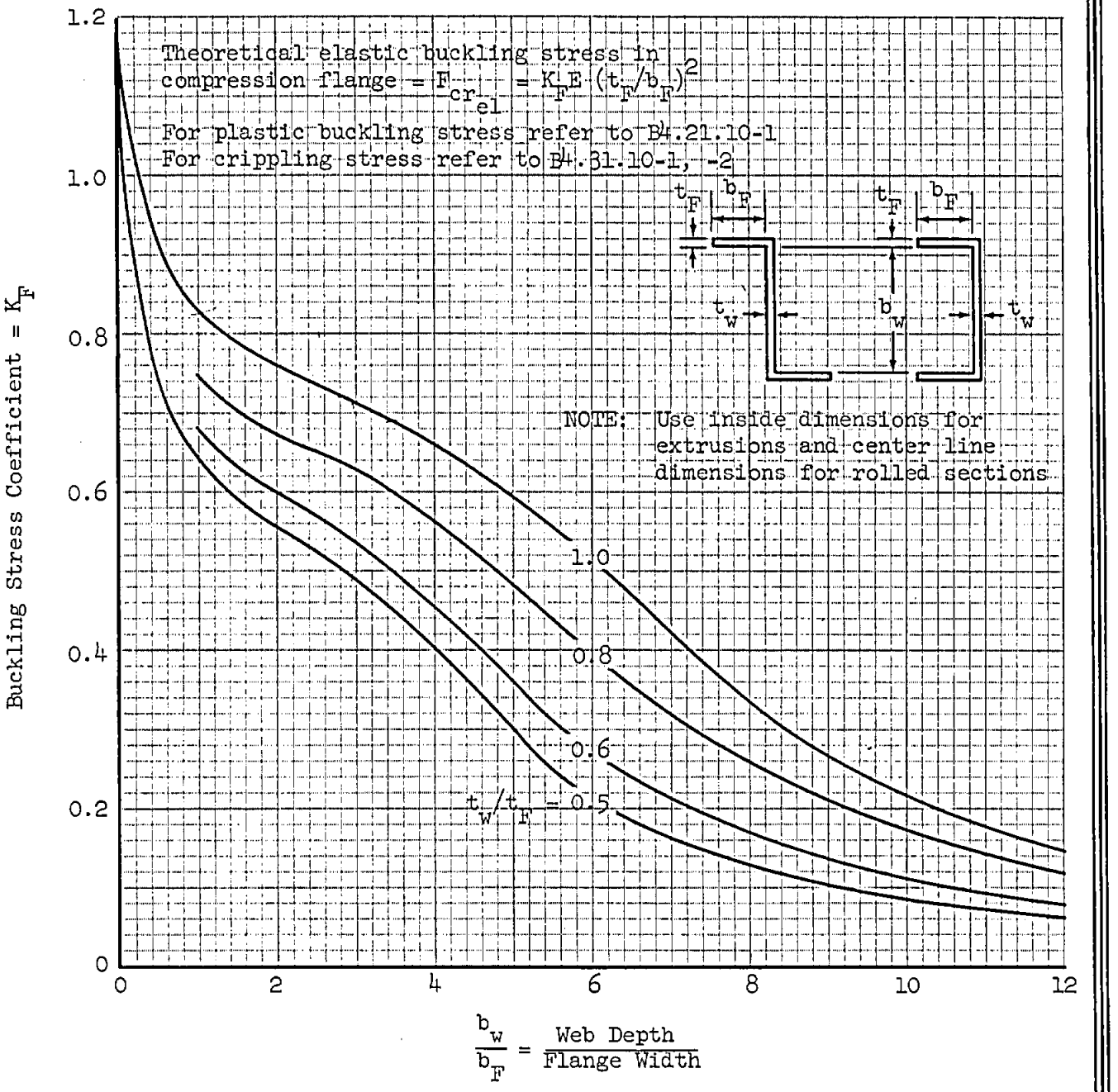

Ref: Grumman Report No. S-2

B4.12 ELASTIC BUCKLING OF ARBITRARY SECTIONS

4.12 Arbitrary Sections With All Corners Stable

This part deals with the local buckling of an arbitrary cross-section with all corners stable. A stable corner in a column cross-section is one that does not move when local buckling takes place over the cross-section. A simple method to determine whether or not a corner is stable is given in B4.13.01, under Sections With Stable Lips.

For the case where all corners are stable, the local buckling stress of the section is determined in the following manner:

(a) Calculate the elastic compressive buckling stress of each individual flat plate element of the section for two types of assumed support conditions at the corners. First, make the calculation assuming the plate elements are hinged at the corners. Then repeat the calculation, assuming the elements are completely fixed at the corners. In both cases the free edges remain free. The elastic buckling stress of any element can be expressed as

$$F_{cr_{el}} = KE\ (t/b)^2$$

where t is the thickness and b is the width of the element (use centerline dimensions for formed sections and inside dimensions for extrusions). The buckling coefficient is

K = 3.62, for elements hinged on both edges

K = .384, for elements hinged on one edge and free on the other edge

K = 6.31, for elements fixed on both edges

K = 1.154, for elements fixed on one edge and free on the other edge.

The flat plate buckling stresses for hinged elements can be obtained directly from the curves on page B5.11.11-3, where curve A applies to an element hinged on one edge and free on the other, and curve B applies to an element hinged on both edges.

The flat plate buckling stresses for elements fixed at the supported edges can be obtained by interpolation from the curves on page B5.11.11-3. Let the lowest of these fixed edge stresses be called F_{lim}. This stress will serve as an upper limit for the buckling of any individual element.

B4.12 ELASTIC BUCKLING OF ARBITRARY SECTIONS (Cont.)

4.12 Arbitrary Sections With All Corners Stable (Cont.)

(b) To find the buckling load of each individual element, multiply the area by either its hinged buckling stress or F_{lim}, whichever is the lower. The local elastic buckling stress for the entire section is then obtained by adding up all the individual element buckling loads and dividing by the entire section area.

The accuracy of this method is greatest when the buckling stresses of the individual elements, as determined in part (a) above, are approximately equal.

Example: Find the local elastic buckling stress in compression of the extruded hat-section at the right. The material is 7075-T6 aluminum alloy. Since this is an extruded section with sharp corners, centerline dimensions are used to obtain the element areas, and inside dimensions are used to obtain the element buckling stresses.

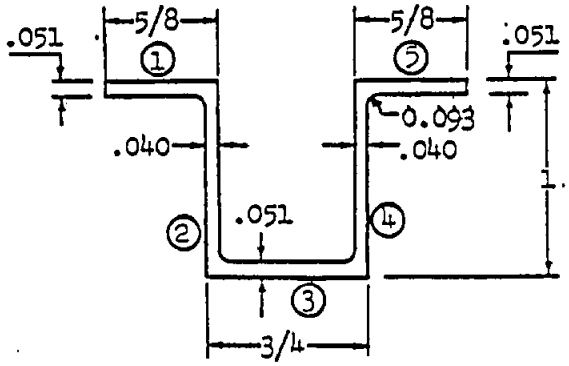

First, the 5/8" flanges will be checked as lips to see whether they stabilize the adjacent corners against any movement in the horizontal plane. Refer to B4.13.01.

$b_L = 5/8 - .040 = .585$; $\quad b_F = 1.00 - .051 - .051 = .898$;

$b_L/b_F = \frac{.585}{.898} = .651$; $\quad b_F/t = \frac{.898}{.040} = 22.5$

Refer to page B4.13.10-1

$R_o = .43$ (from Fig 1)

b_L/b_F is greater than R_o, (the lips are stable).

Therefore, we can determine the local buckling stress of this cross-section according to the method described above for sections with stable corners.

It should be noted here that in most practical applications the flanges of a hat-section would be attached to some other structure (such as wing or fuselage skin), which would probably stabilize the corners of the flange elements regardless of whether or not the flanges are stable as unsupported lips.

B4.12 ELASTIC BUCKLING OF ARBITRARY SECTIONS (Cont.)

4.12 Arbitrary Sections With All Corners Stable (Cont.)

Example (Cont.)

(a)

				Hinged Corners		Fixed Corners	
Element	b_i	t	b_i/t	K	$F_{cr_e\ell}$ B5.11.11-3	K	$F_{cr_e\ell}$ B5.11.11-3
(1) & (5)	.585	.051	11.5	.384	30500	1.154	92000
(2) & (4)	.898	.040	22.5	3.62	75000	6.31	131000*
(3)	.670	.051	13.1	3.62	221000*	6.31	386000*

$\therefore F_{lim}$ = 92000 psi

Maximum value of $F_{cr_e\ell}$ for any element is 92000 psi.

*$F_{cr_e\ell}$ for this element is off the graph on page B5.11.11-3, but it can be determined as follows. (The procedure will be illustrated for element (3), assuming hinged corners.):

(1) Determine the buckling stress $F_{cr_e\ell}$ for an element whose (b/t) is ten times that of element (3).

$b'/t = (10)(13.1) = 131$

$F'_{cr_e\ell}$ = 2210 psi (from page B5.11.11-3)

(2) Multiply $F'_{cr_e\ell}$ by 100 to get the actual elastic buckling stress $F_{cr_e\ell}$ for element (3).

$F_{cr_e\ell} = (100)(2210) = 221000$ psi

Similarly for elements (2), (3), (4), when the fixed corner buckling stresses are to be obtained.

B4.12 ELASTIC BUCKLING OF ARBITRARY SECTIONS (Cont.)

4.12 Arbitrary Sections With All Corners Stable (Cont.)

Example (Cont.)

(b)

Element	$b_{\mathcal{E}}$	t	$A = b_{\mathcal{E}} t$	$F_{cr_{e\ell}}$	$P_{cr_{e\ell}} = F_{cr_{e\ell}} \times A$
(1)	.605	.051	.0309	30500	940
(2)	.949	.040	.0380	75000	2850
(3)	.710	.051	.0362	92000	3330
(4)	.949	.040	.0380	75000	2850
(5)	.605	.051	.0309	30500	940

Section Area = .1740 sq.in. 10910 lbs. = Total Buckling Load

$$F_{cr_{e\ell}} = \frac{10910}{.1740} = 62800 \text{ psi} = \text{Local elastic buckling stress for the section.}$$

This elastic buckling stress has to be corrected for plastic effects according to the method of B4.20 to obtain the true local buckling stress.

The above calculations can be simplified for arbitrary sections of constant thickness.

Example: Find the local elastic buckling stress in compression for the formed hat-section at the right. The material is 7075-T6 bare aluminum alloy sheet. Centerline dimensions are used in determining the element buckling stresses.

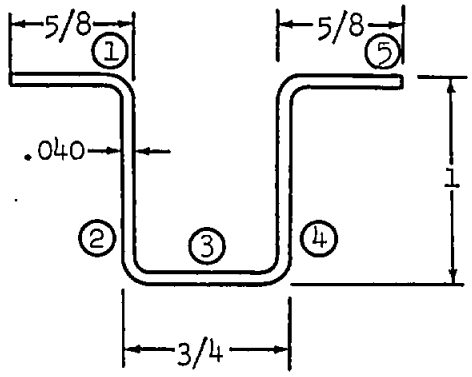

B4.12 ELASTIC BUCKLING OF ARBITRARY SECTIONS (Cont.)

4.12 Arbitrary Sections With All Corners Stable (Cont.)

Example (Cont.)

Refer to B4.13.01 to determine if the corners are stable.

$b_L = 5/8 - .020 = .605$; $b_F = 1.00 - .040 = .960$

$b_L/b_F = \frac{.605}{.960} = .630$; $b_F/t = \frac{.960}{.040} = 24.0$

$R_o = .39$ (from Fig 1, page B4.13.10-1

$b_L/b_F > R$ (the lips are stable).

(a)

Element	$b_{\mathfrak{E}}$	Hinged Corners		Fixed Corners	
		K	$K/(b_{\mathfrak{E}})^2$	K	$K/(b_{\mathfrak{E}})^2$
(1) & (5)	.605	.384	1.05	1.154	3.15
(2) & (4)	.960	3.62	3.93	6.31	6.85
(3)	.710	3.62	7.18	6.31	12.52

$\therefore K/(b_{\mathfrak{E}})^2_{lim} = 3.15$

Maximum value of $K/(b_{\mathfrak{E}})^2$ for any element is 3.15.

(b)

Element	$b_{\mathfrak{E}}$	$K/(b_{\mathfrak{E}})^2$	$K/(b_{\mathfrak{E}})^2 \times b_{\mathfrak{E}}$
(1)	.605	1.05	.64
(2)	.960	3.15	3.02
(3)	.710	3.15	2.24
(4)	.960	3.15	3.02
(5)	.605	1.05	.64
	Σ 3.840		Σ 9.56

$$F_{cr_{e\ell}} = \frac{\Sigma KE\,(t/b)^2\,(bt)}{\Sigma(bt)} = E\,t^2\,\frac{\Sigma(K/b^2)\,(b)}{\Sigma b}$$

$$= (10.5)(10)^6(.040)^2\,\frac{(9.56)}{(3.84)} = 41900 \text{ psi}$$

This stress is in the elastic range so no plastic corrections are necessary.

B4.13 ELASTIC LOCAL BUCKLING OF LIPPED SECTIONS

4.13 Lipped Sections

Many thin-walled sections of arbitrary shape can be classified as lipped sections. A lip is generally a plate element whose main purpose is giving support to the otherwise free edge of the adjacent flange element (see Fig. (a)). Depending upon the relative size of the lip and flange, this edge may or may not move when local buckling occurs.

4.13.01 Sections with Stable Lips

A stable lip will keep the adjacent corner straight when the section buckles locally The adjacent flange element then behaves like a plate supported along both edges instead of like a typical flange element with one edge supported and the other edge free. This is illustrated by the dotted outline in Fig. (a) which shows the buckled shape of a channel section with a stable lip on the lower flange. In this mode of local buckling the web and the lower (stabilized) flange tend to buckle like compressed plates supported at both edges, while the upper flange and the lip itself tend to buckle like typical flange elements, supported along one edge and free on the other edge. The method for determining if a lip is stable and the procedure for calculating the local elastic buckling of an arbitrary section with stable lips are as follows:

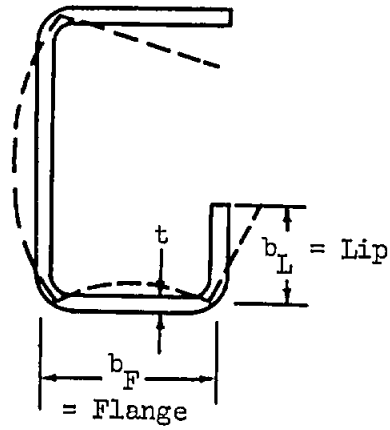

Figure (a)

(1) For the given section, determine the value of b_L/b_F, where b_L is the width of the stabilizing lip, and b_F is the width of the adjacent flange. From Fig. 1 on page B4.13.10-1, determine the value of R_o. If b_L/b_F is equal to or greater than R_o, then the lip is stable. If b_L/b_F happens to be equal to R_o, the lip is the optimum size and the local buckling stress for the entire section is a maximum. The curve in Fig. 1 was drawn for the case where the lip thickness is equal to the flange thickness, and can therefore be expected to give conservative results when the lip is thicker than the flange.

(2) If the lip has been found to be stable, the adjacent corner remains straight when local buckling occurs. For the case where all lips are stable (all corners remain straight), the local buckling stress of the section is determined by the method described in B4.12, under Arbitrary Sections With All Corners Stable.

B4.13 ELASTIC LOCAL BUCKLING OF LIPPED SECTIONS (Cont.)

4.13.02 Sections With Unstable Lips

As mentioned in section B4.13.01, there is an optimum size lip for which the local buckling stress of a section is a maximum; the optimum size lip for a given flange may be determined from the curve of Fig. 1 on page B4.13.10-1.

For lips smaller than the optimum size, the lip-flange intersection moves during local buckling of the section (see Fig. (b). This is called an unstable lip. For b_L/b_F less than 0.15 the section behaves as if there were no lip. A procedure for calculating the local buckling stress of a section having an unstable lip follows:

(1) Calculate $(F_{cr})_{max}$, the local buckling stress of the section, assuming that it has optimum size lips. Use the procedure given in B4.12 for sections with stable corners.

(2) Calculate $(F_{cr})_{min}$. the local buckling stress of the section, assuming that it has no lips. Use the procedure given in B4.11.01 or B4.12, whichever is appropriate.

(3) Using the actual lip width to flange width ratio b_L/b_F, enter the curves of Fig. 2 on page B4.13.10-1 to determine the constant K (for $b_L/b_F < .15$, K = 0).

(4) Calculate the elastic local buckling stress of the section by the formula.

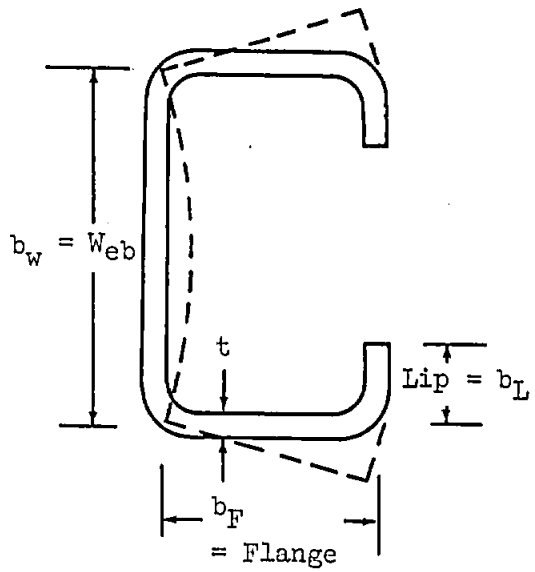

Figure (b)

$$F_{cr_{e\ell}} = (F_{cr})_{min} + K\left[(F_{cr})_{max} - (F_{cr})_{min}\right]$$

B4.13 ELASTIC LOCAL BUCKLING OF LIPPED SECTIONS (Cont.)

4.13.02 Sections With Unstable Lips (Cont.)

Example: Find the elastic local buckling stress in compression for the formed channel section shown at the right. The material is 2014-T6 clad aluminum alloy sheet. Centerline dimensions are used in determining the element buckling stresses and the element areas.

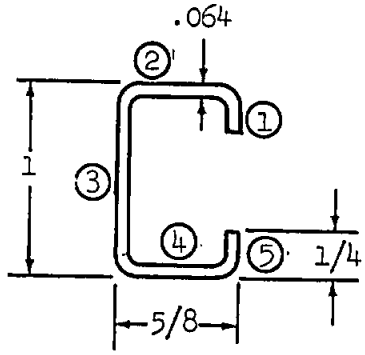

$b_L = 1/4 - .032 = .218$; $b_F = 5/8 - .064 = .561$

$R = b_L/b_F = \frac{.218}{.561} = .389$; $b_F/t = \frac{.561}{.064} = 8.77$

Refer to page B4.13.10-1:

$R_o = (b_L)_{opt}/b_F = .77$; $(b_L)_{opt.} = .77 \times .561 = .432$

The optimum size lip is larger than the actual size lip (.432 > .218), indicating that the actual size lip cannot completely stabilize the flange. Thus the method presented in this section must be used to determine the local buckling stress.

(1) Calculate the local buckling stress of the section assuming it has optimum size lips (see B4.12):

				Hinged Corners		Fixed Corners	
Element	b_{ℓ}	t	b_{ℓ}/t	K	$F_{cr_{\ell}}$ / B5.11.11-3	K	$F_{cr_{\ell}}$ / B5.11.11-3
(1) & (5)	.432	.064	6.75	.384	88500	1.154	266000
(2) & (4)	.561	.064	8.76	3.62	496000	6.31	865000
(3)	.936	.064	14.63	3.62	178000	6.31	310000

$\therefore F_{lim} = 266000$

Maximum value of $F_{cr_{\ell}}$ for any element is 266000 psi.

B4.13 ELASTIC LOCAL BUCKLING OF LIPPED SECTIONS (Cont.)

4.13.02 Sections With Unstable Lips (Cont.)

(b)

Element	$b_{\mathcal{L}}$	t	$A=b_{\mathcal{L}}\,t$	$F_{cr_{e\ell}}$	$P_{cr_{e\ell}} = F_{cr_{e\ell}} \times A$
(1)	.432	.064	.0277	88500	2450
(2)	.561	.064	.0359	266000	9550
(3)	.936	.064	.0600	178000	10700
(4)	.561	.064	.0359	266000	9550
(5)	.432	.064	.0277	88500	2450

Section Area = .1872 sq. in. 34700 lb. = Total Buckling Load

$(F_{cr})_{max} = \frac{34700}{.1872} = 185000$ psi = Local elastic buckling stress for a section with optimum size lips.

(2) Calculate the local buckling stress of the section assuming it has no lips:

The channel with no lips is a standard section, and its elastic local buckling stress is the same as that of the channel section shown on page ~~B4.11.01-1~~ B4.11-1. Thus

$(F_{cr})_{min} = 89300$ psi.

(3) Determine the constant K from the curves of Fig. 2 on page B4.13.10-1:

$R = b_L/b_F = .389$; $R_o = .77$; $K = .58$

(4) Calculate the elastic local buckling stress of the actual section:

$F_{cr_{e\ell}} = 89300 + .58\ [185000 - 89300] = 145000$ psi

LOCAL BUCKLING STRESSES FOR NARROW LIPPED SECTIONS

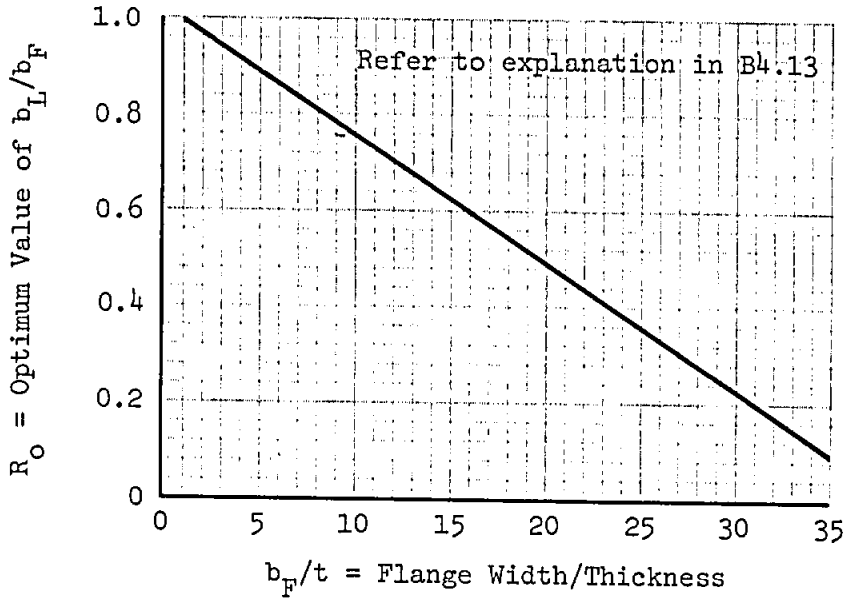

Fig. 1

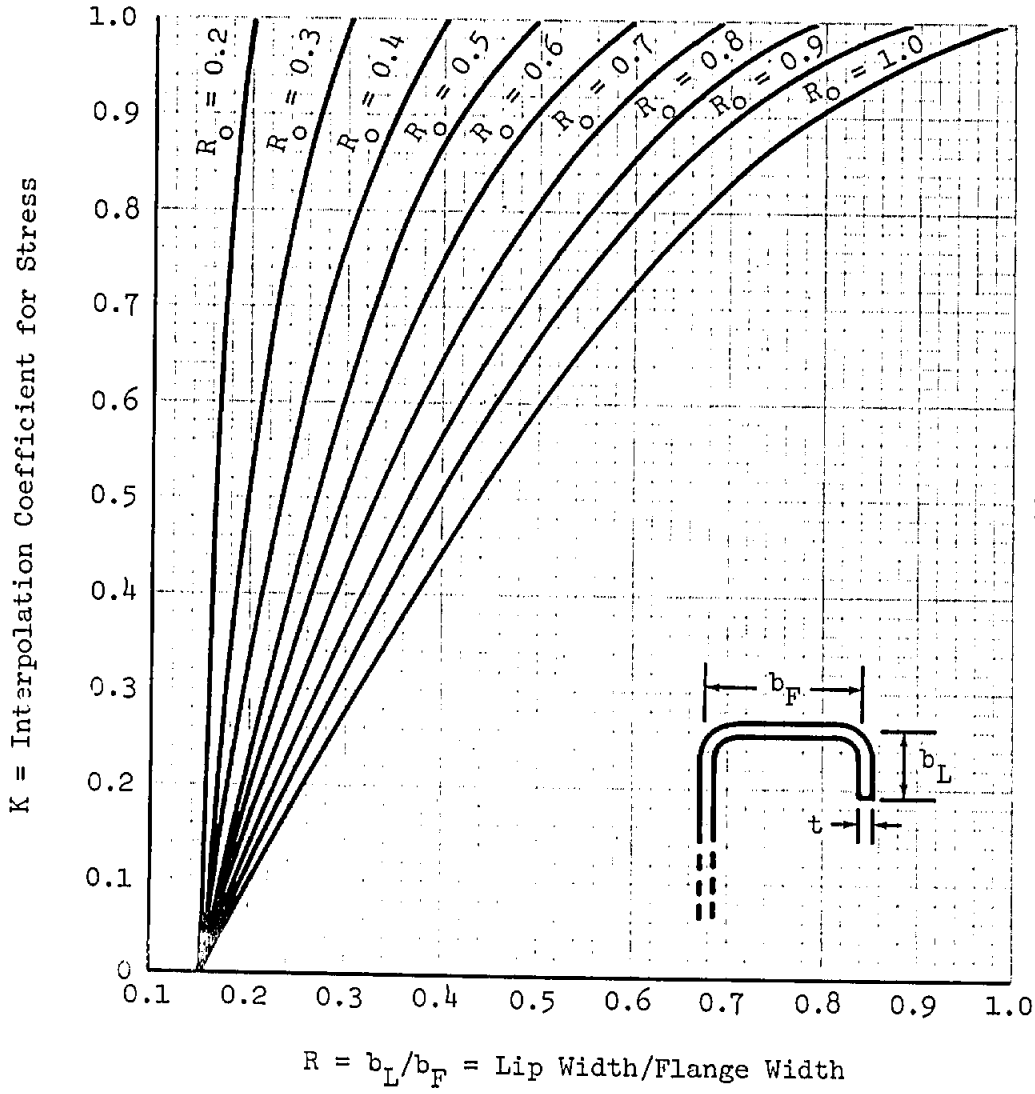

Fig. 2

B4.20 PLASTIC LOCAL BUCKLING OF THIN-WALLED SECTIONS

4.20 Explanation

When $F_{cr\ell}$, the local buckling stress of a thin-walled section, exceeds the proportional limit of the material in compression, the reduced bending stiffness of the material causes the section to buckle at a stress below the theoretical elastic value. This plastic local buckling stress Fc_{cr} can be determined for the various types of thin-walled sections according to the general procedure given below.

General Procedure

(1) Determine $F_{cr\ell}$, the local elastic buckling stress of the section. Use the method in B4.10 which applies to the particular section being considered.

(2) Determine Fc_{cr}, the local plastic buckling stress, from the appropriate curve on page B1.50.1-1 or B1.50.1-2.

Example: Determine the local plastic compressive buckling stress Fc_{cr} of the 7075-T6 formed channel section that was discussed in the example in B4.11.01.

$n = 14.5$

$F_{0.7} = 69800$ psi (from tables of B1.20)

$F_{cr\ell} = 89300$ psi (from example of B4.11.01)

$F_{cr\ell}/F_{0.7} = 89300/69800$

$= 1.28$

$Fc_{cr}/F_{0.7} = 0.905$ (from B1.50.1-2)

$Fc_{cr} = 0.905 \times 69800$

$= 64200$ psi

Example: Determine the local plastic compressive buckling stress F_{ccr} of the 7075-T6 extruded hat section that was discussed in the example in B4.12.

$n = 27.5$

$F_{0.7} = 72000$ psi

$F_{cr\ell} = 62800$ psi

$F_{cr\ell}/F_{0.7} = 62800/72000$

$= 0.872$

$F_{ccr}/F_{0.7} = 0.87$ (from B1.50.1-2)

$F_{ccr} = 0.87 \times 72000$

$= 62600$ psi

PLASTIC LOCAL BUCKLING STRESSES FOR THIN-WALLED ALUMINUM ALLOY SECTIONS IN COMPRESSION

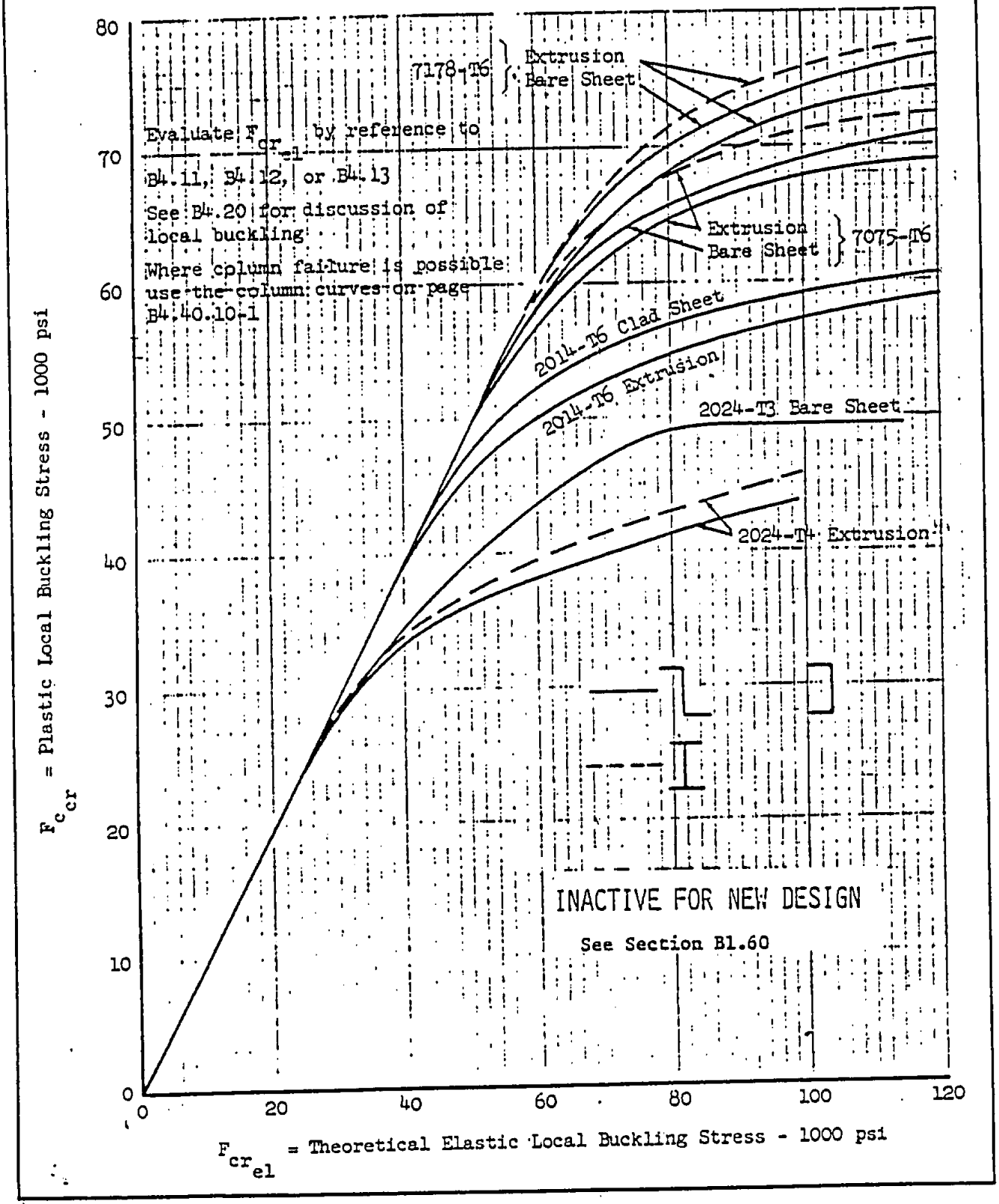

B4.30 CRIPPLING OF THIN-WALLED SECTIONS

4.30 Explanation

When the corners of a thin-walled section in compression are restrained against any lateral movement, the corner material can continue to be loaded even after local buckling has occured in the section. The remaining material is largely ineffective in supporting additional load above the buckling load. The average stress on the section at the maximum attainable compression load is defined as the crippling stress, F_{cc}. Figure (a) below shows the member distortion occuring over one buckle length in a typical thin-walled section. Figure (b) shows the stress distribution over the cross-section when the section is loaded to the crippling stress. The maximum stress on the cross-section, F_e, for any material is a function of the stress-strain characteristics of the material. F_e may be obtained from page B1.60-3. F_e has been determined from the Von Kármán effective width formulation with plasticity based on the secant modulus and evaluated so as to produce the maximum value of F_{cc} consistant with the section geometry.

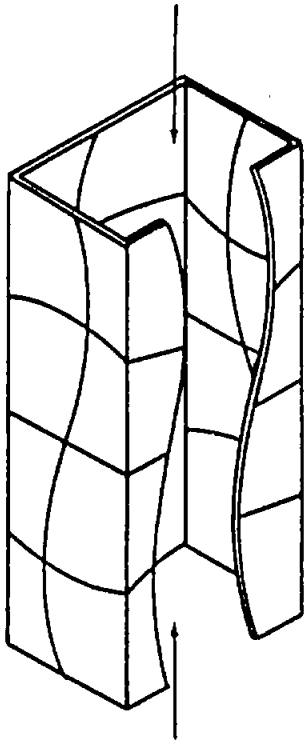

Figure (a)

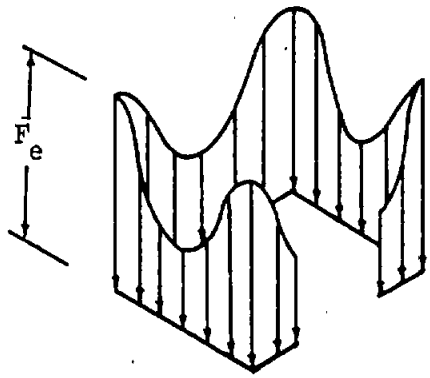

Figure (b)

B4.30 CRIPPLING OF THIN-WALLED SECTIONS (Cont.)

4.30 Explanation (Cont.)

Whereas there is both theoretical and experimental information on the local buckling stresses of various types of thin-walled sections, the information on the crippling stresses is limited mainly to experimental data obtained from tests on a few standard sections. Therefore, until additional information is available, a single procedure is given below for determining the crippling stresses of all types of thin-walled sections made up of flat-plate elements.

General Procedure

(1) Determine $F_{cre\ell}$, the local elastic buckling stress of the section. Use the method in B4.10 that applies to the particular section being considered.

(2) Determine F_{cc}, the local crippling stress from the non-dimensional curve of Section B1.60.

Example: Determine the crippling stress F_{cc} of the 7075-T6 formed channel section that was discussed in the example in B4.11.01.

$n = 14.5$
$F_{0.7} = 69800$ psi (from tables of B1.20)

$F_{cre\ell} = 89300$ psi (from example in B4.11.01)

$F_{cre\ell}/F_{0.7} = 89300/69800$
$= 1.28$

Since this value is off-scale of figure on page B1.60-2, use page B1.50.1-2.

$F_{cc}/F_{0.7} = F_{cr}/F_{0.7} = 0.990$
$F_{cc} = 0.990 \times 69800$
$= 69100$ psi

B4.30 CRIPPLING OF THIN-WALLED SECTIONS (Cont.)

4.30 Explanation (Cont.)

Example: Determine the crippling stress F_{cc} of the 7075-T6 extruded hat section that was discussed in the example on pages B4.12-2,-3, & -4.

$n = 27.5$

$F_{0.7} = 72000$ psi (from tables of B1.20)

$F_{cre\ell} = 62800$ psi (from example on page B4.12-4)

$F_{cre\ell}/F_{0.7} = 62800/72000$

$= 0.872$

$(F_{cc}/F_{0.7})_{Formed} = 0.87$ (from B1.60-2)

$\sum A_{corner} = 4 \times 0.040 \times 0.051 + (4 - \Pi) \times 0.093^2$

$= 0.0156$ in^2

$A = 2\ (0.585 \times 0.051) + 2\ (0.898 \times 0.040) + 0.670 \times 0.051 + 0.0156$

$= 0.181$

$F_e/F_{0.7} = 0.914$ (from B1.60-3)

$(F_{cc}/F_{0.7})_{Extr} = (0.87 \times (0.181 - 0.0156) + (0.914 \times 0.0156))/0.181$

$= 0.874$

$F_{cc} = 0.874 \times 72000$

$= 62913$ psi

CRIPPLING STRESSES FOR THIN-WALLED FORMED ALUMINUM ALLOY SECTIONS IN COMPRESSION

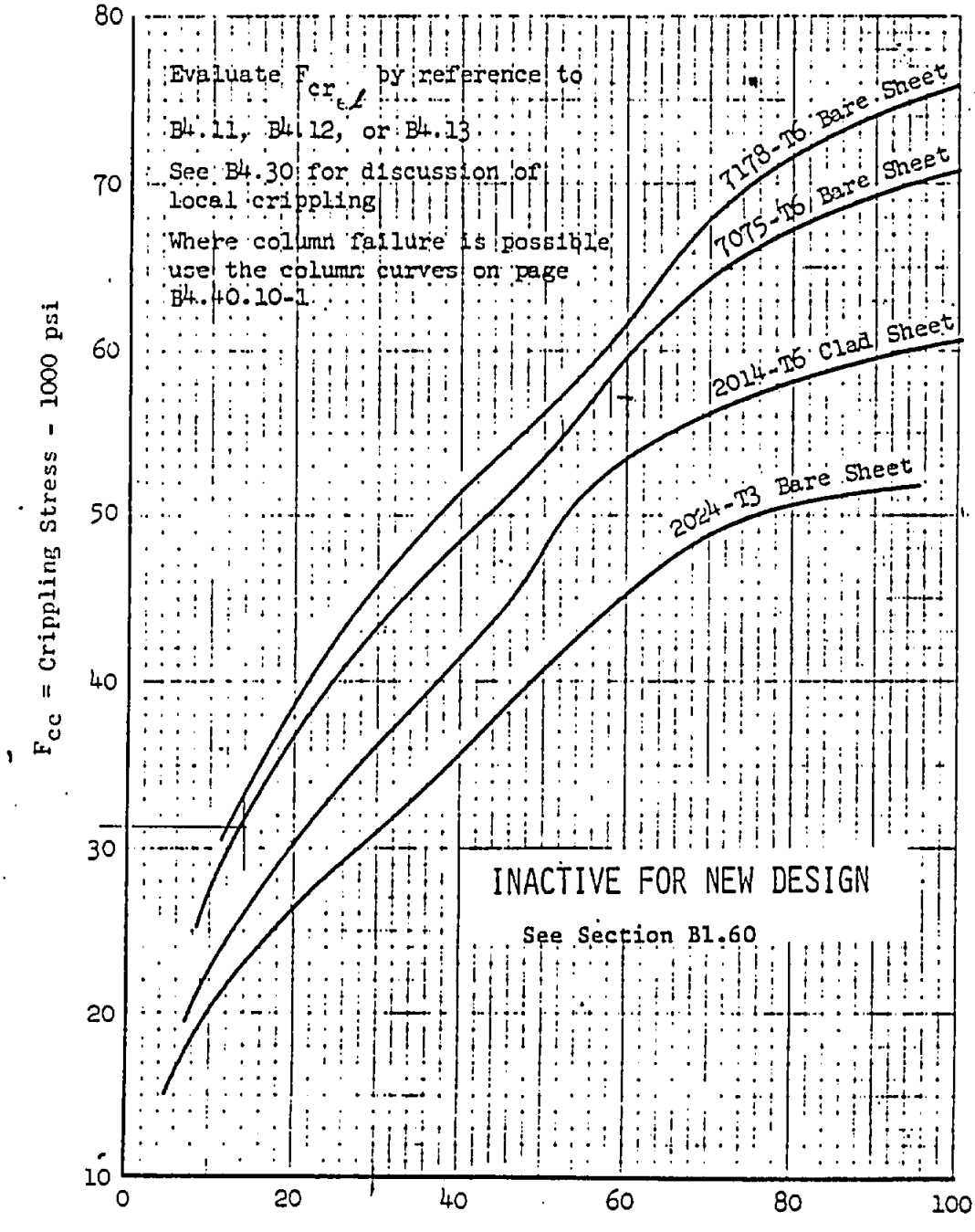

$F_{cr_{e\ell}}$ = Theoretical Elastic Local Buckling Stress - 1000 psi

Ref: ARR No. L5F01; GAEC Report Nos. E33, S4, S5

*GAC 4610 2-74

CRIPPLING STRESSES FOR THIN-WALLED EXTRUDED ALUMINUM ALLOY SECTIONS IN COMPRESSION

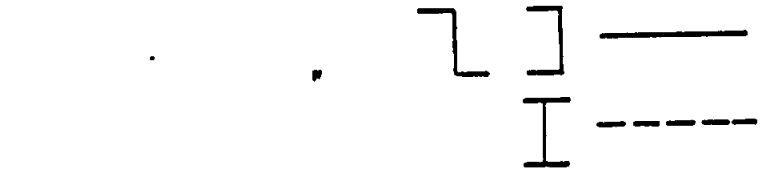

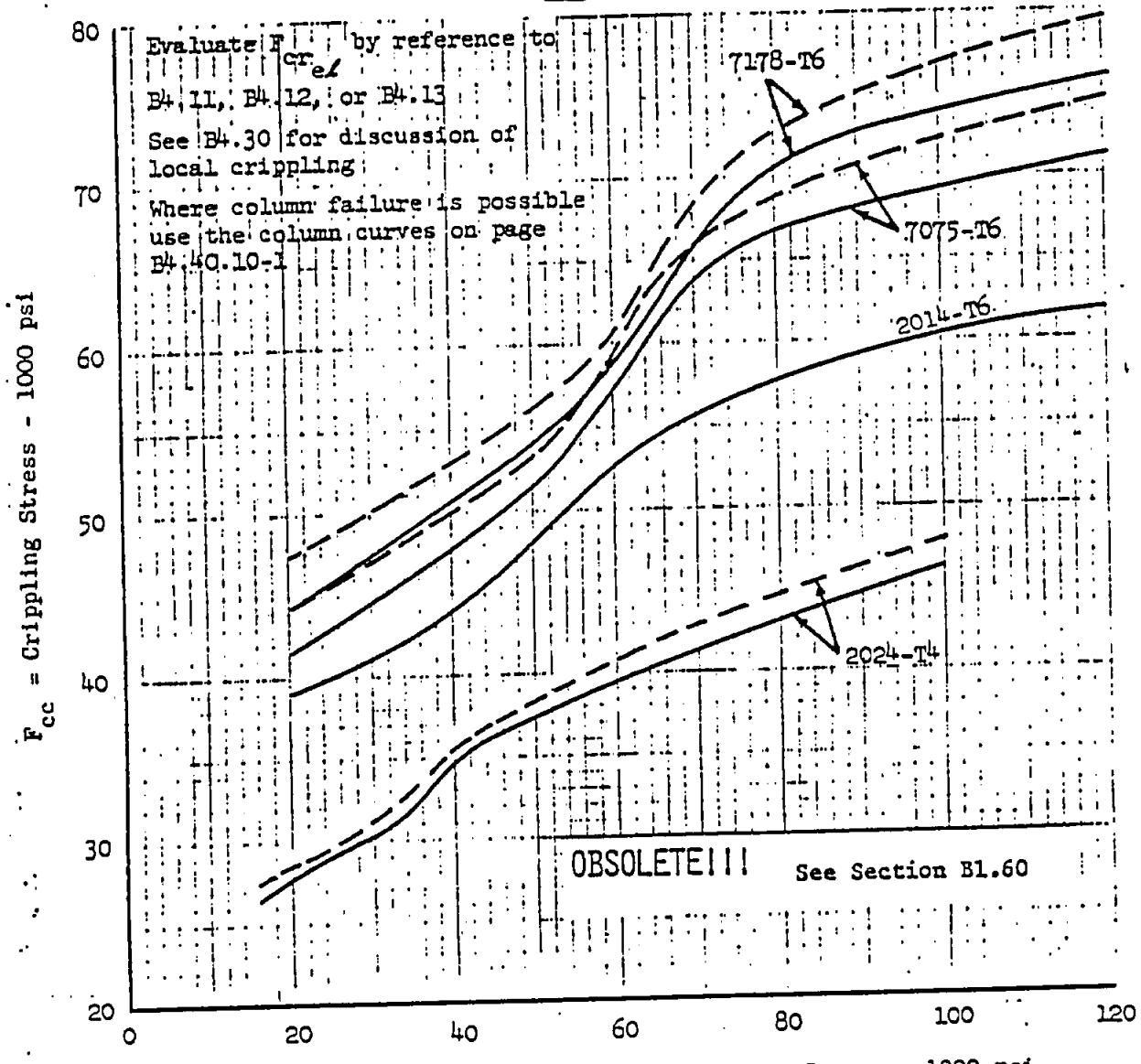

Ref: ARR Nos. L5F08a, L5F08b, L6C19; GAEC Report No. S5

B4.40 INTERACTION OF COLUMN FAILURE WITH LOCAL FAILURE

B4.40 Explanation

Local Failure

If the cross-section of a column contains thin elements, it may be subject to local buckling, which can considerably reduce the column strength. In this type of failure, local distortion of the cross-section accompanies the bowing and twisting typical of column failure. The local strength of a section can be gauged by its local buckling stress F_{ccr} and its crippling stress F_{cc}. Local Buckling will occur below F_{ccr} and Local Crippling will occur below F_{cc} if the column is not restrained against lateral bowing. Local buckling is the stress at which the section begins to distort locally. At this stress the plate elements of the section buckle while the corners remain straight, as is shown in Fig. (a) above. However, the section is capable of sustaining a load greater than the local buckling load because the corners do not fail until their stress reaches yield or slightly above yield, while the stress at points farthest away from the corners remains near the buckling stress. The stress distribution at maximum load is shown in Fig. (b). When the corners fail, the section is said to have crippled, and the maximum load divided by the section area is the crippling stress F_{cc}.

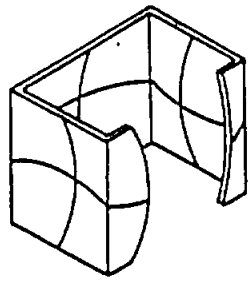

Fig. a

Local Buckling stresses may be found by referring to B4.10 and B4.20, and crippling stresses are given in B4.30.

Column Failure

A column depends primarily on its bending and twisting stiffness for stability. That is, the restoring moment it produces to resist curvature is sufficient to balance the bending moment caused by the c.g. being defected away from the load line when the column is bent. But if the elements of a column are already buckled locally in compression, their stiffnesses in compression are considerably reduced, resulting in a much lower effective moment of inertia for the column. In fact, above the local buckling stress the only significant bending rigidity left is that contributed by the corners; and at crippling even the corners fail. Evidently, in the local buckling range it is the number and the disposition of the corners which determine the strength of the column.

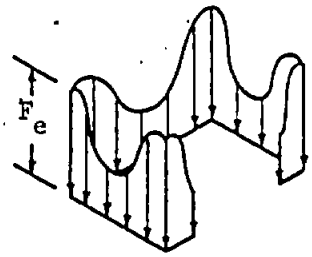

Fig. b

B4.40 INTERACTION OF COLUMN FAILURE WITH LOCAL FAILURE (Cont.)

B4.40 Explanation (Cont.)

Hat sections, square sections, and zee & channel sections having stable lips (see footnote) all have four or more corners. In short columns, the corners of these sections remain straight along the length of the column even after local buckling has taken place. These corners are able to supply the bending stiffness necessary to resist column failure about either principal axis, and, therefore, short columns with these cross-sections remain straight until the corners fail locally. Hence, the upper limit of the column curve for these sections is taken as the crippling stress F_{cc}.

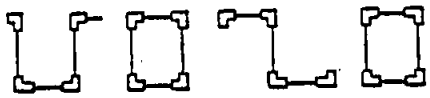

Fig. c

Plain zee and channel sections have only two corners, and when these sections have buckled locally, their corners are able to give them bending stiffness only about axis x-x but not about axis y-y (see Fig. (d)). Therefore, failure naturally tends to occur about axis y-y. The highest stress reached by short lengths of these sections which fail about axis y-y is not much above the local buckling stress. Hence, the upper limit of the column curve for plain zees and channels is normally taken as the local buckling stress $F_{c_{cr}}$.

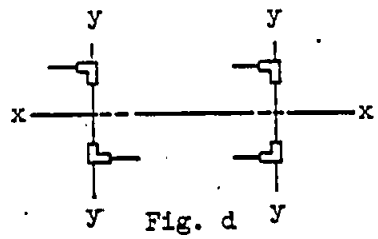

Fig. d

Occasionally a plain zee or channel may be so restrained or supported that it can only fail about axis x-x. Since the corners can supply bending stiffness about axis x-x, even after local buckling has occurred, very short columns with this type of restraint remain straight until the corners cripple. Hence, the upper limit of the column curve for failure in this mode is the local crippling stress F_{cc}.

In general, if the column allowable (neglecting the effect of local buckling) is lower about axis x-x than about y-y, the column should be checked for failure about both axes, with the local crippling stress F_{cc} as the upper limit of the column curve when checking against failure about x-x, and the local buckling stress $F_{c_{cr}}$ as the upper limit when checking against column failure about axis y-y.

NOTE: The lipped zee and channel sections shown in Fig. (c) are not able to develop their full crippling stress, even for short column lengths, unless the lip is wide enough to stabilize the corner. If the lip is very short, the corner behaves as if there were no lip. A procedure for determining the effectiveness of the lip in stabilizing the corner is given in B4.13.01.

B4.40 INTERACTION OF COLUMN FAILURE WITH LOCAL FAILURE (Cont.)

B4.40 Explanation (Cont.)

It should be noted that attaching the stringer along one flange to a sheet will not constrain the column to fail as an Euler column about axis x-x. Instead, the column will fail as shown in Fig. (e) after local buckling has occurred. The sheet prevents an Euler column failure about axis y-y because it restrains the corner of the attached flange against displacement parallel to the plane of the sheet; but the other corner is still free to fail in the weak direction, as shown by the arrow in Fig. (e). Therefore, in the case of a plain zee or channel attached to sheet along one flange, local buckling of the flanges makes the column subject to a torsional instability failure, as shown in Fig. (e), and the upper limit of the column curves must be the local buckling stress. However, if the lower flange of the stringer is also stiffened against failure in the weak direction, perhaps by attaching it to a sheet or by adding a stable lip to the flange, as shown in Fig. (f), the column retains bending stiffness about both axes x-x and y-y until the corners fail. The final column failure may be an Euler column failure about axis x-x in the case of the stinger attached to sheet along both flanges, or a combination of an Euler failure and a torsional instability failure in the case of the stringer with the stabilizing lip. Because the column retains bending stiffness until the corners fail, the upper limit of the column curves should be taken as the crippling stress F_{cc} in both the cases shown in Fig. (f).

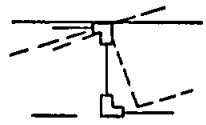

Fig. e

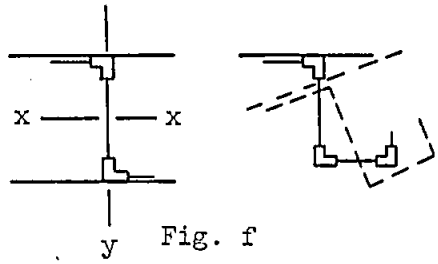

Fig. f

A set of column curves has been provided on page B4.40.10-1, each curve having a different local failing stress as an upper limit. The local failing stress to be used in selecting the proper column curve for any particular problem is either the crippling stress F_{cc} or the local buckling stress of the section $F_{c_{cr}}$ as explained above. These column curves apply specifically to the case where the column failure results from the interaction between local failure and an Euler column type of primary failure.

B4.40 INTERACTION OF COLUMN FAILURE WITH LOCAL FAILURE (Cont.)

The method of analysis of columns subject to local failure can be summarized as follows:

<table>
<tr><td rowspan="5">Type of Section</td><td>a. Sections having four corners.
  </td><td rowspan="2">e. Sections having only two corners (with no restraint in any direction).
 
(Arrow represents direction of column failure.)</td></tr>
<tr><td>b. Sections having three corners, attached to a sheet along one unlipped flange.
 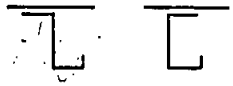 </td></tr>
<tr><td>c. Sections having two corners, attached to sheets along both flanges.
 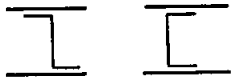 </td><td rowspan="2">f. Sections having only two corners, attached to a sheet.
 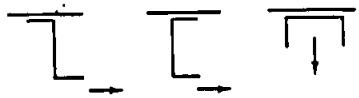
(Arrow represents direction of column failure.)</td></tr>
<tr><td>d. Sections having only two corners, but restrained against column failure about axis thru corners.
 
(Arrow represents direction of column failure.)</td></tr>
<tr><td>Local Failing Stress (Upper Limit of Column Curve)</td><td>Use crippling stress F_{cc}.
Ref. B4.30</td><td>Use local buckling stress $F_{c_{cr}}$.
Ref. B4.20</td></tr>
<tr><td>Column Curve</td><td colspan="2">For columns which fail by Euler buckling, select the proper column curve on page B4.40.10-1 and determine the allowable ultimate stress F_c.</td></tr>
</table>

INTERACTION OF COLUMN FAILURE WITH LOCAL FAILURE

The curves on page B4.40.10-1 have been used to determine the allowable stress F_c of aluminum alloy columns with cross-sections whose local buckling stress is lower than the Euler column buckling stress. However, these curves have been unduly conservative in cases where the value of the local buckling stress $F_{c_{cr}}$ approaches the value of the crippling stress F_{cc} of the section. The curves are therefore being replaced with an analysis procedure which reduces the amount of conservatism for these cases. The principal difference between the two procedures is that in the new procedure the stress at which interaction between local buckling and column buckling begins is slightly below the local buckling stress, whereas in the old procedure interaction began at a stress equal to half of the local failing stress.

The two broad classes of column sections considered remain the same as illustrated in the table on page B4.40-4:

(1) Columns which have F_{cc} as an upper limit to the column curves (section types a through d on page B4.40-4)

The allowable column stress is $F_c = \alpha F_{cc}$ where α is obtained from the figure on page B4.40-6 as a function of $\eta F_{c_{cr}}/F_{cc}$ and $\eta F_{c_{cr}}/F_E$; F_E is the Euler (elastic) buckling stress of the column and η is a reduction factor for which a value of 0.9 is recommended. The local buckling stress $F_{c_{cr}}$ and the crippling stress F_{cc} are calculated according to the procedures outlined in Sections B4.00 through B4.30. If $\eta F_{c_{cr}}/F_{cc}$ is less than 0.5, assume $\eta F_{c_{cr}}/F_E = 0.5 F_{cc}/F_E$ when determining α.

(2) Columns which have $F_{c_{cr}}$ as an upper limit to the column curves (section types e and f on page B4.40-4)

The allowable column stress is $F_c = \alpha F_{c_{cr}}$ where the procedure given previously for determining α is simplified by assuming $\eta F_{c_{cr}}/F_{cc} = 0.9$ for all cases.

Note: In both of the cases a separate check should be made to ensure that the allowable column stress F_c does not exceed the tangent modulus column stress for the material given on page B3.42.10-1.

ULTIMATE STRENGTH OF COLUMNS SUBJECT TO LOCAL FAILURE

E - modulus of elasticity

$F_{c_{cr}}$ - plastic local buckling stress (see B4.20)

F_{cc} - crippling stress (see B4.30)

F_E - Euler column stress, $\pi^2 E (\rho/\ell')^2$

η - reduction factor (0.9 is recommended)

ℓ' - equivalent "pin-ended column" length

ρ - radius of gyration of cross-section

α - allowable strength factor

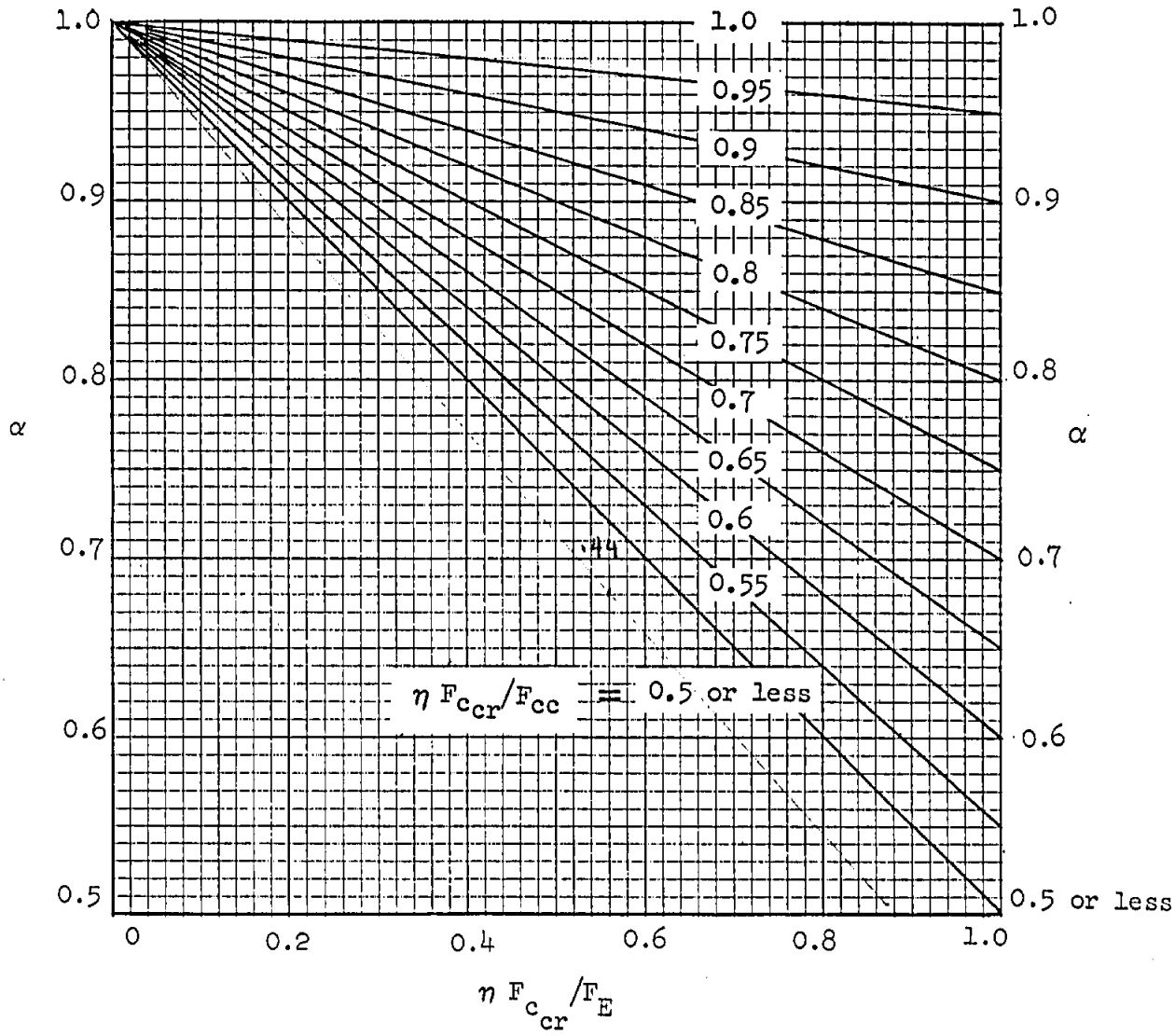

ULTIMATE STRENGTH OF ALUMINUM COLUMNS SUBJECT TO LOCAL FAILURE

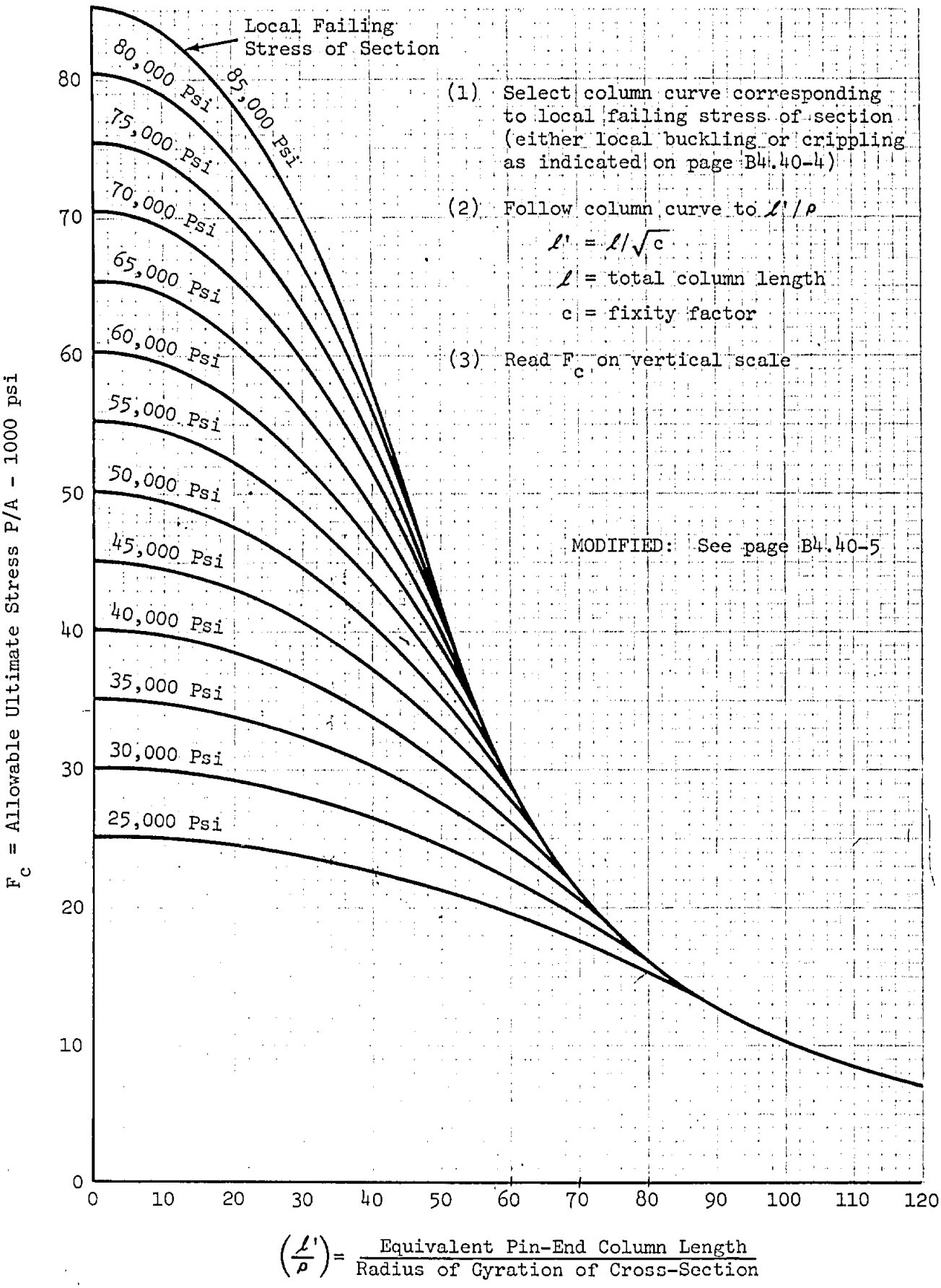

Grumman

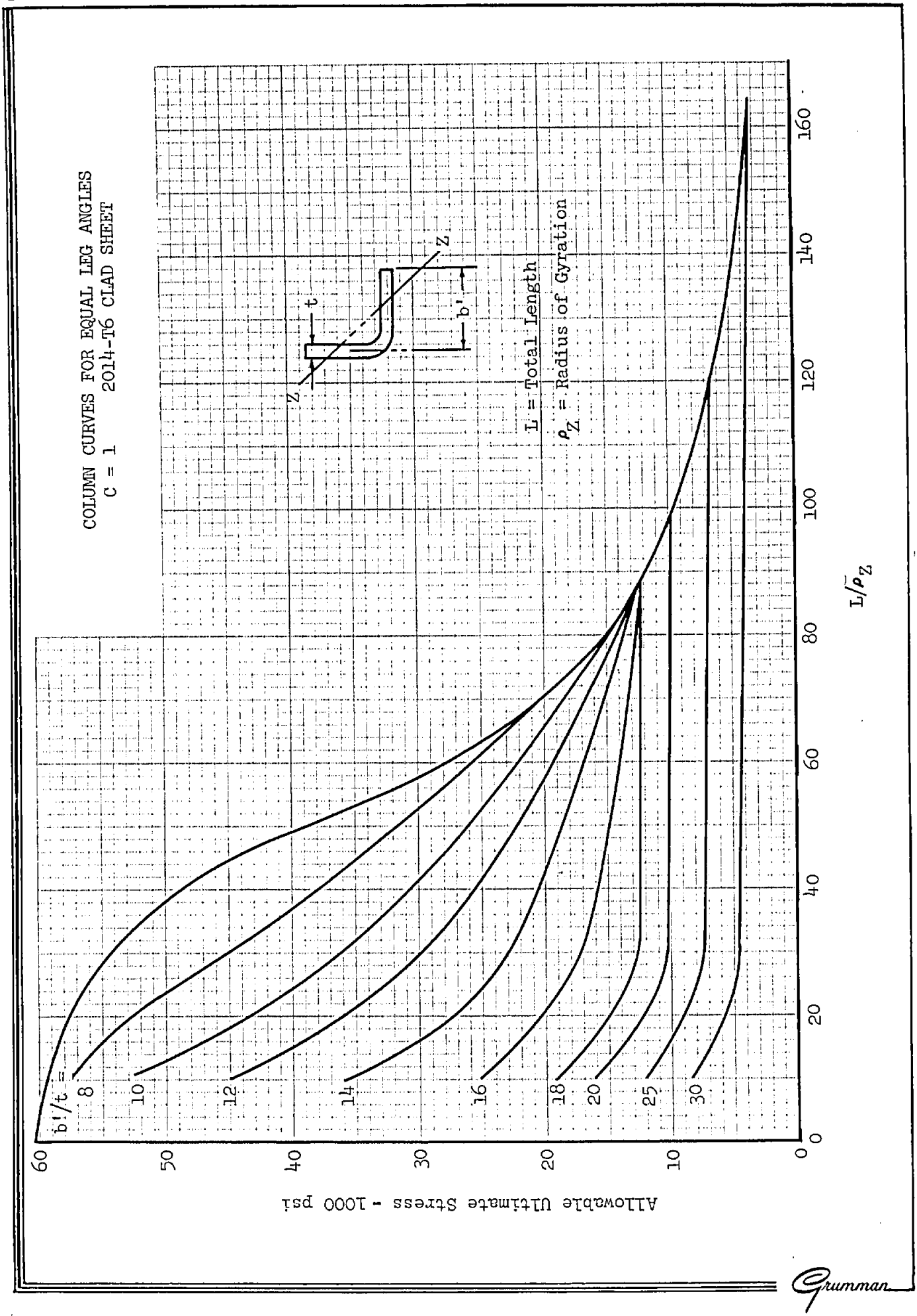
COLUMN CURVES FOR EQUAL LEG ANGLES
C = 1 2014-T6 CLAD SHEET
L = Total Length
ρ_Z = Radius of Gyration
Z
Z
t
b'
b'/t =
8
10
12
14
16
18
20
25
30
0
20
40
60
80
100
120
140
160
L/ρ_Z
60
50
40
30
20
10
0
Allowable Ultimate Stress - 1000 psi

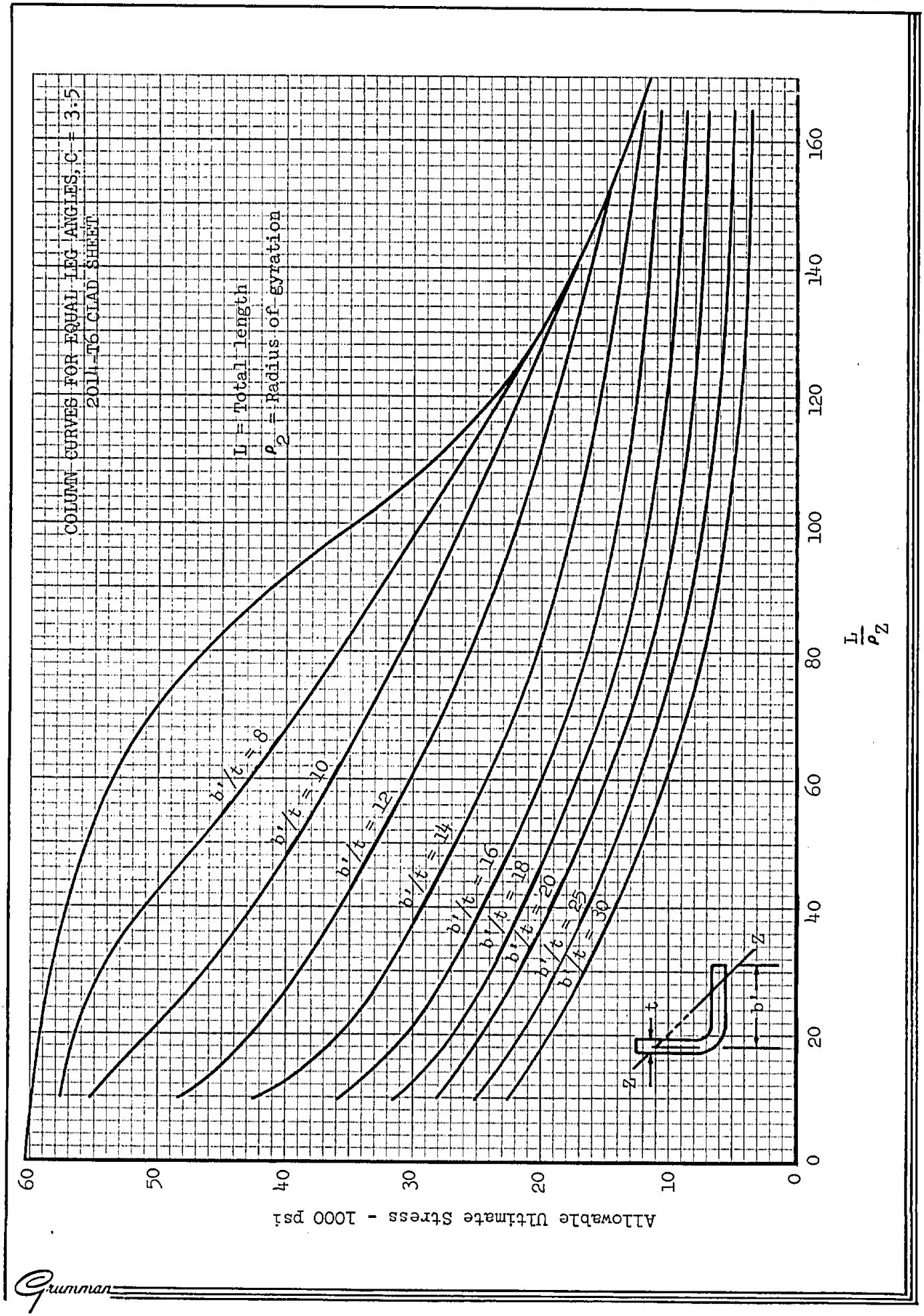
COLUMN CURVES FOR EQUAL LEG ANGLES, c = 3.5
2011-T6 CLAD SHEET
L = Total length
ρ_z = Radius of gyration
b'/t = 8
b'/t = 10
b'/t = 12
b'/t = 14
b'/t = 16
b'/t = 18
b'/t = 20
b'/t = 25
b'/t = 30
Z
t
b'
Allowable Ultimate Stress - 1000 psi
0
10
20
30
40
50
60
0
20
40
60
80
100
120
140
160
$\frac{L}{\rho_z}$

SECTION B5 - THIN SHEET

Table of Contents

BUCKLING STRESS COEFFICIENTS FOR FLAT RECTANGULAR PLATES LOADED IN COMPRESSION ON THE SHORT SIDE

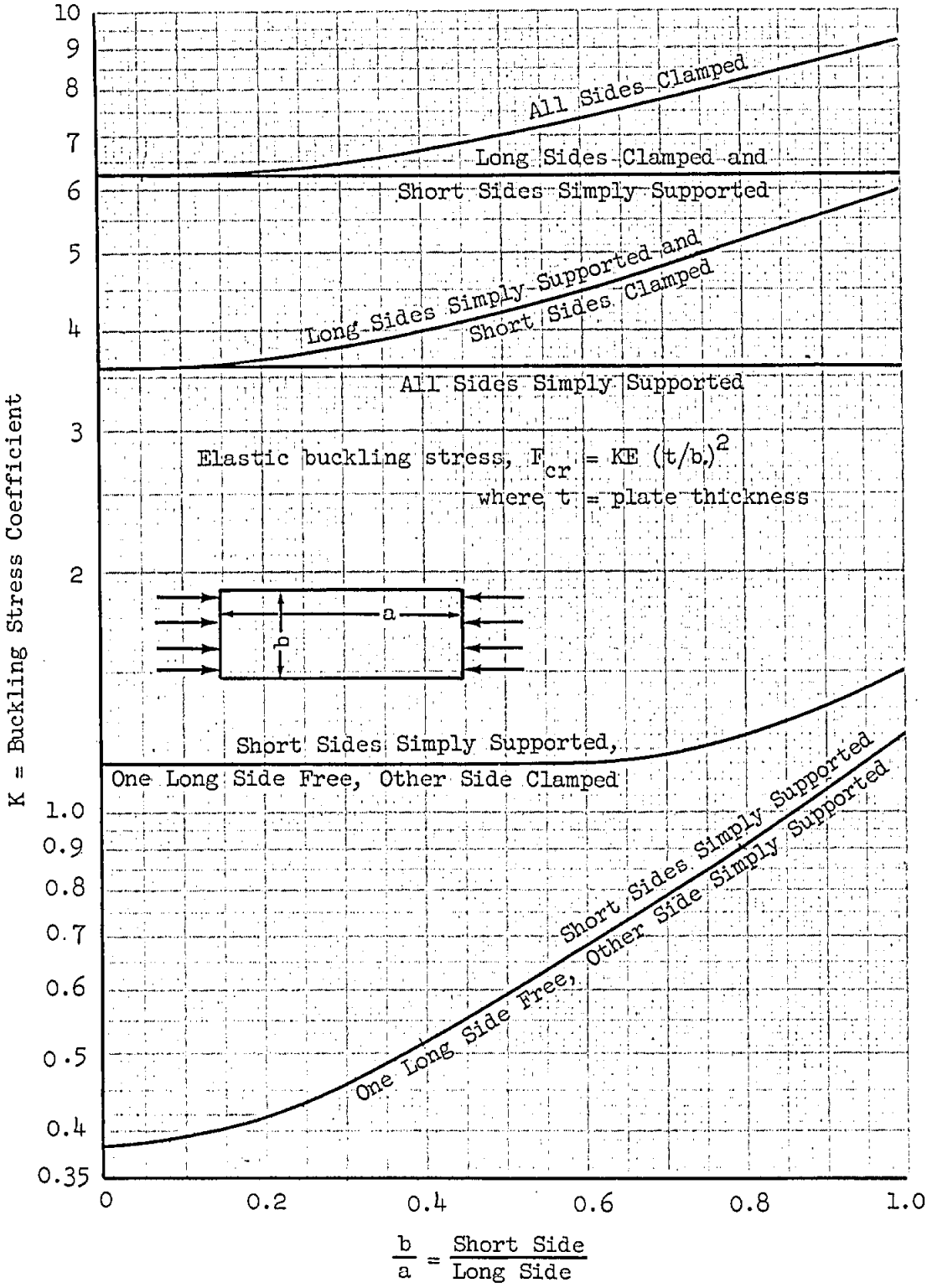

Ref: Timoshenko "Theory of Elastic Stability"
RAS Data Sheets "Stressed Skin Structures"

Grumman

BUCKLING STRESS COEFFICIENTS FOR FLAT RECTANGULAR PLATES LOADED IN COMPRESSION ON THE LONG SIDE

Elastic buckling stress = $F_{cr_{el}} = KE\,(t/b)^2$

where t = plate thickness

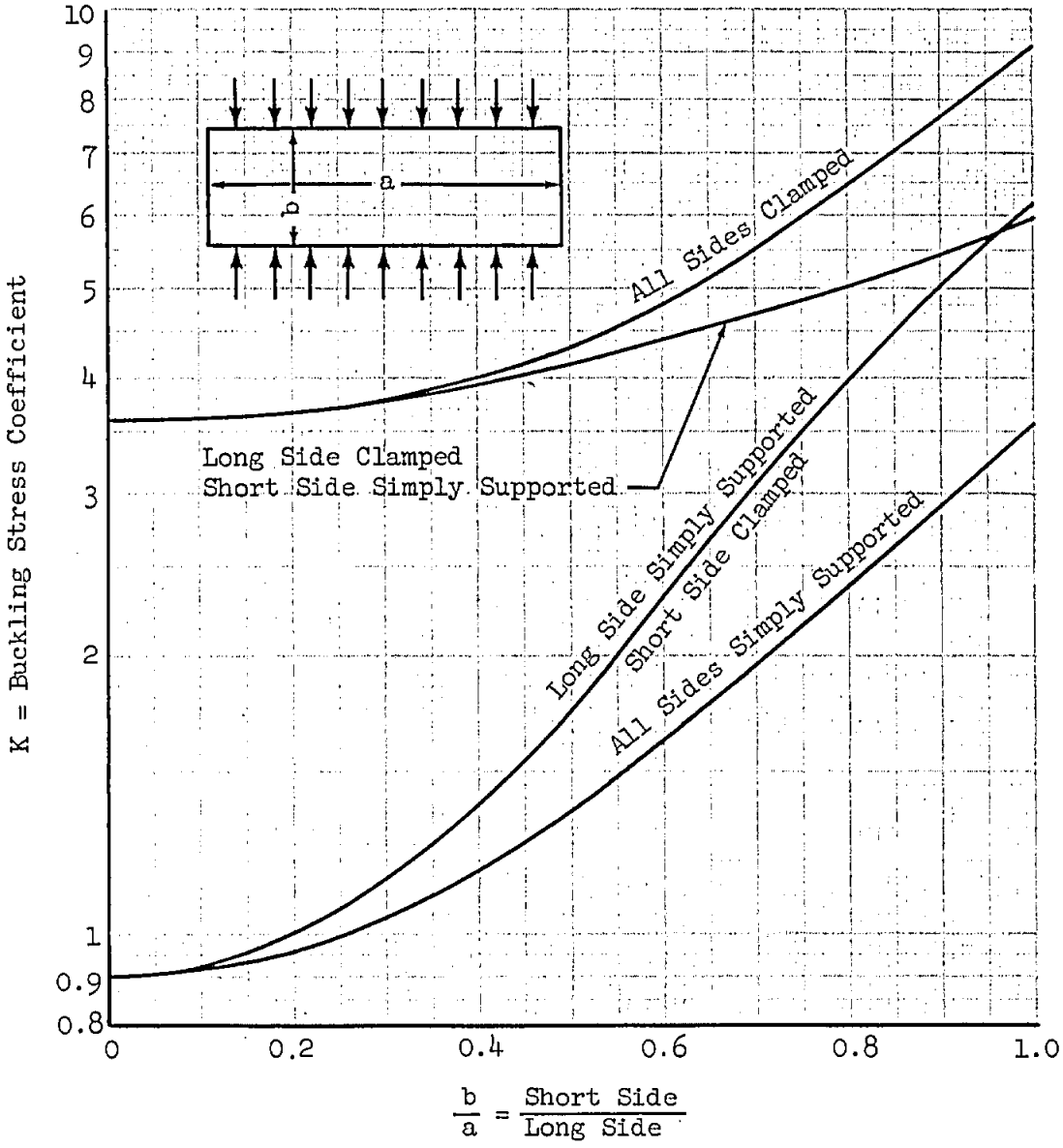

Ref: See page B5.11.11-1

ELASTIC BUCKLING OF FLAT RECTANGULAR ALUMINUM ALLOY PLATES IN COMPRESSION

NOTE: (1) The heavy horizontal lines on the graph separate the elastic region (below the heavy lines) from the plastic region (above the lines) for the various alloys.
(2) In the elastic region the buckling stress is obtained directly from the graph.
(3) In the plastic region the buckling stress = $F_{c_{cr}}$ and is determined as follows: (a) obtain $F_{cr_{el}}$ from this graph; (b) enter the appropriate curve on page B5.12.11-1, -2, or -3 (depending upon the alloy) with $F_{cr_{el}}$ and determine $F_{c_{cr}}$.

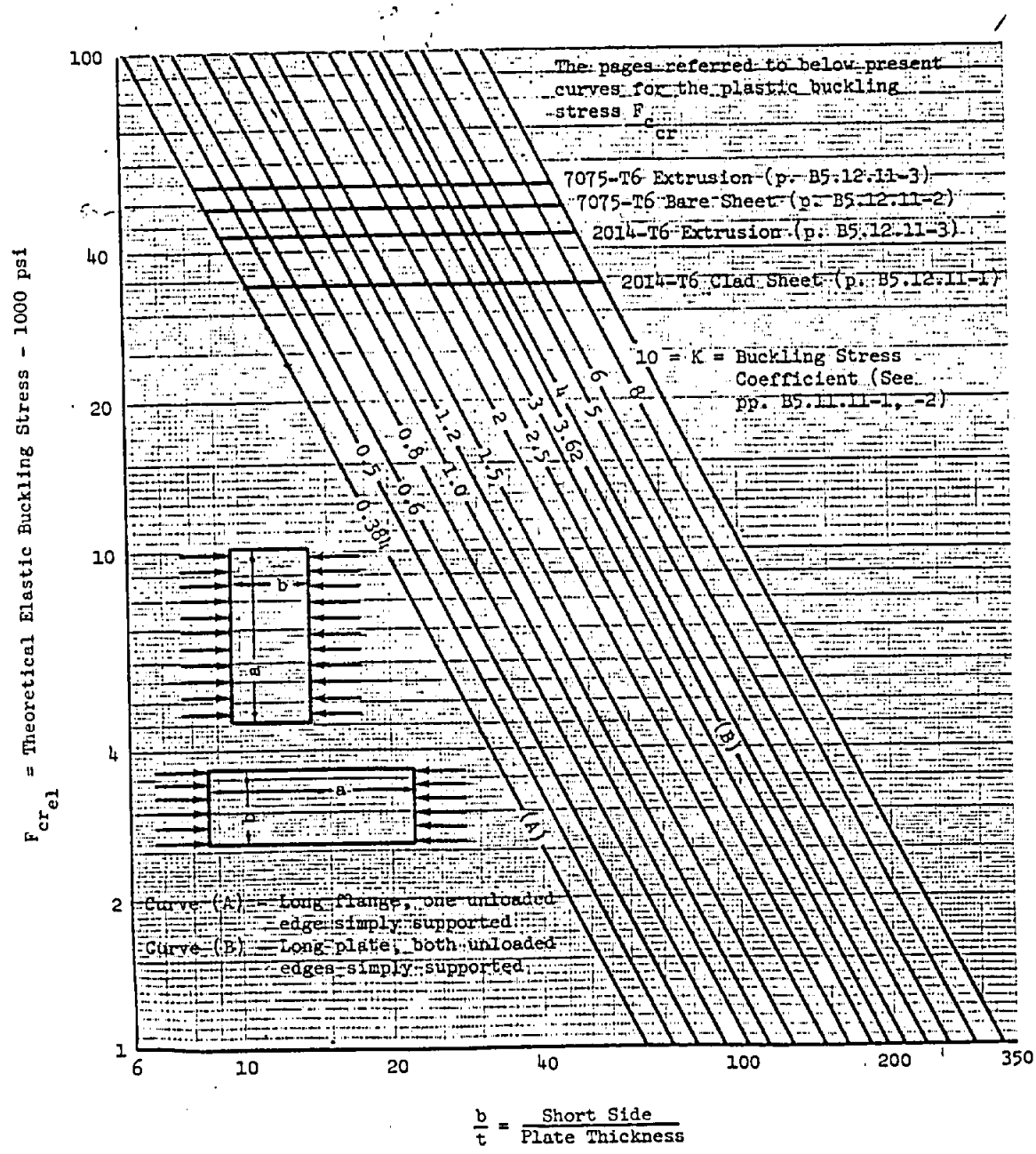

INTERCEPT VALUES

$b/a = 0.0$ $b/a = 1.0$ (B5.11.12-1)

8.12 ← CLAMPED → 13.30

SS/CLAMPED → 11.10

4.84 ← SS → 8.44

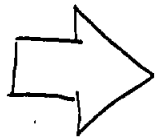

From JIMOSHENKO, THEORY OF ELASTIC STABILITY ARTICLE 9.7

BASED ON $\nu = 0.3$

BUCKLING STRESS COEFFICIENTS FOR FLAT PLATES IN SHEAR

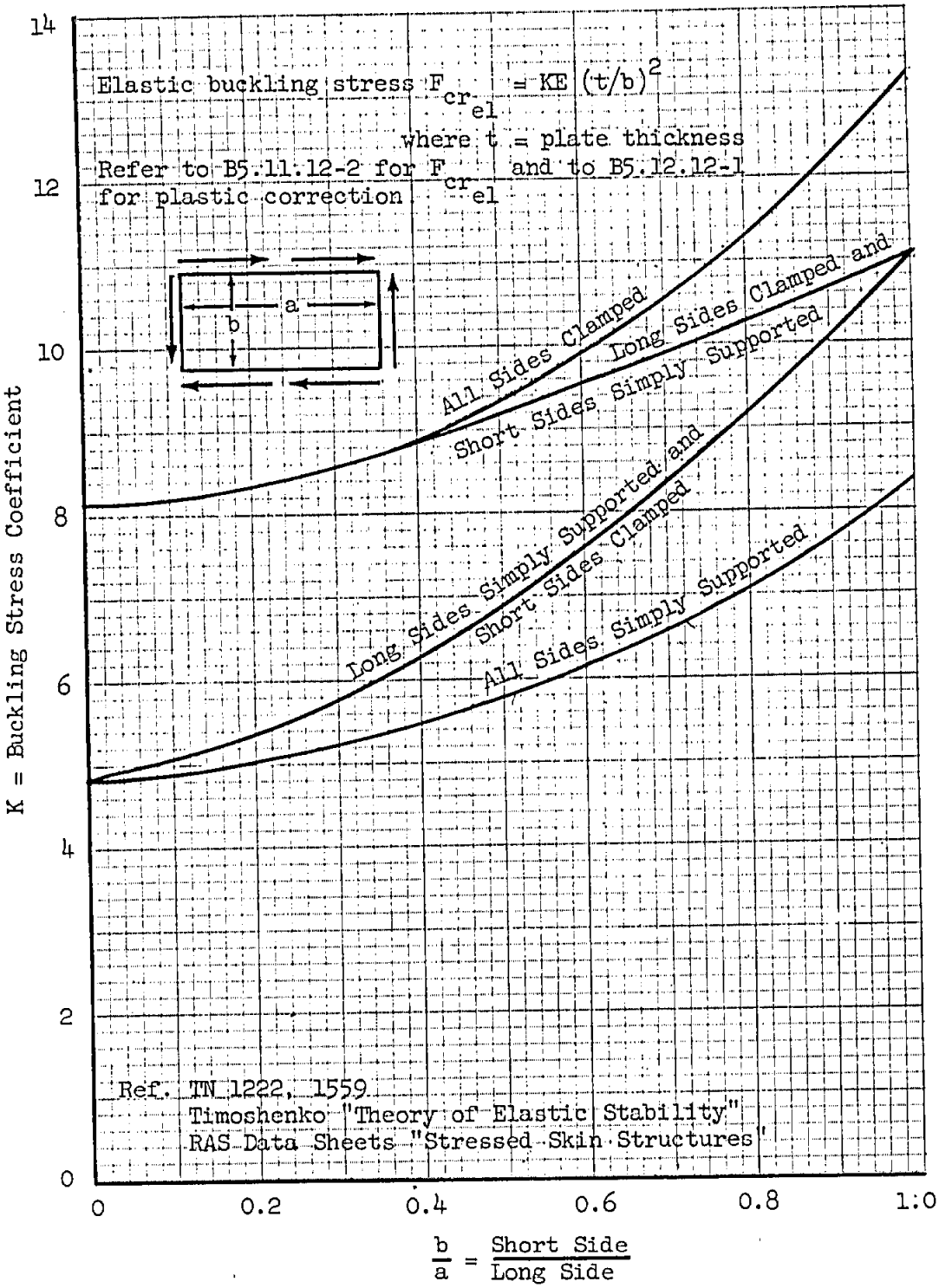

ELASTIC BUCKLING OF FLAT RECTANGULAR ALUMINUM ALLOY PLATES IN SHEAR

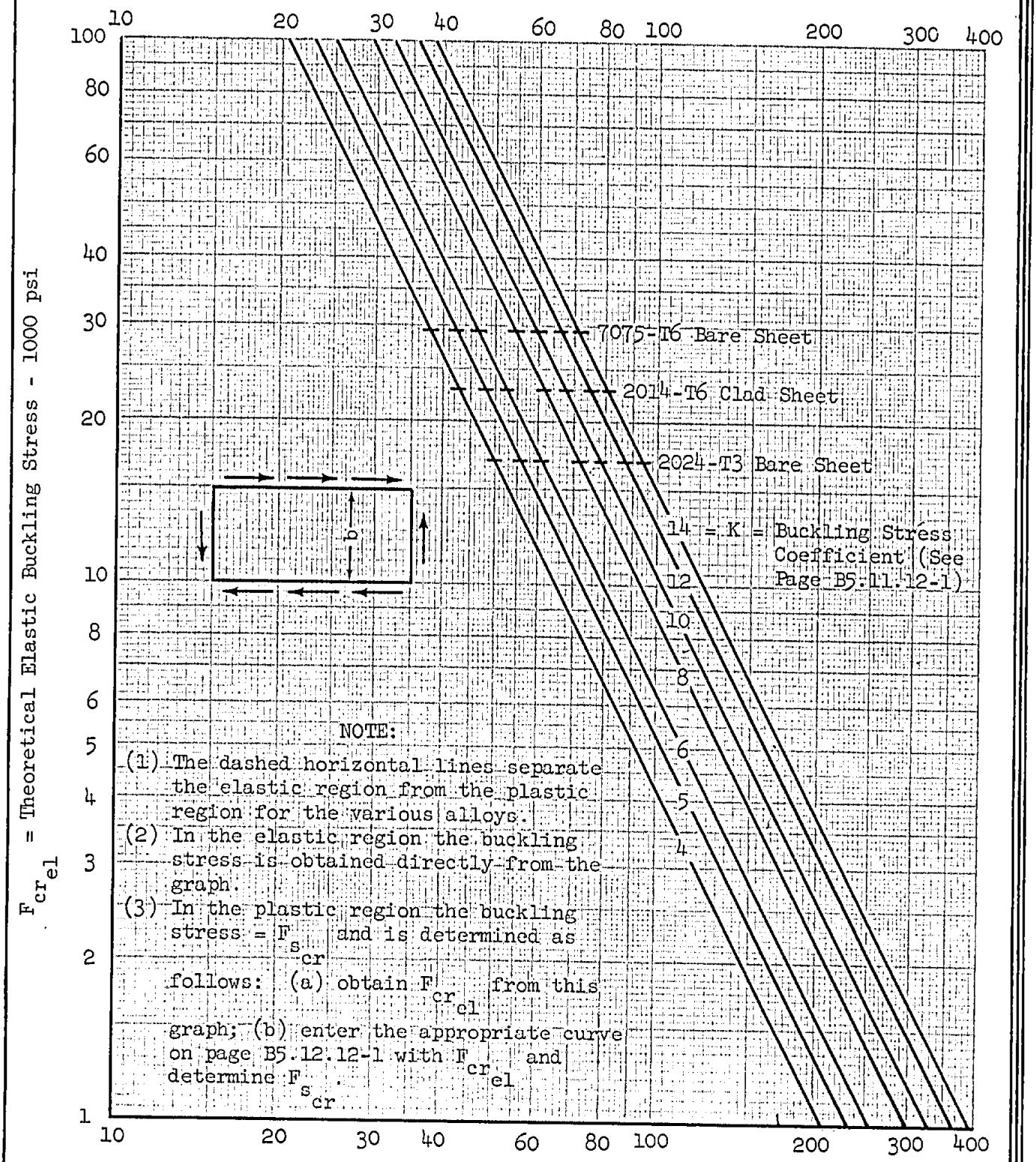

ELASTIC BUCKLING OF LONG PLATES FOR LINEARLY VARYING COMPRESSION

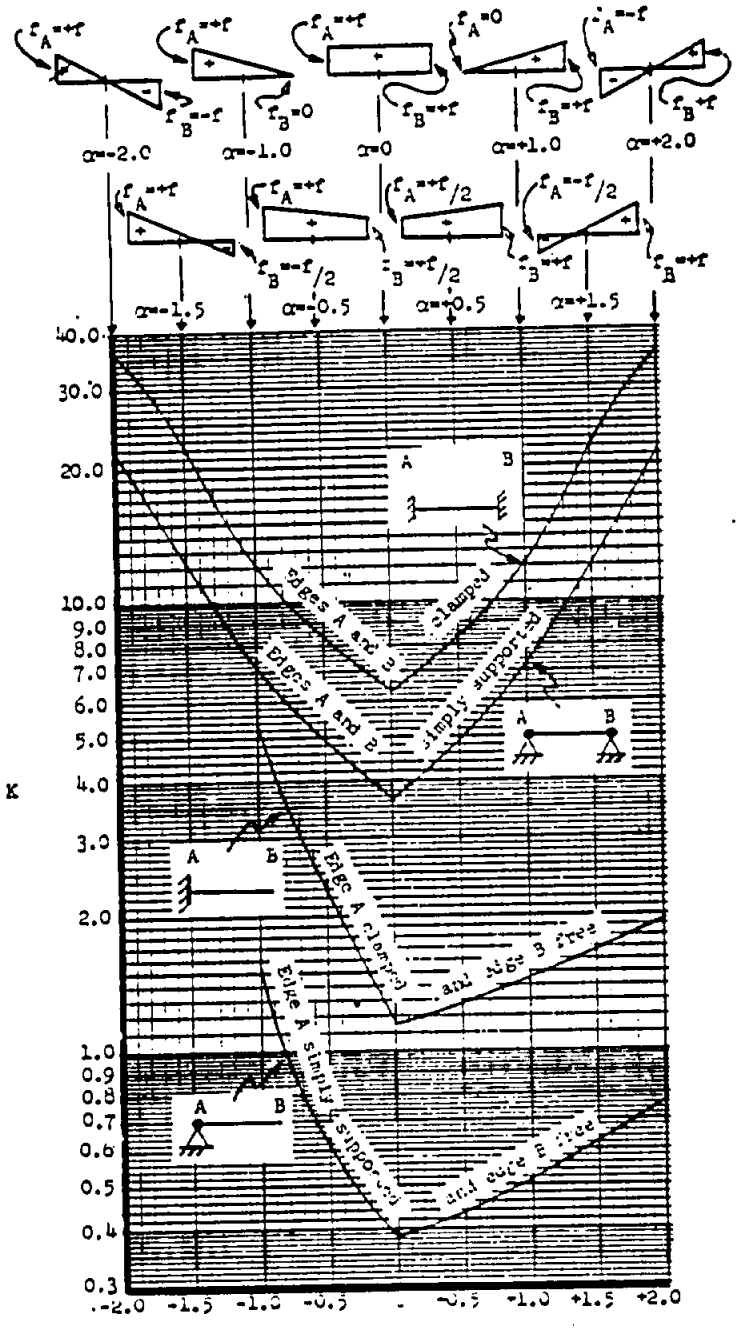

sign convention:

compression ~ positive
tension ~ negative

ELASTIC BUCKLING STRESS

$$F_{e_{cr}} = K\pi^2 (t/b)^2$$

where b = plate width
t = plate thickness
$F_{e_{cr}}$ = maximum allowable value of edge stress f_A or f_B

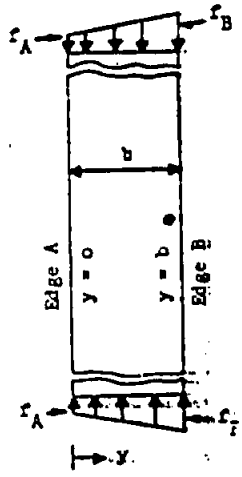

If maximum edge stress at A,

$$|f_A| \geq |f_B|$$

$$f = f_A \left[1 + \alpha\left(\frac{y}{b}\right)\right]$$

where

$$\alpha = \frac{(f_B - f_A)}{f_A}$$

If maximum edge stress at B,

$$|f_B| \geq |f_A|$$

$$f = f_B \left[1 - \frac{\alpha(b-y)}{b}\right]$$

where

$$\alpha = \frac{(f_B - f_A)}{f_B}$$

Ref. Bijlaard, P., "Buckling of Plates Under Non-Homogeneous Stress", Journal of the Engineering Mechanics Division, A.S.C.E., Vol. 83, EM. 3, Proc. Paper 1293, July 1957

ELASTIC BUCKLING OF SHORT PLATES FOR LINEARLY VARYING COMPRESSION

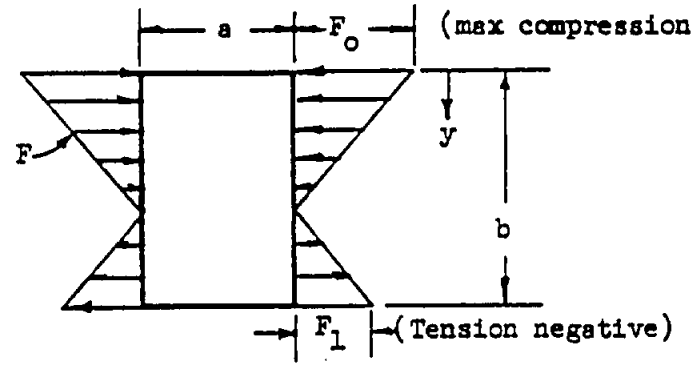

$F = F_o(1 - \alpha y/b)$, $\alpha = (F_o - F_1)/F_o$

$(F_o)_{cr} = KE(t/b)^2$

t = Plate Thickness (inches)

Timoshenko: "Theory of Elastic Stability"

$a/b = \frac{\text{SIDE PARALLEL TO LOAD}}{\text{LOADED SIDE}}$

ELASTIC BUCKLING OF SHORT PLATES FOR LINEARLY VARYING COMPRESSION

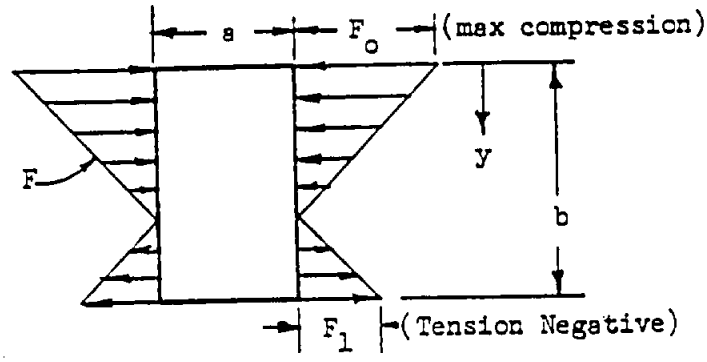

$F = F_o(1 - \alpha y/b)$, $\alpha = (F_o - F_1)/F_o$

$(F_o)_{cr} = KE(t/b)^2$

t = Plate Thickness (inches)

Timoshenko: "Theory of Elastic Stability"

BUCKLING STRESS COEFFICIENTS FOR FLAT, TAPERED PLATES IN COMPRESSION

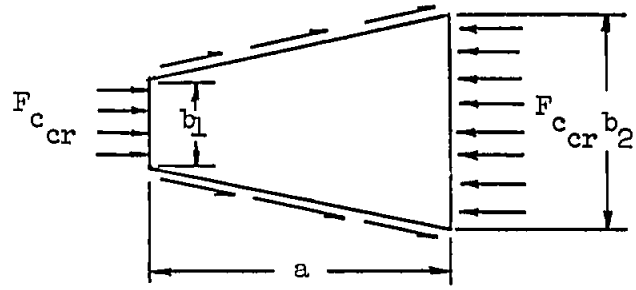

$$F_{c_{cr-el}} = KE\left(\frac{t}{b_2}\right)^2 = \text{Elastic buckling stress}$$

where t = plate thickness

Ref: - RAS Structures Data Sheets (Dec. 1963), p. 02.01.48

PLASTIC BUCKLING OF PLATES OF 2014-T6
ALUMINUM ALLOY SHEET IN COMPRESSION

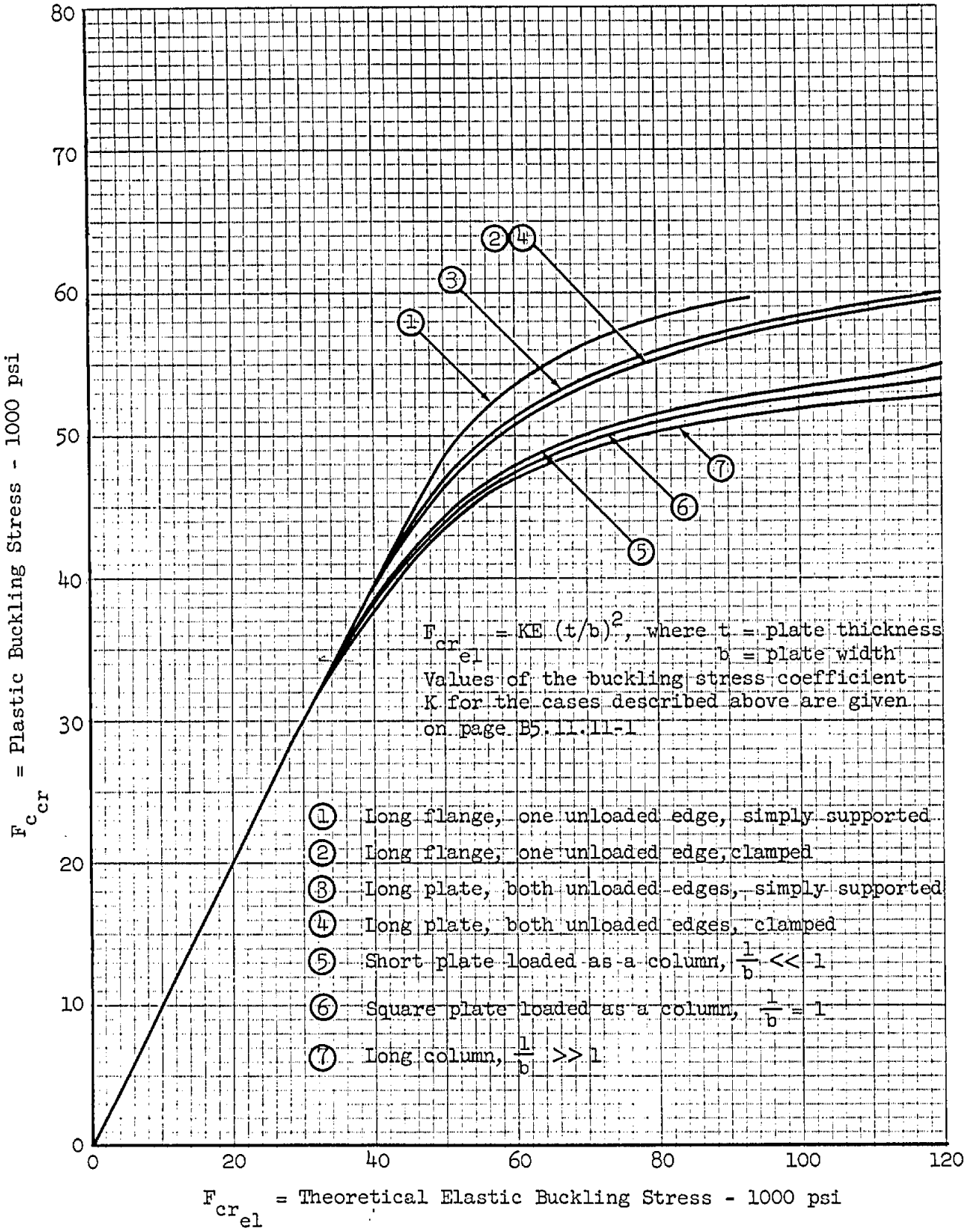

Ref: USDC-28

PLASTIC BUCKLING OF PLATES OF 7075-T6
ALUMINUM ALLOY SHEET IN COMPRESSION

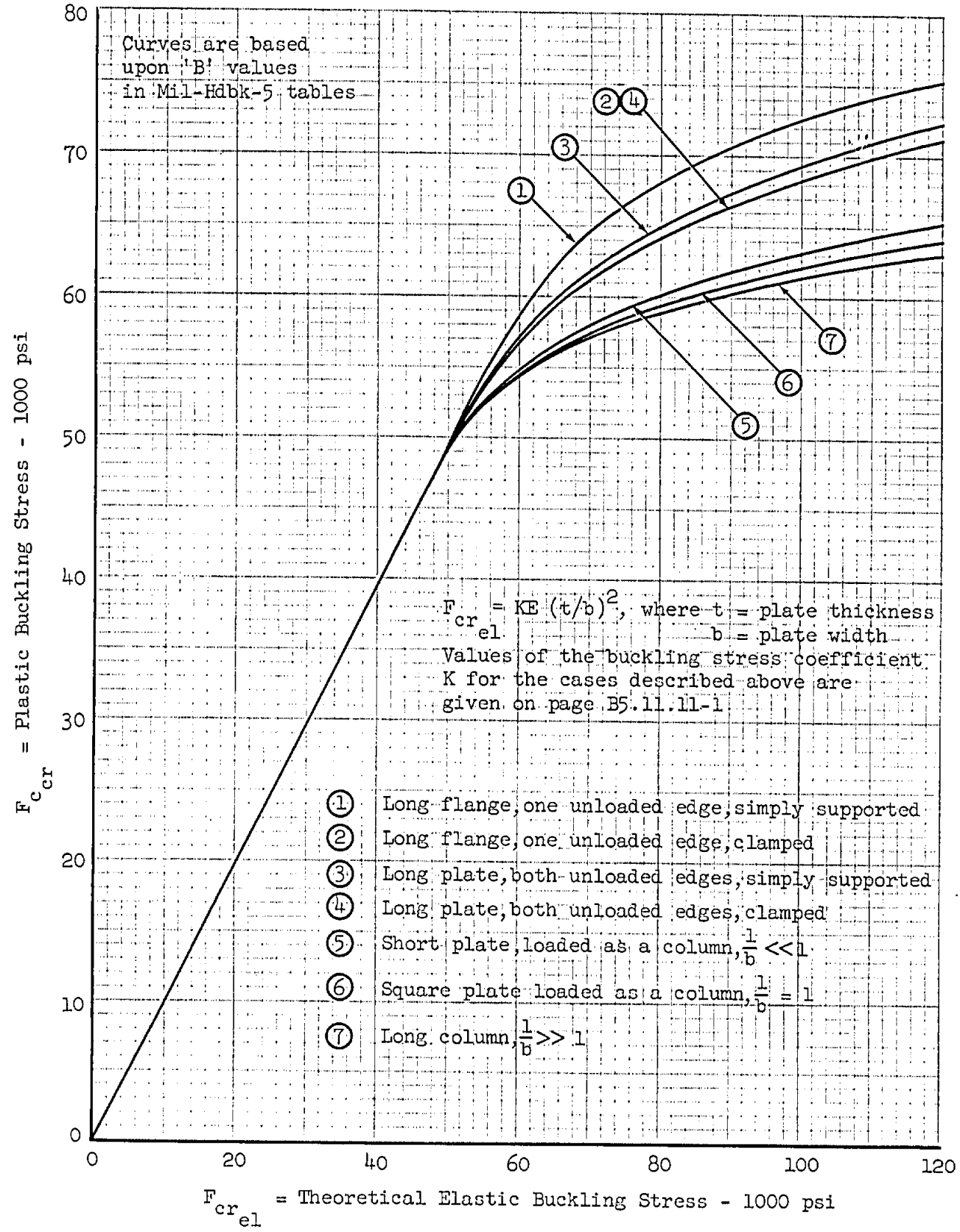

Ref: USDC-28

PLASTIC BUCKLING OF 7075-T6 & 2014-T6 ALUMINUM ALLOY EXTRUSIONS IN COMPRESSION

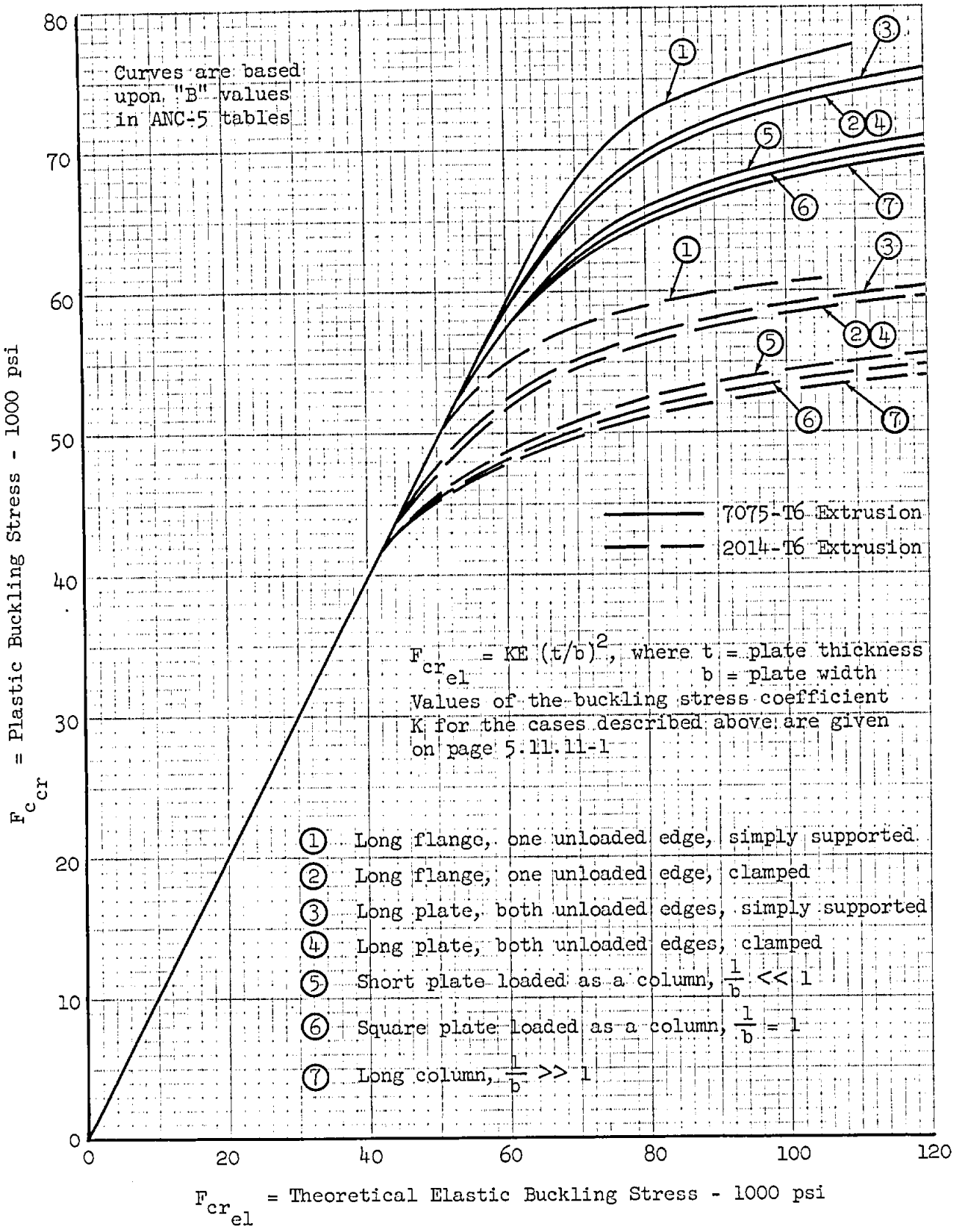

PLASTIC BUCKLING OF ALUMINUM ALLOY SHEET IN SHEAR

$F_{cr_{el}} = KE\,(t/b)^2$, where t = plate thickness
b = plate width

Values of the buckling stress coefficient K for various edge conditions are given on page B5.11.12-1

Curves apply both to simply supported and clamped edge plates

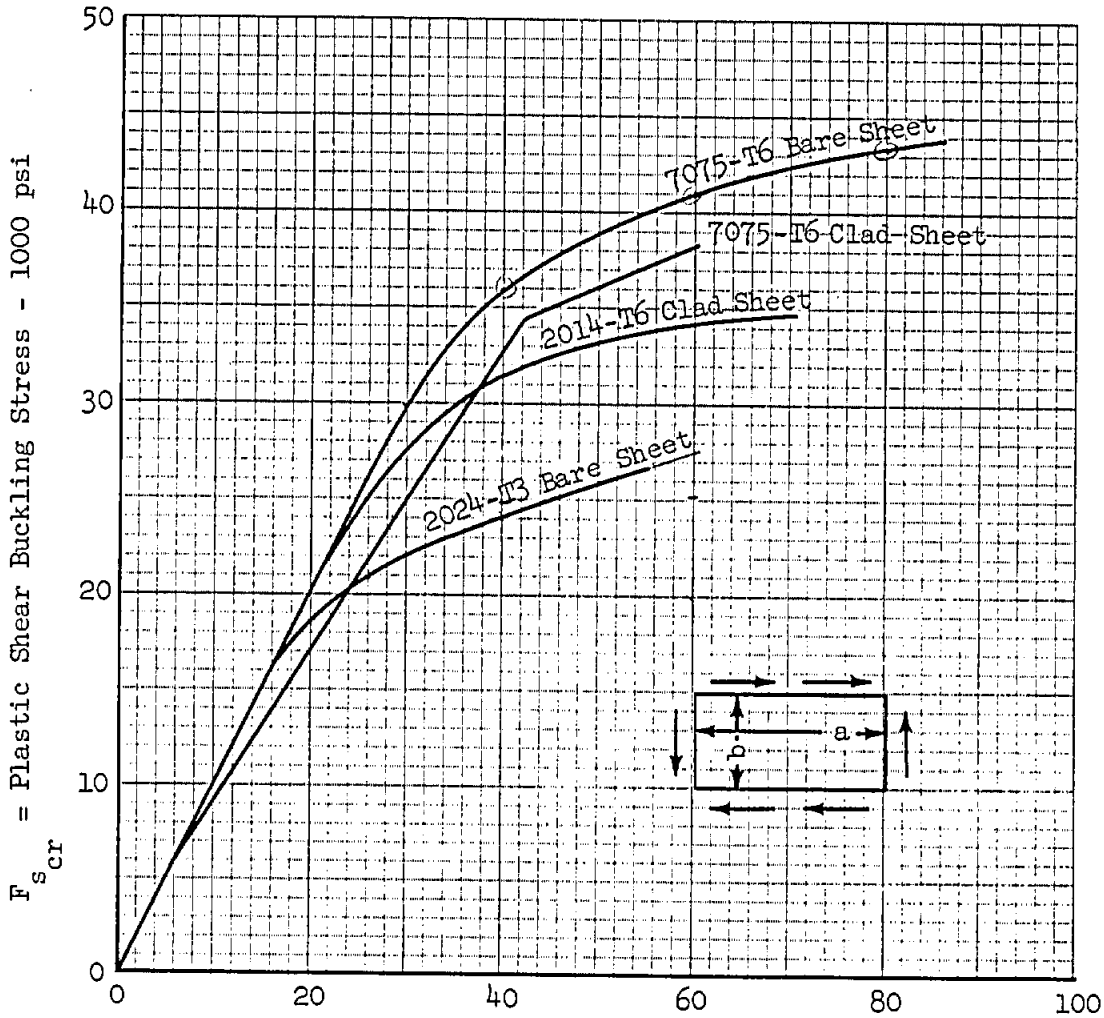

Ref: TN 1956, 2661, 1681

LATERAL DEFLECTION OF FLAT SQUARE PLATE LOADED IN COMPRESSION AND SIMPLY SUPPORTED ON FOUR SIDES

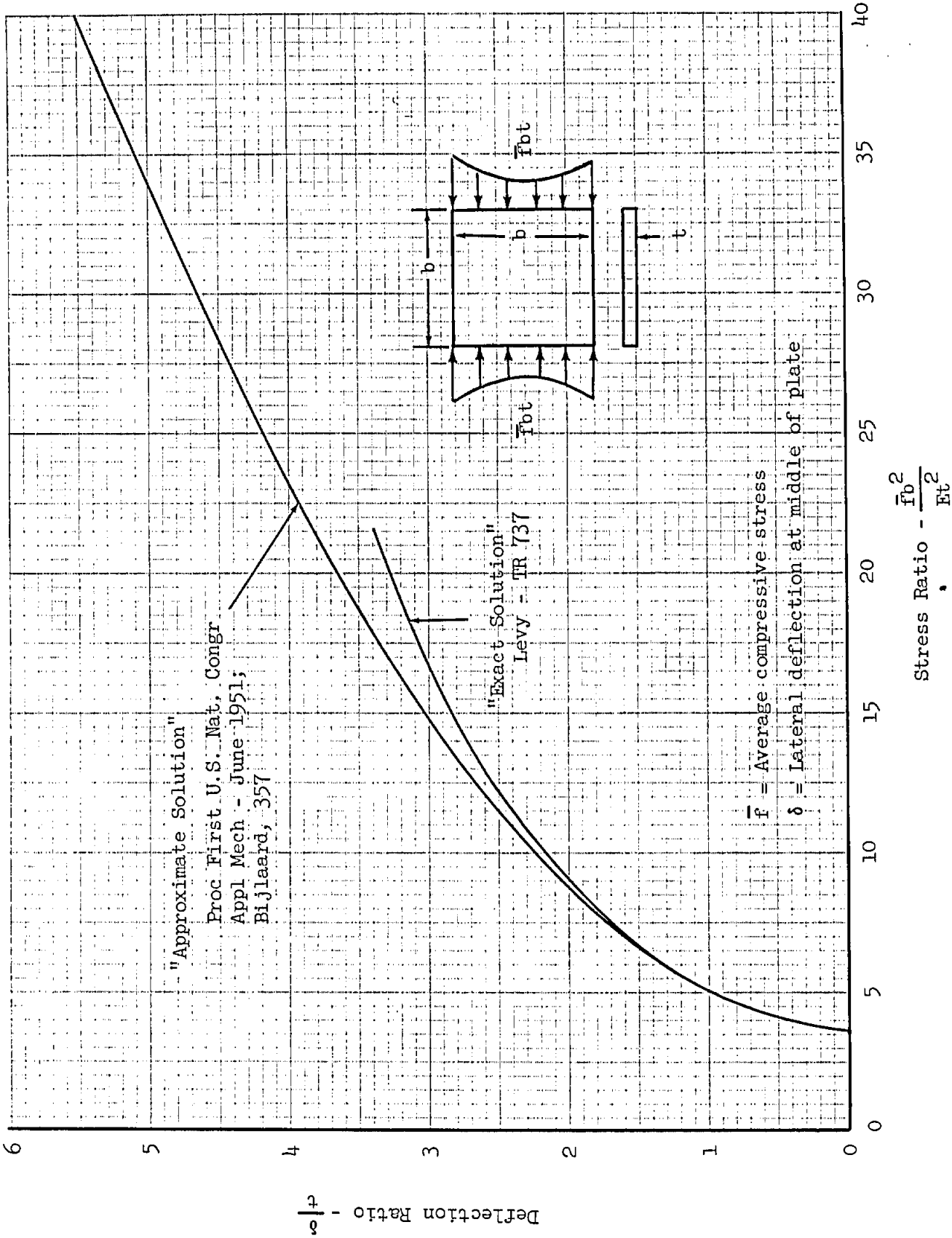

Grumman

TENSION STRESS AND LATERAL DEFLECTION AT CENTER OF FLAT SQUARE PLATE UNDER UNIFORM LOAD WITH SIMPLE SUPPORTS

p - Normal Pressure

f' - Tension Stress in Median Plane of Plate (Membrane Stress Only)

f - Maximum Tension Stress in Plate at Center (Bending Plus Membrane Stress)

δ - Lateral Deflection at Middle of Plate

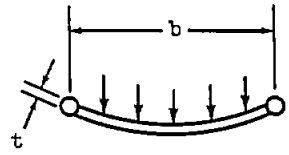

NOTE: Edges are not permitted to move in the plane of the plate.

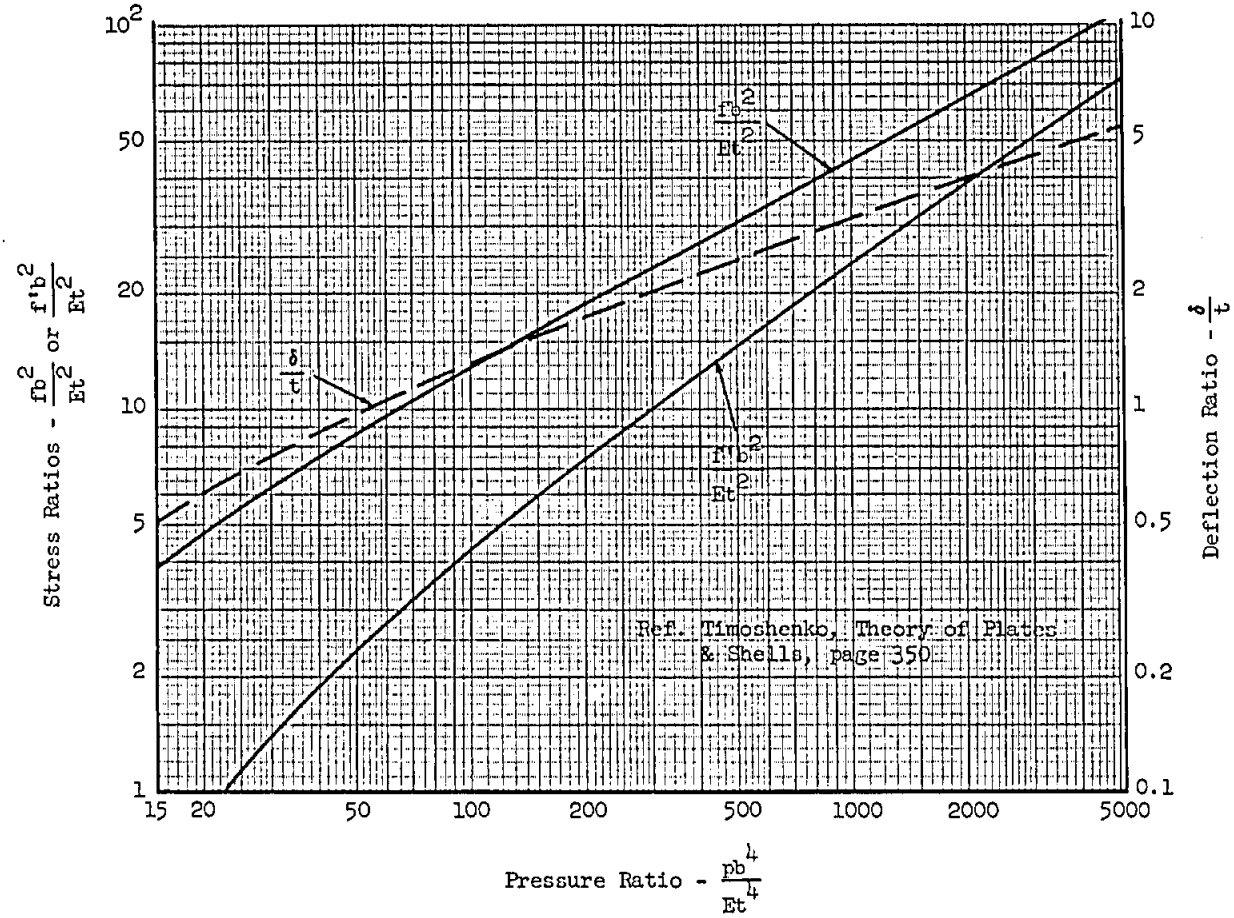

TENSION STRESS AND LATERAL DEFLECTION AT CENTER OF LONG FLAT PLATE UNDER UNIFORM LOAD WITH SIMPLE SUPPORTS

p - Normal Pressure

f' - Tension Stress in Median Plane of Plate (Membrane Stress Only)

f - Maximum Tension Stress in Plate at Center (Bending Plus Membrane Stress)

δ - Lateral Deflection at Middle of Plate

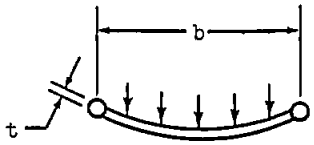

NOTE: Edges are not permitted to move in the plane of the plate.

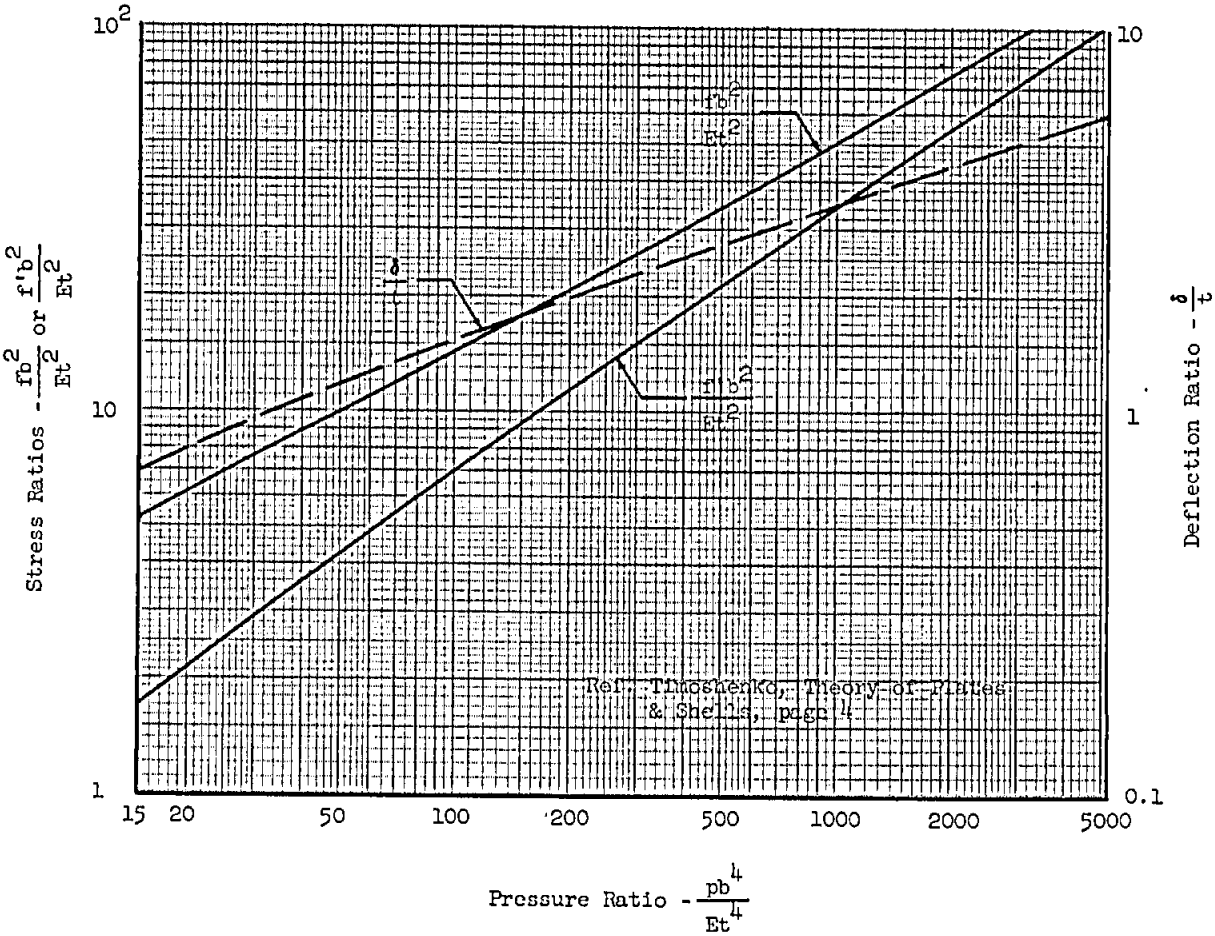

BUCKLING OF CURVED SHEET IN SHEAR AND COMPRESSION

ELASTIC BUCKLING STRESS COEFFICIENTS

Curved Panels with Circumferential Length Greater than Axial Length Loaded in Shear

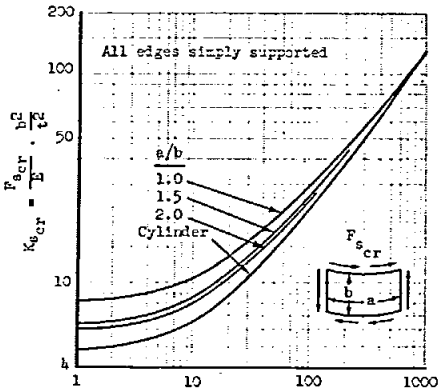

Curved Panels with Axial Length Greater than Circumferential Length Loaded in Shear

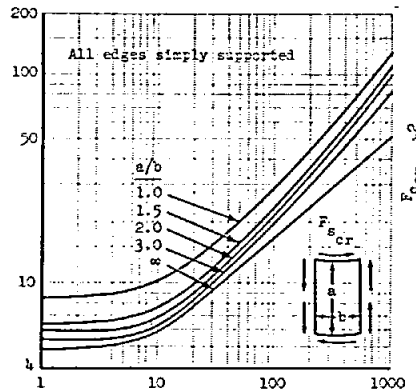

Thin Walled Cylinders Loaded in Axial Compression

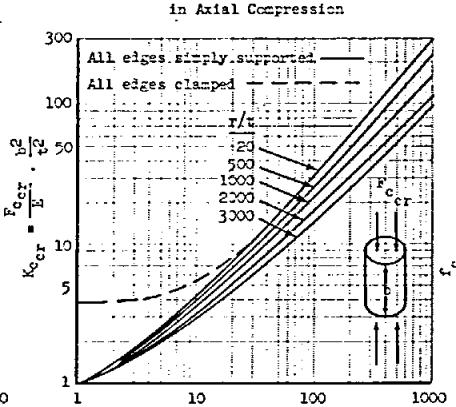

Interaction Curves for Buckling Under Combined Shear and Compression

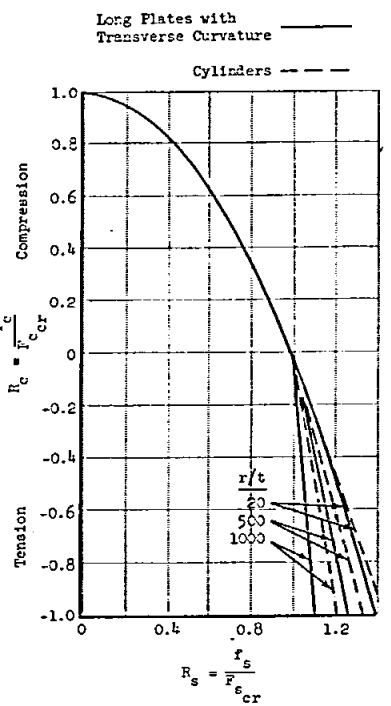

Curved Panels with Circumferential Length Greater than Axial Length Loaded in Shear

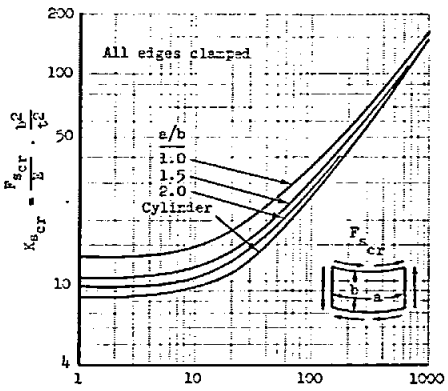

Curved Panels with Axial Length Greater than Circumferential Length Loaded in Shear

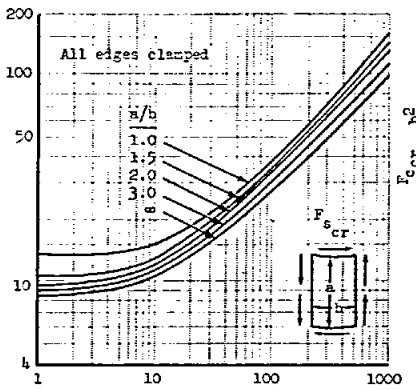

Long Plates with Transverse Curvature in Axial Compression

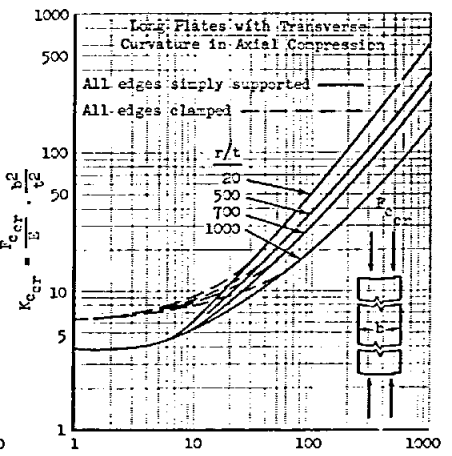

Symbols

- f_s - Applied Shear Stress
- f_c - Applied Axial Compressive Stress
- $F_{s_{cr}}$ - Buckling Stress in Pure Shear
- $F_{c_{cr}}$ - Buckling Stress in Pure Axial Compress.
- r - Radius of Curvature
- t - Panel Thickness

NOTE: When b is the circumferential length Z is a measure of the ratio of panel bulge to panel thickness
Ref. TN No. 1345, 1347, 1348

Grumman

B 5.1.4 Particular Solution of Bents and Semicircular Arches (Cont'd)

Table B 5.1.4-2 Reactions and Constraining Moments in Triangular Bents (Cont'd)

25. HORIZ. UNIFORM RUNNING LOAD 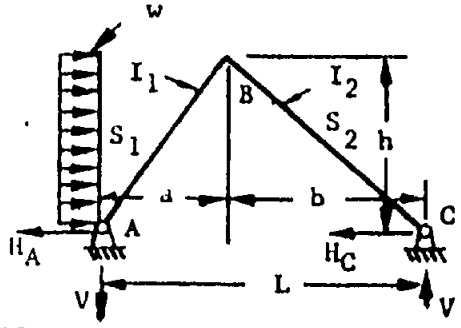	$V = \frac{wh^2}{2L}$ $H_A = wh - H_C$ $H_C = \frac{wh}{8}\left[\frac{4b}{L} + \frac{1}{K+1}\right]$
26. HORIZ. UNIFORM RUNNING LOAD 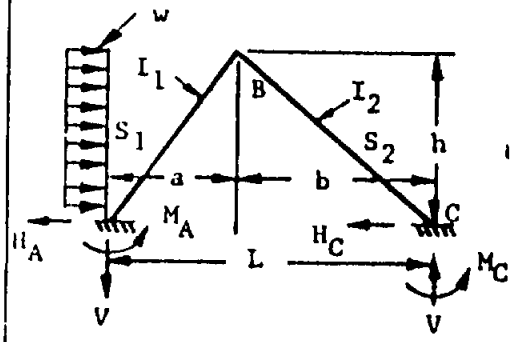	$V = \frac{3wh^2}{8L}$ $H_A = wh - H_C$ $H_C = \frac{wh}{8L(K+1)}\left[b(3K+4) + a\right]$ $M_A = \frac{wh^2(3K+2)}{24(K+1)}$ $\qquad$ $M_C = \frac{wh^2}{24(K+1)}$
27. APPLIED MOMENT AT APEX 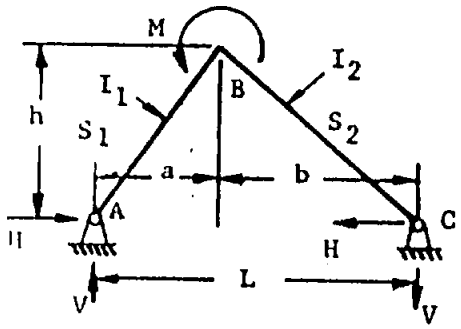	$V = \frac{M}{L}$ $H = \frac{M}{hL}\left[\frac{a - bK}{K+1}\right]$

SECTION B6 - FLAT STIFFENED SHEET

Table of Contents

B6.11 - COMPRESSIVE STRENGTH OF FLAT STIFFENED SHEET

The analysis of stiffened flat panels subjected to in-plane compression loading acting parallel to the stiffening members is presented in the following section.

These analyses are based on the following assumptions:

a) The panel is infinite in width and has identical stiffeners (reinforcing bars) at equal spacing.

b) It is possible to treat a stiffener plus a width of sheet as an individual element whose strength can accurately be predicted. There is no interaction between adjacent stiffeners that will affect the strength calculation. Interaction between the sheet and stiffener is included in the analysis.

Because the strength of a stiffened panel is almost entirely due to the structural characteristics of the stiffening member, most of the analysis effort is directed at the stiffener. The structural function of the sheet is to provide load carrying area that acts with the stiffening member at a stress level usually dictated by the properties of the stiffening member. The sheet area is included with the stiffener in the determination of its structural properties. The amount of sheet included is determined from an effective width formulation.

The analyses and examples are presented for panel structure where sheet and stiffener are of the same material and all elements are at essentially the same temperature (i.e. no thermal gradients).

The effect of a temperature gradient through the depth of the panel (normal to sheet plane) is twofold:

a) To cause induced loads in structure that usually are combined with the applied loads before applied stresses are calculated. These stresses, when treated in this manner, do not affect the allowable stress, are therefore not considered in the following analysis.

b) To change the material mechanical properties applicable to the compression strength prediction. The analysis problem then is the same as one of mixed materials. The following discussion on mixed material structure therefore is applicable to this phase of temperature related effects.

The principles employed in the following allowable stress analysis apply to the case of mixed structural materials. Both the case of different alloys of the same basic material (for instance, an aluminum alloy panel with 2024-T3 sheet and 7075-T6 stiffeners) or the more extreme case of completely different materials (for instance, a 6Al-6V-2Sn titanium alloy sheet and 7075-T6 aluminum alloy stiffener) must be considered. For structure of uniform material (and discounting inter-rivet buckling as an uncommon failure mode), the strength of a stiffened

panel depends on the stiffeners, leading to the philosophy of "sturdy stiffeners" in design. Therefore, in a mixed material structure, if the usable, or working strain, of the stiffeners exceeds that of the sheet material, the principles of the following analyses can be safely employed in predicting the strength of that structure. If the stiffeners are "weaker" (lower working strain) than the sheet, not only will the structural efficiency be low, but the design will not employ "sturdy stiffeners". It is realized that this case could arise from a design environment that resulted in the stiffener temperature exceeding that of the sheet by a significant amount. The stiffeners, even of identical alloy, would be "weaker" than the sheet due to reduced compression properties, particularly F_{cy} ($F_{0.7}$). In this case, the principles of the following analyses can be employed for the strength prediction.

Strength prediction of structures with differing materials requires the basic assumption that when the allowable stress is established, all elements are at equal strain. This is in contrast to the equal stress assumption for uniform material structure. This presents no significant problem in the elastic range since stress and strain are related by a constant. However, in the plastic range (a very significant part of the strength prediction process) the stress-strain relationship is non-linear and the problem solutions can only be obtained by very lengthy iterations. Where the following analyses for uniform material structure can be performed with the aid of a desk calculator, the non-uniform material problem can only be solved with the aid of a computer. Solutions of this problem have been programmed and are available in the Structural Analysis Section.

Historically, compression strength in the wrinkling mode has been the stability strength of the sheet as a column on the elastic foundation provided by the stiffener attached flange. It has been recognized that, as the sheet buckles in the cylindrical shape characteristic of this mode, that the sheet will impose displacements on the stiffener flanges that in conjunction with the axial stresses present will cause failure of the stiffener flange. In addition, it is realized that if the forces causing bending in the stiffener are present, then these same forces in turn will act on the sheet causing bending stress in the sheet that will contribute to possible sheet failure. Therefore, the determination of the compression strength of a stiffened panel in the wrinkling mode has evolved into the calculation of the strength of both sheet and stiffener. Failure strength of the sheet is termed wrinkling and is the minimum of the sheet compression stability strength (page B6.11.5-2) or the sheet transverse bending strength (page B6.11.5-7). The stiffener strength in the wrinkling mode is termed forced crippling and is on page B6.11.6-4.

SYMBOLS

A	Cross sectional area	$inches^2$
B	Area	$inches^2$
b	Stiffener spacing	inch
c	Rivet offset distance	inch
d	Rivet diameter	inch
D	Sheet bending stiffness, $Et^3/12(1 - \nu^2)$	lb inch
E	Young's Modulus	psi
E_s	Secant Modulus	psi
E_t	Tangent Modulus	psi
F	Allowable stress	psi
f	Applied stress	psi
G	Shear modulus	psi
H	Bending modulus reduction factor	
h	Stiffener depth	$inch_4$
I	Moment of inertia	$inch_4$
J	St.Venant torsion constant of stiffener	$inch^4$
k	Torsional restraint afforded by sheet to stiffener	inch lb/inch
K	Buckling stress coefficient	
j	Integer	
L	Panel length between pin ends	inch
m	Applied bending moment	inch lbs.
M	Allowable bending moment	inch lbs.
n	Stress-strain parameter	
P	Flange normal loading	ppi
p	Rivet spacing	inch
R	Strength reduction factor applied to riveted panels	
r	Bend radius of formed part (mean)	inch
t	Thickness of sheet (unless subscripted)	inch
d_{fr}, d_a	Flange width	inch
γ	Ratio of stiffener bending stiffness to sheet bending stiffness	
Γ	Torsion bending constant	$inch^6$
ϵ	Strain	inch/inch
λ	Wave Length	inch
η	Plasticity correction factor	
ψ	Effective stiffness of attached flange of stiffener	psi
ξ	Coupling parameter in flexure/torsion	
ν	Poisson's ratio	

SYMBOLS (continued)

Subscripts:

av	Average
a	Attached flange
b	Stiffener local buckling
cr	Critical, plastic
crel	Critical, elastic
e	Edge (or peak)
eff	Effective
fc	Forced crippling
fr	Free flange
f	Flexure, plastic
fel	Flexure, elastic
ft	Flexure torsion, plastic
ftel	Flexure torsion, elastic
cy	Compression yield
ir	Inter rivet, plastic
irel	Inter rivet, elastic
N	Natural
p	Polar
P	Panel
pb	Tangent (Area)
pc	Secant (Area)
riv	Rivet
s	Stiffener
su,sd	Stiffener twisting springs
t	Torsion, plastic
tel	Torsion, elastic
w	Wrinkling, plastic (interrupted attachment)
w(c)	Wrinkling, continuous attachment, plastic
we	Web
wel	Wrinkling, elastic
x	Axis designation
0.7	Property at secant modulus = 0.7E

B6.11.1 Introduction

For thin sheet supported by sturdy stiffeners, the initial buckling stress can usually be calculated assuming that the skin buckles between stiffeners with some rotational restraint by the stiffeners, while the failing stress can be calculated by considering the stiffener together with an "effective width" of sheet to fail in flexure as an Euler strut. The effective width concept accounts, in a simple way, for the interaction between the sheet and the stiffener.

Where the sheet is thick the initial buckling stress of the sheet may be comparable to the failure stress of the stiffener, and both may approach the yield stress of the material. It may no longer be possible to regard the stiffener as "sturdy" and it becomes necessary to take into account the flexural, torsional, and local deformations of the stiffener. These deformations govern the restraint given by the stiffener to the sheet at initial buckling. They also govern the final mode of failure, where the stiffener fails as a strut with one of the above modes predominating.

Modes of Deformation

The three "pure" modes of sheet and stiffener deformation may be described as follows:

The Flexural Mode is characterized by bending of the sheet, such that a line on the sheet through the stiffener attachments does not remain straight but distorts out of the original plane.

In long buckle lengths, of the order of the frame or rib spacing, this mode is identified as the "Euler" mode and involves bending of the stiffeners without distortion of their cross-sections.

In short buckle lengths, of the order of the stiffener spacing, the mode is called "wrinkling" and "forced crippling" and involves local distortion of the stiffener cross-section without appreciable bending (See B6.11.2).

In very short buckle lengths, of the order of the rivet spacing, the mode is called "inter-rivet" and involves separation of the sheet from the stiffener between rivets. The stiffener remains essentially straight and undistorted (See B6.11.3).

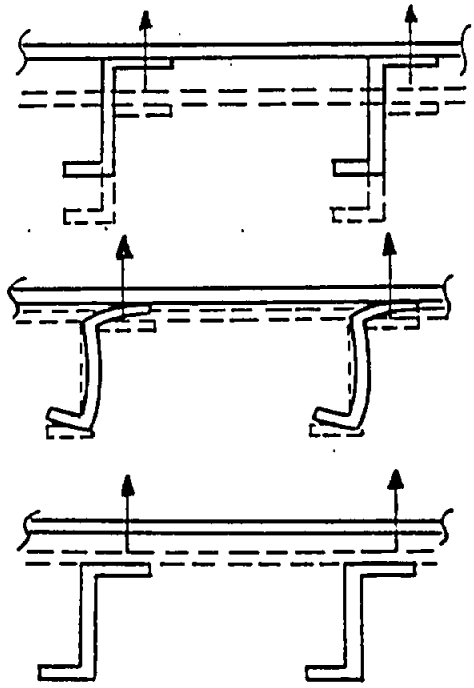

The Torsional Mode is characterized by twisting of the stiffener and rotation of the sheet about the stiffener attachment lines. The stiffener attachment lines remain straight. The buckle length of this mode is an integer fraction (including 1) of the rib or frame spacing. The critical length is a function of stiffener and plate properties (See B6.11.6).

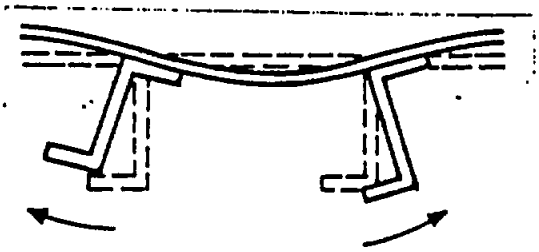

The Local Mode is characterized by distortion of the stiffener cross-section and rotation of the sheet about the stiffener attachment lines. The distortion is such that the junctions of the flat elements comprising the panel-cross-section remain straight. The buckle length is between two-thirds and one times the stiffener spacing.

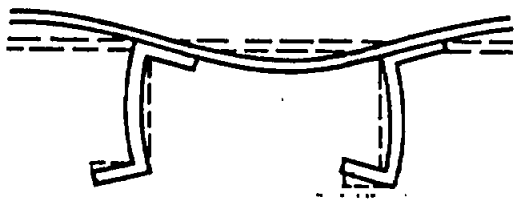

The buckling stress in each of the "pure" modes depends upon the sheet and stiffener geometry and upon the buckle length. There can be significant coupling between modes having the same buckle length, resulting in a lower buckling stress than in the "pure" modes. For example, the flexural, torsional and local modes can couple in buckle lengths of the order of the stiffener spacing (See B6.11.2).

Post-Buckling Behavior

The behavior of the panel after buckling depends upon the instability mode. If the initial instability is predominantly flexural with a buckle length equal to the frame or rib spacing then failure will be coincident with buckling, while if the initial instability is predominantly torsional the growth of the stiffener twist after buckling is usually so rapid that failure occurs soon after buckling. Only if the initial instability is predominantly in the local mode can the panel have any appreciable post-buckled strength. There are several failure modes that must be analyzed at this time in order to adequately determine the post-buckled strength of the panel. These modes for the sheet are the minimum of the wrinkling strength (B6.11.5), inter-rivet buckling strength (B6.11.3 and B6.11.5), or when the peak stress in the buckled sheet approaches the yield stress of the material. The failure modes for the stiffener are in long buckle lengths involving bending and twisting (B6.11.6) or in short lengths involving forced crippling (B6.11.6). For stiffened panel design and analysis local buckling of the stiffener as an individual element is also considered as a failure mode. This criteria is to preclude a severe interaction of stiffener buckling with the plate wrinkling mode.

B6.11.2 Short Wave Buckling

Short wave buckling involves the local, torsional and wrinkling modes in buckle lengths approximately equal to the stiffener spacing. The local and torsional modes are characterized by the stiffener attachment lines remaining straight at buckling, while in the wrinkling mode they distort out of the original plane of the sheet.

The method given here consists of obtaining a buckling stress coefficient which accounts for the coupling between the local and torsional modes. The minimum short-wave buckling stress coefficient is then obtained from Figure 4, which allows for the coupling with the wrinkling mode. The elastic buckling stress is given by:

$$F_{crel} = \frac{F_{cr}}{\eta} = K_{cr} E (t/b)^2 \qquad (1)$$

The buckling stress F_{cr} can be obtained from B1.50.1-1, where the value of η is for a long flat plate with simply-supported edges.

Local Buckling

Curves are given for the local/torsional buckling stress coefficients of flat panels with Z-section (Figure 1) or integral unflanged (Figure 2) stiffeners. Each stiffener deforms by twisting about an axis in the plane of the sheet and by local distortion of its cross-section. Where the curves are convex upwards the stiffener deformation is mainly local, but where the curves are concave upwards (below the dotted line) the deformation is predominantly twisting of the stiffener and failure will be practically coincident with the initial instability.

For closed-section stiffener (such as hats or Ys) the torsional mode can be neglected, and the local buckling stress coefficient can be obtained from R.A.S. Structures Data Sheets 02.01.28 to 37. An approximate value can be obtained by applying the method of B4.12 to the panel cross-section.

Wrinkling Instability

Curves are given in Figure 4 for the minimum value of the short wave buckling stress coefficient. The curves require the value of the local/torsional buckling stress coefficient, and the value of the stiffness of the attached flange of the stiffener against distortion out of the skin plane.

For low values of the attached flange stiffness, the mode is predominantly bending of the stiffener attachment lines out of the original skin plane. This mode is called "wrinkling" and is most likely to occur when thick sheet is supported by relatively thin stiffeners. At high values of the attached flange stiffness the mode is predominantly local with the stiffener attachment lines remaining straight.

The wrinkling mode is characterized by a buckle pattern with troughs and crests extending across the attached stiffener flange. Consequently, the effective stiffness of the supporting flange must take into account two distinct stiffnesses:

The first is associated with the skin pushing in towards the stiffener web (down spring) and is given by:

$$\psi_1 = \frac{E}{(1-\nu^2)}\left(\frac{t_a}{r}\right)^3\left(\frac{2r + c' + h(t_a/t_{we})^3}{4c' - r + (4hc'/r)(t_a/t_{we})^3}\right) \qquad (2)$$

The second is associated with the skin pulling away from the stiffener web (up spring) and is given by:

$$\psi_2 = \frac{E}{(1-\nu^2)}\left(\frac{t_a}{c'}\right)^3\left(\frac{2c' + d_a + h(t_a/t_{we})^3}{4d_a - c' + (4hd_a/c')(t_a/t_{we})^3}\right) \qquad (3)$$

These equations are for Z or channel section stiffeners. Equations for other sections may be derived as shown in GAC Report SAR-71-1. This reference includes on pages 24.1 and 24.2, spring rate and bending moment coefficients for the special case of back to back channel sections.

Also included in Report SAR-71-1 is the clamping effect of the skin to flange attachment fastener on the spring rates and bending moments. This data is presented on B6.11.2-2.1 as a plot of the effective offset distance as a function of the nominal offset distance, fastener pitch and fastener diameter. Use the effective offset distance c', in place of the nominal offset distance c, in the wrinkling spring, rivet load and stiffener flange strength parameters of Equations (2), (3), (11), (14), (20) and (21).

The effective stiffness, ψ, is given in Figure 3.

Figure 3 The Effective Deflectional Stiffness

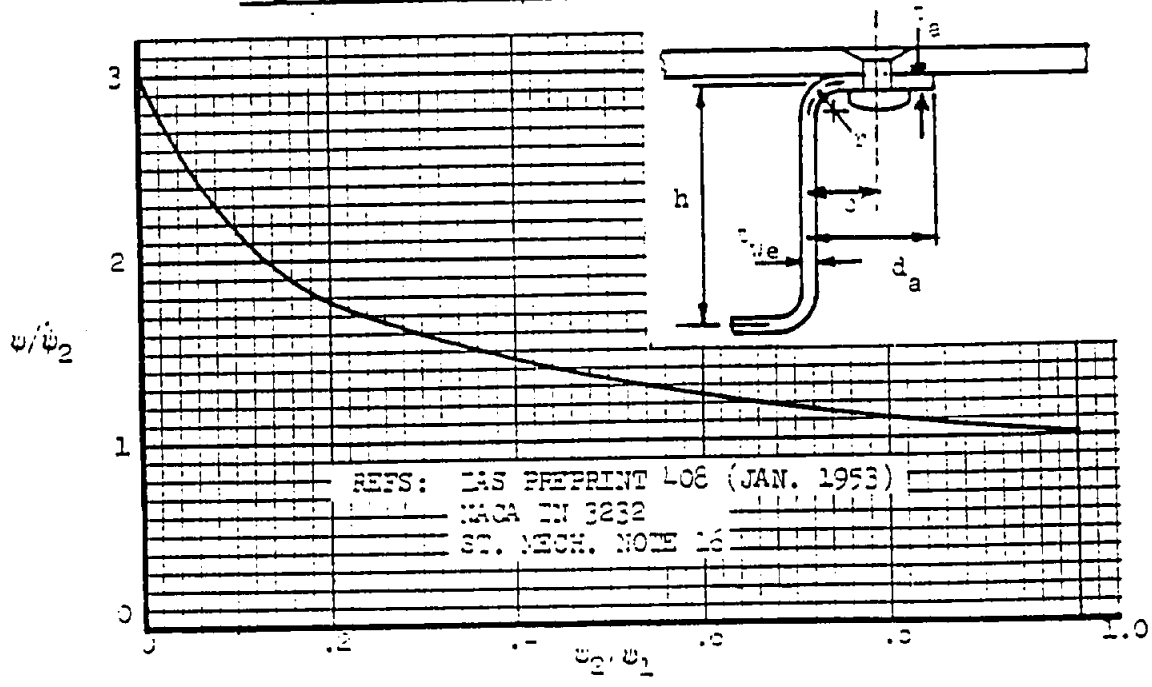

EFFECTIVE FASTENER OFFSET DISTANCE INCLUDING RIVET GEOMETRY LIMIT

Reference NACA TN 3785 Figure 14

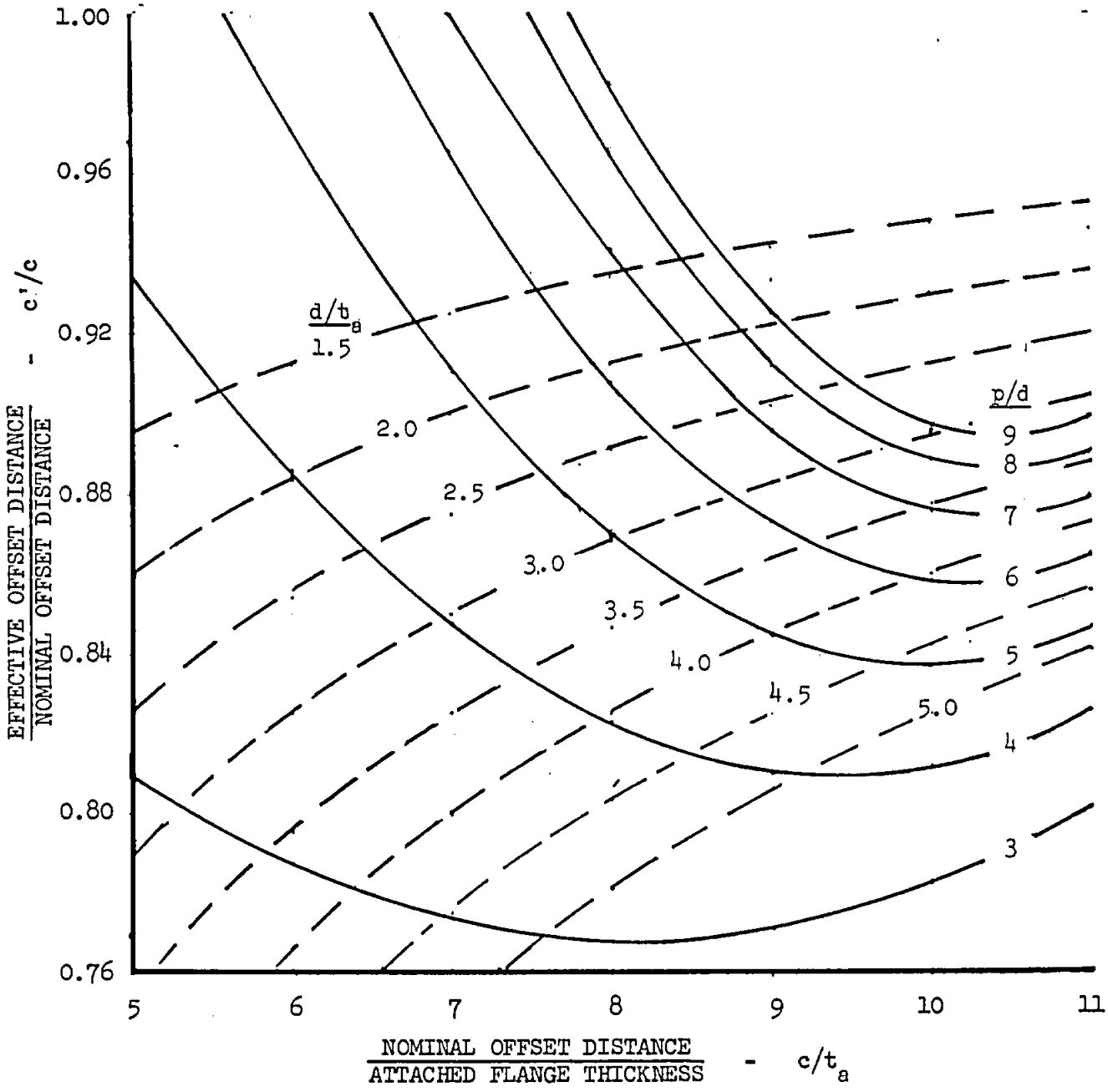

c'/c - Effective Fastener Offset Distance is the maximum value from p/d (fastener pitch/fastener diameter, solid line) or d/t_a (fastener diameter/attached flange thickness, dashed line).

Example: c = 0.496 t_a = 0.070 p = 0.750 d = 0.1875

c/t_a = 7.10 p/d = 4.00 d/t_a = 2.68

The effective fastener offset distance is 0.845 for p/d and 0.868 for d/t_a.

Therefore: c'/c = 0.868 for this geometry.

Figure 4 is then entered with the local/torsional buckling stress coefficient K and the effective stiffness parameter:

$$\frac{\psi b^3}{\pi^4 D} = 0.112 \frac{\psi}{E} \left(\frac{b}{t}\right)^3 \qquad (4)$$

Example

Find the buckling stress of the stiffened panel shown. The material is annealed 6Al-4V titanium alloy sheet, and the rivet diameter = 5/32 in.

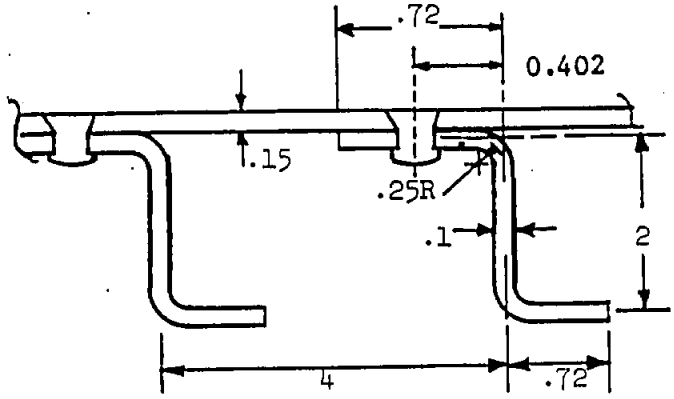

$$\frac{t_{we}}{t} = \frac{.1}{.15} = .67$$

$$\frac{A_s}{bt} \quad \frac{(2 + .72 + .72) \times .1}{4 \times .15} = .57$$

From Figure 1, the local buckling stress coefficient K = 3.92.

This is above the dotted line in Figure 1, therefore the local mode predominates.

From Equation 2, $\psi_1 = \frac{16.3 \times 10^6}{(1 - 0.32^2)} \left(\frac{0.10}{0.25}\right)^3 \frac{(2 \times 0.25 + 0.402 + 2 \times 1)}{(4 \times 0.402 - 0.25 + 4 \times 2 \times 0.402/0.25 \times 1)}$

$= 237150$ psi

From Equation 3, $\psi_2 = \frac{16.3 \times 10^6}{(1 - 0.32^2)} \left(\frac{0.10}{0.402}\right)^3 \frac{(2 \times 0.402 + 0.72 + 2 \times 1)}{(4 \times 0.72 - 0.402 + 4 \times 2 \times 1 \times 0.72/0.402}$

$= 58610$ psi

$\psi_2/\psi_1 = 58612/237150 = .247$

From Figure 3, $\psi/\psi_2 = 1.68$ $\therefore$ $\psi = 1.68 \times 58610 = 98465$ psi

From Figure 4, $\frac{\psi b^3}{\pi^4 D} = 0.112 \times \frac{98465}{16.3 \times 10^6} \left(\frac{4}{0.15}\right)^3 = 12.8$

From Figure 4, the short-wave buckling stress coefficient $K_{cr} = 3.42$

From Equation 1, $F_{crel} = 3.42 \times 16.3 \times 10^6 \ (0.15/4)^2 = 78600$ psi

From B1.20.2, Reference stress $F_{0.7} = 140700$ psi

Stress-strain parameter n = 31

Note: For the effective offset distance, c', from B6.11.2-2.1,
c = 0.402 t_a = 0.100 p = 0.813 d = 0.156
c/t_a = 4.02 p/d = 5.20 d/t_a = 1.56
From B6.11.2-2.1, c', the effective offset distance is 1.00.

$$\frac{\text{Elastic Buckling Stress}}{\text{Reference Stress}} = \frac{F_{crel}}{F_{0.7}} = \frac{78600}{140700} = 0.56$$

from B1.50.1-1 $\quad \frac{\text{Buckling Stress}}{\text{Reference Stress}} = \frac{F_{cr}}{F_{0.7}} = 0.56$

Therefore, buckling stress 0.56 x 140700 = 78600 psi

This example is continued in B6.11.5 (Wrinkling stress of sheet) and B6.11.6 (Failure stress of stiffener). It should be noted that the example was chosen to illustrate the analysis procedure, and is not necessarily indicative of good design.

Figure 1 Local Buckling Stress of Flat Panels With Z-Section Stiffeners Under Compression

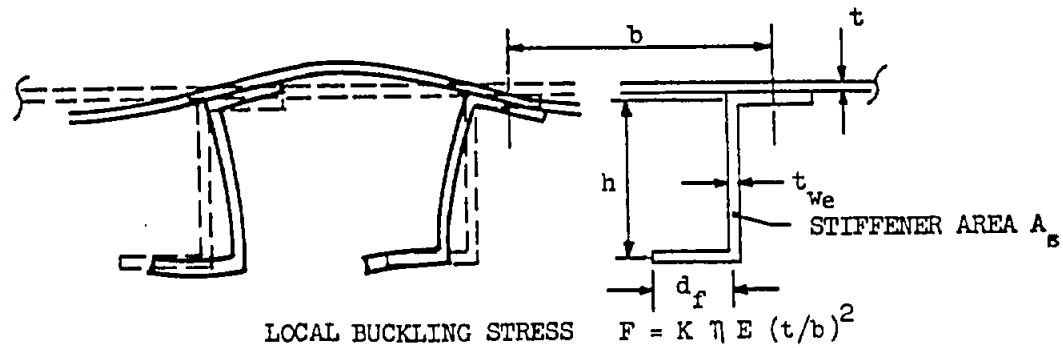

LOCAL BUCKLING STRESS $F = K \eta E (t/b)^2$

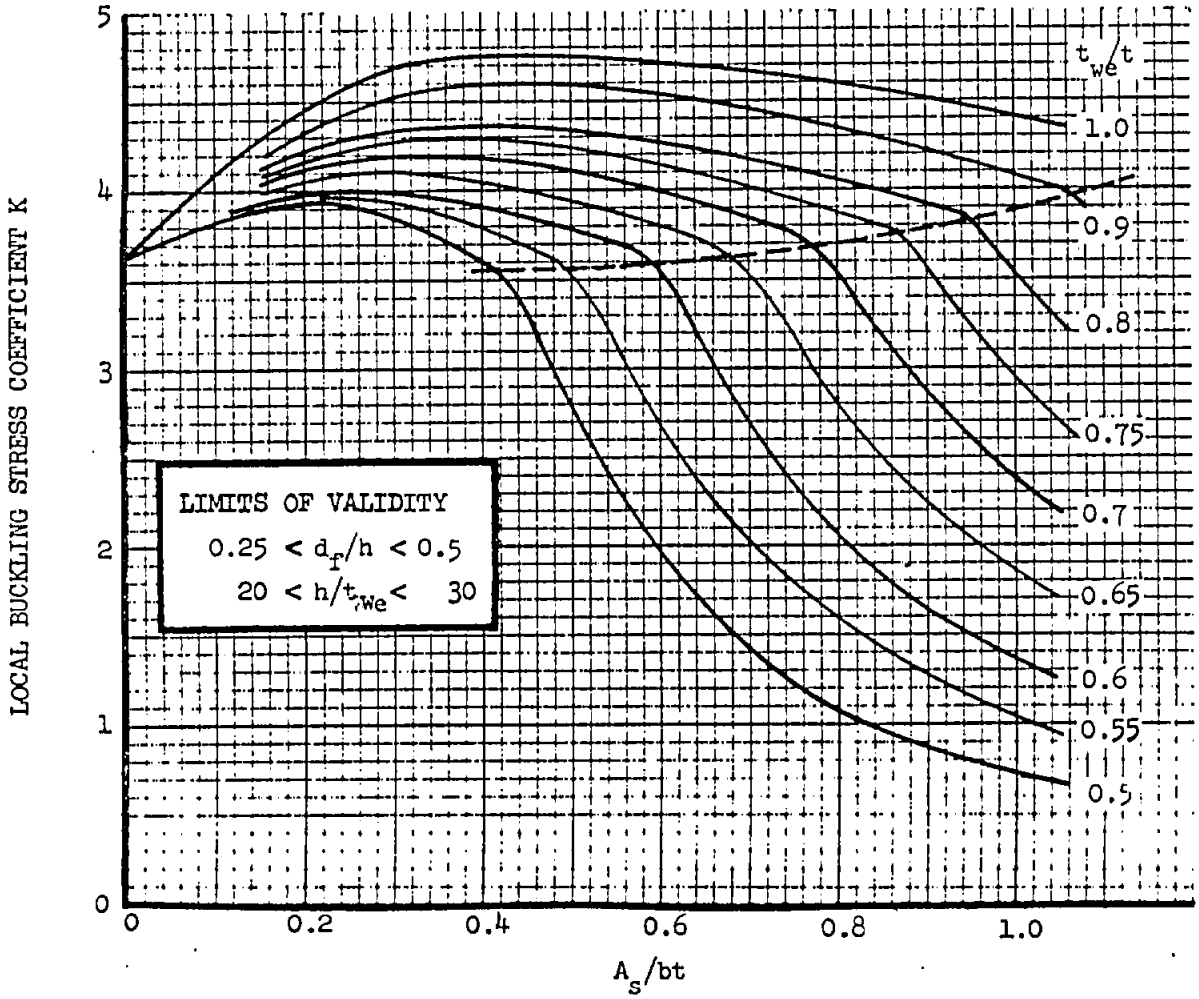

Refs: N.A.C.A. T.N. 1482
RAS Structures Data Sheet 02.01.25
A. Rothwell, JRAS, February 1968

Figure 2 Local Buckling Stress of Flat Panels with Unflanged Stiffeners Under Compression

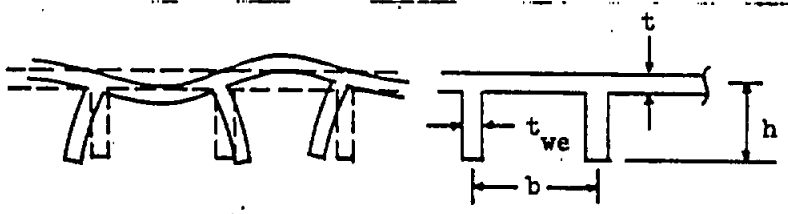

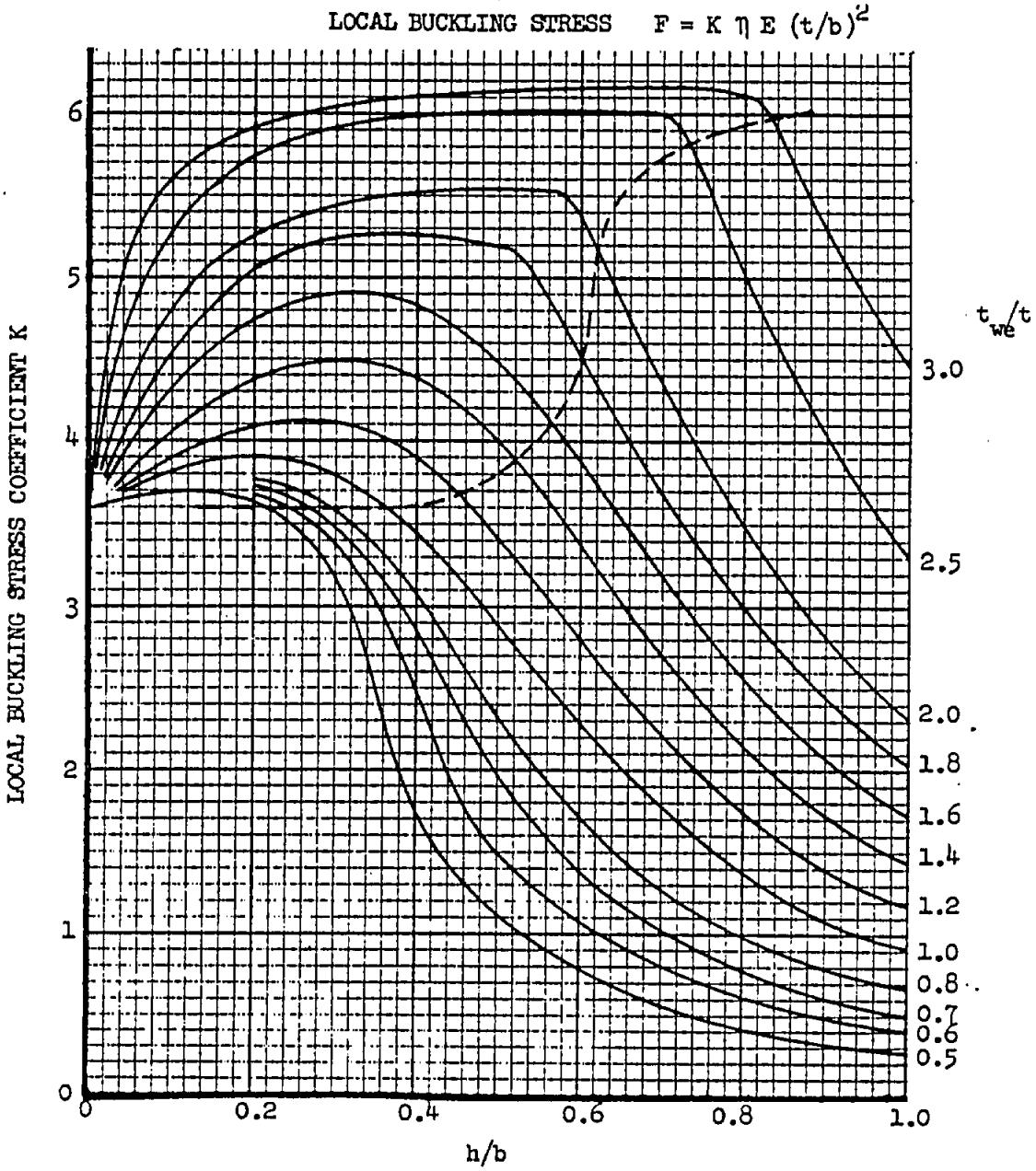

Refs: N.A.C.A. WR L-204
E. J. Catchpole, Journal R. Ae.S. Nov. 1954

Figure 4 Short Wave Buckling of Stiffened Sheet

B6.11.3 Inter-Rivet Buckling

The inter-rivet mode involves buckling of the sheet as a wide column upon essentially undistorted stiffeners so that the sheet separates from the stiffener between the rivets. The length of the column corresponds to the rivet spacing. Because the sheet cannot buckle in the direction of the stiffener, the mode shape is constrained to that of a fixed end column. This mode shape can best be described by the use of an end fixity factor equal 3.75. This factor is derived from results of NACA compression tests.

The elastic inter-rivet buckling stress, which is the limiting compressive stress for the sheet at the rivet line (pg. B6.11.5-9) is given by:

$$F_{irel} = \frac{F_{ir}}{\eta} = \frac{3.75\pi^2 E}{12(1-\nu^2)}\left(\frac{t}{p}\right)^2 \qquad (5)$$

The inter-rivet buckling stress F_{ir} can be obtained from B1.50.2, using the value of η appropriate to a short plate loaded as a column.

Example:

Find the inter-rivet buckling stress of an 0.028 in. 7075-T6 aluminum alloy sheet supported by adequate Z section stiffeners. The rivets are MS20470 AD4 at 9/16 in. spacing.

From Equation (5), $F_{irel} = \dfrac{3.75 \times \pi^2 \times 10.5 \times 10^6}{12\,(1 - 0.32^2)}\left(\dfrac{0.028}{0.5625}\right)^2 = 89400$ psi

From B1.20.2, Reference stress $F_{0.7} = 71800$ psi

Stress-strain parameter n = 14.5

$$\frac{\text{Elastic buckling stress}}{\text{Reference stress}} = \frac{F_{irel}}{F_{0.7}} = \frac{89400.}{71800} = 1.24$$

From B1.50.2 $\dfrac{\text{Buckling stress}}{\text{Reference stress}} = \dfrac{F_{ir}}{F_{0.7}} = 0.84$

$\therefore$ Inter-rivet buckling stress $F_{ir} = 0.84 \times 71800 = \underline{60310 \text{ psi}}$

The inter-rivet buckling stress in the example of B6.11.2 with rivets at 13/16 in spacing is >> than $F_{0.7}$ and therefore not critical.

B6.11.4 Post-Buckling Behavior

The behavior of the panel after buckling depends upon the mode of the initial instability:

1. If the initial instability is predominantly flexural in buckle lengths comparable to the frame or rib spacing then the failure will be coincident with buckling.

2. In the wrinkling mode the buckles run across the stiffeners and distort the attached flanges of the stiffeners. At failure the buckles become almost cylindrical, and the distortion of the attached flange is sufficient to cause collapse of the stiffeners. Although the wrinkling stress is derived from a stability analysis of the sheet, the failing member is the stiffener attached flange.

3. If the skin buckles in the inter-rivet mode then it may be assumed that under continued deformation the sheet will continue to carry the load at buckling but no additional load. Failure occurs when the stiffener fails.

4. If the initial instability is predominantly torsional then the growth of the stiffener twist after buckling is usually so rapid that failure occurs soon after.

5. If the initial instability is predomonantly in the local mode then the sheet is supported by the stiffener and can carry additional load beyond buckling. The stress in the sheet undergoes a redistribution after buckling, with peaks occuring at the stiffener attachment lines. Failure occurs when this peak stress reaches the failing stress of the stiffener or sheet, whichever is critical.

6. In a riveted panel, failure may occur due to the tensile loads induced in the rivets by the post-buckling deformations.

No closed-form analysis of the post-buckling behavior of stiffened flat panels exists. Instead, a failure analysis has evolved which consists of calculating the more critical failing stress of stiffener or sheet (F_e) and the corresponding average stress in the buckled sheet (F_{av}). The two stresses are not independent; the presence of the sheet affects the axes about which the stiffener bends and twists, while the average stress in the buckled sheet depends upon the stiffener stress and the initial buckling stress.

B6.11.4 Post-Buckling Behavior (Cont.)

The failing load of the panel is then given by the sum of the stiffener (or sheet) failing stress times the stiffener area and the average stress in the sheet times the sheet area. This may be expressed as an average panel failing stress (F_p) by dividing by the total area:

$$F_p = \frac{F_e A_s + F_{av} bt}{A_s + bt} = \frac{F_e A_s/bt + F_e b_{eff}/b}{A_s/bt + 1.0}$$

Methods of calculating F_{av} and F_e are given in B6.11.5 and B6.11.6. The peak stress in the sheet at failure is F_e and is the minimum of the sheet failure stress or the stiffener failure stress.

B6.11.5 Failure Stress of Sheet

The failure stress of the sheet is the lowest of the failure stresses calculated for the three modes: crippling, wrinkling and inter-rivet buckling.

Crippling of Sheet

After local buckling, the uniform stress in the sheet is redistributed, with peaks at the stiffener attachment lines, as shown:

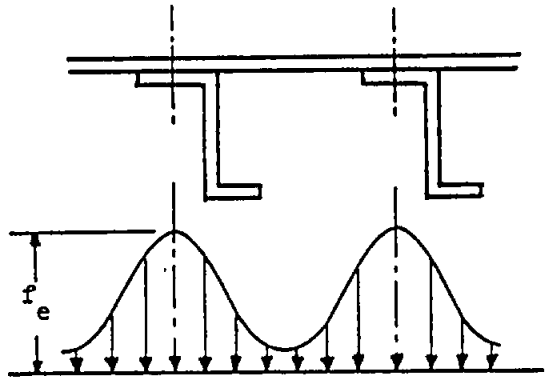

The average stress in the sheet depends upon the buckling stress of the sheet (F_{cr}) and the peak stress (F_e). The limiting value of the peak stress will be either the stiffener failing stress F_s (from B6.11.6), the inter-rivet buckling stress F_{ir} from Equation (5), the wrinkling stress from B6.11.5 or the compressive yield stress of the sheet material F_{cy} whichever is least. If the critical edge stress is F_{cy}, the failure mode is sheet crippling.

The peak stress in the sheet is determined from the load carrying characteristics of the buckled sheet. This is given by the following equation which states the average stress in sheet, the effective width and load carrying area of the sheet.

$$b_{eff}/b = A_{pc}/bt = F_{av}/F_e = 1.2\left(\frac{\epsilon_{cr}}{\epsilon_e}\right)^{2/5} - 0.65\left(\frac{\epsilon_{cr}}{\epsilon_e}\right)^{4/5} + 0.45\left(\frac{\epsilon_{cr}}{\epsilon_e}\right)^{6/5} \quad (7)$$

The stiffness area of the sheet is required in the determination of section properties for stability calculations (Euler column and Wrinkling). The stiffness area is determined from the derivative of the effective width equation and is:

$$b_{eff}'/b = A_{pb}/bt = 0.72\left(\frac{\epsilon_{cr}}{\epsilon_e}\right)^{2/5} - 0.13\left(\frac{\epsilon_{cr}}{\epsilon_e}\right)^{4/5} - 0.09\left(\frac{\epsilon_{cr}}{\epsilon_e}\right)^{6/5} \quad (8)$$

In order that these equations are applicable when the stresses are greater than the material proportional limit, the argument of the equation is given as a strain ratio. The strains are determined from stresses by the following relations:

$$\epsilon_{cr} = F_{cr}/E_s \qquad (E_s \text{ is at stress } F_{cr})$$

$$\epsilon_e = F_e/E_s \qquad (E_s \text{ is at stress } F_e)$$

The secant moduli (E_s) can be determined from Section B.1. Equations 7 and 8 are plotted in Figure 5.

Wrinkling of Sheet

Failure occurs in the wrinkling mode when the sheet buckle becomes almost cylindrical. The peak stress in the sheet at failure is derived from the stability equation for a column supported laterally by an elastic foundation. For the case of a sheet of constant thickness, continuously attached to the stiffener flange, and $F_w < F_{cr}$, the wrinkling stress is:

$$F_{wel} = F_{w(c)}/\eta = 0.61\sqrt{\psi E\, t/b} \qquad (9)$$

For the case of $F_w > F_{cr}$, the wrinkling stress is:

$$F_{wel} = F_{w(c)}/\eta = 0.41\sqrt{\psi E t/b} \cdot \sqrt{b_{eff}/b + b_{eff}'/b}\ \Big/ (b_{eff}/b) \qquad (9a)$$

where ψ is the effective stiffness obtained in B6.11.2 (from Equation 2 and 3, and Figure 3), b_{eff}/b is the load carrying effective width from Equation (7) and b_{eff}'/b is the stiffness effective width from Equation (8). The effective widths are also on Figure 5.

Because the sheet stability is derived from a column analysis, the plasticity correction factor must be a function of E_t (the tangent modulus at a stress equal to $F_{w(c)}$. In the case of wrinkling $\eta = \sqrt{E_t/E_c}$. This plasticity factor is available from page B 1.50.4-2.

To account for the discrete rather than continuous nature of riveted sheet stringer construction, the plastic value of $F_{w(c)}$ is multiplied by the empirically determined factor R to determine F_w. R is given on Figure 6. Therefore:

$$F_w = R \cdot F_{w(c)} \qquad (10)$$

For sheet configurations other than one of constant thickness, the analyst is referred to SAR-71-1. The analyst is cautioned that the wrinkling stress is based on the basic assumption that the sheet stiffness can be conservatively idealized to a concentrated quantity at the stiffener.

FIGURE 5 EFFECTIVE WIDTH OF SHEET LOADED IN COMPRESSION

$$\frac{b_{eff}}{b} = 1.20\left(\frac{\epsilon_{cr}}{\epsilon_e}\right)^{2/5} - 0.65\left(\frac{\epsilon_{cr}}{\epsilon_e}\right)^{4/5} + 0.45\left(\frac{\epsilon_{cr}}{\epsilon_e}\right)^{6/5} \quad \text{(Load)}$$

$$\frac{b_{eff}'}{b} = 0.72\left(\frac{\epsilon_{cr}}{\epsilon_e}\right)^{2/5} - 0.13\left(\frac{\epsilon_{cr}}{\epsilon_e}\right)^{4/5} - 0.09\left(\frac{\epsilon_{cr}}{\epsilon_e}\right)^{6/5} \quad \text{(Stiffness)}$$

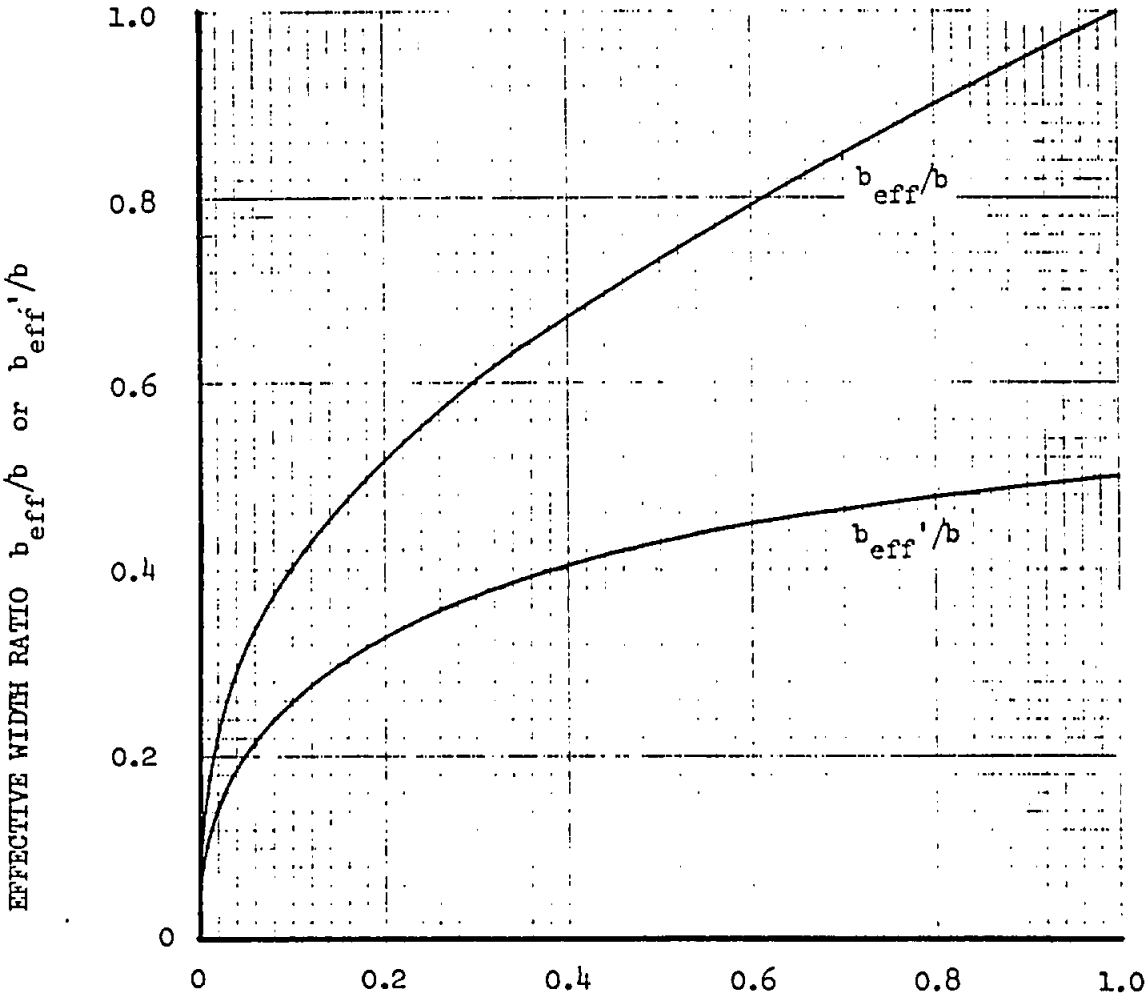

$$\frac{\epsilon_{cr}}{\epsilon_e} = \frac{\text{CRITICAL BUCKLING STRAIN}}{\text{COMPRESSIVE EDGE STRAIN}}$$

Reference: NACA TN 3784

Figure 6. The Reduction Factor R in Equation (10)

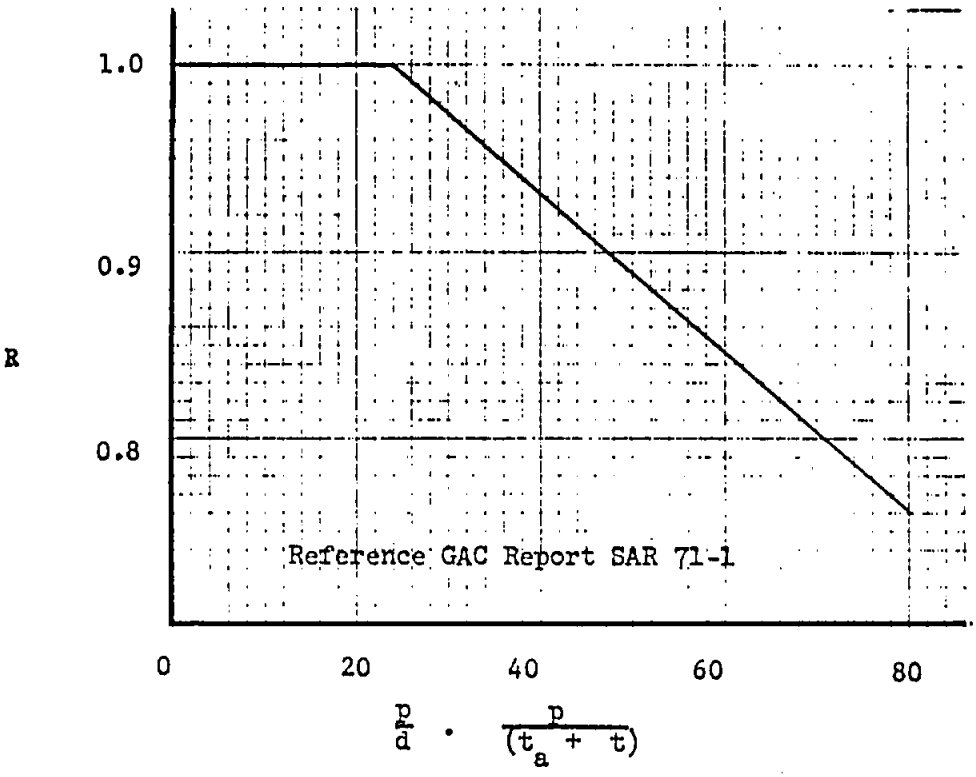

Example:

Find the wrinkling failure stress of the stiffened panel given as the example in B6.11.2. The rivets are 5/32 dia. at 13/16 spacing.

Page B6.11.2-3,	deflection stiffness	ψ	= 98465	psi
	sheet thickness	t	= 0.15	inch
	attached stiffener flange thickness	t_a	= 0.10	inch
	stiffener spacing	b	= 4.0	inch

then $\frac{p}{d} \cdot \frac{p}{(t_a + t)} = \left(\frac{13/16}{5/32}\right) \cdot \left(\frac{13/16}{(0.10 + 0.15)}\right) = 17$

From Figure 6, R = 1.00

From Equation 9, $F_{wel} = 0.61 \times \left(\frac{98465 \times 16.3 \times 10^6 \times 0.15}{4.0}\right)^{\frac{1}{2}} = 149700$ psi

From B1.20.2 Reference stress $F_{0.7}$ = 140700 psi

Stress-strain parameter n = 31

$$\frac{\text{Elastic wrinkling failure stress}}{\text{Reference stress}} = \frac{F_{wel}}{F_{0.7}} = \frac{149700}{140700} = 1.06$$

From B1.50.4-2 $\dfrac{\text{Wrinkling failure stress}}{\text{Reference Stress}} = \dfrac{F_{w(c)}}{F_{0.7}} = 0.88$

$F_{w(c)} = 0.88 \times 140700 = 124950$ psi

This stress exceeds the local buckling stress $F_{cr} = 78600$ and therefore the wrinkling stress must be calculated from Equation 9a. Because b_{eff}/b is a function of $F_{w(c)}$, the solution must be obtained by iteration.

First approximation:	2nd Iteration
Assume $F_{w(c)} = 126000$ psi	(123500)
$\epsilon_{cr} = 78600/E$	
$F_{w(c)}/F_{0.7} = 126000/140700 = 0.896$	(0.878)
$E_s/E = 0.985$ Figure B1.40-2	(0.991)
$\epsilon_{cr}/\epsilon_e = \dfrac{78600 \times 0.985}{126000} = 0.614$	(0.631)
From Fig. 5, $b_{eff}/b = 0.798$	(0.808)
$b_{eff}/b = 0.452$	(0.455)
$F_{wel} = 0.41/0.61 \times 149700 \sqrt{0.798 + 0.452}/0.798$	
$= 140970$ psi	(139950)
$F_{wel}/F_{0.7} = 140970/140700 = 1.002$	(0.995)
$F_{w(c)}/F_{0.7} = 0.878$ (Figure B1.50.4-2)	(0.878)
$F_{w(c)} = 0.878 \times 140700 = 123500$ psi	(123500)

$F_w = R \times F_{w(c)} = 1.0 \times 123500 = 123500$ psi

Calculate the average panel stress, F_p, at wrinkling failure using Equation (6).

$$F_{F_p} = \frac{123500\,[0.57 + 0.798]}{[0.57 + 1.0]}$$

$= 107600$ psi

2nd Example Problem:

Geometry and members same as previous except stiffener spacing = 8.0 in.

The following is the result of the analysis of this panel. Only pertinent results are shown. The following data remain unchanged from the original problem:

$R = 1.0$, $\psi = 98465$ psi, $t = 0.15$ in.

$t_a = 0.10$, $A_s = 0.344$ in., $t_{we}/t = 67$

The following data and results include the effects of the 8.0 in stiffener spacing:

$\psi b^3/\pi^4 D = 102.4$

$A_s/bt = 0.285$

$K = 4.15$ Figure 1

$K_{cr} = 4.08$ Figure 4

$F_{cr} = F_{crel} = 23380$ psi (Equation (1))

$b_{eff}/b = 0.51$

$b'_{eff}/b = 0.325$

$F_{wel} = 127470$ psi

The allowable wrinkling stress (after iteration) is:

$F_W = F_{w(c)} = 119000$ psi

Calculate the average panel stress, F_p, at wrinkling failure. Using Equation (6).

$$F_p = \frac{119000\left[0.285 + 0.51\right]}{\left[0.285 + 1.0\right]}$$

$$= 73600 \text{ psi}$$

Sheet Strength in the Wrinkling Mode

In addition to the primary wrinkling stability stress, the sheet is subjected to transverse bending stress caused by the deflection of the column (sheet) in the cylindrical buckle pattern, that is characteristic of wrinkling. The lateral deflection of the column displaces the elastic foundation (stiffener attached flange) which causes concentrated normal line loads to exist between the sheet and stiffener flange. On the sheet side, these loads are equilibrated by distributed loads that result in bending stresses in the plane of the sheet that act normal to the primary axial stress field. These stresses are critical at the stiffeners where the allowable bending stress must account for the effects of the peak axial stress in the sheet.

The bending moment in the sheet is determined from the following equation for stiffeners with single line of attachment such as a Z.

$$m = \frac{0.022\ t\ \psi_2\ b}{16}\left[1-\frac{4}{\Pi^2}\quad\frac{1-F_{cr}/F_e}{1+F_{cr}F/e}\right] \qquad (10a)$$

The allowable bending moment can be determined from page B6.12.4-6. To use the figure, replace f_{STmax} with F_e. The allowable bending moment is:

$$M = H.F_{cy}.\quad t^2/4.0 \qquad (10b)$$

where

H from page B6.12.4-6

F_{cy} = the sheet material compression yield stress

t = the sheet thickness

Strength in the wrinkling mode F_w, is determined from the more critical of the primary wrinkling instability stress from Equation (10) or from the limiting value of F_e as determined from equations (10a) and (10b).

The calculation required for this analysis is shown in the following example of B6.11.2. As a starting point, let F_e be the value of wrinkling stability strength which is 123500 psi. Then the moment is:

$$m = \frac{0.022 \times 0.15 \times 58612 \times 4.0}{16}\left[1-\frac{4}{\Pi^2}\cdot\frac{1-78600/123500}{1+78600/123500}\right]$$

$$= 48.4 \times 0.91$$

$$= 44.0 \text{ in.lbs./in.}$$

For figure on page B6.12.4-6

F_e/F_{cy} = 123500/138000 = 0.895

H = 0.32

M = $0.32 \times 0.15^2 \times 138000 / 4.0$

248 in lb/in (> m)

Therefore, for this structural configuration, in the wrinkling mode, the sheet is critical for the primary stability stress from equation (10). The transverse bending strength will become more critical in configurations where the thickness ratio of stiffener flange to sheet is nearer unity or greater. In this case, it is necessary to determine the value of F_e that will give a zero margin in the transverse bending strength determination. These calculations are illustrated in an extension of the previous example.

The limiting value of F_e exists when m is equal to the allowable moment, M. Since F_e exists in both m and M, the value is determined by iteration.

A first trial value of F_e can be established by calculating M for H equal 1.0 and then estimating H from ratio of m to the value of M.

		2nd Iteration
M	$= 138000 \times 0.15^2/4.0 = 776$ (For H = 1.0)	
H	$= 44/776 = 0.057$ (Initial trial value)	(0.056)
F_e/F_{cy}	= 0.98 from page B6.12.4-6	(0.985)
F_e	$= 0.98 \times 138000 = 135000$	(136000)
m	$= 48.4 \cdot \left[1 - \frac{4}{\Pi^2} \frac{1-78600/135000}{1+78600/135000}\right]$	
	= 43.2 in lb/in	(43.2)
M	$= 0.057 \times 138000 \times 0.15^2/4$	
	= 44 in lb/in	(43.2)

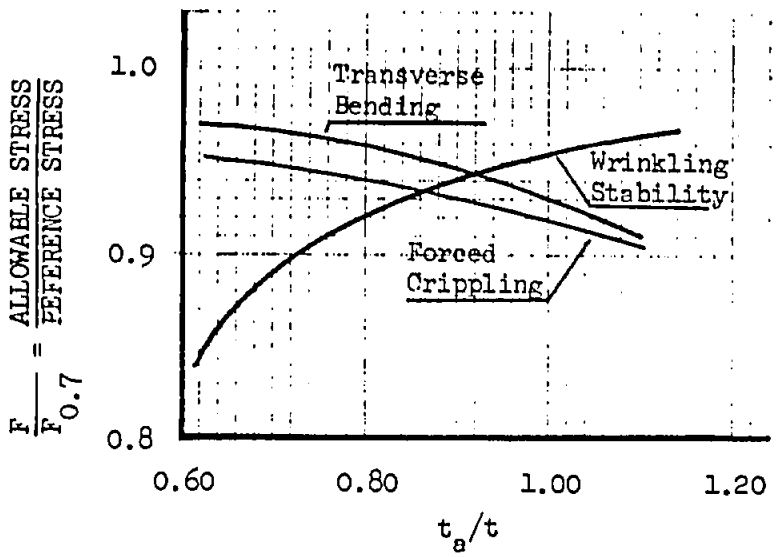

The adjacent figure illustrates the wrinkling stability stress, sheet transverse bending stress and stiffener flange forced crippling stress from B6.11.6-4 as a function of t_a, stiffener attached flange thickness. It can be seen that the sheet bending criteria and stiffener flange forced crippling provide the upper limit of strength to the wrinkling and related failure modes.

Inter-Rivet Failure of Sheet

If the inter-rivet buckling stress F_{ir} given by equation (5) is less than the short-wave buckling stress F_{cr} given in Equation (1), then it may be assumed that, with further increase of load on the panel, the sheet stress will remain constant at F_{ir} and there will be no significant redistribution of stress.

If the inter-rivet buckling stress F_{ir} is greater than the short-wave buckling stress F_{cr}, then the stress in the sheet will be redistributed after buckling at F_{cr}. The peak stress in the sheet cannot exceed F_{ir}, and the average stress in the sheet cannot exceed the value given by Equation (7) with $F_e = F_{ir}$.

Rivet Strength Criteria

The deformation during buckling induces tensile loads on the fasteners attaching the sheet to the stiffeners. A criterion for the rivet strength is that the tensile strength, either in shank failure, head failure, or tearout through the sheet, should not be less than

$$P_{riv} = 0.022\ \psi_2\ t \left[\frac{d_a}{d_a - c'}\right] p \qquad (11)$$

Where:

ψ_2 is from Equation (3)

t is plate thickness

p is the rivet spacing

c' is the effective rivet offset distance from page B6.11.2-2.1

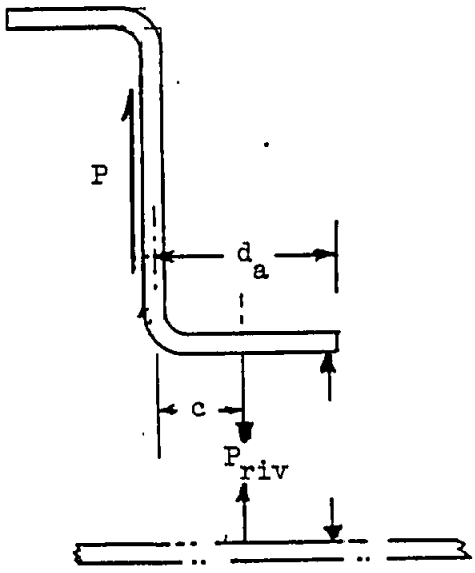

Example:

Find the required tensile strength of the rivets in the example of B6.11.2. The rivets are NAS1200 at 13/16 in. spacing.

ψ_2 = 58612 psi

t = 0.15 in.

d_a = 0.72 in.

c' = 0.402 in.

$$P_{riv} = 0.022 \times 58612 \times 0.15 \times (0.72/(0.72 - 0.402)) \times 0.812$$

$$= 356 \text{ lb/rivet}$$

From Grumman Corporate Titanium Test Program, 5/32 Dia. NAS 1200 rivets of A286 material have an ultimate tensile strength of 1100 lbs. per rivet ∴ Criterion is satisfied.

The shank tensile strength of some steel rivets is available from Grumman Report SAR-71-1, page A-4. Tensile strength for Hi-Lok fasteners is available in MIL-HDBK-5, page 8-85. Sheet pull-through strength for fasteners is given on page B6.12.4-10.

B6.11.6 Failure Stress of Stiffener

Four "pure" modes of stiffener failure may be identified; buckling, forced crippling, twisting, and bending (Euler column). In general, the latter three pure modes will interact to give a stiffener failing stress which decreases with increasing buckle length in the complex manner illustrated in the following sketch.

Although most thin gaged stiffeners will have local strength greater than its local buckling stress, local buckling of the stiffener elements (other than attached flange) is considered to be a failure mode in stiffened panels. The philosophy of "Sturdy Stiffeners", that is, stiffeners unbuckled at ultimate load, is required to prevent coupling with the wrinkling mode. If the stiffener web is permitted to buckle at stresses less than the wrinkling stress (determined in B.6.11.5) the equation for the down spring, ψ_1, is incorrect. The presumed support for the attached flange in the derivation of ψ_1, is essentially a straight, unbuckled (and therefore rigid) web. This is clearly not the case with a buckled stiffener web.

At short buckle lengths, of the order of the stiffener depth h, the failure will be by forced crippling (caused by wrinkling of the sheet). As the buckle length is increased, the torsional mode may be encountered and finally, if sufficiently long buckle lengths can be present in the panel, the flexural failure mode will predominate. For assymetric stiffener cross-sections the flexural mode will couple with the torsional mode.

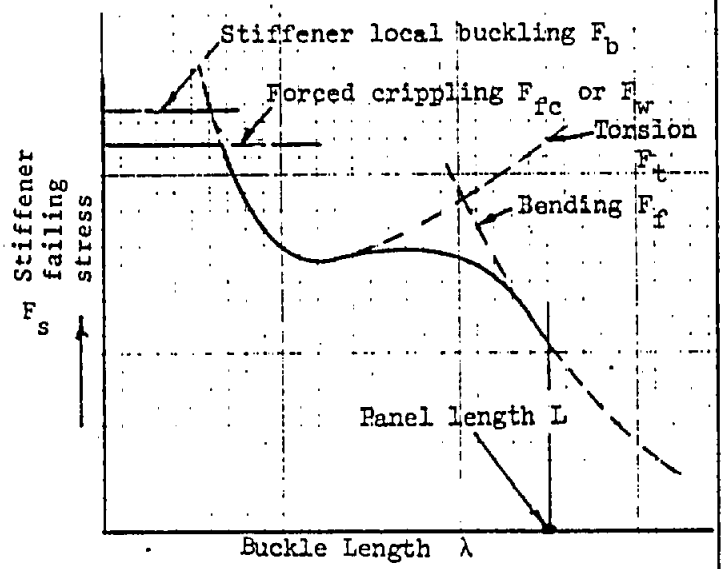

Buckling of the Stiffener Elements

The determination of stiffener buckling stress presented in the following applies only to stiffeners attached to a plate. It is a specific adaptation of Section B4 and in no way is it to be interpreted as an alternate to the general case presented in that section.

For this case, the stiffener local buckling strength is based on the free-standing elements of the member. The attached flange is not to be included in this calculation. The weighted average method or the curves of buckling coefficients, if applicable, of B4 are to be used for these calculations.

The stress in the attached flange (component parallel to axis of stiffener) is assumed to be equal to the stress (edge) in the plate. This stress is potentially higher than the buckling stress on the flange analyzed as a hinged-free element. The load carrying ability of this element is therefore determined from an effective width of flange acting at the plate edge stress. This effective width can be determined from:

$$d_{a(eff)} = 0.62 t_a \cdot \sqrt{E/F_e} \frac{1}{1 + 3/7(F_e/F_{0.7})^{(n-1)}} \leq d_a \qquad (12)$$

The effective load carrying area of the stiffener, A_s, is therefore equal to:

$$A_s = A_s \text{ (gross)} + (d_{a(eff)} - d_a)\, t_a$$

Example 1

Find the local buckling stress of the stiffener section of the example of B6.11.2. The material is annealed 6 AL-4V titanium alloy sheet. The edge stress, F_e, is 110250 Psi, page B6.11.6-12.

Referring to B4.12-1, with

$t_{we} = .10 \quad h = 2.0$

$t_{fr} = .10 \quad d_{fr} = .72$

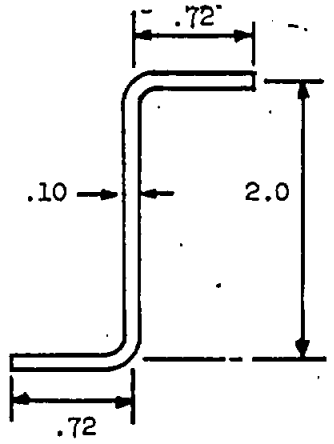

For the weighted average method:

				Hinged		Fixed	
Element	b	t	b/t	K	F_{crel}	K	F_{crel}
2	2.0	0.1	20	3.62	147500	6.31	--
3	0.72	0.1	7.2	0.384	120470	1.154	362000

$$F_{crel} = \frac{147500 \times 2.0 + 120470 \times 0.72}{2.0 + 0.72}$$

$$= 140{,}400 \text{ psi}$$

$F_{0.7}$ = 140700, $F_{crel}/F_{0.7} = 1.00$

$F_{cr}/F_{0.7}$ = 0.91 from B1.50.1-1

Stiffener local Buckling stress $F_b = 0.91 \times 140700$

= 128000 psi > F_e

Determine effective width of flange:

F_e = 110250 psi from B6.11.6

$$d_{a(eff)} = 0.62 \times 0.10 \sqrt{(16.3 \times 10^6/110250)\frac{1}{1 + 3/7\left(\frac{110250}{140700}\right)(31-1)}}$$

$= 0.74 > da = 0.72$

$d_{a(eff)} = d_a = 0.72$

Compute A_s (Stiffener effective area)

$A_s = (2.0 + 2 \times 0.72) \times 0.10 = 0.344$ in.^{2}

Example 2

Increase attached flange dimension to 1.25 in. and repeat determination of stiffener buckling stress and effective properties.

F_b = 128000 psi (same as previous example, since dimensions of free-standing elements were not changed)

Effective width of attached flange of F_e = 110250 psi

$d_{a(eff)}$ = 0.74 in.

$A_s = (2.0 + 0.72 + 0.74) \times 0.1 = 0.346$ in.^{2}

Forced crippling of the stiffener

In the wrinkling mode the buckles run across the stiffeners and distort the attached flanges of the stiffeners. At failure the buckle becomes almost cylindrical and the lateral loads forcing the attached stiffener flange to conform to the buckle shape become sufficiently large to destroy the ability of the stiffener to carry further load. When the sheet is loaded to the stress $F_{w(c)}$, it will impose lateral deflections on the stiffener attached flange.

This deflection will cause transverse bending stress in the flange. Therefore, if the flange is to provide adequate support to the sheet loaded with axial stress, the bending stress cannot exceed the allowable bending stress for the flange. This allowable stress must account for the presence of the axial stress.

The analysis for this failure mode is based on the same criteria that establishes the attachment rivet tensile strength requirements. The net load applied to the stiffener by the sheet is:

$$P_a = 0.022\, \psi_2 t \qquad \text{(ppi)} \qquad (13)$$

where

ψ_2 is from Equation (3)

t = sheet thickness inches

For Z section stiffeners, the critical bending moment is at the rivet attachment line and is equal to:

$$m_a = P_a \frac{c'(1.5c' + h(t_a/t_{we})^3)}{2c' + d_a + h(t_a/t_{we})^3} \qquad (14)$$

The allowable bending moment can be determined from page B6.12.4-6. To use this figure, replace f_{STmax} with F_e.

The allowable bending moment is:

$$M = H.F_{cy}.t_a{}^{2}/4.0 \qquad (15)$$

where

H is from page B6.12.4-6

F_{cy} is the stiffener material compressive yield stress.

t_a is the attached flange thickness,

Equations (13), (14), and (15) can be used to determine a value of F_e for which m_a and M are equal. This value of F_e can then be considered as the allowable stress for the forced crippling failure mode. In this case the critical element is the stiffener attached flange. This mode is identified as F_{fc}. The use of these equations in the forced crippling failure analysis is illustrated in the following example.

The flange bending moment m_a, for other stiffener sections may be derived as shown in GAC Report SAR-71-1.

Example, Part 1

Find the forced-crippling bending moment and allowable bending moment for the example of B6.11.2. Use the limiting edge stress of 110250 psi due to stiffener failure, page B6.11.6-11.

ϕ_2 = 58612 psi t = 0.15 in. F_e = 110250

d_a = 0.72 c' = 0.402 in. F_{cy} = 138000

t_a/t_{we} = 1.0 h = 2.0 in.

From Equation (13)

$$P_a = 0.022 \times 58612 \times 0.15 = 193 \text{ ppi}$$

$$m_a = 193 \times \frac{0.402\ (1.5 \times 0.402 + 2 \times 1.0)}{2 \times 0.402 + 0.72 + 2 \times 1.0}$$

$$= 57 \text{ in.lb/in}$$

For Figure 5, page B6.12.4-6

$$F_e/F_{cy} = 110250/138000 = 0.800$$

$$H = 0.492$$

$$M = 0.492 \times 138000 \times 0.10^2/4 = 170 \text{ in.\#/in.} > m_a$$

Forced crippling is not critical at this axial stress of 110250 psi.

Determine the axial stress, F_{fc}, that will cause a forced crippling failure of this stiffener.

$$M = \frac{H \times F_{cy} \times t_a^2}{4} = \frac{H \times 138000 \times 0.1^2}{4}$$

$$= 345\ H$$

Set the applied moment equal to the allowable moment and solve for H.

$$345\ H = 57$$

$$H = 0.165$$

From Figure B6.12.4-6, the allowable axial stress can be determined.

$$F_e/F_{cy} = 0.96$$

$$F_{fc} = F_e = 0.96 \times 138000$$

$$= 132500 \text{ Psi}$$

Forced crippling is not critical as a stiffener failing stress and therefore not a limiting edge stress.

Flexure/Torsion failure of the stiffener

The coupled flexure/torsion failing stress of the stiffener may be calculated by assuming that the stiffener, with some adjacent sheet, acts as a strut which is restrained against twist by the buckled sheet. The failing stresses of this strut in the pure flexural and pure torsional modes are first calculated, assuming the stiffener cross-section to be unbuckled. The failure stress in the coupled mode can then be derived from the two "pure" failure stresses and a coupling parameter.

It should be noted that the presence of the sheet moves the locations of both the neutral axis in bending and the axis of rotation in torsion away from those for the stiffener alone. The method and graphs given in this section are applicable only to stiffened sheet and must not be used for columns.

a. Pure Flexure

The elastic failure stress in pure flexure is given by the Euler Equation:

$$F_{fe\ell} = \frac{F_f}{\eta} = \frac{\pi^2 E I_{eff}}{\lambda^2 A_{eff}} \qquad (16)$$

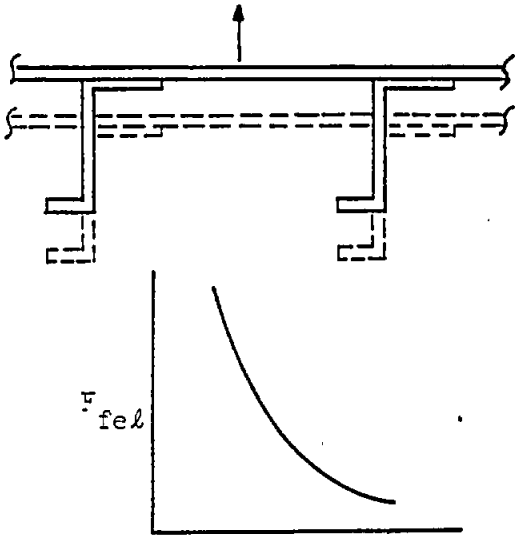

F_f can be obtained from B1.50.4 using the value of η appropriate to a column.

If the skin buckles at a stress F_{cr} before failure, then the moment of inertia I_{eff} and the area A_{eff} are given by

$$\left.\begin{aligned} I_{eff} &= \frac{A_s I_s + A_{pb} I_x}{A_s + A_{pb}} \\ A_{eff} &= A_s + A_{pc} \end{aligned}\right\} \qquad (17)$$

where

I_x = moment of inertia of stiffener about sheet middle plane

I_s = moment of inertia of stiffener about an axis through the stiffener centroid parallel to the sheet middle plane.

A_s = effective stiffener area (see page B6.11.6-1)

A_{pb} = "tangent" area of sheet = $bt(b_{eff}'/b)$

A_{pc} = "secant" area of sheet = $bt(b_{eff}/b)$

b_{eff}/b and b_{eff}'/b are from Figure 5

The moment of inertia I_{eff} is given in Figure 7 for panels with Z-Section stiffeners. (Figure 7 can also be used for hat-section stiffeners as shown).

A requirement of stiffened panel analysis is proof that the stiffeners are adequate to ensure straight node lines at the stiffeners up to the ultimate level of the applied load environment. This requirement is customarily expressed in terms of γ, the ratio of the stiffener EI to the plate stiffness bD. In the case of panels loaded only in compression, it is not necessary to perform this check because satisfaction of the Euler column requirements will provide the stiffener inertia dictated by the γ criteria.

b. Pure Torsion

The elastic failure stress in pure torsion is given by:

$$F_{tel} = \frac{F_t}{\eta} = \frac{GJ + E\Gamma(\pi/\lambda)^2 + k(\lambda/\pi)^2}{I_p} \qquad (18)$$

The plasticity correction factor η for the pure torsion mode shall be obtained from B1.50.4-2.

For closed-section stiffeners the stress given by Equation (18) is usually very high, and its effect on the coupled failing stress can be ignored.

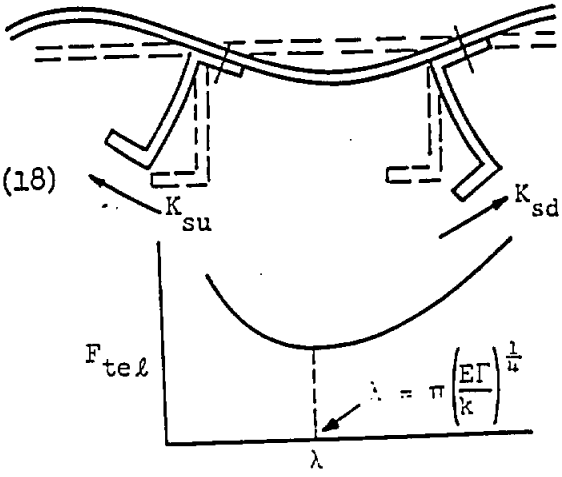

For an open-section stiffener, an approximate value for the St. Venant torsion constant J can be obtained by treating the stiffener section as a number of flat rectangular elements, of width d and thickness t, and calculating the sum $J = \Sigma\, dt^3/3$ or for all the elements.

The presence of the sheet changes the axis of rotation in pure twisting. For stiffener alone the axis passes through the shear centre of the stiffener cross-section; the effect of the skin is to restrain the axis of rotation to lie in the plane of the skin. The torsion-bending constant Γ and the polar moment of inertia I_p about this "restrained" axis can be obtained, for Z-section stiffeners, from Figures 8 and 9 respectively.

The stiffness k represents the restraint against twist afforded to the stiffener, and is given by

$$k = k_s k_p / (k_s + k_p) \qquad (19)$$

where k_s is the stiffness against twist in local deformation of the stiffener and is obtained from the following and is similar to the wrinkling spring of B6.11.2-2.

$$k_{su} = \frac{E}{4(1-\nu^2)} \frac{1}{h/t_{we}^3 + (2c' + d_a)/t_a^3} \qquad (20)$$

$$k_{sd} = \frac{E}{4(1-\nu^2)} \frac{1}{h/t_{we}^3 + (2r + c')/t_a^3} \qquad (21)$$

Enter Figure 3 with the ratio k_{su}/k_{sd} and obtain ψ/ψ_2 to calculate k_s from:

$$k_s = k_{su} \cdot \psi/\psi_2 \qquad (22)$$

and k_p = stiffness against twist of the sheet along the stiffener line

$$= \frac{Et^3}{3b}\,(0.3 + 0.7\,F_e/F_{cr}) \qquad (24)$$

If the bracketed term in Equation (24) exceeds 3, then the value = 3 should be used.

The expressions given in Equations (22) thru (24) are approximations which are valid for long buckle lengths. They are usually sufficiently accurate for practical purposes.

Coupled Flexure/Torsion

The coupling between the flexural and torsional modes is expressed in terms of a "coupling parameter" ξ which may be obtained from Figure 10.

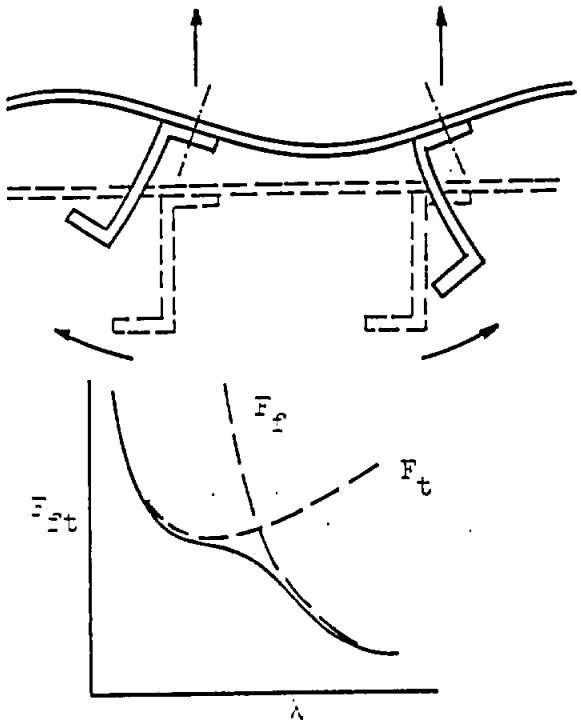

The coupled flexure/torsion failing stress F_{ft} is then given by Figure 11, entering with ξ and F_f/F_t (or F_t/F_f), and obtaining the ratio F_{ft}/F_t (or F_{ft}/F_f).

If the stiffener has an axis of symmetry normal to the sheet plane (such as I, hat, or Y section stiffeners) then the coupling is zero. If one "pure" failure stress is very much higher than the other, than the coupling can be ignored and failure will occur in the mode with the lower failure stress.

When using Figure 11, the 'pure' mode failing stresses, F_{fel} and F_{tel}, must be calculated for the same buckle length λ. In order to determine the critical stiffener stress it is necessary to calculate the coupled failure stress F_{ftel} at the buckle lengths $\lambda = L/j$ where j is all integer values from 1 to $L/\lambda_N + 1$. L is the pin end column length, usually the rib-spacing and λ_N is the natural buckle length for the torsion mode. This buckle length is:

$$\lambda_N = \pi(E\Gamma/k)^{\frac{1}{4}} \qquad (25)$$

Since the stiffness k_p and the effective areas A_{pc} and A_{pb} of the sheet depend upon the peak stress F_e in the sheet, it is necessary to solve the coupled flexure/torsion stress F_{ft} by iteration. Assume a value of F_{ft} to start the iterations. Let F_e equal this value and determine A_{pc}, A_{pb}, and k_p. Compute F_{fel} and F_{tel}. Perform coupling analysis with these elastic stresses and then apply appropriate plasticity correction to obtain F_{ft}. Compare this value with assumed value. If it agrees, this is F_{ft}. If not, repeat cycle with revised assumed value of F_{ft}. Continue this process until agreement is reached.

The plasticity correction factor η for the coupled flexure-torsion mode shall be obtained from B1.50.4-2.

Example:

Find the coupled flexure/torsion failing stress of the stiffener in the example of B6.11.2. The panel length between pin-ends is 20 inch.

$d_{fr} = 0.72$ $t_{fr} = 0.1$

$d_a = 0.72$ $t_a = 0.1$

$h = 2.0$ $t_{we} = 0.1$

$b = 4.0$ $t = 0.15$

$B_a = 0.0$ $B_{fr} = 0.0$

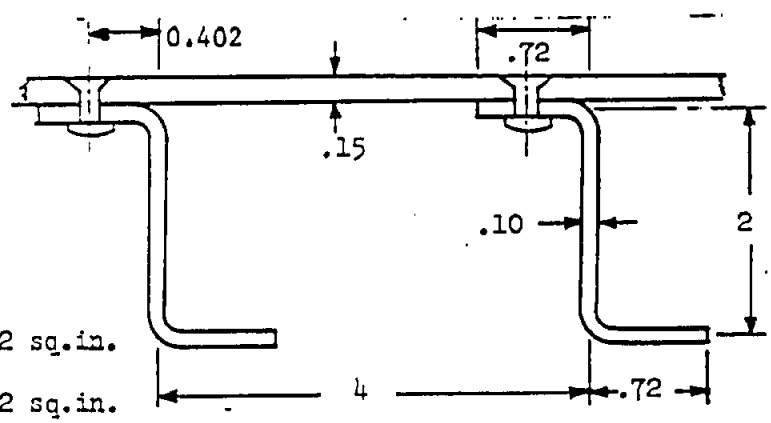

$A_{fr} = 0.72 \times 0.1 + 0.0 = 0.072$ sq.in.

$A_a = 0.72 \times 0.1 + 0.0 = 0.072$ sq.in.

$A_s = 2.0 \times 0.1 + 0.072 + 0.072 = 0.344$ sq.in.

$\Delta = 0.072 - 0.072 = 0.0$

$(d_{fr}t_{fr} + B_{fr}) / ht_{we} = (0.72 \times 0.1 + 0.0)/2.0 \times 0.1 = 0.36$

	2nd Iteration (110,000)
To begin the iteration, assume $F_e = 100{,}000$ psi From B6.11.2, shortwave buckling stress $F_{cr} = 78600$ psi	
$\epsilon_{cr} = 78600/E$	
$E_{S(e)}/E = 1.0/\left(1 + 3/7\left(\frac{100000}{140700}\right)^{(31-1)}\right) = 1.00$	(0.992)
$\therefore \epsilon_{cr}/\epsilon_e = 78600/100{,}000 = 0.786$	(0.720)
From Figure 5, $b_{eff}/b = 0.885$, $b_{eff}'/b = 0.476$	(0.885), (0.470)
$A_{pb} = 0.476 \times 4.0 \times 0.150 = 0.286$	(0.282)
$A_{pc} = 0.885 \times 4.0 \times 0.150 = 0.531$	(0.513)

$$\alpha = \frac{(A_s + \Delta)}{(A_{pb} - \Delta)} = \frac{(0.344 + 0.0)}{(0.286 - 0.0)} = 1.20 \qquad (1.22)$$

from Figure 7,

the effective moment of inertia $I_e = 5.32 \times 2.0^3 \times 0.1/12 = 0.355$ in^4 (.355)

from Figure 8,

the torsion-bending constant $\Gamma = 0.216 \times .72^2 \times 2.0^3 \times .1/3 = 0.0299$ in^6 (.355)

from Figure 9,

the polar moment of inertia $I_p = 2.22 \times 2.0^3 \times 0.1/3 = 0.593$ in^4 (.593)

the St. Venant torsion constant $J = (2.0 + 0.72 + 0.72) \times 0.1^3/3 = 0.00115$ in^4

from B6.11.2,

the short wave buckling stress $F_{cr} = 78600$ psi

from Equations 20 and 21, the stiffness against twist in local deformation of the stiffener

$$k_{su} = \frac{16.3 \times 10^6}{4(1 - 0.32^2)} \quad \frac{0.1^3}{(2.0 + 2.0 \times 0.402 + 0.72)} = 1290 \text{ lb in/in}$$

$$k_{sd} = \frac{16.3 \times 10^6}{4(1-0.32^2)} \quad \frac{0.1^3}{(2.0 + 3.0 \times 0.402 - 2.0 \times 0.25} = 1677 \text{ lb in/in}$$

For a buckle length λ = panel length L = 20.0"

from Equation 16, $F_{fel} = \frac{\pi^2 \times 16.3 \times 10^6 \times 0.355}{20.0^2 \times (0.344 + 0.531)} = 163200$ (166600)

from B1.20.2 Reference stress $F_{0.7} = 140700$ psi

Stress-strain parameter n = 31

$$\frac{\text{Elastic buckling stress}}{\text{Reference stress}} = \frac{F_{fel}}{F_{0.7}} = \frac{163200}{140700} = 1.16 \qquad (1.18)$$

from B1.50.4 $\frac{\text{Buckling stress}}{\text{Reference stress}} = \frac{F_f}{F_{0.7}} = 0.882$ (.89)

∴ Failing stress in pure flexure $F_f = 0.882 \times 140700 = 124100$ psi (125200)

from Equation 24, the stiffness against twist of the sheet along the rivet line $k_p = \frac{16.3 \times 10^6 \times .15^3}{3 \times 4.0} \left(0.3 + 0.7 \times \frac{100{,}000}{78{,}600}\right) = 5460$ lb in/in (5870)

$k_{su}/k_{sd} = 1290/1677 = 0.77$

$\psi/\psi_2 = 1.14$ From Figure 3.

$k_s = k_{su}\, \psi/\psi_2 = 1290 \times 1.14 = 1471$

From Equation 19, $k = (1471 \times 5460)/(1471 + 5460) = 1160$ lb in/in (1174)

Determine natural wave length

$$\lambda_N = \Pi \left(\frac{EI}{k}\right)^{\frac{1}{4}} = \Pi \left(\frac{16.3 \times 10^6 \times 0.0299}{1160}\right)^{\frac{1}{4}}$$

$$= 14.22 \qquad (14.18)$$

$L/\lambda_N = 20.0/14.22 = 1.406$, $j = 1, 2$

$\therefore$ Check F_{tel} for $\lambda = L$ and $L/2$

from Equation 18 ; with $G = E/2(1 + \nu) = 6.18 \times 10^6$ psi and

for $\lambda = L = 20.0$

$$F_{tel} = \frac{6.18 \times 10^6 \times 0.00115 + 16.3 \times 10^6 \times 0.0299\ (\Pi/20)^2 + 1160(20/\Pi)^2}{0.593}$$

$$= 12000 + 20300 + 79300 = 111600 \text{ psi} \quad (112500)$$

Determine F_{tel} for $\lambda = L/2 = 10.0$

$$F_{tel} = \frac{6.18 \times 10^6 \times 0.00115 \quad 16.3 \times 10^6 \times 0.0299(\Pi/(10.0)^2 + 1160(10.0/\Pi)^2}{0.593}$$

$$= 12000 + 81200 + 19800 = 113000 \text{ psi} \quad (113200)$$

$\therefore$ Do coupling at $\lambda = 20.0$

From Figure 10, the coupling parameter = 0.115

$$\xi = 0.115 \left(\frac{0.344 + 0.286}{0.344 + 0.531}\right)^{\frac{1}{2}} = 0.098 \qquad (0.098)$$

$$F_{tel}/F_{fel} = 111600/163200 = 0.683 \qquad (0.675)$$

From Figure 11:

Coupled Flexure/Torsion Elastic Stress $F_{ftel} = 0.98 \times 111600$

$= 109400$ psi (110250)

$$F_{ftel}/F_{0.7} = 109400/140700 = 0.777 \qquad (0.783)$$

$$F_{ft}/F_{0.7} = .777 \text{ (From B1.50.4-2)} \qquad (0.783)$$

$$F_{ft} = 0.777 \times 140700 = 109400 \text{ psi} \qquad (110250)$$

Summary of Failure Mode Stresses for Example of B6.11.2

F_{ir} (Inter-rivet buckling)	>> $F_{0.7}$		B6.11.3-1
F_w (Wrinkling failure stress)	= 123500		B6.11.5-5
F_b (Stiffener local buckling)	= 128000		B6.11.6-2
F_{fc} (Stiffener attached flange forced crippling)	= 132500		B6.11.6-4
F_{ft} (Coupled flexure-torsion)	= 110250		B6.11.6-10

From this summary it can be determined that the limiting value of edge stress is

F_e = 110250 psi

Determine the compression loading and average panel stress at failure.

$$F_p = \frac{110250 \quad (0.344 + 0.855 \times 4. \times 0.15)}{4 \times .15 + .344} = 100100 \text{ psi}$$

The compressive loading in the panel at failure is:

$= F_p \quad (A_s/b + t)$

$= 100100 \times (0.344/4 + 0.15)$

$= 23620$

Figure 7 Moment of Inertia I_e of Stiffened Panel

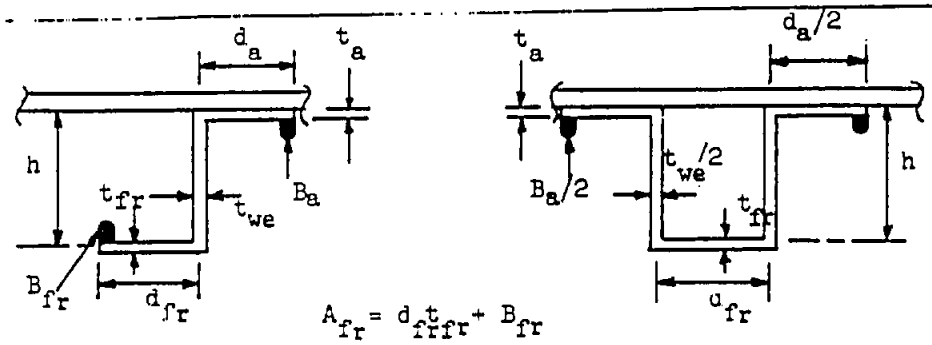

$$A_{fr} = d_{fr}t_{fr} + B_{fr}$$

$$A_a = d_a t_a + B_a$$

$$A_s = ht_w + A_a + A_{fr}$$

$$\Delta = A_{fr} - A_a$$

$$\alpha = \left(\frac{A_s + \Delta}{A_{pb} - \Delta}\right)$$

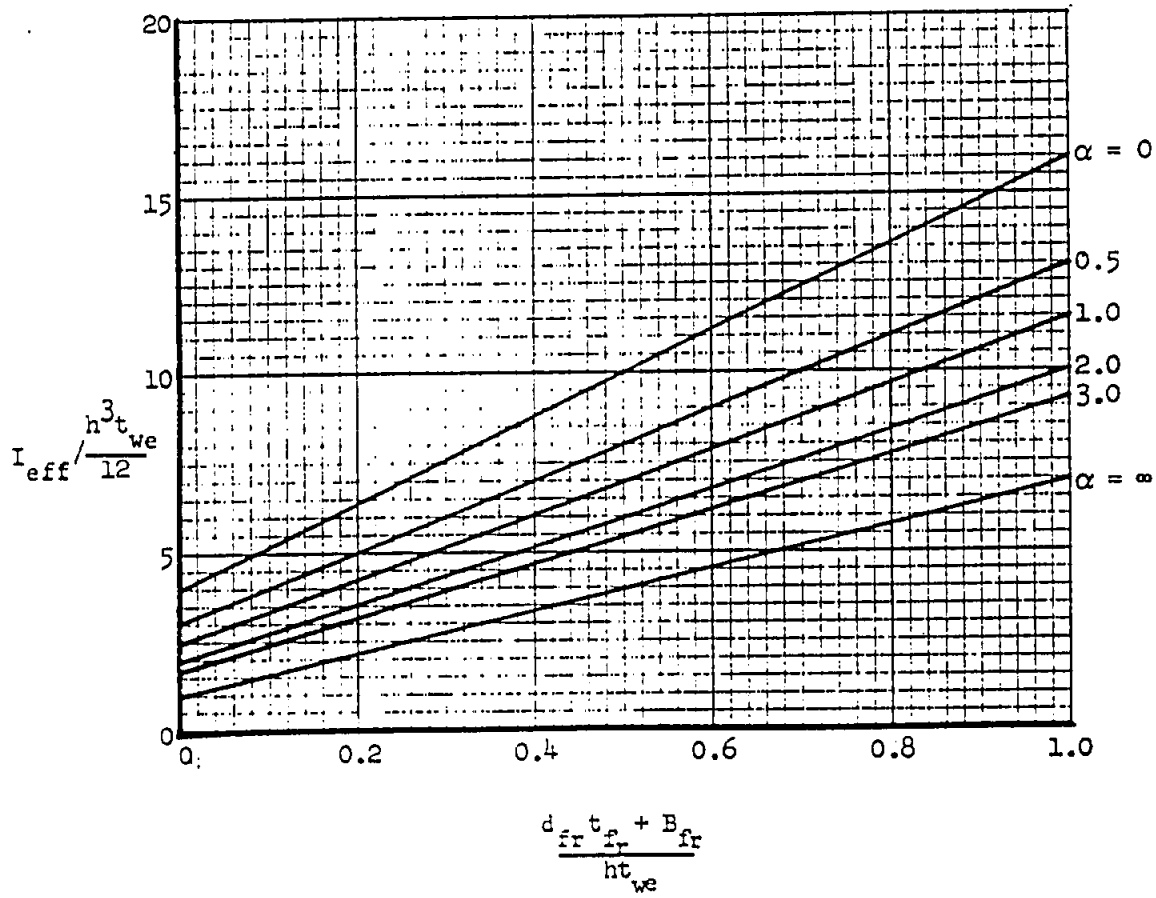

Ref: J.H. Argyris "Flexure Torsion Failure of Panels"
Aircraft Engineering, June - July 1954

Figure 8 Torsion Bending Constant Γ for Z-Section

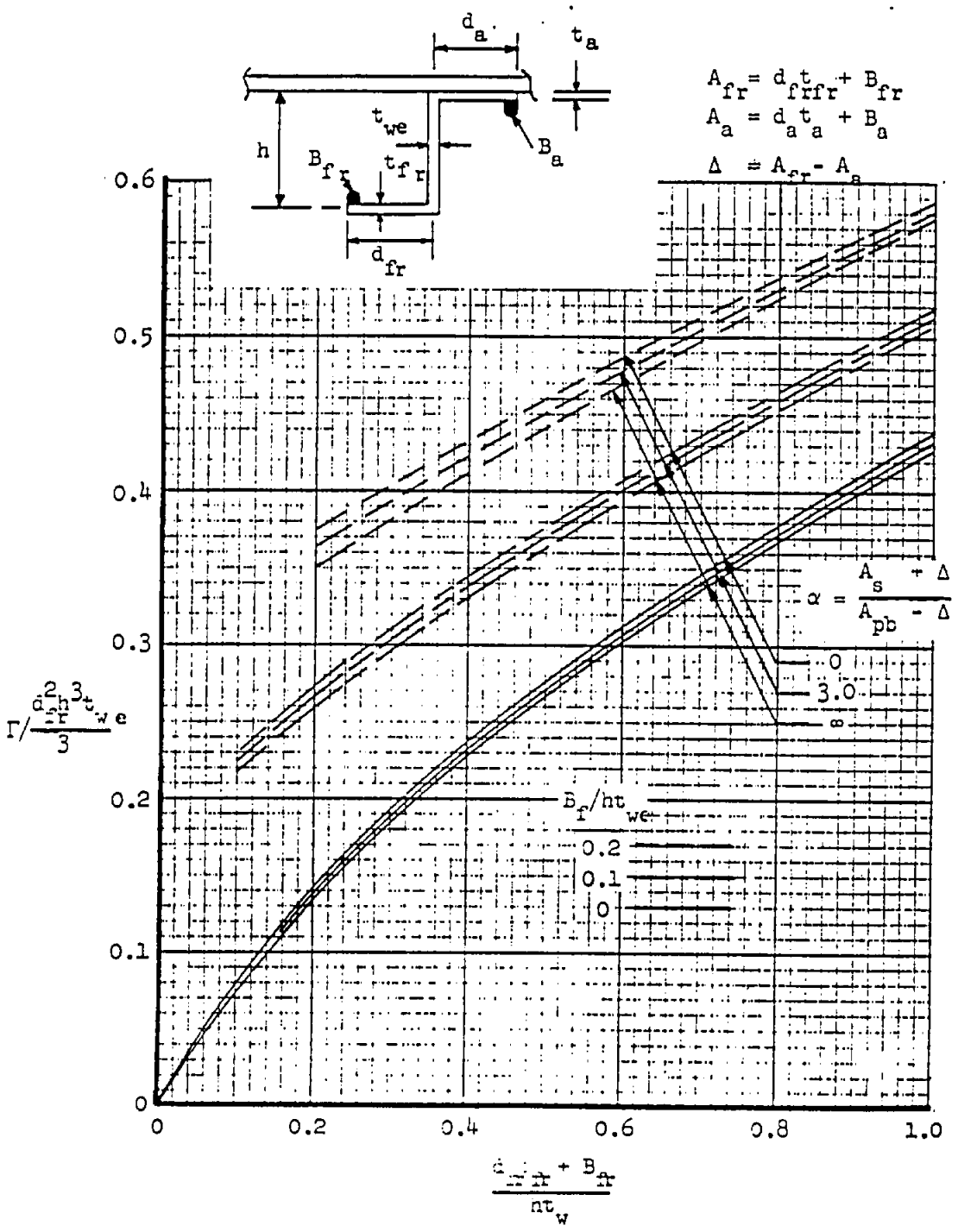

Ref: J.H. Argyris "Flexure Torsion Failure of Panels"
Aircraft Engineering, June - July 1954

Figure 9 Polar Moment of Inertia I_p of Z-Section Stiffener with Equal Flanges

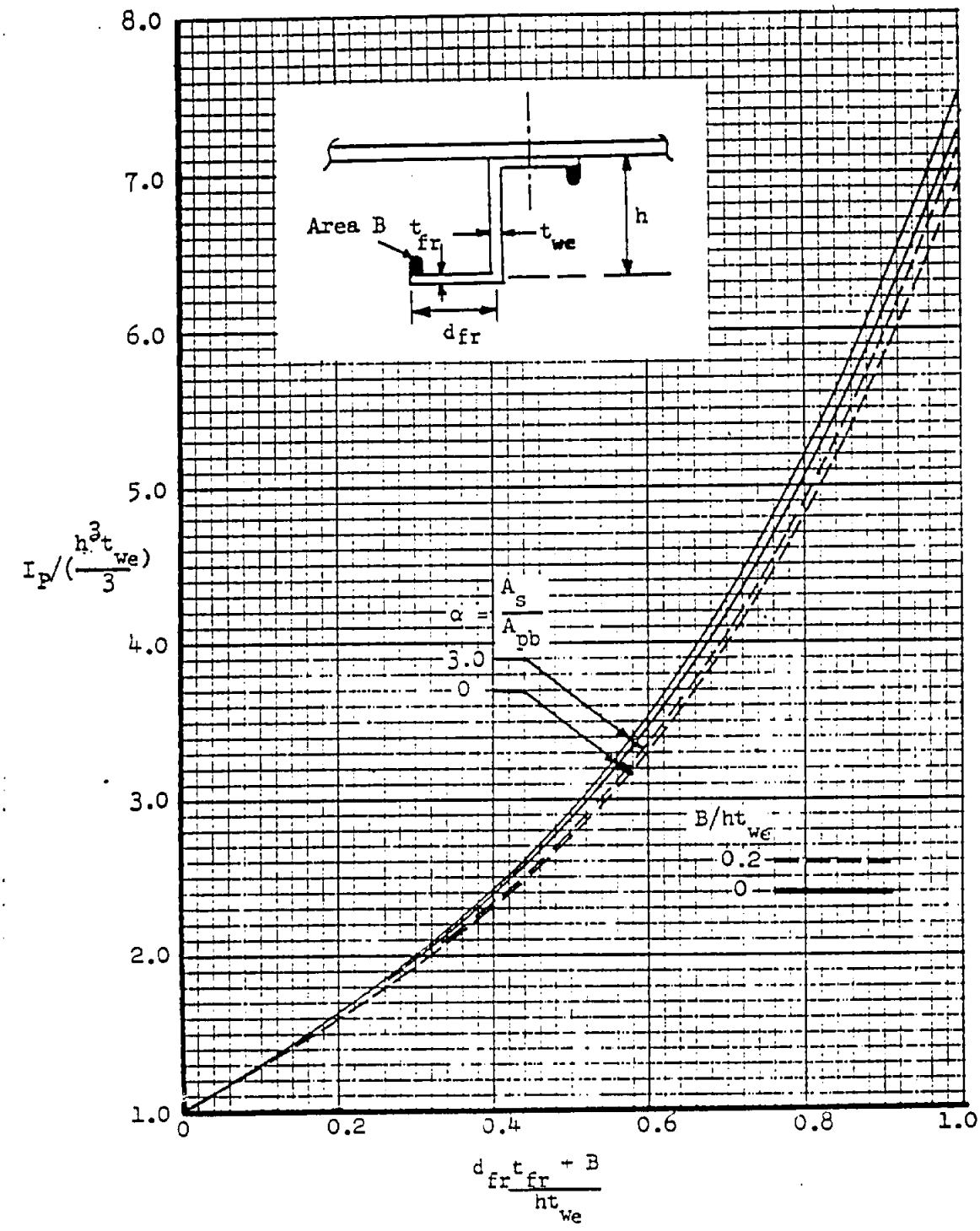

Ref: J.H. Argyris "Flexure Torsion Failure of Panela"
Aircraft Engineering, June - July 1954

Figure 10

Coupling Parameter ξ for Z-Section Stiffeners with Equal Flanges

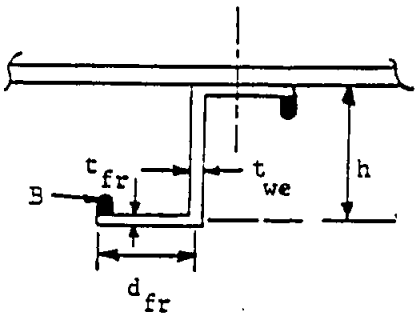

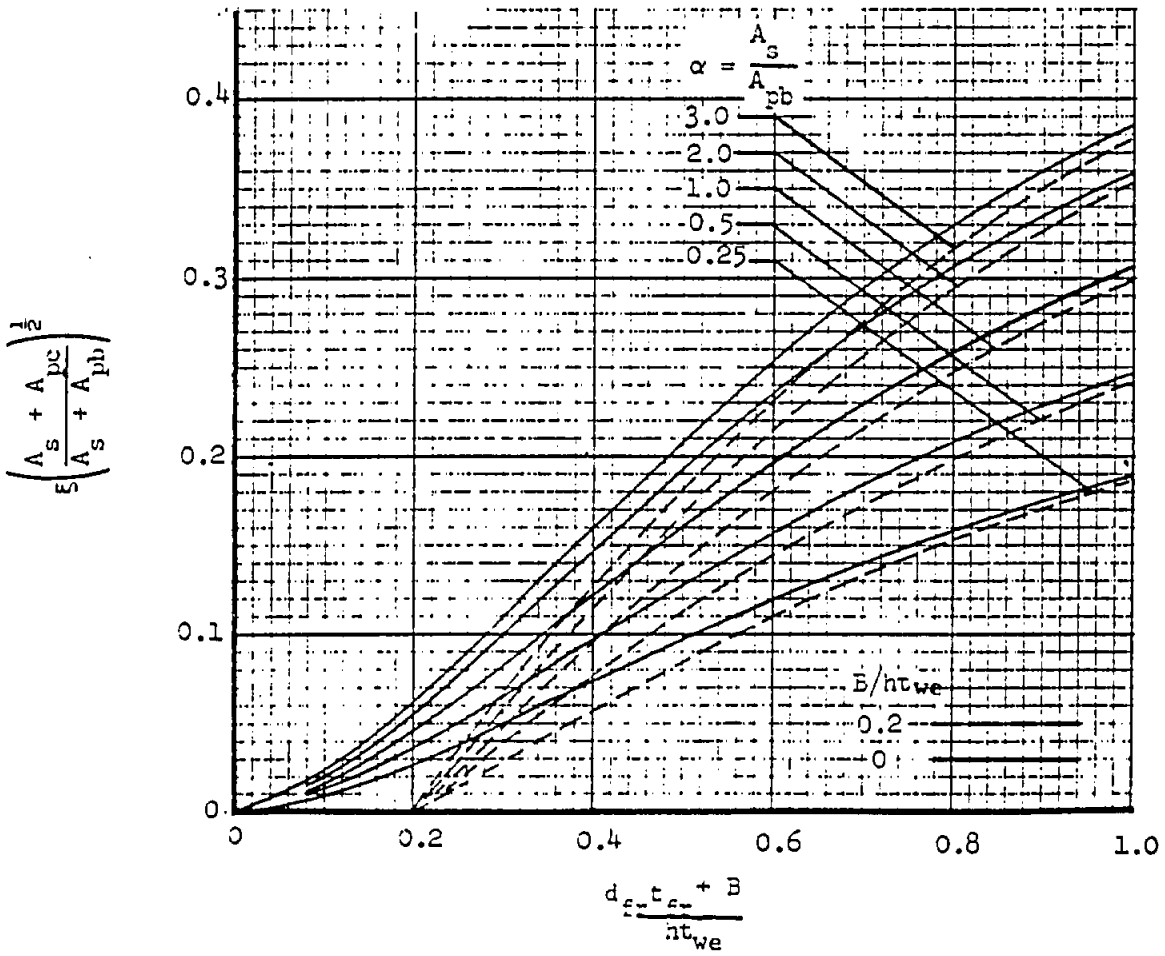

Ref: J.H.Argyris "Flexure Torsion Failure of Panels"
Aircraft Engineering, June - July 1954

Figure 11

Reduction of Failing Stress Due to Coupling of Flexure and Torsion

F_{ft} = failing stress in combined mode
F_f = failing stress in pure flexure
F_t = failing stress in pure torsion
} at wavelength λ

ξ = coupling parameter (from Figure 11)

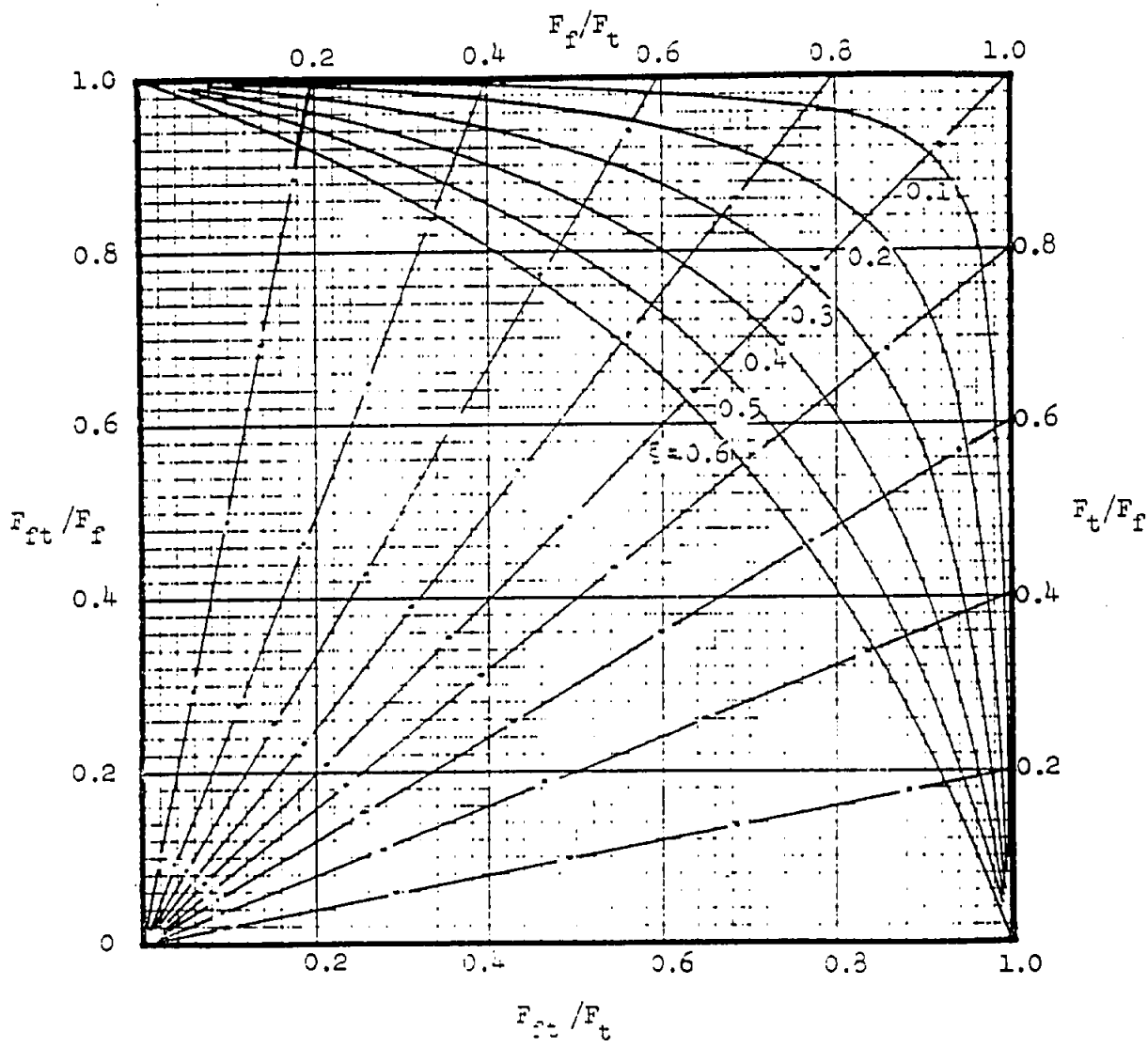

Ref: J.H. Argyris "Flexure Torsion Failure of Panels" Aircraft Engineering, June - July 1954

B6.11.7 Computational Procedure

The following sequence for the complete strength analysis for a stiffened flat panel in compression is suggested:

1. Determine the Local Buckling Stress Coefficient K from Figures (1) or (2) of B6.11.2 or applying the method of B4.12.

2. Calculate the effective stiffness ψ from Equations (2) and (3) and Figure (3).

3. Calculate the effective stiffness parameter $\psi b^3/\Pi^4 D$ from Equation (4)

4. Determine the Minimum Short-Wave Buckling Stress Coefficient K_{cr} from Figure (4) using the values of K from step 1 and $\psi b^3/\Pi^4 D$ from step 3.

5. Calculate the Elastic Short-Wave Buckling Stress F_{crel} from Equation (1)

6. Determine the Plastic Short-Wave Buckling Stress F_{cr} from B1.50.1-1

7. Calculate the Elastic Inter-Rivet Buckling Stress F_{irel} from Equation (5)

8. Determine the Plastic Inter-Rivet Buckling Stress F_{ir} from B1.50.2-1

9. Calculate the Elastic Wrinkling Failure Stress F_{wel} from Equation (9) or (10).

10. Determine the Plastic Wrinkling Failure Stress $F_{w(c)}$ from Figure B1.50.4-2 and F_w from $F_{w(c)}$ and R. Check sheet per B6.11.5-7.

11. Calculate the Elastic Local Buckling Stress of Stiffener F_{bel} from B6.11.6.

12. Determine the Plastic Local Buckling Stress of Stiffener F_b from B1.50.1-1.

13. Calculate the Forced Crippling Strength of Stiffener F_{fc} from Equations (13), (14) and (15).

14. Calculate Geometric Properties of Stiffener/Buckled Sheet Combination. Effective width of sheet b_{eff}/b and b_{eff}'/b from Figure 5
    (a) 'Tangent" area of Sheet $A_{pb} = (b_{eff}'/b) \cdot bt$
    (b) 'Secant' area of sheet $A_{bc} = (b_{eff}/b) \cdot bt$
    (c) Effective moment of inertia I_{eff} from Equation 17 or Figure 7
    (d) St.Venant torsion constant $J (= \Sigma dt^3/3)$
    (e) Torsion bending constant Γ from Figure 8.
    (f) Polar moment of inertia I_p from Figure 9.

15. Calculate the Local Torsional Stiffness of Stiffener k_{su} and k_{sd} from Equations (22) and (23).

B6.11.7 Computational Procedure (continued)

16. Assume a Peak Stress in the Sheet F_e, which must be less than the inter-rivet buckling stress F_{ir} from step 8 and less than the compressive yield stress of the sheet material F_{cy}.

17. Calculate the Twisting Stiffness of the Sheet k_p from Equation (24).

18. Calculate the Effective Twisting Stiffness k from Equation (19).

19. Calculate the Natural Wave Length λ_N from Equation (25).

20. Calculate the Length Ratio j from j = 1 to $L/\lambda_N + 1$ (j is an integer)

21. Calculate the Elastic Pure Flexure Stress F_{fel} from Equation (16) for all values of j.

22. Calculate the Elastic Pure Torsion Stress F_{tel} from Equation (18) for all values of j.

23. Determine the Coupling Parameter ξ from Figure 10.

24. Determine the Coupled Flexure/Torsion Stress F_{ftel} from Figure 11 (Elastic) for all values of j or for the obvious critical value.

25. Calculate the Plastic Coupled Flexure/Torsion Stress F_{ft} from B1.50.1-2 or B1.50-4.

26. Repeat steps 16 through 25 until the assumed $F_e = F_{ft}$

27. The Failing Stress of the Panel F_a is:
The average stress from Equation (7) with F_e equal the minimum of F_{ir} (Step 8), F_w (Step 10), F_b (Step 12), F_{fc} (Step 13) or F_{ft} (Step 26).

28. Calculate the Required Rivet Tensile Strength from B6.11. If this criterion is not met, the panel will fail shortly after exceeding F_{cr} from Step 6 and not achieve the strength indicated in Step 27.

29. Calculate the Average Stress at Failure F_p from Equation (6).

30. Calculate the Failure Loading $P = \dfrac{(F_{sb}A_s + F_{ab}t)}{b}$

B6.12 FLAT STIFFENED SHEET IN SHEAR

INTRODUCTION

A diagonal-tension beam, or flat stiffened shear web, consists of a relatively thin plate with stiffening members designed to carry shear loads applied in the plane of the web sheet. Although the physical behavior of such a structure is well understood, neither the complex state of stresses after initial buckling nor the ultimate strength can be predicted by exact theory. The generally accepted method of analysis and design has been the one presented by the NACA in 1952 [P. Kuhn, J. P. Peterson, L. R. Levin, "A Summary of Diagonal Tension," NACA TN 2661 and 2662, May, 1952]. It is a semi-empirical method based on tests on the types of diagonal tension beams used in aircraft at that time.

The method of analysis given on the following pages is basically the NACA method, but with modifications which make it more up-to-date, more expedient and applicable to various materials and types of construction. (The development of these modifications are discussed in "Instability and Failure Analysis of Flat Stiffened Plates Under Shear," R. T. Ratay, GAEC Structural Mechanics Note No. 14, November, 1968, and in Grumman Aerospace Report SAR-77-2, "The Analyses of Shear Panel Stiffeners with Emphasis on Forced Crippling," E. R. Ranalli and F. E. Bunce, December. 1977.) For users accustomed to the previous issue of this section of the manual the most significant changes are:

- Calculation of Actual Stiffener Stresses using full rather than effective stiffener area
- Prediction of Forced Crippling Allowables of stiffener attached leg (valid for either buckled or unbuckled webs)
- Required Rivet tensile strength consistent with above forced crippling Analysis and fastener tensile strength data for prediction purposes.

Experimental verification of the method consists mainly of the NACA tests [NACA TN 2662] which involved parallel flanges, open-section, uniformly spaced vertical stiffeners, flat web sheets, all of 7075-T6 and 2024-T3 aluminum alloys, and the following dimensional limitations: $115 < h_e/t < 1500$, $0.2 < d/h_e < 1.0$, $t_{ST}/t > 0.6$.

It should be considered a mandatory design practice not to violate the t_a/t ratio, that is, the stiffener attached flange thickness should not be less than 0.6 of the basic web thickness.

Recommendations for the application of this method to chem-milled sheets with lands and to integral construction are given under the Special Conditions.

A computer program, named DITEN3, will be available to perform the complete analysis. The program and user's information will be on file in the

Structures Section ["A Program for Post-Buckling Analysis of Stiffened Flat Plates Under Applied Shear." Grumman Aerospace Report SAR-78-2, F. E. Bunce, A. J. Davidson, December 1978] This program is currently on the Structures Section B-disk, complete with control EXEC DITEN3.

Attention is directed to selection of an apparently unconservative value of ta or F_{sfc} in the forced crippling analysis. The reason why the lower value of t_a or correspondingly the higher value of F_{sfc} is selected is that empirical data correlation gives two distinct solution regions. It can be shown that the above choices give the correct solution values.

SYMBOLS

A	Cross sectional area, sq. inches
A_{ST_t}	Stiffener area including effective width of web, sq. inches
d	Stiffener spacing, inches
d_ℓ	Land width at stiffener, inches
D	Plate bending stiffness, $Et^3/12\ (1-\upsilon^2)$, also Fastener diameter, inches
E	Young's modulus, psi
$\overline{ED}$	Stiffener attach rivet edge distance, inches
f	Applied stress, psi
F	Allowable stress, psi
G	Shear modulus, psi
H	Bending modulus reduction factor due to presence of orthogonal compressive stress
h_e	Effective stiffener height, measured between capstrip centroids, inches
h_ℓ	Width of land, at beam flange, inches
I	Moment of inertia, inches^4
I_{ST_t}	Stiffener moment of inertia including effective width of web, inches^4
K	Buckling coefficient
k	Diagonal tension factor
ℓ'	Effective pin-ended column length, inches
$\overline{OD}$	Rivet offset dimension, inches
P	Applied load, pounds
p	Net load applied by web to stiffener, ppi
q	Running shear load, ppi
R	Stress ratio, applied stress/critical buckling stress

t	Thickness, inches
U	Buckling ratio, Strength Ratio
$\bar{y}$	Stiffener centroid location from web interface, inches
α	Angle between neutral axis of beams and direction of diagonal tension, degrees
γ	Ratio of stiffener bending stiffness to plate bending stiffness, or angle of shear deflection, explanation in text
η	Plasticity correction factor
ν	Poisson's ratio

Subscripts:

a	Stiffener attached flange
all	Allowable
axial	Inplane axial stress
b	Bending
c	Compression
cr	Critical (buckling)
cy	Compression yield
DT	Diagonal tension
IDT	Incomplete diagonal tension
PDT	Pure diagonal tension
t	Total, when used with stiffener, indicates property includes effective width of sheet
el	Elastic
fc	Forced crippling
fℓ	Flange
ℓ	Land
max	Maximum
min	Minimum
o	Buckling stress or stress ratio in uniaxial stress field

req	Required
riv	Rivet
s	Shear
ST	Stiffener
ss	Simple support
tu	Tensile ultimate
ty	Tensile yield
su	Shear ultimate

SPECIAL CONDITIONS

Lands on chem-milled web sheets (Figure 1.c) improve the strength of the panel. For the steps of the analysis procedure, explicitly involving the land, the following recommendations are made. Include effects of the land in the following steps of the procedure:

Step 1.) for calculating the active cross-sectional area of stiffeners (and flanges) plus effective width of sheet, i.e., use $A_{ST} + (t_\ell - t)d_\ell$ + effective width of sheet.

Step 9.) for prediction of allowable web stresses, increase the values given by Figure 10 by 10% provided the thickness of the land, t_ℓ, is greater than the basic web thickness, t, increased by the factor 1/[1 - rivet diameter/rivet pitch].

Step 10.b) for column failure of the stiffener, i.e., do include the land in A_{ST_t}, I_{ST_t} and ρ_{ST}.

Step 13.) for computing load on rivets, i.e., do not include the land area in A_{ST}.

When dealing with integrally stiffened web sheets (such as on Figure 1.b) the following modifications in the analysis procedure are recommended:

Step 9.) for prediction of allowable web stresses, the values given by Figure 10 are conservative because of the absence of rivet or bolt holes, therefore increase the allowables of this figure by 10%.

Step 10.) forced crippling failure is not considered a possibility in integral construction. The limit of the stiffener's capacity is its column strength (in interaction with local buckling), as determined in Section B4.40-5.

Steps 12 to 14.) applying to riveted connections are not applicable here.

COMPUTATIONAL STEPS IN ANALYSIS

1. Basic dimensions and geometric properties

INITIAL BUCKLING STRESSES:

2. Initial web shear buckling stress F_{scr}, initial web axial buckling stress (if combined load problem).

INTERNAL STRESSES:

3. Diagonal-tension factor k
4. Angle of diagonal-tension α_{DT}
5. Maximum web stresses; shear $f_{s\ max}$
6. Stiffener stresses f_{ST} and $f_{ST\ max}$
7. Flange stresses $f_{f\ell}$
8. Equivalent web shear modulus G_{IDT} (if needed)

ALLOWABLE STRESSES:

9. Web $F_{s\ all}$
10. Stiffeners $F_{s\ fc}$, $F_{c\ all}$
11. Flanges $F_{f\ell\ all}$

ATTACHMENT ANALYSIS (Rivets)

12. Shear load, web to flange rivets, $q_{f\ell}$
13. Shear load, stiffenr to flange, . P_{ST}
14. Tension load, stiffener to web, p

PROCEDURE OF INSTABILITY & POST-BUCKLING ANALYSIS

1) Establish basic dimensions and geometric properties:

$$A_{f\ell}, A_{ST}, A_{ST_t}, I_{ST}, \rho_{ST}, EI_{ST_t}/d\ D$$

Determine the required EI_{ST_t}/dD from:

$$\gamma_s = (EI\quad /dD)req = 30\ (h_e/d)^2 - 10\ (1 + h_e/d) \qquad (1)$$

This value will ensure node lines at the stiffener at plate buckling. This requirement is considered essential where significant compressive stresses in the stiffeners are due to externally applied loads, or if it is necessary to achieve the full value of plate buckling (straight node lines). Test data of NACA TN 2662 indicates this value of γ_s is conservative for post buckling strength analysis of beams where the only significant stresses were shear induced. These tests indicate that for a structure loaded in shear only, the following limiting value of EI_{ST_t}/dD from B6.12.4-4 for clamped ends is considered adequate. This value of EI_{ST_t}/dD will not give simply supported buckling, the coefficient for this case must be obtained from Figure 2. When calculating I_{ST_t} for this check, use effective width of sheet = $\frac{1}{2}d$.

Note: on actual aircraft, combinations of bending-stiff and bending-flexible stiffeners are sometimes used. This case, however, requires that additional consideration be given to the bending moment in the beam flange of such designs.

Should the problem of combined shear and in plane axial stress exist, the minimum value of $\frac{EI_{ST_t}}{dD}$ must be increased to account for the presence of these additional stresses. In the case where the inplane stresses do not add axial load to the stiffeners:

$\gamma_s = \frac{EI_{ST_t}}{dD}$ for shear from Equation (1) and $\gamma_{axial} = \frac{EI_{ST_t}}{dD}$ for the axial stress in the web and is equal to:

$$\gamma_{axial} = 39\ (h_e/d\pi)^4 \qquad (2)$$

The value of the required γ under combined load is then

$$\gamma_{req.} = [\ \gamma_s\ (R_s/U) + \gamma_{axial}\ (R_{axial}/U)\ ] \qquad (3)$$

R_s, R_{axial} and U are discussed in the next section.

INITIAL BUCKLING STRESSES

2) Determine <u>initial shear buckling</u> coefficient $K_{scr_{ss}}$ from Figure 2.

The elastic shear buckling stress is:

$$F_{scr\ el} = K_{scr_{ss}}\ E\ (t/d)^2 \qquad (4)$$

Determine the inelastic shear buckling stress F_{scr_o} from page <u>B1.50.3-1.</u>

Note that the value of $K_{scr_{ss}}$ at $EI/dD = \infty$ can be approximated by the following parabola:

$$K_{scr_{ss}} = 0.904\ (4(d/h_e)^2 + 5.34) \qquad (5)$$

If the structure to be analyzed is subject to combined load as indicated in the following sketches, further steps are necessary to determine the initial buckling stress, otherwise proceed to page B.6.12.1-11.

<u>Combined Loadings</u>

The occurrence of other inplane loading conditions, axial stress and bending stress are common occurrences in aerospace shear structures. These typically would appear in free body diagrams as:

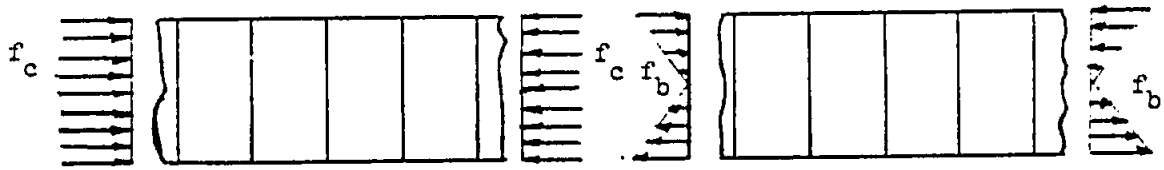

The influence of these stresses on the initial buckling stress can be accounted for by determination of the buckling stress for the case of combined bending and direct stress from Page B5.11.13.2, and then interacting this stress with

the shear stress by the following suggested interaction equation. The value of f_c is the maximum compressive fiber stress.

$$\left[\frac{R_{axial}}{U}\right]+\left[\frac{R_s}{U}\right]^2 = 1.0 \qquad (6)$$

$$R_{axial} = f_c/F_{axial_o} \text{ and}$$

$$R_s = f_s/F_{scr_o}$$

$$F_{axial_o} = K_{axial}\, E\, (t/h_e)^2 \eta \qquad (7)$$

where K_{axial} = K from page B5.11.13-2,3 and η is the plasticity correction factor from page B1.50.1-1.

It is now necessary to calculate the buckling ratio U under combined loads. U may be determined by substitution in the interaction equation above. The following equation results:

$$U = R_{axial/2} + \sqrt{(R_{axial/2})^2 + R_s^2} \qquad (8)$$

When the axial stresses are primarily tension (i.e., $\alpha > 2$ see page B5.11.13-3) the reduction in the shear buckling due to axial stress is reduced. For α greater than 3 this reduction in the shear buckling stress can be ignored but must be included in web combined strength analysis (see equation A-0 page B6.12.1-13). If the web is completely in nonuniform tension the shear buckling stress will be increased. This effect, while not strong, can be accounted for by using appropriate interaction equations from section B8, Grumman Structures Manual and page B5.11.13-2,-3 with sign of R_{axial} negative (indicating tension).

It is now possible to determine the initial shear buckling stress under combined loads by the following:

$$F_{scr} = F_{scr_o} \times (R_s/U) \qquad (9)$$

It is realized that other factors can effect the determination of the

PROCEDURE OF INSTABILITY & POST-BUCKLING ANALYSIS (CONT)

critical buckling stress. The primary effect being that of edge restraint. This effect has not been included because it is believed that it is significantly complex to a point that benefits of edge restraint will be outweighed by the difficulties in their accurate determination. However, if this situation demands investigation of this effect, the user is directed to Structural Analysis Report SAR-77-2, Appendix B.

3) Determine f_s/F_{scr} and then diagonal-tension factor k from Figure 4, or:

$$k = \text{Tanh}\ (0.5 \log\ (f_s/F_{scr})\ ) \tag{10}$$

4) Calculate angle of diagonal-tension α_{DT}

Calculate the angle of pure diagonal tension, α_{PDT}, from:

$$\text{Tan}^4\ \alpha_{PDT} = (1 + h_e t/2A_{f\ell})/(1 + dt/A_{ST}) \tag{11}$$

(or use Figure 6)

Determine α_{DT} from the following interpolation:

$$\alpha_{DT} = 45^\circ - k(45^\circ - \alpha_{PDT}) \tag{12}$$

(The straight line approximation gives slightly low values but less than 5% in error for $A_{ST}/d\ t \geq 0.1$. The lowest possible values of α_{DT} occur at $A_{ST}/d\ t = 0$ and $A_{f\ell}/ht = \infty$)

5) Compute stresses in web:

Maximum shear stress in web.

$$f_{s\ max} = f_s\ (1 + k^2 C_1)\ (1 + kC_2) \tag{13}$$

where

$$C_1 = [1/\text{Sin}2\alpha_{DT} - 1] \tag{14}$$

C_2 is from Figure 7. (web stress magnification due to bending of flanges)

6) Compute compression stress in stiffeners due to diagonal-tension:

$$f_{ST} = \frac{k\ f_s\ \tan\ \alpha_{DT}}{\frac{A_{ST}}{dt} + 0.5\ (1 - k)} \quad \text{(average along stiffener)} \tag{15}$$

PROCEDURE OF INSTABILITY & POST-BUCKLING ANALYSIS (CONT)

Maximum stress at mid-height:

$$f_{ST\,max} = (f_{ST\,max}/f_{ST})\, f_{ST} \qquad (16)$$

where

$f_{ST\,max}/f_{ST}$ is from Figure 8.

7) Compute stresses in flanges due to diagonal tension:

Compression

$$f_{f\ell} = (k\, f_s \cot \alpha_{DT})/(2A_{f\ell}/h_e t + 0.5(1 - k)) \qquad (17)$$

Bending moment near stiffeners

$$M_{f\ell} = C_3\, k\, f_s\, t\, d^2 \tan \alpha_{DT}/12 \qquad (18)$$

where

C_3 is uniform-load reduction due to bending of flanges (Figure 7.)

8) If required the equivalent shear modulus is determined from

$$\frac{G}{G_{IDT}} = (1-k) + \frac{k}{2(1+\nu)} \left[\frac{4}{\sin^2 2\alpha_{DT}} + \frac{\tan^2 \alpha_{DT}}{\frac{A_{ST}}{d\,t} + 0.5(1-k)} + \frac{\cot^2 \alpha_{DT}}{\frac{A_{f\ell}}{2ht} + 0.5(1-k)} \right] \qquad (19)$$

A reasonably accurate value of G/G_{IDT} can be obtained from Figure 9.

Overall shear deformation of buckled web is estimated as:

$$\gamma_{IDT} = f_s/G_{IDT}$$

ALLOWABLE STRESSES AND MARGINS OF SAFETY

Determine Allowable Stresses and Margins of Safety.

Because of the non-linearity of the structural behavior subjected to this type loading condition, the true margin of safety can only be obtained by an iterative calculation that will arbitrarily increase the applied load to such a level that the allowable stress at that level and the internal member stress are equal. The true margin of safety is then the ratio of

the increased applied load to the condition applied load less 1. This of course is a time consuming process unless a suitable computer program is available, and is not recommended for hand calculations unless circumstances demand it. Rather, it is considered acceptable to use the allowable stresses and applied stresses at the condition level as the indication that the part in question has adequate strength for its design condition. This margin should not be used as an accurate predictor of the total strength of the structure. However, margins of safety indicated in this section of the manual will be of this type.

9) Web

Allowable maximum web shear stress $F_{s\ all}$ from Figure 10.

M. S. on web failure $= \dfrac{F_{s\ all}}{f_{s\ max}} - 1.0$ for the shear only case. If there are inplane axial plus shear stresses the web strength can be determined from the following criteria:

$$\text{M.S. on web failure} = 1.0/\sqrt{\left[f_{s\ max}/F_{s\ all}\right]^2 + \left[f_{axial}/F_{tu}\right]^2} - 1.0$$

where f_{axial} is the maximum axial stress in web (tension or compression) at rivet attachment line (see sketch on page B6.12.3-1).

10) Stiffener Analysis

a) Local buckling check

Calculate the local buckling stress of the stringer cross section by the method of B.4 using pages B4.11, 10-1,2, and 3 if applicable or B4.12-1 thru -5 for arbitrary sections. After determining the elastic buckling stress $F_{cr\ el}$, apply the plasticity correction factor of B1.50.1-2, giving F_{ccr}, the allowable buckling stress of the stringer section. Do not use crippling stress in this calculation. Local buckling margin of safety is

$$\text{M.S.} = F_{c\ cr}/f_{ST\ max} - 1.0$$

b) Allowable average compression for column failure of stiffeners (buckling out of the plane of web):

Single stiffeners -- find buckling stress $F_{c\ all}$ of stiffener with effective pin-ended length $\ell' = h_e/2$ from the formula:

$$F_{cr\ el} = \Pi^2\ E\ I_{ST_t}/\ell'^2 A_{ST_t}$$

Use Bl.50.4-1 in plasticity correction to obtain $F_{c\ all}$.

$$f_{ST_{avg}} = f_{ST} \qquad \text{of Step (6)}$$

$$\text{M.S. on column failure} = \frac{F_{c\ all}}{f_{ST\ avg}} - 1.0$$

Double stiffeners -- find buckling stress $F_{c\ all}$ of double stiffener with effective pin-ended length ℓ' from column formula and Bl.50.4-1.

$$\ell' = h_e/\ 1 + k^2\ (3-2d/h_e) \qquad \text{but not to exceed } h_e$$

$$\text{M.S. on column failure} = \frac{F_{c\ all}}{f_{ST\ avg}} - 1.0$$

c) <u>Allowable web load to cause forced crippling failure of stiffener attached flange.</u>

For a defined structure (i.e., an existing design) the allowable shear load that will cause a forced crippling failure of the stiffener attached flange can be determined from the following equation for the normal load applied to the flange by the web.

$$p/q = C_1 + C_2\left[(q/q_{cr})\cdot(\psi_u/1000)\right]^{1/3} \qquad \text{(A-1)}$$

p = Normal load applied by web to stiffener, see sketch, pg. B6.12.1-18.

q = Applied web shear flow.

q_{cr} = Shear flow in web at buckling under combined load.

ψ_u = Stiffener attached flange up-spring, see SAR-77-2, page 9.

If an allowable value of p is substituted in Equation (A-1), that equation can then be solved for q, which is then the allowable web shear that will cause a forced crippling failure of the stiffener flange. The solution to the equation for allowable forced crippling shear is given in Figure 12 in terms of the allowable stiffener normal load p_{all}, the up-spring ψ_u and the web buckling shear flow q_{cr} (= F_{scr} t).

The allowable stiffener flange normal load is determined from:

$$P_{all} = \frac{H F_{cy} t_a^2}{4 \overline{OD}} \qquad (A\text{-}2)$$

where H is obtained from Figure 5, page B6.12.4-6. The shear flow to cause the forced crippling failure can then be determined from Figure 12, page B6.12.4-11. The web shear stress to cause forced crippling is then:

$$F_{s\,fc} = q_{fc}/t \qquad (A\text{-}3)$$

d) Stiffener attached flange thickness t_a, required for forced crippling.

In the design case, Equation (A-1) may also be used to determine the thickness of attached stiffener flange required to prevent a forced crippling failure. In this case it is necessary to know the applied shear flow q, and the buckling shear flow q_{cr}. After substituting the appropriate allowable flange bending stress and geometric quantities into Equation (A-1), a quadratic in t_a is obtained. This equation has the following solution:

$$t_a = \left\{ C_2 \left[(f_s/F_{scr}) \frac{E}{4000(1-\nu^2)} \frac{1}{\overline{OD}^2 (\overline{OD}+\overline{ED})} \right]^{1/3} + \sqrt{ C_2^2 \left[(f_s/F_{scr}) \frac{E}{4000(1-\nu^2)} \frac{1}{\overline{OD}^2 (\overline{OD}+\overline{ED})} \right]^{2/3} + \frac{C_1 H F_{cy}}{f_s t \overline{OD}} } \right\} \Big/ \frac{H F_{cy}}{2 \overline{OD} f_s t} \qquad (A\text{-}4)$$

For single stiffeners $C_1 = -0.0461$ and $C_2 = 0.042624$.
For double stiffeners $C_1 = -0.0400$ and $C_2 = 0.037$

Substitution of these constants in the above equation and adapting the following shorthand, for single stiffeners is obtained:

$$AA = (H F_{cy})/(4 \overline{OD} t f_s)$$

$$BB_1 = 2.77 \times 10^{-3} \left[\frac{E}{\overline{OD}^2 (\overline{OD}+\overline{ED})} \frac{f_s}{F_{scr}} \right]^{1/3}$$

$$t_a = \left[BB_1 + \sqrt{BB_1^2 - 0.1344\ AA} \right] / (2\ AA) \qquad (A\text{-}5)$$

The attached flange thickness t_a, shall also meet the following requirement:

$$2.0 \sqrt{\frac{0.037 f_s t \overline{OD}}{H F_{cy}}} \leq t_a < 2.0 \sqrt{\frac{0.569 f_s t \overline{OD}}{H F_{cy}}} \qquad (A\text{-}6)$$

PROCEDURE OF INSTABILITY & POST-BUCKLING ANALYSIS (CONT)

For double stiffeners, the following is obtained:

$$AA = (H F_{cy})/(4 \overline{OD} t f_s)$$

$$BB_2 = 2.42 \times 10^{-3} \left[\frac{E}{\overline{OD}^2 (\overline{OD}+\overline{ED})} \frac{f_s}{F_{scr}} \right]^{1/3}$$

$$t_a = \left[BB_2 + \sqrt{BB_2^3 - 0.160\ AA} \right] /(2\ AA) \qquad \text{(A-7)}$$

The attached flange thickness t_a, shall also meet the following requirement:

$$2.0\sqrt{\frac{0.029\ f_s\ t\ \overline{OD}}{H\ F_{cy}}} < t_a < 2.0\sqrt{\frac{0.3275\ f_s\ t\ \overline{CD}}{H\ F_{cy}}} \qquad \text{(A-8)}$$

M.S. on forced crippling = $F_{s\ fc}/f_s - 1.0$

11) Flanges

The allowable maximum stress for combined axial combression and flexure (due to $M_{f\ell}$) should be taken as the compression yield of the flange material F_{cy}. Local and overall stability of the flange should also be considered.

$$\text{M.S. on compression yield} = \frac{F_{cy}}{f_{f\ell} + f_{\ell\ B} + f_{f\ell\ A}} - 1.0$$

where

$f_{f\ell\ B}$ - is flexural compression stress from $M_{f\ell}$ (Step 7).

$f_{f\ell\ A}$ - is axial compression in flange due to overall bending of beam.

ATTACHMENT ANALYSIS

12) Design the web-to-flange rivets to transmit the following shear:

$$q_{f\ell} = f_s\ t\ (1.0 + 0.414\ k)$$

13) Design the stiffener to flange rivets to transmit the following load:

$$P_{ST} = f_{ST} A_{ST}$$

In Grumman designs it is customary to include as part of the stiffener-to-flange riveting the rivets attaching the stiffener to the portion of the sheet which can be considered to act as a corner gusset.

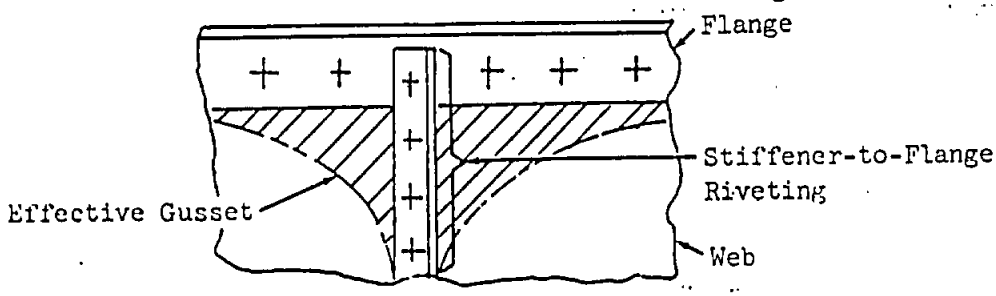

In designs where web stiffeners are not riveted to the flange there is a possibility of twisting failure in the flange. Therefore, the flange should be stabilized against twisting by having a reasonable number of stiffeners connected to the flange, or in any other appropriate manner.

14) The stiffener-to-web rivets must satisfy the following criteria:

a) The rivet pitch must be small enough to prevent inter-rivet buckling of the web at a stress equal to $f_{ST\ max}$ (See Step 6). The inter-rivet buckling curves are given on page B6.11.6-5.

b) The required rivet tensile strength shall be determined from the following:

For Single Stiffeners (one attached flange) the net load applied to the stiffeners is:

$$p = f_s\ t(-0.0461 + BB_1\ t_a) \qquad \text{(A-9)}$$

p also must satisfy:

$$0.037\ f_s\ t \ < \ p \ < \ 0.569\ f_s\ t \qquad \text{(A-10)}$$

For Double Stiffeners (2 attached flanges) the net load p per flange is:

$$p = f_s\ t(-0.040 + BB_2\ t_a) \qquad \text{(A-11)}$$

p also must satisfy:

$$0.029\ f_s\ t \ < \ p \ < \ 0.3275\ f_s\ t \qquad \text{(A-12)}$$

The rivet tensile load (pounds per inch) can be determined from the following equilibrium diagram.

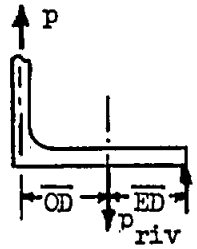

$$p_{riv} = p \frac{(\overline{OD} + \overline{ED})}{\overline{ED}} \qquad \text{(A-13)}$$

It is expected that the rivets selected that will meet the tensile requirement will be used in the normal structural close fitting hole. This will ensure adequate shear connection between the stiffener and web. Rivet tensile allowables are given on Figure 11 and pages B6.12.2-6 and B6.12.3-8.

EXAMPLE ANALYSIS PROBLEM

Consider a diagonal-tension beam with a 7075-T6 bare aluminum alloy web stiffened by 1" x 5/8" x 1/8" angles of 7075-T6 bare aluminum alloy, with the short leg attached to one side of the web. The beam flanges, 2-2" x 2" x $\frac{5}{16}$" $\angle$s, are attached on both sides of the web. The applied shear load is P=37.5 kips. Dimensions are given below.

1) Basic dimensions and geometric properties:

h_e = 11.58 in.

d = 7.0 in.

t_a = 0.125 in. t = 0.104 in. $\overline{ED}$ = .298

A_{ST} = 0.1888 in.^{2} $\bar{y}$ = 0.358 in. $\overline{OD}$ = .264

A_{ℓ} = 2.32 in.^{2} I_{ST} = 0.019 in.^{4} t_F = 0.313 in.

I_{ST_t} including effective width of web = 0.5d

Effective width = 7.0 (0.5)
= 3.50 in.

Centroid of combined section is 0.140 in. from mid plane of web.
Total section area is .5528 in^2

$$I_{ST_t} = .0190 + (3.50 \times .104)(.140)^2 + .1888\ (.358 + .104/2 - .140)^2 = 0.04027$$

$$EI_{ST_t}/dD = E \times 0.04027 = 12(1-.3^2)/7 \times E \times (0.104)^3$$
$$= 56.848$$

From Fig. 2 This will provide simple support

CALCULATION OF STRESSES:

2) Initial shear buckling stress.

d/h_e = 7.0/11.58 = 0.604

$K_{scr_{ss}}$ = 6.15 (Figure 2)

EXAMPLE ANALYSIS PROBLEM (CONT)

$f_{scr\ el} = 6.15 \times 10.5 \times 10^6 \left(\frac{0.104}{7.0}\right)^2 = 14.3$ ksi

$f_{scr} = f_{scr\ el} = 14.3$ ksi from B1.50.3-1

3) Diagonal-tension factor.

$f_s = 37.5/(11.58 \times 0.104) = 31.1$ ksi

$f_s/f_{scr} = 31.1/14.3 = 2.17$

k = 0.170 (from Figure 4)

4) Angle of diagonal tension.

$\frac{A_{ST}}{dt} = \frac{0.1888}{7.0 \times 0.104} = 0.259$ $\qquad \frac{A_{ft}}{h_e t} = \frac{2.32}{11.58 \times 0.104} = 1.93$

$\text{Tan}^4 \alpha_{PDT} = (1.0 + \frac{1}{2 \times 1.93})/(1.0 + 1.0/0.259)$

$\alpha_{PDT} = 35.50$

$\alpha_{DT} = 45 - 0.17(45 - 35.5)$
$= 43.5^\circ$

5) Maximum shear stress in web.

$C_1 = \frac{1}{\sin(2 \times 43.5)} - 1 \approx 0.0$

$\omega_i = 1.37$ (Calculation not shown. Formula on Figure 7)

$C_2 = .02$ (from Figure 7)

$f_{s\ max} = 31.1$ ksi $(1 + 0.17^2 \times 0)(1 + 0.17 \times 0.02) = 31.2$ ksi

6) Compression stress in stiffener

$f_{ST} = \frac{0.17 \times 31.1 \times \tan 43.5^\circ}{0.259 + 0.5(1.0 - 0.17)} = 7.44$ ksi

$f_{ST_{max}} = 1.32 \times 7.44$ (1.32 is from Figure 8)

$= 9.83$ ksi

EXAMPLE ANALYSIS PROBLEM (CONT)

7) Stresses in flanges.

$$f_{f\ell} = \frac{0.17 \times 31.1 \times \text{Cot } 43.5^\circ}{2 \times 1.93 + 0.5\,(1-.17)} = 1.30 \text{ ksi}$$

$$M_{f\ell} = \frac{1.0 \times .17 \times 31.1 \times .104 \times 7.0^2 \times \tan 43.5^\circ}{12} = 2.13 \text{ in-kips}$$

($C_3 = 1.0$ from Figure 7)

8) Equivalent shear modulus.

$$G/G_{IDT} = (1 - 0.17) + \frac{0.17}{2(1+.3)}\left[\frac{4}{\sin^2 87^\circ} + \frac{\tan^2 43.5^\circ}{0.259 + 0.5(1-0.17)} + \frac{\text{Cot}^2 43.5^\circ}{2 \times 2.25 + 0.5(1-0.17)}\right] = 1.19$$

Overall shear deformation of buckled web is

$$\gamma_{IDT} = \frac{31.1}{4.0 \times 10^3} \times 1.19 = 9.25 \times 10^{-3}$$

ALLOWABLE STRESSES:

9) Web allowables.

$$\frac{F_{s\ all}}{F_{ty}} = .512 \qquad @\ k = .17 \qquad \frac{F_{tu}}{F_{ty}} = \frac{77}{67} = 1.15$$

$F_{s\ all} = .512 \times 67 = 34.3$ ksi (Figure 10)

$MS = \frac{34.3}{31.2} - 1 = 0.099$

10.a) Stiffener Local Buckling

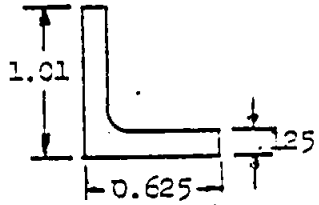

$F_{cr\ el} = 140.5$ ksi (Method of B4.12-1)

$F_{0.7} = 69.0$ ksi

$F_{cr} = 69.4$ ksi (B1.50.1-2)

$MS = 69.4 \div 3.83 =$ - Ample

EXAMPLE ANALYSIS PROBLEM (CONT)

10.b) Column Failure

$f_{ST\ avg} = 7.44$ ksi

I_{ST_t} at (k = 0.17) = 0.0388 in^4

$A_{ST_t} = 0.4909\ in^2$

$$F_{c\ all_{el}} = \frac{\pi^2\ E \times 0.0388}{(11.58)^2 \times 0.4909} = 245 \text{ ksi}$$

$F_{c\ all} = 65.5$ ksi (Bl.50.4-1)

MS = 65.5/7.44 - 1.0 = Ample

10.c) ALLOWABLE SHEAR FOR FORCED CRIPPLING FAILURE

This shear is determined by use of Figure 12. In order to use this figure, the following items must be calculated.

For $f_{ST\ max}/F_{cy} = 9.83/67.0 = 0.147$

H = 0.96 from Figure 5

$$p_{all} = \frac{0.96 \times 67000 \times 0.125^2}{4 \times 0.264}$$ From Equation (A-2)

$= 952.0$

From the reference on page 36.12.1-14, the up-spring for an angle section is determined to be:

$$\psi_u = \frac{E}{4(1-\upsilon^2)} \left[\frac{t_a}{OD}\right]^3 \left[\frac{1}{(1 + \overline{ED}/\overline{OD})}\right]$$

$$\frac{\psi_u}{1000} = \frac{10.5 \times 10^6}{4000(1-0.3^2)} \left[\frac{0.125}{0.264}\right]^3 \left[\frac{1}{(1.0 + 0.298/0.264)}\right]$$

$= 143.9$

$q_{cr} = 14300 \times 0.104$

$= 1487$ ppi

For Figure 12, $\frac{\psi_u\ p_{all}}{1000\ q_{cr}} = = \frac{143.8 \times 952}{1487} = 92$

From Figure 12, $q_{cc}/p_{all} = 3.85$

EXAMPLE ANALYSIS PROBLEM (CONT)

$q_{fc} = 3.85 \times 952$

$= 3662$ ppi

$F_{s\ fc} = 3662/0.104$

$= 35230$ psi

The forced crippling value is $\sim F_{s\ all}$ and therefore this panel is a balanced design.

11) Flange allowables

Numerical calculations are not given here. The computations of $f_{f\ell A}$, $f_{f\ell B}$ and local instability of flanges depend very much on their shape, attachment to the sheet, and the primary axial stresses in the flange.

ATTACHMENT ANALYSIS:

12) The web-to-flange rivets must transmit the following running shear

$q_F = (31.1 \text{ ksi})(0.104)(1 + 0.414 \times 0.17) = 3.46$ kips/in.

13) The stiffener-to-flange rivets must transmit the following load

$P_{ST} = (7.45)(.1888) =$ kips

14) a) From page B6.11.4-1 we see that the stiffener-to-web rivet spacing necessary to prevent inter-rivet buckling of the web at the stress $f_{ST\ max} = 9.83$ ksi exceeds practical upper limit of rivet spacing (7 to 8 diameters).

b) The required tensile strength of the rivets is from

$BB_1 = 2.77 \times 10^{-3} \quad 10.5 \times 10^6 \times (31000/14300)/(0.264^2(0.264+0.298))^{1/3}$

$= 2.2893$

EXAMPLE ANALYSIS PROBLEM (CONT)

14) a) Rivet tensile strength (Cont.)

$p = f_s\ t\ (-0.0461 + BB_1\ t_a)$ Equation (A-9)

$p = 31100 \times 0.104 \times (-0.0461 + 2.2893 \times 0.125)$

$= 776$ lb/in

$P_{riv} = 776 \times (0.264 + 0.298)/0.298$ Equation (A-10)

$= 1464$ ppi

5/32 inch diameter Cherry Buck (160 ksi Titanium) or Huck Blind Rivets (Monel or A286) are possible canditates for this for this application. The fastener shank strength is 1650 lbs for the Cherry Bucks and 1200 lbs for the Huck Blind Rivets. The sheet pull-thru strength for either fastener can be obtained from Figure 11, page B6.12.4-10.

For $D/t = 0.156/0.104$

$= 1.50$

$p/(D^2\ F_{tu}) = 1.11$ (from Figure 11)

Fastener pull-thru strength $= 1.11 \times 0.156^2 \times 77000$

$= 2080$ lbs

The fastener shank is critical and the required spacing for the Cherry Buck fasteners is $= 1650/1464$

$= 1.13$ inch

EXAMPLE DESIGN PROBLEM

Problem: Determine shear structure member sizes for the following geometric and load environment:

From the applicable internal load analysis, the following loads are determined for two possible critical conditions:

	Landing Condition	Flight Condition
q (shear flow, ppi)	4500	2200
f_b (Beam bending at extreme fiber) psi	± 10500	± 55000
f_c (Beam axial stress) psi	- 5000	- 5000

The following is the geometry available at this time of design:

h_e = 17.0 in. $\quad A_{fl}$ = .839 in.^{2}

$I_C = I_T$ = .310 in.^{4}

Material 7075-T6 Aluminum Alloy

F_{tu} = 77 ksi

F_{cy} = 68 ksi

F_{su} = 47 ksi

$F_{0.7}$ = 72.9 ksi

n = 27 (for extrusions)

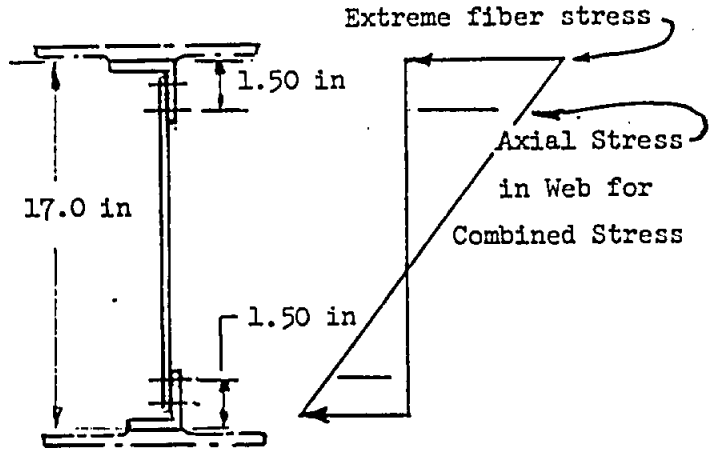

For illustration purposes a stiffener spacing = d = 6.0 in. is used. The stiffeners are extruded sections of 7075-T6 material with corner radius = 0.125 in. Initially assume $\overline{OD}$ = 0.310 and $\overline{ED}$ = 0.342 based on 5/32" attachments.

Start problem by assuming a value of k which will give an allowable shear stress and first approximation of sizes, using the larger (landing condition) shear flow.

Assume the diagonal tension factor k = 0.2, then from Figure 10,

$$F_{s\ all}/F_{cy} = 0.506 \text{ and}$$

$$F_{s\ all} = 34.4 \text{ ksi}$$

The bending stress at the rivet attachment line = $10500 \times \frac{(17-1.5x2)}{17}$

= 8650 psi

Since there are axial stresses present, determine the allowable working shear stress from Equation [A-0] by setting U = 1.0 (M.S. = 0.0).

$$\left(\frac{f_s}{34400}\right)^2 + \left(\frac{8650 + 5000}{77000}\right)^2 = 1.0$$

$$f_s = 33800$$

This will require a web thickness of

t = 4500/33800 = 0.133 in. Before proceeding with stiffener analysis, it is necessary to perform a complete web buckling analysis including the axial stress effects.

$K_{s\ cr_{(ss)}}$ = 5.28 from Figure 2 for d/h = 6/17 = 0.352

$F_{s\ cr_{el}} = 5.28 \times 10.5 \times 10^6 (0.133/6.0)^2 = 27{,}240$ psi

For the figure on page B5.11.13-2, d/h_e = 0.352 and

$\alpha = (10500 + 5000 - (-10500 + 5000))/(10500 + 5000) = 1.35$

$K_{axial} = 20.5$

$F_{axial} = 20.5 \times 10.5 \times 10^6 \left(\frac{0.133}{17}\right)^2 = 13200$ psi

$R_s = 33800/27240 = 1.241$

$R_{axial} = (10500 + 5000)/13200 = 1.174$

$$U = \frac{1.174}{2} + \sqrt{\left(\frac{1.174}{2}\right)^2 + 1.241^2}$$

$$= 1.960$$

$$F_{s_{cr}} = 27240 \times \frac{1.241}{1.960} = 17250$$

EXAMPLE DESIGN PROBLEM (CONT)

f_s/F_{scr} = 33800/17220 = 1.959, k = Tanh(0.5 x Log 1.959) = 0.15.

For F_{su}/F_{tu} = 0.61 and F_{tu}/F_{ty} = 1.13, the shear allowable is 0.515 x F_{ty} = 35020 from Figure 10. With 8650 + 5000 psi axial stress, the working shear stress is 34500 psi from Equation (A-0). The web thickness is 4500/34500 = 0.130 inches.

This only 2% thinner than gage used to this point and is considered adequate to proceed with t = 0.133 inches.

Determine stiffener attached flange thickness for forced crippling from equation [A-5]

Assume H = 0.90, f_s/F_{scr} = 1.959

$$AA = (0.9 \times 68000)/(4 \times 0.31 \times 0.133 \times 33800)$$
$$= 10.979$$
$$BB_1 = 2.77 \times 10^{-3}\left\{\left[(10.5 \times 10^6)/\left(0.310^2(0.310 + 0.343)\right)\right] \cdot 1.959\right\}^{\frac{1}{3}}$$
$$= 1.910$$
$$t_a = (1.910 + \sqrt{1.910^2 - 0.1844 \times 10.979})/(2.0 \times 10.979)$$
$$= 0.145 \text{ inch}$$

Determine limit value from Equation [A-6]

$$2.0\sqrt{(0.037 \times 33800 \times 0.133 \times 0.310)/(0.9 \times 68000)} < t_a < \text{——}$$
$$0.058 < t_a < 0.228 \quad \rightarrow 2.0\sqrt{(0.569 \times 33800 \times 0.133 \times 0.310)/(0.9 \times 68000)}$$

$\therefore t_a$ = 0.145 inch

Determine buckling ratios for the flight condition:

$R_s = (2200/0.133)/27240 = 0.607$

$\gamma = (55000 + 5000 - (-55000 + 5000))/(55000 + 5000) = 1.83$ and from B5.11.13-2, $K_{axial} = 26.6$

$$F_{axial} = 26.6 \times 10.5 \times 10^3 \times \left[\frac{0.133}{17}\right]^2$$
$$= 17095 \text{ psi}$$
$$R_{axial} = \frac{55000 + 5000}{17095} = 3.51$$

EXAMPLE DESIGN PROBLEM (CONT)

$$U = \frac{3.51}{2} + \sqrt{\left(\frac{3.51}{2}\right)^2 + .607^2}$$

$$= 3.612$$

$$F_{s_{cr}} = 27250 \times \frac{0.607}{3.612} = 4580 \qquad \text{From Equation (9)}$$

$$f_s = 2200/.133 = 16540$$

$$f_s/F_{s_{cr}} = 3.611, \; k = 0.272$$

Determine stiffener flange thickness for forced crippling:

Equation [A-1]

$$AA = (0.9 \times 68000)/(4 \times 0.310 \times 0.133 \times 16540)$$

$$= 22.436$$

$$BB_1 = 2.77 \times 10^{-3} \left\{ (10.5 \times 10^6)/\left(0.310^2(.310 + 0.343)\right) \cdot 3.611 \right\}^{\frac{1}{3}}$$

$$= 2.342$$

$$t_a = (2.342 + \sqrt{(2.342)^2 - 0.1644 \times 22.436})/(2.0 \times 22.436)$$

$$= 0.078 \text{ inch}$$

$\therefore$ Landing condition is critical

Since simple support was assumed, the stiffener has to meet the following moment of inertia requirement.

$$\text{Required } \gamma_s = EI_{ST_t}/dD = 30\,(17/6)^2 - 10\,(1 + 17/6) \qquad \text{Equation (1)}$$

$$= 203$$

$$\text{Required } \gamma_{axial} = 39\left(\frac{17}{6}\right)^4 = 26$$

$$\gamma_{req} = \left(203 \times \left(\frac{1.241}{1.960}\right) + 26\left(\frac{1.174}{1.960}\right)\right) = 144$$

The γ required for the flight condition is 55 and is not critical.

For $\gamma_{req} = 144$, determine I_{ST_t} required from $I_{ST_t} = dD\gamma_{req}/E$

$$I_{ST_t} = (144 \times 6 \times 0.133^3 E)/(12(1-0.3^2)E) = 0.188$$

EXAMPLE DESIGN PROBLEM (CONT)

This inertia can be provided by the following section:

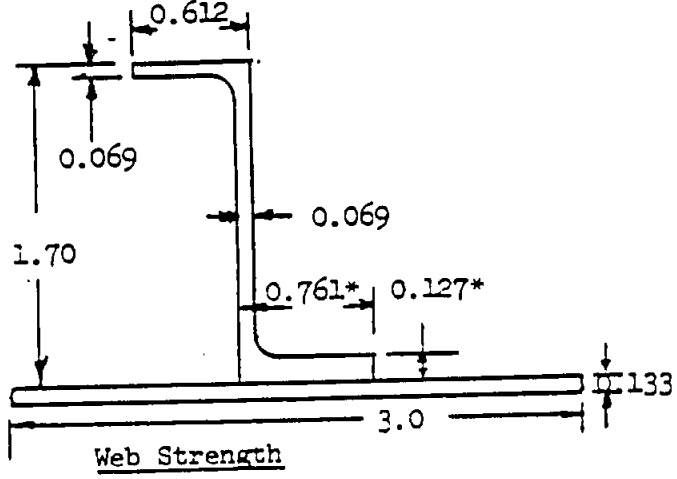

A_{ST} = 0.2487

I_{ST} = 0.1015

I_{ST_t} = 0.1887

$\frac{A_{ST}}{dt} = \frac{0.2487}{6 \times 0.133} = 0.304$

$\frac{A_{\ell}}{h_e t} = \frac{0.839}{17 \times 0.133} = 0.371$

$\text{Tan}\alpha_{FDT} = \sqrt[4]{\frac{1 + 1/(2 \times 0.371)}{1 + 1/0.304}}$

α_{FDT} = 40.7 deg

α_{DT} = 45 - 0.15 (45 - 40.7)
= 44.4 deg

* Note: These dimensions from page B6.12.3-7.

Web Strength

Determine maximum stress in web:

$C_1 = \frac{1}{\sin(2 \times 44.4)} - 1 \approx 0$

$wd = \sin 44.4 \times 6 \sqrt[4]{\frac{0.133}{2 \times .310 \times 17.0}}$

= 1.409

C_2 = 0.02

f_s = 33800 x (1 - .15 x 0.02)
= 33900 psi

$F_{s\ all}$ = 35020

MS = 35020/33900 - 1.0
= 0.033

or

$\left(\frac{33800}{35020}\right)^2 + \left(\frac{8650 - 5000}{77000}\right)^2 = 0.963$

$MS = \frac{1}{\sqrt{0.963}} - 1 = 0.019$

Stiffener/Sheet Rigidity Ratio

$\gamma_s = 12(1 - 0.3^2) \times 0.1887 \div (6.0 \times 0.133^3)$
= 145.98

EXAMPLE DESIGN PROBLEM (CONT)

Stiffener Stress

From previous page, $\alpha_{DT} = 44.4$ deg.

$$f_{st} = - \frac{33800 \tan 44.4^{\circ} \times .15}{.32 + 0.5(1-.15)}$$

$$= - 6664 \text{ psi}$$

$$= - 6664 \times 1.47 \text{ (Figure 8)}$$

$$f_{st\ max} = - 9796 \text{ psi}$$

Above stiffener section was sized so that all elements have buckling stresses the order of yield stress and is therefore not critical for local buckling.

Stiffener Column Allowable

$$F_{c\ all_{el}} = \frac{\pi^2 \times 10.5 \times 10^6 \times .188}{(17/2)^2}$$

$$= 269700$$

For page B1.50.4-1, $F_{crel}/F_{0.7} = 269700/72900 = 3.699$

$F_{cr}/F_{0.7} = 0.96$ and $F_{c\ all} = 0.96 \times 72900 = 69980$ psi

MS = (69980/9796) - 1 = Ample

Riveting Requirements

Calculate net load applied to stiffener from equation [A-9]

p = 33800 x 0.133(-0.0461 + 1.910 x 0.145)

= 1039 ppi

EXAMPLE DESIGN PROBLEM (CONT)

$$P_{riv} = 1039 \times \frac{0.31 + 0.342}{0.342}$$

$$= 1980 \text{ ppi}$$

This loading can be readily satisfied by a 3/16 inch diameter steel or titanium shank fastener at slightly greater than one inch pitch. This change from the assumed 5/32 inch diameter fastener will change the stiffener dimensions critical for forced crippling as well as the riveting requirement itself.

Resize attached flange thickness for actual dimensions:

The calculations for this change of rivet size will be based on the following stiffener attached flange.

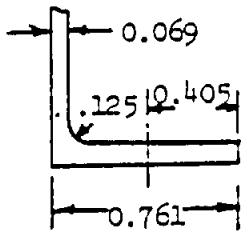

$= \overline{ED} + \overline{OD} + 0.069/2$

Along with this dimensional change and with the stiffener web defined, the value of H can now be determined

For Figure 5:

$F_e/F_{cy} = 9800/68000 = 0.145$ $\quad \overline{ED} = .405 = 2D + 1/32$

$H = 0.96$ $\quad \overline{OD} = .322 = 0.7D + R + 1/16$

Repeating the calculation for t_a, Eqn. [A-2]

$AA = (0.96 \times 68000)/(4.0 \times 0.322 \times 0.133 \times 33800)$

$= 11.274$

$$BB_1 = 2.77 \times 10^{-3} \left\{ \left((10.5 \times 10^6)/(0.322^2(0.322 + 0.405)) \right) \cdot 1.960 \right\}^{\frac{1}{3}}$$

$= 1.797$

$$t_a = (1.797 + \sqrt{1.797^2 - 0.1844 \times 11.274})/(2.0 \times 11.274)$$

$= 0.127$ in

Determine limit value from Equation [A-6]

$2.0 \ (0.037 \times 33800 \times 0.133 \times 0.322)/(0.96 \times 68000) < t_a <$

$0.057 < t_a < 0.225$ $\quad 2.0 \ (0.569 \times 33800 \times 0.133 \times 0.322)/(0.96 \times 68000)$

$\therefore t_a = 0.127$ inch

EXAMPLE DESIGN PROBLEM (CONT)

Repeating riveting requirement:

$$p = 33800 \times .133 \{-0.0461 + 1.797 \times 0.127\}$$

$$= 822 \cdot \text{ppi}$$

$$P_{riv} = \frac{822 \times (.405 + .322)}{0.405}$$

$$= 1475 \text{ \#/in.}$$

Available choices in high strength 3/16 attachments are Cherry Bucks, Hi Loks or Huck Blind rivets or bolts.

For Cherry Bucks or Huck Blind Bolts fastener strength is 2400 lbs.

For Hi Loks 1600 pounds for standard aluminum collars
or 2750 pounds with steel collars or MS21042 nuts

For Huck Blind rivets 1500 pounds

The sheet pull thru strength is:

$$D/t = \frac{0.1875}{0.133} = 1.41 \text{ gives } \frac{P}{D^2 F_{tu}} = 1.19 \text{ for protruding head steel fasteners}$$

or $P = 1.19 \times 0.1875^2 \times 77000 = 3220$ pounds

Using Hi Loks with aluminum collars

$$\text{Required Pitch} = \frac{1600}{1475} = 1.082 \text{ inches}$$

FIGURES

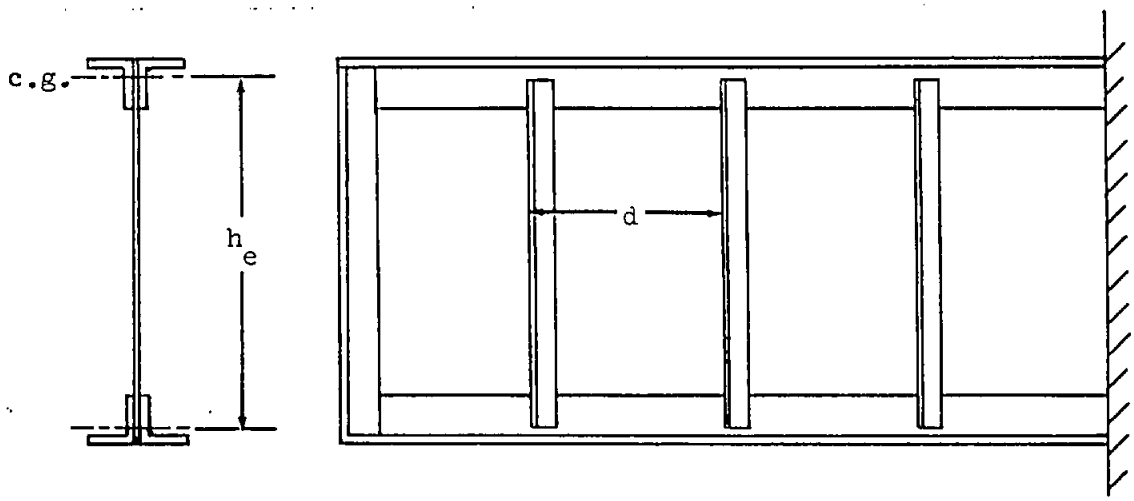

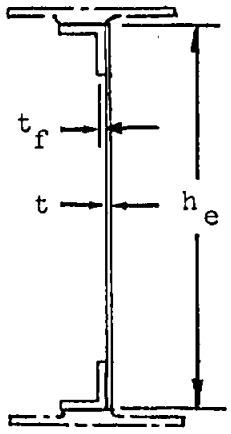

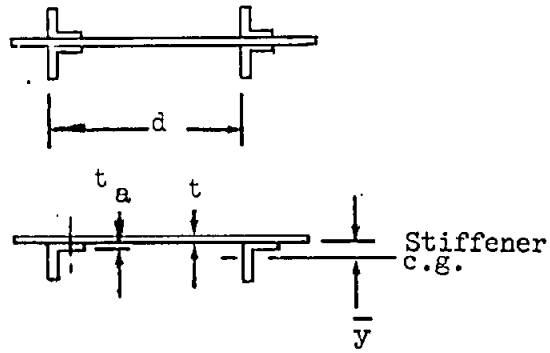

Fig. 1.a Geometry of Typical Plane Diagonal-Tension Beams

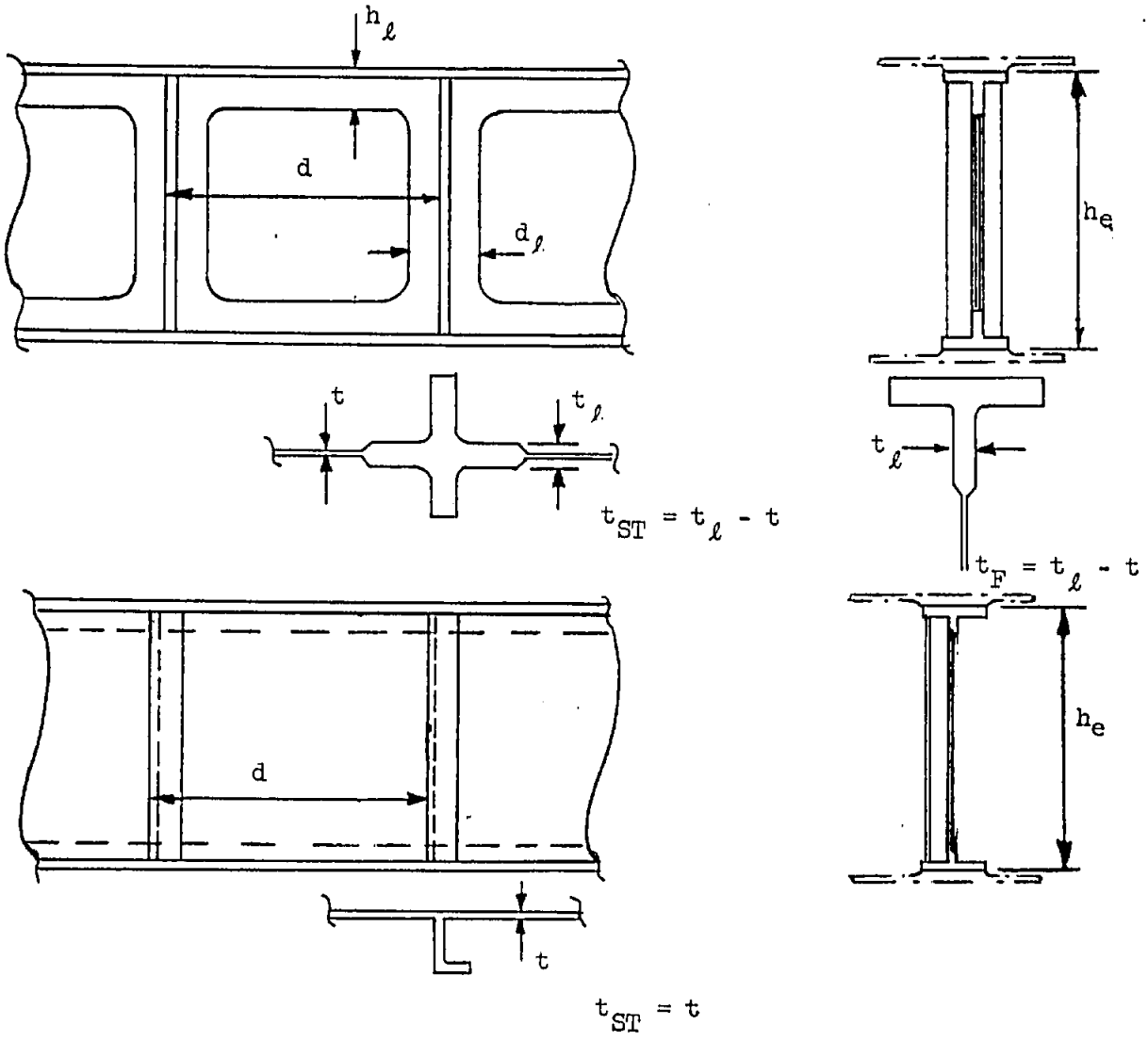

Figure 1.b Dimensions for Integrally Stiffened Beams (Two Configurations Shown)

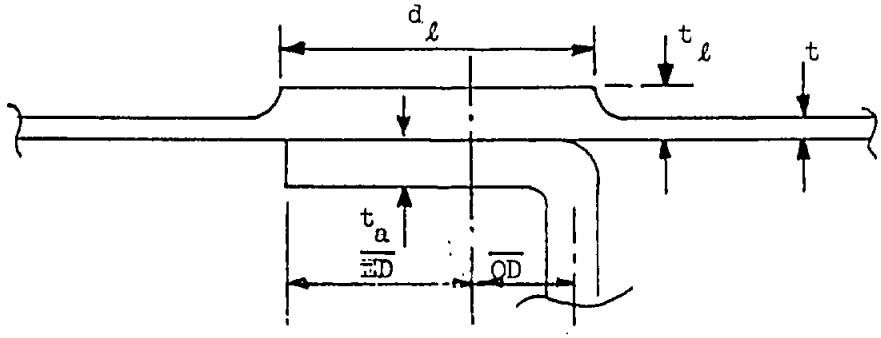

Figure 1.c Attached Stiffeners with Landed Sheet

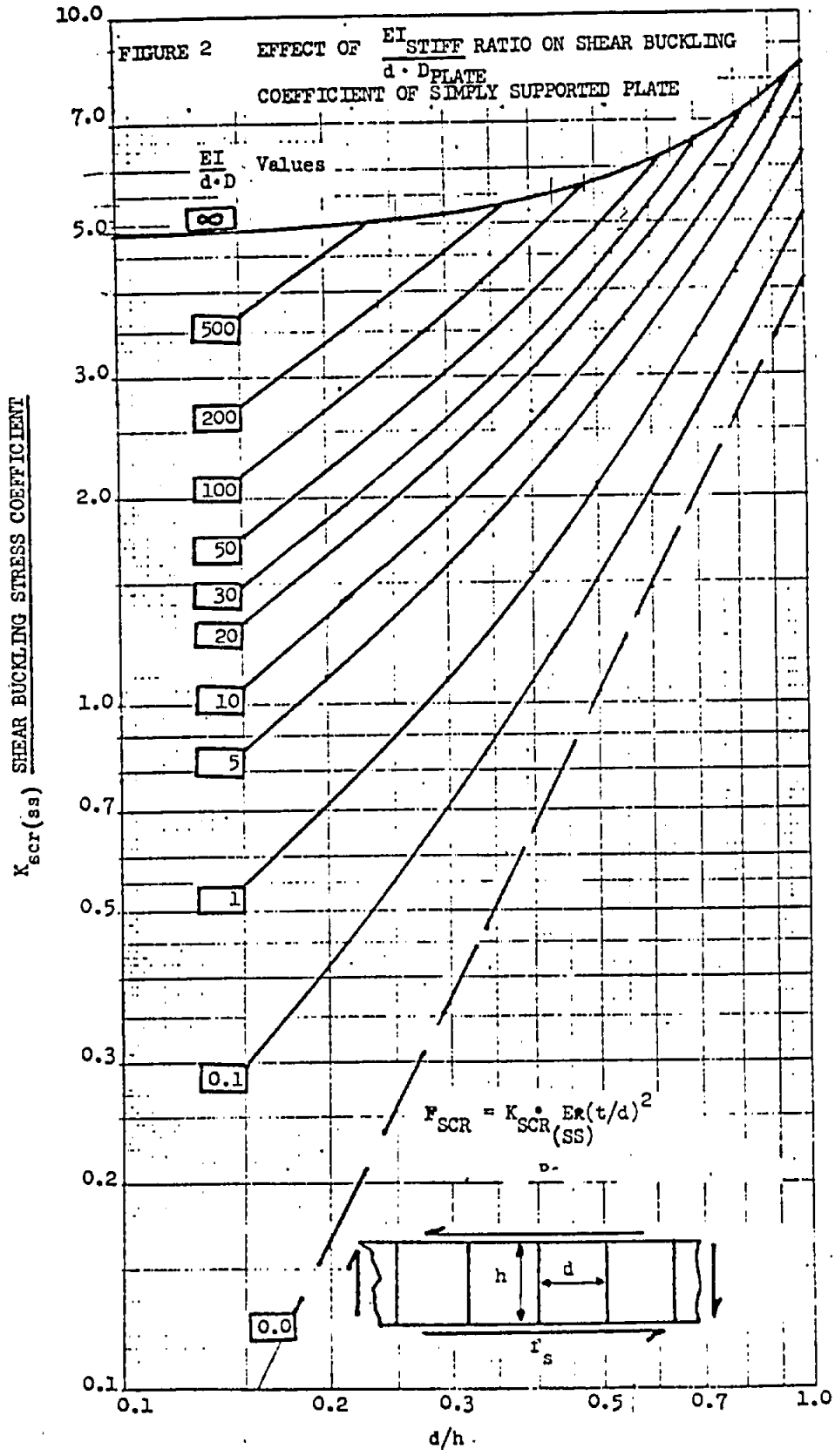
FIGURE 2 EFFECT OF $\frac{EI_{STIFF}}{d \cdot D_{PLATE}}$ RATIO ON SHEAR BUCKLING COEFFICIENT OF SIMPLY SUPPORTED PLATE
$K_{scr(ss)}$ SHEAR BUCKLING STRESS COEFFICIENT
$\frac{EI}{d \cdot D}$ Values
∞
500
200
100
50
30
20
10
5
1
0.1
0.0
10.0
7.0
5.0
3.0
2.0
1.0
0.7
0.5
0.3
0.2
0.1
0.1
0.2
0.3
0.5
0.7
1.0
d/h
$F_{SCR} = K_{SCR_{(SS)}} E_R (t/d)^2$
D
h
d
f_s

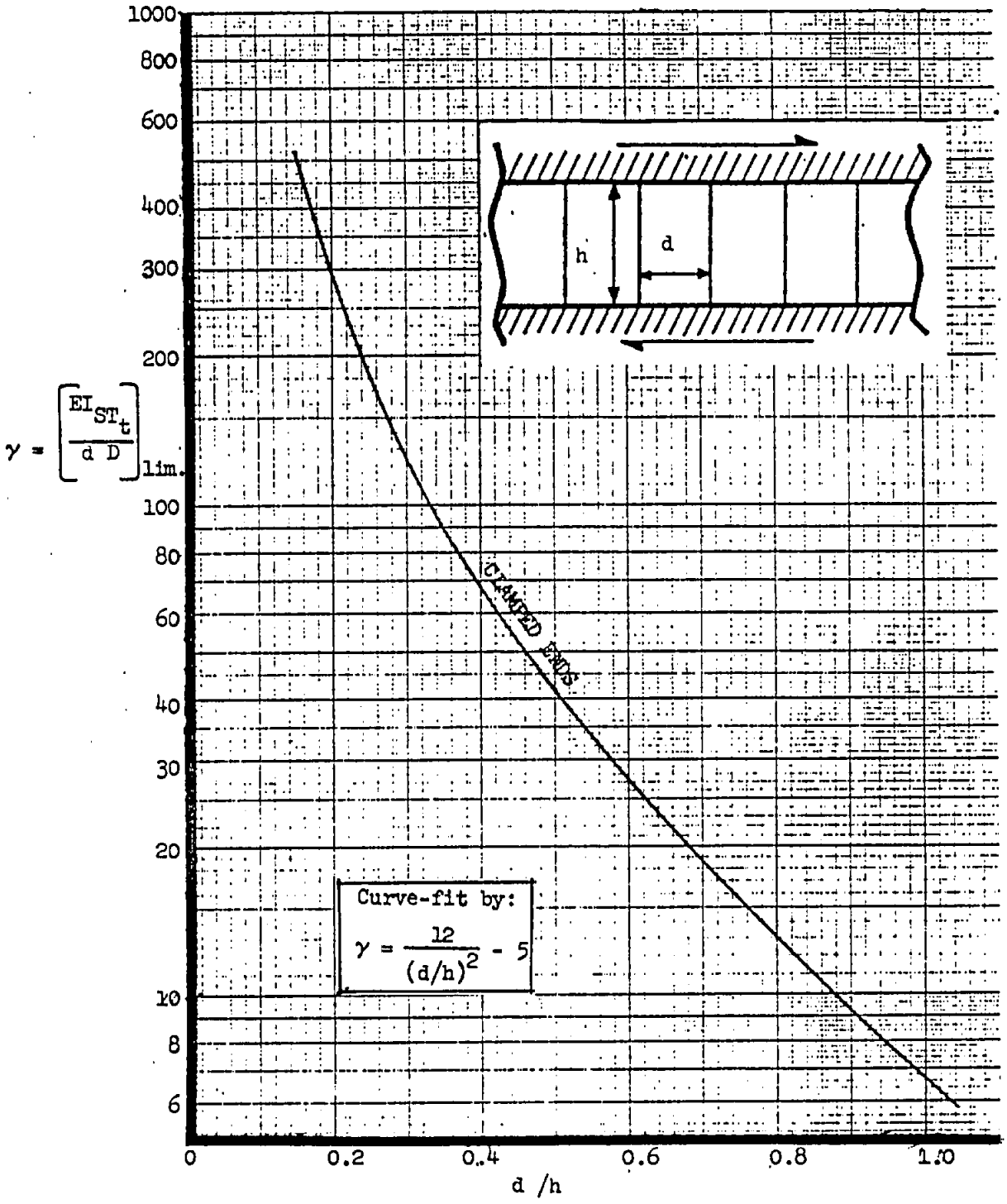

Figure 3 Approximate Minimum Flexural Stiffness of Stiffeners to Enforce Nodal Lines at Shear Buckling

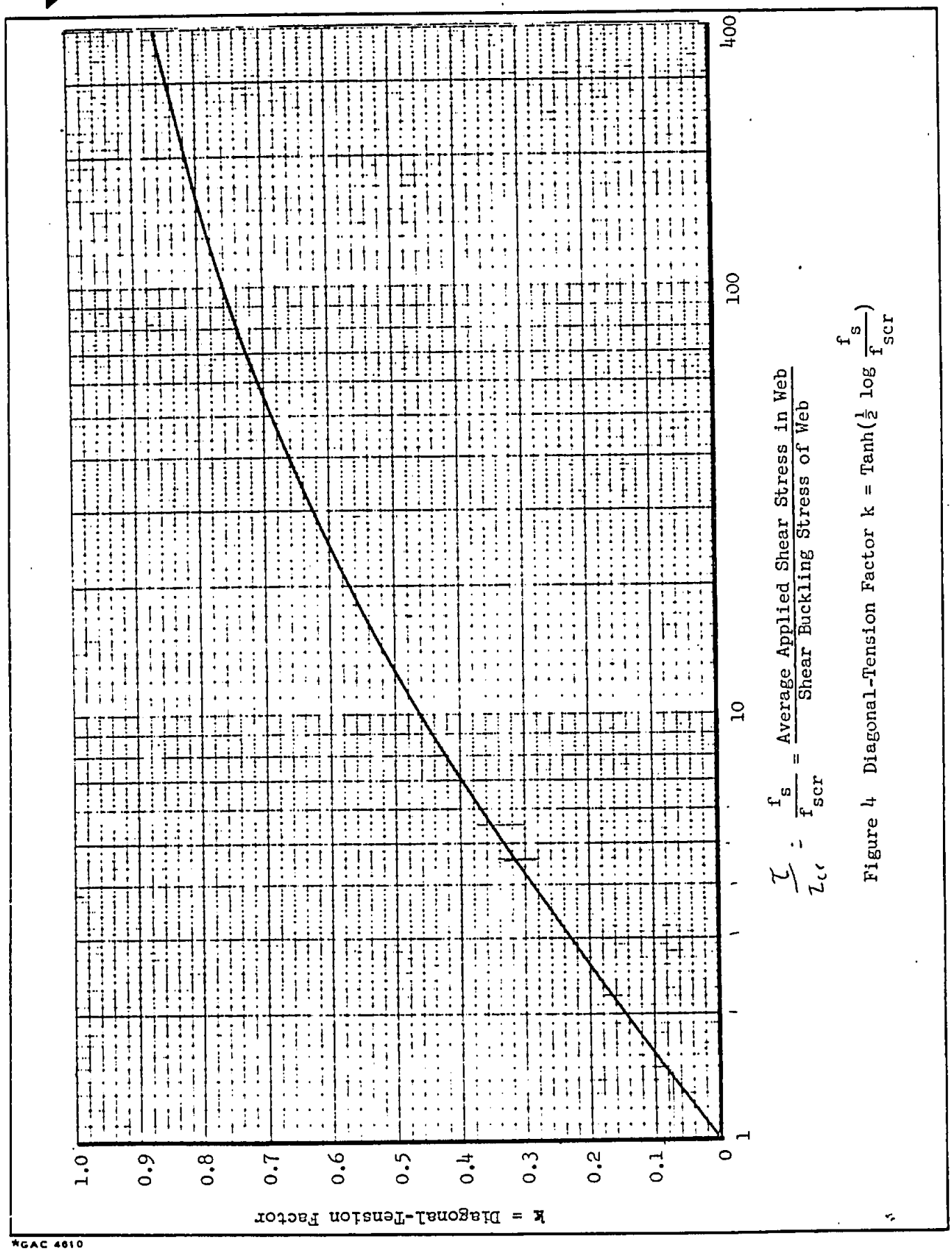

Figure 4 Diagonal-Tension Factor $k = \text{Tanh}(\frac{1}{2} \log \frac{f_s}{f_{scr}})$

FIGURE 5. FLANGE ALLOWABLE TRANSVERSE BENDING MOMENT VERSUS LONGITUDINAL COMPRESSIVE STRESS RATIO

$$M_{all} = \frac{H}{4} \cdot t_a^2 \cdot F_{cy}$$

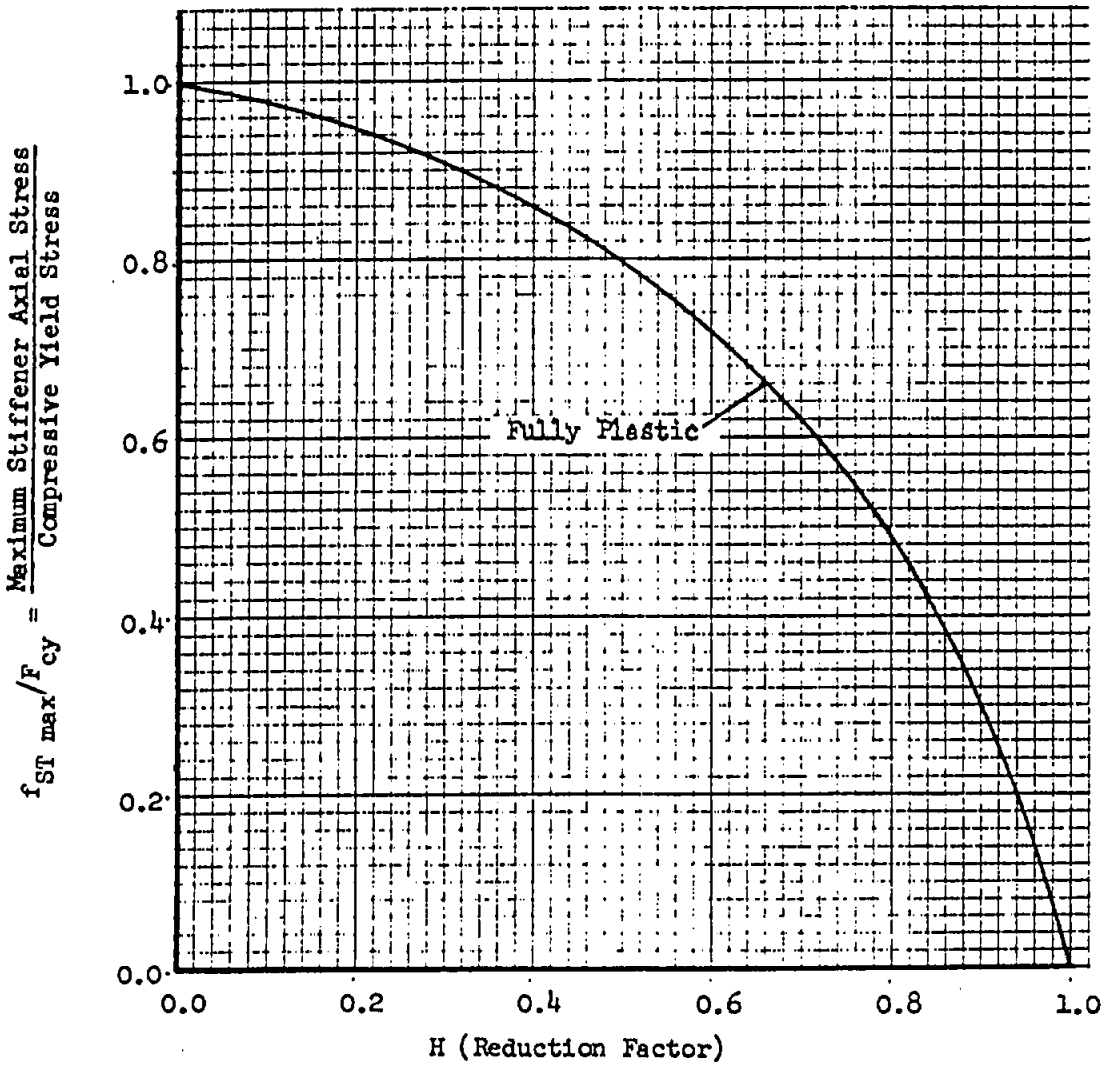

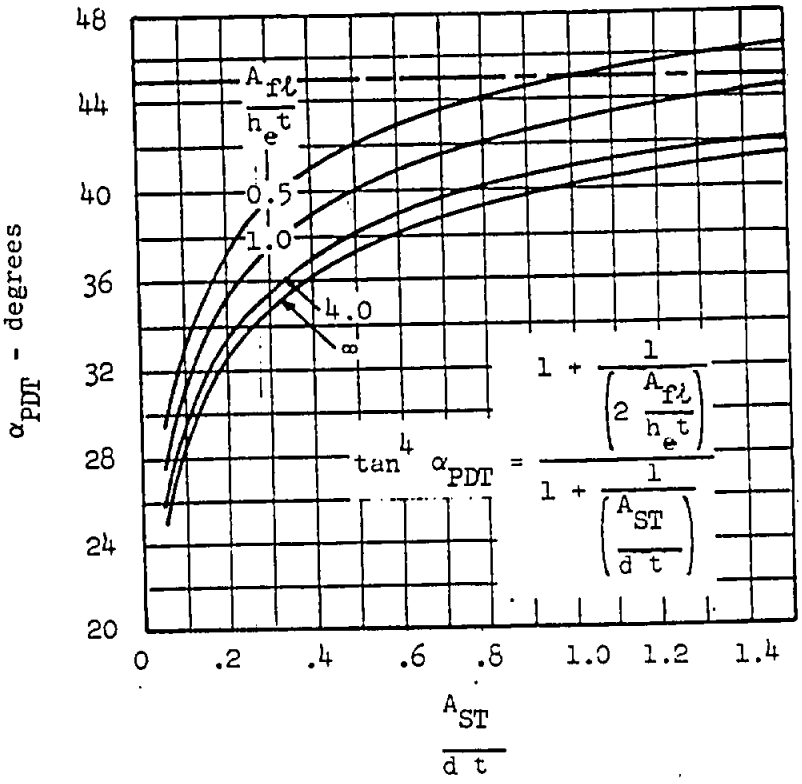

Figure 6 Angle of Pure Diagonal-Tension

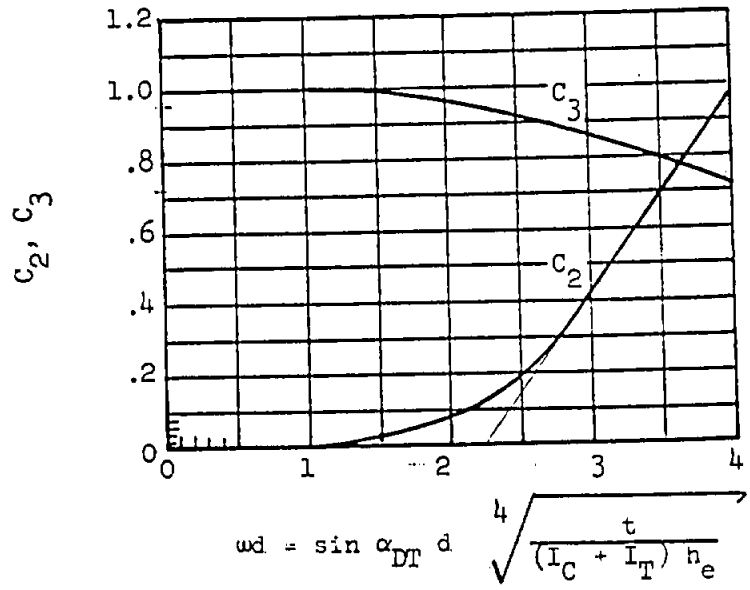

I_C, I_T are moment of inertia of compression and tension flanges about centroid axis normal to web.

Figure 7 Stress Concentration Factors

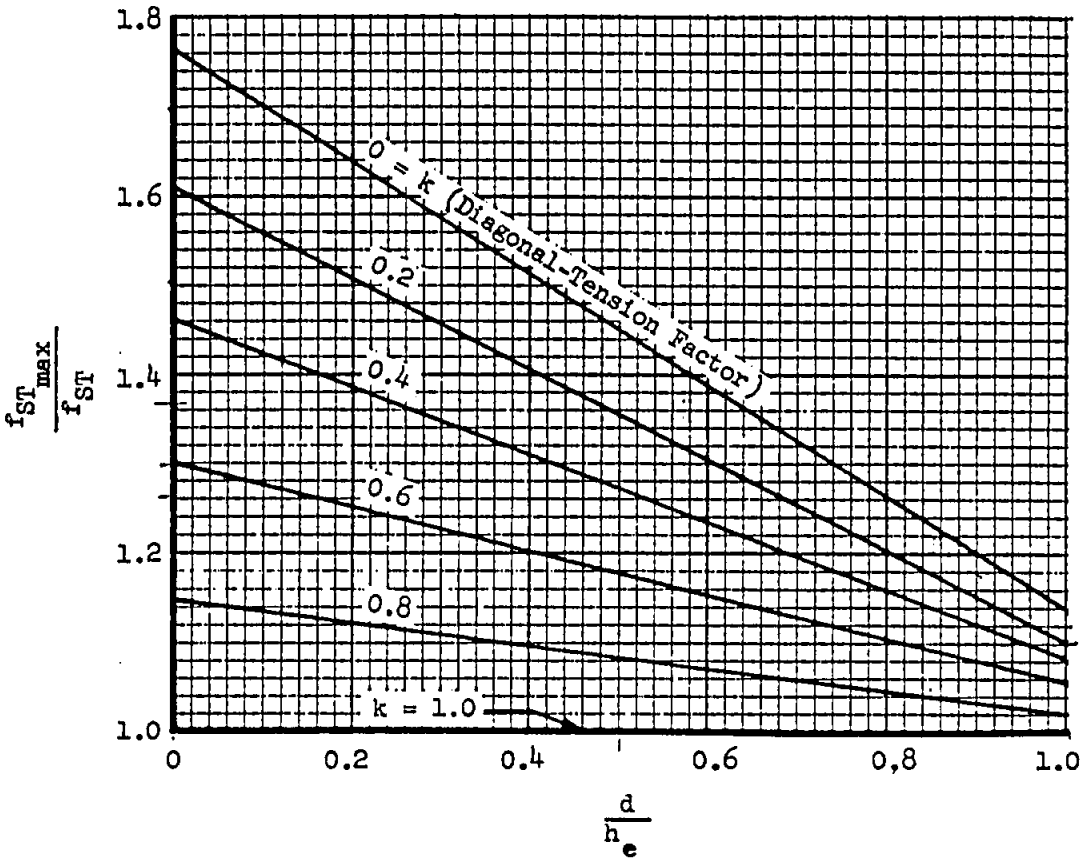

Figure 8 - Ratio of Maximum to Average Stiffener Stress

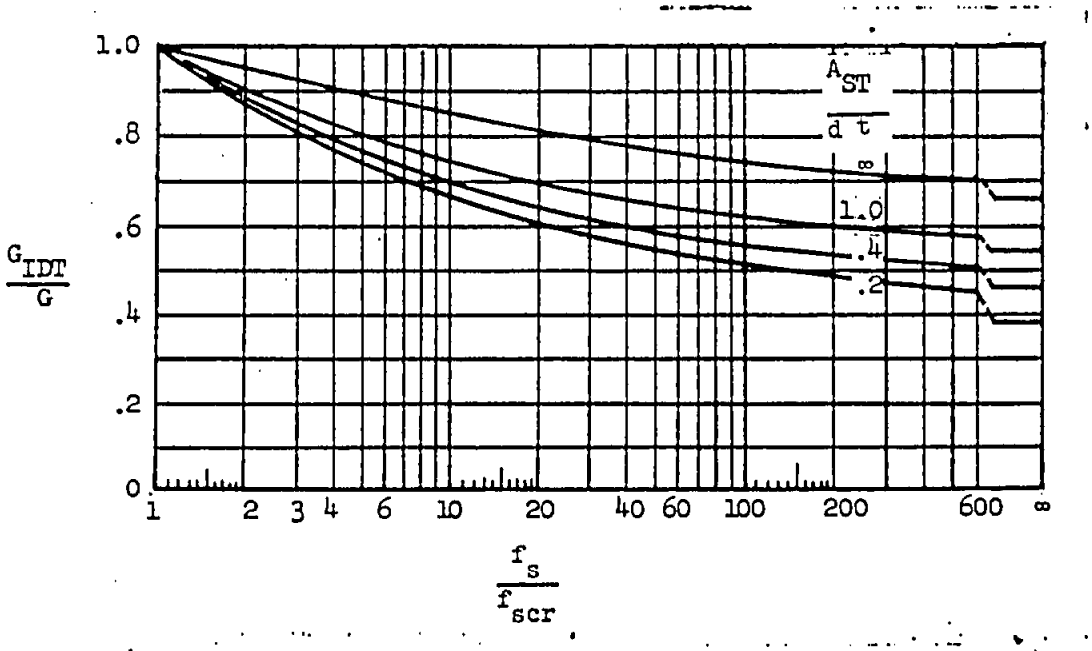

Figure 9 Effective Shear Modulus of Diagonal-Tension Web

$$\frac{F_{s\,all}}{F_{ty}} = 0.9\left[1 + \frac{1}{2}\left(\frac{F_{tu}}{F_{ty}} - 1\right)^2\right]\cdot\left[\frac{1}{2} + (1-k)^3\left(\frac{F_{su}}{F_{tu}} - \frac{1}{2}\right)\right]$$

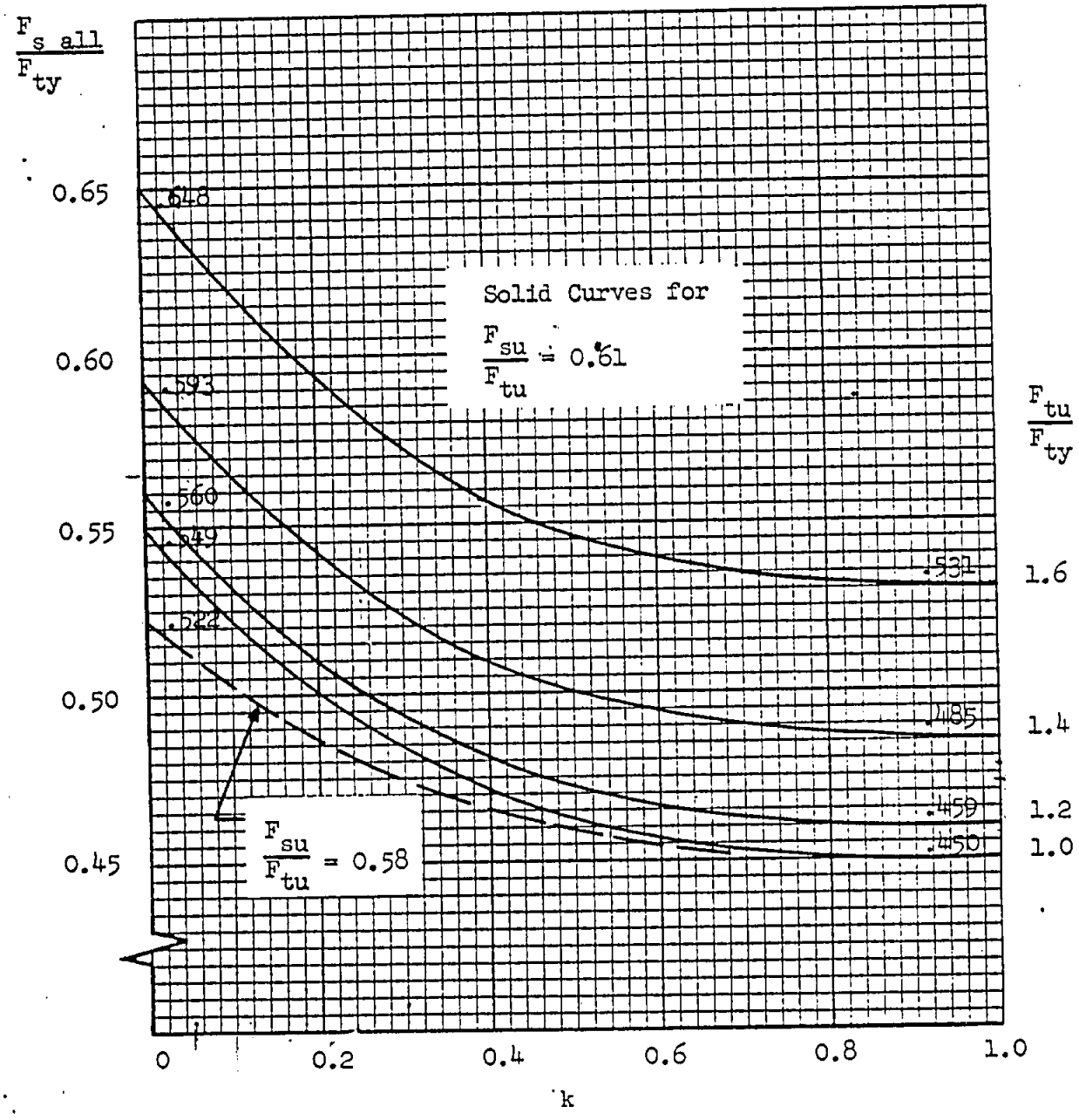

Figure 10. Allowable Maximum Web Shear Stress, $F_{s\,all}$

Figure 11 Normalized Tensile Pull-Thru Strength of Rivet Type Fasteners

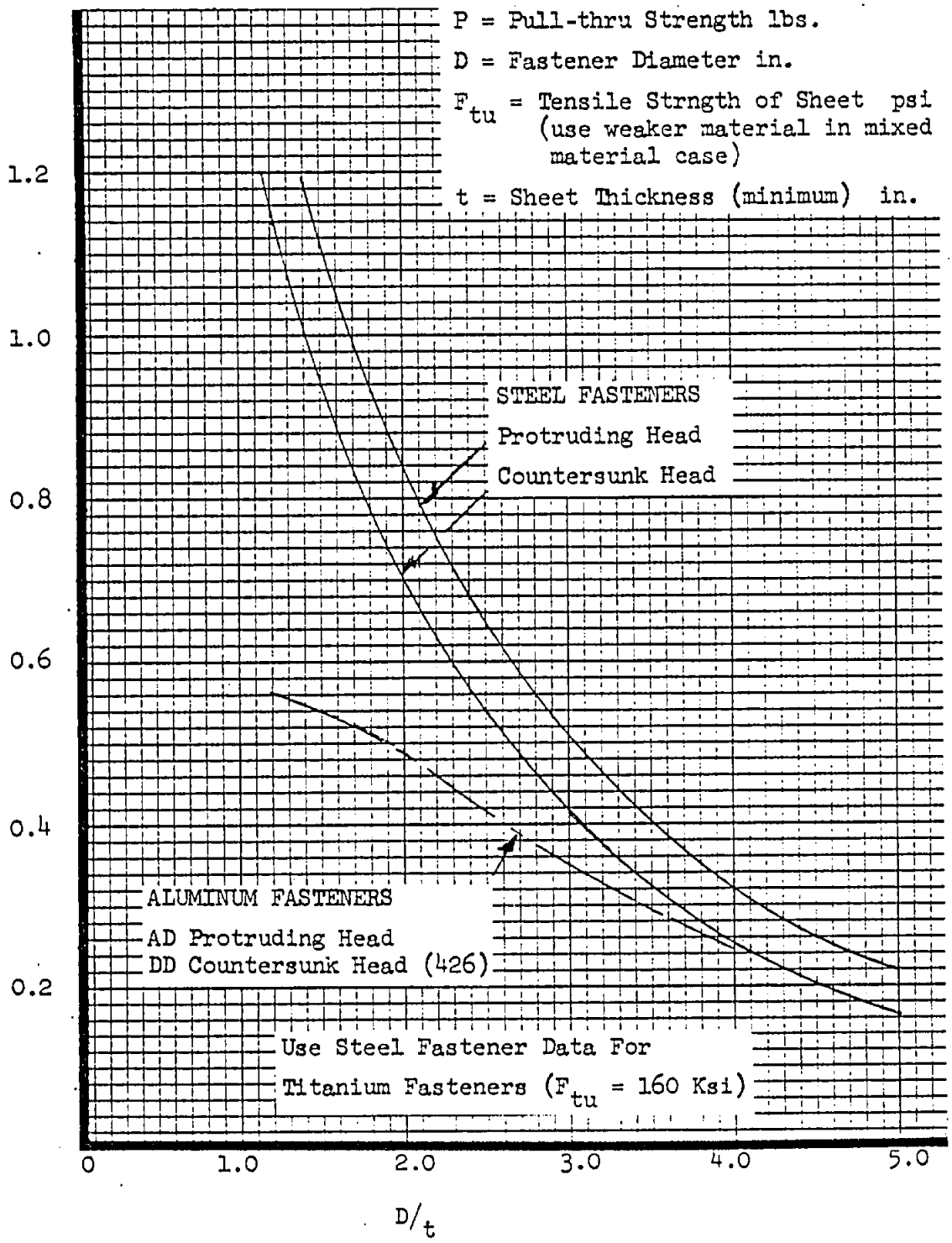

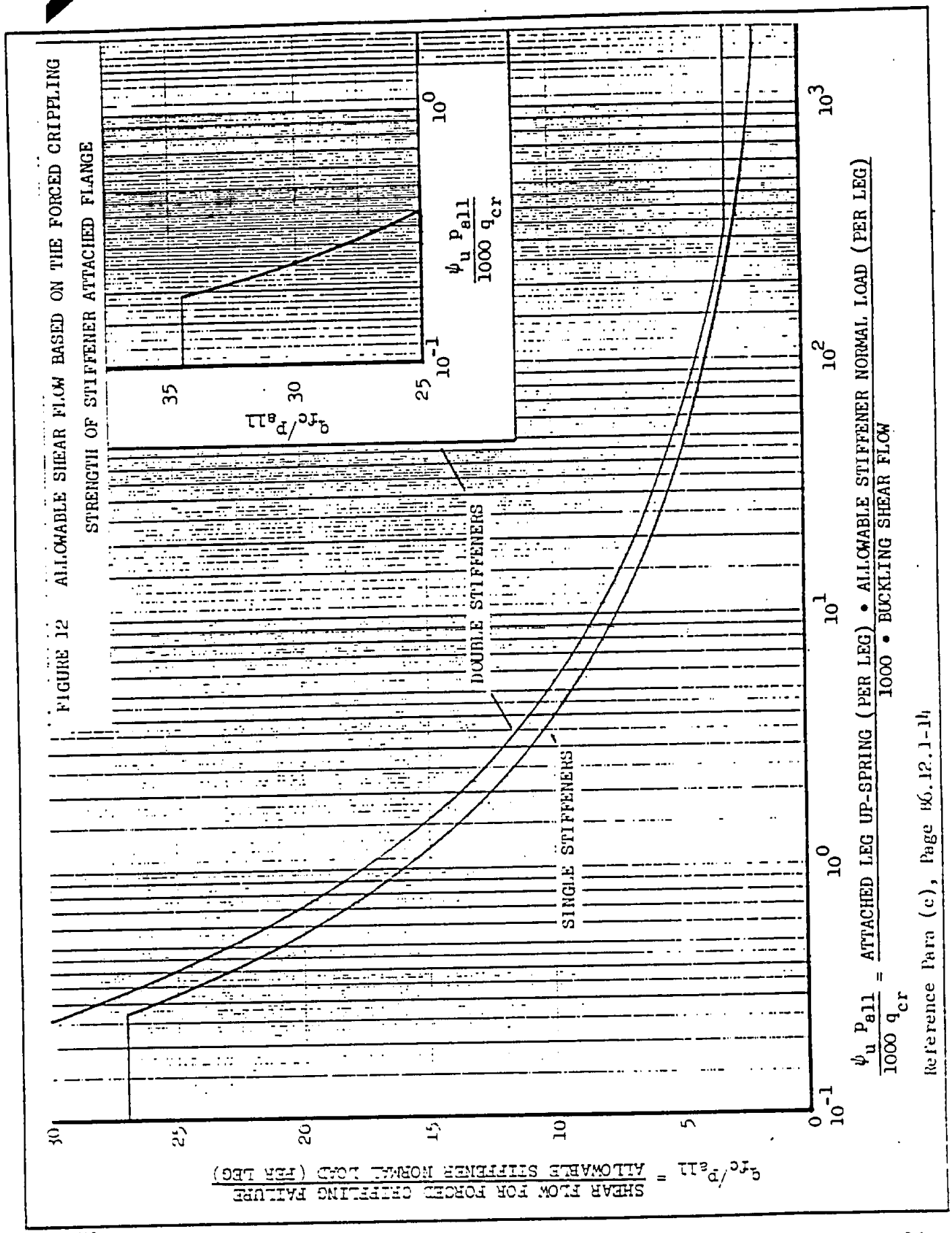
FIGURE 12 ALLOWABLE SHEAR FLOW BASED ON THE FORCED CRIPPLING STRENGTH OF STIFFENER ATTACHED FLANGE
SHEAR FLOW FOR FORCED CRIPPLING FAILURE / ALLOWABLE STIFFENER NORMAL LOAD (PER LEG) = q_{fc}/p_{all}
$\frac{\psi_u P_{all}}{1000\ q_{cr}}$ = ATTACHED LEG UP-SPRING (PER LEG) • ALLOWABLE STIFFENER NORMAL LOAD (PER LEG) / 1000 • BUCKLING SHEAR FLOW
SINGLE STIFFENERS
DOUBLE STIFFENERS
q_{fc}/p_{all}
$\frac{\psi_u p_{all}}{1000\ q_{cr}}$
Reference Para (c), Page 86.12.1-14

ANALYSIS OF ALUMINUM ALLOY WEBS WITH LIGHTENING OR ACCESS HOLES

The dieal construction for most shear-carrying beams is a tension field beam (unperforated web, flanges and stiffeners), designed by the method given on pages B6.12.20-1 through -20 in the Structures Manual. However, in some cases it is advantageous, and in other cases necessary, to incorporate circular, flanged holes in the beam webs. These cases come under two main categories.

I. Lightly loaded or very shallow beams: In such cases it may not be practical to construct an efficiently designed tension field beam because of minimum gage considerations and other restrictions due to the small size of the parts involved. It may then be advantageous from a weight standpoint to omit web stiffeners and, instead, introduce a series of Grumman standard flanged lightening holes, G-H11F, in the webs.

II. Moderately or heavily loaded beams with access holes: Where it is necessary to introduce access holes into the web of a shear-carrying beam, a light, low cost construction is obtained by using a flanged hole with web stiffeners between the holes.

Methods for designing these two main types of perforated webs are given below. These methods are based on a generally conservative evaluation of the data and design procedures given in the following references:

References

(1) Sweden, SAAB TN-29, "Experimental Investigation of Shear Strength and Shear Deformation of Unstiffened Beams of 24S-T Alclad with and without Flanged Lightening Holes", by G. Anevi

(2) NACA Report L-323, "The Strength and Stiffness of Shear Webs with Round Lightening Holes having 45° Flanges", by P. Kuhn

(3) NACA TN-2661, "A Summary of Diagonal Tension", by P. Kuhn, J. P. Peterson and L. R. Levin

Symbols

The definitions of the symbols used in the analysis are as follows:

A_o	Stiffener area, in.^{2}
b	Lightening or access hole spacing, inches.
b_{o1}	Stiffener dimension, inches.
b_{o2}	Stiffener dimension, inches.
b_s	Stiffener spacing, inches.
d	Rivet diameter, inches.
D	Lightening or access hole diameter, inches.

Symbols (Cont.)

F_o	Ultimate allowable web shear stress of a shallow beam without holes, psi.
F_s	Ultimate allowable shear stress on gross section of webs with holes, psi.
F_{su}	Ultimate allowable shear stress of web material, psi.
f_s	Applied shear stress on web gross section, psi.
$f_{s_{net-1}}$	Net-section web shear stress on horizontal section through holes, psi.
$f_{s_{net-2}}$	Net-section web shear stress on vertical section through holes, psi.
$f_{s_{net-3}}$	Net-section web shear stress through attachments, psi.
h	Web height, inches.
H	Total beam height, inches.
I_o	Moment of inertia of stiffener about its center of gravity and parallel to the skin line, $in.^4$
K_1	Correction factor for unstiffened webs with holes.
K_2	Correction factor for stiffened webs with holes.
K_r	Net-area correction factor for web to flange riveting.
q	Applied shear flow, lbs./in.
q_r	Design shear flow for riveting, lbs./in.
s	Rivet spacing, inches.
t	Web thickness, inches.
t_o	Stiffener thickness, inches.
t_{eq}	Equivalent-weight web thickness, inches.

I. LIGHTLY LOADED OR VERY SHALLOW BEAMS

The following two types of beam construction are considered. The Grumman standard flanged lightening holes, G-H11F, are centered and equally spaced.

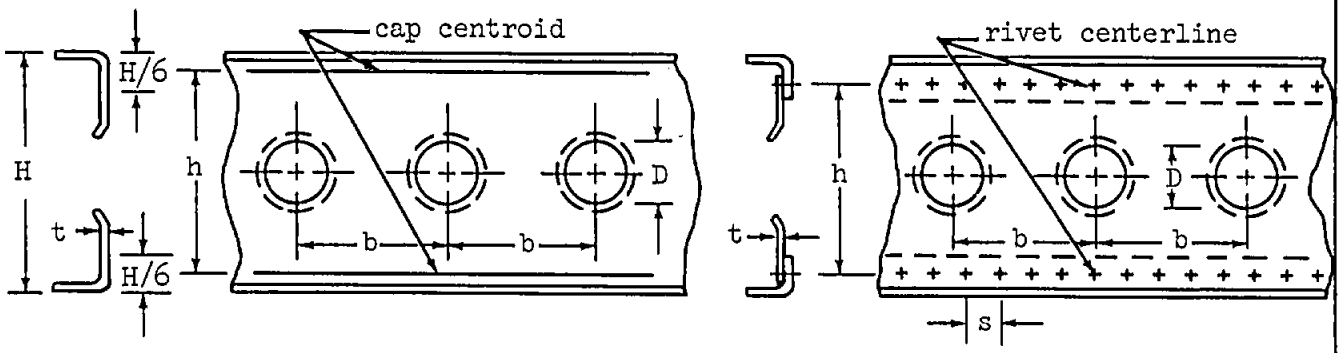

BEAM TYPE I BEAM TYPE II

Note: H/6 is the assumed effective depth of cap.

(1) The limiting conditions for the design curves given in Figure 1, page B6.12.30-14 are:

$$.25 \leq \frac{D}{h} \leq .75 \qquad 40 \leq \frac{h}{t} \leq 250$$

$$.30 \leq \frac{D}{b} \leq .70 \qquad .016 \leq t \leq .125$$

(2) The ultimate allowable gross shear stress of the perforated web is given by:

$$F_s = K_1 F_o \tag{1}$$

where K_1 and F_o are given in Figure 1, page B6.12.30-14. F_o is the ultimate allowable web stress of a shallow beam without holes.

(3) To cover the case of large or closely spaced holes and rivets the net shear stresses should be calculated. These values must not exceed F_{su}.

$$f_{s_{net-1}} = \frac{q}{t}\left[\frac{b}{b-D}\right] \tag{2}$$

$$f_{s_{net-2}} = \frac{q}{t}\left[\frac{h}{h-D}\right] \tag{3}$$

$$f_{s_{net-3}} = \frac{q}{K_r\ t} \tag{4}$$

where $K_r = 1.0$ for beam type I

$$K_r = \frac{s-d}{s} \text{ for beam type II}$$

(4) Because of the non-uniformity of stress caused by the holes, the web-to-flange riveting of the type II beam should be designed by the greater of:

$$q_r = 1.25\ q$$

or (5)

$$q_r = .67\left[\frac{b}{b-D}\right] q$$

(5) The equivalent-weight web thickness of a plane web beam with lightening holes is given by:

$$t_{eq} = t\left[1 - \frac{.785\ D^2}{h\ b}\right] \qquad (6)$$

For a given web height (h), web thickness (t), and loading (q), the equivalent-weight web thickness (t_{eq}) will be a minimum when the hole diameter and hole spacing are chosen so as to lie on the curve for optimum K_1 factor in Figure 1, page B6.12.30-14. The lightest possible beam of height (h) that can support the loading (q) will be obtained by assuming various values of (t) and repeating the above procedure to obtain the corresponding minimum values of (t_{eq}). One of the assumed values of (t) will give the absolute minimum value of (t_{eq}) and, therefore, the lightest beam. This generally will be a beam where D/h is approximately 0.25 and D/b is approximately 0.45. This proceedure is used in example(2).

It should be noted that if the web height (h), hole diameter (D), and loading (q) are given, then the lightest beam will be obtained when the hole spacing (b) is such that D/b is approximately 0.45.

II MODERATELY OR HEAVILY LOADED BEAMS WITH ACCESS HOLES

A sketch of the type construction considered in the design of moderately or heavily loaded beams requiring access holes is given below. The access holes are centered between the single angle stiffeners and are formed from the Grumman standard lightening hole series, G-H11F.

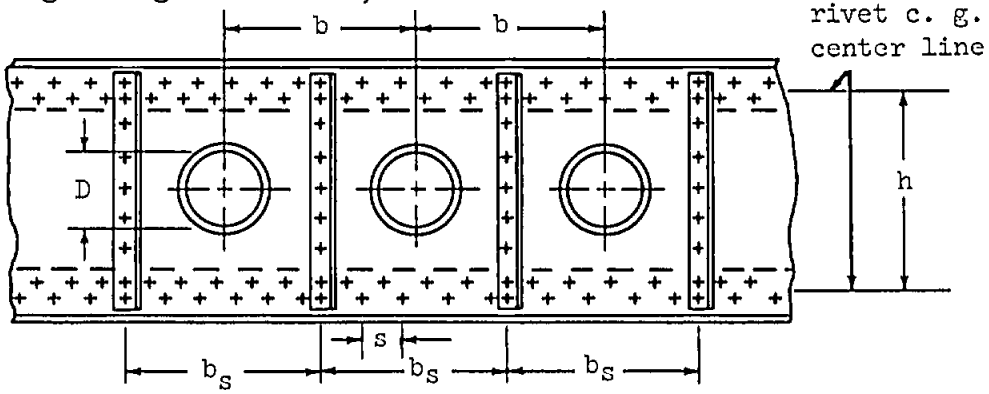

(1) The following limiting conditions must be satisfied when using the design curves on Pages B6.12.30-14 and B6.12.30-15.

(a)
$$.025 \leq t \leq .125$$
$$115 \leq \frac{h}{t} \leq 1500$$
$$.235 \leq \frac{b_s}{h} \leq 1.0$$

(b) To prevent net shear failure between holes, the maximum hole size in relation to panel rectangularity is given by:

$$\frac{D}{b_s} \leq .85 - 0.1 \left[\frac{h}{b_s}\right] \qquad (7)$$

It should be noted that a staggered arrangement of holes between panels is preferred to having them in a single line.

(c) The single angle stiffeners must satisfy the following conditions:

$$t_o \geq t$$
$$\frac{A_o}{b_s t} \geq 0.385 - 0.08\left[\frac{b_s}{h}\right]^3 \qquad (8)$$
$$I_o \geq \frac{F_s\, t\, b_s\, h^3}{10^8\,(h-D)} \qquad (9)$$

where I_o is the moment of inertia of the stiffener about its center of gravity and parallel to the skin line.

$$I_o = \frac{t_o\, b_{o2}^3\, (4b_{o1} + b_{o2})}{12\,(b_{o1} + b_{o2})} \qquad (10)$$

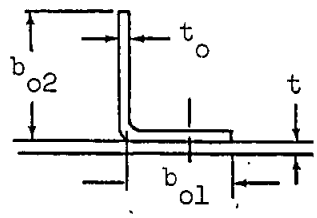

(d) The maximum width-to-thickness ratios of the single angle stiffeners are limited to:

TABLE I

t_o	.032	.040	.051	.064	.072	.081	.091	.102	.125
b_{o1}/t_o	12.5	12.5	11.5	10.0	9.5	9.0	9.0	9.0	9.0
b_{o2}/t_o	16.0	16.0	15.0	13.0	12.0	12.0	12.0	12.0	12.0

(2) If the requirements of 1(a) - 1(d) are satisfied, then the ultimate allowable gross shear stress is given by:

$$F_s = K_2 F_o \qquad (11)$$

F is obtained from Figure 1, page B6.12.30-14, as a function of b_s/t. K_2 is given in Figure 2, page B6.12.30-15.

(3) To provide for the non-uniformity of stress caused by the access holes, the following riveting requirements must be satisified.

(a) Web-to-flange riveting.

$$q_r = 1.25 F_s t \left[\frac{h}{h-D}\right] \qquad (12)$$

(b) Flange-to-stiffener rivets are designed to transmit the following load:

$$P_{st} = \frac{.0024 \text{ Ao } F_s b_s}{t} \left[\frac{h}{h-D}\right] \qquad (13)$$

In Grumman designs it is customary to include as part of the stiffener to flange riveting the rivets attaching the stiffener to the portion of the web which can be considered to act as a corner gusset. (See Page B6.12.20.1-6).

(c) Web-to-stiffener riveting should conform to the following table.

TABLE II

MS 20470 Rivets

Web thickness (t)	.025	.032	.040	.051	.064	.072	.081	.091	.102	.125
Rivet	AD-4	AD-4	AD-4	AD-5	AD-5	AD-6	AD-6	DD-6	DD-6	DD-8
Rivet diameter (d)	1/8	1/8	1/8	5/32	5/32	3/16	3/16	3/16	3/16	1/4
Rivet spacing (s)	1/2	5/8	5/8	7/8	3/4	1.0	7/8	1.0	1.0	1-3/8

For single angle stiffeners, the required tensile strength of the rivets per inch run is:

$$\text{Pten.} = 0.20 \text{ t } F_{tu}$$

Where F_{tu} is the ultimate tensile strength of the web material. This criterion is satisfied by the above table for MS 20470 rivets.

(4) The equivalent-weight web thickness (t_{eq}) for a beam with stiffeners and access holes is given by:

$$t_{eq} = t \left[1 - \frac{.785\ D^2}{h\ b_s} + \frac{A_o}{b_s\ t} \right] \qquad (15)$$

For a given web height (h), hole diameter (D), and loading (q), the minimum equivalent-weight beam (t_{eq}) will usually be obtained when the hole (and stiffener) spacing is the closest permissible value, provided the hole spacing criterion given in (step 1b) is satisfied. The procedure to be followed is outlined in example (4).

EXAMPLES:

1. Consider a formed channel rib that is part of a wing flap.

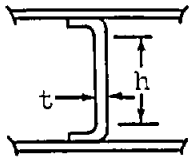

Design q = 300 lbs./in.

h = 6 in., t = .032 in.

material 7075-T6, F_{su} = 45000 psi

Can lightening holes be incorporated in this lightly loaded rib to reduce its overall weight?

The desired allowable stress is:

$$F_s = \frac{q}{t} = \frac{300}{.032} = 9375 \text{ psi}$$

$$\frac{h}{t} = \frac{6}{.032} = 187.5$$

$$F_o = 8100 \text{ psi (Fig. 1b)}$$

Substitution into Equation (1) yields:

$$K_1 = \frac{F_s}{F_o} = \frac{9375}{8100} = 1.16$$

The maximum possible value of K_1 = 0.81 (from Fig. 1a)

Therefore, the magnitude of the design shear does not allow for lightening holes. A lighter web design could be obtained by providing uprights and checking the rib as a diagonal tension beam. Section B6.12.20-1.

2. If, in the above example, access holes are required through the web, the following procedure should be followed in order to find the optimum web thickness, hole size and spacing.

①	②	③	④	⑤	⑥	⑦	⑧	⑨	
t in.	$\frac{h}{t}$	F_o psi	$K_1 = \frac{q/t}{F_o}$	$\frac{D}{h}$	$\frac{D}{b}$	.785 $\frac{D}{h}\frac{D}{b}$		$t_{eq.\ wt.}$ inches	
	$\frac{6}{①}$	Fig.1b	$\frac{300}{① \times ③}$	(1)	(1)	.785 ⑤ ⑥	1-⑦	$\frac{① \times 8}{\text{Eq. (6)}}$	
.032	187	8100	1.16	-	-	-	-	-	
.040	150	9800	.765	.270	.500	.106	.894	.0358	← lightest
.050	120	12000	.500	.490	.600	.231	.769	.0385	
.064	94	15000	.313	.625	.675	.332	.668	.0427	

Note: (1) The values of $\frac{D}{h}$ and $\frac{D}{b}$ are determined from the intersection of the K_1 value tabulated in col. ④ with the optimum K_1 factor curve given in Fig. 1a.

For the lightest web design,

$t = .040$ in.

$D = .270 \times h = .270 \times 6 = 1.62$ in.

$$b = \frac{h}{.500} = \frac{1.62}{.500} = 3.24 \text{ in.}$$

Let D = 1.75 in., Standard Grumman lightening hole G-H11F-16.

Then,

$$\frac{D}{h} = \frac{1.75}{6.0} = .292$$

$F_o = 9800$ psi

$K_1 = .765$

} From the above table.

$$\frac{D}{b} = .44 \text{ (Fig. 1a)}$$

$$b = \frac{1.75}{.44} = 3.98 \text{ in.}$$

If larger access holes are required, one of the thicker webs could be substituted with only a slight weight increase. If the access holes are in a localized area, the overall weight can be reduced by providing stiffeners outside this area and chem-milling the web. This portion of the rib should be checked by the method outlined in B6.12.20-1.

3. Consider the following shallow beam.

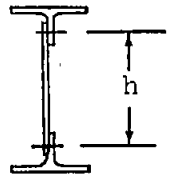

Design q = 600 lbs./in.
h = 3.0 in.
t = .050 in.
material 7075-T6, $F_{su} = 45000$ psi

Determine the optimum hole size and spacing. Check the riveting requirements.

$$F_s = \frac{q}{t} = \frac{600}{.050} = 12000 \text{ psi}$$

$$\frac{h}{t} = \frac{3}{.050} = 60$$ Therefore, $F_o = 22300$ psi (Fig. 1b)

Substitution into Equation (1) yields:

$$K_1 = \frac{F_s}{F_o} = \frac{12000}{22300} = .538$$

$\frac{D}{h} = .465$

$\frac{D}{b} = .590$

} Optimum K_1 factor curve, Fig. 1a

Then, $D = .465 \times 3.0 = 1.395$ in.

$$b = \frac{1.395}{.590} = 2.360 \text{ in.}$$

Grumman standard lightening holes

G-H11F-12 D = 1.25 in.
G-H11F-14 D = 1.50 in.

Either hole diameter could be used with the appropriate spacing, b.

Let D = 1.50 in.

$\frac{D}{h} = \frac{1.50}{3.0} = 0.50$ in. $\frac{D}{b} = .55$ (corresponding to $K_1 = 0.538$, from Fig. 1a)

$$b = \frac{D}{.55} = \frac{1.50}{.55} = 2.73 \text{ in.}$$

$$q_{\text{allow.}} = K_1 F_o t$$

$$q_{\text{allow.}} = .538 \times 22300 \times .050 = 600 \text{ lbs./in.}$$

$$\text{M.S.} = \frac{600}{600} - 1 = .00$$

Web-to-flange riveting, Equation (5)

$$q_r = 1.25\, q = 1.25 \times 600 = 800 \text{ lbs./in.}$$

$$q_r = .67 \left[\frac{2.73}{2.73 - 1.50} \right] 600 = 895 \text{ lbs./in.}$$

Use MS 20470 - DD5 Rivets at 3/4 inch spacing.

$$q_{allow.} = \frac{815}{.750} = 1085 \text{ lbs./in. (From MIL-HDBK-5)}$$

$$M.S. = \frac{1085}{895} - 1 = + .21$$

Net web shear check, Equations (2), (3), and (4)

$$\left[\frac{b}{b - D}\right] = \frac{2.73}{2.73 - 1.50} = 2.23$$

$$\left[\frac{h}{h - D}\right] = \frac{3.0}{3.0 - 1.50} = 2.0$$

$$f_s \text{ net -2} < f_s \text{ net -1} = \frac{600}{.050} \times 2.23 = 26800 \text{ psi} < 45000 \text{ psi}$$

$$K_r = \left[\frac{s - d}{s}\right] = \frac{.750 - .156}{.750} = .792$$

$$f_{s \text{ net -3}} = \frac{q}{K_r t} = \frac{600}{.792 \times .050} = 15180 \text{ psi} < 45000 \text{ psi}$$

4. Consider the following deep beam used to form the closure spar on a wing. Three circular access holes, 5 inches in diameter, are required in an area where the design shear flow equals 1000 lbs./in. The beam height is 12 inches. Determine the web thickness, required stiffener area and spacing.

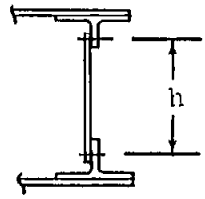

Design q = 1000 lbs./in.
h = 12 in.
D = 5 in. G-H11F-50
Material 7075-T6, F_{su} = 45000 psi

Assuming the closest allowable hole (and stiffener) spacing, Equation (7) yields:

$$\left[\frac{D}{b_s}\right] = 0.85 - 0.1\left[\frac{h}{b_s}\right]$$

$$\frac{5}{b_s} = 0.85 - \frac{(0.01)\ (12)}{b_s}$$

$$b_s = \frac{5 + 1.2}{0.85} = 7.3 \text{ in.}$$

The following procedure is used to obtain the lightest web thickness.

①	②	③	④	⑤	⑥	
t in.	$\frac{b_s}{t}$	F_o psi	K_2	F_s psi	f_s psi	
	$\frac{7.3}{①}$	Fig.1b	Fig.2	$\frac{③ \times ④}{\text{Eq. (11)}}$	$\frac{1000}{①}$	
.072	101	14000	.85	11900	13900	
.081	90	15600	.79	12300	12350	← lightest
.091	80	17400	.73	12700	11000	
.102	71.5	19200	.67	12900	9800	

For the lightest web design, t = .081 in. & $\frac{h}{t} = \frac{12}{.081} = 148$

$$\text{M.S.} = \frac{F_s}{f_s} - 1 = \frac{12300}{12350} - 1 = .00$$

Required stiffener area is determined from Equation (8)

$$A_{o\ min.} = b_s\, t \left[.385 - .08 \left[\frac{b_s}{h} \right]^3 \right] = 7.3 \times .081 \left[.385 - .08 \left[\frac{7.3}{12} \right]^3 \right]$$

$$A_{o\ min.} = .217 \text{ in.}^2$$

Let t_o = .102 in. From Table I, the largest allowable width of stiffener legs is:

$$b_{o1} = 9 \times t_o = 9 \times .102 = .92 \text{ in.}$$

$$b_{o2} = 12 \times t_o = 12 \times .102 = \underline{1.22 \text{ in.}}$$

$$A_o = 2.14 \times .102 - .218 \text{ in.}^2$$

Therefore, O.K.

Required stiffener moment of inertia is given by Equation (9).

$$I_{o\ min.} = \frac{F_s\, t\, b_s\, h^3}{10^8\ (h-D)} = \frac{12350 \times .081 \times 7.3 \times 12^3}{10^8 \times (12 - 5)} = .0180 \text{ in.}^4$$

The assumed stiffener inertia is computed by Equation (10)

$$I_o = \frac{.102 \times 1.223^3\ (4 \times .918 + 1.223)}{12\ (.918 + 1.223)} = .0356 \text{ in.}^4; \text{ therefore O.K.}$$

Web-to-flange riveting, Equation (12)

$$q_r = 1.25\ F_s\ t\left[\frac{h}{h-D}\right] = 1.25 \times 12350 \times .081 \times \frac{12}{12-5}$$

$$q_r = 2140 \text{ lbs./in.}$$

Use a double row of MS 20470-DD6 rivets at 1-1/16 inch spacing.

$$q_{allow.} = \frac{2 \times 1180}{1.0625} = 2230 \text{ lbs./in. (From MIL-HDBK-5)}$$

$$M.S. = \frac{2230}{2140} - 1 = + .04$$

Web-to-stiffener riveting is obtained from Table II. Use MS 20470-AD6 rivets at 7/8 inch spacing.

Flange-to-stiffener load, Equation (13)

$$P_{st} = \frac{.0024 \times .218 \times 12350 \times 7.3 \times 12}{.081 \times (12-5)} = 1000 \text{ lbs.}$$

Use 2 MS 20470-DD6 Rivets.

$$P_{st\ allow.} = 2 \times 1180 = 2360 \text{ lbs. (From MIL-HDBK-5)}$$

$$M.S. = \frac{2360}{1000} - 1 = + 1.36$$

Equivalent weight thickness of web is given by Equation (15)

$$t_{eq} = .081 \left[1 - \frac{785 \times 5^2}{12 \times 7.3} + \frac{.218}{7.3 \times .081}\right]$$

$$t_{eq} = .081 \left[1 - .224 + .369\right] = .081 \times 1.145 = .0926 \text{ in.}$$

ULTIMATE ALLOWABLE GROSS SHEAR STRESS FOR ALUMINUM ALLOY WEBS
WITH GRUMMAN STANDARD FLANGED HOLES
G-H11F

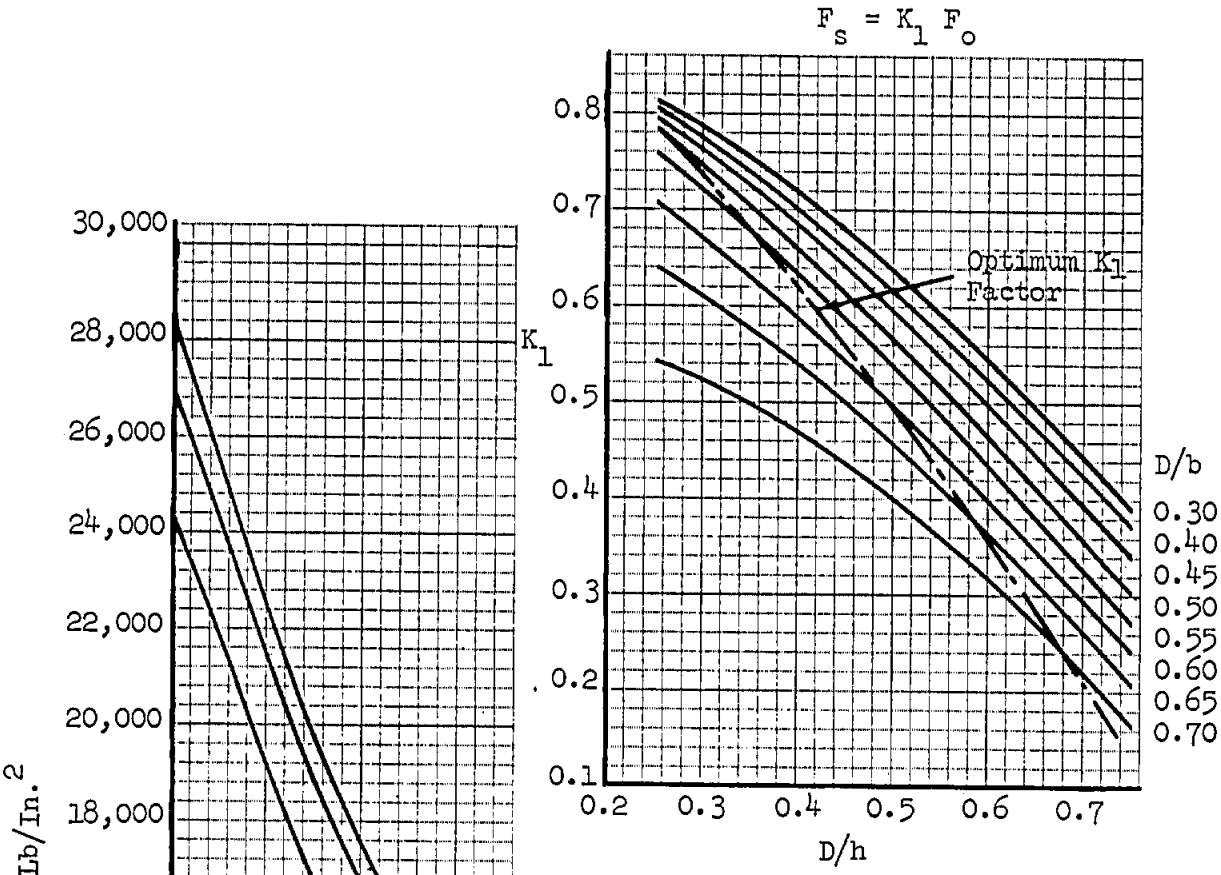

Fig. 1a

Fig. 1b

CORRECTION FACTOR K_2 FOR
ALUMINUM ALLOY WEBS WITH STIFFENERS AND
GRUMMAN STANDARD LIGHTENING HOLES
G-H11F

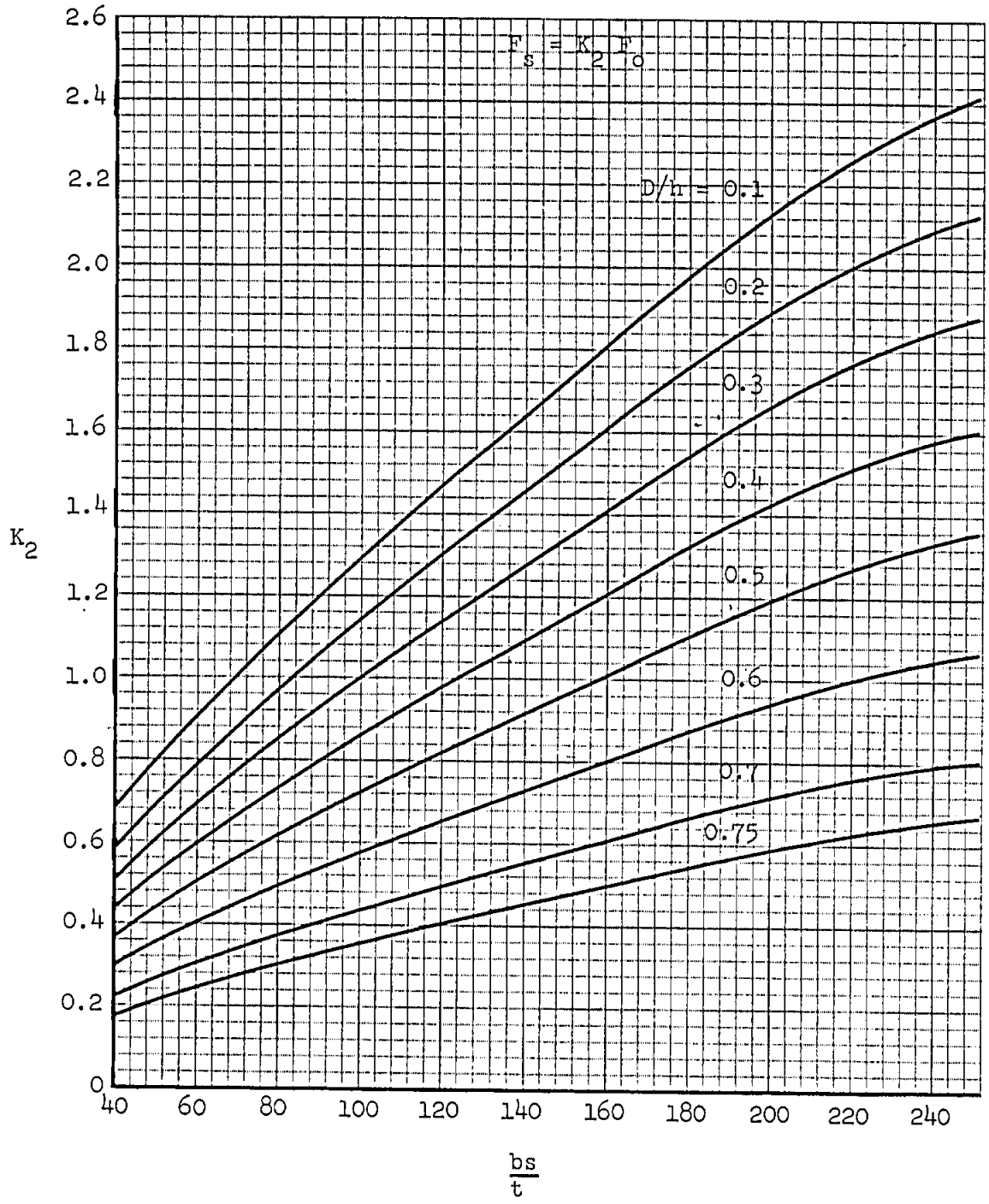

Fig. 2

STRENGTH OF RIB CUTOUTS

Assume this to be a pinned-clamped column with uniformly applied load.

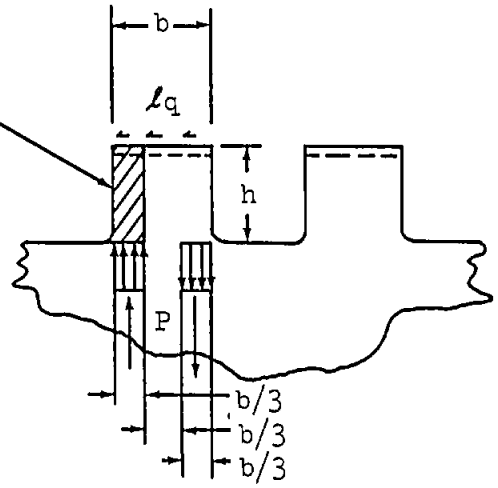

Allowable shear loadings are as follows:

Based on Buckling:

$$q = 7.83 \times 10^6 \frac{bt^3}{h^3}$$ (Ref. Timo, "El. Stab.", p.122)

Based on Compressive Yield:

$$q = .222 F_{c_y} \frac{bt}{h}$$

DESIGN CHARTS FOR STIFFENED PANELS WITH MECHANICALLY ATTACHED STIFFENERS

Data presenting the allowable in-plane biaxial compressive and in-plane shear strength of stiffened panels is given in Reference 1. This reference describes the analysis methods used to obtain the data and describes the stiffener section used.

The results were prepared by actual stress analysis (not Optimum Panel Theory) and account for all critical failure modes for which analysis procedures are available.

Upon request, copies of Reference 1 are available from the Structures Section Administration.

Reference (1), Bunce, F.E., Davidson, A.J., Load Carrying Capabilities of a Series of Stiffened Panels Sbjected to In-plane Biaxial Compressive and In-plane Shear Stresses, Grumman Aerospace Corporation Report SAR-76-4, December 1976.

RIVETED JOINT IN REINFORCED PANEL UNDER COMBINED SHEAR AND TENSION

Applies to portion of loading above buckling where sheet is conservatively assumed to act like a membrane

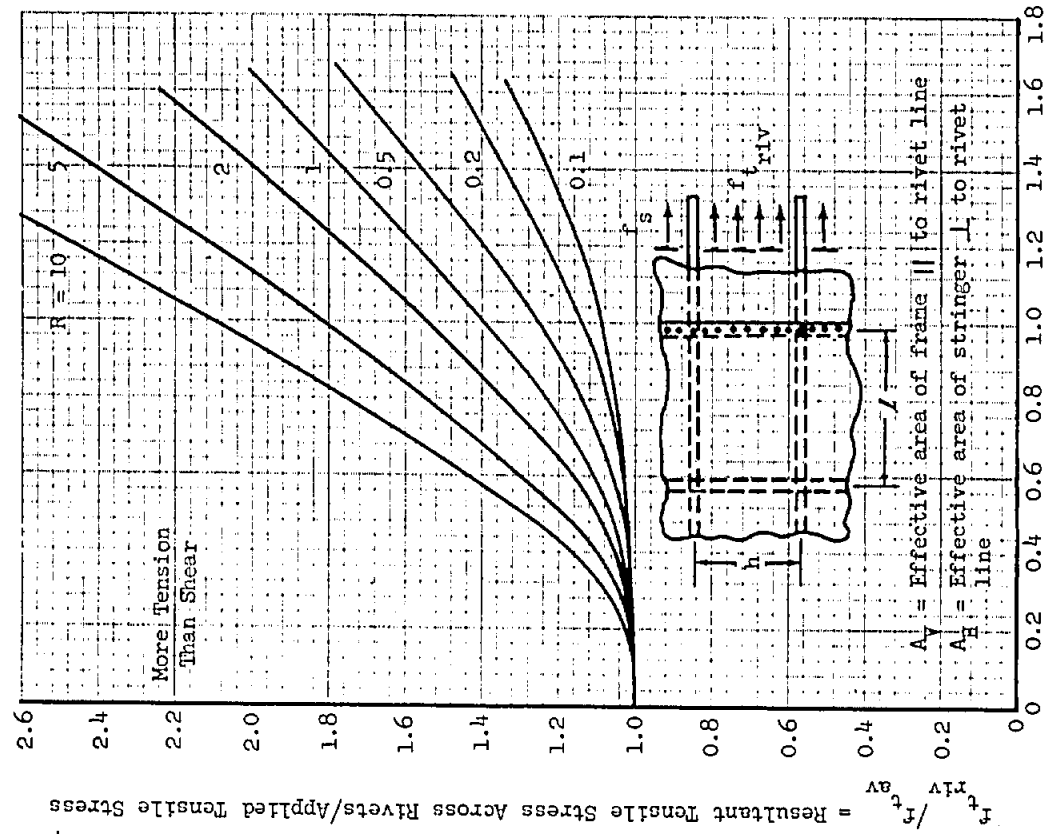

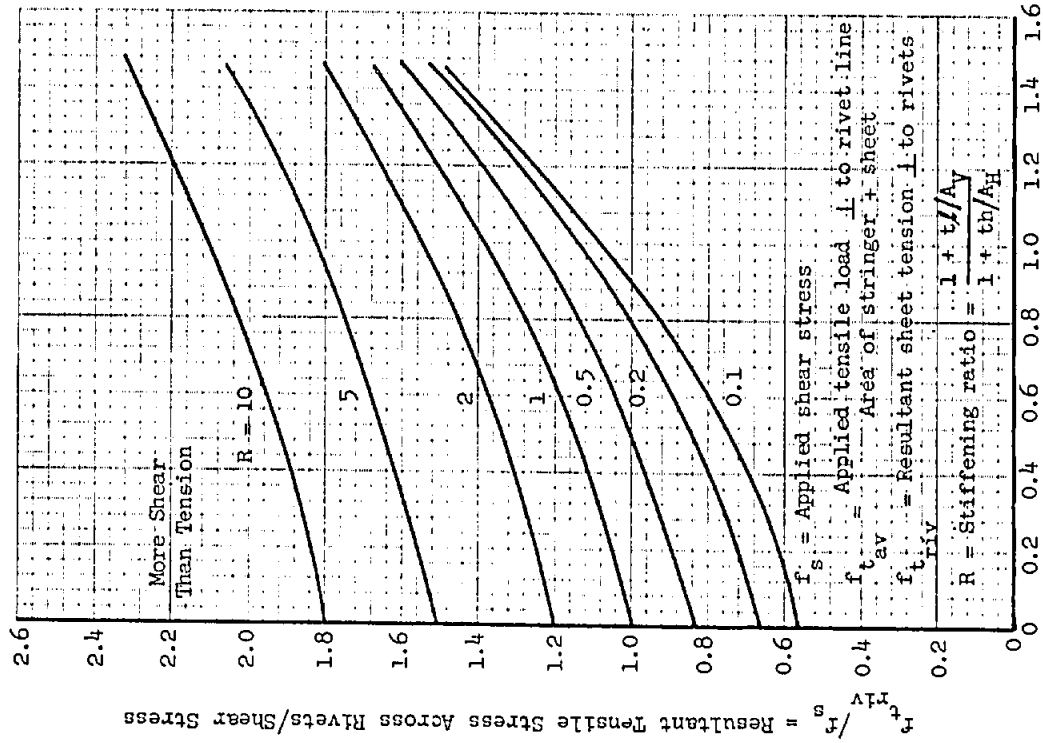

COMPRESSIVE BUCKLING OF A GRID OF STRINGERS AND RIBS

Edges are Simply Supported

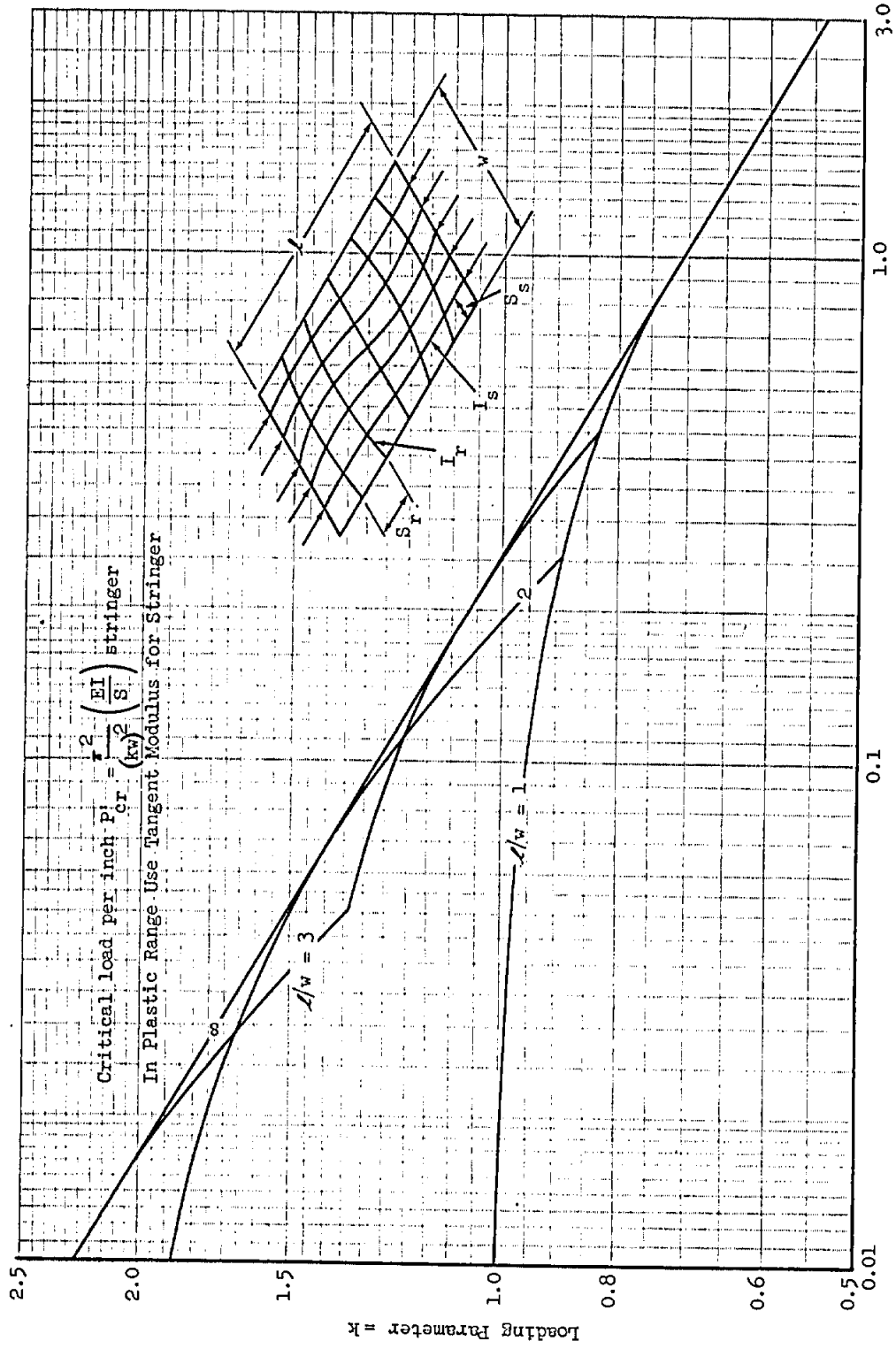

SECTION B7 - FATIGUE

TABLE OF CONTENTS

SECTION B7.030

STRUCTURAL DESIGN FOR FATIGUE

Discussion

This section discusses the general problems of structural fatigue and presents two methods of fatigue life prediction. The method described on pages B7.030-8 through B7.030-26, referred to as the stress-cycling method, has been used on many Grumman designs and has been found to correlate well with fatigue test data in the mid to long life region, It is particularly suited to fatigue life prediction of transport type airplanes, where most of the fatigue damage is due to gust loading and low 'g' maneuvers in the low-stress/high cycle range. The computation procedures are simple and fatigue life predictions for spectra of reasonable length can be quickly performed by hand calculations. A computer program is also available, and is listed on page B7.030-44 under the title "STRESSLF".

The second fatigue life prediction method currently in use at Grumman is referred to as the strain-cycling method, and is described in detail on pages B7.030-27 through B7.030-43.

The general features of the strain-cycling fatigue analysis method are similar to those of the stress-cycling method, but the two methods differ in detail. Basic inputs to the strain cycling method are cyclic stress-strain (S-ϵ) curves rather than monotonic stress-strain curves and cyclic strain-life (ϵ-N) curves rather than cyclic stress-life (S-N) curves. In addition, stress-strain behavior at a notch is approximated by use of a plastic stress concentration factor. The analysis procedure is somewhat more complex than that of the stress-cycling method, but generally results in improved accuracy, especially in the high-stress/low-cycle region. Tabulated forms ENG 818.2 are available for hand calculation, but the strain cycling method is basically suited to computer application and related available programs are listed on page B7.030-44.

REFERENCES

1. Rhode, R. V. and Donely, P.: Frequency of Occurrence of Atmospheric Gusts and of Related Loads on Airplane Structures - NACA WR.L-121, 1944.

2. Military Specification: Airplane Strength and Rigidity Reliability Requirements, Repeated Loads and Fatigue - MIL-A-8866 (ASG), 18 May 1960.

3. Detail Requirements and Status: Air Force Structural Integrity Program - ASD-TN-61-141, Parts 1 & 2, 1963.

4. Military Specification: Airplane Strength and Rigidity Ground Tests - MIL-A-8867 (ASG) 18 May 1960.

5. R. E. Peterson: Stress Concentration Design Factors - John Wiley & Sons Ltd., New York, 1953.

6. G. H. Neugebauer: Stress Concentration Factors and Their Effect on Design - Product Engineering, February 1953.

7. Raymond J. Roark: Formulas for Stress & Strain - McGraw-Hill, New York, 1954.

8. Royal Aeronautical Society Data Sheets on Fatigue, October 1963.

9. Neuber, Heinz: Theory of Notch Stresses: Principals for Exact Stress Calculation - J. W. Edwards (Ann Arbor), 1946.

10. Illg, W.: Fatigue Tests on Notched & Unnotched Sheet Specimens of 2024-T3 & 7075-T6 Aluminum Alloys and of SAE 4130 Steel with Special Considerations of the Life Range from 2 to 10000 cycles NACA-TN-3866, December 1956.

11. Peterson, John G.: Fatigue Behavior of AM-350 Stainless Steel and Titanium 8Al-1Mo-1V Sheet at Room Temperature, 550°F and 800°F - NASA CR-23 (Contractor Report), May 1964.

12. Determination of Design Data for Heat Treated Titanium Alloy Sheet - ASD-TDR-62-335, Volume 3, 1964.

13. Ti-6Al-4V - Titanium Sheet Alloys - Titanium Metals Corporation of America, Bulletin No. 2.

14. Metallic Materials & Elements for Flight Vehicle Structures - MIL - Handbook 5, August 1962.

15. Miner, Milton A.: Cumulative Damage in Fatigue - J. App. Mechanics, 12 September 1945 - p. 159 - 164.

REFERENCES (CONT'D)

16. Results of Spectrum Testing through A6A & BuWeps Positive Maneuver Spectrum - GAEC Report No. 128MT217 1964.

17. Hooson, R. E. - Summary of Fatigue Design Calculation & Test Data on GAEC Airplanes, GAEC Report E206, 1964.

18. Kuhn, Paul & Figge, I. E. - Unified Notch Strength for Wrought Aluminum Alloys, NACA TN D1259, 1964.

19. Grover, H. J. Bishop, S. M. & Jackson, L. R. - Axial Load Fatigue Tests on Notched Sheet Specimens of 24S-T3 & 75S-T6 Aluminum Alloys & of SAE 4130 Steel with Stress Concentration Factors of 5.0, NACA TN 2390, June 1951.

20. Kuhn, Paul & Hardrath, H. F. - An Engineering Method for Estimating Notch Size Effect. NACA TN 2805, October, 1952.

21. Grover, H.J., Hyler, W. S. & Jackson, L. R. - Axial Load Fatigue Tests on Notched Sheet Specimens of 24S-T3 & 75S-T6 Aluminum Alloys & of SAE 4130 Steel with Stress Concentration Factor of 1.5, NACA TN 2639, February, 1952.

22. Grover, H. J., Bishop, S.M. & Jackson, L. R. - Axial Load Fatigue Tests on Notched Sheet Specimens of 24S-T3 & 75S-T6 Aluminum Alloys of SAE 4130 Steel with Stress Concentration Factors of 2.0 and 4.0, NACA TN 2389, June, 1951.

23. Hardrath, H. F. & Illg, W. - Fatigue Tests at Stresses Producing Failure in 2 to 10,000 cycles 24S-T3 & 75S-T6 Aluminum Alloy Sheet Specimens with A Theoretical Stress Concentration Factor of 4.0,

24. Stowell, E. Z. - Stress & Strain Concentration at a Circular Hole in an Infinite Plate, NACA TN 2073, April, 1950.

25. Smith, R. W. Hirshberg, M. H. & Manson, S. S. - Fatigue Behavior of Materials Under Strain Cycling in Low & Intermediate Life Range, NACA TN D.1574, April, 1963.

26. Sines, G. & Waisman, J. L. - Metal Fatigue, McGraw-Hill, New York, 1959.

27. Grover, H.J., Gordon, S. A. & Jackson, L.R. - Fatigue of Metals & Structures, NAVAER 00-25-534, U. S. Government Printing Office, 1954.

28. Ripp, F., Gomza, A. & Adee, T. - Calculation of Fatigue Life by Grumman Method & Comparison with Test Data, GAEC Report GE 168, February, 1959.

29. Heitzmann, R.J. - Effect of Decarburization and Surface Defects on the Notched Fatigue Strength of Steel, GAEC Report ADN 02-01-65.1.

REFERENCES (CONT'D)

30. Stress Memo No. 64-SAM-4, December 3, 1964.

31. Spectrum Fatigue Tests on Specimens with $K_t = 2.5$ and $K_t = 4$. GAEC Structures Development Memo No. 3, January 1965.

32. Hill H. N. & Eaton I. D. Effect of Discontinuities on the Fatigue Strength of 7075-T6 Pin Loaded Lugs. Alcoa Research Laboratories, Report No. 12-60-42 Vellums on File GAEC Engineering Library, Serial No. 4032.

33. Kelsey, A.S. - Fatigue Damage Caused by Loading Distribution. GAEC Report No. GE200, November, 1963.

34. Raynor, G. T. "Spectrum Interpretation Effect on Fatigue Life Prediction", Grumman Aerospace Corporation Report No. 74 SAM-6, December 16, 1974

35. Manson, S.S., and Hirshberg, M.H., "Fatigue Behavior in Strain Cycling in the Low and Intermediate Cycle Range." 10th Sagamore Army Materials Research Conference, August 1963

36. Hardrath, H.F., and Ohman, L., "A Study of Elastic and Plastic Stress Concentration Factors Due to Notches and Fillets in Flat Plates", NACA Report 1117, 1953

37. Silverman, B.S., Hooson, R.E., and Saleme, E. "Fatigue Prediction Methods Based on Strain Cycling", GAC Report No. FSR-AD2-01-68.3, May 1968

38. Ranalli, E.R. "Unified Analytic Fatigue Prediction Method", Unpublished work, Feb. 1964

39. Abcug, I. "Fatigue Prediction Method Based on Strain", GAC IOM No. A51-313-I-69-7, 14 July 1969

40. Neuber, H. "Theory of Notch Stresses: Principals for Exact Calculation of Strength with Reference to Structural Form and Material", AEC-TR-4547, 1961.

41. Endo, T. and Morrow, J.D. "Monotonic and Completed Reversed Cyclic Stress-Strain and Fatigue Behavior of Representative Aircraft Materials" Report No. NAEC-ASL-1105, June 1966.

42. Jaske, C.E.. et al "Analysis of Fatigue, Fatigue Crack Propagation, and Fracture Data" NASA CR-132332, Nov. 1973

43. SAR-76-1 Call Data 360/67 Fatigue Prediction by Stress Method C. Lee, G. Raynor 4/9/1976

44. SAR-76-2, Call Data 360/67 Fatigue Prediction by Strain Method, C. Lee, G. Raynor 6/1976

LIST OF SYMBOLS

A - material constant in Neuber formula.

F - allowable stress, psi

f - nominal average stress, psi

f_N - stress at edge of hole or notch, psi

f_{Nel} - stress at edge of hole or notch in a perfectly elastic material, psi

K_N - Neuber stress concentration factor

K_T - theoretical elastic stress concentration factor

N - allowable number of cycles - number of cycles to failure for a given stress range

n - number of cycles applied

N_{yy} - number of cycles to failure at stress range of + yield to - yield

N_{zu} - maximum load factor, G's

N_{zL} - minimum load factor, G's

P - load

R - (1) radius of hole or notch; (2) stress ratio, $\frac{f_{min}}{f_{max}}$

- nominal average strain, in./in.

N - strain at edge of hole or notch, in./in.

ω - flank angle of notch

SUBSCRIPTS

all - allowable

c - compression

el - elastic

max - maximum

min - minimum

mn - mean

N - (1) Neuber; (2) notch

res - residual

t - tensile

u - ultimate

y - yield

A) - DETERMINATION OF APPLIED LOAD SPECTRUM

General

Wing load factors during a typical mission profile for a military airplane are shown qualitatively in Figure 1. From rest, the airplane will taxi, take off and climb, and will then encounter a variety of maneuver and gust loads according to its function.

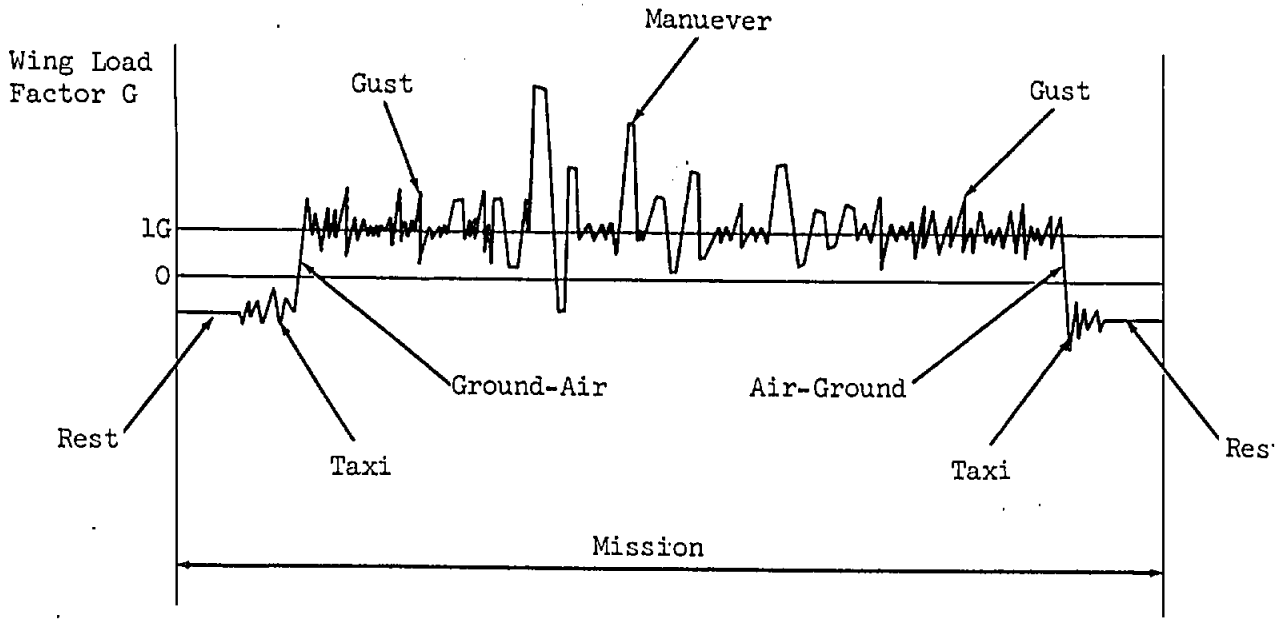

Figure 1.

A military airplane in the attack or fighter category will have a comparatively short service life (perhaps 2500 hours), but will perform relatively severe maneuvers during this time. Fatigue damage due to maneuver loads will generally be much higher than gust damage, and it has in the past been the general practice to design to a spectrum based on the maneuver loads only. This approach has become less valid as the length and complexity of missions has increased. Also, the steady rise in stress level per 'G' and the use of higher strength materials whose fatigue strength, however, has not increased in proportion to their static strength, have all tended to increase the importance of gust fatigue damage, even in fighter aircraft.

Military transports and Civil aircraft in general, are designed for long operating lives (20,000 hours or more). They are not subjected to either the degree or density of maneuver loads normally encountered by a fighter type aircraft, so that gust damage, accumulated over a long period,

is the principal source of fatigue damage to the wing structure. Consideration of pressure cabin fatigue is also of major importance.

Flight Conditions

From data collected by the NASA, the military services, and other sources, it is possible to estimate the intensity and the frequency of gust loads and maneuver loads that an aircraft will experience in a given number of flight hours. Ref. 1 is one of the original references for data of this type. Using these data, flight load spectra have been obtained for various types of aircraft.

The data for military aircraft have been summarized in various military specifications. Mil. Spec. 8866-A (Ref. 2) covers loads and fatigue requirements for military airplane structures and includes the required service lives for various types of Navy aircraft. Because fatigue design and analysis must include consideration of the probable scatter in the fatigue lives of identically manufactured structures, a safety factor should be used on the required service life of the airplane, in order to obtain a reasonably safe design life. Reference 2, Para. 3-1 states that, for Navy procured airplanes, a scatter factor of at least 2.0 on the required service life should be used in design, in lieu of specifically applicable data.

Fatigue requirements for airplanes procured by the Air Force are usually specified for each particular design, but Reference 3 states that a full scale test program shall demonstrate a duration of 4 times the service life.

Flight load spectra for new types of military aircraft not adequately covered by existing specifications are generally arrived at through negotiation with the purchasing agency.

Commercial airplanes are designed for long operating lives, and there are at present no hard and fast rules regarding scatter factors for safe life designs, each commercial type being considered as an individual problem. Fatigue design requirements are negotiated with the Federal Aviation Agency, and extensive full-scale fatigue testing is usually required in addition to calculations.

The Applied Loads Group is primarily responsible for the determination of flight load spectra on any airplane and should be consulted for specific information.

Landing, Catapulting, and Arresting Loads

The frequency of occurrence of various landing sink speeds, which can be expected to occur during the life of an airplane, may be obtained from Reference 2, Table IV, which gives a distribution of sinking speeds per 1000 landings.

This can be used as a basis of fatigue spectra for various parts of a landing gear, and for other parts of the structure affected by landing loads.

Catapult and arresting frequencies are specified in Table 1 of Reference 2, and Reference 4 gives test spectra simulating catapult and arresting loading to which the structure must be subjected.

Ground-Air-Ground Cycle

This combination of conditions, indicated in Figure 1. occurs on take off, and in reverse order on landing. The stress reversals which occur during this operation contribute a significant element of fatigue damage.

Mechanical Operation Loads

Frequency of loading for such items as doors, wing fold mechanisms, controls etc. must include any impact loading which may occur during the operation of such devices.

The frequency of occurrence of loads of this nature must be determined by consideration of the basic planned usage of the airplane.

B - CALCULATION OF STRESSES AT POINTS OF STRESS CONCENTRATION

The Grumman procedure for the calculation of fatigue life is based on the use of smooth, unnotched specimen data, which is provided on pages B7.031-1 through B7.031-12. In a case where no stress concentration is present, and the stress distribution is known, the curves provided can be used directly to determine the fatigue life.

When a notch or some other point of stress concentration is present, it is necessary to determine the peak stress at the point of stress concentration, and also to determine the range of this stress as the loading is varied. It is assumed that the notched part will have the same fatigue life as a plain, unnotched specimen that is stressed through this same range of stress. This concept allows the fatigue lives of notched parts to be determined from unnotched fatigue data.

Stress Concentration Factors

Theoretical elastic stress concentration factors, K_T, have been determined mathematically for some cases and have been closely approximated by photoelastic methods for other cases. Values are given in Section B7.040 of the Manual and in References 5 through 8. The use of theoretical elastic stress concentration factors in calculating peak stresses at a hole or notch in actual structural members is usually conservative, since the factors have been obtained on the assumption that the material is perfectly homogeneous and elastic, whereas actual engineering materials have a granular structure which tends to reduce the effective stress concentration factor. Neuber (Ref. 9), proposed that the material structure be considered as an aggregate of building blocks, of 'radius' A, where A is a different constant for different materials. Based on the assumption that no stress gradient could develop across such a block, Neuber derived an effective elastic stress concentration factor, K_N, generally called the Neuber Factor, which is given by the formula:

$$K_N = 1 + \frac{K_T - 1}{1 + \frac{\pi}{\pi - \omega}\frac{\sqrt{A}}{\sqrt{R}}} \qquad (1)$$

where

K_T = Theoretical elastic stress concentration factor

ω = Flank angle of a notch, in radians (ω = 0 for holes and notches with parallel sides, see figure 2)

R = Radius of hole, or radius at bottom of notch (inches)

A = Material constant, (inches) see pg B7.030-26

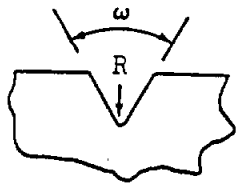

Figure 2.

The material constant, A, is generally obtained by comparing the endurance strengths of notched and unnotched fatigue test specimens of the same material. Values of $\sqrt{A}$ are given on page B7.030-26 for aluminum and steel alloys. It should be noted that the Neuber correction is considerably smaller for steel than for aluminum alloy, especially for the higher strength steels where the A value is very small.

Stresses at Point of Stress Concentration

If all stresses are elastic, the stress f_N at the point of stress concentration is:

$$f_N = f_{Nel} = K_N f \qquad (2)$$

where f is the nominal average stress applied to the section.

When the stress at the point of stress concentration exceeds the elastic limit (nominally defined as the yield stress), equation (2) can no longer be used to determine f_N. Instead, it is assumed that the strain at the point of stress concentration can be determined as follows:

$$\epsilon_N = K_N \epsilon \qquad (3)$$

where ϵ is the strain corresponding to the nominal average stress applied to the section. Equation (3) is not exact but is sufficiently accurate

for our analysis method (more accurate values of ϵ_N can be obtained from Ref. 24). The value of f_N corresponding to ϵ_N can now be obtained from a stress-strain curve of the material as shown in Fig. 3a. If a simplified stress-strain diagram as shown in Figure 3b is assumed, then f_N cannot exceed F_y. The use of this simplified stress-strain diagram simplifies subsequent fatigue life calculations and is, in many cases, a reasonable assumption.

In both figures the value of f_N that would have been attained if the material were completely elastic is shown by f_{Nel}.

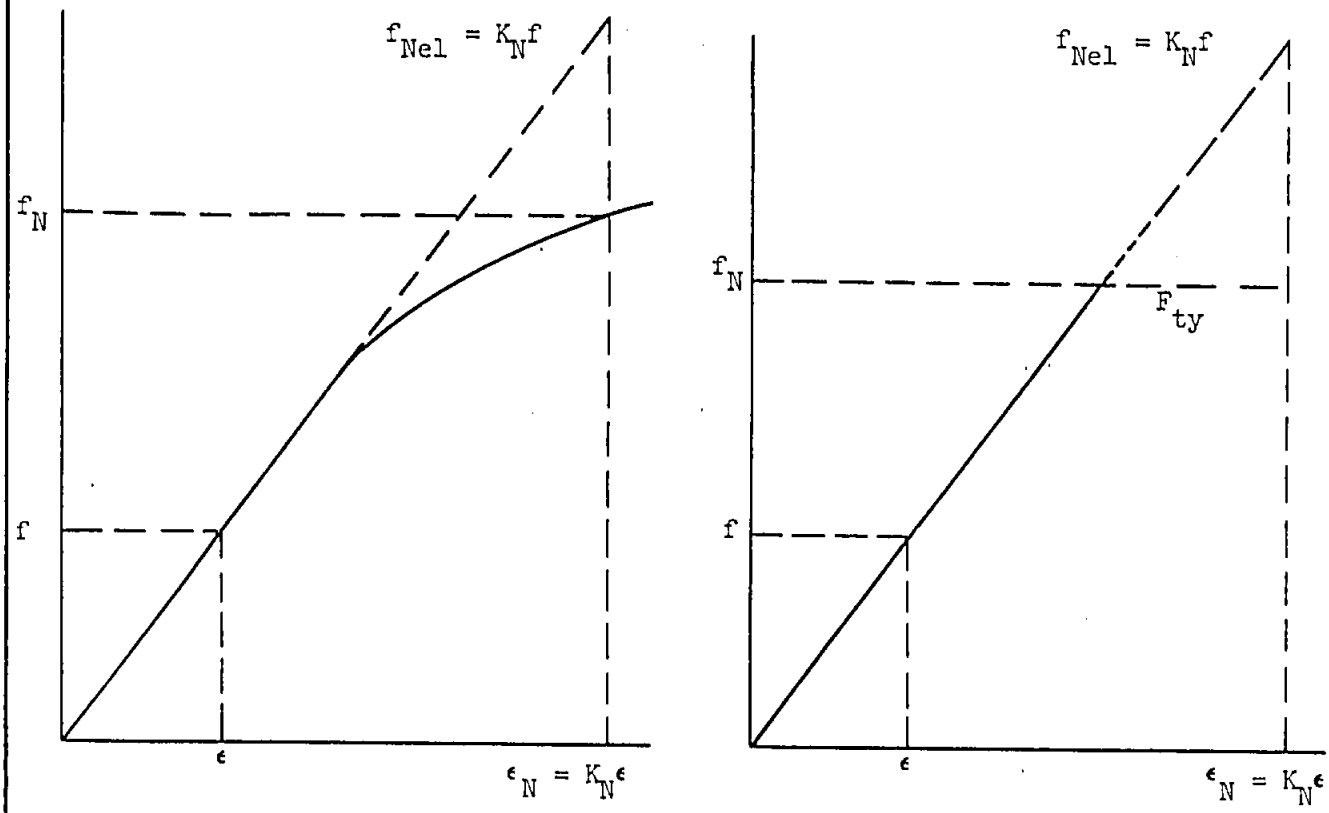

Figure 3.

If, after initial loading, the load is decreased to some lower value, the stresses and strains are assumed to decrease elastically throughout the entire section. Therefore, the resulting stress at a point of stress concentration is:

$$f_N = f_{Nmax} - K_N \Delta f \tag{4}$$

where f_{Nmax} = the maximum value of f_N attained during the initial loading, psi

Δf = the decrease in the value of nominal applied stress from the peak value, f_{max}, attained during the initial loading, psi

For the special case where the stresses, during loading and unloading, have nowhere exceeded the elastic limit, the value of f_N obtained by equations (2) and (4) will be identical, and equation (2) can be used throughout the loading and unloading cycle.

For the case where the material stress-strain curve is similar to that shown in Figure 3b, equation (4) takes the following form, if f_{Nmax} has exceeded the elastic limit during initial loading:

$$f_N = F_{ty} - K_N \cdot \Delta f \tag{4a}$$

If the part is completely unloaded, then $\Delta f = f_{max}$ and the resulting residual stress at the notch, designated by f_{Nres}, is:

$$f_{Nres} = F_{ty} - K_N f_{max} \tag{4b}$$

Since $K_N f_{max}$ is greater than F_{ty}, the resulting residual stress will be of opposite sign to the original applied stress.

Figure 4 illustrates the stress-strain cycle at the notch in a part that has first been loaded to a nominal stress, f_{max}, where f_{max} is a sufficiently high value to cause yielding at the notch, and then unloaded. The simplified stress-strain curve of Figure 3b. is assumed.

During loading, the nominal stress-strain curve goes elastically from Ⓐ to Ⓑ. At the same time the stress-strain curve at the notch goes from Ⓐ to Ⓒ, first elastically and then plastically.

If the nominal applied stress is decreased by Δf, the nominal stress-strain curve goes back elastically to point Ⓑ' and the stress-strain curve at the notch goes back elastically by an amount $K_N \Delta f$ to Ⓒ'.

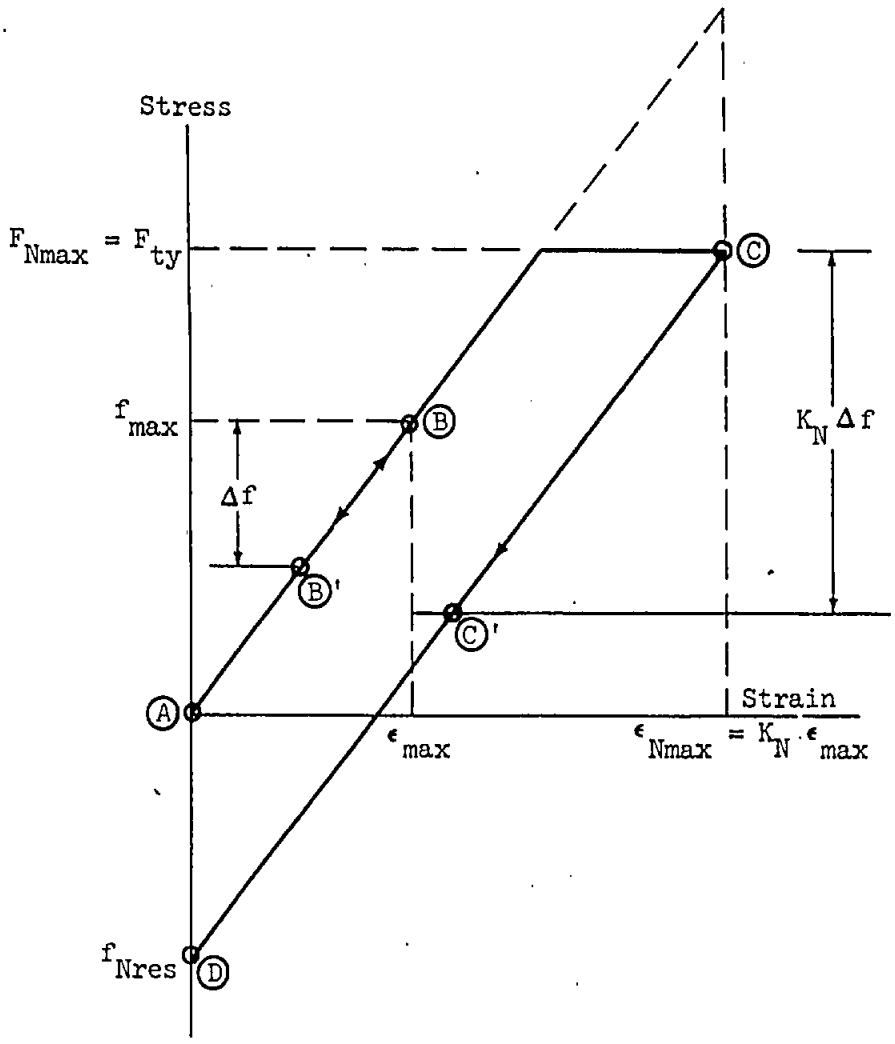

Figure 4.

If the part is then completely unloaded ($\Delta f = f_{max}$) the nominal stress-strain curve returns to point (A) and the stress-strain curve at the notch goes to (D), where f_{Nres} is given by equation (4b).

The notch stress resulting from any subsequent loading or unloading of the part can be determined from a more general restatement of equation (4).

$$f_N = f_N' + K_N \Delta f \qquad (4c)$$

where f_N' = the value of f_N just prior to the loading or unloading, psi

Δf = the change (positive or negative) in nominal applied stress resulting from the loading or unloading, psi

Equation (4c) applies within the elastic range (from compression yield to tension yield).

If any of the subsequent loadings or unloadings cause the stress at the notch to go outside the elastic range, the maximum value of f_N is again limited to $\pm F_{ty}$ if the simplified stress-strain curve of Figure 3b is assumed. If the actual stress-strain curve (Figure 3a) is used, the strains at the notch must be determined, using successive applications of equation (3) to determine the strains at the notch, and the stress-strain curve to determine the stresses.

Examples

The procedure is best illustrated by a series of numerical examples. Consider a simple structural element, as shown in Figure 5., consisting of a 1/8" thick 7075-T6 plate (with F_{ty} = 75000 psi and F_{tu} = 82500 psi) having a circular hole at the center, subjected to a cyclic tensile load P. Assume a simplified material stress-strain curve, as shown in Figure 3b, with the curve horizontal after yield.

Cross sectional area at Ⓐ-Ⓐ = .125 x (3 3/16-1 3/16) = 0.25 sq ins. K_T = 2.27 (Page B7.11.1-1). $\sqrt{A}$ = 0.128 (Page B7.030.-26).

$$K_N = 1 + \frac{2.27-1}{1 + \frac{.128}{\sqrt{.594}}} = 2.09$$

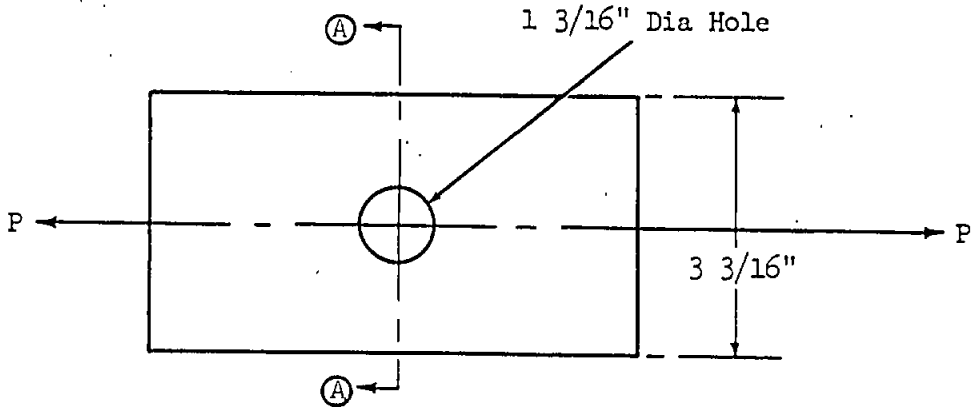

Figure 5.

Case 1: P = 0 to 5000 pounds, and back to 0.

At P = 0, f = 0, f_N = 0.

At P = 5000 lbs, f = f_{max} = 5000/.25 = 20,000 psi.

f_{Nel} = 2.09 x 20,000 = 41,800 psi (eq 2). Since this value of f_{Nel} is less than F_{ty}, all stresses are elastic, and $F_N = f_{Nel}$ = 41,800 psi.

At P = 0, f and f_N both return to 0 stress.

Case 2: P = 0 to 12,000 pounds, then back to 0.

At P = 0, f = 0, f_N = 0

At P = 12,000 lbs, f = f_{max} = 12,000/.25 = 48,000 psi

f_{Nel} = 2.09 x 48,000 = 100,320 psi (eq 2)

However, since the material yields at 75,000 psi, the stresses at the notch are no longer elastic, so that f_N = f_{Nmax} = 75,000 psi.

If an actual stress-strain curve for the material (Fig. 3a) had been assumed instead of the simplified stress-strain curve, equation 3 would be used to determine the strain at the edge of the hole, and the corresponding value of f_{Nmax} determined from the actual stress-strain curve.

At P = 12,000 lbs; ϵ_{max} = 48,000/10.3 x 10^6 = 0.00466 in./in.

ϵ_{Nmax} = 2.09 x 0.00466 = 0.00974 in./in. (eq 3)

The notch stress, f_{Nmax} is then determined from the stress-strain curve.

Now, as the load is decreased to zero, the stresses and strains are assumed to decrease elastically throughout the net section. Equation (4b) is used to determine the final residual stress at the notch when the nominal stress f returns to zero.

f_{Nres} = 75,000 - 2.09 x 48,000 = - 25,320 psi (eq 4b)

The stress-strain cycle at the edge of the hole is traced in Figure 6, starting at the point (A) where the load is zero, then following the stress-strain curve to the point (B) where, at a load of 9000 lbs, yielding first occurs at the edge of the hole.

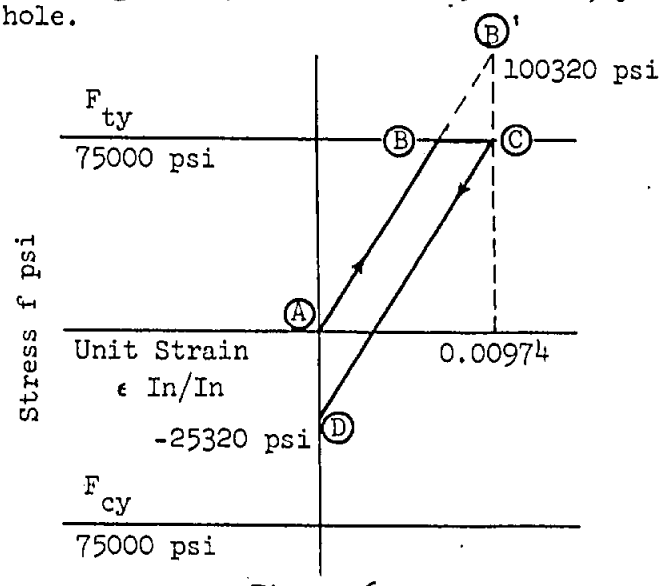

Figure 6.

As the load is increased to 12,000 pounds, the stress-strain cycle continues at constant stress to point Ⓒ, corresponding to the strain of 0.00974 determined from equation 3. (Point Ⓑ represents the maximum stress that would have been reached at the edge of the hole if yielding had not occurred.) As the load is decreased to zero, the stress-strain cycle at the edge of the hole decreases elastically to Ⓕ.

Under the assumptions made, the strains are zero across the entire net section when the load returns to zero.

Case 3: Initial preload of 12,000 pounds, followed by cyclic loading between 0 and 5000 lb.

In this case, the first loading cycle, zero up to 12,000 lb and down to zero, leaves the material at the edge of the hole with a residual compressive stress of -25320 psi. This is the same condition as existed at the end of the cycle in Case 2. When the part is now loaded to 5000 lb, the stresses will all be within the elastic range, so that equation (4C) can be used to determine the increase in stress at the edge of the hole. (f'_N = - 25,320 psi, Δf = 5000/.25 = 20,000 psi)

$$f_N = -25{,}320 + (2.09) \times (20{,}000) = 16{,}480 \text{ psi}$$

Figure 7 shows the cycle, where point Ⓓ is the residual stress left after the 12,000 lb load was removed (this corresponds to point Ⓓ in Figure 5). Loading to 5000 lb takes the stress to point Ⓔ and the material at the edge of the hole then cycles between points Ⓓ and Ⓔ. Therefore, the effect of the 12,000 pound preload is to introduce a 25,320 psi residual compressive stress at the edge of the hole when the preload is removed. Subsequent load cycling between 0 and 5000 pounds results in a stress cycle at the edge of the hole of -25,320 psi to + 16,480 psi. With no preload, the same load cycle resulted in a stress cycle at the edge of the hole of 0 to 41,800 psi (Case 1). The amplitude of the stress range is the same in both cases, but the values of the stresses differ by 25,320 psi, the magnitude of the residual stress.

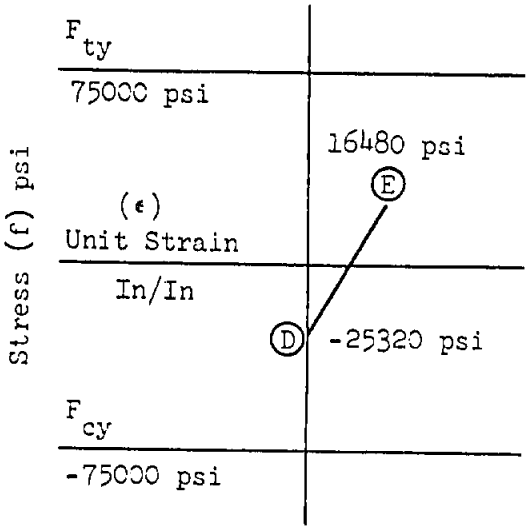

Figure 7.

Effect of Loading Direction on Stress Concentrations

If a part with a stress concentration is subjected to compressive loading, the stress concentration factor may or may not be the same as when it is subjected to tension loading.

A part with an open hole, for example, would have the same K_T for both tensile and compressive loadings. If, however, the hole were filled with a close tolerance bolt or a rivet, the K_T would be applied for tensile loads only, since a compressive load would tend to be uniformly distributed across the entire section.

C) - DETERMINATION OF FATIGUE LIFE AND FATIGUE DAMAGE

Fatigue Test Data

A considerable amount of experimental data on the fatigue properties of various materials are available, and the more commonly used steels and aluminum alloys have been fairly well covered. Information on titanium alloys has been somewhat more limited, but the increasing use of this material has resulted in extensive laboratory testing programs, and a reasonable amount of data now exists, for example, References 11, 12, and 13.

In selecting data to use in a given case, both the form of the material (plate, extrusion, etc.) and the grain direction should be considered The effect of these items is by no means constant for the range of materials. Steel and aluminum do not, for instance, exhibit the same magnitude of fatigue life reduction in the transverse grain direction from the fatigue life in the longitudinal direction.

Fatigue data are generally presented in the form of a stress-life curve, commonly called an S-N curve. There are several variations in the methods of plotting such curves, each of which has its uses.

Wide variations in stress range may be shown on a plot like that on page B7.031-1, called a modified Goodman diagram. Constant minimum stress curves are frequently plotted against maximum stress, as on page B7.031-2 and the effect on fatigue life due to variations in these parameters is readily seen.

Fatigue data have been obtained both for unnotched polished specimens ($K_T = 1$) and for specimens with notches, holes or other discontinuities ($K_T > 1$). This discussion is mainly concerned with unnotched specimen data which are used in the Grumman fatigue life prediction method.

Surface Finish

The quality of the surface finish on a part can have a significant effect on the fatigue life under certain circumstances. Normally accepted standard machine finishes are generally satisfactory. Sub-standard finishes are more likely to reduce the fatigue strength of a notched part if the hole or notch is large, since the area affected by the stress concentration is also relatively large. If the radius of the notch or hole is small (perhaps less than 1/4") the possibility of substantial reduction of fatigue strength is likely to be much less. The effect of surface finish on fatigue strength also varies with the material, the effect being generally greater in steel than in aluminum. In addition, decarburization on the surface of a steel part can reduce its fatigue life significantly, particularly in the long life region (Ref. 29).

A further consideration is that of surface damage incurred during handling and servicing of various components. An unnotched part or one with a small concentration factor may show little or no theoretical fatigue damage in a calculation, but scratches or marks received in service could result in significant local stress concentrations. Reference 30 gives an example of this type of stress concentration factor, and reference 31 shows, on a limited scale, the effect of scratches on the fatigue life of specimens with stress concentrations when scratches are present in the area of the notch. Further investigations in this field are in progress.

Fatigue Symbols and Definitions

Reference 14, paragraph 1.4.9.2, defines the terms in general use in fatigue. Examples of fatigue loadings are shown in Figure 8. below. Most of the terms are self-explanatory and will not be repeated here, but it may be of use to mention the following items specifically:

a) Stress Range (f_r) = The algebraic difference between the maximum and minimum stresses in one cycle, that is, $f_r = f_{max} - f_{min}$.

b) Stress Amplitude (f_a) - This is also known as alternating stress, alternating stress amplitude, or variable stress component. It is half the total stress range, that is, $f_a = 1/2\ f_r$.

c) Stress Ratio (R) - The algebraic ratio of the minimum stress to the maximum stress in one cycle, $R = \frac{f_{min}}{f_{max}}$.

d) Endurance Limit or Fatigue Limit - The limiting value of the maximum stress below which a material can presumably endure an infinite number of stress cycles. At this value, the stress vs. life curve for a material becomes essentially horizontal for most structural materials. The endurance limit is usually specified for R = 0. If not, it is necessary to indicate the value of the stress ratio for which the endurance limit is given. For many materials the endurance limit is reached between 10^6 cycles and 10^7 cycles of stress. It should be noted that for certain materials there is no fatigue limit, and the fatigue strength decreases continually as the number of cycles is increased.

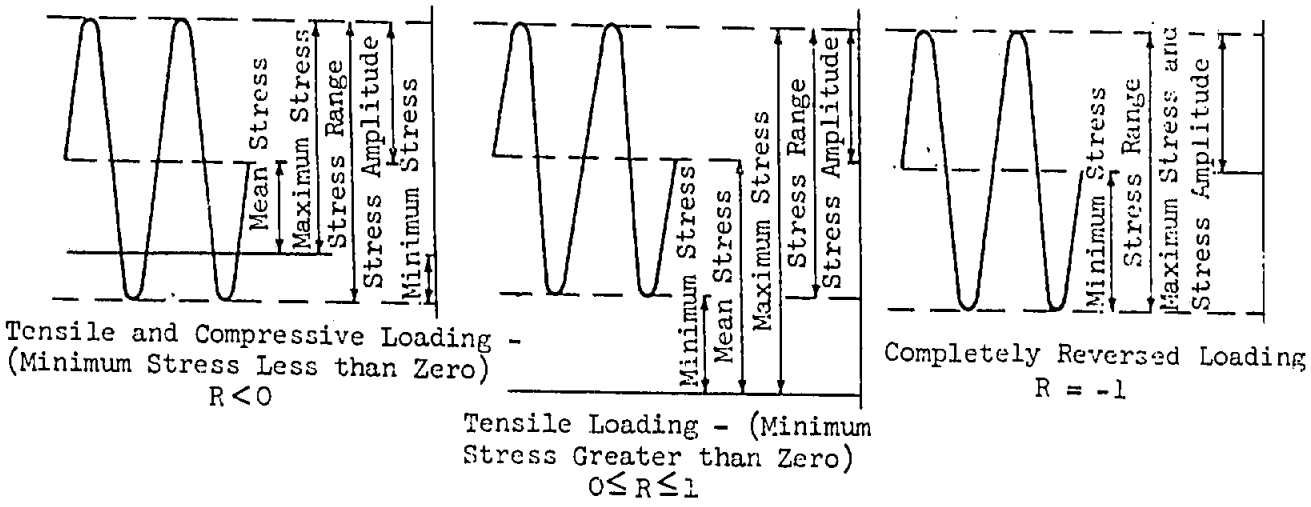

Figure 8.

Constant Amplitude Fatigue Life

The fatigue life of a smooth, unnotched ($K_T = 1$) structural component can be obtained directly from the S-N curves for smooth specimens, if there is only one loading cycle that is continuously repeated.

If the component is notched, the stress range at the notch is computed as described in Section B, "Calculation of Stresses at Points of Stress Concentration." The fatigue life is then determined from the S-N curves for smooth specimens, provided that the curves are entered with the stresses at the notch, and not the nominal stresses in the component. Therefore, the following fatigue lives are obtained for the cases described on pages B7.030-13 through B7.030-15

Case 1: $f_{Nmax} = 41{,}800$ psi, $f_{Nmin} = 0$

$N = 180{,}000$ cycles (from page B7.031-8)

Case 2: $f_{Nmax} = 75{,}000$ psi, $f_{Nmin} = -25{,}320$

$N = 2000$ cycles (from page B7.031-8)

Case 3: $f_{Nmax} = 16{,}480$ psi, $f_{Nmin} = -25{,}320$ psi

$N = > 10^8$ cycles (from page B7.031-8)

A comparison of cases (1) and (3) illustrates the beneficial effect sometimes obtained from a tensile preload that produces residual compression stresses at the hole. This is discussed more fully at the end of this section.

It should be pointed out that the reverse effect may be expected from a compressive preload. For example, had the load in the first cycle in case (3) been 12,000 pounds compression instead of 12,000 pounds tension, and compression yield assumed identical to tensile yield, the residual stress would have been +25,320 psi, and the stress range +25,320 to +67,120 psi.

The life of the part is thus reduced to 50,000 cycles. So called compression fatigue failures are not frequent, but the possibility of occurrence should be kept in mind.

Recent experimental evidence indicates that the yield stress of some materials is affected by cyclic loading in the plastic region (Ref. 25). Other tests have been started by the NASA to determine whether there is any comparable effect on the residual stresses at the edge of notches in such materials. Until further evidence is available, however, no cyclic changes in yield stress or residual stress will be assumed when using the fatigue analysis procedure described here.

Fatigue Life when Stress Varies from Compressive Yield to Tensile Yield

The fatigue life calculation procedure described above is reasonably accurate in the intermediate-life and long-life region of the fatigue curves, but has definite limitations in the short-life region, particularly when the stress at the hole varies from compression yield to tension yield.

To illustrate this condition of extreme stress range, consider the following case.

Case 4: A part made of 2024-T3 material, with $F_{ty} = F_{cy} = 52{,}000$ psi, and $K_N = 2.50$, is subjected to a nominal stress range of zero to + 48,000 psi nominal. Assume the stress strain curve is horizontal after yield. Determine the fatigue life.

At maximum load, $f_{Nel} = (K_N \times f_{max}) = 2.50 \times 48{,}000 = 120{,}000$ psi (eq 2)

Therefore, yielding occurs at the edge of the stress concentration, and $f_{Nmax} =$ 52,000 psi.

As the load is decreased back to zero the stress at the edge of the stress concentration would decrease elastically by an amount equal to $K_N f_{max}$, to a value of (52,000 - 120,000) = -68,000 psi, (eq 4b), if compression yielding did not occur. Since compression yield is exceeded, the stress at the edge of the hole or notch varies from F_{cy} to F_{ty}.

N = 7000 Cycles

It has been assumed in the previous examples that the stress-strain curve became horizontal at yield. Therefore, the allowable number of cycles would remain constant once the condition of compressive yield stress to tensile yield stress was reached, regardless of how much the yield strain was exceeded in tension or compression.

In fact, however, fatigue damage is closely related to strain range, and will increase with increases in strain beyond the initial yield strain, even if the stress does not significantly exceed the yield stress.

The use of an actual stress-strain curve (Fig. 3a) in place of the simplified version of Fig. 3b will give more realistic results, since an increase in strain beyond yield would correspond to an increase in stress, resulting in a shorter fatigue life.

However, comparison with test data indicates this latter method becomes very conservative if the strain range goes appreciably beyond the initial tensile yield to compressive yield range. Therefore, the following empirical procedure for the region beyond initial yield-to-yield is recommended.

Fatigue Life Prediction Beyond the Yield-to-Yield Range

1) Determine N_{yy}, the number of cycles to failure corresponding to a stress range of F_{cy} to F_{ty} for the particular material (i.e. 7000 cycles for 2024-T3), using unnotched data. Typical values of N_{yy} for several materials are listed below.

   2024-T3: N_{yy} = 7000 Cycles
   7075-T6: N_{yy} = 120 Cycles
   SAE 4340 (F_{t_u} = 230,000 KSI) N_{yy} = 120 Cycles

2) For cases where the stress range at the stress concentration exceeds the yield-to-yield range, the fatigue life will be less than N_{yy} cycles, and can be approximated by the following, generally conservative, expression.

$$\log N = \frac{(F_{tu} - f_{max}) \times \log N_{yy}}{\left(F_{tu} - \frac{F_{ty}}{K_N} - f_{mean}\right)} \qquad (5)$$

This expression for N represents a straight line variation of f_{max} vs log N, between N = 1 (static failure), and N = N_{yy}.

Case 5: Assuming the same part as in Case 4, determine the fatigue life using equation (5)

F_{t_u} = 72,000 psi, F_{ty} = 52,000 psi, N_{yy} = 7000 Cycles, K_N = 2.5

$$\log N = \frac{(72{,}000 - 48{,}000) \times 3.845}{\left(72{,}000 - \frac{52{,}000}{2.5} - 24{,}000\right)} = 3.39$$

N = 2450 Cycles

Constant Cyclic Loading Fatigue Damage

If a structural component can be subjected to N repetitions of a constant loading cycle before failure, then the fatigue damage to the component resulting from n repetitions of the loading cycle is defined by the damage ratio, n/N. Fatigue failure will not occur until the damage ratio, n/N equals 1.0.

Spectrum Loading Fatigue Damage

If the structural component is subjected to a spectrum of cyclic loadings, the fatigue life calculation procedure is essentially the same as described above.

1) The stress range for each range of cyclic loads is determined.
2) The fatigue life, N, is obtained for each stress range.
3) The damage ratio, n/N, is obtained for each stress range. The damage ratios are then summed up, so that the fatigue damage ratio for the entire spectrum is Σ n/N. Failure is assumed to occur when $\Sigma n/N = 1.0$. This is known as Miner's Law. (Reference 15)
4) If $\Sigma n/N$ is less than 1.0, the factor of safety on fatigue life is $\frac{1}{\Sigma \frac{n}{N}} - 1.$

It should be noted that a small change in applied stress level can often result in a relatively large change in fatigue life.

Effect of Load Sequence on Fatigue Damage

Most of the cyclic loads sustained by an airplane have a random character, as illustrated in Figure 1. Design load spectra, such as given in Reference 2, generally indicate the number of times various specific load levels are likely to be exceeded during a given number of flight hours, for different classes of airplane. In effect, such design load spectra count the number and magnitude of all the individual load peaks in a load spectrum, such as shown in Figure 1, and present the results in a simplified tabular form.

However, such design load spectra do not, in general, define the order in which the individual loads in the spectrum are applied. Since, as has already been shown, the order of load application can significantly affect the fatigue life of any structure, care must be taken to avoid assuming an order of load application that may lead to overly optimistic fatigue life predictions. Specifically, when running a fatigue life analysis, or a fatigue test program, the highest positive gust or maneuver loads should not be introduced too early in the load spectrum. This is because the compressive residual stress at a notch, resulting from the application of high positive loads, will lead to an underprediction of the fatigue damage calculated for the remainder of the service life of the structure.

The current trend in estimating order of load application is towards the use of statistical procedures, based on the assumption that the actual loading process is random. (Ref.32) A simplified version of this procedure is to break up the total load spectrum into a number of identical "loading blocks" or "loading stages", each one having its proportionate share of the total number

of cycles at each of the critical load levels in the spectrum. Load levels which do not contribute significantly to fatigue damage, as is often the case with the lower load levels, are generally omitted. Within any one load block the positive loads are applied in ascending order of magnitude. This "loading block" concept has generally been adopted both for fatigue analysis and for fatigue test purposes.

The manner in which the positive load and negative load spectra are combined also has a significant effect on fatigue life. Here, too, statistical procedures can be employed to determine reasonable load combinations. In the past, however, a simplified, conservative approach has been adopted for fatigue damage calculations, in which a positive load in any cycle was immediately followed by a negative load. The combinations of positive and negative loads were chosen so that the smallest positive loads were combined with the smallest negative loads, and so on up to the largest positive loads being combined with the largest negative loads. It has been shown, both by analysis and test, that this procedure is more conservative than the use of a procedure which analyzes the fatigue damage for the positive load spectrum and the negative load spectrum separately. However, because of difficulties in reversing the directions of applied loads in full-scale fatigue tests on airplanes, most tests of this type have separated the positive load spectrum from the negative load spectrum.

Case 6: A cyclic load of 0 to 5000 lb will be applied 20,000 times to the specimen in Case 1, followed by 200 applications of a 0 to 12,000 lb load cycle. This combination of cyclic loads will be considered as one loading block. The stress ranges at the edge of the hole will be as calculated in Cases 1 and 2. The fatigue damage in one loading block will be determined as follows:

1	2	3	4	5	6	7
f_{max} psi	f_{min} psi	f_{Nmax} psi	f_{Nmin} psi	Allowable Number of Cycles N	Applied Number of Cycles n	Damage Ratio $\frac{n}{N}$
20,000	0	41,800	0	200,000	20,000	0.1
48,000	0	75,000	-25,320	2000	200	0.1

$$\Sigma \frac{n}{N} = 0.2$$

If these loading blocks were repeated, and if the residual stresses resulting from the 12,000 lb load were arbitrarily assumed to be wiped out before the start of the next loading block, the element would have a fatigue life equal to $\frac{1.0}{0.2}$ = 5 loading blocks, or 101,000 cycles. However, if the residual stress of -25,320 psi sustained after application of the 12,000 lb load is assumed to remain after the first loading block is completed, any subsequent block would be affected by it. The stress ranges at the edge of the hole would now correspond to a combination of Cases 2 and 3, and the life calculation for the second, and any following block would be as shown.

1	2	3	4	5	6	7
f_{max}	f_{min}	f_{Nmax}	f_{Nmin}	N	n	$\frac{n}{N}$
psi	psi	psi	psi	Cycles	Cycles	
20,000	0	16,480	-25,320	10^8	20,000	0
48,000	0	75,000	-25,320	2000	200	0.1

$$\Sigma \frac{n}{N} = 0.1$$

Therefore, the damage for the second, and any subsequent loading block will be 0.1, and the life of the element will be

$$1 + \frac{1 - 0.2}{0.1} = 9 \text{ blocks.} \quad (181,800 \text{ Cycles})$$

This compares with the 5 blocks previously calculated, and indicates the beneficial effect of a compression residual stress mentioned on page B7.030-18.

Case 7

Component. Test Specimen (Fig. 9)
Material. Alum. Alloy 7075-T6
F_{tu} = 83000 psi F_{ty} = 75000 psi
Neuber Stress Concentration Factor, K_N = 2.18
Maximum Stress in Spectrum = 72000 psi
Source S/N Data Structures Manual, Page B7.031-3
Base Load: 1g
1 Complete Loading Block = 100 Hours Service Life

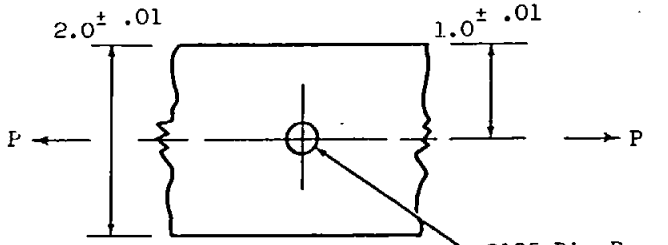

Figure 9

1	2	3	4	5	6	7	8	9	10	11	12	13	14	15	16	17
$N_{z_{max}}$ g's	$N_{z_{min}}$ g's	f_{max} psi	f_{min} psi	Δf = ③ - ④ psi	f_{Nelmax} = K_N x ③ psi	f_{Nelmin} = K_N x ④ psi	f_{Nmax} psi	f_{Nmin} psi	Allow. Number of Cycles N	Applied Number of Cycles n	Damage Ratio $\frac{n}{N}$	f_{Nmin} psi	f_{Nmax} psi	Allow. Number of Cycles N	Applied Number of Cycles n	Damage Ratio $\frac{n}{N}$
3.5	1.0	32300	9230	23070	70400	20100	70400	20100	25000	810	0.0324	-61800	-11500	$>10^8$	810	0
4.5	1.0	41500	↓	32270	90500	↓	75000	4600	7600	260	0.0342	↓	8600	300000	260	0.00087
5.5	1.0	51000	↓	41770	110700	↓	↓	-16100	2300	65	0.0282	↓	28800	40000	65	0.00162
6.5	1.0	60000	↓	50770	130800	↓	↓	-35700	1000	13	.013	↓	48900	12000	13	0.00108
7.8	1.0	72000	9230	62770	157000	20100	75000	-61800	210	2	0.0095	-61800	75000	210	2	0.0095

⑧ $f_{Nmax} = f_{Nelmax}$, if $f_{Nelmax} < F_{ty}$

$f_{Nmax} = F_{ty}$, if $f_{Nelmax} > F_{ty}$

⑨ $f_{Nmin} = f_{Nmax} - K_N \Delta f$ (equation 4)

⑬ f_{Nmin} = -61800 psi = Stress (at 1g) Remaining After Application of 6.5 g Loads in 1st Block)

⑭ $f_{Nmax} = ⑬ + K_N \Delta f = ⑬ + ⑥ - ⑦$

$\Sigma \frac{n}{N} = 0.1173$ $\Sigma \frac{n}{N} = 0.01307$

Total Damage for 1st Block = 0.1173

Total Damage for 2nd and Subs. Blocks = 0.01307

Life = $\left[1 + \frac{1-0.1173}{0.01307}\right] 100$ = 6850 Hours

Fatigue Design Curves

Additional calculations of the type made in Cases 6 and 7 can be used to obtain fatigue design curves such as shown in Figures 10a and 10b.

In Figure 10a the fatigue lives of notched parts are plotted, for different values of K_N, as a function of the maximum nominal stress applied in a loading block. The curves in Figure 10a were drawn for the particular load spectrum assumed in Case 6, but similar curves could be drawn for any given loading spectrum.

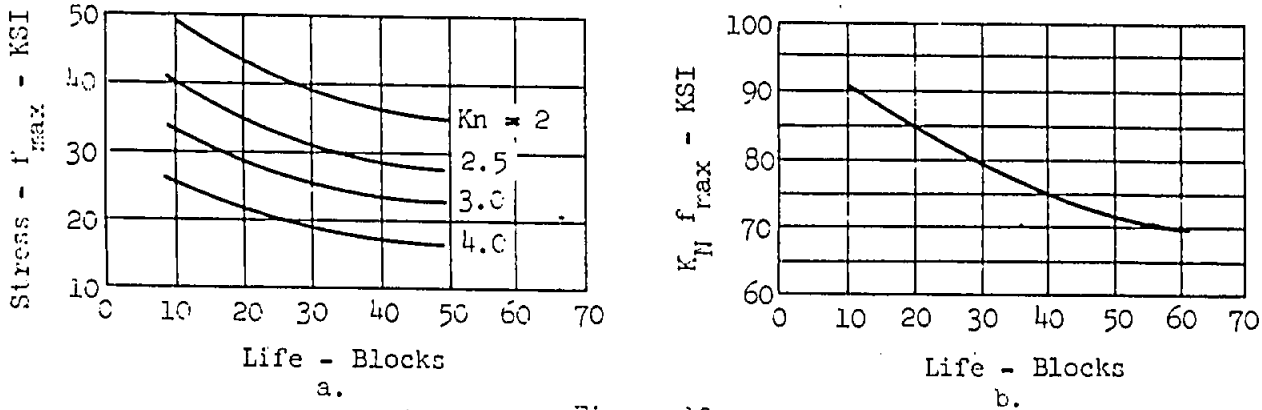

Figure 10.

These curves can be used in design to determine the allowable values of f_{max} for any required service life. For example, if for Case 6 a service life of 20 blocks was required, an allowable value of f_{max} = 41,200 psi can be determined from Figure 10a by interpolation, between curves for K_N = 2 and K_N = 3

An examination of Figure 10a indicates that the values of f_{max}, for any given fatigue life, are inversely proportional to the values of K_N. This results from our basic assumption that the fatigue life of any notched part is a function only of the stress at the notch. However, as can be seen from equations (4) through (4c), the stress at the notch is a function only of the product $K_N f$ (or $K_N \epsilon$). Therefore, the information presented by the three curves in Figure 10a can be represented by the single curve of Figure 10b which shows the variation in fatigue life of notched parts as a function of $K_N f_{max}$, for the particular spectrum being considered.

Considering the previous example again, where a life of 20 blocks is required for case 6, we obtain, from Figure 10b, a value of 89,800 psi for $K_N f_{max}$, therefore $f_{max} = \frac{86,000}{2.09} = 41,200$ psi.

It should be noted that presentation of fatigue data with just a single curve, as shown in Figure 10b, is possible only if the stress range at the notch is less than tension yield-to-compression yield. However, much of the range of practical interest can be covered by a single curve as in Figure 10b.

A computer program is available for fatigue life calculations, and the above curves can be obtained for any loading spectrum, and for a number of different materials.

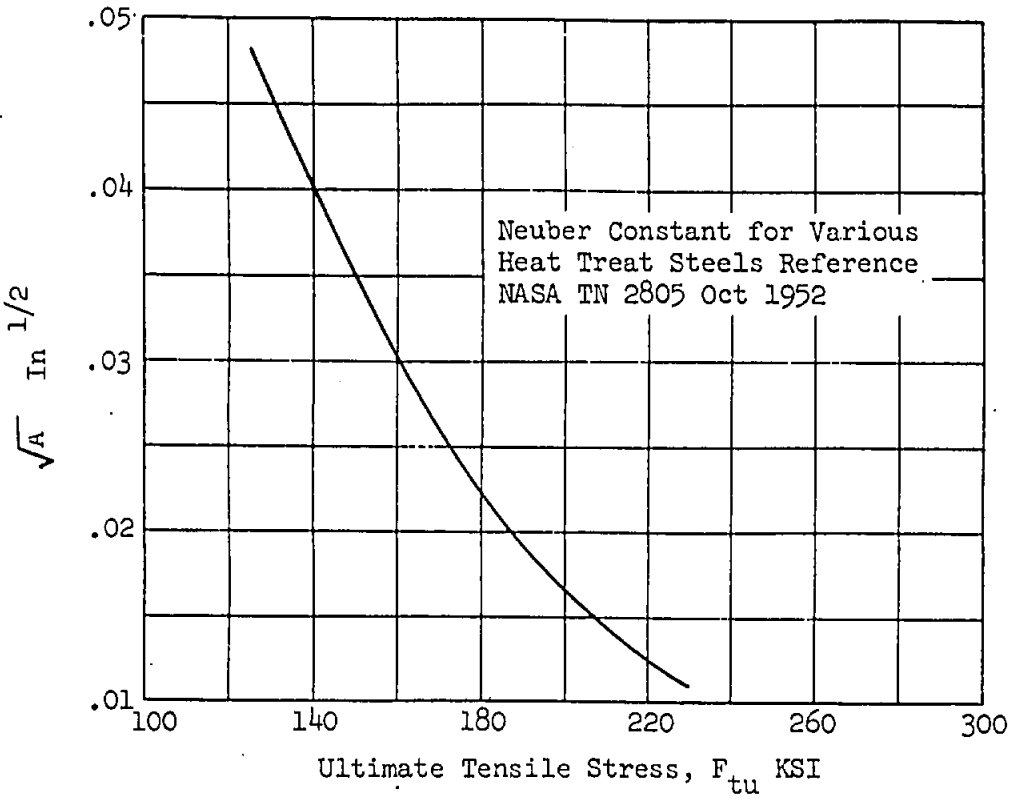
.05
.04
.03
.02
.01
100
140
180
220
260
300
$\sqrt{A}$ In $^{1/2}$
Neuber Constant for Various
Heat Treat Steels Reference
NASA TN 2805 Oct 1952
Ultimate Tensile Stress, F_{tu} KSI

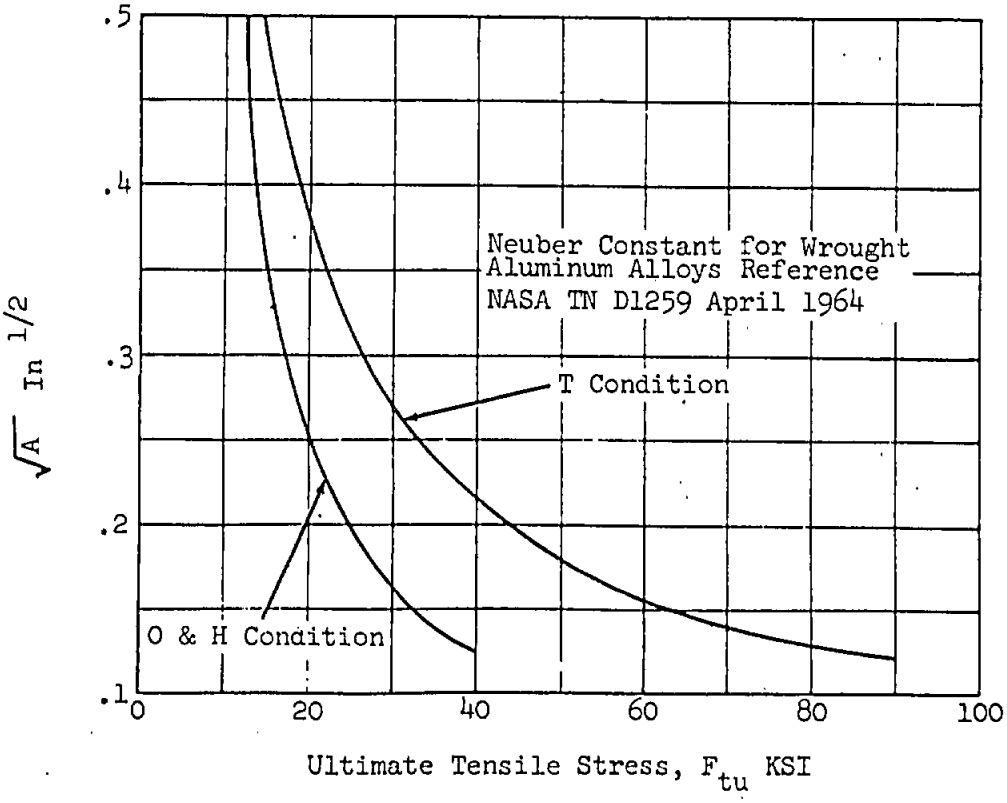
.5
.4
.3
.2
.1
0
20
40
60
80
100
$\sqrt{A}$ In $^{1/2}$
Neuber Constant for Wrought
Aluminum Alloys Reference
NASA TN D1259 April 1964
T Condition
O & H Condition
Ultimate Tensile Stress, F_{tu} KSI

D) STRAIN-CYCLING FATIGUE PREDICTION METHOD

The strain-cycling fatigue prediction method is based on the concepts of references 25,35 & 36 and on the modifications and extensions to these concepts described in reference 37 and 38. Reference 39 is specifically concerned with the application of the method.

Some general features of the strain-cycling method are similar to those of the stress cycling method but there are differences in basic inputs and analysis procedure, resulting in improved predictions in fatigue life, especially in the high-stress/low-cycle field. A discussion of the principal features of the strain cycling method follows:

a) Cyclic Stress-Strain Curves

Many structural materials undergo significant changes in stress-strain behavior during fatigue cycling, especially in the high-stress/low-cycle region. Materials are referred to as "cyclically strain hardening" or "cyclically strain -softening" and cyclic stress-strain curves can be generated for either class of material by running strain-controlled fatigue tests, in which smooth, unnotched specimens are subjected to fully reversed constant amplitude fatigue loading. For a cyclically strain-hardening material, the stress required to produce a given strain will increase with each loading cycle until a stabilized value is reached, usually in about 20% of the specimen fatigue life at that value of cyclic straining. In a strain-softening material, the stress required to produce a given strain decreases with loading cycles until a stabilized value is reached. For materials having no significant cyclic strain-hardening or cyclic strain-softening characteristics, strain-controlled fatigue data is directly comparable to stress-controlled fatigue data. Cyclic effects on the stress-strain curve are primarily felt at the higher stress levels, therefore, these effects will generally be significant in local highly stresses regions near notches. However, the notch strains will be controlled by the strains in the surrounding bulk structure and if these strains are essentially constant for a given load level, then the notch strains will be constant also. Therefore, cyclic fatigue tests on smooth specimens give fatigue data representative of material behavior near notches. Cyclic stress-strain curves are used to establish stress-strain relationships used in the strain cycling method and the assumption is made that the local material adjacent to a notch is fully stabilized.

b) Cyclic Strain-Life Curves

In the original stress cycling method, the fatigue life obtained for a given stress cycle is obtained from the fatigue S-N curves on pages B7.031-1 through B7.031-26 of the Structures Manual. The high stress/low cycle end of the S-N curve tends to become very flat, with large percentages changes in life for small changes in cyclic stress. Predictions in this region are therefore very sensitive to small errors in cyclic stress. The strain-cycling method employs strain-life (e-N) curves which are not flat in the

low-cycle region, making the curves less sensitive to errors in strain.

c) Plastic Stress Concentration Factor

Both the stress-cycling and strain-cycling methods approximate the stress-strain behavior at the root of a notch by the use of effective stress concentration factors. In the stress method, the material is assumed to behave elastically throughout the cycle and the theoretical elastic stress concentration factor, K_T, is modified by Neuber's theory (reference 9) to obtain an effective elastic stress concentration factor, K_N. This factor is then utilized to obtain stresses at a point of stress concentration (pages B7.030-8 through B7.030-16). The strain-cycling method also employs the Neuber factor, K_N, but as an input to the generalized Stowell formula (reference 36) to obtain a plastic stress concentration factor , Kf_p, which is then used to obtain stresses at a notch. This procedure will be presented in detail later in the text.

The foregoing items (a) through (c) cover the major differences in input data between the two fatigue life prediction methods. The strain cycling method will now be discussed in detail.

Reference 25, 35, 41 & 42 present data for cyclic stress-strain and cyclic strain-life curves obtained from strain-controlled fatigue tests, developed for reversed cyclic loading ($R = \frac{f_{min}}{f_{max}} = -1$). These data are relatively difficult to obtain and are not available for all aerospace materials, however, Manson, et al in references 25 & 35 observed that the elastic and plastic components of cyclic strain could, for many materials, be related to cycles to failure, by the following expressions for reversed cyclic loading

$$\epsilon_e = \frac{\sigma a}{E} = C_1 N_f^{-\beta} \qquad (1)$$

$$\epsilon_p = C_2 N_f^{-\gamma} \qquad (2)$$

where ϵ_e, ϵ_p are the elastic and plastic components of the total strain amplitude ϵ_t

σ_a	is the stabilized stress amplitude
E	is Young's Modulus
N_f	is the number of cycles to failure
C_1, C_2, β, γ	are constants for a given material

Equations (1) and (2) represent straight lines drawn through elastic and plastic strain-life data on a log-log plot. When test data are available, the material constants can be determined by best-fit

straight lines representing ϵ_e and ϵ_p. Reference 35 noted that if test data are not available for a particular material, reasonable values for the material constants can be obtained by making use of static test properties Evaluation of test data on a wide variety of materials led to the following approximations for material constants:

Elastic Strains

1. At $N = \frac{1}{4}$ cycle, elastic strain amplitude, ϵ_e, is estimated as $1.25 \frac{\sigma f}{E}$ where σ_f = true stress at fracture as determined in a static tensile test.

2. At $N = 10^5$ cycles, the elastic strain amplitude is approximately $0.45 \frac{F_{tu}}{E}$ where F_{tu} is the nominal ultimate tensile strength of the material.

Plastic Strains

3. At 10 cycles, the plastic strain amplitude can be assumed equal to $.125\ D^{3/4}$ where D is the true ductility.

4. At 10^4 cycles, the elastic and plastic strain amplitudes satisfy the following empirical relation

$$\epsilon_p = 0.00345 - 0.52\ \epsilon_e$$

These relationships lead to the following equations for the material constants.

$$C_1 = 1.12 \frac{F_{TU}}{E} \left(\frac{\sigma f}{F_{TU}}\right)^{0.893}$$

$$C_2 \doteq \frac{0.414\ D}{\sqrt[3]{1 - 81.4 \frac{F_{TU}}{E} \left(\frac{\sigma f}{F_{TU}}\right)^{0.179}}} \approx 0.125\ D^{0.75}\ (10)^{\gamma}$$

$$\beta = 0.792 + 0.179 \log\left(\frac{\sigma f}{F_{TU}}\right)$$

$$\gamma = \log \left\{ \frac{3.31 \sqrt[4]{D}}{\sqrt[3]{1 - 81.4 \frac{F_{TU}}{E} \left(\frac{\sigma f}{F_{TU}}\right)^{0.179}}} \right.$$

where:

F_{TU} = nominal ultimate tensile strength based on the original cross-sectional area of a static tensile specimen

σ_f = true stress at fracture, taking into account the reduction in cross-sectional area of the tensile specimen when it necks down

E = elastic modulus of elasticity of the material

$D = \ln\left(\frac{A_o}{A_f}\right)$ = ductility of the material (A_o and A_f are the initial and final areas of the fracture cross-section in the tensile specimen)

Values of material constants are given, for some of the more common aircraft structural materials, in reference 37.

It is therefore possible to obtain approximate cyclic stress-strain and strain life curves for any material for which the required static properties are available. The total strain, from equations (1) and (2) is:

$$\epsilon_t = \epsilon_e + \epsilon_p = C_1 N_f^{-\beta} + C_2 N_f^{-\gamma} \qquad (3)$$

from equation (1):

$$N_f = \left(\frac{C_1 E}{\sigma_a}\right)^{\frac{1}{\beta}} \qquad (4)$$

and substituting equation (4) into equation (3):

$$\epsilon_t = \frac{\sigma_a}{E} + C_2 \left(\frac{\sigma_a}{C_1 E}\right)^{\frac{\gamma}{\beta}} \qquad (5)$$

where σ_a represents the stabilized stress amplitude.

Equations (4) and (5) represent approximations to cyclic strain-life curves and cyclic stress-strain curves for the material. Pages B7.030-39 & B7.030-40 show typical cyclic strain-life and cyclic stress-strain curves for an aluminum alloy 7075-T6, calculated using equations (4) and(5).

The curves so obtained are related to fully reversed cyclic loading (R = -1). In order to allow for stress ratios other than R = -1, the Goodman-type concept illustrated on page B7.030-42 is used. The total strain amplitude for a fully reversed loading condition, corresponding to a given life, N_f, in a smooth specimen is represented as ϵ_t on the R = -1 line in the diagram. A straight constant life-line is then assumed between ϵ_t (R = -1) and $\sigma_m = \sigma_f$ (fracture stress), at R = +1. Then if ϵ_a is the strain amplitude for any given non-fully reversed loading condition (R= -1), the corresponding fully-reversed loading strain in a smooth specimen for the same life will be, from page B7.030-40.

$$\epsilon_t = \frac{\epsilon_a}{1 - \frac{\sigma_m}{\sigma_f}} \qquad (6)$$

where ϵ_t = "equivalent" strain amplitude

σ_m = mean stress = $\frac{\sigma_{max} + \sigma_{min}}{2}$, in cycle

σ_f = fracture stress, as defined on page B7.030-30

Using the cyclic strain-life and cyclic stress-strain curves in conjunction with the mean stress correction given by equation (6), the fatigue life of any unnotched (K_T = 1) part of specimen may be predicted directly. For example, consider a 7075-T6 part, with K_T = 1, subjected to a cyclic stress of 50,000 psi at R = 0.1. In this case:

σ_{max} = 50,000 psi

$\sigma_{min} = R\sigma_{max}$ = 5000 psi

$\sigma_{mean} = \frac{\sigma_{max} + \sigma_{min}}{2}$ = 27500 psi

The corresponding cyclic strains are, from page B7.030-39

ϵ_{max} = 0.0067 ins/inch

ϵ_{min} = 0.0005 ins/inch

$\epsilon_{amp} = \frac{0.0067 - 0.0005}{2} = 0.0031$ in/in

using equation (6):

$$\epsilon_t = \frac{0.0031}{1 - \frac{27500}{110000}} = 0.00413 \text{ in/in}$$

entering the cyclic strain-life curve on page B7.030-40 with ϵ_t = 0.00413 in/in, the value

N_f = 90,000 cycles

The S-N curve for 7075-T6, K_T = 1 on page B7.031-8 gives a life of 100,000 cycles for an applied stress range of 50000 to 5000 psi.

The fatigue life of a notched specimen is calculated on the basic assumption that a part of specimen which is subjected to a given cyclic strain range at the base of a notch or hole, will fail in fatigue at the same number of cycles as a smooth (K_T = 1) specimen, subjected to the same strain range. This assumption is similar to that made in the stress-cycling method (page B7.030-8) and is commonly used in other methods of fatigue life prediction.

The calculation of fatigue life for notched parts, using unnotched data, requires that stresses at points of stress concentration be determined. The values of the mean stress, σ_m and the strain amplitude, ϵ_a, to which the material at the base of a notch is subjected during a loading cycle, is a function of the stress-strain curve the material follows during the loading and unloading phases. In the stress-cycling method, the stresses at a notch were calculated in the manner described on pages B7.030-9 through B7.030-16. In the strain cycling method, the pattern of material behavior at a notch is established in the following manner:

The peak stress at the notch is determined using a plastic stress concentration factor, K_{f_p}, obtained from the generalized Stowell equation (reference 36).

$$K_{f_p} = \frac{\text{stress at notch}}{\text{nominal stress}} = \frac{\sigma}{f} = 1 + \left[(K_N - 1) \left(\frac{E_2}{E_1}\right)\right] \quad (7)$$

where K_N = Neuber stress concentration factor

E_1, E_2 = secant moduli associated with the nominal and notch stress, f and σ, respectively.

Curves for K_{f_p}, such as those shown on page B7.030-38, can be drawn for different materials.

For the particular case when the material remote from the notch is stressed into the plastic range, a value for the secant modulus, E_1, for the material away from the notch, is obtained from the appropriate monotonic stress-strain curve. In the computerized version of the strain-life method, this is accomplished by inputting values of $f_{0.7}$ and n, enabling the program to calculate the material stress-strain curve by the Ramberg-Osgood approximation.

Referring to page B7.030-43 let OM represent the cyclic stress-strain curve. The nominal net section stress varies from 0 to f_{max} (point A) and the corresponding stress at the root of the notch is assumed to vary

from 0 to σ_{max} (point A'), where

$$\sigma_{max} = K_{f_p} \times f_{max} \tag{8}$$

When the section remote from the notch unloads from f_{max} (Point A) to f_{min} (Point C), the material adjacent to the notch unloads from point A' to point C'. The material at the notch is first assumed to unload elastically from point A' to point B'. This corresponds to a nominal stress of f_1 (point B). The stress f_1 is found using either of the following equations:

$$f_1 = \frac{f_{max}}{2} \quad (\text{if } f_{min} \leq 0) \tag{9a}$$

or

$$f_1 = \frac{f_{max} + f_{min}}{2} \quad (\text{if } f_{min} \geq 0) \tag{9b}$$

The notch stress decreased by an amount

$$\Delta\sigma_1 = K_N \frac{f_{max}}{2} \quad (\text{if } f_{min} \leq 0) \tag{10a}$$

$$\Delta\sigma_1 = K_N \frac{f_{max} - f_{min}}{2} \quad (\text{if } f_{min} \geq 0) \tag{10b}$$

The notch strain decreases by

$$\Delta\epsilon_1 = \frac{\Delta\sigma_1}{E} \tag{11}$$

During the remainder of the unloading cycle the nominal stress decreases by an amount

$$\Delta f_2 = f_1 - f_{min} \tag{12}$$

To determine the remaining part of the unloading cycle at the notch, it is assumed that from point B' the material follows the same stress-strain curve as during the initial loading, and that the strain concentration factor at the bottom of thenotch during this unloading is the same as that corresponding to point A' on the initial loading curve. Therefore, the strain at the notch will decrease by an additional amount

$$\Delta\epsilon_2 = \frac{\Delta f_2}{f_{max}} \epsilon_{max} \tag{13}$$

where ϵ_{max} is the strain at point A', corresponding to σ_{max} on the cyclic stress-strain curve. Consequently, the stress at the notch will decrease by an amount $\Delta\sigma_2$, the stress corresponding to $\Delta\epsilon_2$ on the cyclic stress-strain curve. This is the stress at the notch (point C') existing when element is subjected to the minimum load in the cycle.

At this stage of the calculation, the maximum stress at the notch is known (equation 8). The minimum stress and the mean stress at the notch can be determined by

$$\sigma_{min} = \sigma_{max} - (\Delta\sigma_1 + \Delta\sigma_2) \tag{14}$$

$$\sigma_{mean} = \frac{\sigma_{max} + \sigma_{min}}{2} = \sigma_{max} - \left(\frac{\Delta\sigma_1 + \Delta\sigma_2}{2}\right) \tag{15}$$

The strain amplitude at the notch is given by

$$\epsilon_a = \frac{\Delta\epsilon_1 + \Delta\epsilon_2}{2} \tag{16}$$

The corresponding strain amplitude for fully reversed loading in a smooth ($K_T = 1$) specimen will be as before, from equation (6)

$$\epsilon_t = \frac{\epsilon_a}{1 - \frac{\sigma_m}{\sigma_f}}$$

The life is obtained by entering the strain-life curve for the material (unnotched specimen, fully reversed loading) with ϵ_t as the total strain amplitude and finding the corresponding value of N_f.

In order to determine the residual stress remaining at the notch when the element is unloaded, it is necessary to complete the hysterisis load to the point of zero applied load. For the case when $f_{min} \geq 0$, this is accomplished by unloading the element from f_{max} (point A) to zero, and determining the corresponding stress-strain behavior at the notch. It follows that if $f_{min} \geq 0$, the residual stress level will be that remaining after unloading to zero from the maximum applied load. The material at the notch is first assumed to unload elastically from σ_{max} (point A') by

$$\Delta\sigma_1 Res_1 = \frac{K_N f_{max}}{2} \tag{17}$$

which corresponds to a nominal stress unloading of $\frac{f_{max}}{2}$. To determine the

remaining part of the unload cycle at the notch, it is assumed that the material again follows the same stress-strain curve as during initial loading. Therefore, the stress at the notch will decrease by an additional amount $\Delta\sigma_{Res_2}$, obtained by entering the cyclic stress-strain curve with a strain

$$\Delta\epsilon_{Res_2} = \frac{\epsilon_{max}}{2} \quad \text{and reading the corresponding stress level, } \Delta\sigma_{Res_2} \text{ from the curve} \tag{18}$$

The residual stress at zero load is then

$$\sigma_{Res} = \sigma_{max} - \Delta\sigma_{1Res_1} - \Delta\sigma_{1Res_2} \tag{19}$$

For the case when $f_{min} \leq 0$, the residual stress is determined by unloading the section from f_{min} (point C) to zero applied load. This is accomplished in the same manner as unloading from f_{max} (point A). The first part of the unloading cycle is assumed to be elastic, and the stress is given by

$$\Delta\sigma_{Res_1} = \frac{K_N f_{min}}{2} \tag{20}$$

During the remainder of the cycle, the nominal stress decreases by an amount $\Delta\sigma_{Res_2}$, corresponding to a strain

$$\Delta\epsilon_{Res_2} = \frac{f_{min}}{2f_{max}} \quad (\epsilon_{max}) \tag{21}$$

and $\Delta\sigma_{Res_2}$ can be read from the cyclic stress-strain curve. The residual stress at zero applied load is then

$$\sigma_{res} = \sigma_{min} - \Delta\sigma_{res_1} - \Delta\sigma_{Res_2} \tag{22}$$

Application to Spectrum Loading

In a spectrum containing a number of different load levels, residual stresses will interact from one level to another, affecting the values of cyclic stress at a notch and, therefore, the fatigue life of the element. When a spectrum is applied in a series of loading blocks, the residual stress remaining at the end of a block is 'carried over' to the next block and applied as an initial loading stress at each level. It is assumed in the strain cycling method that the 'carry-over' residual is that associated with the level containing the largest strain range in the block.

The residual stress carried over from the first block is used as an input to each level of the second block. If the maximum stress, σ_{max}, (calculated with the effect of the carry-over residual included) exceeds the allowable ultimate stress for the material at any level the residual stress is modified

on the assumption the σ_{max} cannot exceed F_{t_u}. The modified residual stress value is then substituted for the carry-over residual, and used as an input to subsequent levels. The procedure is followed at each level of the spectrum in which $\sigma_{max} > F_{tu}$. This particular case is discussed in detail later in the text.

To determine the fatigue life for a given loading cycle, the method objective is to calculate the mean stress and total strain amplitude in the cycle (equations 15 and 16). It is therefore convenient to include the effect of the established residual stress on subsequently applied load levels in the form of a modification to the mean stress. A new equivalent strain amplitude for the level, which includes the residual stress effect, is then obtained from equation (6).

The procedure is best explained by reference to the illustrative example on page B7.030-41 . The computation represents a simple five-level fighter-type spectrum, with a constant minimum stress of zero. The appropriate plastic stress concentration curves and the cyclic stress-strain and strain-life curves for the material are shown on pages B7.030-39 and B7.030-40 . The material is aluminum 7075-T6 and the elastic stress concentration factor, $K_T = 2.96$.

Referring to the table on page B7.030-41 , columns (1) through (18) represent a 'first block' calculation, in which the cyclic stresses and strains are calculated on an individual level basis, with no interaction from one level to the next. The mean stress in the cycle is computed in column 13 (equation 15). The residual stress for each level, again computed on a non-interactive basis, is shown in either column 23 ($f_{min} \leq 0$) or column 28 ($f_{min} \geq 0$). The residual stress corresponding to the load level with the maximum strain range is assumed to apply after the first loading block, (as previously discussed) and is designated σ_{res}^*. In the example, σ_{res}^* is shown in column 28 (level 5) and is calculated to be -61690 psi.

The mean stress levels calculated for each load level (column 13) in the first block are now shifted by the amount $(\sigma_{res}^* - \sigma_{res})$ where σ_{res} is the residual stress for any particular load level, and σ_{res}^* is the carry-over residual stress. The new mean stress for any level in the second block is now

$$\sigma_{mean_2} = \sigma_{mean_1} + \sigma_{res}^* - \sigma_{res} \qquad (23)$$

This operation does not affect the strain amplitude, ϵ_a, calculated in column 14 but the new value for σ_{mean} causes a change in the value of ϵ_t (column 31) when the new mean stress is substituted in equation (6).

As in the stress-cycling method, the Miner-Palmgren cumulative damage rule is assumed to apply for the case of spectrum loading. The fatigue damage for each load level is calculated in columns 18 and 33.

For load levels in which the calculated maximum stress at the notch exceeds the material ultimate tensile strength, the method assumes that the maximum stress in the cycle to be 'cut off' at F_{tu}, and the mean stress and residual stress are accordingly changed by an increment

$$\Delta\sigma_{mean} = \sigma_{max} - F_{tu} \tag{24}$$

The mean stress in the cycle will become:

$$\sigma_{mean_2} = \sigma_{mean_1} - \Delta\sigma_{mean} \tag{25}$$

and the residual stress:

$$\sigma_{res_2} = \sigma_{res_1} - \Delta\sigma_{mean} \tag{26}$$

In the computer program FATLF, the machine performs the identical calculations shown in table on page B7.030-41 , for the first block, and enters the second block with the 'carry-over' residual stress, corresponding to the level with the largest strain range. The maximum stress at the notch is computed at each level, with the residual stress included. If, at one or more levels, the maximum notch stress exceeds F_{tu}, the program proceeds to a third block calculation, in which all levels are re-calculated using the 'cut-off' procedure previously discussed. Subsequent loading blocks are assumed to be identical with the third. The life prediction is obtained by use of the first, second and third block damages i.e.:

$$\text{Life} = \left[\frac{1 - \sum\left(\frac{n}{N}\right)_1 - \sum\left(\frac{n}{N}\right)_2}{\sum\left(\frac{n}{N}\right)_3} + 2 \right] H$$

where H = loading block size (27)

STRESS CONCENTRATION FACTOR K_{fp} VS. K_N CURVES FOR 7075-T6 ALUMINUM ALLOY

F_{TU} = 83 ksi; σ_f = 110 ksi; E = 10×10^3 ksi

C_1 = 0.012; C_2 = 0.208; β = 0.102; γ = 0.543

K_{fp} Curves Based on Cyclic Stress-Strain Curve Calculated from Ref. 37, Equation (5) and the Generalized Stowell Formula given in Ref. 37, Equation (12)

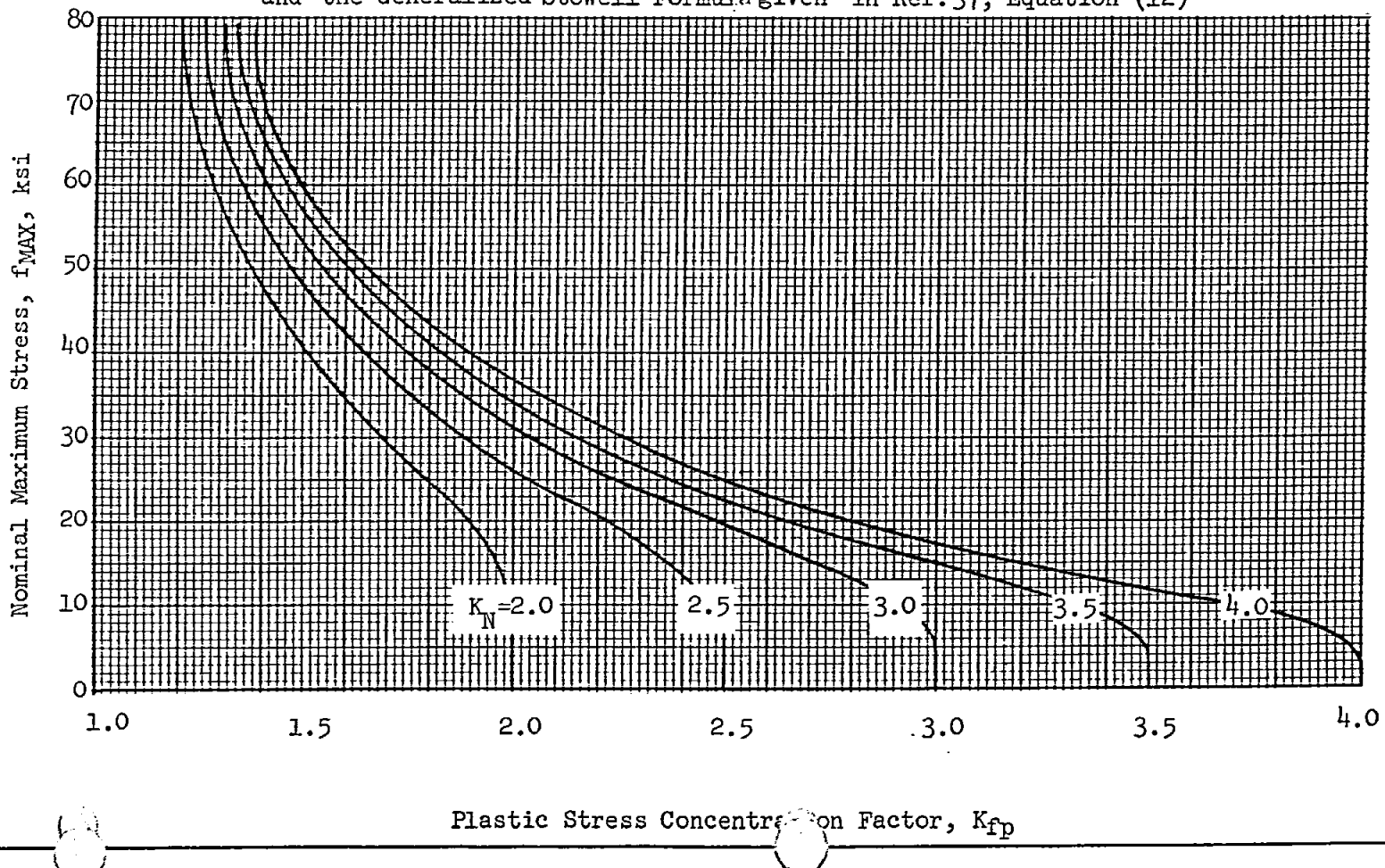

CYCLIC STRESS-STRAIN CURVE, 7075-T6 ALUMINUM ALLOY-BARE SHEET

F_{TU} = 83 ksi; σ_f = 110 ksi; E = 10×10^3 ksi

C_1 = 0.012; C_2 = 0.208; β = 0.102; γ = 0.543

Curve Calculated from Ref. 37, Equation (5)

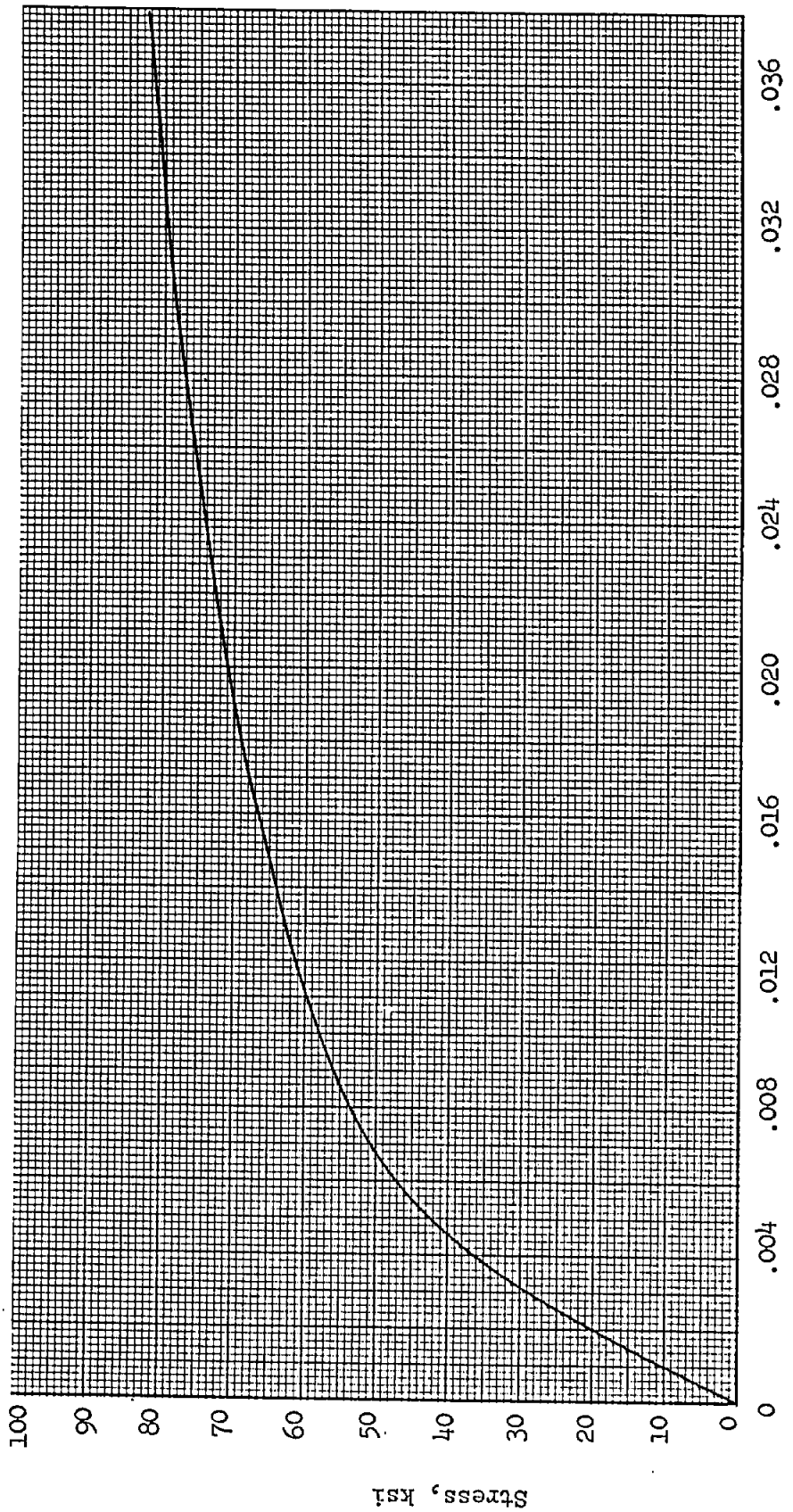

VARIATION OF TOTAL STRAIN AMPLITUDE WITH FATIGUE LIFE FOR COMPLETELY REVERSED CYCLIC LOADING, 7075-T6 ALUMINUM ALLOY-BARE SHEET

F_{TU} = 83 ksi; σ_f = 110 ksi; E = 10×10^3 ksi

C_1 = 0.012; C_2 = 0.208; β = 0.102; γ = 0.543

Curve Calculated from Ref. 37, Equation (3)

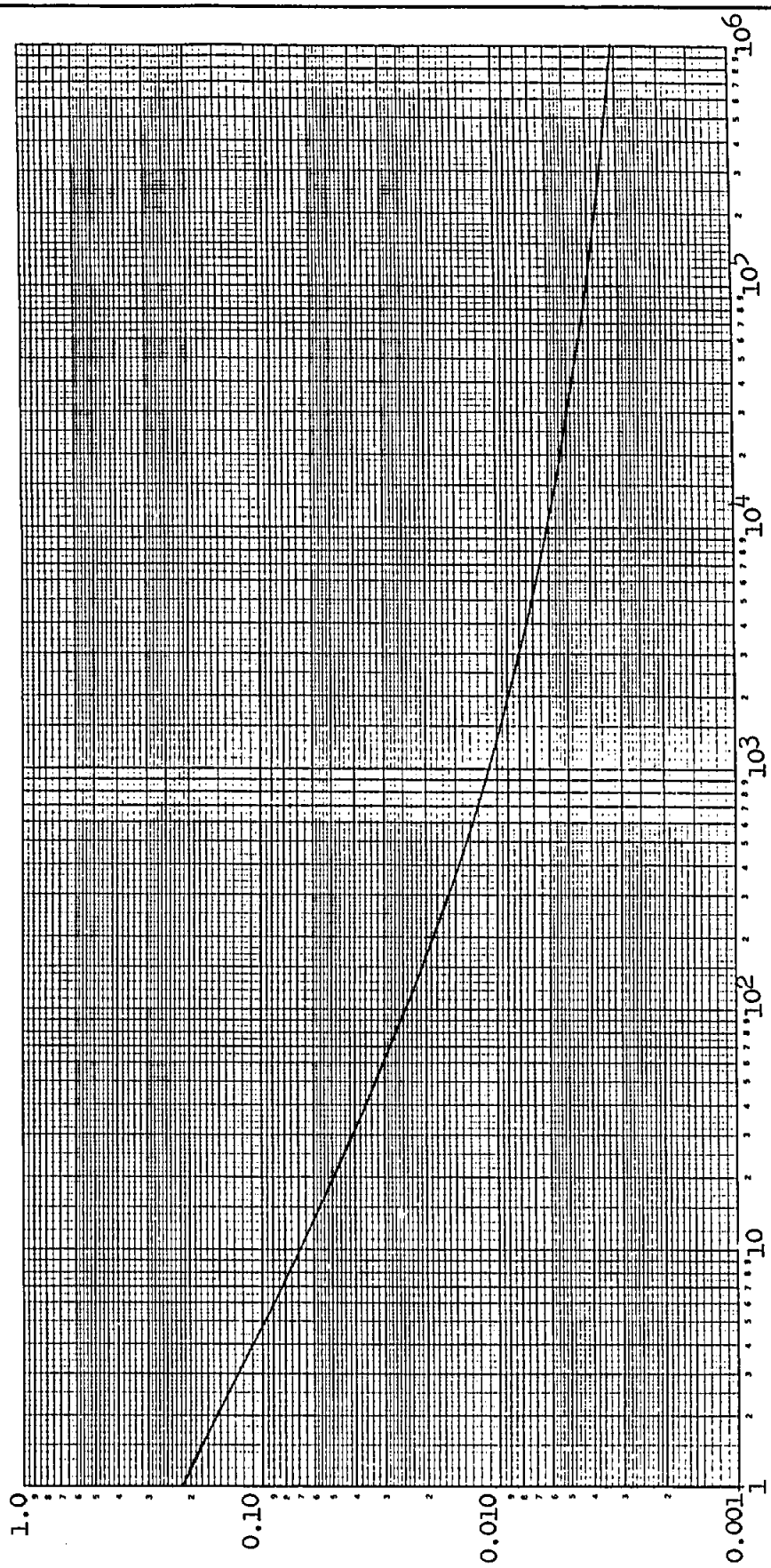

ILLUSTRATIVE EXAMPLE FOR STRAIN CYCLING FATIGUE PREDICTION METHOD

A-6A Wing Fatigue Test Spectrum — 7075-T6 Aluminum Alloy - Bare Sheet

Reference Load Factor = 6.5 g's, Limit Load Factor; Reference Stress = 42100 psi at Limit Load Factor

$K_N = 2.96$; $K_N \cdot f_{REF} = 124616$ psi; H = One Complete Loading Block = 100 Hours Service Life

$F_{TU} = 83$ ksi; $\sigma_f = 110$ ksi; $E = 10 \times 10^3$ ksi; $C_1 = 0.012$; $C_2 = 0.208$; $\beta = 0.102$; $\gamma = 0.543$

	1	2	3	4	5	6	7	8	9	10	11	12	13	14	15	16	17	18
NUMBER OF LOAD CYCLE LEVELS	f_{MAX} NOMINAL NET SECTION STRESS	f_{MIN} NOMINAL NET SECTION STRESS	K_{fp}	σ_{MAX} ① x ③	ϵ_{MAX} FROM CYCLIC STRESS-STRAIN CURVE	f_1	Δf_2 ⑥ - ②	$\Delta\sigma_1'$ K_H[① - ⑥]	$\Delta\epsilon_1$ ⑧ / E	$\Delta\epsilon_2$ ⑦ x ⑤ / ①	$\Delta\sigma_2$ FROM CYCLIC STRESS-STRAIN CURVE	σ_{MIN} ④ - ⑧ - ⑪	σ_{MEAN} (④ + ⑫) / 2.0	ϵ_a (⑨ + ⑩) / 2.0	ϵ_t ⑭ / (1 - σ_{MEAN}/σ_{FRACT})	N_1 CYCLES TO FAILURE	n APPLIED CYCLES PER BLOCK	n/N_1 ⑯ / ⑮
1	22669	0	2.3175	52535	.0078142	11335	11335	33550	.0033550	.0039071	35776	-16791	17872	.0036311	.0043355	69630	810	.011633
2	29146	0	2.0544	59877	.0111256	14573	14573	43136	.0043136	.0055628	44752	-28011	15933	.0049382	.0057746	12990	260	.020015
3	35623	0	1.8510	65938	.0151782	17812	17812	52722	.0052722	.0075891	51906	-38690	13624	.0064307	.0073398	4263	65	.015247
4	42100	0	1.6933	71289	.0201338	21050	21050	62308	.0062308	.0100669	57865	-48884	11202	.0081489	.0090728	1846	13	.007042
5	50529	0	1.5379	77693	.0283277	25260	25260	74770	.0074770	.0141639	64613	-61690	8002	.0108205	.0116694	782	2	.002559
6																		
7																		
8																		
9																		
10																		

$\sum \left[\frac{n}{N}\right]_1 = 0.0564966$

	f_{MIN} IS OPPOSITE SIGN FROM f_{MAX}					f_{MIN} IS ZERO OR SAME SIGN AS f_{MAX}									
	19	20	21	22	23	24	25	26	27	28	29	30	31	32	33
	f_{MIN} / 2	$\Delta\sigma'_{RES_1}$ K_N x ⑲	$\Delta\epsilon_{RES_2}$ ⑲ x ⑤ / ①	$\Delta\sigma'_{RES_2}$ FROM CYCLIC STRESS-STRAIN CURVE	σ_{RES} ⑫ - ⑳ - ㉒	f_{MIN}	$\Delta\sigma'_{RES_1}$ K_N x ① / 2.0	$\Delta\epsilon'_{RES_2}$ ⑤ / 2.0	$\Delta\sigma'_{RES_2}$ FROM CYCLIC STRESS-STRAIN CURVE	σ_{RES} ④ - ㉕ - ㉗	$\Delta\epsilon$ RANGE ⑨ + ⑲	σ_{MEAN} ⑬ + σ^*_{RES} - σ_{RES}	-ϵ_t ⑭ / (1 - σ_{MEAN}/σ_{FRACT})	N_2 CYCLES TO FAILURE	n/N_2 ⑰ / ㉜
1						O	33550	.0039071	35776	-16791	.0078621	-27027	.0029149	1459000	.000555
2						↕	43136	.0055628	44752	-28011	.0093764	-17746	.0042522	79190	.003283
3						↕	52722	.0075891	51906	-38690	.0123613	- 9376	.0059256	11410	.005698
4						↕	62308	.0100669	57865	-48884	.0162977	- 1604	.0080318	2045	.004414
5						↕	74770	.0141639	64613	-61690	.0216409	8002	.0116694	782	.002559
6						↕									
7						↕									
8						↕									
9						↕									
10						O									

$$\text{LIFE} = \left[\frac{1 - \sum\left[\frac{n}{N}\right]_1}{\sum\left[\frac{n}{N}\right]_2} + 1\right] H$$

= 5815 hours

FATIGUE PREDICTION METHOD BASED ON STRAIN — $\sigma^*_{RES} = 61690$ — $\sum\left[\frac{n}{N}\right]_2 = 0.0165094$

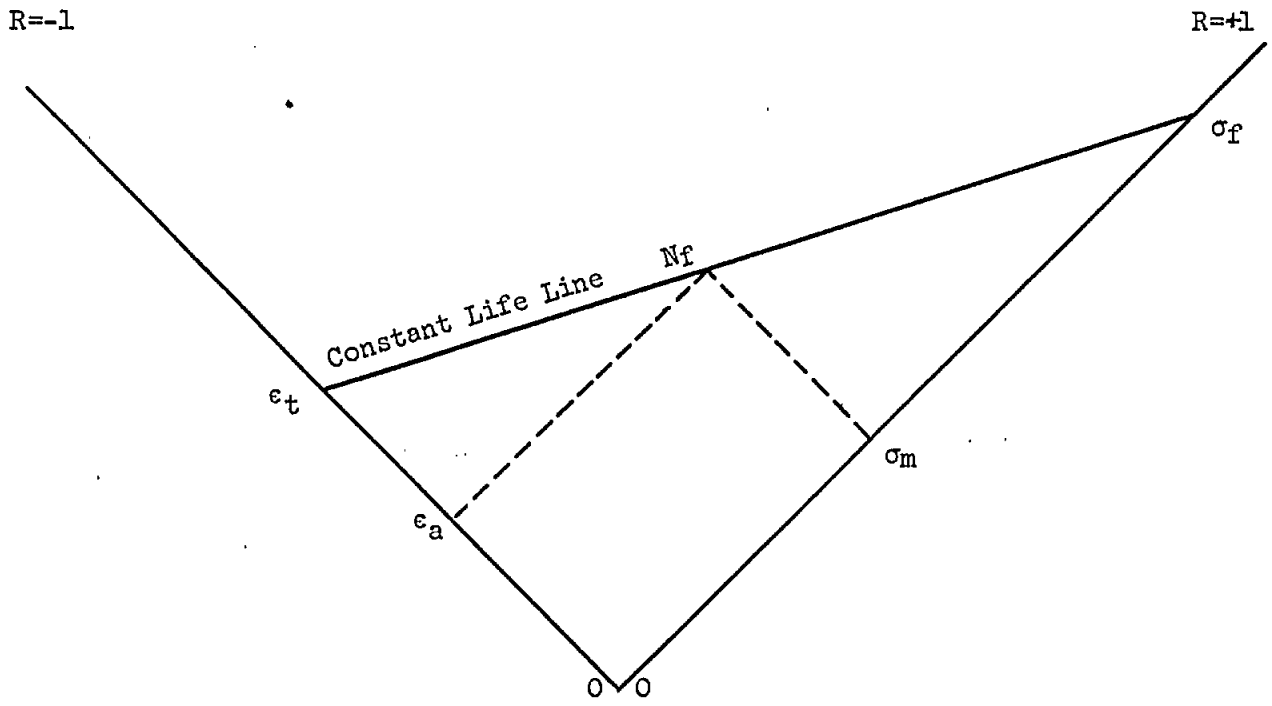

Modified Goodman Diagram

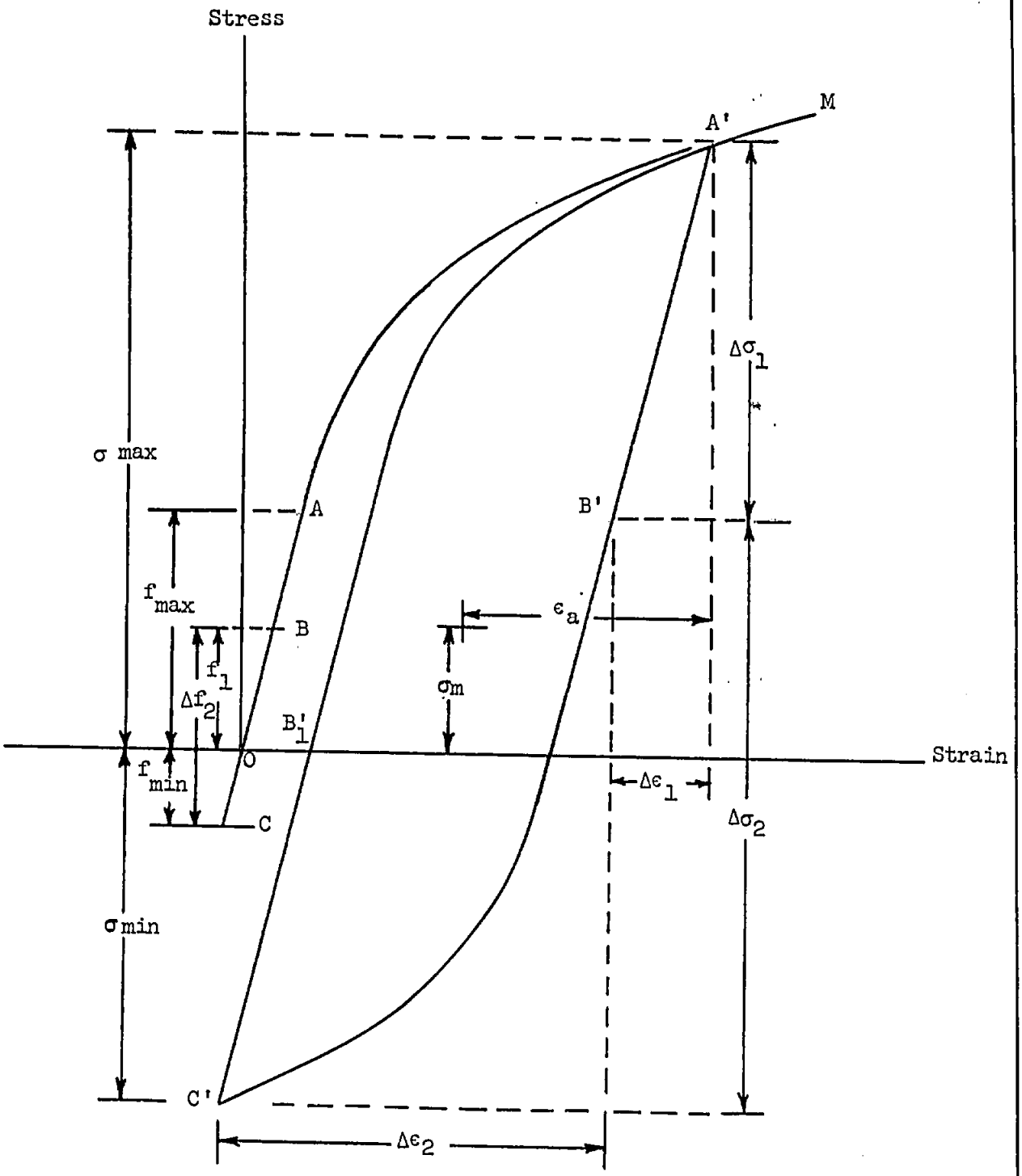

Hysteresis Curve for Strain Method

E. COMPUTER PROGRAMS FOR FATIGUE LIFE PREDICTION

Several computer programs are available to facilitate the tedious arithmetic involved in making fatigue life predictions of multiple level spectra. The programs are stored using computer language titles for the type program desired.

The stress method of fatigue life prediction as defined by Grumman Structures Manual pages B7.030-8 through B7.030-26 is presented in users manual form by report SAR-76-1.(Ref.43) The strain method of fatigue life prediction as defined by pages B7.030-27 through B7.030-43 is likewise presented in users manual form by report SAR-76-2.(Ref.44) The strain method has available several auxilary programs attached to facilitate presentation features. The general strain life prediction program is titled FATLF , attached to this program is another program titled PCENT,this is a damage presentation analysis. One other program for preliminary spectrum review is the program CHECK . This program produces a column output of the input spectrum data.

PREPARATION OF DESIGN FATIGUE SPECTRA

Introduction

Since military aircraft are required to meet many design conditions, a problem the stress analyst encounters occurs when a given part is affected by the loads of more than one design spectrum. The magnitudes of the various levels in a spectrum are usually a specified quantity or dependent on events outside the analysts control, however, the analyst can influence the design spectrum when spectra combination is necessary. Spectra combination has a strong influence on the stress range of a given cycle. For example a positive load spectrum can be arbritrarily combined with a negative load spectrum so that a cycle goes from negative maximum to positive maximum. This can be overly conservative and not realistic for loading conditions whose combination is statistically improbable. It is therefore necessary to follow a more rational proceedure when combining the levels of several spectra.

Discussion

The method offered in this section for the combination of levels of different spectra is based on the assumption that each spectrum is statistically independent. This assumption then permits a random combination of levels based on joint probability calculations. It must be recognized that the combination of levels must be limited to levels that can be randomily combined. For example, spectra levels that should not be separated, such as catapult buffer load followed by catapult launch loads must be combined separately, before the catapult sequence (buffer to launch, Reference(a), for example) can be combined with other possible loading spectra.

For each level in the spectrum, the probability of the level occuring in a given cycle is the number of cycles at the level divided by the total number of cycles in the spectrum. This is true for the individual spectrum or for spectra combined from several lesser spectra. Therefore, when combining spectra, the probabilities of two levels occurring in a given cycle is the joint probability, which is the product of the individual probabilities. The number of cycles of this combination is the total number of cycles times the joint probability of occurance. In order to combine several spectra, the cycles of one individual spectrum must at least equal the sum of the cycles of all the other spectra. The dominate spectrum is then the one to which all the other spectra are combined. If the cycles of the dominate spectrum exceed the sum of cycles of the other spectra, then another spectra must be added so that the cycles of the dominate spectrum will equal the total number of cycles of the other spectra to be combined.

This process can be illustrated by the following example. Given three combinable spectra A, B, and C of load levels up to L and total cycles N_A, N_B, and N_C respectively. For this example $N_C > (N_A + N_B)$.

Preparation of Design Fatigue Spectra (Continued)

Each individual spectra can be illustrated in the following tabular presentation:

Level	Occurances
1	a
2	b
.	.
.	.
.	.
L	n
	$\Sigma = N$

For example, the probability of level 2 occurring in a given cycle is:

$$P(2) = \frac{b}{N}$$

In tabular form, the spectra to be combined will appear as:

Level	Spectrum A	Spectrum B	Spectrum Base	Spectrum C
1	a_A	a_B	$a_C - a_A - a_B$	a_C
2	b_A	b_B	$b_C - b_A - b_C$	b_C
.	.	.	.	.
.	.	.	.	.
.	.	.	.	.
L	n_A	n_B	$n_C - n_A - n_B$	n_C
	$\Sigma = N_A$	$\Sigma = N_B$	$\Sigma = N_C - N_A - N_B$	$\Sigma = N_C$

} occurrances

Notice that another spectrum called Base has been added to the definition of the original problem. The magnitude of the level in this spectrum may be arbitrarily defined or possibly be stipulated by the procuring agency. However, the number of cycles (total and at each level) are derived so that $N_A + N_B + N_{BASE} = N_C$ and similarly at each level: $a_A + a_B + a_{BASE} = a_C$ etc.

Preparation of Design Fatigue Spectra (Continued)

The probability of level 2 of Spectrum B occuring in a given cycle of the joint spectrum is:

$$P_B(2) = \frac{b_B}{N_C}$$ and the probability of

level 1 of spectrum C occuring in a given cycle of the combined spectrum is:

$$P_C(1) = \frac{a_C}{N_C}$$

The probability of level 2, Spectrum B and level 1, Spectrum C occuring in a given cycle is then:

$$P_B(2) \times P_C(1) = \frac{b_B \cdot a_C}{(N_C)^2}$$ (this is the joint probability)

The number of cycles of this combination of events is the joint probability times the number of cycles in the combined spectrum:

$$n_{(B,2)(C,1)} = \frac{b_B \cdot a_C}{(N_C)^2} \cdot N_C = \frac{b_B \cdot a_C}{N_C}$$

If each level of the four spectra in the above example is of different magnitude, a tabulation of the combined spectra will expand from 5 columns to a table containing (3 x Levels + 2) columns. This can be seen by listing the calculations made for each spectrum. Spectrum B is shown below as an example.

Spectrum B				Spectrum C	Level
1	2	. . .	L		
$a_B\ a_C/N_C$	$b_B\ a_C/N_C$	. . .	$n_B\ a_C/N_C$	a_C	1
$a_B\ b_C/N_C$	$b_B\ b_C/N_C$	. . .	$n_B\ b_C/N_C$	b_C	2
.	.	. . .	.	.	.
.	.	. . .	.	.	.
.	.	. . .	.	.	.
$a_B\ n_C/N_C$	$b_B\ n_C/N_C$	. . .	$n_B\ n_C/N_C$	n_C	L
$\Sigma = a_B$	$\Sigma = b_B$		$\Sigma = n_B$	ΣN_C	

$\Sigma\Sigma = N_B$

Preparation of Design Fatigue Spectra (Continued)

The value in each column under spectrum B is cycles of occurance of that level (column heading) with the event in that row of spectrum C.

At this point a numerical example is in order. In the following example assume Spectra A, B, and C are specified and Spectrum Base is derived. Spectra A, B, and Base are to be combined with spectrum C. It is also assumed that all levels of the Base spectrum are of the same magnitude. The spectra will appear as follows (before combining):

Level	Spectra			
	A	B	Base	C
1	12000	70000	All	150000
2	7000	30000	Levels	80000
3	400	15000	Same	20000
4	100	2000	Magnitude	4000
5	20	100		300
$\sum$ N =	19520	117100	117680	254300

Performing the arithmetic operations discussed above will result in the following combined spectra.

	Spectrum A					Spectrum B					Spectrum Base	Spectrum C	
Level→	1	2	3	4	5	1	2	3	4	5		Cycles	Level
cycles	7078	4129	236	59	12	41290	17695	8848	1180	59	69414	150000	1
	3775	2202	126	31	6	22021	9438	4719	630	31	37021	80000	2
	944	551	31	8	2	5505	2360	1179	157	8	9255	20000	3
	189	110	6	2	0	1101	472	236	31	2	1851	4000	4
	14	8	1	0	0	83	35	18	2	0	139	300	5
$\sum$	12000	7000	400	100	20	70000	30000	15000	2000	100	117680	254300	
	$\sum\sum$ = 19520					$\sum\sum$ = 117100							

References:

(a) Raynor, G.T. "Spectrum Interpretation Effect on Fatigue Life Prediction", Grumman Aerospace Corporation Report No. 74-SAM-6, December 16, 1974

Symbols:

A, B, C	Spectrum designations
a, b, n	Occurances at different spectrum levels
N	Total occurances in one spectrum
P	Probability of occurance
L	Maximum level in given spectrum

Subscripts:

A, B, C	Pertaining to spectrum of that designation
1, 2	Pertaining to that level number

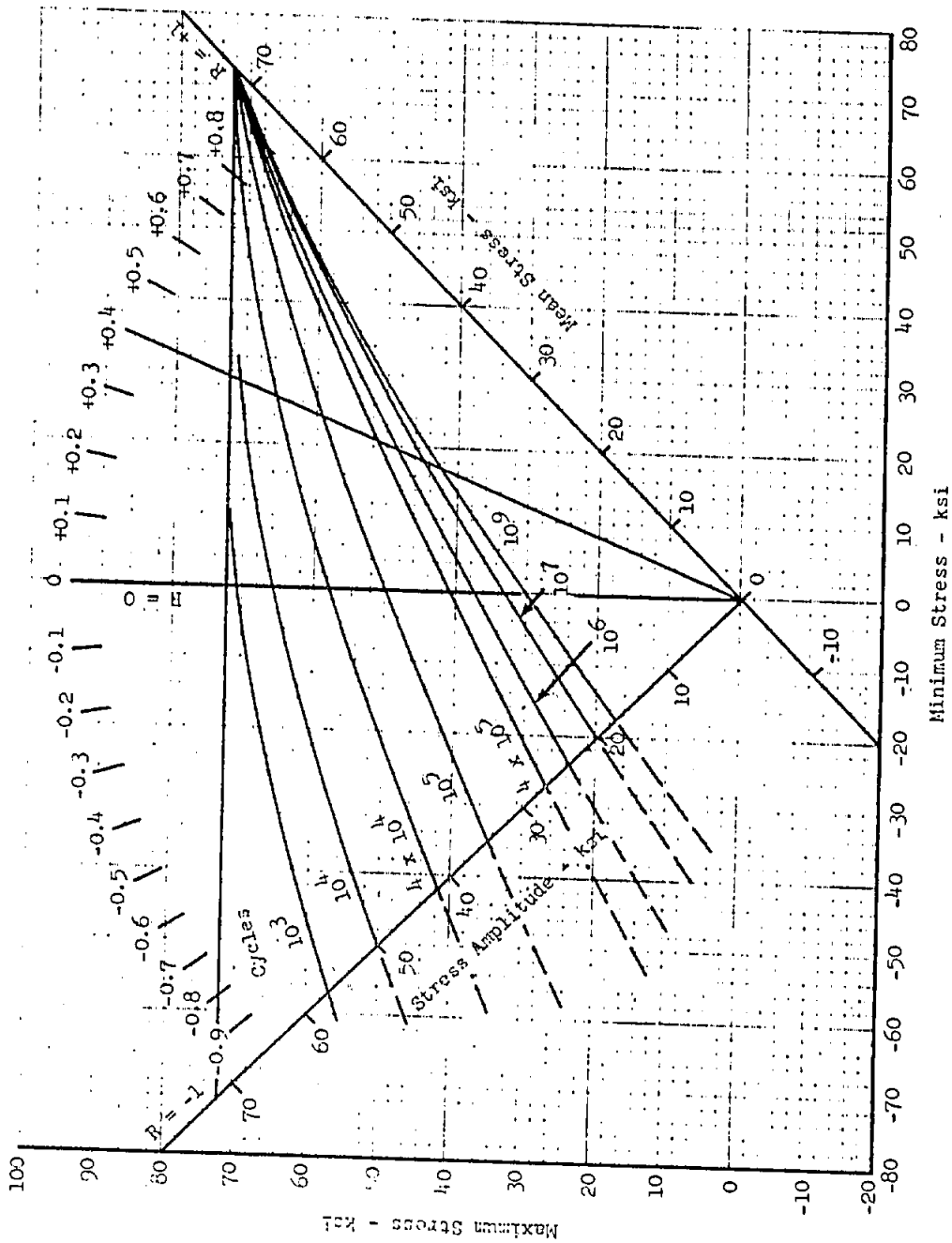

CONSTANT LIFE CURVES

Rolled and Drawn Sheet and Bar
Axially Loaded
Polished Specimens
Curves Represent Average of Test Data

Ref: Report GE-144

FATIGUE CURVES

Bare 2024-T3, 2024-T4
and 2014-T6
Aluminum Alloys

Material	Ult.Tens.Str.	Yield Str.
2024	72000 psi	52000 psi
2014	71500 psi	63500 psi

Grumman

FATIGUE CURVES

Bare 2024-T3,
2024-T4 & 2014-T6
Aluminum Alloys

Material	Ult.Tens.Str.	Yield Str.
2024	72000 psi	52000 psi
2014	71500 psi	63500 psi

CONSTANT MINIMUM STRESS CURVES

Rolled and Drawn Sheet and Bar
Axially Loaded
Polished Specimens
Curves Represent Average of Test Data

Ref: Report GE-144

NOTE: For clad materials subjected to a loading cycle of f_{min} to f_{max}, the fatigue life can be determined by entering the bare material curves below with an equivalent loading cycle of f_{min} to f_{max} ①, where f_{max} ① $= f_{max} + \Delta f$, and the correction stress Δf is given in the table below.

CORRECTION STRESS FOR CLAD MATERIAL				
Material	Δf, in 1,000 psi			
	$n \leq 10^3$	$n = 10^4$	$n = 5 \times 10^4$	$n \geq 10^5$
2024-T3,-T4	6	8	9	9
2014-T6	2	3	6	9

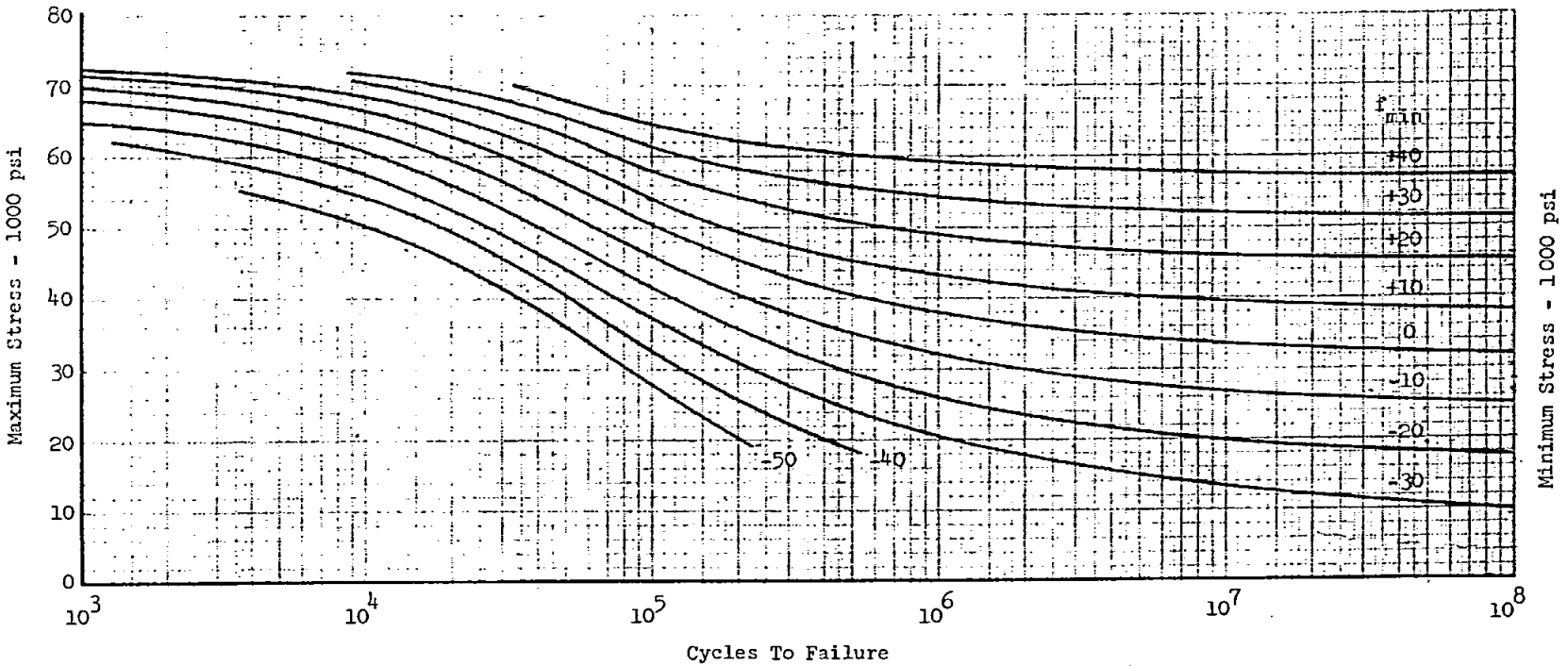

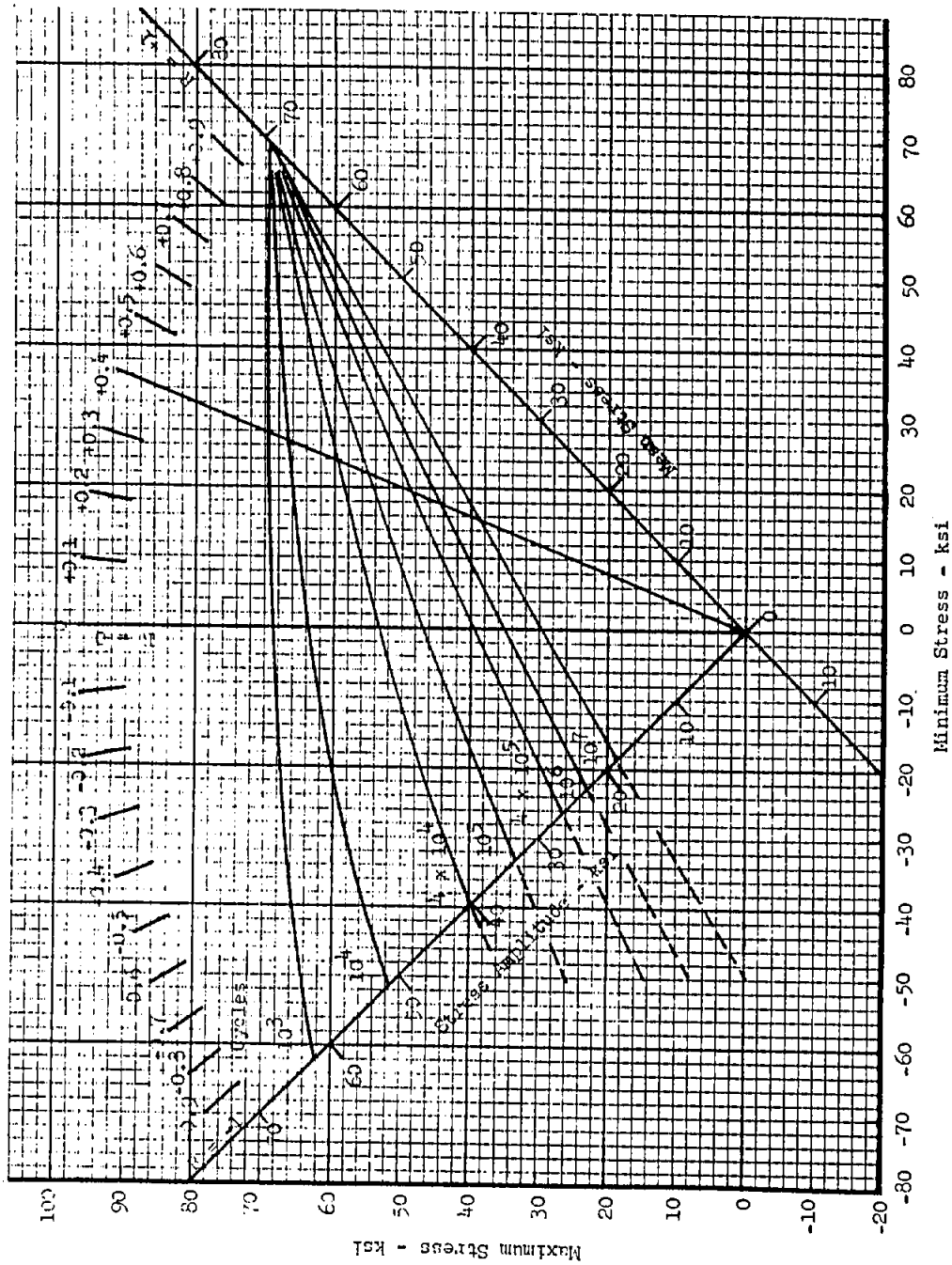

CONSTANT LIFE CURVES

7/8 in. Thick Plate
Axially Loaded
Polished Specimens

Ref: Alcoa Research Labs.
M.T. No. 030662-C

FATIGUE CURVES

Bare 2024-T851 Aluminum Alloy

Material	Ult. Tens. Str.	Yield Str.
2024	69000 psi	61700 psi

FATIGUE CURVES

Bare 2024-T851 Aluminum Alloy

Material	Ult. Tens. Str.	Yield Str.
2024	69000 psi	61700 psi

CONSTANT MINIMUM STRESS CURVES

7/8 in. Thick Plate
Axially Loaded
Polished Specimens

Ref: Alcoa Research Labs. M.T. No. 030662-C

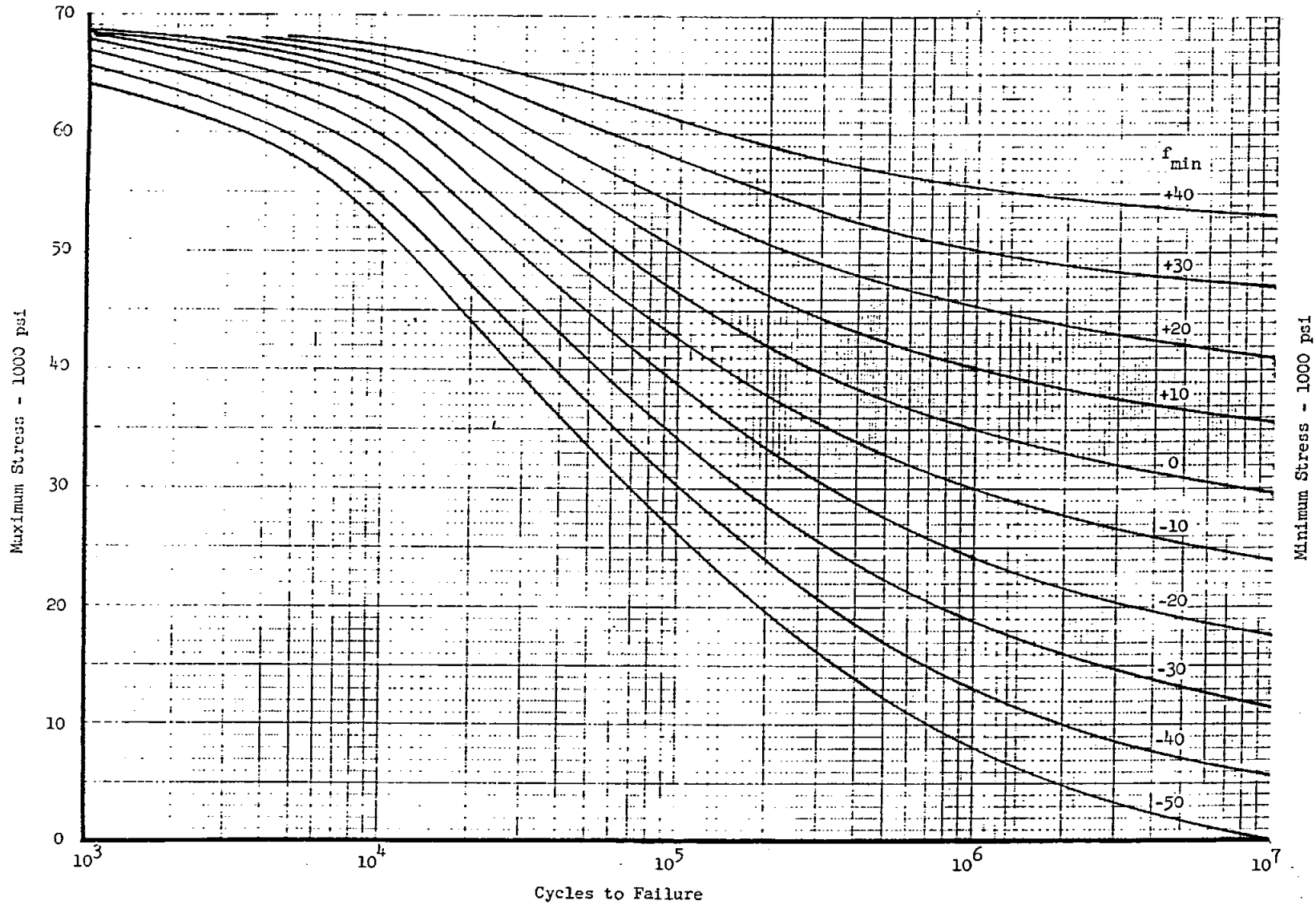

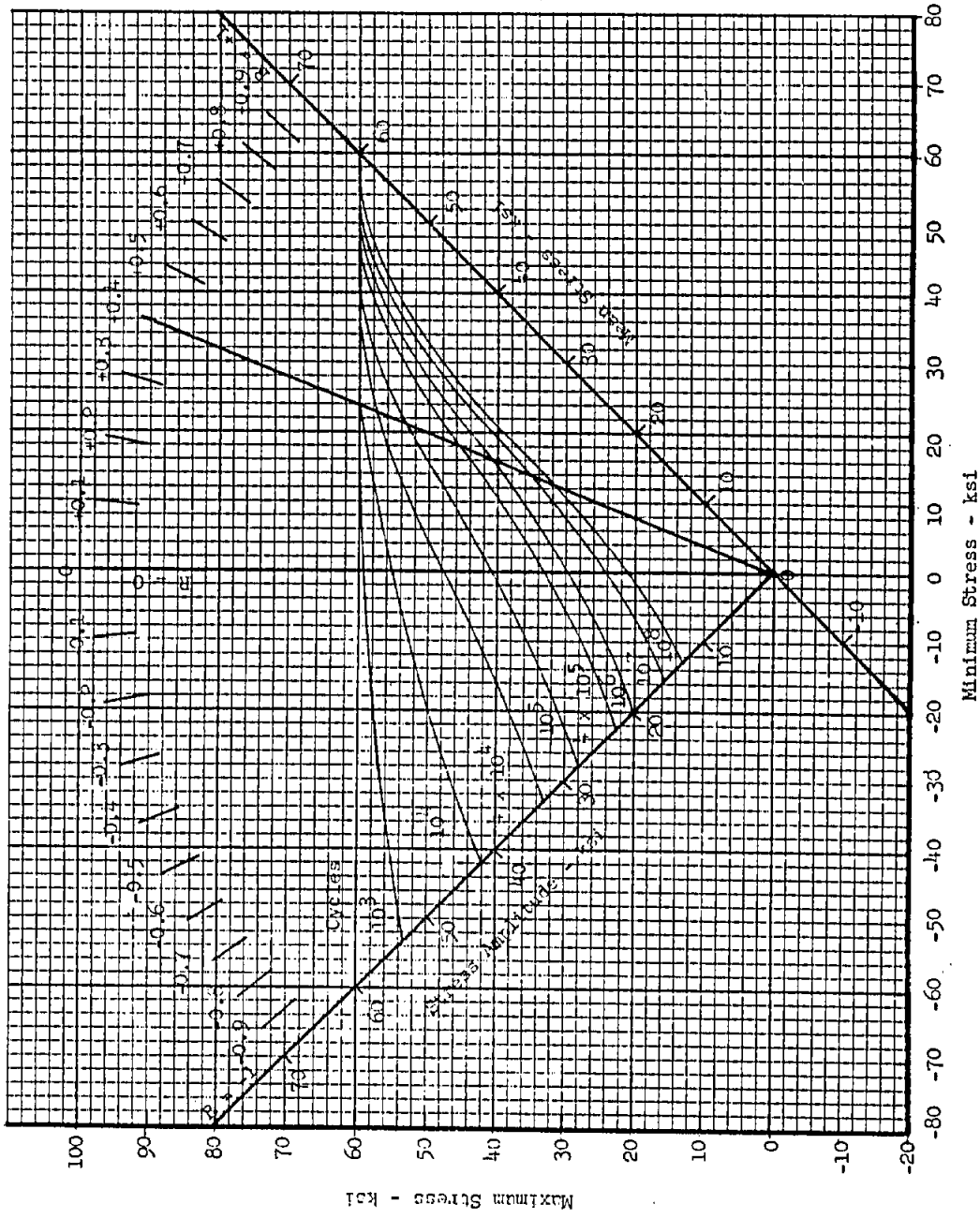

FATIGUE CURVES

Bare 2024-T851 Aluminum
Alloy at 300° F

Material	Ult. Tens. Str.	Yield Str.
2024	60100 psi	55300 psi

CONSTANT LIFE CURVES

7/8 in. Thick Plate
Axially Loaded
Polished Specimens

Ref: Alcoa Research Labs. M. T. No. 030662-C

FATIGUE CURVES

Bare 2024-T851 Aluminum Alloy at 300°F

Material	Ult. Tens. Str.	Yield Str.
2024	60100 psi	55300 psi

CONSTANT MINIMUM STRESS CURVES

7/8 in. Thick Plate
Axially Loaded
Polished Specimens

Ref: Alcoa Research Labs. M. T. No. 030662-C

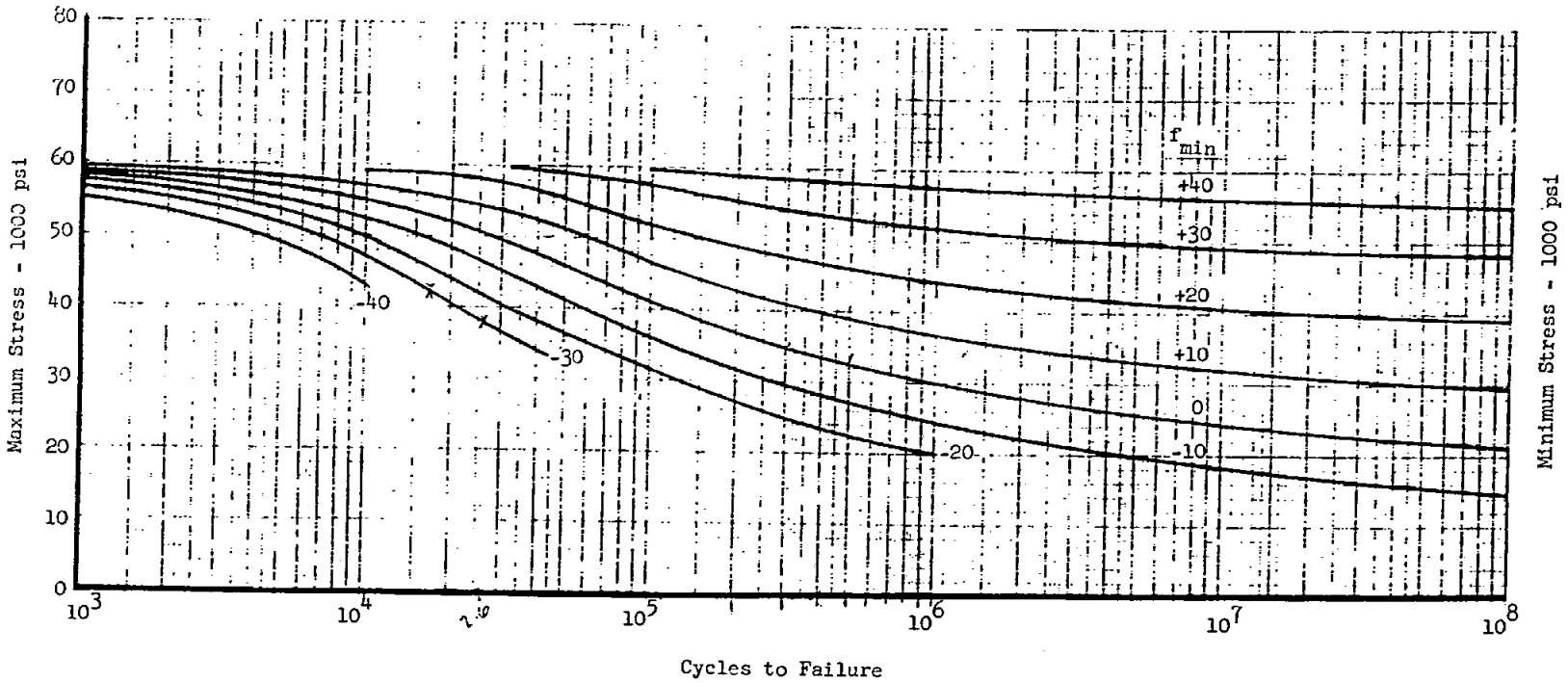

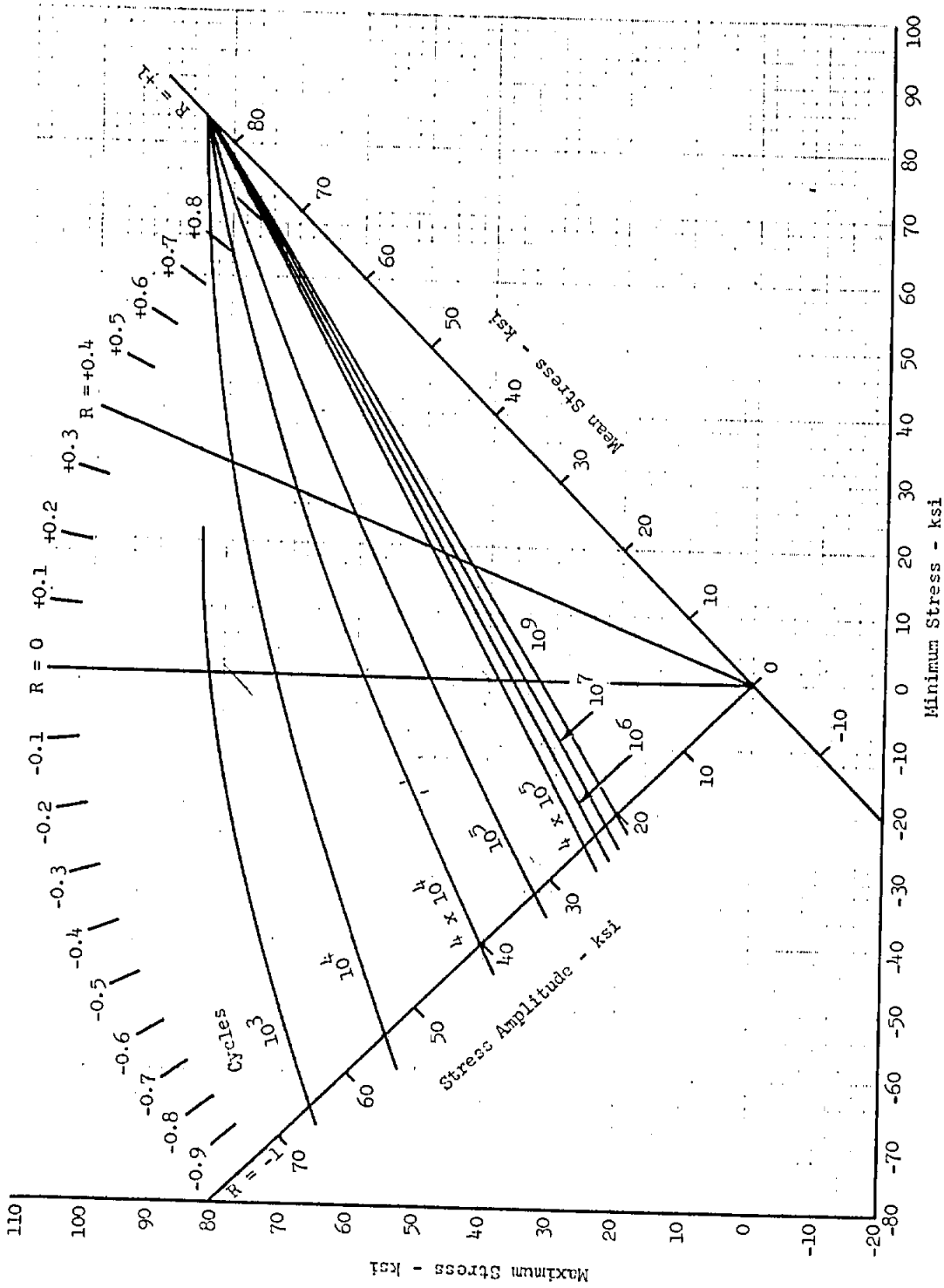

CONSTANT LIFE CURVES

Rolled and Drawn Sheet and Bar
Axially Loaded
Polished Specimens
Curves Represent Average of Test Data
Ref: Report GE-144

FATIGUE CURVES
Bare 7075-T6 Aluminum Alloys

Material	Ult.Tens.Str.	Yield Str.
7075	82500 psi	75000 psi

Grumman

Grumman

FATIGUE CURVES
Bare 7075-T6
Aluminum Alloys

Material	Ult.Tens.Str.	Yield Str.
7075	82500 psi	75000 psi

CONSTANT MINIMUM STRESS CURVES

Rolled and Drawn Sheet and Bar
Axially Loaded
Polished Specimens
Curves Represent Average of Test Data
Ref: Report GE-144

NOTE: For clad 7075-T6 subjected to a loading cycle of f_{min} to f_{max}, the fatigue life can be determined by entering the bare material curves below with an equivalent loading cycle of f_{min} to f_{max}①, where f_{max}① = f_{max} + Δf, and the correction stress Δf is given in the table below.

CORRECTION STRESS FOR CLAD MATERIAL		
Δf, in 1000 psi		
$n \leq 10^3$	$n = 10^4$	$n \geq 10^5$
6	8	9

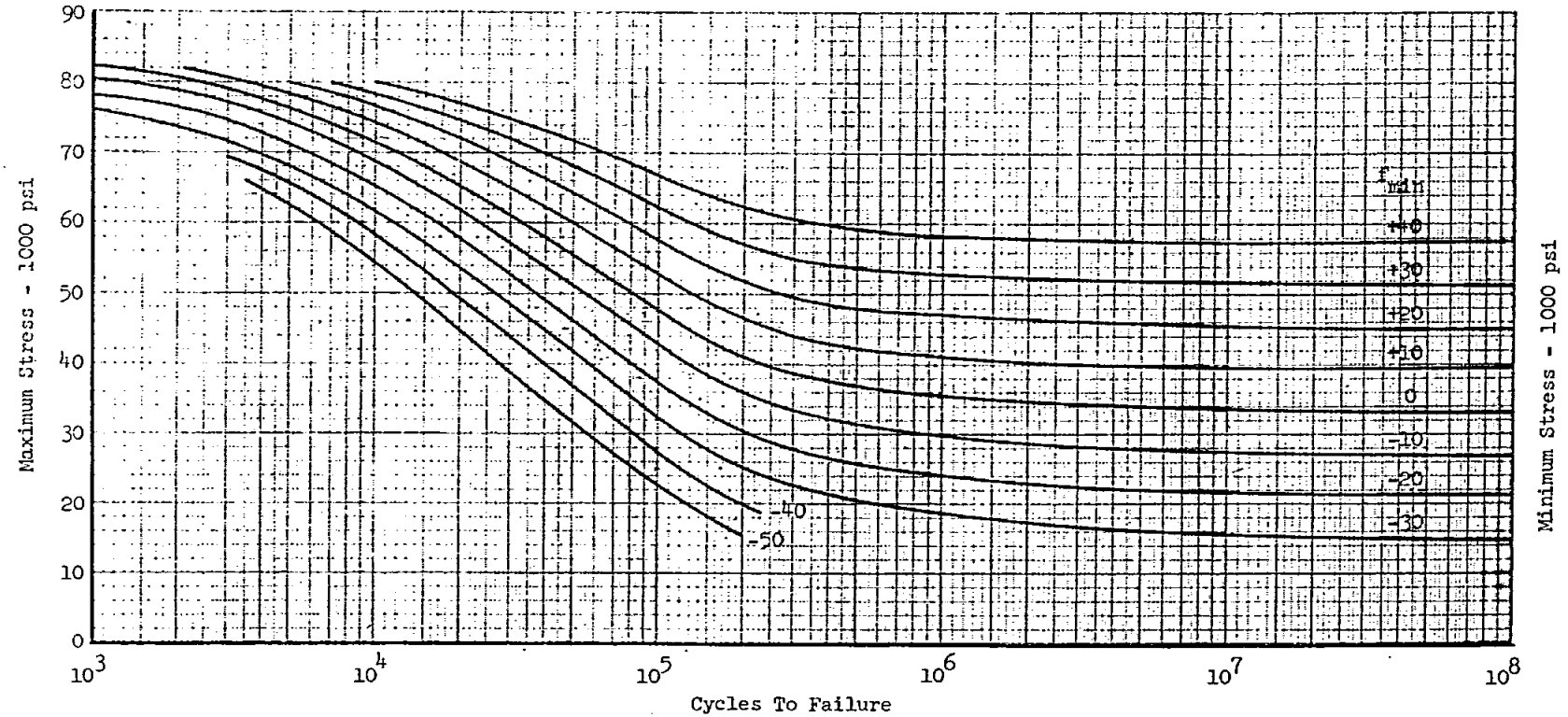

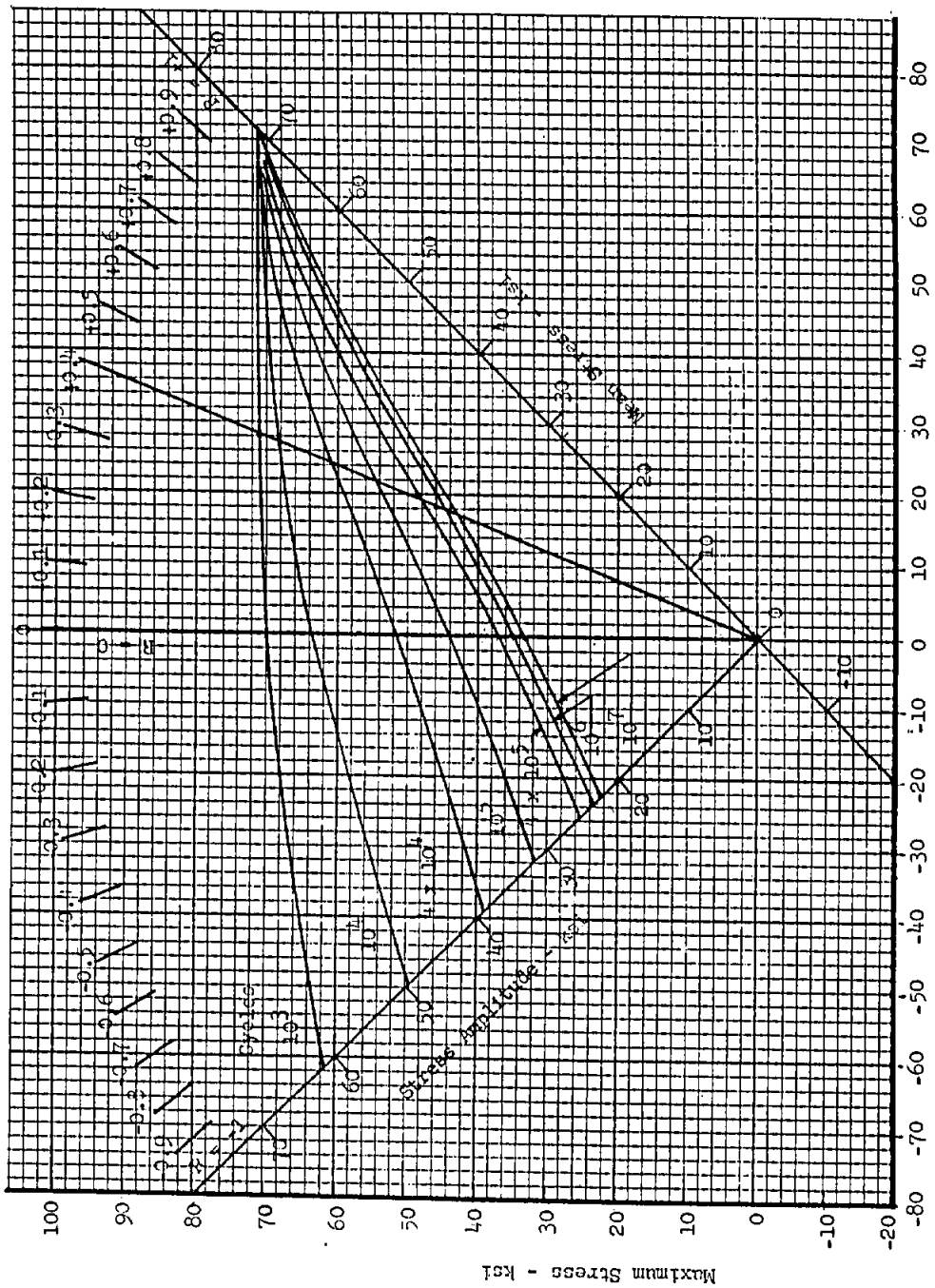

FATIGUE CURVES

7075-T7351 Aluminum Alloy

CONSTANT LIFE CURVES

1 3/8 in. Thick Plate
Axially Loaded
Polished Specimens

Ref: Alcoa Research Labs.
M.T. No. 060567-A

Material	Ult. Tens. Str.	Yield Str.
7075	71000 psi	59000 psi

FATIGUE CURVES

7075-T7351 Aluminum Alloy

Material	Ult. Tens. Str.	Yield Str.
7075	71000 psi	59000 psi

CONSTANT MINIMUM STRESS CURVES

1 3/8 in. Thick Plate
Axially Loaded
Polished Specimens

Ref: Alcoa Research Labs. M.T. No. 060567-A

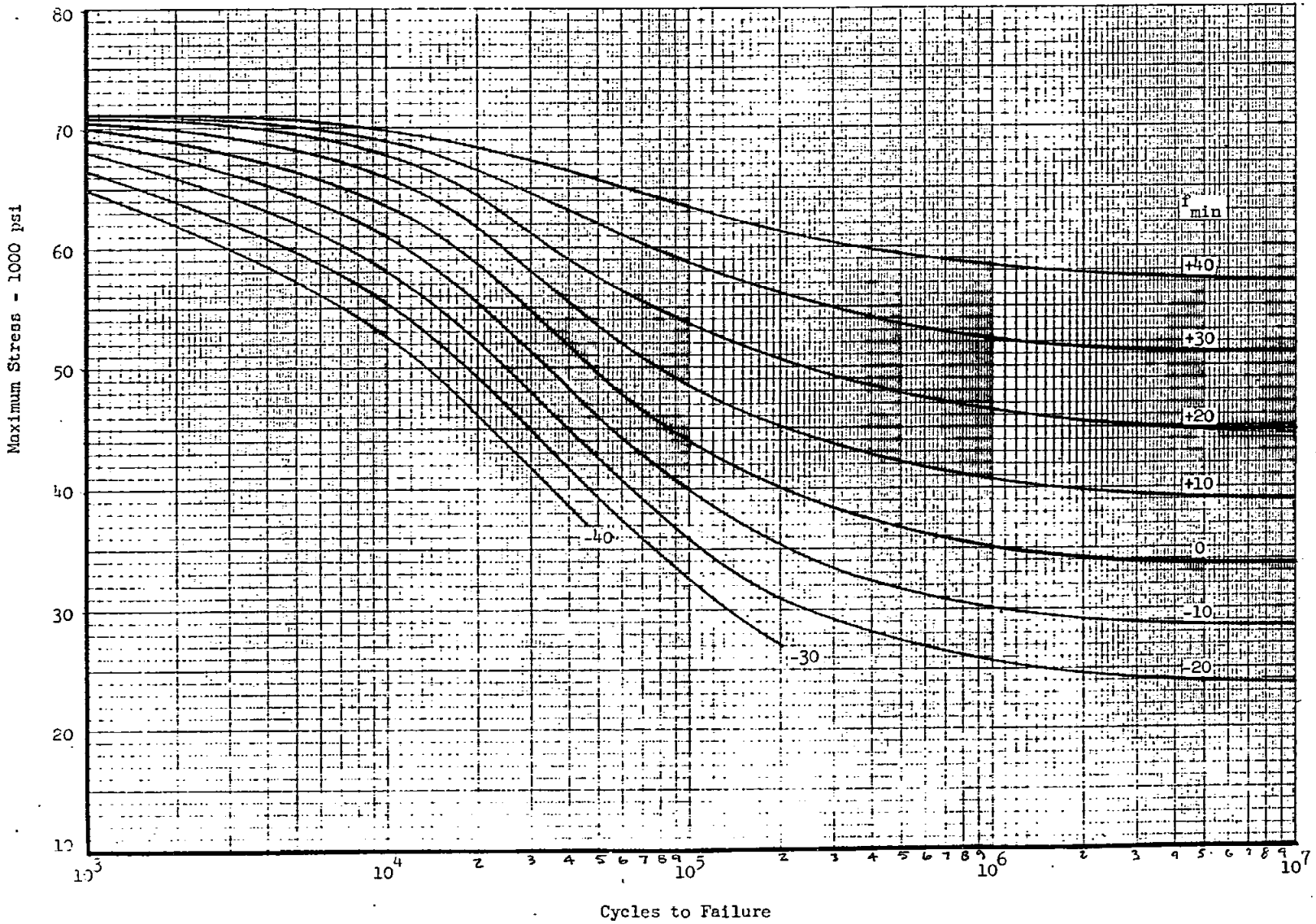

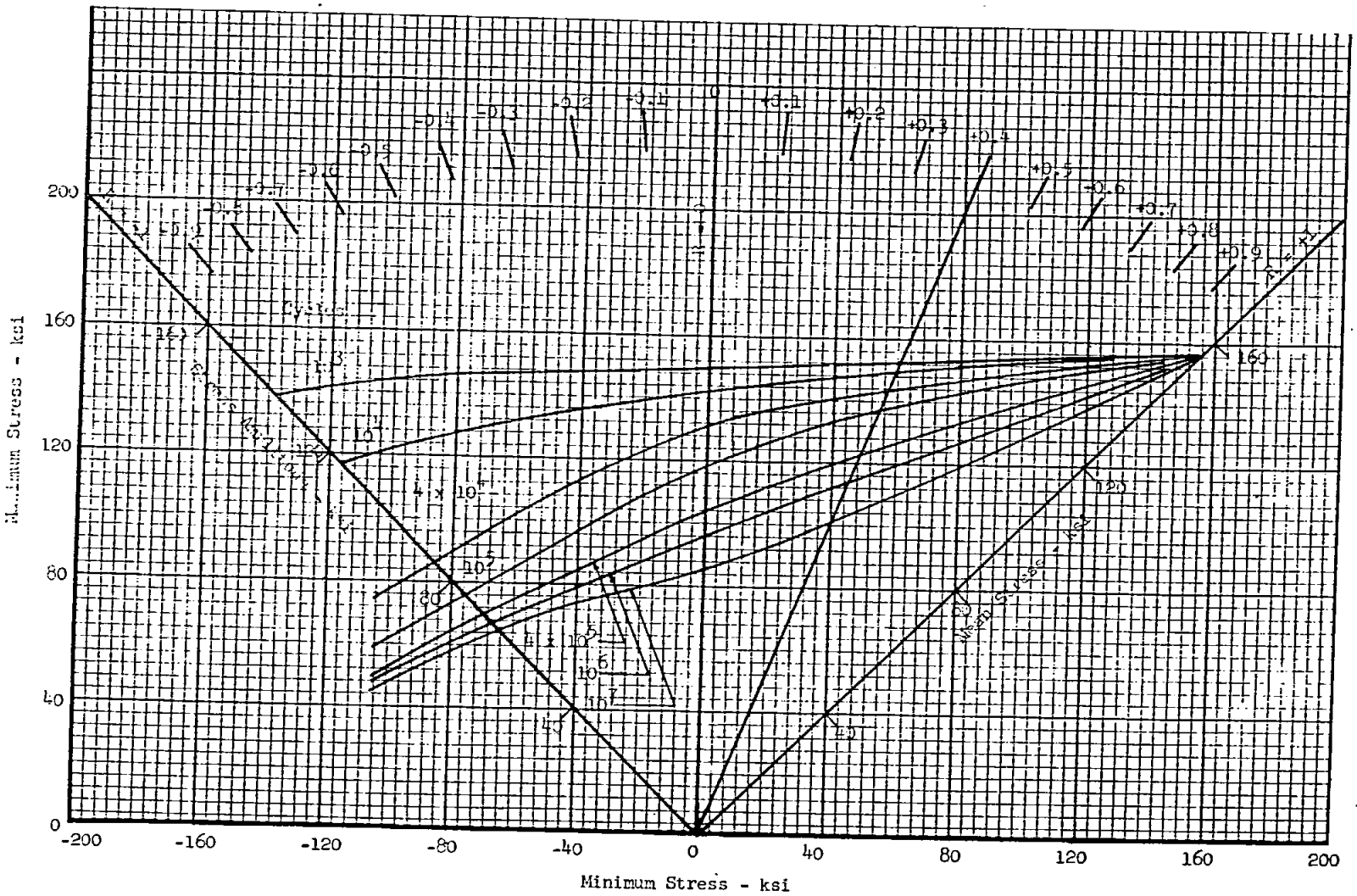

FATIGUE CURVES

6Al-6V-2Sn Annealed Titanium Alloy

Material	Ult. Tens. Str.	Yield Str.
6Al-6V-2Sn Annealed	156000 psi	146000 psi

CONSTANT LIFE CURVES

1 in. Thick Plate
Axially Loaded
Polished Specimens

Ref: Report FSN-AD2-06-68.1 and Unpublished G.A.E.C. Tests

FATIGUE CURVES

6Al-6V-2Sn Annealed
Titanium Alloy

Material	Ult. Tens. Str.	Yield Str.
6Al-6V-2Sn Annealed	156000 psi	146000 psi

CONSTANT MINIMUM STRESS CURVES

1 in. Thick Plate
Axially Loaded
Polished Specimens

Ref: Report FSN-AD2-06-68.1 and
Unpublished G.A.E.C. Tests

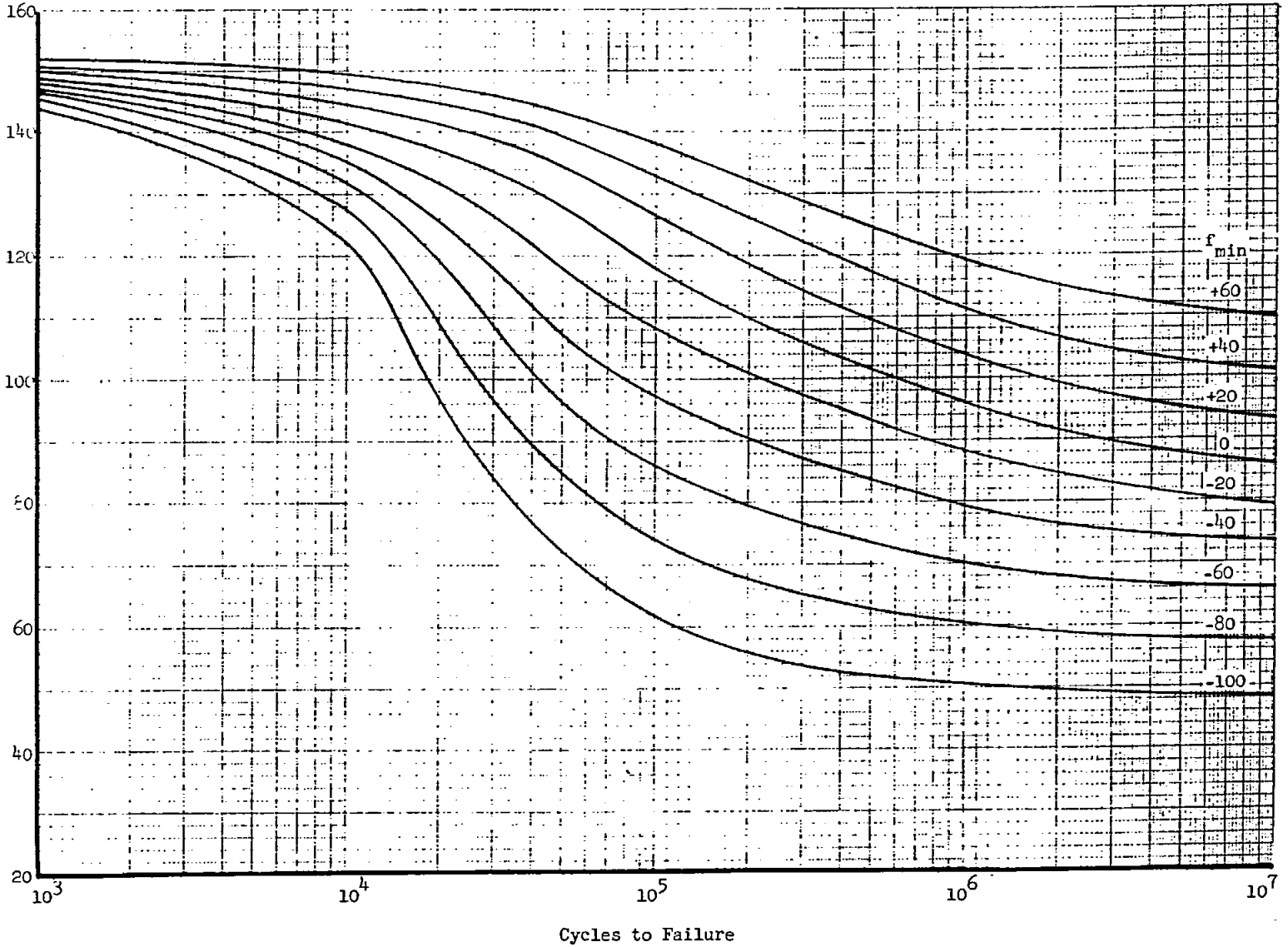

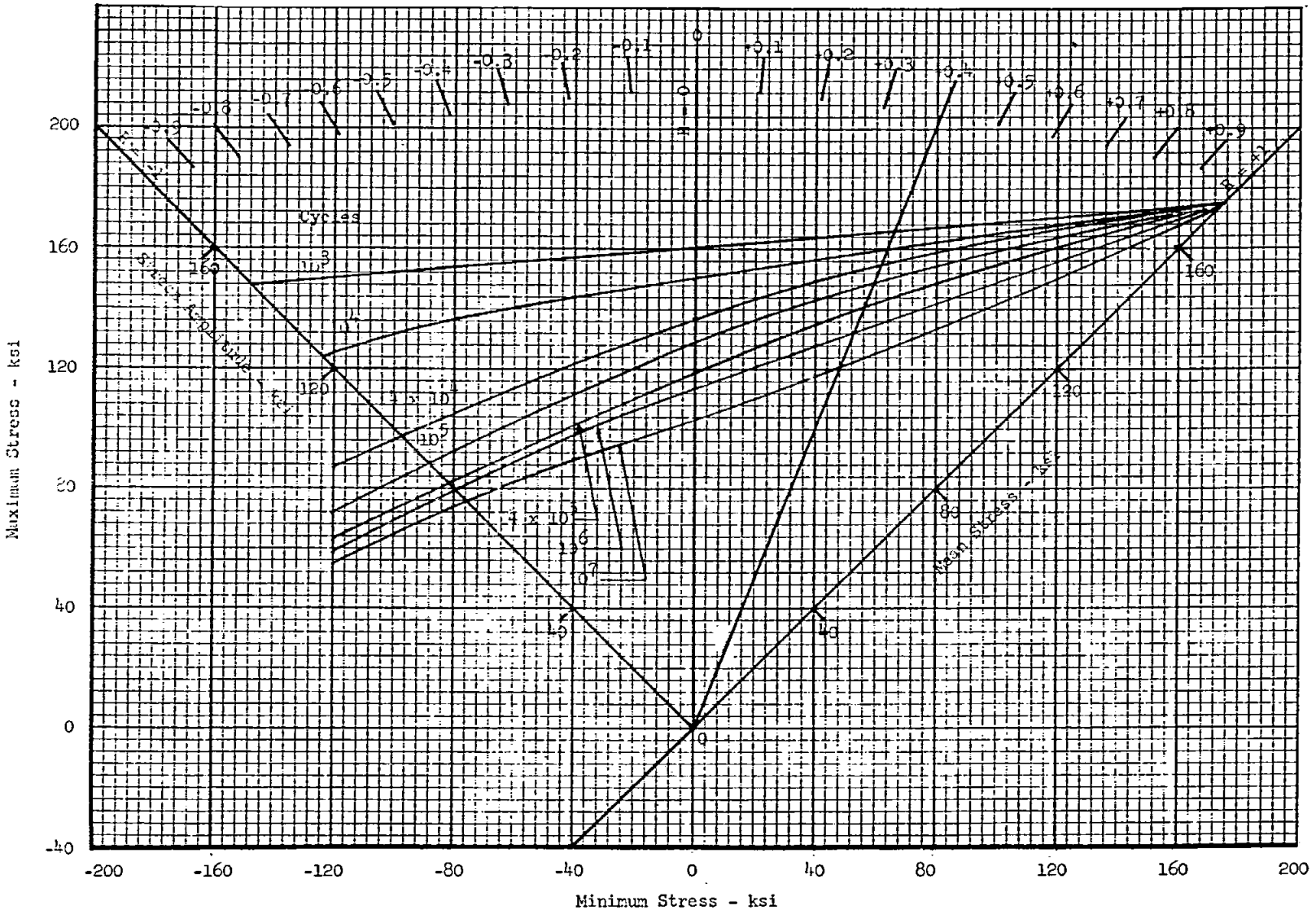

FATIGUE CURVES

6Al-6V-2Sn STA Titanium Alloy

Material	Ult. Tens. Str.	Yield Str.
6Al-6V-2Sn STA	175000 psi	165000 psi

CONSTANT LIFE CURVES

1 in. Thick Plate
Axially Loaded
Polished Specimens

Ref: Report FSN-AD2-06-68.1 and Unpublished G.A.E.C. Tests

FATIGUE CURVES

6Al-6V-2Sn STA
Titanium Alloy

Material	Ult. Tens. Str.	Yield Str.
6Al-6V-2Sn STA	175000 psi	165000 psi

CONSTANT MINIMUM STRESS CURVES

1 in. Thick Plate
Axially Loaded
Polished Specimens

Ref: Report FSN-AD2-06-68.1 and
Unpublished G.A.E.C. Tests

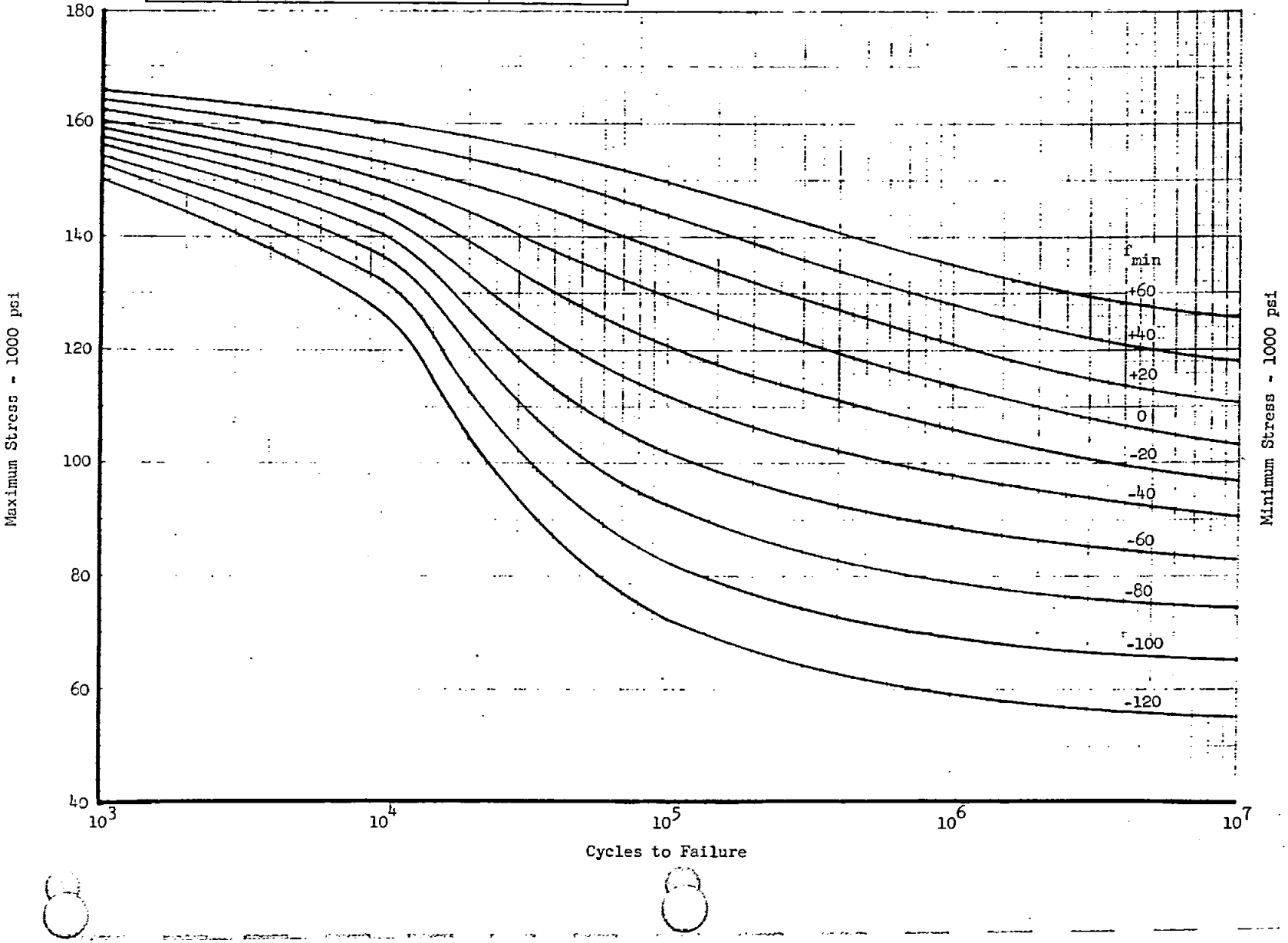

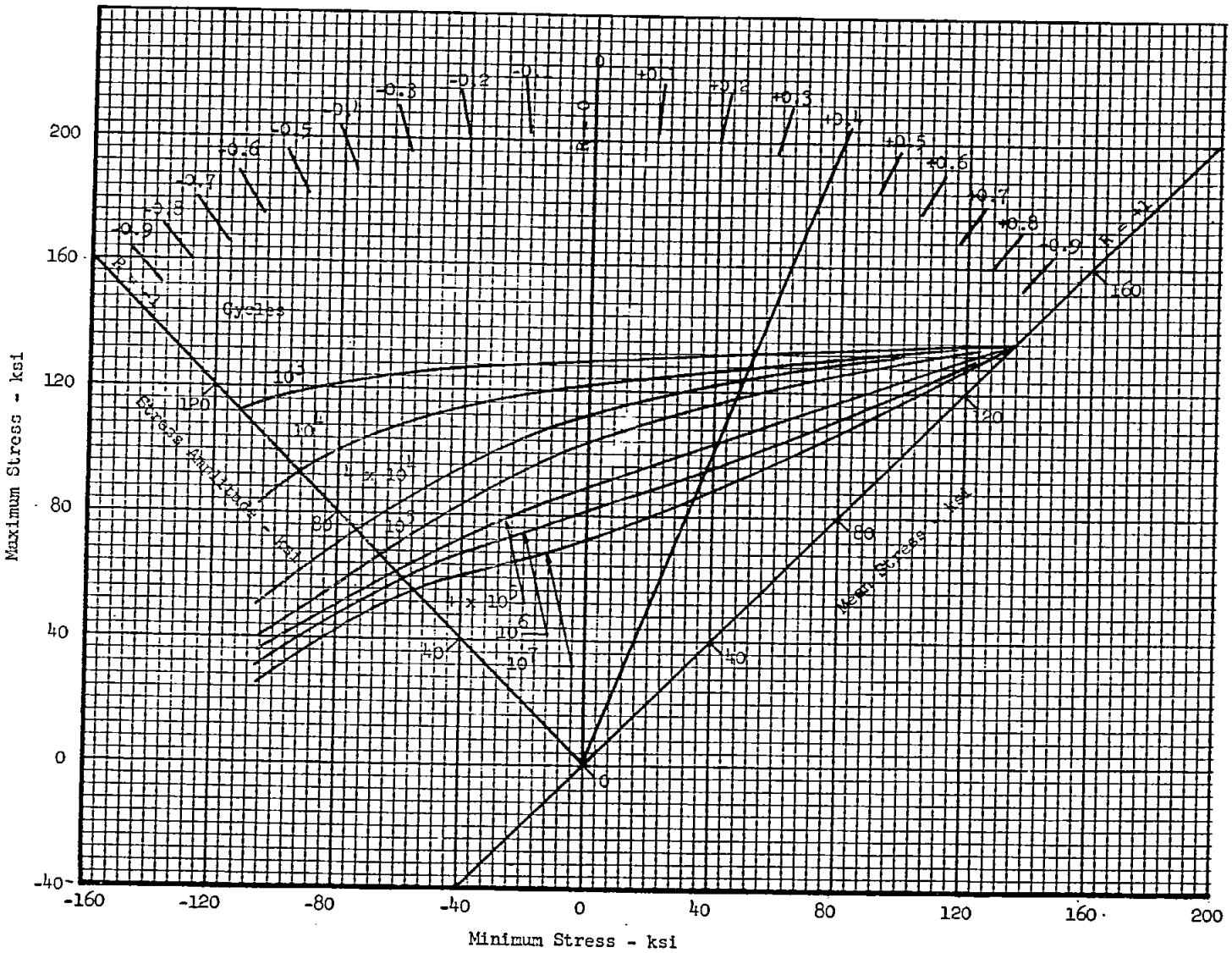

FATIGUE CURVES

6Al-4V Annealed Titanium Alloy

Material	Ult. Tens. Str.	Yield Str.
6Al-4V Annealed	136000 psi	128000 psi

CONSTANT LIFE CURVES

1 in. Thick Plate
Axially Loaded
Polished Specimens

Ref: Report FSN-AD2-06-68.1 and Unpublished G.A.E.C. Tests

FATIGUE CURVES

6Al-4V Annealed
Titanium Alloy

Material	Ult. Tens. Str.	Yield Str.
6Al-4V Annealed	136000 psi	128000 psi

CONSTANT MINIMUM STRESS CURVES

1 in. Thick Plate
Axially Loaded
Polished Specimens

Ref: Report FSN-AD2-06-68.1 and
Unpublished G.A.E.C. Tests

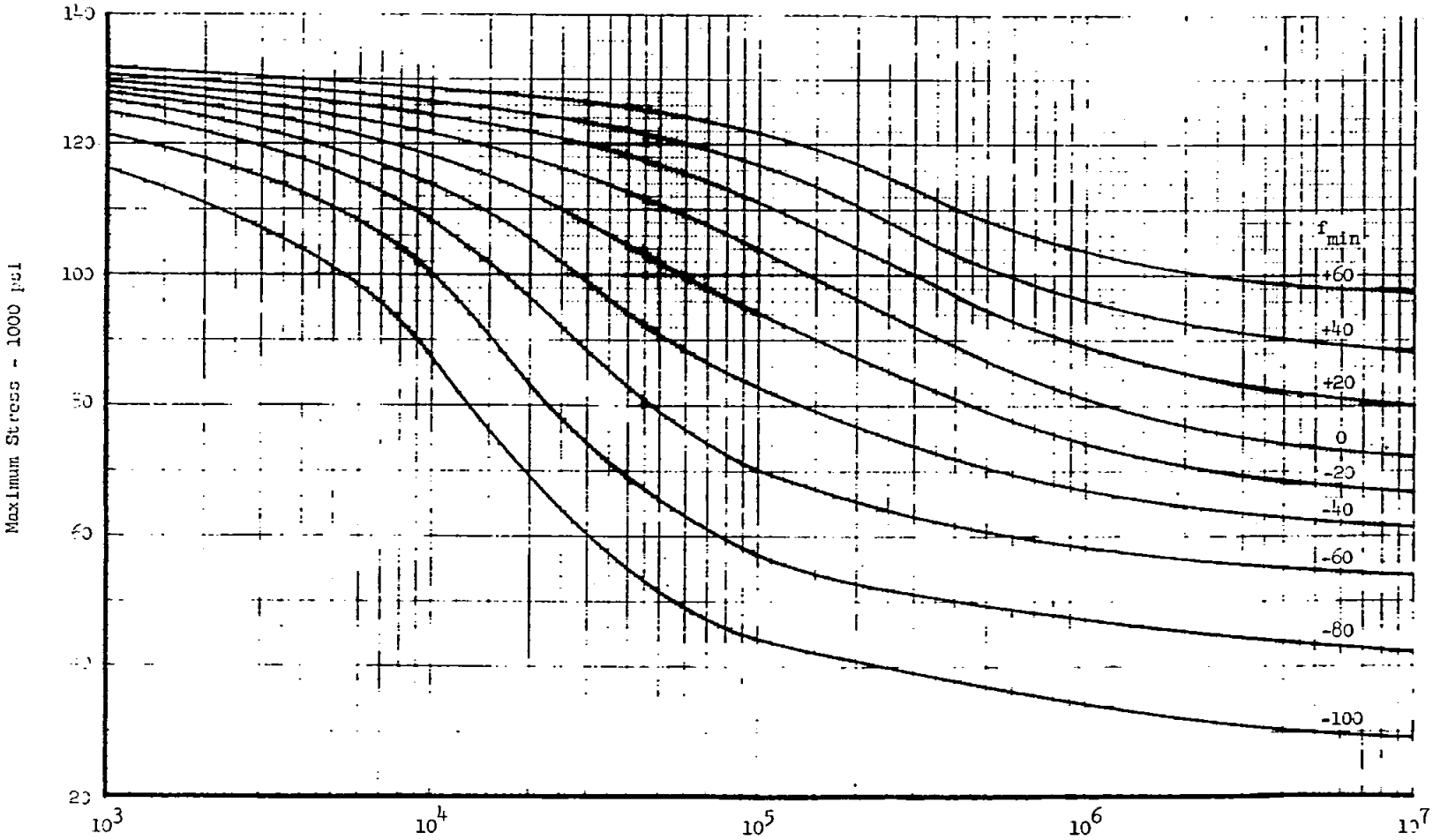

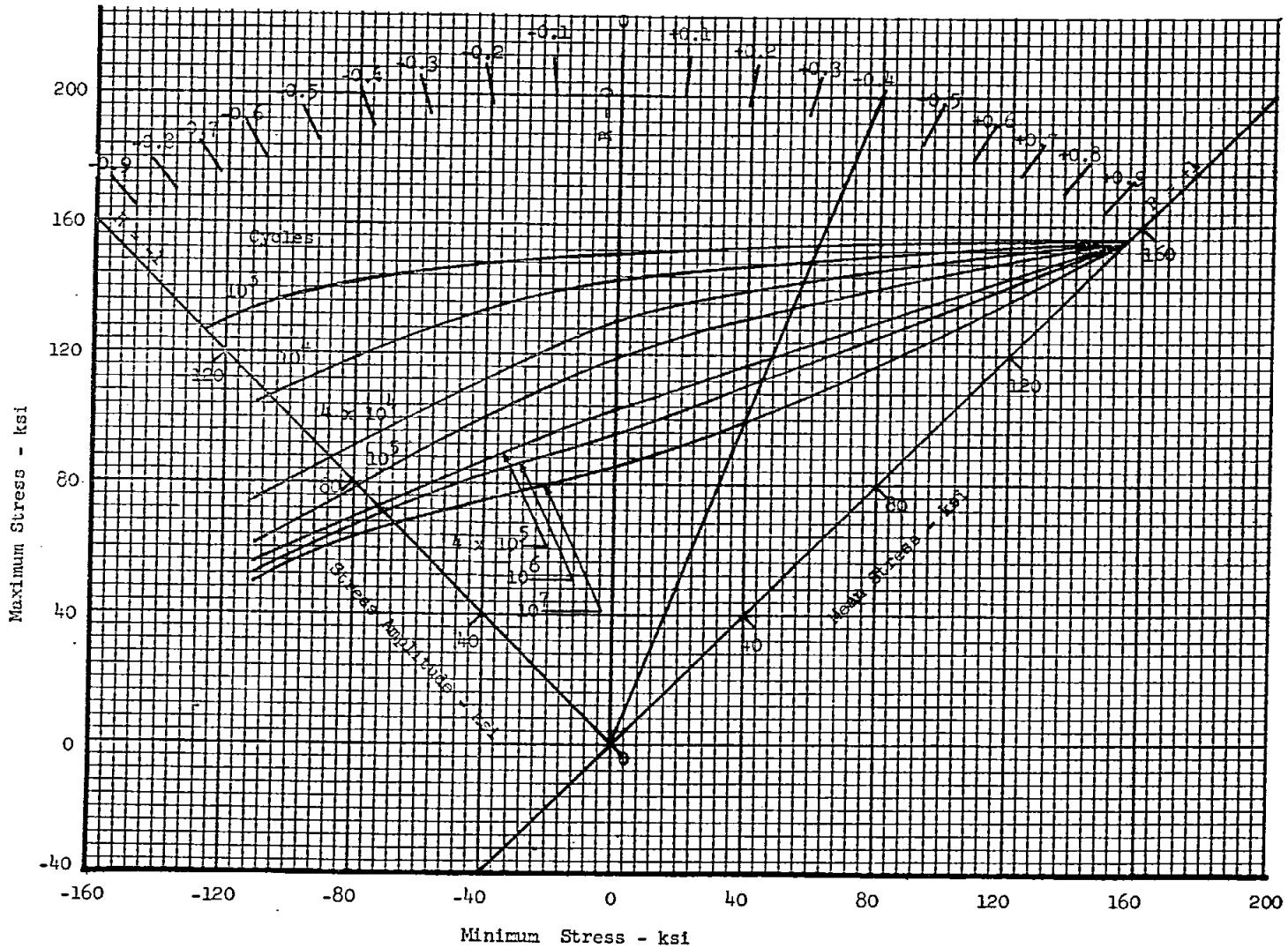

FATIGUE CURVES

6Al-4V STA Titanium Alloy

Material	Ult. Tens. Str.	Yield Str.
6Al-4V STA	155000 psi	145000 psi

CONSTANT LIFE CURVES

1 in. Thick Plate
Axially Loaded
Polished Specimens
Ref: Report FSN-AD2-06-68.1 and
Unpublished G.A.E.C. Tests

FATIGUE CURVES

6Al-4V STA Titanium Alloy

Material	Ult. Tens. Str.	Yield Str.
6Al-4V STA	155000 psi	145000 psi

CONSTANT MINIMUM STRESS CURVES

1 in. Thick Plate
Axially Loaded
Polished Specimens

Ref: Report FSN-AD2-06-68.1 and
Unpublished G.A.E.C. Tests

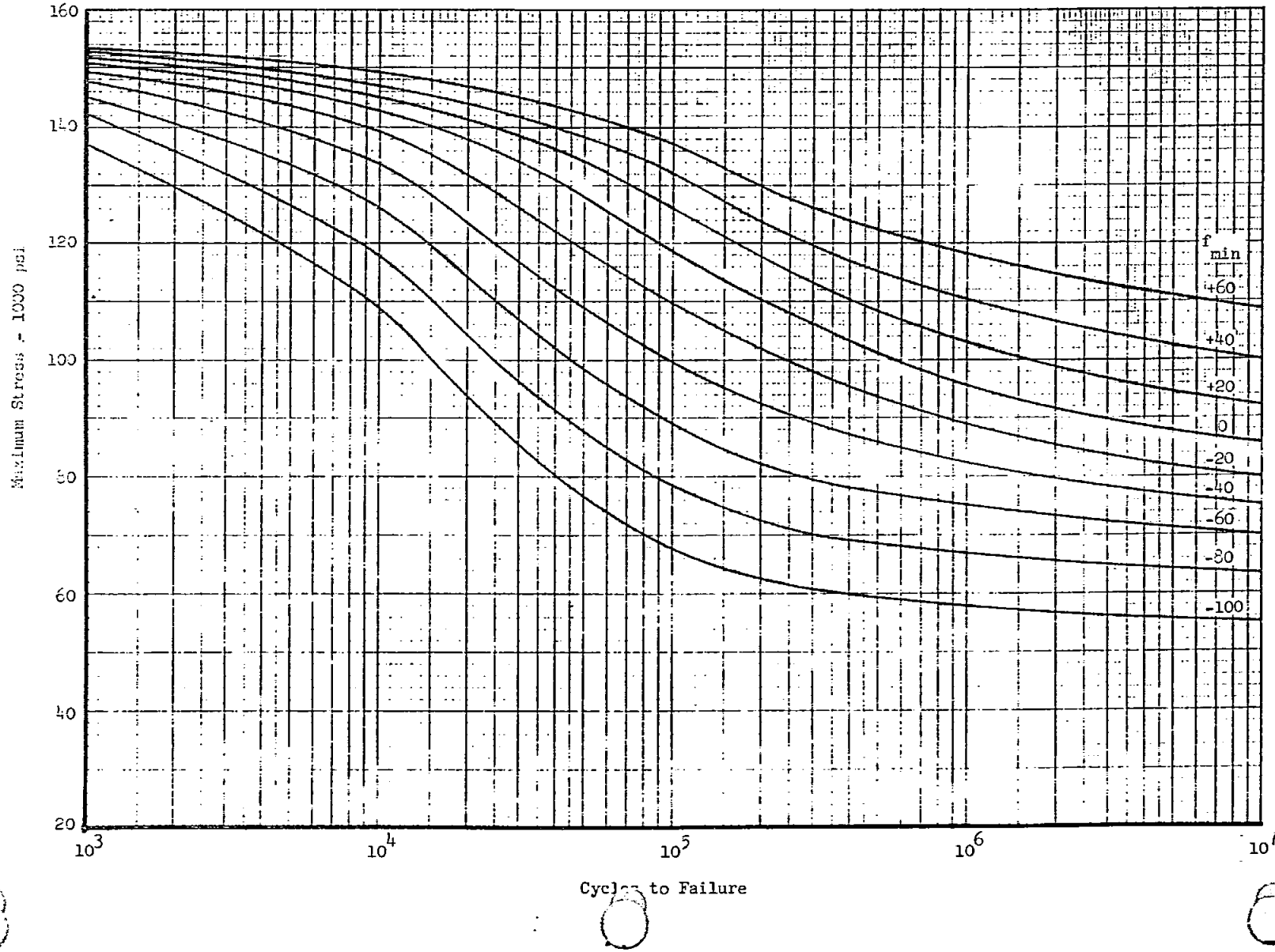

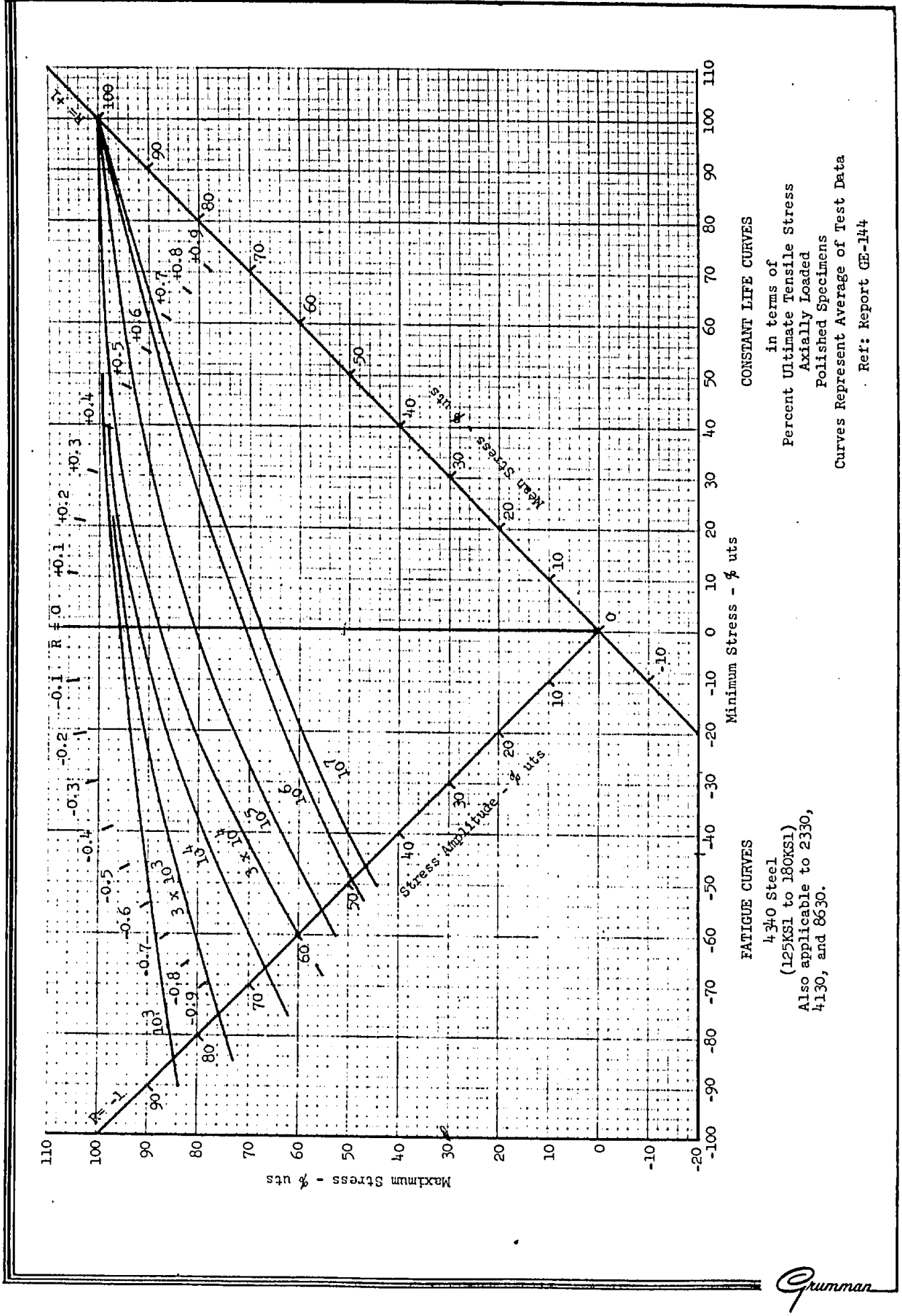

CONSTANT LIFE CURVES
in terms of
Percent Ultimate Tensile Stress
Axially Loaded
Polished Specimens
Curves Represent Average of Test Data
Ref: Report GE-144

FATIGUE CURVES
4340 Steel
(125KSI to 180KSI)
Also applicable to 2330,
4130, and 8630.

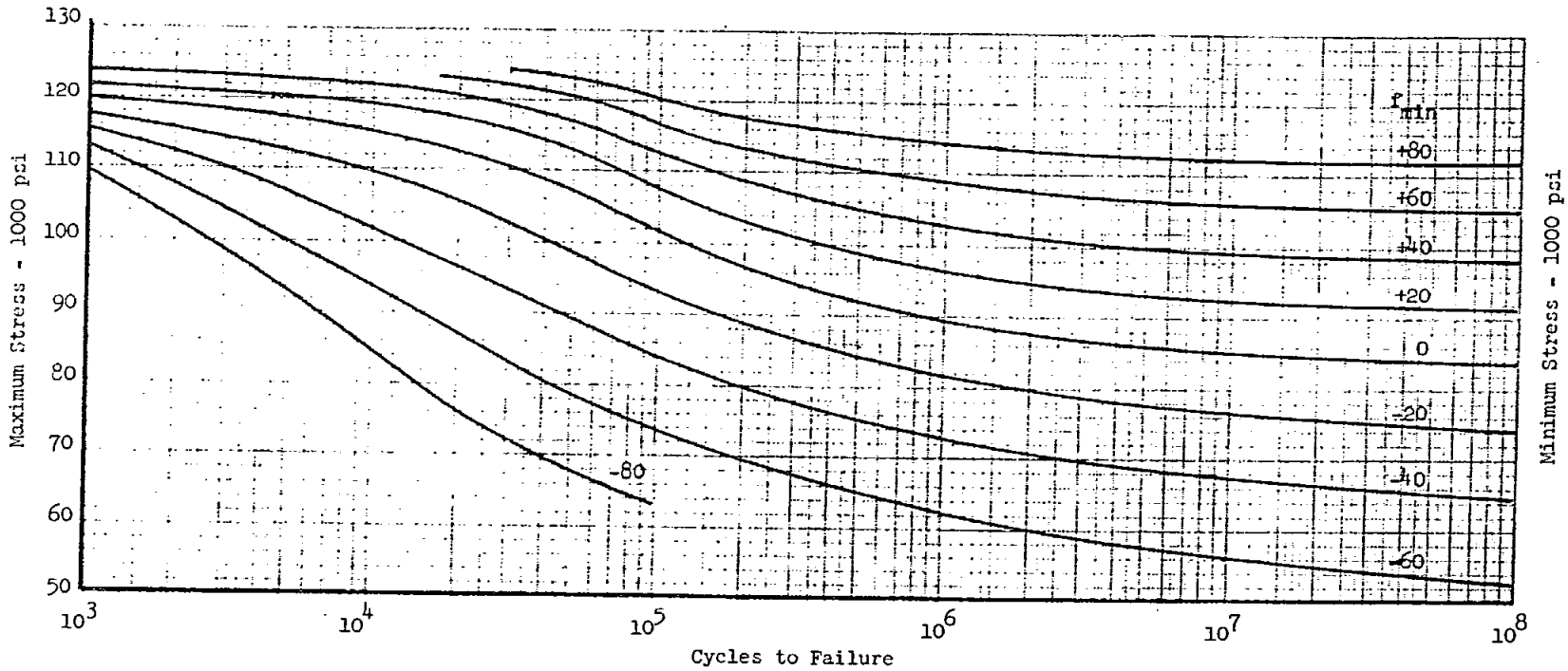

FATIGUE CURVES
125,000 psi
4340 STEEL

CONSTANT MINIMUM STRESS CURVES

Axially Loaded
Polished Specimens
Curves Represent Average of Test Data
Also Applicable to 2330, 4130, and 8630

Ref: Report GE-144

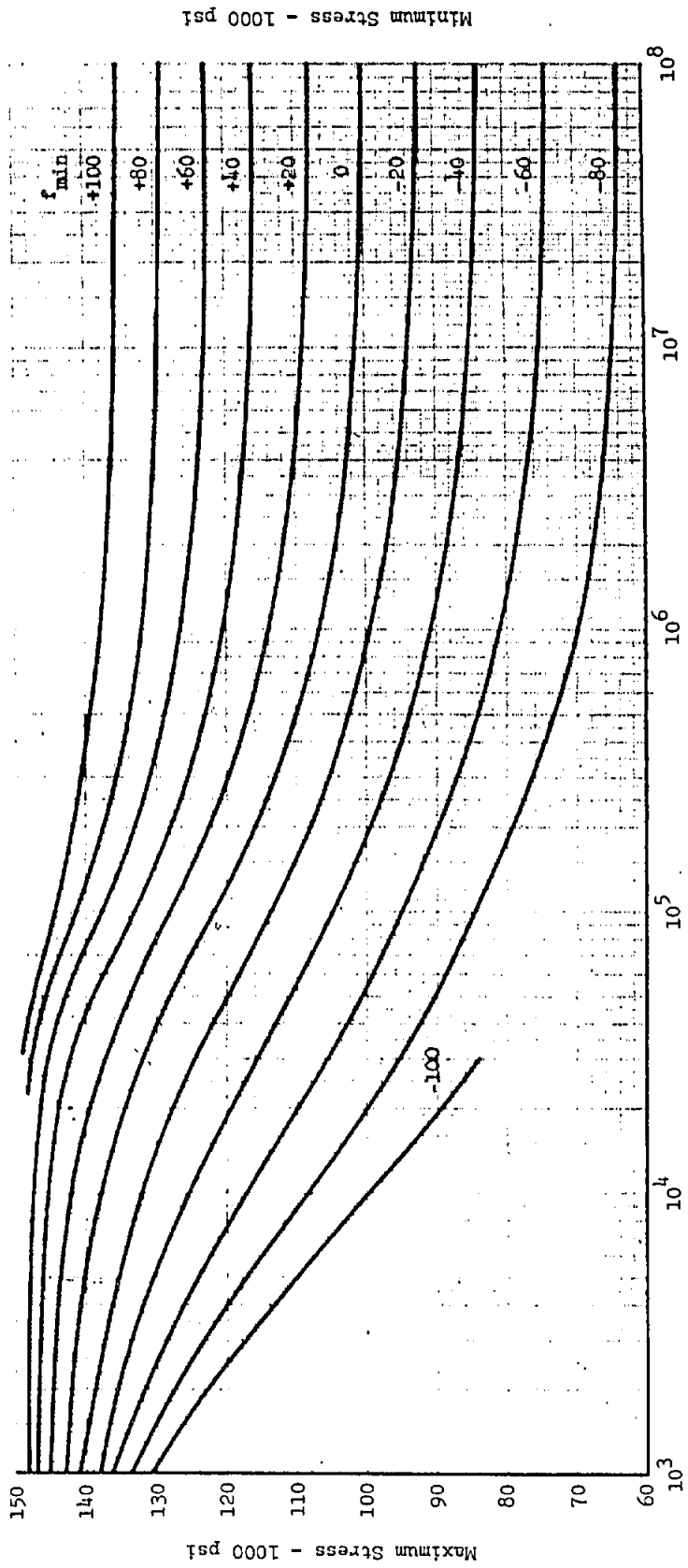

FATIGUE CURVES

150,000 psi
4340 Steel

CONSTANT MINIMUM STRESS CURVES

Axially Loaded - Polished Specimens
Curves Represent Average of Test Data
Also Applicable to 2330, 4130, and 8630
Ref: Report GE-144

Grumman

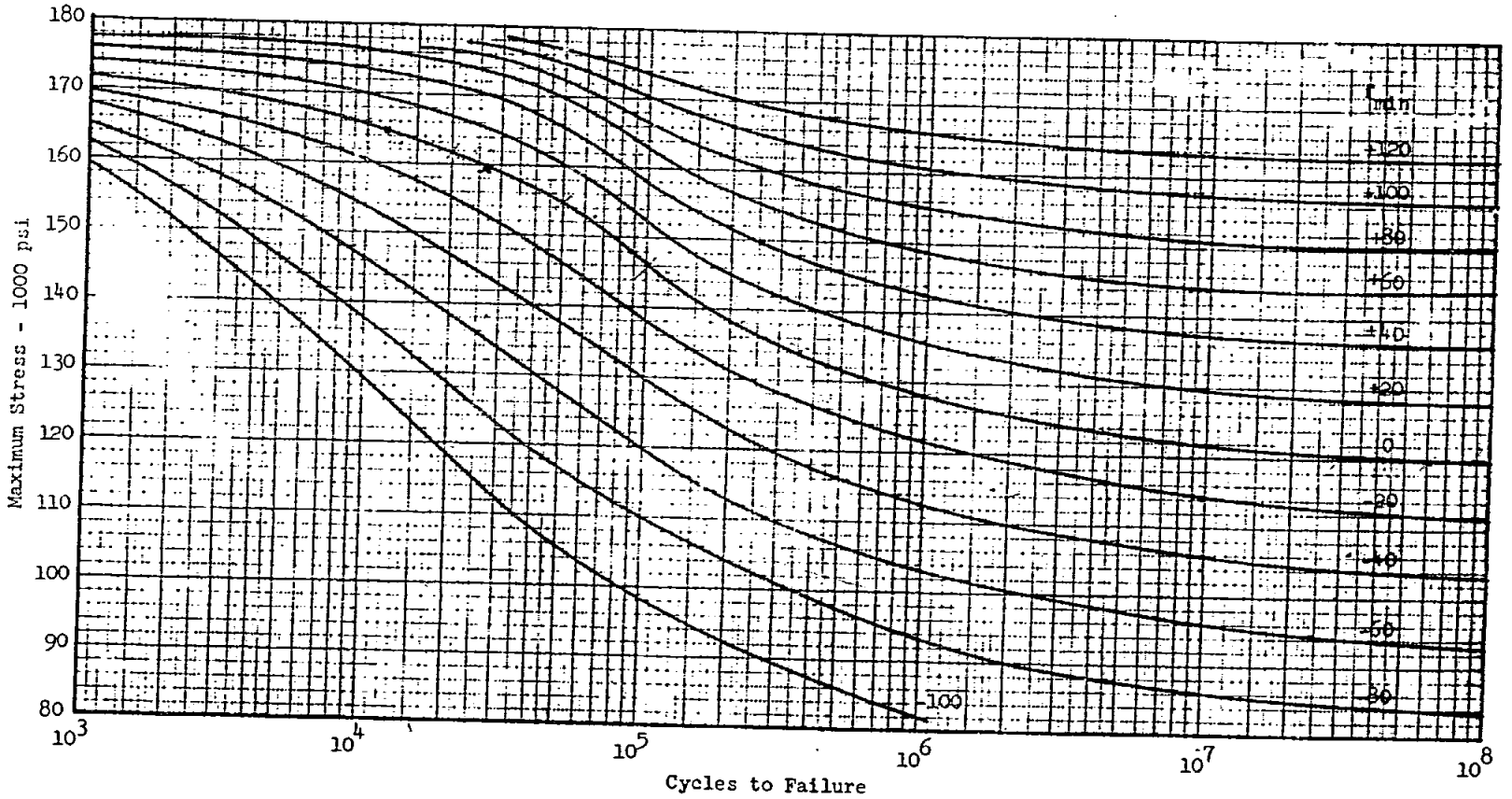

FATIGUE CURVES

180,000 psi
4340 STEEL

CONSTANT MINIMUM STRESS CURVES

Axially Loaded - Polished Specimens
Curves Represent Average of Test Data
Also Applicable to 2330, 4130, and 8630
Ref: Report GE-144

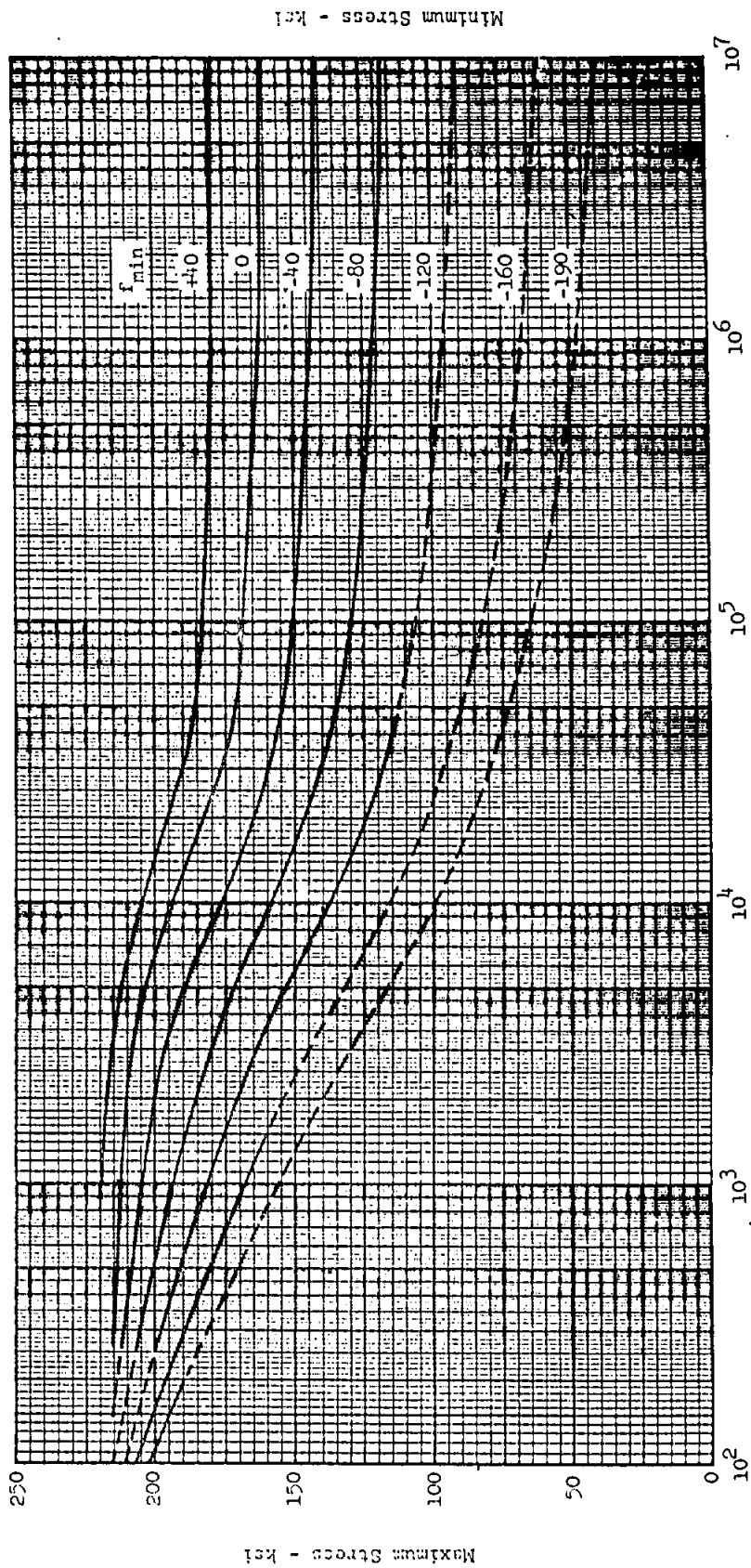

CONSTANT MINIMUM STRESS CURVES
Axially Loaded
Unnotched Polished Specimens
4330 V(Mod) Steel Bars, Billets & Die Forgings
Vacuum Melted
Longitudinal Grain Direction
Curves Represent Average of Test Data
Ref: Report GE-202

FATIGUE CURVES
4330 V(Mod) Steel
Heat Treated to 220-240 ksi

Curves May Also be Used for D6AC Steel

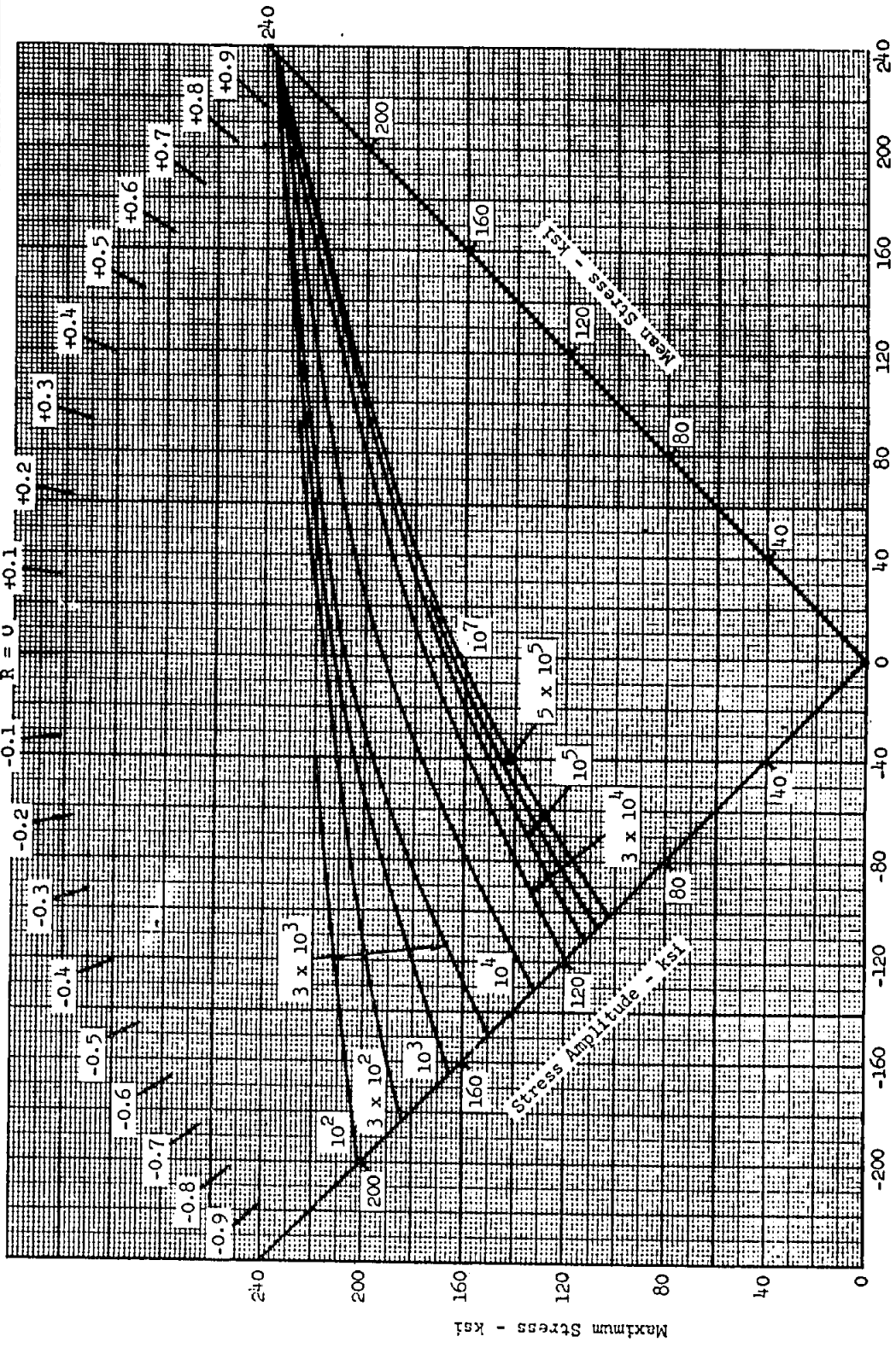

CONSTANT LIFE FATIGUE CURVES
Unnotched Polished Specimens
Axially Loaded
4330 V(Mod) Steel Bars, Billets & Die Forgings
Vacuum Melted
Longitudinal Grain Direction
Curves Represent Average of Test Data
Ref: Report GE-202

FATIGUE CURVES
4330 V(Mod) Steel
Heat Treated to 220-240 ksi
Curves May Also be Used for D6AC Steel

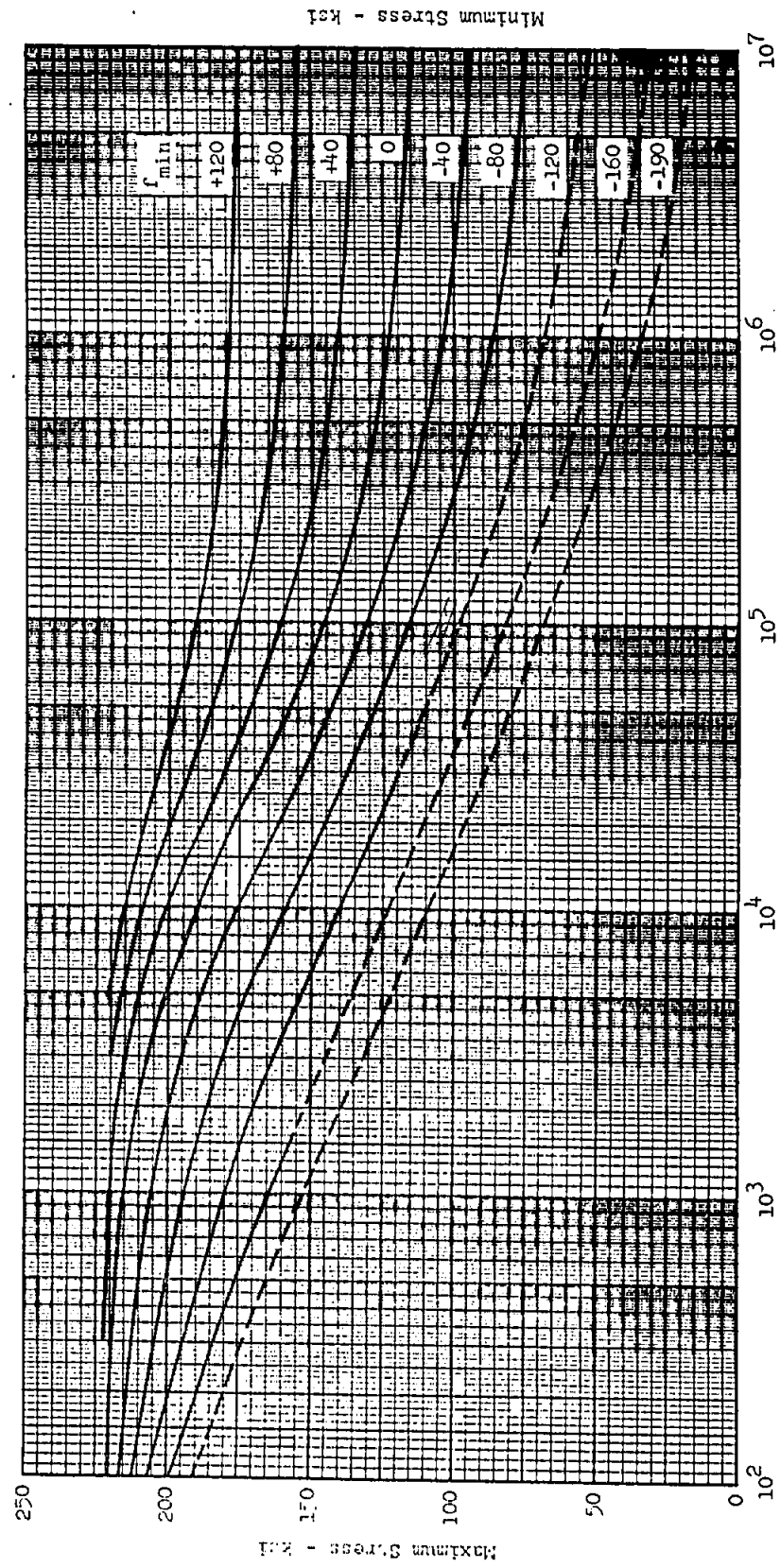

CONSTANT MINIMUM STRESS CURVES

Axially Loaded
Unnotched Polished Specimens
4330 V(Mod) Steel Bars, Billets & Die Forgings
Vacuum Melted
Short Transverse Grain Direction
(Also Applicable to Long Transverse)
Curves Represent Average of Test Data

Ref: Report GE-202

FATIGUE CURVES

4330 V(Mod) Steel
Heat Treated to 220-240 ksi

Curves May Also be Used for D6AC Steel

Grumman

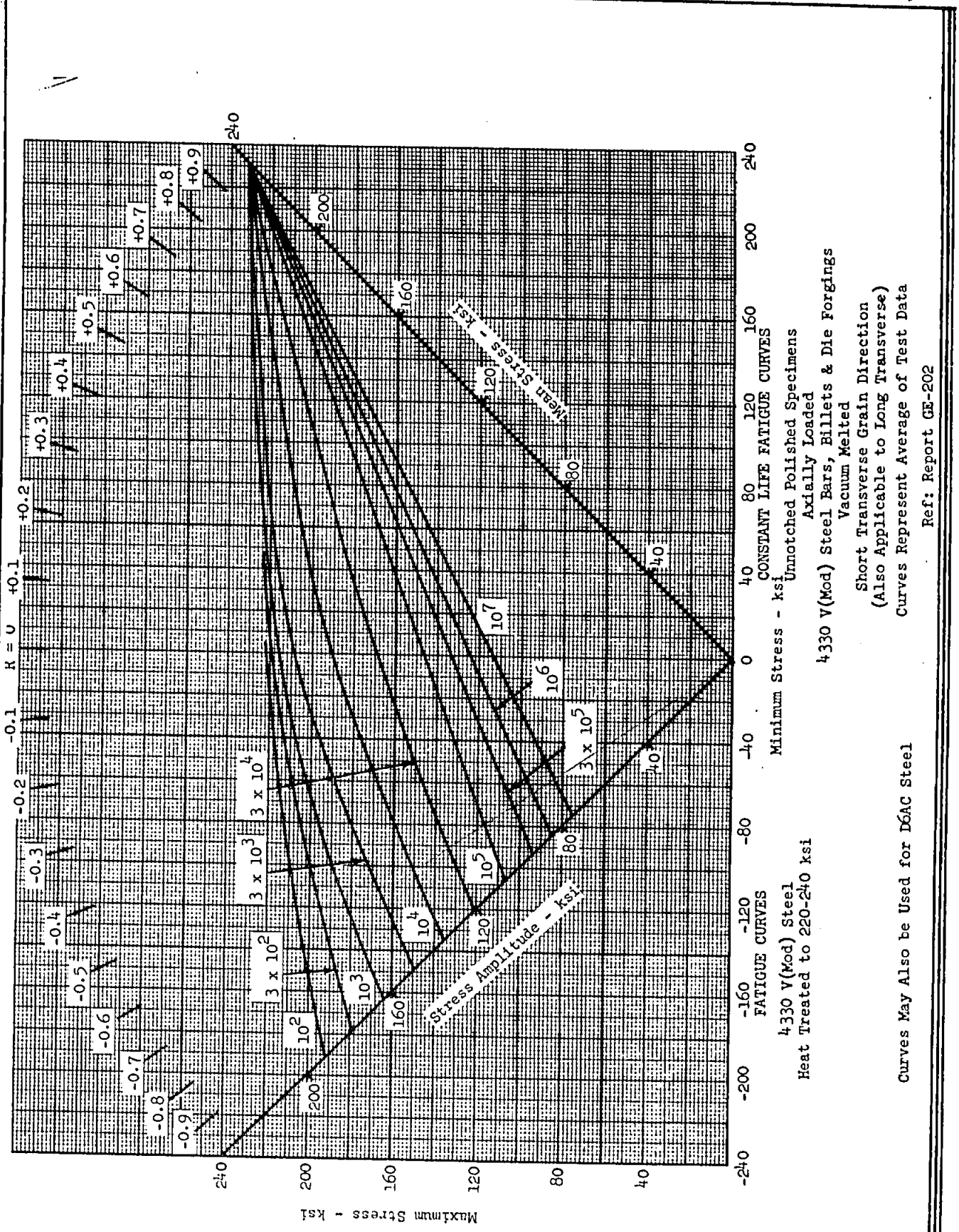

Minimum Stress - ksi CONSTANT LIFE FATIGUE CURVES

Unnotched Polished Specimens
Axially Loaded
4330 V(Mod) Steel Bars, Billets & Die Forgings
Vacuum Melted
Short Transverse Grain Direction
(Also Applicable to Long Transverse)
Curves Represent Average of Test Data
Ref: Report GE-202

4330 V(Mod) Steel
Heat Treated to 220-240 ksi
FATIGUE CURVES

Curves May Also be Used for D6AC Steel

FATIGUE STRENGTH OF LOW CARBON STEEL AND TITANIUM ALLOY LUGS

The following section presents a method for the determination of the fatigue strength of low alloy steel and annealed 6Al-4V or 6Al-6V-2Sn titanium lugs. Although the method was originally developed for the fatigue analysis of axially loaded lugs, it can be used with certain restrictions for obliquely loaded lugs.

Analysis of Axially Loaded Lugs

The method is based on the use of constant amplitude lug fatigue data for the above alloys and the use of Miner's Law to determine the cumulative damage for the case of spectrum loading.

The test data was normalized to the ultimate engineering tensile strength of the particular material after multiplying the tested alternating stress across the lug net section, $\left(\frac{f_{max} - f_{min}}{2}\right) = f_a$, by the stress concentration factor for the lug test specimen, KN, This fatigue stress concentration factor is determined from page B7.040.3-1 with the Neuber correction applied as described on pages B7.030-8 and -9. This procedure provides the constant amplitude fatigue life curves of pages B7.032-13 thru B7.032-16 for a family of curves covering a range of R $(= f_{min}/f_{max})$ from 0 to 0.6. These curves supply the data for damage calculations of 10^4 cycles and greater. Below this cycle range, a linear cutoff is applied to the data so that at one cycle the ultimate static strength of the lug as determined from page B3.13-28 will not be exceeded. The other point locating the cut off line intersects the data curve at a maximum stress equal to the allowable yield stress for the lug as determined from page B3.13-28. In this case of axially loaded lugs, the lug static strength is based on the net section factor of page B3.13-28 even though the lug may be critical for a static load as determined from page B3.13-27. This procedure is followed because most axially loaded lugs fail in fatigue across the net section even though static analysis might predict a hoop tension/shear out failure mode.

It is assumed in the method that compressive loads on the lug cause no fatigue damage across the net section. Therefore any negative (compressive) load in the applied spectrum has to be set equal to zero before the fatigue life calculation is made.

Determination of Low Cycle Cut-Off Values

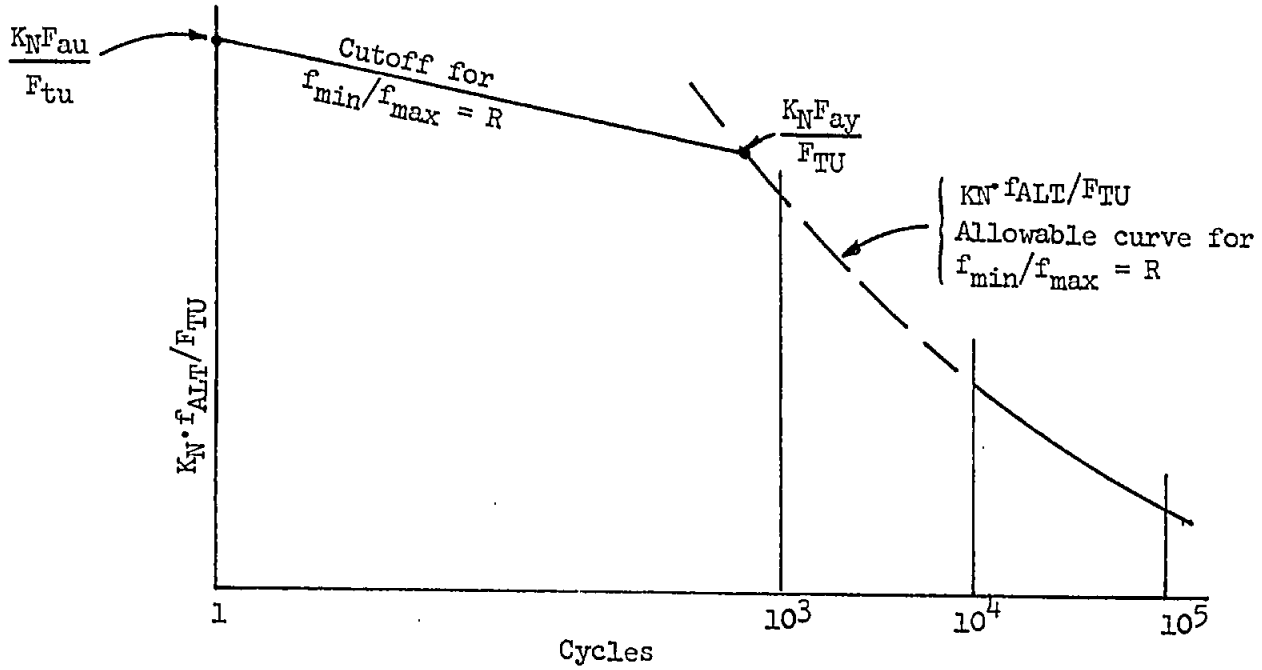

Determine the lug net section strength factor, K_L, from page B3.13-28 for particular lug geometry and material. Determine lug stress concentration factor, K_N, from page B7.040.3-1 including the Neuber correction of page B7.030-8, 9.

The cut-off values are then:

$$\frac{K_N F_{au}}{F_{tu}} = \frac{K_N \cdot K_L \cdot F_{tu}}{2 F_{tu}} \cdot (1-R) \qquad \text{since } F_{au} = \frac{K_L \cdot (F_{tu} - R \cdot F_{tu})}{2}$$

$$\frac{K_N F_{ay}}{F_{tu}} = \frac{K_N \cdot K_L \cdot F_{ty}}{2 F_{tu}} \cdot (1-R) \qquad \text{since } F_{ay} = \frac{K_L \cdot (F_{ty} - R \cdot F_{ty})}{2}$$

These values can then be located on the appropriate data curves to complete the fatigue data cut-off for the lug in question.

Analysis of Obliquely Loaded Lugs

The method of analysis of obliquely loaded lugs is derived from the method for axially loaded lugs, reference page B7.032-8 for sketch of lug. To do this, it was necessary to assume the allowable fatigue data for axially loaded lugs applies to obliquely loaded lugs provided the proper stress concentration factors are used such as page B7.040.3-2.

Obliquely Loaded Lugs (Continued)

Since the lug test data is for $R \geq 0$, the obliquely loaded lug is restricted to applied positive load ratios $(P_{min}/P_{max}) \geq 0$. The assumption that negative loads do no fatigue damage cannot be made in the case of obliquely loaded lugs.

As in the case of the axially loaded lugs, the maximum static strength both ultimate and yield, must be determined and applied as cut-offs to the lug fatigue strength curves. The static strength values are determined as described on page B3.13-15. These strength values are located on the fatigue allowable curves in the same manner as described for the case of axially loaded lug.

As opposed to the case of the axially loaded lugs where the strength of the lug is based on the net section, it is recommended that page B3.13-15 be followed exactly. This will ensure that the axial strength of the lug will be based on the critical failure mode of either net section failure or combined hoop stress/shear out. This added conservatism is recommended because the adaptation of the axially loaded lug fatigue data to obliquely loaded lugs is not adequately supported by test results at this time.

Determination of Low-Cycle Cut-Off Values

Determine the static strength of the obliquely loaded lug, both ultimate and yield. This procedure is clearly given on page B3.13-15, item 1. Following this procedure the allowable oblique lug strength, $P_{\alpha\, u}$ or $P_{\alpha\, y}$ will be determined.

The cutoff values are then:

$$\frac{K_N \cdot F_{au}}{F_{tu}} = \frac{P_{\alpha\, u} \cdot K_N}{(W-D) \cdot t \cdot F_{tu}} \times \left(\frac{1}{2}\right) \times (1-R)$$

$$\frac{K_N \cdot F_{ay}}{F_{tu}} = \frac{P_{\alpha\, y} \cdot K_N}{(W-D) \cdot t \cdot F_{tu}} \times \left(\frac{1}{2}\right) \times (1-R)$$

The K_N value is for the lug loaded at the oblique angle (from page B7.040-3.2) including the Neuber correction of pages B7.030-8, -9.

Illustrative Examples

The following pages illustrate the application of this method for the determination of the fatigue life of a titanium alloy lug for both the axial load case and the oblique load case.

Symbols

R	=	Stress ratio, f_{min}/f_{max}
f_{min}	=	Minimum cyclic stress on net section of lug, (= $P_{min}/(W-D)\cdot t$) lbs/in.^{2}
f_{max}	=	Maximum cyclic stress on net section of lug, (= $P_{max}/(W-D)\cdot t$) lbs/in.^{2}
f_a or f_{alt}	=	Cyclic stress amplitude on net section of lug, lb/in.^{2}
	=	$(f_{max} - f_{min})/2 = \frac{f_{max}}{2} \cdot (1-R)$
N	=	Allowable number of cycles-number of cycles to failure for a given stress range
F_{ty}	=	Lug material tensile yield stress, lb/in.^{2}
F_{tu}	=	Lug material tensile ultimate stress, lb/in.^{2}
K_L	=	Lug net section strength factor from page B3.13-28
P	=	Lug load, either applied or allowable, see sketch for description including lug geometry on pages B7.032-4,8
K_T	=	Theoretical elastic stress concentration factor
K_N	=	Fatigue stress concentration factor including Neuber correction, page B7.030-8, -9
n	=	Number of cycles applied

Subscripts

u	=	designates ultimate strength
y	=	designates yield strength
α	=	direction of load line on obliquely loaded lug
L	=	denotes lug strength when used with primary symbol, P
a, alt	=	alternating stress

Example Problem 1

Axial Load Case

Lug Geometry

W = 2.0 in
e = 1.0 in
D = 1.0 in
a = (e-D/2)= 0.50 in
t = 1.0 in
D/W = 0.5
e/D = 1.0

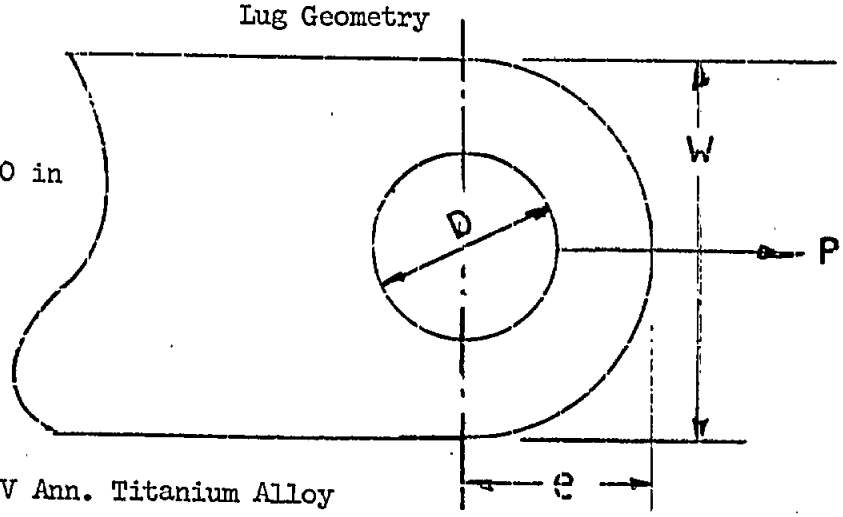

Material: 6Al-4V Ann. Titanium Alloy

F_{tu} = 130000 psi

F_{ty} = 120000 psi

E = 16.0 x 10^6 psi

ϵ_u = 0.10

(Material properties from MIL-HDBK-5B)

Determine Lug Net Section Static Strength

From page B3.13-28

$$\frac{F_{tu}}{E\,\epsilon_u} = \frac{130000}{16x10^6x.10} = .081$$

$$\frac{F_{ty}}{F_{tu}} = 0.92$$

K_L =0.92 (interpolated)

Determine Non Dimensional Fatigue Factors

From page B7.040.3-1

K_T = 2.80

Example Problem 1 (Continued)

From page B7.030-26

$\sqrt{A} = 0.08$

$K_N = 1 + (2.8-1.0)/(1+.08/\sqrt{0.5}$ (Page B7.030-9)

$= 2.62$

Load Spectrum and Damage Calculation

Level	Loads (Kips) Max	Loads (Kips) Min	n Cycles/ 1000 hrs.	R	Stress f_{max}	$\frac{K_N f_a}{F_{tu}}$	Allowable Cycles N	Damage n/N
1	65.2	34.5	1000	0.530	65200	.309	14070	0.0711
2	78.6	28.8	300	0.366	78600	.502	6450	0.0465
3	92.0	24.9	100	0.270	92000	.676	3170	0.0315
4	103.5	21.0	30	0.203	103500	.831	1770	0.0170
5	115	19.2	10	0.167	115000	.966	35	0.2859
6	115	0	3	0	115000	1.159	31	0.0976
7	115	-1.0*	1	0	115000	1.159	31	0.0326

*This level is set equal to 0.0, therefore R for level = 0.0

$$\sum \frac{n}{N} = 0.5822$$

Life = 1000/0.5822 = 1718 hrs.

Cutoff Values - Levels 6, 7

$$\frac{K_N F_{au}}{F_{tu}} = \frac{2.62 \times 0.92}{2} = 1.205$$

$$\frac{K_N F_{ay}}{F_{tu}} = \frac{2.62 \times 0.92 \times 120000}{2 \times 130000} = 1.112$$

Cutoff Values - Level 5

$$\frac{K_N F_{au}}{F_{tu}} = \frac{2.62 \times 0.92}{2} \times (1 - 0.167) = 1.012$$

Example Problem 1 (continued)

$$\frac{K_N F_{ay}}{F_{tu}} = \frac{2.62 \times 0.92}{2} \times \frac{120000}{130000} \quad (1-0.167) = 0.934$$

Cutoff Values - Level 4

$$\frac{K_N F_{au}}{F_{tu}} = \frac{2.62 \times .92}{2} \times (1-0.203) = 0.961$$

$$\frac{K_N F_{ay}}{F_{tu}} = \frac{2.62 \times .92}{2} \times \frac{120000}{130000} \quad (1-0.203 = 0.887)$$

These cutoff values are shown on the following plot:

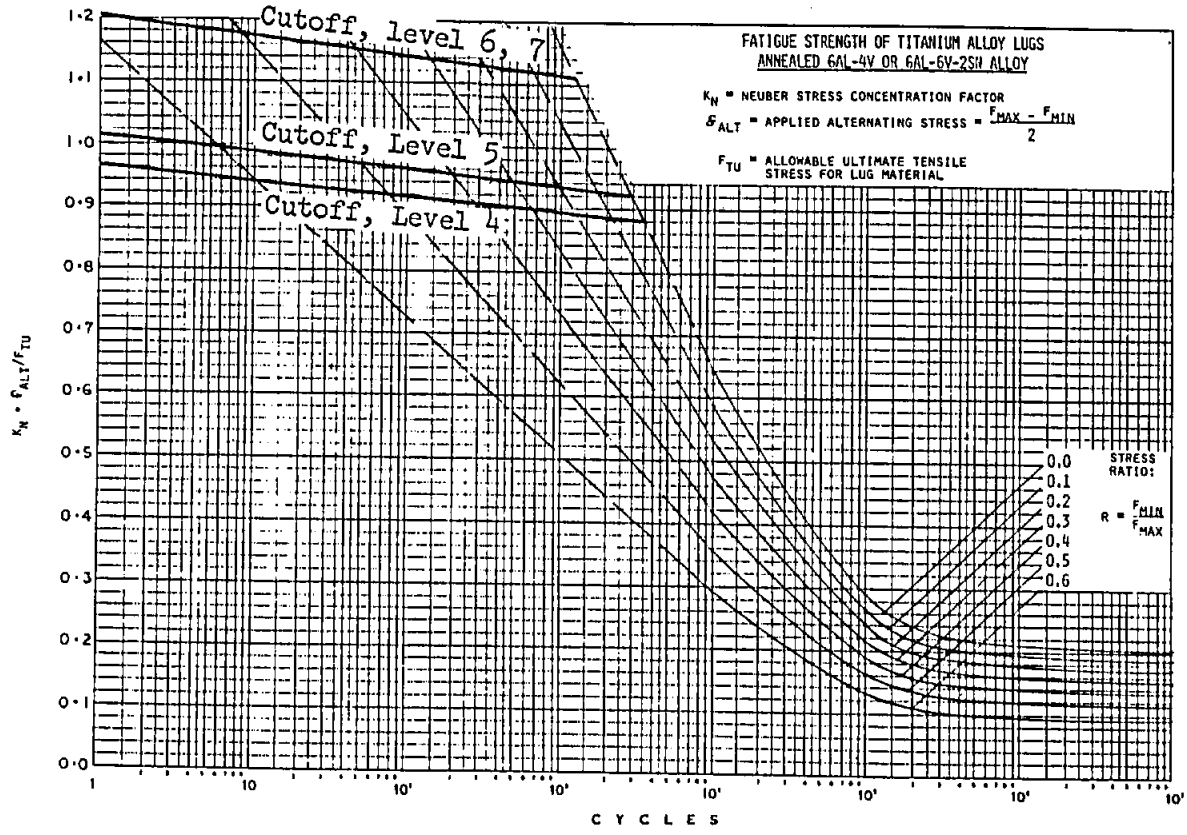

Example Problem 2

Obliquely Loaded Lug

(Same lug as problem 1)

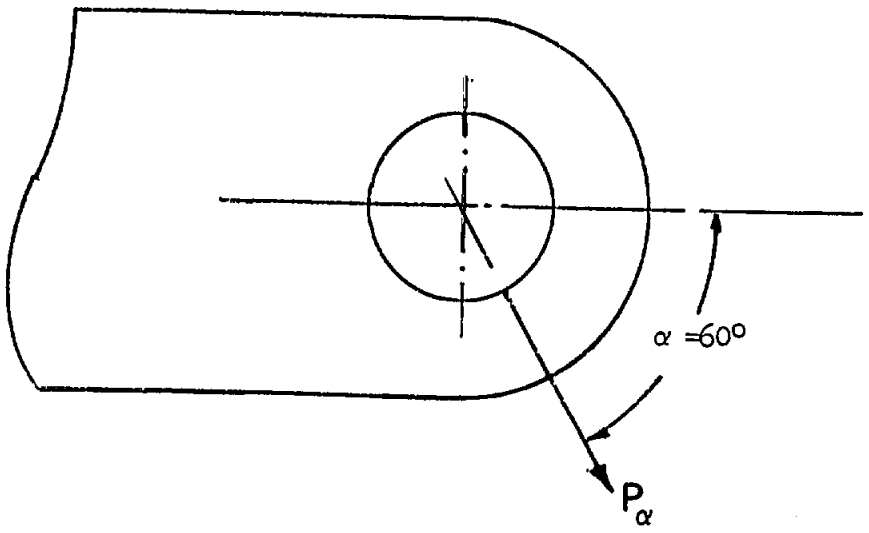

e/D = 1.0
D/W = 0.50
t = 1.0 in
a = 0.50 in

Determination of Lug Static Strength, P

Start at Page B3.13-15, Item 1

For P_L, Reference page B3-13-5

K_L for Eqns. 4 thru 6b from Problem 1, page B7.032-5

Next determine P_{brl}, B3.13-4, Item 1

Determine K for Eqns 1a and 1b from page B3.13-27

K = 1.61

Lug strength (axial) based on hoop tension/shear out is:

$P_{brL} = K \cdot a \cdot t \cdot F_{tu} = 1.61 \times 0.50 \times 1.0 \times F_{tu}$

$= 0.805\ F_{tu}$

$P_{nL} = K_L \cdot A_{net} \cdot F_{tu} = 0.92 \times (2.0 - 1.0) \times 1.0 \times F_{tu}$

$= 0.92\ F_{tu}$

$\therefore P_L = 0.805\ F_{tu}$

Example Problem 2 (continued)

For P_{tr}, Reference Page B3.13-15

From page B3.13-30, $h_{av}/D = 0.589$

From B3.13-29

$K_{tru} = 0.720$

$P_{trL} = K_{tru} \cdot D \cdot t \cdot F_{tu}$

$P_{trL} = 0.720 \times 1.00 \times 1.00 \times F_{tu}$

$= 0.720\ F_{tu}$

Then by either solving the interaction equation of page B3.13-31 or by plotting on that diagram,

$\frac{P}{P_L} = 0.4286$

$\frac{P_{tr}}{P_{tr_L}} = 0.8300$

$P = 0.4286 \times 0.805\ F_{tu} = 0.3450\ F_{tu}$

$P_{tr} = 0.8300 \times 0.720\ F_{tu} = 0.5976\ F_{tu}$

$P_{\alpha L} = \sqrt{P^2 + P_{tr}^2} = 0.690\ F_{tu}$

Because the fatigue allowables are referenced to the net section stress, the net section factor, K_L, must be calculated for the obliquely loaded lug from the following definition;

$P_{\alpha L} = K_L \cdot A_{Net} \cdot F_{tu}$

$K_L = P_{\alpha L}/(A_{net} \cdot F_{tu}) = 0.690\ F_{tu}/(2.0 - 1.0) \times 1.0 \times F_{tu}$

$= 0.690$

The factor 0.690 is identical in meaning to the K_L used in the axially loaded lug fatigue analysis.

Determination of Cutoff Values for Fatigue Allowables:

From page B7.040.3-2

Example Problem 2 (continued)

$K_T = 4.10$

From page B7.030-26

$\sqrt{A} = 0.08$

$K_N = 1 + (4.10 - 1.0)/(1 + .08/\sqrt{0.5}) = 3.785$ (page B7.030-9)

Load Spectrum and Damage Calculation

Levels	Load (Kips) Max	Load (Kips) Min	n Cycles 1000 hrs	R	Stress f_{max}	$\frac{K_N F_a}{F_{tu}}$	N Allow Cycles	Damage n/N
1	48900	25920	1000	0.530	48900	0.335	10570	0.0946
2	58950	21575	300	0.366	58950	0.544	4810	0.0624
3	69000	18630	100	0.270	69000	0.733	2230	0.0449
4	77625	15530	30	0.200	77625	0.904	1180	0.0255
5	86230	13800	10	0.160	86250	1.055	28	0.3568
6	86250	0	4	0	86250	1.256	24	0.1643

$\sum \frac{n}{N} = 0.7485$

$$\text{Life} = \frac{1000}{0.7485} = 1336 \text{ hrs}$$

Cutoff value, Level 6

$$\frac{K_N F_{au}}{F_{tu}} = \frac{3.785 \times 0.69}{2} = 1.306$$

$$\frac{K_N F_{ay}}{F_{tu}} = \frac{3.785 \times 0.69 \times 120000}{2 \times 130000} = 1.206$$

Cutoff value, Level 5

$$\frac{K_N F_{au}}{F_{tu}} = \frac{3.785 \times 0.69}{2} (1-0.16) = 1.097$$

$$\frac{K_N F_{ay}}{F_{tu}} = \frac{3.785 \times 0.69 \times 120000}{2 \times 130000} (1-0.16) = 1.013$$

Cutoff value, Level 4

$$\frac{K_N F_{au}}{F_{tu}} = \frac{3.785 \times 0.69}{2} = (1-0.20) = 1.0448$$

$$\frac{K_N F_{ay}}{F_{tu}} = \frac{3.785 \times 0.69 \times 120000}{2 \times 130000} \quad (1-0.20) = 0.9648$$

These cutoff values are shown on the following plot:

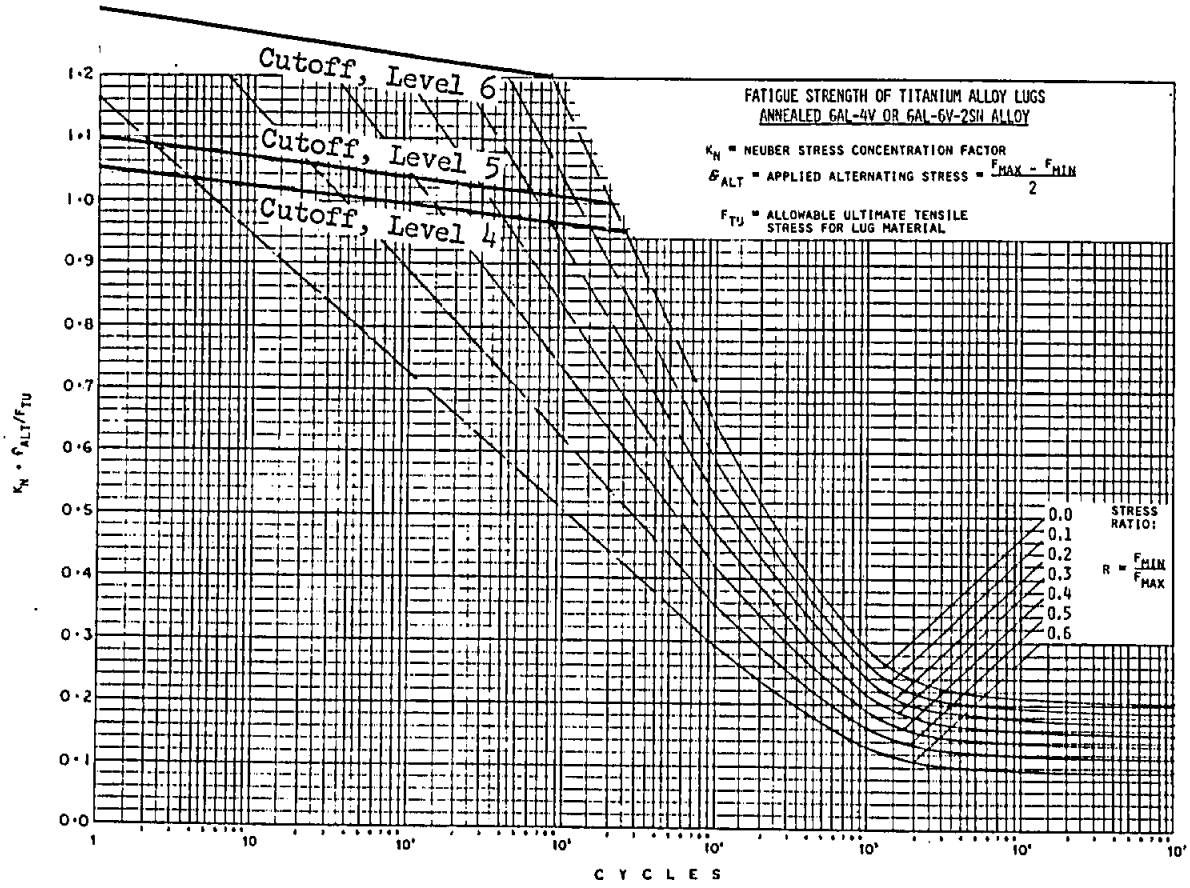

THIS PAGE UNINTENTIONALLY LEFT BLANK.

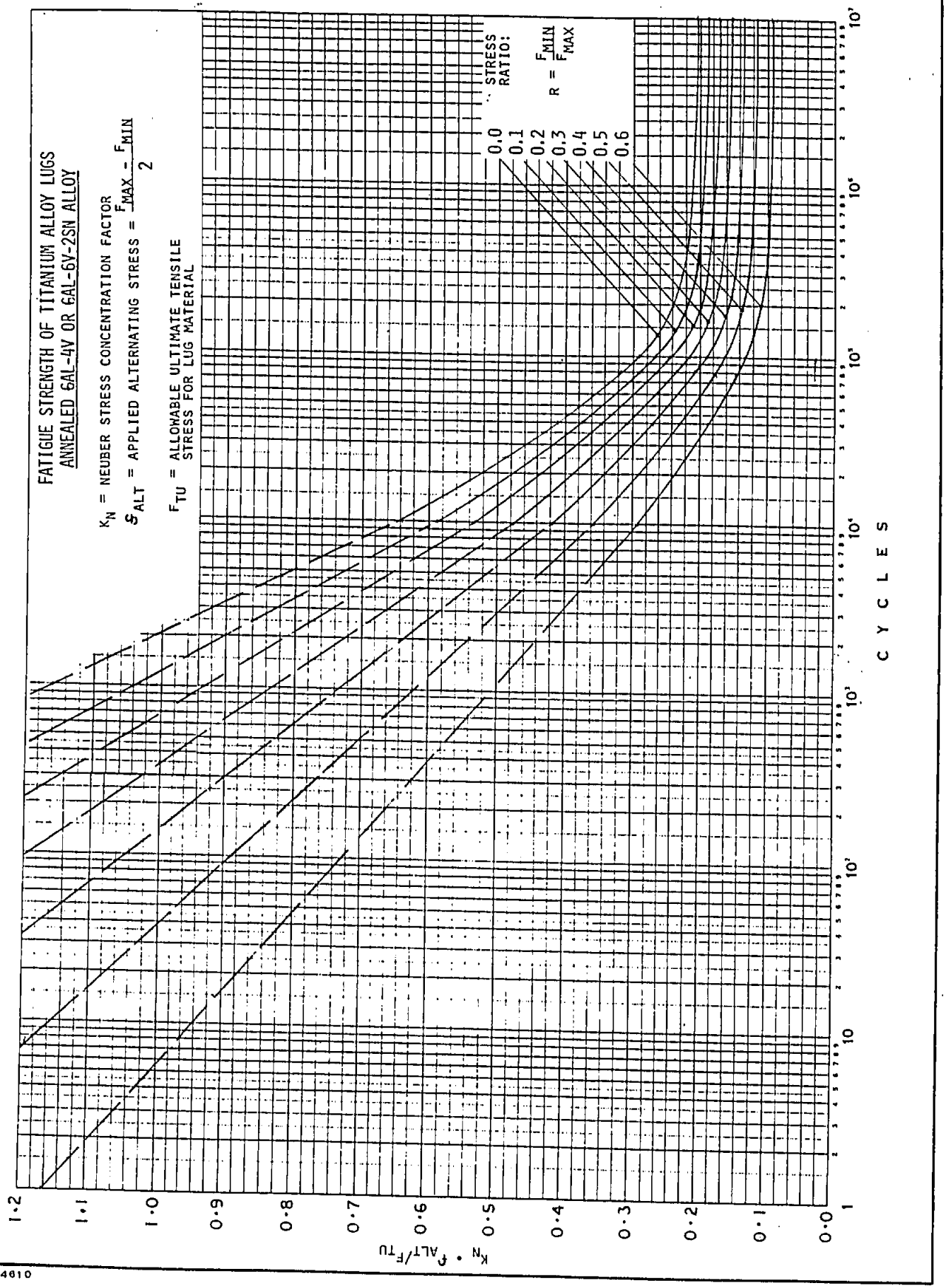
FATIGUE STRENGTH OF TITANIUM ALLOY LUGS
ANNEALED 6AL-4V OR 6AL-6V-2SN ALLOY
K_N = NEUBER STRESS CONCENTRATION FACTOR
S_{ALT} = APPLIED ALTERNATING STRESS = $\frac{F_{MAX} - F_{MIN}}{2}$
F_{TU} = ALLOWABLE ULTIMATE TENSILE STRESS FOR LUG MATERIAL
STRESS RATIO: $R = \frac{F_{MIN}}{F_{MAX}}$
0.0
0.1
0.2
0.3
0.4
0.5
0.6
$K_N \cdot F_{ALT}/F_{TU}$
1·2
1·1
1·0
0·9
0·8
0·7
0·6
0·5
0·4
0·3
0·2
0·1
0·0
1
10
10²
10³
10⁴
10⁵
10⁶
10⁷
CYCLES

*GAC 4610
2-74

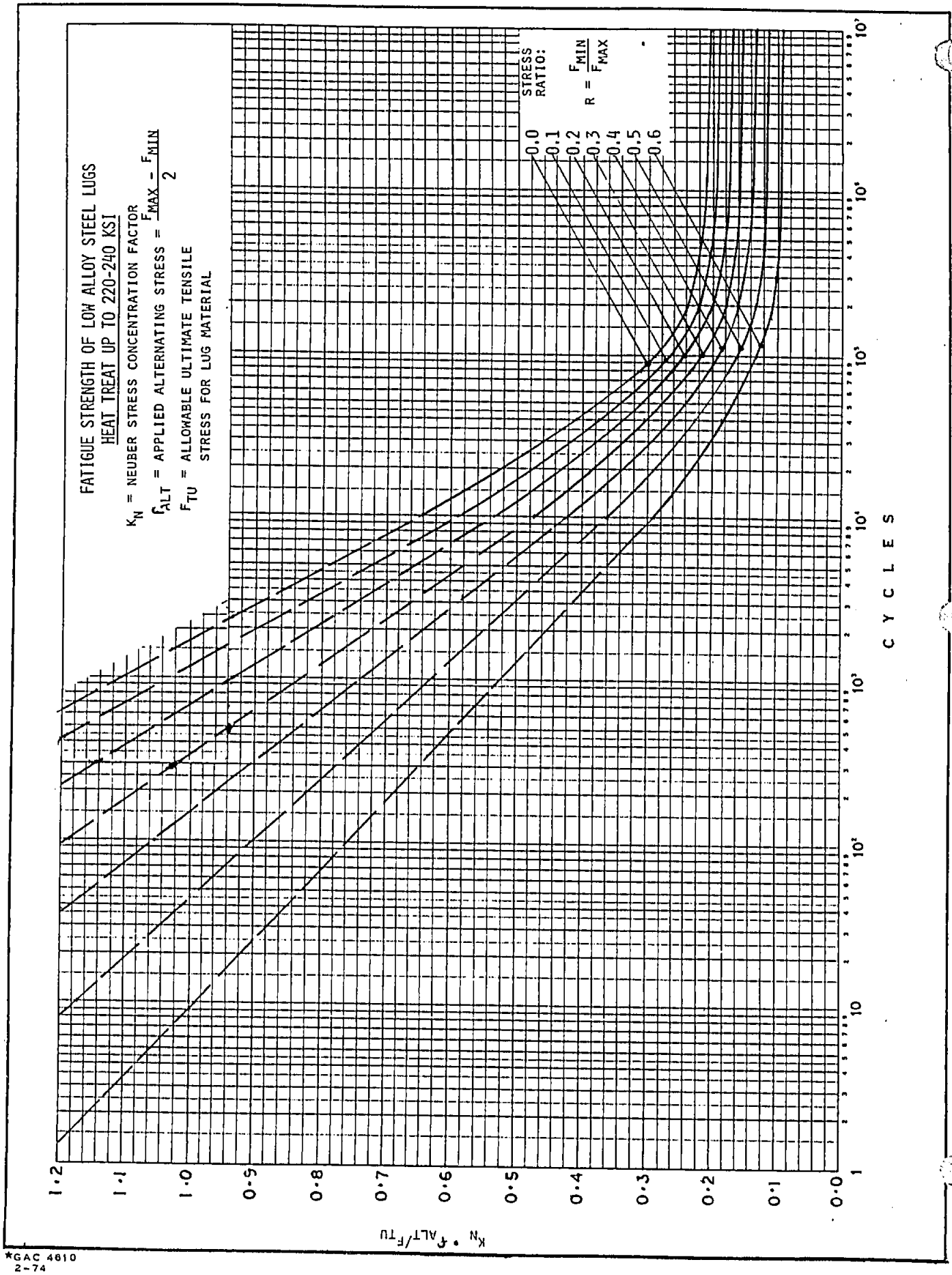
FATIGUE STRENGTH OF LOW ALLOY STEEL LUGS
HEAT TREAT UP TO 220-240 KSI
K_N = NEUBER STRESS CONCENTRATION FACTOR
f_{ALT} = APPLIED ALTERNATING STRESS = $\frac{F_{MAX} - F_{MIN}}{2}$
F_{TU} = ALLOWABLE ULTIMATE TENSILE STRESS FOR LUG MATERIAL
STRESS RATIO: $R = \frac{F_{MIN}}{F_{MAX}}$
0.0
0.1
0.2
0.3
0.4
0.5
0.6
$K_N \cdot f_{ALT}/F_{TU}$
1.2
1.1
1.0
0.9
0.8
0.7
0.6
0.5
0.4
0.3
0.2
0.1
0.0
1
10
10^2
10^3
10^4
10^5
10^6
10^7
CYCLES

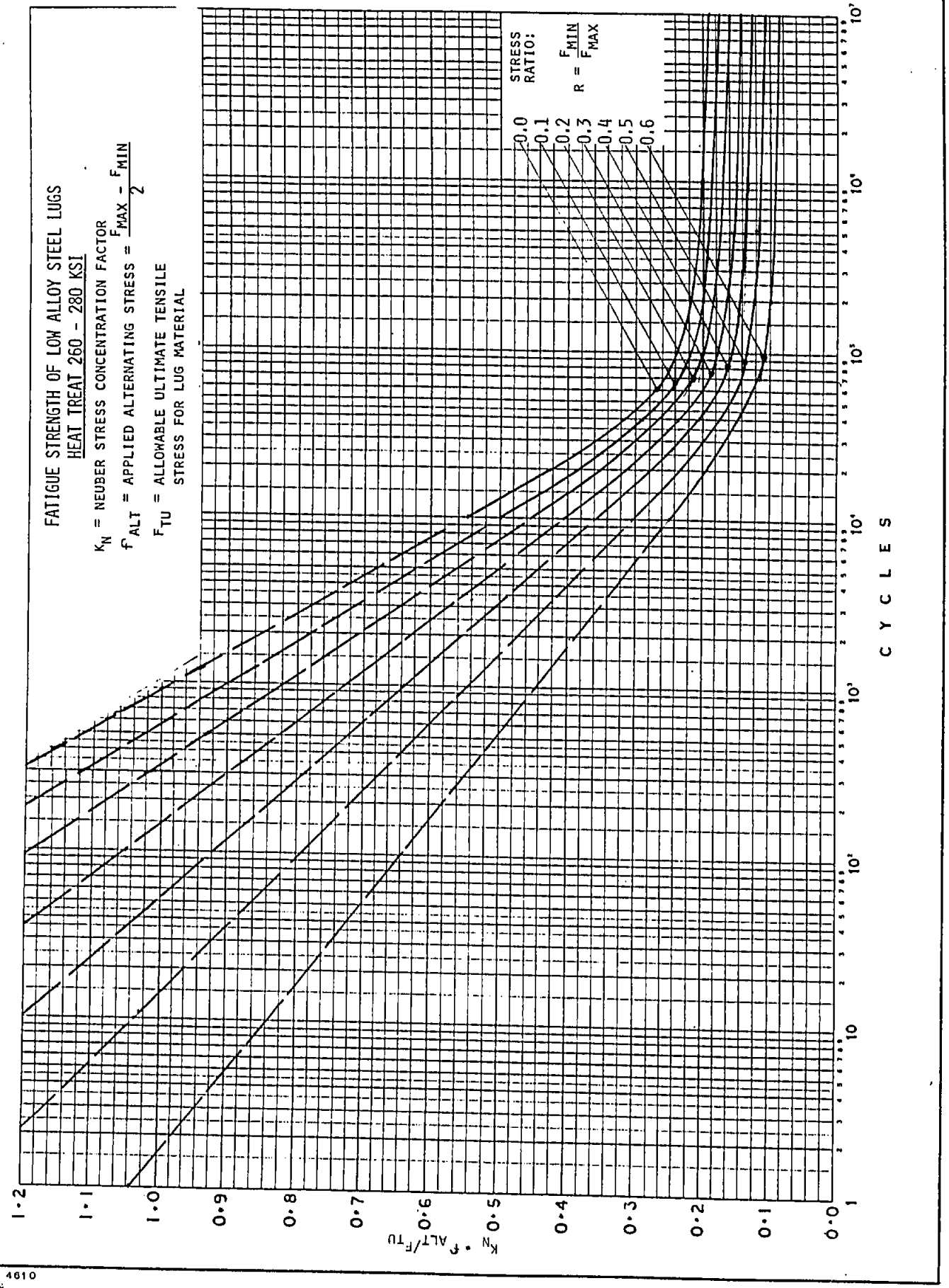
FATIGUE STRENGTH OF LOW ALLOY STEEL LUGS
HEAT TREAT 260 - 280 KSI
K_N = NEUBER STRESS CONCENTRATION FACTOR
f_{ALT} = APPLIED ALTERNATING STRESS = $\frac{F_{MAX} - F_{MIN}}{2}$
F_{TU} = ALLOWABLE ULTIMATE TENSILE STRESS FOR LUG MATERIAL
STRESS RATIO:
$R = \frac{F_{MIN}}{F_{MAX}}$
0.0
0.1
0.2
0.3
0.4
0.5
0.6
$K_N \cdot f_{ALT}/F_{TU}$
1.2
1.1
1.0
0.9
0.8
0.7
0.6
0.5
0.4
0.3
0.2
0.1
0.0
1
10
10^2
10^3
10^4
10^5
10^6
10^7
CYCLES

*GAC 4610
2-74

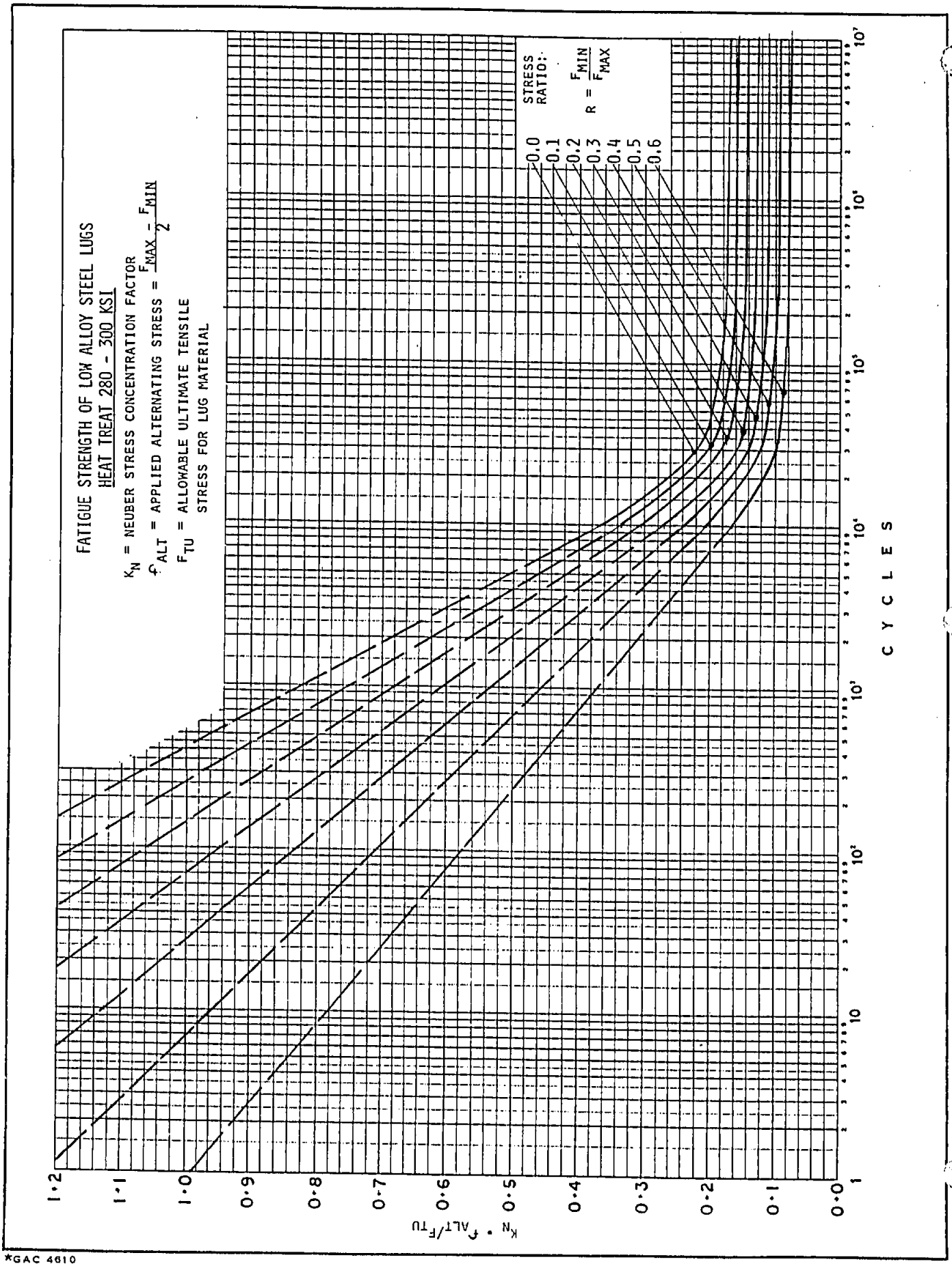
FATIGUE STRENGTH OF LOW ALLOY STEEL LUGS
HEAT TREAT 280 - 300 KSI
K_N = NEUBER STRESS CONCENTRATION FACTOR
f_{ALT} = APPLIED ALTERNATING STRESS = $\frac{F_{MAX} - F_{MIN}}{2}$
F_{TU} = ALLOWABLE ULTIMATE TENSILE STRESS FOR LUG MATERIAL
STRESS RATIO: $R = \frac{F_{MIN}}{F_{MAX}}$
0.0
0.1
0.2
0.3
0.4
0.5
0.6
$K_N \cdot f_{ALT}/F_{TU}$
1.2
1.1
1.0
0.9
0.8
0.7
0.6
0.5
0.4
0.3
0.2
0.1
0.0
1
10
10^2
10^3
10^4
10^5
10^6
10^7
CYCLES

*GAC 4610
2-74

SECTION B7.040

STRESS CONCENTRATION FACTORS

	FORM OF DISCONTINUITY		LOADING	PAGE
BARS, STRIPS, PLATES	Single circular hole		end load transverse bending (central hole)	B7.040.1-1
	Reinforced circular hole	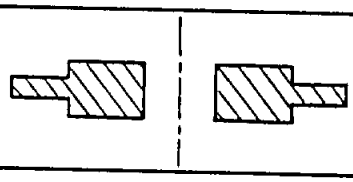	tensile stress shear stress	B7.040.1-3
	Central line of circular holes	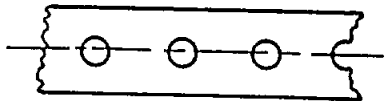	end load	B7.040.1-5
	Wide sheet with double row of holes	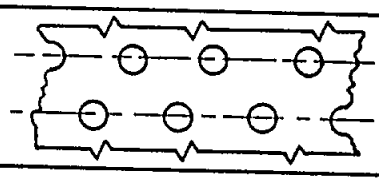	end load perpendicular to lines of holes	B7.040.1-6
	Transverse slot	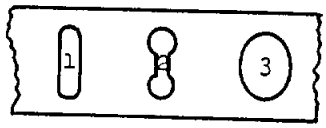	end load (types 1, 2, 3) bending (types 1, 3)	B7.040.1-7
	Notch on both sides	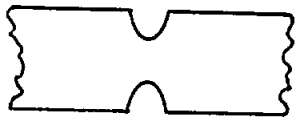	end load bending transverse bending	B7.040.1-9
	Notch on one side	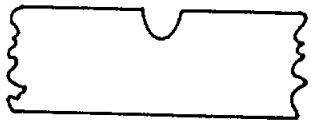	end load bending a. effect of notch angle	B7.040.1-12
	Multiple notches on one or both sides	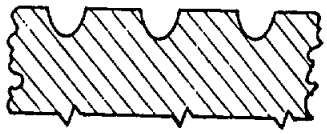	end load bending	B7.040.1-14
	Shoulder fillet		end load bending	B7.040.1-15
	T-Head with distributed reactions	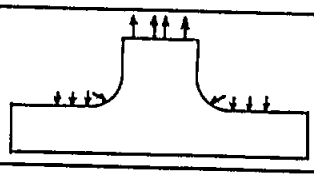	as shown	B7.040.1-17
	Fillets (effect of shoulder width, L)	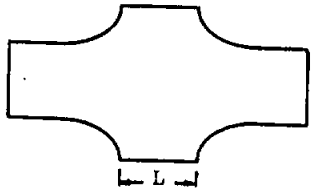	bending	B7.040.1-18

SECTION B7.040

STRESS CONCENTRATION FACTORS

	FORM OF DISCONTINUITY		LOADING	PAGE
SHAFTS AND TUBES	Diametrical Circular Hole	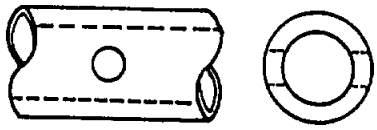	end load torsion bending	B7.040.2-1
	Groove (in solid shaft)	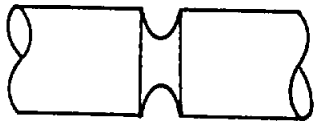	end load bending torsion	B7.040.2-5
	Fillet	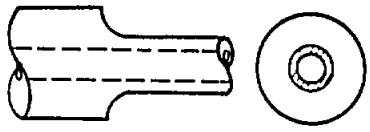	end load - solid shaft hollow shaft torsion - solid shaft hollow shaft bending - solid shaft	B7.040.2-8
JOINTS	Bar loaded by a close fitting pin	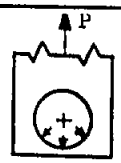	tension	B7.040.3-1
MISCELLANEOUS	Angle	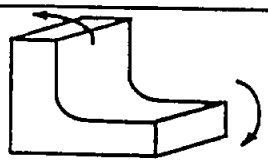	bending	B7.040.4-1

ADDITIONAL REFERENCES	B7.040.7-1

STRESS CONCENTRATION FACTORS FOR AN AXIALLY-LOADED PLATE WITH AN ECCENTRIC CIRCULAR HOLE

NOTE: These factors apply to stresses in the elastic region.

$f_{max} = K \times f_{net}$ = maximum stress (at point "n")

$f_{net} = P/(d_1 + d_2)\ (t)$ = average net section stress

t = plate thickness

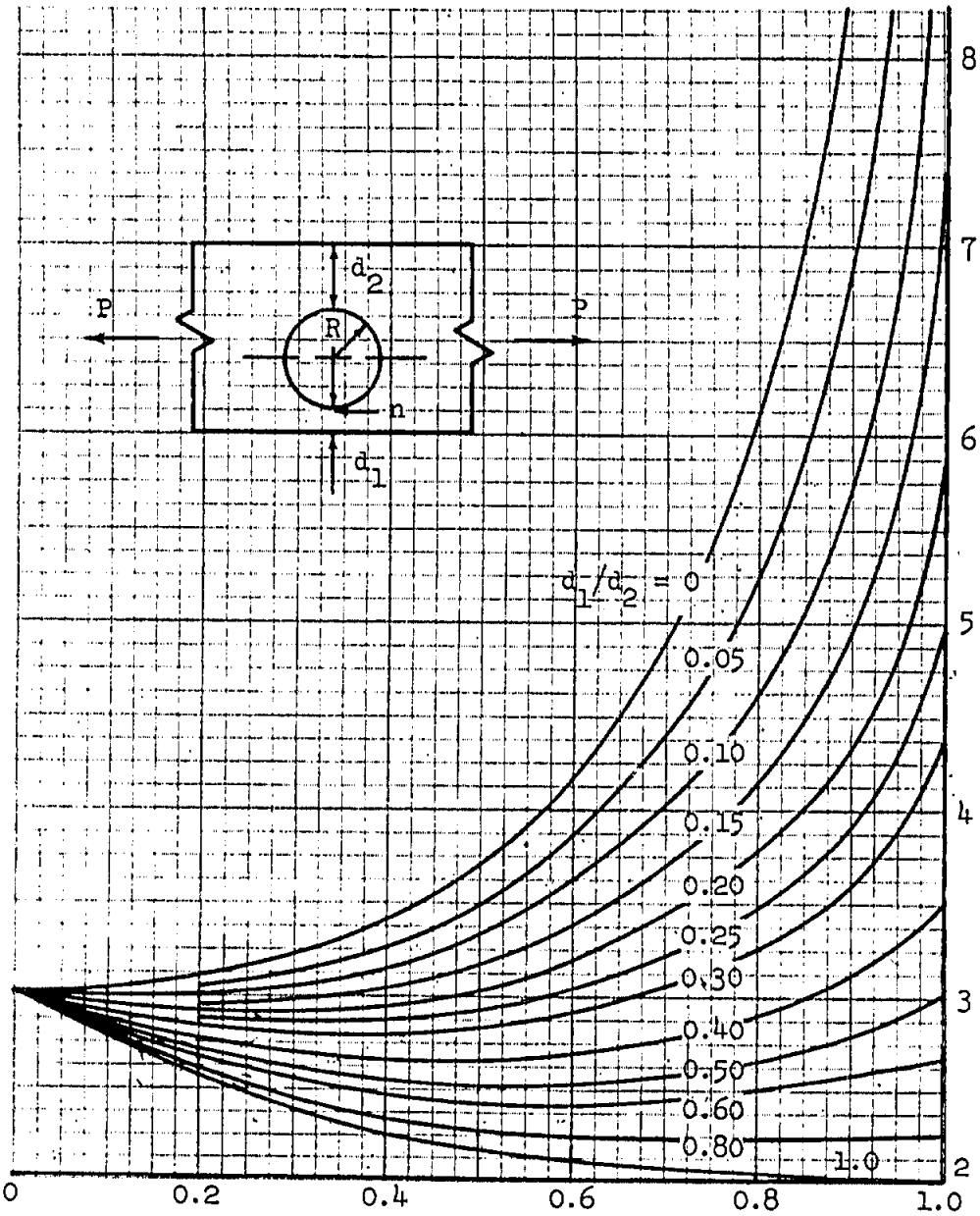

$K = \frac{f_{max}}{f_{net}}$ = Stress Concentration Factor

$\frac{R}{d_1 + R} = \frac{\text{Radius of Hole}}{\text{Minimum Edge Distance}}$

Ref: Aero. Res. Inst. of Sweden - Report No. 36

STRESS CONCENTRATION FACTORS FOR A PLATE IN BENDING WITH A CENTRAL CIRCULAR HOLE

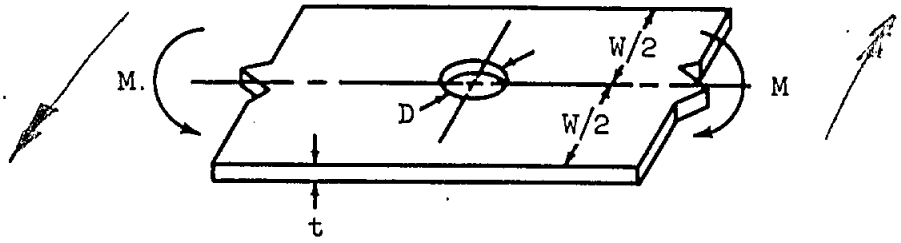

$f_{max} = K f_{nom}$ = maximum stress at edge of hole

$f_{nom} = \frac{6M}{(W - D)t^2}$ = nominal bending stress in outer fibers of plate

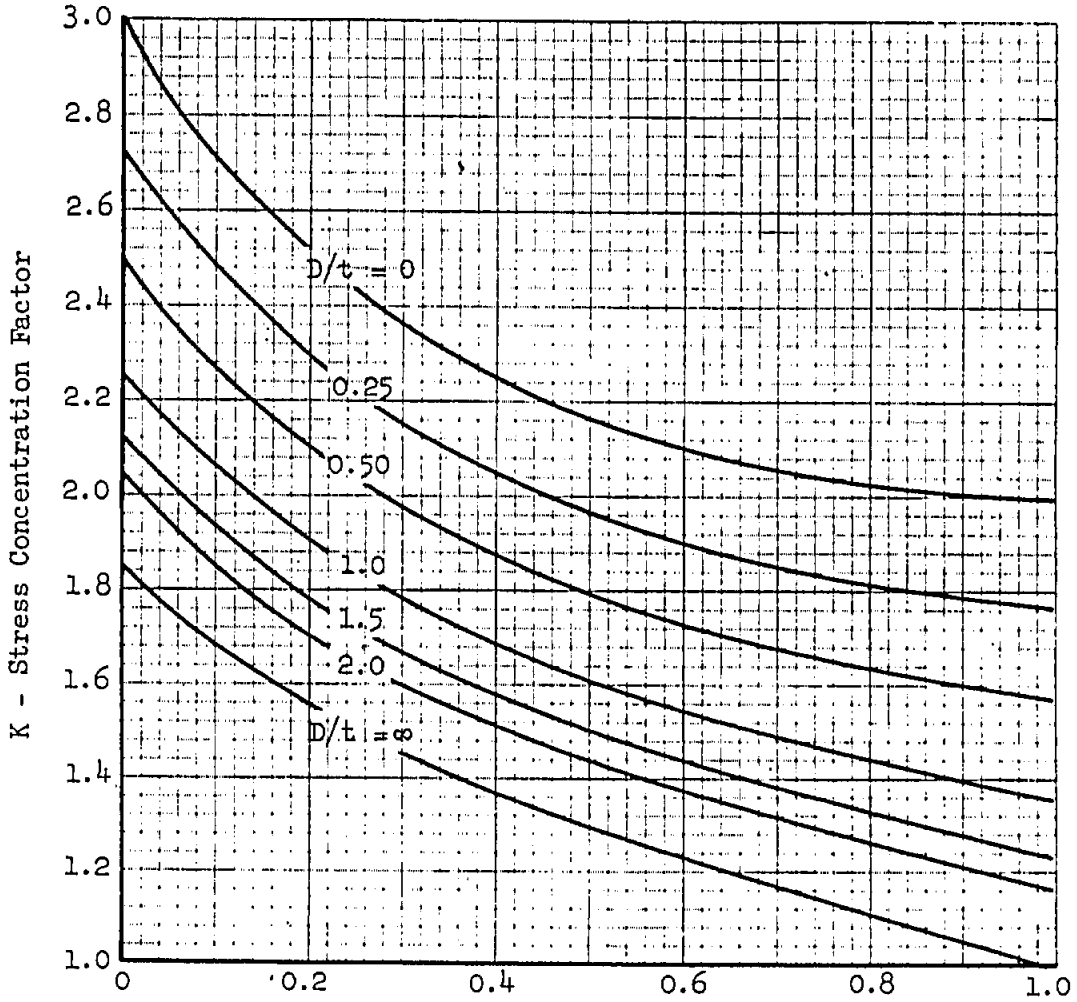

$\frac{D}{W} = \frac{\text{Hole Diameter}}{\text{Plate Width}}$

Ref: R. E. Peterson, "Stress Concentration Design Factors," Fig. 86 & GAEC Calculations

THE EFFECT OF REINFORCEMENT ON THE STRESS CONCENTRATION AT A HOLE IN A PLATE

NOTATION

d = diameter of hole (in.)

D = outside diameter of reinforcing ring (in.)

t = thickness of plate (in.)

t_r = thickness of reinforcement (in.) (*see* sketch)

f = direct stress in plate, neglecting hole and reinforcement (lb./in.^{2})

q = shear stress in plate, neglecting hole and reinforcement (lb./in.^{2})

f_{max} = maximum principal stress in reinforced plate (lb./in.^{2})

NOTES

The ratios f_{max}/f and f_{max}/q are plotted against the ratio t_r/t for various values of D/d.

Two cases are considered: in one a single direct stress f is applied to the plate, in the other a shear stress q.

It is assumed that the plate is large compared with the hole; but the results may be applied with sufficient accuracy to plates the smallest dimension of which is not less than four times d. The deformations of the ring reinforcement are assumed to be equal to those of the plate in both the radial and tangential directions, and the stress is assumed to be uniformly distributed over the thickness of the ring and plate. In practice, if the ring is riveted to the plate, stress concentrations will occur at each rivet and the deformations and stresses in ring and plate will not be equal. The plotted results may be used as a guide, the accuracy of which depends upon the number and position of the rivets.

For small values of t_r/t the maximum principal stress occurs at the edge of the hole but for higher values it occurs at the junction of the plate and reinforcing ring. This change in location causes the discontinuity in the slope of the curves.

In the case of a single direct stress and with the lower values of t_r/t, f_{max} occurs at the edge of the hole on a diameter drawn perpendicular to the direction of the applied stress. In the same case but with higher value of t_r/t, f_{max} occurs at the junction of the plate and the reinforcing ring at four points located within 10° of the two diameters drawn at 45° and −45° to the direction of the applied stress.

In the case of pure shear and with the lower values of t_r/t, f_{max} occurs at the edge of the hole at four points located on the two diameters drawn in the directions of the maximum applied tension and compression stresses. In the same case but with higher values of t_r/t, f_{max} occurs at eight points on the junction of the plate and the reinforcing ring. These eight points are grouped in four pairs and for the range of t_r/t covered in this data sheet these points occur within 10° on each side of the two diameters drawn at 45° to the directions of the maximum applied tension and compression stresses.

It is assumed that f_{max} is within the elastic range and that buckling of the plate or reinforcement out of its plane does not occur.

DERIVATION

Gurney. An analysis of the stresses in a flat plate with a reinforced circular hole under edge forces. R. and M. No. 1834 (1938).

Heaps. Unpublished work at the R.A.E. (1952).

EXAMPLE

Find the dimensions of a circular reinforcing ring when the maximum stress is limited to 1.5 times the undisturbed stress in the plate under direct load, and:—

$$D = 4.0 \text{ in., } d = 2.0 \text{ in., and } t = 0.036 \text{ in.}$$

From the diagram, with

$$D/d = 2.0,\ t_r/t = 2.42.$$

Therefore a ring with $t_r = 2.42 \times 0.036 = 0.087$ in., satisfies the requirements.

Ref. RAS Structural Data Sheets (Dec. 1963) pp. 02.04.03

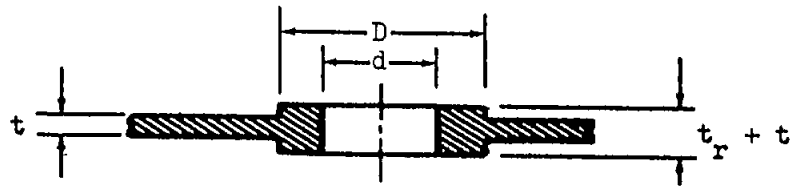

f_{max}/q

f_{max}/f

f_{max}/q

f_{max}/f

D/d
1.25
1.5
2.0
1.25
1.5
2.0

4.0
3.5
3.0
2.5
2.0
1.5
1.0
0.5
0

0 1 2 3 4 5 6

t_r/t

Ref. RAS Structures Data Sheets (Dec. 1963) pp. 02.04.03
Reproduced by Royalty Agreement.

STRESS CONCENTRATION FACTORS FOR AN AXIALLY LOADED PLATE WITH A CENTRAL LINE OF HOLES

$f_{max} = K\, f_{nom}$ = maximum stress at edge of holes

$f_{nom} = \dfrac{P}{(W - D)t}$ = nominal stress in net section

t = plate thickness

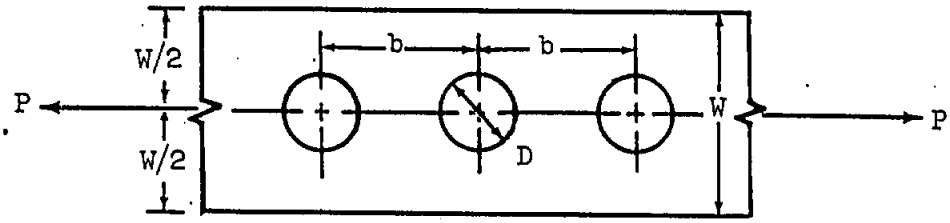

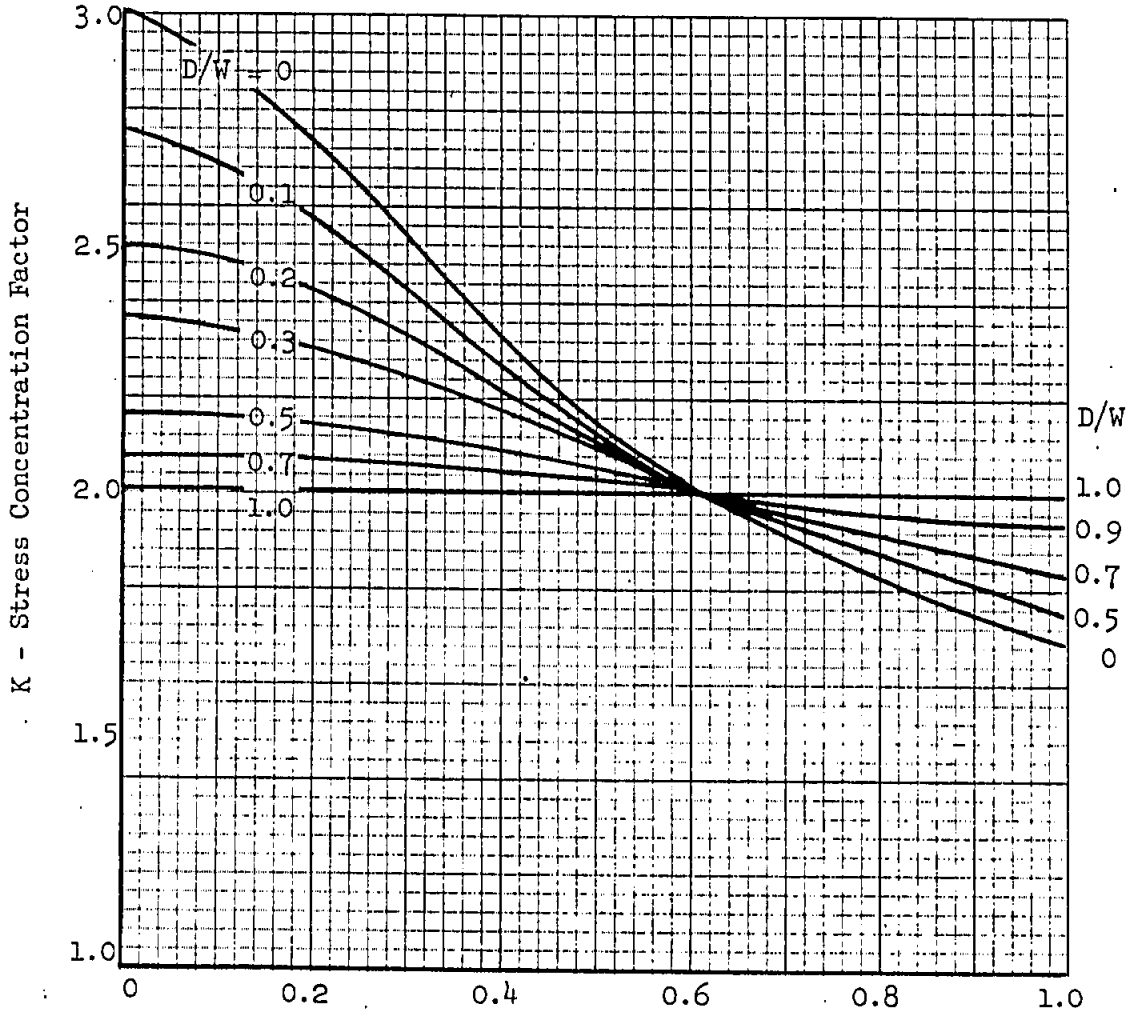

$\dfrac{D}{b} = \dfrac{\text{Hole Diameter}}{\text{Hole Spacing}}$

Ref: R.E. Peterson, "Stress Concentration Design Factors," Fig. 78 & GAEC Calculations

STRESS CONCENTRATION FACTORS FOR A WIDE SHEET WITH A DOUBLE ROW OF HOLES PERPENDICULAR TO THE LOAD

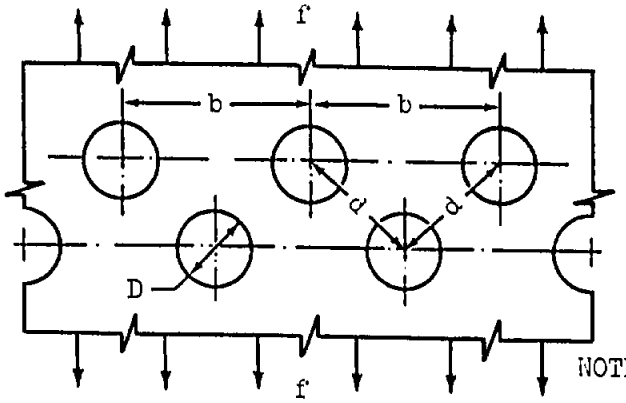

NOTE: f = average stress on cross section

$f_{max} = Kf\left(\frac{b}{b-D}\right)$ $f_{max} = Kf\left(\frac{d}{d-D}\right)$

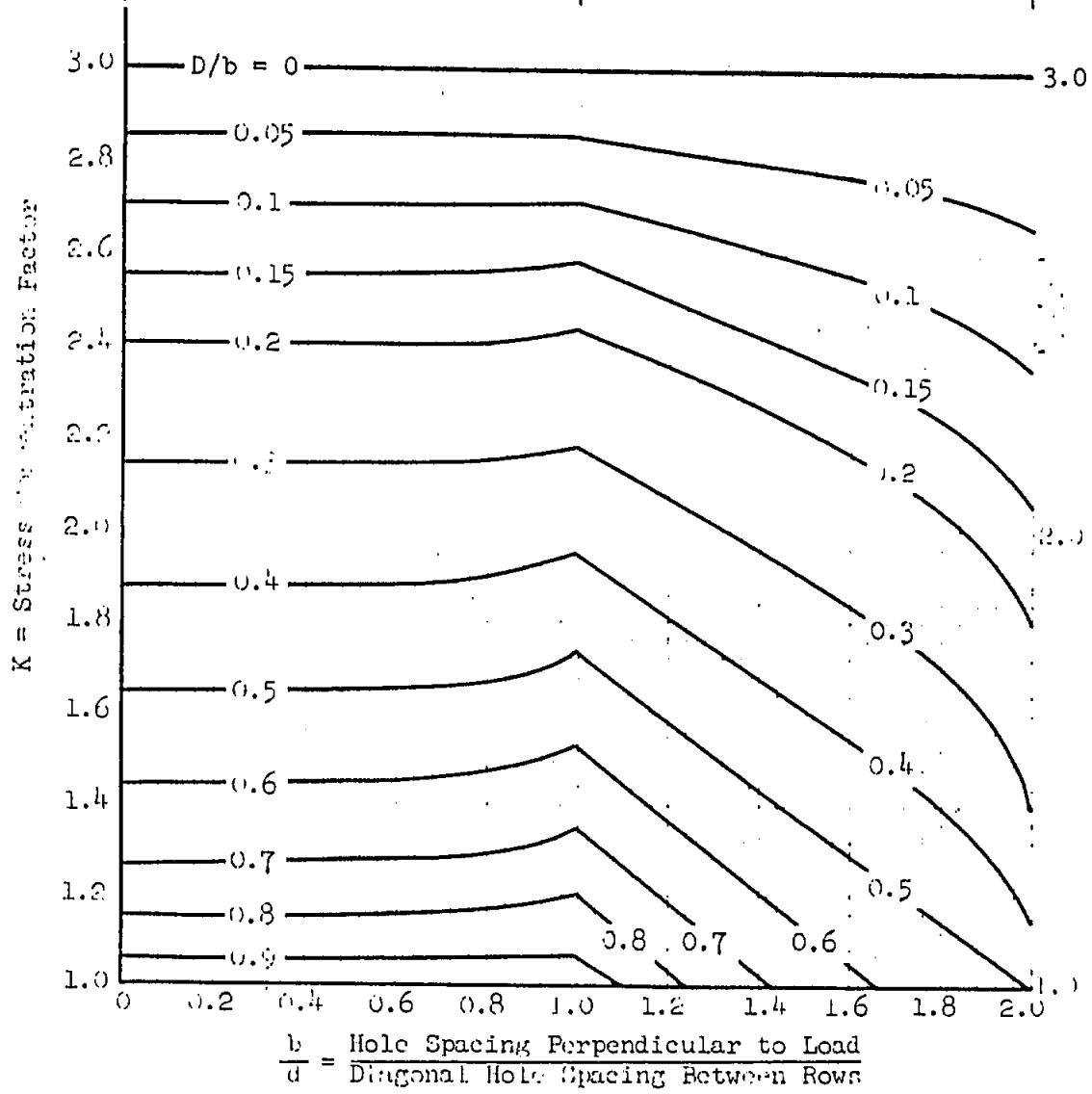

$\frac{b}{d} = \frac{\text{Hole Spacing Perpendicular to Load}}{\text{Diagonal Hole Spacing Between Rows}}$

Ref: R. E. Peterson, "Stress Concentration Design Factors", Fig. 30

STRESS CONCENTRATION FACTORS FOR SLOTTED BARS UNDER AXIAL LOAD

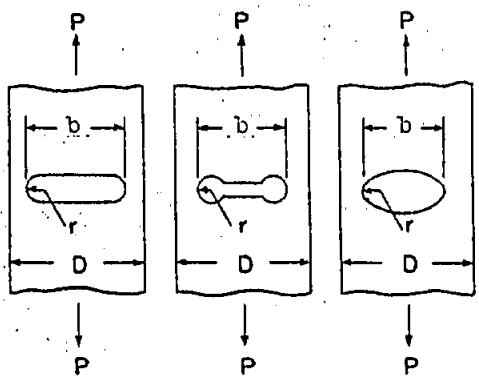

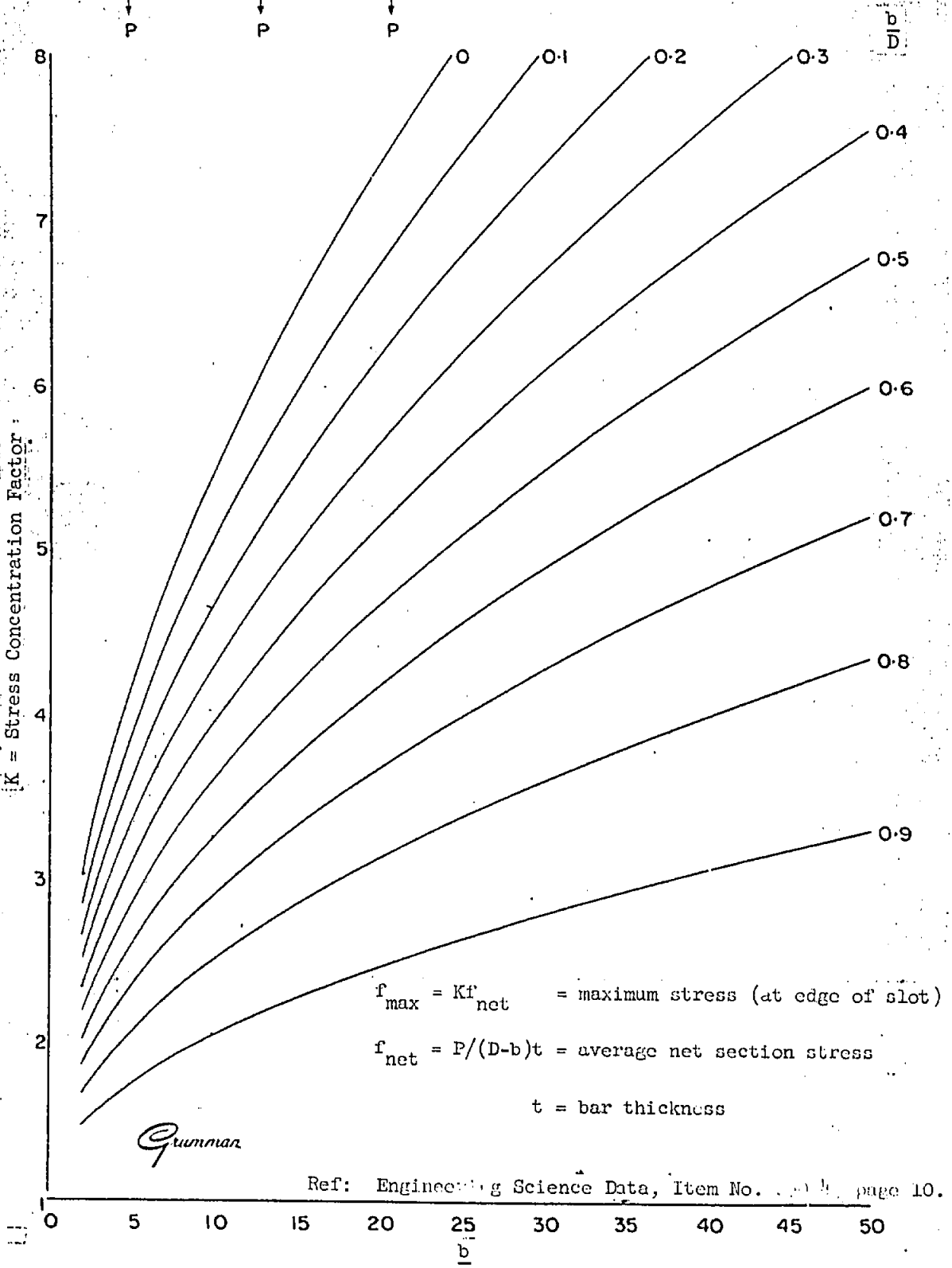

$f_{max} = Kf_{net}$ = maximum stress (at edge of slot)

$f_{net} = P/(D-b)t$ = average net section stress

t = bar thickness

Grumman

Ref: Engineering Science Data, Item No. [illegible] page 10.

STRESS CONCENTRATION FACTORS FOR SLOTTED BARS IN PURE BENDING

1. $f_A = KMc/I$ = maximum value of stress along edge of slot (at point "A")
2. $f_B = Mc/I$ = maximum value of outer fiber stress (at points "B")

c = semi-depth of bar (see figure below)

I = moment of inertia of net area through slot, taken about an axis through the middle of the bar.

These factors apply to stresses in elastic region.

In an elliptical slot R is the minimum radius.

NOTE: 1. Solid lines indicate that the maximum stress in the bar is obtained at the edge of the slot. (Use equation 1 above.)
2. Dashed lines indicate maximum stress in bar is at the outer fiber. (Use equation 2 above.)

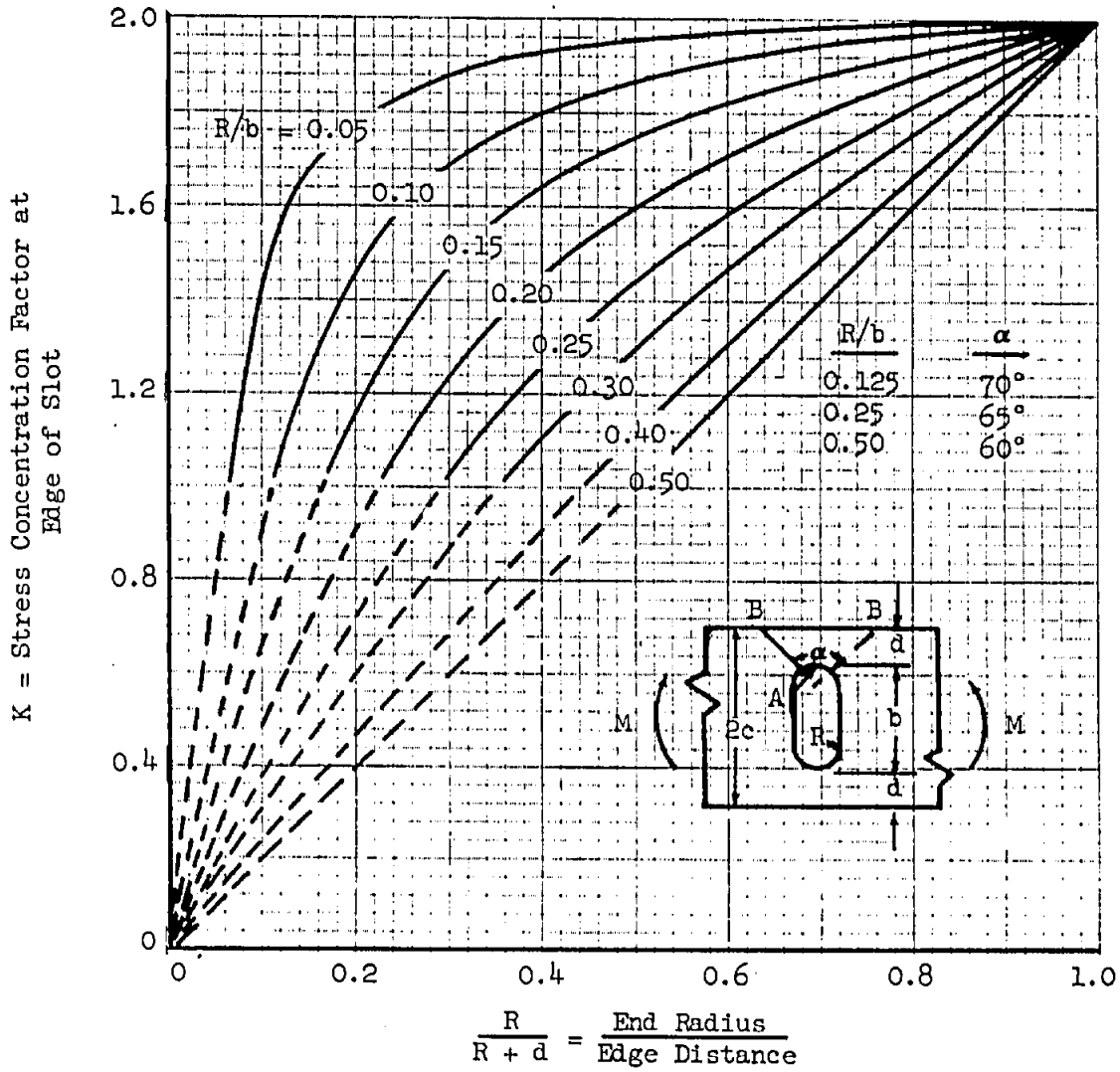

Ref: Journal of Applied Mechanics, March 1951, pages 107, 108

Grumman

STRESS CONCENTRATION FACTORS FOR A NOTCHED FLAT PLATE UNDER AXIAL LOAD

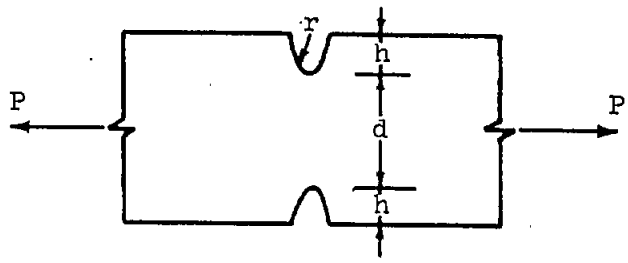

$f_{max} = K\, f_{ave}$

$f_{ave} = P/dt$ average net section stress

t = plate thickness

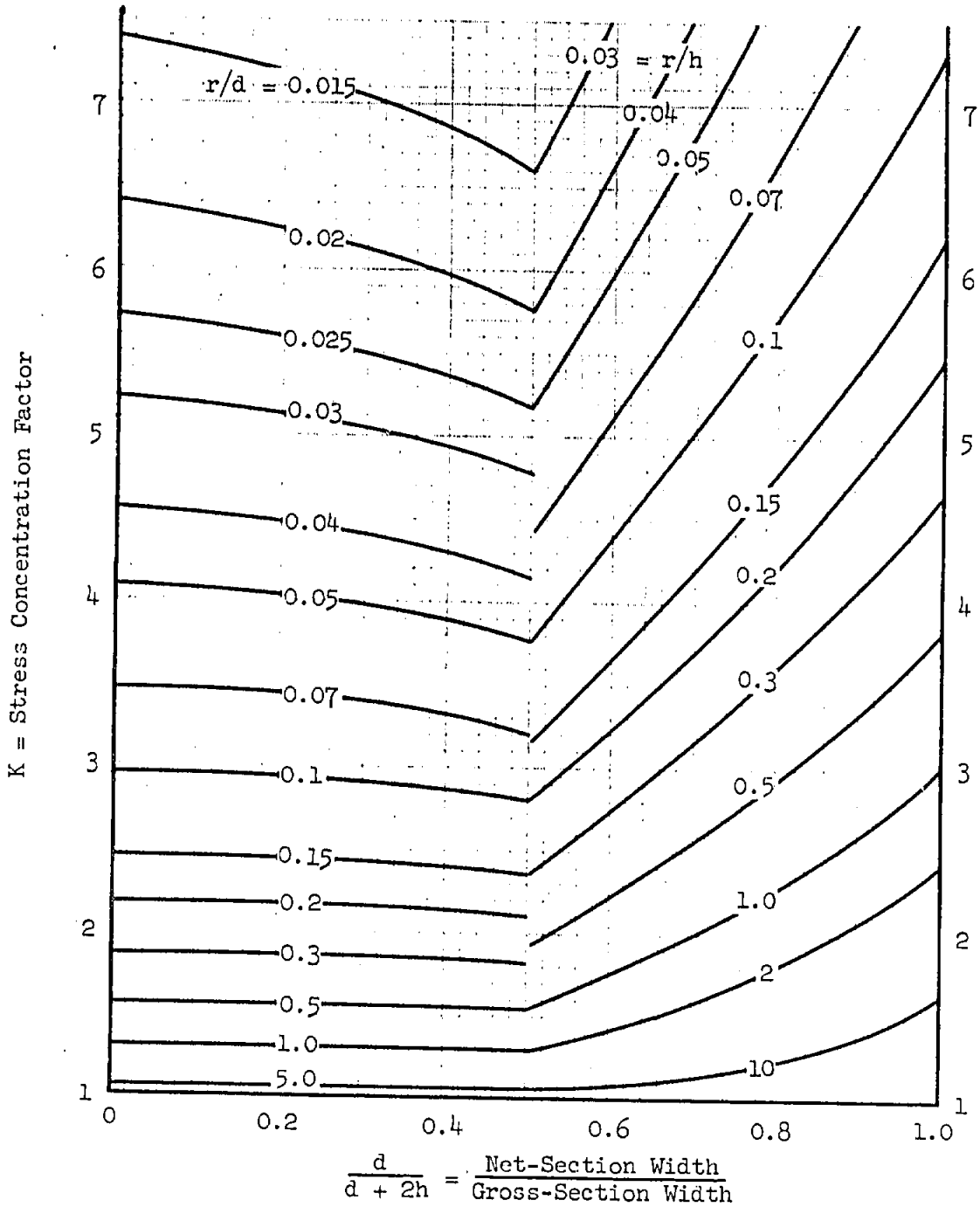

Ref: R. E. Peterson, "Stress Concentration Design Factors," Fig 16-19

STRESS CONCENTRATION FACTORS FOR A NOTCHED FLAT PLATE IN BENDING

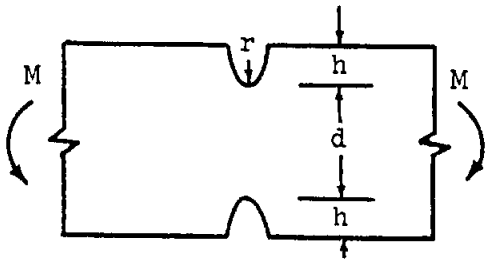

$f_{max.} = K\, f_{nom.}$

$f_{nom.} = \frac{6M}{d^2 t}$ = nominal outer fiber bending stress at net section

t = plate thickness

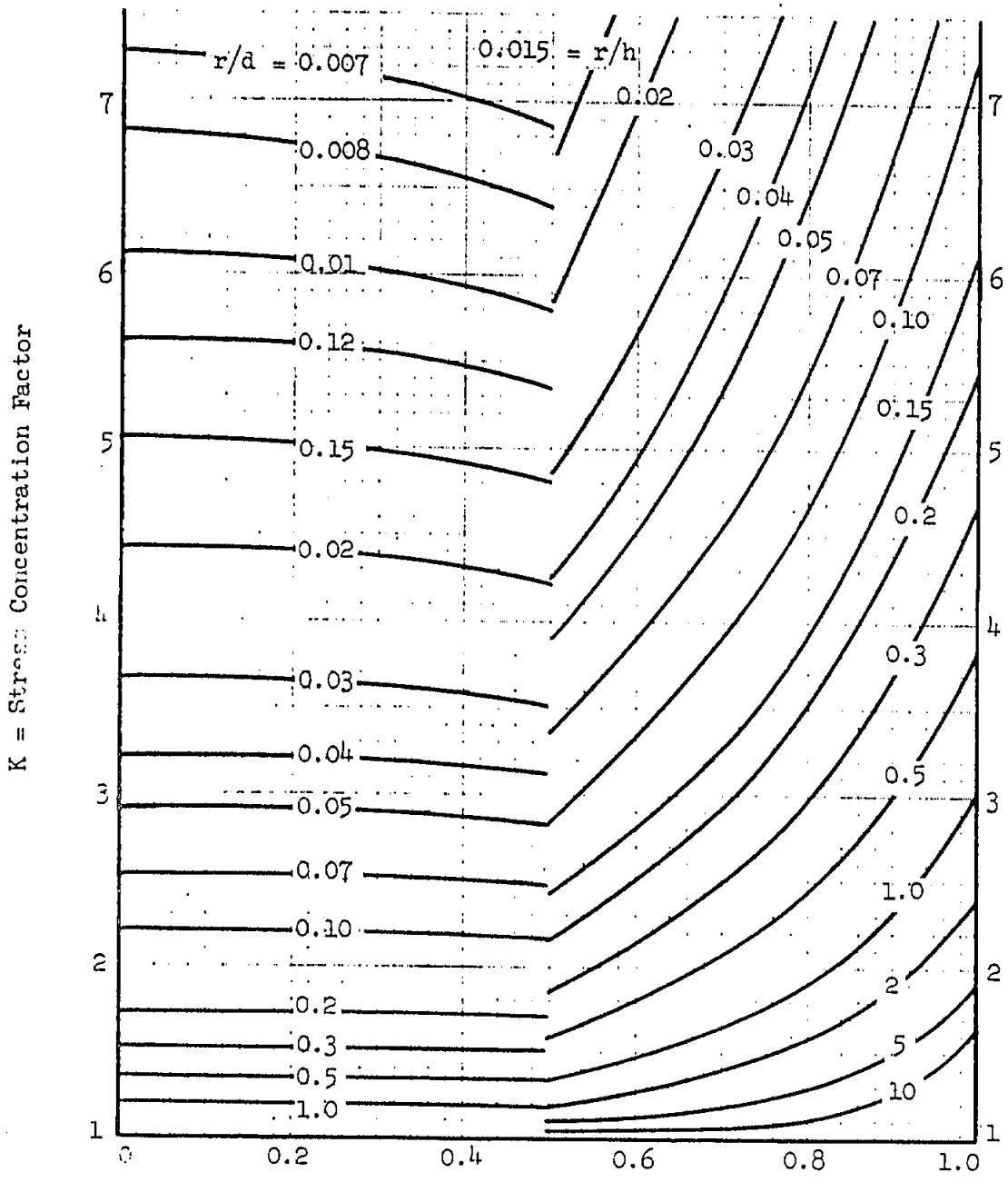

$$\frac{d}{d + 2h} = \frac{\text{Net-Section Depth}}{\text{Gross-Section Depth}}$$

Ref: R. E. Peterson, "Stress Concentration Design Factors", Fig. 32-35

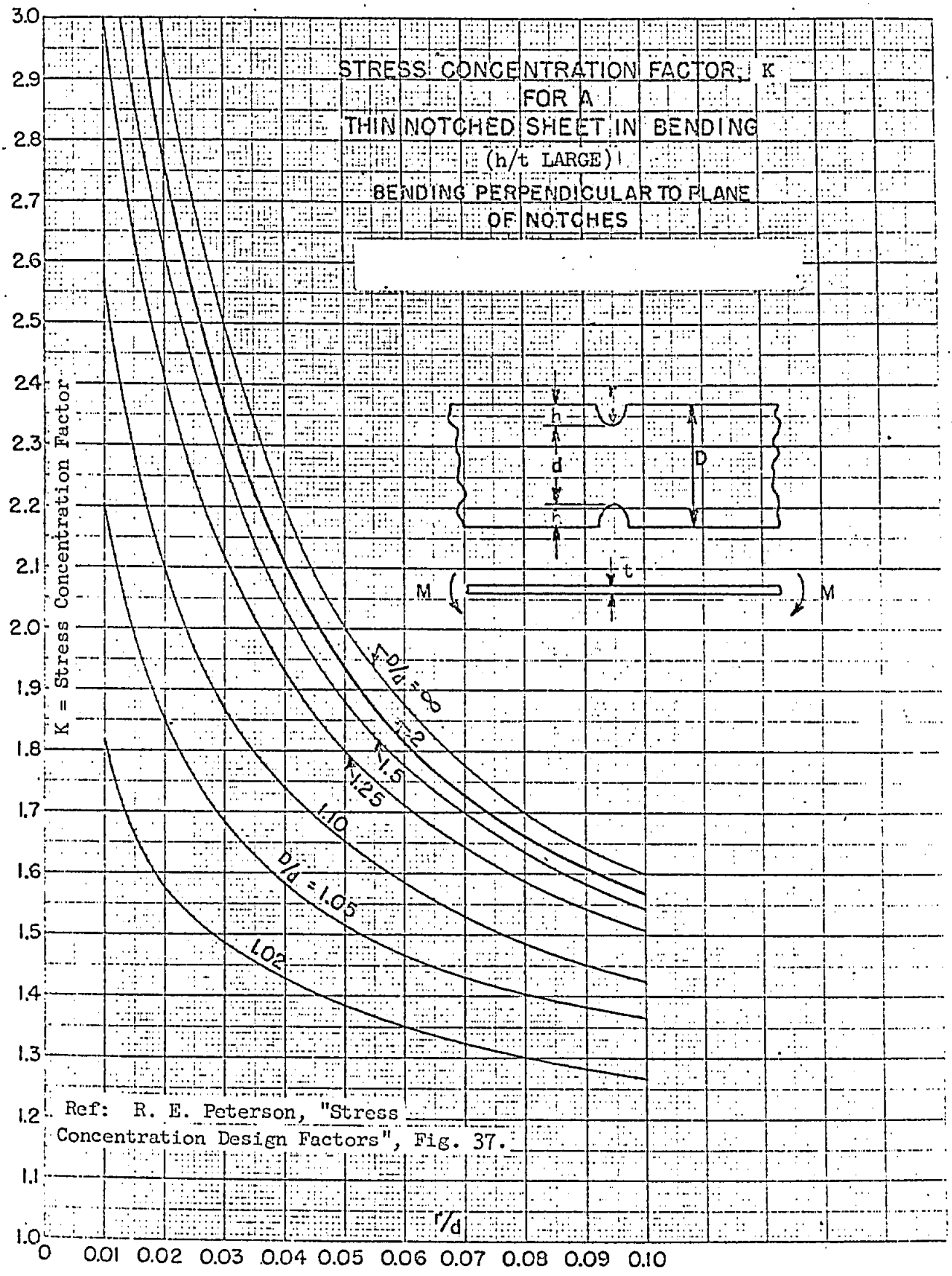

Ref: R. E. Peterson, "Stress Concentration Design Factors", Fig. 37.

STRESS CONCENTRATION FACTORS FOR "U" TYPE NOTCH IN FLAT BAR

$f_{max} = Kf_{net}$ = maximum stress (at root of notch)

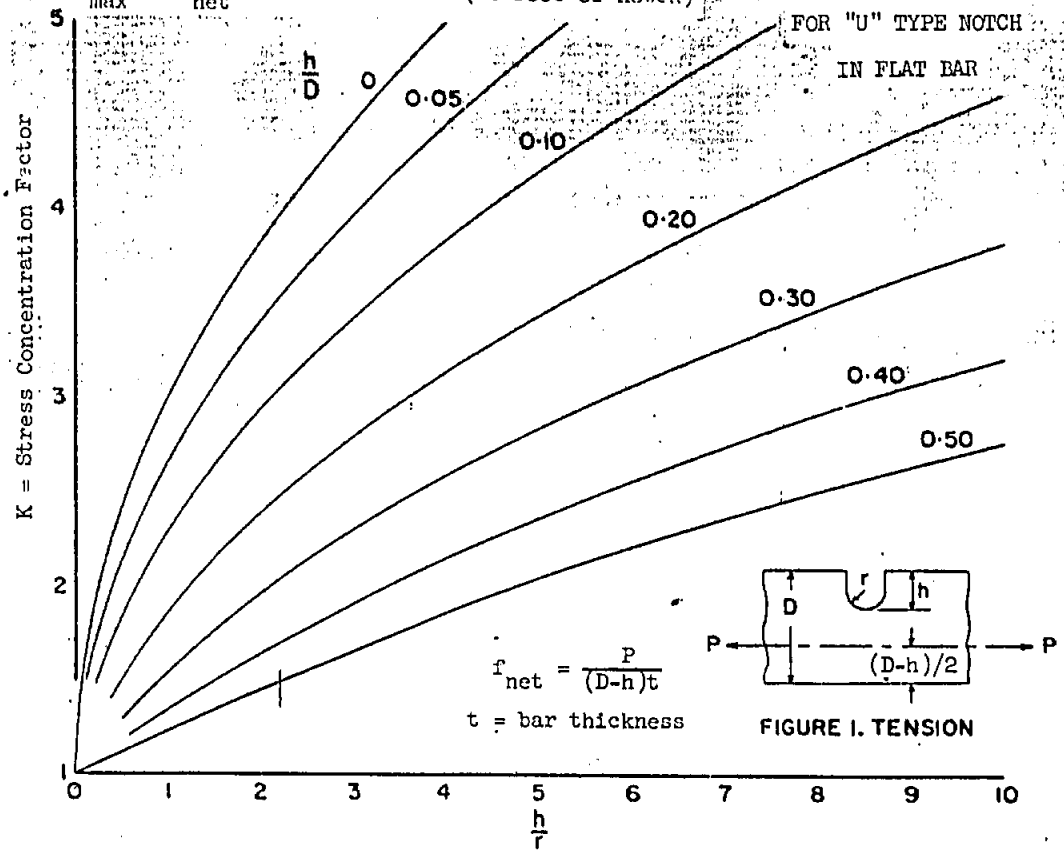

$$f_{net} = \frac{P}{(D-h)t}$$

t = bar thickness

FIGURE 1. TENSION

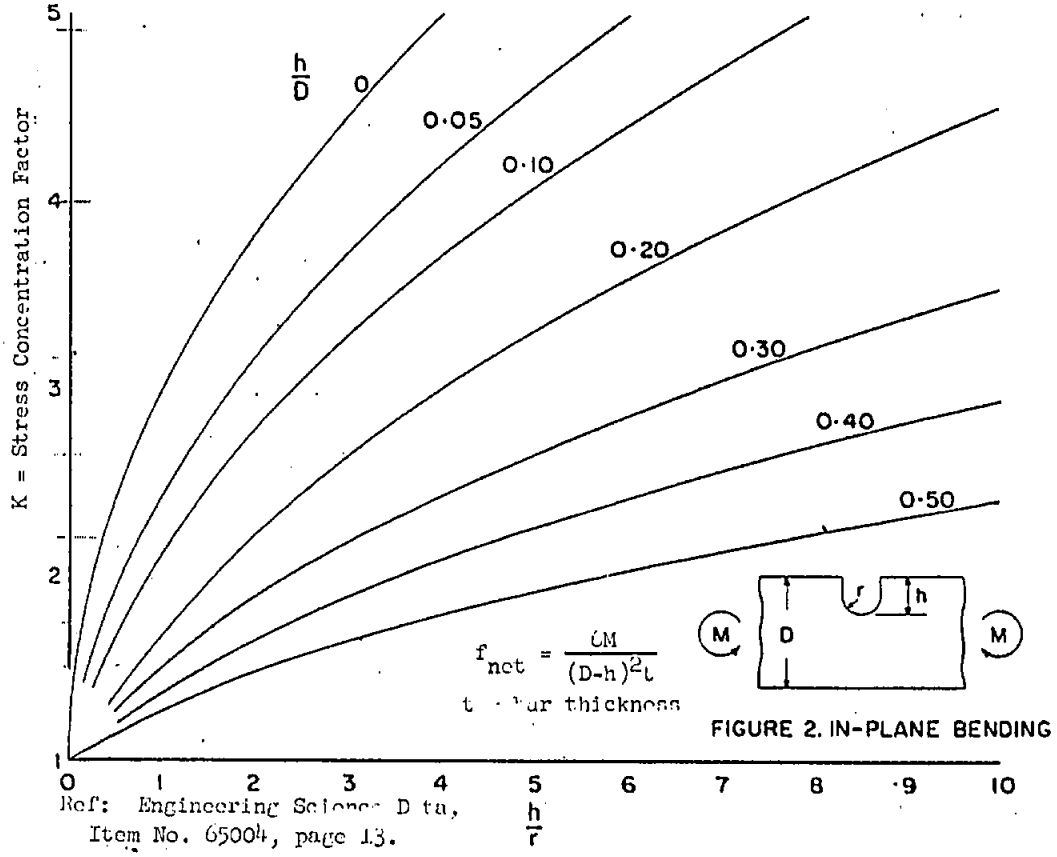

$$f_{net} = \frac{6M}{(D-h)^2 t}$$

t = bar thickness

FIGURE 2. IN-PLANE BENDING

Ref: Engineering Science Data, Item No. 65004, page 13.

EFFECT OF NOTCH ANGLE ON STRESS CONCENTRATION FACTOR FOR A BAR IN BENDING WITH A NOTCH ON ONE SIDE

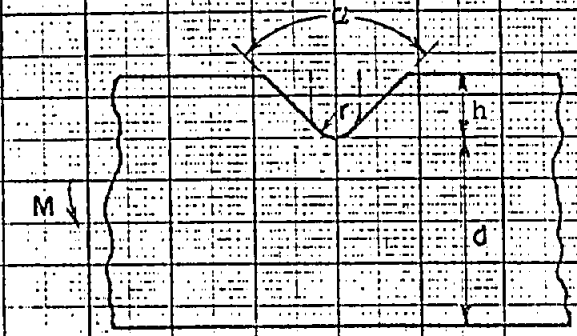

K = STRESS CONC. FACTOR FOR STRAIGHT-SIDED NOTCH WITH SEMI-CIRCULAR BOTTOM (DASHED LINES IN ABOVE SKETCH)

K_α = STRESS CONC. FACTOR FOR NOTCH OF ANGLE α, WITH OTHER DIMENSIONS SAME

Ref: R. E. Peterson, "Stress Concentration Design Factors", Fig. 36.

STRESS CONCENTRATION FACTORS FOR BARS WITH MULTIPLE NOTCHES

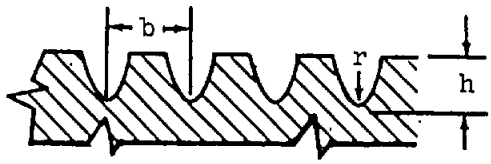

Case (a)
Multiple Notch

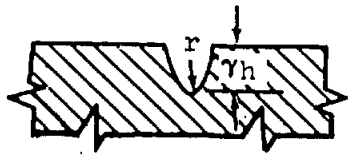

Case (b)
Equivalent Single Notch

For a given loading the stress concentration factor for the multiple notch, case (a), is the same as the factor for the equivalent single notch, case (b), with the same root radius r, but a depth γh. Determine γ from the curve below and then obtain the stress concentration factor for the equivalent single notch, from pages B7.040.1-9, B7.040.1-10 or B7.040.1-12 .

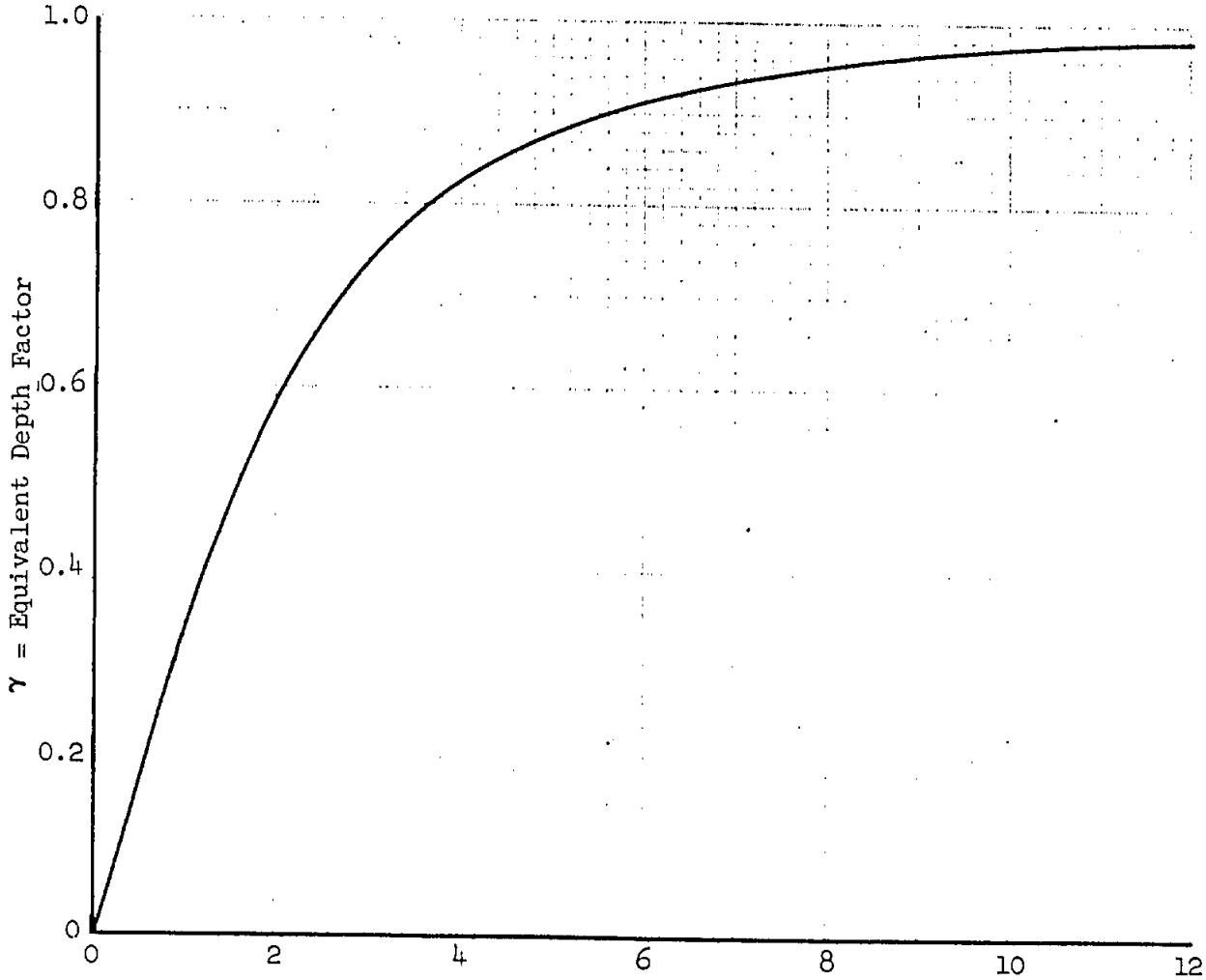

Ref: R. E. Peterson, "Stress Concentration Design Factors", Fig. 23

STRESS CONCENTRATION FACTORS FOR A FLAT PLATE WITH A SHOULDER FILLET UNDER AXIAL LOAD

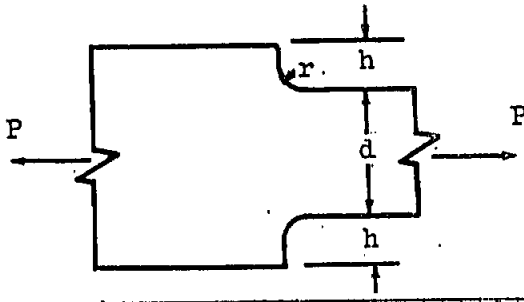

$f_{max} = K f_{ave}$

$f_{ave} = \frac{P}{dt}$ average stress in shank

t = plate thickness

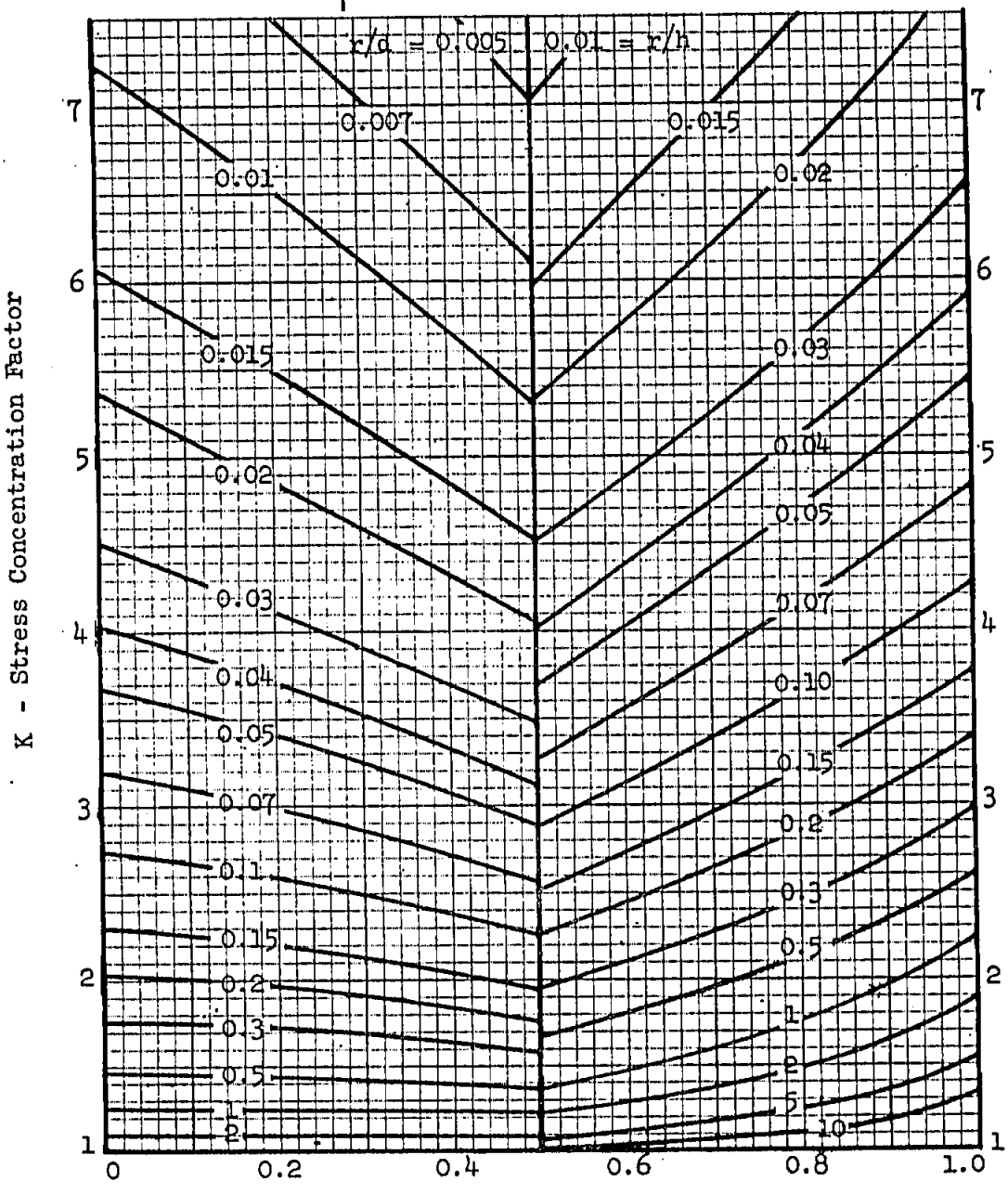

$$\frac{d}{d + 2h} = \frac{\text{Shank Width}}{\text{Shoulder Width}}$$

Ref: R. E. Peterson, "Stress Concentration Factors," Fig. 57; T.N. 2442; GAEC Data

Grumman

STRESS CONCENTRATION FACTORS FOR A FLAT PLATE WITH A SHOULDER FILLET IN BENDING

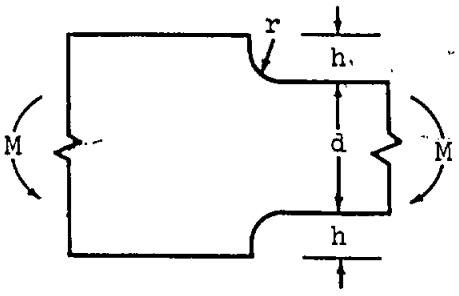

$f_{max.} = K f_{nom.}$

$f_{nom.} = \frac{6M}{d^2 t}$ = nominal outer fiber bending stress in shank

t = plate thickness

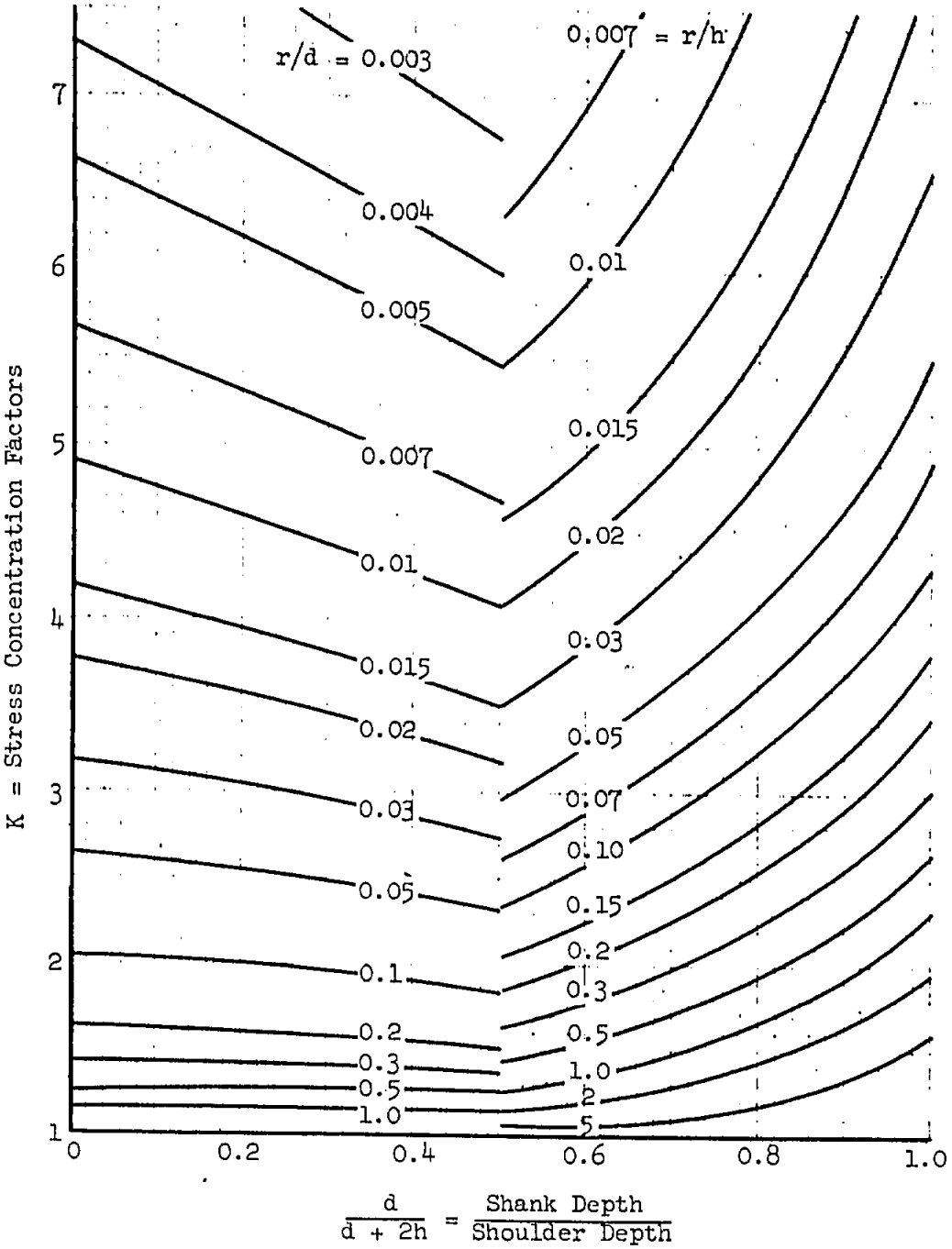

$\frac{d}{d + 2h} = \frac{\text{Shank Depth}}{\text{Shoulder Depth}}$

Ref: R. E. Peterson, "Stress Concentration Design Factors", Fig. 60, GAEC Data

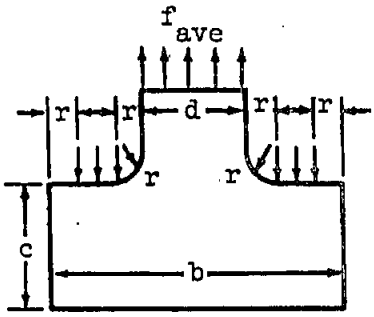

STRESS CONCENTRATION FACTORS FOR A T-HEAD WITH DISTRIBUTED REACTIONS

Ref: R. E. Peterson, "Stress Concentration Design Factors," Figs. 103-108

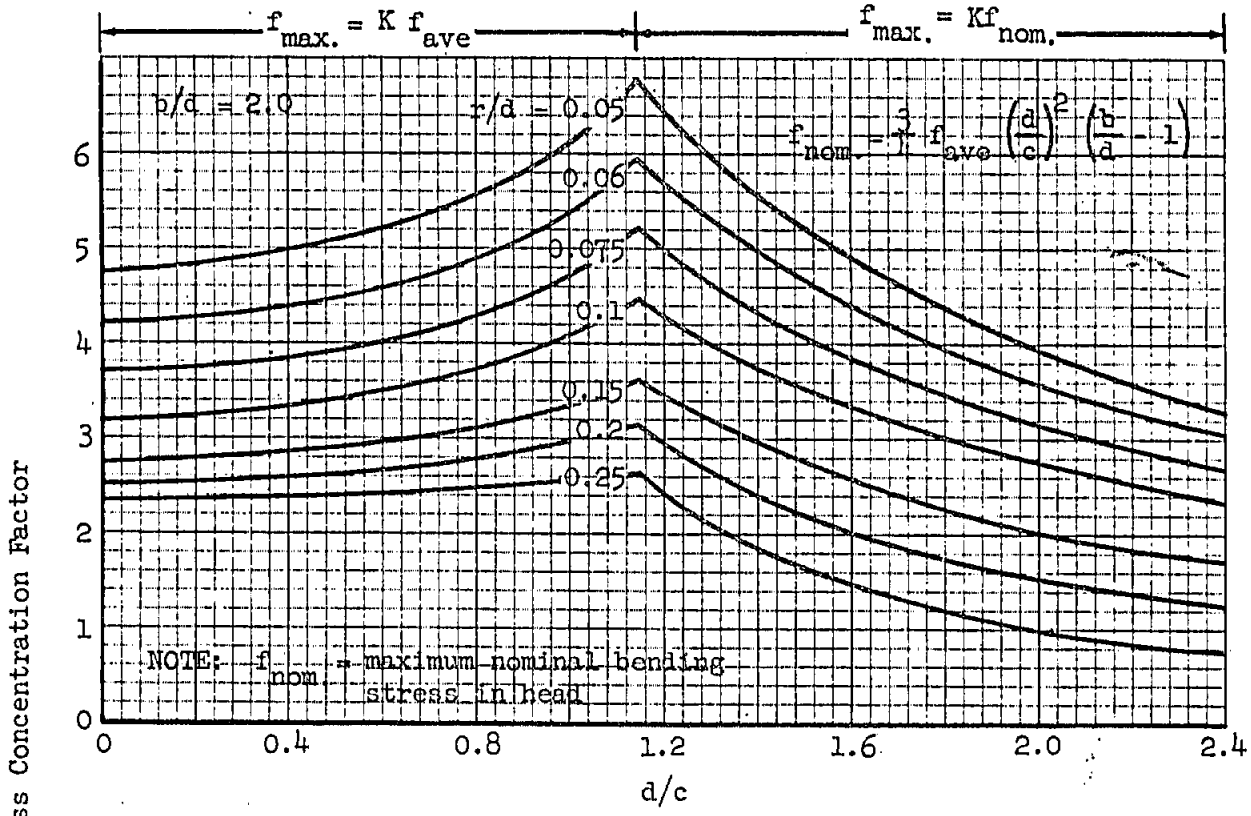

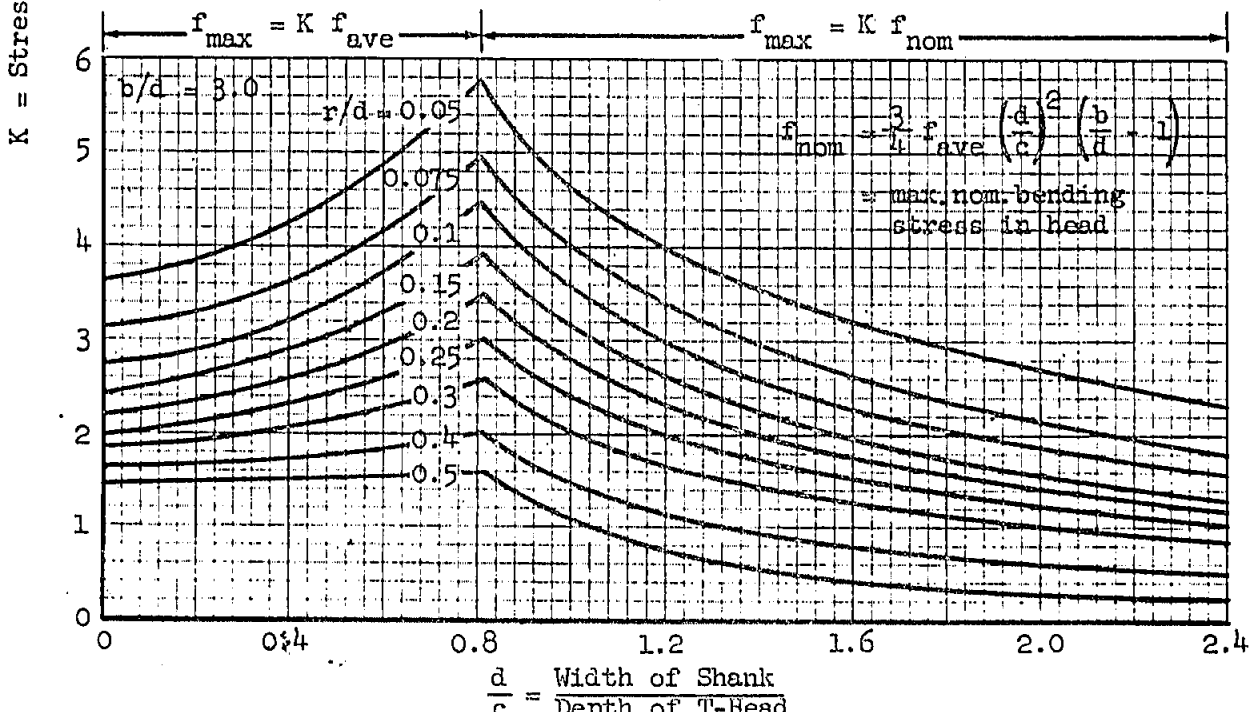

Grumman

EFFECT OF SHOULDER WIDTH, L, ON STRESS CONCENTRATION FACTOR FOR FILLETED BARS IN BENDING

$$f_{max} = Kf_{nom}$$

$$f_{nom} = \frac{6M}{d^2t}$$

t = plate thickness

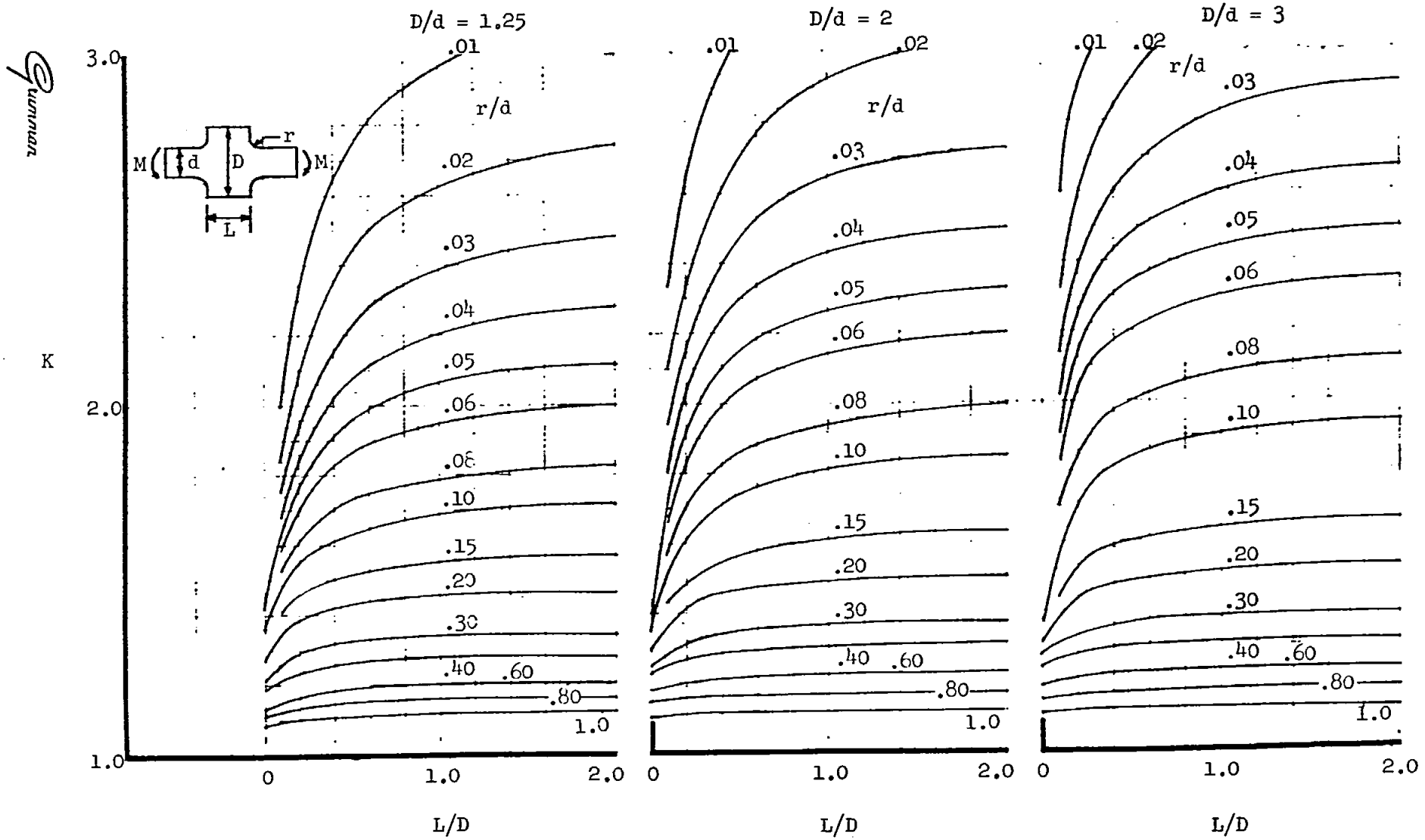

Ref: R. E. Peterson, "Stress Concentration Design Factors", Figs. 61-63

GEOMETRIC STRESS CONCENTRATION FACTORS
DIAMETRAL CIRCULAR HOLES IN ROUND TUBES UNDER TENSION OR TORSION

NOTATION

d = diameter of hole (in.)
D_I = inner diameter of tube (in.)
D_0 = outer diameter of tube (in.)
P = direct load in tube (lb.)
T = torque in tube (lb. in.)
f_{max} = maximum direct stress in tube (lb./in.^{2})
K = stress concentration factor defined by

$$f_{max} = \frac{4KP}{\pi (D_0^2 - D_I^2)} \qquad \text{(for Case 1)}$$

$$f_{max} = \frac{16KT D_0}{\pi (D_0^4 - D_I^4)} \qquad \text{(for Case 2)}$$

NOTES

CASE 1. Values of K are plotted against d/D_0 for various values of D_I/D_0, for a diametral hole in a round tube in tension. The maximum stress occurs in the bore of the hole slightly below the outer surface of the tube, at, or near to, the intersections between the bore of the hole and a plane at right angles to the axis of the tube containing the hole centre line.

CASE 2. Values of K are plotted against d/D_0 for various values of D_I/D_0, for a diametral hole in a round tube in torsion. The maximum direct stress occurs in the bore of the hole slightly below the outer surface of the tube, at points on planes at approximately 45° from the plane through the axis of the tube containing the hole centre line.

DERIVATION*

Results of Strain Gauge Tests:—

THUM and KIRMSER.[1, 2] Tension, Bending, and Torsion of Bars containing a Transverse Hole and Combinations thereof. *V.D.I. Forschungsheft* 419. Vol. 14(*b*), 1943.

Results of Photoelastic Tests:—

FROCHT.[1] Studies in Three-Dimensional Photoelasticity—Stress Concentrations in Shafts with Transverse Circular Holes in Tension. *Journal of Applied Physics*, January, 1944.

LEVEN.[1] Quantitative Three-Dimensional Photoelasticity. *Proceedings of the Society for Experimental Stress Analysis*. Vol. 12, No. 2, 1955.

JESSOP, SNELL and ALLISON.[1, 2] The Investigation of the Stress Concentration Factors in Cylindrical Tubes with Transverse Circular Holes. (To be published).

*[1] Relates to Case 1.
[2] Relates to Case 2.

Ref. RAS Structural Data Sheets (Dec. 1963) pp. 06.00.04
Reproduced by Royalty Agreement.

GEOMETRIC STRESS CONCENTRATION FACTORS

Diametral Circular Holes in Round Tubes Under Tension or Torsion

CASE 1

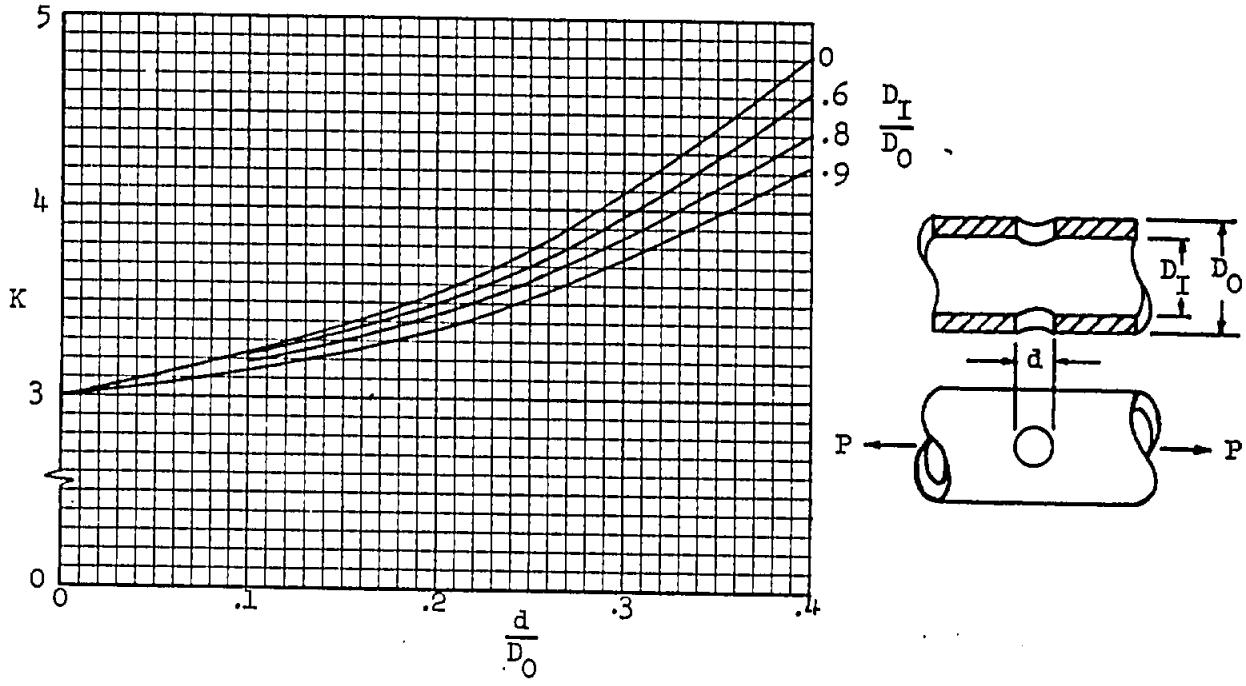

CASE 2

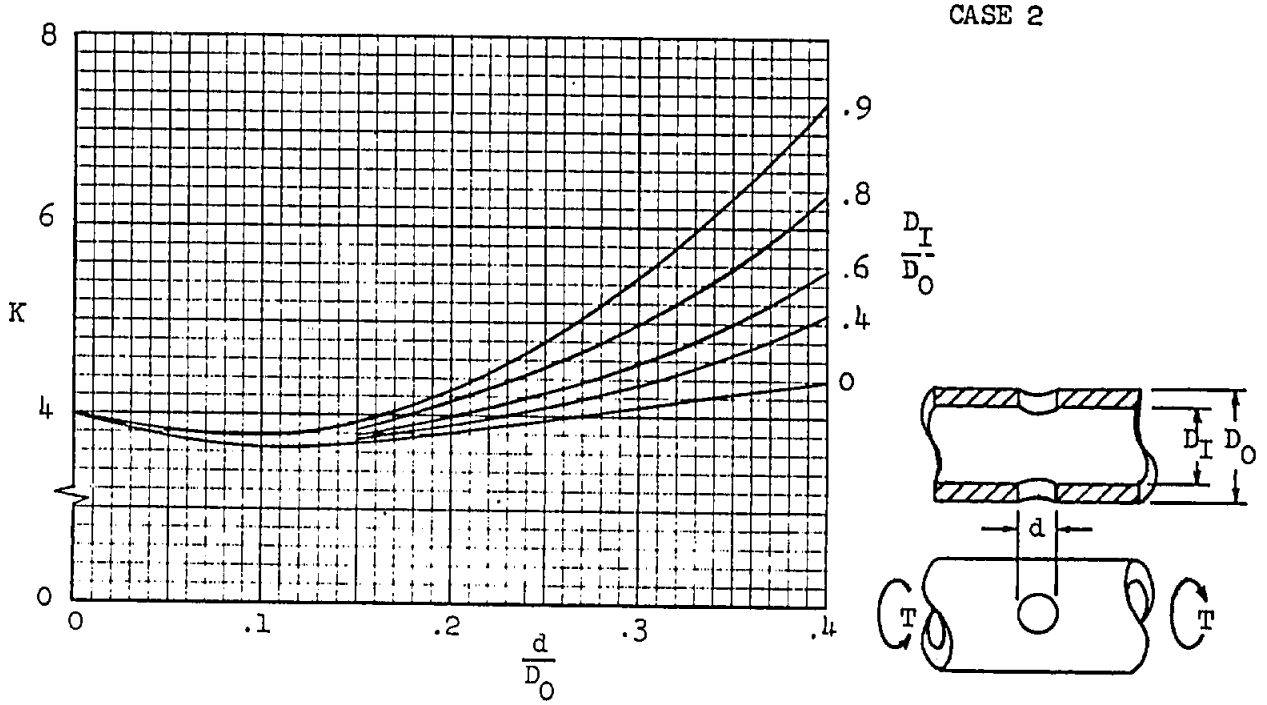

Ref. RAS Structural Data Sheets (Dec. 1963) pp. 06.00.04

GEOMETRIC STRESS CONCENTRATION FACTORS DIAMETRAL CIRCULAR HOLES IN ROUND TUBES IN BENDING

NOTATION

d = diameter of hole (in.)
D_I = inner diameter of tube (in.)
D_O = outer diameter of tube (in.)
M = bending moment in tube (lb. in.)
f_{max} = maximum direct stress in tube (lb./in.^{2})
K = stress concentration factor defined by:

$$f_{max} = \frac{32\,KMD_O}{\pi\,(D_O^4 - D_I^4)}$$

NOTES

Values of K are plotted against d/D_O for various values of D_I/D_O, for a diametral hole in a round tube in bending. The applied bending moment lies in a plane containing the hole centre line.

The maximum stress occurs in the bore of the hole slightly below the outer surface of the tube, at, or near to, the intersections between the edge of the hole and a plane at right angles to the axis of the tube containing the hole centre line.

DERIVATION

Results of Strain Gauge Tests:—

PETERSON and WAHL. Two and three Dimensional Cases of Stress Concentration and Comparison with Fatigue Tests. *Journal of Applied Mechanics*, March, 1936.

THUM and KIRMSER. Tension, Bending and Torsion of Bars containing a Transverse Hole and Combinations thereof *V.D.I. Forschungsheft* 419. March and April, 1943.

Results of Photoelastic Tests: —

FROCHT. Studies in Three-Dimensional Photoelasticity—Stresses in Bent Circular Shafts with Transverse Holes—Correlation with Results from Fatigue and Strain Measurements. *Proceedings of the Society for Experimental Stress Analysis*, Vol. 2, No. 1, 1945.

JESSOP, SNELL and ALLISON. The Investigation of the Stress Concentration Factors in Cylindrical Tubes with Transverse Circular Holes. (To be published in the *Aeronautical Quarterly*).

Results of Electroplating tests:—

OKUBO and TAKAI. Stress Concentration Factors in Shafts Containing Transverse Holes and Subjected to Bending. *Journal of Applied Mechanics*, September 1956.

Ref. RAS Structural Data Sheets (Dec. 1963) pp. 06.06.04
Reproduced by Royalty Agreement.

GEOMETRIC STRESS CONCENTRATION FACTORS

DIAMETRAL CIRCULAR HOLES IN ROUND TUBES IN BENDING

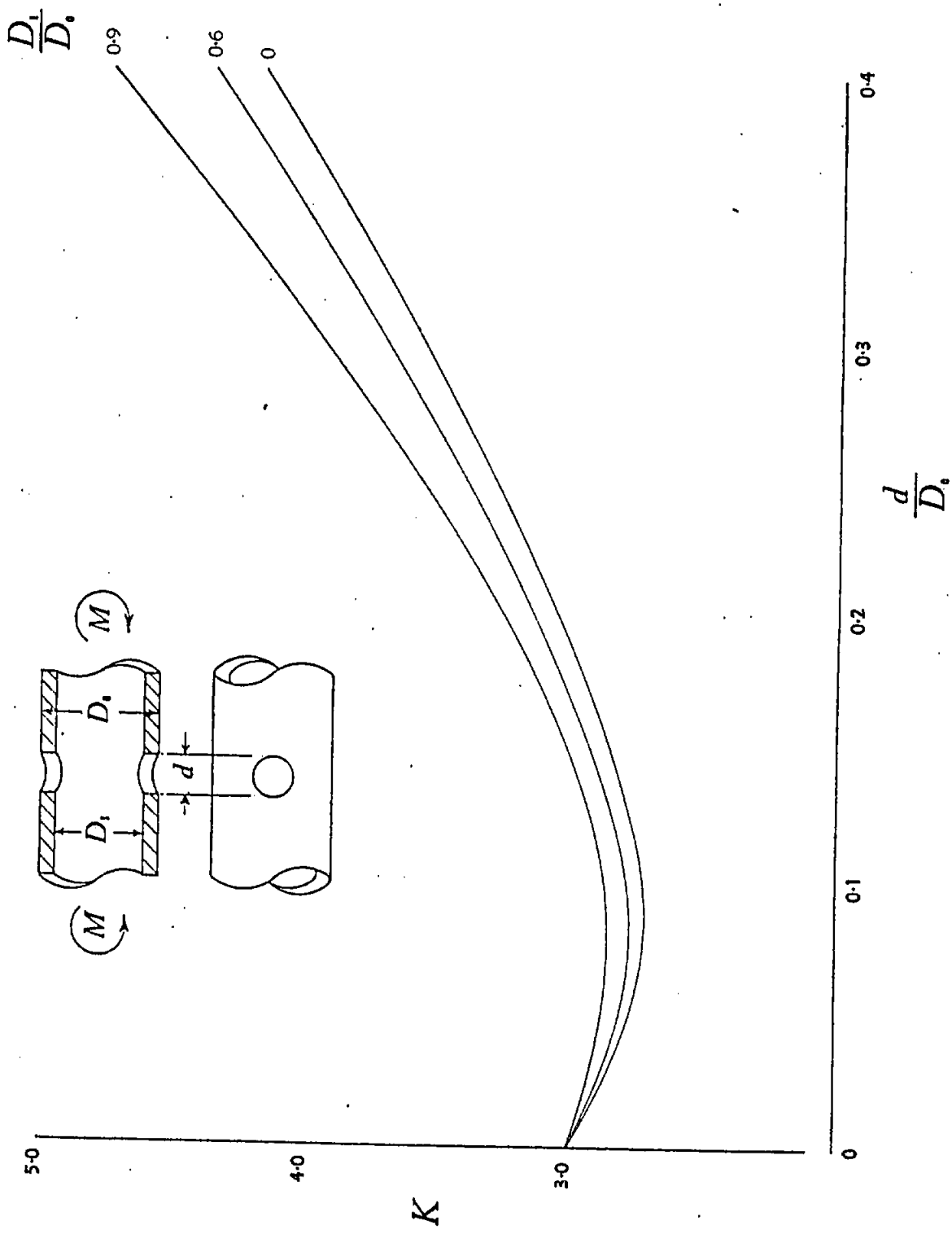

Ref. RAS Structural Data Sheets (Dec. 1963) pp. 06.06.04
Reproduced by Royalty Agreement.

STRESS CONCENTRATION FACTORS FOR A GROOVED SHAFT IN TENSION

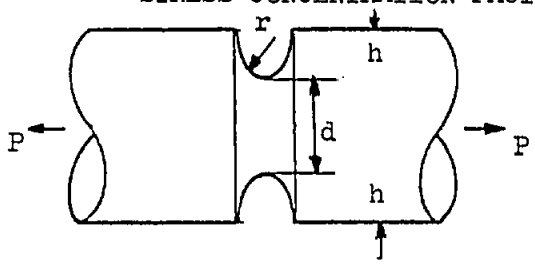

$f_{max} = K f_{ave}$

$f_{ave} = 4P/\pi d^2$ = average net section stress

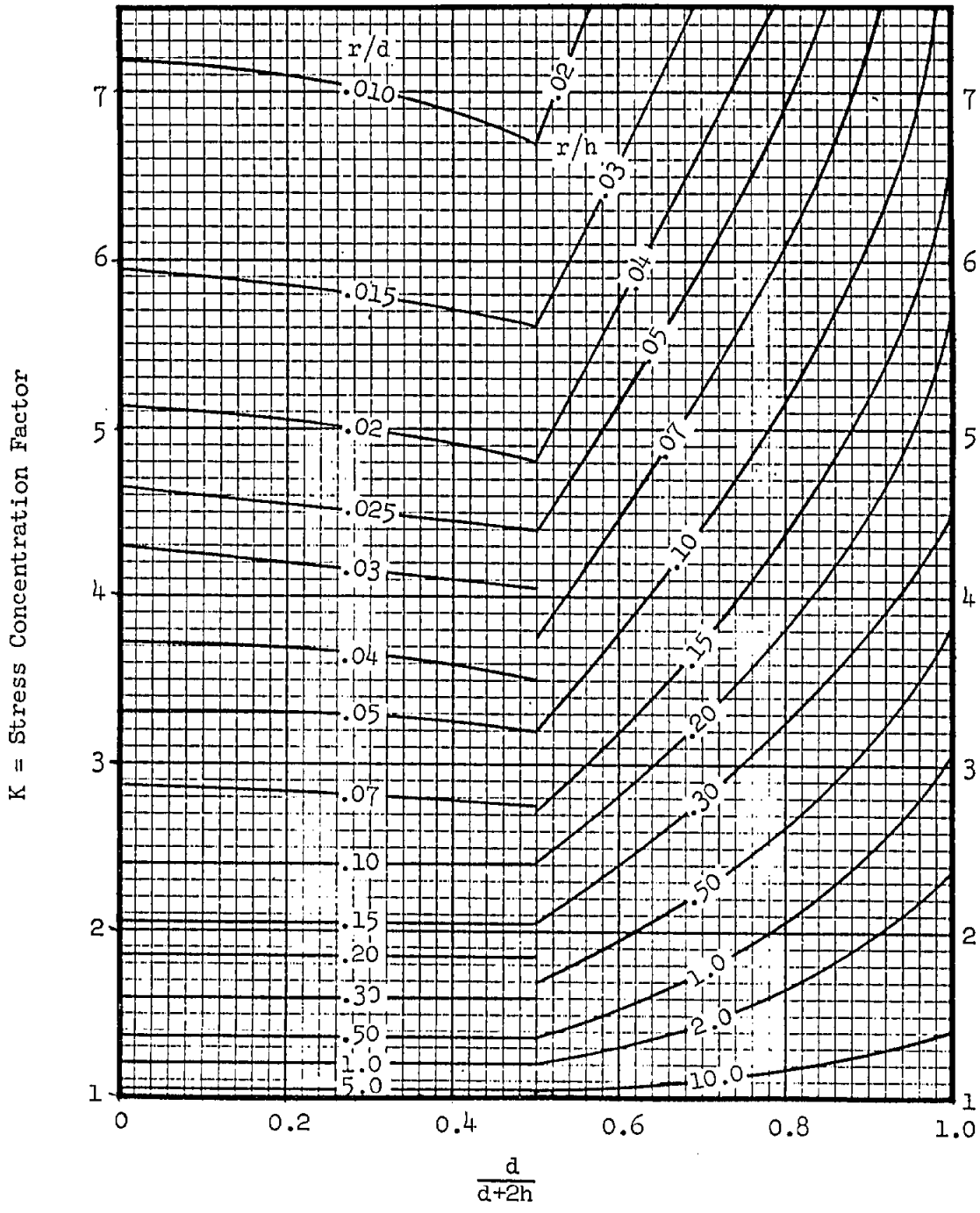

Ref: R. E. Peterson, "Stress Concentration Design Factors", Fig. 24-27

STRESS CONCENTRATION FACTORS FOR A GROOVED SHAFT IN BENDING

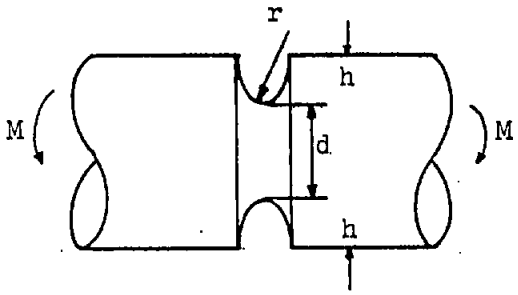

$f_{max} = K\, f_{nom}$

$f_{nom} = \frac{32M}{\pi d^3}$ = nominal outer fiber bending stress at net section

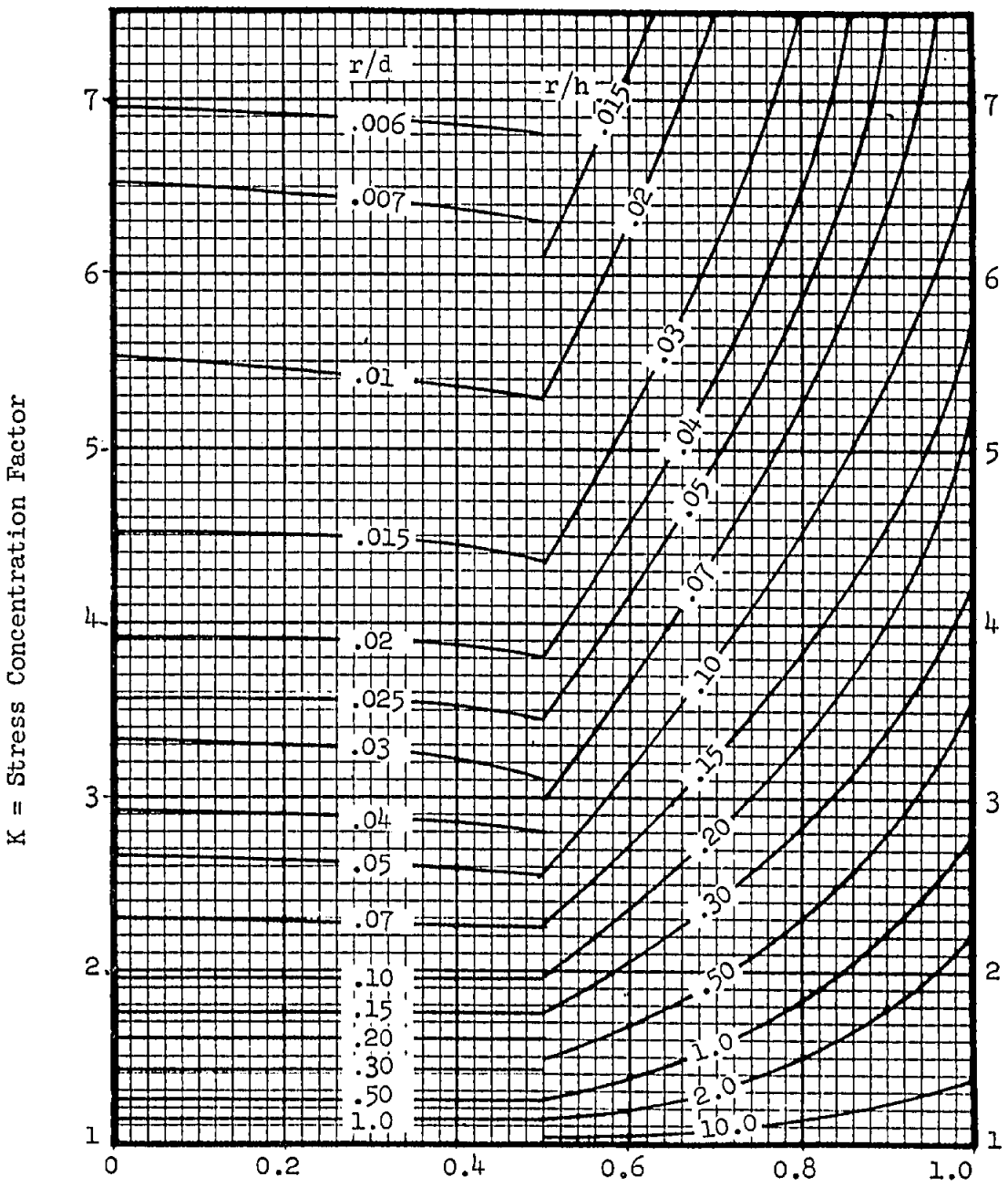

$\frac{d}{d+2h} = \frac{\text{Net-Section Diameter}}{\text{Gross-Section Diameter}}$

Ref: R. E. Peterson, "Stress Concentration Design Factors", Fig. 38-41

STRESS CONCENTRATION FACTOR FOR A GROOVED SHAFT IN TORSION

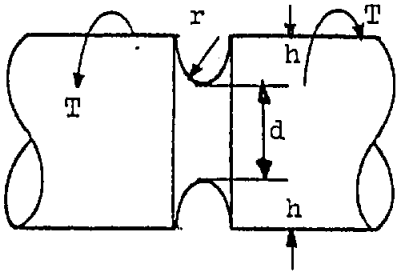

$$\tau_{max} = K_{TS}\ \tau_{nom}$$

$$\tau_{nom} = \frac{16T}{\pi d^3} = \text{nominal shear stress at net section}$$

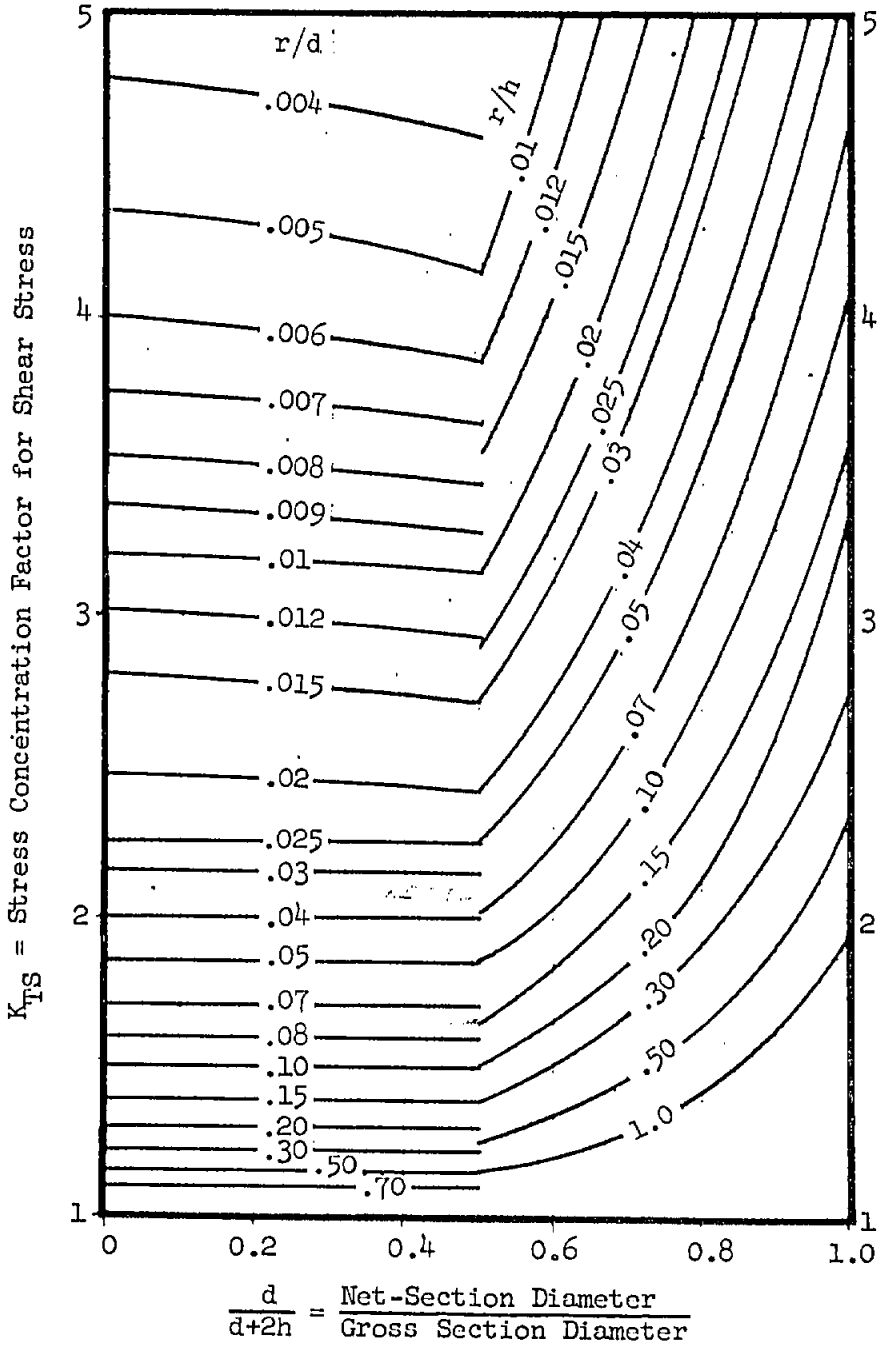

Ref: R. E. Peterson, "Stress Concentration Design Factors", Fig. 46-49

STRESS CONCENTRATION FACTORS FOR FILLETS IN SOLID AND HOLLOW CIRCULAR SHAFTS UNDER AXIAL LOAD

$f_{max} = Kf_{net}$ = maximum stress

FIGURE 1. TENSION (Solid Shaft)

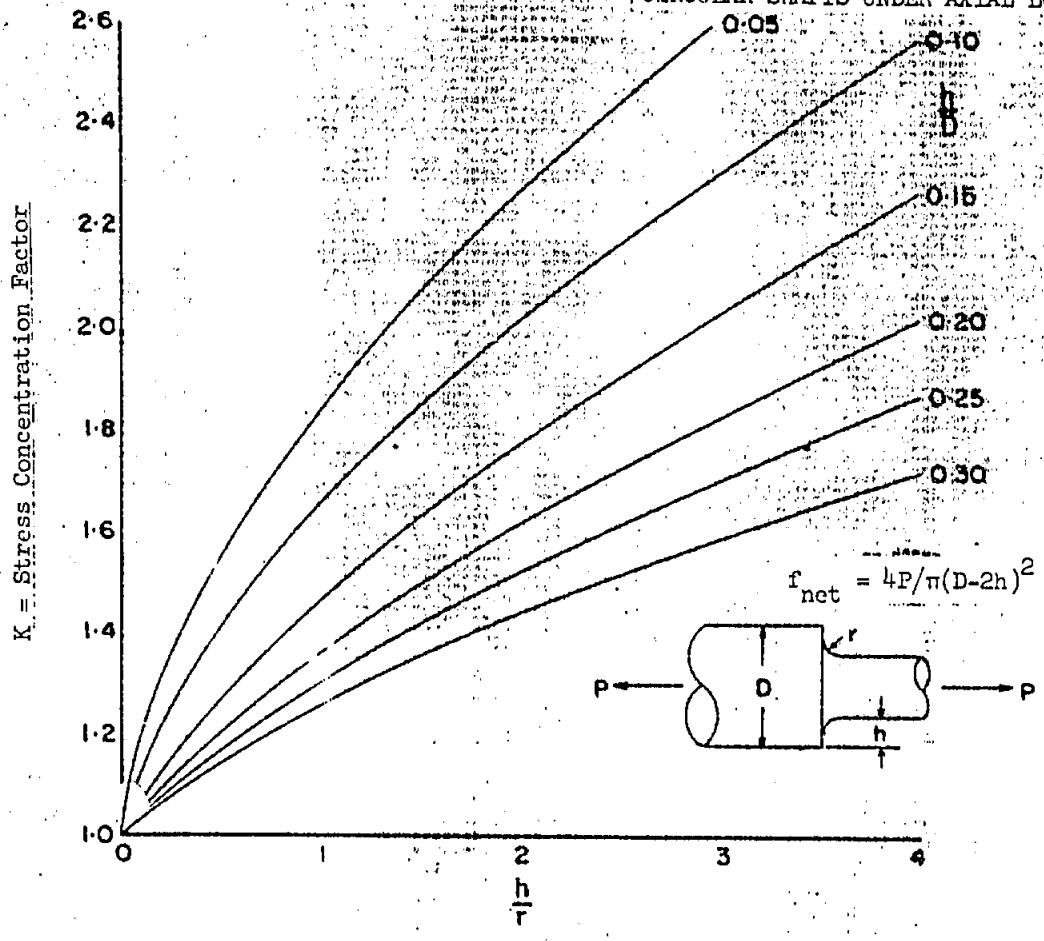

FIGURE 2. TENSION (Hollow Shaft $\frac{D_i}{t} > \frac{28}{1+t/h}$)

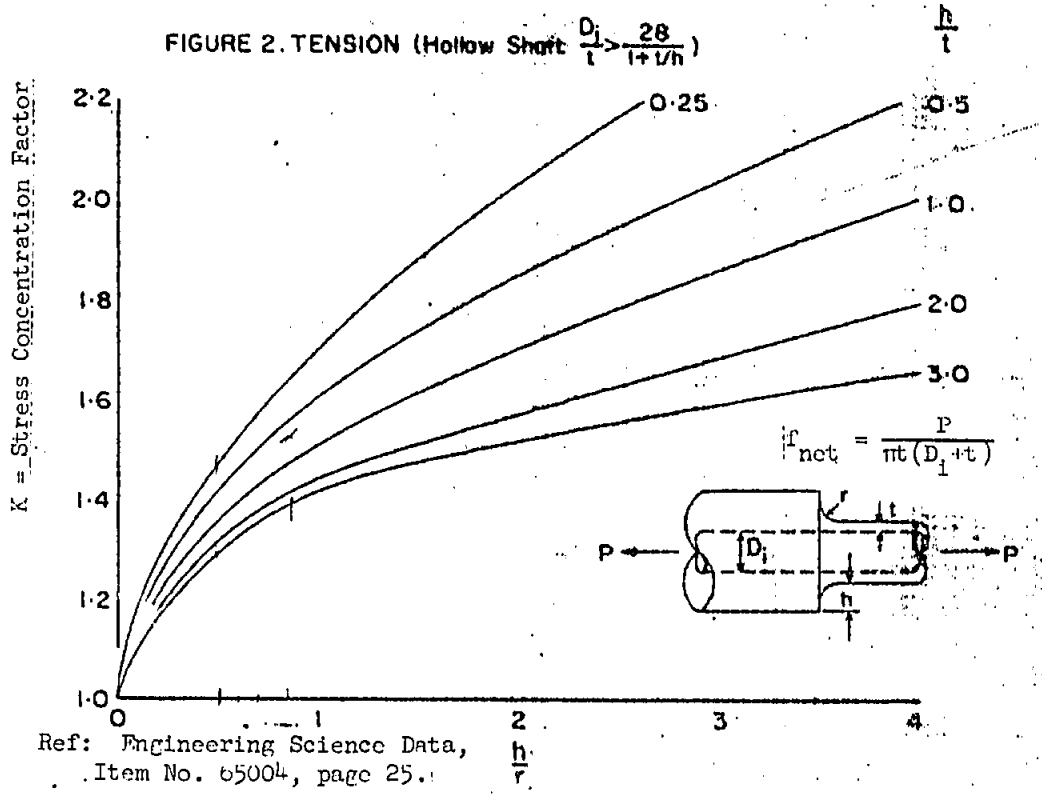

Ref: Engineering Science Data, Item No. 65004, page 25.

STRESS CONCENTRATION FACTORS FOR FILLETS IN CIRCULAR SHAFTS

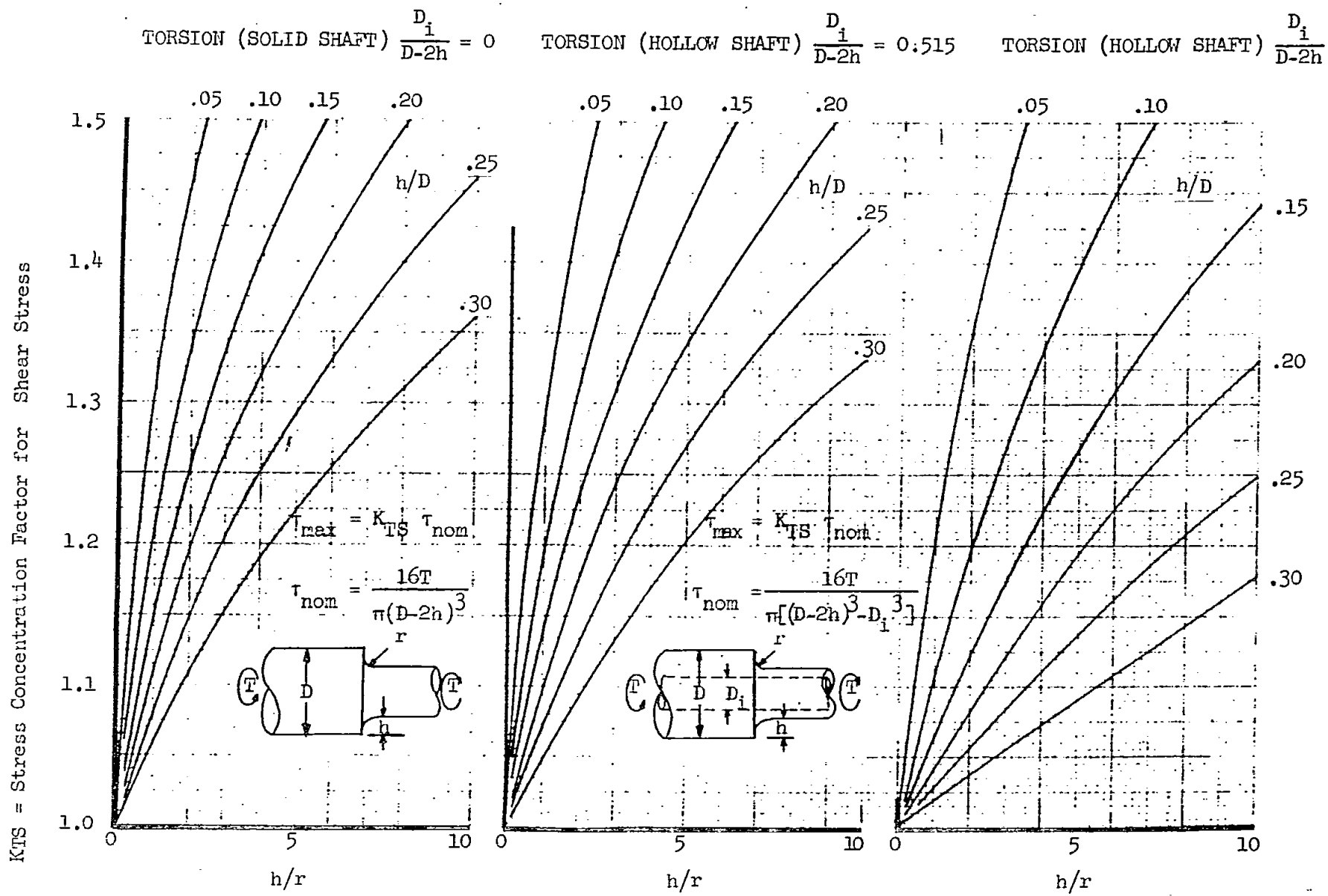

Ref: Engineering Science Data, Item No. 65004, pages 27, 28.

B7.040.2-10

December 1968

STRESS CONCENTRATION FACTORS FOR FILLETS IN SOLID CIRCULAR SHAFTS IN BENDING

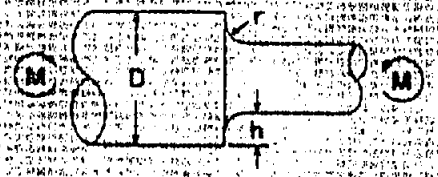

$f_{max} = Kf_{net}$ = maximum stress

$$f_{net} = \frac{32M}{\pi(D-2h)^3}$$

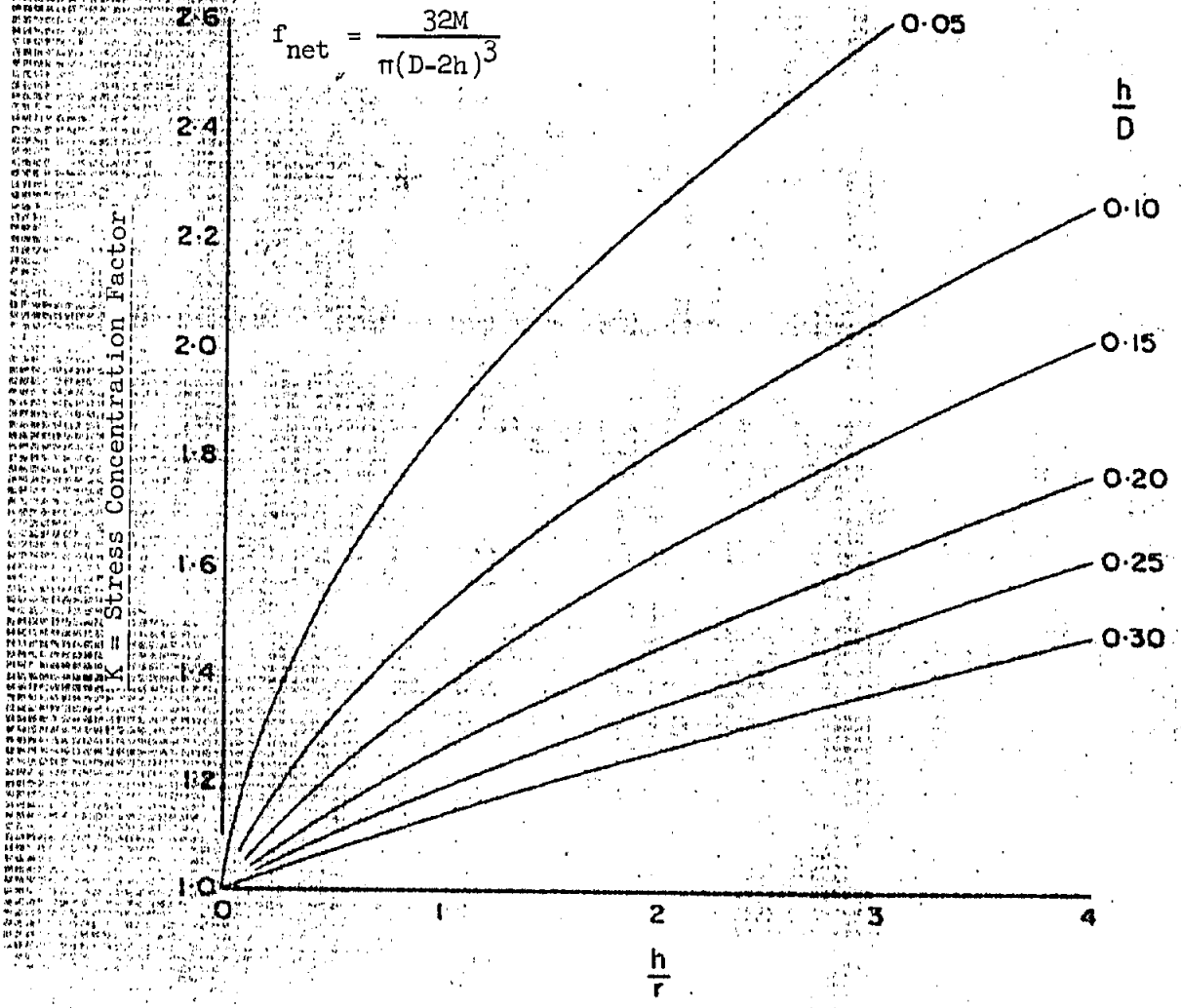

Ref: Engineering Science Data, Item No. 65004, page 26.

STRESS CONCENTRATION FACTORS FOR A BAR LOADED BY A CLOSE-FITTING PIN

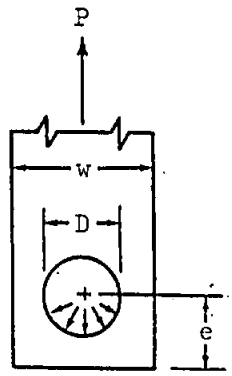

$f_{max} = K f_{net}$ = maximum stress at edge of hole

$f_{net} = \frac{P}{(w - D)t}$ = average net-section stress

t = bar thickness

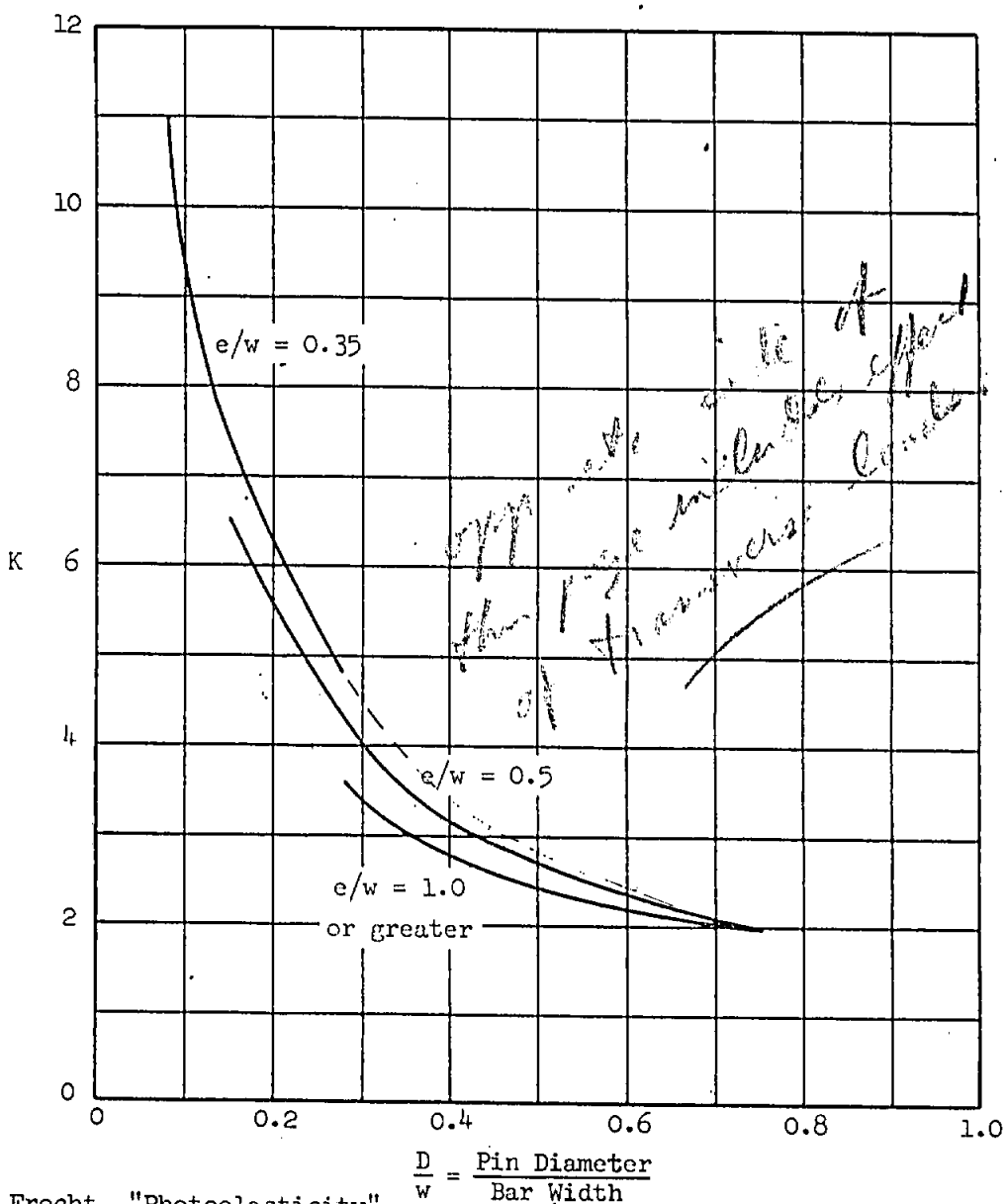

Ref: Frocht, "Photoelasticity"

STRESS CONCENTRATION FACTORS FOR A BAR LOADED BY A CLOSE-FITTING PIN (e/w = 0.5)

$f_{max.} = Kf_{net}$ = max. Stress at Edge of Hole

$f_{net} = \frac{P}{(W-D)t}$ = Average Net-Section Stress

t = Bar Thickness

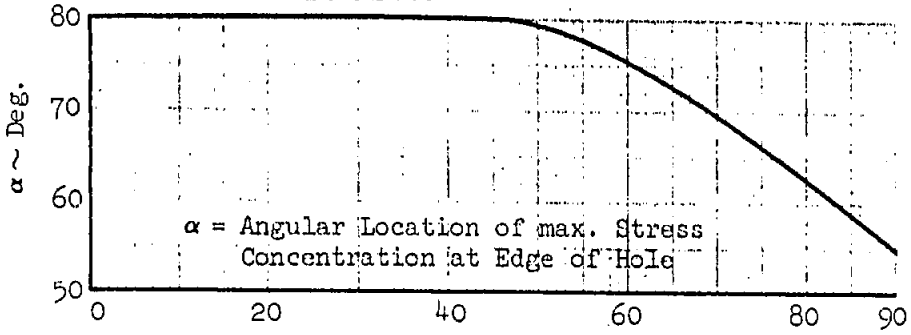

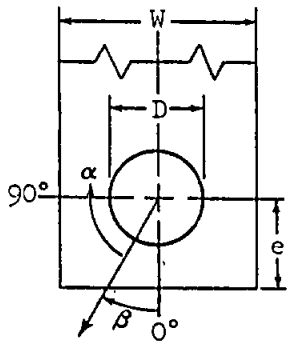

β = Position of Load Line ~ Degrees

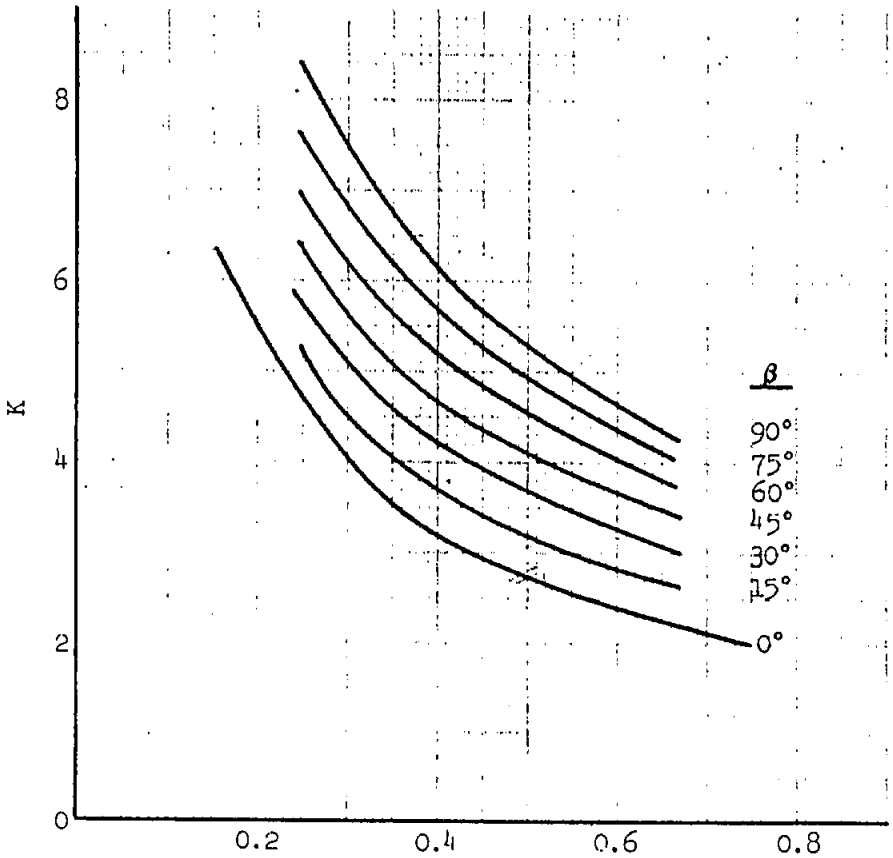

$\frac{D}{W} = \frac{\text{Pin Diameter}}{\text{Bar Width}}$

Ref. R. Melts, M.S. Thesis, PIB, June 1964, "Photoelastic Study of Stress Concentrations of Single Pin Loaded Lugs in Tension."

STRESS CONCENTRATION FACTORS FOR A LUG LOADED AT OBLIQUE ANGLE INCLUDING EFFECTS OF LUG PROFILE GEOMETRY (FLANK ANGLE)

$(0.30 < D/W < 0.65)$

$f_{max} = K_\beta \cdot f_{net}$ = Maximum Stress at Edge of Hole

$f_{net} = P/(W-D) \cdot t$ = Average Net-Section Stress

t = Lug Thickness

$K_\beta = K \cdot (K_\beta / K_{to})$

K from page B7.040.3-1

K_β / K_{to} from figure below

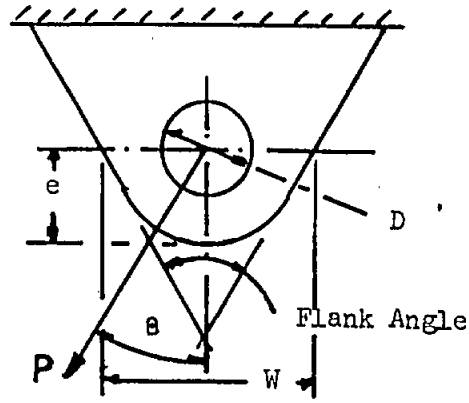

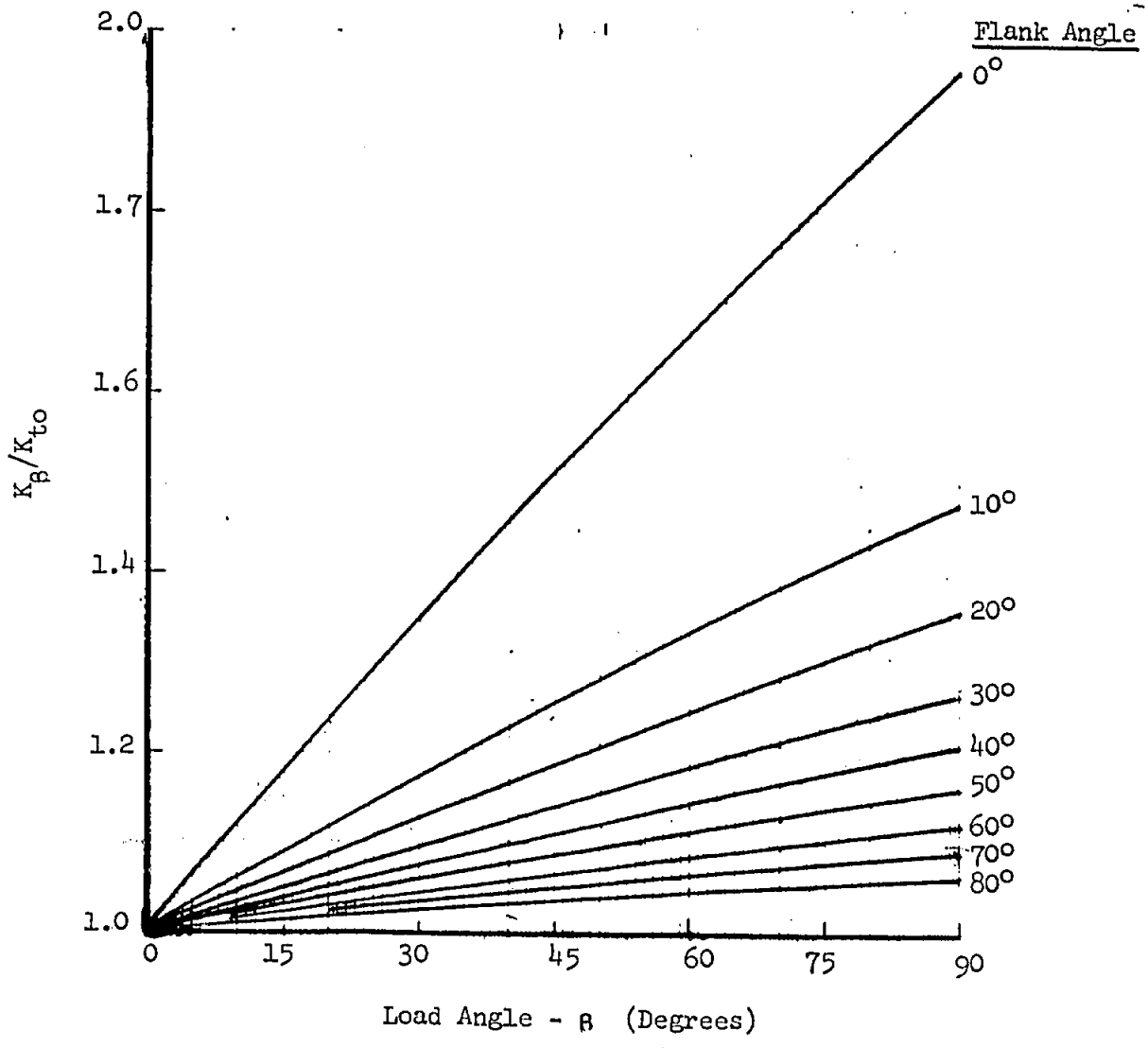

*GAC 4610
2-74

STRESS CONCENTRATION FACTORS FOR AN ANGLE IN BENDING

$f_{max.} = K\, f_{nom.}$ = maximum stress at the fillet

$f_{nom.} = \frac{6M}{bt^2}$ = nominal bending stress in outer fiber

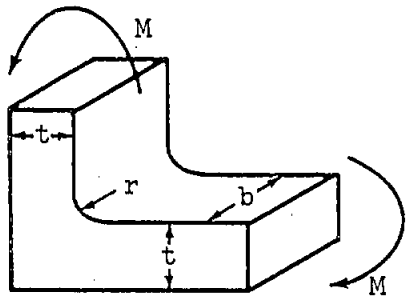

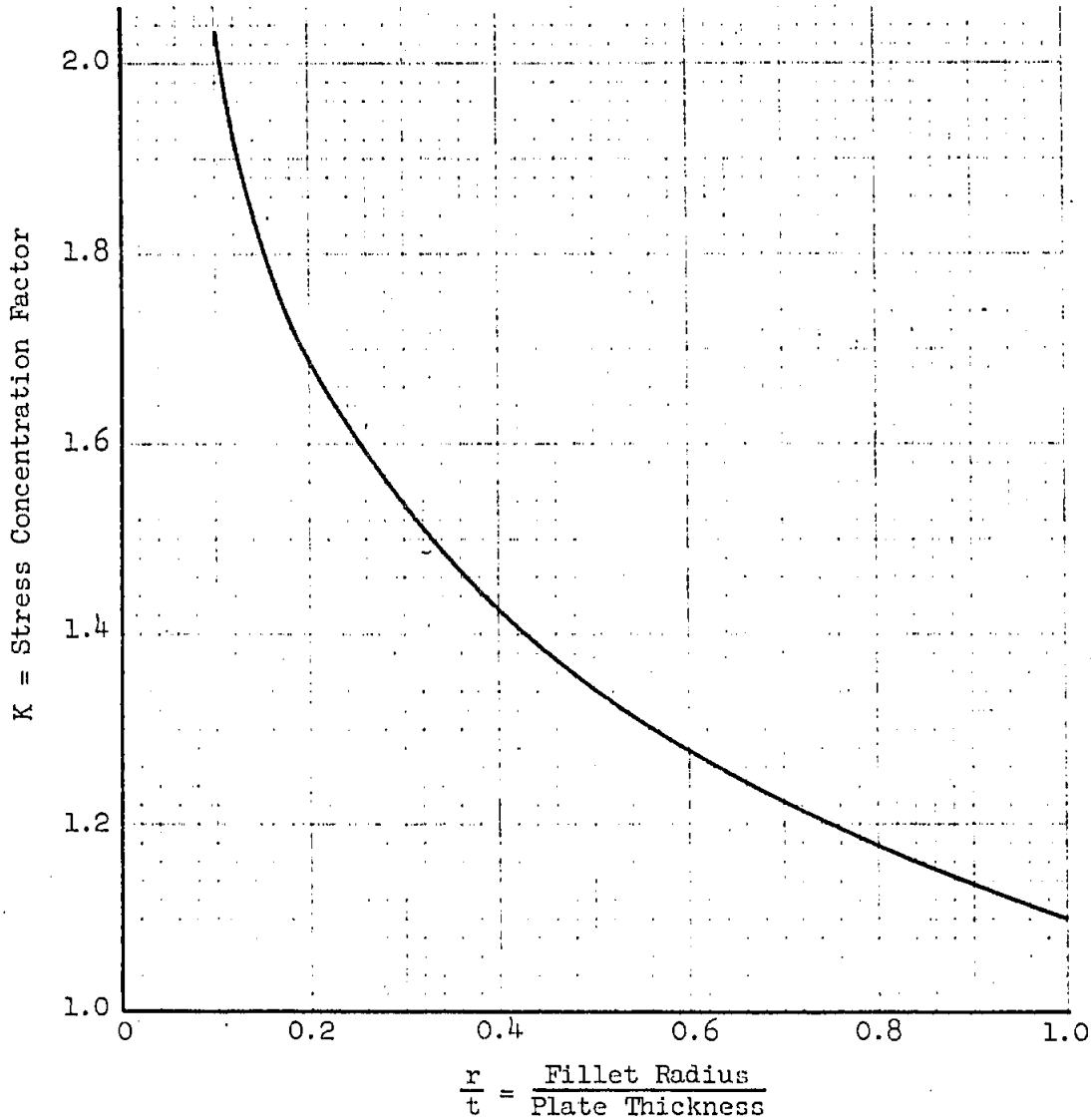

Ref: Lipson, Noll & Clock, "Stress & Strength of Manufactured Parts", Page 101

STRESS CONCENTRATION FACTORS-ADDITIONAL REFERENCES

	FORM OF DISCONTINUITY		LOADING	REFERENCE *
BARS, STRIPS, PLATES	Single and Multiple Holes	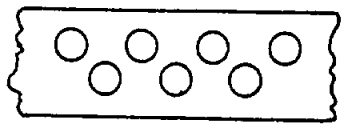	uniaxial biaxial	1 Pages 84-98
	Infinitely Wide Sheet With Elliptical Hole	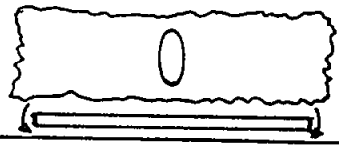	transverse bending	1 Page 103
	Shallow Elliptical Notch (in infinitely wide plate)		tension bending	1 Page 139
	Deep Hyperbolic Notch (in an infinitely wide plate)	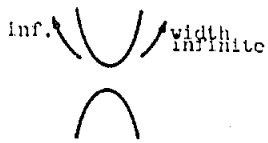	bending transverse bending	1 Page 140 Page 142
	Reinforced Holes (circular, elliptical, square)	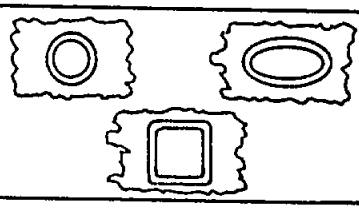	biaxial shear	2 Pages 33-44
	Unreinforced Rectangular Hole	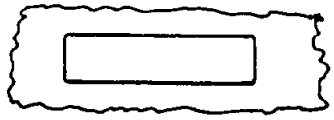	biaxial shear	2 Pages 45-50
	Semi-circular Notches	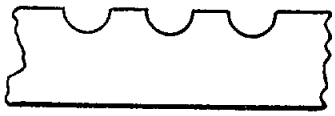	end load	1 Pages 29-31
	Elliptical Fillet	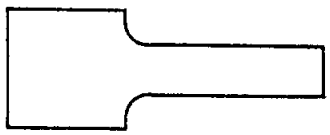	bending	1 Page 73
	Curved Bar		bending	1 Page 127
JOINTS	Pin	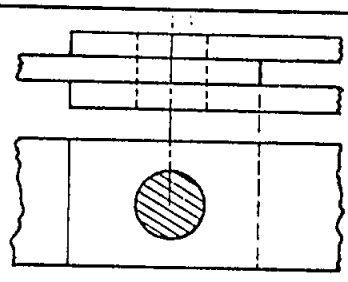	end load interference fit	2 Pages 51-52 Pages 53-55

* See page B7.040.1-2

STRESS CONCENTRATION FACTORS-ADDITIONAL REFERENCES

	FORM OF DISCONTINUITY		LOADING	REFERENCE
JOINTS	Bushing	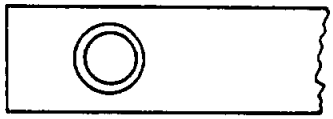	interference fit	2 Pages 57-59
MISCELLANEOUS	Helical Spring	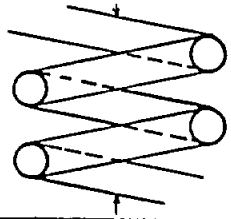	end loading	1 Page 128
	Rotating Disk With Central Hole	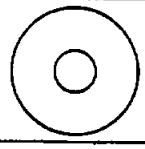	rotation	1 Page 132
	Rotating Disk With Non-central Hole	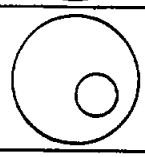	rotation	1 Page 133
	Ring or Hollow Roller	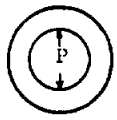	diametrically opposite internal concentrated loads	1 Page 134
		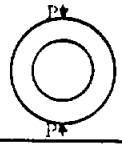	diametrically opposite external concentrated loads	1 Page 135
	Angle or Box Section		torsion	1 Page 131
	Tee or I Beam	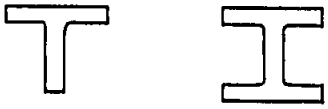	torsion	3
	U Shaped Member	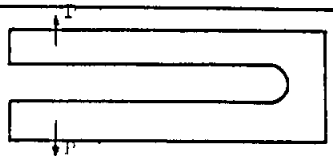	as shown	1 Pages 129,130

REFERENCES

1. R.E. Peterson, Stress Concentration Design Factors, John Wiley & Sons, Inc., 1953.
2. Engineering Science Data, Aeronautical Series, Item No. 64004.
3. Beadle, C. W. and Conway, H. D., "Conducting Sheet Analogy for Stress Concentrations in Twisted Structural Sections", Proc. Society for Experimental Stress Analysis, Vol. XX, No. 2, page 198.

THE ANALYSIS OF ECCENTRIC REINFORCEMENT ON TENSION STRUCTURE

The problems associated with the reinforcement of axially loaded members are frequently complicated by geometric constraints that restrict the placement of the reinforcing material. This problem is almost always encountered in aircraft structure on the tension side of the wing structure (or tail structure) at the transverse rib attachment attachment holes. In order to ensure the design fatigue life at these points of stress concentration at a minimum weight penalty, it is necessary to depress the stress level in the vicinity of these holes. Ideally, the added material would be placed symmetrically about the basic wing skin, and extend only a short distance in the direction of the tension stress on either side of the stress raiser. Aerodynamic cleanliness requirements prevent this ideal design and it is therefore necessary to contend with the inefficiency of eccentric reinforcement. Even in the best of conditions, the efficiency of the reinforcement will be low, and it is therefore necessary to minimize the conservatisms in the analysis as well as prepare the best design possible.

Tension wing skins usually employ integral construction techniques and are therefore milled from plate material where the thickness can be designed to meet the load requirements. This construction readily permits integral reinforcement material at points of stress raisers. In a typical wing skin, the problem is illustrated by the following sections. The section is cut parallel to the direction of the tension stress midway between the longitudinal stiffening members.

IDEAL CASE

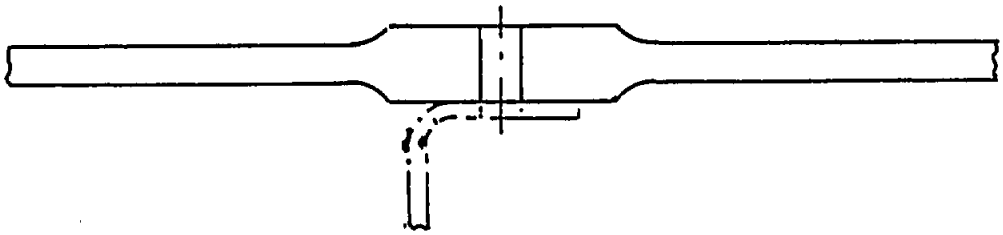

WITH REALISTIC GEOMETRY

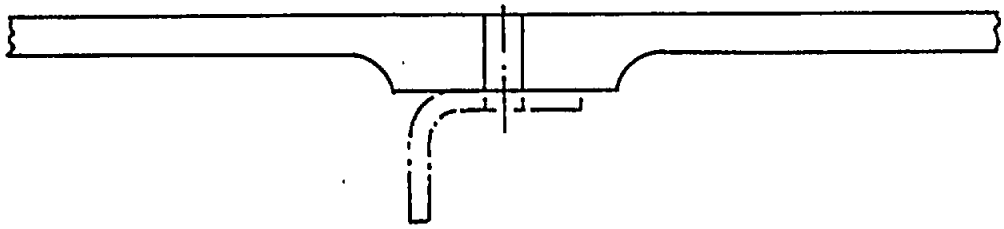

REALISTIC GEOMETRY WITH ALTERNATE CONFIGURATION

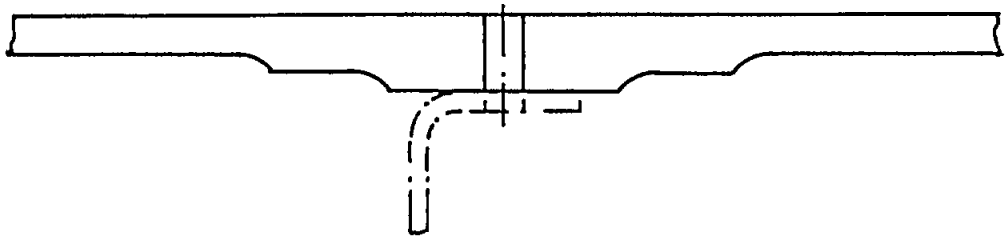

THE ANALYSIS OF ECCENTRIC REINFORCEMENT ON TENSION STRUCTURE (CONT)

The analysis of stresses at critical sections in the reinforced skin depends primarily on an accurate determination of the bending moment at the section and an equally accurate assessment of the stress concentration factor that accounts for the geometric variations along the member.

The bending moments are determined from a two dimensional model of the structure as indicated in the previous sketches. The bending moment analysis, to be of any value, must include the effects of the structural deflections as well as the constructed eccentricities. A two dimensional analysis (as opposed to a plate) is used because the effects of the adjacent longitudinal stiffening members is considered to be negligible. It is also assumed that the transverse ribs are spaced far enough apart so that there is no interaction from rib to rib. These assumptions then permit the development of the following idealized structural model for a reinforcement with two thicknesses. The actual structure will appear as shown in the following sketch.

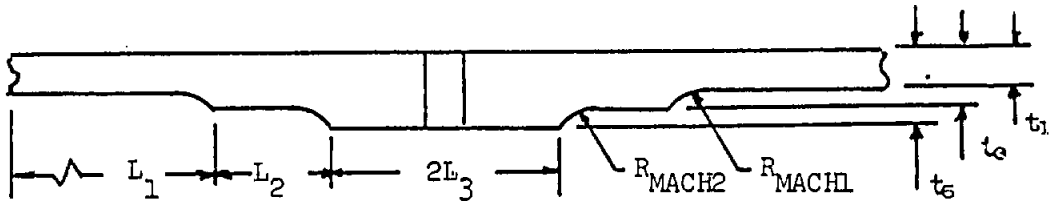

For the bending moment analysis, the fillet region is idealized as a constant thickness element whose geometry is constructed as shown in the following sketch. The basic assumption in the construction is that the limit of the effective material is established by the line tangent to the fillet at the angle of 30 degrees.

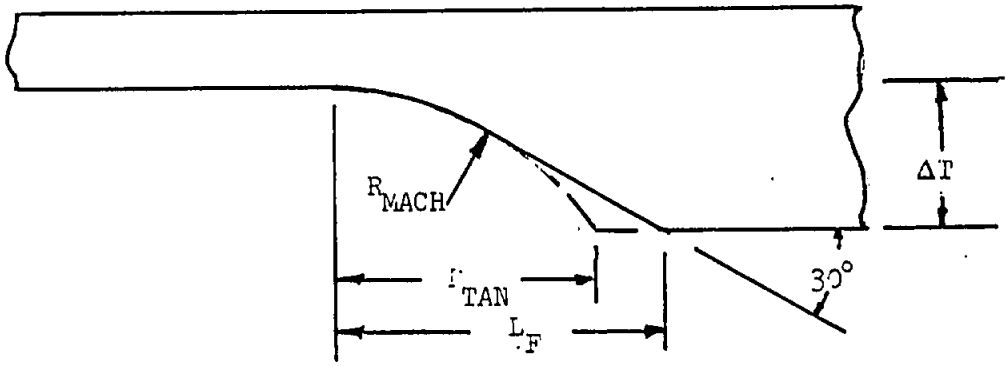

$$L_F = 0.268\ R_{MACH} + 1.732\ \Delta T$$

The idealized structure will now appear as shown in the following sketch.

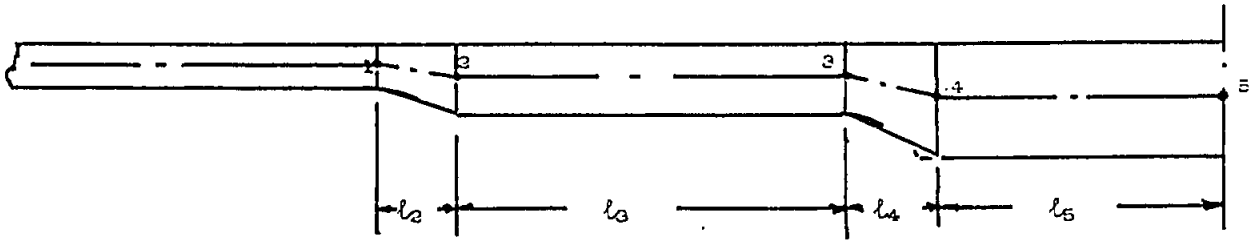

THE ANALYSIS OF ECCENTRIC REINFORCEMENT ON TENSION STRUCTURE (CONT)

The dimensions of the idealized structural model are:

When R_{MACH} is greater than the thickness change:

$$R_{TAN1} = (t_3 - t_1)\sqrt{2\ R_{MACH1}/(t_3 - t_1) - 1.0}$$

$$R_{TAN2} = (t_5 - t_3)\sqrt{2\ R_{MACH2}/(t_5 - t_3) - 1.0}$$

When R_{MACH} is less than the thickness change:

$$R_{TAN1} = R_{MACH1}$$

$$R_{TAN2} = R_{MACH2}$$

$$\ell_2 = 0.268\ R_{MACH1} + 1.732\ (t_3 - t_1)$$

$$\ell_3 = L_2 + R_{TAN1} - \ell_2 - R_{TAN2}$$

$$\ell_4 = 0.268\ R_{MACH2} + 1.732\ (t_5 - t_3)$$

$$\ell_5 = L_3 + R_{TAN2} - \ell_4$$

The thickness of the structural element at each fillet is a weighted average of the thickness at the ends of the fillet.

$$t_3 = t_1 + 0.8\ (t_3 - t_1)$$

$$t_4 = t_3 + 0.8\ (t_5 - t_3)$$

The internal load designation for the members of the structural model are shown in the following sketch. The bending moments are about the centroid of the structural element.

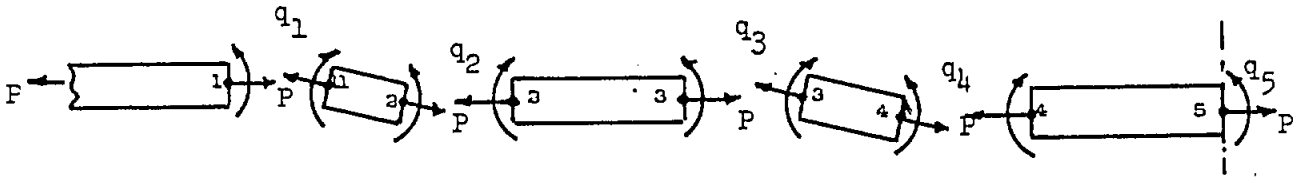

The problem is solved by formulating the displacement continuity equations at each node, 1 thru 4. Structural symmetry is present at node 5 which yields a boundary condition of zero rotation at this point. At the left end of the structural model, the boundary conditions are zero bending moment and zero linear displacement. The displacements of the elements are determined from the beam-column equations readily available in structural engineering texts such as Reference 1. The following constants are required in order to solve for the internal loads.

Reference 1: Niles, A. S., and Newell, J. S.: Aircraft Structures, Volume II, Third Edition, John Wiley & Sons, Inc., 1943.

THE ANALYSIS OF ECCENTRIC REINFORCEMENT ON TENSION STRUCTURE (CONT)

$$k_i = \sqrt{\frac{12\ P}{E\ t_i^3}} \qquad \text{for } i = 1,2,3,4,5$$

$A = k_1/P$ $\qquad$ $H = (k_5 \text{ Coth } k_5\ell_5)/P$

$B = (k_2 \text{ Coth } k_2\ell_2)/P$ $\qquad$ $I = k_5/(P \text{ Sinh } k_5\ell_5)$

$C = k_2/(P \text{ Sinh } k_2\ell_2)$ $\qquad$ $J = B + D - C^2/(A + B)$

$D = (k_3 \text{ Coth } k_3\ell_3)/P$ $\qquad$ $K = D + F - G^2/(F + H - I^2/H)$

$E' = k_3/(P \text{ Sinh } k_3\ell_3)$ $\qquad$ $e_1 = \frac{1}{2}(t_1 + t_3)$

$F = (k_4 \text{ Coth } k_4\ell_4)/P$ $\qquad$ $e_2 = \frac{1}{2}(t_3 + t_5)$

$G = k_4/(P \text{ Sinh } k_4\ell_4)$

The internal loads are now calculated from the following equations.

$$q_3 = \left[E'J/(JK - E'^2)\right] \cdot \left[\{e_1/(J\ell_2)\} \cdot \{C/(A + B) - 1.0\} + \{e_2/(E'\ \ell_4)\} \cdot \{1.0 - G/(F + H - I^2/H)\}\right]$$

$$q_2 = \{e_1/(J\ell_2)\} \cdot \{C/(A + B) - 1.0\} + E'\ q_3/J$$

$$q_4 = (G\ q_3 - e_2/\ell_4)/(F + H - I^2/H)$$

$$q_5 = I\ q_4/H$$

$$q_1 = C\ q_2/(A + B) + e_1/(\ell_2\ (A + B))$$

Stresses in the actual structure

The points of interest in the actual structure are at locations of geometric stress concentration and at points of net section stress. In this structure, these points are at the fillet radius tangency points and at the rivet hole. The structural idealization provides the bending moment for each of these locations.

Single step reinforcement

The equations in the previous text can be used for the single step reinforcement case by setting $t_1 = t_3$. Assign an arbitrary value to R_{TAN1} (say 0.10) if R_{MACH1} is equal to zero, otherwise, determine from equation on page
In the single step case, the value of ℓ_2 is not significant to the critical answers because the moments q_1 and q_2 are not at points of stress concentration. The analysis of a single step reinforcement is included in the illustrative example.

THE ANALYSIS OF ECCENTRIC REINFORCEMENT ON TENSION STRUCURE (CONT)

Increased accuracy and special cases

The idealization of the fillet area for the closed form solution of this problem presented in the previous text can be expected to give acceptable accuracy for the geometries resulting from normal aircraft strucure manufacturing techniques. The accuracy of the preceeding analysis can be improved by using a finer grid in the structural idealization. This step will preclude hand calculations, but if this increased accuracy is required, computer aid is available. A system of programs controlled by EXEC REINFORC is available on the Structural Analysis Section B-DISK. This program analyzes eccentric reinforcements as described in the previous text and also includes the analysis of linear taper reinforcement and the analysis for normal pressure loading. The description of this program and instructions for its use are available in a separate Structural Analysis Section memo. Should special problems arise involving geometry significantly different than the straightforward cases discussed previously or the analyst wish to dictate the structural idealization, the Structural Analysis Section beam-column computer program must then be used. This program is available on the section B-DISK and is titled DG002 VSBASIC. The program description and instructions for its use are given in Reference 2. In addition to the advantages noted above, this program, due to its flexiblity in description of EI variations along the beam and in location of section centroids relative to load-lines, is an extremely powerful analysis tool for the special case problem.

The output of both programs includes, in addition to bending moments, the deflections and stresses at each node of the idealized structure. The axial shortening of the member due to bending is also included as program output.

Illustrative example

The use of the equations presented in the preceeding text is shown in the following example. The section chosen for the example is geometrically similar to the F-14 wing lower cover at about Rib #14 (Sta. 85). The material for the example is 6Al-4V annealed titanium alloy plate with an F_{tu} of 135 ksi (B value). In the following problems, the gross section stress is 115 ksi which is approximately the design tension stress level for the F-14. This stress level will result in critical section stresses at about the material ultimate strength when a bending modulus of rupture is included in the static strength analysis. Although the F-14 is not fatigue critical at this location because of the use of interference fit fasteners, it is probable that in an other application, the design would be fatigue critical. The calculation of the applied stresses therefore includes the applicable stress concentration factor. This will permit a comparison, on a fatigue basis, of the two step configuration to other possible designs. The strength analysis, static or fatigue, is not included in this section since these analyses are adequately covered in other sections of the Structures Manual.

Reference 2: Aerospace Strucures II. Grumman Aerospace Corporation Report

(This report is the Structures Section Stress Analysis course notes that are scheduled for publication in 1983)

THE ANALYSIS OF ECCENTRIC REINFORCEMENT ON TENSION STRUCTURE (CONT)

Illustrative example (Cont)

Material: Titanium alloy, machine milled plate

$E = 16.0 \times 10^6$ psi

Section thru structure

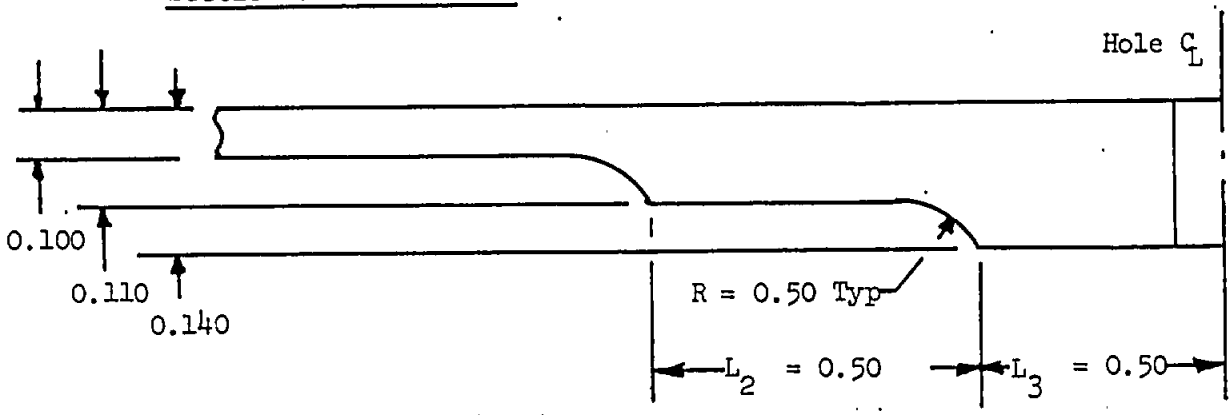

Dimensions of idealized structure:

$$\ell_2 = 0.268 \times 0.50 + 1.732 \times (0.110 - 0.100)$$
$$= 0.151 \text{ in}$$
$$\ell_4 = 0.268 \times 0.50 + 1.732 \times (0.140 - 0.110)$$
$$= 0.186 \text{ in}$$
$$R_{MACH1} > (t_3 - t_1)$$
$$R_{TAN1} = (0.110 - 0.100)\sqrt{2 \times 0.50/(0.110 - 0.100) - 1.0}$$
$$= 0.0995 \text{ in}$$
$$R_{MACH2} > (t_5 - t_3)$$
$$R_{TAN2} = (0.140 - 0.110)\sqrt{2 \times 0.50/(0.140 - 0.110) - 1.0}$$
$$= 0.171 \text{ in}$$
$$\ell_3 = 0.500 + 0.0995 - 0.151 - 0.171$$
$$= 0.276 \text{ in}$$
$$\ell_5 = 0.500 + 0.171 - 0.186$$
$$= 0.485 \text{ in}$$
$$t_2 = 0.100 + 0.8\ (0.110 - 0.100)$$
$$= 0.108 \text{ in}$$
$$t_4 = 0.110 + 0.8\ (0.140 - 0.110)$$
$$= 0.134 \text{ in}$$

THE ANALYSIS OF ECCENTRIC REINFORCEMENT ON TENSION STRUCTURE (CONT)

Illustrative example (Cont)

$P = 115000 \times 0.100 = 11500$ lb

$$k_1 = \sqrt{\frac{12 \times 11500}{16 \times 10^6 \times 0.100^3}} = 2.936837$$

$$k_2 = \sqrt{\frac{12 \times 11500}{16 \times 10^6 \times}} = 2.616643$$

$$k_3 = \sqrt{\frac{12 \times 11500}{16 \times 10^6 \times 0.110^3}} = 2.545605$$

$$k_4 = \sqrt{\frac{12 \times 11500}{16 \times 10^6 \times}} = 1.893314$$

$$k_5 = \sqrt{\frac{12 \times 11500}{16 \times 10^6 \times 0.140^3}} = 1.772914$$

$A = 2.936837/P = 0.255377 \times 10^{-3}$

$B = (2.616643 \text{ Coth } 0.151 \times 2.616643)/P = 0.604375 \times 10^{-3}$

$C = (2.616643/\text{Sinh } 0.151 \times 2.616643)/P = 0.559908 \times 10^{-3}$

$D = (2.545605 \text{ Coth } 0.276 \times 2.545605)/P = 0.363736 \times 10^{-3}$

$E' = (2.545605/\text{Sinh } 0.276 \times 2.545605)/P = 0.288626 \times 10^{-3}$

$F = (1.893314 \text{ Coth } 0.186 \times 1.893314)/P = 0.486773 \times 10^{-3}$

$G = (1.893314/\text{Sinh } 0.186 \times 1.893314)/P = 0.458086 \times 10^{-3}$

$H = (1.772914 \text{ Coth } 0.485 \times 1.772914)/P = 0.221552 \times 10^{-3}$

$I = (1.772914/\text{Sinh } 0.485 \times 1.772914)/P = 0.159117 \times 10^{-3}$

$J = (0.604375 + 0.363736 - 0.559908^2/(0.255377 + 0.604375)) \times 10^{-3}$

$= 0.603474 \times 10^{-3}$

$K = (0.363736 + 0.486773 - 0.458086^2/(0.486773 + 0.221552 - 0.159117^2/0.221552)) \times 10^{-3}$

$= 0.497267 \times 10^{-3}$

$e_1 = \frac{1}{2}(0.110 - 0.100)$

$= 0.005$ in

$e_2 = \frac{1}{2}(0.140 - 0.110)$

$= 0.015$ in

THE ANALYSIS OF ECCENTRIC REINFORCEMENT ON TENSION STRUCTURE (CONT)

Illustrative example (Cont)

Calculate internal loads

$$q_3 = \left[(0.288626 \times 0.603474)/(0.603474 \times 0.497267 - 0.288626^2)\right] \times \left[\{0.005/(0.603474 \times 10^{-3} \times 0.151)\}\{0.559908/(0.255377 + 0.604375) - 1.0\} + \{0.015/(0.288626 \times 10^{-3} \times 0.186)\} \times \{1.0 - 0.458086/(0.486773 + 0.221522 - 0.159117^2/0.221522)\}\right]$$

$$= 36.050 \text{ in lb}$$

$$q_2 = \{0.005/(0.603474 \times 10^{-3} \times 0.151)\}\{0.559908/(0.255377 + 0.604375) - 1.0\} + 0.288626 \times 36.050/0.603474$$

$$= -1.854 \text{ in lb}$$

$$q_4 = (0.458086 \times 36.050 + 0.015 \times 10^3/0.186)/(0.486773 + 0.221522 - 0.159117^2/0.221522)$$

$$= -107.985 \text{ in lb}$$

$$q_5 = -0.159117 \times 107.985/0.221522$$

$$= -77.554 \text{ in lb}$$

$$q_1 = -0.559908 \times 1.854/(0.255377 + 0.604375) + 0.005 \times 10^3 \div (0.151 \times (0.255377 + 0.604375))$$

$$= 37.225 \text{ in lb}$$

Summary of moments

(Moments about centroid of element)

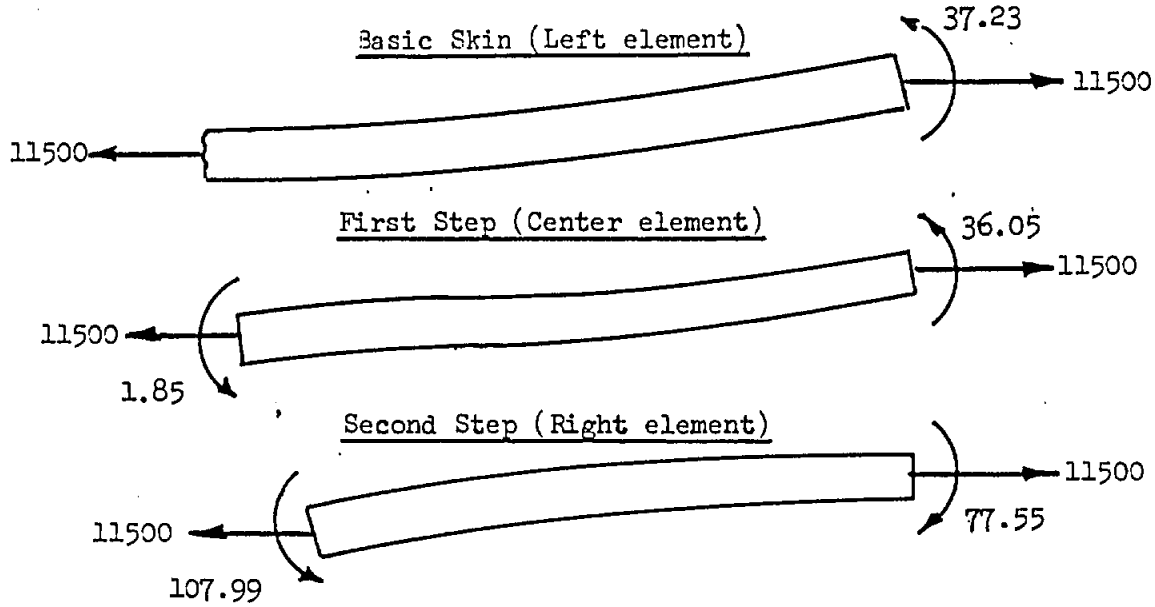

THE ANALYSIS OF ECCENTRIC REINFORCEMENT ON TENSION STRUCTURE (CONT)

Illustrative example (Cont)

Calculate stresses at points of stress concentration

Basic skin at first step

Obtain the stress concentration factors from B7.040.1-15, -16. For these figures, $h = 0.110 - 0.100 = 0.010$, $d = 2 \times 0.100 = 0.200$, $r = 0.500$, $d/(d + 2h) = 0.20/(0.20 + 0.020) = 0.910$, $r/h = 0.50/0.01 = 50.0$.

K_T for direct load < 1.05 use 1.05

K_T for bending moment < 1.05 use 1.05

Total raised stress:

$$K_T \sigma = 1.05 \times 11500/0.100 + 1.05 \times 6 \times 37.23/0.100^2$$
$$= 144204 \text{ psi}$$

First step to second transition

For B7.040.1-15, -16: $h = 0.140 - 0.110 = 0.030$, $d = 2 \times 0.110 = 0.220$, $r = 0.50$, $d/(d + 2h) = 0.220/(0.220 + 0.060) = 0.786$, $r/h = 0.50/0.030 = 16.7$

K_T for direct load < 1.05, use 1.05

K_T for bending moment < 1.05, use 1.05

Total raised stress

$$K_T \sigma = 1.05 \times 11500/0.110 + 1.05 \times 6 \times 36.05/0.110^2$$
$$= 128542 \text{ psi}$$

Net stress at rivet hole, second step

Obtain stress concentration factors from B7.040.1-1, -2. Base the stress calculation on 3/16 in diam fasteners at 0.813 in pitch. For B7.040.1-1, $d_1 = \frac{1}{2}(0.813 - 0.190) = 0.3115$, $R/(R + d_1) = 0.095/(0.095 + 0.3115) = 0.2337$.

$K_{T(net)}$ for direct load = 2.40

For B7.040.1-2, $D/W = 0.190/0.813 = 0.234$, $D/t = 0.190/0.140 = 1.36$.

$K_{T(net)}$ for bending moment = 1.77

Total raised stress

$$K_T \sigma = (2.40 \times 11500/0.140 + 1.77 \times 6 \times 77.55/0.140^2) \times 0.813/(0.813 - 0.190)$$
$$= 312090 \text{ psi}$$

THE ANALYSIS OF ECCENTRIC REINFORCEMENT ON TENSION STRUCTURE (CONT)

Illustrative example (Cont)

What has the reinforcement accomplished? This can best be answered by calculating the stress at the rivet hole for the basic skin with no reinforcement. This stress is:

$$K_T \sigma = 2.40 \times 11500/0.100 \times 0.813/(0.813 - 0.190)$$
$$= 360173 \text{ psi}$$

The magnitude of this stress shows a 13% reduction in notch stress due to the reinforcement. This change, for a given load spectrum, will translate into a significant increase in fatigue life. If the reinforcing material could be symmetrically placed, the raised net stress at the holes would be 257300 psi. This, compared to 312090 psi indicates the measure of inefficiency of the one-sided reinforcement and the necessity of good design in conjunction with the best possible analysis.

Two step reinforcement with chem-mill radius

In order to demonstrate the design sensitivity to the magnitude of the fillet radius, change the manufacturing process from machine milling to chemical milling. In chemical milling, it is conventional to assume the fillet radius equal to the thickness of material removed by the chemical milling operation. This will lead to the structural configuration shown in the following sketch.

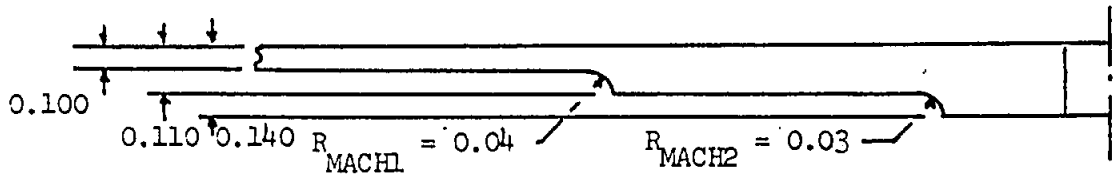

For this revision in structural configuration, it is necessary to recalculate the geometry of the idealized structure and the constants B thru K. The values of k_i, e_1 and e_2 are the same as for the machine mill case. The calculation of the geometry, constants and internal loads is the same as for the machine mill configuration and only the results are summarized here.

$R_{MACH1} = 0.040$	$R_{TAN1} = 0.265$	$e_1 = 0.005$
$R_{MACH2} = 0.030$	$R_{TAN2} = 0.030$	$e_2 = 0.015$
$\ell_2 = 0.028$	$\ell_4 = 0.060$	$t_3 = 0.108$
$\ell_3 = 0.468$	$\ell_5 = 0.470$	$t_4 = 0.134$
$k_1 = 2.936837$	$k_3 = 2.545605$	$k_5 = 1.772914$
$k_2 = 2.616643$	$k_4 = 1.893314$	
$A = 0.255377 \times 10^{-3}$	$E' = 0.147990 \times 10^{-3}$	$I = 0.165219 \times 10^{-3}$
$B = 0.310673 \times 10^{-2}$	$F = 0.145550 \times 10^{-2}$	$J = 0.517650 \times 10^{-3}$
$C = 0.309839 \times 10^{-2}$	$G = 0.144616 \times 10^{-2}$	$K = 0.385741 \times 10^{-3}$
$D = 0.266271 \times 10^{-3}$	$H = 0.225975 \times 10^{-2}$	
$q_1 = 39.27$ in lb	$q_3 = 42.26$ in lb	$q_5 = -88.48$ in lb
$q_2 = -14.93$ in lb	$q_4 = -121.02$ in lb	

THE ANALYSIS OF ECCENTRIC REINFORCEMENT ON TENSION STRUCTURE (CONT)

Illustrative example (Cont)

Two step chem-mill configuration (Cont)

Calculate stress at points of stress concentration

Basic skin at first step

Stress concentration factors are from B7.040.1-15 and -16.
For these figures, $h = 0.010$, $d = 2 \times 0.10 = 0.20$, $r = 0.040$,
$d/(d + 2h) = 0.20/(0.20 + 0.020) = 0.910$, $r/h = 0.040/0.010 = 4.00$.

K_T for direct load = 1.63

K_T for bending moment = 1.58

Total raised stress

$$K_T \sigma = 1.63 \times 11500/0.100 + 1.58 \times 6 \times 39.27/0.100^2$$
$$= 224678 \text{ psi}$$

First to second step

Stress concentration factors from B7.040.1-15 and -16.
For these figures, $h = 0.030$, d 2 x 0.1 0 = 0.220, $r = 0.030$,
$d/(d + 2h) = 0.220/(0.220 + 0.060) = 0.786$, $r/h = 0.030/0.030 = 1.00$.

K_T for direct load = 1.75

K_T for bending moment = 1.67

Total raised stress

$$K_T \sigma = 1.75 \times 11500/0.110 + 1.67 \times 6 \times 42.26/0.110^2$$
$$= 217950 \text{ psi}$$

Net stress at rivet holes

The stress concentration factors are the same as for the machine mill configuration. These factors are:

$K_{T(net)}$ for direct load = 2.40

$K_{T(net)}$ for bending moment = 1.77

Total raised stress

$$K_T \sigma = (2.40 \times 11500/0.140 + 1.77 \times 6 \times 88.48/0.140^3) \times 0.813/(0.813 - 0.190)$$
$$= 319818 \text{ psi}$$

The stress at the rivet hole is 3% greater than for the machine mill configuration. This stress is still the critical stress and the change to chemical milling is only slightly detrimental to the design at this location, UNLESS it is attempted to reduce the stress at the rivet holes by redesigning the reinforcement geometry. If a stress reduction at the rivet holes is obtained by a redesign, the stress at the fillet radius tangency points will increase. The chemical mill configuration because of its high (compared to machine mill) stresses will have considerably less tolerance to accomodate an overall satisfactory design.

THE ANALYSIS OF ECCENTRIC REINFORCEMENT ON TENSION STRUCTURE (CONT)

Illustrative example (Cont)

One step configuration (Reference Page B7.050-4)

Modify the machine mill configuration to eliminate the first step. In order to use the equations developed for the two step case, it is necessary to evaluate all geometry, constants and internal loads. The structural configuration will appear as shown in the following sketch.

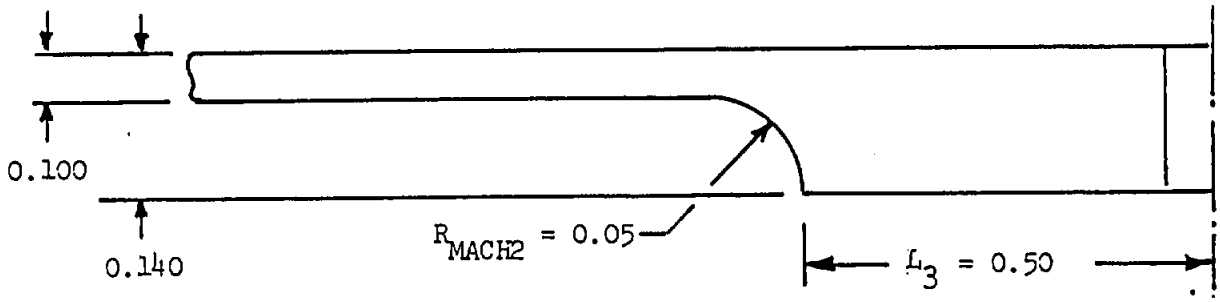

The calculated geometry, constants and internal loads are summarized in the following table.

R_{MACH1} = 0.500	R_{TAN1} = 0.100	e_1 = 0.000
R_{MACH2} = 0.500	R_{TAN2} = 0.196	e_2 = 0.015
ℓ_2 = 0.134	ℓ_4 = 0.204	t_2 = 0.100
ℓ_3 = 0.270	ℓ_6 = 0.493	t_4 = 0.132
k_1 = 2.936837	k_3 = 2.936837	k_5 = 1.772914
k_2 = 2.936837	k_4 = 1.936506	
A = 0.255377 x 10^{-3}	E' = 0.290580 x 10^{-3}	I = 0.155902 x 10^{-3}
B = 0.682088 x 10^{-3}	F = 0.449638 x 10^{-3}	J = 0.642228 x 10^{-3}
C = 0.632477 x 10^{-3}	G = 0.416916 x 10^{-3}	K = 0.525008 x 10^{-3}
D = 0.386851 x 10^{-3}	H = 0.219255 x 10^{-3}	
q_1 = 19.30 in lb	q_3 = 63.22 in lb	q_5 = -91.78 in lb
q_2 = 28.61 in lb	q_4 = -129.07 in lb	

Summary of moments in idealized structure

Basic skin (left Element)

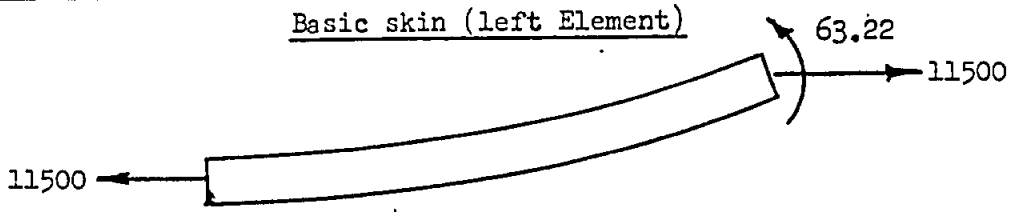

First step (Right element)

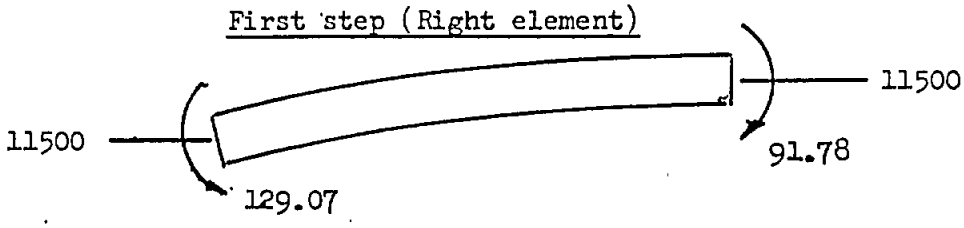

THE ANALYSIS OF ECCENTRIC REINFORCEMENT ON TENSION STRUCTURE (CONT)

Illustrative example (Cont)

One step reinforcement (Cont)

Calculate stresses at points of stress concentration

Basic skin at first step

Stress concentration factors from B7.040.1-15 and -16. For these figures, $h = (0.140 - 0.100) = 0.040$, $d = 2 \times 0.100 = 0.200$, $r = 0.50$, $d/(d + 2h) = 0.20/(0.20 + 0.080) = 0.714$, $r/h = 0.50/0.040 = 12.5$.

K_T for direct load < 1.05, use 1.05

K_T for bending moment < 1.05, use 1.05

Total raised stress:

$$K_T \sigma = 1.05 \times 11500/0.100 + 1.05 \times 6 \times 63.22/0.100^2 = 160578 \text{ psi}$$

Net stress at rivet hole

The stress concentration factors are the same as for the two step case on page

Total raised stress:

$$K_T \sigma = (2.40 \times 11500/0.140 + 1.77 \times 6 \times 91.78/0.140^2) \times 0.813/(0.813 - 0.190) = 322151 \text{ psi}$$

The raised stress at the basic skin transition to the step is 11% higher than in the two step case and at the fastener hole is 3% higher. The net benefit of the single step reinforcement over no reinforcement is 11% as compared to 13% in the two step case. Before condemning the one step design based on these results, other combinations of reinforcement thickness and length should be investigated to assure some resemblence of an optimum design.

SECTION B8 - MEMBERS UNDER COMBINED LOADING

Table of Contents

MEMBERS UNDER COMBINED LOADING

B8.10 INTRODUCTION

Aircraft structural members are often subjected to the simultaneous action of different external loadings resulting in combinations of axial, bending, and shearing stresses. The purpose of this section to present a simple and straightforward method of determining the minimum (buckling, yield, or ultimate) structural capacity of a member when it is subjected to a combined load system.

B8.11 STRESS RATIOS, INTERACTION, AND MARGIN OF SAFETY

The critical strength (yield, ultimate, and buckling) of structural members subjected to a single type of loading such as pure axial compression or tension, pure bending, or pure shear, is, in general, sufficiently and accurately defined. On the other hand, the critical strength of members subjected to simultaneous action of various combinations of these loads is difficult to predict, even if the true stresses are known. This is especially true in cases which involve the effects of overall or local elastic or inelastic instability and cases involving plastic bending or torsion. The stress ratio or interaction method has been developed to predict the ultimate strength of members subjected to combined loads. The basis for the method is given as follows:

1. The allowable stress under a simple loading condition (tension, shear, bending, buckling, etc.) is determined by test or theory.

2. Each load of the combined load conditions is represented by stress (or load) ratios which are ratios of applied stress to allowable stress. The stress ratio, R, is expressed as follows:

$$R = f/F \qquad \text{(B8.11.1)}$$

where:

f = applied stress or load

F = allowable stress or load.

3. The interaction relationship of the loading conditions, that is, the effect of one condition on other(s), is governed by the interaction curve whose shape is generally derived from theory or test or by a combination of both. Generally, for a combined system of loadings, the general interaction relationship can be equations of the following type:

$$R_1^{\,x} + R_2^{\,y} + R_3^{\,z} + \ldots = 1 \qquad \text{(B8.11.2)}$$

where:

R_1, R_2, R_3 = stress ratios for various loadings such as compression, bending, and shear

x,y,z = exponents defining interaction relationships.

Equation (B8.11.2) indicates failure when the sum of the left-hand side is equal to or greater than 1.0

Considering only two loading conditions, such as bending and torsion, equation (B8.11.2) can be plotted as a single interaction curve as R_b against R_{st}. When three or more loading conditions exist, the interaction equation represents an interaction surface which can be plotted as a family of curves. Typical two-parameter curves corresponding to various exponents are shown in Figure (B8.12.1). When both exponents are equal to 1, the interaction curve is a straight line and is indicative of the most interaction possible. Making one exponent equal to 2 gives a parabola. Making each exponent equal to 2 yields a circle. With an increase in the exponents, the curves approach the boundaries given by $R_1 = 1$ and $R_2 = 1$. Therefore, complete independence or zero interaction is obtained with infinite exponents.

The effect of one loading, R_1, on another simultaneous loading, R_2, is represented by an equation or interaction curve like that shown in figure B8.11.1 This curve represents all the possible combinations of R_1 and R_2 that will cause failure. Explanation of the interaction curve (figure B8.11.1), is given as follows:

1. Point "a" is given by R_1 and R_2 and indicates a positive margin of safety because it is "inside" the interaction curve.

2. Failure can occur at 3 points and for the reasons noted:
   (1) at Point "d" by a proportionate increase in R_1 and R_2
   (2) at Point "h" by an increase in R_1 while R_2 remains constant
   (3) at Point "g" by an increase in R_2 while R_1 remains constant.

3. The additional strength available results in the following margins of safety:
   (1) Point "d"; MS = od/oa − 1
   (2) Point "h"; MS = bh/ba − 1
   (3) Point "g"; MS = cg/ca − 1.

Values od, bh, and cg are referred to as allowable stress (or load) ratios and oa, ba, and ca are referred to as applied stress (or load) ratios.

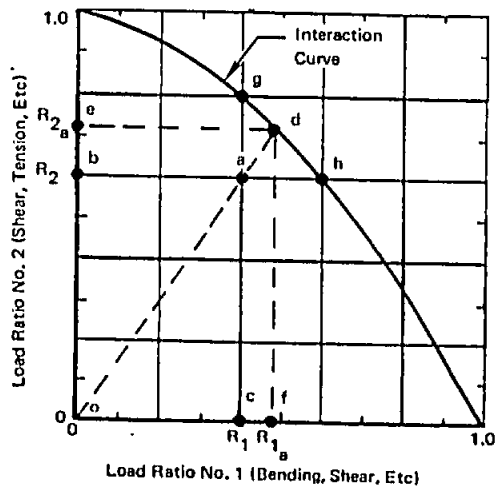

Figure B8.11.1 Typical two-loads-acting interaction curve.

B8.11.1 Procedure for Margin-of-Safety Determination for Two Loads Acting

1. Using buckling, yield, or ultimate criteria and equation (B8.11.1), calculate the stress ratio for each load acting alone.

2. Using the calculated stress ratios, locate point "a" on the proper interaction curve (Figure B8.11.1).

3. Draw a straight line from the origin "o" through point "a," and at the intersection of this line and the interaction curve read the corresponding allowable stress ratios, R_{1_a} and R_{2_a}.

4. Compute the margin of safety from the following equation:

$$MS = R_{1_a}/R_1 - 1 = R_{2_a}/R_2 - 1. \qquad (B8.11.3)$$

B8.11.2 Procedure for Margin-of-Safety Determination for Three Loads Acting

1. Same as Step (1) for two-loads-acting procedure, subsection B8.11.1.

2. Using the appropriate interaction family of curves, locate point "a" corresponding to the calculated stress ratios, R_1 and R_2, as shown in figure B8.11.2.

3. Draw a straight line from the origin "o" through point "a."

4. Extend this line to locate the allowable point "x" which must satisfy the following relationships:

$$R_1/R_{1_a} = R_2/R_{2_a} = R_3/R_{3_a}, \qquad (B8.11.4)$$

or

$$R_{3_a} = (R_3/R_1)\, R_{1_a}. \qquad (B8.11.5)$$

Point "x" is obtained by a trial-and-error procedure utilizing the following steps:

(1) Select an arbitrary value of R_{1_a}

(2) Calculate R_{3_a} from equation (B8.11.5) using the known values of R_1 and R_3 and the arbitrary value of R_{1_a}.

(3) Locate point "x" on line oa using the calculated R_{3_a} from step (2) and compare the corresponding R_{1_a} with the assumed R_{1_a}.

(4) Repeat steps (1) through (3) until the assumed R_{1_a} and the "x" value of R_{1_a} converge. At convergence, R_{1_a}, R_{2_a}, and R_{3_a} will be at a common point on line oa.

(5) Compute the margin of safety from the following equation:

$$MS = R_{1_a}/R_1 - 1 = R_{2_a}/R_2 - 1 = R_{3_a}/R_3 - 1. \qquad (B8.11.6)$$

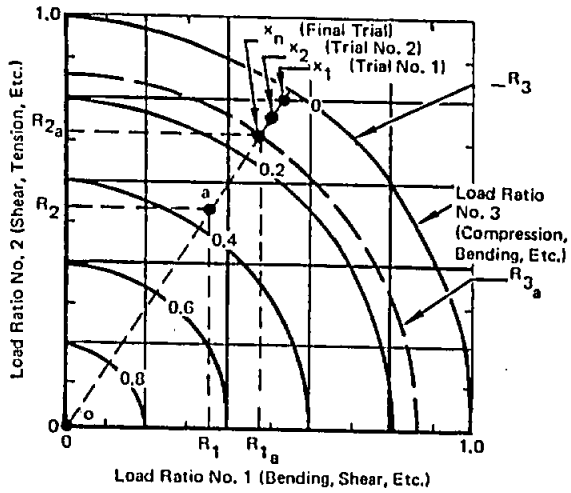

B8.11.2 Typical three-loads-acting interaction curve.

B8.12 GENERAL INTERACTION RELATIONSHIPS

A single general interaction curve will often apply to a variety of geometrical proportions (plates, tubes, and cylinders), edge-fixity conditions (simply supported and fixed), applied loadings (torsion, bending, and tension) and failure criteria (yield, elastic stability, inelastic stability, and fracture). The interaction curves presented in figures B8.12.1 through B8.12.5 are such a set of general curves. For the interaction curves (figures B8.12.1 through B8.12.4) determined from general equations, the parameters to substitute for R_1 and R_2 are determined from known equations and can be determined for most cases from the tables in sections B8.13 through B8.17. For the cases involving direct tension stress (figures B8.12.4 and B8.12.5), the interaction curves have been derived by considering tension as negative compression and utilizing the critical compressive allowable stress. The interaction curves presented in figure B8.12.5 represent special cases as indicated and are, except for curve (1), of a nonequation form.

B8.13 COMPACT (STABLE) STRUCTURES

A compact structure is one in which failure does not occur by crippling or buckling. This section presents interaction criteria for compact structures subjected to two types of stress conditions: the biaxial stress condition of a rectangular volume, such as that found in plates, membranes, and shells of revolution; and the uniaxial stress condition on a plane, such as that found in beams, round bars, and bolts.

B8.13.1 Biaxial (Volume) Stress Condition — Interaction Relationships

Tests have indicated that the maximum shear stress theory and the octahedral shear stress theory adequately predict the yield and ultimate strengths of biaxially loaded isotropic ductile materials — if the compression and tension allowables are in close agreement and the structures are compact.

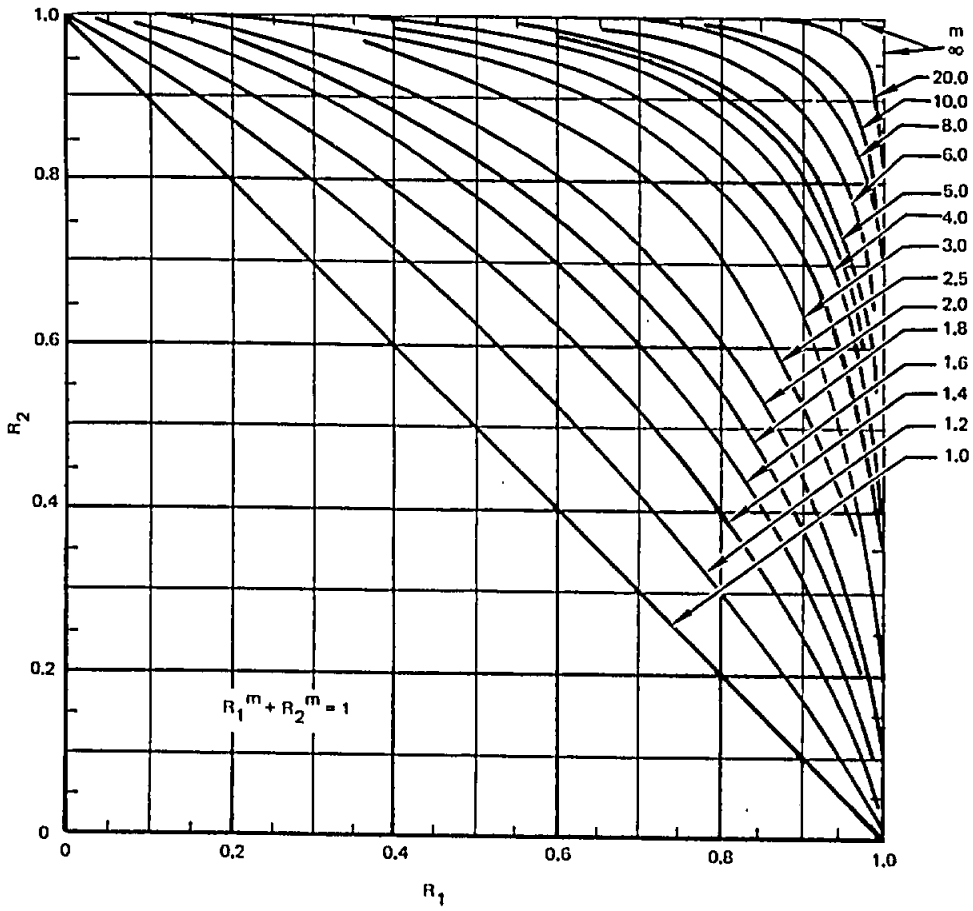

B8.12.1 General interaction curves—symmetrical form.

The interaction equations and curves presented in this section are applicable to the yield and ultimate conditions of failure by a utilization of the interaction parameters given in table B8.13.1. The method is applicable to stress conditions that combine in a two-dimensional fashion like that shown in figure B8.13.1. It is emphasized that the stress condition exists in a rectangular volume and not on a single plane. The element can be chosen at any convenient angle without regard to the actual plane of failure. Unless otherwise stated, the sign convention is: tension is positive; compression is negative.

As indicated in table B8.13.2, there are only a few cases of the compact structure type where convenient margin of safety equations are derivable. Thus, a general interaction method in curve form is presented in figure B8.13.2 to include all of the possible combinations of biaxial stress.

In order to derive the interaction equation in terms of tension or shear strength allowables, the following material constant is defined:

$$K = F_{su}/F_{tu}. \qquad \text{(B8.13.1)}$$

Tests of most materials show K to vary from approximately 0.5 to 0.75.

The transverse shear and torsional stress ratios combine as follows:

$$R_s = R_{ss} + R_{st}. \qquad \text{(B8.13.2)}$$

The directional tension and bending stress ratios combine as follows:

$$\left.\begin{aligned} R_x &= R_{tx} + R_{bx} \\ R_y &= R_{ty} + R_{by} \end{aligned}\right\}. \qquad \text{(B8.13.3)}$$

The directional compression and bending stress ratios combine as follows:

$$\left.\begin{aligned} R_x &= R_{cx} + R_{bx} \\ R_y &= R_{cy} + R_{by} \end{aligned}\right\}. \qquad \text{(B8.13.4)}$$

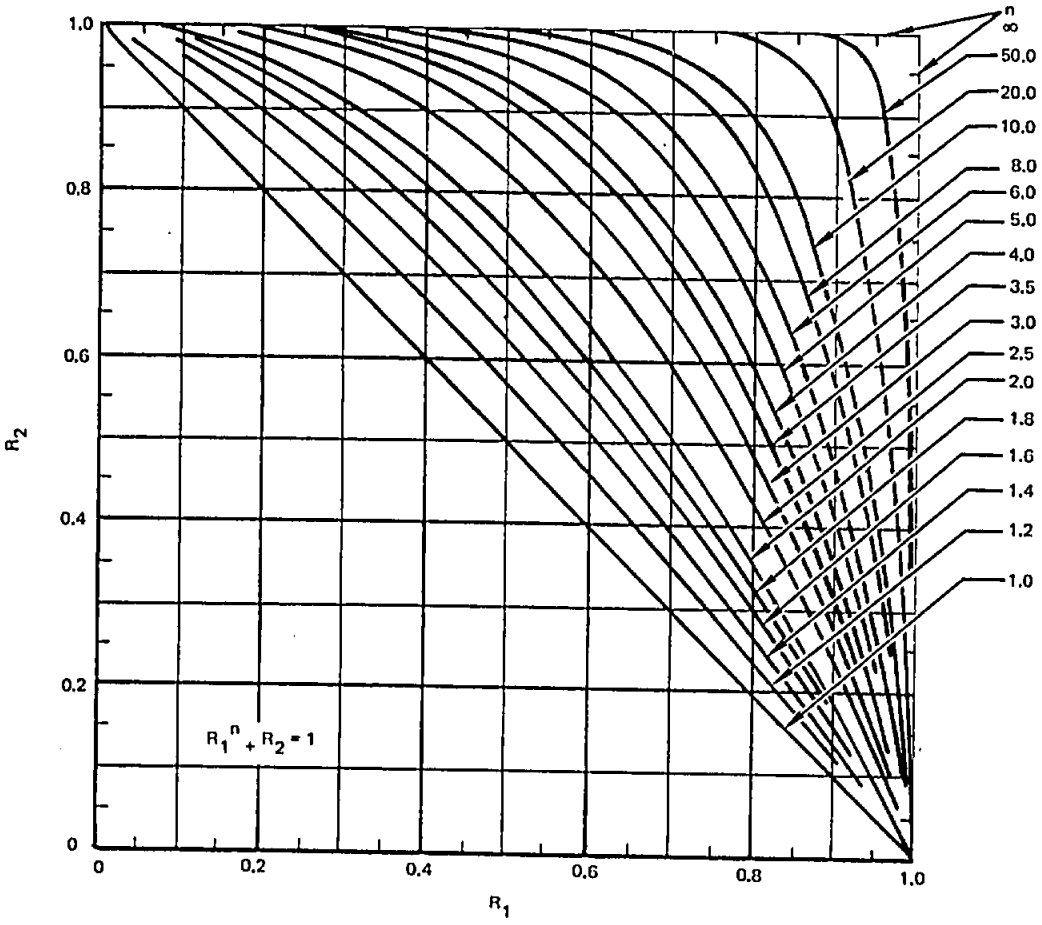

Figure B8.12.2. General interaction curves—unsymmetrical form.

It is convenient to derive the maximum shear stress and octahedral shear stress interaction equations in terms of the following principal stress ratios:

$$R_{n_{max}} = \frac{R_x + R_y}{2} + \sqrt{\left(\frac{R_x - R_y}{2}\right)^2 + K^2 R_s^2} \qquad (B8.13.5)$$

and

$$R_{n_{min}} = \frac{R_x + R_y}{2} - \sqrt{\left(\frac{R_x - R_y}{2}\right)^2 + K^2 R_s^2} \qquad (B8.13.6)$$

B8.13.1.1 Theories of Failure Interaction Curves

The maximum shear stress theory states that yielding or fracture occurs when the maximum shear stress in a combined stress element equals the maximum shear stress in a pure tension test specimen subjected to the yielding (F_{ty}) or fracture (F_{tu}) stress of the material. This results in K = 1/2 and the maximum shear stress theory interaction curve (the dashed line in figure B8.13.2.

The octahedral shear stress theory states that yielding or fracture occurs when the octahedral shear stress in a combined stress element equals the octahedral shear stress in a pure tension test specimen subjected to the yielding (F_{ty}) or fracture (F_{tu}) stress of the material. This results in $K = (1/\sqrt{3}) = 0.577$ and the maximum octahedral shear stress theory interaction curve (the solid line in Figure B8.13.2).

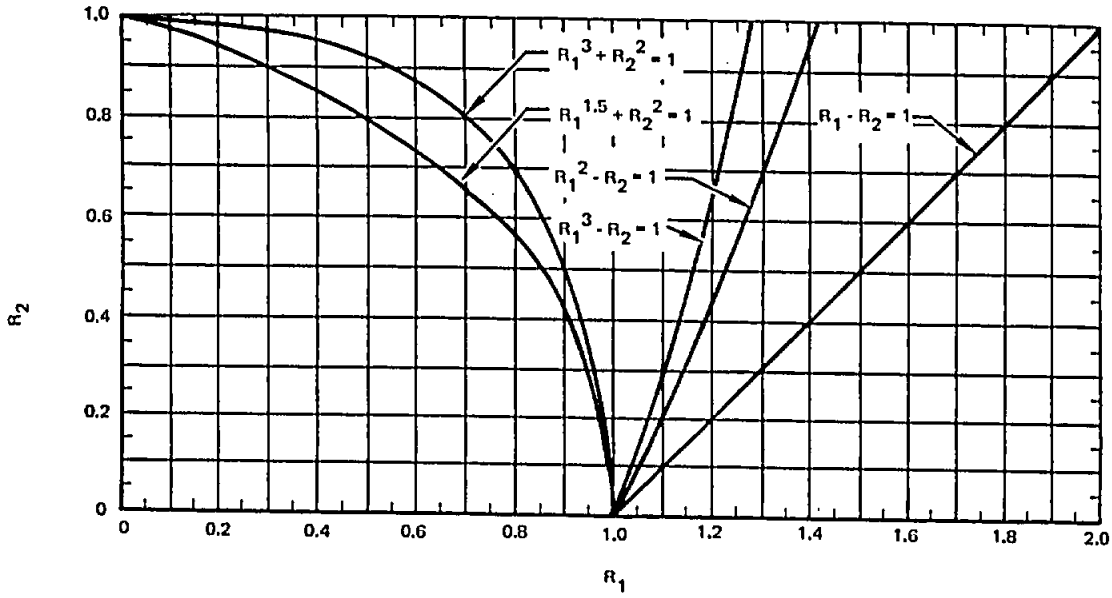

B8.12.3 **General interaction curves—special form.**

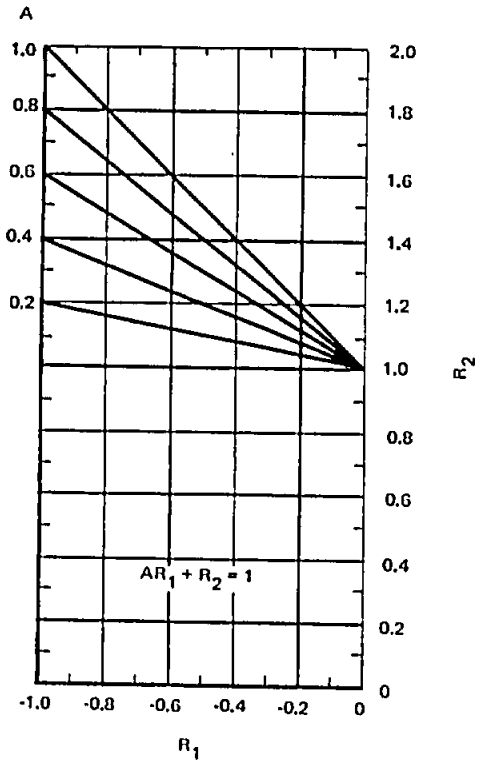

B8.12.4 **General interaction curves – linear form.**

B8.13.1.2 **Procedure for Margin-of-Safety Determination**

1. For cases where orientation of applied stress with respect to the grain direction is unknown:

   (1) Assume the allowable stresses in each direction of applied stress are the same as in the weaker direction of the material.

   (2) Evaluate

   $$K' = F_{su}/F_{tu}. \qquad \text{B8.13.7}$$

   (3) If $0.5 \leq K' < 0.577$, use $K = 0.5$ in calculating the pincipal stress ratios (equations B8.13.5 and B8.13.6) and use the maximum shear stress interaction curve (figure B8.13.2).

   (4) If $0.577 \leq K'$, use $K = 0.577$ in calculating the principal stress ratios (equations B8.13.5 and B8.13.6) and use the octahedral shear stress interaction curve (figure B8.13.2).

   (5) In evaluating R_x and R_y, the allowable axial stress is taken to be F_{ty} (yield) or F_{tu} (ultimate) regardless of whether the applied stress is tension or compression. Applied tension is positive, applied compression is negative.

   (6) Calculate the margin of safety using the two-parameter interaction procedure outlined in subsection B8.11.1.

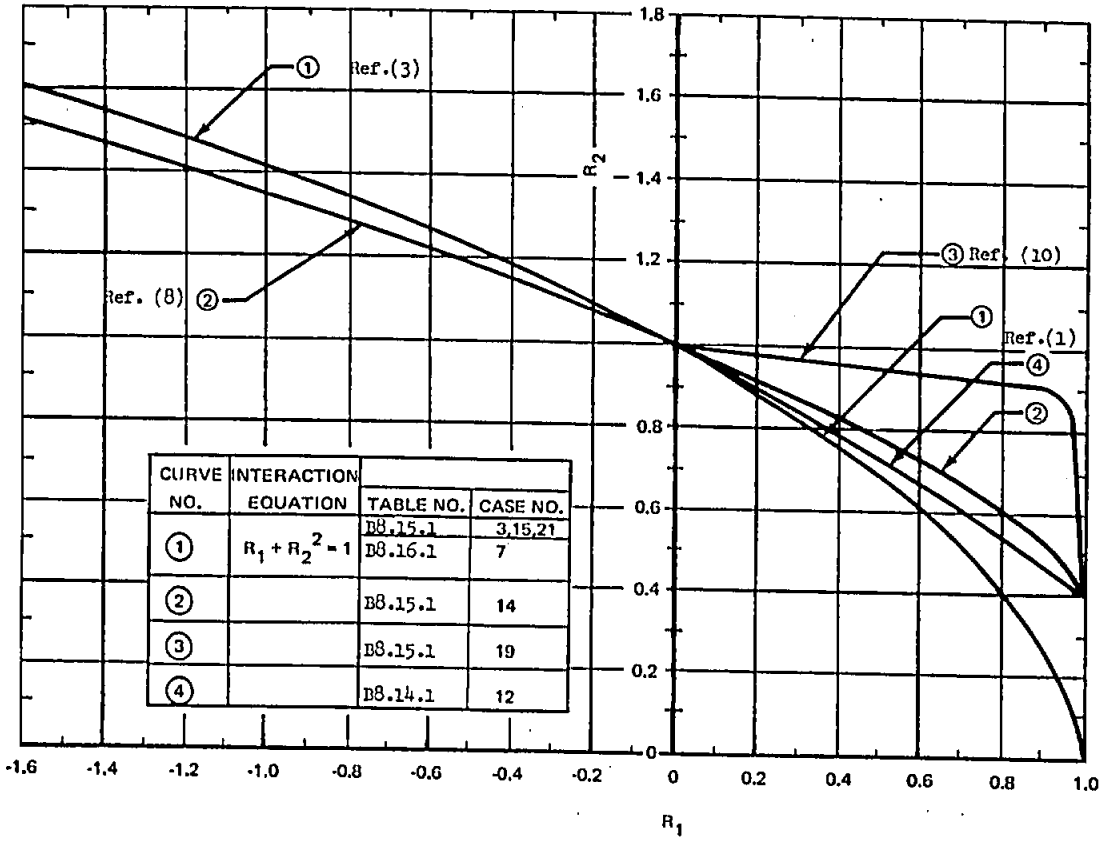

CURVE NO.	INTERACTION EQUATION	TABLE NO.	CASE NO.
①	$R_1 + R_2^2 = 1$	B8.15.1	3,15,21
		B8.16.1	7
②		B8.15.1	14
③		B8.15.1	19
④		B8.14.1	12

Figure B8.12.5. General interaction curves--special form.

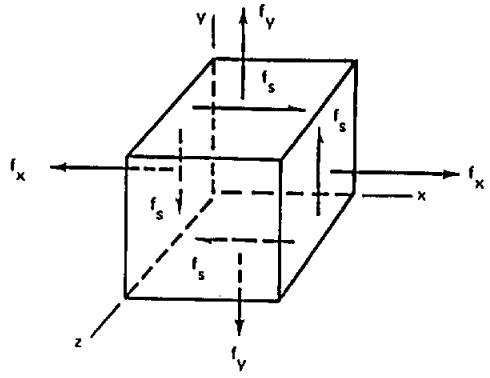

Figure B8.13.1. Biaxial stress condition for compact structures.

MEMBERS UNDER COMBINED LOADING

Table B8.13.1 Stress ratio parameters

STRESS TYPE	STRESS RATIO PARAMETER	
	YIELD CONDITION	ULTIMATE CONDITION
Tension - "x" Direction	$R_{tx} = f_{tx}/F_{ty}$	$R_{tx} = f_{tx}/F_{tu}$
Tension - "y" Direction	$R_{ty} = f_{ty}/F_{ty}$	$R_{ty} = f_{ty}/F_{tu}$
Compression - "x" Direction	$R_{cx} = f_{cx}/F_{cy}$	$R_{cx} = f_{cx}/F_{cu}$ (1)
Compression - "y" Direction	$R_{cy} = f_{cy}/F_{cy}$	$R_{cy} = f_{cy}/F_{cu}$ (1)
Bending - "x" Direction	$R_{bx} = f_{bx}/F_{by}$	$R_{bx} = f_{bx}/F_{bu}$
Bending - "y" Direction	$R_{by} = f_{by}/F_{by}$	$R_{by} = f_{by}/F_{bu}$
Transverse Shear	$R_{ss} = f_{ss}/F_{sy}$ (2)	$R_{ss} = f_{ss}/F_{su}$
Torsional Shear	$R_{st} = f_{st}/F_{sty}$ (2)	$R_{st} = f_{st}/F_{stu}$

Explanation of Subscripts:

t = tension
c = compression
b = bending
ss = transverse shear
st = torsional shear
s = shear

Subscripts x and y on R and f refer to x and y directions, respectively.
Subscripts y and u on F refer to yield and ultimate strength conditions, respectively.

Notes:
(1) Assume $F_{cu} = F_{tu}$
(2) Assume $F_{sy} = F_{sty} = KF_{ty}$
$K \approx 0.5$–0.75 for most isotropic ductile materials

2. For cases where orientation of applied stress with respect to the grain direction is known:

(1) Determine applied stress on an element with sides parallel and perpendicular to the grain direction.

(2) Evaluate

$$K' = F_{su}/F_{tu} \sqrt{\frac{1 + \left(\frac{F_{tu_T}}{F_{tu_L}}\right)^2}{2}} \qquad \text{(B8.13.8)}$$

where:

subscripts T and L refer to the transverse and longitudinal grain direction, respectively.

(3) If $0.5 \leq K' \leq 0.577$, use $K = 0.5$ and the appropriate transverse and longitudinal allowable stresses in calculating the principal stress ratios (equations B8.13.5 and B8.13.6) and use the maximum shear stress interaction curve (figure B8.13.2).

(4) If $0.577 \leq K'$, use $K = 0.577$ and the appropriate transverse and longitudinal allowable stresses in calculating the principal stress ratios (equations B8.13.5 and B8.13.6) and use the octahedral shear stress interaction curve (figure B8.13.2).

(5) In evaluating R_x and R_y, the allowable axial stress is taken to be F_{ty} (yield) or F_{tu} (ultimate) regardless of whether the applied stress is tension or compression. Applied tension is positive, applied compression is negative.

(6) Calculate the margin of safety using the two-parameter interaction procedure outlined in subsection B8.11.1.

Table B8.13.2 **Compact structures—biaxial interaction criteria (no crippling or buckling)—yield and ultimate conditions of strength**

CASE	LOADING PICTURE	LOADING DESCRIPTION	INTERACTION CURVE		MARGIN-OF-SAFETY EQUATION	REMARKS
			EQUATION	FIGURE		
1	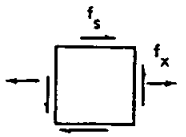	Uniaxial Tension + Shear	$R_x^2 + R_s^2 = 1$	B8.13.2 or B8.12.1	$\frac{1}{\sqrt{R_x^2 + R_s^2}} - 1$	
2	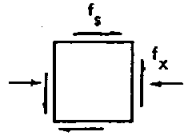	Uniaxial Compression + Shear	$R_x^2 + R_s^2 = 1$	B8.13.2 or B8.12.1	$\frac{1}{\sqrt{R_x^2 + R_s^2}} - 1$	
3	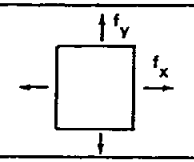	Biaxial Tension (Principal Stresses)		B8.13.2	$\frac{1}{R} - 1$	R is greater of R_x or R_y
4	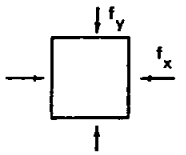	Biaxial Compression (Principal Stresses)		B8.13.2	$\frac{1}{R} - 1$	R is greater of R_x or R_y
5	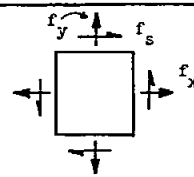	All other states of biaxial stress		B8.13.2		Refer to subsection B8.13.1 and use: (1) Table B8.13.1 (2) Equations B8.13.5 and B8.13.6 (3) Figure B8.13.2

NOTES:

(1) Tension is positive, compression is negetive

(2) $R_s = R_{ss} + R_{st}$

(3) $R_x = R_{tx} + R_{bx}$ (tension); $R_x = R_{cx} + R_{bx}$ (compression)

(4) $R_y = R_{ty} + R_{by}$ (tension); $R_y = R_{cy} + R_{by}$ (compression)

(5) $\{R_t = f_t/F_{ty},\ R_c = f_c/F_{ty},\ R_b = f_b/F_{by},\ R_{ss} = f_s/F_{sy},\ R_{st} = f_{st}/F_{sty}\}$ (YIELD)

(6) $\{R_t = f_t/F_{tu},\ R_c = f_c/F_{tu},\ R_b = f_b/F_{bu},\ R_{ss} = f_s/F_{su},\ R_{st} = f_{st}/F_{stu}\}$ (ULTIMATE)

MEMBERS UNDER COMBINED LOADING

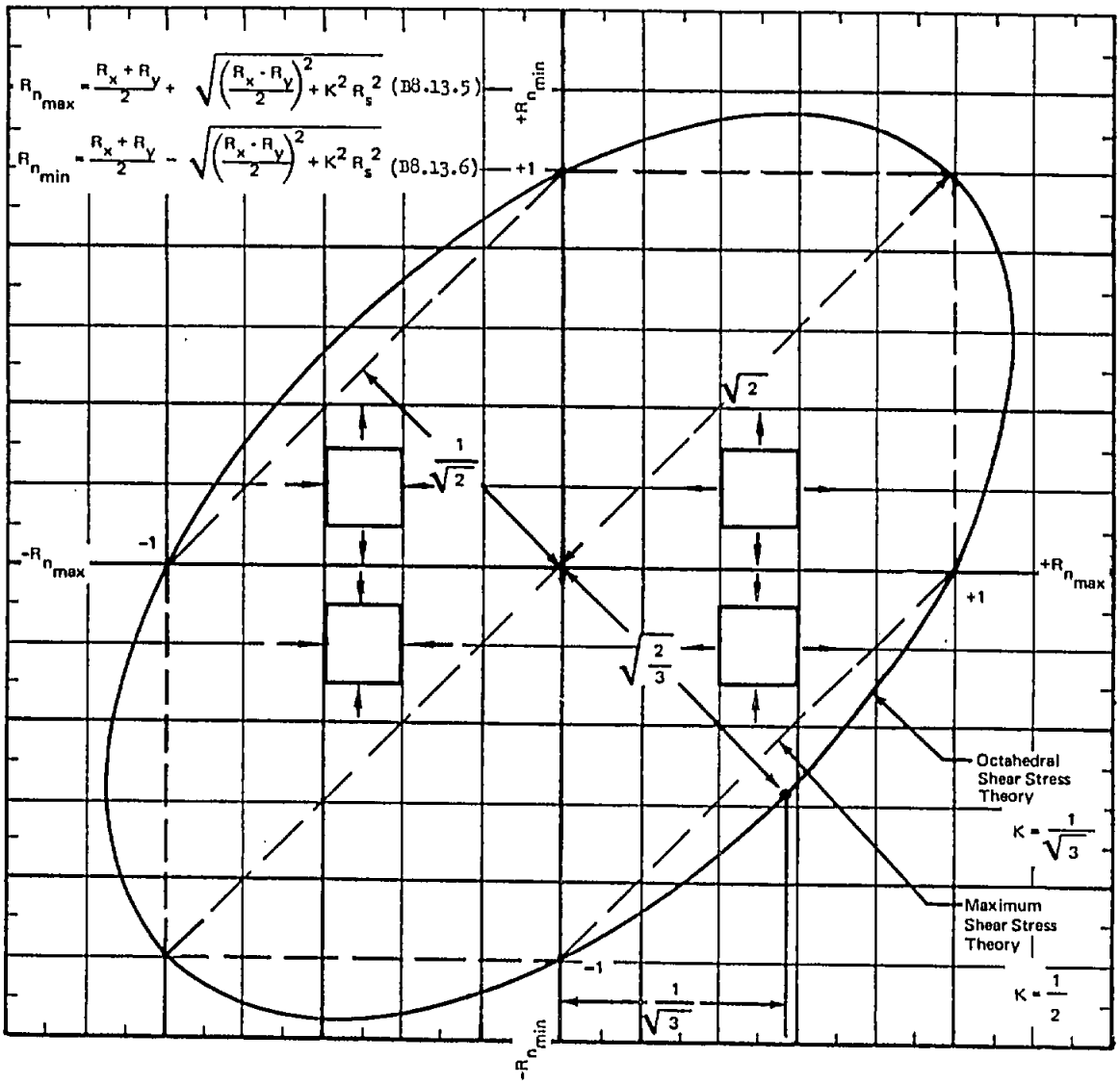

Figure B8.13.2. **Interaction curves for biaxially stressed compact structures.**

B8.13.2 Uniaxial (Plane) Stress Condition — Interaction Relationships

When compact structures such as beams (symmetrical and unsymmetrical) are loaded by axial loads, bending moments (simple and complex) and shear loads (simple and complex) that do not combine in a biaxial two-dimensional fashion like that shown in figure B8.13.1, methods other than those presented in subsection B8.13.1 must be utilized. Analysis involving the bending strengths of beams loaded into the inelastic range by bending moments or by a combination of bending moments and axial load is contained in section B3.32.

B8.14 THICK-WALLED TUBULAR STRUCTURES

This section presents combined loads-interaction data for the design and analysis of thick-walled tubular structures. The interaction stress ratios (R_t, R_b, R_{st}, etc.) must be determined from critical tube strength and stability criteria. Bending stress calculations must include the effects of secondary bending, if any, and compressive stress ratios must be based on column stability criteria.

Table B8.14.1 lists the applicable interaction equations and margin-of-safety equations along with a reference to the pertinent interaction curve.

Figures B8.14.1 and B8.14.3 represent loading conditions as a three-load nature, but the margin of safety is determined by the two loads acting procedure as given in subsection B8.11.1.

B8.15 UNSTIFFENED PANEL STRUCTURES (INITIAL BUCKLING CRITERIA)

This section presents combined loads-interaction data for the design and analysis of unstiffened flat rectangular panels and unstiffened curved panels. In this instance a panel is a member whose thickness is small compared to its other dimensions. The interaction stress ratios (R_c, R_b, R_s, etc.) must be based on elastic initial buckling criteria. For panels subjected to direct axial stress, tension is included as negative compression using the critical compression allowable. For panels in which geometry governs, the interaction curves are plotted as a parametric function of aspect ratio (a/b; a = long-side dimension, b = short-side dimension). Table B8.15.1 lists the applicable interaction equations and margin-of-safety equations along with a reference to the pertinent interaction curve.

B8.16 UNSTIFFENED CYLINDRICAL SHELL STRUCTURES (INITIAL BUCKLING CRITERIA)

This section presents combined loads-interaction data for the design and analysis of unpressurized and pressurized unstiffened cylindrical shell structures. A shell is defined as a member whose radius-to-thickness ratio is greater than ten. Interaction criteria are presented for circular and elliptical cylinders. The interaction stress ratios (R_t, R_c, R_s, etc.) must be based on initial buckling criteria. For cylindrical shells subjected to direct axial stress, tension is included as negative compression using the compression buckling allowable. Table B8.16.1 lists the applicable interaction equations, margin-of-safety equations, and a reference to the appropriate interaction curve.

B8.17 STIFFENED STRUCTURES (STABILITY CRITERIA)

This section presents combined loads-interaction data for the design and analysis of stiffened panel and cylindrical shell structures. The interaction stress ratios (R_c, R_b, R_s, and R_{st}) must be based on stability criteria. Table B8.17.1 lists the applicable interaction equations along with a reference to the pertinent interaction curve.

Table B8.14.1 **Thick-walled tubular structures—interaction criteria—yield and ultimate conditions of strength, including the effects of column stability**

CASE	LOADING PICTURE	LOADING DESCRIPTION	INTERACTION CURVE EQUATION	INTERACTION CURVE FIGURE	MARGIN-OF-SAFETY EQUATION	REMARKS
ROUND TUBES						
1	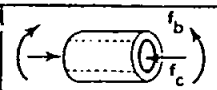	Compression + Bending	$R_c + R_b = 1$	B8.12.1 Ref.(25)	$\frac{1}{R_c + R_b} - 1$	
2	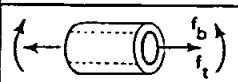	Tension + Bending				Refer to Section B3.32 for analysis of this case of loading
3	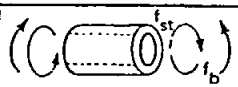	Bending + Torsion	$R_b^2 + R_{st}^2 = 1$	B8.12.1 Ref.(25)	$\frac{1}{\sqrt{R_b^2 + R_{st}^2}} - 1$	
		OMITTED				
7	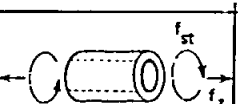	Tension + Torsion	$R_t^2 + R_{st}^2 = 1$	B8.12.1 Ref. (26)	$\frac{1}{\sqrt{R_t^2 + R_{st}^2}} - 1$	
8	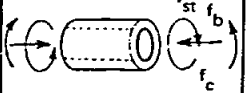	Compression + Bending + Torsion	$R_b^2 + R_{st}^2 = (1-R_c)^2$	B8.14.1 Ref.(26)	$\frac{1}{R_c + \sqrt{R_b^2 + R_{st}^2}} - 1$	In using figure B8.14.1. follow two-loads-acting procedure as outlined in subsection B8.11.1.

Grumman

Table B8.14.1. Thick-walled tubular structures-interaction criteria-yield and ultimate conditions of strength, including the effects of column stability (concluded)

CASE	LOADING PICTURE	LOADING DESCRIPTION	INTERACTION CURVE EQUATION	INTERACTION CURVE FIGURE	MARGIN-OF-SAFETY EQUATION	REMARKS
OMITTED						
10		Tension + Torsion + Internal Pressure	$R_t^2 + R_{st}^2 + R_p^2 = 1$	B8.14.3 Ref.(26)	$\frac{1}{\sqrt{R_t^2 + R_{st}^2 + R_p^2}} - 1$	
STREAMLINE TUBES						
11	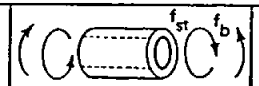	Bending + Torsion	$R_b + R_{st} = 1$	B8.12.1 Ref.(25)	$\frac{1}{\sqrt{R_b + R_{st}}} - 1$	
SQUARE TUBES						
12	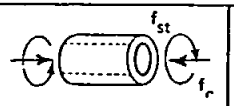	Compression + Torsion		B8.12.5 Ref.(1)		Let $R_c = R_1$ $R_s = R_2$

NOTES:

(1) R_c must be based on the tube column allowable.

(2) R_t must be based on the material strength allowable.

(3) R_b and R_{st} must be based on tube strength allowables.

(4) R_b must include the effects of secondary bending.

(5) For shear-bending analysis use $f_s = f_{smax}$ and $f_b = f_{bmax}$ even though the locations of the two maxima do not coincide. The allowable transverse shear stress is equal to the lower of 1.20 times the allowable torsional-shear stress and the material allowable shear stress.

(6) $R_p = pd/2t\,F_{tu}$, d = tube mean diameter, t = wall thickness.

MEMBERS UNDER
COMBINED LOADING

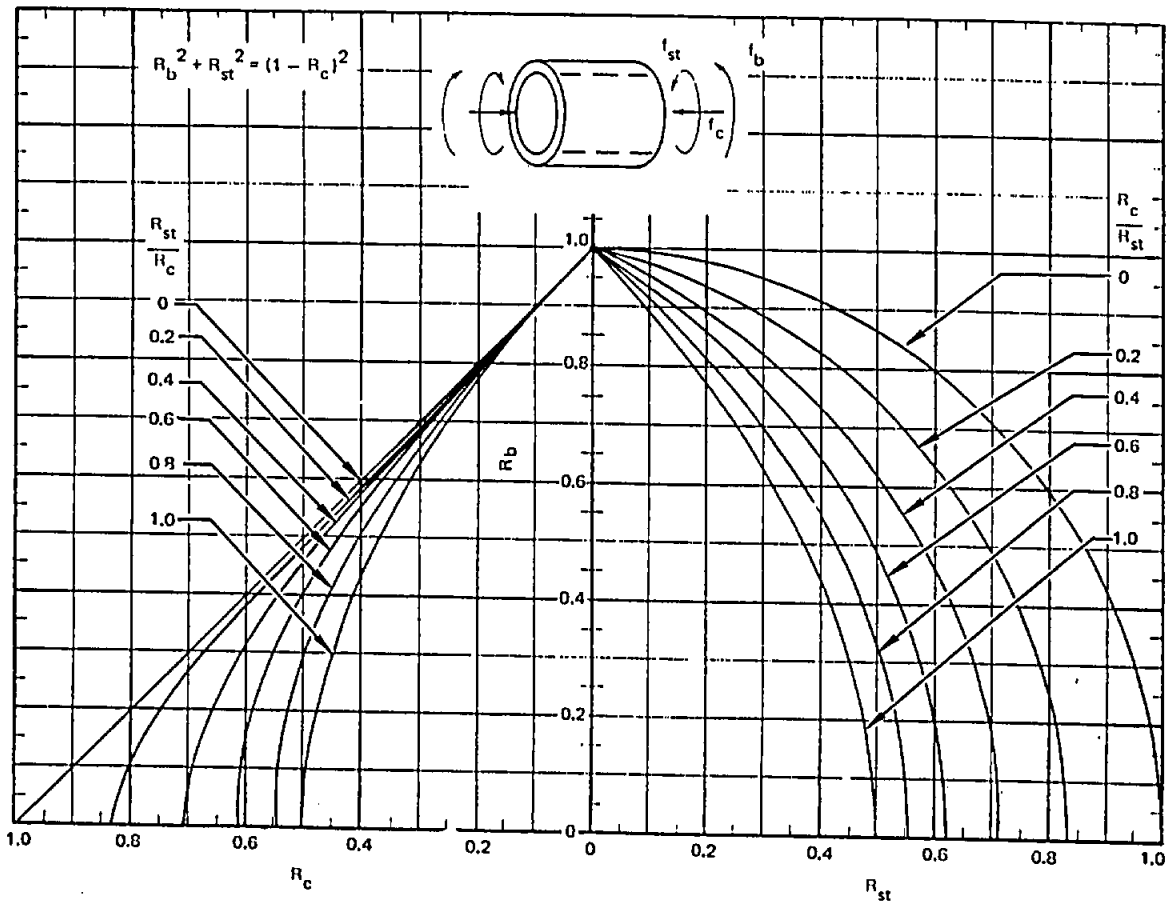

Figure B8.14.1. Interaction curves for thick-walled round tubes — compression, bending, and torsion (ref B8.14.1, Case 8).

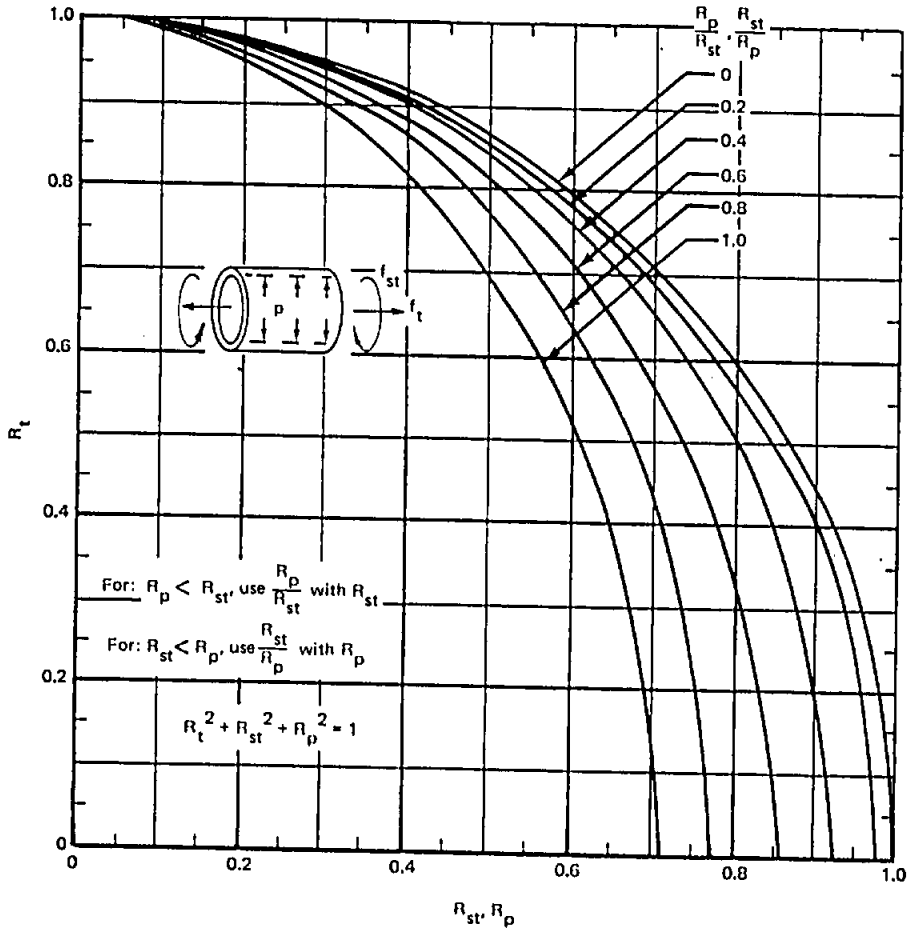

Figure B8.14.3. Interaction curves for thick-walled round tubes—tension, torsion, and internal pressure (ref Table B8.14.1, Case 10).

Table B8.15.1 Unstiffened panel structures interaction criteria (initial buckling)

CASE	LOADING PICTURE	LOADING DESCRIPTION	INTERACTION CURVE EQUATION	INTERACTION CURVE FIGURE	MARGIN-OF-SAFETY EQUATION	REMARKS
FLAT RECTANGULAR PANELS						
1	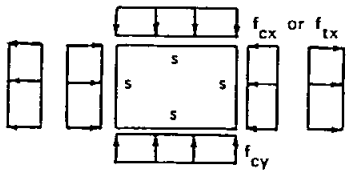	Longitudinal Compression or Tension + Transverse Compression		B8.15.1 Ref.(2)		
2	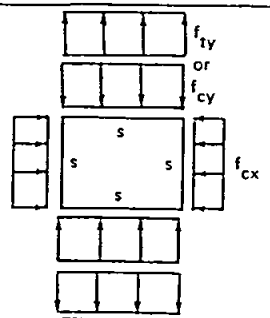	Longitudinal Compression + Transverse Compression or Tension		B8.15.1 Ref. (2)		
3	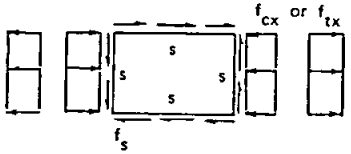	Longitudinal Compression or Tension + Shear	$R_{cx} + R_s^2 = 1$ or $R_{tx} + R_s^2 = 1$	B8.12.5 ① Ref. (3)	$\frac{2}{R_{cx} + \sqrt{R_{cx}^2 + 4R_s^2}} - 1$ or $\frac{2}{R_{tx} + \sqrt{R_{tx}^2 + 4R_s^2}} - 1$	Let R_{cx} or $R_{tx} = R_1$ $R_s = R_2$
4	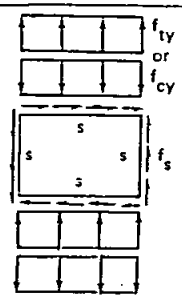	Transverse Compression or Tension + Shear		B8.15.2 Ref. (4)		

Grumman

Table B8.15.1 Unstiffened panel structures—interaction criteria (initial buckling) (continued)

CASE	LOADING PICTURE	LOADING DESCRIPTION	INTERACTION CURVE		MARGIN OF SAFETY EQUATION	REMARKS
			EQUATION	FIGURE		
OMITTED						
6	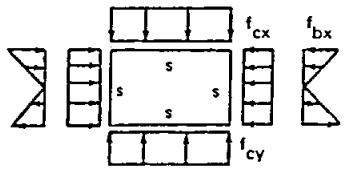	Longitudinal Compression + Transverse Compression + Longitudinal Bending		B8.15.4 Ref. (5)		In using figure B8.15.4 follow three-loads-acting procedure as outlined in subsection B8.11.2
7	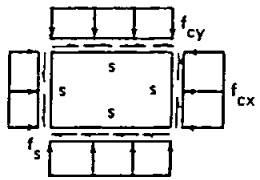	Longitudinal Compression + Transverse Compression + Shear		B8.15.5 Ref. (6)		
OMITTED						

Table B8.15.1 Unstiffened panel structures—interaction criteria (initial buckling) (continued)

CASE	LOADING PICTURE	LOADING DESCRIPTION	INTERACTION CURVE EQUATION	INTERACTION CURVE FIGURE	MARGIN-OF-SAFETY EQUATION	REMARKS
10	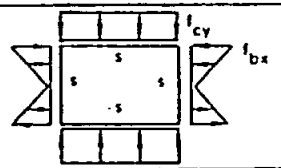	Longitudinal Bending + Transverse Compression		B8.15.4 Ref. (7)		In using figure B8.15.4 use $R_{cx} = 0$ curve and follow two-loads-acting procedure as outlined in sub section B8.11.1
11	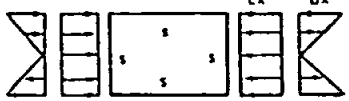	Longitudinal Compression + Longitudinal Bending	$R_{cx} + R_{bx}^{1.75} = 1$	B8.12.2 Ref. (3)		Let $R_{bx} = R_1$ $R_{cx} = R_2$
12	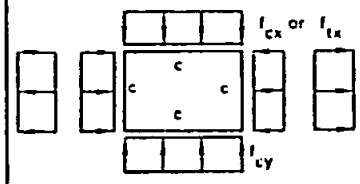	Longitudinal Compression or Tension + Transverse Compression		B8.15.7 Ref. (2)		
13	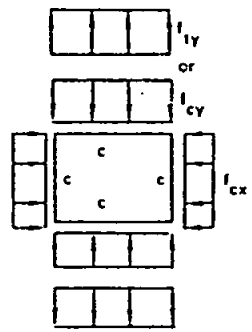	Longitudinal Compression + Transverse Compression or Tension		B8.15.7 Ref. (2)		

Table B8.15.1 Unstiffened panel structures—interaction criteria (initial buckling) (continued)

CASE	LOADING PICTURE	LOADING DESCRIPTION	INTERACTION CURVE EQUATION	INTERACTION CURVE FIGURE	MARGIN-OF-SAFETY EQUATION	REMARKS
14	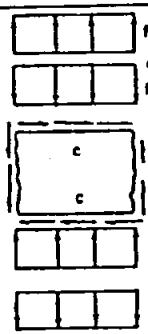	Transverse Compression or Tension + Shear		B8.12.5 ② Ref. (8)		Let $R_{cy} = R_1$ $R_s = R_2$
15	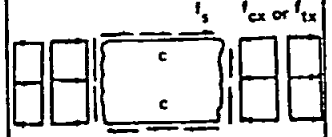	Longitudinal Compression or Tension + Shear	$R_{cx} + R_s^2 = 1$ or $R_{tx} + R_s^2 = 1$	B8.12.5 ① Ref. (3)	$\frac{2}{R_{cx} + \sqrt{R_{cx}^2 + 4R_s^2}} - 1$ or $\frac{2}{R_{tx} + \sqrt{R_{tx}^2 + 4R_s^2}} - 1$	Let $R_{cx} = R_1$ $R_s = R_2$ or $R_{tx} = R_1$ $R_s = R_2$
16	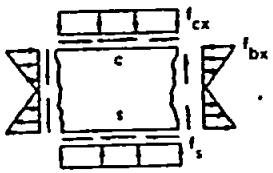	Longitudinal Bending + Transverse Compression + Shear		B8.15.8 B8.15.9 Ref.(27)		
17	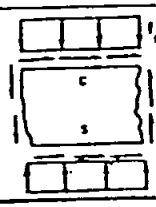	Transverse Compression + Shear	$R_{cy} + R_s^2 = 1$	B8.12.2 Ref. (9)	$\frac{2}{R_{cy} + \sqrt{R_{cy}^2 + 4R_s^2}} - 1$	Let $R_s = R_1$ $R_{cy} = R_2$

Table B8.15.1 Unstiffened panel structures--interaction criteria (initial buckling)(continued)

CASE	LOADING PICTURE	LOADING DESCRIPTION	INTERACTION CURVE EQUATION	INTERACTION CURVE FIGURE	MARGIN-OF-SAFETY EQUATION	REMARKS
18	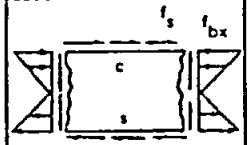	Longitudinal Bending + Shear		B8.15.8 B8.15.9 Ref.(27)		In using figure B8.15.8 use $R_{cy} = 0$ curve and follow two-loads-acting procedure as outlined in sub-section B5.11.1
19	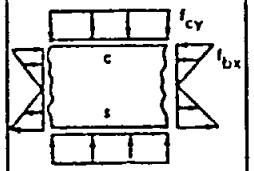	Longitudinal Bending + Transverse Compression		B8.12.5 Ref. (3)		Let $R_{cy} = R_1$ $R_{bx} = R_2$
20	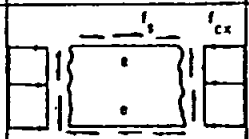	Longitudinal Compression + Shear	$R_{cx} + R_s^2 = 1$	B8.12.2 Ref. (4)	$\frac{2}{R_{cx} + \sqrt{R_{cx}^2 + 4R_s^2}} - 1$	Let $R_s = R_1$ $R_{cx} = R_2$
ADDITIONAL FLAT RECTANGULAR PANEL CASES						
21	Longitudinal and transverse direct stress, long edges simply supported, short edges clamped. Interaction criteria are given in terms of buckling coefficients in reference 2.					
22	Longitudinal and transverse direct stress, long edges clamped, short edges simply supported. Interaction criteria are given in terms of buckling coefficients in reference 2.					
CURVED RECTANGULAR PANELS						
23		Longitudinal Compression or Tension + Shear		B5.21.1		

Table B8.15.1 Unstiffened panel structures--interaction criteria (initial buckling)(continued)

CASE	LOADING PICTURE	LOADING DESCRIPTION	INTERACTION CURVE		MARGIN-OF-SAFETY EQUATION	REMARKS
			EQUATION	FIGURE		
24	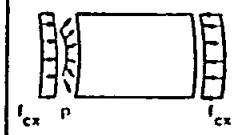	Longitudinal Compression + Internal Pressure	$R_{cx}^2 - \lvert R_p \rvert = 1$	B8.12.3 Ref. (10)		Let $R_{cx} = R_1$ $R_p = R_2$
25	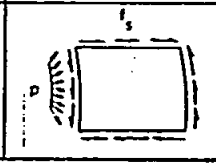	Shear + Internal Pressure	$R_s^2 - \lvert R_p \rvert = 1$	B8.12.3 Ref. (11)		Let $R_s = R_1$ $R_p = R_2$

NOTES

(1) R_c, R_b, and R_s must be based on panel initial buckling allowables.

(2) R_t is negative and is based on compression allowable.

(3) R_p is negative and is based on external collapsing pressure.

(4) S = simple supports, c = clamped supports, e = elastic supports.

(5) Dimensions; a = long side, b = short side.

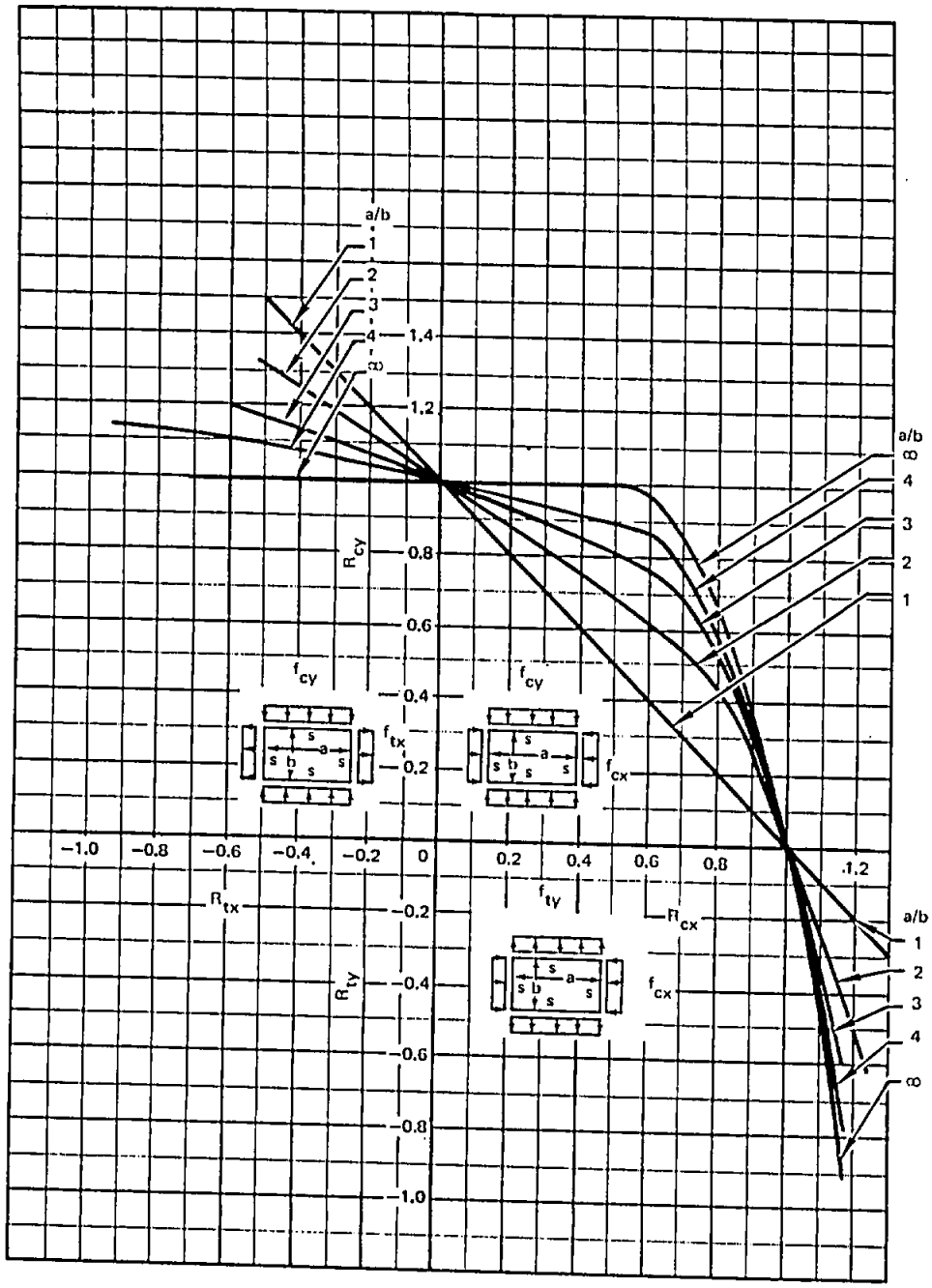

Figure B8.15.1. Interaction curves for flat rectangular panels-longitudinal compression or tension and transverse compression or tension (ref Table B8.15.1, Cases 1 and 2).

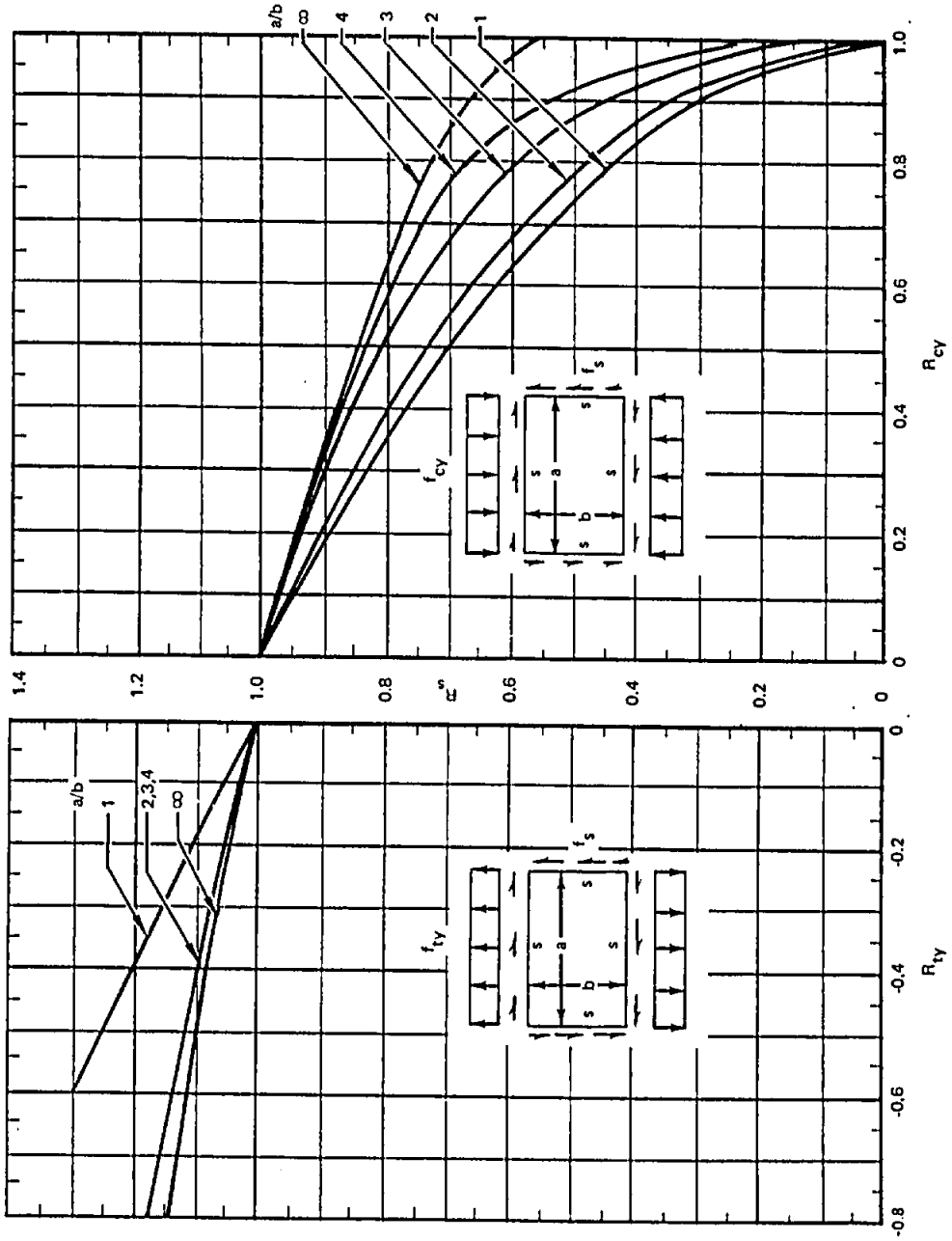

Figure B8.15.2. Interaction curves for flat rectangular panels-transverse compression or tension and shear (ref Table B8.15.1, Case 4).

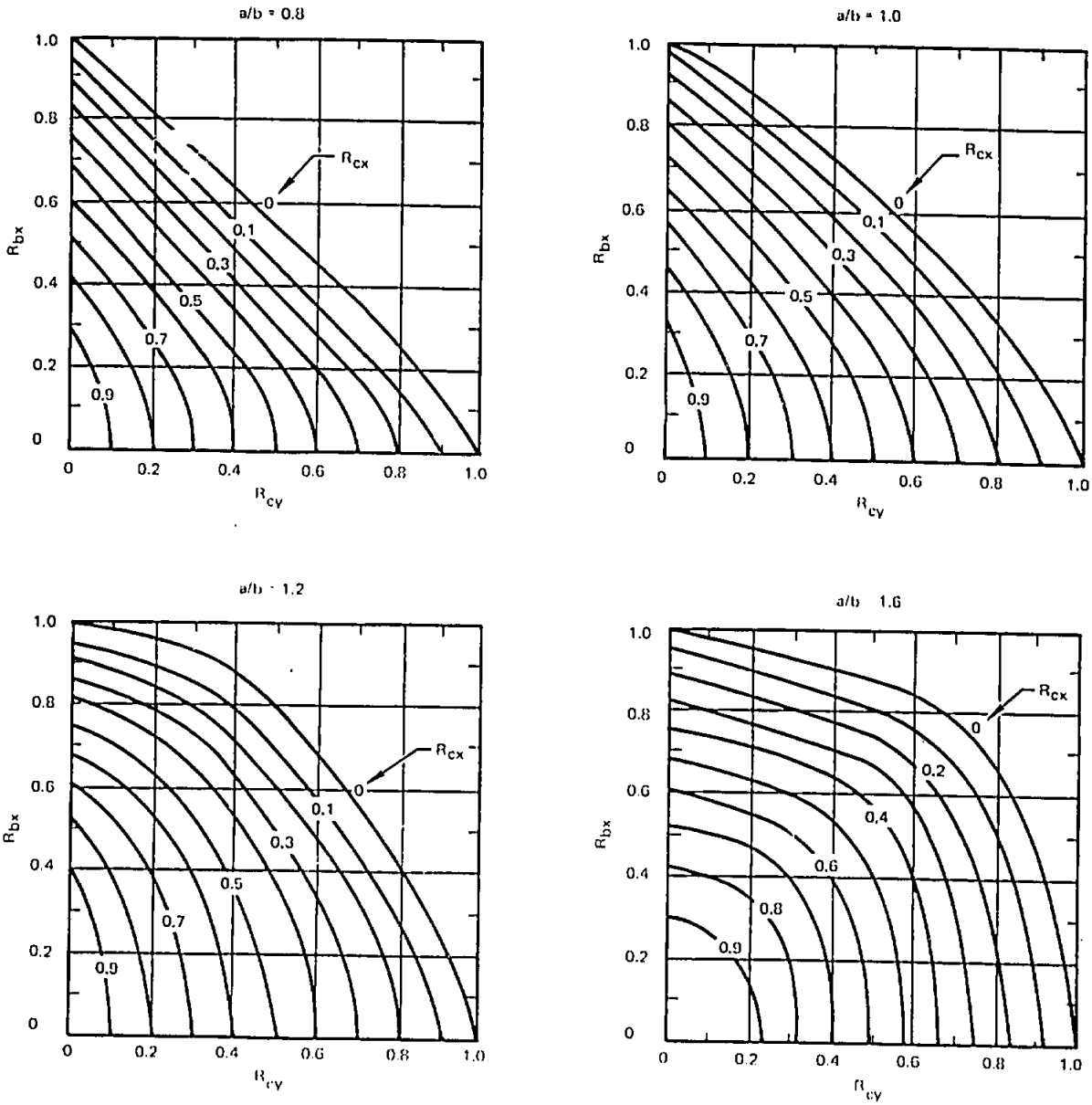

Figure B8.15.4. Interaction curves for flat rectangular panels-longitudinal compression, longitudinal bending, and transverse compression (ref Table B8.15.1, Cases 6 and 10)

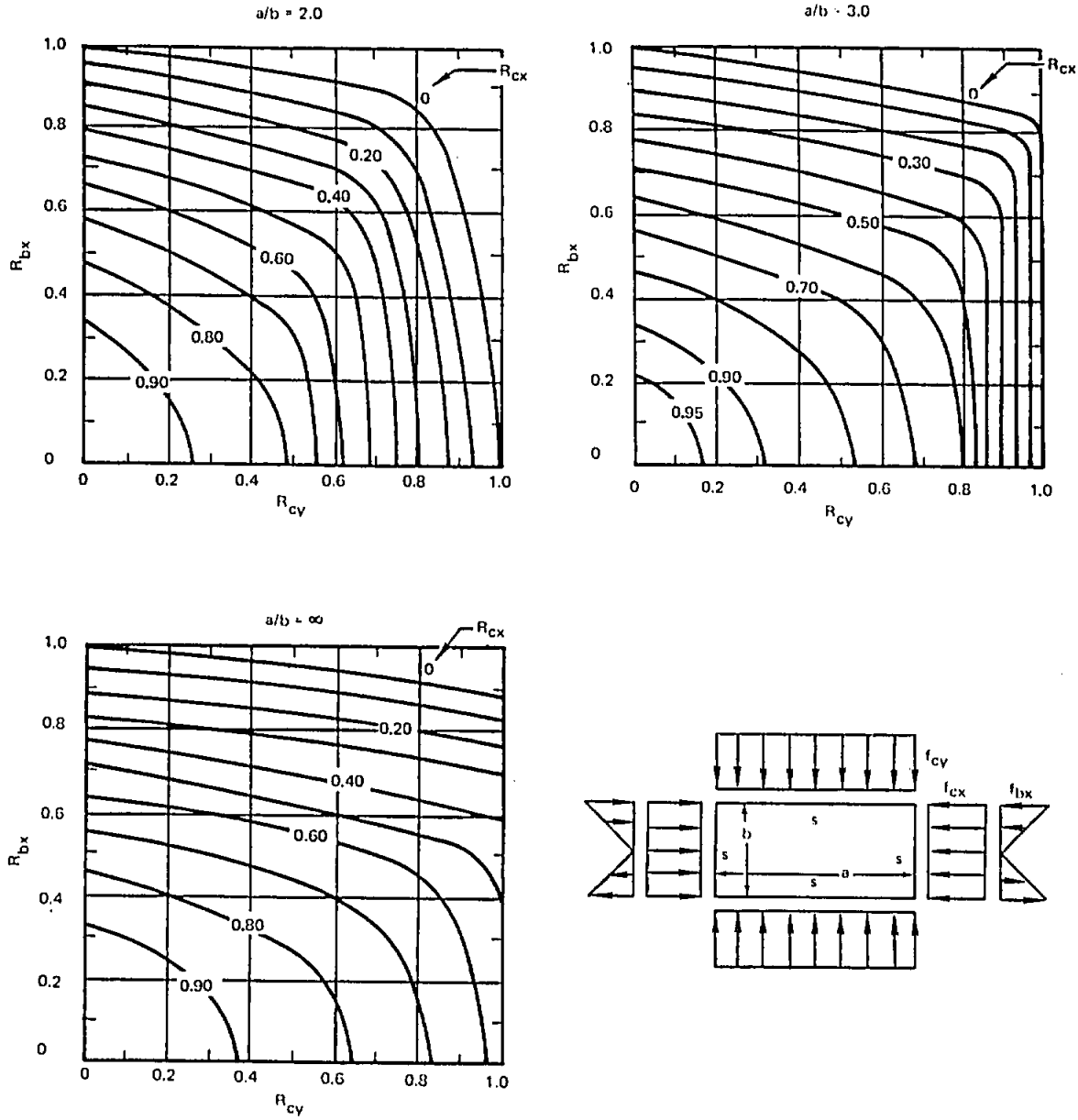

Figure B8.15.4. Interaction curves for flat rectangular panels-longitudinal compression, longitudinal bending, and transverse compression (ref Table B8.15.1, Cases 6 and 10) (concluded).

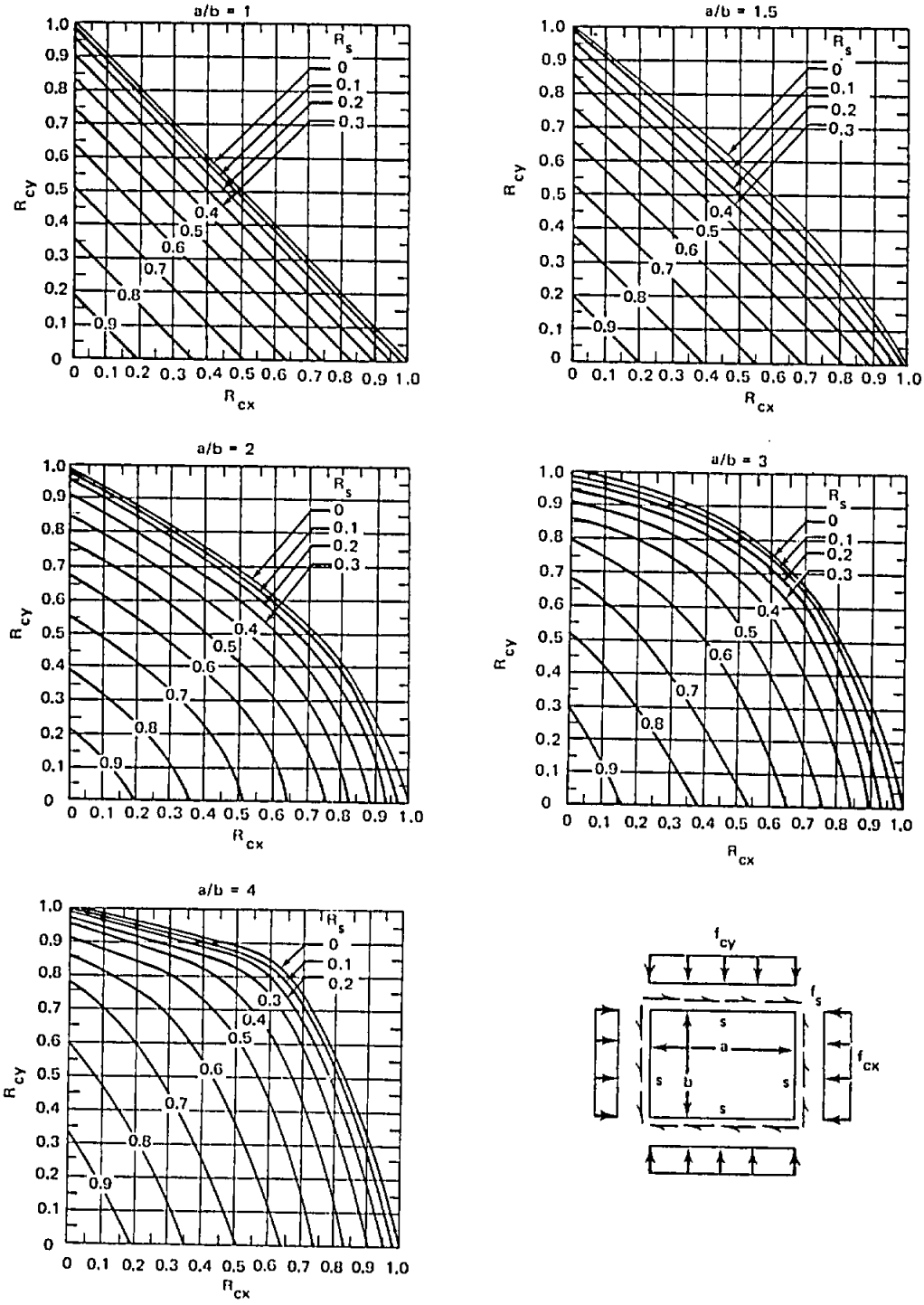

Figure B8.15.5. Interaction curves for flat rectangular panels - longitudinal compression, transverse compression, and shear (ref Table B8.15.1, Case 7).

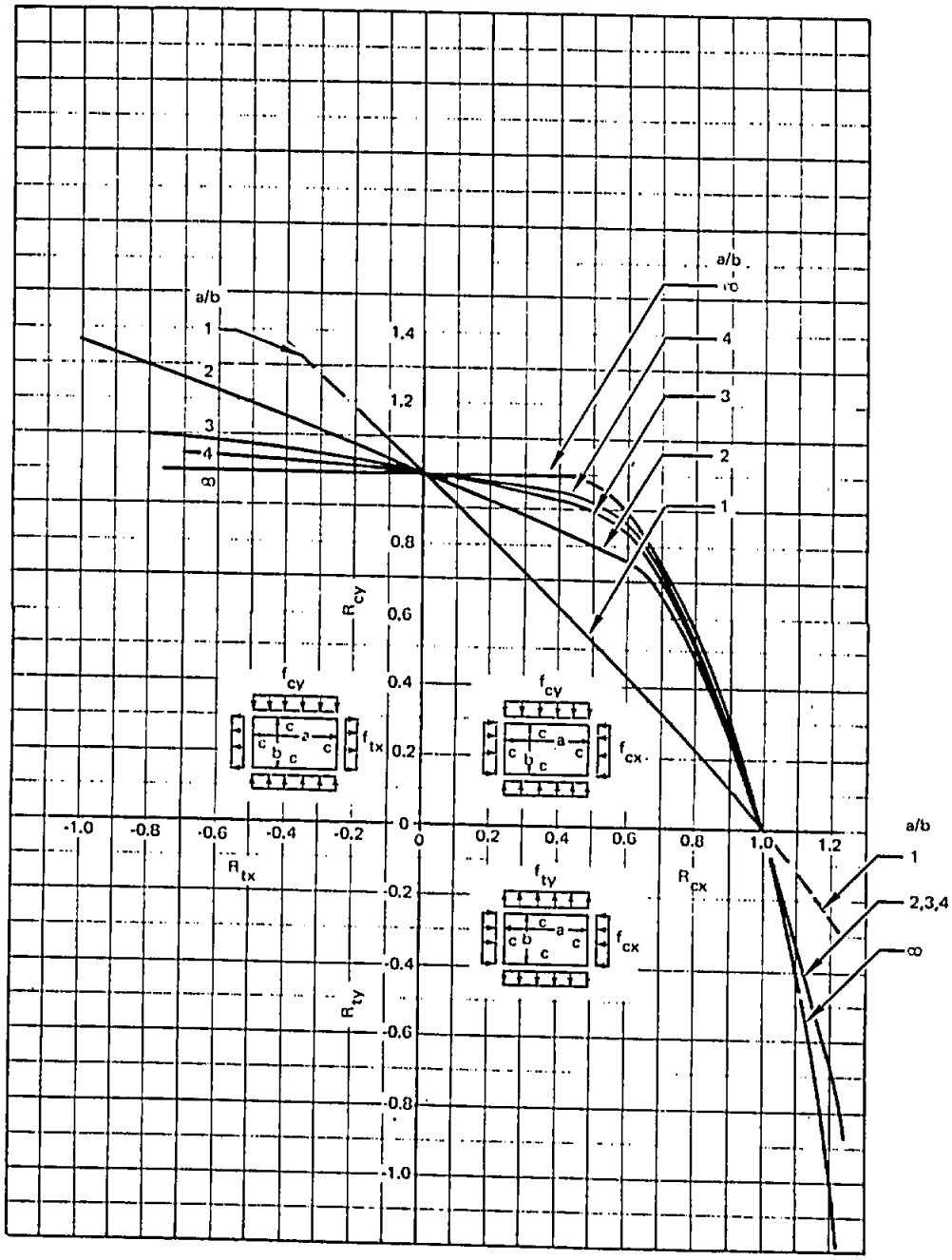

Figure B8.15.7. Interaction curves for flat rectangular panels - longitudinal compression or tension and transverse compression or tension (ref Table B8.15.1, Cases 12 and 13).

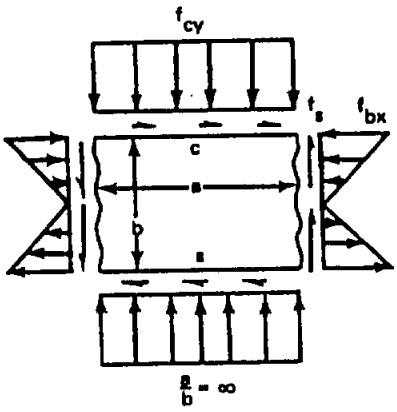

NOTE: Bending moment direction is not reversible with respect to clamped edge.

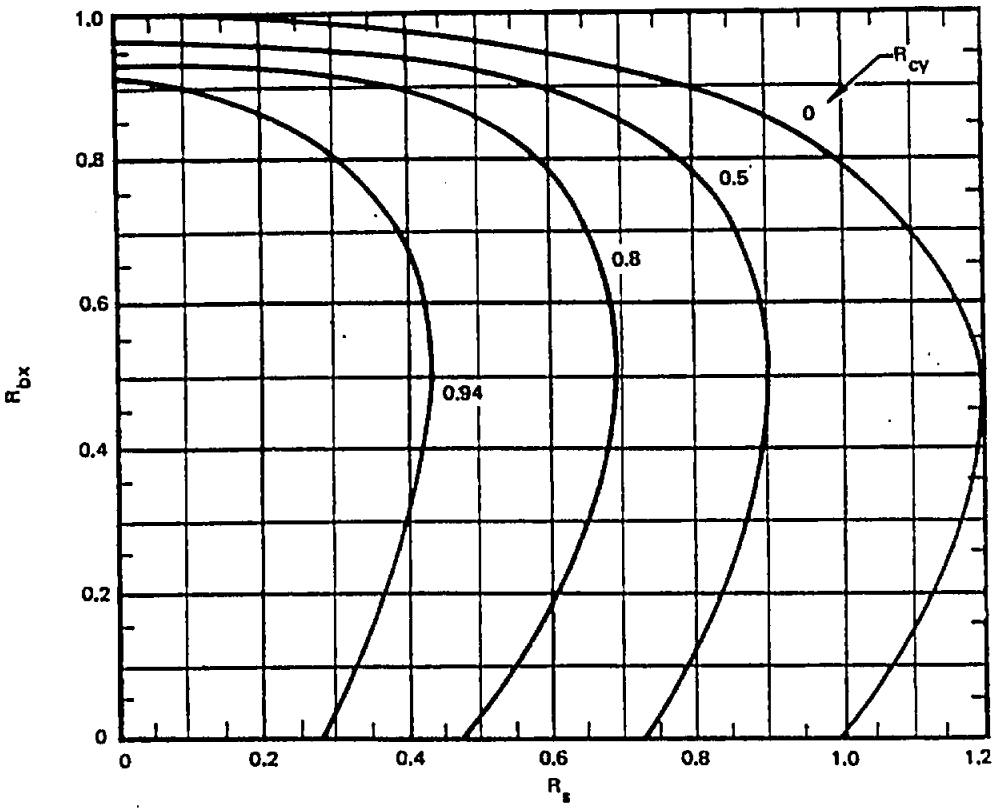

Figure B8.15.8. Interaction curves for flat rectangular panels - longitudinal bending, transverse compression, and shear with lower edge simply supported and upper edge clamped (ref. Table B8.15.1, Case 16 and 18).

MEMBERS UNDER
COMBINED LOADING

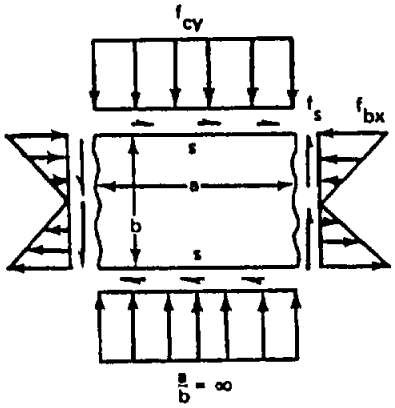

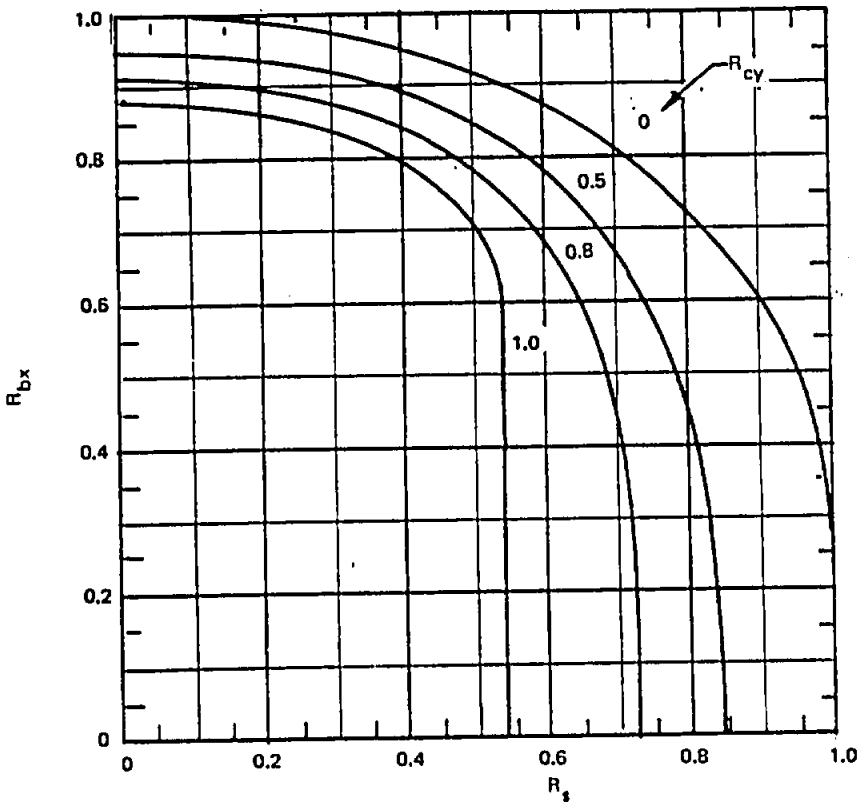

Figure B8.15.9. Interaction curves for flat rectangular panels - longitudinal bending, transverse compression, and shear with simply supported edges (ref. Table B8.15.1, Case 16 and 18).

Table B8.16.1 Unstiffened cylindrical shell structures-interaction criteria (initial buckling)

CASE	LOADING PICTURE	LOADING DESCRIPTION	INTERACTION CURVE EQUATION	INTERACTION CURVE FIGURE	MARGIN-OF-SAFETY EQUATION	REMARKS
1	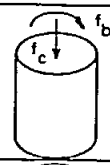	Longitudinal Compression + Longitudinal Bending	$R_c + R_b = 1$	B8.12.1 Refs.(10, 12)	$\frac{1}{R_c + R_b} - 1$	Applicable for all values of Z_L and for all edge constraints.
2	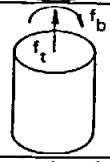	Longitudinal Tension + Longitudinal Bending	$R_b + 0.9\,R_t = 1$	B8.12.4 Ref. (12)		Let $R_t = R_1$ $R_b = R_2$
3	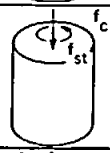	Longitudinal Compression + Torsion	$R_c + R_{st}^2 = 1$	B8.12.2 Refs.(10, 13)	$\frac{2}{R_c + \sqrt{R_c^2 + 4R_{st}^2}} - 1$	Applicable range: (1) Using theoretical σ_{cr} & τ_{cr} $Z_L<1$ SS $Z_L<5$ C (2) Using empirical σ_{cr} & τ_{cr} $1<Z_L<7.7(r/t)^2$ SS $5<Z_L<7.7(r/t)^2$ C Let $R_{st} = R_1$ $R_c = R_2$
4	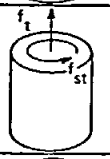	Longitudinal Tension + Torsion	$R_{st}^3 - \lvert R_t \rvert = 1$	B8.12.3 Refs.(12, 14)		$\lvert R_t \rvert < 0.8$ Let $R_{st} = R_1$ $\lvert R_t \rvert = R_2$
5	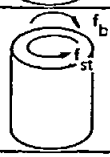	Longitudinal Bending + Torsion	$R_b^{1.5} + R_{st}^2 = 1$	B8.12.3 Ref.(10)		Let $R_b = R_1$ $R_{st} = R_2$
6	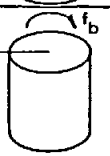	Longitudinal Bending + Transverse Shear				

Table B8.16.1 Unstiffened cylindrical shell structures-interaction criteria (initial buckling)(continued)

CASE	LOADING PICTURE	LOADING DESCRIPTION	INTERACTION CURVE		MARGIN-OF-SAFETY EQUATION	REMARKS
			EQUATION	FIGURE		
7	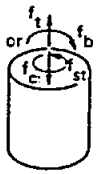	Longitudinal Compression or Tension + Longitudinal Bending + Torsion	$R_c + R_b + R_{st}^2 = 1$ or $R_t + R_b + R_{st}^2 = 1$	B8.12.5 ① Refs. (10, 12)	$\frac{2}{R_c+R_b+\sqrt{(R_c+R_b)^2+4R_{st}^2}}-1$ or $\frac{2}{R_t+R_b+\sqrt{(R_c+R_b)^2+4R_{st}^2}}-1$	Let $R_c + R_b = R_1$, $R_{st} = R_2$ or $R_t + R_b = R_1$, $R_{st} = R_2$

OMITTED

Table B8.16.1 Unstiffened cylindrical shell structures-interaction criteria (initial buckling)(concluded)

CASE	LOADING PICTURE	LOADING DESCRIPTION	INTERACTION CURVE EQUATION	INTERACTION CURVE FIGURE	MARGIN-OF-SAFETY EQUATION	REMARKS
11	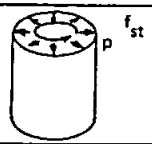	Torsion + Internal Pressure	$R_{st}^2 - \lvert R_p \rvert = 1$	B8.12.3 Refs.(15, 16)		Let $R_{st} = R_1$ $R_p = R_2$
12	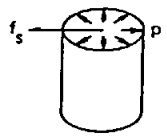	Transverse Shear + Internal Pressure	$R_s - \lvert R_p \rvert = 1$	B8.12.3		Interaction equation is conservative form of that given in Ref.(17) Let $R_s = R_1$ $R_p = R_2$
ELLIPTIC CYLINDER						
		OMITTED				
14	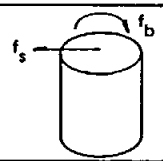	Longitudinal Bending + Transverse Shear	$R_b^2 + R_s^2 = 1$	B8.12.1 Ref.(10)	$\frac{1}{\sqrt{R_b^2 + R_s^2}} - 1$	
15		Longitudinal Bending + Torsion	$R_b^2 + R_{st}^2 = 1$	B8.12.1 Ref.(18)	$\frac{1}{\sqrt{R_b^2 + R_{st}^2}} - 1$	

NOTES:

(1) R_c, R_b, R_{st}, and R_s must be based on cylindrical shell initial buckling allowables.

(2) R_t is negative and is based on compression buckling allowable.

(3) For shear-bending analysis, use $f_s = f_{s_{max}}$ and $f_b = f_{b_{max}}$ even though the locations of the maxima do not coincide. The transverse shear buckling allowable stress is equal to 1.20 times the torsional buckling allowable.

(4) The interaction equations are applicable to both internally pressurized and unpressurized cylinders.

(5) $Z_L = L^2(1-\nu^2)^{\frac{1}{2}}/rt$

Grumman

Table B8.17.1 Stiffened structures-interaction criteria (stability)

CASE	LOADING PICTURE	LOADING DESCRIPTION	INTERACTION CURVE EQUATION	INTERACTION CURVE FIGURE	MARGIN-OF-SAFETY EQUATION	REMARKS
FLAT RECTANGULAR CORRUGATED PANELS						
1	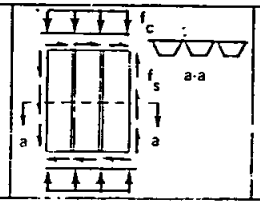	Longitudinal Compression + Shear	$R_c + R_s^{1.7} = 1$	B8.12.2		Interaction equation is derived from tests of "omega"-type corrugated panels (ref 19).
CURVED PANELS						
2	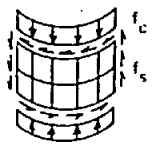	Longitudinal Compression + Shear	$R_c + R_s^2 = 1$	B8.12.2 Refs.(20, 21,22)	$\frac{2}{R_c + \sqrt{R_c^2 + 4R_s^2}} - 1$	Failure mode is given by stringer instability criteria.
CIRCULAR CYLINDERS						
3	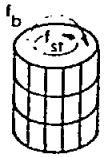	Longitudinal Bending + Torsion	$R_b + R_{st}^2 = 1$	B8.12.2 Refs.(23, 24)	$\frac{2}{R_b + \sqrt{R_b^2 + 4R_{st}^2}} - 1$	Failure mode is given by general instability criteria.
4	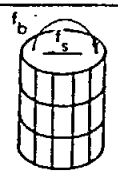	Longitudinal Bending + Shear	$R_b^\infty + R_s^\infty = 1$ (Zero interaction)	B8.12.1 Refs.(20, 25)	$\frac{1}{R_b} - 1$ or $\frac{1}{R_s} - 1$	Failure mode is given by general instability criteria.
5	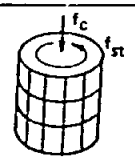	Longitudinal Compression + Torsion	$R_c + R_{st}^{1.5} = 1$	B.8.12.2 Refs.(22, 26)		Failure mode is given by stringer crippling criteria.

NOTES:

(1) R_c, R_p, R_s, and R_{st} must be based on stiffened structures stability criteria.

(2) For shear-bending analysis of circular cylinders use $f_s = f_{s_{max}}$ and $f_b = f_{b_{max}}$ even though the locations of the maxima do not coincide. For circular cylinder general instability failure criteria the allowable transverse shear stress is assumed to be equal to 0.80 times the allowable torsional shear stress.

B8.18 REFERENCES

1. Budiansky, B., Stein, M., and Gilbert, A., "Buckling of a Long Square Tube in Torsion and Compression", NACA TN 1751, 1948.

2. Libove, C., and Stein, Manuel, "Charts for Critical Combinations of Longitudinal and Transverse Direct Stress for Flat Rectangular Plates", NACA WR L-224 (Formerly NACA ARR No. L6A05), 1946.

3. Gerard, G., and Becker, H., "Handbook of Structural Stability - Part I - Buckling of Flat Plates", NACA TN 3781, 1957.

4. Batdorf, B., and Stein, M., "Critical Combinations of Shear and Direct Stress for Simply Supported Rectangular Flat Plates", NACA TN 1223, 1947.

5. Noel, R., "Elastic Stability of Simply Supported Flat Rectangular Plates Under Critical Combinations of Longitudinal Bending, Longitudinal Compression, and Lateral Compression, Jour. Aero. Sci., Vol. 19, No. 12, Dec. 1952, pp. 829-834.

6. Johnson, James, "Critical Buckling Stresses of Simply Supported Rectangular Plates Under Combined Longitudinal Compression, Transverse Compression and Shear", Jour. Aero. Sci., Vol. 21, 1954, pp. 411-416.

7. Grossman, N., "Elastic Stability of Simply Supported Flat Rectangular Plates Under Critical Combinations of Transverse Compression and Longitudinal Bending", Jour. Aero. Sci., Vol. 16, 1949, pp. 272-276.

8. Batdorf, S., and Houbolt, J., "Critical Combinations of Shear and Transverse Direct Stress for an Infinitely Long Flat Plate with Edges Elastically Restrained Against Rotation", NACA Rep. 847, 1946.

9. Stowell, E., and Schwartz, E., "Critical Stress for an Infinitely Long Flat Plate with Elastically Restrained Edges Under Combined Shear and Direct Stress", NACA WR L-340, 1943 (Formerly NACA ARR-3K13).

10. Gerard, G., and Becker, H., "Handbook of Structural Stability", Part III - Buckling of Curved Plates and Shells, NACA TN 3783, 1957.

11. Brown, E. and Hopkins, H., "The Initial Buckling of a Long and Slightly Bowed Panel Under Combined Shear and Normal Pressure", R and M 2766, 1949, pp. 1013-1031.

12. Bruhn, E., "Tests on Thin-Walled Celluloid Cylinders to Determine the Interaction Curves Under Combined Bending, Torsion, and Compression or Tension Loads", NACA TN 951, 1945.

13. Bridget, F., Jerome, C., and Vosseller, A., "Some New Experiments on Buckling of Thin-Wall Construction", Trans. A.S.M.E. Vol. 56, No. 8, Aug. 1934, pp. 569-578.

14. Batdorf, B., Stein, M., and Schildcrout, M., "Critical Combinations of Torsion and Direct Axial Stress for Thin-Walled Cylinders", NACA TN 1345, 1947.

B8.18 REFERENCES (Continued)

15. Hopkins, H., and Brown, E., "The Effect of Internal Pressure on the Initial Buckling of Thin Walled Circular Cylinders Under Torsion", R & M 2423, Jan. 1946, pp. 2165-2177.

16. Crate, H., Batdorf, S., and Baab, G., "Effect of Internal Pressure on the Buckling Stress of Thin Walled Circular Cylinders Under Torsion", NACA WR L-67 (Formerly NACA ARR No. L4 E27), 1944.

17. Abraham, Lewis, "Structural Design of Missiles and Spacecraft", McGraw Hill, New York, N. Y., 1962, pp. 195-197.

18. Lundguist, E., and Stowell, E., "Strength Tests of Thin-Walled Elliptic Duralumin Cylinders in Pure Bending and in Combined Pure Bending and Torsion", NACA TN 851, 1942.

19. Sanderson, P., and Fischel, R., "Corrugated Panels Under Combined Compression and Shear", Jour. Aero. Sci., Vol. 7, Feb. 1940, pp. 148-153.

20. Becker, H., "Handbook of Structural Stability", Part. IV - Strength of Stiffened Curved Plates and Shells, NACA TN 3786, 1958.

21. Melcon, M., and Ensrud, A., "Analysis of Stiffened Curved Panels Under Shear and Compression", Jour. Aero. Sci., Vol. 20, No. 2, Feb. 1953, pp. 111-119,126.

22. Peterson, J., "Experimental Investigation of Stiffened Circular Cylinders Subjected to Combined Torsion and Compression", NACA TN 2188, 1950.

23. Dunn, L., "Some Investigations of the General Instability of Stiffened Metal Cylinders IX - Criterions for the Design of Stiffened Metal Cylinders Subject to General Instability Failures", NACA TN 1198, 1947.

24. Kuhn, P., Peterson, J., and Ross, L., "A Summary of Diagonal Tension, Part I - Method of Analysis", NACA TN 2661, 1952.

25. Military Handbook, MIL-HDBK-5A, February 1966.

26. Sadowsky, M. A., "A Principle of Maximum Plastic Resistance", Journal of the Applied Mechanics, Vol. 10, No. 2, June 1943, pp. A65-A68.

27. Johnson, A. E., Jr., and Buchert, K. P., "Critical Combination of Bending, Shear, and Transverse Compressive Stresses for Buckling of Infinetly Long Flap Plates", NACA TN 2536, July 1951.

SECTION C - STRESS AND LOAD DISTRIBUTION

Table of Contents

SECTION C2 - SHEAR LAG IN FLAT PANELS

Table of Contents

DISCUSSION

The effect of shearing deformations upon stress distributions in continuous sheet structures is commonly known as "shear lag". The term was originated to describe the redistribution of bending stresses in box beams; currently it is also applied to the diffusion of any concentrated load into sheet material.

Exact Theory

There are a few exact shear lag solutions available based upon the theory of elasticity. These are mainly for unreinforced flat plate and are usually not directly applicable in design, but can sometimes be useful as a guide in making approximations. Several cases are included on the pages following this discussion. One is for a long plate bounded by constant stress edge members; the others are for deep beams.

Approximate Shear Lag Theory

Several approximate shear lag theory solutions are available for reinforced flat panels: The simplifying assumption is that the panels are rigid in the transverse direction. This makes the peak shear stress values artificially high locally, but does not materially affect the direct, longitudinal stresses.

A representative case from the RAS Data Sheets is included. It is for a long, reinforced panel bounded by constant stress edge members. Note that the accompanying discussion also covers approximate corrections for the post-buckling range. Titles of additional cases included in the RAS Data Sheets are given in Section A of this manual.

Another excellent reference for this class of problem is the book by P. Kuhn,* which includes a summary of the work done on shear lag by the NASA. The methods outlined have been used to advantage on several Grumman wing designs where a digital computer solution was not warranted.

Redundant Structure Solutions

A third approach to the analysis of shear lag is via the theory of redundant structures. Here the panel is idealized as consisting of a number of interacting bars and shear panels, or other simple structural elements.

When the idealization is very much simplified, the results may be presented in the form of design charts. Several are given in this section for reinforced plates subjected to opposing concentrated loads.

When the application justifies it, a more refined redundant structure analysis may be performed. The results can be expected to approach an exact solution for a reasonably detailed analysis. See Structural Methods Memo. 13, "Shear Lag in Unreinforced Flat Plates", 1959 and 1961.

* Kuhn, P., "Stress in Aircraft and Shell Structures", McGraw-Hill, 1956

STRESS DISTRIBUTION IN AN ELASTIC FLAT PANEL BOUNDED BY CONSTANT STRESS EDGE MEMBERS

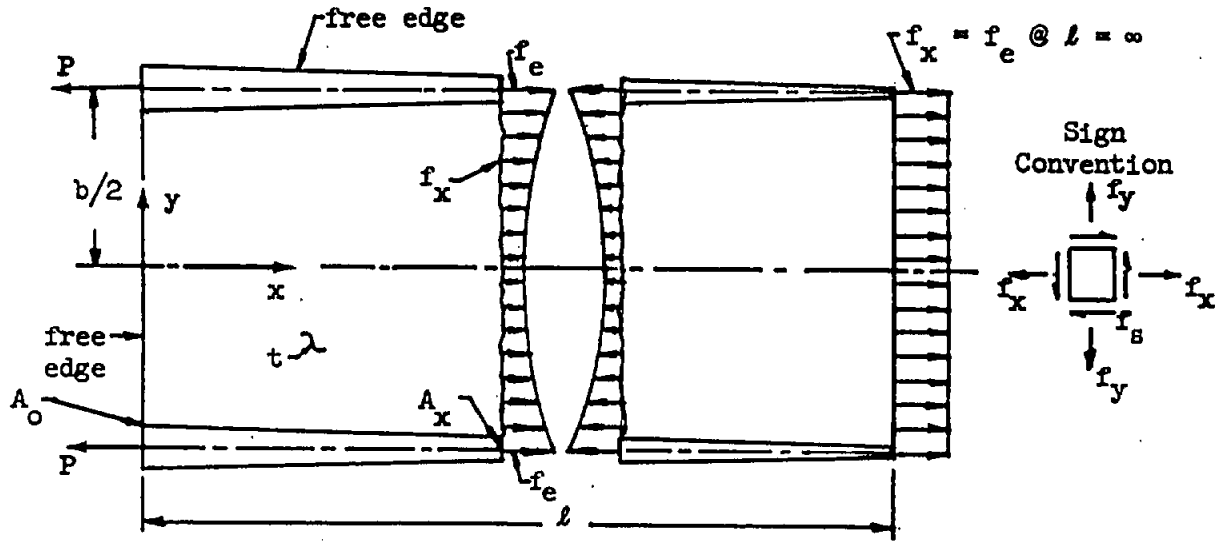

ℓ = Length of panel

b = Width of panel

P = Applied load

A_o = Area of edge member at x = 0

A_x = Area of edge member at x

t = Panel thickness

f_e = Stress in edge member

f_x, f_y, f_s = Stress in panel at (x, y)

The curves on the following two pages are based on an exact solution of the elasticity equations. These curves are valid for $\ell/b \geq 3$ and $A_o \geq bt/2$. The solution assumes no transverse support exists at the edge member so that $f_y = 0$ along its entire length.

EXAMPLE

Given: P = 33,200 lbs, b = 10 t = .036 in., A_o = 0.95 in.^{2}, ℓ = 30 in.

Find: f_x, f_y, f_s and A_x at the point (5, 2.5)

Solution: $\frac{\ell}{b} = 3$ $f_e = \frac{33,200}{0.95} = 35,000$ psi $\frac{x}{b} = 0.5$ $\frac{y}{b} = 0.25$

From figures 1, 2, 3 and 4 on the next two pages, the following are determined:

$$\frac{f_x}{f_e} = 0.5, \quad \frac{f_y}{f_e} = 0.12, \quad \frac{f_s}{f_e} = -0.28, \quad \frac{A_o - A_x}{\left(\frac{bt}{2}\right)} = 0.54$$

Then

f_x = 17,500 psi f_y = 4,200 psi f_s = -9,800 psi A_x = 0.853 in.^{2}

Reference - Mansfield, E. H.; "The Stress Distribution in Panels Bounded By Constant Stress Edge Members", Aeronautical Research Council R & M No. 2965, Jan. 1954.

STRESS DISTRIBUTION IN AN ELASTIC FLAT PANEL BOUNDED BY CONSTANT STRESS EDGE MEMBERS

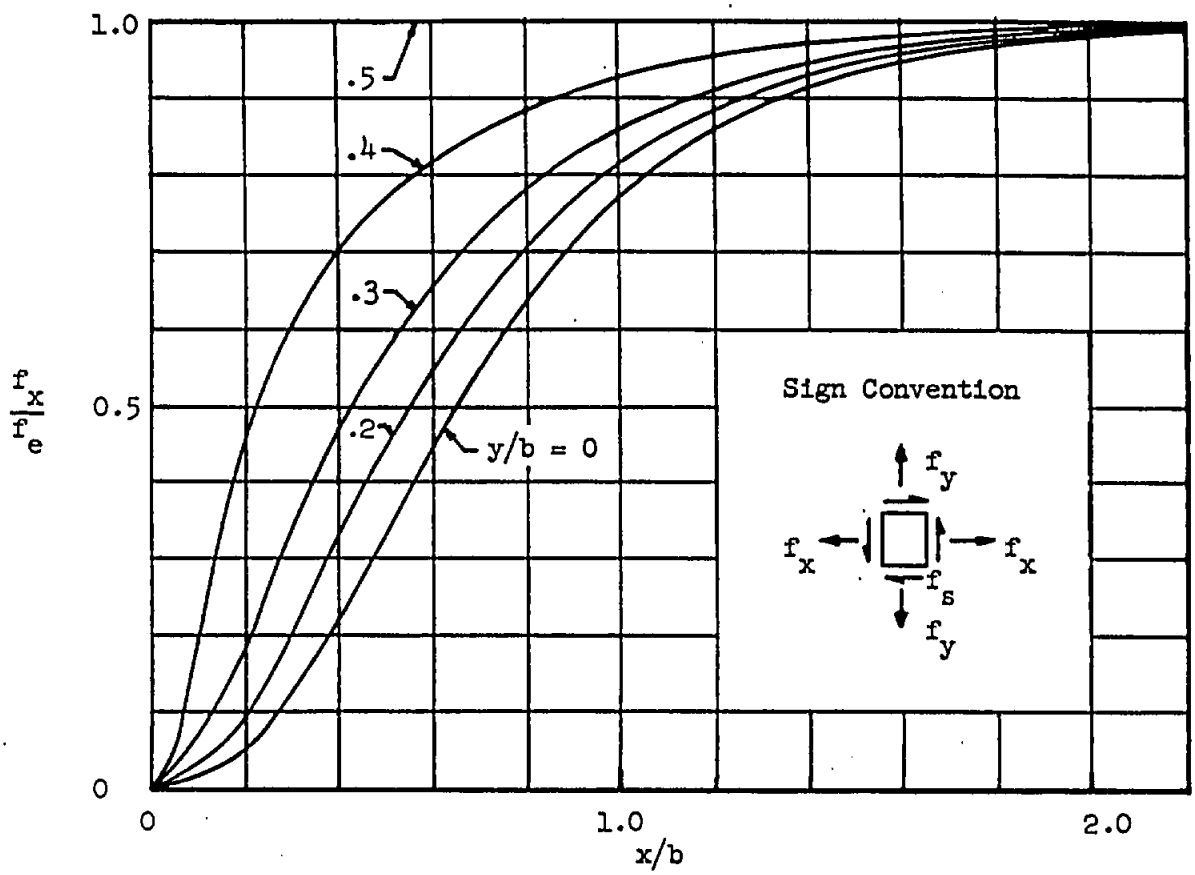

Fig. 1 Longitudinal Stress Ratio vs. x/b

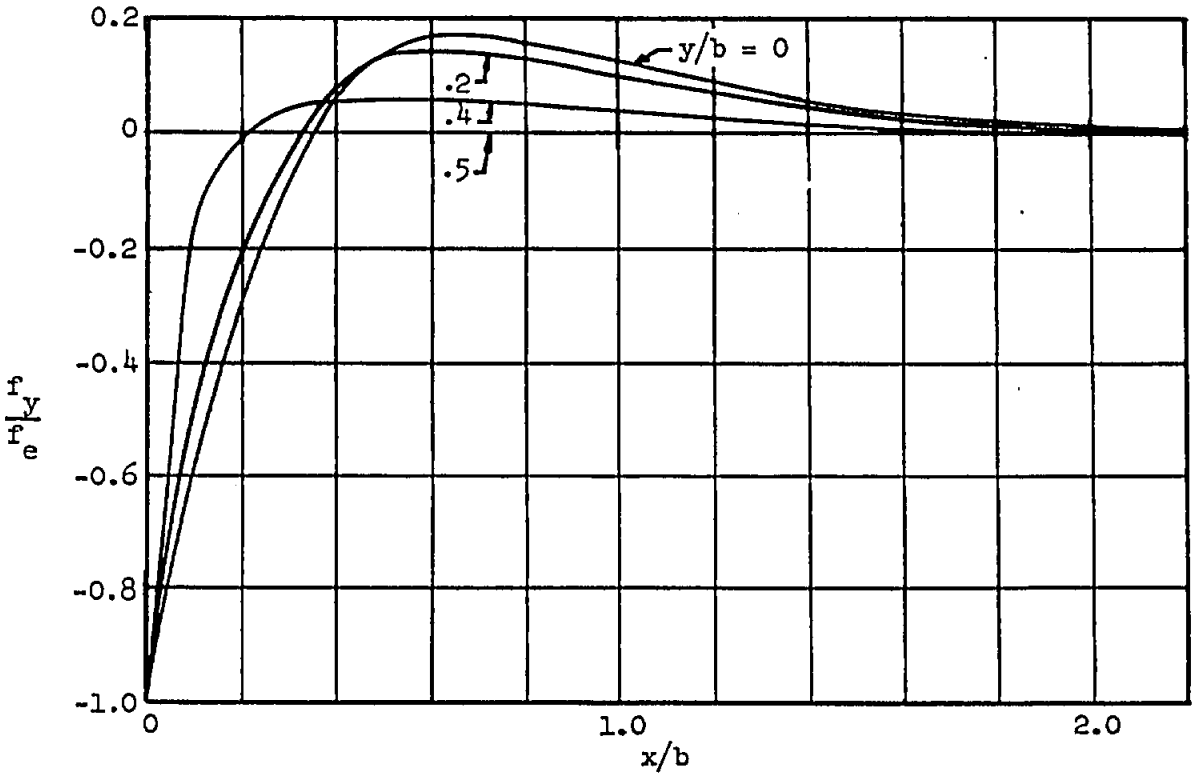

Fig. 2 Transverse Stress Ratio vs. x/b

STRESS DISTRIBUTION IN AN ELASTIC FLAT PLATE BOUNDED BY CONSTANT STRESS EDGE MEMBERS

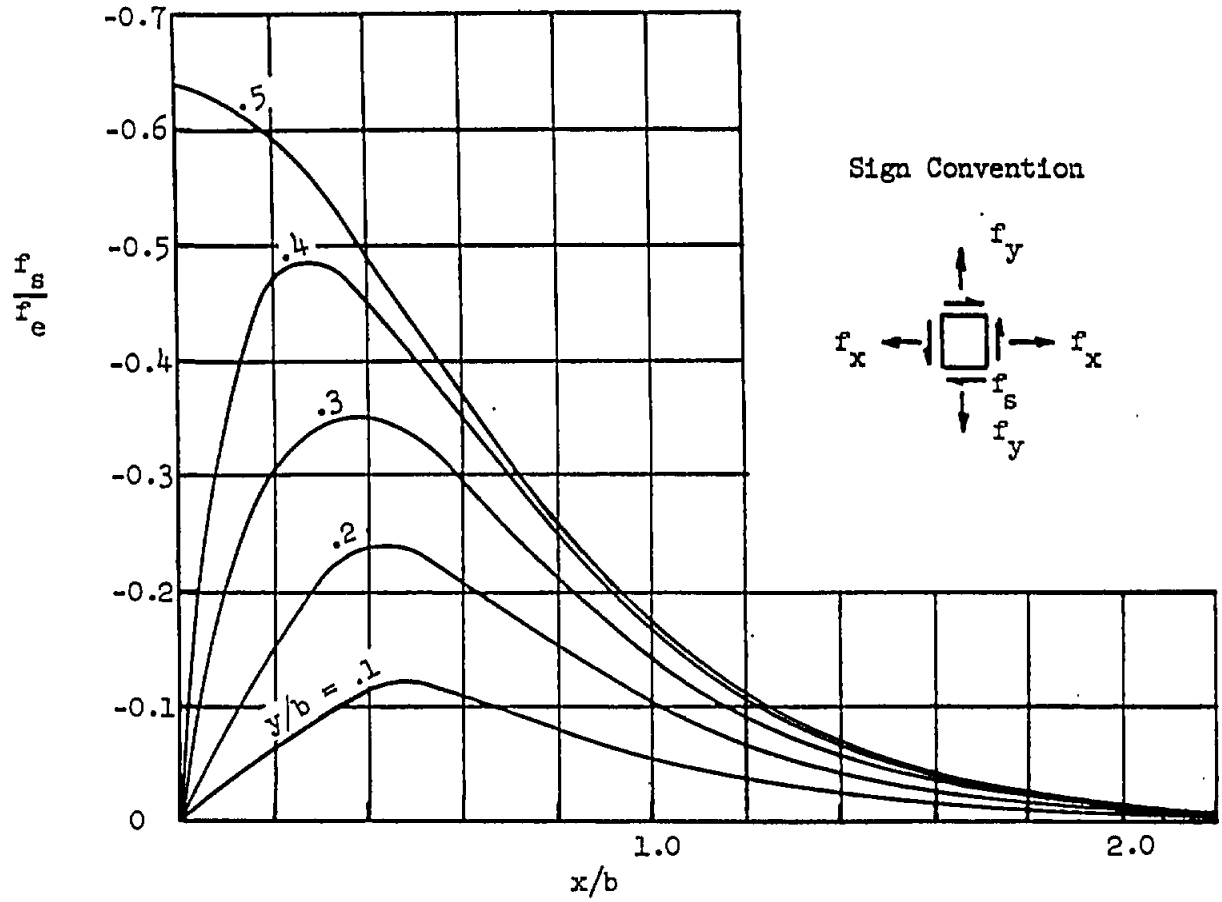

Fig. 3 Shear Stress vs. x/b

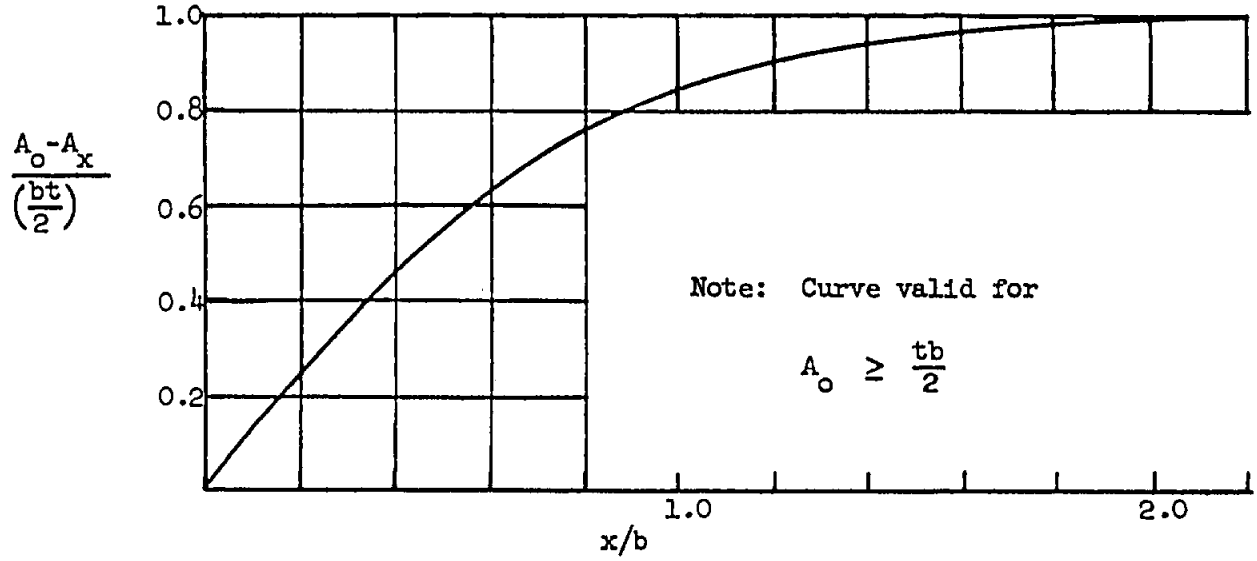

Fig. 4 Area of Edge Member vs. x/b

BENDING STRESS IN A DEEP BEAM OF INFINITE LENGTH WITH ALTERNATING LOADS ALONG AN EDGE

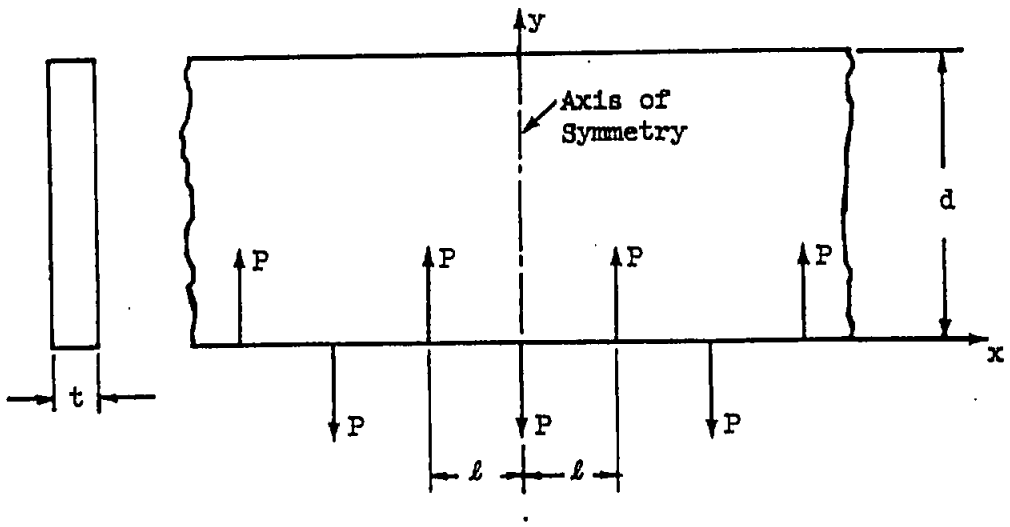

P = Applied load (lbs)
ℓ = Distance between applied loads (in.)
t = Beam thickness (in.)
d = Beam depth (in.)
I = Beam moment of inertia, $\frac{td^3}{12}$ $(in.^4)$
f_x = Stress in the x direction at the axis of symmetry $(lbs/in.^2)$

The graph shown below is a plot of the stress distribution on a beam section at the axis of symmetry. The stress f_o is the $\frac{"Mc"}{I}$ bending stress defined by equation (1). These curves are based on a solution of the elasticity equations for an elastic structure. The results are valid for P distributed over $\ell/10$. For P distributed less than $\ell/10$ the curves are unconservative. For P distributed greater than $\ell/10$ the curves are conservative. For the limiting case of P distributed over ℓ see the following page.

$$f_o = \left(\frac{P\ell}{4}\right)\left(\frac{d}{2I}\right) \qquad (1)$$

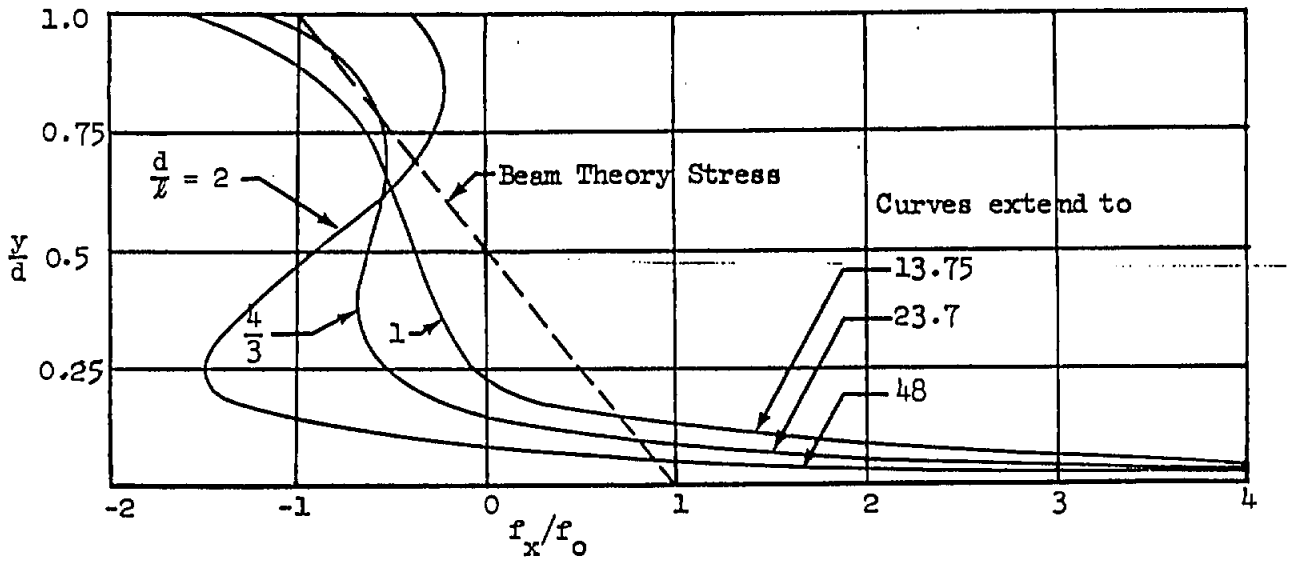

Ref. Portland Cement Assoc., "Design of Deep Girders", 1951

Grumman

BENDING STRESS IN A DEEP BEAM OF INFINITE LENGTH WITH ALTERNATING LOADS ALONG AN EDGE

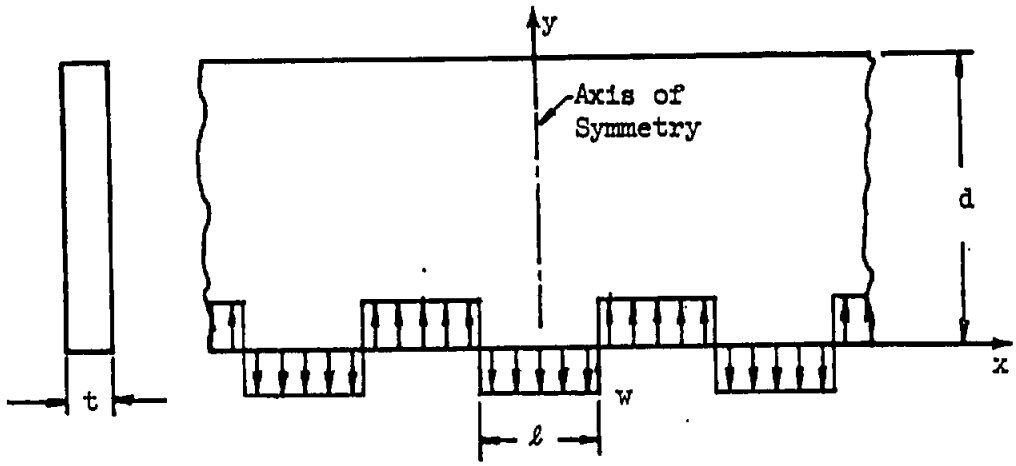

w = Uniform load (lbs/in.)
ℓ = Length of uniform load (in.)
t = Beam thickness (in.)
d = Beam depth (in.)
I = Moment of inertia, $\frac{td^3}{12}$ ($in.^4$)
f_x = Stress in the x direction at the axis of symmetry

The graph shown below is a plot of the stress distribution on a beam section at the axis of symmetry. The stress f_o, is the $\frac{"Mc"}{I}$ bending stress defined by equation (1). These curves are based on a solution of the elasticity equations for an elastic structure.

$$f_o = \left(\frac{w\ell^2}{8}\right)\left(\frac{d}{2I}\right) \qquad (1)$$

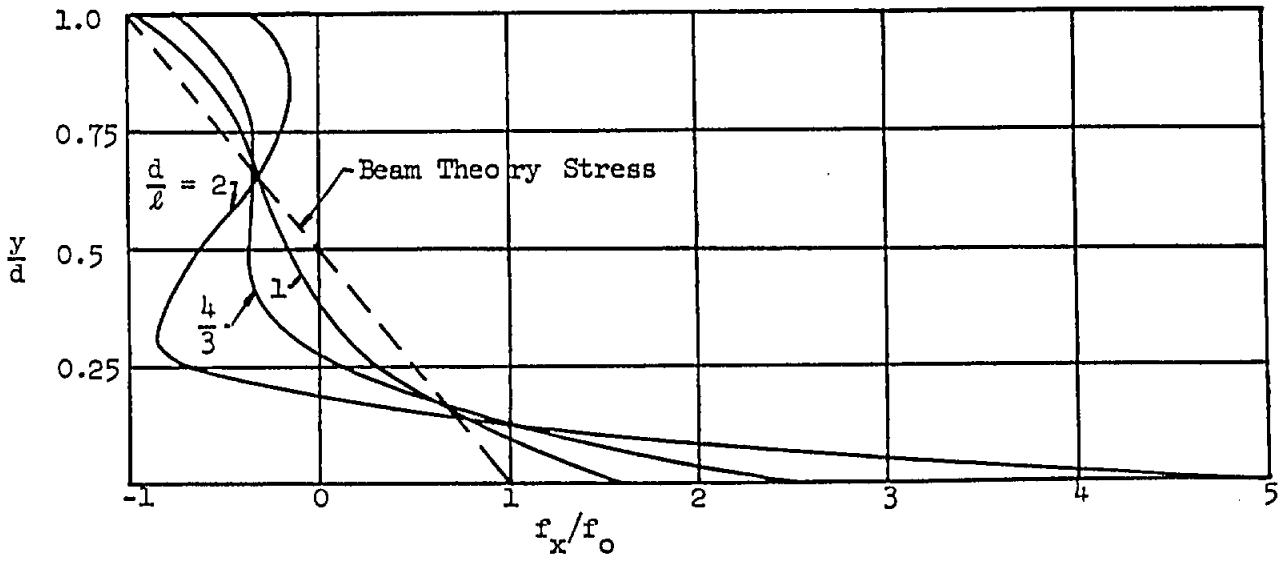

Ref. Portland Cement Association; "Design of Deep Girders", 1951

02.05.00

INFORMATION ON THE USE OF DATA SHEETS 02.05.

(Second Issue, July 1948)
(Second Reprint, February 1961)

1. Data Sheets 02.05 deal with the diffusion of loads into a flat uniform panel symmetrical about its centre line with equal stringers spaced uniformly across its width. The panel is assumed to be built-in at one end and free to warp in its plane at the other end. The loads are applied to special members, such as spar flanges or fuselage longerons, bordering the longitudinal edges of the panel; from these members the loads are diffused into the panel.

2. The data sheets are based upon the following assumptions:

   (*a*) The lateral direct strains are zero.

   (*b*) At any cross section the shear stress between adjacent stringers is constant; thus the effective sheet area under direct stress is concentrated along the line of attachment to the stringer.

   These assumptions are known to give good accuracy in panels typical of aircraft structures, in particular the exact condition of lateral restraint is relatively unimportant.

3. The sheets relate to two particular cases. In one the areas of section of the edge members are assumed to be constant. In the other the areas of the edge members are adjusted so that their strain is either uniform or varies linearly along their length.

   The loads which are diffused into the panel may be externally applied or may arise from a concentration of forces within the structure, due to openings or other sudden changes of section. The loading may be either symmetrical or anti-symmetrical about the centre line of the panel. Symmetrical load conditions arise for instance in the covers of rectangular doubly-symmetrical box beams under vertical lift loads. Anti-symmetrical load conditions occur in the cover when the box is under transverse (drag) loads or under torque. Other loadings may be represented by a combination of symmetrical and anti-symmetrical loadings.

4. The sheets relating to edge members of constant area deal with three types of applied loading:—concentrated end loads, uniform edge loads, and linearly varying edge loads. In those relating to edge members with constant or linearly varying strain the loading applied to the panel is completely specified by that strain, and the correlation between applied loading and strain of the edge members must be achieved by appropriate variation of their areas of section. In all these cases both symmetrical and anti-symmetrical loadings are treated. Sheets are also given showing how to calculate the stresses in a panel under constant edge strain when both ends are free to warp.

5. It is assumed that the ratio of the stiffness of the plate in shear to the stiffness of the stringers and sheet in tension or compression is constant over the whole panel. This assumption is strictly valid before buckling begins, and may be applied after buckling by the adoption of an average value of the stiffness ratio. Owing to the present limited knowledge of the stress distribution in a panel buckled under combined direct and shear stresses, in estimating the ratio of the two stiffnesses, the shear stiffness may be calculated as if the sheet were buckled under pure shear, and the contribution of the sheet to the compression stiffness may be calculated as if the sheet were buckled under pure compression. In the example of each individual data sheet a suitable procedure to obtain an average value of the stiffnesses is given.

6. The data sheets deal specifically with rectangular panels but may also be applied to panels of moderate taper, say not more than 3/2. For such cases the value of μl (*see* Data Sheet 02.05.01), the total load carried by the panel, and the edge shear stresses, can be calculated as for a rectangular panel of the same length and with cross-dimensions the same as those at the mid-section of the tapered panel.

7. Curvature of the panel has no effect on the diffusion provided that the edge members are constrained to remain straight. When the panel forms part of a structure in bending, and is subjected to symmetrical loading, allowance for curvature can be made by assuming an equivalent flat panel having stringer areas increased in the ratio

$$\left(1+\frac{2}{3}\frac{e}{h}\right)^2,$$

   where h = mean distance of edges from the neutral axis of the structure
   e = maximum rise of panel (cover) above line joining edges.

   The edge shear stress is then obtained directly from the flat panel data sheets, but the average stringer stress as calculated for the equivalent panel must be increased by the factor

$$\left(1+\frac{2}{3}\frac{e}{h}\right).$$

8. In the regions of high shear stress, as in the sheet adjoining the points of application of concentrated loads, the relief afforded by buckling and yielding of the plate may be supplemented by the give of the rivets or other forms of jointing. Special care must be taken in the design of the joints in these regions.

Reference - Royal Aeronautical Society Data Sheets, Volume 4, December 1963. Reproduced by Royalty agreement.

02.05.01

COEFFICIENT OF DIFFUSION FOR A UNIFORM PARALLEL PANEL

(*Third Issue, July 1947*)
(*Second Reprint, July 1962*)

NOTATION

l = length of panel (in)
t = sheet thickness (in)
a = distance between centroids of transverse members (in)
b = distance between centroids of adjacent stringers (in)
n = number of stringers
w = width of panel $= (n+1)\,b$ (in)
A_s = area of one stringer (in^2)
A_e = area of one stringer plus effective sheet (in^2)
E = Young's modulus of stringer (lbf/in^2)
G = shear modulus of material of sheet (lbf/in^2)
G_s = secant shear modulus of sheet (lbf/in^2)
μ = coefficient of diffusion $= (2/w)\{G_s bt/(EA_e)\}^{\frac{1}{4}}$ (in^{-1})

NOTES

The product μl is plotted against the ratio l/w for various values of the stiffness ratio $EA_e/(G_s bt)$.

The coefficient of diffusion μ determines the rate at which loads, acting along the length of the panel, are spread by means of shear in the sheet as direct stresses across the width of the panel.

It is assumed that the panel is of constant section along its length and has n uniformly spaced stringers.

As long as the sheet does not buckle $A_e = A_s + bt$ and $G_s = G$. After buckling A_e and G_s will be reduced. Since the sheet between the stringers is buckling under direct and shear stresses which vary over the panel, A_e and G_s will likewise vary. However, to apply this sheet in cases where buckling occurs, average values of A_e and G_s have to be adopted. Owing to the present limited knowledge of the stress distribution in a panel buckled under combined direct and shear stresses, an average value of A_e is calculated as if the sheet were buckled under pure compression. Accordingly, from Data Sheet 02.01.02 or 02.01.03,

$$A_e = A_s + bt(f_{\text{average}}/f_{\text{edge}})$$

where the appropriate value of f_{edge} depends on the edge strains or edge loadings of the panel as specified in each particular data sheet. Similarly a value of G_s is calculated from Data Sheet 02.03.10 as if the sheet were buckled under pure shear on the basis of an equivalent average shear stress as specified in each particular data sheet.

It should be noted that, on Data Sheets 02.01.02 and 02.01.03, f_{average} and f_{edge} are written f_a and f_e.

DERIVATIONS

COX. Diffusion of Concentrated Loads into Monocoque Structures, III, R. & M. 1860, 1938.

HADJI-ARGYRIS and COX. Diffusion of Load into Flat Stiffened Panels of Varying Cross-section. R. & M. 1969, 1944.

HADJI-ARGYRIS. Diffusion of Symmetrical Loads into Stiffened Parallel Panels with Constant Area Edge Members. R. & M. 2038, 1944.

HADJI-ARGYRIS. Diffusion of Anti-Symmetrical Concentrated End Loads and Edge Loads into Parallel Stiffened Panels and Analysis of Parallel Panels under Transverse Loads. A.R.C. 9662, 1946.

EXAMPLE

To find μl for a panel when

$l = 90$ in, $t = 0{\cdot}036$ in, $b = 6{\cdot}25$ in, $n = 7$, $A_s = 0{\cdot}247$ in^2,
$E = 10 \times 10^6$ lbf/in^2, $G_s = 1{\cdot}85 \times 10^6$ lbf/in^2.

Then $w = (n+1)b = 50$ in, $l/w = 1{\cdot}80$ and $EA_e/(G_s bt) = 5{\cdot}93$.

From diagram, $\mu l = 1{\cdot}5$.

Reference - Royal Aeronautical Society Data Sheets, Volume 4, December 1963. Reproduced by Royalty Agreement.

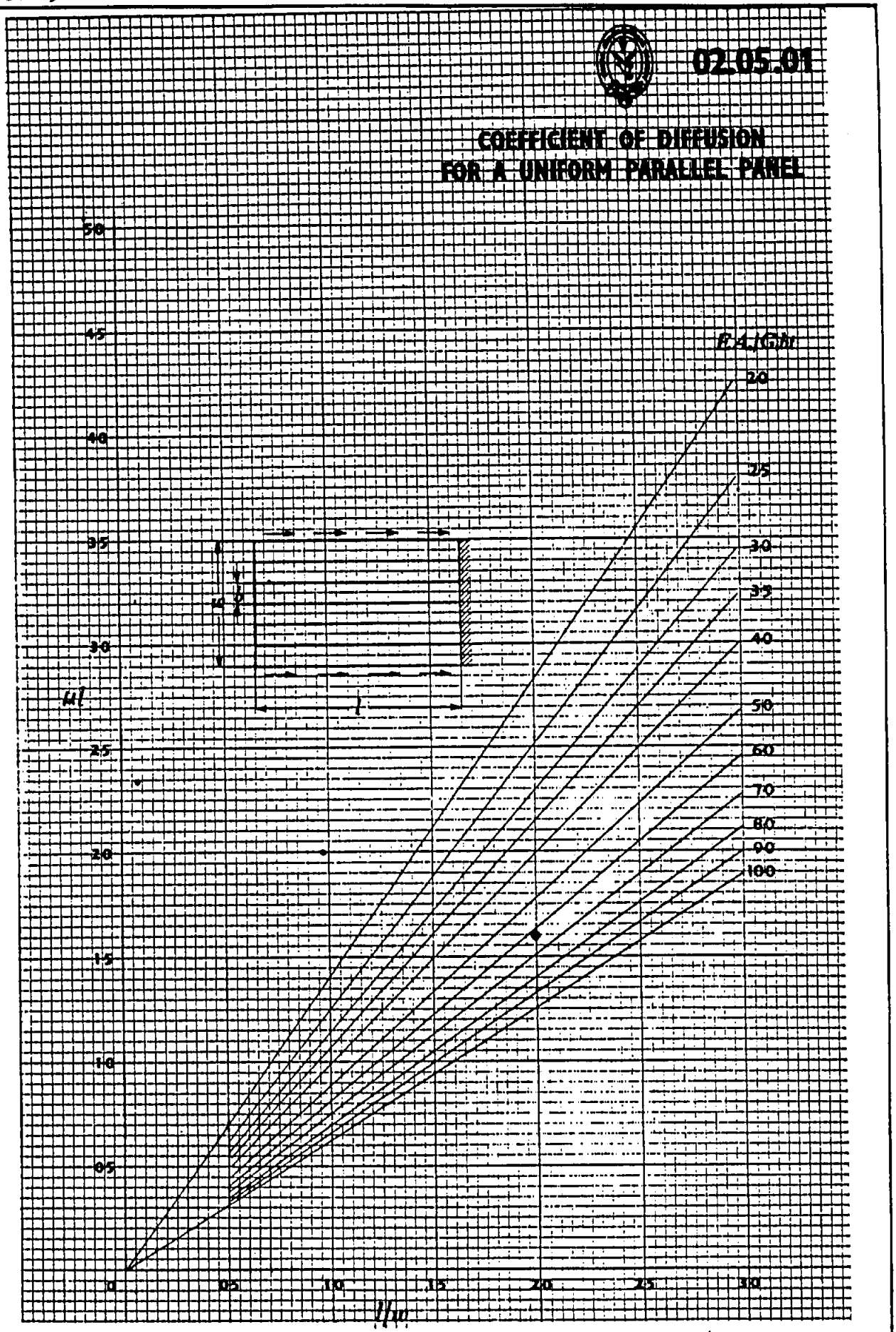

Reference - Royal Aeronautical Society Data Sheets, Volume 4, December 1963. Reproduced by Royalty Agreement.

Grumman

02.05.02

AVERAGE STRINGER STRESS FOR A UNIFORM PANEL WITH CONSTANT EDGE STRAIN

(*Third Issue, July 1947*)
(*Second Reprint, May 1962*)

NOTATION

l = panel length (in)
x = distance of cross section from free end of panel (in)
t = sheet thickness (in)
a = distance between centroids of transverse members (in)
b = distance between centroids of adjacent stringers (in)
n = number of stringers
w = width of panel $= (n+1)\,b$ (in)
A_s = area of one stringer (in^2)
A_e = area of one stringer plus effective sheet (in^2)
f = constant direct stress along edges of panel (lbf/in^2)
f_s = average direct stress in stringers and effective sheet at section x (lbf/in^2)
q_s = equivalent average shear stress $= nA_sf/(2lt)$ (lbf/in^2)
G = shear modulus of material of sheet (lbf/in^2)
G_s = secant shear modulus of sheet (lbf/in^2)
μ = coefficient of diffusion from Data Sheet 02.05.01 (in^{-1})

NOTES

The ratio f_s/f is plotted against the ratio x/l for various values of μl.

It is assumed that the panel is of constant section along its length and that the edge members are subjected to constant and equal strains corresponding to a stress f. The data sheet is based on a seven stringer panel, but may be applied to panels with four or more stringers with little loss of accuracy. The end section at $x=0$ is unconstrained, and the other end section (at $x=l$) is constrained to remain plane. This constraint may result from a symmetrical arrangement of the structure and its loading about the section at $x=l$.

The average value of A_s may be found on the lines indicated in Data Sheet 02.05.01 taking $f_{stgr}=f$. An average value of G_s, corresponding to q_s, may be found from Data Sheet 02.03.10 on the assumption that the shear stress at the edge is uniform and ordinary engineering theory applies at $x=l$. For large values of μl, f_s approaches f.

DERIVATIONS

HADJI-ARGYRIS and COX. Diffusion of Load into Flat Stiffened Panels of Varying Cross Section, R. & M. 1969 (1944).

COX. Diffusion of Concentrated Loads into Monocoque Structures, III, R. & M. 1860 (1938).

EXAMPLE

To find the average stringer stress in a panel at $x=0{\cdot}75l$ when
$l=90$ in, $b=6{\cdot}25$ in, $a=15$ in, $t=0{\cdot}036$ in, $n=11$, $A_s=0{\cdot}175$ in^2,
A_t = cross-sectional area of edge member $=1{\cdot}2$ in^2 at $x/l=0{\cdot}75$,
I_t = second moment of area of edge member about an axis through its centroid normal to the panel $=0{\cdot}72$ in^4 at $x/l=0{\cdot}75$,
$E=10\times10^6$ lbf/in^2, $G=3{\cdot}85\times10^6$ lbf/in^2, $f=35{,}000$ lbf/in^2.

To obtain μl, A_e and G_s must be known.

From Data Sheet 02.01.03, $A_e=A_s+bt\,(f_{s\,average}/f_{stgr})$.

Taking $f_{stgr}=f=35{,}000$ lbf/in^2, for $b/t=174$, from Data Sheet 02.01.03, $f_{s\,average}=11{,}300$ lbf/in^2.

Then $bt\,(f_{s\,average}/f_{stgr})=0{\cdot}073$ in^2, and $A_e=0{\cdot}175+0{\cdot}073=0{\cdot}248$ in^2.

From Data Sheet 02.03.01 curve (4) for $b/a=0{\cdot}42$, $q_b=1{,}860$ lbf/in^2.

Continuing, $w=12b=75$ in, $l/w=1{\cdot}2$, and the equivalent average shear stress is
$q_s=nA_sf/(2lt)=11\times0{\cdot}248\times35{,}000/(2\times90\times0{\cdot}036)=14{,}700$ lbf/in^2.

Thus $q_s/q_b=7{\cdot}9$.

From Data Sheet 02.03.10, for $A_s/bt=0{\cdot}8$, and $A_t/ht=A_t/wt=0{\cdot}45$, $G_s/G=0{\cdot}65$, whence $G_s=2{\cdot}50\times10^6$ lbf/in^2, and $EA_s/(G_sbt)=4{\cdot}41$.

The flange flexibility parameter $B=0{\cdot}003$; therefore the effect of flange flexibility may be ignored.

From Data Sheet 02.05.01, $\mu l=1{\cdot}14$,

From diagram, by interpolation,
$f_s/f=0{\cdot}66$ and $f_s=0{\cdot}66\times35{,}000=23{,}100$ lbf/in^2.

Reference - Royal Aeronautical Society Data Sheets, Volume 4, December 1963. Reproduced by Royalty Agreement.

02.05.02

AVERAGE STRINGER STRESS FOR A UNIFORM PANEL WITH CONSTANT EDGE STRAIN

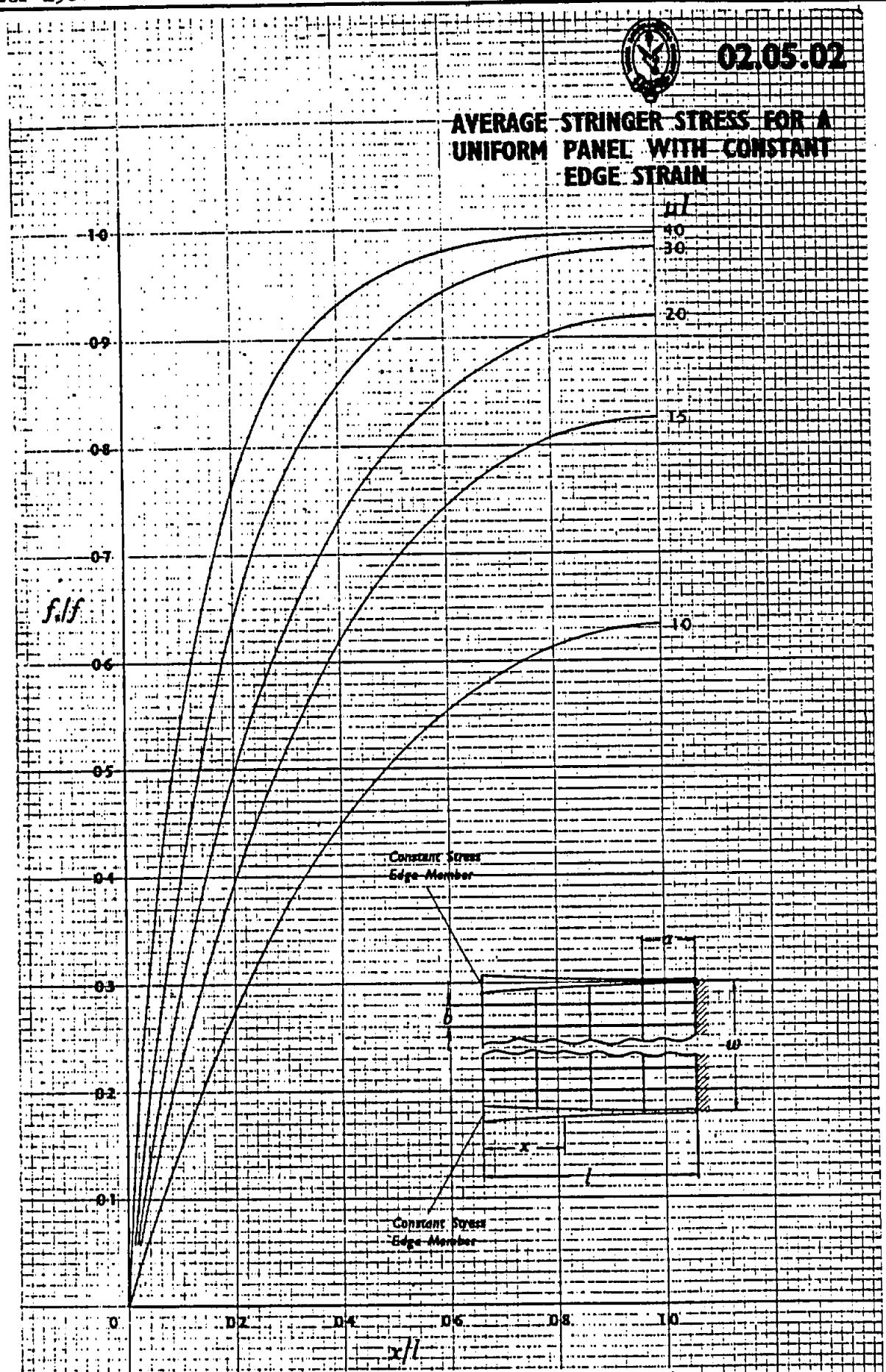

Reference - Royal Aeronautical Society Data Sheets, Volume 4, December 1963. Reproduced by Royalty Agreement.

Grumman

02.05.03

EDGE SHEAR STRESSES IN A UNIFORM 5 STRINGER PANEL WITH CONSTANT EDGE STRAIN

(Third Issue, July 1947)
(Second Reprint, July 1962)

NOTATION

l = panel length (in)
x = distance of cross section from free end of panel (in)
t = sheet thickness (in)
a = distance between centroids of transverse members (in)
b = distance between centroids of adjacent stringers (in)
w = width of panel (in)
A_s = area of one stringer (in²)
A_e = area of one stringer plus effective sheet (in²)
f = constant direct stress along edges of panel (lbf/in²)
q = shear stress in sheet adjacent to edge members at section x (lbf/in²)
q_a = equivalent average shear stress $= 5A_s f/(2lt)$ (lbf/in²)
E = Young's modulus of stringer (lbf/in²)
G = shear modulus of material of sheet (lbf/in²)
G_s = secant shear modulus of sheet (lbf/in²)
μ = coefficient of diffusion from Data Sheet 02.05.01 (in⁻¹)

NOTES

The ratio $(q/f)\{Ebt/(G_sA_e)\}^{\frac{1}{2}}$ is plotted against the ratio x/l for various values of μl, and can also be written in the form

$$(q/f)\,(G_s/E)\,(\mu w/2).$$

It is assumed that the panel is of constant section along its length with 5 equally spaced stringers, and that the edge members are subjected to constant and equal strains corresponding to a stress f. The end section of the panel at $x=0$ is unconstrained and the other end section (at $x=l$) is constrained to remain plane. This constraint may result from an arrangement of the structure and its loading symmetrical about the section at $x=l$.

The shear stress varies anti-symmetrically across the width of the panel and at any section is a maximum at the edges. The shear stress along the edge increases rapidly towards the free end of the panel, where in practice it may be relieved by buckling, yielding of the sheet, or give of the joint.

An average value of A_e may be found on the lines indicated in Data Sheet 02.05.01 taking $f_{edge}=f$. An average value of G_s, corresponding to q_a, may be found from Data Sheet 02.03.10 on the assumption that the shear stress at the edge is uniform and the ordinary engineering theory applies at $x=l$.

For shear stresses in panels with 10 or 30 stringers *see* Data Sheets 02.05.04 and 02.05.05.

DERIVATION

HADJI-ARGYRIS and COX. Diffusion of Load into Flat Stiffened Panels of Varying Cross Section. R. & M. 1969, 1944.

COX. Diffusion of Concentrated Loads into Monocoque Structures, III. R. & M. 1860, 1938.

EXAMPLE

To find the edge shear stress in a 5 stringer panel at $x=a/2$ when
$l=60$ in, $b=6{\cdot}1$ in, $a=12$ in, $t=0{\cdot}036$ in, $A_s=0{\cdot}13$ in², A_t = cross-sectional area of edge member $=0{\cdot}4$ in² at $x=a/2$, I_t = second moment of area of edge member about an axis through its centroid normal to the panel $=0{\cdot}069$ in⁴ at $x=a/2$, $E=10\times10^6$ lbf/in², $G=3{\cdot}85\times10^6$ lbf/in², $f=39{,}000$ lbf/in².

To obtain μl, A_e and G_s must be known.

From Data Sheet 02.01.03, $A_e=A_s+bt\,(f_{average}/f_{edge})$.

Taking $f_{edge}=f=39{,}000$ lbf/in², for $b/t=170$, from Data Sheet 02.01.03, $f_{average}=12{,}500$ lbf/in².

Then $bt(f_{average}/f_{edge})=0{\cdot}071$ in², and $A_e=0{\cdot}13+0{\cdot}071=0{\cdot}201$ in².

From Data Sheet 02.03.01, curve (4), for $b/t=170$ and $b/a=0{\cdot}5$, $q_b=2{,}030$ lbf/in².

Continuing, $x/l=0{\cdot}1$, $w=6b=36{\cdot}6$ in, $l/w=1{\cdot}64$,
and the equivalent average shear stress is

$$q_a=5A_sf/(2lt)=5\times0{\cdot}201\times39{,}000/(2\times60\times0{\cdot}036)=9{,}070\text{ lbf/in}^2.$$

Thus $q_a/q_b=4{\cdot}5$.

From Data Sheet 02.03.10, for $A_s/bt=0{\cdot}6$ and $A_t/ht=A_t/wt=0{\cdot}30$,
$G_s/G=0{\cdot}68$, whence $G_s=2{\cdot}62\times10^6$ lbf/in², and $EA_s/(G_sbt)=3{\cdot}5$.

Flange flexibility parameter $B=0{\cdot}05$, therefore the effect of flange flexibility may be ignored.

From Data Sheet 02.05.01, $\mu l=1{\cdot}77$.

From diagram, by interpolation,

$$(q/f)\{Ebt/(G_sA_e)\}^{\frac{1}{2}}=1{\cdot}03.$$

Hence, since $Ebt/(G_sA_e)=4{\cdot}17$,

$$q/f=0{\cdot}51 \text{ and } q=0{\cdot}51\times39{,}000=19{,}900\text{ lbf/in}^2.$$

If G_s were calculated with the local value of q the corresponding result would be

$$q=18{,}400\text{ lbf/in}^2.$$

Reference - Royal Aeronautical Society Data Sheets, Volume 4, December 1963. Reproduced by Royalty Agreement.

02.05.03

EDGE SHEAR STRESSES IN A UNIFORM 5-STRINGER PANEL WITH CONSTANT EDGE STRAIN

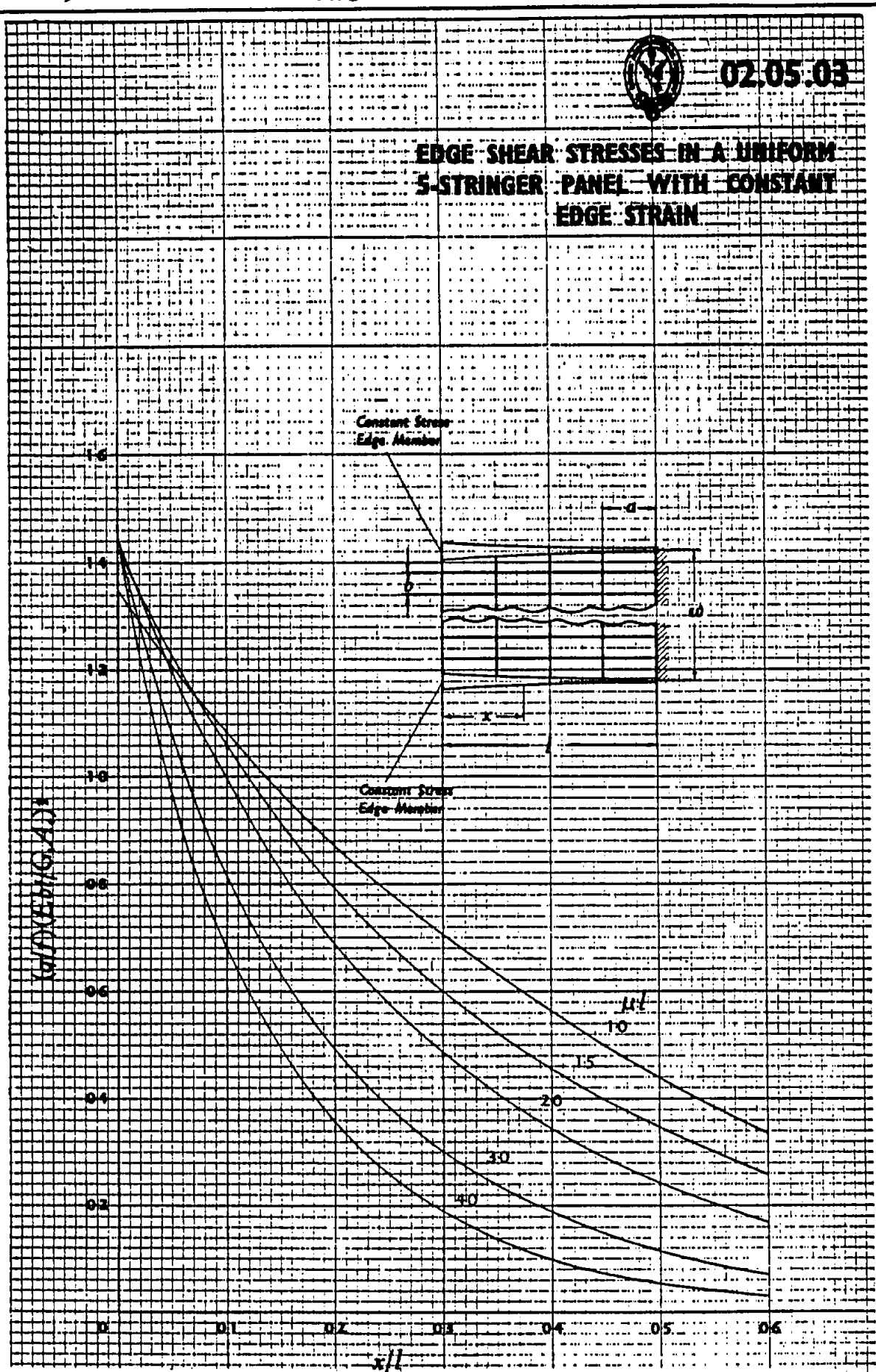

Reference - Royal Aeronautical Society Data Sheets, Volume 4, December 1963. Reproduced by Royalty Agreement.

Grumman

SHEAR LAG IN A FOUR BAY PANEL DUE TO OPPOSING EDGE LOADS

True Structure

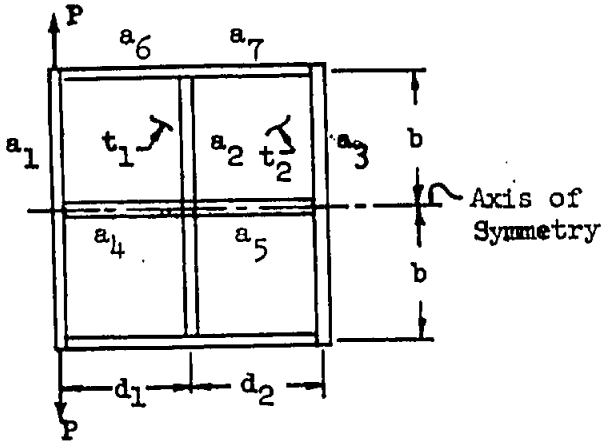

Idealized Structure

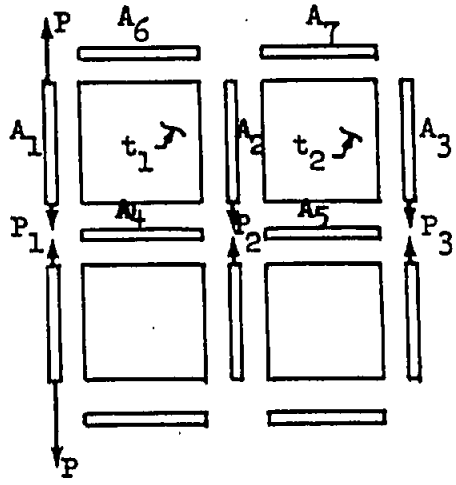

$a_1, \ldots a_7$ - True stringer area (in.^{2})

$A_1, \ldots A_7$ - Effective stringer area; true area plus effective skin (in.^{2})

t_1, t_2 - Panel skin thickness (in.)

d_1, d_2 - Panel length (in.)

b - Panel width (in.)

E - Young's Modulus (lbs/in.^{2})

G - Shear Modulus (lbs/in.^{2})

P_1, P_2, P_3 - Axial load in members 1, 2 and 3 at the axis at symmetry (lbs)

The graph on the following page is a plot of the ratio P_1/P vs β, where β is defined by equation (1). The ratios P_2/P and P_3/P are defined by equations (2) and (3). The curves are based on a redundant analysis which assumes the structure is in the elastic non-buckled state. Interaction effects between the longitudinal and transverse stringer stresses are small for this type of structure and are neglected. The curves are valid for $0.5 \leq d_1/b \leq 2$ and $0.5 \leq d_2/b \leq 2$.

$$\beta = \frac{2d_1}{d_2} + \left(\frac{d_1}{d_2}\right)^2 \left(1 + \frac{A_2}{A_3}\right) + \frac{3EA_2d_1}{Gb^2t_1}\left(1 + \frac{d_1t_1}{d_2t_2}\right) + \left(\frac{d_1}{b}\right)^3 \left[\frac{2A_2}{A_4} + \frac{A_2}{A_6} + \left(\frac{d_2}{d_1}\right)\left(\frac{2A_2}{A_5} + \frac{A_2}{A_7}\right)\right] \quad (1)$$

$$\frac{P_2}{P} = \left(1 + \frac{d_1}{d_2}\right)\left(1 - \frac{P_1}{P}\right) \quad (2)$$

$$\frac{P_3}{P} = \frac{d_1}{d_2}\left(\frac{P_1}{P} - 1\right) \quad (3)$$

SHEAR LAG IN A FOUR BAY PANEL DUE TO OPPOSING EDGE LOADS

Ratio of Stringer Loads vs β

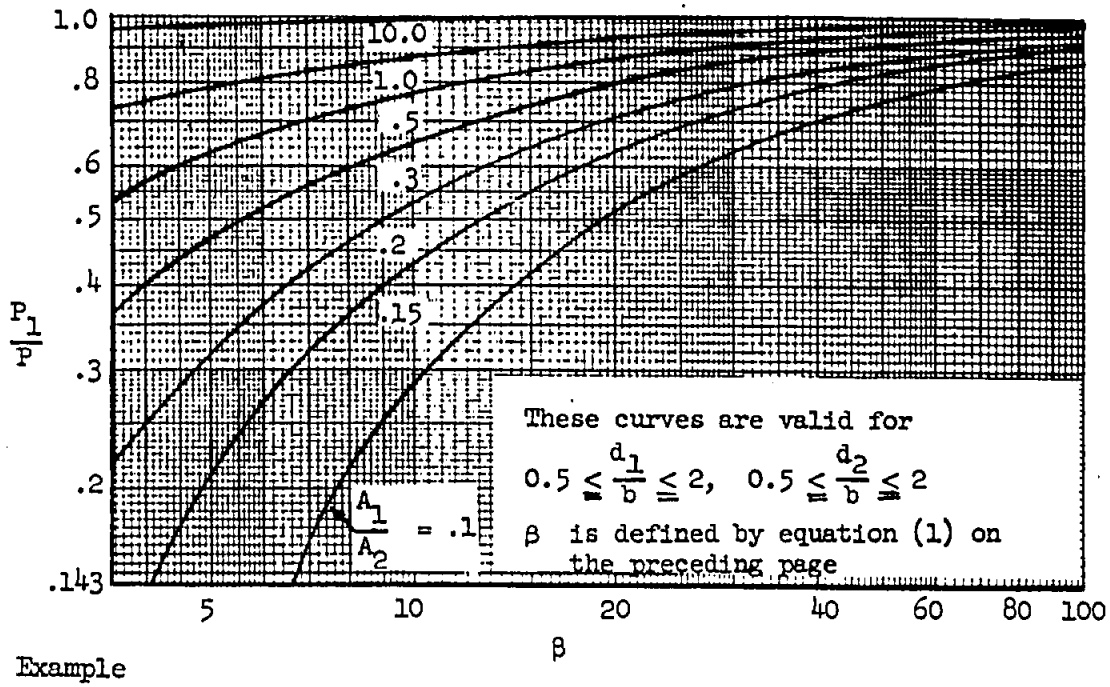

Example

Determine the stress distribution at the axis of symmetry for the structure shown below.

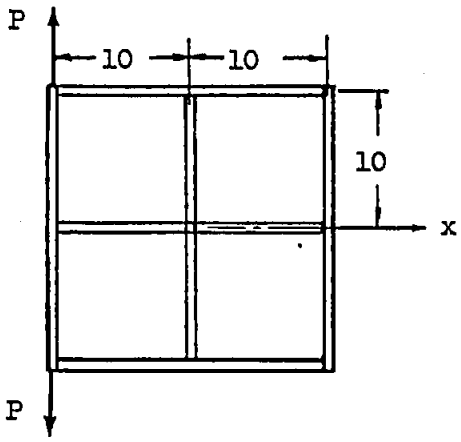

Plot of Stress at Symmetry Axis

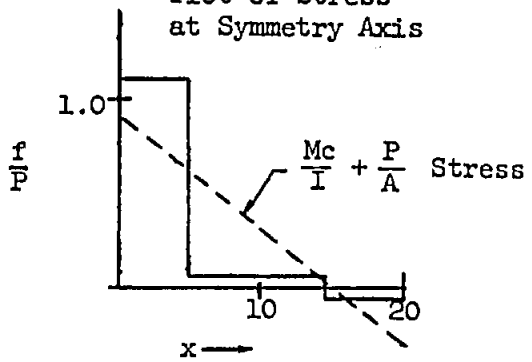

Given: $a_1 = a_3 = a_6 = a_7 = 0.5$ in.^{2} $\frac{E}{G} = 2.6$

$a_4 = a_5 = a_2 = 1.0$ in.^{2}

$t_1 = t_2 = .070$ in.

$d_1 = d_2 = b = 10$

Compute:

$A_1 = A_3 = A_6 = A_7 = 0.5 + 5\,(.070) = 0.85$ in.^{2}

$A_4 = A_5 = A_2 = 1.0 + 10\,(.070) = 1.70$ in.^{2}

from (1) $\beta = 50.9$

from curve, $\frac{P_1}{P} = 0.94$

from (2) & (3) $\frac{P_2}{P} = 0.12$, $\frac{P_3}{P} = -0.06$

then, $f_1 = \frac{P_1}{A_1} = 1.105P$

$f_2 = \frac{P_2}{A_2} = .071P$

$f_3 = \frac{P_3}{A_3} = -.071P$

SHEAR LAG IN A FOUR BAY PANEL DUE TO OPPOSING INTERIOR LOADS

True Structure

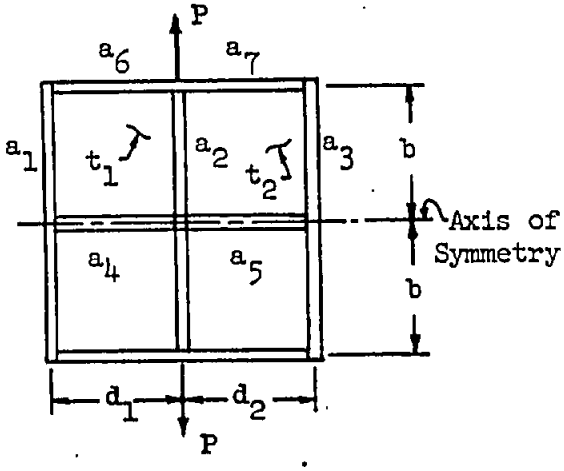

Idealized Structure

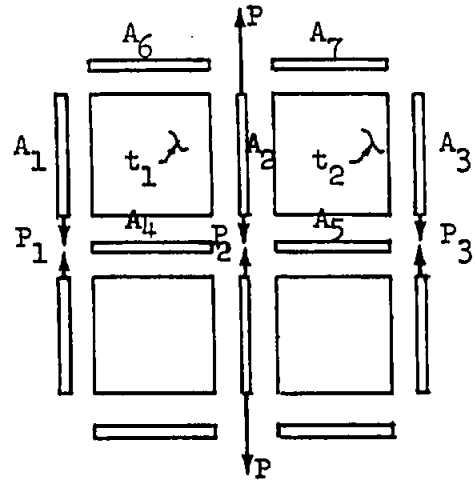

$a_1, \ldots a_7$ - True stringer area (in.^{2})

$A_1, \ldots A_7$ - Effective stringer area; true area plus effective skin. (in.^{2})

t_1, t_2 - Panel skin thickness (in.)

d_1, d_2 - Panel length (in.)

b - Panel width (in.)

E - Young's Modulus (lbs/in.^{2})

G - Shear Modulus (lbs/in.^{2})

P_1, P_2, P_3 - Axial load in members 1, 2 and 3 at the axis of symmetry (lbs)

The graph on the following page is a plot of the ratio $\left[2/(1 + d_1/d_2)\right]P_1/P$ vs β, where β is defined by equation (1). The ratios P_2/P and P_3/P are defined by equations (2) and (3). The curves are based upon a redundant analysis which assumes the structure is in the elastic non-buckled state. Interaction effects between the longitudinal and transverse stringer stresses are small for this type of structure and are neglected. The curves are valid for $0.5 \leq d_1/b \leq 2$ and $0.5 \leq d_2/b \leq 2$.

$$\beta = \frac{2d_1}{d_2} + \left(\frac{d_1}{d_2}\right)^2 \left(1 + \frac{A_2}{A_3}\right) + \frac{3EA_2d_1}{Gb^2t_1}\left(1 + \frac{d_1t_1}{d_2t_2}\right) + \left(\frac{d_1}{b}\right)^3 \left[\frac{2A_2}{A_4} + \frac{A_2}{A_6} + \left(\frac{d_2}{d_1}\right)\left(\frac{2A_2}{A_5} + \frac{A_2}{A_7}\right)\right] \qquad (1)$$

$$\frac{P_2}{P} = 1 - \left(1 + \frac{d_1}{d_2}\right)\left(\frac{P_1}{P}\right) \qquad (2)$$

$$\frac{P_3}{P} = \frac{d_1}{d_2}\,\frac{P_1}{P} \qquad (3)$$

SHEAR LAG IN A FOUR BAY PANEL DUE TO OPPOSING INTERIOR LOADS

Ratio of Stringer Loads vs β

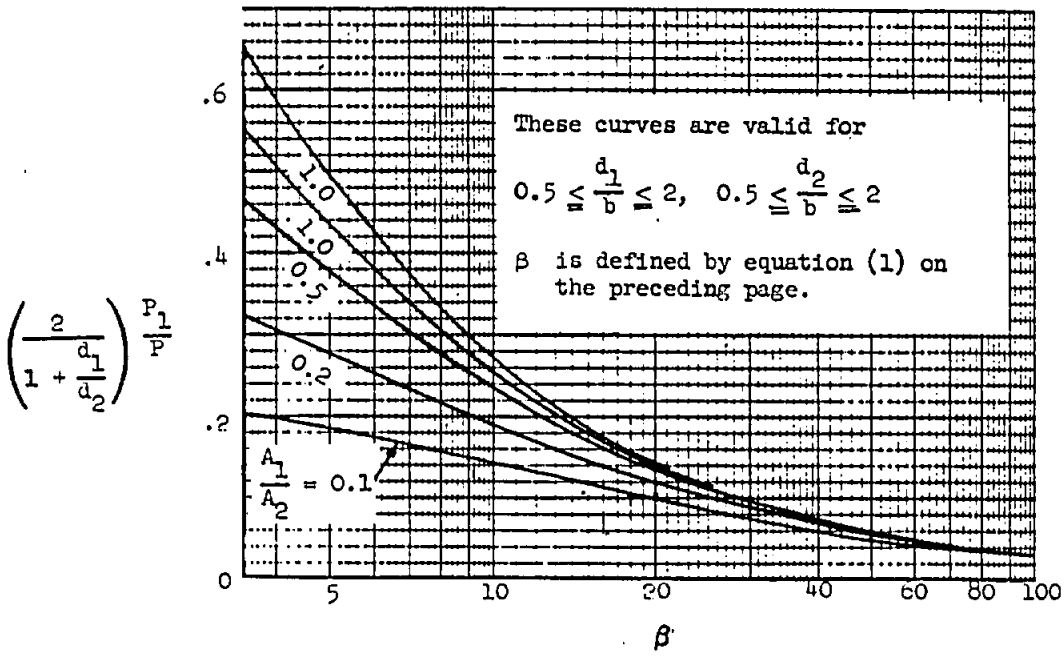

Example

Compare the prediction of the present method with a solution of an infinite unreinforced plate given in Timoshenko's "Theory of Elasticity", 1934 Ed., Page 48.

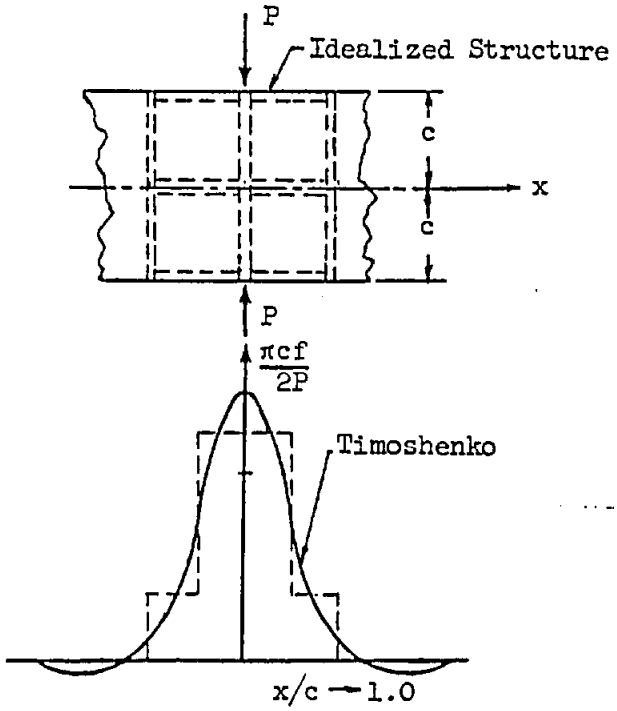

Idealized Structure Geometry

$d_1 = d_2 = b = c \qquad \frac{E}{G} = 2 \qquad t = 1.0$

$A_1 = A_3 = A_6 = A_7 = \frac{c}{2}$

$A_2 = A_4 = A_5 = c$

Solution:

From (1) $\beta = 25$

From graph $\frac{P_1}{P_2} = 0.11$

From (2) & (3) $\frac{P_2}{P} = 0.78, \quad \frac{P_3}{P} = 0.11$

Then

$f_1 = f_3 = \frac{.22P}{C}$

$f_2 = \frac{.78P}{C}$

SECTION C3 - FRAMES AND SEMIMONOCOQUE SHELLS

Table of Contents

DISCUSSION

The determination of stress distributions in semimonocoque structures constitutes one of the major problems in aerospace structural analysis. These structures are frequently highly redundant, and a wide variety of approaches is available for their solution. The one selected should depend heavily upon the specific circumstances.

Early Design Stage

Early in the design stage, rough analyses are usually adequate, and redundancies are partially or entirely removed by assumption. The most elaborate analysis possible cannot make a poor design into a good one - any time available at this stage might better be spent on improving the design.*

During this period, fuselage stringer loads may be calculated based upon an assumed Mc/I stress distribution, modified by assumed effectiveness factors if necessary. From these, skin shears can be obtained by equilibrium alone for single cell construction; for multi-cells, the redundant shears may be determined by assuring compatibility of twist between the various cells.

The loads acting upon the frames are now known, coming from adjacent shell structure and external applied loads, if any. The frames themselves are usually redundant structures, in the form of closed non-circular rings. At this stage it is usually sufficient to assume locations for the inflection points; thereafter bending moment, shear and axial load distributions can be calculated by statics.

Incidentally the circular ring bending moment curves given in this section may be helpful in picking the locations for zero bending.

These calculations are described in the standard texts on aircraft stress analysis.** They can be carried out either by hand or by available computer programs, depending upon circumstances.

Large cutouts in semimonocoque structures pose a special problem. A rapid technique suitable for early design is given in Section C3.06.

There are analytical solutions available for cutouts in circular shells, see references in Section C3.06. Their treatment of the reinforcement required is necessarily somewhat restricted, and limits their general applicability.

The design curves and procedures for uniform circular shells given in this section may prove useful in the early design stage. This will obviously be so if the shell structure in question is circular or nearly so, and reasonably uniform and continuous. In such cases the information available conceivably may be all that is required even for the final design. In the more usual situation however, where these conditions are not met, the design curves must be used with due caution.

* Structures Section Memo, "Stress Analysis Procedures," 12 May 1964

** Bruhn and Schmitt, "Analysis and Design of Aircraft Structures," TRI-State Offset Company, 1958
Peery, "Aircraft Structures," McGraw-Hill, 1950

One way in which the curves, nevertheless, may be useful is in indicating qualitatively whether or not frame flexibility will affect significantly the stress distribution in the structure. As is well known, when the frames are relatively flexible as compared to the shell, the stress distribution in the shell will be profoundly different from Mc/I, VQ/I and T/2A in the neighborhood of concentrated applied loads. Also, the frame internal loads will be very different from those obtained assuming beam theory shell shears to hold. If frame flexibility is a factor with which to reckon, the curves will so indicate, and will give a rough estimate of how much, as well.

Detail Design Stage

Once the framing has been reasonably well established and preliminary section properties have been selected using the rough methods mentioned previously, a more detailed analysis is usually required. In cases where the entire structure or a part of it is reasonably continuous and has relatively stiff frames, a careful re-run of the previous rough calculations may suffice. Various computer programs are available for this purpose; see section G. Included is a very useful program which treats the frames as redundant structures subjected to known self-balancing shear flows and concentrated loads.

When flexible frames and/or significant discontinuities exist in a good sized region of the structure, and the circular cross section shell analyses mentioned previously do not apply, a comprehensive redundant analysis may be justified. Its execution is a rather formidable task and should not be undertaken lightly. In order to benefit from previous company experience, these analyses should be a joint venture by the Structures Project Group and Structural Methods Group.

CIRCULAR RING LOADS AND DISPLACEMENTS FOR VARIOUS LOADING CONDITIONS

The curves on the following 24 pages are based upon simple bending theory. Where required, balancing skin shears are distributed according to "VQ/I" and "T/2A".

Reference — Bornscheuer: "Circular Ring Frame Bending Moments, Transverse and Axial Forces Under Various Loading Conditions", Peenemunde Army Proving Grounds, Germany, June 1944.

INDEX OF LOADING CASES

1 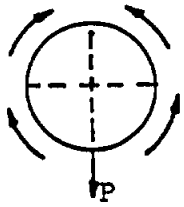	2 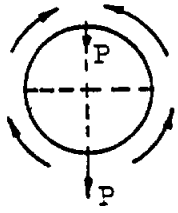	3 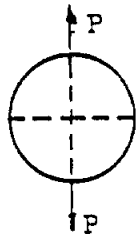	4 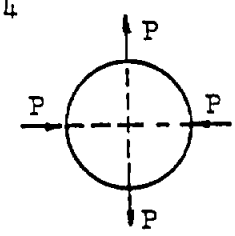	5 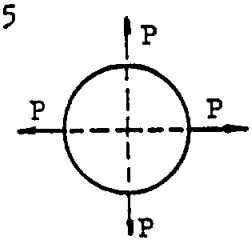
6 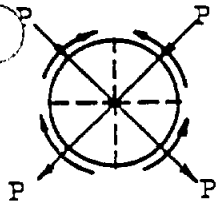	7 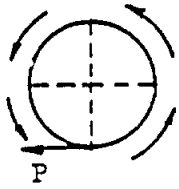	8 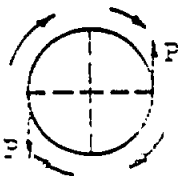	9 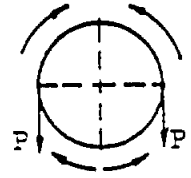	10 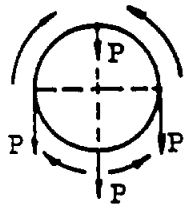
11 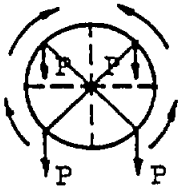	12 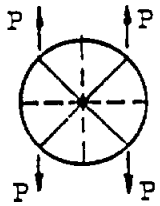	13 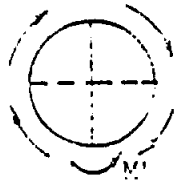	14 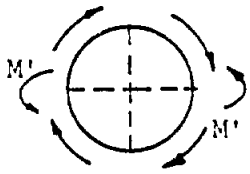	15 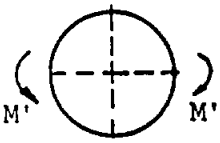
16 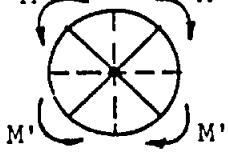	17 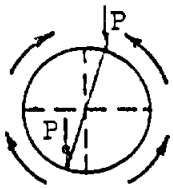	18  $p = p_{max} \cos \phi$	19  $p = p_{max} \cos \phi$	20  $p = p_{max} \cos 2\phi$
21 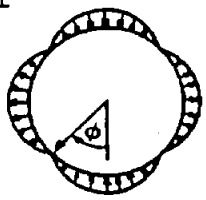 $p = p_{max} \cos 2\phi$	22 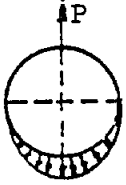 $p = p_{max} \cos \phi$	23 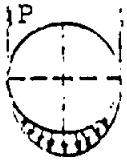 $p = p_{max} \cos \phi$	24 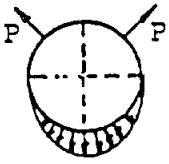 $p = p_{max} \cos \phi$	

CIRCULAR RING LOADS AND DISPLACEMENTS

Loading Condition (1)

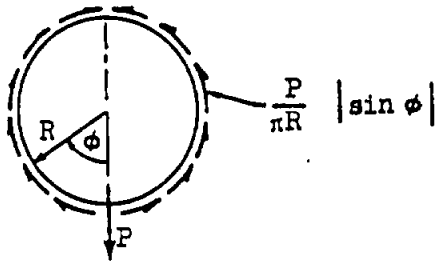

Internal Loads

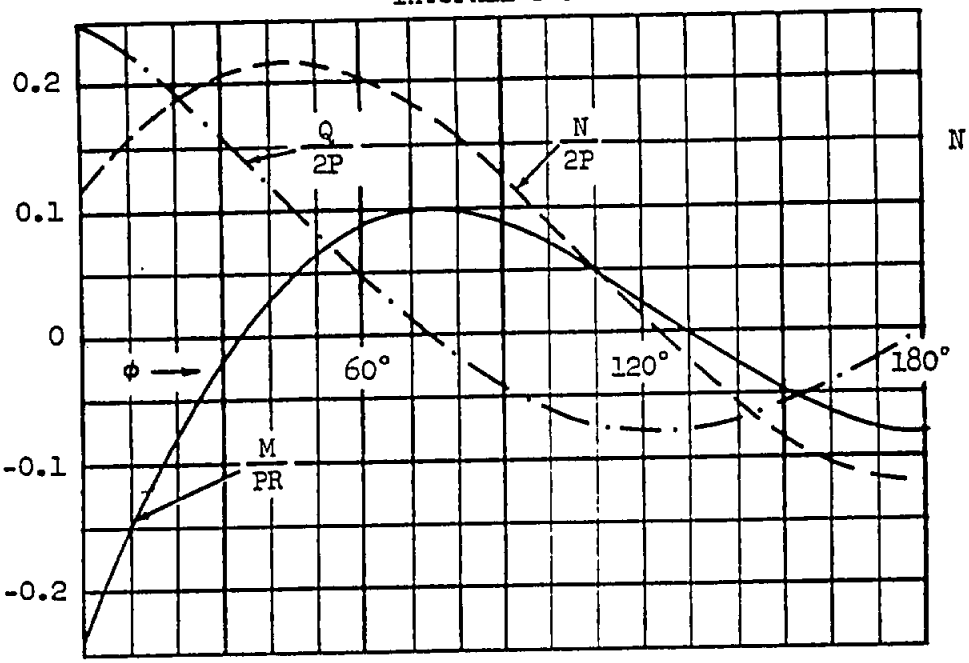

Sign Convention

$M(\phi) = M(-\phi)$
$N(\phi) = N(-\phi)$
$Q(\phi) = -Q(-\phi)$

Displacements

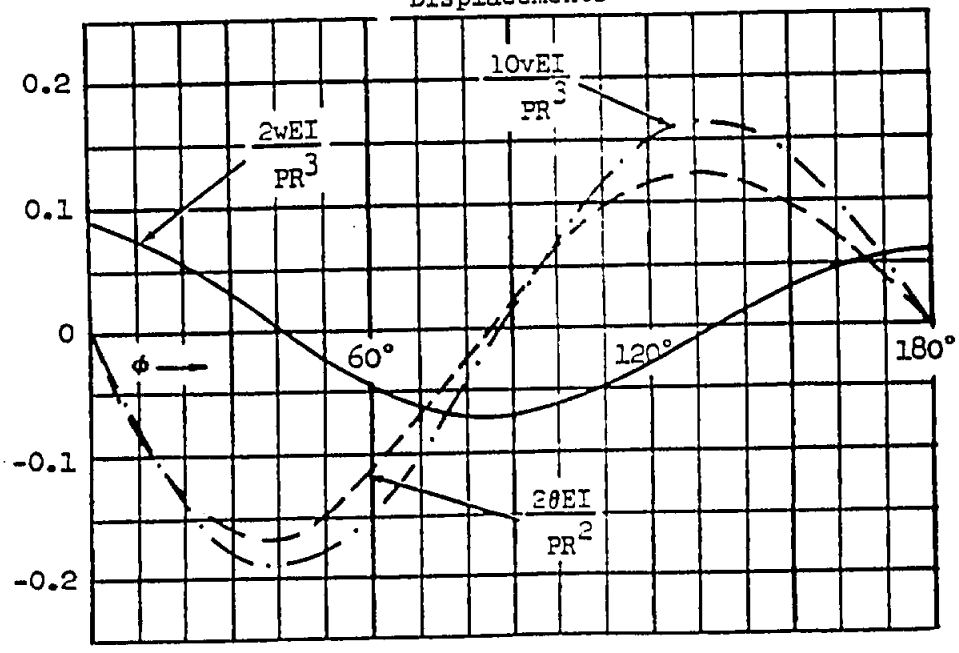

Sign Convention

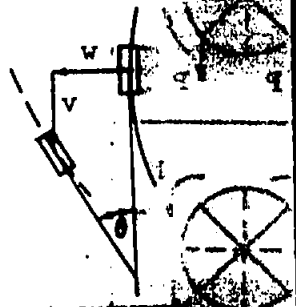

w = + outward
θ = + counter-clockwise
v = + counter-clockwise
$w(\phi) = w(-\phi)$
$\theta(\phi) = -\theta(-\phi)$
$v(\phi) = -v(-\phi)$

CIRCULAR RING LOADS AND DISPLACEMENTS

Loading Condition (2)

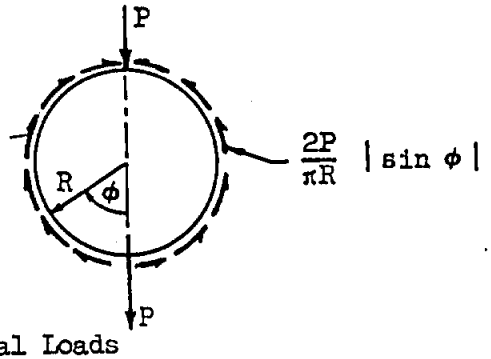

Internal Loads

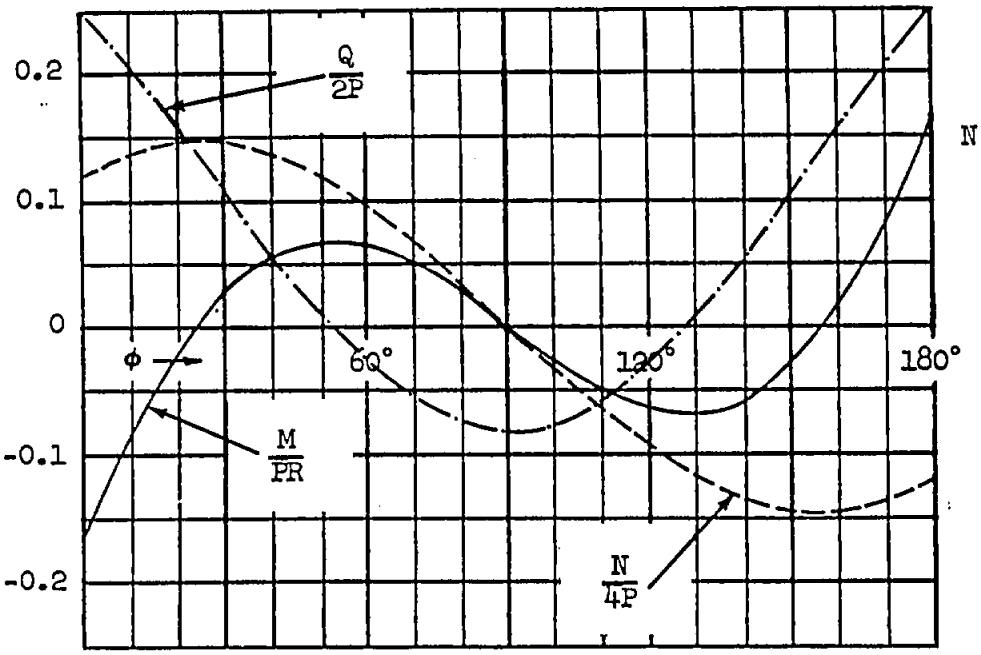

Sign Convention

$M(\phi) = M(-\phi)$
$N(\phi) = N(-\phi)$
$Q(\phi) = -Q(-\phi)$

Displacements

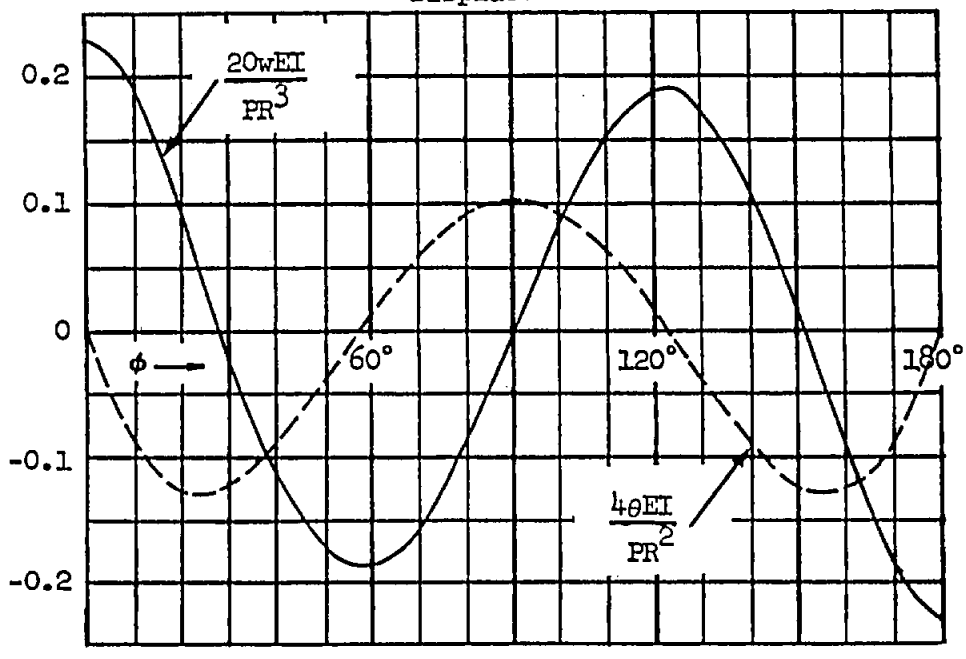

Sign Convention

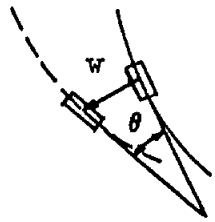

w = + outward

θ = + counter clockwise

$w(\phi) = w(-\phi)$

$\theta(\phi) = -\theta(-\phi)$

CIRCULAR RING LOADS AND DISPLACEMENTS

Loading Condition (3)

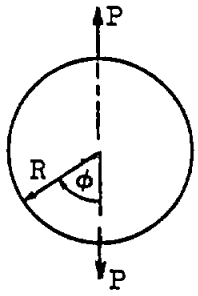

Internal Loads

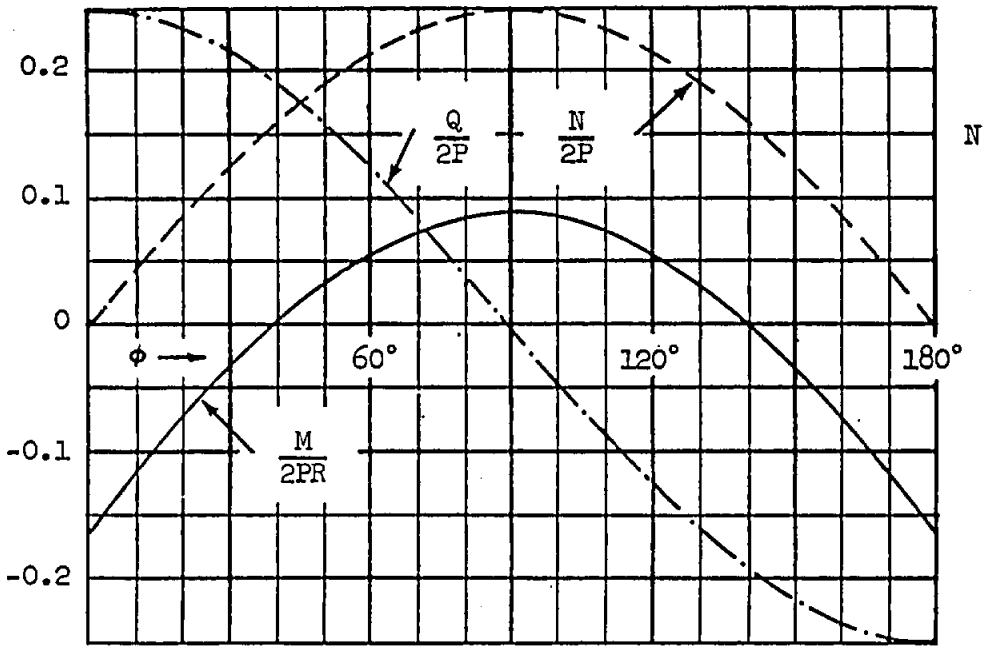

Sign Convention

$M(\phi) = M(-\phi)$
$N(\phi) = N(-\phi)$
$Q(\phi) = -Q(-\phi)$

Displacements

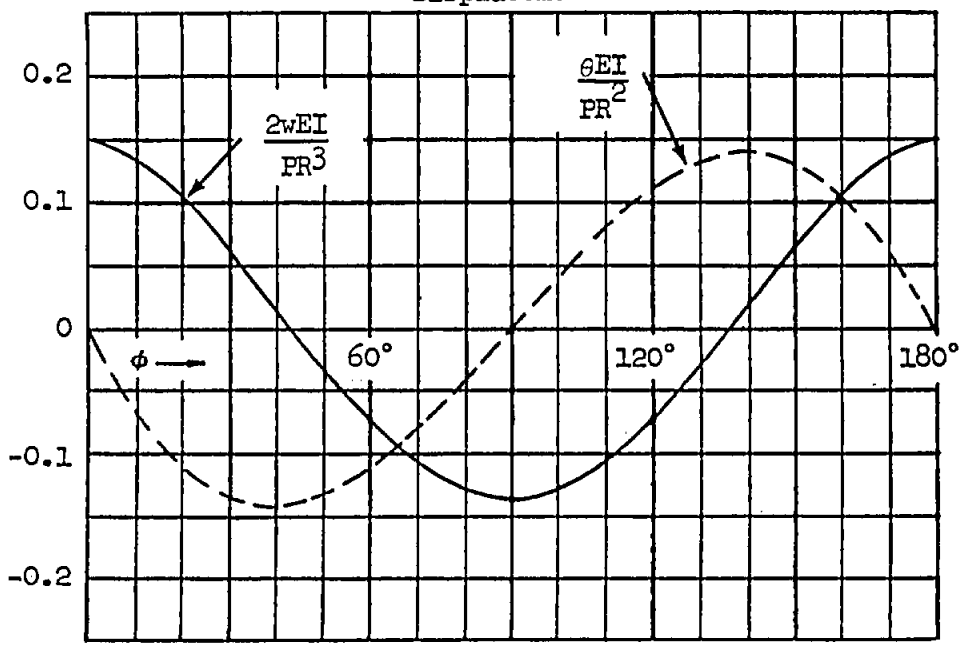

Sign Convention

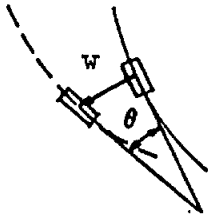

w = + outward

θ = + counter clockwise

$w(\phi) = w(-\phi)$

$\theta(\phi) = -\theta(-\phi)$

CIRCULAR RING LOADS AND DISPLACEMENTS

Loading Condition (4)

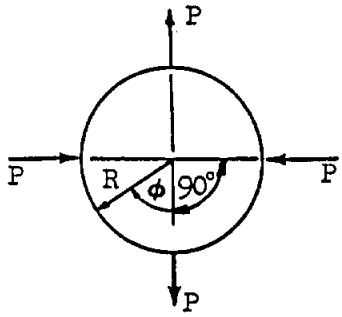

Internal Loads

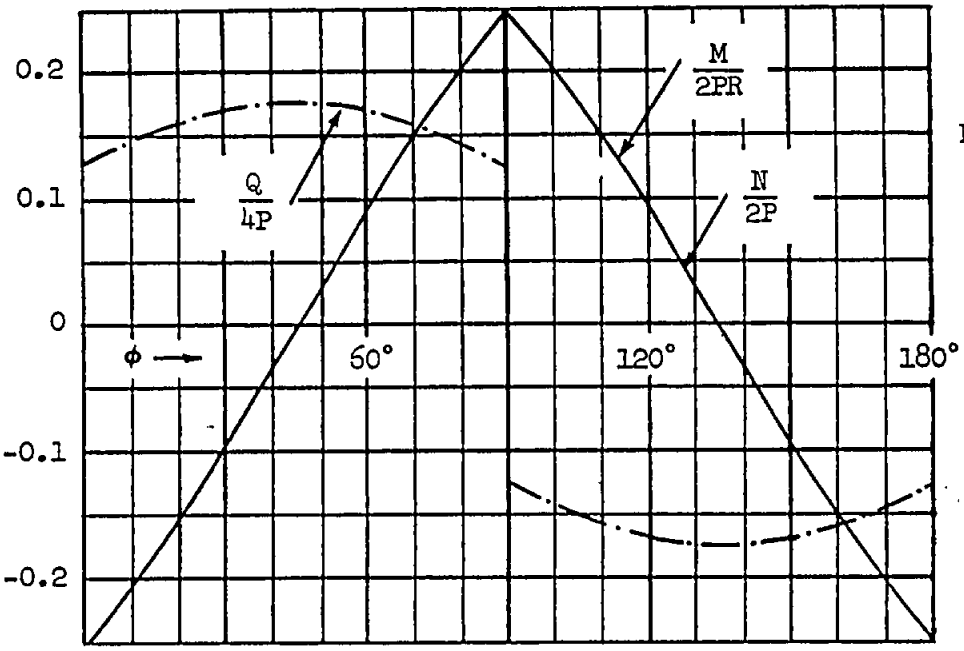

Sign Convention

$M(\phi) = M(-\phi)$
$N(\phi) = N(-\phi)$
$Q(\phi) = -Q(-\phi)$

Displacements

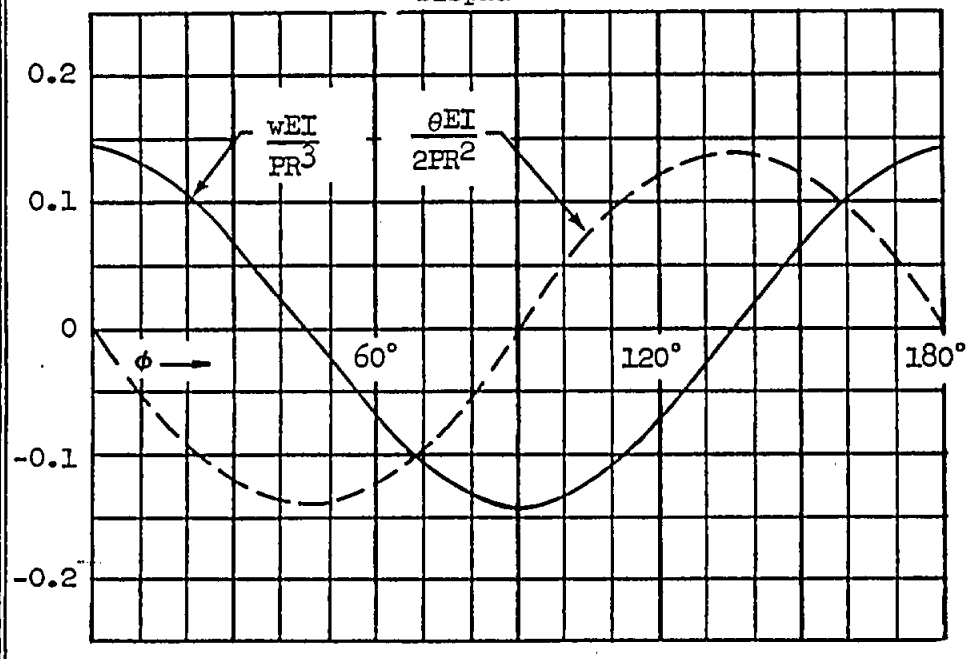

Sign Convention

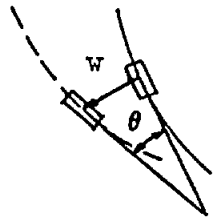

w = + outward

θ = + counter clockwise

$w(\phi) = w(-\phi)$

$\theta(\phi) = -\theta(-\phi)$

CIRCULAR RING LOADS AND DISPLACEMENTS

Loading Condition (5)

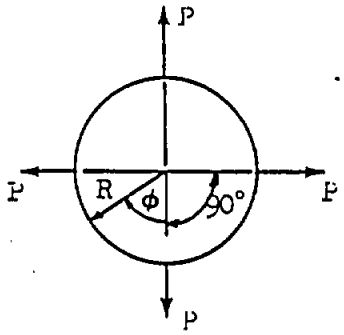

Internal Loads

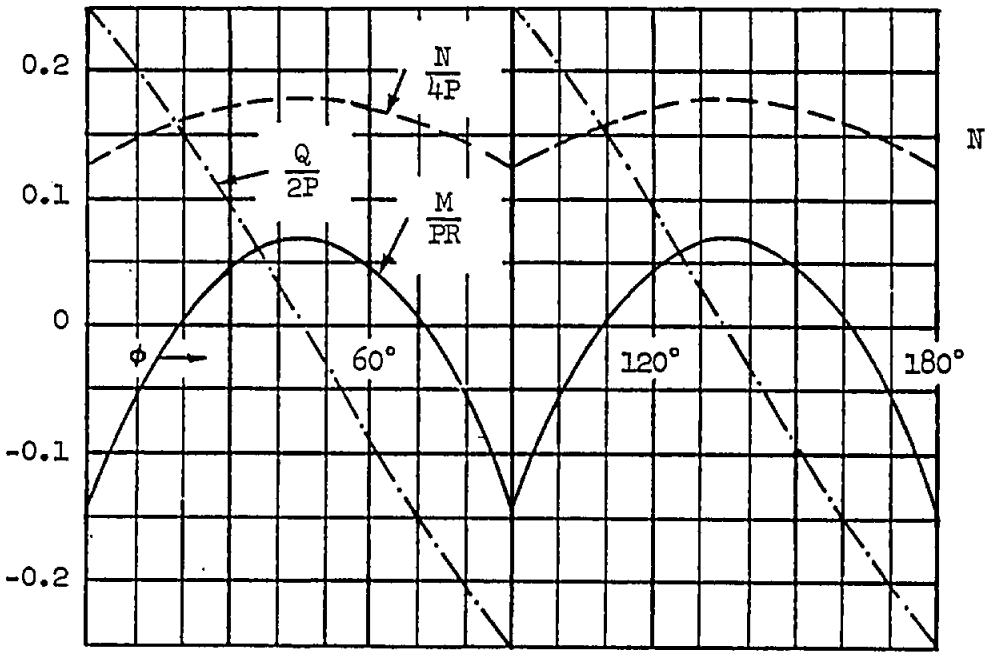

Sign Convention

$M(\phi) = M(-\phi)$
$N(\phi) = N(-\phi)$
$Q(\phi) = -Q(-\phi)$

Displacements

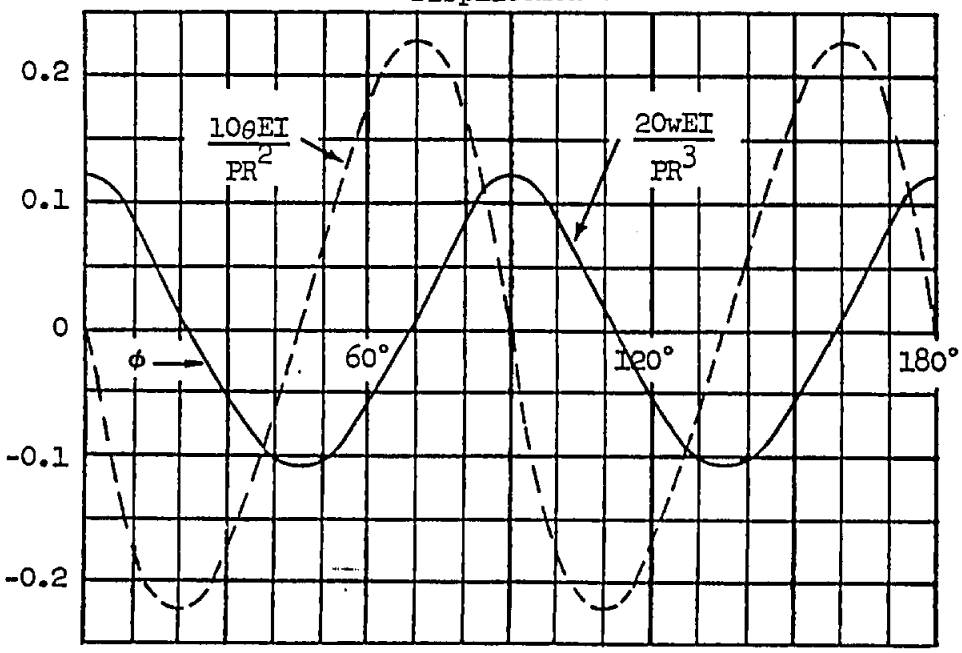

Sign Convention

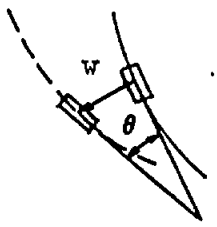

w = + outward

θ = + counter clockwise

$w(\phi) = w(-\phi)$

$\theta(\phi) = -\theta(-\phi)$

CIRCULAR RING LOADS AND DISPLACEMENTS

Loading Condition (6)

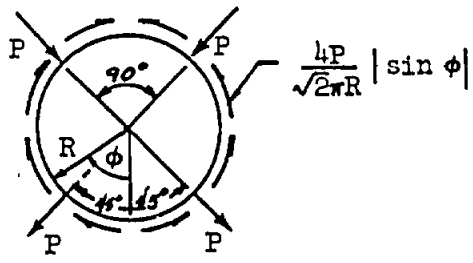

Internal Loads

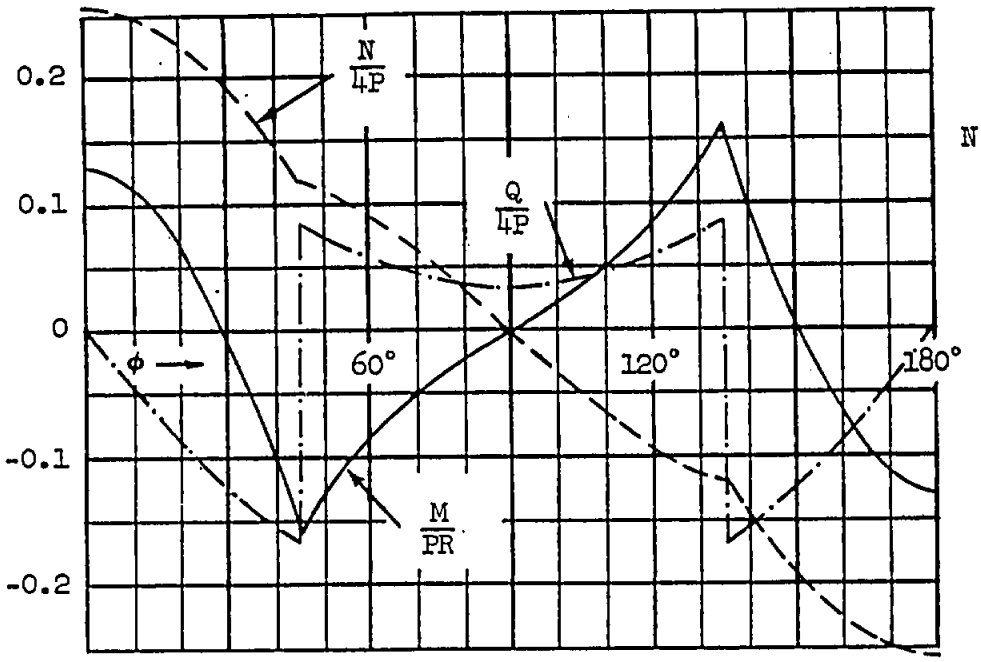

Sign Convention

$M(\phi) = M(-\phi)$
$N(\phi) = N(-\phi)$
$Q(\phi) = -Q(-\phi)$

Displacements

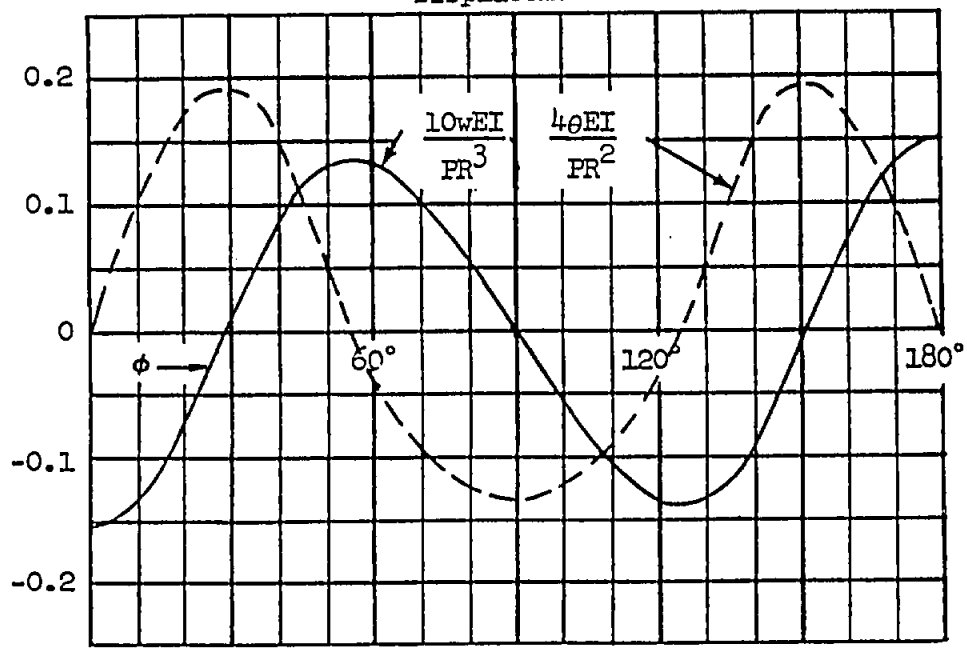

Sign Convention

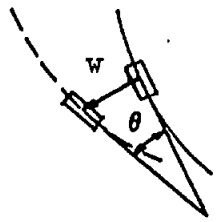

w = + outward

θ = + counter clockwise

$w(\phi) = w(-\phi)$

$\theta(\phi) = -\theta(-\phi)$

CIRCULAR RING LOADS AND DISPLACEMENTS

Loading Condition (.7)

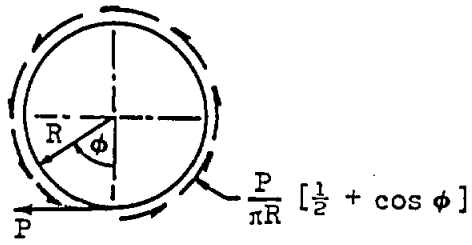

Internal Loads

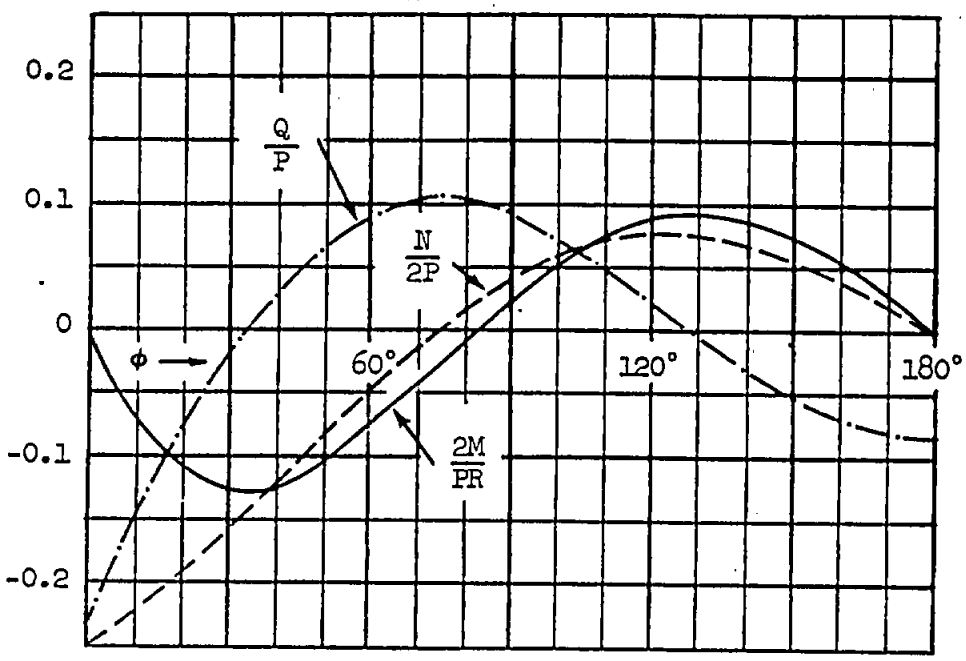

Sign Convention

$M(\phi) = -M(-\phi)$

$N(\phi) = -N(-\phi)$

$Q(\phi) = Q(-\phi)$

Displacements

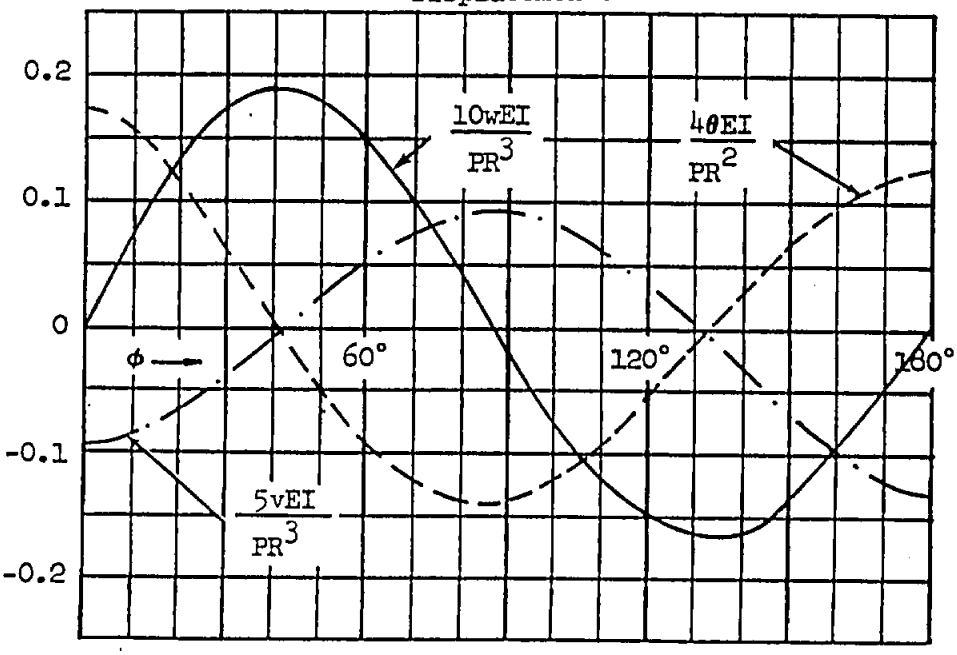

Sign Convention

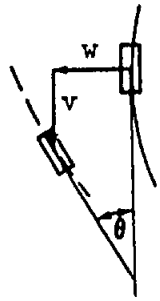

w = + outward
θ = + counter clockwise
v = + counter clockwise

$w(\phi) = -w(-\phi)$
$\theta(\phi) = \theta(-\phi)$
$v(\phi) = v(-\phi)$

CIRCULAR RING LOADS AND DISPLACEMENTS

Loading Condition (8)

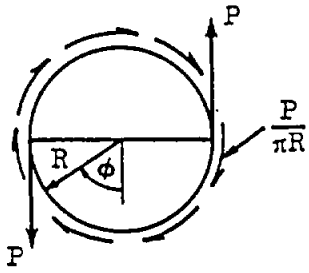

Internal Loads

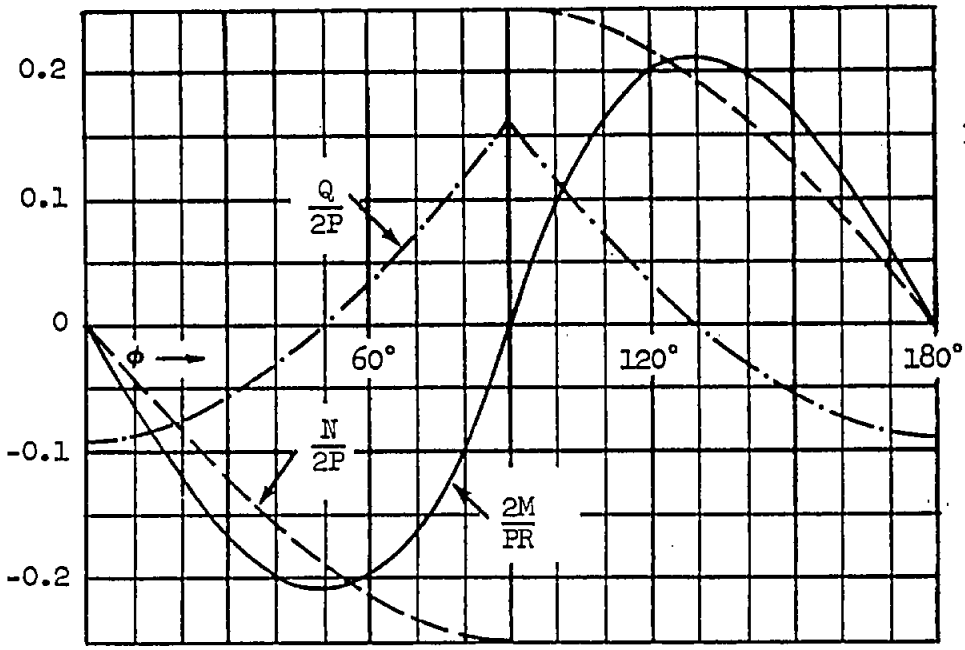

Sign Convention

$M(\phi) = -M(-\phi)$
$N(\phi) = -N(-\phi)$
$Q(\phi) = Q(-\phi)$

Displacements

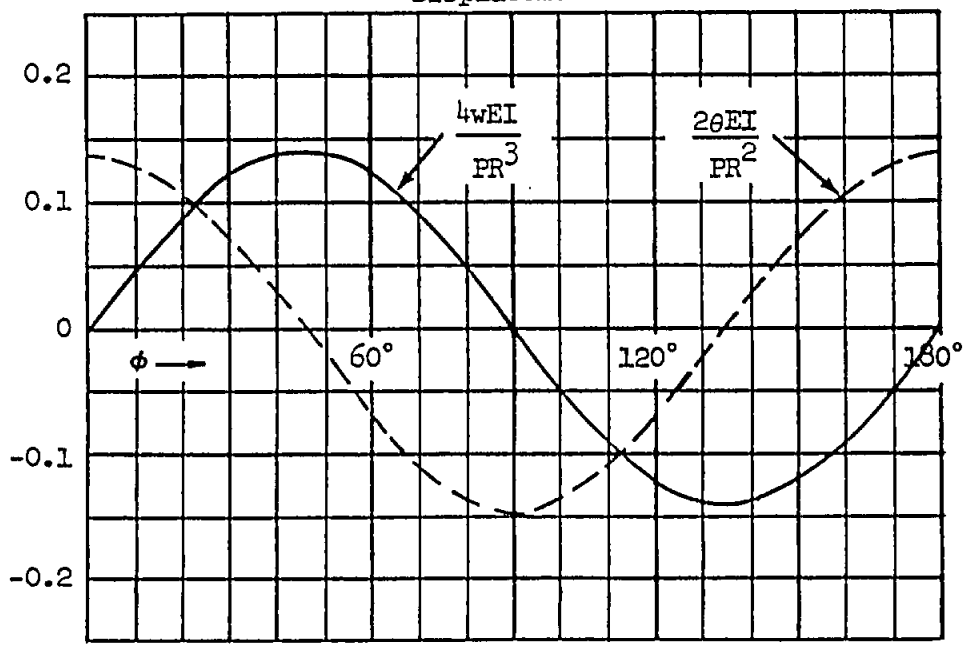

Sign Convention

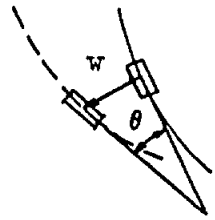

w = + outward

θ = + counter clockwise

$w(\phi) = -w(-\phi)$

$\theta(\phi) = \theta(-\phi)$

CIRCULAR RING LOADS AND DISPLACEMENTS

Loading Condition (9)

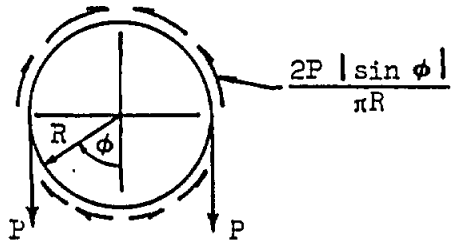

Internal Loads

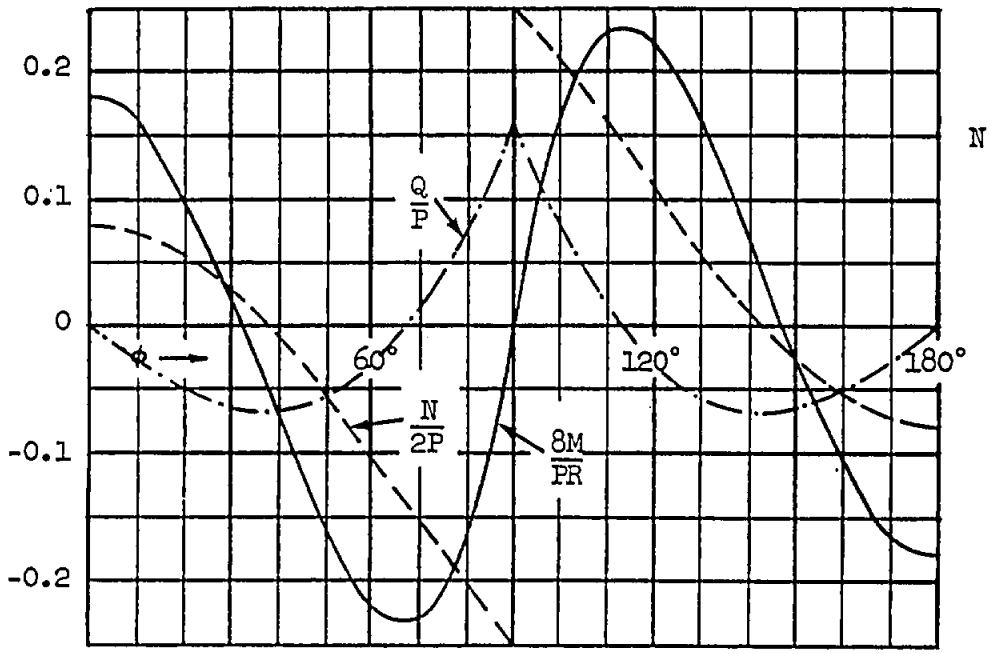

Sign Convention

$M(\phi) = M(-\phi)$
$N(\phi) = N(-\phi)$
$Q(\phi) = -Q(-\phi)$

Displacements

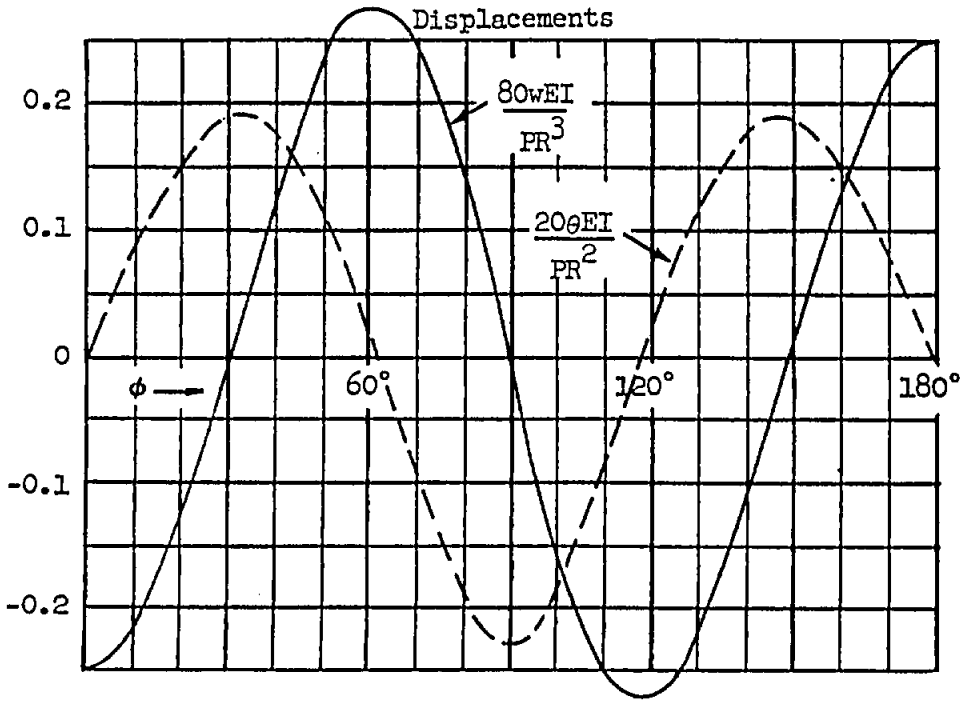

Sign Convention

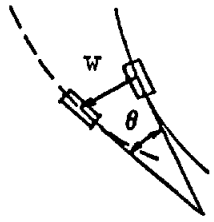

w = + outward

θ = + counter clockwise

$w(\phi) = w(-\phi)$

$\theta(\phi) = -\theta(-\phi)$

CIRCULAR RING LOADS AND DISPLACEMENTS

Loading Condition (10)

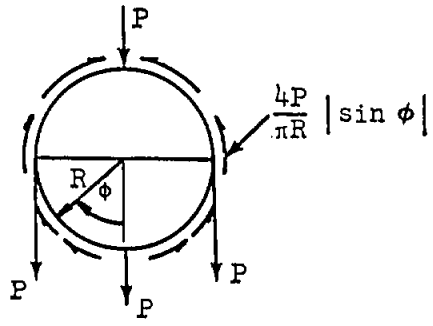

Internal Loads

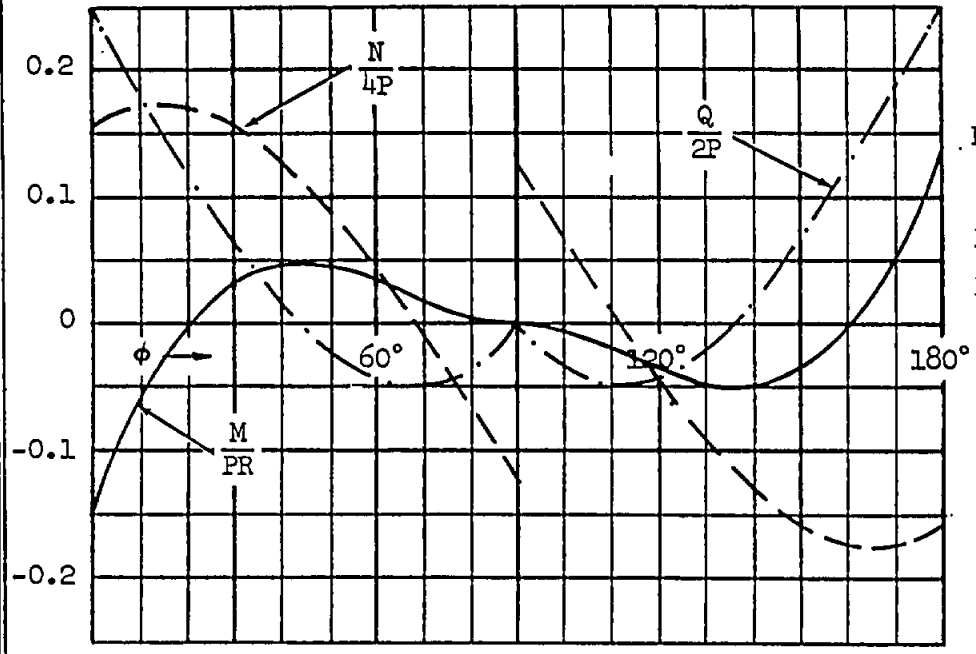

Sign Convention

$M(\phi) = M(-\phi)$

$N(\phi) = N(-\phi)$

$Q(\phi) = -Q(-\phi)$

Displacements

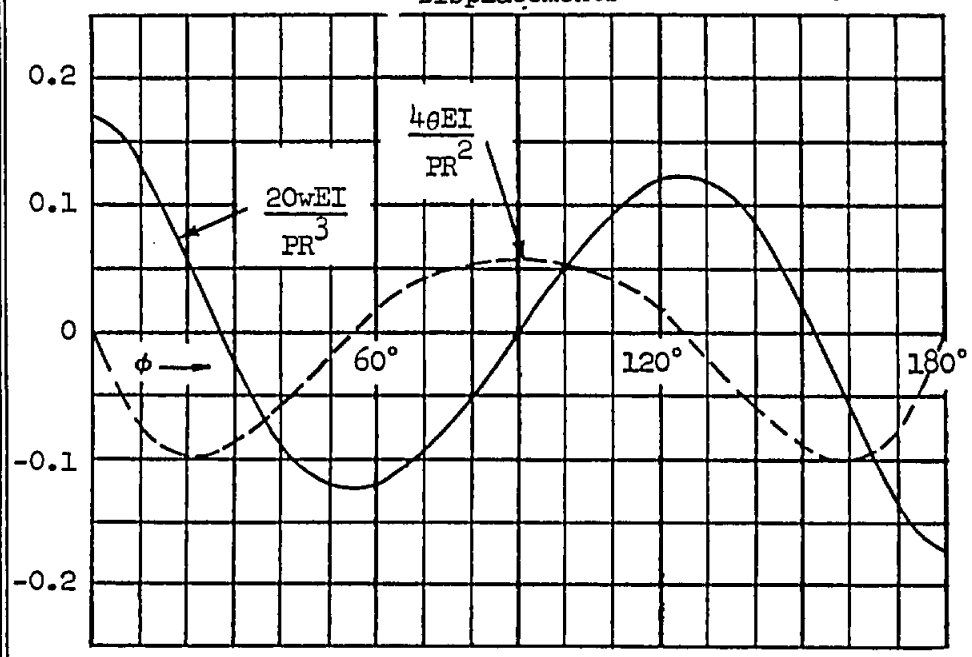

Sign Convention

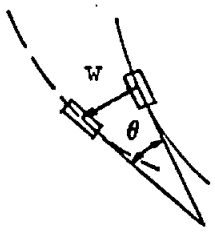

w = + outward

θ = + counter clockwise

$w(\phi) = w(-\phi)$

$\theta(\phi) = -\theta(-\phi)$

CIRCULAR RING LOADS AND DISPLACEMENTS

Loading Condition (11)

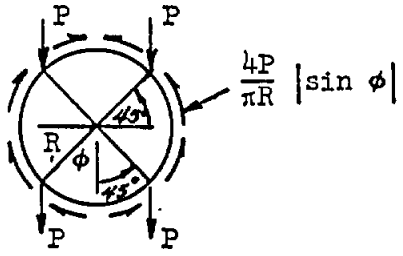

Internal Loads

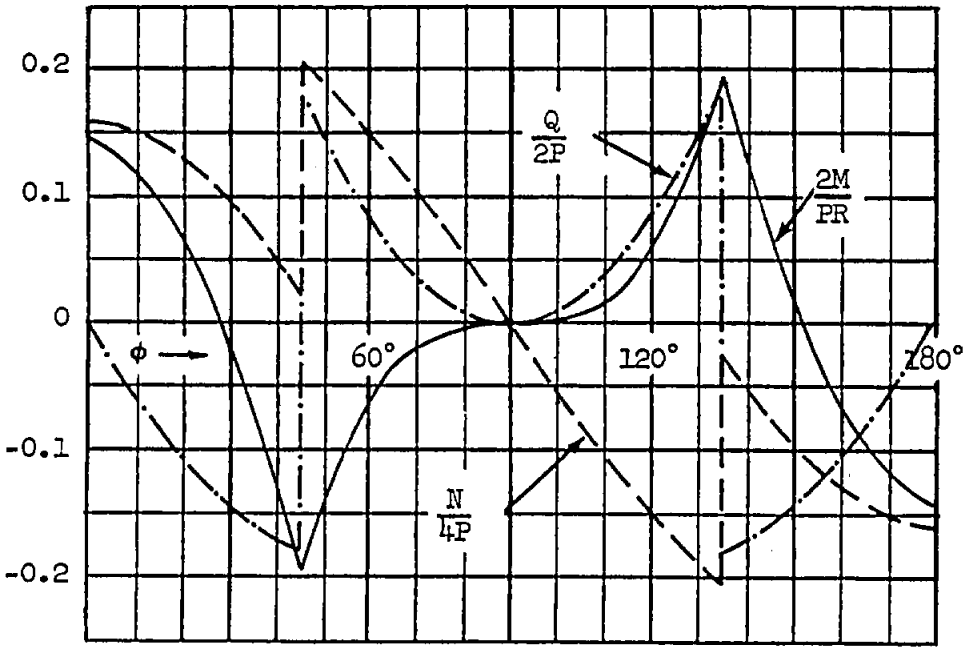

Sign Convention

$M(\phi) = M(-\phi)$

$N(\phi) = N(-\phi)$

$Q(\phi) = -Q(-\phi)$

Displacements

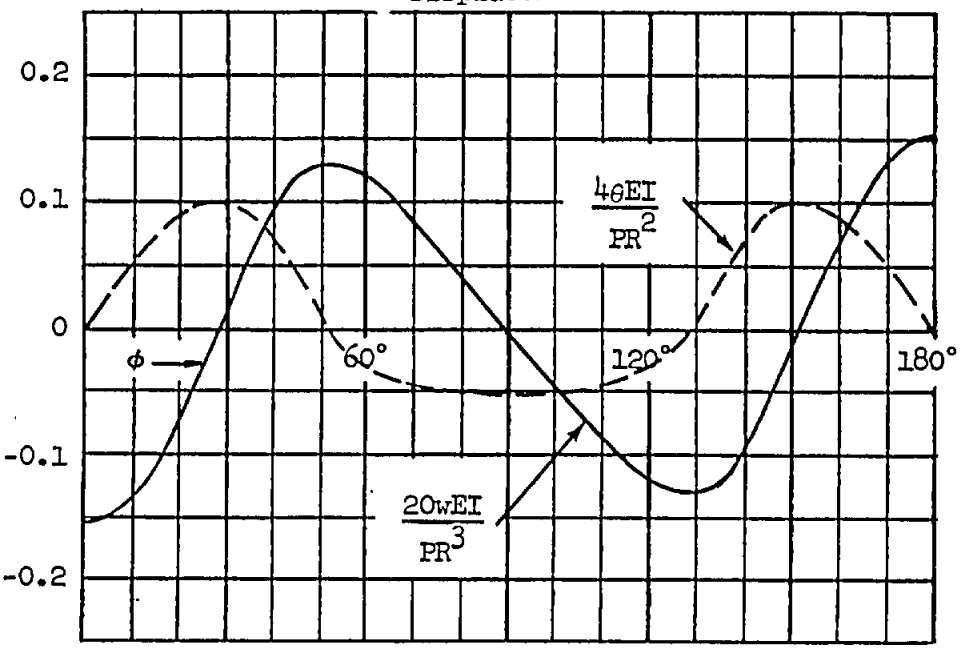

Sign Convention

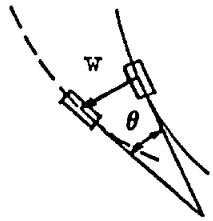

w = + outward

θ = + counter clockwise

$w(\phi) = w(-\phi)$

$\theta(\phi) = -\theta(-\phi)$

CIRCULAR RING LOADS AND DISPLACEMENTS

Loading Condition (12)

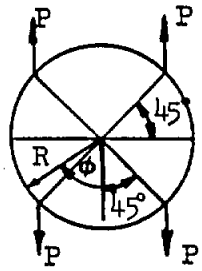

Internal Loads

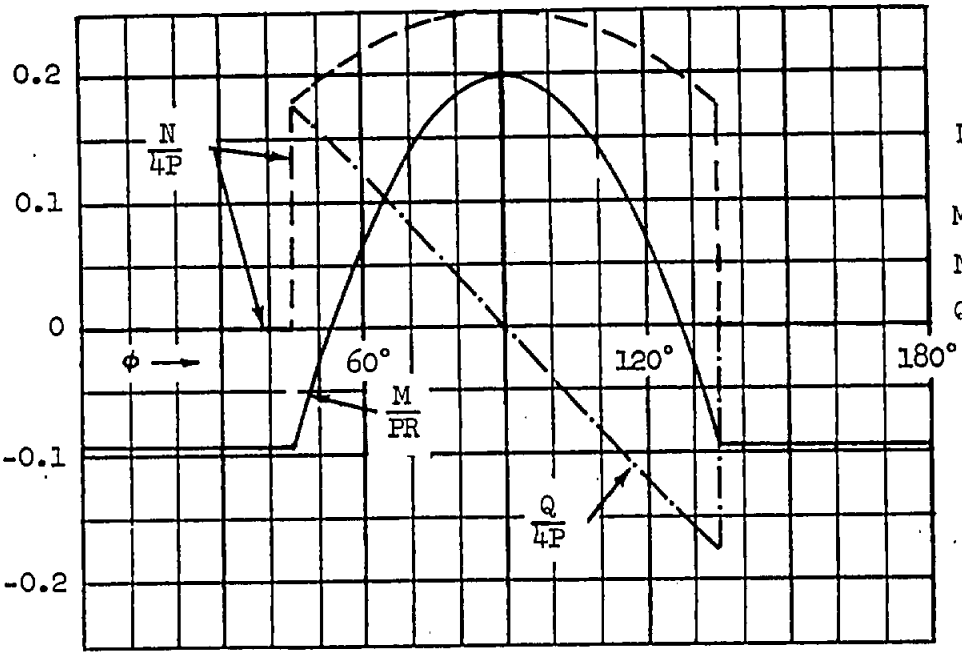

Sign Convention

$M(\phi) = M(-\phi)$

$N(\phi) = N(-\phi)$

$Q(\phi) = -Q(-\phi)$

Displacements

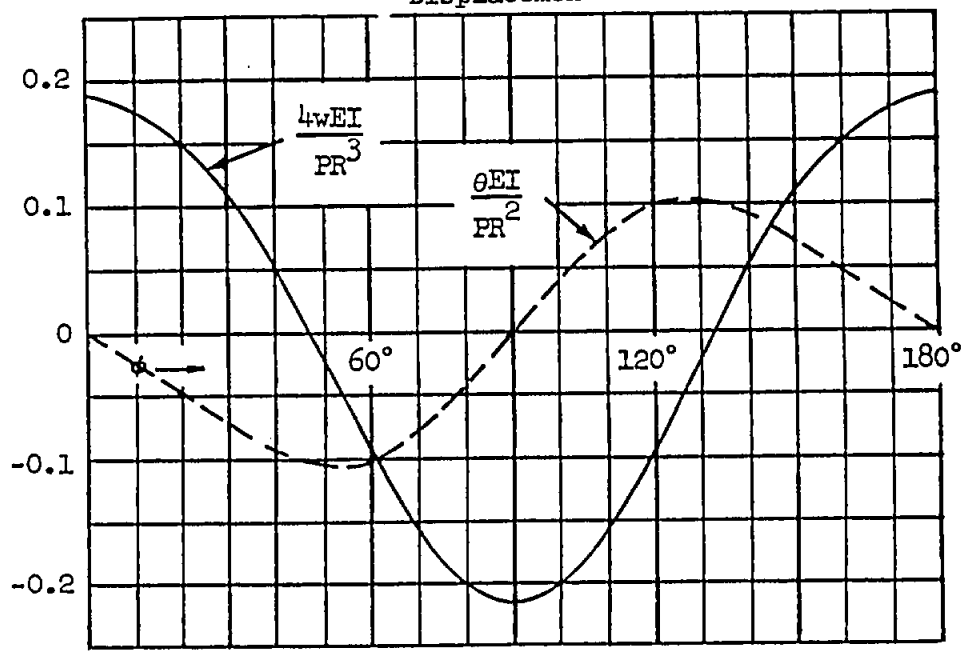

Sign Convention

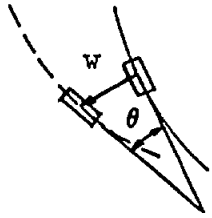

w = + outward

θ = + counter clockwise

$w(\phi) = w(-\phi)$

$\theta(\phi) = -\theta(-\phi)$

CIRCULAR RING LOADS AND DISPLACEMENTS

Loading Condition (13)

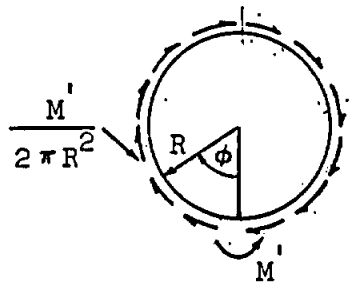

Internal Loads

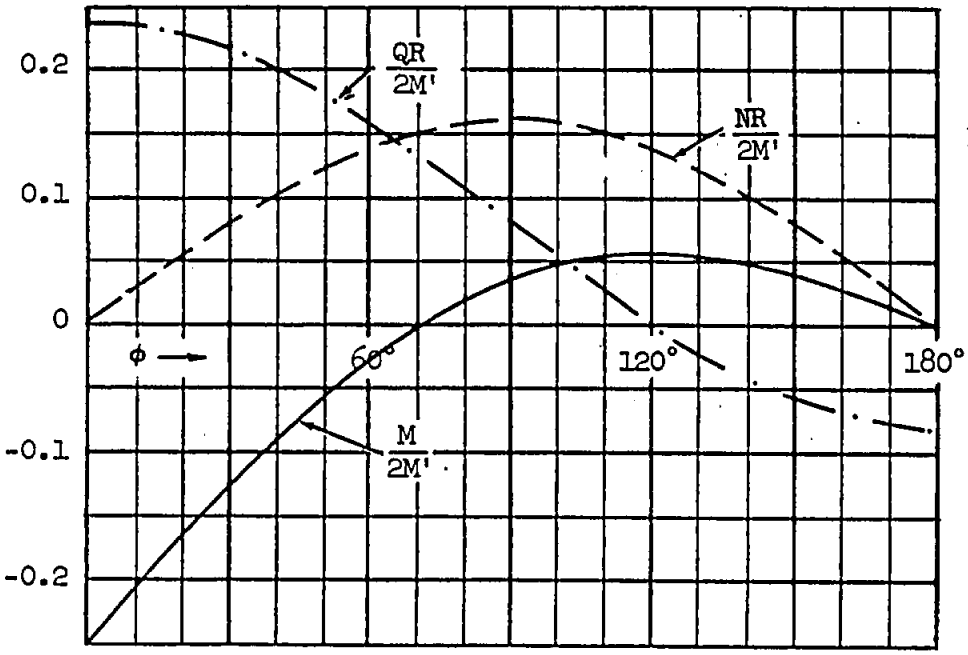

Sign Convention

$M(\phi) = -M(-\phi)$

$N(\phi) = -N(-\phi)$

$Q(\phi) = Q(-\phi)$

Displacements

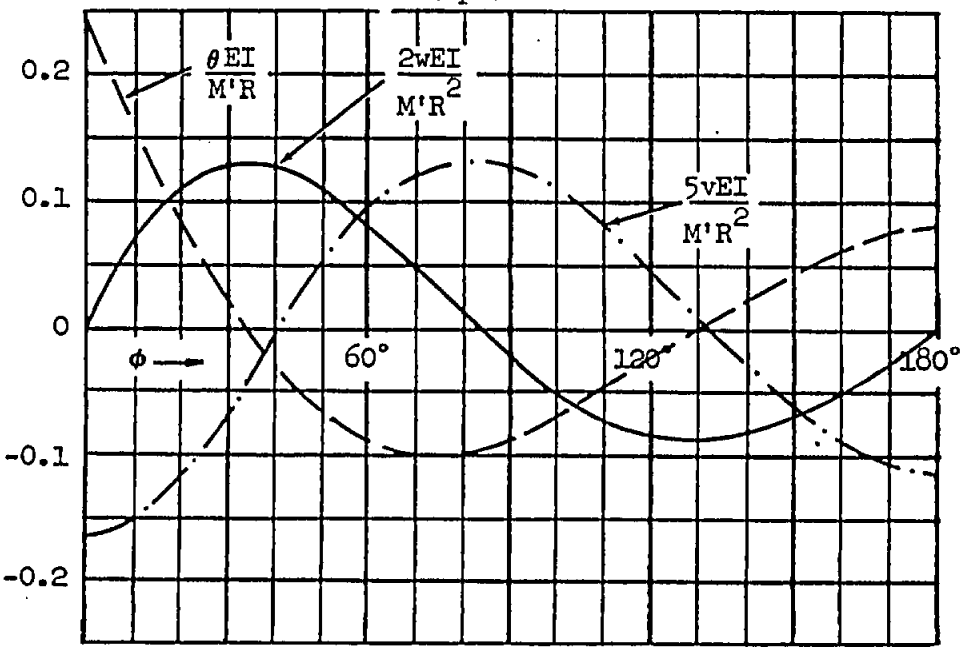

Sign Convention

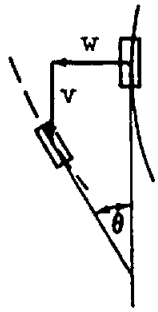

w = + outward
θ = + counter clockwise
v = + counter clockwise

$w(\phi) = -w(-\phi)$
$\theta(\phi) = \theta(-\phi)$
$v(\phi) = v(-\phi)$

CIRCULAR RING LOADS AND DISPLACEMENTS

Loading Condition (14)

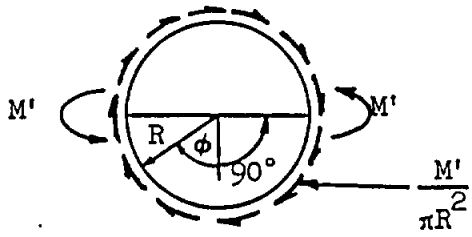

Internal Loads

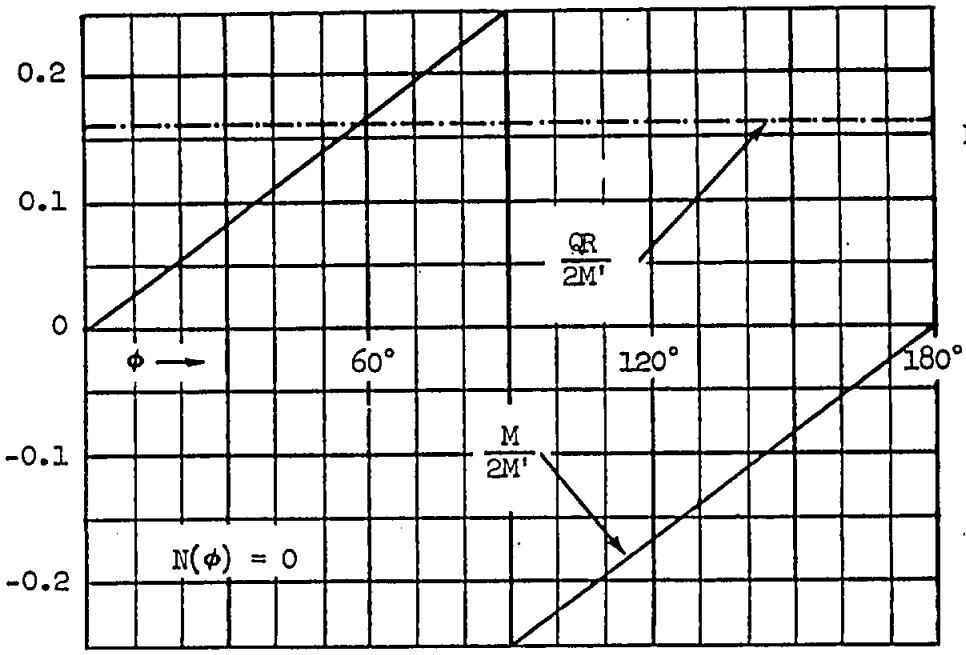

Sign Convention

$M(\phi) = -M(-\phi)$

$N(\phi) = -N(-\phi)$

$Q(\phi) = Q(-\phi)$

Displacements

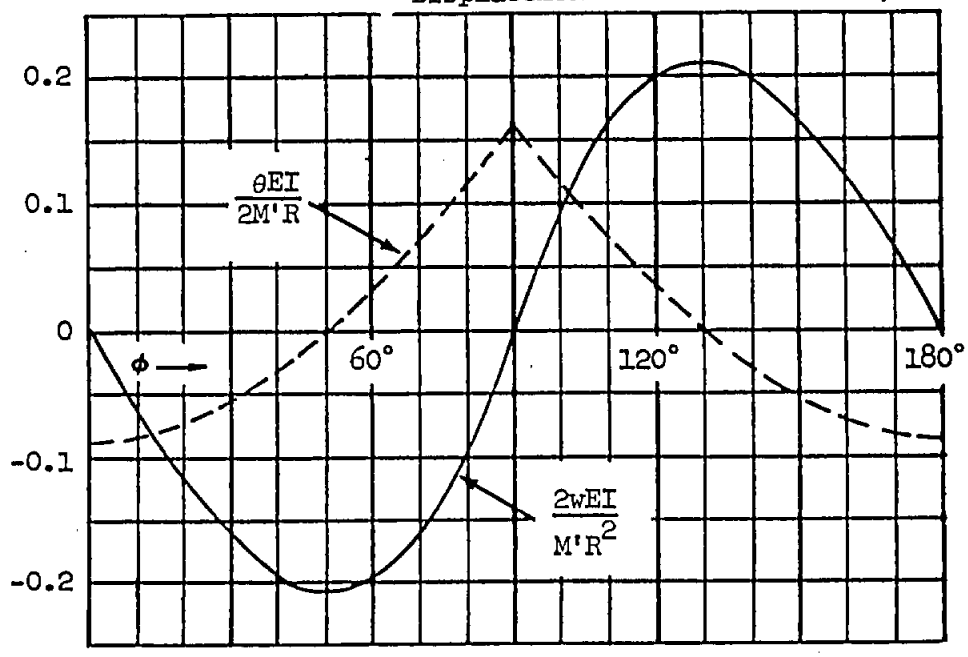

Sign Convention

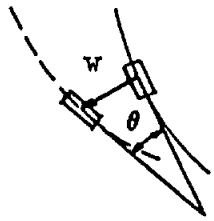

w = + outward

θ = + counter clockwise

$w(\phi) = -w(-\phi)$

$\theta(\phi) = \theta(-\phi)$

CIRCULAR RING LOADS AND DISPLACEMENTS

Loading Condition (15)

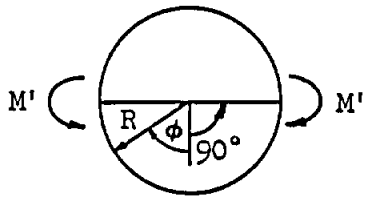

Internal Loads

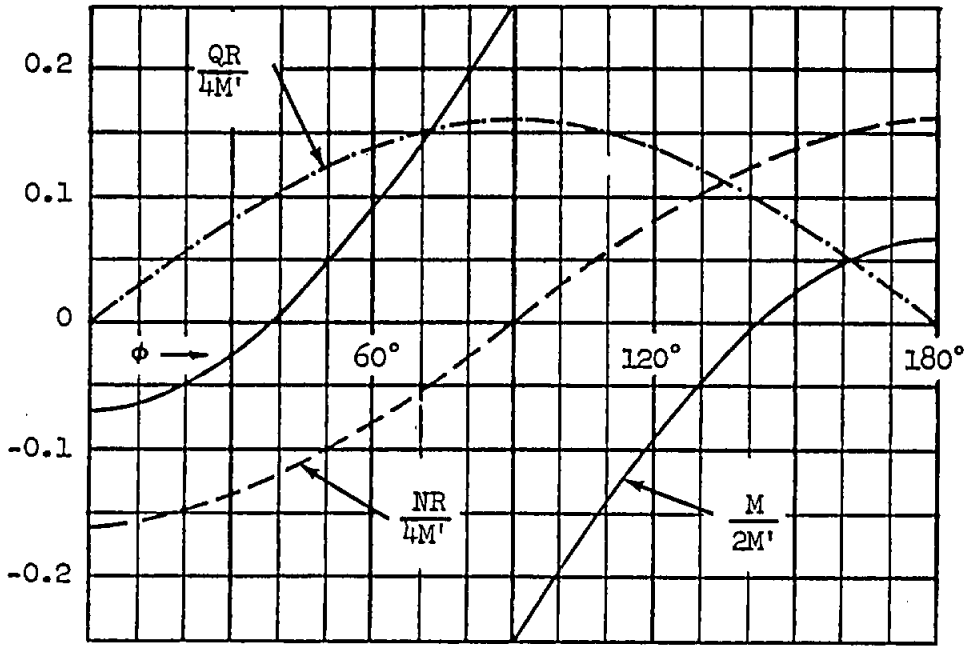

Sign Convention

$M(\phi) = M(-\phi)$

$N(\phi) = N(-\phi)$

$Q(\phi) = -Q(-\phi)$

Displacements

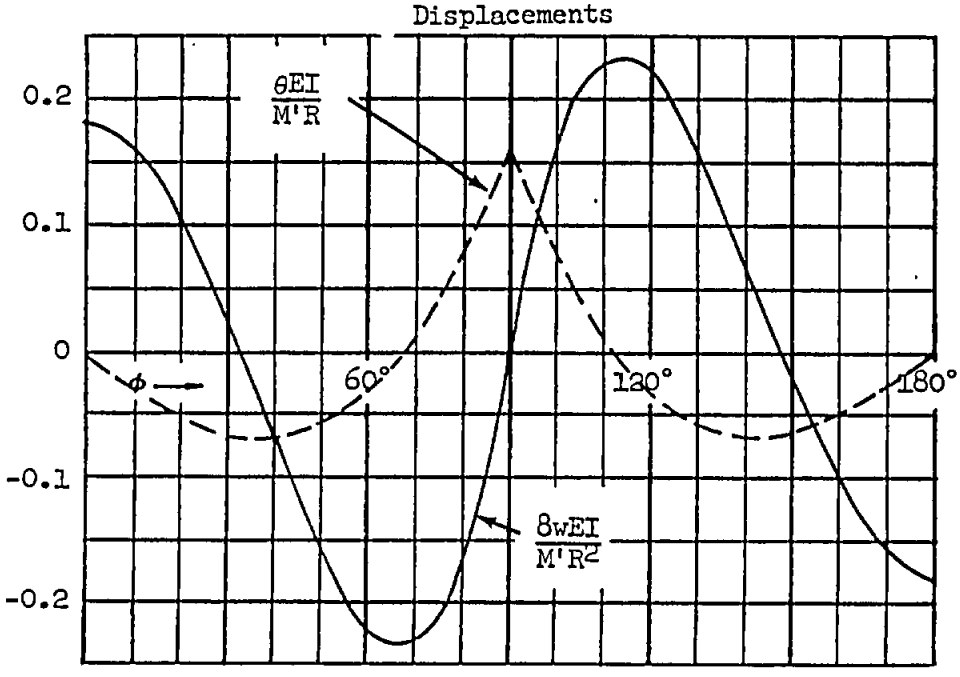

Sign Convention

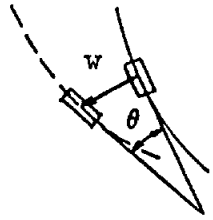

w = + outward

θ = + counter clockwise

$w(\phi) = w(-\phi)$

$\theta(\phi) = -\theta(-\phi)$

CIRCULAR RING LOADS AND DISPLACEMENTS

Loading Condition (16)

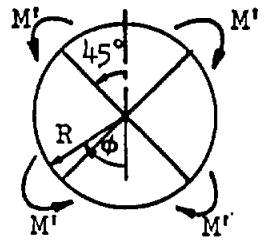

Internal Loads

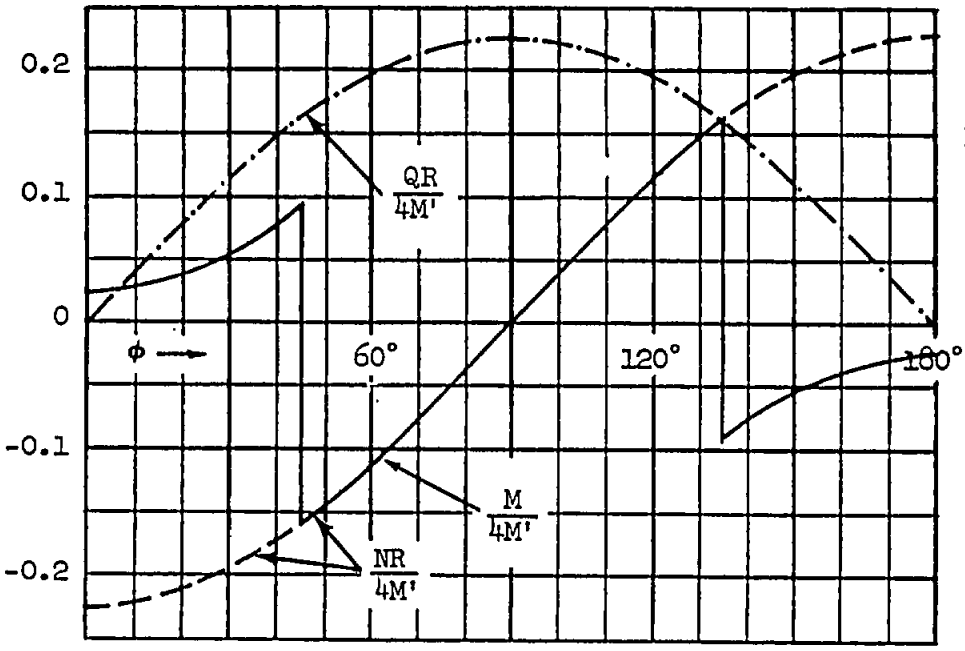

Sign Convention

$M(\phi) = M(-\phi)$

$N(\phi) = N(-\phi)$

$Q(\phi) = -Q(-\phi)$

Displacements

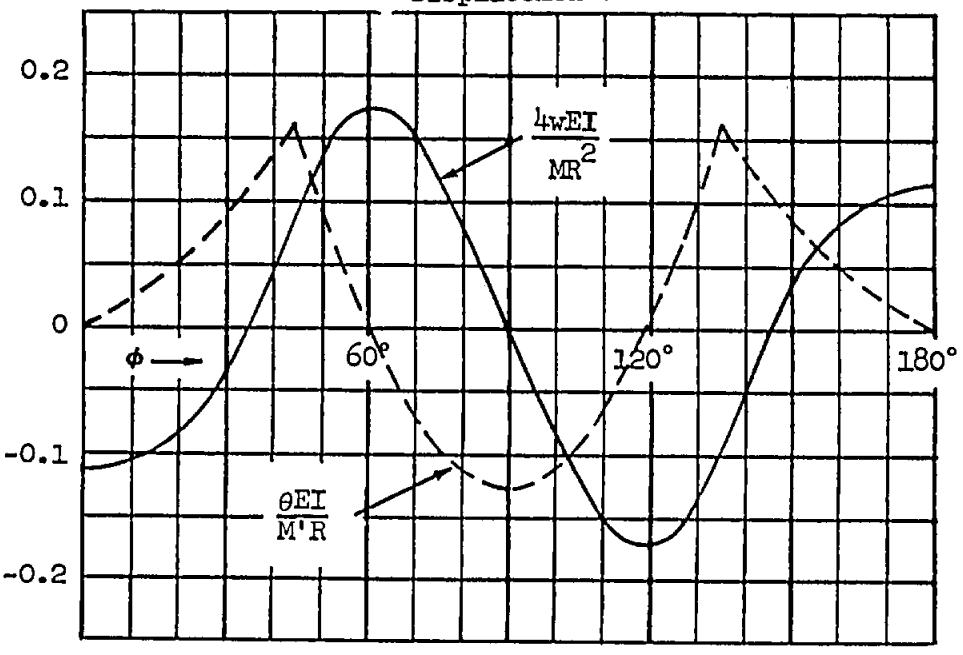

Sign Convention

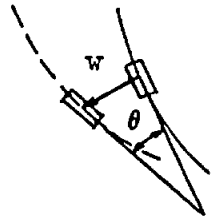

w = + outward

θ = + counter clockwise

$w(\phi) = w(-\phi)$

$\theta(\phi) = -\theta(-\phi)$

CIRCULAR RING LOADS AND DISPLACEMENTS

Loading Condition (17)

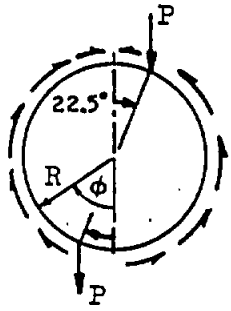

$$\frac{2P}{\pi R}\left|\sin\phi\right|$$

Internal Loads

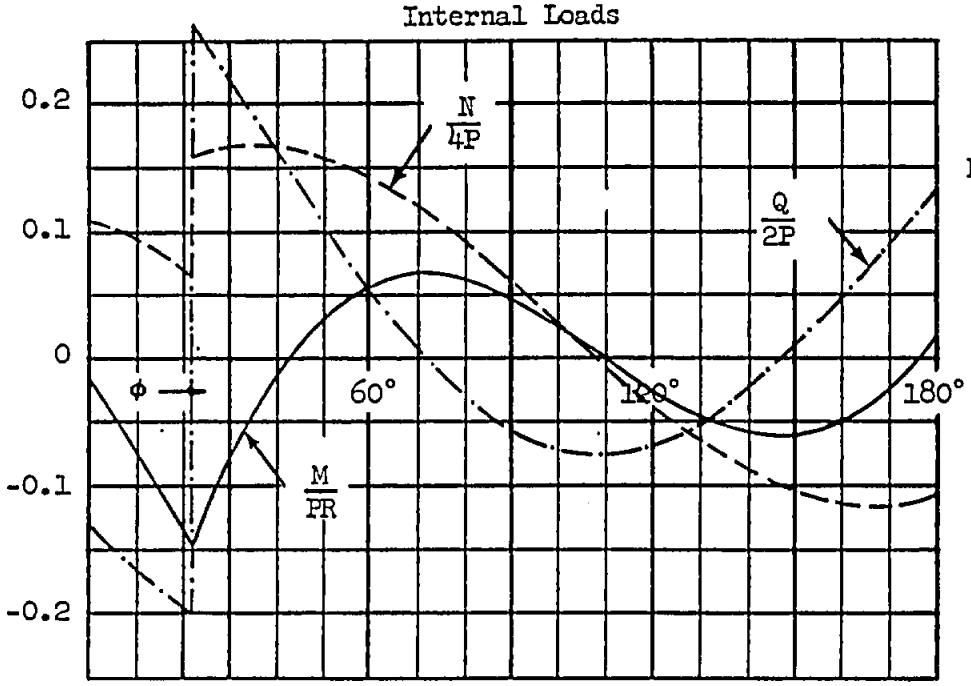

Sign Convention

$M(\phi) = -M(-180 + \phi)$

$N(\phi) = -N(-180 + \phi)$

$Q(\phi) = -Q(-180 + \phi)$

Displacements

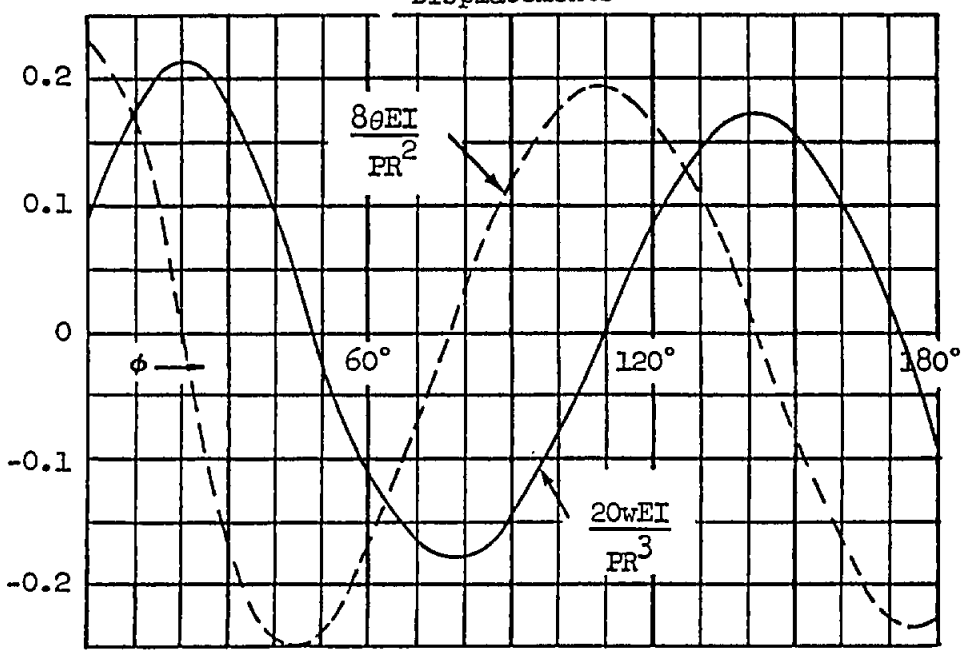

Sign Convention

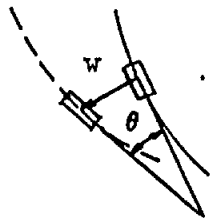

w = + outward

θ = + counter clockwise

$w(\phi) = -w(-180 + \phi)$

$\theta(\phi) = -\theta(-180 + \phi)$

CIRCULAR RING LOADS AND DISPLACEMENTS

Loading Condition (18)

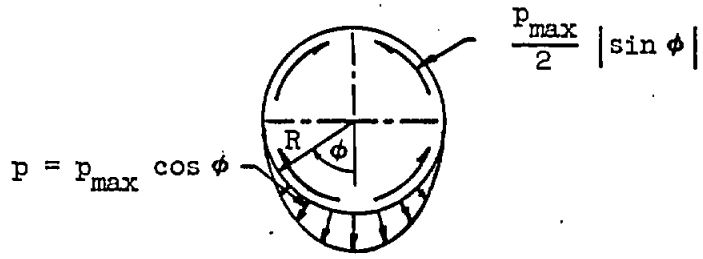

Internal Loads

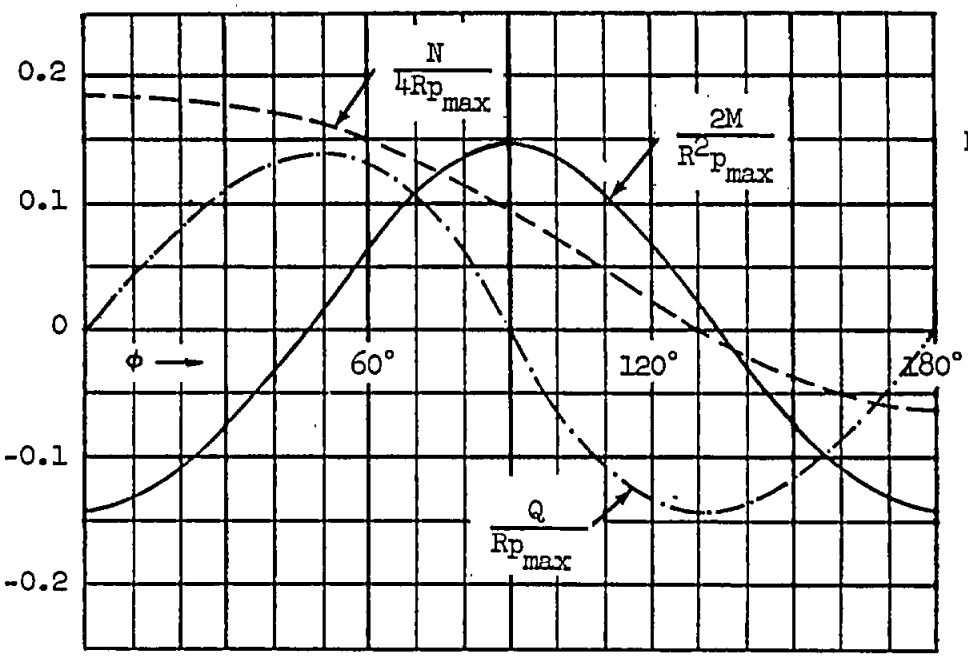

Sign Convention

$M(\phi) = M(-\phi)$

$N(\phi) = N(-\phi)$

$Q(\phi) = -Q(-\phi)$

Displacements

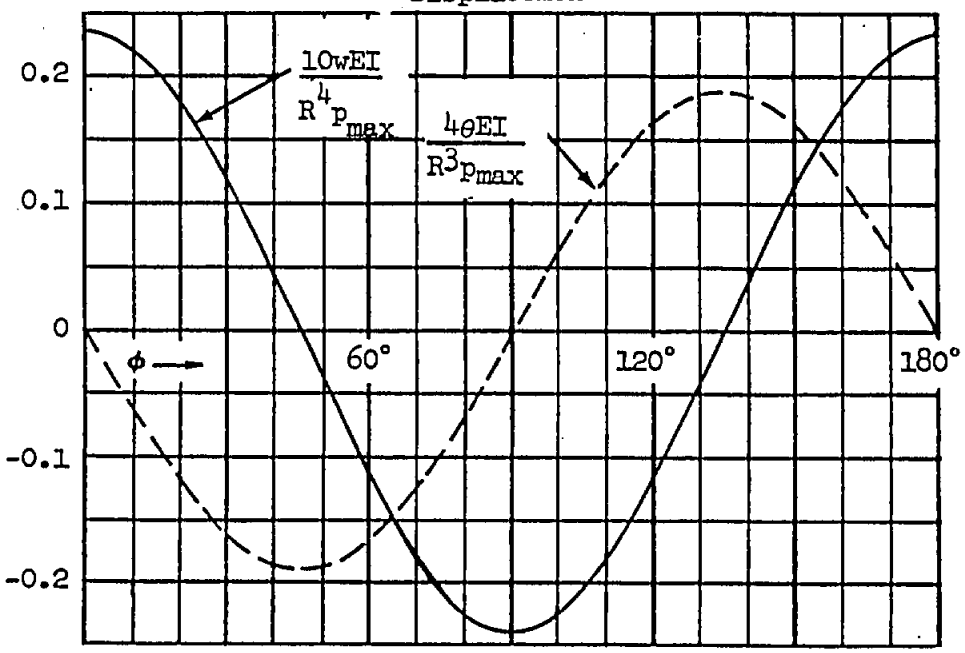

Sign Convention

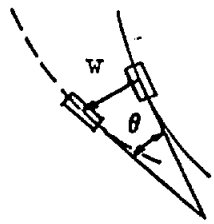

w = + outward

θ = + counter clockwise

$w(\phi) = w(-\phi)$

$\theta(\phi) = -\theta(-\phi)$

CIRCULAR RING LOADS AND DISPLACEMENTS

Loading Condition (19)

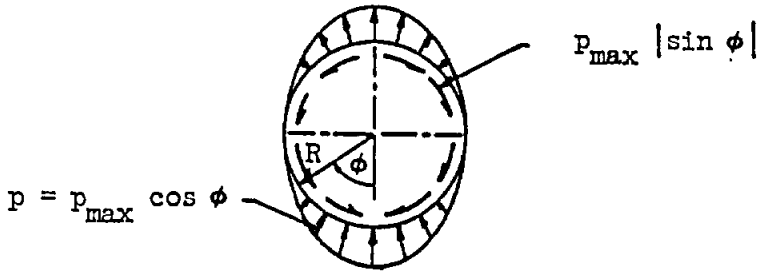

Internal Loads

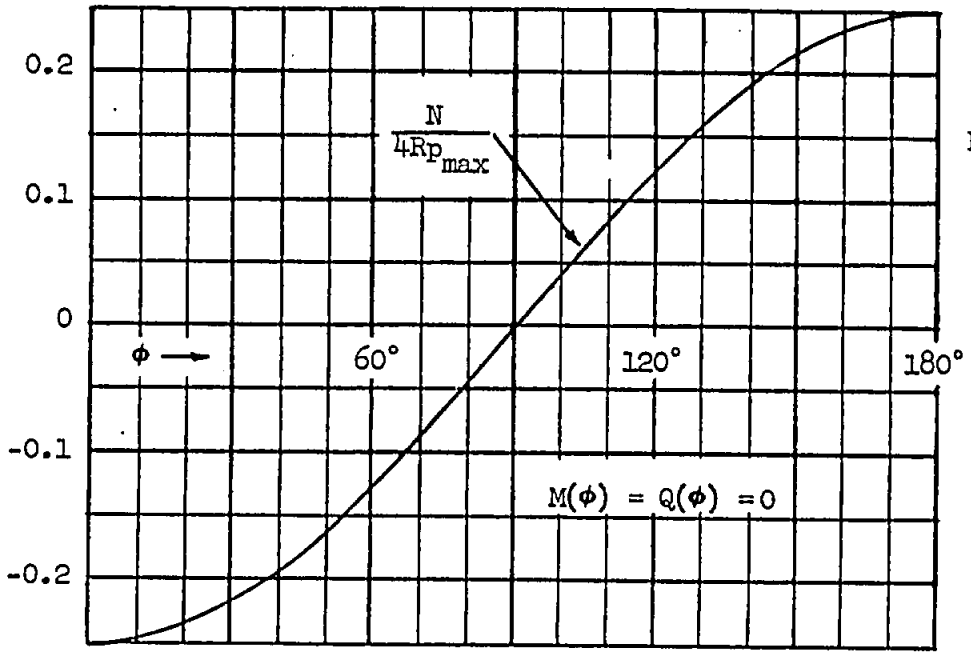

Sign Convention

$M(\phi) = M(-\phi) = 0$

$N(\phi) = N(-\phi)$

$Q(\phi) = Q(-\phi) = 0$

Displacements

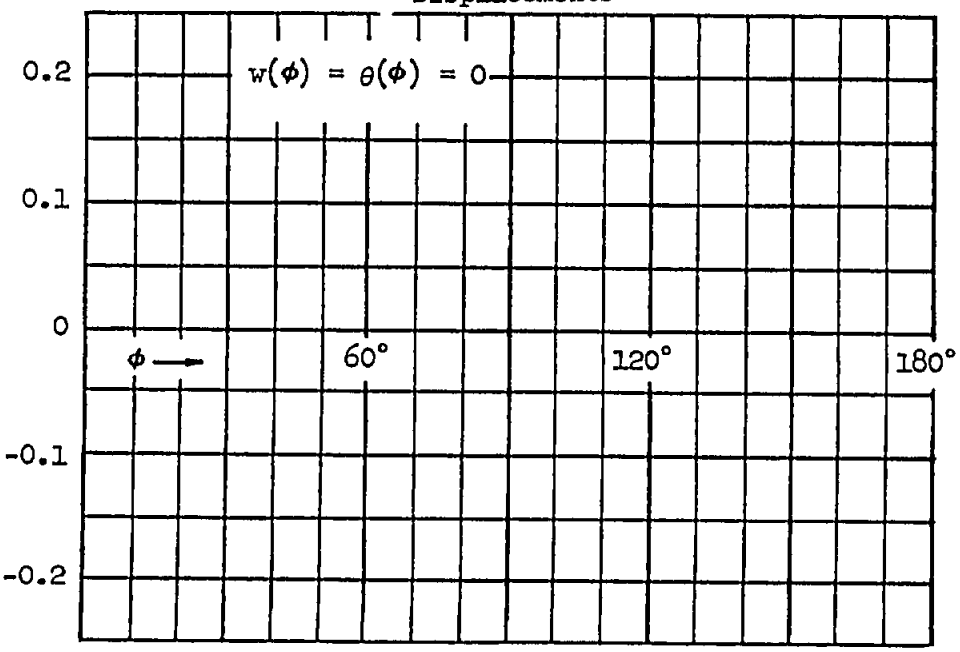

Sign Convention

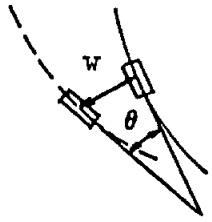

w = + outward

θ = + counter clockwise

$w(\phi) = w(-\phi) = 0$

$\theta(\phi) = \theta(-\phi) = 0$

CIRCULAR RING LOADS AND DISPLACEMENTS

Loading Condition (20)

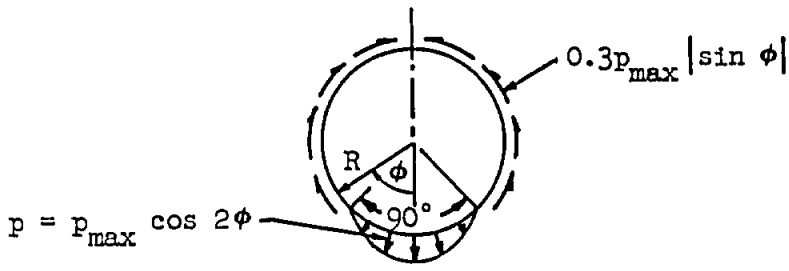

Internal Loads

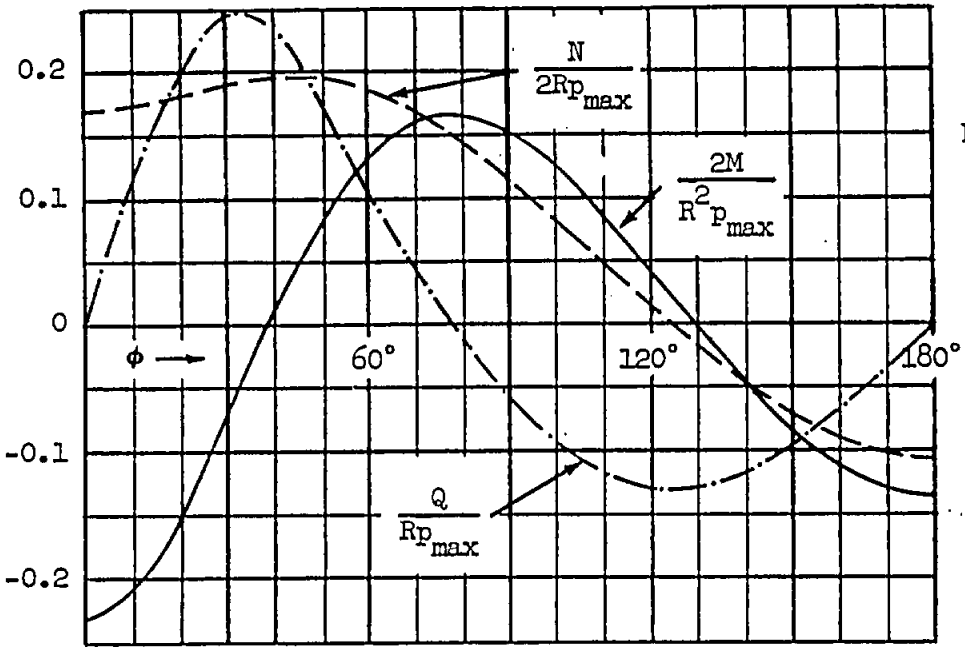

Sign Convention

$M(\phi) = M(-\phi)$

$N(\phi) = N(-\phi)$

$Q(\phi) = -Q(-\phi)$

Displacements

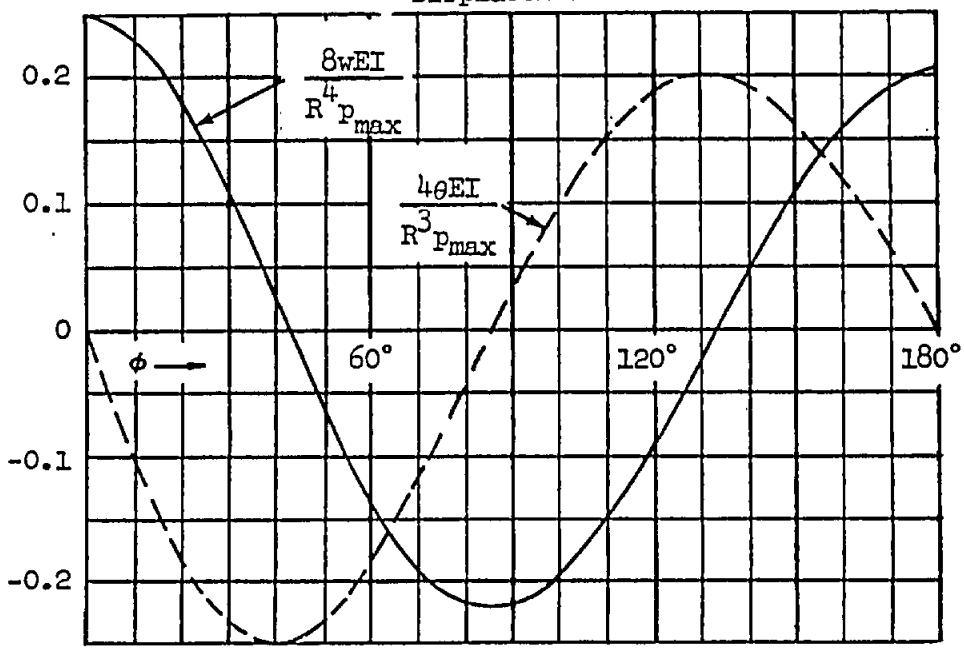

Sign Convention

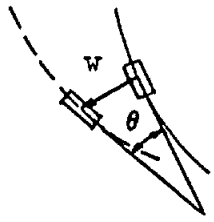

w = + outward

θ = + counter clockwise

$w(\phi) = w(-\phi)$

$\theta(\phi) = -\theta(-\phi)$

CIRCULAR RING LOADS AND DISPLACEMENTS

Loading Condition (21)

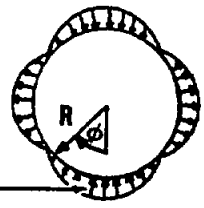

$p = p_{max} \cos 2\phi$

Internal Loads

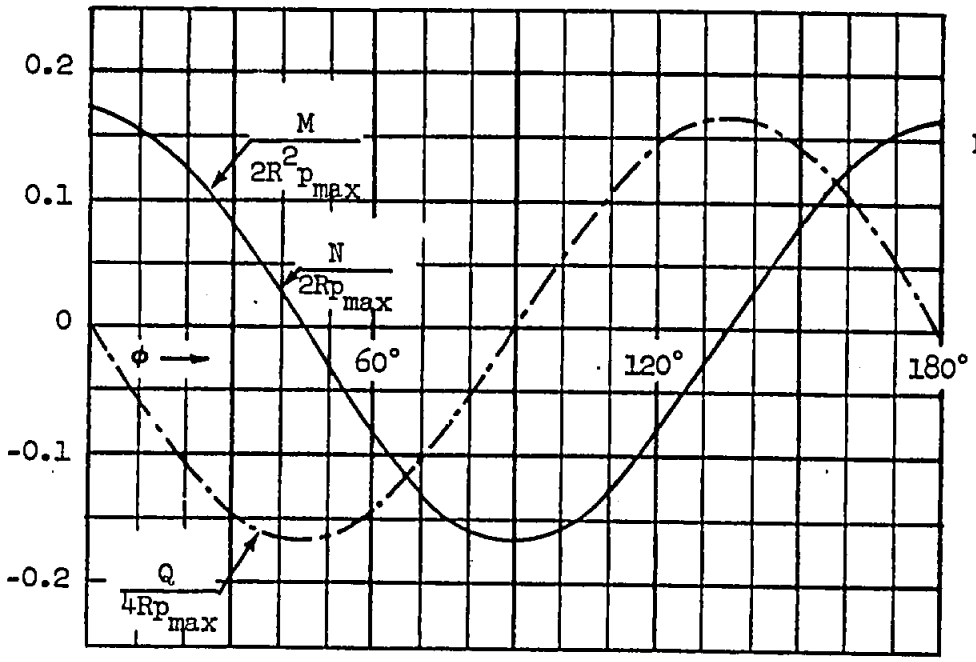

Sign Convention

$M(\phi) = M(-\phi)$
$N(\phi) = N(-\phi)$
$Q(\phi) = -Q(-\phi)$

Displacements

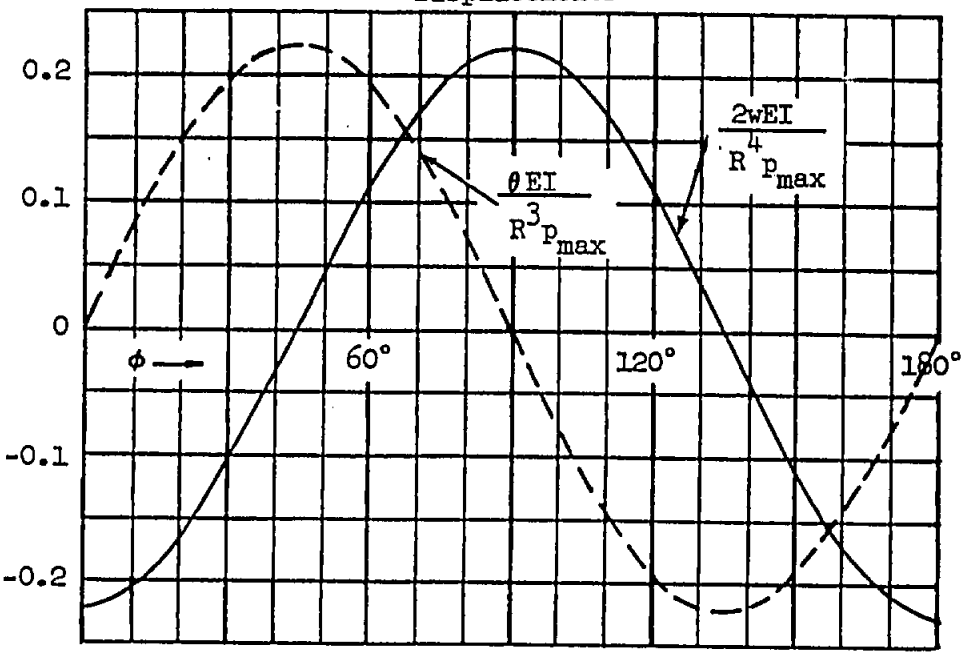

Sign Convention

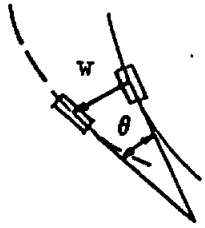

w = + outward

θ = + counter clockwise

$w(\phi) = w(-\phi)$
$\theta(\phi) = -\theta(-\phi)$

CIRCULAR RING LOADS AND DISPLACEMENTS

Loading Condition (22)

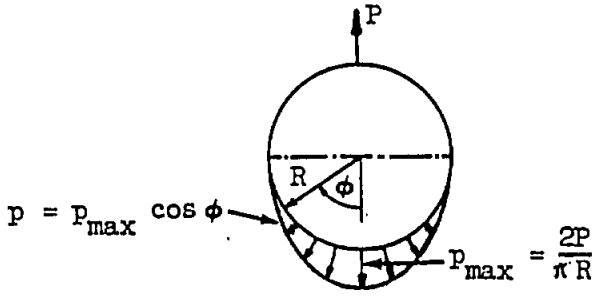

Internal Loads

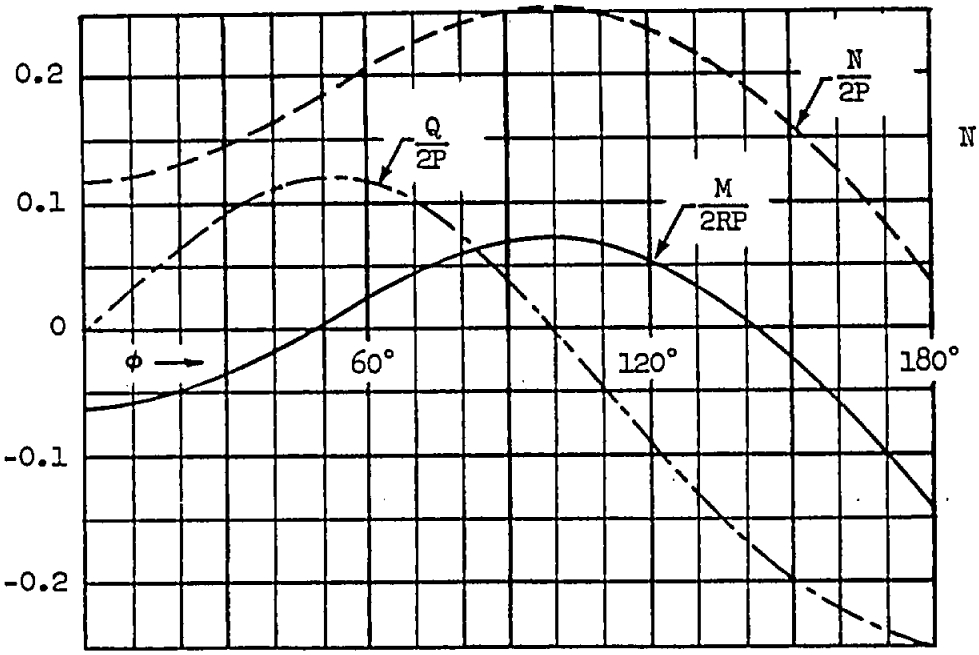

Sign Convention

$M(\phi) = M(-\phi)$
$N(\phi) = N(-\phi)$
$Q(\phi) = -Q(-\phi)$

Displacements

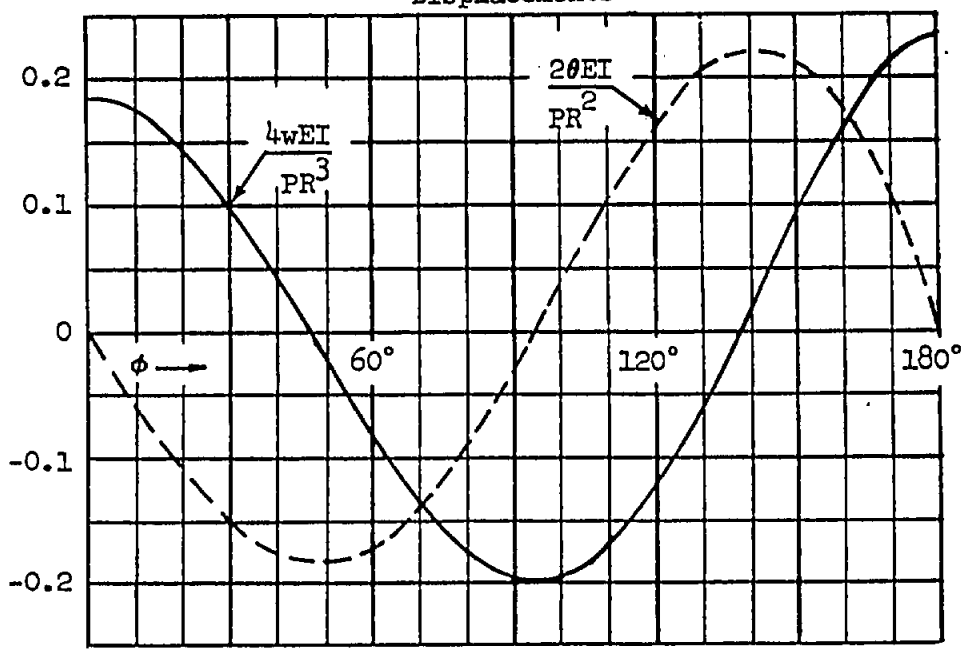

Sign Convention

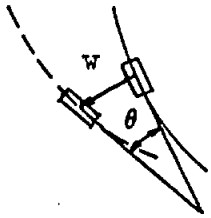

w = + outward

θ = + counter clockwise

$w(\phi) = w(-\phi)$
$\theta(\phi) = -\theta(-\phi)$

Grumman

CIRCULAR RING LOADS AND DISPLACEMENTS

Loading Condition (23)

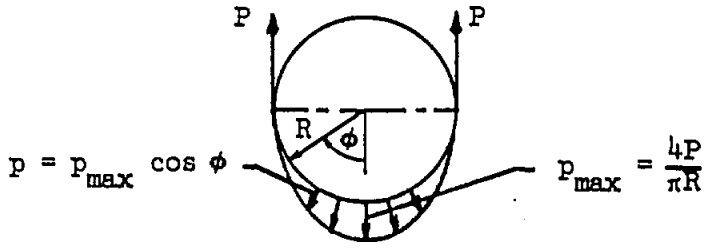

Internal Loads

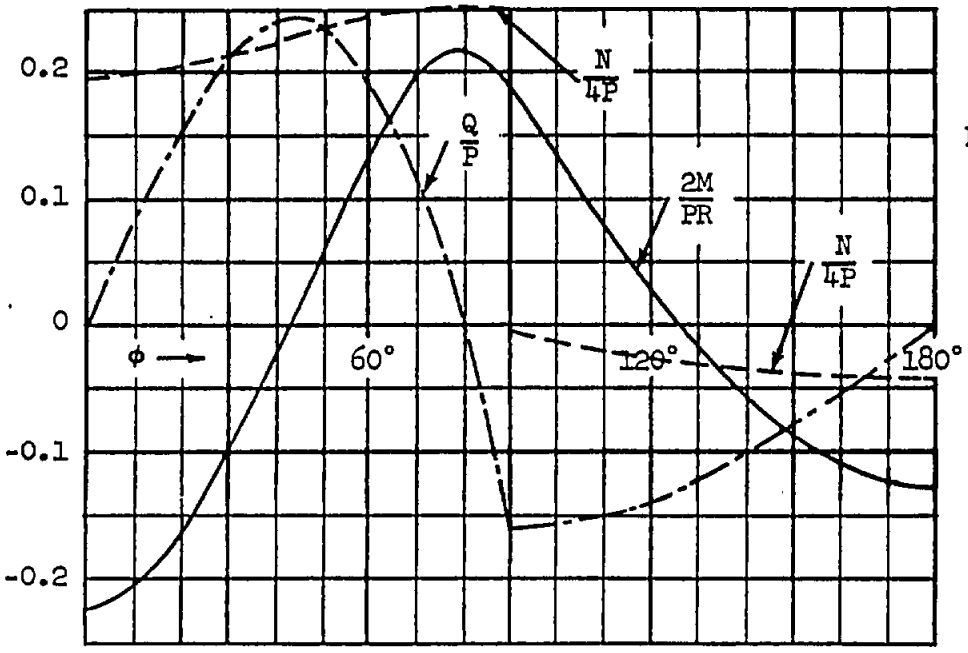

Sign Convention

$M(\phi) = M(-\phi)$
$N(\phi) = N(-\phi)$
$Q(\phi) = -Q(-\phi)$

Displacements

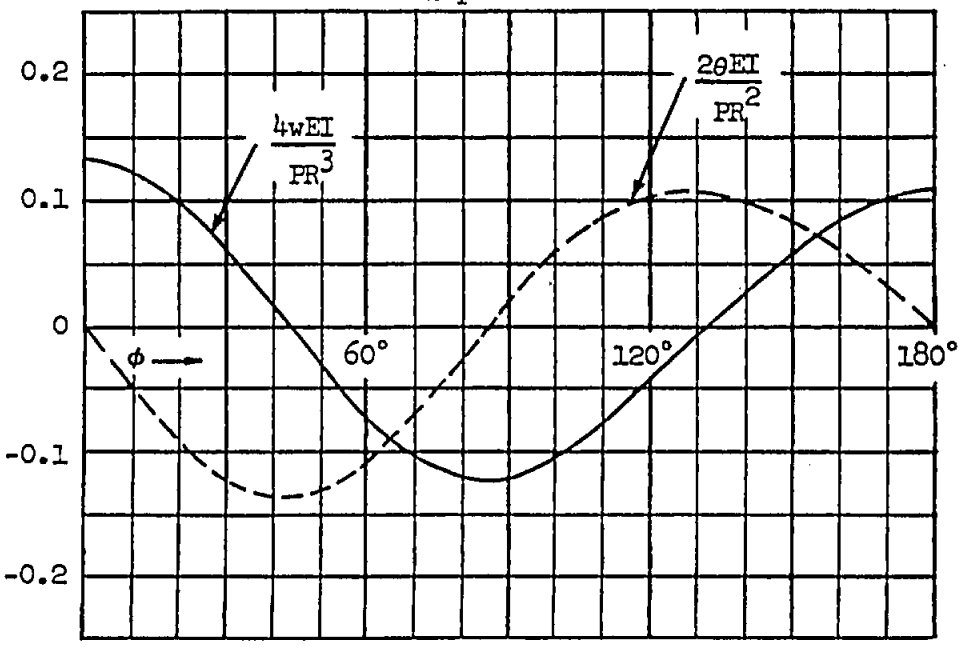

Sign Convention

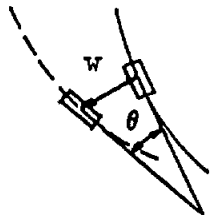

w = + outward

θ = + counter clockwise

$w(\phi) = w(-\phi)$

$\theta(\phi) = -\theta(-\phi)$

CIRCULAR RING LOADS AND DISPLACEMENTS

Loading Condition (24)

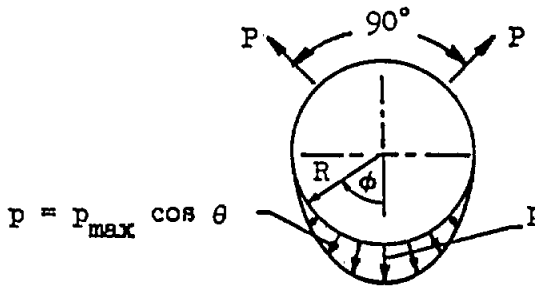

$p = p_{max} \cos \theta$

$p_{max} = \frac{2\sqrt{2}\,P}{\pi R}$

Internal Loads

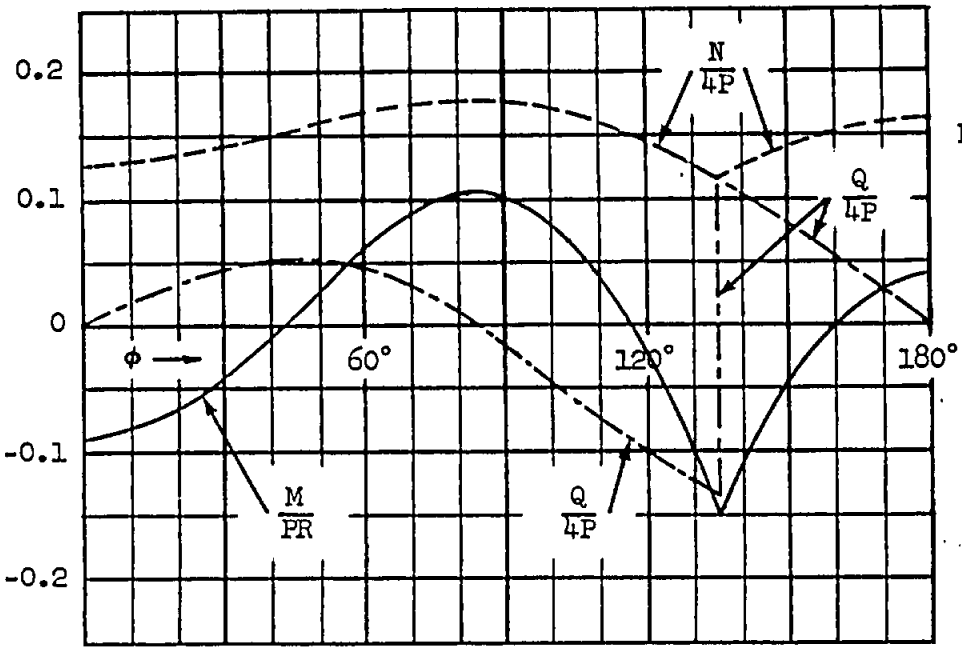

Sign Convention

$M(\phi) = M(-\phi)$
$N(\phi) = N(-\phi)$
$Q(\phi) = -Q(-\phi)$

Displacements

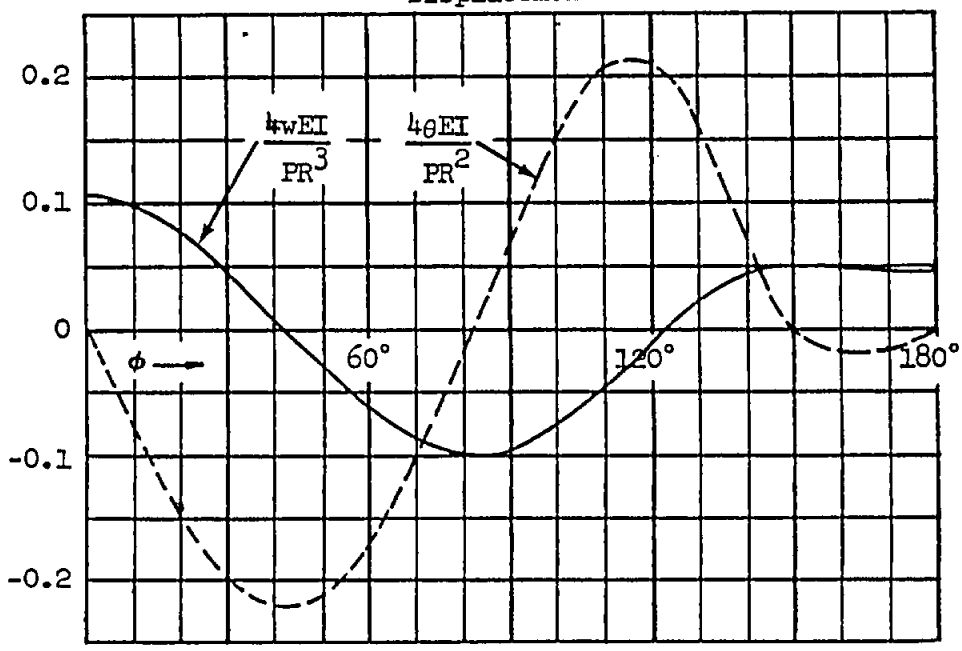

Sign Convention

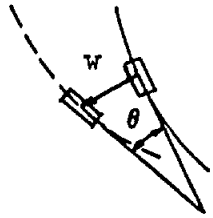

w = + outward

θ = + counter clockwise

$w(\phi) = w(-\phi)$

$\theta(\phi) = -\theta(-\phi)$

BENDING MOMENT IN A PRESSURIZED THIN RING

M = Bending moment, positive when it produces tension in the inner fibers.
R = Ring radius
EI = Ring bending rigidity
p = Internal pressure
b = Ring width

Bending Moment with an Applied Radial Load

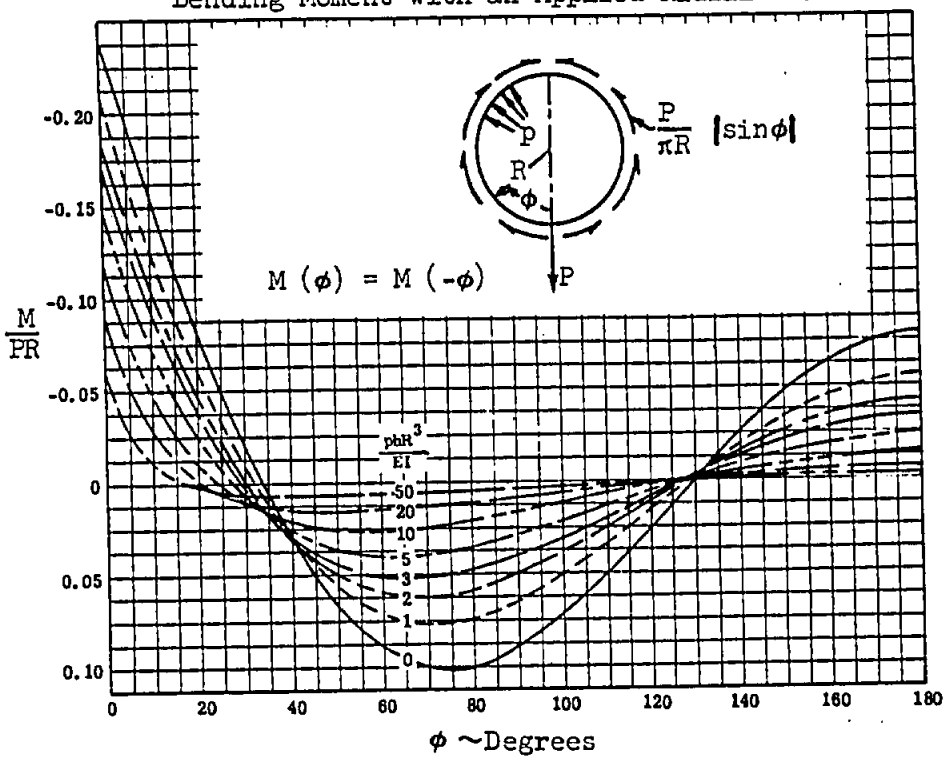

Bending Moment with an Applied Tangential Load

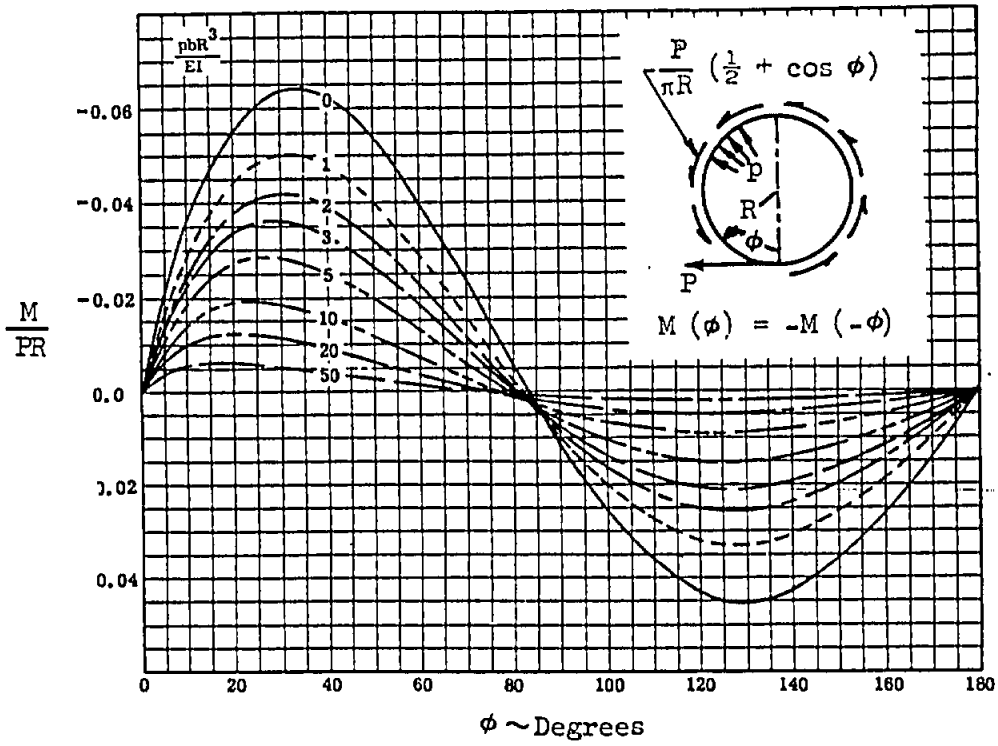

Ref: Grumman Report ADR 04-03c-61.1, August 1961

BENDING MOMENT IN A PRESSURIZED THIN RING

M = Bending moment, positive when it produces tension in the inner fibers

R = Ring radius

EI = Ring bending rigidity

p = Internal pressure

b = Ring width

Bending Moment with an Applied Couple Load

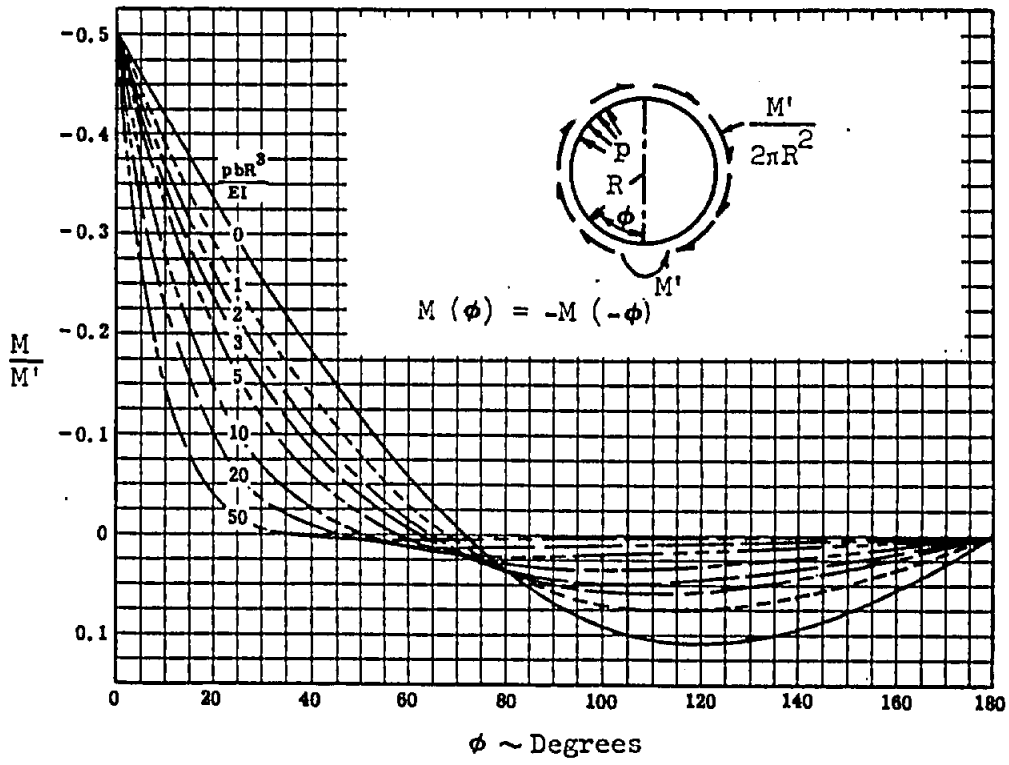

Ref: Grumman Report ADR 04-03c-61.1, August 1961

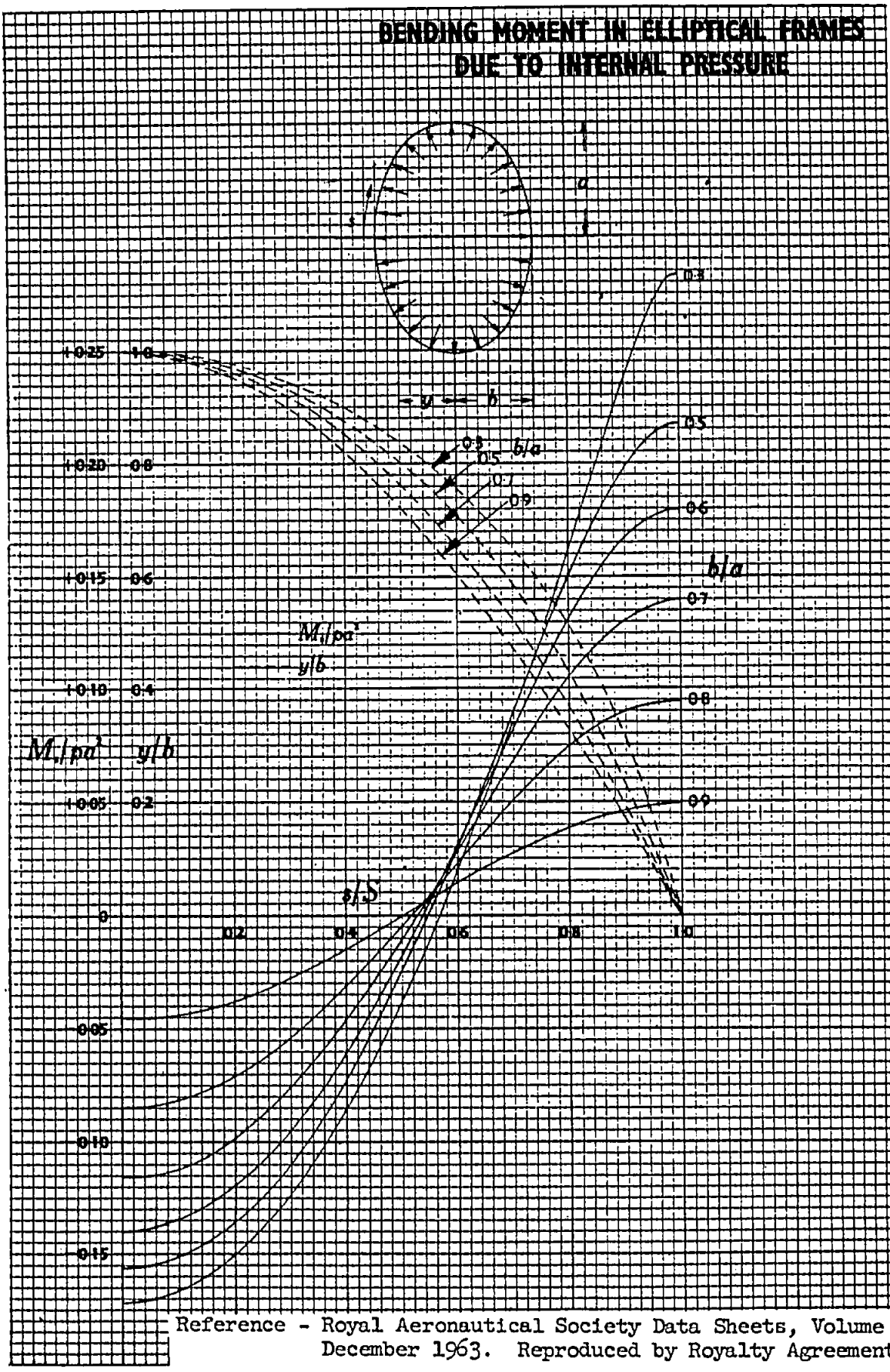

Reference - Royal Aeronautical Society Data Sheets, Volume 4, December 1963. Reproduced by Royalty Agreement.

03.06.05

BENDING MOMENT IN ELLIPTICAL FRAMES DUE TO INTERNAL PRESSURE

(Second Issue June, 1948)

NOTATION

$2a$ = length of major axis of elliptical frame (in.).
$2b$ = length of minor axis of elliptical frame (in.).
s = distance along perimeter from minor axis (in.).
S = quarter of perimeter (in.).
y = distance of point on perimeter from major axis (in.).
p = uniform normal internal loading on frame (lb./in.).
I_s = moment of inertia of cross-section of frame at point s (in.^{4}).
I_o = moment of inertia of cross-section of frame at minor axis (in.^{4}).
M_s = bending moment at point s of frame with constant moment of inertia, positive if it produces tension on the inside of the frame (lb.in.).
M_c = constant correction to bending moment in frame with variable moment of inertia (lb.in.).
$M_s' = M_s + M_c$ = bending moment at point s of frame with variable moment of inertia (lb.in.).

NOTES

The ratios M_s/pa^2 and y/b are plotted against the ratio s/S for various values of b/a.

The moments M_s refer to bending moments in an elliptical frame with constant moment of inertia. The curves can also be used to obtain the bending moment in any elliptical frame of varying moment of inertia provided the major and minor axes are axes of symmetry. The effect of this variation of moment of inertia is simply to add a constant bending moment M_c, where

$$M_c = -\int_0^S (M_s/I_s)\,ds \Big/ \int_0^S ds/I_s \qquad \ldots \quad \ldots \quad \ldots \quad (1)$$

No allowance is made for transverse shear deflection or circumferential extension of the frame centre line, but these effects are not important provided the depth of the section of the frame is less than one-tenth of the radius of curvature.

The contribution of the skin to the stiffness of the frame must be taken into account.

DERIVATION

Timoshenko, Strength of materials, Part II (second edition) p. 90, 1941.

EXAMPLES

(1) Find the maximum bending moment in the frame of a fuselage of elliptical cross-section with frames equally spaced at 15 in. pitch when the internal pressure is 10 lb./in.^{2}, $a = 55$ in., and $b = 43$ in..

Then, $p = 10 \times 15 = 150$ lb./in. and $b/a = 0.782$.

From diagram the maximum bending moment occurs at $s/S = 1$ and by interpolation,

$M_s/pa^2 = 0.103$, hence $M_s = 0.103 \times 150 \times 55^2 = 46{,}700$ lb.in..

(2) Find the bending moment correction and the bending moments at the major and minor axes of an elliptical frame when $a = 62$ in., $b = 31$ in., $p = 120$ lb./in. and the moment of inertia varies as in the following table:

s/S	0	0.1	0.2	0.3	0.4	0.5	0.6	0.7	0.8	0.9	1.0
I_s/I_o	1	1.01	1.04	1.09	1.16	1.25	1.36	1.49	1.64	1.81	2.0

Then $b/a = 0.5$.

From diagram for $b/a = 0.5$ and from the above values of I_s/I_o the following table is obtained:

s/S	0	0.1	0.2	0.3	0.4	0.5	0.6	0.7	0.8	0.9	1.0
M_s/pa^2	−.158	−.151	−.136	−.110	−.073	−.024	.030	.090	.149	.197	.218
$1/(I_s/I_o)$	1	.990	.962	.917	.862	.800	.735	.671	.610	.552	.5
$(M_s/pa^2)/(I_s/I_o)$	−.158	−.150	−.131	−.102	−.063	−.019	.022	.060	.091	.109	.109

Rewriting formula (1) in a non-dimensional form,

$$M_c/pa^2 = -\frac{\int_0^S \frac{M_s/pa^2}{I_s/I_o}\,d(s/S)}{\int_0^S \frac{d(s/S)}{I_s/I_o}}$$

and integrating by Simpson's rule, or otherwise, one finds,

$$M_c/pa^2 = -\frac{-6.10}{141.4} = 0.043.$$

Thus $M_c = 0.043 \times 120 \times 62^2 = 19{,}800$ lb.in..

From table and notation the bending moments at the minor and major axes are respectively,

$$M_o' = -0.158 \times 120 \times 62^2 + 19{,}800 = -53{,}000 \text{ lb.in.}.$$

and

$$M_a' = 0.218 \times 120 \times 62^2 + 19{,}800 = 120{,}300 \text{ lb.in.}.$$

Reference - Royal Aeronautical Society Data Sheets, Volume 4, December 1963. Reproduced by Royalty Agreement.

SECTION C3.05--SHELL SUPPORTED CIRCULAR RINGS

Table of Contents

DISCUSSION

As already noted in the discussion on page C3.01-1, the stress distributions and displacements in shell supported rings are strongly influenced by the relative stiffnesses of ring and supporting shell. If the ring is relatively rigid, the stress distributions and deflections on pages C3.02-1 thru -25 are applicable. For relatively more flexible rings, the design curves of this subsection are applicable.

Three Important References

There are three important references available in the literature on shell supported rings. They give exact analyses for idealized structures of varying complexity and are summarized briefly in the next paragraphs. In situations where the structure to be designed is sufficiently like one of the idealized structures treated, i.e., structural parameters lie within the range given and the desired structural proportions are covered, it is advantageous to go directly to the appropriate report. Otherwise, the approximate design procedure proposed in the third reference and described subsequently may be used.

NACA TN 929 (Ref. 1, see page C3.05.3-1)

The structural idealization of this report is shown on the accompanying sketch. The analysis assumptions made are:

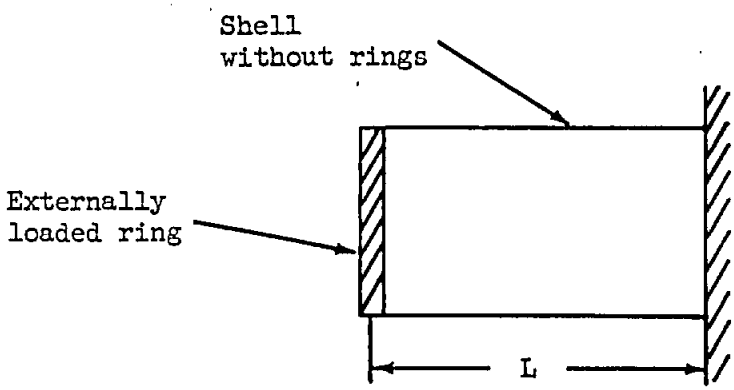

(1) The shell is cylindrical, uniform and of length L.

(2) Only shell shearing deformations are considered, i.e., the skin can undergo shearing strain but not direct strain.

(3) The ring has bending flexibility only and is uniform. Its neutral axis coincides with the shell skin line, to which it is continuously attached.

(4) The structure behaves linearly and is elastic.

The simplicity of the idealization allows the analysis results to be presented as families of curves in a single parameter d, where $d = GtR^4/EIL$. These curves are reproduced on pages C3.05.5-2 thru -10, and show frame internal loads and displacements for unit applied radial, tangential, and couple loads.

The basic weakness of the approach as originally proposed is the uncertainty regarding the selection of length L. As originally defined, it is to be taken as the distance from the loaded frame to the nearest effective bulkhead or stiff frame where the locally induced perturbations are negligible. This weakness has been largely overcome in NASA TN D-402 (to be discussed later) which gives a still approximate but somewhat more rational method for evaluating L.

NACA TN 1310 (Ref. 2, page C3.05.3-1)

This report is an improvement over TN 929 in that the unrealistic assumption of zero direct strain in the skin is eliminated, and the reinforcing rings are accounted for in an entirely rational manner. Specifically, the assumptions are:

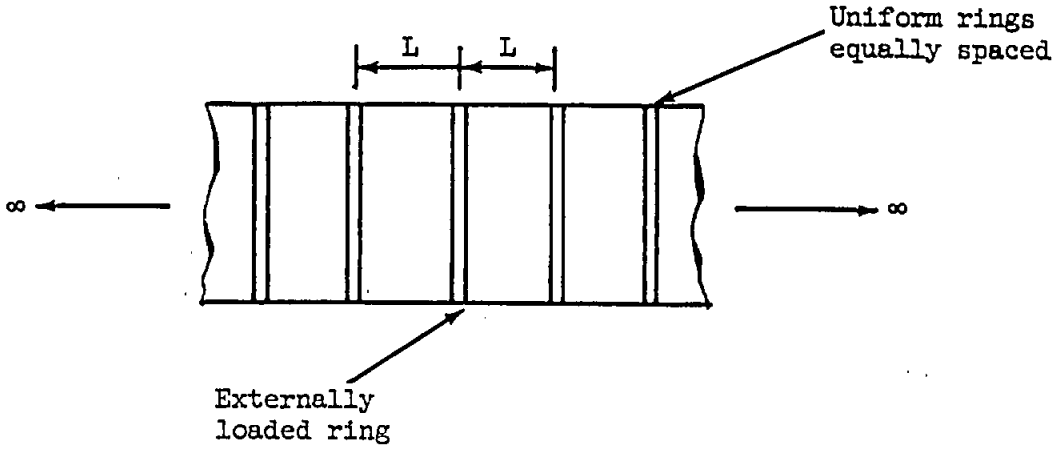

(1) The shell is cylindrical, uniform and extends to infinity on both sides of the loaded ring.

(2) The externally loaded ring and the reinforcing rings are identical. They are of uniform moment of inertia, uniformly spaced, and their neutral axes coincide with the shell skin.

(3) Longerons are smeared out circumferentially creating an effective skin thickness t' which resists the longitudinal direct stresses. The true skin thickness t resists the shear stresses. This effective skin thus acts as an orthotropic membrane.

(4) The structure behaves linearly and is elastic.

Due to the additional complexity of this idealization the results must be presented as families of curves in two parameters A and A/B, where $A = t'R^6/IL^3$ and $A/B = GtR^4/EIL$. These curves show the loaded frame and adjacent frame internal

loads, and the axial stresses induced in the skin. The assumption that the shell extends to infinity is not unduly restricting since the effect of the perturbation caused by the loaded ring is actually confined to a region extending only several diameters to either side. The range of parameters covered by the curves is

$$2 \times 10^2 \leq A \leq 2 \times 10^6$$

$$0 \leq A/B \leq \infty$$

NASA TN D-402 (Ref. 3, page C3.05.3-1)

The essential difference between the idealized structure of TN 1310 and that of this reference is the provision for the moment of inertia of the loaded ring to be different from that of the reinforcing rings. The detailed assumptions are:

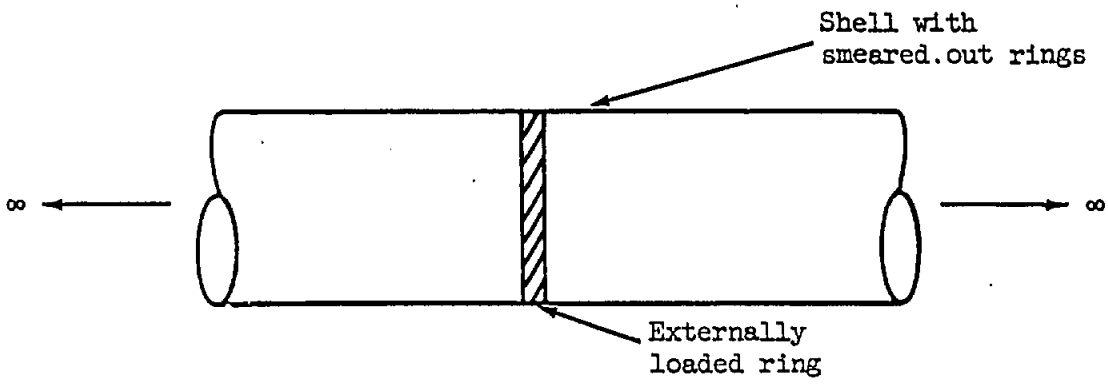

(1) The shell is cylindrical, uniform and extends to infinity on both sides of the loaded ring.

(2) The externally loaded ring is of uniform moment of inertia, and its neutral axis coincides with the shell skin.

(3) Longerons are smeared out circumferentially, creating an effective skin thickness t_e ($=t'$ of TN 1310) which resists the longitudinal direct stresses. The true skin thickness t resists the shear stresses.

(4) The shell reinforcing rings are smeared out longitudinally creating an equivalent uniform skin moment of inertia. The shell skin thus acts as an orthotropic curved plate.

(5) The structure behaves linearly and is elastic.

The analysis results are presented in tabular form as functions of the new parameters γ, L_r, and L_c, to be defined later. The coefficients given define the stress distribution in the frame and in the shell within a distance L_c of the frame. The range of parameters covered is

$$0.02 \leq \gamma \leq 3$$

$$0.2 \leq L_r/L_c \leq 1$$

The report also redefines the parameters d of TN 929 and A and A/B of TN 1310 in terms of γ, L_r and L_c, and shows how the predictions of the three reports for ring loads can be made to agree reasonably well. This permits the use of the relatively simple curves of TN 929 in a somewhat rational design procedure, and is the basis for the discussion which follows. Recommended procedures are also given in TN D-402 and here for the usual situation in which the actual structure deviates from complete uniformity.

Limitations of the Design Procedure

The design procedure given in the next paragraph applies to structure which is reasonably circular, integral and uniform, such as is found in some missile tanks and aircraft fuselages. It does not account for the following features, which may be significant in some structures:

(1) non-circular cross sections

(2) shells where the cross sections vary longitudinally

(3) presence of major discontinuities such as door cutouts, or large access holes, near the loaded ring

(4) bending stiffness of longerons

(5) axial and shear flexibility of rings

The effects of (4) and (5) are generally small. Their omission yields ring loads which are conservative. For structures that are decidedly non-circular or non-uniform as indicated by items 1, 2 and 3, the predictions of the procedure are questionable.

Use of the Design Curves

The graphs on pages 3.04.5-2 through -10 show curves for ring internal loads and displacements, and supporting skin shears, for unit radial, tangential, and couple loads, as functions of the stiffness parameter d. On page 3.05.5-1, d is defined in terms of L_r, L_c, and γ. To enter this curve, L_r, L_c, and γ must be evaluated from formulas (1), (2) and (3):

$$L_c = \frac{R}{\sqrt{6}} \left[\frac{E_{sk}\, t_e\, R^2}{E_f i} \right]^{1/4} \qquad (1)$$

$$L_r = \frac{R}{2} \sqrt{\frac{E_{sk}\, t_e}{Gt}} \qquad (2)$$

$$\frac{1}{\gamma} = \frac{2\, E_f i L_c}{E_o\, I_o} \qquad (3)$$

See page C3.05.4-1 for explanation of symbols used.

L_c is the distance from the loaded ring within which the effect of the shell perturbations substantially die out. To approximate moderately non-uniform structure the stiffness factors Gt, $E_{sk}t_e$, and $E_f i$ should be averaged in the region of the loaded ring. The average of Gt, and $E_{sk}t_e$ should be taken for a distance $L_c/2$ on both sides of the loaded frame. $E_f i$ can be evaluated from equations (4), (5) and (6).

$$E_f i = (E_f i)_{fwd} + (E_f i)_{aft} \qquad (4)$$

$$(E_f i)_{fwd} = \frac{1}{L_c} \sum_{fwd} W\, E_f\, I_f \qquad (5)$$

$$(E_f i)_{aft} = \frac{1}{L_c} \sum_{aft} W\, E_f\, I_f \qquad (6)$$

where

$$W = 1 - \frac{X}{L_c} \text{ for } X < L_c$$

$$W = 0 \text{ for } X > L_c$$

X is the distance from the loaded ring to a reinforcing ring. Since L_c is a function of $E_f i$ (note equation (1)), an initial estimate of L_c is required to evaluate (4), (5) and (6), (see illustrative problem). For the situation where

a rigid bulkhead or exceptionally stiff frame or the free end of the shell is within a distance L_c of the loaded ring, TN D-402 describes how to evaluate γ, and L_c. The use of the curves for ring internal loads is straightforward. Additional comments concerning the application of the shear flow and the displacements curves are necessary, however.

Shear Flow

The ring shear flow q determined from pages 3.05.5-3, -6, and -9 can be considered to be composed of two parts:

(1) Shears defined by VQ/I and T/2A. This distribution is shown by the curve for d = 0.

(2) Induced self-balancing shears due to ring-shell distortions.

Shears defined by (1) are distributed in the shell as dictated by equilibrium. The induced shear flow is reacted on both sides of the loaded ring in proportion to the shell relative stiffness. For reasonably non-uniform shells this distribution can be approximated by equations (7) and (8).

$$q \text{ induced fwd} = \frac{(E_f i)_{fwd}}{E_f i} (q_d - q_o) \qquad (7)$$

$$q \text{ induced aft} = \frac{(E_f i)_{aft}}{E_f i} (q_d - q_o) \qquad (8)$$

Ring Displacements

The displacements shown on pages 3.05.5-3, -4, -6, -7, -9 and -10, can also be considered to be composed of two parts:

(1) Translation and rotation of the ring as a rigid body, due to shell skin shear deformations (note idealized structure sketch for TN 929).

(2) Ring bending distortions.

The value normally required for design purposes is the deflection due to ring bending distortions. For values of $d > 300$ the effects of (1) are relatively small and can be neglected. When $d < 300$ the effects of (1) can approximately be eliminated by subtracting the corresponding value from the d = 0 curve. This latter curve consists of ring translational displacement as a rigid body.

Illustrative Problem

Given: A segment of a cylindrical semi-monocoque aluminum fuselage structure shown in the accompanying sketch with an externally applied radial load of 1000 pounds. All units are in inches and pounds.

Find: (1) The frame maximum moment, axial load, and shear load, and their respective locations.

(2) The maximum radial, rotational, and tangential displacements, and their respective locations.

(3) Compare these results with those shown on page C3.02-2.

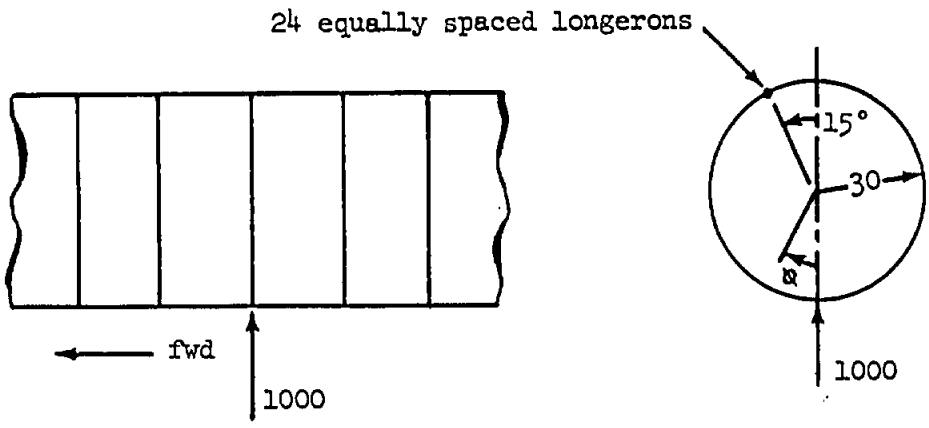

I_o = 3.0, frame spacing = 24"

I of frames fwd of the loaded frame = 2.0

I of frames aft of the loaded frame = 1.0

Area of one longeron fwd of the loaded frame = 0.30

Area of one longeron aft of the loaded frame = 0.20

Skin thickness fwd of the loaded frame = .040

Skin thickness aft of the loaded frame = .030

$E = 10^7$, $G = 4 \times 10^6$

Solution:

Compute

$$(Gt)_{avg} = \frac{G\,(t_{aft} + t_{fwd})}{2} = 0.14 \times 10^6$$

$$(t_e)_{fwd} = 0.040 + \frac{24(.30)}{2\pi(30)} = 0.078$$

$$(t_e)_{aft} = 0.030 + \frac{24(.20)}{2\pi(30)} = 0.056$$

then

$$E_{sk}t_e = \frac{10^7}{2}\,(0.078 + 0.056) = 0.67 \times 10^6$$

Compute L_c

To obtain a first approximation for L_c assume,

$$E_f i = \frac{10^7}{2}\,\left(\frac{2}{24} + \frac{1}{24}\right) = 0.625 \times 10^6$$

From equation (1),

$$L_c = \frac{R}{\sqrt{6}}\left[\frac{E_{sk}t_e R2}{E_f i}\right]^{1/4} = 68.2$$

From equations (5) and (6),

$$(E_f i)_{fwd} = \frac{2 \times 10^7}{68.2}\left[\left(1 - \frac{24}{68.2}\right) + \left(1 - \frac{48}{68.2}\right)\right] = 0.277 \times 10^6$$

$$(E_f i)_{aft} = \frac{(E_f i)_{fwd}}{2} = 0.139 \times 10^6$$

$$E_f i = 0.416 \times 10^6$$

Recomputing L_c from (1)

$$L_c = 75.6$$

From equations (2) and (3)

$L_r = 32.8$

$\frac{l}{\gamma} = 2.1 \qquad L_r/L_c = 0.434$

From page C3.05.5-1

$d = 60$

From page C3.02-2 and the curves on pages C3.05.5-2 through C3.05.5-4 (for stiffness parameter d = 50) the following table is obtained:

	Shell Supported Ring		Relatively Stiff Ring	
	Load or Deflection	Location, ϕ	Load or Deflection	Location, ϕ
Moment, M	5250	0°	7,200	0°
Axial Load, N	-580	15°	-435	45°
Shear Load, Q	-500	0°	-500	0°
Shear flow, q	-21.6	43°	- 11	90°
Radial Deflec., w	$.022 \frac{PR^3}{EI}$	0°	$.043 \frac{PR^3}{EI}$	0°
Rotational deflec., θ	$-.036 \frac{PR^2}{EI}$	26°	$-.083 \frac{PR^2}{EI}$	35°
Tangential deflec., v	$.0086 \frac{PR^3}{EI}$	43°	$.019 \frac{PR^3}{EI}$	40°
Skin Axial Stress in Longitudinal Direction	34.4 psi (Comp.)	0°	0	

*See TN D-402, tables 83 and 92 for $\gamma = .476$, $\frac{L_r}{L_c} = .400$

REFERENCES

1. Wignot, J.E., E., Combs, H. and Ensrud, A.F.: "Analysis of Circular Shell-Supported Frames", NACA TN 929, July 1943.

2. Duberg, J.E., Kempner, J.: "Charts for the Stress Analysis of Reinforced Circular Cylinders Under Lateral Loads", NACA TN 1310, May 1947.

3. MacNeal, Richard H., and Bailie, John A.: "Analysis of Frame Reinforced Cylindrical Shells - Part III - Applications", NASA TN D-402, May 1960.

4. Royal Aeronautical Society Data Sheets, Volume 4, December 1963.

5. Jensen, W.R., "Bending Moments for the Design of Pressurized Shell Reinforcing Rings at Concentrated Loads", Grumman Report No. ADR 04-03c-61.1, August 1961.

6. Jensen, W.R., "On Simplified Fuselage Structure Stress Distributions", J. Aero/Space Sciences, 25, No. 10, October 1958.

LIST OF SYMBOLS

P	applied load, either radial or tangential
M'	applied couple load; positive clockwise
M	frame internal bending moment; positive when inner fibers are in tension
N	frame axial load; positive in tension
Q	frame shear load; positive when up on the left of an elemental cut (see page 3.05.5-3)
R	radius of the shell
w	radial displacement; positive inward
θ	rotational displacement; positive clockwise
v	tangential displacement; positive clockwise
q	shear flow acting on frame; positive clockwise
q_o	shear flow acting on frame for d = 0
d	stiffness parameter determined from page C3.05.5-1
E_o	Young's modulus of the loaded frame
E_f	Young's modulus of an unloaded frame
E_{sk}	Young's modulus of the skin
I_o	moment of inertia of the loaded frame
I_f	moment of inertia of an unloaded frame
i	cross-sectional moment of inertia of unloaded frames per unit length of shell
G	shear modulus of shell skin
t	effective shell skin thickness for shear loads
t_e	weighted average of all bending material including skin and longerons assumed uniformly distributed around the circumference

L_c $\frac{R}{\sqrt{6}}\left[\frac{E_{sk}t_e R^2}{E_f i}\right]^{1/4}$, the length from the loaded frame to where the shell stress deviation from the "Mc/I" and "VQ/I" distribution are small.

L_r $\frac{R}{2}\sqrt{\frac{E_{sk}t_e}{Gt}}$

$\frac{1}{\gamma}$ $\frac{2E_f i L_c}{E_o I_o}$, ratio of the stiffness of the unloaded frames to the loaded frame

A parameter in TN 1310

$\frac{A}{B}$ parameter in TN 1310

X distance from loaded frame to unloaded frame

SHELL SUPPORTED CIRCULAR FRAMES

Chart to Determine Stiffness Parameter d

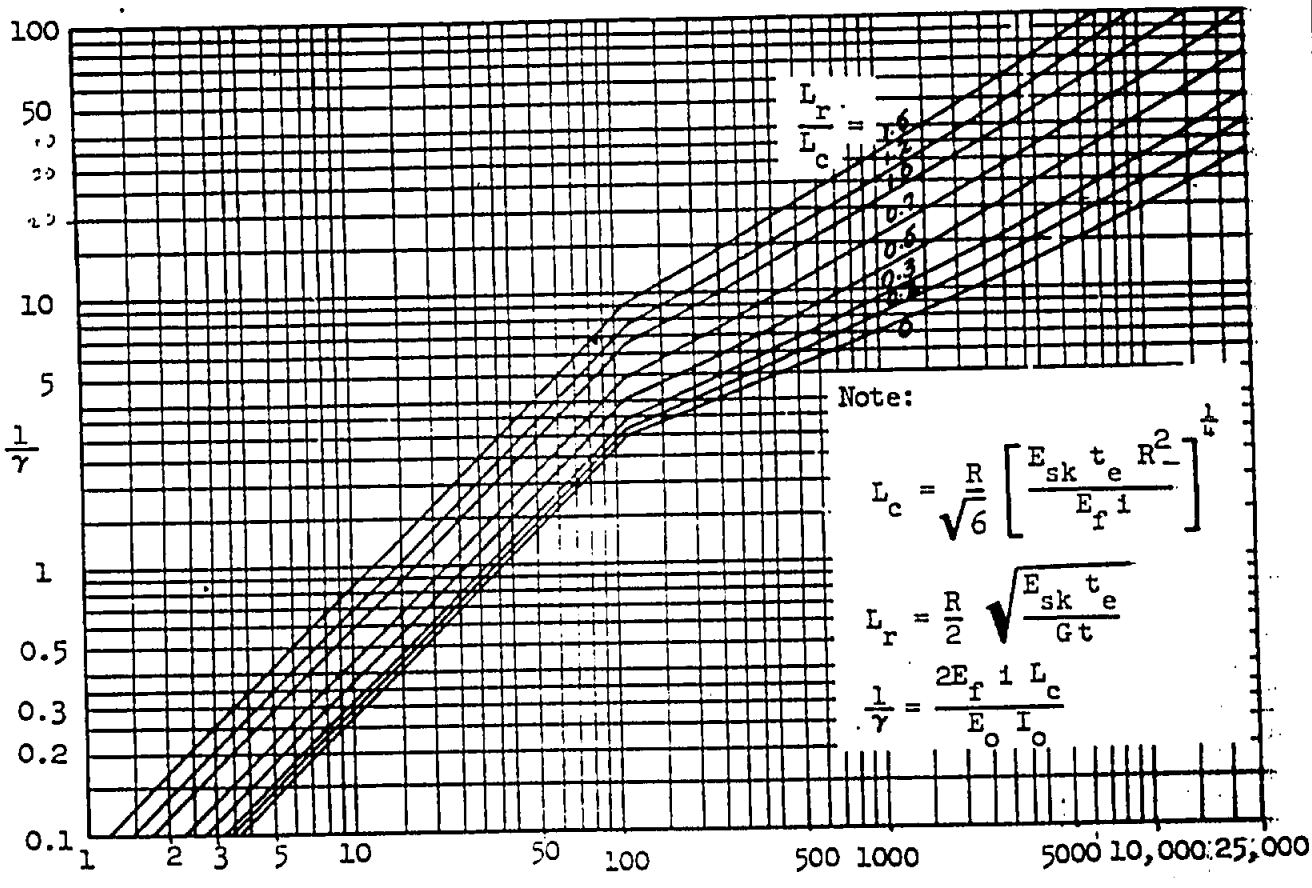

Reference - NASA TN D-402

SHELL SUPPORTED CIRCULAR RINGS

Bending Moments for an Applied Radial Load

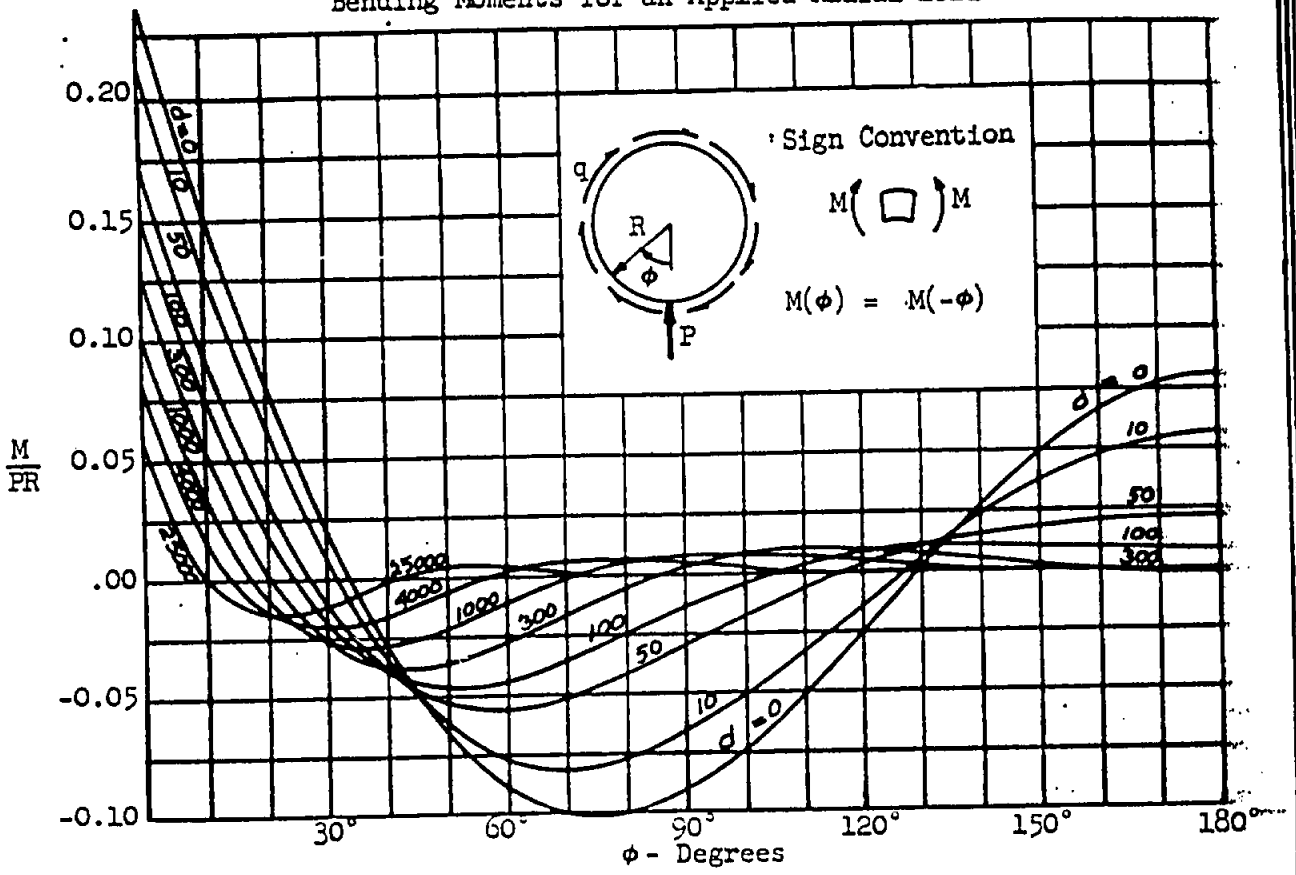

Axial Loads for an Applied Radial Load

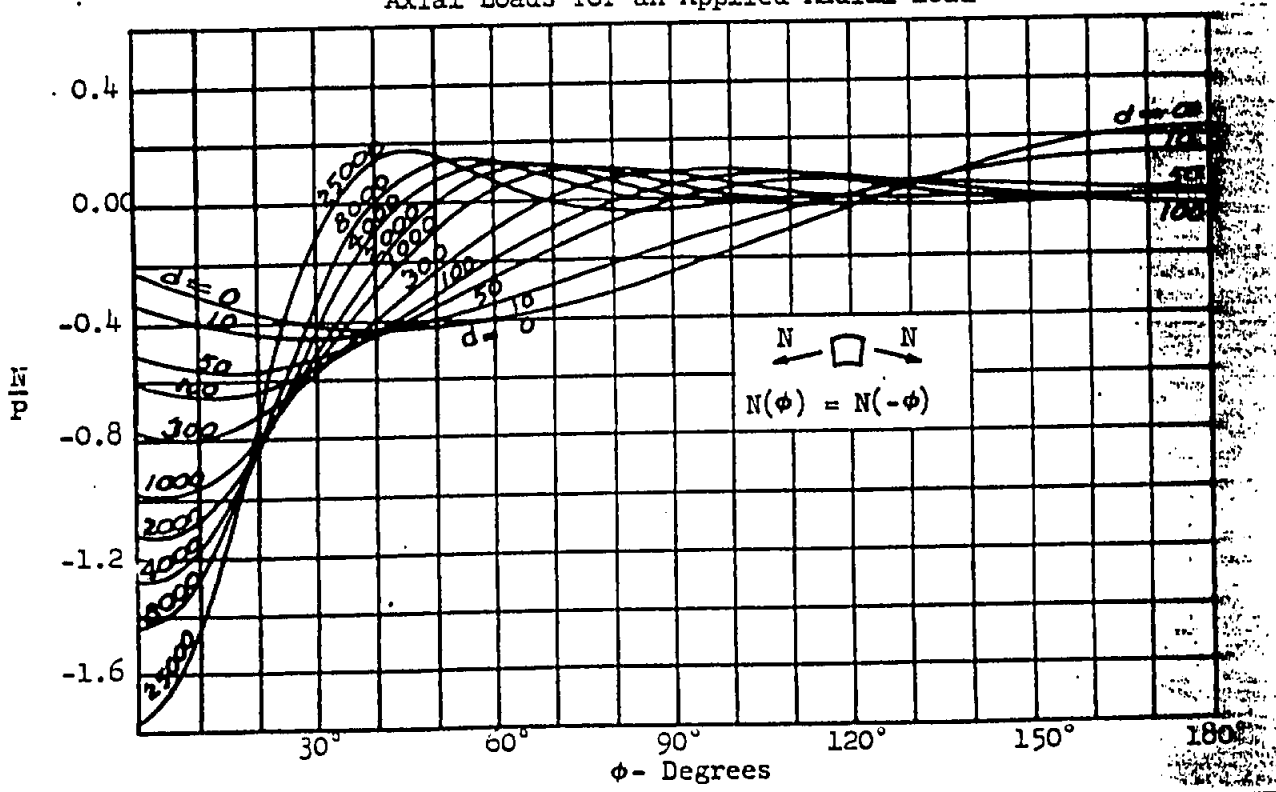

SHELL SUPPORTED CIRCULAR RINGS

Shear Load For An Applied Radial Load

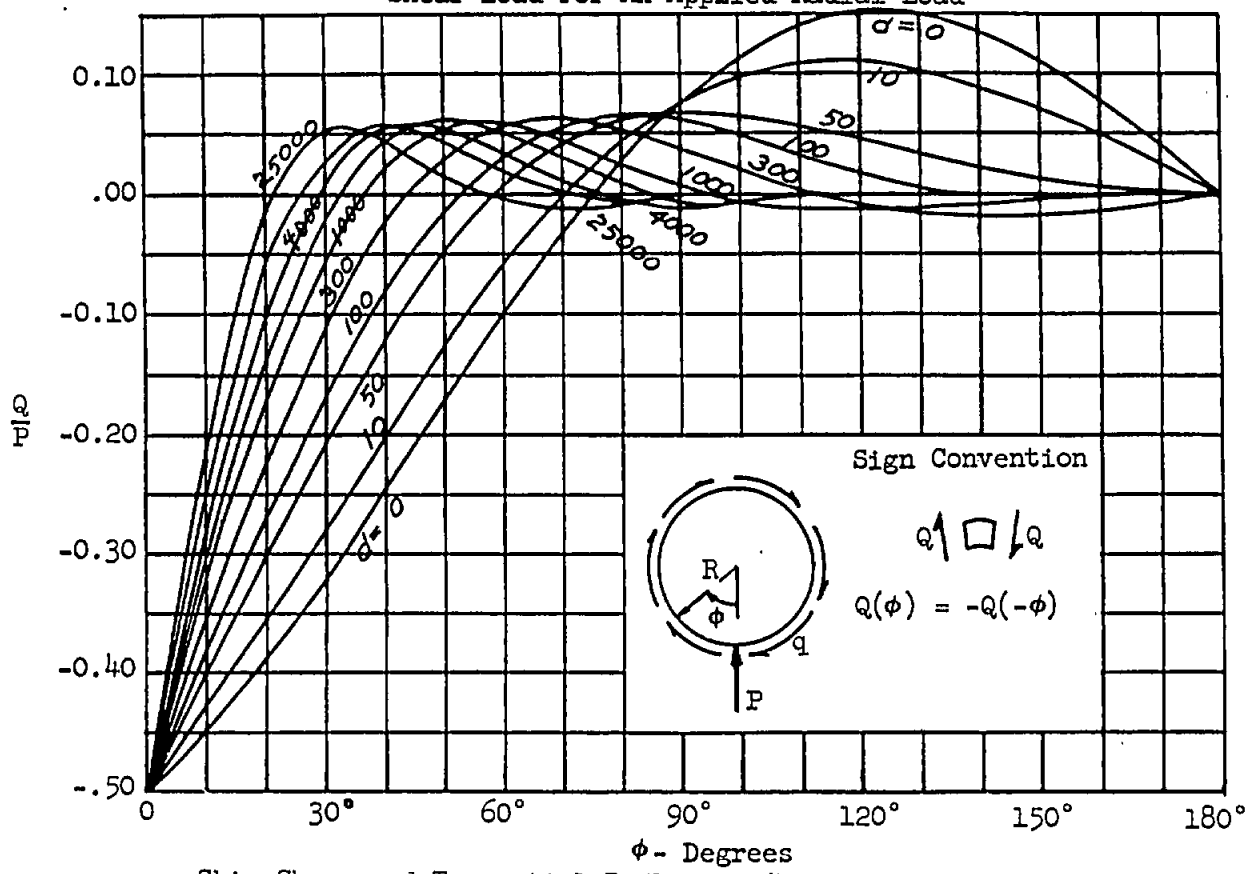

φ - Degrees

Skin Shear and Tangential Deflection For An Applied Radial Load

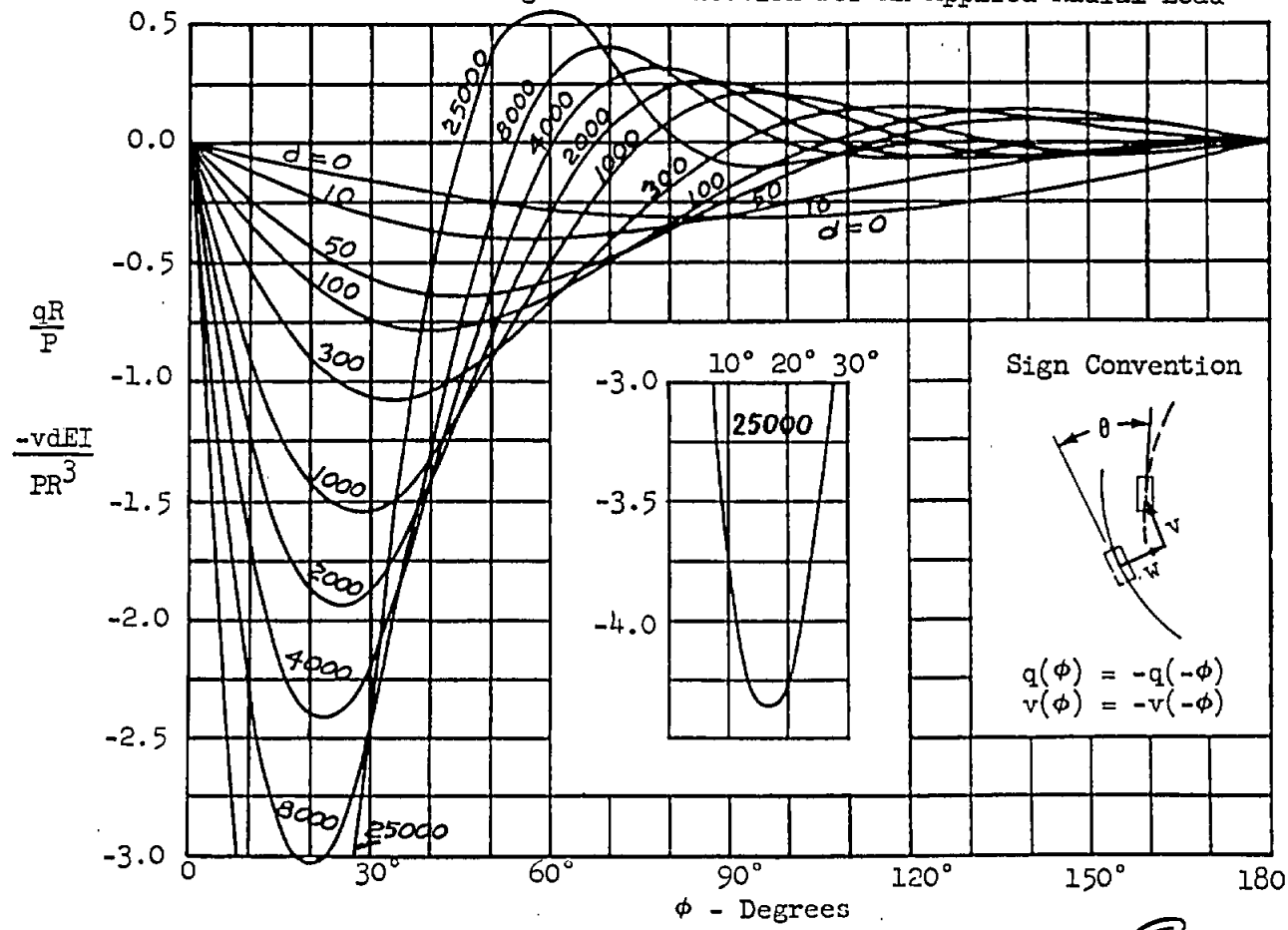

φ - Degrees

Grumman

SHELL SUPPORTED CIRCULAR RINGS

Radial Deflection For An Applied Radial Load

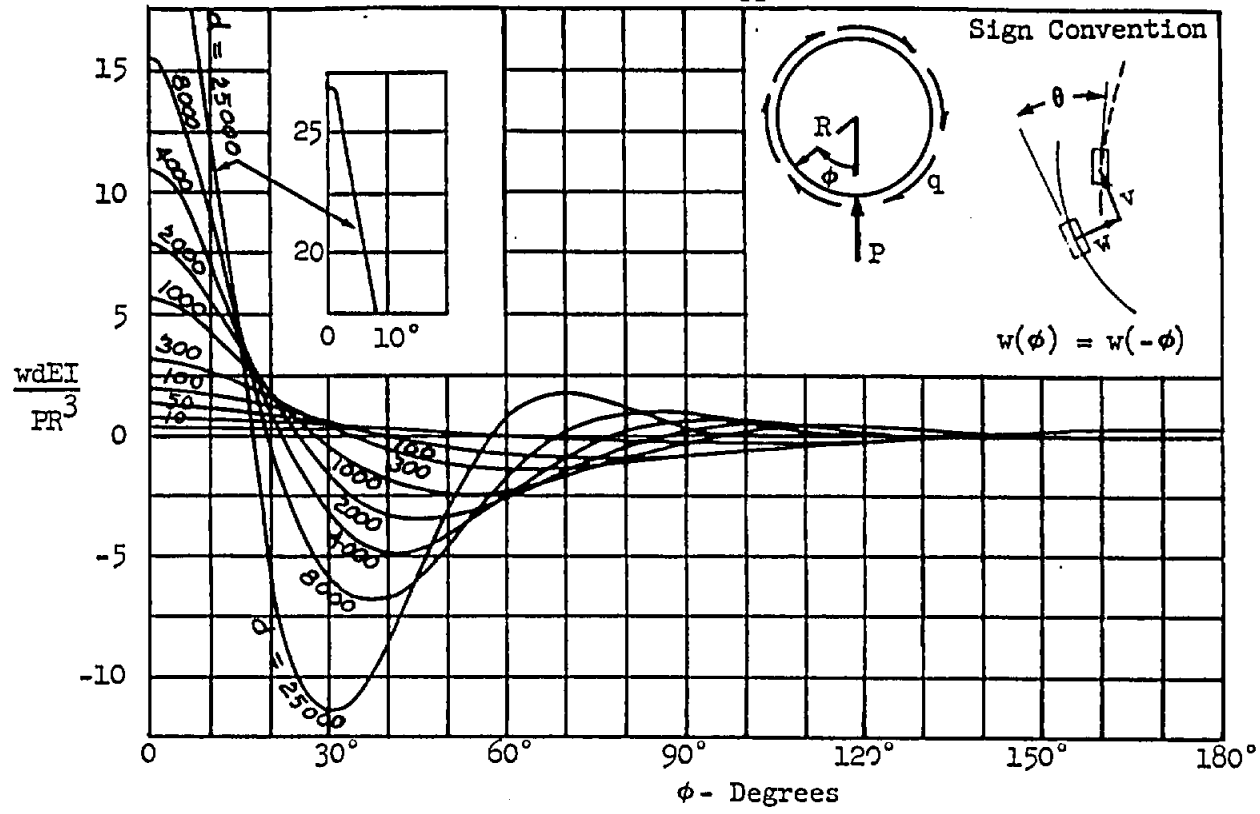

Rotational Deflection For An Applied Radial Load

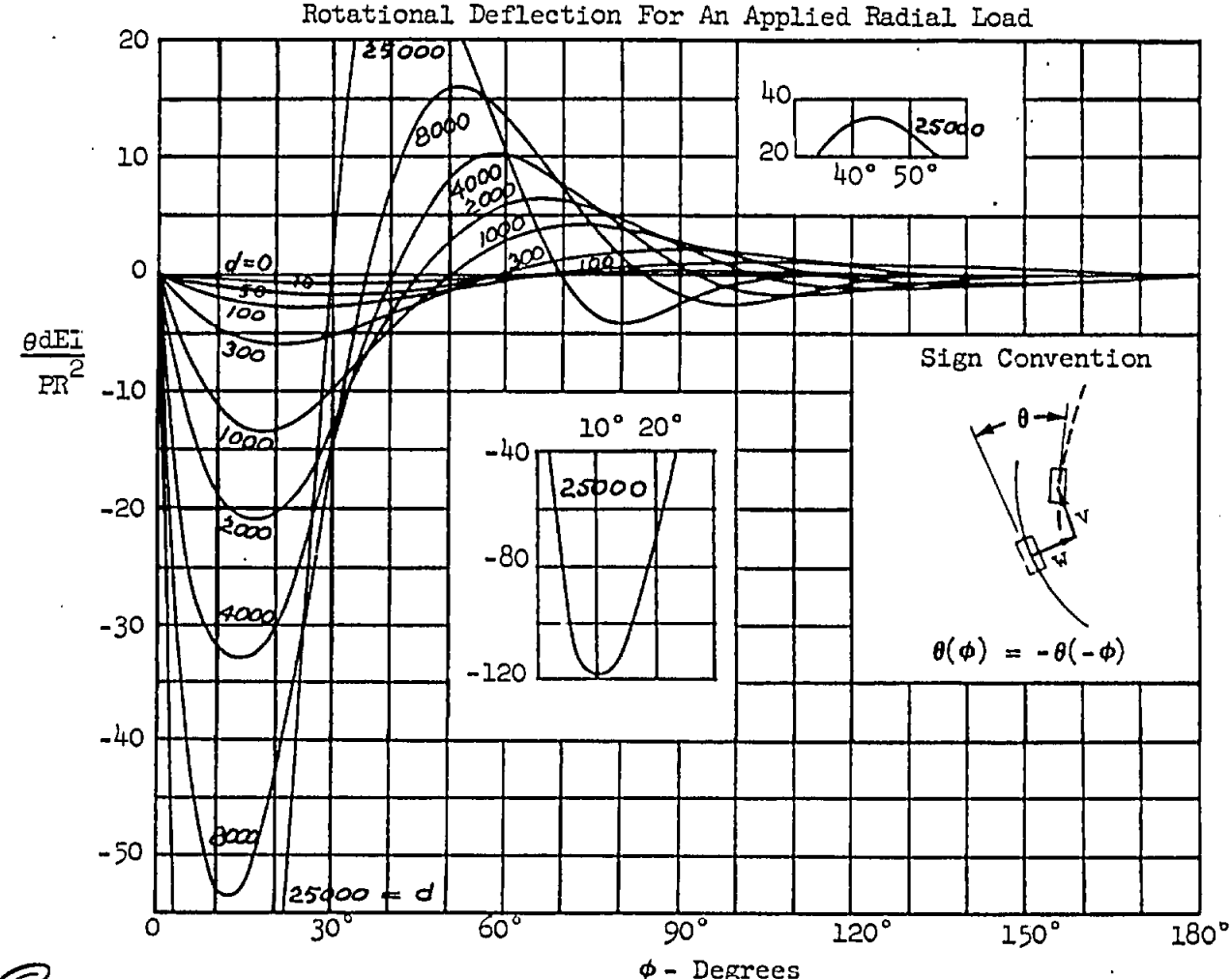

SHELL SUPPORTED CIRCULAR RINGS

Bending Moment For An Applied Tangential Load

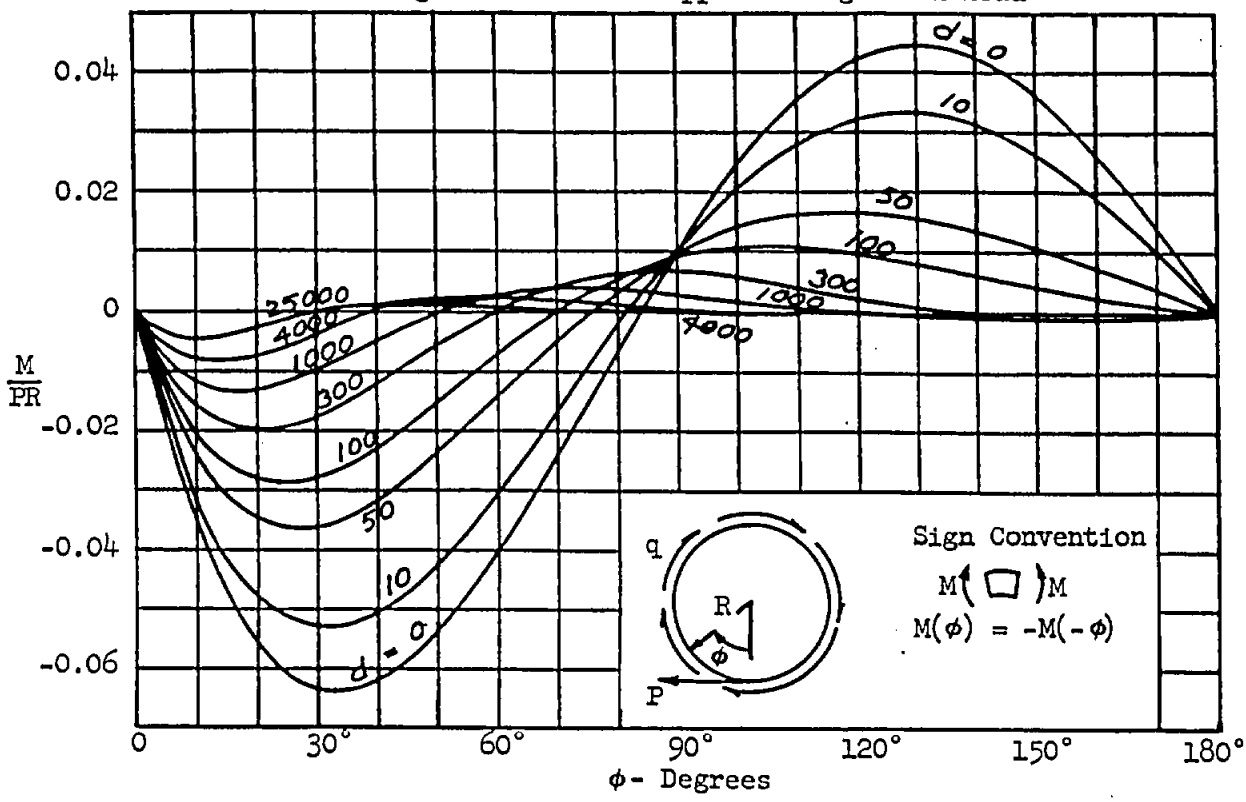

Axial Load For An Applied Tangential Load

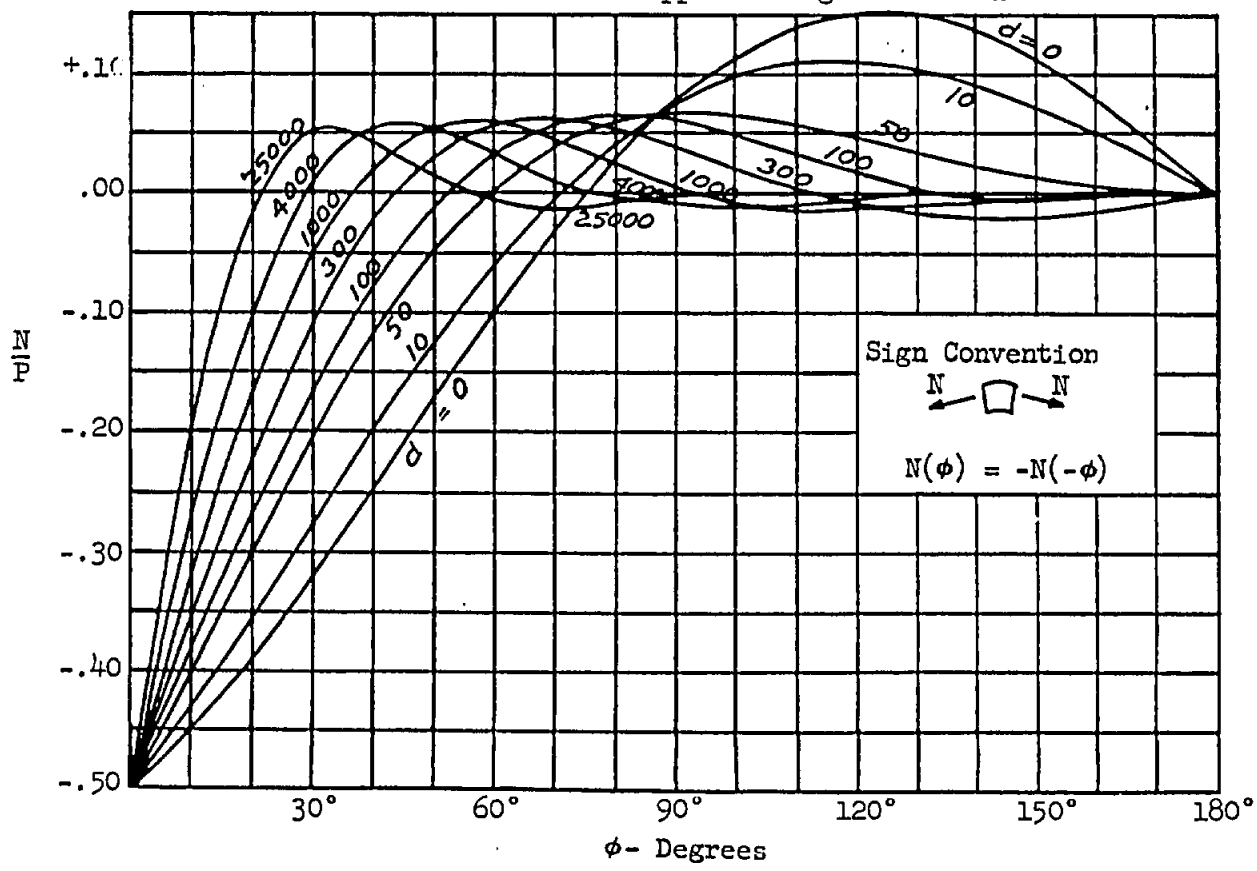

SHELL SUPPORTED CIRCULAR RINGS

Shear Load For An Applied Tangential Load

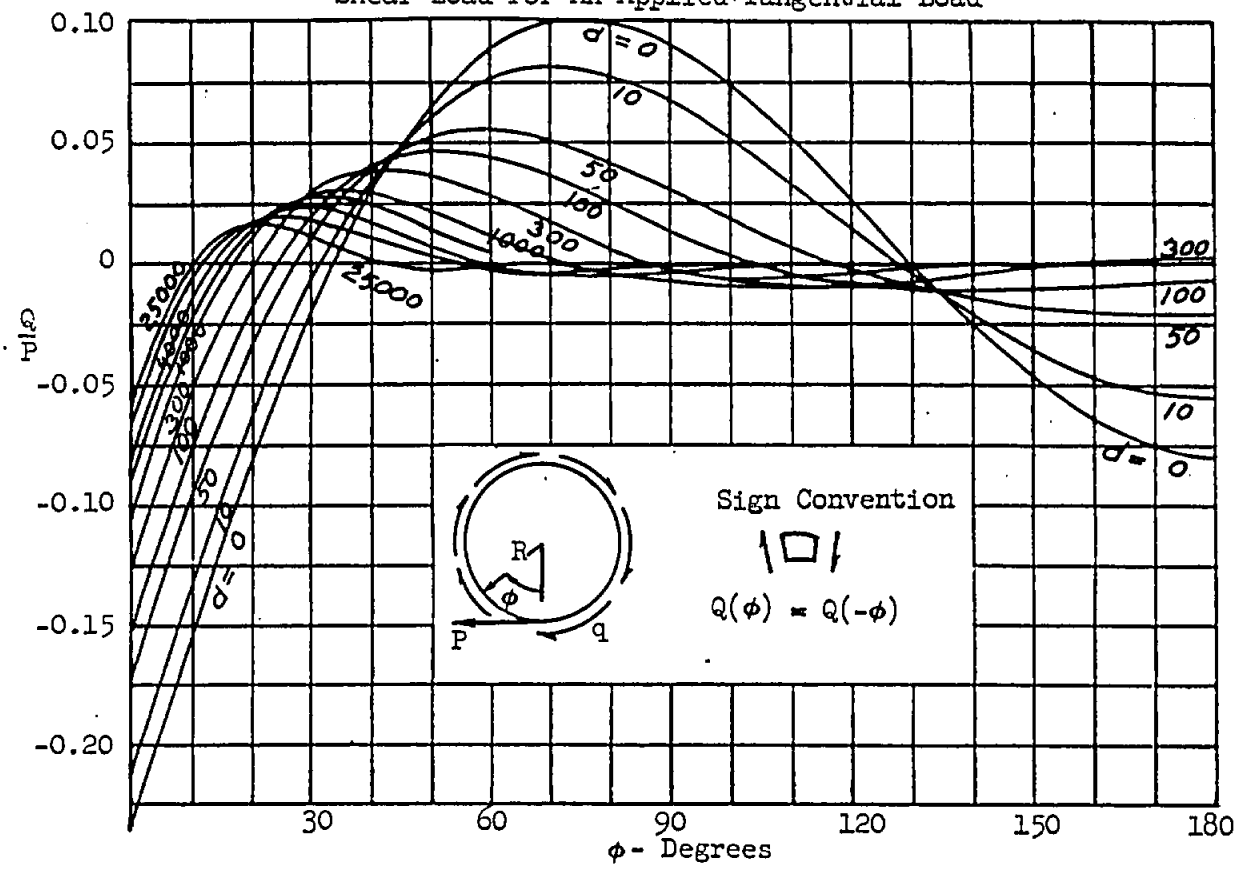

Skin Shear and Tangential Deflection For An Applied Tangential Load

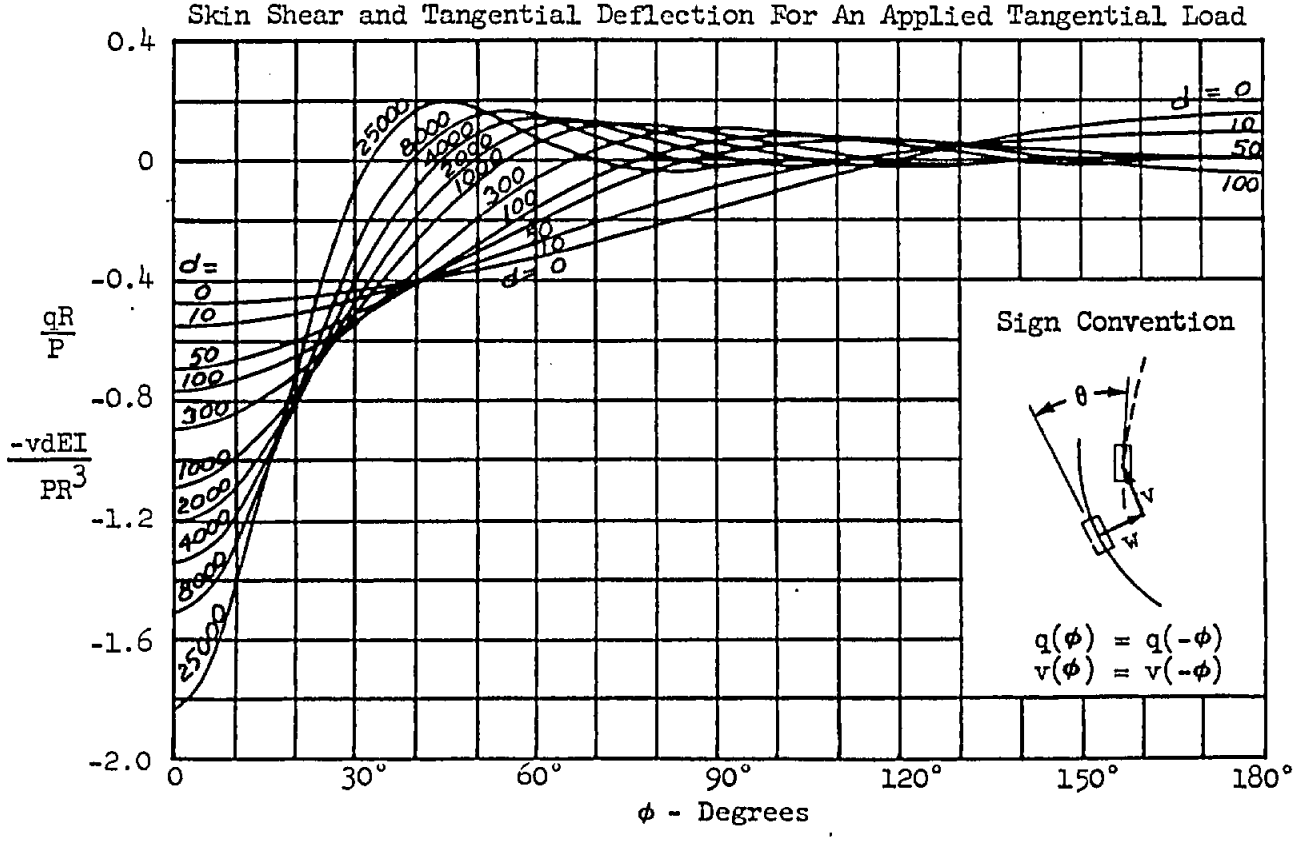

SHELL SUPPORTED CIRCULAR RINGS

Radial Deflection For An Applied Tangential Load

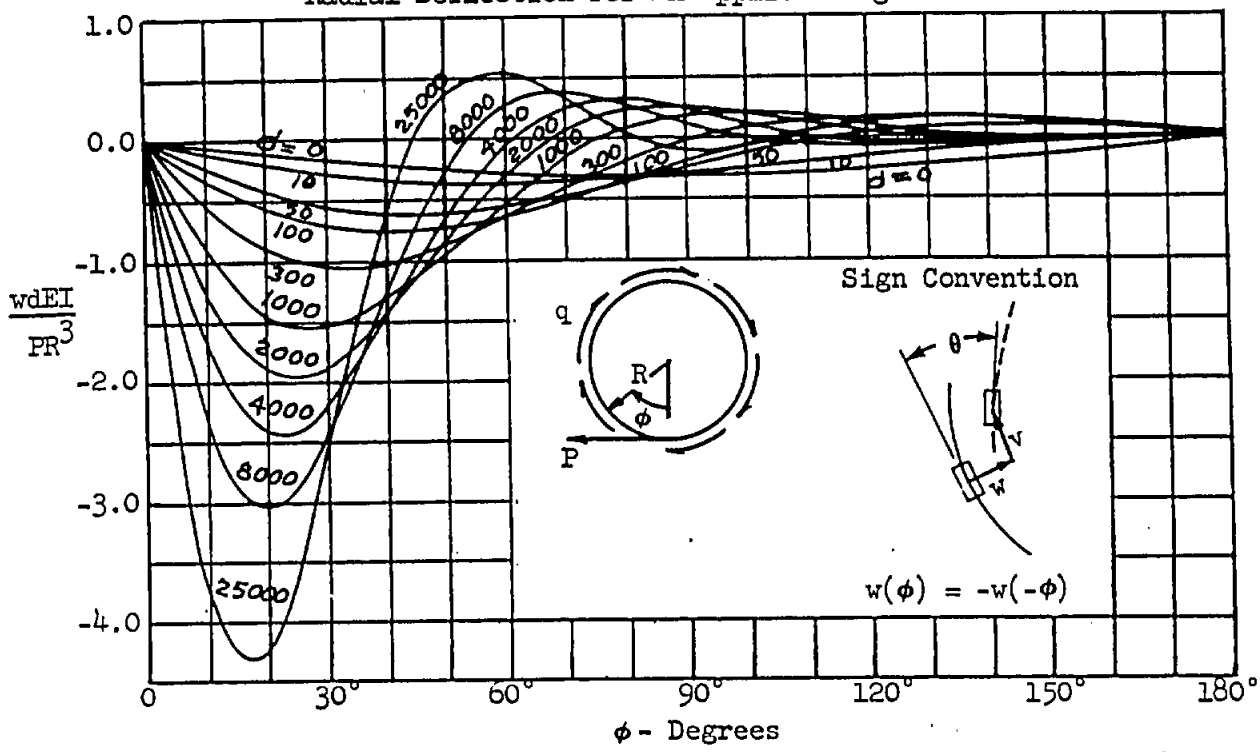

Rotational Deflection For An Applied Tangential Load

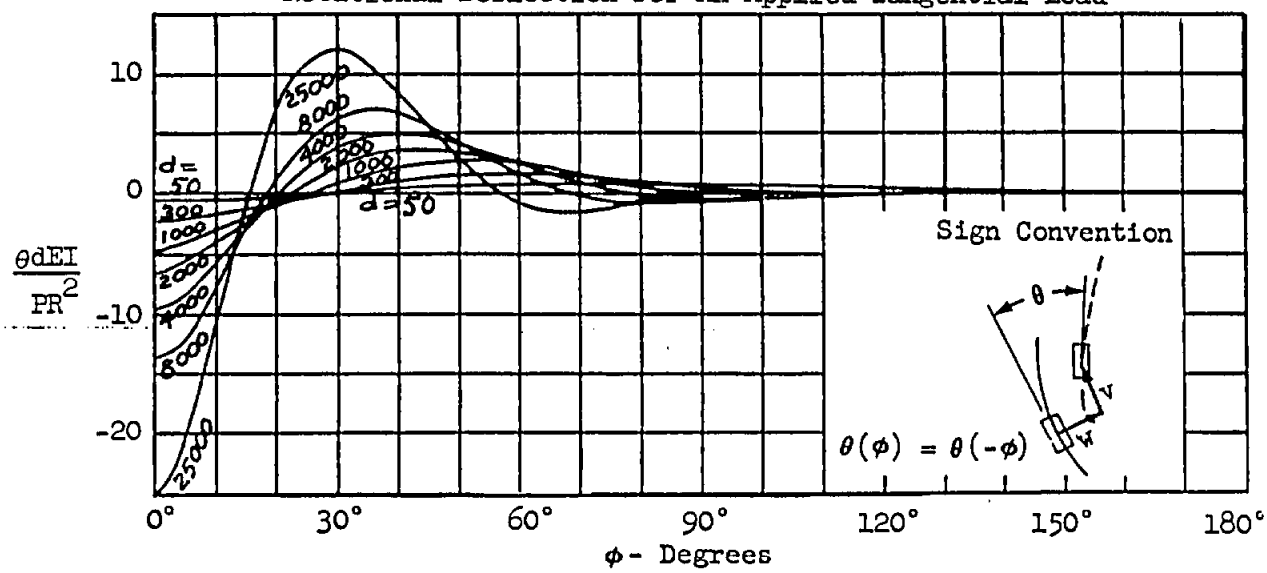

Grumman

SHELL SUPPORTED CIRCULAR RINGS

Bending Moment For An Applied Couple Load

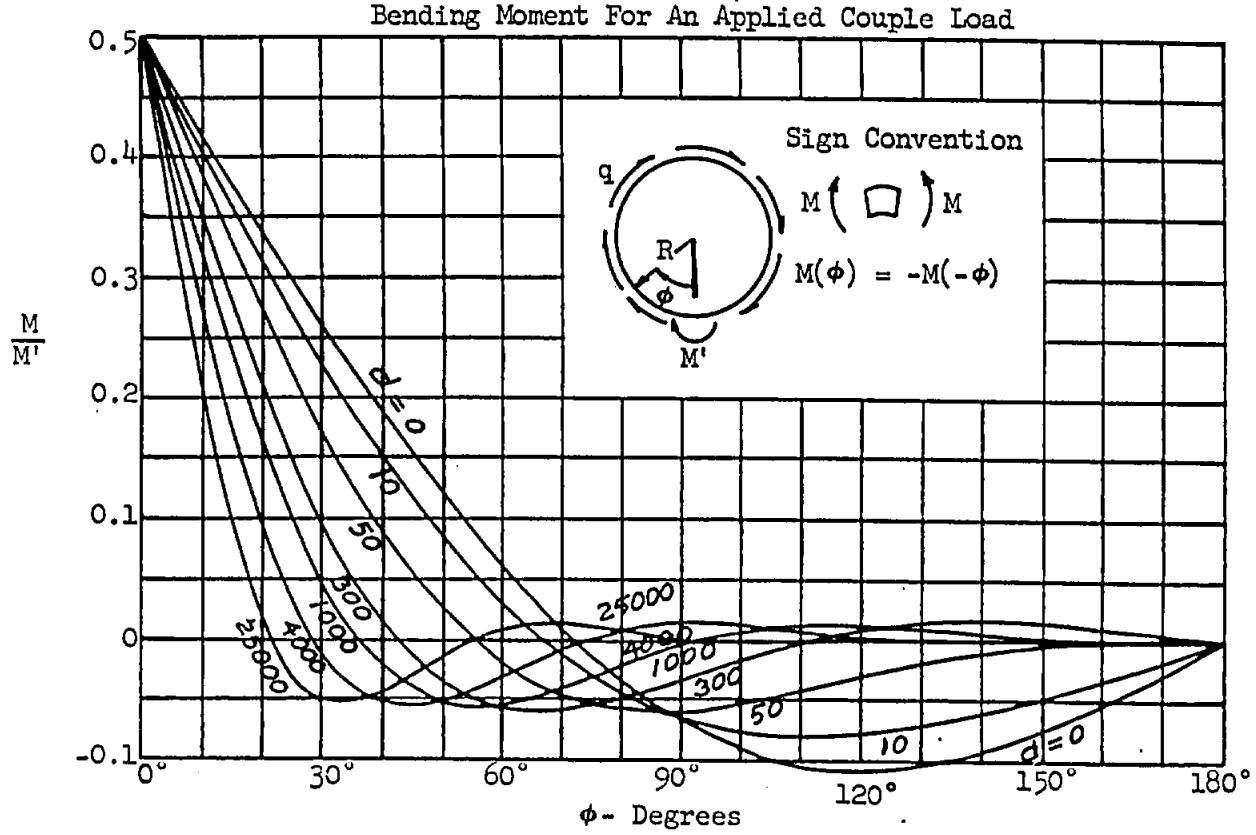

Axial Load For An Applied Couple Load

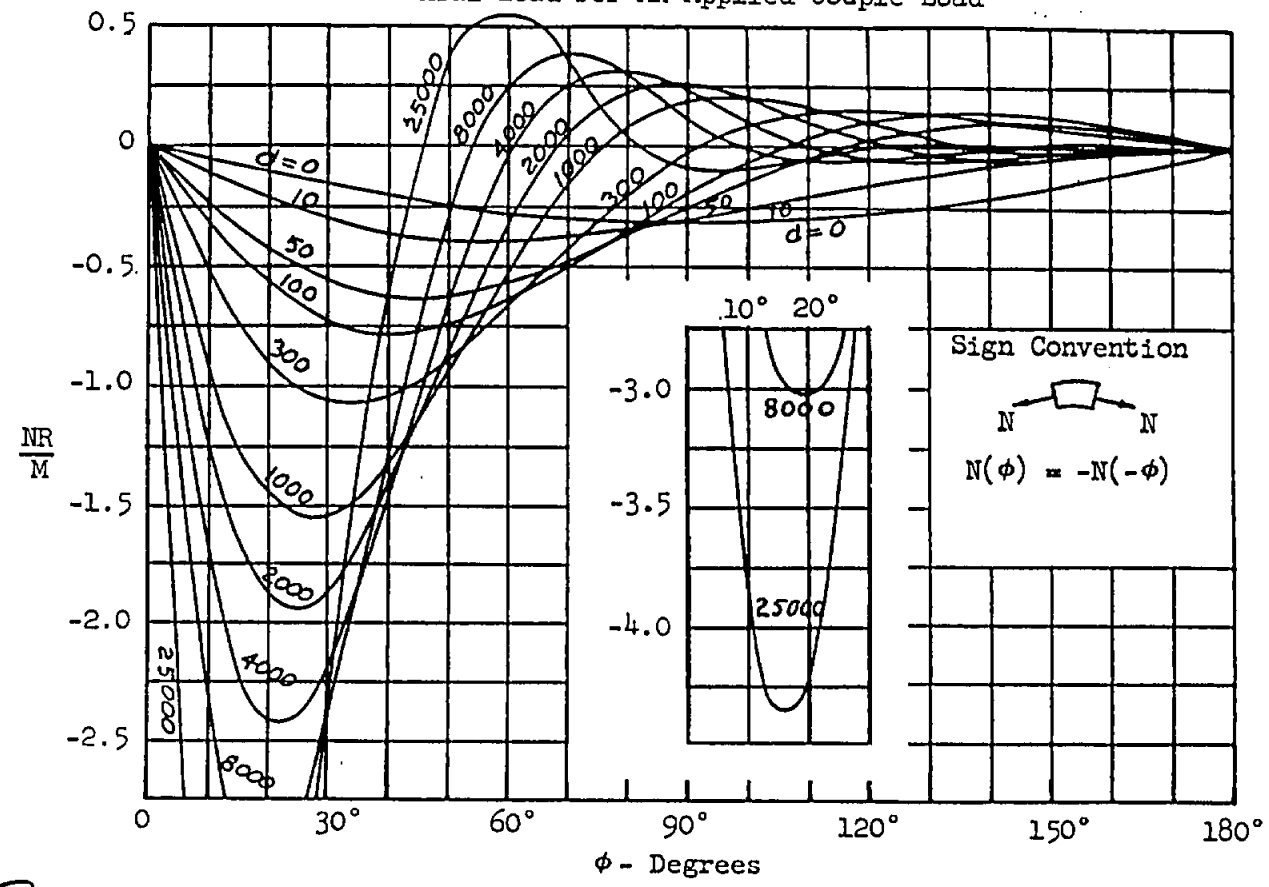

SHELL SUPPORTED CIRCULAR RINGS

Shear Load For An Applied Moment

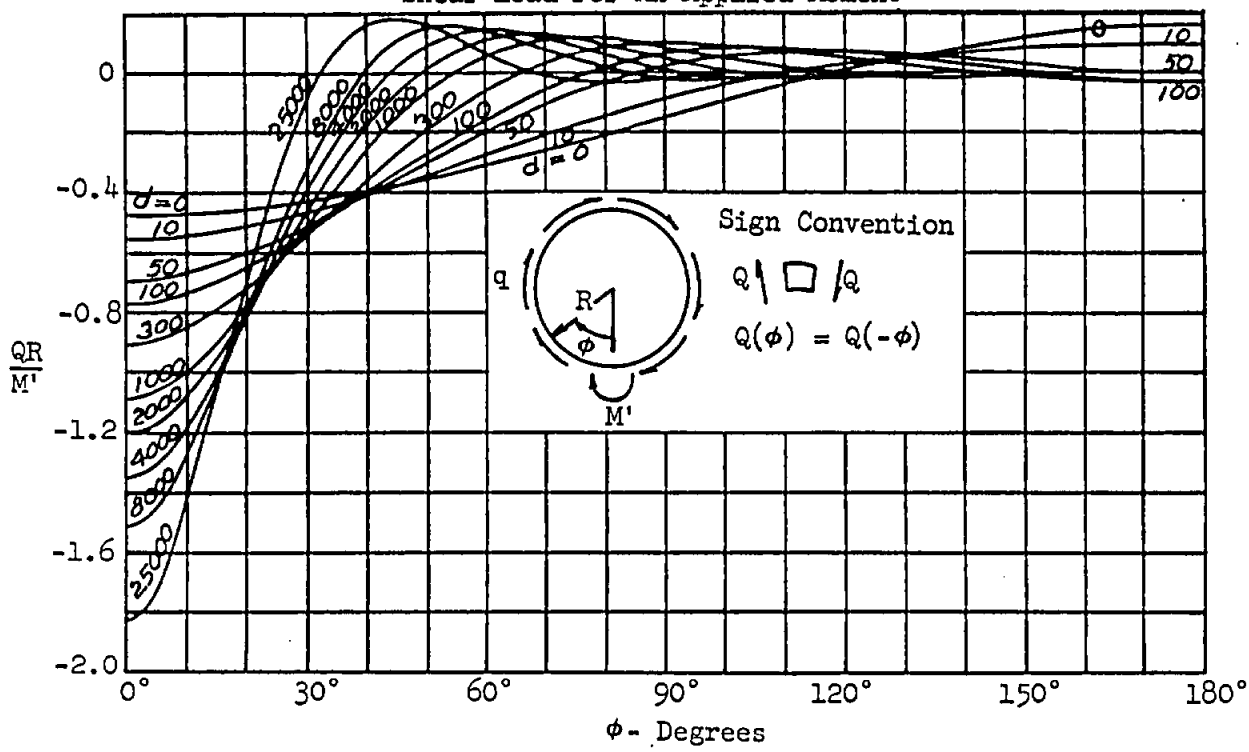

Shear Flow and Tangential Deflection for an Applied Moment

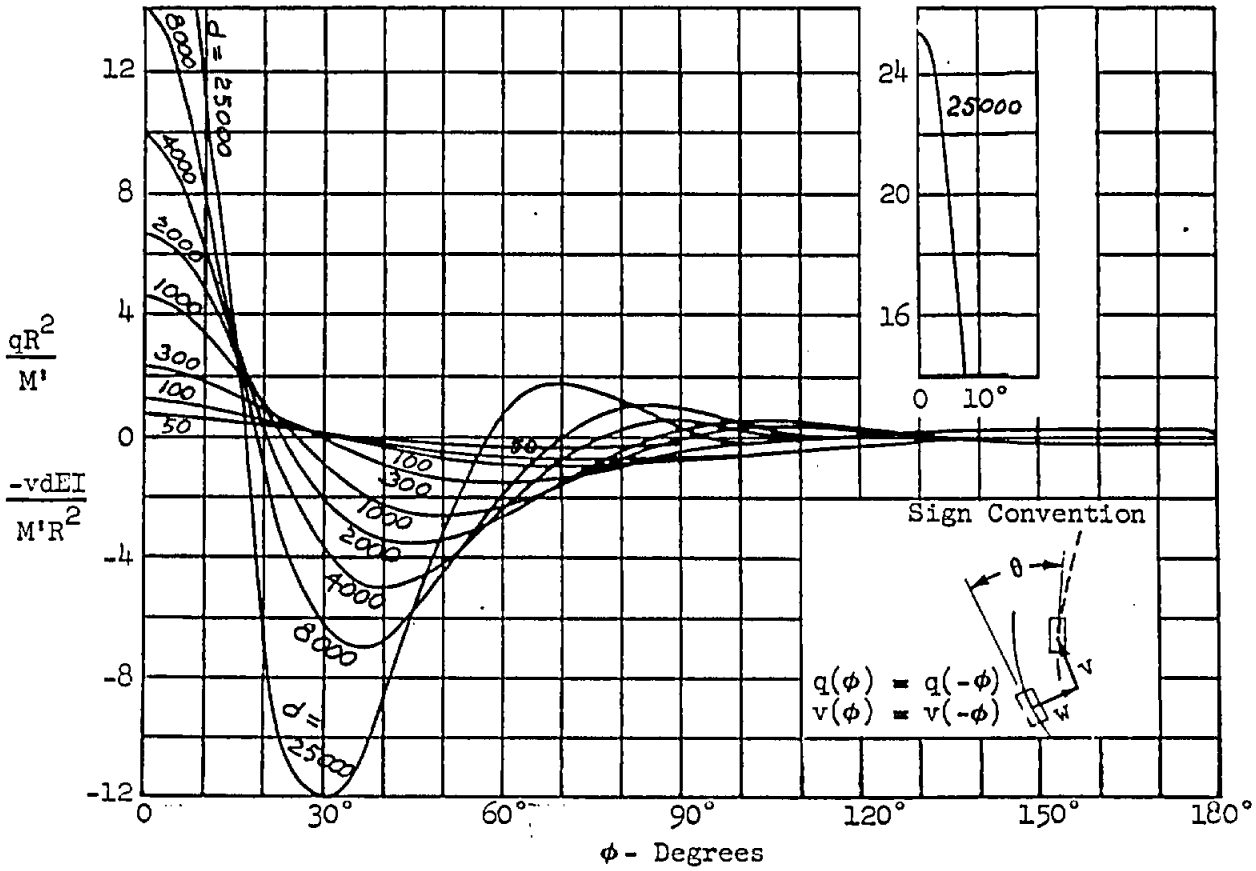

Grumman

SHELL SUPPORTED CIRCULAR RINGS

Radial Deflection For An Applied Moment

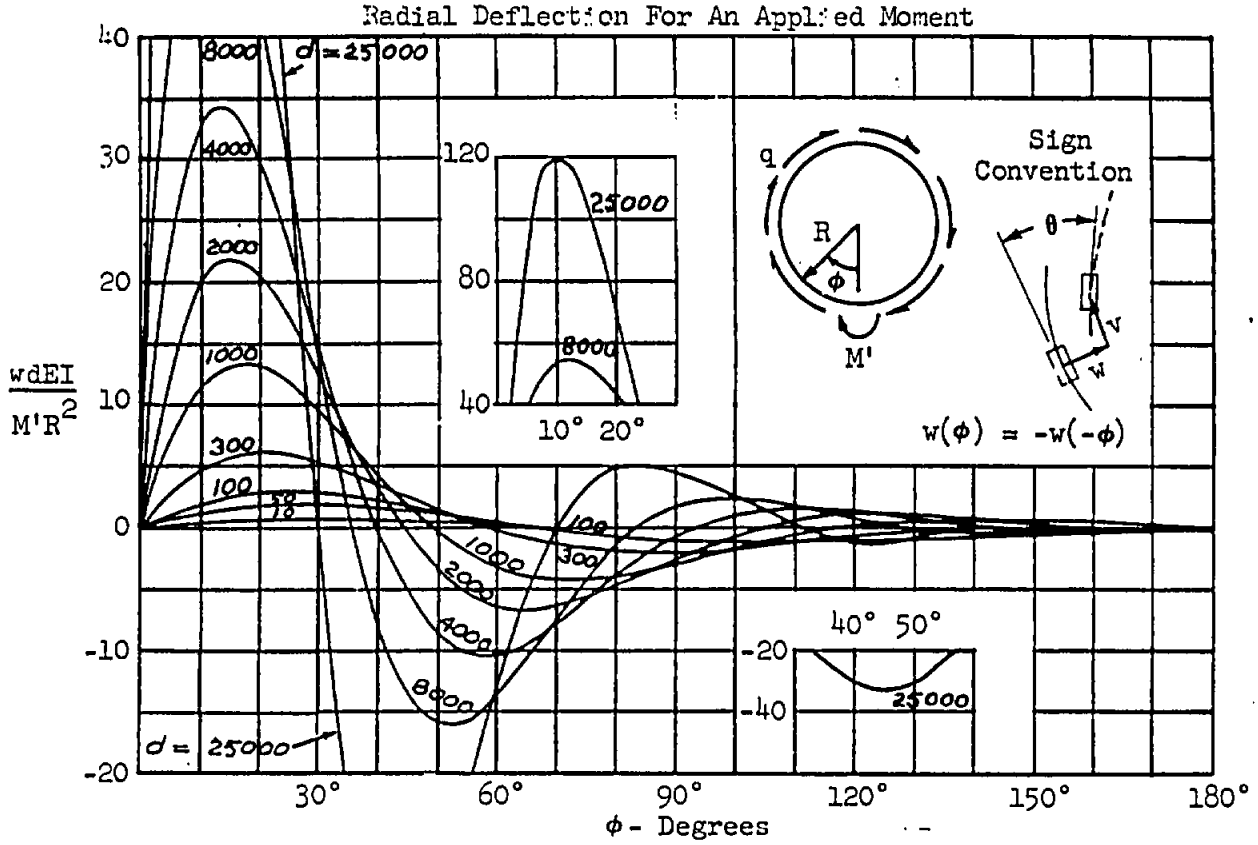

Rotation Deflection for an Applied Moment

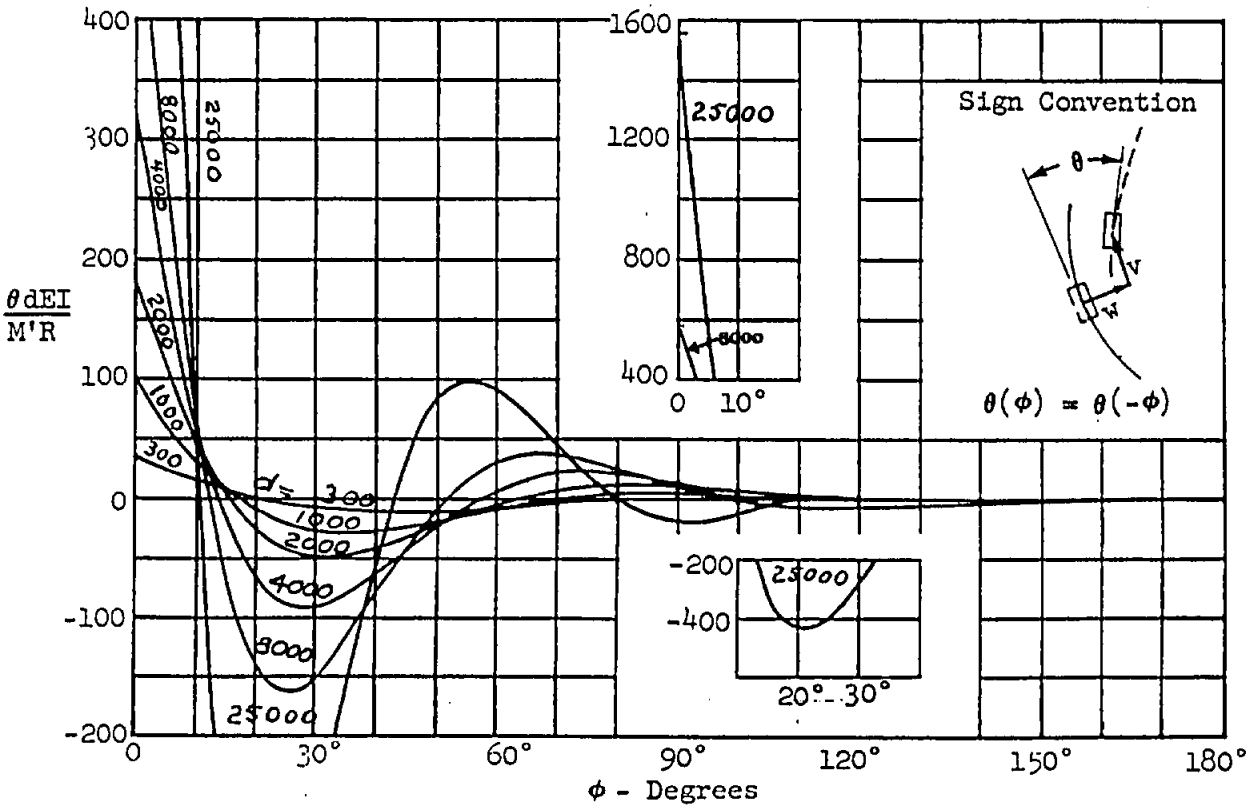

SECTION C4 - DETERMINATION OF BEAM DEFLECTIONS AND MOMENTS

Table of Contents

DEFLECTIONS OF BEAMS USING THE METHOD OF SEMI-GRAPHIC INTEGRATION

Discussion:

The method applies in cases where the consideration of bending energy can be assumed to give acceptable results.

The deflections of beams, frames, and similar structures which resist bending moments are often obtained by methods of virtual work. It is assumed that the reader is familiar with the latter. Usually, the use of such methods requires the evaluation of the $\int_0^L M_1 M_2 \, dx$ along a span(s) of structure. The quick evaluation of this integral is the subject of this section.

Derivation:*

In many practical problems the bending moment diagrams may be readily plotted, but they cannot be expressed as simple algebraic expressions. The integrals involving such bending moments may often be evaluated more readily by semigraphic methods than by direct integration. The expression $\int M_1 M_2 \, dx$, in which either M_1 or M_2 is a linear function of x, will be evaluated. Assuming M_1 to be linear between two points a and b, it may be expressed as follows:

$$M_1 = M_a + \frac{x}{L}(M_b - M_a) \qquad (a)$$

where L is the distance between a and b and M_a and M_b are the values of M_1 at these points, as shown in Figure 1. Substituting the value of M_1 into the integral and expanding, the following values are obtained:

$$\int M_1 M_2 \, dx - M_a \int_a^b M_2 \, dx + \frac{M_b - M_a}{L} \int_a^b M_2 x \, dx$$

* Extracted from textbook "Aircraft Structures" by David J. Peery - McGraw Hill, 1950

The first integral on the right side represents the area of the M_2 diagram and will be designated as A. The second integral represents the moment of the M_2 diagram about point a and will be designated as $A\bar{x}$, where $\bar{x}$ is the distance to the centroid of the M_2 diagram area, as shown in Figure 1. The integral becomes

$$\int_a^b M_1 M_2 \, dx = A\left[M_a + \frac{\bar{x}}{L}(M_b - M_a)\right]$$

where the term in brackets may be compared with Eq. (a) and is seen to represent the value of M_1 at a point opposite the centroid of the area of the M_2 diagram. This value is designated as $\overline{M}_1$ in Figure 1. The integral is therefore evaluated by the following equation:

$$\boxed{\int_a^b M_1 M_2 \, dx = A\overline{M}_1}$$

where the M_1 diagram is a straight line between a and b, A is the area of the M_2 diagram between a and b, and $\overline{M}_1$ is the value of M_1 opposite the centroid of the area of the M_2 diagram.

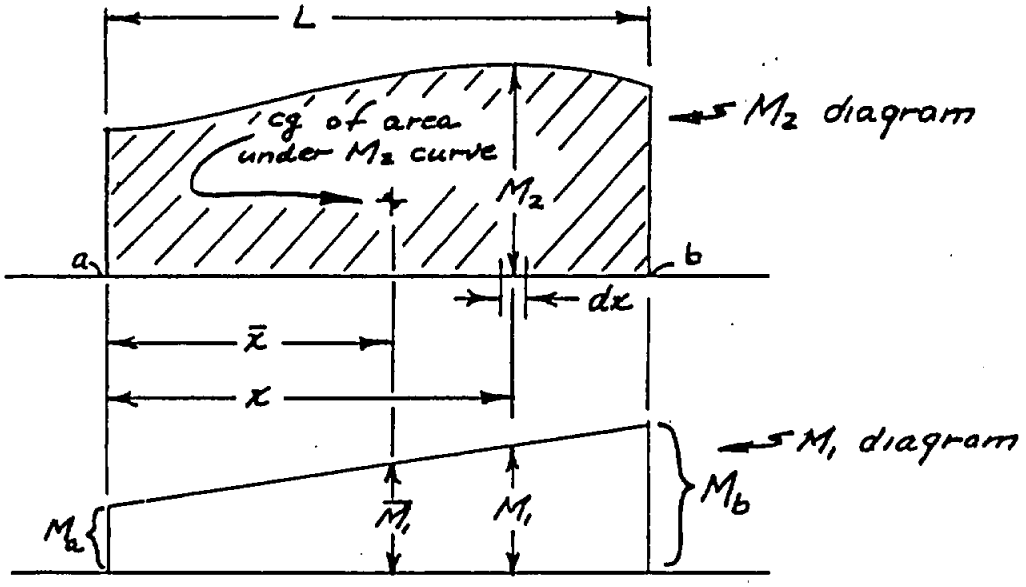

Figure 1

Several commonly used values of $\int_a^b M_1 M_2 \, dx$ have been computed as definite integrals. These are presented in Table 1.

Examples illustrating the use of this method are presented on pages C4.02-4 thru -9.

February 1974

TABLE 1

C4.02-3

VALUES OF INTEGRALS: $\int_0^L M_1 M_2\, dx$

1

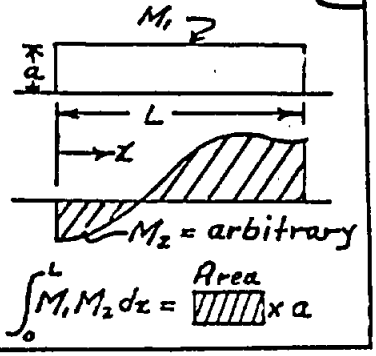

$\int_0^L M_1 M_2\, dx = \text{Area} \times a$

2

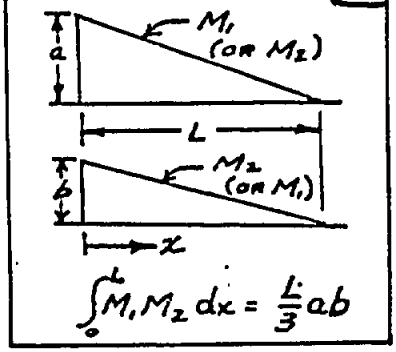

$\int_0^L M_1 M_2\, dx = \frac{L}{3} ab$

3

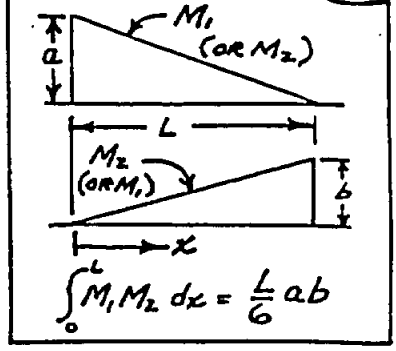

$\int_0^L M_1 M_2\, dx = \frac{L}{6} ab$

4

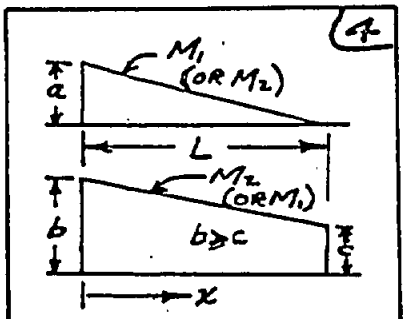

$\int_0^L M_1 M_2\, dx = \frac{L}{6} a[2b+c]$

5

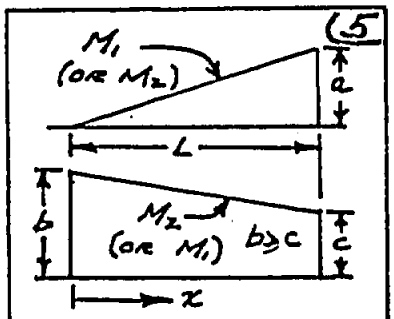

$\int_0^L M_1 M_2\, dx = \frac{L}{6} a[2c+b]$

6

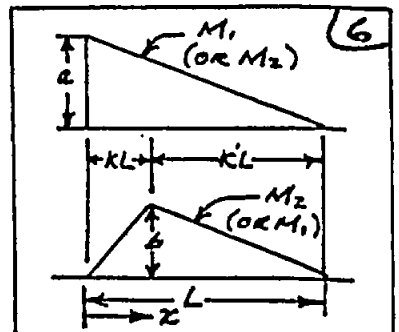

$\int_0^L M_1 M_2\, dx = \frac{L}{6} ab[1+k']$

7

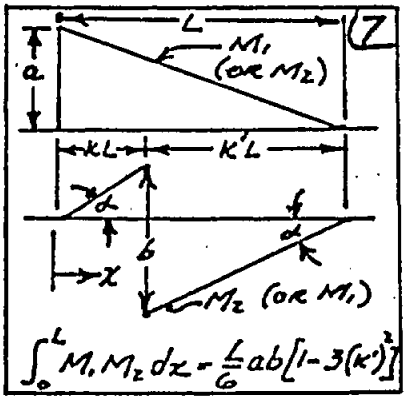

$\int_0^L M_1 M_2\, dx = \frac{L}{6} ab[1-3(k')^2]$

8

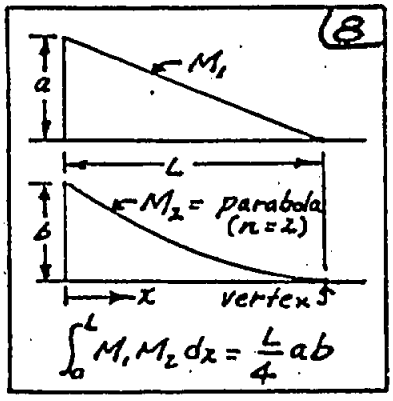

$\int_0^L M_1 M_2\, dx = \frac{L}{4} ab$

9

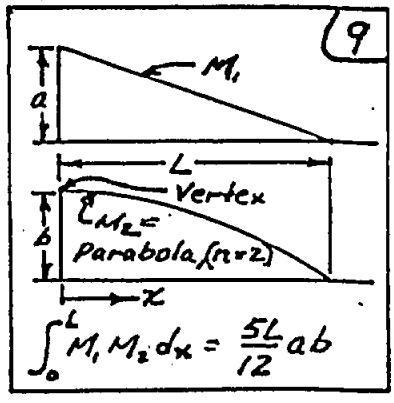

$\int_0^L M_1 M_2\, dx = \frac{5L}{12} ab$

10

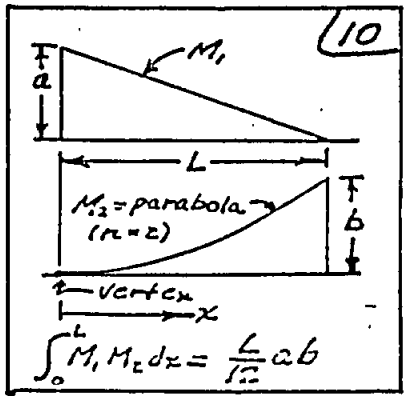

$\int_0^L M_1 M_2\, dx = \frac{L}{n+2} ab$

11

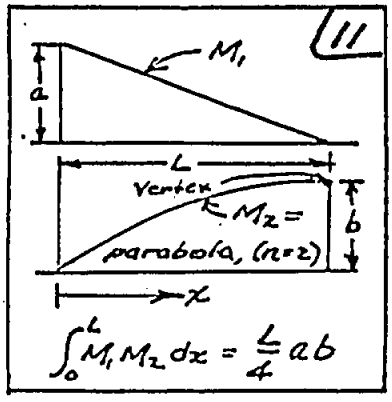

$\int_0^L M_1 M_2\, dx = \frac{L}{4} ab$

12

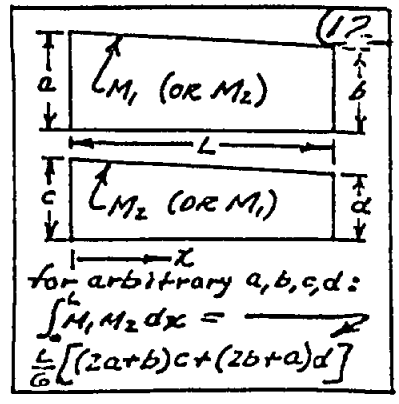

for arbitrary a, b, c, d:

$\int_0^L M_1 M_2\, dx = \frac{L}{6}[(2a+b)c+(2b+a)d]$

GRUMMAN

The illustrative examples which follow are presented in an effort to highlight the versatility, simplicity, and accuracy of this method.

Example 1:

Cantilever beam - constant EI - uniform load w lbs/inch - length L. Find Δ and θ by semi-graphic integration (This simple example is chosen only because the reader undoubtedly has access to formulas for Δ and θ, thus the method is easily verified independently.)

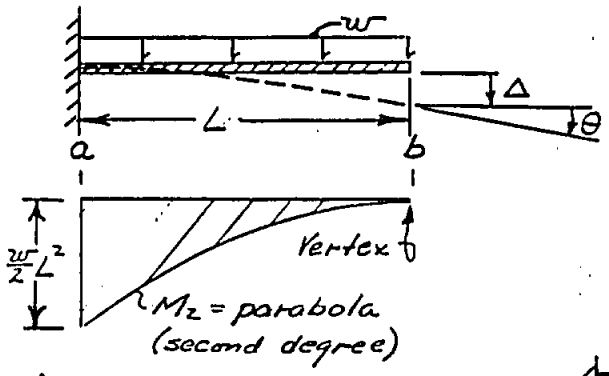

Calculation of Δ :

- Determine the bending moment diagram for a 1 lb. virtual load acting down at point b on the beam. This is the M_1 diagram.

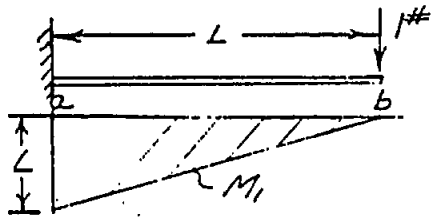

- Using case 8, the deflection Δ is determined from:

$$EI\Delta = \int_a^b M_1 M_2 \, dx :$$

then $EI\Delta = \frac{L}{4} a b$ where $a = L$ and $b = \frac{w}{2}L^2$

thus, $EI\Delta = \frac{L}{4}(L)\frac{w}{2}L^2 = \frac{wL^4}{8}$ and $\boxed{\Delta = \frac{wL^4}{8EI}}$

Calculation of θ :

- Determine the bending moment diagram for a 1 inch-lb. virtual moment acting clockwise at point b on the beam. This is the M_1 diagram.

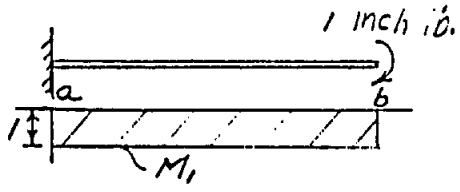

- Using case 1, the rotation θ is determined from:

$$EI\theta = \int_a^b M_1 M_2 \, dx :$$

then $EI\theta = (\overbrace{\text{AREA OF } M_2 \text{ DIAGRAM}}^{A_{M_2}}) \times M_1$ where $A_{M_2} = \frac{L}{3} \times \frac{w}{2}L^2$, $M_1 = 1$

thus $EI\theta = \frac{wL^3}{6} \times 1$ and,

$$\boxed{\theta = \frac{wL^3}{6EI}}$$

GRUMMAN

Example 2

Single span simply supported beam - constant EI - length ℓ. Assume a 1 lb. transverse load is applied at any point "C" a distance "n" from the right support. Determine the deflection under the 1 lb. load, and thus the flexibility of the beam at point C.

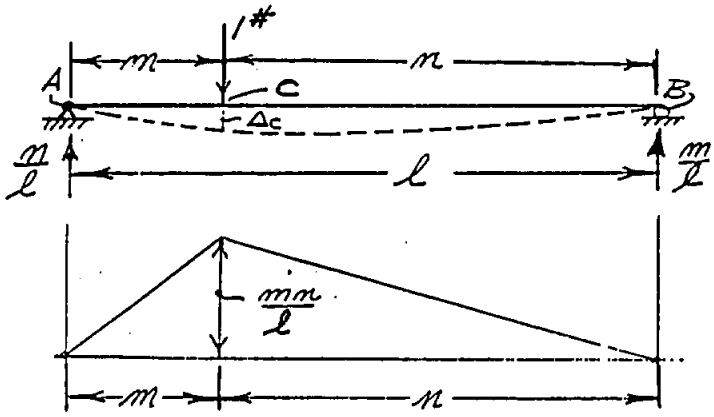

The bending moment diagram shown above is for the 1 lb. load applied at point C and will be designated as M_2. To determine the deflection under this load, we can place a 1 lb. virtual load at point C and proceed with semi-graphic integration. Obviously, the bending moment due to this virtual load is numerically identical to M_2, however it will be designated as M_1.

The deflection under the 1 lb. load applied at point C will now be determined:

Table 1 does not present a case which specifically covers the $\int M_1 M_2 dx$ in which we are presently interested. However, if the composite span $\overline{A\text{-}B\text{-}C}$ is treated as two spans, $\overline{A\text{-}C}$ + $\overline{C\text{-}B}$, then Case 2 can be used. The calculations are as follows:

CASE 2 GIVES $\int_0^L M_1 M_2 dx = \frac{L}{3} ab$ FOR THE GENERAL CASE.

FOR OUR PROBLEM:

SPAN $\overline{A\text{-}C}$: $L = m$, $a = \frac{mn}{\ell}$, $b = \frac{mn}{\ell}$

SPAN $\overline{C\text{-}B}$: $L = n$, $a = \frac{mn}{\ell}$, $b = \frac{mn}{\ell}$

THUS: $EI\Delta_C = \left[\frac{m}{3}\left(\frac{mn}{\ell}\right)^2\right] + \left[\frac{n}{3}\left(\frac{mn}{\ell}\right)^2\right] = \left(\frac{mn}{\ell}\right)^2 \frac{m+n}{3}$

OR $\boxed{\Delta_C = \frac{m^2 n^2}{3EI\ell}}$

CONTRIBUTION OF SPAN $\overline{C\text{-}B}$

CONTRIBUTION OF SPAN $\overline{A\text{-}C}$

Examples 1 and 2 have been intentionally explained in greater detail than what might seem necessary. Actually, as the user of this method becomes familiar with it, such problems can be solved quickly with very little computation.

The following examples are intentionally explained in somewhat less detail than that noted in Examples 1 and 2.

Example 3

Beam on several supports - bending moment diagram is known - constant EI. Find the deflection of point B in span A-D.

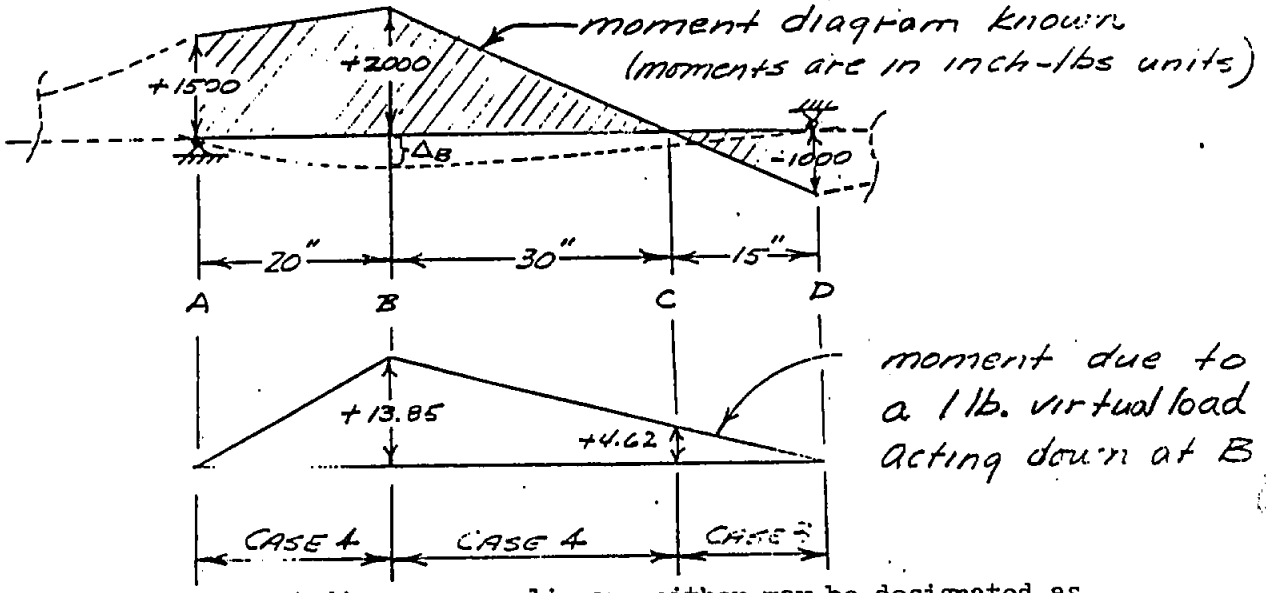

Since both moment diagrams are linear, either may be designated as M_1 and the other M_2.

$$EI\Delta_B = \overbrace{\frac{20}{6}(13.85)[2\times2000+1500]}^{\text{SPAN } \overline{A\text{-}B}} + \overbrace{\frac{30}{6}(2000)[2\times13.85+4.62]}^{\text{SPAN } \overline{B\text{-}C}} + \overbrace{\frac{15}{6}(-1000)(4.62)}^{\text{SPAN } \overline{C\text{-}D}}$$

$$EI\Delta_B = 565617 \quad \text{and} \quad \boxed{\Delta_B = \frac{565617}{EI}}$$

The following two illustrative examples, 4 and 5, deal with structures having variable EI.

Example 5 solves the typical "design problem" as opposed to the typical "textbook problem" and is offered to portray the versatility of this method. Many such problems occur during the course of designing typical aerospace component structures.

Example 4

Cantilever beam - uniform load w = 200 lbs/inch - I varies linearly from 2.0 in^4 (at the fixed end) to 1.0 in^4 - E is constant - L = 10 in. Determine the deflection Δ_B

Before starting the calculations, it is best to reflect on some fundamentals.

The idealization of the structure is very important. Since we wish to save time, we should use the least number of segments (sub-spans) consistent with desired accuracy. Often, a small number of judiciously selected segments will give acceptable accuracy. It is not necessarily true that we should select segments which are all the same length. A reasonable approach is to plot both the M_1 diagram and, in cases of variable EI, the $\frac{M_1}{EI}$ diagram. An "eyeball" comparison of the two diagrams is valuable in judging how the structure should be idealized. It is best to consult an experienced person when making this judgement. For the problem at hand, the M_1 and $\frac{M_1}{EI}$ diagrams were plotted and then the five segments shown below were selected for the idealization. When we perform the semi-graphic integration we will be evaluating $\int_0^L M_1\left(\frac{M_2}{EI}\right)dx$ instead of $\int_0^L M_1 M_2 dx$ as was the case for constant EI beams. The values in Table 1 still apply except that we substitute $\left(\frac{M_1}{EI}\right)$ where M_2 appears.

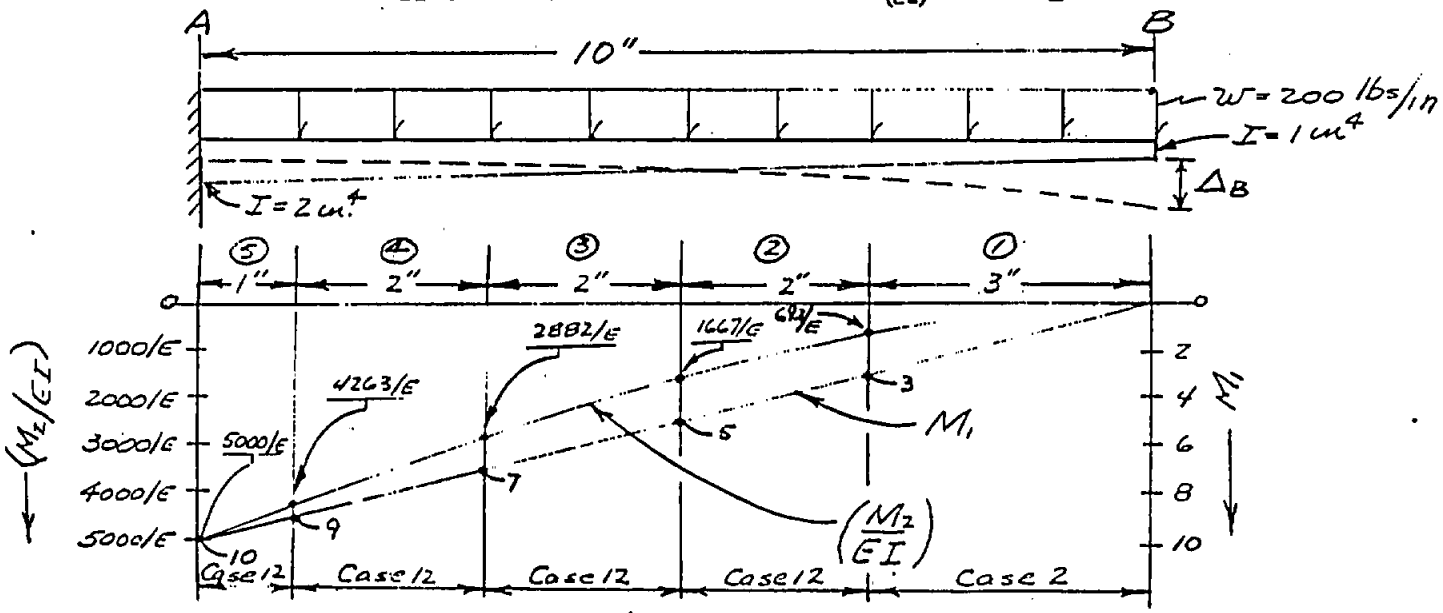

Making the assumption that the $\left(\frac{M_2}{EI}\right)$ diagram is linear along each of the five segments, we can use Cases 2 and 12 to solve for Δ_B:

$$\Delta_B = \underbrace{\frac{3}{4}[3(692/E)]}_{\text{Segment ①}} + \underbrace{\frac{2}{6}[(10+3)(1667/E)+(6+5)(692/E)]}_{\text{Segment ②}} + \underbrace{\frac{2}{6}[(14+5)(2882/E)+(10+7)(1667/E)]}_{\text{Segment ③}}$$

$$+ \underbrace{\frac{2}{6}[(18+7)(4263/E)+(14+9)(2882/E)]}_{\text{Segment ④}} + \underbrace{\frac{1}{6}[(20+9)(5000/E)+(18+10)(4263/E)]}_{\text{Segment ⑤}} = \underbrace{\frac{140698}{E}}_{\Delta_B}$$

To check the accuracy of the answer, this problem was solved via an existing computer program which calculates the deflection using the Area-Moment method. The program assumes 1000 equal length segments. Δ_B obtained via computer program = 140186/E. Thus the semi-graphic integration of only 5 segments has yielded a 0.37% error compared to the more accurate solution. The computer solution, however, involves the usual punching of cards, checking of data etc. and consumes more total time.

Example 5

This is an hypothetical design problem. It has been decided that at point A the "y" deflection of the existing fuselage frame, shown below, must be restrained. The frame supports the ultimate loads noted and is aluminum with E = 10.5 x 10^6 psi. The following question has been asked:

How much y load must be applied at point A to prevent displacement in the y direction, assuming no redesign of the frame?

Solution

In order to determine the required load R_y at point A, we must determine Δ_{yA} and α_{yA} where Δ_{yA} is the y deflection due to the applied loads and where α_{yA} is the flexibility of the frame for y load at A.

(a) $\Delta_{yA} + R_y \alpha_{yA} = 0$ $\Big\}$ $\Delta_{yA} = \int M_1 \left(\frac{M_2}{EI}\right) dx$ and $\alpha_{yA} = \int M_1 \left(\frac{M_1}{EI}\right) dx$

Since we have a variable EI beam, we plot the M_1 and the $\left(\frac{M_2}{EI}\right)$ diagrams where M_1 is due to a 1lb. virtual load applied in the +y direction at point A and where M_2 is due to the applied loads. The diagrams have been plotted along the developed neutral axis of the frame. Note that although neither diagram is linear, the six segments chosen enable us to assume linearity within any segment and we proceed with semi-graphic integration.

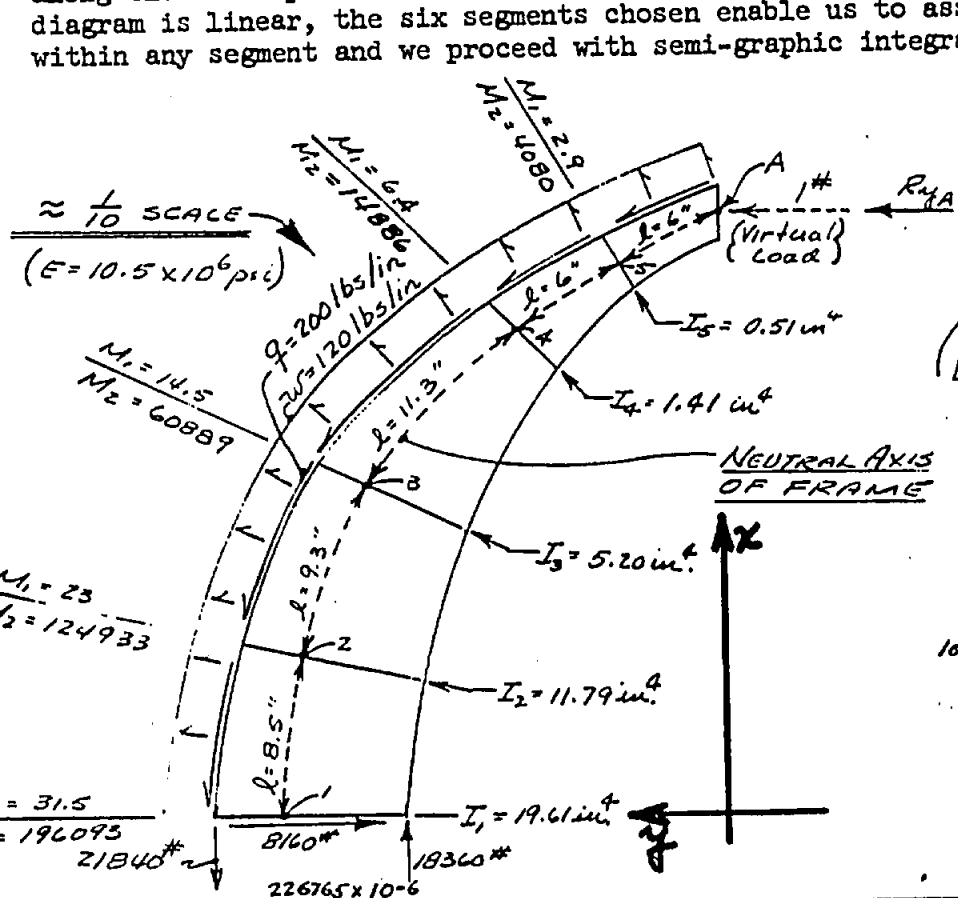

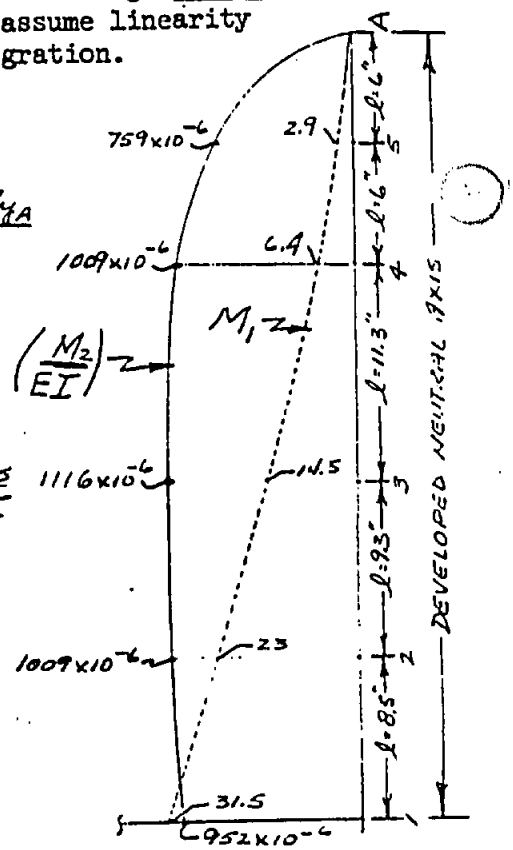

$$\Delta_{yA} = \underbrace{\frac{8.5}{6}\left[(2\times952+1009)31.5+(2\times1009+952)23\right]\times10^{-6}}_{126281\times10^{-6}} + \underbrace{\frac{9.3}{6}\left[(2\times1009+1116)23+(2\times1116+1009)14.5\right]\times10^{-6}}_{25101\times10^{-6}}$$

$$+ \underbrace{\frac{11.3}{6}\left[(2\times1116+1009)14.5+(2\times1009+1116)6.4\right]\times10^{-6}}_{4402\times10^{-6}} + \underbrace{\frac{6}{6}\left[(2\times1009+759)6.4+(2\times759+1009)2.9\right]\times10^{-6}}_{} + \underbrace{\frac{6}{3}(2)759\times10^{-6}}_{}$$

thus $\boxed{\Delta_{yA} = 567118 \times 10^{-6} \text{ in.}}$ ← $\int M_1 \left(\frac{M_2}{EI}\right) dx$

GRUMMAN

Example 5 - continued

To evaluate α_{y_A} we must determine $\int M_1 \left(\frac{M_1}{EI}\right) dx$ along each of the six segments. Rather than plot the $\left(\frac{M_1}{EI}\right)$ diagram, we will substitute the correct values directly into the appropriate formulas:

$$\alpha_{y_A} = \overbrace{\frac{8.5}{6}\left[(2\times 31.5+23)\frac{31.5}{19.61}+(2\times 23+31.5)\frac{23}{11.79}\right]\frac{1}{E}}^{409.88\times\frac{1}{E}} + \overbrace{\frac{9.3}{6}\left[(2\times 23+14.5)\frac{23}{11.79}+(2\times 14.5+23)\frac{14.5}{5.2}\right]\frac{1}{E}}^{407.69\times\frac{1}{E}}$$

$$+ \overbrace{\frac{11.3}{6}\left[(2\times 14.5+6.4)\frac{14.5}{5.2}+(2\times 6.4+14.5)\frac{6.4}{1.405}\right]\frac{1}{E}}^{420.11\times\frac{1}{E}} + \overbrace{\frac{6}{6}\left[(2\times 6.4+2.9)\frac{6.4}{1.405}+(2\times 2.9+6.4)\frac{2.9}{.51}\right]\frac{1}{E}}^{140.889\times\frac{1}{E}}$$

$$+ \overbrace{\frac{6}{3}\left[(2.9)2.9\right]\frac{1}{E}}^{16.82\times\frac{1}{E}} = 1395.389\times\frac{1}{E} \quad \text{and} \quad \boxed{\alpha_{y_A} = 132.89\times10^{-6}\ \text{in/\#}} \leftarrow \int M_1\left(\frac{M_1}{EI}\right)dx$$

$E = 10.5\times10^6$

then from equation (a) we solve for R_{y_A}:

$$\Delta_{y_A} + R_{y_A}\alpha_{y_A} = 0 = 567118\times10^{-6} + R_{y_A}\times 132.89\times10^{-6}$$

hence, $\boxed{R_{y_A} = -4267^{\#}}$

THUS IT TAKES A LOAD OF 4267#, ACTING TO THE RIGHT AT POINT A, TO PREVENT "y" DIRECTION DISPLACEMENT OF POINT A.

PROCEDURES AND DATA WHICH CAN BE USED TO SAVE TIME WHEN SOLVING STRUCTURES BY THE METHOD OF MOMENT DISTRIBUTION.

Summary

This subject is presented in two sections. Section 1 contains a review of the moment distribution method and outlines a time saving approach to solving spans with linearly varying EI. Section 2 deals with spans having arbitrary EI. A computer program is available to reduce analysis time for such spans (Reference a). Axially loaded members are not included in the material of Sections 1 and 2. Such structures are covered separately under the subject entitled "Beam Columns".

Section 1 Moment Distribution for Structures with spans of Linearly Varying EI

The intent of this writing is to present a compact review of the procedures used in moment distribution and to give the analyst data which can be used to save time when using the procedure. Comprehensive discussions of moment distribution are presented in many publications. For those who need more review than that offered herein, the following two references may be helpful:

Peery, David J.: "Aircraft Structures", McGraw Hill Book Company, New York, 1950.

Niles, A. S., and J. S. Newell: "Airplane Structures", Volume II, John Wiley and Sons, New York, 1955.

Review

The method is usually used to solve beams or frames having more than three redundants and in which the consideration of bending energy can be assumed to give acceptable results. It is not necessary to remove the redundant supports to obtain a statically determinate structure and then to write and solve the simultaneous equations which determine the redundants. Instead, the structure is imagined as comprising several interconnected single-span fixed-end beams. Fixed-end moments for each span are calculated. At the points where two or more spans interconnect, the fixed-end moments usually are not equal. By the moment distribution procedure, the net unbalanced moment at each such joint is successively altered until the conditions for the actual structure are obtained.

Reference (a) SACP-5, G1.01-1 and -2 of this manual.

Review continued:

The application of this method is simplified if certain steps can be prescribed and followed automatically. Before going over these steps, a review of the following fundamentals may prove helpful.

A. Sign convention: Unless an alternate convention is more convenient, the one which follows is recommended

M_L and M_R are the bending moments applied to the beam span at its left and right ends respectively.

B. Stiffness factor K_j: The stiffness factor is defined as the magnitude of bending moment required to produce a unit angle θ_j with the beam span supported as shown:

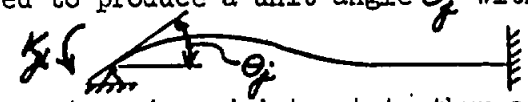

Assuming all spans meeting at a given joint rotate thru a commom angle θ_j the total joint moment M_j is then distributed to each span according to:

$$M_j = K_1\theta_j + K_2\theta_j + \ldots + K_n\theta_j = \theta_j \Sigma K_j$$ where

K_1, K_2, etc. are the stiffness factors for the individual spans. Stiffness factors can be obtained quickly from the curve of Figure 1.

C. Distribution factor: The distribution factor for a given span is defined as the fraction of the total joint moment M_j which is resisted by that span.

$$\text{Distribution Factor} = \frac{K_j}{\Sigma K_j} = \text{DF}$$

D. Carry-over factor: For a span of beam supported as shown below, the carry-over factor is defined as the ratio of M_R to M_L. Carry-over factors can be obtained quickly from the curve of Figure 2.

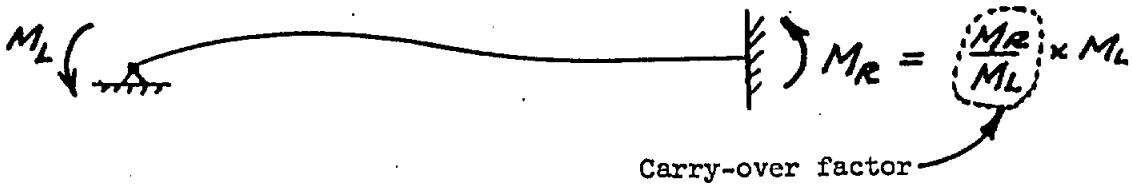

An outline of the steps to follow when performing moment distribution is presented on page 3. Two illustrative examples are presented on pages C4.03-11 thru -15. The first example is treated in deeper detail than the second for the benefit of those who may profit from same.

Review continued:

The Moment Distribution Procedure:

The steps outlined below should be followed in sequence. To clarify the operations, Illustrative Example 1 is presented in a manner such that each step is cross referenced.

Step 1: Calculate the fixed-end moments for each loaded span. Figure 3 & Tables 1 thru 5 can be used for quick computation of same if spans are of linearly varying EI*.

Step 2: Compute the stiffness factors K_L and K_R for each span. Use Figure 1 for beams of linearly varying EI*.

Step 3: Using the stiffness factors determined in Step 2, calculate the distribution factors $K_j \div \Sigma K_j$ for the members meeting at each joint. K_j is the stiffness factor for any individual member at a given joint and ΣK_j is the sum of all individual stiffness factors at that joint.

Step 4: Determine the carry-over factors C_L and C_R for each span. Use Figure 2 for beams of linearly varying EI.*

Step 5: Calculate the unbalanced moment at each joint. This is simply the algebraic sum of the fixed-end moments at a joint.

Step 6: Balance the moments at each joint by multiplying the unbalanced moment by the distribution factor for each span, changing the sign, and recording the balancing moment below each fixed-end moment. If a support is fixed against rotation, the unbalanced moment is resisted by the support and the balancing moment is zero because the joint is not free to rotate in the balancing process. Now draw a horizontal line below the balancing moments.

Step 7: Calculate the carry-over moments at the opposite ends of each individual span indicating the carry-over process by diagonal arrows. The carry-over moments have the same sign as the corresponding balancing moments and have magnitudes determined by the carry-over factors determined in Step 4.

Step 8: Repeat the process of "balance and carry-over" of moments for as many cycles as desired. The final moment at the end of each span is the algebraic sum of all moments in the table at the point in question. The sum of the final moments for all spans meeting at a given joint must be either zero or equal to the externally applied moment at the joint.

* See Section 2 for problems involving spans of arbitrary EI.

TABLE I

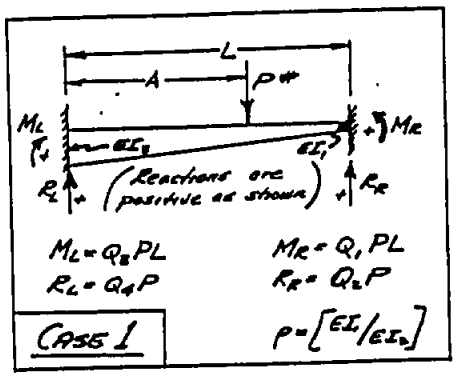

ρ=.2

A/L	Q1	Q2	Q3	Q4
0.05000	-0.10117	0.04483	-0.04633	0.99517
0.10000	-0.00453	0.01996	-0.08547	0.98094
0.15000	-0.20587	0.04223	-0.11764	0.95777
0.20000	-0.01894	0.07385	-0.14308	0.92615
0.25000	-0.02548	0.11339	-0.16258	0.88661
0.30000	-0.03523	0.16032	-0.17688	0.83968
0.35000	-0.04580	0.21461	-0.18179	0.78539
0.40000	-0.05684	0.27370	-0.18319	0.72630
0.45000	-0.06809	0.33824	-0.17954	0.66176
0.50000	-0.07897	0.40772	-0.17125	0.59228
0.55000	-0.08897	0.48017	-0.15880	0.51983
0.60000	-0.09769	0.55472	-0.14277	0.44528
0.65000	-0.10388	0.63003	-0.12385	0.36997
0.70000	-0.10750	0.70469	-0.10281	0.29531
0.75000	-0.10748	0.77721	-0.08028	0.22279
0.80000	-0.10246	0.84448	-0.05797	0.15552
0.85000	-0.09108	0.90417	-0.03692	0.09583
0.90000	-0.07174	0.95291	-0.01883	0.04709
0.95000	-0.04258	0.98682	-0.00572	0.01318
1.00000	-0.00000	1.00000	-0.00000	0.0

ρ=.3

A/L	Q1	Q2	Q3	Q4
0.05000	-0.00138	0.00527	-0.04612	0.99473
0.10000	-0.00534	0.02070	-0.08465	0.97930
0.15000	-0.01160	0.04571	-0.11568	0.95429
0.20000	-0.01963	0.07968	-0.14015	0.92032
0.25000	-0.02969	0.12191	-0.15779	0.87809
0.30000	-0.04083	0.17166	-0.16917	0.82834
0.35000	-0.05284	0.22919	-0.17465	0.77181
0.40000	-0.06528	0.29061	-0.17467	0.70939
0.45000	-0.07707	0.35793	-0.16974	0.64207
0.50000	-0.08968	0.42903	-0.16045	0.57097
0.55000	-0.10016	0.50283	-0.14733	0.49717
0.60000	-0.10901	0.57799	-0.13102	0.42201
0.65000	-0.11524	0.65295	-0.11229	0.34705
0.70000	-0.11796	0.72569	-0.09197	0.27401
0.75000	-0.11648	0.79338	-0.07152	0.20662
0.80000	-0.10961	0.85926	-0.05235	0.14074
0.85000	-0.09641	0.91563	-0.03498	0.08457
0.90000	-0.07584	0.96007	-0.01497	0.03993
0.95000	-0.04369	0.98974	-0.00305	0.01026
1.00000	-0.00000	1.00000	0.00000	-0.00000

ρ=.4

A/L	Q1	Q2	Q3	Q4
0.05000	-0.00156	0.00563	-0.04593	0.99437
0.10000	-0.00603	0.02207	-0.08394	0.97793
0.15000	-0.01304	0.04660	-0.11444	0.95140
0.20000	-0.02221	0.08444	-0.13777	0.91556
0.25000	-0.03313	0.12878	-0.15434	0.87122
0.30000	-0.04536	0.18074	-0.16463	0.81926
0.35000	-0.05844	0.23937	-0.16907	0.76063
0.40000	-0.07187	0.30372	-0.16815	0.69628
0.45000	-0.08509	0.37269	-0.16241	0.62732
0.50000	-0.09748	0.44505	-0.15243	0.55495
0.55000	-0.10845	0.51947	-0.13898	0.48053
0.60000	-0.11731	0.59464	-0.12267	0.40536
0.65000	-0.12332	0.66968	-0.10424	0.33092
0.70000	-0.12556	0.74109	-0.08456	0.25900
0.75000	-0.12301	0.80938	-0.06463	0.19162
0.80000	-0.11458	0.86909	-0.04549	0.13091
0.85000	-0.09918	0.92388	-0.02853	0.07912
0.90000	-0.07598	0.96189	-0.01408	0.03811
0.95000	-0.04343	0.98924	-0.00418	0.01076
1.00000	-0.00000	1.00000	0.00000	-0.00000

ρ=.5

A/L	Q1	Q2	Q3	Q4
0.05000	-0.00174	0.00598	-0.04576	0.99402
0.10000	-0.00668	0.02336	-0.08332	0.97664
0.15000	-0.01439	0.05129	-0.11310	0.94871
0.20000	-0.02441	0.08889	-0.13555	0.91112
0.25000	-0.03631	0.13512	-0.15116	0.86485
0.30000	-0.04955	0.18911	-0.16044	0.81089
0.35000	-0.06359	0.24968	-0.16391	0.75032
0.40000	-0.07789	0.31573	-0.16216	0.68427
0.45000	-0.09185	0.38612	-0.15572	0.61388
0.50000	-0.10481	0.45954	-0.14527	0.54046
0.55000	-0.11607	0.53459	-0.13147	0.46541
0.60000	-0.12487	0.60978	-0.11508	0.39022
0.65000	-0.13053	0.68358	-0.09694	0.31642
0.70000	-0.13220	0.75437	-0.07783	0.24563
0.75000	-0.12900	0.82039	-0.05861	0.17961
0.80000	-0.12002	0.87981	-0.04020	0.12019
0.85000	-0.10386	0.92992	-0.02393	0.07008
0.90000	-0.07946	0.96852	-0.01085	0.03148
0.95000	-0.04531	0.99290	-0.00241	0.00710
1.00000	-0.00000	1.00000	-0.00000	0.0

ρ=.6

A/L	Q1	Q2	Q3	Q4
0.05000	-0.00187	0.00624	-0.04553	0.99376
0.10000	-0.00716	0.02433	-0.08283	0.97567
0.15000	-0.01539	0.05329	-0.11210	0.94671
0.20000	-0.02603	0.09210	-0.13394	0.90790
0.25000	-0.03856	0.13968	-0.14889	0.86032
0.30000	-0.05242	0.19491	-0.15751	0.80509
0.35000	-0.06703	0.25664	-0.16040	0.74336
0.40000	-0.08178	0.32363	-0.15815	0.67637
0.45000	-0.09603	0.39462	-0.15142	0.60538
0.50000	-0.10913	0.46827	-0.14087	0.53173
0.55000	-0.12035	0.54319	-0.12716	0.45681
0.60000	-0.12894	0.61788	-0.11106	0.38212
0.65000	-0.13416	0.69073	-0.09336	0.30927
0.70000	-0.13497	0.76006	-0.07491	0.23994
0.75000	-0.13063	0.82404	-0.05660	0.17596
0.80000	-0.12043	0.88113	-0.03930	0.11887
0.85000	-0.10328	0.92931	-0.02397	0.07069
0.90000	-0.07820	0.96660	-0.01161	0.03340
0.95000	-0.04415	0.99090	-0.00325	0.00910
1.00000	-0.00000	1.00000	0.00000	-0.00000

ρ=.7

A/L	Q1	Q2	Q3	Q4
0.05000	-0.00201	0.00653	-0.04549	0.99347
0.10000	-0.00769	0.02538	-0.08231	0.97462
0.15000	-0.01648	0.05545	-0.11193	0.94455
0.20000	-0.02779	0.09558	-0.13221	0.90442
0.25000	-0.04105	0.14459	-0.14646	0.85541
0.30000	-0.05563	0.20125	-0.15438	0.79875
0.35000	-0.07091	0.26430	-0.15661	0.73570
0.40000	-0.08622	0.33242	-0.15380	0.66758
0.45000	-0.10091	0.40427	-0.14664	0.59573
0.50000	-0.11426	0.47845	-0.13581	0.52155
0.55000	-0.12557	0.55353	-0.12204	0.44647
0.60000	-0.13410	0.62851	-0.10609	0.37199
0.65000	-0.13907	0.70236	-0.08871	0.29964
0.70000	-0.13964	0.76854	-0.07070	0.23106
0.75000	-0.13495	0.83203	-0.05293	0.16797
0.80000	-0.12417	0.88786	-0.03626	0.11214
0.85000	-0.10623	0.93458	-0.02164	0.06542
0.90000	-0.08028	0.97224	-0.01004	0.02976
0.95000	-0.04523	0.99277	-0.00246	0.00723
1.00000	-0.00000	1.00000	-0.00000	-0.00000

ρ=.8

A/L	Q1	Q2	Q3	Q4
0.05000	-0.00212	0.00674	-0.04538	0.99326
0.10000	-0.00807	0.02616	-0.08191	0.97384
0.15000	-0.01724	0.05702	-0.11022	0.94298
0.20000	-0.02904	0.09867	-0.13093	0.90193
0.25000	-0.04270	0.14901	-0.14469	0.85199
0.30000	-0.05789	0.20553	-0.15216	0.79447
0.35000	-0.07329	0.26929	-0.15401	0.73071
0.40000	-0.08883	0.33791	-0.15092	0.66209
0.45000	-0.10366	0.41000	-0.14359	0.59000
0.50000	-0.11689	0.48413	-0.13276	0.51587
0.55000	-0.12796	0.55863	-0.11913	0.44117
0.60000	-0.13668	0.63261	-0.10347	0.36739
0.65000	-0.14249	0.70396	-0.08653	0.29604
0.70000	-0.14041	0.77130	-0.06910	0.22870
0.75000	-0.13504	0.83306	-0.05198	0.16694
0.80000	-0.12358	0.88761	-0.03597	0.11239
0.85000	-0.10520	0.93329	-0.02191	0.06671
0.90000	-0.07906	0.96841	-0.01064	0.03159
0.95000	-0.04428	0.99124	-0.00305	0.00876
1.00000	-0.00000	1.00000	-0.00000	0.0

ρ=.9

A/L	Q1	Q2	Q3	Q4
0.05000	-0.00220	0.00702	-0.04524	0.99298
0.10000	-0.00840	0.02718	-0.08142	0.97282
0.15000	-0.01831	0.05909	-0.10922	0.94091
0.20000	-0.03072	0.10139	-0.12933	0.89861
0.25000	-0.04512	0.15266	-0.14246	0.84734
0.30000	-0.06079	0.21149	-0.14910	0.78851
0.35000	-0.07703	0.27645	-0.15058	0.72355
0.40000	-0.09312	0.34609	-0.14702	0.65391
0.45000	-0.10831	0.41909	-0.13935	0.58164
0.50000	-0.12188	0.49350	-0.12830	0.50642
0.55000	-0.13307	0.56845	-0.11462	0.43155
0.60000	-0.14113	0.64267	-0.09906	0.35793
0.65000	-0.14531	0.71292	-0.08239	0.28708
0.70000	-0.14482	0.77946	-0.06536	0.22054
0.75000	-0.13941	0.84011	-0.04877	0.15987
0.80000	-0.12777	0.89417	-0.03339	0.10583
0.85000	-0.10781	0.93759	-0.02002	0.06241
0.90000	-0.08004	0.97118	-0.00946	0.02882
0.95000	-0.04504	0.99251	-0.00251	0.00747
1.00000	-0.00000	1.00000	-0.00000	0.00000

ρ=1.0

A/L	Q1	Q2	Q3	Q4
0.05000	-0.00237	0.00725	-0.04513	0.99275
0.10000	-0.00900	0.02800	-0.08100	0.97200
0.15000	-0.01912	0.06075	-0.10937	0.93925
0.20000	-0.03209	0.10400	-0.12800	0.89600
0.25000	-0.04687	0.15625	-0.14063	0.84375
0.30000	-0.06300	0.21600	-0.14700	0.78400
0.35000	-0.07962	0.28175	-0.14788	0.71825
0.40000	-0.09600	0.35200	-0.14400	0.64800
0.45000	-0.11137	0.42525	-0.13613	0.57475
0.50000	-0.12500	0.50000	-0.12500	0.50000
0.55000	-0.13612	0.57475	-0.11138	0.42525
0.60000	-0.14400	0.64800	-0.09600	0.35200
0.65000	-0.14787	0.71825	-0.07963	0.28175
0.70000	-0.14700	0.78400	-0.06300	0.21600
0.75000	-0.14062	0.84375	-0.04688	0.15625
0.80000	-0.12800	0.89600	-0.03200	0.10400
0.85000	-0.10837	0.93925	-0.01913	0.06075
0.90000	-0.08100	0.97200	-0.00900	0.02800
0.95000	-0.04513	0.99275	-0.00238	0.00725
1.00000	-0.00000	1.00000	-0.00000	0.00000

GRUMMAN

TABLE 2

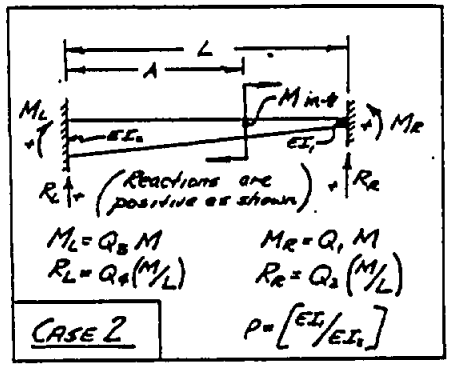

ρ=.2

A/L	Q1	Q2	Q3	Q4
0.05000	-0.06596	0.19185	-0.85412	-0.19185
0.10000	-0.09771	0.37525	-0.71246	-0.37525
0.15000	-0.12488	0.54953	-0.57535	-0.54953
0.20000	-0.15765	0.71387	-0.44318	-0.71387
0.25000	-0.18371	0.86732	-0.31639	-0.86732
0.30000	-0.20429	1.00429	-0.19596	-1.00429
0.35000	-0.21810	1.13578	-0.08213	-1.13578
0.40000	-0.22451	1.24835	0.02386	-1.24835
0.45000	-0.22744	1.34406	0.12162	-1.34406
0.50000	-0.21886	1.42560	0.20999	-1.42560
0.55000	-0.18951	1.47609	0.28757	-1.47609
0.60000	-0.15398	1.50717	0.35319	-1.50717
0.65000	-0.10511	1.50965	0.40455	-1.50965
0.70000	-0.03909	1.47760	0.43981	-1.47760
0.75000	0.04746	1.40498	0.46244	-1.40498
0.80000	0.15780	1.28377	0.44157	-1.28377
0.85000	0.29821	1.10264	0.40115	-1.10294
0.90000	0.47629	0.86659	0.32288	-0.86659
0.95000	0.70292	0.49217	0.19510	-0.49217
1.00000	0.99999	0.00001	0.00000	-0.00001

ρ=.3

A/L	Q1	Q2	Q3	Q4
0.05000	-0.05435	0.20872	-0.84563	-0.20872
0.10000	-0.10319	0.40624	-0.69686	-0.40624
0.15000	-0.14584	0.59174	-0.55411	-0.59174
0.20000	-0.18209	0.76429	-0.41780	-0.76429
0.25000	-0.21130	0.92283	-0.28847	-0.92283
0.30000	-0.23291	1.06603	-0.16678	-1.06603
0.35000	-0.24597	1.19227	-0.05369	-1.19227
0.40000	-0.25006	1.30029	0.05023	-1.30029
0.45000	-0.24418	1.38834	0.14416	-1.38834
0.50000	-0.22710	1.45402	0.22693	-1.45402
0.55000	-0.19757	1.49494	0.29737	-1.49494
0.60000	-0.15429	1.50833	0.35404	-1.50833
0.65000	-0.09575	1.49120	0.39545	-1.49120
0.70000	-0.01967	1.43971	0.41984	-1.43971
0.75000	0.07619	1.34771	0.42389	-1.34771
0.80000	0.19561	1.20877	0.40438	-1.20877
0.85000	0.34263	1.01506	0.35768	-1.01506
0.90000	0.52677	0.75831	0.27907	-0.75831
0.95000	0.73673	0.42592	0.16765	-0.42592
1.00000	1.00000	0.00001	0.00000	-0.00001

ρ=.4

A/L	Q1	Q2	Q3	Q4
0.05000	-0.06163	0.22287	-0.83856	-0.22287
0.10000	-0.11591	0.43183	-0.68498	-0.43183
0.15000	-0.16305	0.62601	-0.53699	-0.62601
0.20000	-0.20221	0.80445	-0.39778	-0.80445
0.25000	-0.23299	0.96606	-0.26692	-0.96606
0.30000	-0.25469	1.10980	-0.14509	-1.10980
0.35000	-0.26661	1.23359	-0.03332	-1.23359
0.40000	-0.26808	1.33646	0.06838	-1.33646
0.45000	-0.25833	1.41680	0.15966	-1.41680
0.50000	-0.23653	1.47296	0.23643	-1.47296
0.55000	-0.20121	1.50214	0.30092	-1.50214
0.60000	-0.15125	1.50208	0.35082	-1.50208
0.65000	-0.08514	1.46984	0.38466	-1.46984
0.70000	-0.00156	1.40262	0.40104	-1.40262
0.75000	0.10111	1.29714	0.39825	-1.29714
0.80000	0.22521	1.14908	0.37429	-1.14908
0.85000	0.37361	0.95291	0.32634	-0.95291
0.90000	0.54921	0.70119	0.25039	-0.70119
0.95000	0.75637	0.38685	0.14121	-0.38685
1.00000	0.99999	0.00001	0.00000	-0.00001

ρ=.5

A/L	Q1	Q2	Q3	Q4
0.05000	-0.06812	0.23623	-0.83189	-0.23623
0.10000	-0.12792	0.45580	-0.67212	-0.45580
0.15000	-0.17995	0.65764	-0.52111	-0.65784
0.20000	-0.22675	0.84141	-0.37934	-0.84141
0.25000	-0.25278	1.00548	-0.24730	-1.00548
0.30000	-0.27446	1.14889	-0.12557	-1.14889
0.35000	-0.28814	1.27036	-0.01478	-1.27036
0.40000	-0.28468	1.36845	0.08437	-1.36845
0.45000	-0.27671	1.44167	0.17096	-1.44167
0.50000	-0.26424	1.48862	0.24438	-1.48862
0.55000	-0.20387	1.50770	0.30383	-1.50770
0.60000	-0.16873	1.49720	0.34847	-1.49720
0.65000	-0.07714	1.45385	0.37671	-1.45385
0.70000	0.01191	1.37561	0.38752	-1.37561
0.75000	0.11989	1.25961	0.37949	-1.25961
0.80000	0.24868	1.10250	0.35098	-1.10250
0.85000	0.39962	0.90250	0.30091	-0.90250
0.90000	0.57210	0.65509	0.22719	-0.65509
0.95000	0.77176	0.35595	0.12771	-0.35595
1.00000	0.99999	0.00001	0.00000	-0.00001

ρ=.6

A/L	Q1	Q2	Q3	Q4
0.05000	-0.07319	0.24868	-0.82679	-0.24868
0.10000	-0.13674	0.47356	-0.66320	-0.47356
0.15000	-0.19033	0.68769	-0.50984	-0.68769
0.20000	-0.23345	0.88695	-0.36651	-0.88695
0.25000	-0.26568	1.03142	-0.23426	-1.03142
0.30000	-0.28652	1.17312	-0.11340	-1.17312
0.35000	-0.29546	1.29097	-0.00444	-1.29097
0.40000	-0.29176	1.38379	0.09203	-1.38379
0.45000	-0.27493	1.45330	0.17534	-1.45330
0.50000	-0.24421	1.48912	0.24491	-1.48912
0.55000	-0.19922	1.49915	0.29993	-1.49915
0.60000	-0.13915	1.47895	0.33980	-1.47895
0.65000	-0.06326	1.42706	0.36380	-1.42706
0.70000	0.02923	1.34192	0.37115	-1.34192
0.75000	0.13915	1.22168	0.36103	-1.22168
0.80000	0.26840	1.06324	0.33164	-1.06324
0.85000	0.41771	0.86450	0.28221	-0.86450
0.90000	0.58839	0.62306	0.21145	-0.62306
0.95000	0.78194	0.33598	0.11792	-0.33598
1.00000	0.99999	0.00001	0.00000	-0.00001

ρ=.7

A/L	Q1	Q2	Q3	Q4
0.05000	-0.07871	0.25715	-0.82136	-0.25715
0.10000	-0.14645	0.49273	-0.65371	-0.49273
0.15000	-0.20286	0.70549	-0.49738	-0.70549
0.20000	-0.24761	0.89490	-0.35271	-0.89490
0.25000	-0.28031	1.06023	-0.22008	-1.06023
0.30000	-0.30057	1.20070	-0.09987	-1.20070
0.35000	-0.30797	1.31547	0.00790	-1.31547
0.40000	-0.30206	1.40364	0.10158	-1.40364
0.45000	-0.28235	1.46426	0.18190	-1.46426
0.50000	-0.24835	1.49633	0.24797	-1.49633
0.55000	-0.19950	1.49875	0.29925	-1.49875
0.60000	-0.13523	1.47038	0.33516	-1.47038
0.65000	-0.05480	1.40998	0.35508	-1.40998
0.70000	0.04175	1.31682	0.35847	-1.31682
0.75000	0.15524	1.18985	0.34500	-1.18985
0.80000	0.28831	1.02764	0.31397	-1.02764
0.85000	0.43567	0.82942	0.26450	-0.82892
0.90000	0.60191	0.59216	0.19627	-0.59216
0.95000	0.79177	0.31695	0.10819	-0.31695
1.00000	1.00000	0.00001	0.00000	-0.00001

ρ=.8

A/L	Q1	Q2	Q3	Q4
0.05000	-0.08274	0.26563	-0.81711	-0.26563
0.10000	-0.15326	0.50679	-0.64667	-0.50679
0.15000	-0.21131	0.72296	-0.48831	-0.72296
0.20000	-0.25664	0.91372	-0.34292	-0.91372
0.25000	-0.28899	1.07846	-0.21053	-1.07846
0.30000	-0.30808	1.21667	-0.09141	-1.21667
0.35000	-0.31363	1.32777	0.01415	-1.32777
0.40000	-0.30534	1.41119	0.10585	-1.41119
0.45000	-0.28290	1.46630	0.18340	-1.46630
0.50000	-0.24600	1.49246	0.24646	-1.49246
0.55000	-0.19418	1.48902	0.29471	-1.48902
0.60000	-0.12745	1.45526	0.32781	-1.45526
0.65000	-0.04509	1.39048	0.34539	-1.39048
0.70000	0.05317	1.29391	0.34707	-1.29391
0.75000	0.16771	1.16475	0.33247	-1.16475
0.80000	0.29898	1.00220	0.30116	-1.00220
0.85000	0.44735	0.80537	0.25272	-0.80537
0.90000	0.61333	0.57337	0.18670	-0.57337
0.95000	0.79738	0.30324	0.10262	-0.30324
1.00000	0.99999	0.00001	0.00	-0.00001

ρ=.9

A/L	Q1	Q2	Q3	Q4
0.05000	-0.08823	0.27629	-0.81194	-0.27629
0.10000	-0.16278	0.52524	-0.63754	-0.52524
0.15000	-0.22392	0.74835	-0.47693	-0.74835
0.20000	-0.27042	0.94006	-0.33026	-0.94006
0.25000	-0.30303	1.10519	-0.19765	-1.10519
0.30000	-0.32182	1.24226	-0.07926	-1.24226
0.35000	-0.32563	1.35042	0.02479	-1.35042
0.40000	-0.31523	1.42955	0.11432	-1.42955
0.45000	-0.29016	1.47837	0.18921	-1.47917
0.50000	-0.25026	1.49955	0.24929	-1.49955
0.55000	-0.19538	1.48180	0.29442	-1.48180
0.60000	-0.12537	1.44479	0.32442	-1.44479
0.65000	-0.04005	1.37919	0.33914	-1.37919
0.70000	0.06073	1.27768	0.33841	-1.27768
0.75000	0.17715	1.14462	0.32207	-1.14462
0.80000	0.30939	0.98056	0.28995	-0.98056
0.85000	0.45760	0.78425	0.24186	-0.78425
0.90000	0.62199	0.55563	0.17762	-0.55563
0.95000	0.80272	0.29434	0.09707	-0.29434
1.00000	1.00000	0.00000	0.00000	-0.00000

ρ=1.0

A/L	Q1	Q2	Q3	Q4
0.05000	-0.09297	0.28500	-0.80750	-0.28500
0.10000	-0.17001	0.54000	-0.63000	-0.54000
0.15000	-0.23250	0.77000	-0.46750	-0.76000
0.20000	-0.28000	0.96000	-0.32000	-0.96000
0.25000	-0.31250	1.12500	-0.18750	-1.12500
0.30000	-0.33000	1.26000	-0.07000	-1.26000
0.35000	-0.33250	1.36500	-0.03250	-1.36500
0.40000	-0.32000	1.44000	0.12000	-1.44000
0.45000	-0.29250	1.48500	0.19250	-1.48500
0.50000	-0.25000	1.50000	0.25000	-1.50000
0.55000	-0.19250	1.48500	0.29250	-1.48500
0.60000	-0.12000	1.44000	0.32000	-1.44000
0.65000	-0.03250	1.36500	0.33250	-1.36500
0.70000	0.07000	1.26000	0.33000	-1.26000
0.75000	0.18750	1.12500	0.31250	-1.12500
0.80000	0.32000	0.96000	0.28000	-0.96000
0.85000	0.46750	0.76500	0.23250	-0.76500
0.90000	0.63000	0.54000	0.17000	-0.54000
0.95000	0.80750	0.28500	0.09250	-0.28500
1.00000	1.00000	0.00000	0.00000	-0.00000

GRUMMAN

TABLE 3

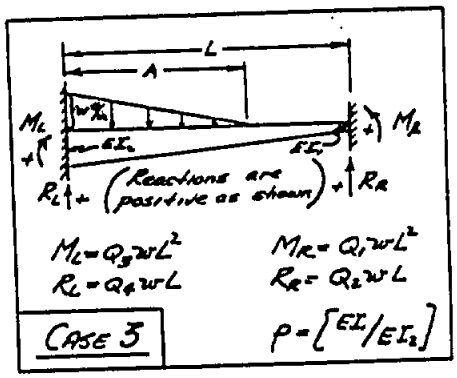

$\rho = .2$

A/L	Q1	Q2	Q3	Q4
0.05000	-0.00006	0.00002	-0.00040	0.02498
0.10000	-0.00004	0.00016	-0.00154	0.04984
0.15000	-0.00013	0.00354	-0.00334	0.07446
0.20000	-0.00030	0.00626	-0.00576	0.09874
0.25000	-0.00057	0.00944	-0.00854	0.12256
0.30000	-0.00097	0.00418	-0.01178	0.14582
0.35000	-0.00150	0.00657	-0.01536	0.16843
0.40000	-0.00219	0.00971	-0.01915	0.19029
0.45000	-0.00304	0.01366	-0.02312	0.21134
0.50000	-0.00406	0.01852	-0.02720	0.23147
0.55000	-0.00525	0.02435	-0.03132	0.25065
0.60000	-0.00661	0.03119	-0.03542	0.26881
0.65000	-0.00813	0.03911	-0.03944	0.28589
0.70000	-0.00982	0.04818	-0.04331	0.30182
0.75000	-0.01164	0.05843	-0.04697	0.31657
0.80000	-0.01357	0.06979	-0.05045	0.33021
0.85000	-0.01557	0.08229	-0.05370	0.34272
0.90000	-0.01759	0.09588	-0.05671	0.35412
0.95000	-0.01957	0.11053	-0.05946	0.36447
1.00000	-0.02141	0.12612	-0.06196	0.37387

$\rho = .3$

A/L	Q1	Q2	Q3	Q4
0.05000	-0.00001	0.00002	-0.00040	0.02498
0.10000	-0.00005	0.00017	-0.00154	0.04983
0.15000	-0.00015	0.00358	-0.00332	0.07442
0.20000	-0.00035	0.00137	-0.00565	0.09863
0.25000	-0.00067	0.00265	-0.00844	0.12235
0.30000	-0.00113	0.00452	-0.01161	0.14545
0.35000	-0.00175	0.00709	-0.01508	0.16791
0.40000	-0.00255	0.01044	-0.01878	0.18956
0.45000	-0.00353	0.01467	-0.02262	0.21033
0.50000	-0.00470	0.01983	-0.02654	0.23016
0.55000	-0.00607	0.02601	-0.03047	0.24899
0.60000	-0.00762	0.03325	-0.03437	0.26675
0.65000	-0.00935	0.04159	-0.03818	0.28341
0.70000	-0.01124	0.05105	-0.04186	0.29895
0.75000	-0.01328	0.06166	-0.04535	0.31332
0.80000	-0.01543	0.07350	-0.04860	0.32650
0.85000	-0.01766	0.08651	-0.05157	0.33849
0.90000	-0.01991	0.10059	-0.05432	0.34941
0.95000	-0.02211	0.11568	-0.05684	0.35932
1.00000	-0.02418	0.13170	-0.05915	0.36830

$\rho = .4$

A/L	Q1	Q2	Q3	Q4
0.05000	-0.00001	0.00002	-0.00040	0.02498
0.10000	-0.00005	0.00019	-0.00153	0.04981
0.15000	-0.00017	0.00062	-0.00330	0.07436
0.20000	-0.00040	0.00146	-0.00560	0.09854
0.25000	-0.00075	0.00281	-0.00836	0.12219
0.30000	-0.00127	0.00479	-0.01148	0.14521
0.35000	-0.00196	0.00781	-0.01487	0.16749
0.40000	-0.00285	0.01164	-0.01848	0.18896
0.45000	-0.00394	0.01568	-0.02221	0.20952
0.50000	-0.00523	0.02089	-0.02601	0.22911
0.55000	-0.00673	0.02734	-0.02981	0.24766
0.60000	-0.00843	0.03487	-0.03356	0.26513
0.65000	-0.01032	0.04353	-0.03720	0.28147
0.70000	-0.01237	0.05333	-0.04070	0.29667
0.75000	-0.01457	0.06428	-0.04403	0.31072
0.80000	-0.01687	0.07636	-0.04716	0.32362
0.85000	-0.01924	0.08960	-0.05005	0.33540
0.90000	-0.02163	0.10395	-0.05268	0.34605
0.95000	-0.02398	0.11936	-0.05504	0.35564
1.00000	-0.02621	0.13578	-0.05711	0.36422

$\rho = .5$

A/L	Q1	Q2	Q3	Q4
0.05000	-0.00001	0.00003	-0.00040	0.02497
0.10000	-0.00006	0.00020	-0.00153	0.04980
0.15000	-0.00019	0.00066	-0.00328	0.07434
0.20000	-0.00044	0.00156	-0.00556	0.09846
0.25000	-0.00083	0.00297	-0.00828	0.12203
0.30000	-0.00140	0.00505	-0.01135	0.14495
0.35000	-0.00216	0.00789	-0.01468	0.16719
0.40000	-0.00313	0.01159	-0.01820	0.18841
0.45000	-0.00431	0.01623	-0.02184	0.20877
0.50000	-0.00572	0.02186	-0.02552	0.22813
0.55000	-0.00734	0.02856	-0.02920	0.24644
0.60000	-0.00918	0.03636	-0.03281	0.26364
0.65000	-0.01121	0.04531	-0.03631	0.27969
0.70000	-0.01341	0.05541	-0.03966	0.29459
0.75000	-0.01575	0.06667	-0.04283	0.30833
0.80000	-0.01820	0.07909	-0.04578	0.32091
0.85000	-0.02071	0.09261	-0.04852	0.33239
0.90000	-0.02323	0.10719	-0.05104	0.34281
0.95000	-0.02569	0.12277	-0.05333	0.35223
1.00000	-0.02802	0.13928	-0.05541	0.36072

$\rho = .6$

A/L	Q1	Q2	Q3	Q4
0.05000	-0.00001	0.00003	-0.00040	0.02497
0.10000	-0.00006	0.00021	-0.00152	0.04979
0.15000	-0.00020	0.00069	-0.00327	0.07431
0.20000	-0.00047	0.00160	-0.00553	0.09840
0.25000	-0.00089	0.00309	-0.00822	0.12192
0.30000	-0.00149	0.00524	-0.01125	0.14476
0.35000	-0.00230	0.00818	-0.01454	0.16682
0.40000	-0.00332	0.01193	-0.01800	0.18801
0.45000	-0.00457	0.01675	-0.02157	0.20825
0.50000	-0.00606	0.02254	-0.02518	0.22746
0.55000	-0.00776	0.02941	-0.02877	0.24559
0.60000	-0.00968	0.03739	-0.03229	0.26261
0.65000	-0.01180	0.04652	-0.03570	0.27848
0.70000	-0.01409	0.05680	-0.03896	0.29320
0.75000	-0.01651	0.06822	-0.04204	0.30678
0.80000	-0.01904	0.08079	-0.04492	0.31921
0.85000	-0.02162	0.09446	-0.04758	0.33054
0.90000	-0.02419	0.10918	-0.05001	0.34082
0.95000	-0.02670	0.12489	-0.05222	0.35011
1.00000	-0.02905	0.14149	-0.05423	0.35851

$\rho = .7$

A/L	Q1	Q2	Q3	Q4
0.05000	-0.00001	0.00003	-0.00040	0.02497
0.10000	-0.00007	0.00022	-0.00152	0.04978
0.15000	-0.00022	0.00072	-0.00325	0.07426
0.20000	-0.00050	0.00167	-0.00550	0.09833
0.25000	-0.00095	0.00321	-0.00816	0.12179
0.30000	-0.00160	0.00544	-0.01115	0.14456
0.35000	-0.00245	0.00844	-0.01439	0.16652
0.40000	-0.00354	0.01241	-0.01779	0.18759
0.45000	-0.00486	0.01732	-0.02129	0.20768
0.50000	-0.00643	0.02328	-0.02482	0.22672
0.55000	-0.00823	0.03032	-0.02832	0.24468
0.60000	-0.01025	0.03851	-0.03174	0.26149
0.65000	-0.01248	0.04785	-0.03504	0.27715
0.70000	-0.01488	0.05836	-0.03819	0.29164
0.75000	-0.01742	0.07002	-0.04115	0.30496
0.80000	-0.02007	0.08282	-0.04391	0.31718
0.85000	-0.02275	0.09671	-0.04646	0.32829
0.90000	-0.02543	0.11161	-0.04880	0.33837
0.95000	-0.02802	0.12751	-0.05093	0.34749
1.00000	-0.03044	0.14424	-0.05287	0.35576

$\rho = .8$

A/L	Q1	Q2	Q3	Q4
0.05000	-0.00001	0.00003	-0.00040	0.02497
0.10000	-0.00007	0.00022	-0.00151	0.04978
0.15000	-0.00023	0.00074	-0.00324	0.07426
0.20000	-0.00053	0.00172	-0.00547	0.09829
0.25000	-0.00100	0.00330	-0.00811	0.12170
0.30000	-0.00167	0.00559	-0.01108	0.14441
0.35000	-0.00256	0.00870	-0.01428	0.16630
0.40000	-0.00369	0.01271	-0.01764	0.18729
0.45000	-0.00506	0.01772	-0.02109	0.20728
0.50000	-0.00667	0.02377	-0.02456	0.22623
0.55000	-0.00852	0.03093	-0.02801	0.24407
0.60000	-0.01059	0.03922	-0.03137	0.26078
0.65000	-0.01287	0.04867	-0.03462	0.27633
0.70000	-0.01533	0.05929	-0.03770	0.29071
0.75000	-0.01792	0.07104	-0.04061	0.30394
0.80000	-0.02061	0.08387	-0.04331	0.31603
0.85000	-0.02335	0.09767	-0.04580	0.32703
0.90000	-0.02608	0.11231	-0.04808	0.33699
0.95000	-0.02872	0.12782	-0.05012	0.34599
1.00000	-0.03121	0.14391	-0.05197	0.35409

$\rho = .9$

A/L	Q1	Q2	Q3	Q4
0.05000	-0.00001	0.00003	-0.00040	0.02497
0.10000	-0.00007	0.00021	-0.00151	0.04977
0.15000	-0.00024	0.00077	-0.00322	0.07423
0.20000	-0.00056	0.00179	-0.00544	0.09821
0.25000	-0.00106	0.00342	-0.00806	0.12158
0.30000	-0.00177	0.00579	-0.01098	0.14421
0.35000	-0.00271	0.00899	-0.01414	0.16601
0.40000	-0.00390	0.01312	-0.01744	0.18689
0.45000	-0.00534	0.01826	-0.02083	0.20674
0.50000	-0.00703	0.02447	-0.02423	0.22553
0.55000	-0.00897	0.03179	-0.02760	0.24321
0.60000	-0.01114	0.04026	-0.03088	0.25974
0.65000	-0.01352	0.04990	-0.03403	0.27510
0.70000	-0.01607	0.06070	-0.03703	0.28929
0.75000	-0.01877	0.07267	-0.03985	0.30233
0.80000	-0.02156	0.08576	-0.04247	0.31424
0.85000	-0.02440	0.09994	-0.04487	0.32506
0.90000	-0.02721	0.11514	-0.04707	0.33486
0.95000	-0.02994	0.13130	-0.04906	0.34370
1.00000	-0.03251	0.14833	-0.05085	0.35167

$\rho = 1.0$

A/L	Q1	Q2	Q3	Q4
0.05000	-0.00001	0.00003	-0.00040	0.02497
0.10000	-0.00008	0.00024	-0.00150	0.04976
0.15000	-0.00026	0.00079	-0.00321	0.07421
0.20000	-0.00059	0.00184	-0.00541	0.09816
0.25000	-0.00111	0.00352	-0.00801	0.12148
0.30000	-0.00184	0.00594	-0.01090	0.14406
0.35000	-0.00282	0.00922	-0.01402	0.16578
0.40000	-0.00405	0.01344	-0.01728	0.18656
0.45000	-0.00554	0.01868	-0.02061	0.20632
0.50000	-0.00729	0.02506	-0.02396	0.22500
0.55000	-0.00929	0.03244	-0.02726	0.24256
0.60000	-0.01152	0.04104	-0.03048	0.25896
0.65000	-0.01396	0.05081	-0.03357	0.27419
0.70000	-0.01658	0.06174	-0.03650	0.28826
0.75000	-0.01936	0.07383	-0.03926	0.30117
0.80000	-0.02219	0.08704	-0.04181	0.31296
0.85000	-0.02508	0.10133	-0.04416	0.32367
0.90000	-0.02795	0.11664	-0.04631	0.33336
0.95000	-0.03077	0.13289	-0.04825	0.34211
1.00000	-0.03333	0.15000	-0.05000	0.35000

GRUMMAN

TABLE 4

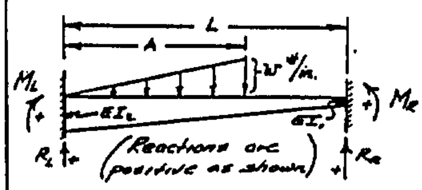

$M_L = Q_3 wL^2$ $M_R = Q_1 wL^2$

$R_L = Q_4 wL$ $R_R = Q_2 wL$

CASE 4 $\rho = [EI_1/EI_2]$

$\rho = .2$

A/L	Q1	Q2	Q3	Q4
0.05000	-0.00001	0.00006	-0.00079	0.02496
0.10000	-0.00011	0.00046	-0.00297	0.04952
0.15000	-0.00038	0.00160	-0.00628	0.07360
0.20000	-0.00087	0.00374	-0.01046	0.09626
0.25000	-0.00165	0.00721	-0.01527	0.11779
0.30000	-0.00277	0.01229	-0.02048	0.13771
0.35000	-0.00426	0.01923	-0.02586	0.15577
0.40000	-0.00614	0.02827	-0.03120	0.17171
0.45000	-0.00841	0.03959	-0.03632	0.18561
0.50000	-0.01107	0.05337	-0.04103	0.19651
0.55000	-0.01407	0.06970	-0.04520	0.20530
0.60000	-0.01737	0.08867	-0.04870	0.21133
0.65000	-0.02089	0.11032	-0.05140	0.21468
0.70000	-0.02453	0.13466	-0.05319	0.21546
0.75000	-0.02814	0.16165	-0.05399	0.21335
0.80000	-0.03151	0.19088	-0.05396	0.20912
0.85000	-0.03438	0.22212	-0.05310	0.20288
0.90000	-0.03645	0.25494	-0.05152	0.19506
0.95000	-0.03734	0.28883	-0.04935	0.18617
1.00000	-0.03645	0.32296	-0.04682	0.17704

$\rho = .3$

A/L	Q1	Q2	Q3	Q4
0.05000	-0.00002	0.00007	-0.00078	0.02493
0.10000	-0.00014	0.00052	-0.00295	0.04948
0.15000	-0.00044	0.00173	-0.00621	0.07327
0.20000	-0.00102	0.00405	-0.01031	0.09595
0.25000	-0.00194	0.00778	-0.01499	0.11722
0.30000	-0.00323	0.01322	-0.02001	0.13678
0.35000	-0.00495	0.02063	-0.02516	0.15437
0.40000	-0.00711	0.03022	-0.03022	0.16978
0.45000	-0.00970	0.04219	-0.03501	0.18281
0.50000	-0.01270	0.05667	-0.03937	0.19333
0.55000	-0.01608	0.07377	-0.04314	0.20123
0.60000	-0.01976	0.09353	-0.04623	0.20647
0.65000	-0.02364	0.11592	-0.04855	0.20908
0.70000	-0.02758	0.14086	-0.05006	0.20918
0.75000	-0.03144	0.16826	-0.05068	0.20678
0.80000	-0.03501	0.19793	-0.05042	0.20207
0.85000	-0.03805	0.22958	-0.04930	0.19542
0.90000	-0.04018	0.26257	-0.04761	0.18743
0.95000	-0.04102	0.29631	-0.04555	0.17869
1.00000	-0.04006	0.33000	-0.04339	0.17000

$\rho = .4$

A/L	Q1	Q2	Q3	Q4
0.05000	-0.00002	0.00007	-0.00078	0.02493
0.10000	-0.00015	0.00056	-0.00293	0.04944
0.15000	-0.00050	0.00185	-0.00615	0.07318
0.20000	-0.00115	0.00430	-0.01018	0.09570
0.25000	-0.00217	0.00825	-0.01476	0.11675
0.30000	-0.00361	0.01398	-0.01963	0.13602
0.35000	-0.00551	0.02174	-0.02460	0.15325
0.40000	-0.00788	0.03177	-0.02944	0.16823
0.45000	-0.01072	0.04423	-0.03399	0.18077
0.50000	-0.01399	0.05924	-0.03808	0.19076
0.55000	-0.01764	0.07689	-0.04158	0.19811
0.60000	-0.02159	0.09720	-0.04440	0.20280
0.65000	-0.02573	0.12012	-0.04644	0.20488
0.70000	-0.02990	0.14555	-0.04768	0.20445
0.75000	-0.03392	0.17328	-0.04814	0.20172
0.80000	-0.03758	0.20307	-0.04784	0.19693
0.85000	-0.04060	0.23458	-0.04685	0.19061
0.90000	-0.04270	0.26746	-0.04524	0.18254
0.95000	-0.04349	0.30115	-0.04318	0.17385
1.00000	-0.04255	0.33501	-0.04087	0.16499

$\rho = .5$

A/L	Q1	Q2	Q3	Q4
0.05000	-0.00002	0.00008	-0.00078	0.02492
0.10000	-0.00017	0.00059	-0.00291	0.04941
0.15000	-0.00055	0.00195	-0.00610	0.07305
0.20000	-0.00127	0.00454	-0.01006	0.09546
0.25000	-0.00239	0.00868	-0.01456	0.11632
0.30000	-0.00398	0.01468	-0.01929	0.13532
0.35000	-0.00603	0.02278	-0.02408	0.15222
0.40000	-0.00860	0.03320	-0.02873	0.16680
0.45000	-0.01166	0.04611	-0.03305	0.17889
0.50000	-0.01517	0.06160	-0.03690	0.18840
0.55000	-0.01907	0.07975	-0.04016	0.19525
0.60000	-0.02326	0.10054	-0.04272	0.19946
0.65000	-0.02763	0.12392	-0.04454	0.20108
0.70000	-0.03200	0.14976	-0.04558	0.20026
0.75000	-0.03619	0.17786	-0.04584	0.19714
0.80000	-0.03994	0.20795	-0.04536	0.19205
0.85000	-0.04307	0.23963	-0.04427	0.18547
0.90000	-0.04515	0.27246	-0.04269	0.17784
0.95000	-0.04585	0.30598	-0.04081	0.16912
1.00000	-0.04474	0.33922	-0.03886	0.16078

$\rho = .6$

A/L	Q1	Q2	Q3	Q4
0.05000	-0.00002	0.00008	-0.00078	0.02492
0.10000	-0.00018	0.00061	-0.00290	0.04939
0.15000	-0.00059	0.00203	-0.00606	0.07297
0.20000	-0.00135	0.00471	-0.00998	0.09529
0.25000	-0.00256	0.00899	-0.01438	0.11601
0.30000	-0.00421	0.01517	-0.01903	0.13482
0.35000	-0.00640	0.02351	-0.02372	0.15144
0.40000	-0.00909	0.03419	-0.02823	0.16561
0.45000	-0.01229	0.04747	-0.03242	0.17763
0.50000	-0.01596	0.06315	-0.03612	0.18665
0.55000	-0.01997	0.08157	-0.03926	0.19363
0.60000	-0.02429	0.10261	-0.04166	0.19739
0.65000	-0.02875	0.12620	-0.04338	0.19880
0.70000	-0.03319	0.15218	-0.04434	0.19782
0.75000	-0.03740	0.18043	-0.04457	0.19466
0.80000	-0.04116	0.21039	-0.04411	0.18961
0.85000	-0.04419	0.24198	-0.04305	0.18302
0.90000	-0.04617	0.27465	-0.04152	0.17535
0.95000	-0.04674	0.30788	-0.03966	0.16712
1.00000	-0.04548	0.34105	-0.03777	0.15895

$\rho = .7$

A/L	Q1	Q2	Q3	Q4
0.05000	-0.00003	0.00008	-0.00078	0.02492
0.10000	-0.00020	0.00064	-0.00289	0.04936
0.15000	-0.00066	0.00212	-0.00602	0.07288
0.20000	-0.00145	0.00490	-0.00988	0.09510
0.25000	-0.00271	0.00913	-0.01421	0.11567
0.30000	-0.00448	0.01572	-0.01877	0.13428
0.35000	-0.00679	0.02430	-0.02333	0.15070
0.40000	-0.00963	0.03527	-0.02770	0.16473
0.45000	-0.01299	0.04877	-0.03173	0.17623
0.50000	-0.01681	0.06480	-0.03527	0.18512
0.55000	-0.02107	0.08364	-0.03842	0.19136
0.60000	-0.02550	0.10501	-0.04050	0.19499
0.65000	-0.03012	0.12889	-0.04206	0.19611
0.70000	-0.03469	0.15513	-0.04290	0.19487
0.75000	-0.03902	0.18349	-0.04302	0.19151
0.80000	-0.04286	0.21360	-0.04249	0.18641
0.85000	-0.04591	0.24540	-0.04140	0.17966
0.90000	-0.04790	0.27800	-0.04008	0.17200
0.95000	-0.04861	0.31115	-0.03810	0.16345
1.00000	-0.04704	0.34415	-0.03626	[illegible]

$\rho = .8$

A/L	Q1	Q2	Q3	Q4
0.05000	-0.00003	0.00008	-0.00078	0.02492
0.10000	-0.00021	0.00066	-0.00288	0.04934
0.15000	-0.00067	0.00218	-0.00599	0.07282
0.20000	-0.00152	0.00504	-0.00981	0.09496
0.25000	-0.00283	0.00958	-0.01409	0.11542
0.30000	-0.00467	0.01610	-0.01857	0.13390
0.35000	-0.00705	0.02484	-0.02305	0.15016
0.40000	-0.00998	0.03599	-0.02733	0.16401
0.45000	-0.01343	0.04967	-0.03125	0.17533
0.50000	-0.01733	0.06597	-0.03470	0.18403
0.55000	-0.02162	0.08489	-0.03755	0.19011
0.60000	-0.02616	0.10640	-0.03975	0.19360
0.65000	-0.03081	0.13038	-0.04126	0.19462
0.70000	-0.03540	0.15667	-0.04206	0.19332
0.75000	-0.03971	0.18504	-0.04217	0.18996
0.80000	-0.04350	0.21518	-0.04165	0.18482
0.85000	-0.04650	0.24674	-0.04060	0.17826
0.90000	-0.04840	0.27947	-0.03913	0.17073
0.95000	-0.04885	0.31228	-0.03740	0.16272
1.00000	-0.04766	0.34510	-0.03562	0.15482

$\rho = .9$

A/L	Q1	Q2	Q3	Q4
0.05000	-0.00003	0.00009	-0.00077	0.02491
0.10000	-0.00022	0.00069	-0.00286	0.04931
0.15000	-0.00071	0.00226	-0.00595	0.07276
0.20000	-0.00161	0.00522	-0.00973	0.09478
0.25000	-0.00300	0.00990	-0.01393	0.11510
0.30000	-0.00493	0.01661	-0.01832	0.13339
0.35000	-0.00744	0.02558	-0.02269	0.14942
0.40000	-0.01051	0.03700	-0.02684	0.16300
0.45000	-0.01411	0.05098	-0.03063	0.17402
0.50000	-0.01818	0.06758	-0.03393	0.18242
0.55000	-0.02263	0.08682	-0.03664	0.18818
0.60000	-0.02743	0.10862	-0.03071	0.19138
0.65000	-0.03213	0.13288	-0.04008	0.19212
0.70000	-0.03685	0.15941	-0.04077	0.19059
0.75000	-0.04127	0.18797	-0.04080	0.18703
0.80000	-0.04515	0.21826	-0.04022	0.18174
0.85000	-0.04821	0.24991	-0.03914	0.17509
0.90000	-0.05013	0.28248	-0.03766	0.16752
0.95000	-0.05058	0.31547	-0.03594	0.15953
1.00000	-0.04917	0.34833	-0.03418	0.15167

$\rho = 1.0$

A/L	Q1	Q2	Q3	Q4
0.05000	-0.00003	0.00009	-0.00077	0.02491
0.10000	-0.00023	0.00071	-0.00285	0.04929
0.15000	-0.00074	0.00233	-0.00591	0.07267
0.20000	-0.00168	0.00536	-0.00965	0.09464
0.25000	-0.00312	0.01016	-0.01380	0.11484
0.30000	-0.00513	0.01701	-0.01812	0.13299
0.35000	-0.00772	0.02615	-0.02240	0.14885
0.40000	-0.01088	0.03776	-0.02645	0.16224
0.45000	-0.01458	0.05194	-0.03014	0.17306
0.50000	-0.01875	0.06875	-0.03333	0.18125
0.55000	-0.02329	0.08818	-0.03595	0.18682
0.60000	-0.02808	0.11016	-0.03792	0.18984
0.65000	-0.03295	0.13457	-0.03922	0.19043
0.70000	-0.03773	0.16121	-0.03985	0.18879
0.75000	-0.04219	0.18984	-0.03984	0.18516
0.80000	-0.04608	0.22016	-0.03925	0.17984
0.85000	-0.04913	0.25179	-0.03817	0.17321
0.90000	-0.05103	0.28431	-0.03672	0.16569
0.95000	-0.05144	0.31773	-0.03505	0.15777
1.00000	-0.05000	0.35000	-0.03333	0.15000

TABLE 5

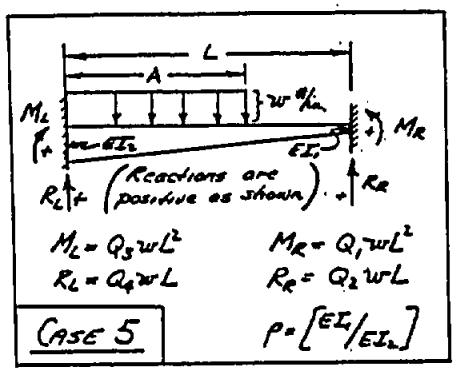

$\rho = .2$

A/L	Q1	Q2	Q3	Q4
0.05000	-0.00002	0.00008	-0.00119	0.04992
0.10000	-0.00015	0.00064	-0.00481	0.09936
0.15000	-0.00051	0.00214	-0.00967	0.14786
0.20000	-0.00117	0.00500	-0.01416	0.19499
0.25000	-0.00227	0.00944	-0.01862	0.24034
0.30000	-0.00374	0.01647	-0.02226	0.28353
0.35000	-0.00579	0.02581	-0.02412	0.32410
0.40000	-0.00832	0.03797	-0.02503	0.36202
0.45000	-0.01145	0.05326	-0.02446	0.39674
0.50000	-0.01512	0.07190	-0.02823	0.42810
0.55000	-0.01932	0.09405	-0.02652	0.46595
0.60000	-0.02398	0.11986	-0.02412	0.48014
0.65000	-0.02902	0.14943	-0.02084	0.50057
0.70000	-0.03434	0.18284	-0.02650	0.51716
0.75000	-0.03979	0.22008	-0.02996	0.52992
0.80000	-0.04508	0.26068	-0.03446	0.53932
0.85000	-0.04995	0.30440	-0.03680	0.54560
0.90000	-0.05404	0.35081	-0.03823	0.54919
0.95000	-0.05691	0.39935	-0.03881	0.55065
1.00000	-0.05786	0.44908	-0.03878	0.55092

$\rho = .3$

A/L	Q1	Q2	Q3	Q4
0.05000	-0.00002	0.00009	-0.00119	0.04991
0.10000	-0.00018	0.00076	-0.00449	0.09930
0.15000	-0.00066	0.00232	-0.00953	0.14768
0.20000	-0.00137	0.00542	-0.01396	0.19458
0.25000	-0.00261	0.01041	-0.02343	0.23957
0.30000	-0.00437	0.01774	-0.03163	0.28226
0.35000	-0.00671	0.02771	-0.04024	0.32229
0.40000	-0.00966	0.04066	-0.04899	0.35934
0.45000	-0.01323	0.05685	-0.05763	0.39315
0.50000	-0.01741	0.07651	-0.06590	0.42349
0.55000	-0.02215	0.09979	-0.07362	0.45021
0.60000	-0.02738	0.12678	-0.08060	0.47322
0.65000	-0.03299	0.15751	-0.08674	0.49249
0.70000	-0.03883	0.19191	-0.09191	0.50809
0.75000	-0.04472	0.22994	-0.09603	0.52006
0.80000	-0.05044	0.27142	-0.09902	0.52858
0.85000	-0.05571	0.31609	-0.10087	0.53391
0.90000	-0.06009	0.36318	-0.10193	0.53684
0.95000	-0.06313	0.41199	-0.10239	0.53801
1.00000	-0.06425	0.46171	-0.10254	0.53829

$\rho = .4$

A/L	Q1	Q2	Q3	Q4
0.05000	-0.00003	0.00009	-0.00118	0.04991
0.10000	-0.00020	0.00074	-0.00446	0.09926
0.15000	-0.00067	0.00247	-0.00945	0.14753
0.20000	-0.00185	0.00576	-0.01579	0.19424
0.25000	-0.00392	0.01106	-0.02311	0.23894
0.30000	-0.00698	0.01877	-0.03111	0.28123
0.35000	-0.00747	0.02925	-0.03947	0.32075
0.40000	-0.01073	0.04281	-0.04792	0.35719
0.45000	-0.01466	0.05971	-0.05620	0.39029
0.50000	-0.01922	0.08013	-0.06409	0.41987
0.55000	-0.02437	0.10423	-0.07139	0.44577
0.60000	-0.03002	0.13207	-0.07795	0.46793
0.65000	-0.03604	0.16365	-0.08364	0.48635
0.70000	-0.04227	0.19888	-0.08839	0.50112
0.75000	-0.04849	0.23756	-0.09217	0.51244
0.80000	-0.05445	0.27945	-0.09500	0.52055
0.85000	-0.05984	0.32418	-0.09691	0.52581
0.90000	-0.06433	0.37141	-0.09792	0.52859
0.95000	-0.06747	0.42051	-0.09821	0.52949
1.00000	-0.06876	0.47078	-0.09798	0.52922

$\rho = .5$

A/L	Q1	Q2	Q3	Q4
0.05000	-0.00003	0.00010	-0.00118	0.04990
0.10000	-0.00023	0.00079	-0.00444	0.09921
0.15000	-0.00074	0.00261	-0.00938	0.14739
0.20000	-0.00171	0.00604	-0.01563	0.19392
0.25000	-0.00322	0.01165	-0.02282	0.23815
0.30000	-0.00536	0.01973	-0.03063	0.28027
0.35000	-0.00819	0.03067	-0.03876	0.31933
0.40000	-0.01173	0.04488	-0.04693	0.35820
0.45000	-0.01597	0.06233	-0.05499	0.38767
0.50000	-0.02089	0.08347	-0.06242	0.41653
0.55000	-0.02641	0.10831	-0.06936	0.44169
0.60000	-0.03244	0.13690	-0.07554	0.46310
0.65000	-0.03883	0.16923	-0.08085	0.48077
0.70000	-0.04541	0.20517	-0.08524	0.49483
0.75000	-0.05195	0.24451	-0.08866	0.50547
0.80000	-0.05818	0.28704	-0.09114	0.51296
0.85000	-0.06378	0.33224	-0.09279	0.51776
0.90000	-0.06838	0.37965	-0.09373	0.52035
0.95000	-0.07154	0.42865	-0.09414	0.52135
1.00000	-0.07277	0.47859	-0.09427	0.52150

$\rho = .6$

A/L	Q1	Q2	Q3	Q4
0.05000	-0.00003	0.00010	-0.00118	0.04990
0.10000	-0.00024	0.00082	-0.00442	0.09918
0.15000	-0.00080	0.00272	-0.00933	0.14728
0.20000	-0.00182	0.00632	-0.01551	0.19368
0.25000	-0.00343	0.01209	-0.02261	0.23792
0.30000	-0.00570	0.02041	-0.03029	0.27959
0.35000	-0.00869	0.03168	-0.03826	0.31832
0.40000	-0.01241	0.04617	-0.04624	0.35381
0.45000	-0.01686	0.06412	-0.05399	0.38588
0.50000	-0.02199	0.08569	-0.06130	0.41431
0.55000	-0.02774	0.11098	-0.06801	0.43902
0.60000	-0.03397	0.14001	-0.07397	0.45999
0.65000	-0.04055	0.17272	-0.07908	0.47729
0.70000	-0.04728	0.20898	-0.08330	0.49102
0.75000	-0.05392	0.24855	-0.08661	0.50145
0.80000	-0.06021	0.29118	-0.08903	0.50982
0.85000	-0.06581	0.33644	-0.09062	0.51356
0.90000	-0.07036	0.38383	-0.09153	0.51617
0.95000	-0.07343	0.43277	-0.09191	0.51723
1.00000	-0.07453	0.48253	-0.09200	0.51747

$\rho = .7$

A/L	Q1	Q2	Q3	Q4
0.05000	-0.00003	0.00011	-0.00117	0.04989
0.10000	-0.00024	0.00086	-0.00440	0.09914
0.15000	-0.00085	0.00283	-0.00927	0.14717
0.20000	-0.00195	0.00657	-0.01538	0.19343
0.25000	-0.00367	0.01254	-0.02219	0.23746
0.30000	-0.00608	0.02116	-0.02992	0.27884
0.35000	-0.00924	0.03278	-0.03772	0.31722
0.40000	-0.01317	0.04768	-0.04549	0.35232
0.45000	-0.01784	0.06609	-0.05302	0.38391
0.50000	-0.02324	0.08816	-0.06009	0.41184
0.55000	-0.02925	0.11396	-0.06654	0.43604
0.60000	-0.03575	0.14351	-0.07224	0.45649
0.65000	-0.04259	0.17674	-0.07711	0.47326
0.70000	-0.04957	0.21348	-0.08109	0.48652
0.75000	-0.05644	0.25351	-0.08418	0.49649
0.80000	-0.06291	0.29641	-0.08641	0.50359
0.85000	-0.06867	0.34205	-0.08787	0.50795
0.90000	-0.07331	0.38961	-0.08868	0.51036
0.95000	-0.07642	0.43865	-0.08902	0.51135
1.00000	-0.07752	0.48838	-0.08914	0.51162

$\rho = .8$

A/L	Q1	Q2	Q3	Q4
0.05000	-0.00004	0.00011	-0.00117	0.04989
0.10000	-0.00026	0.00089	-0.00439	0.09911
0.15000	-0.00090	0.00292	-0.00923	0.14708
0.20000	-0.00204	0.00676	-0.01529	0.19324
0.25000	-0.00383	0.01288	-0.02220	0.23712
0.30000	-0.00634	0.02149	-0.02965	0.27831
0.35000	-0.00961	0.03334	-0.03732	0.31666
0.40000	-0.01366	0.04876	-0.04496	0.35130
0.45000	-0.01846	0.06739	-0.05234	0.38261
0.50000	-0.02400	0.08974	-0.05926	0.41126
0.55000	-0.03011	0.11582	-0.06556	0.43618
0.60000	-0.03674	0.14562	-0.07113	0.45438
0.65000	-0.04368	0.17908	-0.07588	0.47094
0.70000	-0.05072	0.21566	-0.07976	0.48604
0.75000	-0.05741	0.25510	-0.08278	0.49390
0.80000	-0.06412	0.29815	-0.08496	0.50085
0.85000	-0.06985	0.34471	-0.08639	0.50529
0.90000	-0.07448	0.39328	-0.08719	0.50772
0.95000	-0.07757	0.44139	-0.08757	0.50870
1.00000	-0.07868	0.49109	-0.08756	0.50891

$\rho = .9$

A/L	Q1	Q2	Q3	Q4
0.05000	-0.00004	0.00012	-0.00117	0.04988
0.10000	-0.00029	0.00092	-0.00437	0.09909
0.15000	-0.00095	0.00303	-0.00917	0.14697
0.20000	-0.00217	0.00700	-0.01517	0.19390
0.25000	-0.00406	0.01332	-0.02199	0.23868
0.30000	-0.00670	0.02240	-0.02931	0.27760
0.35000	-0.01015	0.03487	-0.03683	0.31543
0.40000	-0.01441	0.05012	-0.04428	0.34988
0.45000	-0.01945	0.06924	-0.05148	0.38078
0.50000	-0.02521	0.09205	-0.05816	0.40795
0.55000	-0.03160	0.11861	-0.06424	0.43139
0.60000	-0.03847	0.14888	-0.06958	0.45112
0.65000	-0.04565	0.18278	-0.07412	0.46722
0.70000	-0.05292	0.22012	-0.07781	0.47986
0.75000	-0.06004	0.26064	-0.08065	0.48936
0.80000	-0.06671	0.30402	-0.08269	0.49598
0.85000	-0.07260	0.34984	-0.08401	0.50016
0.90000	-0.07735	0.39762	-0.08473	0.50238
0.95000	-0.08052	0.44677	-0.08500	0.50323
1.00000	-0.08169	0.49665	-0.08503	0.50335

$\rho = 1.0$

A/L	Q1	Q2	Q3	Q4
0.05000	-0.00004	0.00012	-0.00117	0.04988
0.10000	-0.00031	0.00095	-0.00436	0.09905
0.15000	-0.00100	0.00312	-0.00913	0.14688
0.20000	-0.00227	0.00725	-0.01507	0.19280
0.25000	-0.00423	0.01367	-0.02181	0.23633
0.30000	-0.00697	0.02295	-0.02902	0.27765
0.35000	-0.01054	0.03537	-0.03642	0.31603
0.40000	-0.01493	0.05120	-0.04373	0.34880
0.45000	-0.02012	0.07062	-0.05075	0.37938
0.50000	-0.02604	0.09375	-0.05729	0.40625
0.55000	-0.03258	0.12062	-0.06321	0.42938
0.60000	-0.03960	0.15120	-0.06840	0.44880
0.65000	-0.04691	0.18537	-0.07279	0.46463
0.70000	-0.05431	0.22295	-0.07636	0.47705
0.75000	-0.06152	0.26367	-0.07910	0.48633
0.80000	-0.06827	0.30720	-0.08107	0.49280
0.85000	-0.07421	0.35312	-0.08234	0.49686
0.90000	-0.07897	0.40095	-0.08303	0.49905
0.95000	-0.08217	0.45012	-0.08329	0.49986
1.00000	-0.08333	0.50000	-0.08333	0.50000

GRUMMAN

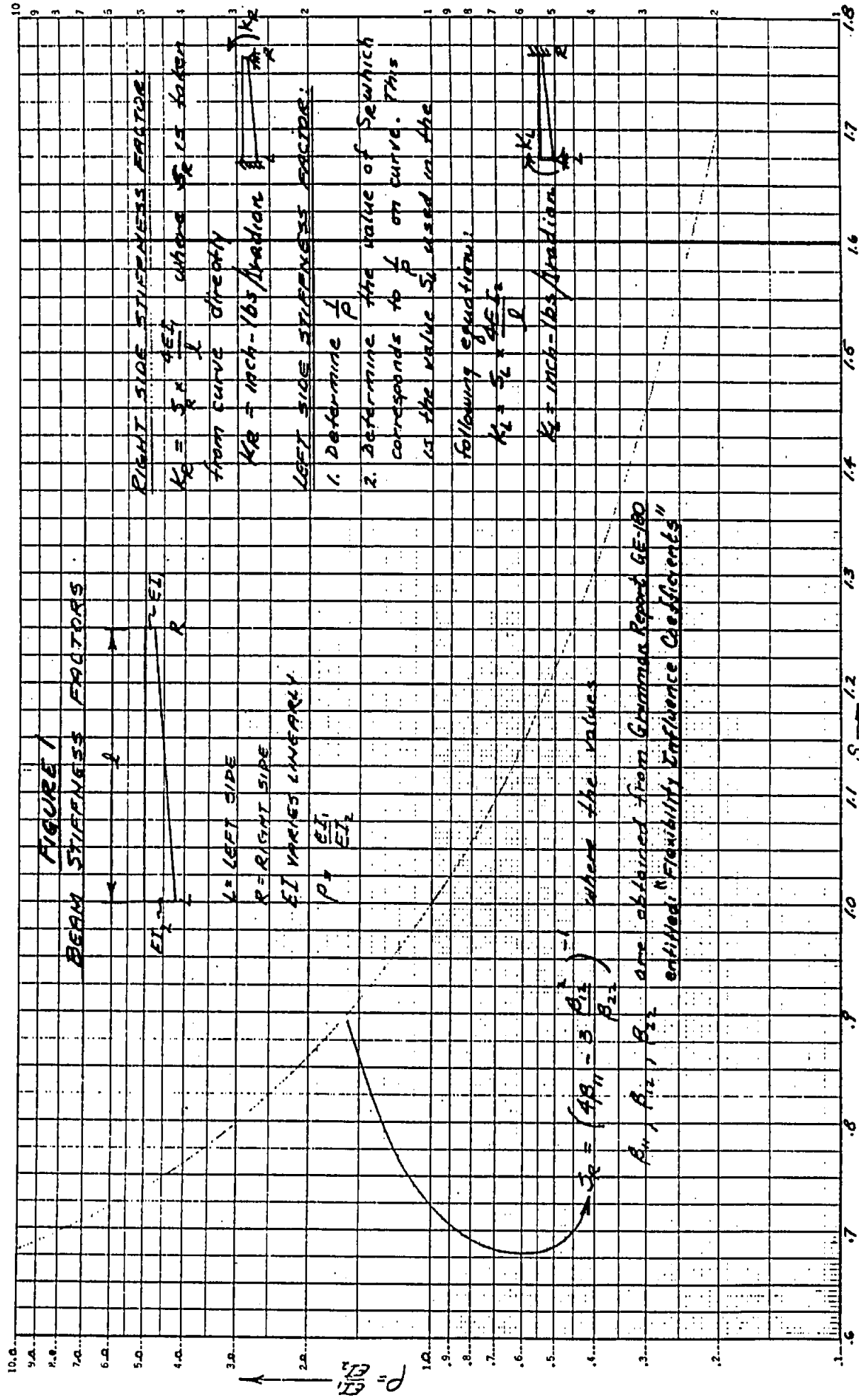
FIGURE 1
BEAM STIFFNESS FACTORS
L = LEFT SIDE
R = RIGHT SIDE
EI VARIES LINEARLY
$P = \frac{EI_1}{EI_2}$
EI_1
EI_2
$\frac{EI}{R}$
RIGHT SIDE STIFFNESS FACTOR:
$K_R = S_R \frac{4EI}{L}$ where S_R is taken from curve directly
K_R = inch-lbs/radian
LEFT SIDE STIFFNESS FACTOR:
1. Determine $\frac{L}{P}$
2. Determine the value of S_L which corresponds to $\frac{L}{P}$ on curve. This is the value S_L used in the following equations:
$K_L = S_L \times \frac{4EI_2}{L}$
K_L = inch-lbs/radian
$S_R = \left(4\beta_{11} - 3\frac{\beta_{12}^2}{\beta_{22}} - 1\right)$ where the values β_{11}, β_{12}, β_{22} are abbreviated from Grumman Report GE-180 entitled "Flexibility Influence Coefficients"
$P = \frac{EI_1}{EI_2}$
S_R

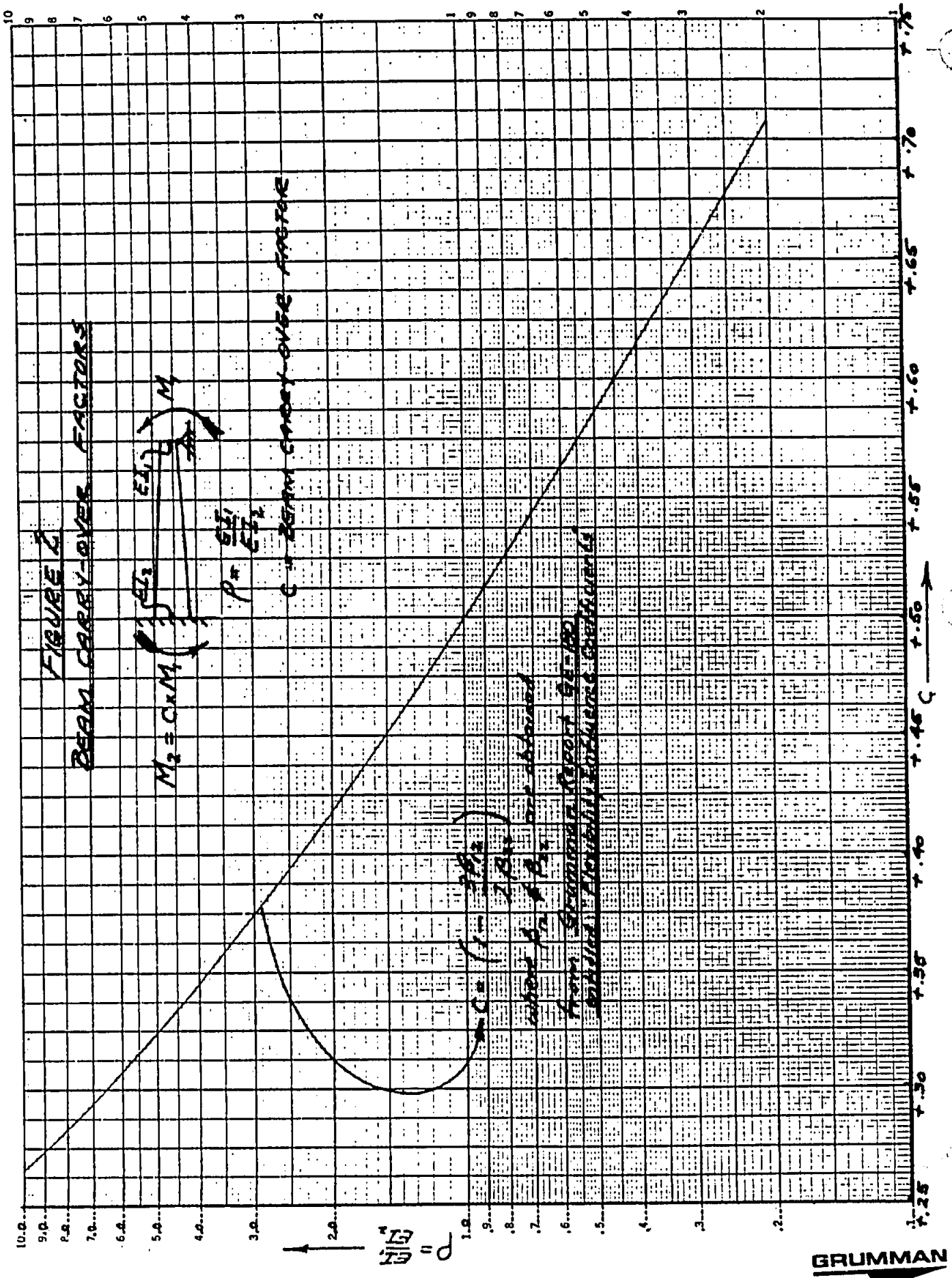

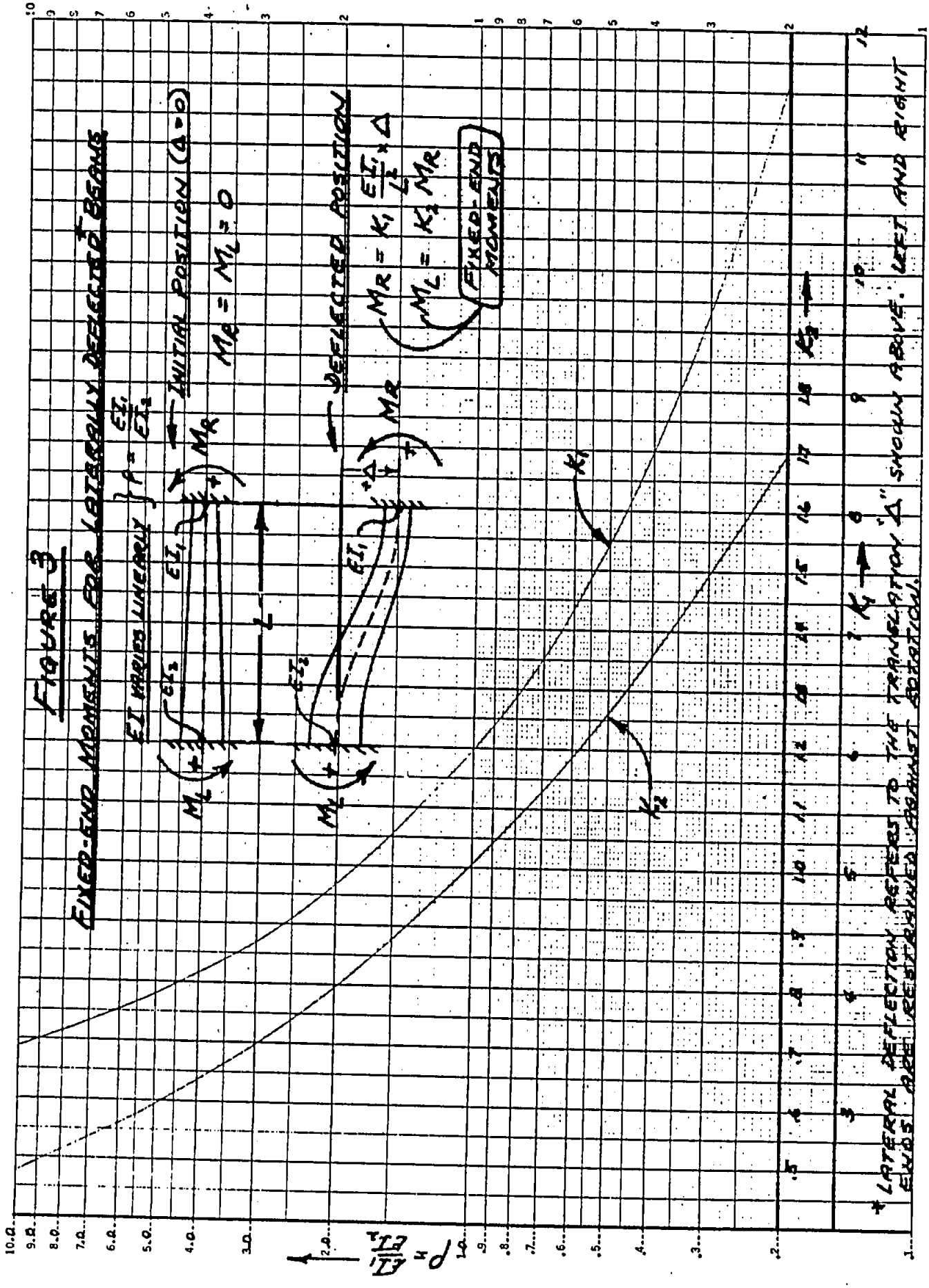

Illustrative Example 1:

For the beam sketched below, determine the internal bending moments at the supports. Also determine the external reactions. Solve the structure via moment distribution. (This is a three redundant structure which the analyst would not necessarily elect to solve by moment distribution, however it provides a good illustration of the procedure.)

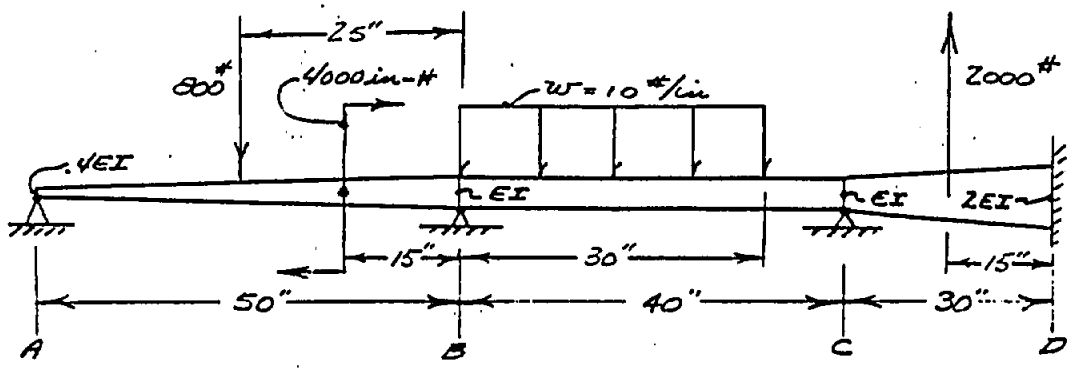

See pgs. 12, 13

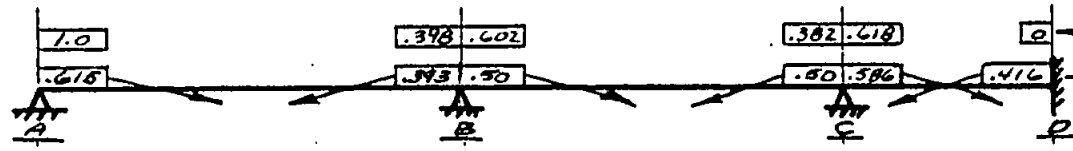

Steps 2 & 3

Step 4

+2881	−5520	+1266	−984	−6290	+8720	← Step 1
−2881	+1700	+2554	+2780	+4494	0	
+670	−1770	+1390	+1277	0	2630	
−670	+151	+228	−488	−789	0	
+60	−411	−245	+114	0	−462	
−60	+261	+395	−43	−71	0	
+103	−37	−21	+198	0	−42	
−103	+23	+35	−76	−119	0	
0	−5603	+5602	+2777	−2775	+10846	← Totals: these are the final internal moments

Steps 5, 6, 7 & 8

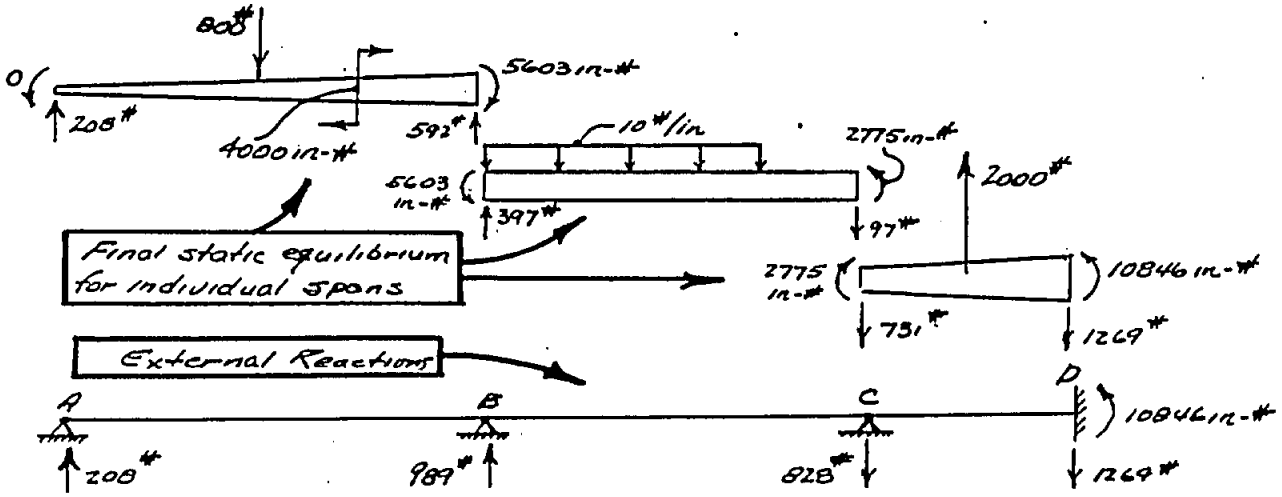

GRUMMAN

ILLUSTRATIVE EXAMPLE 1 ~ Continued

STEP 1: Calculation of fixed-end moments:

Span AB: Use Tables 1 & 2

Table 1: $\frac{A}{L} = \frac{25}{50} = .5$; $\rho = \frac{.4EI}{EI} = .4$; $P = +800^{\#}$

$M_A = Q_1 PL = (-.09748)(800)(50) = -3900 \text{ in-\#}$

$M_B = Q_3 PL = (-.15243)(800)(50) = -6100 \text{ in-\#}$

Table 2: $\frac{A}{L} = \frac{15}{30} = .3$; $\rho = .4$; $M = -4000 \text{ in-\#}$

$M_A = Q_1 M = (-.25469)(-4000) = +1019 \text{ in-\#}$

$M_B = Q_3 M = (-.14509)(-4000) = +580 \text{ in-\#}$

NET $M_A = -2881 \text{ in-\#}$

NET $M_B = -5520 \text{ in-\#}$

Span BC: Use Table 5

Table 5: $\frac{A}{L} = \frac{30}{40} = .75$; $\rho = \frac{EI}{EI} = 1.0$; $w = +10 \text{ \#/in.}$

$M_B = Q_3 wL^2 = (-.07910)10(40)^2 = -1266 \text{ in-\#}$

$M_C = Q_1 wL^2 = (-.06152)10(40)^2 = -984 \text{ in-\#}$

Span CD: Use Table 1

Table 1: $\frac{A}{L} = \frac{15}{30} = .5$; $\rho = \frac{EI}{2EI} = .5$; $P = -2000^{\#}$

$M_C = Q_1 PL = (-.10481)(-2000)30 = +6290 \text{ in-\#}$

$M_D = Q_3 PL = (-.14527)(2000)30 = +8720 \text{ in-\#}$

The sign convention for the moments computed above is noted in Tables 1 thru 5. To adopt the sign convention recommended on page 2, we change the sign of the left fixed-end moment in each span and obtain the following:

Span AB:	$M_A = +2881 \text{ in-\#}$;	$M_B = -5520 \text{ in-\#}$	} fixed-end moments
Span BC:	$M_B = +1266 \text{ in-\#}$;	$M_C = -984 \text{ in-\#}$	
Span CD:	$M_C = -6290 \text{ in-\#}$;	$M_D = +8720 \text{ in-\#}$	

STEP 2: Calculation of stiffness factors: Use Figure 1

Span AB: $\rho = \frac{EI}{.4EI} = 2.5$; from curve: $S_R = .825$ and $S_C = .1308$

$K_R = K_B = S_R \times \frac{4EI_1}{L} = .825 \times \frac{4(EI)}{50} = .066EI$

$K_L = K_A = S_L \times \frac{4EI_2}{L} = .1308 \times \frac{4(.4EI)}{50} = .00418EI$

Continued next page:

GRUMMAN

Illustrative Example 1 ~ continued

Step 2: continued

Span BC: since $\rho = 1.0$, then $K_B = K_C = \frac{4EI}{L} = \frac{4(EI)}{40} = .100EI$

Span CD: $\rho = \frac{2EI}{EI} = 2.0$; from curves: $S_R = .858$ and $S_L = 1.214$

$$K_R = K_D = S_R \times \frac{4EI_1}{L} = .858 \times \frac{4(2EI)}{30} = .2288\,EI$$

$$K_L = K_C = S_L \times \frac{4EI_2}{L} = 1.214 \times \frac{4(EI)}{30} = .1619\,EI$$

Step 3: Calculation of distribution factors for joints:

Span AB: Joint A $DF = \frac{.0042EI}{.0042EI} = 1.0$

Joint B $DF = \frac{.066EI}{.066EI + .100EI} = .398$

Span BC: Joint B $DF = \frac{.100EI}{.066EI + .100EI} = .602$

Joint C $DF = \frac{.100EI}{.100EI + .1619EI} = .382$

Span CD: Joint C $DF = \frac{.1619EI}{.100EI + .1619EI} = .618$

Joint D: since joint D is fixed against rotation, the DF = 0.

Step 4: Calculation of Carry-Over factors for spans:

For each span, C_L & C_R have been obtained from Figure 2

Span AB: to obtain C_L, use $\rho = \frac{.4EI}{EI} = .4$ } $C_L = +.615$

to obtain C_R, use $\rho = \frac{EI}{.4EI} = 2.5$ } $C_R = +.393$

Span BC: to obtain C_L and C_R, use $\rho = \frac{EI}{EI} = 1.0$ } $C_L = C_R = +.50$

Span CD: to obtain C_L, use $\rho = \frac{EI}{2EI} = .5$ } $C_L = +.586$

to obtain C_R, use $\rho = \frac{2EI}{EI} = 2.0$ } $C_R = +.414$

Step 5: Calculation of unbalanced moments at joints:

see Step 1~ Pg 12

Joint A: $M = +2881$ in-#

Joint B: $M = -5520$ in-# (from span AB) $+ 1266$ in-# (from span BC) $= -4254$ in-#

Joint C: $M = -984$ in-# (from span BC) -6290 in-# (from span CD) $= -7274$ in-#

Joint D: $M = +8720$ in-#

GRUMMAN

Illustrative Example 2:

The structure sketched below is initially unloaded. When joint B is displaced downward a distance of .500 inches by load P_B, the structure becomes loaded. Determine P_B and the external reactions.

Note that the fixed-end moments for spans CD and CE are zero by inspection. The fixed-end moments for spans AB and BC have been determined from Figure 3.

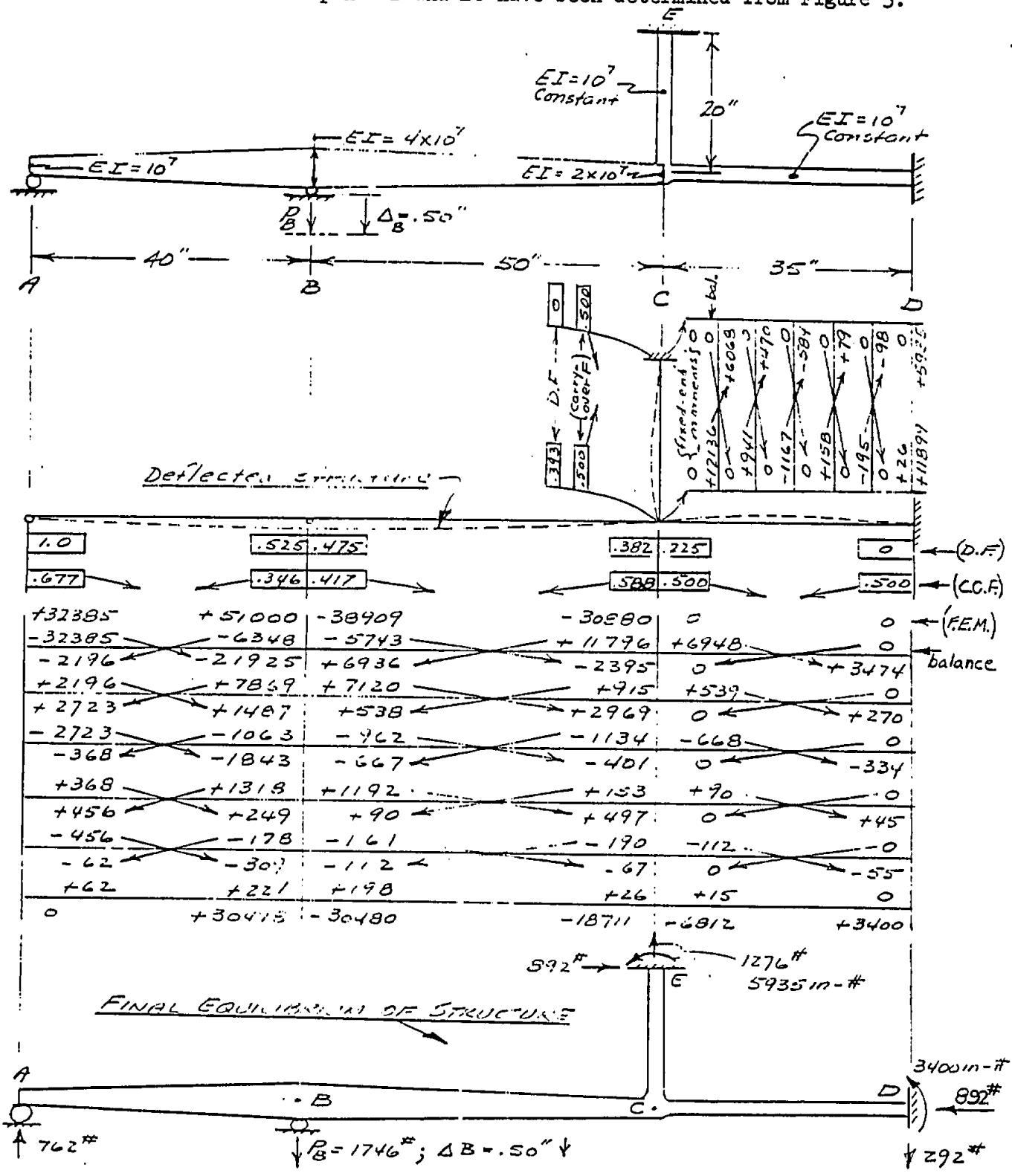

GRUMMAN

Section 2: Moment Distribution for Structures with Spans of Arbitrary EI.

The same fundamentals defined on page 2 and the same 8 steps outlined on page 3 apply to structures with spans of arbitrary EI.

The calculations indicated in Steps 1 thru 4, page C4.03-13 can be accomplished quickly if use is made of the computer program described in Reference (a). Instructions for access to and use of this program are described in the Reference.

No illustrative examples are presented herein for problems involving structures with spans of arbitrary EI. The procedure is sufficiently covered in Section 1 and the paragraphs above.

SECTION C5 - LOAD DISTRIBUTIONS IN MULTIPLE FASTENER JOINTS

Table of Contents

LOAD DISTRIBUTION IN SINGLE SHEAR MULTIPLE FASTENER LAP JOINTS

Discussion

The load distribution in the members of several basic structural connections has been determined and the significant results presented on pages C5.02-4 thru C5.02-10. The structural configurations consist of axially loaded members joined by multiple mechanical type fasteners loaded in single shear. Two cases of overall joint load were considered: (I) end loaded, and (II) shear loaded. The most significant observation for the end loaded case is that the load distribution to the fasteners is not uniform since the distribution is wholly controlled by the relative flexibility of the fastener to the axial load member. The load on the critical fastener exceeds the average load by significant amounts. As expected, no significant load concentrations are developed in the shear load case. This is illustrated on pages C5.02-4 and C5.02-5.

The load distributions were determined by linear-elastic analyses which predict the most conservative fastener load concentration because the nonlinear effects of the fastener load deflection curve are not accounted for. The results therefore are only directly applicable to joints where the load levels at the fastener are within the linear portions of the fastener load deflection curve which should be the case for fatigue critical joints. If the determination of total static strength is the problem, then an analysis such as described in Reference (a) is required.

SACP-19 (S M Pages G1.01-1 and -2) was the primary elastic analysis method used for the load calculations. Use was also made of an adaptation Kuhn's shear-lag equation, Reference (b), for the calculation of load distributions of page C5.02-8. A version of this approach is also described in Reference (c). The modification required to the Kuhn equations is in the shear-lag parameter, K, where it is necessary to replace the terms that are a function of the shear web stiffness with a set that are a function of the fastener stiffness. This method is most effective for constant area members, and is not readily adaptable to cases involving members of varying section other than the specific case of a constant stress edge member.

Symbols and Definitions

P - member axial load, pounds
N - number of fasteners
T - taper ratio measured as an area ratio (or thickness ratio for constant width members) with dimensions taken at the end fasteners
A - cross-section area of axial load members, square inches
L - total or overall length of joint that is significant to load distribution, inches

Symbols and Definitions (Continued)

R - ratio of fastener flexibility to axial member flexibility
q - applied shear load, pounds/inch
t - member thickness, inches
E - Young's modulus, pounds/square inch
K - Kuhn's shear lag parameter, 1/inches
ℓ - length of axial member between fastener centerlines. For evenly spaced fasteners the value will approach L/N, inches
σ - axial stress, pounds/square inch

Subscripts

L - pertaining to primary member
D - pertaining to doubler

Definitions

Fastener flexibility is the inverse of the slope of the load deflection curve obtained experimentally for appropriate specimens. The conventional test specimen used is the single shear, single fastener, lap joint configuration. For the most conservative estimate of fastener load concentration, the initial or straight line portion of the curve is usually taken. Data of this type is available from References (d) and (e). Member axial flexibility is defined as ℓ/AE, inches/pound.

References

(a) Torczyner, R. D. Computerized Method for Calculating Load Distribution in Multiple Fastener Joints, Grumman Aerospace Corporation Report No. ADR 02-01-71.3, June 1971.

(b) Kuhn, P., Stresses in Aircraft and Shell Structures, McGraw-Hill Book Co., Inc., 1956.

(c) Niles, A. S., and Newell, J.S. Airplane Structure, Volume 1, Fourth Edition, John Wiley and Sons, Inc., 1954.

(d) Harris, H. G., Ojalvo, I. U. and Hooson, R. E., Stress and Deflection Analysis of Mechanically Fastened Joints, AFFDL-TR-70-49, May 1970.

(e) Page B2.50-1 thru B2.50-7

LOAD DISTRIBUTION IN AN AXIALLY LOADED MEMBER REINFORCED WITH A MULTI-THICKNESS DOUBLER

The load distribution for an axially loaded member reinforced with a multi-thickness doubler is shown on pages C5.02-4 and C5.02-5 for six doubler configurations for each of the two loading cases. The joint configuration is shown in the following sketch. The load distribution is given for only the first nine fasteners of a continuing line. The total length of the members and the number of fasteners in each joint are such that the stresses in both members become equal. The value plotted is the load in the doubler, P_D, normalized with respect to the total applied load. From this information the fastener loads and load in reinforced member is easily obtained.

Loading Conditions: The doubler load is shown for two loading cases: Case I is when the total load exists in the primary member before the doubler, and Case II is when the total load is applied to the primary member as a uniformly distributed load over the length the structure as shown. The doubler load is introduced by shear loads in the joining fasteners from the primary member. The load distributions for the two cases may be superposed. This permits analysis for any case of linear load variation in the reinforced member.

JOINT CONFIGURATION:

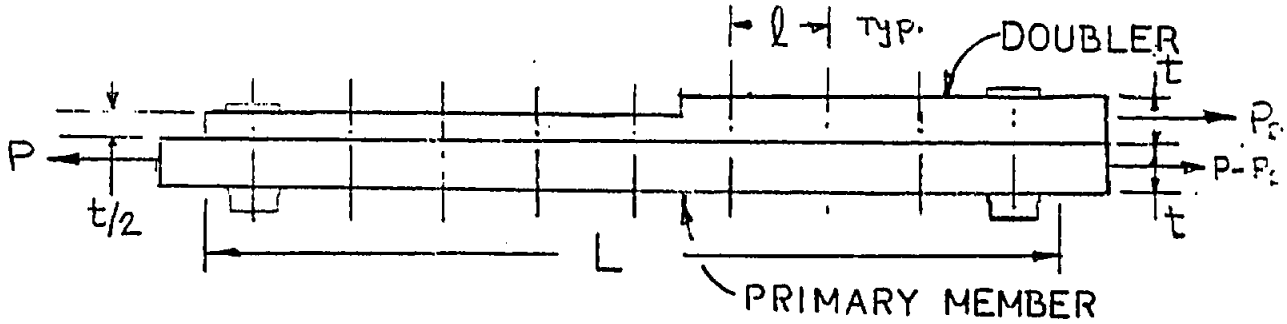

(R = 2.5 TO 4.0)

Note: This configuration is limited to like materials in both members.

LOAD DISTRIBUTION IN AN AXIALLY LOADED MEMBER WITH A MULTI-THICKNESS DOUBLER

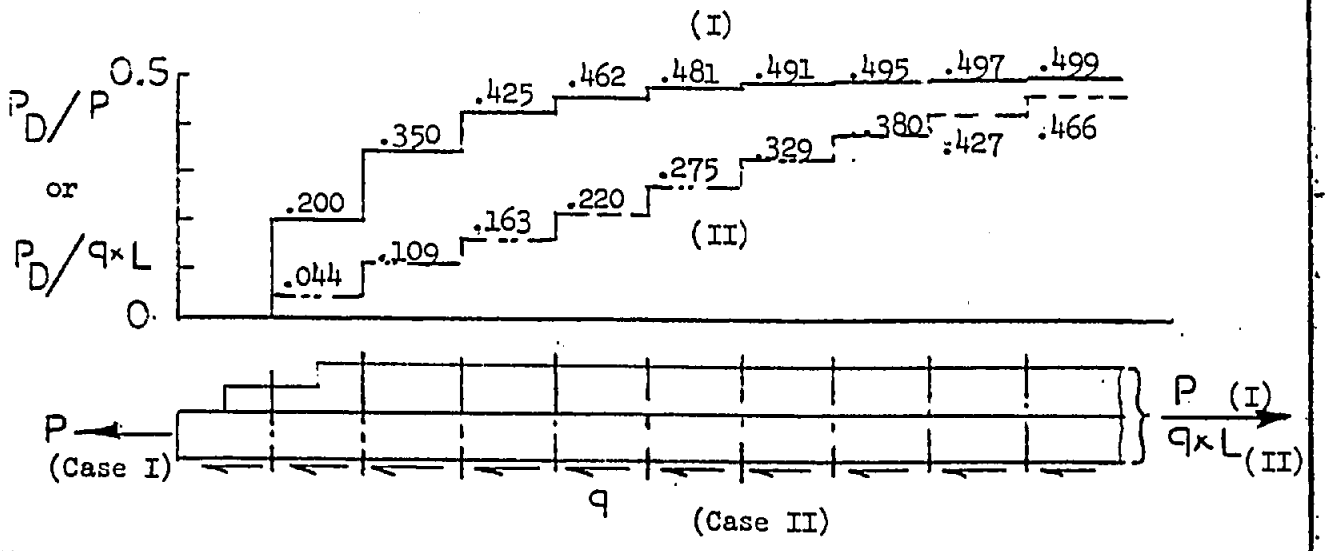

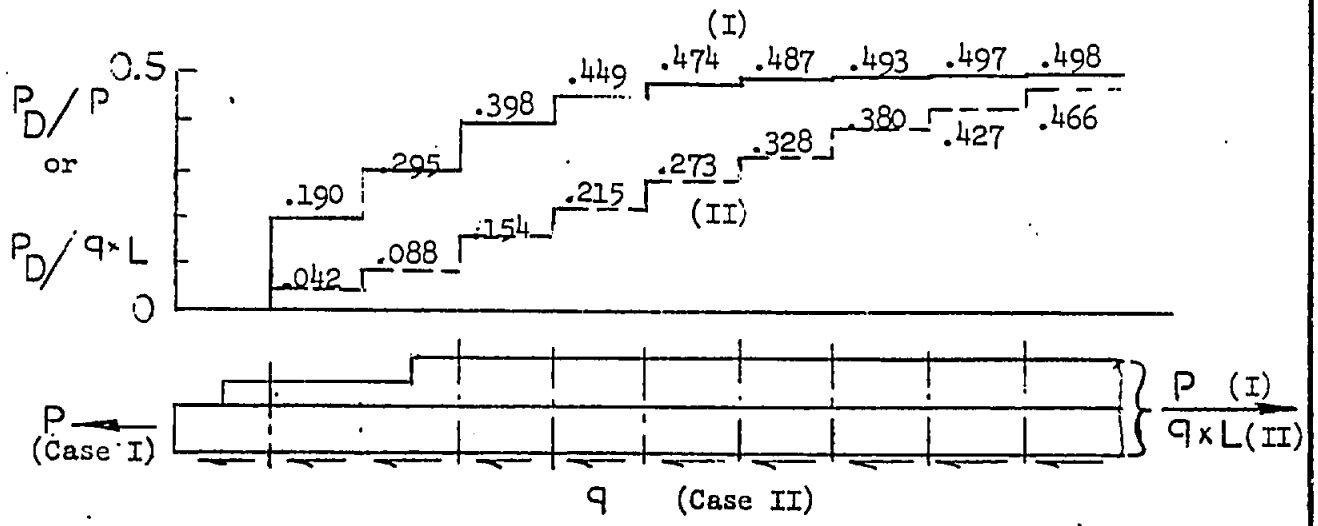

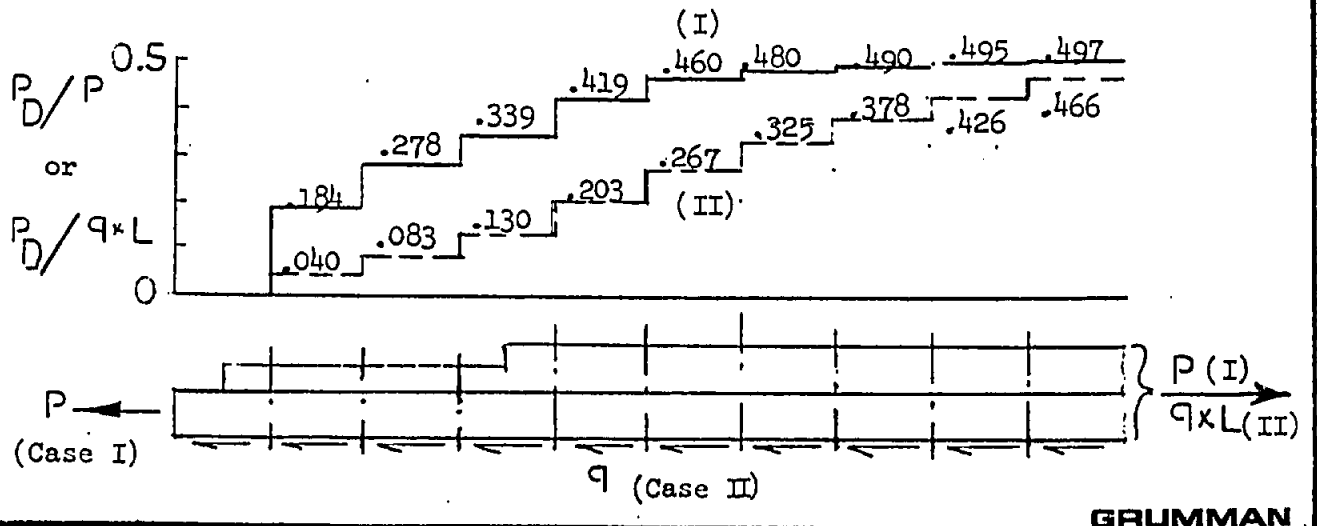

GRUMMAN

LOAD DISTRIBUTION IN AN AXIALLY LOADED MEMBER WITH A MULTI-THICKNESS DOUBLER

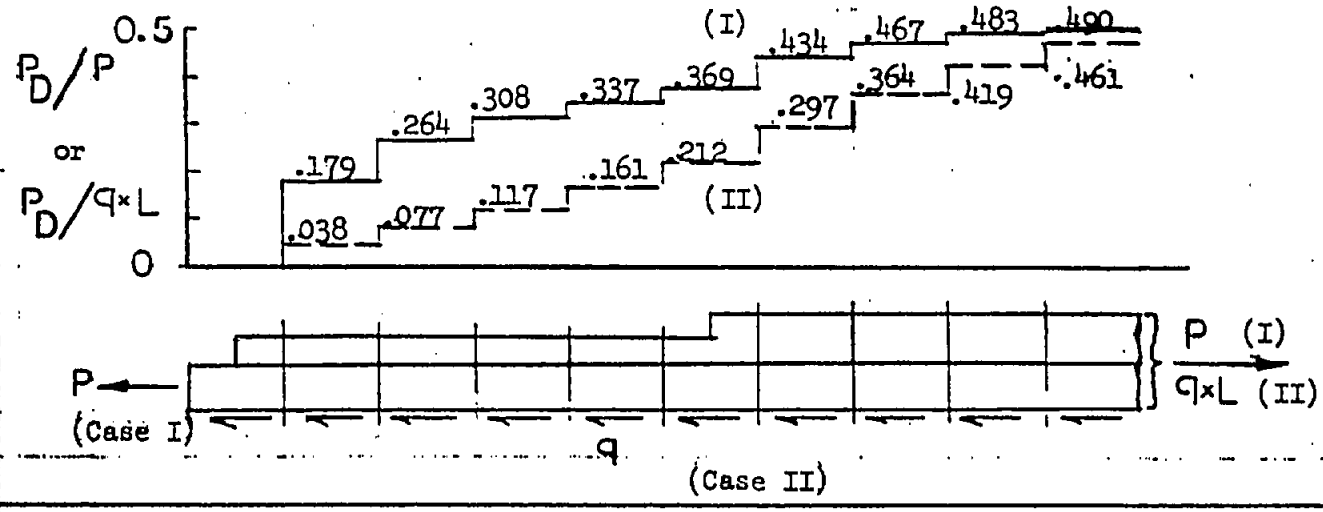

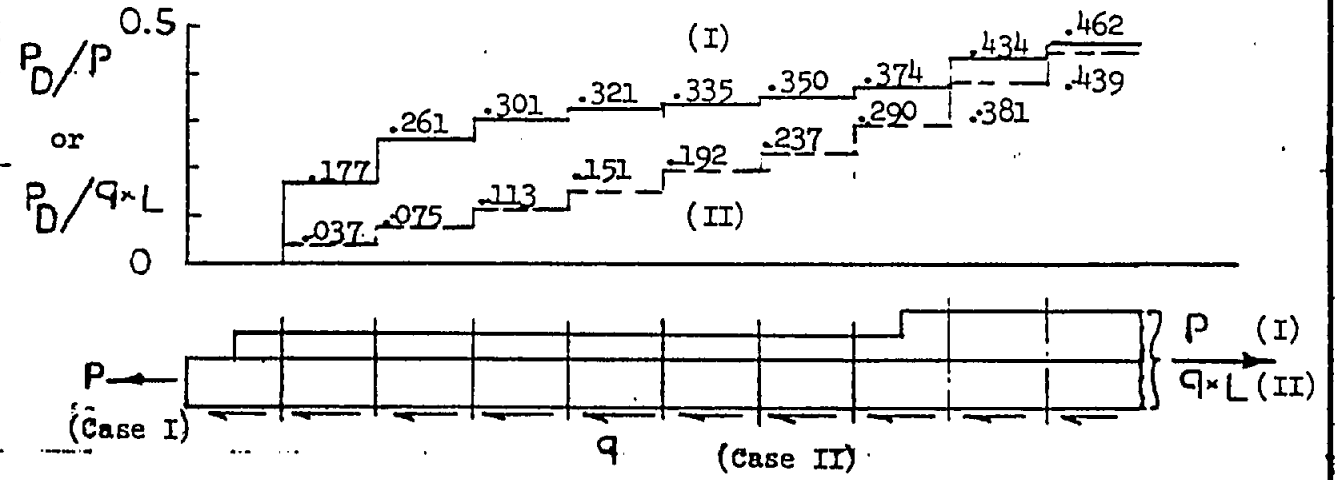

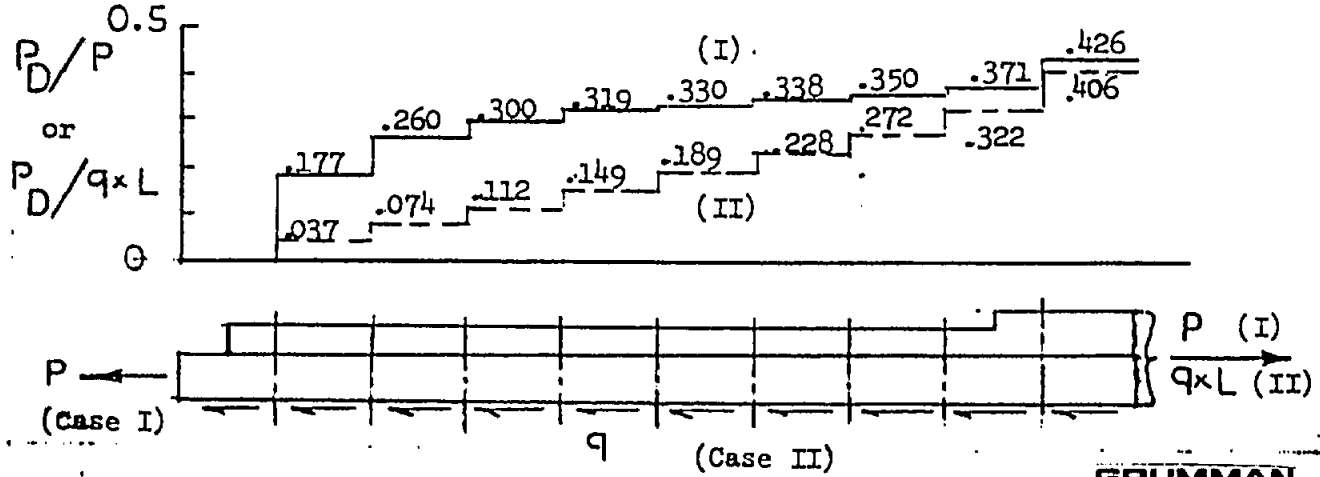

GRUMMAN

LOAD DISTRIBUTION IN SINGLE SHEAR LAP JOINTS WITH MULTIPLE FASTENERS

The following figures present the critical fastener load in a single shear lap splice for both constant area and linear tapering area members. The plotted value is the critical fastener load normalized with respect to the total splice load. The fastener load is plotted as a function of R, the ratio of fastener flexibility to axial member flexibility. In the case of the splice with tapered members, this ratio is determined at the end fastener relative to the thinner member. The member area is average between the two end fasteners. The flexibility for the intermediate fasteners was adjusted from this value to reflect the effect of the thickness change of the axial members.

CRITICAL FASTENER LOAD IN LAP SPLICE WITH TAPERED MEMBERS

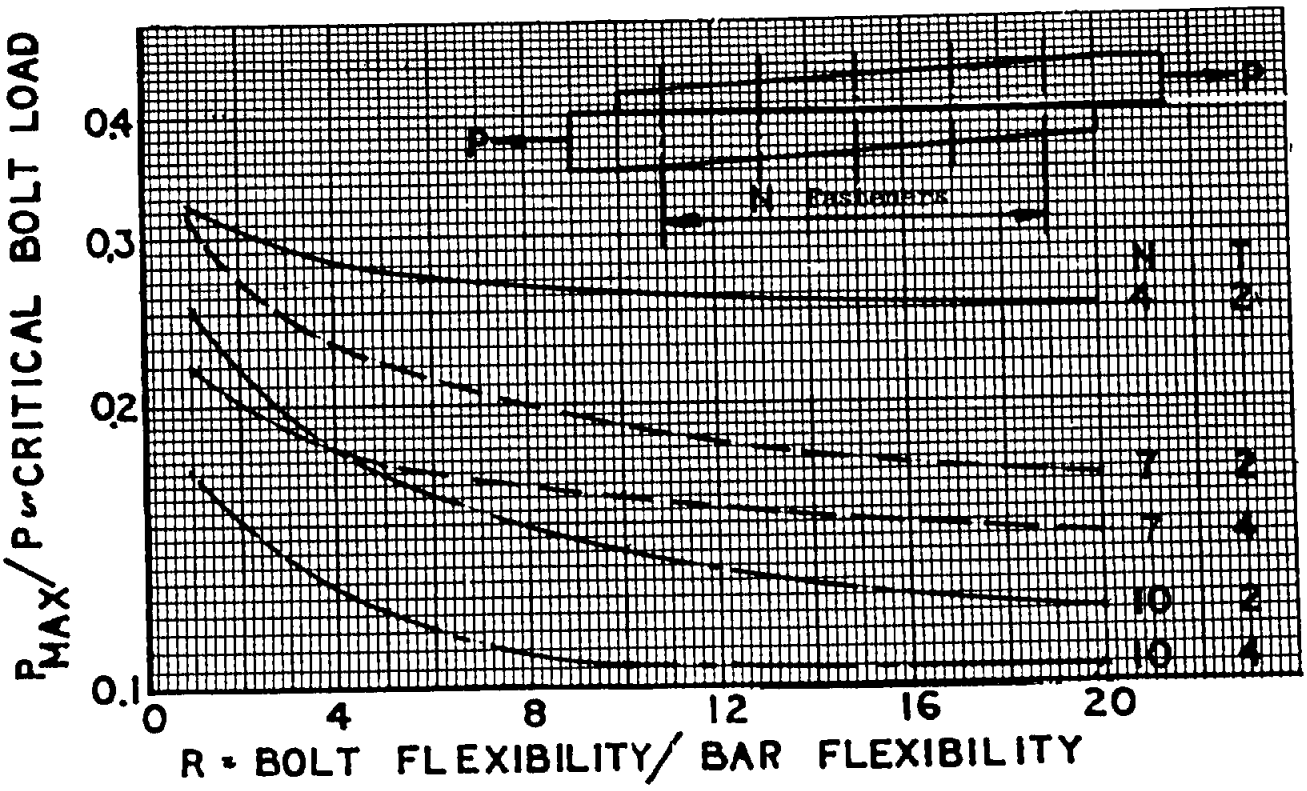

Note: This configuration is limited to like materials in both members.

CRITICAL FASTENER LOAD IN SINGLE SHEAR LAP SPLICE WITH CONSTANT AREA MEMBERS

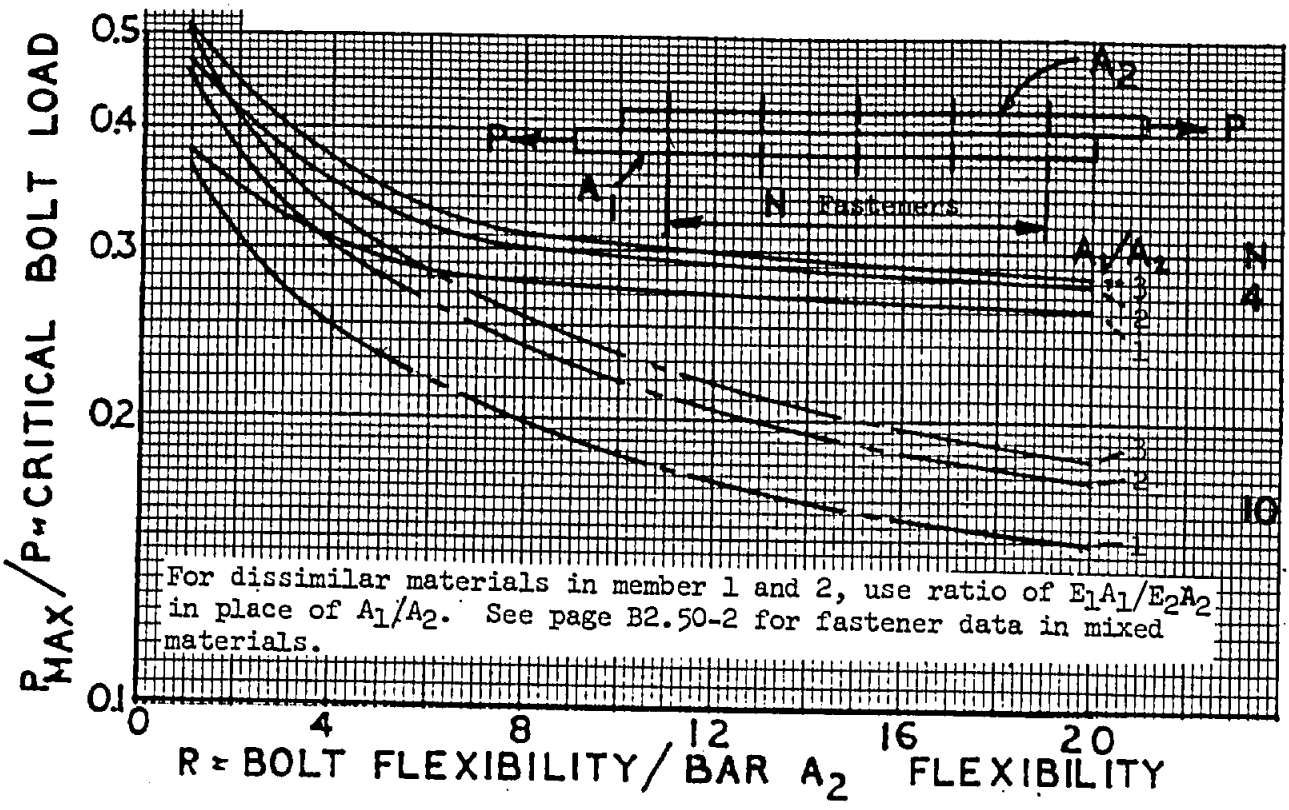

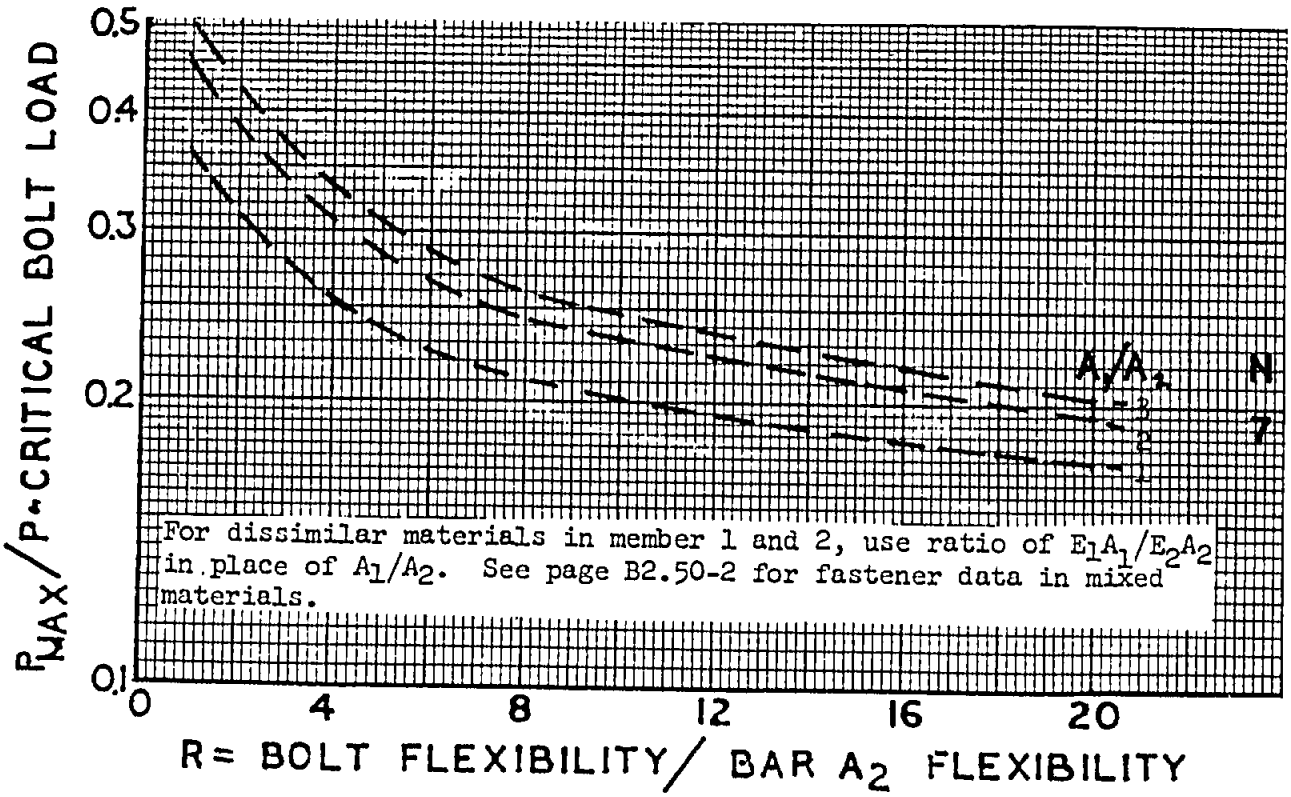

AXIAL LOAD MEMBER WITH SINGLE SHEAR LAP DOUBLER AND MULTIPLE FASTENERS

The following figure and pages C5.02-9 and -10 present the load distribution data for several configurations of an axially loaded member of constant area reinforced with a constant area doubler. The critical fastener load is normalized with respect to the total load and is shown below. The doubler effectiveness measured as the ratio of doubler stress to primary member stress at the doubler mid-length is given on page C5.02-9 and C5.02-10. Both variables are plotted as a function of R, the ratio of fastener flexibility to axial member flexibility.

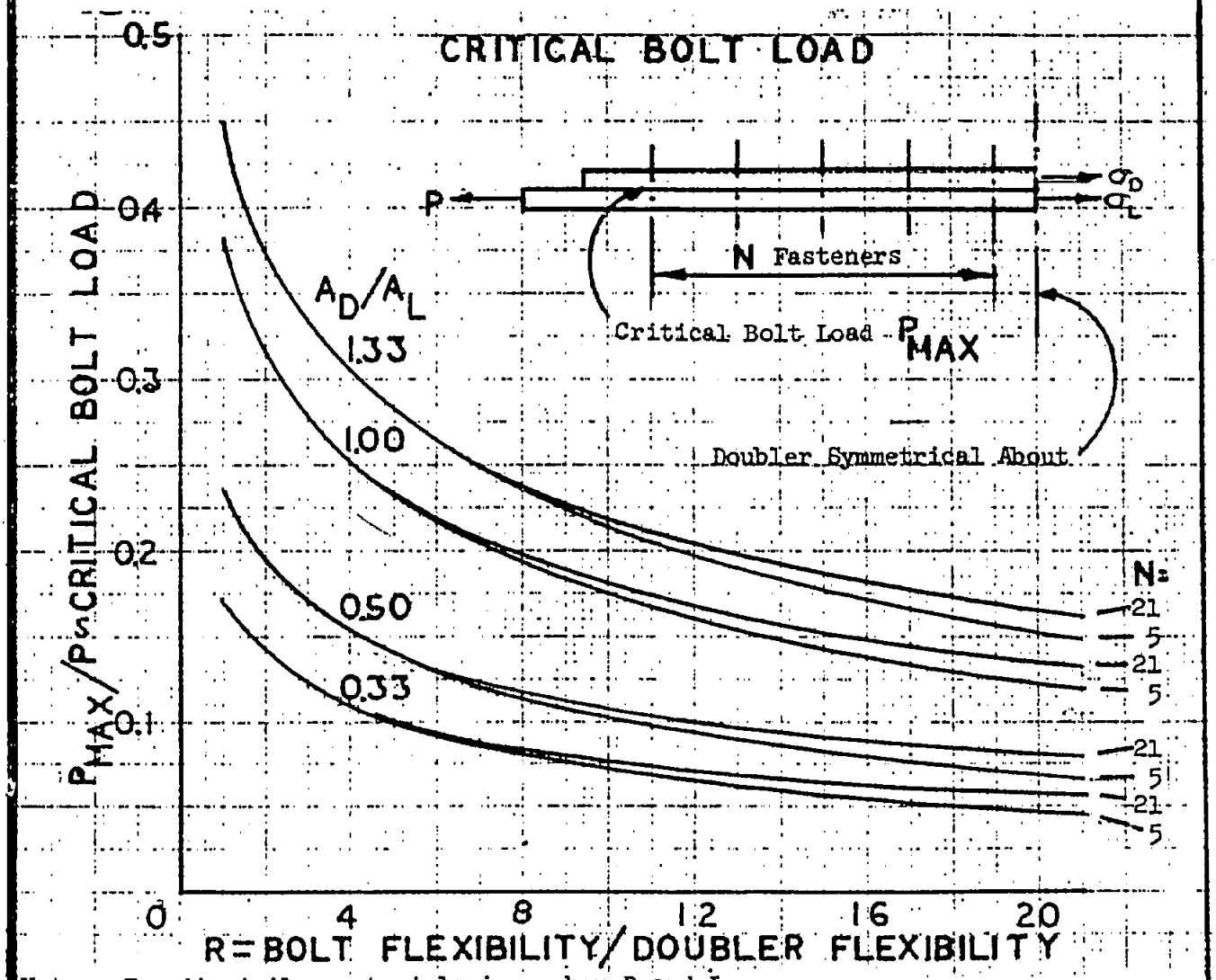

Note: For dissimilar materials in member D and L use $E_D A_D / E_L A_L$ in place of A_D/A_L. See page B2.50-2 for fastener data in mixed materials.

GRUMMAN

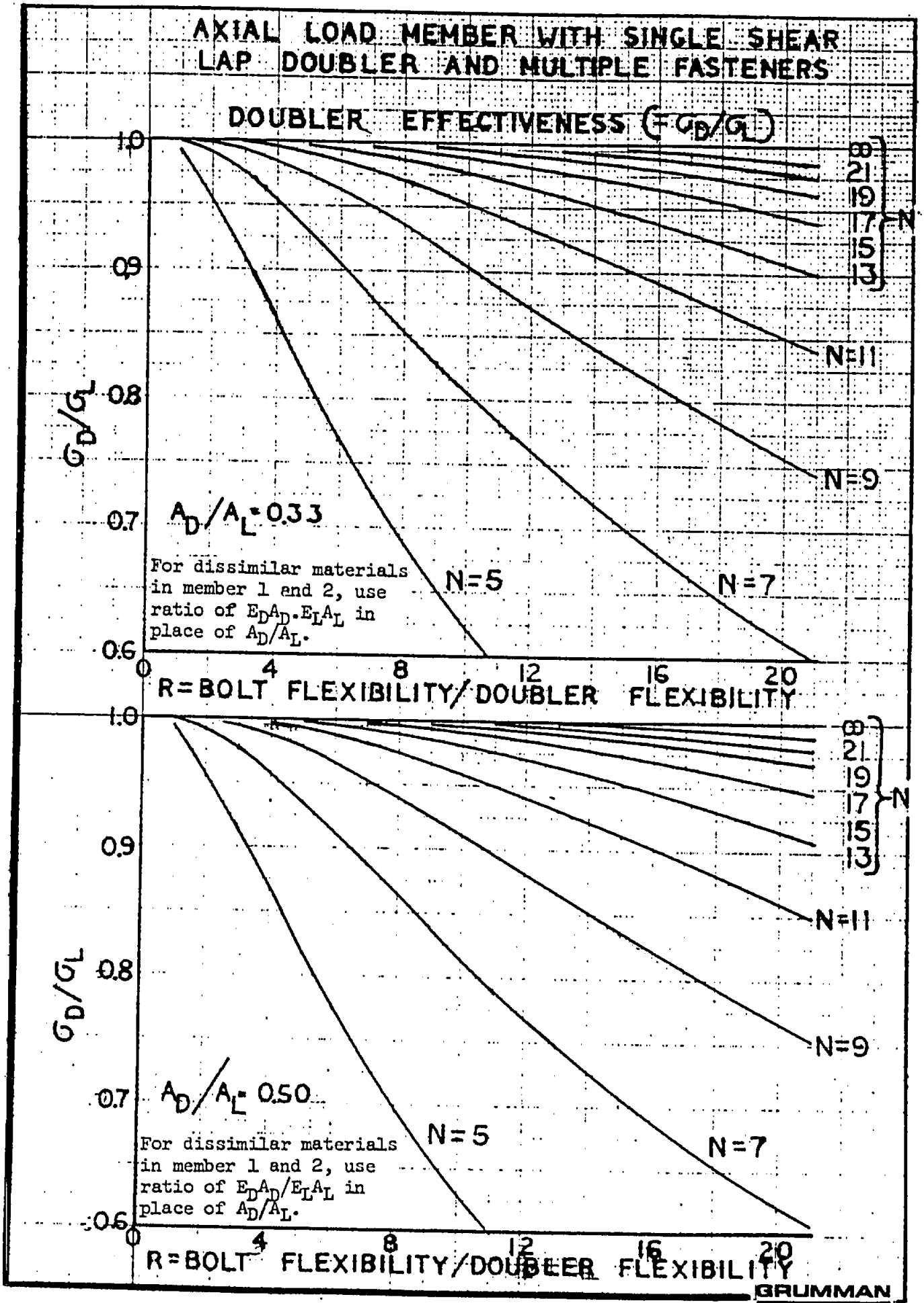
AXIAL LOAD MEMBER WITH SINGLE SHEAR LAP DOUBLER AND MULTIPLE FASTENERS
DOUBLER EFFECTIVENESS (= σ_D/σ_L)
σ_D/σ_L
1.0
0.9
0.8
0.7
0.6
A_D/A_L = 0.33
For dissimilar materials in member 1 and 2, use ratio of $E_D A_D . E_L A_L$ in place of A_D/A_L.
N=5
N=7
N=9
N=11
∞
21
19
17
15
13
N
0
4
8
12
16
20
R = BOLT FLEXIBILITY / DOUBLER FLEXIBILITY
σ_D/σ_L
1.0
0.9
0.8
0.7
0.6
A_D/A_L = 0.50
For dissimilar materials in member 1 and 2, use ratio of $E_D A_D/E_L A_L$ in place of A_D/A_L.
N=5
N=7
N=9
N=11
∞
21
19
17
15
13
N
0
4
8
12
16
20
R = BOLT FLEXIBILITY / DOUBLER FLEXIBILITY
GRUMMAN

AXIAL LOAD MEMBER WITH SINGLE SHEAR LAP DOUBLER AND MULTIPLE FASTENERS

DOUBLER EFFECTIVENESS (σ_D/σ_L)

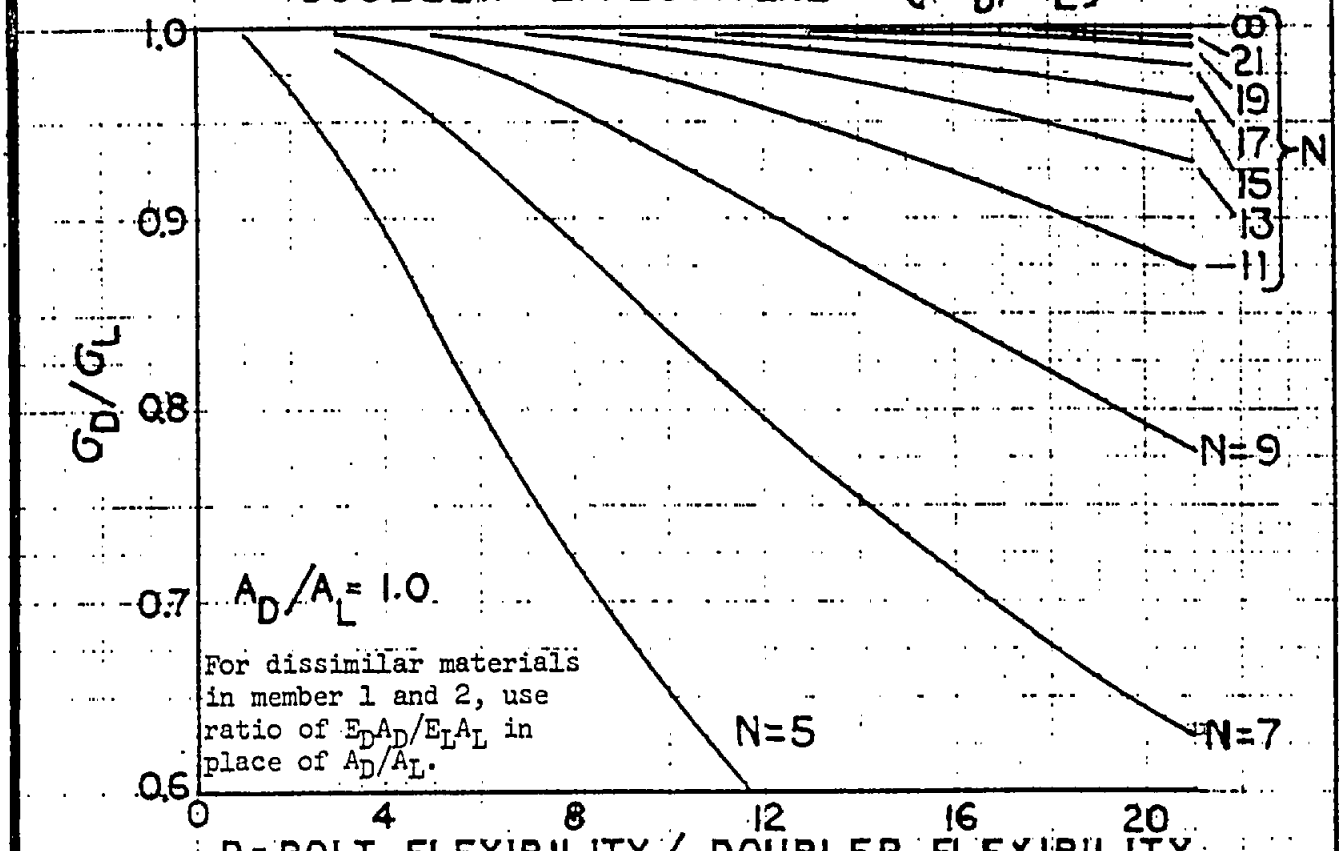

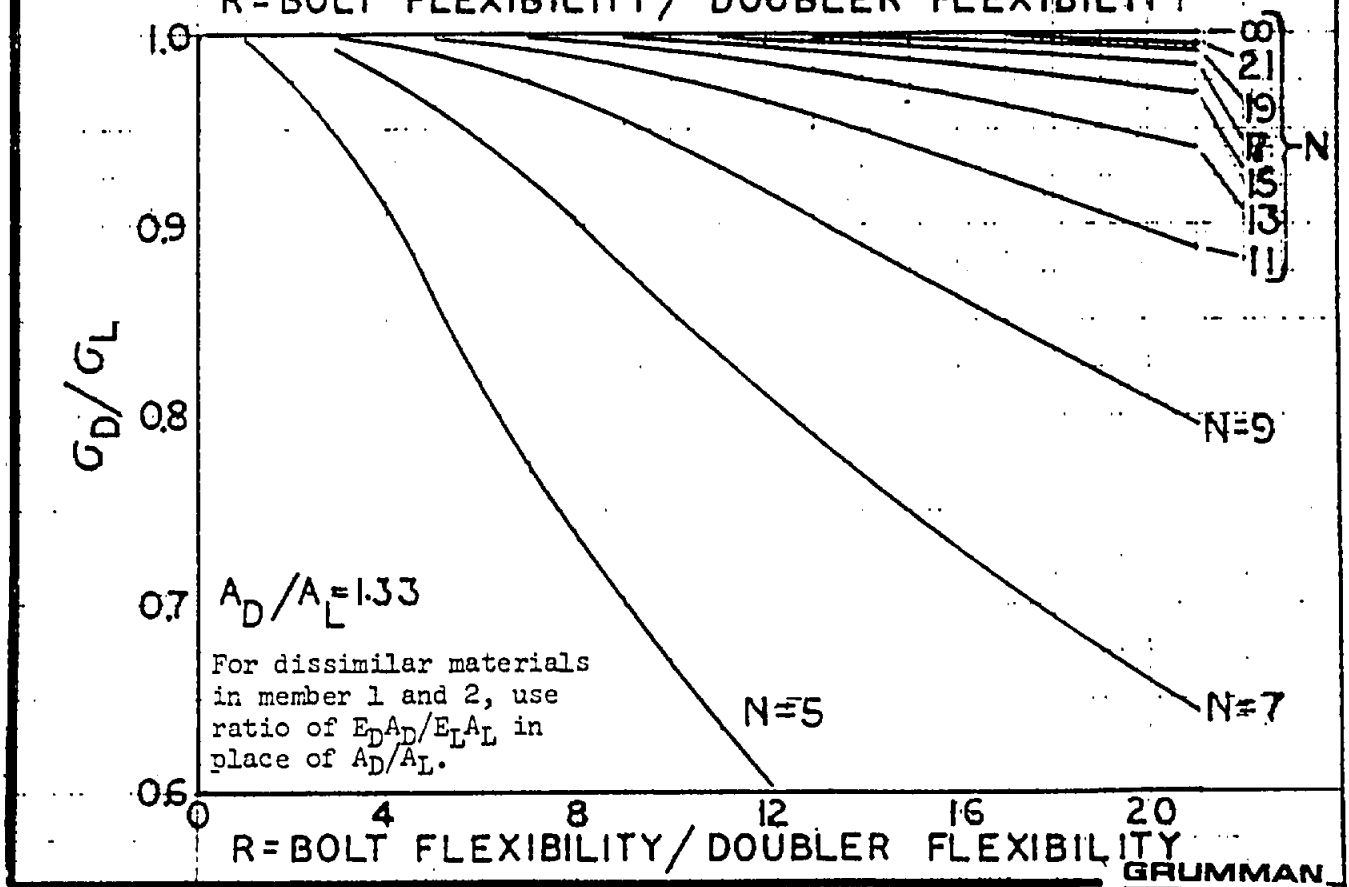

GRUMMAN

SECTION C11 - WEIGHT OPTIMIZATION

Table of Contents

WEIGHT OPTIMIZATION PROCEDURE FOR STIFFNESS DESIGN STRUCTURES

Practical Application

This procedure can be used when a structure has been sized for strength but has a stiffness requirement which can only be satisfied by adding material. The procedure determines where to add material so as to obtain a specified stiffness at minimum weight. This method applies to statically determinate structures and to redundant structure where the internal load distribution is not significantly sensitive to stiffness changes in selected structural elements.

Assumptions:

- The structure is idealized as an appropriate assemblage of bars, panels, truss members, etc.
- Each structural member is sized for strength or is minimum gage.
- Each structural member has a weight W_{io} and contributes a deflection δ_{io} to the stiffness parameter being optimized; $W_{io} \times \delta_{io} =$ constant $= K_i$ - i.e. if the weight of a member is doubled, then its contribution to the total deflection will be halved.

Procedure:

Since $W \times \delta = K$, then $\frac{dW}{d\delta} = -\frac{K}{\delta^2} = -\frac{W\delta}{\delta^2} = -\frac{W}{\delta}$

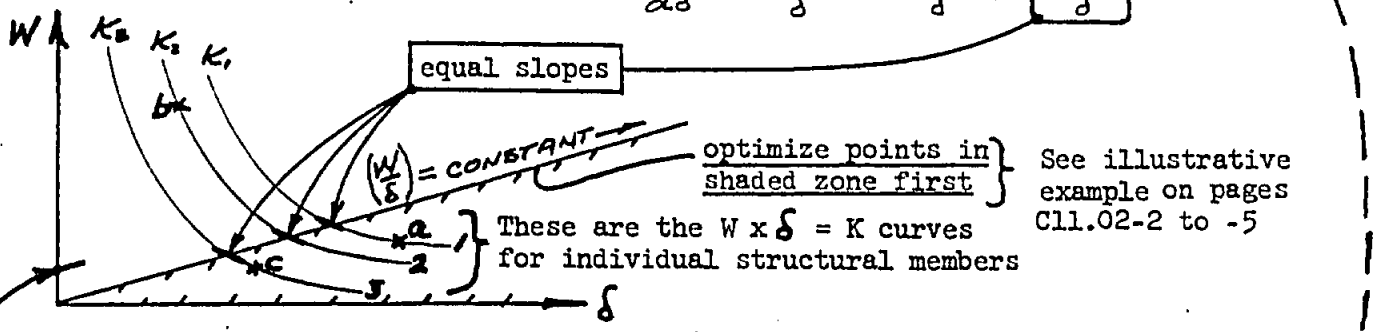

See illustrative example on pages C11.02-2 to -5

Points a, b, and c represent the baseline (sized for strength) structure.

- Successively bring the low (W/δ) values for individual members up to higher values - continue until the desired stiffness is achieved.
  - Use a table similar to the one provided in the illustrative example
    - Obtain revised δ's from the equation: $\delta_{revised} = \sqrt{\frac{K_i}{(W/\delta)_{revised}}}$ (K_i DOES NOT CHANGE)
    - Obtain revised W's from the equation: $W_{revised} = K_i \div \delta_{revised}$

An illustrative example follows.

Illustrative Example:

The structure is in the XY plane. The member sizes noted in Figure 1 are those resulting from strength or minimum gage requirements associated with the single design condition shown. The "X" deflection at point 1, hereafter referred to as Δ_{1x}, is 3.716 inches. Impose the design requirement that Δ_{1x} be limited to 3.333 inches, under the same loads, and determine the optimum weight structure for this requirement.

Figure 1

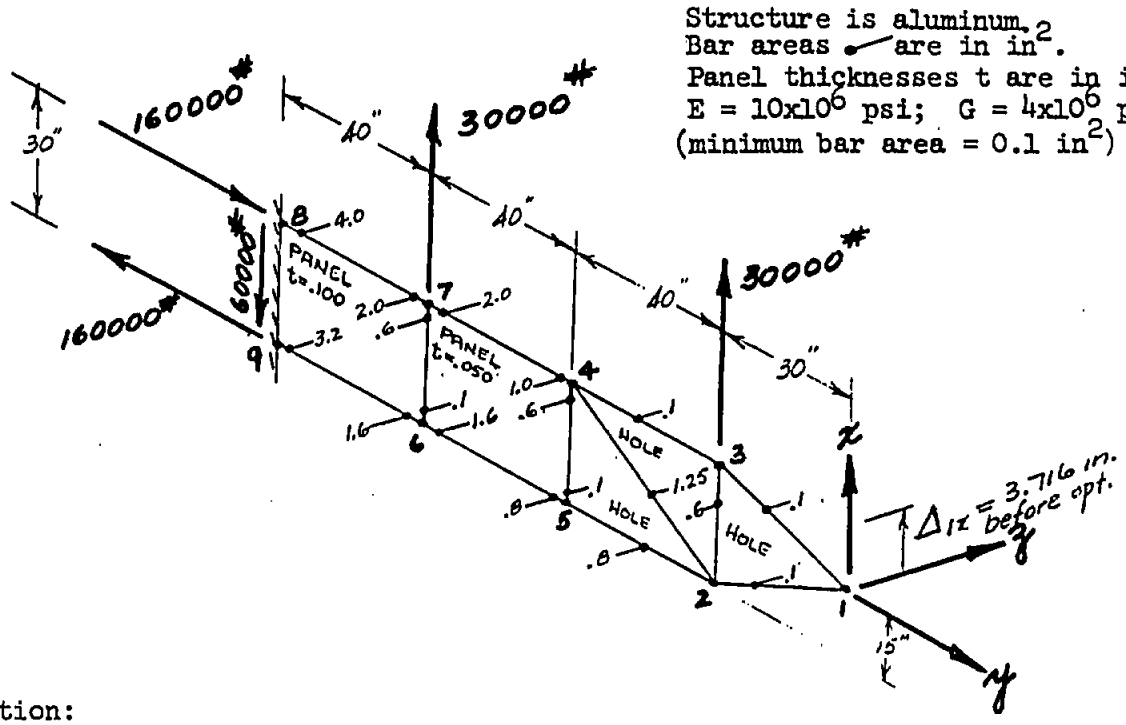

Problem Solution:

1. The structure is idealized, for this problem, as comprising twelve axially loaded bars plus two shear panels. (See Figure 1 and Table 1)

   - The contribution, δ_{io}, of each of the above noted structural elements to the total deflection Δ_{1x} has been determined by virtual work and is recorded in Table 1.

2. The structural weight, W_{io}, of each individual element, as sized for strength/mimimum-gage, has been determined and is recorded in Table 1.

   - $K_i = W_{io} \times \delta_{io}$ and values of $\left(\frac{W_{io}}{\delta_{io}}\right)$ have been computed and are recorded in Table 1.

3. The optimization procedure starts at this point. Figure 2 has been prepared only to assist the reader in understanding the fundamentals of this method. It is not necessary or recommended that time be spent plotting curves such as those in Figure 2 if the method is understood.

Illustrative Example (Continued)

- Members whose "$\left(\frac{W}{\delta}\right)$" values are low are the first to be stiffened. This is simply because the rate of change of Δ_{1x} with structural weight is highest for such members. (Although it does not occur in this problem there can exist negative values of "$\left(\frac{W}{\delta}\right)$". When this occurs, it is because the members with such values have a negative influence on the deflection in question. We are not at liberty to decrease the stiffness of these members to obtain our goal since this would violate either strength or minimum gage requirements.)

4. From this point on, common sense must be the guide. The revised values of $\left(\frac{W}{\delta}\right)$ for individual members are selected on a trial-and-error basis. Table 1 and Figure 2 speak for themselves in this respect.

Concluding Remarks:

At a cost of 4.38 lbs, the deflection Δ_{1x} has been reduced from 3.716 inches to the required 3.333 inches. Without this method, one might have decided to arbitrarily ratio up all member sizes by $\left(\frac{3.716}{3.333}\right)$ to obtain the required Δ_{1x}. This would have cost 7.45 lbs.

Figure 3 shows a comparison of the initial and final member sizes for this problem. Only the members whose sizes have been changed from those noted in Figure 1 are recorded below.

Figure 3

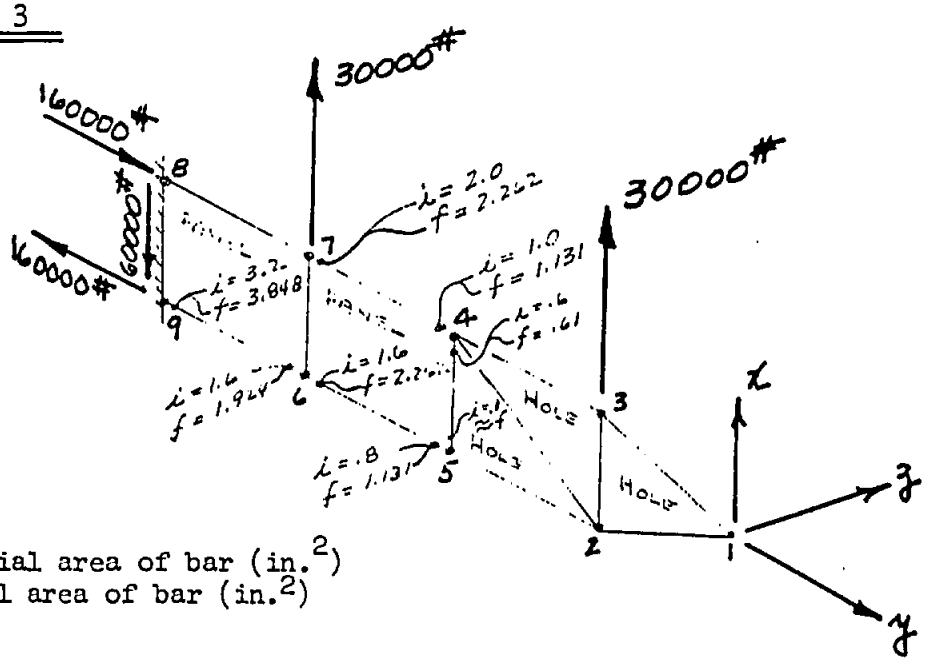

i = initial area of bar (in.^{2})
f = final area of bar (in.^{2})

GRUMMAN

Table 1: Weight vs Stiffness Optimization Procedure - Tabularized

Illustrative Example (Continued)

Structural Member	Initial Sizing (Fig. 1)				1st Optimization Pass			2nd Optimization Pass			Final Optimization Pass		
	①	②	③	④	⑤	⑥	⑦	⑧	⑨	⑩	⑪	⑫	⑬
	W_{i_o} (lbs)	δ_{i_o} (inches)	K_i ① × ②	$(W/\delta)_o$ ① ÷ ②	Revised $(W/\delta)_1 \geq 11.1111$	$\delta_1 = \sqrt{③/⑤}$	$W_1 = ③/⑥$	Revised $(W/\delta)_2 \geq 13.3333$	$\delta_2 = \sqrt{③/⑧}$	$W_2 = ③/⑨$	Revised $(W/\delta)_3 \geq 16.0000$	$\delta_3 = \sqrt{③/⑪}$	$W_3 = ③/⑫$
Bar 1-2	.335	0				.335	0		.335	0		0	0
" 2-3	1.800	.075	.1350	24.0000	24.000	.075	1.800	24.0000	.075	1.800	24.0000	.075	1.800
" 1-3	.335	0				0	.335		0	.335		0	.335
" 3-4	.400	0				0	.400		0	.400		0	.400
" 2-4	6.250	.333	2.0813	18.7688	18.7688	.333	6.250	18.7688	.333	6.250	18.7688	.333	6.250
" 2-5	3.200	.200	.6400	16.0000	16.0000	.200	3.200	16.0000	.200	3.200	16.0000	.200	3.200
" 9-5	1.050	.067	.0704	15.6716	15.6716	.067	1.050	15.6716	.067	1.050	16.0000	.0663	1.062
" 4-7	6.000	.480	2.8800	12.5000	12.5000	.480	6.000	13.333	.4648	6.196	16.0000	.4243	6.783
" 5-6	4.600	.600	2.880	8.0000	11.1111	.509	5.657	13.333	.4648	6.196	16.0000	.4243	6.783
" 6-7	1.050	0				0	1.050		0	1.050		0	1.050
" 7-8	12.000	.694	8.3280	17.2911	17.2911	.694	12.000	17.2911	.694	12.000	17.2911	.694	12.000
" 6-9	9.600	.867	8.3236	11.0716	11.1111	.867	9.600	13.333	.7900	10.536	16.0000	.7217	11.541
Panel 4-5-6-7	6.000	.200	1.2000	30.0000	30.0000	.200	6.000	30.0000	.200	6.000	30.0000	.200	6.000
" 6-7-8-9	12.000	.200	2.4000	60.0000	60.0000	.200	12.000	60.0000	.200	12.000	60.0000	.200	12.000
$\Sigma \rightarrow$	64.820	3.716				3.625	65.677		3.489	67.348		3.338	69.204
	Initial Sizing					1st Optimization			2nd Optimization			Final Optimization	

NOTES:
- o W_{i_o} = Initial weight of structural element in lbs.
- o δ_{i_o} = Initial contribution, of structural element, to Δ_{1x}. (see Fig. 1) The values of are initially determined by virtual work.
- o $K_i = W_{i_o} \times \delta_{i_o}$; note that members having $K_i = 0$ <u>are not included in the optimization procedure</u> but are carried thru the table.
- o Boxes marked [ ] pertain to those members which have been altered in the optimization process.

GRUMMAN

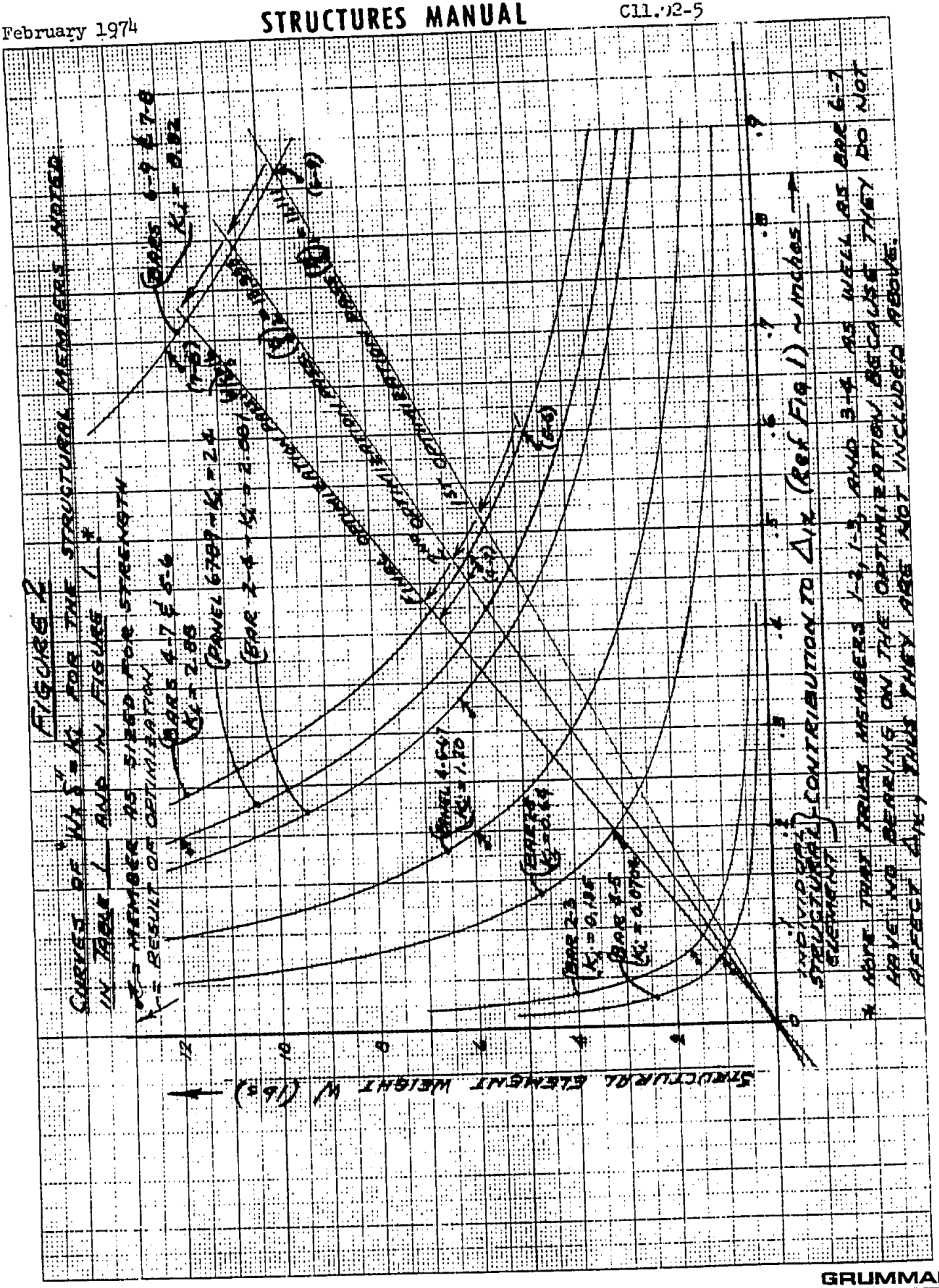

SECTION C12 - MISCELLANEOUS TOPICS

Table of Contents

VERTICAL COMPRESSION IN RIB DUE TO WING BENDING DEFLECTION

Case I - Single Stringer or Capstrip in Wing

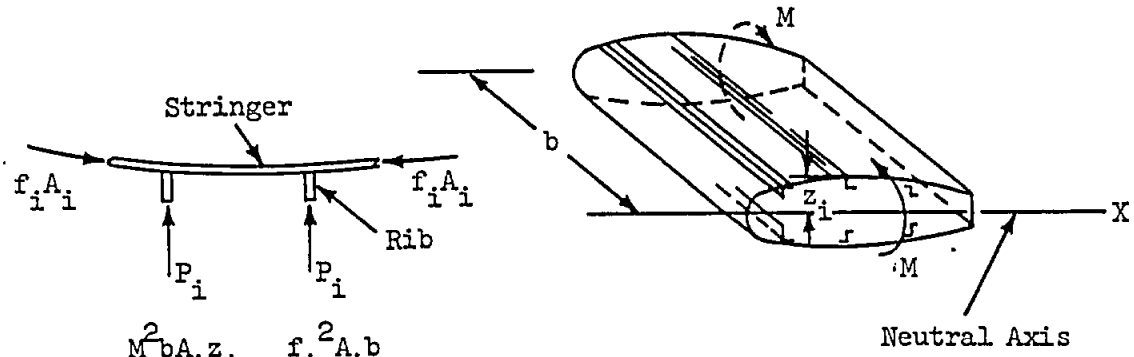

$$P_i = \frac{M^2 b A_i z_i}{EI^2} = \frac{f_i^2 A_i b}{E z_i}$$

where

P_i = vertical load exerted by one capstrip or stringer

M = external bending moment

b = rib spacing

I = bending inertia of entire wing section

z_i = distance from neutral axis to centroid of capstrip or stringer

f_i = flexural stress in capstrip or stringer

A_i = area of capstrip or stringer

E = Young's modulus

Case II - Beam Composed of a Web Plus Two Flanges

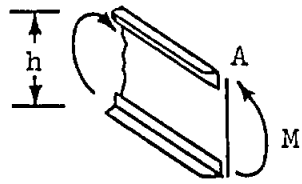

$$P = \frac{M^2 b}{EIh} = 2\,\frac{f^2 Ab}{Eh}$$

where

h = distance between centroids of flanges

Case III - Full Wing Section

$$P = \Sigma P_i = \frac{M^2 bQ}{EI^2} = \frac{MbP_t}{EI}$$

where

P = total vertical force exerted by all top surface capstrips and stringers

Q = static moment of all bending area above neutral axis

P_t = total load in top surface bending material

NOTE: The force P is balanced by an equal force applied by the lower wing surface.

10. The matrix form for the shear flows q_a, q_b, q_c as given on page C1.20-5 could be rearranged;

$$\begin{bmatrix} q_a & q_b & q_c \end{bmatrix} = \begin{bmatrix} V & D & T \end{bmatrix} \begin{bmatrix} .01079 & .01956 & .08570 \\ -.05572 & .03200 & .02063 \\ .00606 & .00606 & -.00606 \end{bmatrix}$$

It is seen that the order of multiplication of the matrices on the right hand side is now reversed; also, the rows and columns of each matrix are interchanged. The latter defines the "transpose" of a matrix. The transpose is designated by a prime ('). For example,

$$\begin{bmatrix} .01079 & .01956 & .08570 \\ -.05572 & .03200 & .02063 \\ .00606 & .00606 & -.00606 \end{bmatrix} = \begin{bmatrix} .01079 & -.05572 & .00606 \\ .01956 & .03200 & .00606 \\ .08570 & .02063 & -.00606 \end{bmatrix}$$

In general, it may be noted that

$$\begin{bmatrix} A \end{bmatrix} \begin{bmatrix} B \end{bmatrix} = \begin{bmatrix} C \end{bmatrix} \neq \begin{bmatrix} B \end{bmatrix} \begin{bmatrix} A \end{bmatrix},$$

but instead, as illustrated above,

$$\begin{bmatrix} B \end{bmatrix}' \begin{bmatrix} A \end{bmatrix}' = \begin{bmatrix} C \end{bmatrix}'$$

11. The numbers in any individual row of the first three rows of the table on page C1.20-6 are of different order of magnitude. This can be a disadvantage in the calculations which follow.

We have already pointed out that all numbers in the table (except for those entering the original equations) are carried out to the same number of decimal places; in this way we are able to add up each row and obtain a running check on the smaller numbers as well as the larger ones. An undesirable feature is thereby introduced; in order to obtain a solution which is accurate to three or four significant figures, we must deal with numbers containing as many as eight significant figures in the intermediate stages of the calculation.

3. The shears for the two design conditions can be given by the equations:

Cond. 1

$$q_{a1} = .01079 \times 10000 - .05572 \times 500 - .00606 \times 30000$$

$$q_{b1} = .01956 \times 10000 + .03200 \times 500 - .00606 \times 30000$$

$$q_{c1} = .08570 \times 10000 + .02063 \times 500 + .00606 \times 30000$$

Cond. 2

$$q_{a2} = .01079 \times 7000 - .05572 \times 2000 + .00606 \times 10000$$

$$q_{b2} = .01956 \times 7000 + .03200 \times 2000 + .00606 \times 10000$$

$$q_{c2} = .08570 \times 7000 + .02063 \times 2000 - .00606 \times 10000$$

4. When these six equations are written in matrix form, they become a single matrix equation:

$$\begin{bmatrix} q_{a1} & q_{a2} \\ q_{b1} & q_{b2} \\ q_{c1} & q_{c2} \end{bmatrix} = \begin{bmatrix} .01079 & -.05572 & .00606 \\ .01956 & .03200 & .00606 \\ .08570 & .02063 & -.00606 \end{bmatrix} \begin{bmatrix} 10000 & 7000 \\ 500 & 2000 \\ -30000 & 10000 \end{bmatrix}$$

(Product Matrix) (Premultiplier) (Postmultiplier)

5. Each of the three arrays of numbers is a matrix, and the two matrices on the right are to be multiplied together. The rule for multiplying matrices together is as follows: An element in the product matrix is found by multiplying the elements in the corresponding row of the pre-multiplier by the elements in the corresponding column of the post-multiplier and then adding these products together. Thus, q_{b2} is found by multiplying each element in the second row of the unit load matrix (.01956 .03200 .00606) by the corresponding element in the second column of the net load matrix $\begin{pmatrix} 7000 \\ 2000 \\ 10000 \end{pmatrix}$ and adding. This is seen to be identical to the equation for q_{b2} in section 3. The rule can be indicated schematically, thus:

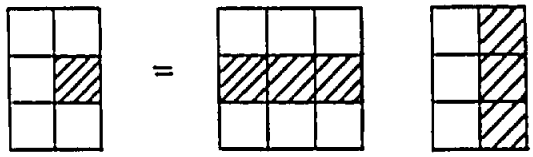

6. A matrix multiplication can be checked without repeating all of the individual steps, simply by adding a check row to the pre-multiplier. The elements of this additional row are the sums of the columns above. The columns of the post-multiplier are now multiplied by this row, yielding an additional row in the product matrix.

$$\left[\begin{array}{ccc} .01079 & -.05572 & .00606 \\ .01956 & .03200 & .00606 \\ .08570 & .02063 & -.00606 \\ \hline .11605 & -.00309 & .00606 \end{array}\right] \left[\begin{array}{cc} 10000 & 7000 \\ 500 & 2000 \\ -30000 & 10000 \end{array}\right] = \left[\begin{array}{cc} -101.8 & 24.7 \\ 29.8 & 261.5 \\ 1049.1 & 580.6 \\ \hline 977.2 & 866.8 \end{array}\right]$$

$$-.1 \qquad \checkmark$$

If the matrix multiplication has been carried through without error, it will be found upon checking that the elements in the additional row in the product matrix are equal to the sums of the columns above. Certain uncommon types of errors are not detected by this check, but are found if a check column is also added to the post-multiplier. Both check row and check column should be used in all matrix multiplications, even if the work is done by I.B.M. machines.

USE OF MATRIX METHODS IN STRUCTURES PROBLEMS (Cont.)

7. The unit loads shown in (2) can be obtained by means of the three equilibrium equations:

$$\Sigma V = 0: \quad 6q_a + 4q_b + 10q_c = V$$
$$\Sigma D = 0: \quad -12q_a + 11q_b - q_c = D$$
$$\Sigma M = 0: \quad 50q_a + 60q_b - 55q_c = -3V - 2D + T$$

about point A

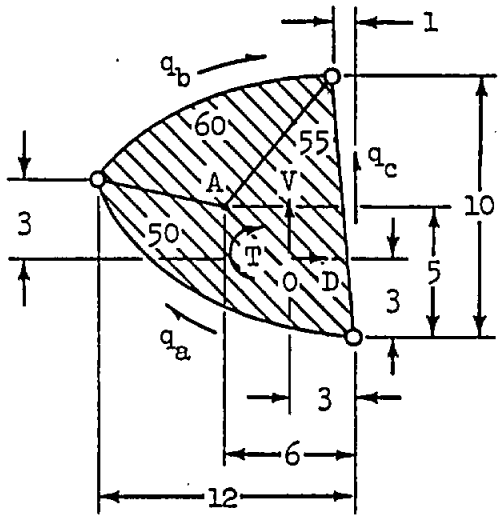

These three equations can also be put into matrix form, thus:

$$\begin{bmatrix} 6 & 4 & 10 \\ -12 & 11 & -1 \\ 50 & 60 & -55 \end{bmatrix} \begin{bmatrix} q_a \\ q_b \\ q_c \end{bmatrix} = \begin{bmatrix} 1 & 0 & 0 \\ 0 & 1 & 0 \\ -3 & -2 & 1 \end{bmatrix} \begin{bmatrix} V \\ D \\ T \end{bmatrix}$$

8. The three equations in three unknowns given above may be solved by the method of successive eliminations, which is the same whether the equations are in algebraic or in matrix form. These equations are solved in a compact table on page C1.20-6; the following points may be noted about this solution:

   a. The instruction column tells what row is to be multiplied by what constant, or which rows are to be added together. For example, the instructions for obtaining row 4 are -(1) x (2.1)/(1.1). The interpretation is: multiply row 1 by

$$-\frac{\text{number in second row, first column}}{\text{number in first row, first column}} = -\frac{-12}{6} = 2$$

b. The Σ column provides a running check so that most of the numerical errors may be picked up as soon as they are made. In each of the first three rows the Σ number is the sum of the numbers in that row. In the fourth row and thereafter, the Σ number is obtained by the same procedure as the other numbers of the row. The check consists of adding the numbers in any row and comparing the sum with the corresponding Σ number. If they are identical, a (✓) mark is put in the check column. If they are different, the difference is recorded.

Notice that all of the numbers in the table except for those entering the original equations are carried out to the same number of decimal places. This is essential in order that the smaller numbers (as well as the larger ones) actually receive a check.

c. The result is given on lines 16...18 of the table. It may be written in the matrix form:

$$\begin{bmatrix} q_a \\ q_b \\ q_c \end{bmatrix} = \begin{bmatrix} .01079 & -.05572 & .00606 \\ .01956 & .03200 & .00606 \\ .08570 & .02063 & -.00606 \end{bmatrix} \begin{bmatrix} V \\ D \\ T \end{bmatrix}$$

The solution of a set of simultaneous equations may be checked by substituting it back into the original equations:

$$\begin{bmatrix} 6 & 4 & 10 \\ -12 & 11 & -1 \\ 50 & 60 & -55 \end{bmatrix} \begin{bmatrix} .01079 & -.05572 & .00606 \\ .01956 & .03200 & .00606 \\ .08570 & .02063 & -.00606 \end{bmatrix} \begin{bmatrix} V \\ D \\ T \end{bmatrix} = \begin{bmatrix} 1 & 0 & 0 \\ 0 & 1 & 0 \\ -3 & -2 & 1 \end{bmatrix} \begin{bmatrix} V \\ D \\ T \end{bmatrix}$$

The result of multiplying the first and second matrices on the left hand side of the preceding equation is given at the bottom of page C1.20-6. Since the elements of this matrix are identical to those of the right hand side of the preceding equation except for round-off errors, the solution is correct.

8. TABLE FORM FOR SOLVING AND CHECKING SIMULTANEOUS EQUATIONS

		Instruction	(1) q_a	(2) q_b	(3) q_c	(4) V	(5) D	(6) T	Σ	Check
	1		6	4	10	1	0	0	21	-
	2	Original Equations	-12	11	-1	0	1	0	-1	-
	3		50	60	-55	-3	-2	1	51	-
2.00	4	-(1)x(2.1)/(1.1)	12.00000	8.00000	20.00000	2.00000	0	0	42.00000	v
-8.33333	5	-(1)x(3.1)/(1.1)	-50.00000	-33.33333	-83.33333	-8.33333	0	0	-174.99999	v
	6	(2)+(4)	0	19.00000	19.00000	2.00000	1.00000	0	41.00000	v
	7	(3)+(5)	0	26.66667	-138.33333	-11.33333	-2.00000	1.00000	-123.99999	v
-1.40351	8	-(6)x(7.2)/(6.2)	0	-26.66667	-26.66667	-2.80702	-1.40351	0	-57.54387	v
	9	(7)+(8)	0	0	-165.00000	-14.14035	-3.40351	1.00000	-181.54386	v
.060606	10	-(9)x(1.3)/(9.3)	0	0	-10.00000	-.85699	-.20627	.06061	-11.00265	v
.11515	11	-(9)x(6.3)/(9.3)	0	0	-19.00000	-1.62828	-.39192	.11515	-20.90505	v
	12	(1)+(10)	6.00000	4.00000	0	.14301	-.20627	.06061	9.99735	v
	13	(6)+(11)	0	19.00000	0	.37172	.60808	.11515	20.09495	v
-.21053	14	-(13)x(12.2)/(13.2)	0	-4.00000	0	-.07826	-.12802	-.02424	-4.23052	v
	15	(12)+(14)	6	0	0	.06475	-.33429	.03637	5.76683	v
	16	(15)/(15.1)	1.00000	0	0	.01079	-.05572	.00606	.96113	v
.052631	17	(13)/(13.2)	0	1.00000	0	.01956	.03200	.00606	1.05762	v
.0060606	18	(9)/(9.3)	0	0	1.00000	.08570	.02063	-.00606	1.10027	v

Check:

.99998	-.00002	0
-.00002	1.00001	0
-3.00040	-2.00065	.99990

9. The notion of the "inverse" of a matrix is sometimes useful. The solution of the simple algebraic equation a x y = b may be written $y = a^{-1} \times b$. As an extension of this, the solution of the equations on page C1.20-4 may be written

$$\begin{bmatrix} q_a \\ q_b \\ q_c \end{bmatrix} = \begin{bmatrix} 6 & 4 & 10 \\ -12 & 11 & -1 \\ 50 & 60 & -55 \end{bmatrix}^{-1} \begin{bmatrix} 1 & 0 & 0 \\ 0 & 1 & 0 \\ -3 & -2 & 1 \end{bmatrix} \begin{bmatrix} V \\ D \\ T \end{bmatrix}$$

in which $\begin{bmatrix} 6 & 4 & 10 \\ -12 & 11 & -1 \\ 50 & 60 & -55 \end{bmatrix}^{-1}$ is the symbol for the inverse of the matrix $\begin{bmatrix} 6 & 4 & 10 \\ -12 & 11 & -1 \\ 50 & 60 & -55 \end{bmatrix}$

The inverse may be found by the following trick. The matrix equation

$$\begin{bmatrix} 6 & 4 & 10 \\ -12 & 11 & -1 \\ 50 & 60 & -55 \end{bmatrix} \begin{bmatrix} q_a \\ q_b \\ q_c \end{bmatrix} = \begin{bmatrix} 1 & 0 & 0 \\ 0 & 1 & 0 \\ 0 & 0 & 1 \end{bmatrix} \begin{bmatrix} x_a \\ x_b \\ x_c \end{bmatrix}$$

is really a set of simultaneous algebraic equations. Its solution

$$\begin{bmatrix} q_a \\ q_b \\ q_c \end{bmatrix} = \begin{bmatrix} 6 & 4 & 10 \\ -12 & 11 & -1 \\ 50 & 60 & -55 \end{bmatrix}^{-1} \begin{bmatrix} 1 & 0 & 0 \\ 0 & 1 & 0 \\ 0 & 0 & 1 \end{bmatrix} \begin{bmatrix} x_a \\ x_b \\ x_c \end{bmatrix}$$

is just the solution of these simultaneous equations. Because of the property of the "unit matrix" $\begin{bmatrix} 1 & 0 & 0 \\ 0 & 1 & 0 \\ 0 & 0 & 1 \end{bmatrix}$ that

$$\begin{bmatrix} 1 & 0 & 0 \\ 0 & 1 & 0 \\ 0 & 0 & 1 \end{bmatrix} \begin{bmatrix} x_a \\ x_b \\ x_c \end{bmatrix} = \begin{bmatrix} x_a \\ x_b \\ x_c \end{bmatrix}$$

, The preceding solution may be

simplified to $\begin{bmatrix} q_a \\ q_b \\ q_c \end{bmatrix} \begin{bmatrix} 6 & 4 & 10 \\ -12 & 11 & -1 \\ 50 & 60 & -55 \end{bmatrix}^{-1} \begin{bmatrix} x_a \\ x_b \\ x_c \end{bmatrix}$

When the equations are solved by the method of successive eliminations (page C1.20-6), the coefficients on the right hand side thus constitute the inverse of the original matrix.

It should be noted that only a square matrix can have an inverse. If you are unable to find the inverse of a matrix, it may not actually exist because there is something wrong with the original equations.

The solution of the original equations is now obtained when we multiply the inverse by the matrix representing the right hand side of the original equations.

Use of the inverse in solving simultaneous equations is only advantageous under the following circumstances:

a. When the number of applied loads is considerably larger than the number of equations, or more generally, when the number of known quantities is considerably larger than the number of unknowns.

b. If there is a possibility that in the future, additional applied loads (or known quantities) may need to be considered.

When these conditions do not hold, the equations should be solved directly by the simpler method of page C1.20-6.

In general, it should be noted that

$$[A]\,[A]^{-1} = [A]^{-1}\,[A] = [I]$$

where $[I]$ is merely $\begin{bmatrix} 1 & 0 & 0\ldots \\ 0 & 1 & 0 \\ 0 & 0 & 1 \\ \cdot & & \\ \cdot & & \\ \cdot & & \end{bmatrix}$

The unit matrix I has the property that $[A]\,[I] = [A]$.

10. The matrix form for the shear flows q_a, q_b, q_c as given on page C1.20-5 could be rearranged;

$$\begin{bmatrix} q_a & q_b & q_c \end{bmatrix} = \begin{bmatrix} V & D & T \end{bmatrix} \begin{bmatrix} .01079 & .01956 & .08570 \\ -.05572 & .03200 & .02063 \\ .00606 & .00606 & -.00606 \end{bmatrix}$$

It is seen that the order of multiplication of the matrices on the right hand side is now reversed; also, the rows and columns of each matrix are interchanged. The latter defines the "transpose" of a matrix. The transpose is designated by a prime ('). For example,

$$\begin{bmatrix} .01079 & .01956 & .08570 \\ -.05572 & .03200 & .02063 \\ .00606 & .00606 & -.00606 \end{bmatrix} = \begin{bmatrix} .01079 & -.05572 & .00606 \\ .01956 & .03200 & .00606 \\ .08570 & .02063 & -.00606 \end{bmatrix}$$

In general, it may be noted that

$$\begin{bmatrix} A \end{bmatrix} \begin{bmatrix} B \end{bmatrix} = \begin{bmatrix} C \end{bmatrix} \neq \begin{bmatrix} B \end{bmatrix} \begin{bmatrix} A \end{bmatrix},$$

but instead, as illustrated above,

$$\begin{bmatrix} B \end{bmatrix}' \begin{bmatrix} A \end{bmatrix}' = \begin{bmatrix} C \end{bmatrix}'$$

11. The numbers in any individual row of the first three rows of the table on page C1.20-6 are of different order of magnitude. This can be a disadvantage in the calculations which follow.

We have already pointed out that all numbers in the table (except for those entering the original equations) are carried out to the same number of decimal places; in this way we are able to add up each row and obtain a running check on the smaller numbers as well as the larger ones. An undesirable feature is thereby introduced; in order to obtain a solution which is accurate to three or four significant figures, we must deal with numbers containing as many as eight significant figures in the intermediate stages of the calculation.

The tendency just described can usually be minimized by a proper choice of units for the applied loads. In order to illustrate this, suppose we multiply all of the numbers of columns (4) and (5) by 10, and all of the numbers of column (6) by 100. It is seen that now the solution will be sufficiently accurate using only three decimal places throughout instead of five.

To show that the preceding is equivalent to a change in the units of the applied loads, re-write the equilibrium equations of page C1.20-4 in the following way:

$$\begin{bmatrix} 6 & 4 & 10 \\ -12 & 11 & -1 \\ 50 & 60 & -55 \end{bmatrix} \begin{bmatrix} q_a \\ q_b \\ q_c \end{bmatrix} = \begin{bmatrix} (1x10) & (0x10) & (0x100) \\ (0x10) & (1x10) & (0x100) \\ (-3x10) & (-2x10) & (1x100) \end{bmatrix} \begin{bmatrix} (V \times \frac{1}{10}) \\ (D \times \frac{1}{10}) \\ (T \times \frac{1}{100}) \end{bmatrix}$$

$$= \begin{bmatrix} 10 & 0 & 0 \\ 0 & 10 & 0 \\ -30 & -20 & 100 \end{bmatrix} \begin{bmatrix} V' \\ D' \\ T' \end{bmatrix}$$

where $V' = \frac{V}{10}$, $D' = \frac{D}{10}$, $T' = \frac{T}{100}$.

The new vertical shear V' and drag shear D' are measured in units of 10 lb., while the new torsion T' is measured in units of 100 in. lb.

12. References

Scanlan, R.H., and Rosenbaum, R., "Aircraft Vibration and Flutter" 1st Ed.; MacMullan, New York, 1951.

Frazer, R.A., Duncan, W.J., and Collar, A.R., Elementary Matrices, 1st Ed.; University Press, Cambridge, 1938.

SECTION D - APPLIED LOADS

Table of Contents

STANDARD ATMOSPHERE PROPERTIES

(Ref. NACA TR 837)

Altitude h ft.	Pressure P psf	Pressure P psi	$\sqrt{P/P_o}$ (1)	Temperature t (°F)	Temperature T (°Fabs)	Density Ratio $\sigma = \rho/\rho_o$	$\sqrt{1/\sigma}$ (2)	Speed of Sound True kts.	Speed of Sound Equiv. kts.
0	2116	14.69	1.000	59.0	518.4	1.0000	1.0000	660.8	660.8
1,000	2041	14.17	.982	55.4	514.8	.9710	1.015	658.5	648.8
2,000	1968	13.67	.964	51.8	511.2	.9428	1.030	656.2	637.1
3,000	1896	13.17	.946	48.3	507.7	.9151	1.045	653.9	625.7
4,000	1828	12.69	.929	44.7	504.1	.8881	1.061	651.6	614.1
5,000	1760	12.22	.912	41.2	500.6	.8616	1.077	649.3	602.9
6,000	1696	11.78	.895	37.6	497.0	.8358	1.094	647.0	591.4
7,000	1633	11.34	.878	34.0	493.4	.8106	1.111	644.6	580.2
8,000	1572	10.92	.862	30.5	489.9	.7859	1.128	642.3	569.4
9,000	1512	10.50	.845	26.9	486.3	.7619	1.146	640.0	558.5
10,000	1455	10.10	.829	23.3	482.7	.7384	1.164	637.7	547.9
11,000	1399	9.72	.813	19.8	479.2	.7154	1.182	635.3	537.5
12,000	1346	9.35	.798	16.2	475.6	.6931	1.201	632.9	527.0
13,000	1293	8.98	.782	12.6	472.0	.6712	1.220	630.5	516.8
14,000	1243	8.63	.766	9.1	468.5	.6499	1.240	628.2	506.6
15,000	1194	8.29	.751	5.5	464.9	.6291	1.261	625.8	496.3
16,000	1146	7.96	.736	1.9	461.3	.6088	1.282	623.3	486.2
17,000	1101	7.65	.721	-1.6	457.8	.5891	1.303	620.9	476.5
18,000	1056	7.33	.706	-5.2	454.2	.5698	1.325	618.5	466.8
19,000	1014	7.04	.692	-8.8	450.6	.5509	1.347	616.0	457.3
20,000	972.1	6.751	.678	-12.3	447.1	.5327	1.370	613.6	447.9
21,000	932.0	6.472	.664	-15.9	443.5	.5148	1.394	611.2	438.4
22,000	893.3	6.203	.650	-19.5	439.9	.4974	1.418	608.7	429.3
23,000	855.9	5.944	.636	-23.0	436.4	.4805	1.443	606.2	420.1
24,000	819.8	5.693	.622	-26.6	432.8	.4640	1.468	603.8	411.3
25,000	784.9	5.451	.609	-30.2	429.2	.4480	1.494	601.3	402.5
26,000	751.2	5.217	.596	-33.7	425.7	.4323	1.521	598.8	393.7
27,000	718.7	4.991	.583	-37.3	422.1	.4171	1.548	596.2	385.1
28,000	687.4	4.774	.570	-40.9	418.5	.4023	1.577	593.7	376.5
29,000	657.1	4.563	.557	-44.4	415.0	.3879	1.606	591.2	368.1
30,000	628.0	4.361	.545	-48.0	411.4	.3740	1.635	588.7	360.1
31,000	599.9	4.166	.533	-51.6	407.8	.3603	1.666	586.1	351.8
32,000	572.9	3.978	.520	-55.1	404.3	.3472	1.697	583.6	343.9
33,000	546.8	3.797	.508	-58.7	400.7	.3343	1.730	581.0	335.8
34,000	521.7	3.623	.496	-62.2	397.2	.3218	1.763	578.3	328.0
35,000	497.6	3.456	.485	-65.8	393.6	.3098	1.797	575.7	320.4
36,000	474.4	3.294	.473	-67.0	392.4	.2963	1.837	574.9	313.0
37,000	452.2	3.140	.462	-67.0	392.4	.2824	1.881	574.9	305.6
38,000	431.1	2.994	.451	-67.0	392.4	.2692	1.927	574.9	298.3
39,000	411.0	2.854	.441	-67.0	392.4	.2567	1.974	574.9	291.2
40,000	391.9	2.722	.430	-67.0	392.4	.2448	2.021	574.9	284.5
41,000	373.6	2.594	.420	-67.0	392.4	.2333	2.070	574.9	277.7
42,000	356.2	2.474	.410	-67.0	392.4	.2225	2.120	574.9	271.2
43,000	339.6	2.358	.401	-67.0	392.4	.2120	2.172	574.9	264.7
44,000	323.7	2.248	.391	-67.0	392.4	.2021	2.224	574.9	258.5
45,000	308.6	2.143	.382	-67.0	392.4	.1927	2.278	574.9	252.4
46,000	294.2	2.043	.373	-67.0	392.4	.1838	2.333	574.9	246.4
47,000	280.5	1.948	.364	-67.0	392.4	.1752	2.389	574.9	240.6
48,000	267.4	1.857	.356	-67.0	392.4	.1670	2.447	574.9	234.9
49,000	255.0	1.771	.347	-67.0	392.4	.1592	2.506	574.9	229.4
50,000	243.1	1.688	.339	-67.0	392.4	.1518	2.567	574.9	224.0
51,000	231.7	1.609	.331	-67.0	392.4	.1447	2.629	574.9	218.7
52,000	220.9	1.534	.323	-67.0	392.4	.1379	2.692	574.9	213.6
53,000	210.6	1.462	.315	-67.0	392.4	.1315	2.758	574.9	208.4
54,000	200.8	1.394	.308	-67.0	392.4	.1254	2.824	574.9	203.6
55,000	191.4	1.329	.301	-67.0	392.4	.1195	2.893	574.9	198.7
56,000	182.5	1.267	.294	-67.0	392.4	.1140	2.962	574.9	194.1
57,000	174.0	1.208	.287	-67.0	392.4	.1087	3.033	574.9	189.5
58,000	165.9	1.152	.280	-67.0	392.4	.1036	3.107	574.9	185.0
59,000	158.1	1.098	.273	-67.0	392.4	.0988	3.182	574.9	180.7
60,000	150.8	1.047	.267	-67.0	392.4	.0942	3.259	574.9	176.4

(1) V_e variation with altitude at constant Mach No.

(2) Ratio between true airspeed and equivalent airspeed.

Grumman

V_A means design maneuvering speed.

V_B means design speed for maximum gust intensity.

V_C means design cruising speed.

V_D means design diving speed.

V_{DF}/M_{DF} means demonstrated flight diving speed.

V_F means design flap speed.

V_{FC}/M_{FC} means maximum speed for stability characteristics.

V_{FE} means maximum flap extended speed.

V_H means maximum speed in level flight with maximum continuous power.

V_{LE} means maximum landing gear extended speed.

V_{LO} means maximum landing gear operating speed.

V_{LOF} means lift-off speed.

V_{MC} means minimum control speed with the critical engine inoperative.

V_{MO}/M_{MO} means maximum operating limit speed.

V_{MU} means minimum unstick speed.

V_{NE} means never-exceed speed.

V_{NO} means maximum structural cruising speed.

V_R means rotation speed.

V_S means the stalling speed or the minimum steady flight speed at which the airplane is controllable.

V_{S0} means the stalling speed or the minimum steady flight speed in the landing configuration.

V_{S1} means the stalling speed or the minimum steady flight speed obtained in a specific configuration.

V_{TOSS} means takeoff safety speed for Category A rotorcraft.

V_X means speed for best angle of climb.

V_Y means speed for best rate of climb.

V_1 means takeoff decision speed (formerly denoted as critical engine failure speed).

V_2 means takeoff safety speed.

V_2 min means minimum takeoff safety speed.

"VFR" means visual flight rules.

"VHF" means very high frequency.

"VOR" means very high frequency omnirange station.

AIRSPEED NOMENCLATURE

The following are not exact definitions but are intended to provide a physical picture of the relationships between the various airspeeds. For a complete discussion, see NACA TR No. 837(1946).

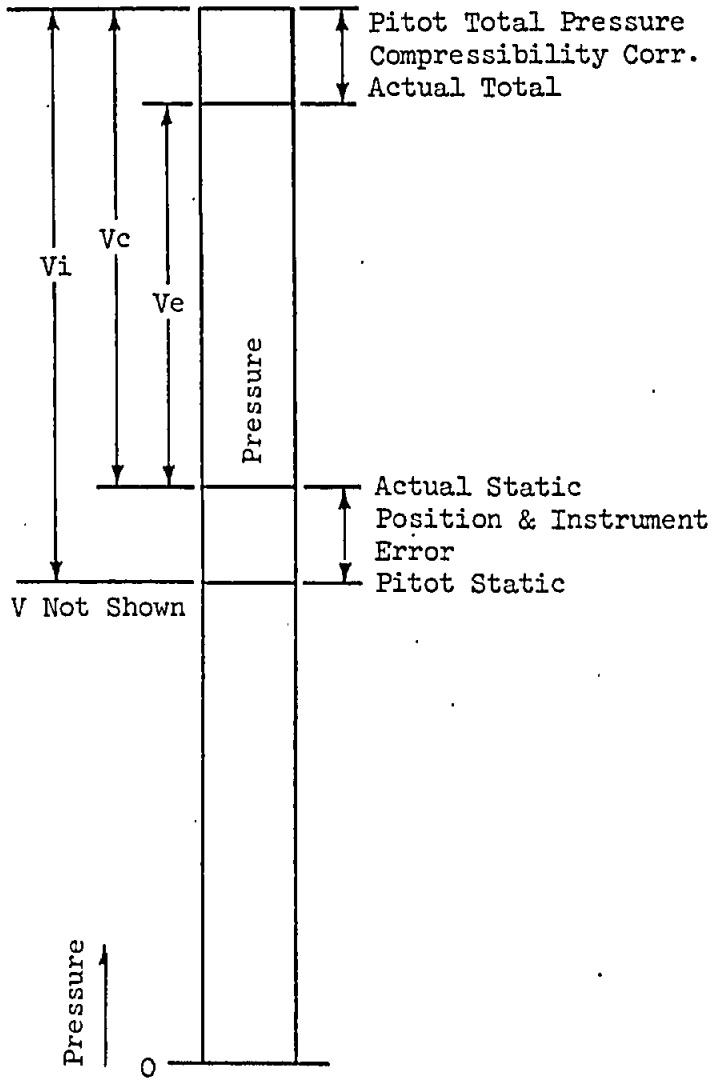

Vi = Indicated Airspeed
= Uncorrected instrument reading.

Vc = Calibrated Airspeed
= Vi corrected for position and instrument errors.

Ve = Equivalent Airspeed
= Vc corrected for Compressibility error.

V = True speed
= Ve corrected for density; (identical to ground speed in still air.)

To convert from Vc to V and to obtain Mach number, use page D2.03-1.

To convert from V to Ve, use page D2.03-2. Ve is used principally in structural design.

AIRSPEED-MACH NUMBER CHART

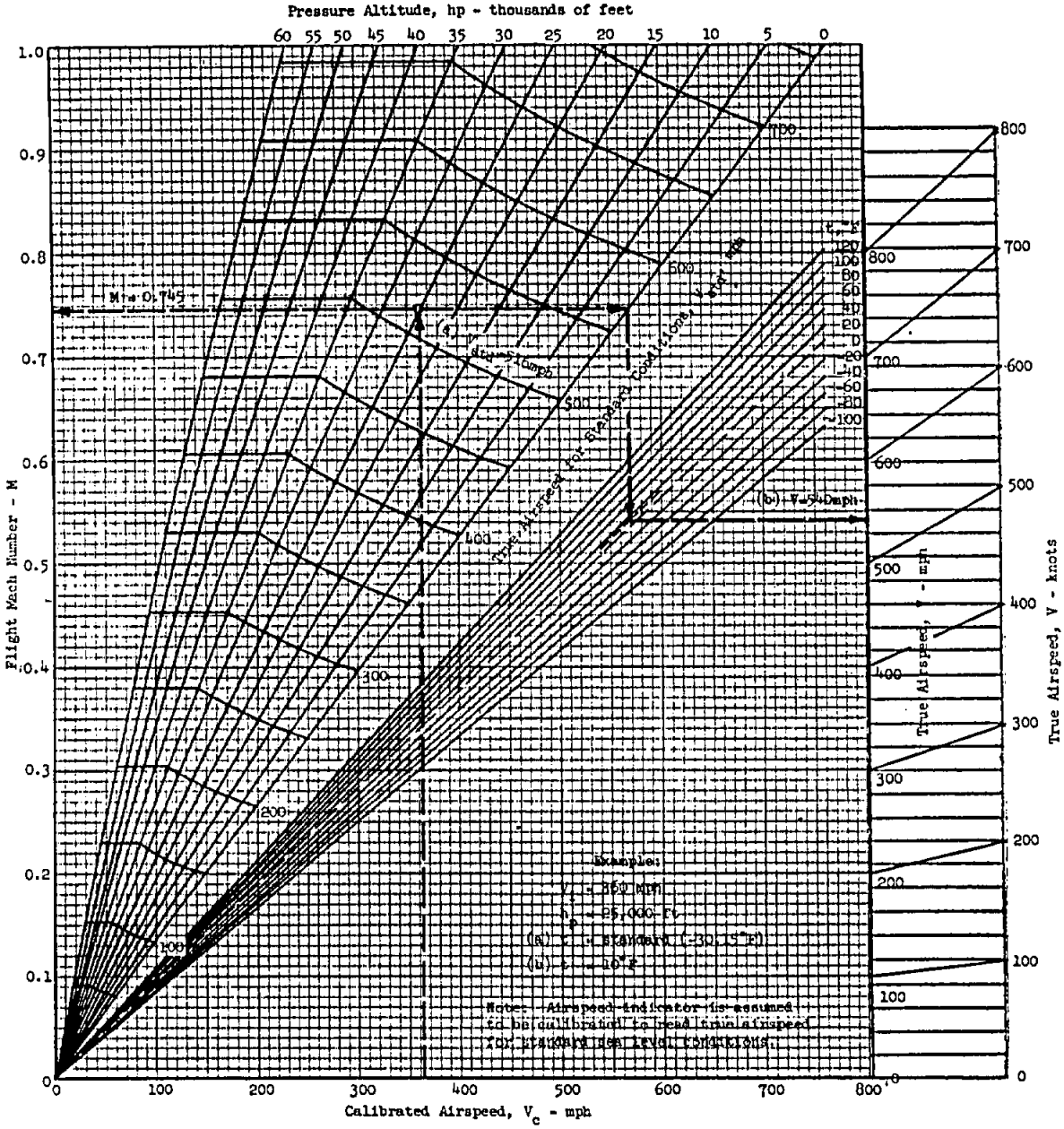

AIRSPEED - MACH NUMBER CHART
FOR STANDARD ATMOSPHERE

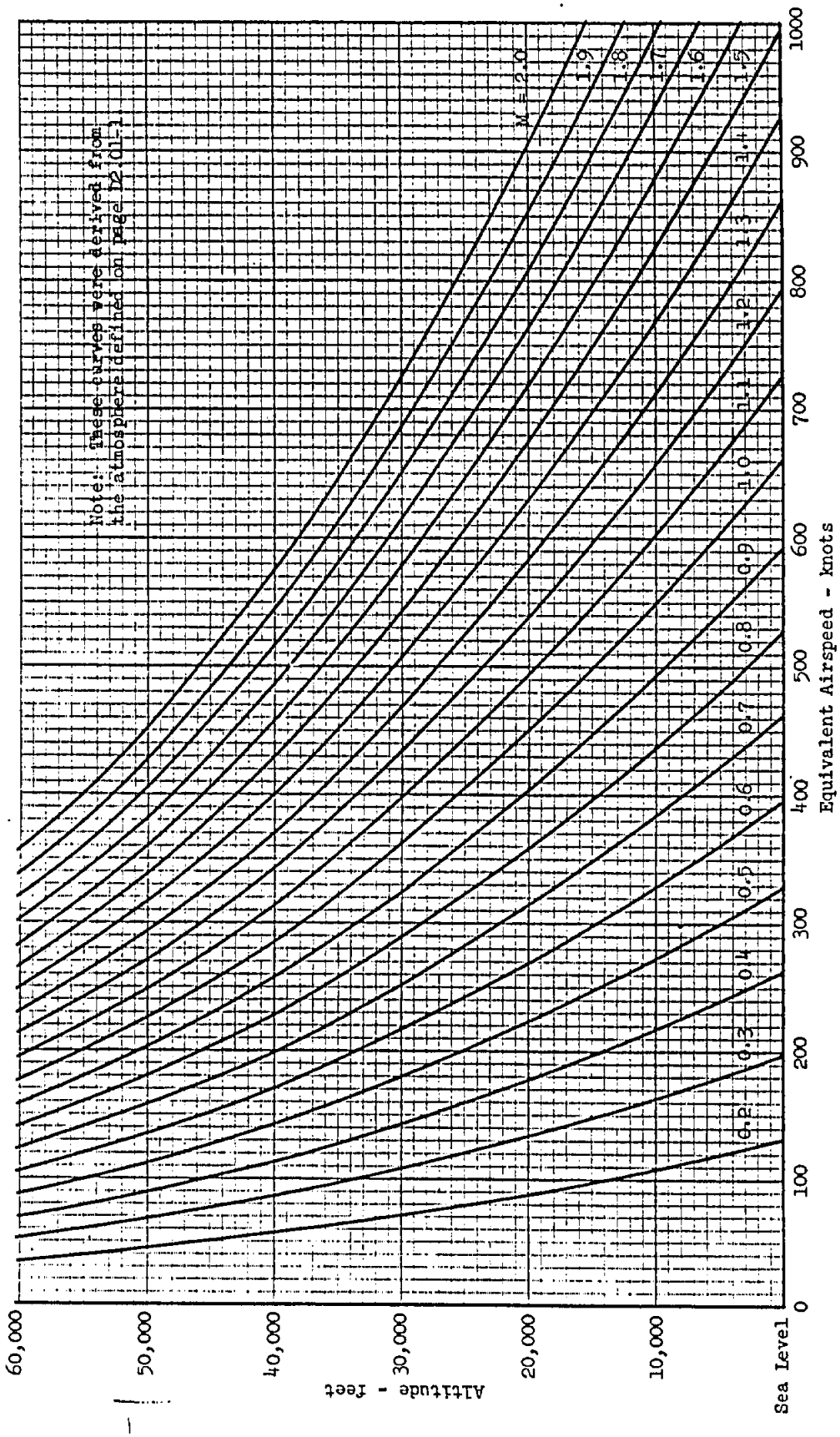

SECTION E - DYNAMIC LOADS

Table of Contents

INTRODUCTION

General

In the analysis of linear elastic systems excited by dynamic forces, two general mathematical representations are available. The more common, the "lumped parameter" idealization, breaks the structure up into a finite number of concentrated masses, connected by weightless rods or springs which provide restoring and dissipative forces. The resulting equations of motion are ordinary differential equations. The "distributed parameters" idealization treats the structure as a continuous elastic body which is homogeneous, isotropic, and follows Hooke's law. The motion equations in this case are partial differential equations. The following material is based primarily upon the lumped parameter idealization.

Use of Section

The intent of this section is to provide an outline of the basic dynamic load techniques required by structures personnel. Emphasis is placed upon the fundamental single degree of freedom system, this being useful in its own right as well as being a prerequisite to handling more complex systems. Tables and charts are provided which give the important response characteristics of the simple system. In addition, considerable space has been allotted to random vibrations, since this subject has not been included in structural engineering curricula until recently. For more details of the general theory or of Structures Section practice, see the references below.

References

a. Karman and Biot, "Mathematical Methods in Engineering," McGraw-Hill, 1940

b. Yeh and Abrams, "Principles of Mechanics of Solids and Fluids" Vol. 1. Particle and Rigid-Body Mechanics, McGraw-Hill, 1960

c. Crandall, "Random Vibration" Tech. Press, MIT, 1958

d. Grumman Structures Manual:
Section A: List of Structural Methods Publications
Section G: List of Computer Programs

SINGLE DEGREE OF FREEDOM SYSTEM

General

A single degree of freedom system is one whose response can be completely described by one coordinate. Simple examples would include a "black box" on vibration isolators subjected to uniaxial motion, or a mass at the tip of a weightless cantilever beam. The latter case is sometimes used to simulate a landing gear in preliminary spin up and spring back load calculations. The structure is idealized as a concentrated mass, a linear spring, and a dissipative linear dashpot. Two versions of the model are of interest, described by (a) a fixed base with force applied to the mass, and (b) a free base subjected to a motion input.

(a) Force input - fixed base

$$m\ddot{x} + c\dot{x} + kx = f(t)$$

or

$$\ddot{x} + 2\gamma\omega_n\dot{x} + \omega_n^2 x = \frac{1}{m} f(t)$$

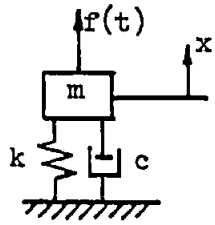

(b) Motion input - free base

$$m\ddot{x} + c(\dot{x} - \dot{y}) + k(x - y) = 0$$

or

$$m\ddot{z} + c\dot{z} + kz = -m\ddot{y}(t)$$

where $z = x - y$

$$\ddot{z} + 2\gamma\omega_n\dot{z} + \omega_n^2 z = -\ddot{y}(t)$$

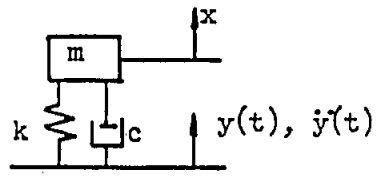

where

m = model mass, [mass]

k = spring rate, [force/unit displacement]

c = viscous damping rate, [force/unit velocity]

c_{cr} = critical damping rate = $2\omega_n m$

γ = ratio of damping to critical damping = c/c_{cr}

ω_n = natural undamped circular frequency, [radians/sec.] = $\sqrt{k/m}$

ω_d = damped circular frequency = $\omega_n\sqrt{1-\gamma^2}$

x = displacement of mass from static equilibrium position

z = relative displacement of base = $x - y$, tension position

$f(t)$ = applied force

$y(t), \dot{y}(t)$ = input displacement, acceleration of free base

$x_o, z_o, \dot{x}_o, \dot{z}_o$ = initial conditions on displacements and velocities

While the single degree of freedom system is a somewhat restricted case, it is often useful in supplying preliminary design load data, and in predicting the degree of dynamic magnification of rigid body load levels. In addition, more complex systems can often be treated as a superposition of single degree systems using normal mode techniques. The solutions to various types of excitation are discussed in the following paragraphs.

Steady State Vibration

Frequently the response to a single sinusoid is desirable. This is described in detail below. In general, any periodic excitation can be broken up into a sum of sinusoidal terms using a Fourier series approach. In this case the total response of the linear system is simply the sum of the responses to the individual terms.

If we let the excitation $f(t) = F_o \sin \omega t$ for the fixed base model, the general solution for the response $x(t)$ consists of two terms: a particular (steady state) solution at the same frequency as the excitation, and a complementary (transient) solution at the damped natural frequency of the system. The transient motion is soon damped out and is consequently ignored in the steady state response analysis.

Amplification Factor: The amplification factor (magnification factor) is defined as the ratio of the steady state response amplitude to the static response. Thus

$$AF = \frac{|x_{max}|}{x_o} = \left\{ \left[1 - \left(\frac{\omega}{\omega_n} \right)^2 \right]^2 + 4\gamma^2 \left(\frac{\omega}{\omega_n} \right)^2 \right\}^{-\frac{1}{2}}$$

where x_o is the static displacement corresponding to a static force F_o.

Transmissibility: The transmissibility is the ratio of force transmitted through the flexible supports to the force transmitted with rigid supports.

$$TR = \frac{|F_{tr\ max}|}{F_o} = \frac{\sqrt{1 + 4\gamma^2 \left(\frac{\omega}{\omega_n} \right)^2}}{\sqrt{\left[1 - \left(\frac{\omega}{\omega_n} \right)^2 \right]^2 + 4\gamma^2 \left(\frac{\omega}{\omega_n} \right)^2}}$$

The AF and TR charts have been plotted on the following page. While these have been developed for the fixed base model they can be used for the base motion model with the proper interpretation. For base motion input, use

$$\left| \frac{\ddot{x}_{max}}{\ddot{y}_{max}} \right| = TR, \quad \text{and} \quad \left| \frac{z_{max}}{y_{max}} \right| = \left(\frac{\omega}{\omega_n} \right)^2 AF,$$

Steady State Vibration*: Amplification Factor and Transmissibility Curves for a Linear Single Degree of Freedom System

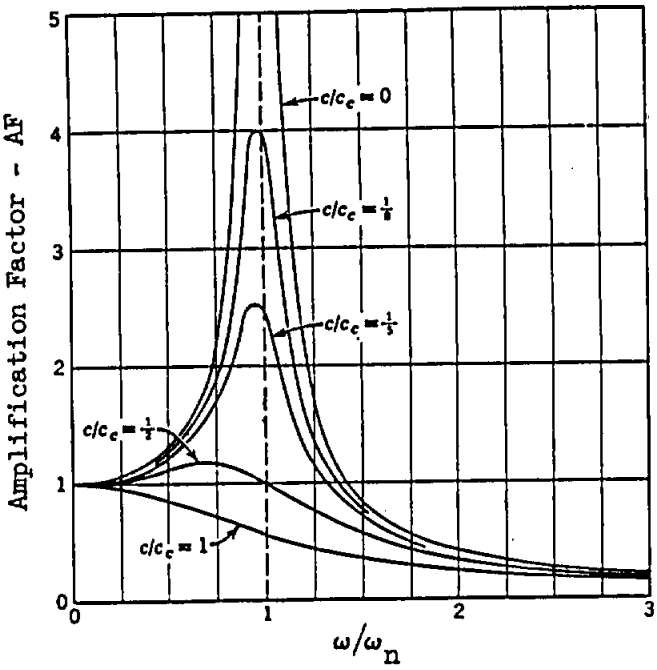

Force Input: $F(t) = F_o \sin \omega t$

$x_o = F_o/k$

$AF = |x_{max}|/x_o$

$TR = |(c\dot{x}+kx)_{max}|/F_o$

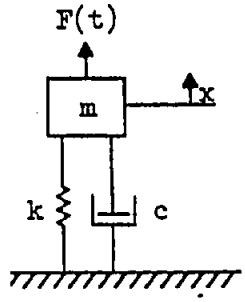

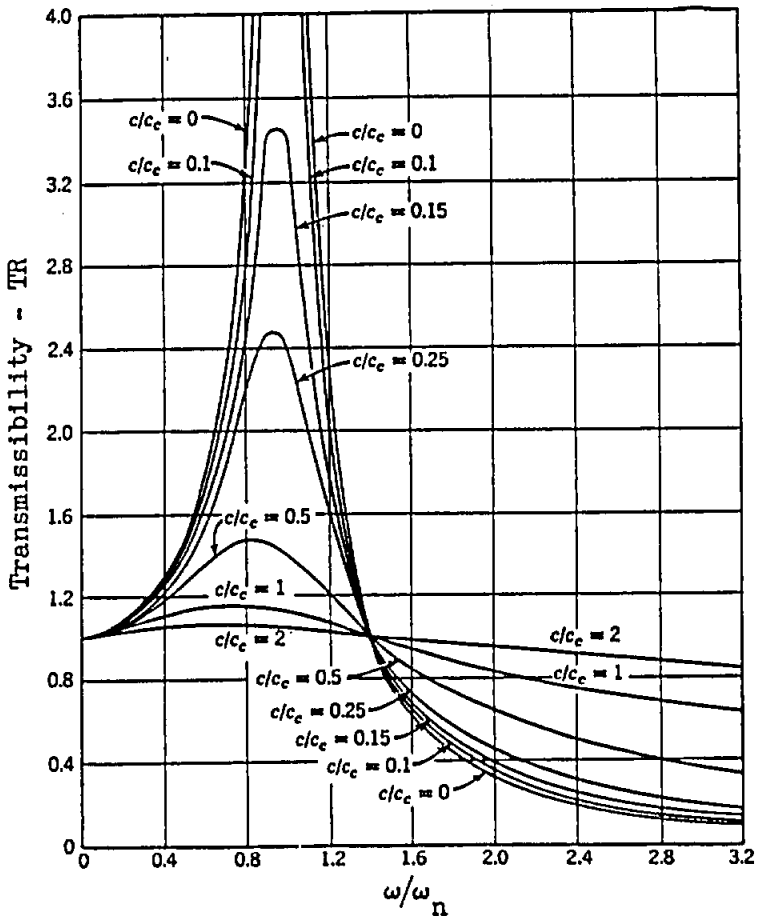

Motion Input: $\ddot{y}(t) = \ddot{Y}_o \sin \omega t$

$|\ddot{x}_{max}|/\ddot{Y}_o = TR$

$|z_{max}|/|y_o| = (\omega/\omega_n)^2 \, AF$

$y_o = -\ddot{Y}_o/\omega^2$

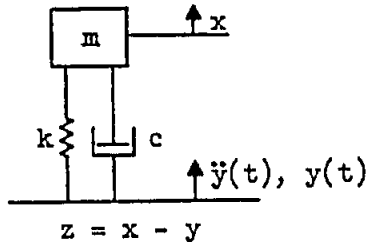

* Curves reproduced from "Theory of Mechanical Vibration", by K. N. Tong, John Wiley and Sons, Inc., New York, 1960; with permission of the publishers.

VIBRATION NOMOGRAPH FOR SIMPLE HARMONIC MOTION

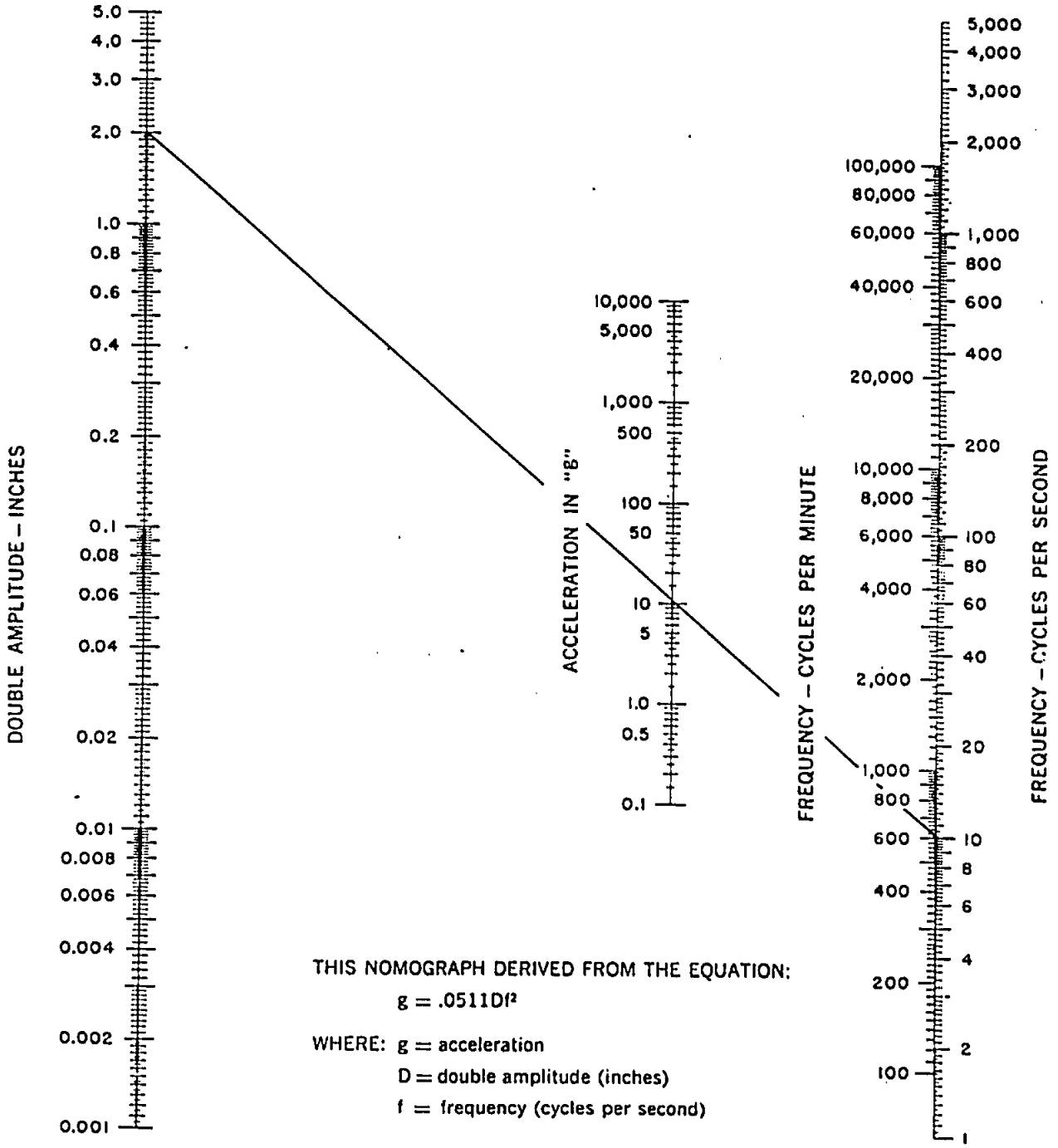

THIS NOMOGRAPH DERIVED FROM THE EQUATION:

$$g = .0511Df^2$$

WHERE: g = acceleration

D = double amplitude (inches)

f = frequency (cycles per second)

Example: Given D = 2 inches and f = 10 cps. Then the acceleration equals 10 g's (single amplitude).

Transient Response to Analytic Functions

The response to non-harmonic functions is useful in many applications, e.g., aircraft landing shock. If the forcing functions are analytic, the response can be readily obtained in closed form using techniques such as the Laplace transform. The results for several forcing functions are presented based upon Grumman Report GE-90A.

The single degree of freedom system models and the notation used here are consistent with the previous discussions. In addition

a = characteristic time parameter of forcing function

T_n = natural undamped period of system

TR = transmissibility = $|F_{tr\ max}|/F_o$ for force input

= $|\ddot{x}_{max}|/\ddot{Y}_o$ for motion input

$F_{tr} = (c\dot{x} + kx)$ for force input = $\ddot{x}$ for motion input

I. Transmissibility Curves

A. Ramp-Step Force

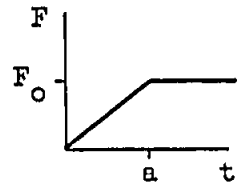

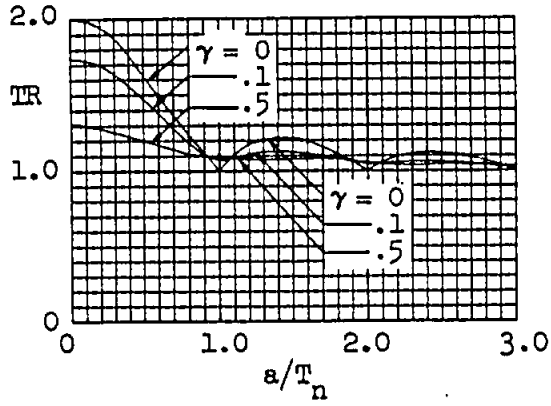

B. Step Pulse

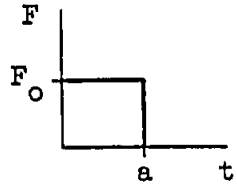

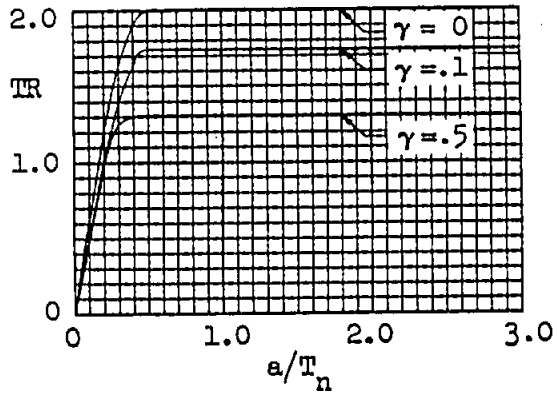

C. Ramp Pulse

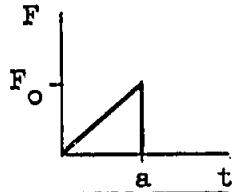

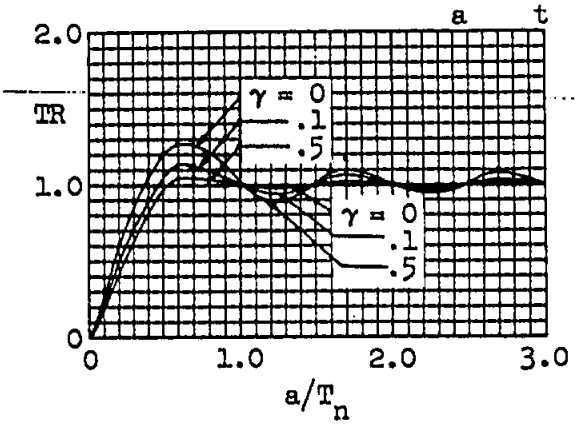

D. Isosceles Triangular Pulse

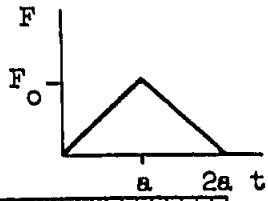

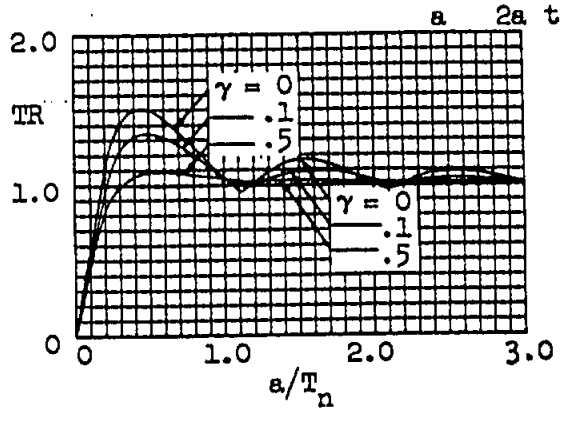

E. Sine Pulse

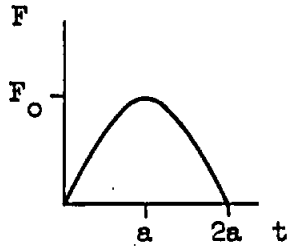

F. Sine-Squared Pulse

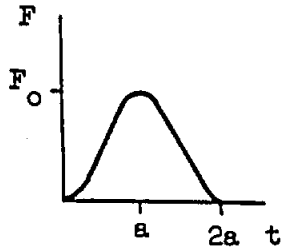

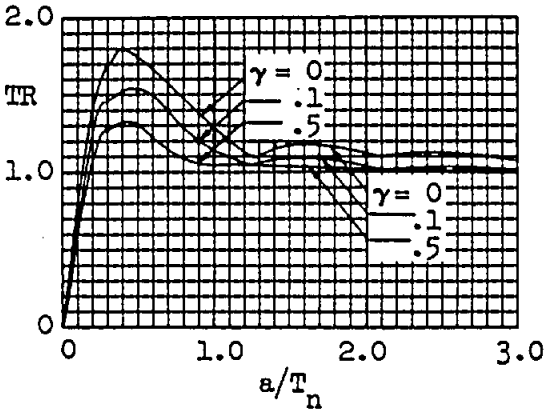

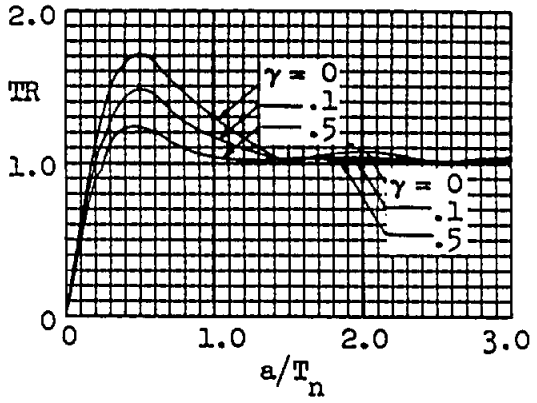

II. Time-Histories of Dynamic Response

A. Step Force

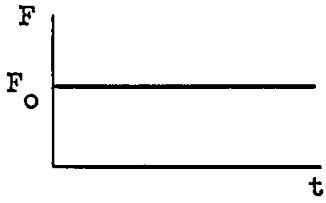

B. Ramp Force

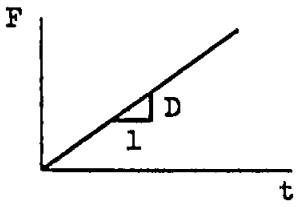

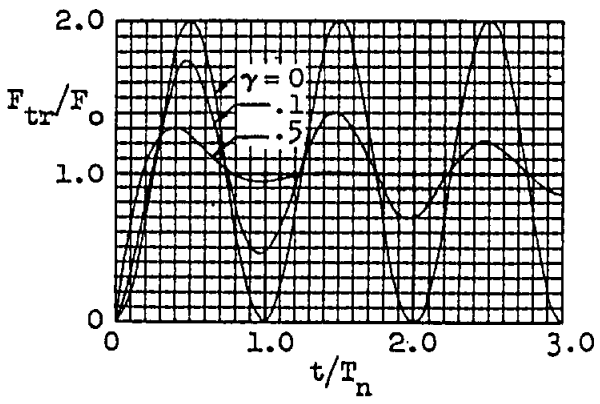

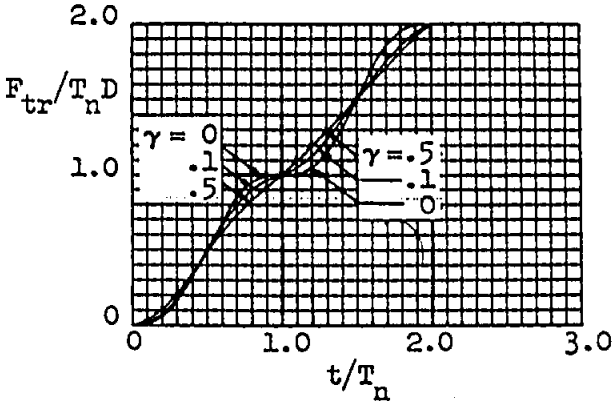

Transient Response to Non-Analytic Functions

In general, the response to arbitrary forcing functions must be obtained by numerical methods. While various methods are available these are usually quite tedious for hand solution and should be handled by computer. However, the function can often be approximated adequately by smooth analytic functions in the area of interest, depending on the system's characteristics and nature of the function.

One graphical approach provides a reasonable hand solution in addition to shedding some insight into the problem. This is the phase plane technique. While it is applied here to a linear system without damping, it can be extended to non-linear damped systems. The added complexity is usually not warranted, however, where computer facilities are readily available.

The construction is simply a plot of the system's displacement vs velocity. The forcing function is approximated by a series of step pulses. The response to each pulse is a circular arc which is a function of the pulse magnitude and the initial conditions at the start of the pulse. In mathematical terms, for the i^{th} pulse

$$M\ddot{x} + kx = F_i$$

where F_i is the step magnitude. The initial conditions are $x(0) = x_i$ and $\dot{x}(0) = \dot{x}_i$, the values at the end of the preceeding pulse. All parameters are expressed in displacements units, i.e.,

$$\frac{\ddot{x}}{\omega^2} + x = \frac{F_i}{k}, \quad \text{where } k = M\omega^2$$

The solution for this pulse in the interval Δt_i is

$$\left(x - \frac{F_i}{k}\right)^2 + \left(\frac{\dot{x}}{\omega}\right)^2 = \left(x_i - \frac{F_i}{k}\right)^2 + \left(\frac{\dot{x}_i}{\omega}\right)^2$$

This represents a circular arc with its center at $\left(\frac{F_i}{k}, 0\right)$, a radius equal to the square root of the right hand side, and a central angle given by $\theta = \omega \Delta t_i$. The displacement and velocity can be projected onto time axes to give the desired time histories. The acceleration can then be obtained directly by

$$\frac{\ddot{x}}{\omega^2} = \frac{F(t)}{k} - x$$

The method is illustrated on the next page.

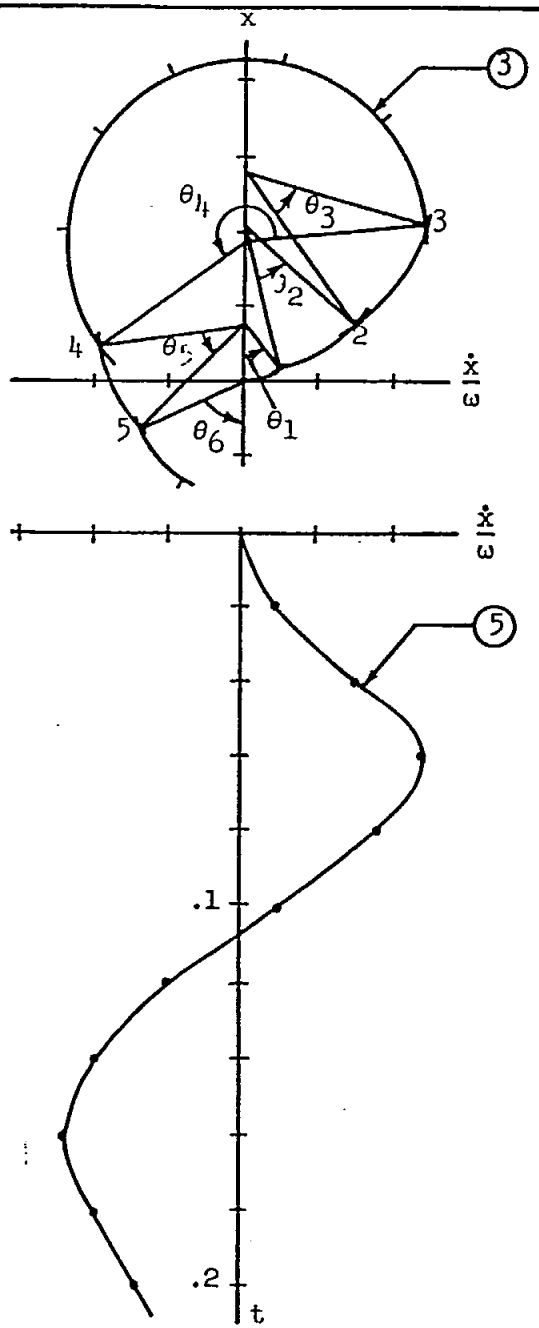

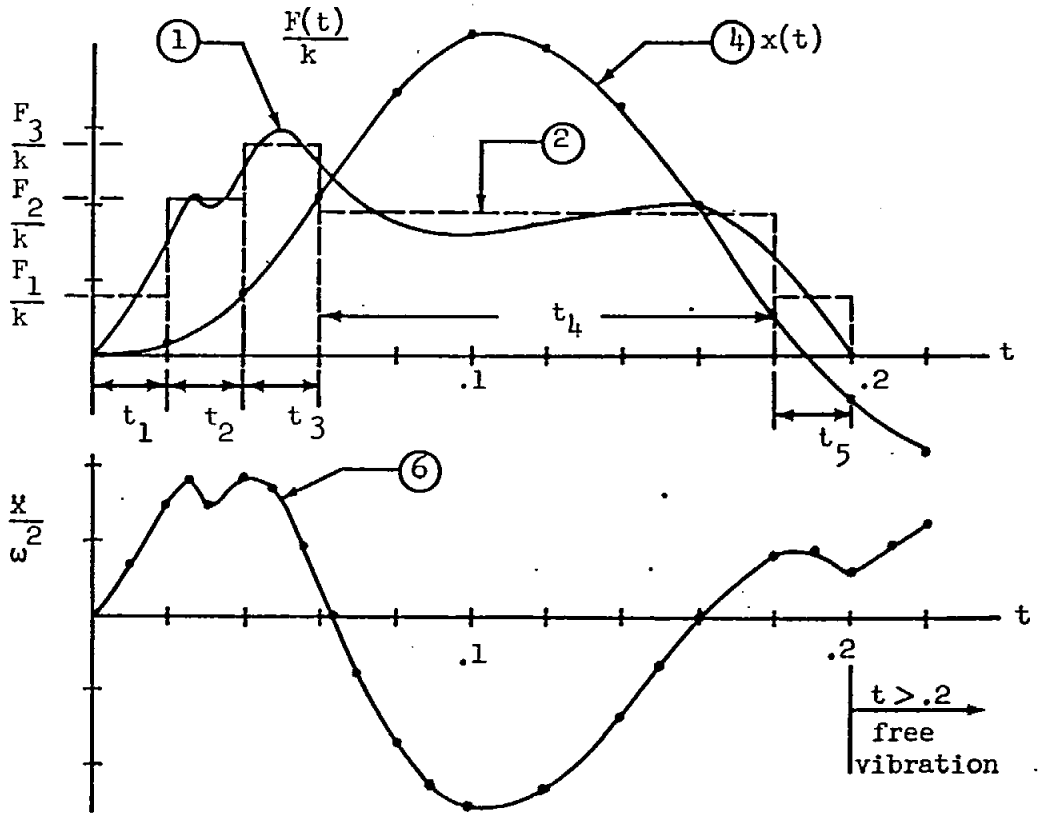

Phase Plane Solution for $M\ddot{x} + kx = F(t)$, or $\frac{\ddot{x}}{\omega^2} + x = \frac{F(t)}{k}$,
with $x(0) = \dot{x}(0) = 0$ and $\omega = 2\pi f = 10\pi$.

1. Approximate forcing function F(t)/k (curve 1) by step pulses (curve 2).
2. Construct phase plane plot, curve 3:
   a) Draw arc with radius F_1/k and center $(F_1/k, 0)$ for $\theta_1 = \omega t_1$, from point 0 to 1.
   b) Draw arc with radius from center $(F_2/k, 0)$ to point 1 for $\theta_2 = \omega t_2$, from point 1 to 2.
   c) Continue as in b) for θ_3, etc.
3. Project displacements horizontally generating curve 4; project velocities vertically for curve 5.
4. Subtract curve 4 from curve 1 to obtain acceleration, $\frac{\ddot{x}}{\omega^2}$, curve 6.

MULTI-DEGREE OF FREEDOM SYSTEMS

General

Many typical dynamic load problems are too complex to be handled by the elementary techniques of the preceeding paragraphs. The details of the procedures for the more complex systems are too lengthly to be included here. However, many standard procedures have been routinized for various classes of problems; references to these are listed in Sections A and G of this manual.

In many applications a quick means of estimating the natural frequencies (normal modes) of structural elements is desirable. The mode shapes for several simple beam configurations are shown below. On the following pages, tables are presented listing the frequencies for various beams, plates, and ring elements.

Mode Shapes for Simple Beams

Beam Type	Mode I	Mode II	Mode III	Mode IV
Cantilever	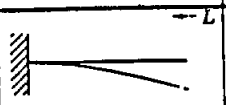	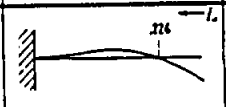	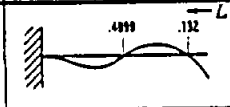	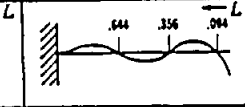
Simply supported ends	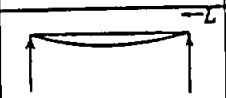	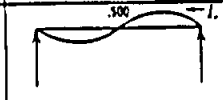	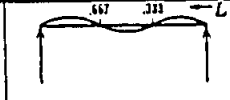	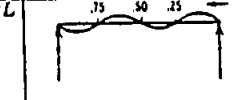
Fixed ends	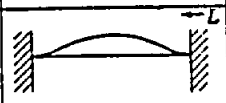	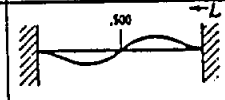	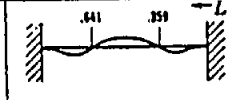	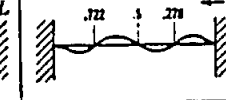
Free ends	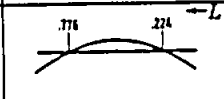	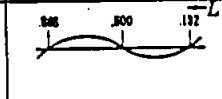	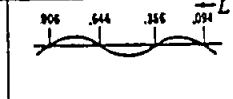	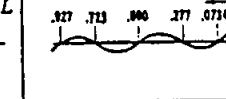
Fixed-hinged		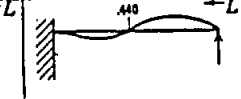	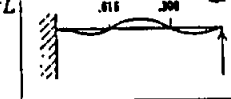	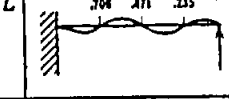
Hinged-free	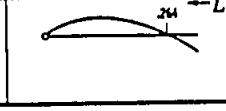	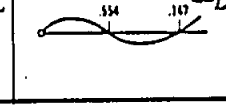	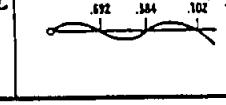	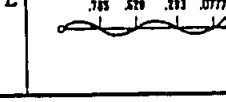

VIBRATION FREQUENCY TABLES FOR BEAMS, PLATES AND RINGS

These tables provide a quick means for estimating the natural frequencies of simple structural elements. They are for steel at room temperature; see page E3-8 for other materials and other temperatures. References are given for the frequencies of less common structural elements.

TABLE I

FREQUENCY CONSTANT $C = fL^2/r$ FOR UNIFORM STEEL BEAMS

f = NATURAL FREQUENCY, cps
L = BEAM LENGTH, inches
r = RADIUS OF GYRATION $\sqrt{I/A}$

$C/10^4 = (fL^2/r)/10^4$

BEAMS	MODE NUMBER				
	1	2	3	4	5
 CLAMPED - CLAMPED FREE - FREE	71.95	198.29	388.73	642.60	959.94
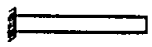 CLAMPED - FREE	11.30	70.85	198.30	388.73	642.60
 CLAMPED - HINGED FREE - HINGED	49.57	160.65	335.17	573.20	874.65
 CLAMPED - GUIDED FREE - GUIDED	17.98	97.18	239.98	446.25	715.98
 HINGED - HINGED GUIDED - GUIDED	31.73	126.93	285.60	507.73	793.33
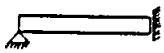 HINGED - GUIDED	7.93	71.40	198.33	388.73	642.60

TABLE 2

FREQUENCY CONSTANT $C=fL^2/r$ FOR VARIABLE SECTION STEEL BEAMS

f = NATURAL FREQUENCY, cps
L = BEAM LENGTH, inches
r = RADIUS OF GYRATION = $\sqrt{I/A}$ inches

$C/10^4=(fL^2/r)/10^4$

VARIABLE SECTION BEAMS	b/b_o	h/h_o	MODE 1	2	3
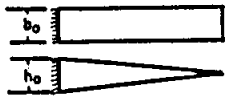	1	x/L	17.09	48.89	96.57
	x/L	x/L	26.08	68.08	123.64
	$(x/L)^{1/2}$	x/L	22.30	58.18	109.90
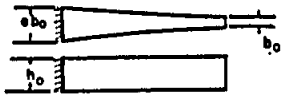	$e^{x/L}$	1	15.23	77.78	206.07
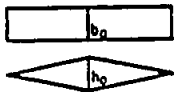	1	x/L	21.21 35.05	56.97	SYMMETRIC ANTISYMMETRIC
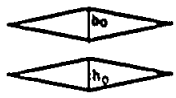	x/L	x/L	32.73 49.50	76.57	SYMMETRIC ANTISYMMETRIC
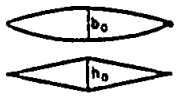	$(x/L)^{1/2}$	x/L	25.66 42.02	66.06	SYMMETRIC ANTISYMMETRIC

TABLE 3

FREQUENCY FUNCTION = fL FOR LONGITUDINAL VIBRATION OF STEEL BEAMS

f = NATURAL FREQUENCY, cps
L = LENGTH OF BEAM, inches

$fL/10^4$

BEAMS	n = NUMBER OF HALF WAVES ALONG LENGTH 0	1	2	3	4	5
 CLAMPED-FREE	5.05	15.15	25.25	35.35	45.46	55.56
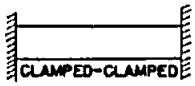 CLAMPED-CLAMPED		10.10	20.20	30.30	40.41	50.51

TABLE 4

FREQUENCY CONSTANT $C = fL^2/r$ FOR CONTINUOUS STEEL BEAM OF k EQUAL SPANS
EXTREME ENDS SIMPLY SUPPORTED

f = NATURAL FREQUENCY, cps
L = SPAN LENGTH, inches
r = RADIUS OF GYRATION = $\sqrt{I/A}$ inches

$C/10^4 = (fL^2/r)/10^4$

UNIFORM BEAM EXTREME ENDS SIMPLY SUPPORTED	NUMBER OF SPANS = k	MODE NUMBERS 1	2	3	4	5
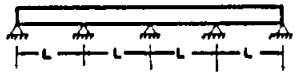	1	31.73	126.94	285.61	507.76	793.37
	2	31.73	49.59	126.94	160.66	285.61
	3	31.73	40.52	59.56	126.94	143.98
	4	31.73	37.02	49.59	63.99	126.94
	5	31.73	34.99	44.19	55.29	66.72
	6	31.73	34.32	40.52	49.59	59.56
	7	31.73	33.67	38.40	45.70	53.63
	8	31.73	33.02	37.02	42.70	49.59
	9	31.73	33.02	35.66	40.52	46.46
	10	31.73	33.02	34.99	39.10	44.19
	11	31.73	32.37	34.32	37.70	41.97
	12	31.73	32.37	34.32	37.02	40.52

TABLE 5

FREQUENCY CONSTANT $C = fL^2/r$ FOR CONTINUOUS STEEL BEAM OF k EQUAL SPANS
EXTREME ENDS CLAMPED

f = NATURAL FREQUENCY, cps
L = SPAN LENGTH, inches
r = RADIUS OF GYRATION = $\sqrt{I/A}$ inches

$C/10^4 = (fL^2/r)/10^4$

UNIFORM BEAM EXTREME ENDS CLAMPED	NUMBER OF SPANS = k	MODE NUMBERS 1	2	3	4	5
	1	72.36	198.34	388.75	642.63	959.98
	2	49.59	72.36	160.66	198.34	335.20
	3	40.52	59.56	72.36	143.98	178.25
	4	37.02	49.59	63.99	72.36	137.30
	5	34.99	44.19	55.29	66.72	72.36
	6	34.32	40.52	49.59	59.56	67.65
	7	33.67	38.40	45.70	53.63	62.20
	8	33.02	37.02	42.70	49.59	56.98
	9	33.02	35.66	40.52	46.46	52.81
	10	33.02	34.99	39.10	44.19	49.59
	11	32.37	34.32	37.70	41.97	47.23
	12	32.37	34.32	37.02	40.52	44.94

TABLE 6

FREQUENCY CONSTANT $C = fL^2/r$ FOR CONTINUOUS STEEL BEAM OF k EQUAL SPANS. EXTREME ENDS CLAMPED - SUPPORTED.

f = NATURAL FREQUENCY, cps
L = SPAN LENGTH, inches
r = RADIUS OF GYRATION = $\sqrt{I/A}$ inches

$C/10^4 = (fL^2/r)/10^4$

UNIFORM BEAM EXTREME ENDS CLAMPED - SUPPORTED	NUMBER OF SPANS = K	MODE NUMBERS 1	2	3	4	5
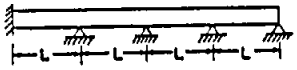	1	49.59	160.66	335.2	573.21	874.69
	2	37.02	63.99	137.30	185.85	301.05
	3	34.32	49.59	67.65	132.07	160.66
	4	33.02	42.70	56.98	69.51	129.49
	5	33.02	39.10	49.59	61.31	70.45
	6	32.37	37.02	44.94	54.46	63.99
	7	32.37	35.66	41.97	49.59	57.84
	8	32.37	34.99	39.81	45.70	53.63
	9	31.73	34.32	38.40	43.44	49.59
	10	31.73	33.67	37.02	41.24	46.46
	11	31.73	33.67	36.33	39.81	44.19
	12	31.73	33.02	35.66	39.10	42.70

TABLE 7

FREQUENCY CONSTANT $C = fr^2/h$ FOR CIRCULAR STEEL PLATES

f = NATURAL FREQUENCY, cps
r = RADIUS OF PLATE, inches
h = THICKNESS OF PLATE, inches

$C/10^4 = (fr^2/h)/10^4$

CIRCULAR PLATE CLAMPED AT BOUNDARY	m = NUMBER OF NODAL CIRCLES	n = NUMBER OF NODAL DIAMETERS n = 0	1	2	3
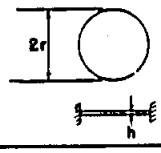	0	9.936	20.651	33.906	
	1	38.713			
	2	86.516			

CIRCULAR PLATE WITH FREE BOUNDARY	m = NUMBER OF NODAL CIRCLES	n = NUMBER OF NODAL DIAMETERS n = 0	1	2	3
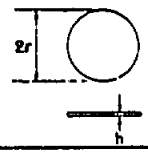	0			5.110	11.902
	1	8.832	19.970	34.295	51.491
	2	37.487	58.255		

CIRCULAR PLATE CLAMPED AT ITS CENTER	m = NUMBER OF NODAL CIRCLES 0	1	2	3
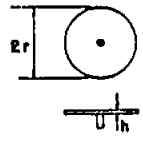	3.649	20.349	59.053	116.490

TABLE 8

FREQUENCY CONSTANT $C = fa^2/h$ FOR SQUARE STEEL PLATES

f = NATURAL FREQUENCY, cps
a = SIDE OF PLATE, inches
h = PLATE THICKNESS, inches

F = FREE
S = SUPPORTED
C = CLAMPED

$C/10^4 = (fa^2/h)/10^4$

SQUARE PLATES	MODE NUMBERS					
	1	2	3	4	5	6
F F C	3.40	8.32	20.86	26.71	30.32	
F C F C	6.77	23.43	26.07	46.75	61.44	
F F F	13.72	19.99	23.26	34.98	59.93	63.47
S S S	19.20	48.00	76.82	96.01	124.82	163.25
S S C	23.01	50.28	57.06	83.79	97.58	110.13
C C S	28.16	53.26	67.44	92.02	99.43	125.60
C C C	35.01	71.42	105.36	128.03	128.71	160.72

TABLE 9

FREQUENCY CONSTANT $C = fa^2/h$ FOR CANTILEVER STEEL PLATES

f = NATURAL FREQUENCY, cps
a = SIDE OF PLATE, inches
h = PLATE THICKNESS, inches

F = FREE
C = CLAMPED

$C/10^4 = (fa^2/h)/10^4$

RECTANGULAR CANTILEVER PLATE	a/b	MODE NUMBER				
		1	2	3	4	5
a, C F F F, b	1/2	3.41	5.23	21.36	9.98	24.18
	1	3.40	8.32	20.86	26.71	30.32
	2	3.38	14.52	21.02	91.92	47.39
	5	3.36	33.79	20.94	548.60	103.03
SKEWED CANTILEVER PLATE	SKEW ANGLE θ DEGREES	MODE NUMBER				
		1	2	3	4	5
a, C F F F, a, θ	15°	3.50	8.63			
	30°	3.85	9.91			
	45°	4.69	13.38			

TABLE 10

FREQUENCY CONSTANT $C = f a^2/h$ FOR RECTANGULAR STEEL PLATES

f = NATURAL FREQUENCY, cps
a = SIDE OF PLATE, inches
h = PLATE THICKNESS, inches
F = FREE
S = SUPPORTED
C = CLAMPED

$C/10^4 = (f a^2/h)/10^4$

RECTANGULAR PLATES	FIRST MODE						
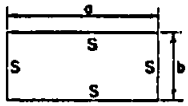	b/a	1.0	1.5	2.0	2.5	3.0	INFINITE
	$C/10^4$	19.20	13.87	12.00	11.14	10.67	9.60
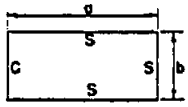	b/a	1.0	1.5	2.0	2.5	3.0	INFINITE
	$C/10^4$	23.01	18.39	16.86	16.18	15.82	15.01
	a/b	1.0	1.5	2.0	2.5	3.0	INFINITE
	$C/10^4$	23.01	15.15	12.57	11.43	10.84	9.60
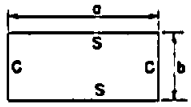	b/a	1.0	1.5	2.0	2.5	3.0	INFINITE
	$C/10^4$	28.16	24.37	23.17	22.64	22.37	21.76
	a/b	1.0	1.5	2.0	2.5	3.0	INFINITE
	$C/10^4$	28.16	16.90	13.32	11.80	11.05	9.60
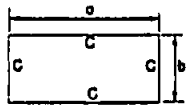	b/a	1.0	1.5	2.0	2.5	3.0	INFINITE
	$C/10^4$	35.00	26.27	23.90	23.12	22.56	21.76

TABLE 11

FREQUENCY FUNCTION = $fr/(s/h)^{1/2}$ FOR CIRCULAR STEEL MEMBRANES

f = NATURAL FREQUENCY, cps
r = MEMBRANE RADIUS, inches
s = TENSION, lb/in AT PERIPHERY
h = MEMBRANE THICKNESS, inches

$fr/(s/h)^{1/2}$

CIRCULAR MEMBRANE	m = NUMBER OF NODAL CIRCLES	n = NUMBER OF NODAL DIAMETERS					
		0	1	2	3	4	5
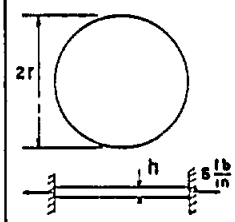	1	14.09	22.49	30.12	37.46	44.56	51.55
	2	32.41	41.22	49.44	57.30	64.94	72.22
	3	50.79	59.71	64.94	76.45	84.55	92.18
	4	69.28	78.09	86.90	95.12	103.34	111.56
	5	87.48	96.88	105.68	113.91	122.13	130.35
	6	106.27	115.08	123.89	132.69	140.91	149.13
	7	124.47	133.87	142.68	150.90	159.70	167.92
	8	143.26	152.07	160.88	169.68	178.49	186.71

TABLE 12

FREQUENCY CONSTANT $C=fr^2/h$ FOR STEEL RING VIBRATING IN ITS OWN PLANE

f = NATURAL FREQUENCY, cps
r = MEAN RADIUS, inches
h = RING THICKNESS, inches

$C/10^4=(fr^2/h)/10^4$

CIRCULAR RING	n = NUMBER OF FULL WAVES AROUND PERIPHERY					
	2	3	4	5	6	7
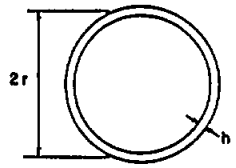	54.21	153.33	240.00	475.46	697.48	

Table 13 Loaded Uniform Beams - First Vibration Mode
Notation - See Table 2 r = ratio of load to beam weight

Beam Structure		$C/10^4 = (f_s L^2/r)/10^4$					
		r → 0	.5	1	5	10	100
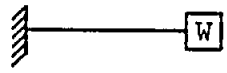	Cantilever End Load	11.30	6.49	5.02	2.44	1.75	.56
	Hinged Ends Center Load	31.73	22.4	18.29	9.55	6.91	2.24
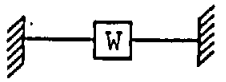	Clamped Ends Center Load	71.95	48.1	38.1	19.35	13.92	4.49

Other Materials and Non-Room Temperatures

The tables provided are accurate to within 6% for aluminum, magnesium, nickel, and titanium at room temperatures. For other temperatures or other materials the frequency obtained is multiplied by a correction factor, k, where

$$K = \frac{\sqrt{E/\omega}}{\sqrt{E_s/\omega_s}}$$

E = Youngs modulus for the material at the operating temperature
ω = material density
E_s = 30×10^6 lbs/in^2, for steel
ω_s = .284 lbs/in^3, for steel

Other Structural Elements

Similar tables are available in the references below for continuous beams, longitudinal vibrations of beams, circular membranes, curved rectangular plates, and cylindrical shells.

1. "Vibration Frequency Charts", Macduff and Felgar, Machine Design, Vol. 29, 2/7/57.
2. "The Natural Frequency of Vibration of Curved Rectangular Plates", Palmer, Aero. Quarterly, Vol. V, July 1954.
3. "Tables for Frequencies and Modes of Free Vibration of Infinitely Long Thin Cylindrical Shells", Baron and Bleich, J. App. Mech., June 1954.

RANDOM VIBRATION

Introduction

In various modern applications the vibrational energy in the excitation is distributed in a random manner over a wide range of frequencies. This is characteristic of the environments associated with rocket and jet noise, atmospheric turbulence, aerodynamic noise, and rough terrain. The instantaneous value of the resulting random displacement, acceleration, stress, etc., can be specified only in terms of the probability that the value will be in a given range during a given time interval.

The intent of this section is to briefly discuss the basic concepts involved in the analysis of random phenomena. The basic statistical concepts are covered in Section F of this manual and are not repeated here. To simplify the discussion, the mathematical relationships have been deleted wherever possible; two simple examples have been included to illustrate the discussion.

Discussion

Inspection of a typical random time history, such as the force input of figure 1, reveals a completely irregular wave pattern with no apparent amplitude, frequency, or phase relationships. Equal duration samples of this history will vary considerably in their instantaneous values; however, the average characteristics will be equal. Such a time history can only be described in terms of statistical and probabilistic parameters. The mathematical model used for this is the Gaussian random process subjected to various mathematical restrictions. As used here it is applicable only to linear structural systems. Having assumed a Gaussian or normal probability distribution, the only other parameter needed to completely define the random process is its spectral density.

While there are many other types of probability distributions, the Gaussian mathematical model is commonly used in many physical problems. This is due not only to its wide applicability, but also to its relatively simple mathematical formulation. One should consequently be aware that it is sometimes used where the justification is questionable merely because of its ease of handling.

Average Values: For the random functions considered here the mean value is zero. The mean-square value is the main average of interest. Literally, it is simply the average of the function squared evaluated for the sample time duration T. The root-mean-square (rms) value is merely the positive square root of the mean square value. Since the mean value is zero here, the mean-square is equivalent to the variance σ^2, and the rms value is equivalent to the standard deviation σ. Thus for the random function $x(t)$:

$$\overline{x^2} = \sigma^2 = \frac{1}{T}\int_0^T x^2(t)\,dt, \text{ and } x_{rms} = \sigma = \sqrt{\overline{x^2}}.$$ In random vibration applications the mean-square is obtained by computing the area under the spectral density curve as described later.

Gaussian Probability Density: The Gaussian or normal probability density function is the familiar bell shaped curve, symmetrical about its mean value. This is described in detail in Section F. Briefly, the area under the density curve equals the probability. Specifically, the probability that a value of a random function x will occur between two limits x_1 and x_2, is the area under the density curve bounded by x_1 and x_2. For example, the probability of $|x|$ exceeding its rms value (or standard deviation) is 31.7%, of exceeding twice its rms value is 4.6%, and of exceeding 3 times the rms value is only 0.3%. Since the mean value is zero, the probability density depends only on the standard deviation which equals the rms value. Knowing the density function, the relative frequency of occurrence of the various amplitudes of x are completely known. Note that the probability density function deals only with amplitudes and has nothing to do with the harmonic content of the random function.

Based upon the normal distribution, various relationships useful in fatigue analysis have been derived. Knowing the relative frequency of occurrences of the instantaneous amplitudes of x, the frequency of occurrences of the peak values of x can be obtained. Relating this to the conventional SN curves, an estimate of the time to failure can be calculated. For lightly damped, single degree of freedom systems, the envelope of the peak values is described by the Rayleigh probability density function (derived from the Gaussian distribution); this is often used in acoustic fatigue analyses.

Spectral Density: The spectral density function may be interpreted as the measure of the energy distribution in a variable as a function of frequency. In practice it may be measured by passing a signal corresponding to the sample time history through a tuneable narrow band pass filter 1 cycle wide, and measuring the mean-square response at each frequency over the entire frequency range. Dimensionally the response is in mean-square unit/cps. Actually the band pass is not 1 cycle wide so each response point must be divided by the actual band width at that point.

For most random excitations the spectral density must be obtained by test procedures. However, there are some special cases where the spectral density has been expressed analytically, e.g., for atmospheric turbulence in gust load analyses. In such cases, however, these are empirical expressions based upon exhaustive test data. One important special case is that of a constant or uniform spectral density corresponding to "white noise". Here every frequency component from 0 to ∞ is present with equal amplitude. (This is impossible physically, implying infinite power.) A uniform spectral density is often called out in random vibration specifications, where a specific frequency range is used, e.g., 20 to 20,000 cps.

Mathematically the spectral density is defined in terms of the Fourier Integral, an extension of the Fourier series. The Fourier series is used to express a periodic function in terms of discrete frequency components. The Fourier Integral extends this procedure to nonperiodic functions and leads to a continuous functional relationship between amplitude and frequency. In practice the mean-square value of the original time variable is equal to the total area under the spectral density curve.

The term power spectral density is often used, a carry-over from its original electrical engineering applications. "Power" is applicable in a generalized sense. For example the power generated in a resistance is proportional to the mean-square of the current through the resistor. Similarly, the power dissipated in a viscous dashpot is proportional to the mean-square of the velocity across the dashpot.

Note that the spectral density describes only the average energy or mean-square amplitude at each frequency component. It says nothing about the individual magnitudes of the time history waveform. Thus the spectral density and probability density functions are complementary; between them they completely define the random function characteristics.

Transfer Function: In random motion analysis the characteristics of the physical structure are described by the system transfer function. This can be loosely defined as the ratio of the response of a linear system to the applied excitation, where the excitation is simple harmonic motion. The response and excitation correspond to specific points of the structure. The terms impedance, mobility, admittance, etc. are simply special types of transfer functions. For a single degree of freedom system the transfer function is directly proportional to the steady state amplification factor or transmissibility.

The transfer function is used to relate the spectral density of the response to the spectral density of the excitation. Since the spectral densities are in terms of mean-square units, the squared absolute value of the transfer function is used. Thus

$$S_x(\omega) = \left|H(\omega)\right|^2 \quad S_f(\omega)$$

where $H(\omega)$ is the transfer function relating the excitation $S_f(\omega)$ to the response spectral density $S_x(\omega)$. In general the transfer function can be obtained both analytically and by test.

Notched Beam Fatigue - Example

The following example, based upon NASA Memo 4-12-59L, illustrates much of the preceding discussion. This study investigated the fatigue life of a cantilever beam notched near the root and excited at the tip by a lateral random force. The stress response measured at the root acts like a very lightly damped single degree of freedom system.

Sample time histories of the force input and stress response are shown in Fig. 1. Note that the force input appears completely irregular with no apparent periodicities or phase relationships, while the response appears to be a sine wave with random amplitude and phase. The beam thus acts like a narrow band filter tuned to its natural frequency. This is also illustrated in the spectral density curves (figures 2 and 3) obtained by test from the corresponding time histories; note that the force has frequency components from 0-350 cps while the response has a narrow band of frequencies about its natural frequency of 119 cps.

To check the probability distribution of the stress response, the number of times/second that various stress levels were crossed with positive slope were electronically measured. The results were plotted in Fig. 4 along with the theoretical number for a Gaussian distribution. The test data was considered close enough to the theoretical curves; consequently the process was treated as a Gaussian phenomena. This assumption seems open to question here, since the deviation from the theoretical curve is fairly large percentagewise.

Having the stress response spectral density (measured directly), and the probability distribution of the stress levels (assumed Gaussian with calculated parameter σ), the response has been completely specified. The probable time to failure for this random loading was calculated based upon Miner's rule for cumulative fatigue damage in the form

$$(T_f)^{-1} = \int_0^\infty \frac{N(x)\,dx}{N_f(x)}$$

where T_f = time to failure in seconds,

$N_f(x)$ = number of cycles to failure for stress reversals with constant amplitude x, (from standard SN curve),

$N(x)\,dx$ = probable number of stress reversals/second with amplitudes between x and x + dx.

Typical results are shown in Figure 5. The difference between the test and theoretical curves may be due to the fact that the Gaussian assumption was not very good.

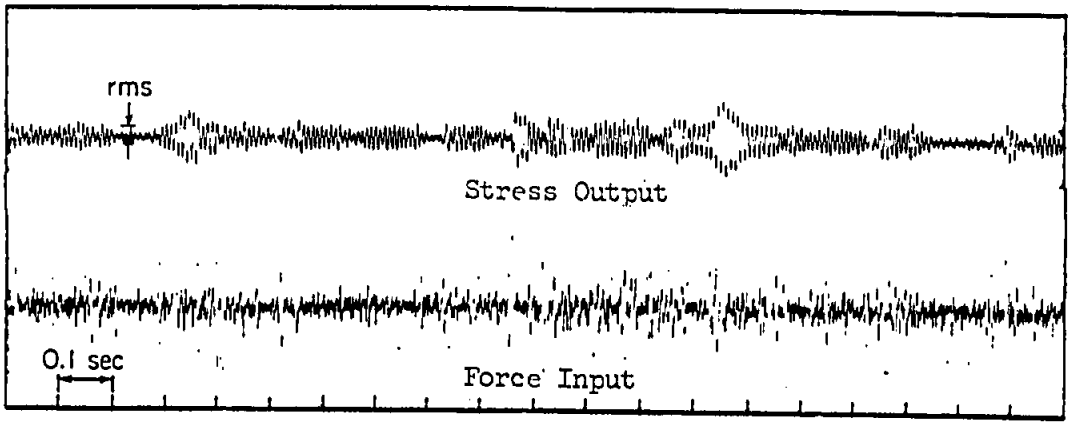

Figure 1. Sample time histories of force input and stress output.

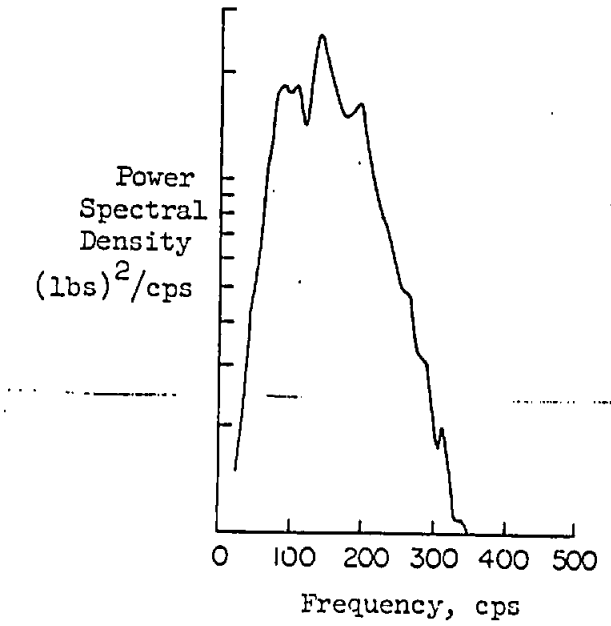

Figure 2. Power spectrum of force input.

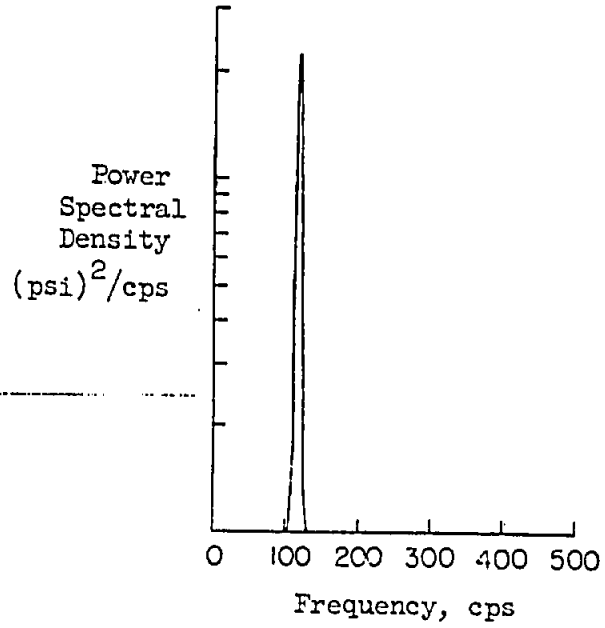

Figure 3. Power spectrum of stress output.

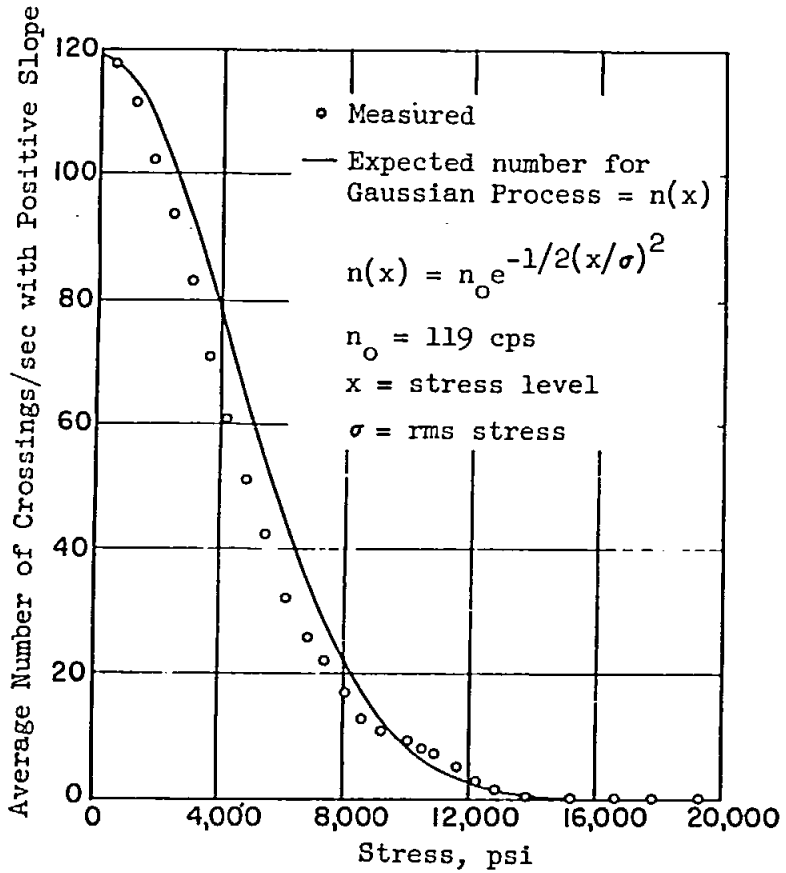

Figure 4. Average number of crossings/sec of stress level with positive slope for test with rms stress of 4330 psi.

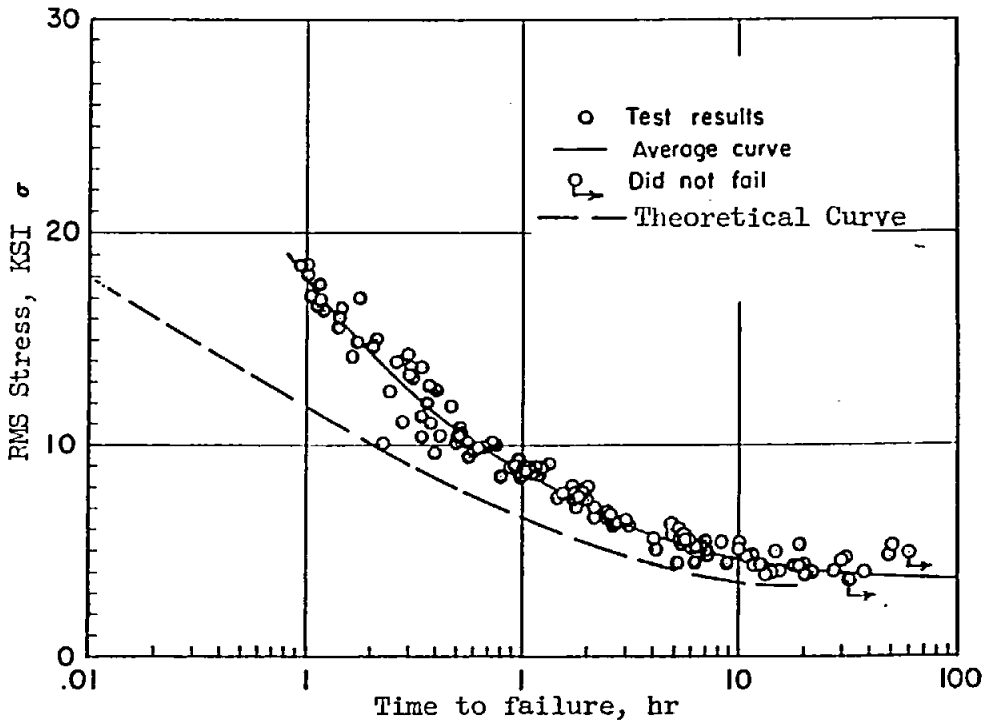

Figure 5. Fatigue results of random loading tests. For rms peak stress use $\sigma_p = \sqrt{2}\,\sigma$.

$$(T_f)^{-1} = \frac{2f_o}{\sigma_p^2} \int_0^\infty \frac{x\, e^{-(x/\sigma_p)^2}\, dx}{N_f(x)}$$

T_f = time to failure, sec.

f_o = natural frequency

x = stress level

σ_p = rms peak stress

$N_f(x)$ = no. cycles to failure for stress reversals with constant amplitude x

Grumman

Response to Uniform Spectral Density - Example

The random concepts can be further illustrated using the example of a uniform spectral density applied to a linear damped oscillator. This could represent the acceleration response of a black box on vibration isolators, where the base is excited by a random acceleration.

Referring to the free base, single degree of freedom model of Section 2 (Page E2-2), let the base motion $\ddot{y}(t)$ be a random Gaussian function with a constant spectral density, $S_{\ddot{y}}(\omega) = S_o$. The transfer function for the acceleration response is equivalent to the transmissibility, i.e.,

$$|H(\omega)| = \frac{|\ddot{x}\ \max|}{|\ddot{y}\ \max|} = TR = \left[\frac{1 + 4\gamma^2 \left(\frac{\omega}{\omega_n}\right)^2}{\left[1 - \left(\frac{\omega}{\omega_n}\right)^2\right]^2 + 4\gamma^2 \left(\frac{\omega}{\omega_n}\right)^2}\right]^{\frac{1}{2}}$$

The response spectral density is given by

$$S_{\ddot{x}}(\omega) = S_o\ |H(\omega)|^2,$$

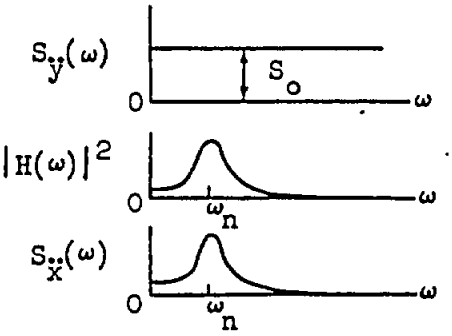

and the mean square acceleration is:

$$\overline{\ddot{x}^2} = \frac{1}{2\pi} \int_0^\infty S_{\ddot{x}}(\omega)\ d\omega$$

$$= S_o \left[\frac{1}{2\pi} \int_0^\infty \frac{1 + 4\gamma^2 \left(\frac{\omega}{\omega_n}\right)^2}{\left[1 - \left(\frac{\omega}{\omega_n}\right)^2\right]^2 + 4\gamma^2 \left(\frac{\omega}{\omega_n}\right)^2}\ d\omega\right]$$

$$\overline{\ddot{x}^2} = S_o \left[\frac{\omega_n}{8\gamma}\right]$$

and $$\ddot{x}_{rms} = \left[\frac{S_o\ \omega_n}{8\gamma}\right]^{\frac{1}{2}}$$

Since the response is Gaussian, we know that $\ddot{x}(t)$ will exceed $2\ddot{x}_{rms}$ 4.6% of the time, $3\ddot{x}_{rms}$ about .3% of the time, etc. This solution assumes

a narrow band width (light damping) and constant excitation density. Actually, if the spectral density is flat near the system natural frequency, the above results still hold, replacing S_o by $S_{\ddot{y}}(\omega_n)$. This same procedure can be applied to multi-degree of freedom systems using a normal mode approach, providing again that the system is lightly damped.

In most cases the integration above would be performed numerically. However in this case of a uniform spectral density excitation, it can be integrated analytically (by the method of residues). The value of the integral is the same if the integrand is equal to either $|TR|^2$ or $|AF|^2$, i.e.,

$$\frac{1}{2\pi}\int_0^\infty |TR|^2\, d\omega = \frac{1}{2\pi}\int_0^\infty |AF|^2\, d\omega = \frac{\omega_n}{8\gamma}$$

It is also applicable to other transfer functions which are proportional to either AF or TR. For example, the displacement response of the fixed base model to a random force input having a constant spectral density S_o can be found immediately. Thus:

$$|H(\omega)| = \frac{|x_{max}|}{F_o} = \frac{|x_{max}|}{k\, x_o} = \frac{1}{k}(AF)$$

and $$\overline{x^2} = \frac{S_o}{k^2}\left[\frac{\omega_n}{8\gamma}\right]$$

SECTION F - STATISTICS

Table of Contents

INTRODUCTION

General

This section has been added to the Structures Manual in response to the increased importance of statistical techniques in structural design. The current trend toward probabilistic design criteria will undoubtedly continue, resulting in more contractual specifications based upon statistical procedures. It is anticipated that this section will be frequently revised to reflect new applications as they arise.

The intent here is to outline the basic statistical concepts and to define the terminology and parameters which are currently of general interest. The statistical terminology is quite specialized; consequently familiarity with it is essential to its proper usage. Since this area is relatively new to many structures personnel, more details are presented here than is usual for a manual of this type. However, due to the very specialized nature of the subject matter, the coverage is of necessity limited to fundamental applications. The material is supplemented by an extensive reference list, covering both general and specific statistical practice.

In a broad sense statistics deals with the collection, analysis, interpretation, and presentation of numerical data. Statistical methods may be divided into two general classes - descriptive and inductive. Descriptive methods are used to summarize or describe large bodies of data. Inductive methods are used to generalize from a small body of data to a larger body of similar data. This manual is concerned mainly with inductive statistical methods.

The inductive generalizations about characteristics of a population are termed statistical inferences. These take two forms: estimates of the magnitudes of population characteristics, and tests of hypotheses. Emphasis in this section centers on the former. The high degree of specialization makes the latter category largely beyond the scope of this manual.

Two facets of statistical usage should be noted. First, the recent popularization of statistical techniques in "practical" engineering problems has led to many questionable practices, particularly in regard to the inherent assumptions and limitations of the statistical model. Second, but on the positive side, the simple fact that the statistical processes are precise and reproducible is often enough to justify their application. The knowledge that results of different tests have been analyzed in the same way may permit rational modification of the inferences from one set of results in the light of experience with previous sets of results.

REFERENCES

Numerous general statistical texts are available in the Grumman library. The references below have been selected on the basis of some specialized feature, described if not obvious by the title. Numbered references are referred to in the text.

A. Introductory and General

1. Moroney, "Facts from Figures," a Penguin Book (paperback), 1960. An excellent discussion for the layman.
2. Spiegel, "Theory and Problems of Statistics," (paperback), Schaum Publ. Co., New York, 1961. Strong on illustrative examples.
3. Natrella, "Experimental Statistics," NBS Handbook 91, 1966 (revised). Excellent handbook, very extensive coverage, extensive tables.
4. Burlington and May, "A Handbook of Probability and Statistics with Tables," Handbook Publishers, 1958. Extensive tables.
5. Kelsey, "Introduction to Statistical Techniques Pertinent to Structural Analysis," Grumman Report No. ADR 02-12-64.1, September 1964.
6. Kelsey, "A Statistical Approach to Aircraft Landing Design Criteria, - Statistical Applications I," Grumman SMM No. 29, March 1966. Random Sampling Technique.
7. Kelsey, "Statistical Analysis of Suspended Tests - Statistical Applications III," Grumman STMECH No. 67.57, June 1967.
8. Kelsey, "Weibull Distribution - Statistical Application IV," Grumman, STMECH 67.81, September 1967.
9. King, "Graphical Data Analysis with Probability Papers," Technical and Engineering Aids for Management, Lowell, Mass., 1966.

B. Reliability and Designed Experiments

10. Pieruschka, "Principles of Reliability," Prentice Hall, 1963.
11. Lloyd and Lipow, "Reliability: Management, Methods, and Mathematics," Prentice Hall, 1962.
12. Shainin, Everdell, "Statistical Engineering Tools for Reliability," Lecture Series Notes by Rath and Strong, Inc., given at Grumman 1962 (two series).
13. Sprey and Van Gelder, "Small Sample Reliability Testing," Grumman GRD-105, 1964. Non-parametric confidence bands.
14. Cochran and Cox, "Experimental Design," Wiley, 1957.

C. Fatigue

15. ASTM STP #91-A, "Tentative Guide for Fatigue Testing and Statistical Analysis of Fatigue Data," 1958.
16. Kelsey, "Analysis of Fatigue Data - Statistical Applications II, Grumman SMM No. 44, August 1966.

D. Gust Loads and Power Spectral Density Techniques

17. Kelsey, "A Physical Interpretation of Generalized Harmonic Analysis," Grumman SMM No. 14, December 1959.
18. Crandall and Mark, "Random Vibration," Academic Press, 1963.
19. Press and Steiner, "An Approach to the Problem of Estimating Severe and Repeated Gust Loads for Missile Operation," NACA TN 4332, September 1958.
20. Press, Meadows, and Hadlock, "Reevaluation of Data on Atmospheric Turbulence and Airplane Gust Loads for Application Spectral Calculations," NACA Report 1272, 1956.
21. Press and Tukey, "Power Spectral Methods of Analysis and their Application to Problems in Airplane Dynamics," AGARD Flight Test Manual, Vol. IV, Pt. IVC.

Symbol List

The symbols are grouped according to their most common usage. Standard notation is used wherever possible, although this leads to some duplication of notation.

Population parameters:

μ	mean value
σ^2	variance
σ	standard deviation
N	size of a finite population (populations usually assumed infinite)

Sample statistics:

$\bar{x}$	the bar denotes the mean value (of the random variable x)
x_k	k^{th} percentile of probability distribution of x, e.g., x_{10} is the 10^{th} percentile
s^2	variance
s	standard deviation; when used with sampling distribution called standard error
V	coefficient of variation (also applicable to populations)
n	sample size

Distributions:

f_i	frequency (number of occurrences) of the i^{th} value of a discrete variable; frequency of the variable in the i^{th} interval for a continuous variable
f(x)	probability density function for random variable x
F(x)	cumulative probability distribution function

Normal Distribution:

μ, σ	mean, standard deviation; the two parameters completely defining a normal distribution
z	standard normal deviate (Table 1) = $(x-\mu)/\sigma$, where x is normally distributed

x_L, x_A, x_B one-sided lower tolerance limits; the A and B limits are the strength allowables of MIL-HDBK-5

K one-sided tolerance factor (Table 6)

Log-normal Distribution:

N cycles to failure (for fatigue data)

$\hat{N}$ geometric mean of random variable N

g geometric dispersion

Weibull Distribution:

x_o origin of distribution

θ characteristic value

m Weibull slope or shape parameter

Binomial Distribution:

p probability of a single random event

q compliment to p = 1-p

n number of independent trials

r number of occurrences in n trials

$P_n(r)$ probability of r occurrences in n trials; binomial probability density function.

Poisson Distribution:

r number of occurrences (per unit time)

m expected number of occurrences

P(r) probability of exactly r occurrences; Poisson probability density function.

Confidence Levels:

γ confidence level

α significance level

f degrees of freedom

x_ℓ, x_u lower, upper confidence limit of statistic x

The t Distribution - sampling distribution of the sample means:

$t_{\alpha,f}$ — t percentile at α significance level for f degrees of freedom

The χ^2 Distribution - sampling distribution of the sample variances:

$\chi^2_{\alpha,f}$ — χ^2 percentile at the α significance level for f degrees of freedom

E_i — expected frequency in i^{th} class or interval

O_i — observed frequency in i^{th} class or interval

Probability:

$P\{A\}$ — probability of occurrence of event A

$P\{A|B\}$ — conditional probability, probability of occurrence of event A given the occurrence of event B

$E\{x\}$, $E\{g(x)\}$ — expected value of the random variable x, of the function g(x); equivalent to mean value

R — reliability, probability of non-failure; for structures, the probability that the strength exceeds the applied load

Miscellaneous:

C_n^r — combinations of n things taken r at a time

P_n^r — permutations of n things taken r at a time

$n!$ — n factorial $= n(n-1)(n-2).....3.2.1$

$\sum$ — Greek capital sigma, denotes summation, i.e.,

$$\sum_{i=1}^{k} x_i = x_1 + x_2 + \ldots + x_{k-1} + x_k$$

$\prod$ — Greek capital pi, denotes multiplication, i.e.,

$$\prod_{i=1}^{k} x_i = x_1 x_2 x_3 \cdots x_{k-1} x_k$$

DISCUSSION

Terminology and Definitions

In many engineering applications data is obtainable for only a limited number of any particular component. Statistics provides a mathematical basis for inferring the characteristics of the entire theoretical population of such components and for setting probabilistic limits to the accuracy of these predicted characteristics. Proper use of the statistical techniques requires a familiarity with the basic terminology; a brief discussion of the more important terms follows.

The population or universe is an entire class of objects having some common observable characteristics; such characteristics are called the population parameters. Populations can be either discrete or continuous depending on whether they contain enumerated or measured data. A set of items chosen from the population is called a sample. The sample is generally considered large if it contains 30 or more data points, small if it contains less than 30 points. If all the members of the population have an equal chance of being selected, the set is a random sample; if some members are more likely to be selected, the sample is said to be biased. Two random samples or random variables are independent if the selection of one has no effect on the characteristics of the other. A statistic is a characteristic calculated from the sample; it is used as an estimate of the corresponding population parameter.

The frequency of the data is the number of observations falling within some specified measurement interval. A frequency diagram, histogram, or bar diagram is a block representation of the data showing the frequency of the data measurements within some class interval. A probability density function can be pictured as a continuous relative frequency diagram showing the expected relative frequency of the data per unit measurement interval. The area under a portion of the probability density curve bounded by two abscissa values is the probability (or relative frequency) of occurrence of the variable between those limits. The cumulative probability distribution function is the total probability of occurrence of all the values of the variable up to and including the

specific value in question. Numerous probability density and distribution functions have been evaluated and tabulated; the most common and useful of these is the Gaussian or Normal probability density function.

Consideration of one, two, or more characteristics of an individual leads to a univariate, bivariate, or multivariate distribution in the population. Unless specifically stated to the contrary, further discussion is restricted to univariate distributions.

Measures of Central Tendency and Scatter - The basic statistical measures deal with the central values and the scatter of the data. Greek letters are conventionally used to denote population parameters and Latin letters are used for the sample statistics.

The mean value is the simple arithmetic average of the data points. It corresponds physically to the coordinate of the center of gravity of the area under the probability density curve. The population mean μ and the sample mean $\bar{x}$ are given by

$$\mu = \frac{1}{N}\sum_{i=1}^{N} x_i \quad \text{and} \quad \bar{x} = \frac{1}{n}\sum_{i=1}^{n} x_i$$

where N and n are the number of discrete points in the population and sample respectively. When multiple values of x_i occur, the weighted mean is more convenient. Letting f_i be the frequency of x_i gives

$$\bar{x} = \frac{1}{n}\sum_{i=1}^{k} f_i x_i, \text{ where } i = 1, 2, \ldots, k, \text{ and } n = \sum_{i=1}^{k} f_i$$

The geometric mean value of a sample of size n is the n^{th} root of the product of the n data points,

$$\hat{x} = \left\{\prod_{i=1}^{n} x_i\right\}^{1/n}$$

This is equivalent to the antilog of the mean value of the logarithms of the data points. Thus

$$\log \hat{x} = \frac{1}{n}\sum_{i=1}^{n} \log x_i = \overline{\log x_i}$$

(This is commonly used in the analysis of fatigue data with the assumption of a log-normal distribution.)

The median is the halfway point in the sample readings when they are ordered by size. It is the 50th percentile, dividing the area under the probability density curve into two equal parts. In general, the k^{th} percentile divides the data into two parts with k% being below and (100-k)% above the percentile. For a discrete sample of size n, the median equals $x_{(n+1)/2}$ for n odd, and equals $\frac{1}{2}(x_{n/2} + x_{n/2+1})$ for n even.

The mode is the most frequent value in a set of observations. For symmetrical distributions having a single mode, the mean, median, and mode coincide.

The midrange of a sample is the arithmetic average of the smallest and largest values in the sample. The range is the difference between the largest and smallest values.

The most useful measure of the data spread or scatter about the central value is the standard deviation. For a population of N points this is given by

$$\sigma = \left[\frac{1}{N}\sum_{i=1}^{N} (x_i - \mu)^2\right]^{\frac{1}{2}},$$

the square root of the average of the squared deviations from the mean.

The population variance, σ^2, is the square of the standard deviation; it is physically equivalent to the moment of inertia about the mean value. Variances are calculated for various statistics or functions of statistics, where the variance of the function F is commonly denoted by Var F, $\sigma^2(F)$, or σ_F^2. The sample standard deviation and variance, denoted by s and s^2, are defined by

$$s^2 = \frac{1}{n-1}\sum_{i=1}^{n} (x_i - \bar{x})^2$$

Rearranging,

$$s^2 = \frac{1}{n-1}\left[\sum x_i^2 - \frac{1}{n}(\Sigma x_i)^2\right] = \frac{1}{n-1}\left[\sum x_i^2 - n(\bar{x})^2\right]$$

The latter form is more convenient for computation. As defined above with (n-1) rather than (n), s^2 is an unbiased estimate of σ^2. Care must be taken in using the formulas involving s^2 as some authors define the sample variance with (n) rather than (n-1); this must be reflected in all equations using s^2.

The terms mean-square and root-mean-square value (rms) are often used in random vibration applications. They are similar to the variance and standard deviation except that the deviations are taken relative to the zero value rather than the mean. In the case where the mean value is zero the terms become equivalent.

The coefficient of variation, V, shows the relative scatter between different sets of data. It is defined as the ratio of the standard deviation to the mean value, thus

$$V = \frac{s}{\bar{x}}, \text{ or } V = \frac{\sigma}{\mu}$$

The expectation is used (by the theorist) in referring to the various averages of probability distributions. The expected value of a random variable x, denoted E{x}, is identical to the mean value of x. Thus

$$E\{x\} = \mu$$

For the case of discrete data

$$E\{x\} = \mu = \frac{1}{N}\sum_i f_i x_i = \sum_i (f_i/N)x_i = \sum_i f(x_i)x_i ,$$

where $f_i/N = f(x_i)$ is the relative frequency of x_i, or equivalently, the probability density function of x. The expected value is merely the summation of all values of the variable weighted by the corresponding probabilities.

For a continuous random variable x, with probability density function f(x), the expected value of x is defined by

$$E\{x\} = \int_{-\infty}^{\infty} f(x)x\,dx$$

Similarly, the expected value of any real-valued function of x, say g(x), is given by

$$E\{g(x)\} = \int_{-\infty}^{\infty} f(x)\ g(x)\,dx.$$

The variance, for example, is given by

$$\sigma^2 = E\{(x-\mu)^2\} = \int_{-\infty}^{\infty} f(x)\ (x-\mu)^2\,dx$$

Since E{ } is a linear operator, this can be simplified. Thus

$$\sigma^2 = E\{(x-\mu)^2\} = E\{x^2-2\mu x+\mu^2\} = E\{x^2\} - E\{2\mu x\} + E\{\mu^2\}$$

$$= E\{x^2\} - 2\mu\ E\{x\} + \mu^2$$

$$= E\{x^2\} - \mu^2$$

Combination of Independent Random Variables - Several fundamental relationships for the mean value and variance follow:

a. Coded values. To simplify computation, coded values are often used which allow the use of smaller numbers, whole numbers rather than decimals, etc. The set of measurements x_i are evaluated in terms of the coded values y_i, and the results are then transformed back into the x_i. Specifically:

1. Let $y_i = (x_i - a)/b$, where a and b are any convenient constants.
2. Compute $\bar{y}$ and s_y^2.
3. Then $\bar{x} = a + b\bar{y}$ and $s_x^2 = b^2 s_y^2$.

Note that this procedure is very useful for hand calculations, but becomes of marginal value with a desk calculator.

b. Linear combination of independent random variables. Let z_i represent several independent random variables with means and variances denoted by μ_i and σ_i^2. The individual frequency distributions are unspecified. Let y be some linear combination of these variables, i.e.,

$$y = \sum_i c_i z_i \text{ , where the } c_i\text{'s are constants.}$$

The combined population is also a random variable with parameters μ_y and σ_y^2, where

$$\mu_y = \sum_i c_i \mu_i \quad \text{and} \quad \sigma_y^2 = \sum_i c_i^2 \sigma_i^2$$

In the special case where the z_i's are normally distributed, y will also be normally distributed.

c. General (non-linear) function of independent random variables.

Let z_i represent several independent random variables with means and variances denoted by μ_i and σ_i^2. If Z is some function of the z_i, $Z = Z(z_i)$, then the mean and variance of Z are given approximately by

$$\bar{Z} = Z(\mu_i) + \tfrac{1}{2} \sum_i \sigma_i^2 \frac{\partial^2 Z}{\partial z_i^2}$$

$$\sigma_Z^2 = \sum_i \sigma_i^2 \left(\frac{\partial Z}{\partial z_i}\right)^2$$

where the partial derivatives are evaluated at the means values of the z_i. (Assumes Z is reasonable smooth within $\pm 3\sigma_i$ for each z_i).

Sampling Distribution

Consider an infinite population with parameters μ and σ and with an arbitrary probability distribution. Take all possible samples of size n from this population. Calculate the mean value $\bar{x}$ for each sample. The distribution of the resulting $\bar{x}$'s is known as the sampling distribution for the means. The mean value and standard deviation (often called standard error) for this new distribution are denoted $\mu_{\bar{x}}$ and $\sigma_{\bar{x}}$. The sampling distribution for the means is the t-distribution. It approaches the normal distribution for large samples. In the special case where the original population is normally distributed, the sampling distribution for the means is also normally distributed.

Similarly there are sampling distributions for all the other major statistics. The most important after the t-distribution is the χ^2-distribution, the sampling distribution for the variances.

The mean value for these sampling distributions is the statistic itself, e.g., $\mu_{\bar{x}} = \mu$. Several common standard errors are listed below.

Mean: $\sigma_{\bar{x}} = \sigma/\sqrt{n}$

Variance: $\sigma_s^2 = \sigma^2\sqrt{2/(n-1)}$

Std. Dev: $\sigma_s = \sigma/\sqrt{2(n-1)}$

Median: $\sigma_{med} = 1.25\,\sigma/\sqrt{n}$

Degrees of Freedom

The number of independent measurements available for calculating a statistic is called the degrees of freedom for that statistic. For example, in estimating the variance from a sample of size n, 1 degree has been used in calculating the mean. There are (n-1) degrees left for the variance. In general, if k independent linear

relations are imposed on a sample of n values, there are (n-k) degrees of freedom left for a further estimate. Several statistical tables refer to degrees of freedom rather than sample size.

Confidence Level

The sample statistics as defined in the previous section represent best point estimates of the true, but unknown population parameters. While estimates calculated from other samples will differ, one would expect these differences to become smaller as the samples become larger, approaching the true value in the limit. If an estimate is unbiased, it should overestimate the true parameter 50% of the time and underestimate it 50% of the time.

To be meaningful the accuracy of the estimate must accompany the statistic. This is done by computing a confidence interval about the statistic. This interval depends on the desired confidence level and on the sample size. The confidence level (γ) defines the probability that the true population parameter will be within the computed interval. More generally, we may define the confidence level as the probability that the accompanying statistical statement is true.

The confidence level commonly used in engineering practice is 95%. This is reasonable providing the sample is sufficiently large. For very small samples a smaller level, such as 85%, is more reasonable; otherwise the interval becomes too large to be of practical use. In the typical case of estimating a mean value, a confidence level of 95% says that we are 95% confident that the true population mean lies in the calculated interval. In other words, if we took a large number of samples of size n from the given population, in 95% of these samples the true mean would lie in the calculated interval; in 5% of the samples the interval would not contain μ . This possible error of 5% is called the significance level (α).

The confidence interval is obtained by using tables based upon the sampling distribution of the particular statistic together with the standard error of the statistic. The confidence level corresponds to the area under the probability density curve of the sampling distribution bounded by the confidence limits defining the interval. These limits may be symmetrical about the statistic or one-sided depending on the particular case.

The most common confidence interval is that associated with a mean value. For a population with unknown parameters μ and σ, the population mean value would be estimated as

$$\mu = \bar{x} \pm t_{\alpha,f}\, s_{\bar{x}} = \bar{x} \pm t_{\alpha,f}\, \frac{s}{\sqrt{n}}$$

where $\bar{x}$ = sample mean value

$s_{\bar{x}}$ = the standard error of the sample means $= s/\sqrt{n}$

s = sample standard deviation

$t_{\alpha,f}$ = t-distribution value for a significance level of α, i.e., a confidence level of $(1-\alpha)$, and for $f = n-1$ degrees of freedom (from Table 3).

This represents a two-sided symmetrical confidence interval about the mean value. Note that α, the signficance level, represents the total area under the t-distribution curve <u>outside</u> the interval, with $\alpha/2$ being the area under each excluded tail.

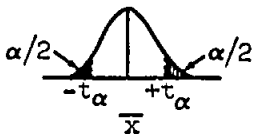

γ = Confidence Level = $1-\alpha$

α = Significance Level

Thus for a single-sided confidence limit (upper or lower), $\alpha/2$ represents the total significance level; the tabular t-value must be selected accordingly. This is illustrated in the section labelled "Calculation of Sample Statistics."

Referring to the sketch above, the limiting cases are instructive. For a 100% confidence level, $\alpha = 0$, and the confidence interval extends to infinity on both sides of the sample mean. On the opposite extreme $\alpha = 100\%$, and the confidence interval shrinks to zero. Thus in predicting the population mean using the sample mean alone, the associated confidence level is 0%. While somewhat ambiguous, this merely says that the probability of the population mean being <u>exactly</u> equal to the sample mean is zero. It is more meaningful to consider a single sided interval, say the lower bound. For a 100% confidence level, we can say the population mean is no less than $-\infty$. As the confidence level is lowered the interval decreases, until at a 50% confidence level ($t = 0$), we can say the population mean is <u>no less than</u> the sample mean at the 50% confidence level. Similarly we can say the population mean is <u>no more than</u> the sample mean at the 50% confidence level. In other words,

point estimates derived from sample data can be interpreted as "median" values, which will overestimate the true value 50% of the time and underestimate the true value 50% of the time.

Sample Size as a Function of Confidence Level: Since the confidence interval depends on sample size, the problem can be reversed as follows. Given a maximum allowable error in a mean value estimate at a specific confidence level, what is the minimum sample size required to produce this interval? Letting 2R be the length of the symmetrical interval, the minimum size is found by rearranging the last equation.

$$2R = 2\left|\mu - \bar{x}\right| = 2\, t_{\alpha,f}\, \frac{s}{\sqrt{n}}$$

$$\text{so} \quad n = \left[\frac{t_{\alpha,f}\, s}{R}\right]^2 \text{, (rounded up to next integer).}$$

If σ is known the required sample size can be immediately calculated. For σ unknown,

1. Using a best estimate (guess) for σ, calculate n_{est}.
2. Choose $n_1 < n_{est}$, say about $.5n_{est}$, depending on expected accuracy of n_{est}.
3. Perform required measurements on sample of size n_1. Calculate s_1.
4. Compute required value of n using new estimate s_1.
5. Complete tests on balance of required sample.

In some cases the population standard deviation may be known from prior (extensive) data. As expected, this results in a smaller confidence interval. A known standard deviation allows the use of the normal distribution rather than the t-distribution, giving for the symmetrical interval.

$$\mu = \bar{x} \pm z_{\alpha/2}\, \sigma_{\bar{x}} = \bar{x} \pm z_{\alpha/2}\, \sigma/\sqrt{n}$$

where $z_{\alpha/2}$ is the value of the normal deviate at the $\alpha/2$ percentile.

Confidence intervals for the variance (and thus the standard deviation) make use of the chi-squared distribution (Table 5). For a two-sided interval at the $100(1-2\alpha)\%$ confidence level, the limits are given by

$$\frac{f}{\chi^2_{\alpha}} s^2 \leq \sigma^2 \leq \frac{f}{\chi^2_{1-\alpha}} s^2.$$

Confidence intervals can in general be constructed about any statistic. Tables derived from the sampling distributions are available for the more important cases, e.g., variance, standard deviation, proportions, etc. (Reference 3). In addition, but of less importance, confidence bands can be constructed for sample distributions (Ref. 3, 4, 13).

For the general case of a statistic which is some function of one (or more) random variable(s), confidence intervals can also be constructed, again using the t-distribution. Let $G_{u,\ell}(x)$ be the upper and lower confidence limits for the function $G(x)$. Then

$$G_{u,\ell}(x) = G(x) \pm t_{\alpha,f}\, s_{G(x)}$$

where $s_{G(x)}$, is the standard error of $G(x)$ (See page 2-7).

Tolerance Limits - Design Allowables - Tolerance limits enclose at least P% of the population at a specified confidence level. The percentage P is variously referred to as the population coverage, proportion, or conformance level. Tables are available for both symmetrical (Ref. 3) and one-sided limits (Table 6) based on the normal distribution. The tables give a K-factor as a function of the confidence level, proportion, and sample size. For one-sided limits at least P% of the population will lie above $\bar{x}$ - Ks with the given confidence.

The "A" and "B" design allowable strength levels of MIL-HDBK-5 are common one-sided (lower) tolerance limits. They are defined as follows:

"A" level - that strength which would be exceeded by at least 99% of the entire population with a confidence of 95%.

"B" level - that strength which would be exceeded by at least 90% of the population with a confidence of 95%.

This is illustrated in the sample problem section.

The difference between confidence limits, statistical tolerance limits, and engineering tolerance limits should be noted. Confidence limits bound a point statistical estimate. Statistical tolerance limits bound a stated proportion of a population. Engineering tolerance limits are outer limits of acceptability usually prescribed by a design engineer.

Note that these tolerance limits are applicable only to normal distributions. For other type distributions one can use distribution-free tolerance limits (Reference 3). However, unless a large sample is available, these of necessity lead to fairly broad limits.

Reliability - In general, reliability is the probability of the successful operation of a device for a specific time under specific conditions of use and environment. As applied to structural elements, the reliability is the probability that the strength will exceed the applied load under specific service usage. In general, both load and strength levels are represented by probability density functions. See sample problem section.

Design of Experiments - An experiment is generally conducted to determine if a suspected effect exists, and if so, to determine the magnitude of the effect. When only the effect of one factor upon another is of interest the experiment is usually simple. When several factors are involved the design of the experiment can become important. The classical method restricts attention to one variable at a time, the other factors being held fixed. While appearing simple, this procedure is generally inefficient and restricts the conclusions that can be drawn from the data.

Recent statistical techniques have been developed to optimize the design of experiments from the viewpoint of obtaining a maximum amount of information with a minimum of experimental cost. These techniques allow several factors to vary simultaneously in a specific integrated experimental design. This permits the determination of not only the main effects (as in the classical approach) but also provides information about the interactions present, the existence of unsuspected factors, and the experimental error.

Various statistical procedures are available for analyzing the data obtained from a multi-factor designed experiment. One of the more important of these techniques is called the analysis of variance. This consists essentially of dividing the total variance of the test results into components which can be associated with the various main effects, interactions, and residual effects. The variance ratio test (F test) is used to determine the significance of the various results.

A detailed discussion of this subject can be found in References 3, 12 and 14.

Probability Distributions

One of the simplest ways to reveal the general nature of a population distribution is to construct a histogram or bar diagram. Suppose we had a large number of material strength measurements. We would first divide the range of the strength data into equal-sized intervals and tabulate the number of times (i.e., frequency) that the data fell into each interval. A bar diagram is then drawn where the height of each rectangle equals the frequency of the data in that interval (see sketch). The frequency is usually divided by the total sample size, giving a relative frequency ordinate. The area in each rectangle is then the proportion of the total sample having values in that particular interval. As the sample size is increased and interval width decreased, the histogram will approach a continuous curve (dashed curve). The probability density function is such a curve where the area under the curve between two abcissa's represents the probability that a random value of the variable will fall between those values. Since the total probability must be unity, the ordinate scale is normalized so that the total area under the curve equals unity. The sketch above is typical of symmetrical unimodal probability density functions, and is the most common shape for physical applications. Other possible shapes are sketched below.

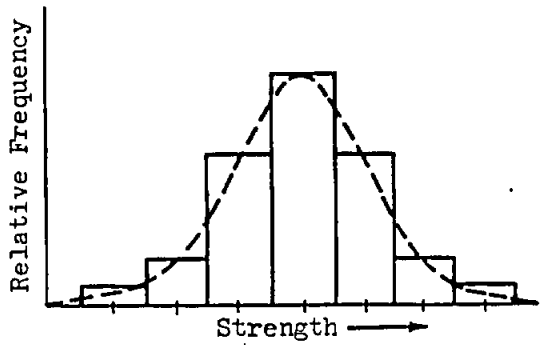

Figure 2.2-1 Typical Histogram, Symmetrical Probability Density Function (Dashed)

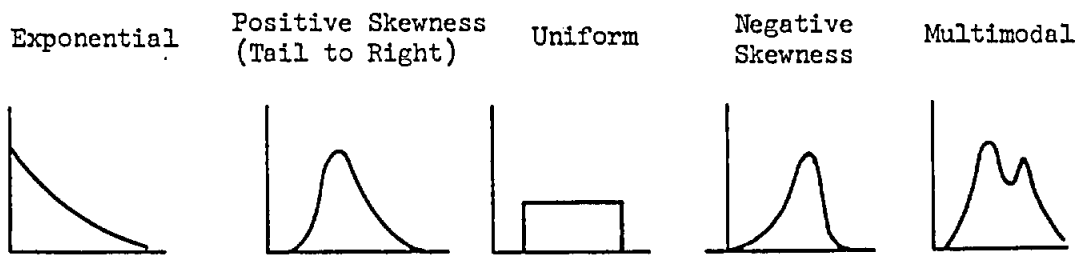

Figure 2.2-2 Probability Density Functions of Various Shapes

The two modes in the last sketch usually indicate a mixed sample, containing data from two different populations. These shapes are for continuous density functions. The same general shapes can apply to discrete functions, but the curves would be discontinuous as in the histogram.

Note that the density function is not a direct measure of the probability; however, the area under the density curve is. The cumulative probability distribution is the direct measure of probability, being the integral of the density function from $-\infty$ to a specific value of the variable. While the density function shows the general nature of the function, the distribution is more useful.

Analytic expressions have been found which fit many common physical distributions. To simplify treatment, special probability paper has been designed for many of these. This is discussed in Section F3. Several of the more important distributions are discussed in the following paragraphs.

Gaussian Probability Density Function

The most useful probability density function in applied statistics is the Gaussian or Normal function. This provides a good approximation to many actual physical distributions, and is the basis for many applications such as tests of significance, quality control work, etc. Because of its mathematical simplicity, transformations are often made upon non-normal data so that the transformed data is normal. For example, material static strength is usually normally distributed, whereas fatigue life frequently has a log-normal distribution, i.e., the log (life) is normally distributed.

The Gaussian probability density function, f(x), is given by

$$f(x) = \frac{1}{\sqrt{2\pi}\,\sigma}\, e^{-\frac{1}{2}\left(\frac{x-\mu}{\sigma}\right)^2}$$

where μ and σ are the mean and standard deviation of the random variable x. This is the familiar bell-shaped curve symmetrical about its mean value, as shown in Fig. 2.2-3a.

The area under the curve represents the probability of occurrence or the relative frequency of the variable x. The total area under f(x) between $\pm\infty$ is unity by definition. Note that 68.2% of the distribution lies within $\pm 1\ \sigma$ of the mean, 95.4% within $\pm 2\ \sigma$'s, and 99.7% within $\pm 3\ \sigma$'s.

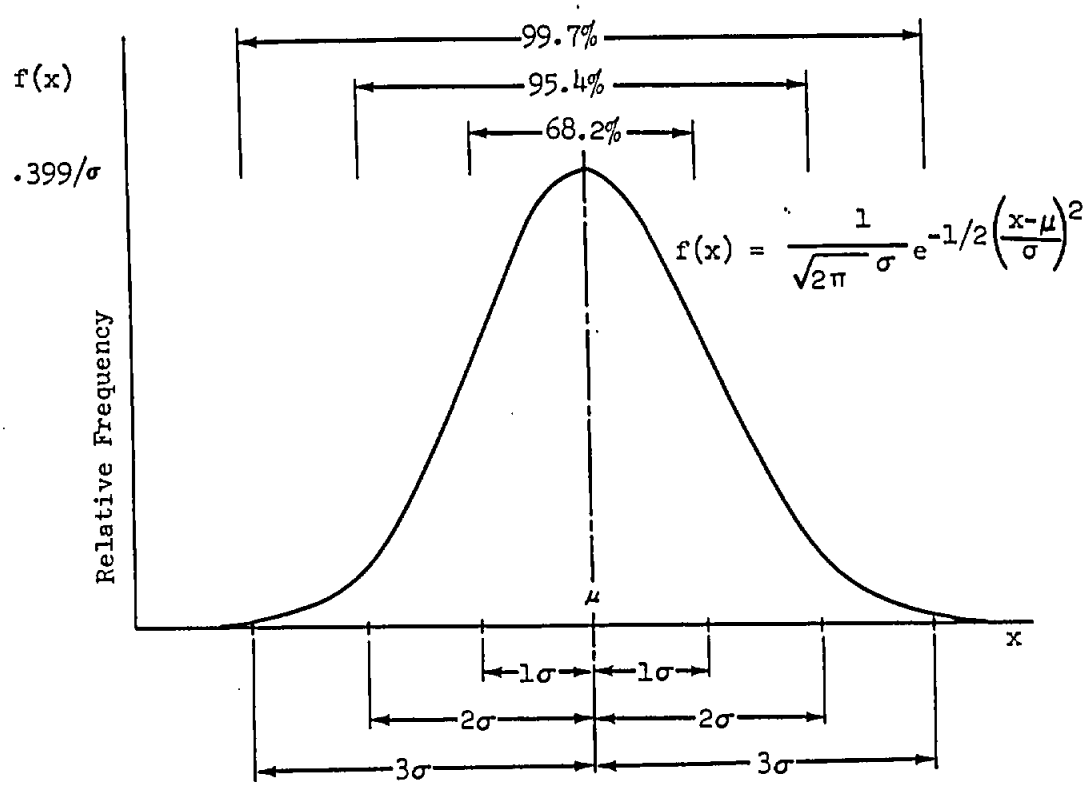

Figure 2.2-3a Normal Probability Density Function

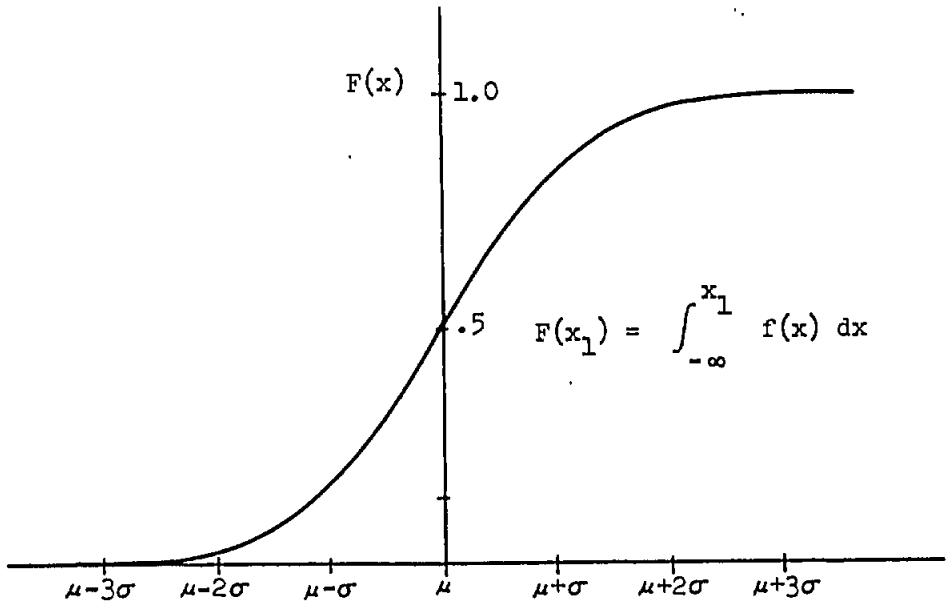

Figure 2.2-3b Cumulative Normal Distribution Function

The cumulative normal probability distribution function, $F(x)$, is a direct measure of the probability, being the total area under the density curve from $-\infty$ to the point x (Figure 2.2-3b).

$$F(x) = \int_{-\infty}^{x} f(x)dx$$

Both the density and cumulative distribution functions are commonly expressed in standardized form in terms of the standard normal deviate z, where $z = (x-\mu)/\sigma$. The resulting standardized functions then become:

$$f(z) = \frac{1}{\sqrt{2\pi}} e^{-z^2/2}, \text{ and } F(z) = \int_{-\infty}^{z} f(z)dz,$$

where now the mean is zero and standard deviation unity. These standard normal functions are readily available in tabulated form (Tables 1 & 2).

In practice, sample data is often plotted on normal probability paper. This paper has been designed so that the cumulative distribution will plot as a straight line rather than the curve of Figure 2.2-3b. This application is illustrated later.

Log Normal Distribution - The logarithmic transformation is the most common type of transformation made upon data to allow use of the normal distribution; it is used primarily as a first approximation to fatigue failure distributions. The equations and discussion for the normal distribution apply directly, where x is now interpreted as the logarithm of the random variable. The log-normal distribution is positively skewed (tail to the right), with a zero origin rising steeply to its maximum, and then tailing off to infinity. For the log distribution the (arithmetic) mean, mode and median coincide. In terms of the original data, the geometric mean and median coincide. In fatigue applications $x = \log N$, N being the cycles to failure. All statistics are calculated with the log data, i.e., in terms of x, and the results then transformed back into the original data, N.

The basic parameters for the log-normal distribution in terms of the original data are the geometric mean and geometric dispersion, where:

$$\text{Geometric mean} = \hat{N} = \text{antilog } \bar{x}$$

$$\text{Geometric dispersion} = g = \text{antilog } s$$

The percentage of the population in the interval

$$\hat{N}\, g^{-z} < N \leq \hat{N}\, g^{z}$$

is identical to that of the normal distribution for the interval

$$\mu - z\sigma < x \leq \mu + z\sigma$$

where z is the standard normal deviate for both cases. For example, 95.4% of a normal population falls within $\pm 2\,\sigma$ of the mean value. For a log-normal population, 95.4% falls between $\hat{N}\, g^{-2}$ and $\hat{N}\, g^{2}$. See reference 16 for several applications of the log-normal distribution to fatigue data.

Weibull Distribution - This is an "extreme value" type distribution adaptable to a wide spectrum of probability density functions, ranging from exponential to highly skewed shapes. It is often applicable to material strength and fatigue. The cumulative distribution function is given by:

$$F(x) = 1 - e^{-\left(\frac{x-x_o}{\theta-x_o}\right)^m}$$

where $F(x)$ = fraction at or below the strength x, where $x \geq x_o$.

x_o = origin of distribution, often equal to zero in structures applications.

θ = "characteristic strength," the measure of central tendency, where $F(\theta) = .632$ independent of the other parameters.

m = "Weibull slope," the shape parameter, $m > 0$.

The wide range of possible shapes for the density function is illustrated in the following sketches:

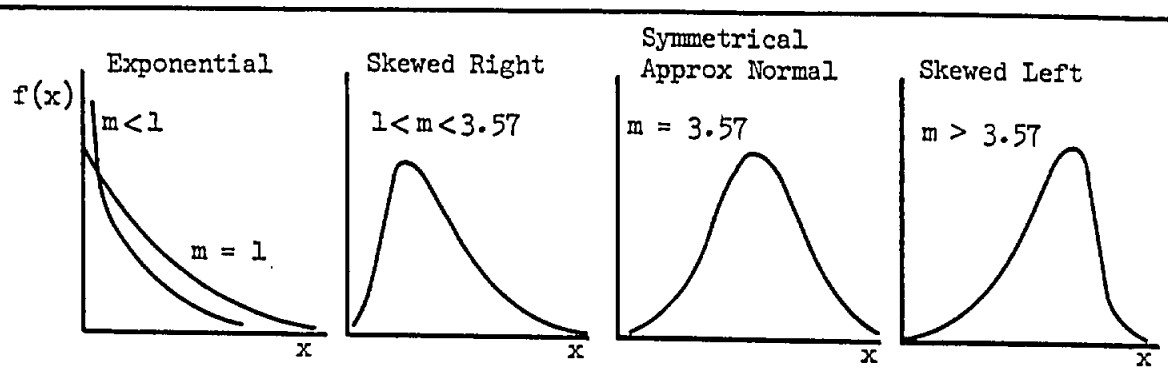

Figure 2.2-4 Typical Weibull Probability Density Curves

Because of the analytic complexity, Weibull distributions are always handled graphically on special Weibull probability paper. A unique feature of the graphical treatment is the fact that samples containing multiple failure mechanisms are immediately apparent when the data is plotted.

A detailed discussion of this distribution is available in Reference 8.

Rayleigh Distribution - Also called the radial normal or the two-dimensional error distribution. As used in acoustic fatigue applications, it represents the distribution of the response peaks (or envelope) of a lightly damped single-degree-of-freedom system to random Gaussian excitation. It is a special case of the Weibull distribution with a zero origin and Weibull slope of 2. The distribution function is given by:

$$F(x) = 1 - e^{-x^2/2}$$

where x = ratio of peak response to rms response, $x \geq 0$.

$F(x)$ = probability of a random value being equal to or less than x

μ_x = 1.257, mean value

σ_x^2 = .429, variance

Binomial Distribution - This is one of the most common discrete distributions in applied statistics. It applies where each sample member is judged on some go - no go basis, such as heads or tails, a good or defective item, etc. It is derived from the binomial expansion:

$$(q + p)^n = q^n + npq^{n-1} + \frac{n(n-1)}{2!} p^2 q^{n-2} + \ldots + p^n$$

$$= \sum_{r=0}^{n} C_r^n p^r q^{n-r}$$

where C_r^n = number of combinations of n things taken r at a time

$$= \frac{n!}{r!(n-r)!}$$

If p is the probability of a single random event occurring and q = 1 - p is the probability that the event does not occur, then the probability that the event will occur exactly r times in n independent trials is given by $P_n(r)$, where

$$P_n(r) = C_r^n p^r q^{n-r}$$

This is the binomial probability density function for the integers r running from 0 to n. The cumulative distribution is the sum of successive terms starting with r = 0. Thus the probability that the event will occur k times or less in n trials is

$$\sum_{r=0}^{k} P_n(r) = \sum_{r=0}^{k} C_r^n p^r q^{n-r}$$

The mean and variance of the binomial distribution are given by $\mu = np$ and $\sigma^2 = npq$.

Tables are available for the density function, distribution function and for several confidence levels, Reference 4. Special probability paper is also available to simplify computation, Reference 12.

For large samples or for $p \approx q$, the binomial distribution can be approximated by the normal distribution. For large samples and very small p, it can be approximated by the Poisson distribution.

Poisson Distribution - This is used when the number of occurrences of an isolated event in some specific period is known and when non-occurrences may be meaningless. For example, it could represent the number of meteorites striking a specific area of the moon per month, or the number of auto fatalities in New York City per year. It assumes the conditions of the experiment are invariant with time, the number of occurrences is proportional to the time interval, and non-overlapping time intervals are independent.

The Poisson density function is given by

$$P(r) = \frac{m^r e^{-m}}{r!}$$

where $P(r)$ = probability of exactly r occurrences (per unit time)

m = expected or average number of occurrences (per unit time)

The cumulative distribution for k or less occurrences is $\sum_{r=0}^{k} P(r)$.

The mean and variance are equal, i.e., $\mu = \sigma^2 = m$. Tables and charts are available for the distribution functions (Ref. 4, 12).

The Poisson distribution can be used to approximate the Binomial distribution when the sample is large and probability of success small. In this case the expected value of the Poisson distribution is equated to the mean value of the Binomial distribution, i.e., $m = np$.

Graphical Treatment - Probability Paper

Sample data should always be plotted. In some cases approximate graphical results may be adequate in themselves; more important, the plot immediately gives information as to the nature of the distribution.

The simplest type of plot is the basic histogram, discussed on page F2.2-1, which approximates the probability density function. The shape of the distribution is readily apparent - the degree of symmetry or type of skewness, single or multi-modal nature, etc.; one can also get a rough estimate of the mode, median and mean values. However, little useful numerical data can be obtained from the histogram.

The preferred procedure is to plot the cumulative distribution directly on probability graph paper. Special probability paper has been developed for most of the common distributions, the most useful for structural applications being normal, log-normal, and Weibull paper. The advantageous feature of this graph paper is the fact that an exact probability distribution will plot as a straight line. Having such a straight line plot, the basic statistics and percentiles of the distribution can be read directly from the graph. A general discussion of the application of probability paper is found in Reference 9; additional discussion of Weibull paper is contained in Reference 8. Further discussion in this section is restricted to normal probability paper unless otherwise stated.

A sample sheet of normal probability paper is reproduced on Page F3.2-3. Note that the right hand probability scale F(x) represents the cumulative frequency or percentiles of the distribution, and runs between .01% to 99.99%. This is interpreted as the probability that a random value of the normal variable is equal to or less than x. The left hand scale is the complimentary probability, 1 - F(x), i.e., the probability of a random value being greater than x. The bottom linear scale is for the random variable x.

In practice, the sample data is plotted against its assigned cumulative frequency and a best fit curve is drawn thru the points. If a reasonably satisfactory straight line fit exists[1,2], normalcy is assumed and the desired statistics or percentiles can be read directly from the graph. For example, the mean value (equal to the median) is at the 50th percentile; the standard deviation is the difference between the mean value and the abcissa corresponding to the 84.13 (or 15.87) percentile point. If a straight line fit does not exist, one could then plot the data on some other type of probability paper. Note, however, that percentiles (but not statistics) can still be read off the curved line within the range of the data.

Two cases arise in the assignment of cumulative frequencies to the data points. For large samples (over 30 points), the data is grouped into equal length intervals, with one more significant figure being assigned to the boundaries than the data. While somewhat arbitrary, the number of intervals which provides the best fit depends on the sample size. The recommended number of intervals is 6 for 30-45 data points, 7 for 46-100 points, 8 for 100-200 points, and 9 for 200-400 points. The intervals are arranged in ascending order, and the frequency and cumulative frequency of the data tabulated for each interval. The cumulative frequencies are then plotted against the upper boundary of each interval.

For small samples the data is arranged in ascending order and a cumulative frequency assigned to each point. Either median ranks or mean ranks are satisfactory. The former are theoretically better, but the latter are simpler to use. Tables are available for the median ranks (Ref. 12). Where j is the order of the sample point in a sample of n points, the median rank is given by $(j-.3)/(n+.4)$ and the mean rank by $j/(n+1)$.

Confidence bands are often drawn about the plotted data. Various approximate methods appear in the engineering literature; these are not recommended in general. Non-parametric bands can be drawn if desired; these give a good indication of the extent of information possible from the sample (See Refs. 3, 12, and 14).

Cumulative frequencies are occasionally plotted on semi-log paper rather than on probability paper. This is done when the type of distri- is of no interest, and when it is desirable to expand the scale of one tail of the distribution. Load exceedance curves are typical.

---

1 See Section F2.4 for a Goodness-of-Fit statistical test.

2 The ideal best straight line fit would be the linear regression line of F(x) on x, equivalent to obtaining the straight line which minimizes the squared deviations of the percentiles from the line. The additional effort required to obtain this is usually not warranted. A "practical" best fit line can be obtained as follows:

1. Draw a good "eyeball" straight line thru the data.
2. Place the pencil point on the line across from the smallest plotted value; rotate a straight edge about this point so as to divide the points <u>above</u> the 50th percentile into 2 equal parts, i.e., half above and half below the line. Draw the new line.
3. Place the pencil point on the new line across from the top data point; repeat (2) for the points <u>below</u> the 50th percentile. Repeat steps 2 and 3 until convergence.

Statistical Decision Making

Tests of Significance - (Tests of Statistical Hypotheses) - Statistical decision making conventionally uses tests of significance. These tests are applicable to a wide variety of problems involving the evaluation of different processes. This is accomplished in various ways - by comparing the primary statistics, by comparing multiple categories of data, or by comparing an entire sample distribution to some standard distribution. Unfortunately, there are many such tests and many variations upon them, all of which are highly specialized. Consequently, proper usage becomes rather difficult. Because of the broad scope of the subject, the following discussion is restricted to general philosophy with one particular test described in detail. An alternative and much simpler approach to one type of these tests is discussed in the following section.

Suppose we wish to compare a new (presumably superior) manufacturing process to a standard process. The statistician adopts a Null Hypothesis, i.e., he assumes there is no real difference between the processes. He also tentatively assumes the new sample could have come from the standard population by chance and calculates the probability of this happening. If the probability of occurrence is reasonably high, he accepts the null hypothesis and concludes there is no real difference between the processes. On the other hand, if the probability of obtaining the sample from the population is very low, say under 5%, he would reject the null hypothesis at the 5% significance level as being an unlikely explanation. The significance level (α), selected in advance for the rejection of the hypothesis, represents an error of the first kind, that is, there is a 5% chance of rejecting the null hypothesis when it is true.

Failure to reject the null hypothesis when it is false is called an error of the second kind. This type error is summarized in the Operating Characteristic (OC) Curve for the specific test as a function of the significance level and sample size. The particular application dictates the optimum compromise between the two type errors and associated sample size.

All of the standard texts describe such tests in considerable detail; Reference 3 is particularly recommended. Reference 16 gives several examples in comparing the means and variances of two samples of fatigue data.

The Chi-squared (χ^2) Goodness of Fit Test - This is used to test the deviation of measured or enumerated data from some hypothesized model. For example, we might wish to determine if a sample of data was normally distributed, or whether the number of rejections in a production lot was excessive compared to the theoretical rejection rate. The χ^2 statistic is a measure of the deviation, where

$$\chi^2 = \sum_{i=1}^{k} \frac{(O_i - E_i)^2}{E_i}$$

O_i = observed frequency

E_i = expected (theoretical) frequency, (must be ≥ 5)

k = number of classes or intervals of the data.

The maximum values of $\chi^2_{\alpha,f}$ that can be expected with probability α for f degrees of freedom are tabulated (Table 5). The degrees of freedom is given by $f = (k-1) - j$, where j is the number of parameters in the theoretical model which had to be estimated from the sample data.

There are two restrictions. The expected frequency in each class or interval should be at least 5; intervals may be combined to satisfy this requirement. This implies a reasonably large sample -- the test accuracy falls off rapidly for samples under 30 in size. Second, an adjusted χ^2 statistic must be used where there is only one degree of freedom to correct for bias. In this case, use

$$\chi^2 \text{ (adjusted)} = \sum_{i=1}^{k} \frac{(|O_i - E_i| - .5)^2}{E_i}$$

If the expectation in one of the two classes is less than 5, even for large samples, the accuracy of the test decreases. This might occur for a large sample with only one degree of freedom. However, the test may be performed and if the calculated is sufficiently different from the tabulated value (say less than half or greater than twice) the test conclusions are reasonable. Otherwise the test should not be used.

Suppose we have a sample of strength data which appears normally distributed. We want to determine if the assumption of normalcy is valid at a 5% significance level. Procedure:

1. Calculate $\bar{x}$ and s from sample. Assume sample comes from a population with $\mu = \bar{x}$ and $\sigma \doteq s$.

2. Divide data range into intervals in terms of normal deviate z. Since at least 5 points are required in each interval, the z boundary values must be at least 10 percentiles apart, i.e., at least 10% of the population must be in each interval. Choose convenient z's satisfying this requirement. (In general the maximum number of intervals is desirable.)

3. Calculate expected and observed frequencies in each interval.

4. Calculate χ^2 statistic.

5. Find $\chi^2_{\alpha,f}$ from table, for $\alpha = .05$ and $f = (8-1) - 2 = 5$ degrees of freedom.

6. If $\chi^2 < \chi^2_{\alpha,f}$ the assumption of normalcy is valid at the 5% significance level. If $\chi^2 > \chi^2_{\alpha,f}$, reject assumption.

Confidence Level Approach - An alternate method of statistical decision making uses the confidence interval; because of its simplicity is should be used whenever applicable (in preference to tests of significance). Suppose a sample of data from a new manufacturing process is to be compared to the standard process. Assuming that the mean value is the parameter of interest, we could calculate a confidence interval about the new mean, say at a 95% confidence level. If this interval lies completely above the standard mean value, we are justified in concluding that the new process is, on the average, better than the standard, with only a 5% risk of error. Depending on the application, a lower confidence level, e.g., 90% or 85%, giving a smaller interval might be satisfactory. In any case the size of the interval gives an indication of how large the difference is between the two processes.

Whenever the decision can be evaluated in terms of a confidence level, this approach is recommended in preference to the test-of-significance approach because of its basic simplicity. Refer to Section F2.1 of this manual for a discussion of confidence levels.

Random Sampling

In order to make accurate predictions of population characteristics from sample data, the sample must be selected at random. Simple random sampling is defined by the requirement that each member of the population have an equal chance of being the first member of the sample; each of the remaining members has an equal chance of being drawn second, etc. It is necessary that each possible sample from the population have an equal chance of being selected.

This is not quite as simple as it seems. Randomness is a property of the sampling scheme and not of the sample itself. It is virtually impossible to unconsciously draw a sample at random; a sample drawn haphazardly, without any conscious plan, seldom is a valid random sample. Consequently, some mechanical randomization scheme is required.

The simplest random sampling scheme makes use of random number tables; two such tables are included for illustration in Section F4 in excerpted form. (Much larger tables should be used for any large problem; repeated use of the same portion of a random number table destroys the randomness.) Referring to Table 7, page F4-7, note that the random number table consists of rows and columns of two-digited numbers. These can be treated as decimals or whole numbers using as many digits (significant figures) as required. One enters the table at some arbitrary point and reads down a column consecutively the desired number of random numbers. Note that 0 can be interpreted as the first or last number in a population of 10; similarly 00 can be interpreted as 0 or 100 in a population of 100, etc.

For example, if we have a finite population of 750 members, we would assign one number (from 1 - 750) to each member. To obtain a random sample of 20 members, we would enter the table at some arbitrary point, and read off 20 consecutive 3 digited numbers falling between 001 and 750. Numbers outside the range and duplicated numbers would be skipped over.

Under some circumstances it might be desirable to divide a large population into intervals with 1 number assigned to each interval. In this case the intervals must be selected so that each has the same probability of occurrence.

In the case of sampling from a normal population one would use the Table of Random Normal Deviates, page F4-8. The selection procedure is the same as above except that each tabulated value (the standard normal deviate z_i) must be transformed into corresponding values of the actual random normal variable x_i, using $x_i = \bar{x} + z_i s$.

Basic Probability Relationships

Probability Laws - The fundamental probability laws, necessary for many statistical applications, are summarized below.

Definition: If N events are possible, and n_A is the number having an attribute A, then the probability of A occurring in any single trial is denoted by $P\{A\}$, where

$$P\{A\} = \frac{n_A}{N}$$

The events must be mutually exclusive and equally likely.

Laws:

1. Multiplication: If A and B are independent events, the probability of both events occurring is

$$P\{A \text{ and } B\} = P\{AB\} = P\{A\}\ P\{B\}$$

Similarly

$$P\{A_1 A_2 \ldots A_r\} = \prod_{i=1}^{r} P\{A_i\}$$

2. Addition

a) If A and B are independent and mutually exclusive, i.e., $P\{AB\} = 0$, the probability of either A or B occurring is

$$P\{A \text{ or } B\} = P\{A\} + P\{B\} .$$

Similarly $P\{A_1 \text{ or } A_2 \ldots \text{ or } A_r\} = \sum_i P\{A_i\}$

b) For A and B independent but not mutually exclusive, the probability of at least one occurring is $P\{A \text{ and/or } B\} = P\{A\} + P\{B\} - P\{AB\}$

Similarly $P\{A \text{ and/or } B \text{ and/or } C\} = P\{A\} + P\{B\} + P\{C\} - P\{AB\} - P\{BC\} - P\{AC\} + P\{ABC\}$

This can be extended to any number of terms where terms having an odd number of events are positive, an even number negative.

3. Conditional Probability - If an event B is contingent upon the prior occurrence of an event A, the probability of B occurring is called a conditional probability, denoted $P\{B|A\}$. The probability of the combined event is

$$P\{AB\} = P\{A\}\ P\{B|A\}$$

4. Bayes' theorum on Inverse Probability - If event A is dependent on one of several mutually exclusive events B_1, B_2 ..., B_n, and if A has occurred, then the probability that B_k has occurred is

$$P\{B_k|A\} = \frac{P\{B_k\}\ P\{A|B_k\}}{P\{B_i\}\ P\{A|B_i\}}$$

Permutations and Combinations - The solution of problems based on an a priori probability involves the determination of the number of events whose probability is to be found and the total number of events possible for the particular situation. The calculation of the number of events is facilitated by recourse to the rules of permutations and combinations. In a sample of discrete items from a large population, the sample represents a combination of items drawn, while the order of drawing is a permutation of the items.

Definition: A permutation is an arrangement of items where the order of selection is noted - usually restricted to items taken without replacement. A combination is a group of items where order is not regarded.

Basic Formulae

1. The number of arrangements of n different things taken r at a time, with replacement, is n^r, where $1 \leq r \leq n$.

2. The number of arrangements of n different things taken r at a time, without replacement, is P_r^n, where

$$P_r^n = \frac{n!}{(n-r)!}$$

3. The number of permutations of n things taken all at one time, where there are n_1 of one kind, n_2 of another kind, ..., up to n_k, and where $\Sigma n_i = n$, is

$$\frac{n!}{n_1!n_2!\ldots n_k!}$$

4. The number of combinations of n things taken r at a time is

$$C_r^n = \frac{n!}{r!(n-r)!}$$

5. Factorials $n! = n(n-1)(n-2)(n-3) \ldots 2.1$

$1! = 1$ and $0! = 1$

Tables are readily available for factorials, their reciprocals, and their logs. For large values of n, the factorial can be approximated by Stirlings formula:

$$n! \approx \sqrt{2\pi}\ e^{-n}\ n^{n+\frac{1}{2}}$$

For n = 10, the error is less than 1%; the error approaches zero as n increases.

EXAMPLES

Calculation of Sample Statistics

The calculation of the more common statistics is illustrated using a small sample of test data. These procedures, discussed in Section F2.1, apply in general, For large samples (over 30 data points) the data may be grouped for computational convenience; in this case the weighted versions of the formulae are used.

Example #1

Given Ultimate tensile strength data for 6 specimens of an 0.040 sheet titanium sheet alloy: 182.50, 181.30, 183.50, 184.75, 189.90, and 187.75 KSI.

Calculate 1) median

2) mean value

3) variance, standard deviation

4) two-sided 95% confidence limits about mean value

5) one-sided lower 95% confidence limit on mean value

6) sample size required for a lower confidence limit on the mean, no more than 1% below sample mean at 95% confidence level.

7) "A" and "B" strength levels

Procedure:

Tabulate data in rank order (ascending values). Circled numbers identify columns used in the various calculations. Alternate methods are used in several cases for illustration. Definition of terms can be located on pages within parenthesis.

① Rank i	② F_{tu}, ksi x_i	③ $(x_i-\bar{x})$	④ $(x_i-\bar{x})^2$	⑤ x_i^2	⑥ y_i	⑦ y_i^2
1	181.30	-3.63	13.1769	3.286969×10^4	-7.4	54.76
2	182.50	-2.43	5.9049	3.330625	-5.0	25.00
3	183.50	-1.43	2.0449	3.367225	-3.0	9.00
4	184.75	- .18	.0324	3.413256	- .5	.25
5	187.75	+2.82	7.9524	3.525006	+5.5	30.25
6	189.80	+4.87	23.7169	3.602404	+9.6	92.16
Sums:	1109.60		52.8284	20.525485×10^4	- .8	211.42

1. Median = $\frac{1}{2}(x_3 + x_4)$ = 184.13 ksi (F2.1-4), ②

2. Mean Value (by direct use of definition, Page F2.1-3), ②

$$\bar{x} = \frac{1}{n}\sum_{i=1}^{6} x_i = 1109.60/6 = 184.93 \text{ ksi}$$

3. Variance and Standard Deviation (by direct use of definition, page F2.1-4), ③ and ④.

$$s^2 = \frac{1}{n-1}\sum_{i} (x_i-\bar{x})^2 = 52.8284/5 = 10.566$$

$$s = (10.566)^{\frac{1}{2}} = 3.25 \text{ ksi}$$

3. Variance and Standard Deviation - Alternate Method (page F2.1-5) ⑤

$$s^2 = \frac{1}{n-1}\left[\sum x_i^2 - n\bar{x}^2\right] = \frac{1}{5}\left[20.5255 \times 10^4 - 6(184.93)^2\right]$$

$$= \frac{10^4}{5}\left[20.525485 - 20.520202\right] = 52.83/5 = 10.566$$

$$s = 3.25\text{ksi}$$

Note that this latter method is much quicker, assuming the use of a desk calculator.

2.&3. Mean, Variance and Standard Deviation by coded values (F2.1-7). Useful only for hand calculations. ⑥ and ⑦

$y_i = (x_i - a)/b$, where a and b are any convenient constants chosen to simplify the calculation.

$= (x_i - 185)/.5$

$$\bar{y} = \frac{1}{n}\sum y_i = -.8/6 = -.1333$$

$$s_y^2 = \frac{1}{n-1}\left[\sum y_i^2 - n\bar{y}^2\right] = 1/5\left[211.42 - 6(.1333)^2\right] = 211.313/5$$

$= 42.263$

$$\bar{x} = a + b\bar{y} = 185 + .5(-.1333) = 184.93\text{ksi}$$

$$s_x^2 = b^2 s_y^2 = \tfrac{1}{4}s_y^2 = 42.263/4 = 10.566$$

$$s_x = 3.25\text{ksi}$$

4. Symmetrical 95% confidence interval about the mean value (F2.1-9). For a confidence level of 95%, the significance level α is .05. The population mean is then estimated by

$$\mu = \bar{x} \pm t_{\alpha,f}\frac{s}{\sqrt{n}}$$

From Table 3 for $\alpha = .05$ and $f = n-1 = 5$, $t_{.05,5} = 2.5706$, giving

$$\mu = 184.93 \pm 2.5706\,(3.25)/\sqrt{6}$$

$$= 184.93 \pm 3.41$$

The symmetrical (two-sided) 95% confidence interval is then

$$\underline{181.52 < \mu < 188.34 \text{ ksi}}$$

5. The 95% lower confidence limit on the mean is given by

$$\mu_\ell = \bar{x} - t_{\alpha,f} \frac{s}{\sqrt{n}} \quad \text{(F2.1-10)}$$

where now the 5% significance level corresponds to the area under the lower tail (see sketch Table 3), i.e., $\alpha/2$. The t-table is thus entered with an α of 10%, giving $t_{.10,5} = 2.015$. The lower bound on the mean is

$$\mu_\ell = 184.93 - 2.015\ (3.25)/\sqrt{6} = 184.93 - 2.67$$

$$= 182.26 \text{ ksi minimum}$$

$$\underline{\text{Thus } 182.26 \leq \mu \text{ at the 95\% confidence level.}}$$

6. The required sample size so that the lower limit at the 95% confidence level is no more than 1% below the sample mean (F2.1-11). Rearranging the equation in calculation 5 above,

$$\bar{x} - \mu_\ell \geq t_{\alpha,f} \frac{s}{\sqrt{n}}$$

$$.01(184.93) \geq 3.25 \frac{t_{\alpha,f}}{\sqrt{n}}$$

$$\text{or } \frac{3.25\ t_{\alpha,f}}{\sqrt{n}} \leq 1.8493\ (=R)$$

The required sample size, n, is found by trial and error, as below.

n	f	$t_{.10,f}$	R
7	6	1.943	2.38
9	8	1.869	2.01
10	9	1.833	1.885
11	10	1.813	1.775

Note: For the single tail test, a confidence level of 95% corresponds to $\alpha/2 = .05$, or $\alpha = .10$. Table 3 is thus entered with $t_{.10,f}$.

The necessary value of n is 11.

7. "A" and "B" strength levels:

Referring to one-sided tolerance tables (Table 6) for a confidence of 95%, a sample size of 6, and a proportion of .99, the K-factor is 5.062; for a proportion of .90, the K-factor is 3.006. The lower tolerance limit is given by $\bar{x}$ - Ks (F2.1-13).

"A" level: $\bar{x}$ - Ks = 184.93-16.45 = 168.48 KSI

"B" level: $\bar{x}$ - Ks = 184.93-9.77 = 175.16 KSI

For a confidence level of 95%, at least 99% of the specimens will have an ultimate strength greater than 168.48 ksi., and at least 90% will be over 175.16 ksi. Note that the tolerance limits are based on the assumption that the parent population is normal. With this sample of only six points the assumption cannot be justified from a statistical viewpoint; however, past data shows that strength values are usually normally distributed. It follows that the extrapolation to the A and B values is only as good as the assumption of normalcy. In the event that such calculations are required, these reservations should be carefully noted.

Example #2

Given: Fatigue life test data for a sample of 5 shot peened test specimens: 11,943; 10,545; 10,280; 13,555; 11,931 cycles to failure. Assume a log-normal distribution for the fatigue life.

Calculate:
1) geometric mean
2) geometric dispersion
3) range of population containing 95% of the distribution
4) 10^{th} percentile of fatigue life
5) "B" value of fatigue life

Solution:

Rank i	Cycles to Failure N_i	x_i log N_i	$(x_i-\bar{x})$ $(\log N_i - \overline{\log N})$	$(x_i-\bar{x})^2$
1	10,280	4.01199	-.05219	27.2380×10^{-4}
2	10,545	4.02305	-.04113	16.9168×10^{-4}
3	11,931	4.07668	+.01250	1.5625×10^{-4}
4	11,943	4.07711	+.01293	1.6718×10^{-4}
5	13,555	4.13209	+.06791	46.1177×10^{-4}
Sums		20.32092		93.5068×10^{-4}

1) Mean log $= \bar{x} = \frac{1}{n}\sum \log N_i = 20.32092/5 = 4.06418$ (F2.1-3; F2.2-4)

Geometric mean $= N = 11,593$ cycles.

2) Variance of logs $= s^2 = \frac{1}{n-1}\sum(x_i-\bar{x})^2 = (93.5068/4)10^{-4}$

Std. log deviation $= s = .04835$
Geometric dispersion $= g = 1.118$

3) The geometric dispersion for a log-normal distribution corresponds to σ for a normal distribution. For a normal distribution 95% of the population falls within $\pm 2\sigma$ of the mean; for the log-normal distribution, 95% of the population is bounded by $\hat{N}g^{\pm 2}$, or

$$11,593(1.118)^{-2} < N < 11,593(1.118)^{2}$$

$$9.275 < N < 14,490$$

Thus 95% of the fatigue distribution falls between 9,275 and 14,490 cycles. (F2.2-5)

4) The 10^{th} percentile level is given by

$$x_{10} = \bar{x} - z_{10}s = 4.06418 - 1.282(.04835) = 4.00220$$

$$N_{10} = 10,051 \text{ cycles}$$

5) "B" value of fatigue life. For a conformance of 90%, a confidence level of 95%, and sample size of 5, the tolerance factor (Table 6) is 3.407, (F2.1-13).

$$x_B = \bar{x} - Ks = 4.06418 - 3.407(.04835) = 3.89945$$

$$N_B = 7930 \text{ cycles}$$

Graphical Treatment

Example 1 - The strength data from Example 1 in the previous section is retabulated below with the associated mean rank values (F2.3-2).

i	F_{t_u} x_i	Mean Rank i/(n 1)
1	181.30 ksi	14.3%
2	182.50	28.6
3	183.50	42.9
4	184.75	57.1
5	187.75	71.5
6	189.80	85.7

The data has been plotted on normal probability paper, page F3.2-3, and a "best fit" straight line drawn through the data. The mean value and standard deviation can be read directly from the curve as indicated, giving $\bar{x}$ = 184.9 ksi and s = 4.3 ksi. The poor straight line fit makes the assumption of a normal distribution questionable; extrapolation to lower percentiles wolld clearly be poor practice in this case.

Example 2 - The fatigue data of Example 2 in the previous section is retabulated below and mean ranks assigned. Note that a log-normal distribution has been assumed.

i	N_i	x_i $\log N_i$	Mean Rank :i/(n+1)
1	10,280	4.012	16.7%
2	10,545	4.023	33.3
3	11,931	4.077	50.0
4	11,943	4.077	66.7
5	13,555	4.132	83.3

Two procedures are available. The logs can be plotted on normal probability paper. This has been done on page F2.3-3. The mean log and standard log

deviation are read from the plot, giving $\bar{x} = 4.065$ and $s = .063$. Converting back to cycles results in a geometric mean of 11,620 cycles and a geometric dispersion of 1.16.

The more direct procedure is to plot the fatigue data directly on log-normal probability paper, thus eliminating the steps involving the logs. This has been done on page F3.2-4. The geometric mean can be read directly from the plot. The geometric dispersion can be found by taking the square root of the ratio of the cycles to failure at the 84.1 and 15.9 percentile points. Thus

$$g^2 = \frac{N_{84.1}}{N_{15.9}} = \frac{13,400}{10,100} = 1.328$$

or $g = 1.15$

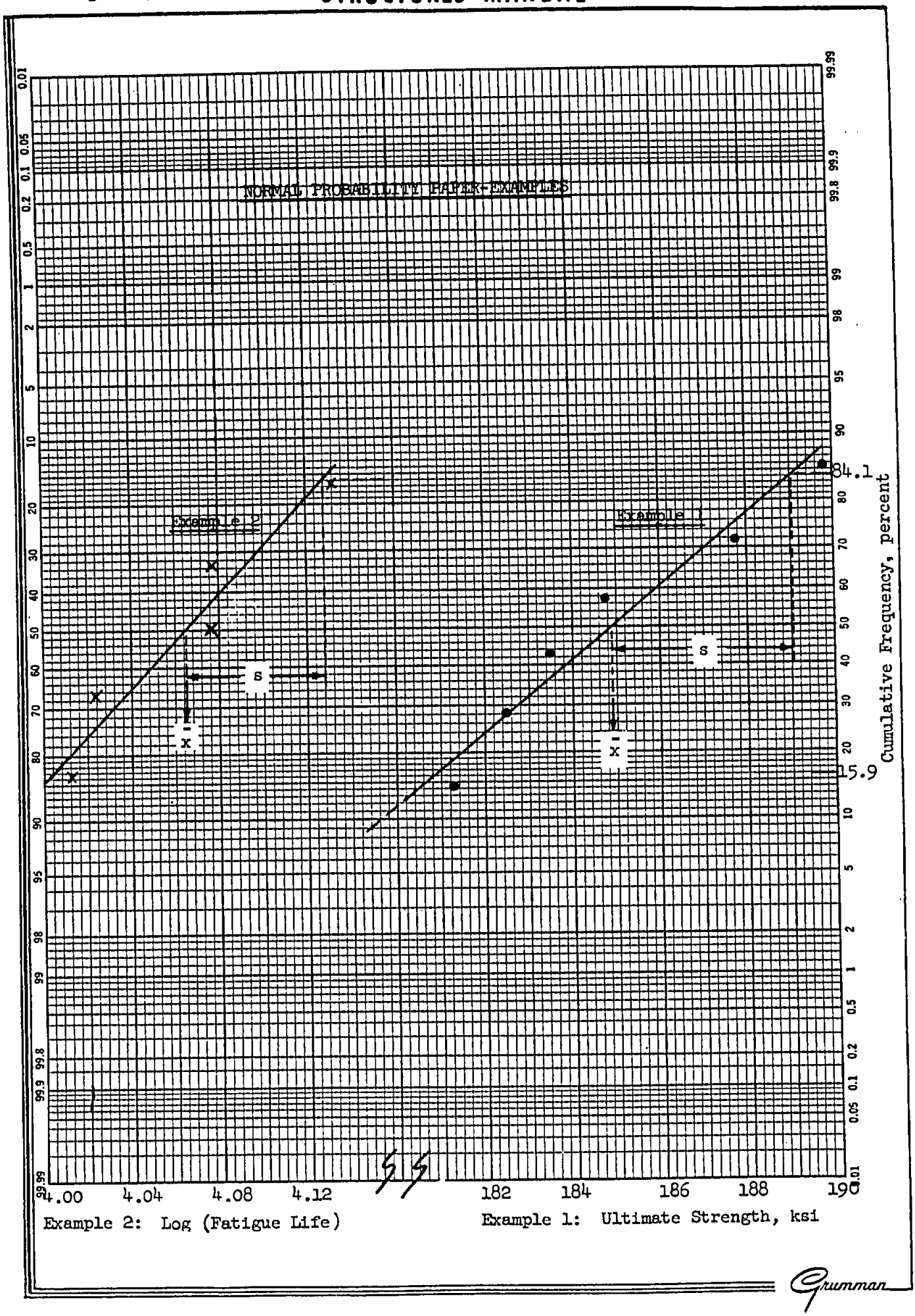
NORMAL PROBABILITY PAPER-EXAMPLES
Example 2
Example 1
s
x
s
x
84.1
15.9
Cumulative Frequency, percent
0.01 0.05 0.1 0.2 0.5 1 2 5 10 20 30 40 50 60 70 80 90 95 98 99 99.8 99.9 99.99
4.00 4.04 4.08 4.12
182 184 186 188 190
Example 2: Log (Fatigue Life)
Example 1: Ultimate Strength, ksi

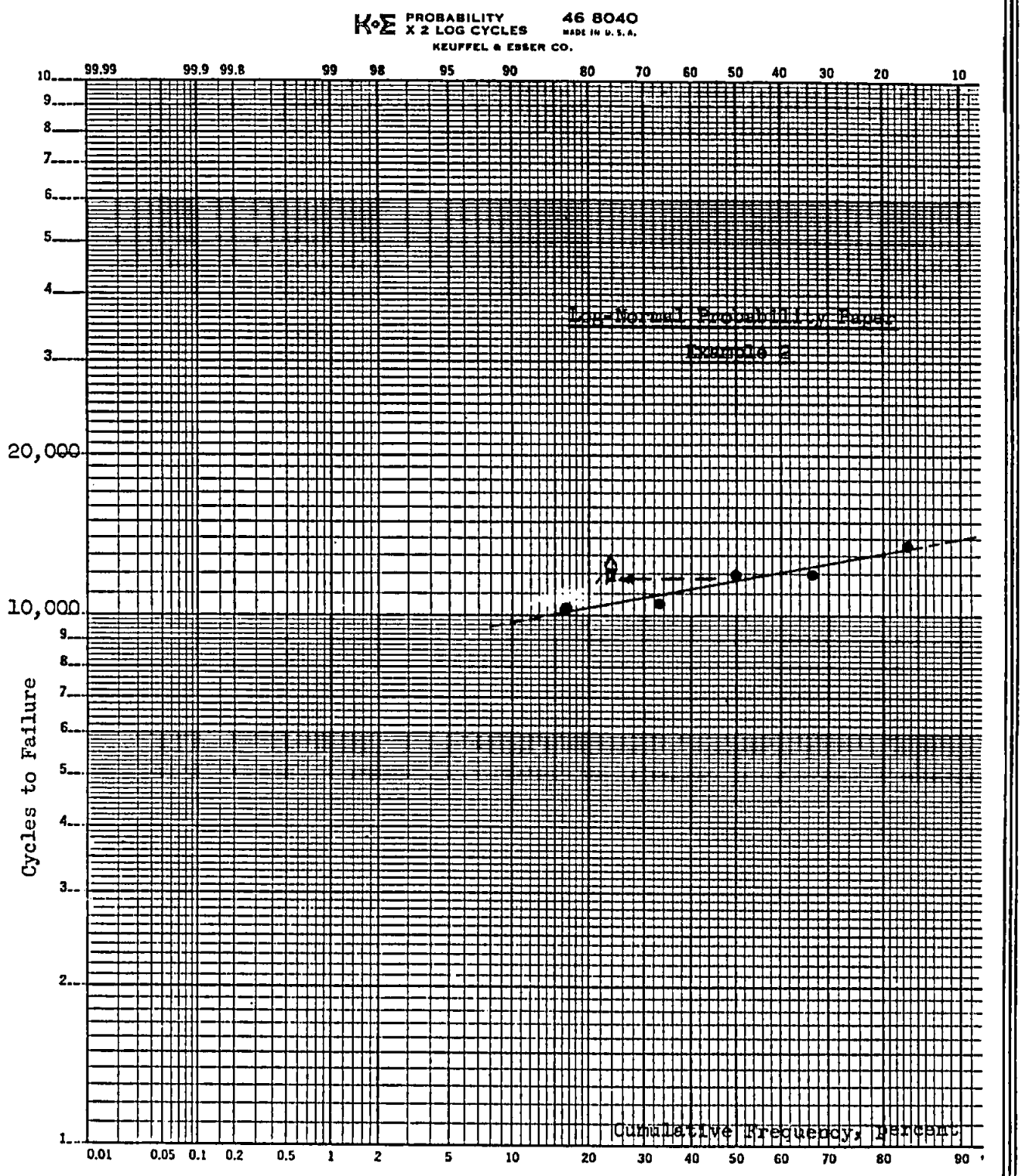
K•Σ PROBABILITY X 2 LOG CYCLES 46 8040
MADE IN U. S. A.
KEUFFEL & ESSER CO.
99.99 99.9 99.8 99 98 95 90 80 70 60 50 40 30 20 10
10 9 8 7 6 5 4 3
20,000
10,000
9 8 7 6 5 4 3 2 1
Cycles to Failure
Log-Normal Probability Paper
Example 2
0.01 0.05 0.1 0.2 0.5 1 2 5 10 20 30 40 50 60 70 80 90
Cumulative Frequency, Percent

Structural Reliability

In conventional design practice a safety factor is applied to the maximum expected service load to obtain a design load. The design load is taken as some minimum allowable strength level such as the "A" value of MIL-HDBK-5. This procedure does not account for the variation in spread of either load or strength distributions and can lead to a wide range in "survival probabilities." The statistical or reliability approach, on the other hand, depends on the actual probability distributions of both the load and strength.

Since this type of calculation has achieved a degree of popularity in some areas, it is worth describing briefly. However, the reservations noted below as to its applicability to major structural sections should be noted.

For the fundamental "stress vs. strength" analysis, the structural reliability can be defined as the probability of survival, or one minus the probability of failure. The reliability is thus the probability that the strength level will exceed the applied load level. While the general procedure is applicable to any type of probability distribution, it is restricted here to cases where both load and strength are normally distributed random variables (NDRV's)*. The means and standard deviations are either known or can be estimated from large samples. Since reliability type calculations are concerned with extreme values, i.e., the tails of the distributions, knowledge of the distributions is critical. Unless the data is based on very large samples, the results are relatively meaningless. Unfortunately from a statistical viewpoint, small samples are the rule when dealing with major structural components.

Assume both load and strength are NDRV's denoted by x_ℓ and x_s with known parameters (μ_ℓ, σ_ℓ) and (μ_s, σ_s). The reliability (R) is the probability (P) that the strength will exceed the load, i.e.,

$$R = P\{x_s - x_\ell > 0\}$$

The difference between two NDRV's is another NDRV, say x, with parameters (μ, σ).

---

* This assumption results in a closed form analytic solution. Non-normal distributions require the use of relatively lengthy numerical techniques.

From page F2.1-7(b),

$$\text{if } x = x_s - x_\ell,$$
$$\text{then } \mu = \mu_s - \mu_\ell$$
$$\text{and } \sigma^2 = \sigma_s^2 + \sigma_\ell^2.$$

The reliability, $P\{x > 0\}$, is thus equal to the area under the probability density curve $f(x)$ for x between 0 and ∞. In terms of the standard deviate, z, where $z = \frac{x-\mu}{\sigma}$, this is the area under the standard normal density curve from $-\frac{\mu}{\sigma}$ to ∞, or by symmetry from $-\infty$ to $\frac{\mu}{\sigma}$. Thus the reliability is given by

$$R = P\{z > -\frac{\mu}{\sigma}\} = P\{z < \frac{\mu}{\sigma}\}$$

or,
$$R = F\left(\frac{\mu}{\sigma}\right), \text{ where } \frac{\mu}{\sigma} = \frac{\mu_s - \mu_\ell}{\sqrt{\sigma_s^2 + \sigma_\ell^2}},$$

and where $F\left(\frac{\mu}{\sigma}\right)$ is the standardized normal distribution function, Table 1.

Note that this relation holds for the limiting case where one of the distributions is a single value. For example, the applied load might be a single known value L, with zero variance. In this case the reliability is given by $R = F\left(\frac{\mu_s - L}{\sigma_s}\right)$.

The steps described are illustrated in the sketch below, showing the various probability density functions.

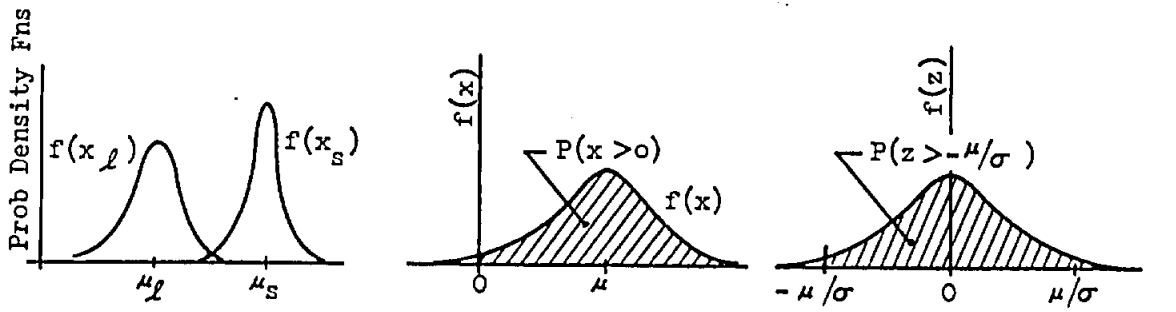

Strength, x_s; Load, x_ℓ | Strength Minus Load | Reliability = $P(z > -\mu/\sigma)$ = $P(z < \mu/\sigma)$ = $F(\mu/\sigma)$

Since both distributions are based upon known populations, the calculated reliability is a known parameter of the combined distribution. It has a zero variance and consequently an associated confidence level of 100%. In the case where one of the distributions is based on sample data, the μ and σ would be replaced by the statistics $\bar{x}$ and s with the appropriate subscripts. The calculation for R is identical, but now R is an estimate of the true reliability and should be so expressed, i.e., as an estimate with an appropriate confidence interval. Thus the best estimate of the reliability would be $F\left(\frac{\bar{x}}{s}\right)$, where $\bar{x}$ and s are the estimated mean and standard deviation of the combined distribution. Then

$$R = F\left(\frac{\bar{x}}{s}\right) \pm t_{\alpha,f}\, \sigma_R$$

where

σ_R = standard error of R (see page F2.1-7c.),
$t_{\alpha,f}$ = t-distribution value for a confidence level of $(1-\alpha)$ and f degrees of freedom (Table 3).

An example of this calculation is found in Reference 5.

In the case where the load distribution is known and the required reliability is specified, the procedure is merely worked backwards. That is, Table 1 is entered with the value of $F\left(\frac{\mu}{\sigma}\right)$ to obtain the corresponding value of $\frac{\mu}{\sigma}$. Using

$$\frac{\mu}{\sigma} = \frac{\mu_s - \mu_\ell}{\sqrt{\sigma_s^2 + \sigma_\ell^2}}$$

the values of the strength distribution parameters can be found. The solution to be above may be simplified by recourse to the coefficient of variation, $V_s = \frac{\sigma_s}{\mu_s}$, which is approximately constant for a given material and process. For example, V runs between .02 to .05 for standard aluminum alloys; the smaller value corresponds to sheet plate forms, while the latter applies to extruded forms. For materials where the "A" and "B" values are known, $V \approx .9(B-A)/B$.

Table 1.

The Standardized Normal Distribution Function

$$F(z) = \int_{-\infty}^{z} \frac{1}{\sqrt{2\pi}} e^{-t^2/2}\, dt$$

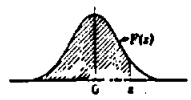

z	0.00	0.01	0.02	0.03	0.04	0.05	0.06	0.07	0.08	0.09
0.0	0.5000	0.5040	0.5080	0.5120	0.5160	0.5199	0.5239	0.5279	0.5319	0.5359
0.1	0.5398	0.5438	0.5478	0.5517	0.5557	0.5596	0.5636	0.5675	0.5714	0.5753
0.2	0.5793	0.5832	0.5871	0.5910	0.5948	0.5987	0.6026	0.6064	0.6103	0.6141
0.3	0.6179	0.6217	0.6255	0.6293	0.6331	0.6368	0.6406	0.6443	0.6480	0.6517
0.4	0.6554	0.6591	0.6628	0.6664	0.6700	0.6736	0.6772	0.6808	0.6844	0.6879
0.5	0.6915	0.6950	0.6985	0.7019	0.7054	0.7088	0.7123	0.7157	0.7190	0.7224
0.6	0.7257	0.7291	0.7324	0.7357	0.7389	0.7422	0.7454	0.7486	0.7517	0.7549
0.7	0.7580	0.7611	0.7642	0.7673	0.7703	0.7734	0.7764	0.7794	0.7823	0.7852
0.8	0.7881	0.7910	0.7939	0.7967	0.7995	0.8023	0.8051	0.8078	0.8106	0.8133
0.9	0.8159	0.8186	0.8212	0.8238	0.8264	0.8289	0.8315	0.8340	0.8365	0.8389
1.0	0.8413	0.8438	0.8461	0.8485	0.8508	0.8531	0.8554	0.8577	0.8599	0.8621
1.1	0.8643	0.8665	0.8686	0.8708	0.8729	0.8749	0.8770	0.8790	0.8810	0.8830
1.2	0.8849	0.8869	0.8888	0.8907	0.8925	0.8944	0.8962	0.8980	0.8997	0.90147
1.3	0.90320	0.90490	0.90658	0.90824	0.90988	0.91149	0.91309	0.91466	0.91621	0.91774
1.4	0.91924	0.92073	0.92220	0.92364	0.92507	0.92647	0.92785	0.92922	0.93056	0.93189
1.5	0.93319	0.93448	0.93574	0.93699	0.93822	0.93943	0.94062	0.94179	0.94295	0.94408
1.6	0.94520	0.94630	0.94738	0.94845	0.94950	0.95053	0.95154	0.95254	0.95352	0.95449
1.7	0.95543	0.95637	0.95728	0.95818	0.95907	0.95994	0.96080	0.96164	0.96246	0.96327
1.8	0.96407	0.96485	0.96562	0.96638	0.96712	0.96784	0.96856	0.96926	0.96995	0.97062
1.9	0.97128	0.97193	0.97257	0.97320	0.97381	0.97441	0.97500	0.97558	0.97615	0.97670
2.0	0.97725	0.97778	0.97831	0.97882	0.97932	0.97982	0.98030	0.98077	0.98124	0.98169
2.1	0.98214	0.98257	0.98300	0.98341	0.98382	0.98422	0.98461	0.98500	0.98537	0.98574
2.2	0.98610	0.98645	0.98679	0.98713	0.98745	0.98778	0.98809	0.98840	0.98870	0.98899
2.3	0.98928	0.98956	0.98983	0.9^20097	0.9^20358	0.9^20613	0.9^20863	0.9^21106	0.9^21344	0.9^21576
2.4	0.9^21802	0.9^22024	0.9^22240	0.9^22451	0.9^22656	0.9^22857	0.9^23053	0.9^23244	0.9^23431	0.9^23613
2.5	0.9^23790	0.9^23963	0.9^24132	0.9^24297	0.9^24457	0.9^24614	0.9^24766	0.9^24915	0.9^25060	0.9^25201
2.6	0.9^25339	0.9^25473	0.9^25604	0.9^25731	0.9^25855	0.9^25975	0.9^26093	0.9^26207	0.9^26319	0.9^26427
2.7	0.9^26533	0.9^26636	0.9^26736	0.9^26833	0.9^26928	0.9^27020	0.9^27110	0.9^27197	0.9^27282	0.9^27365
2.8	0.9^27445	0.9^27523	0.9^27599	0.9^27673	0.9^27744	0.9^27814	0.9^27882	0.9^27948	0.9^28012	0.9^28074
2.9	0.9^28134	0.9^28193	0.9^28250	0.9^28305	0.9^28359	0.9^28411	0.9^28462	0.9^28511	0.9^28559	0.9^28605
3.0	0.9^28650	0.9^28694	0.9^28736	0.9^28777	0.9^28817	0.9^28856	0.9^28893	0.9^28930	0.9^28965	0.9^28999
3.1	0.9^30324	0.9^30646	0.9^30957	0.9^31260	0.9^31553	0.9^31836	0.9^32112	0.9^32378	0.9^32636	0.9^32886
3.2	0.9^33129	0.9^33363	0.9^33590	0.9^33810	0.9^34024	0.9^34230	0.9^34429	0.9^34623	0.9^34810	0.9^34991
3.3	0.9^35166	0.9^35335	0.9^35499	0.9^35658	0.9^35811	0.9^35959	0.9^36103	0.9^36242	0.9^36376	0.9^36505
3.4	0.9^36631	0.9^36752	0.9^36869	0.9^36982	0.9^37091	0.9^37197	0.9^37299	0.9^37398	0.9^37493	0.9^37585
3.5	0.9^37674	0.9^37759	0.9^37842	0.9^37922	0.9^37999	0.9^38074	0.9^38146	0.9^38215	0.9^38282	0.9^38347
3.6	0.9^38409	0.9^38469	0.9^38527	0.9^38583	0.9^38637	0.9^38689	0.9^38739	0.9^38787	0.9^38834	0.9^38879
3.7	0.9^38922	0.9^38964	0.9^40039	0.9^40426	0.9^40799	0.9^41158	0.9^41504	0.9^41838	0.9^42159	0.9^42468
3.8	0.9^42765	0.9^43052	0.9^43327	0.9^43593	0.9^43848	0.9^44094	0.9^44331	0.9^44558	0.9^44777	0.9^44988
3.9	0.9^45190	0.9^45385	0.9^45573	0.9^45753	0.9^45926	0.9^46092	0.9^46253	0.9^46406	0.9^46554	0.9^46696
4.0	0.9^46833	0.9^46964	0.9^47090	0.9^47211	0.9^47327	0.9^47439	0.9^47546	0.9^47649	0.9^47748	0.9^47843

For example: $F(3.82) = 0.9^43327 = 0.99993327 = 1 - 0.00006673 = 1 - F(-3.82)$.

† From *Statistical Tables and Formulas*, by A. Hald, John Wiley and Sons, New York, 1952; reproduced by permission of Professor A. Hald and the publishers.

Table 2.

Percentiles of the Normal Distribution

$F(z)$	.75	.90	.95	.975	.99	.995	.999	.9995	.99995	.999995
$\alpha = 2[1 - F(z)]$	.50	.20	.10	.05	.02	.01	.002	.001	.0001	.00001
z	0.674	1.282	1.645	1.960	2.326	2.576	3.090	3.291	3.891	4.417

Table 3.
Percentages Points t_α of the t Distribution

f \ α	0.50	0.25	0.10	0.05	0.025	0.01	0.005
1	1.00000	2.4142	6.3138	12.706	25.452	63.657	127.32
2	0.81650	1.6036	2.9200	4.3027	6.2053	9.9248	14.089
3	0.76489	1.4226	2.3534	3.1825	4.1765	5.8409	7.4533
4	0.74070	1.3444	2.1318	2.7764	3.4954	4.6041	5.5976
5	0.72669	1.3009	2.0150	2.5706	3.1634	4.0321	4.7733
6	0.71756	1.2733	1.9432	2.4469	2.9687	3.7074	4.3168
7	0.71114	1.2543	1.8946	2.3646	2.8412	3.4995	4.0293
8	0.70639	1.2403	1.8595	2.3060	2.7515	3.3554	3.8325
9	0.70272	1.2297	1.8331	2.2622	2.6850	3.2498	3.6897
10	0.69981	1.2213	1.8125	2.2281	2.6338	3.1693	3.5814
11	0.69745	1.2145	1.7959	2.2010	2.5931	3.1058	3.4966
12	0.69548	1.2089	1.7823	2.1788	2.5600	3.0545	3.4284
13	0.69384	1.2041	1.7709	2.1604	2.5326	3.0123	3.3725
14	0.69242	1.2001	1.7613	2.1448	2.5096	2.9768	3.3257
15	0.69120	1.1967	1.7530	2.1315	2.4899	2.9467	3.2860
16	0.69013	1.1937	1.7459	2.1199	2.4729	2.9208	3.2520
17	0.68919	1.1910	1.7396	2.1098	2.4581	2.8982	3.2225
18	0.68837	1.1887	1.7341	2.1009	2.4450	2.8784	3.1966
19	0.68763	1.1866	1.7291	2.0930	2.4334	2.8609	3.1737
20	0.68696	1.1848	1.7247	2.0860	2.4231	2.8453	3.1534
21	0.68635	1.1831	1.7207	2.0796	2.4138	2.8314	3.1352
22	0.68580	1.1816	1.7171	2.0739	2.4055	2.8188	3.1188
23	0.68531	1.1802	1.7139	2.0687	2.3979	2.8073	3.1040
24	0.68485	1.1789	1.7109	2.0639	2.3910	2.7969	3.0905
25	0.68443	1.1777	1.7081	2.0595	2.3846	2.7874	3.0782
26	0.68405	1.1766	1.7056	2.0555	2.3788	2.7787	3.0669
27	0.68370	1.1757	1.7033	2.0518	2.3734	2.7707	3.0565
28	0.68335	1.1748	1.7011	2.0484	2.3685	2.7633	3.0469
29	0.68304	1.1739	1.6991	2.0452	2.3638	2.7564	3.0380
30	0.68276	1.1731	1.6973	2.0423	2.3596	2.7500	3.0298
40	0.68066	1.1673	1.6839	2.0211	2.3289	2.7045	2.9712
60	0.67862	1.1616	1.6707	2.0003	2.2991	2.6603	2.9146
120	0.67656	1.1559	1.6577	1.9799	2.2699	2.6174	2.8599
∞	0.67449	1.1503	1.6449	1.9600	2.2414	2.5758	2.8070

Computed by Maxime Merrington from "Tables of percentage points of the incomplete beta function," Biometrika, Vol. 32(1941), pp. 168-181, by Catherine M. Thompson, Cambridge University Press; reproduced by permision of the author and publisher.

Table 4.

Percentages Points F of the F Distribution

α - 0.05

f_2 \ f_1	1	2	3	4	5	6	7	8	9	10	12	15	20	24	30	40	60	120	∞
1	161.45	199.50	215.71	224.58	230.16	233.99	236.77	238.88	240.54	241.88	243.91	245.95	248.01	249.05	250.09	251.14	252.20	253.25	254.32
2	18.513	19.000	19.164	19.247	19.296	19.330	19.353	19.371	19.385	19.396	19.413	19.429	19.446	19.454	19.462	19.471	19.479	19.487	19.496
3	10.128	9.5521	9.2766	9.1172	9.0135	8.9406	8.8868	8.8452	8.8123	8.7855	8.7446	8.7029	8.6602	8.6385	8.6166	8.5944	8.5720	8.5494	8.5265
4	7.7086	6.9443	6.5914	6.3883	6.2560	6.1631	6.0942	6.0410	5.9988	5.9644	5.9117	5.8578	5.8025	5.7744	5.7459	5.7170	5.6878	5.6581	5.6281
5	6.6079	5.7861	5.4095	5.1922	5.0503	4.9503	4.8759	4.8183	4.7725	4.7351	4.6777	4.6188	4.5581	4.5272	4.4957	4.4638	4.4314	4.3984	4.3650
6	5.9874	5.1433	4.7571	4.5337	4.3874	4.2839	4.2066	4.1468	4.0990	4.0600	3.9999	3.9381	3.8742	3.8415	3.8082	3.7743	3.7398	3.7047	3.6688
7	5.5914	4.7374	4.3468	4.1203	3.9715	3.8660	3.7870	3.7257	3.6767	3.6365	3.5747	3.5108	3.4445	3.4105	3.3758	3.3404	3.3043	3.2674	3.2298
8	5.3177	4.4590	4.0662	3.8378	3.6875	3.5806	3.5005	3.4381	3.3881	3.3472	3.2840	3.2184	3.1503	3.1152	3.0794	3.0428	3.0053	2.9669	2.9276
9	5.1174	4.2565	3.8626	3.6331	3.4817	3.3738	3.2927	3.2296	3.1789	3.1373	3.0729	3.0061	2.9365	2.9005	2.8637	2.8259	2.7872	2.7475	2.7067
10	4.9646	4.1028	3.7083	3.4780	3.3258	3.2172	3.1355	3.0717	3.0204	2.9782	2.9130	2.8450	2.7740	2.7372	2.6996	2.6609	2.6211	2.5801	2.5379
11	4.8443	3.9823	3.5874	3.3567	3.2039	3.0946	3.0123	2.9480	2.8962	2.8536	2.7876	2.7186	2.6464	2.6090	2.5705	2.5309	2.4901	2.4480	2.4045
12	4.7472	3.8853	3.4903	3.2592	3.1059	2.9961	2.9134	2.8486	2.7964	2.7534	2.6866	2.6169	2.5436	2.5055	2.4663	2.4259	2.3842	2.3410	2.2962
13	4.6672	3.8056	3.4105	3.1791	3.0254	2.9153	2.8321	2.7669	2.7144	2.6710	2.6037	2.5331	2.4589	2.4202	2.3803	2.3392	2.2966	2.2524	2.2064
14	4.6001	3.7389	3.3439	3.1122	2.9582	2.8477	2.7642	2.6987	2.6458	2.6021	2.5342	2.4630	2.3879	2.3487	2.3082	2.2664	2.2230	2.1778	2.1307
15	4.5431	3.6823	3.2874	3.0556	2.9013	2.7905	2.7066	2.6408	2.5876	2.5437	2.4753	2.4035	2.3275	2.2878	2.2468	2.2043	2.1601	2.1141	2.0658
16	4.4940	3.6337	3.2389	3.0069	2.8524	2.7413	2.6572	2.5911	2.5377	2.4935	2.4247	2.3522	2.2756	2.2354	2.1938	2.1507	2.1058	2.0589	2.0096
17	4.4513	3.5915	3.1968	2.9647	2.8100	2.6987	2.6143	2.5480	2.4943	2.4499	2.3807	2.3077	2.2304	2.1898	2.1477	2.1040	2.0584	2.0107	1.9604
18	4.4139	3.5546	3.1599	2.9277	2.7729	2.6613	2.5767	2.5102	2.4563	2.4117	2.3421	2.2686	2.1906	2.1497	2.1071	2.0629	2.0166	1.9681	1.9168
19	4.3808	3.5219	3.1274	2.8951	2.7401	2.6283	2.5435	2.4768	2.4227	2.3779	2.3080	2.2341	2.1555	2.1141	2.0712	2.0264	1.9796	1.9302	1.8780
20	4.3513	3.4928	3.0984	2.8661	2.7109	2.5990	2.5140	2.4471	2.3928	2.3479	2.2776	2.2033	2.1242	2.0825	2.0391	1.9938	1.9464	1.8963	1.8432
21	4.3248	3.4668	3.0725	2.8401	2.6848	2.5727	2.4876	2.4205	2.3661	2.3210	2.2504	2.1757	2.0960	2.0540	2.0102	1.9645	1.9165	1.8657	1.8117
22	4.3009	3.4434	3.0491	2.8167	2.6613	2.5491	2.4638	2.3965	2.3419	2.2967	2.2258	2.1508	2.0707	2.0283	1.9842	1.9380	1.8895	1.8380	1.7831
23	4.2793	3.4221	3.0280	2.7955	2.6400	2.5277	2.4422	2.3748	2.3201	2.2747	2.2036	2.1282	2.0476	2.0050	1.9605	1.9139	1.8649	1.8128	1.7570
24	4.2597	3.4028	3.0088	2.7763	2.6207	2.5082	2.4226	2.3551	2.3002	2.2547	2.1834	2.1077	2.0267	1.9838	1.9390	1.8920	1.8424	1.7897	1.7331
25	4.2417	3.3852	2.9912	2.7587	2.6030	2.4904	2.4047	2.3371	2.2821	2.2365	2.1649	2.0889	2.0075	1.9643	1.9192	1.8718	1.8217	1.7684	1.7110
26	4.2252	3.3690	2.9751	2.7426	2.5868	2.4741	2.3883	2.3205	2.2655	2.2197	2.1479	2.0716	1.9898	1.9464	1.9010	1.8533	1.8027	1.7488	1.6906
27	4.2100	3.3541	2.9604	2.7278	2.5719	2.4591	2.3732	2.3053	2.2501	2.2043	2.1323	2.0558	1.9736	1.9299	1.8842	1.8361	1.7851	1.7307	1.6717
28	4.1960	3.3404	2.9467	2.7141	2.5581	2.4453	2.3593	2.2913	2.2360	2.1900	2.1179	2.0411	1.9586	1.9147	1.8687	1.8203	1.7689	1.7138	1.6541
29	4.1830	3.3277	2.9340	2.7014	2.5454	2.4324	2.3463	2.2782	2.2229	2.1768	2.1045	2.0275	1.9446	1.9005	1.8543	1.8055	1.7537	1.6981	1.6377
30	4.1709	3.3158	2.9223	2.6896	2.5336	2.4205	2.3343	2.2662	2.2107	2.1646	2.0921	2.0148	1.9317	1.8874	1.8409	1.7918	1.7396	1.6835	1.6223
40	4.0848	3.2317	2.8387	2.6060	2.4495	2.3359	2.2490	2.1802	2.1240	2.0772	2.0035	1.9245	1.8389	1.7929	1.7444	1.6928	1.6373	1.5766	1.5089
60	4.0012	3.1504	2.7581	2.5252	2.3683	2.2540	2.1665	2.0970	2.0401	1.9926	1.9174	1.8364	1.7480	1.7001	1.6491	1.5943	1.5343	1.4673	1.3893
120	3.9201	3.0718	2.6802	2.4472	2.2900	2.1750	2.0867	2.0164	1.9588	1.9105	1.8337	1.7505	1.6587	1.6084	1.5543	1.4952	1.4290	1.3519	1.2539
∞	3.8415	2.9957	2.6049	2.3719	2.2141	2.0986	2.0096	1.9384	1.8799	1.8307	1.7522	1.6664	1.5705	1.5173	1.4591	1.3940	1.3180	1.2214	1.0000

From "Tables of percentage points of the inverted beta (F) distribution, Biometrika, Vol. 33(1943), pp. 73-88, by Maxine Merrington and Catherine M. Thompson, Cambridge University Press; reprinted by permission of the authors and publishers.

Table 4. (Continued)

$\alpha = 0.01$

f_2 \ f_1	1	2	3	4	5	6	7	8	9	10	12	15	20	24	30	40	60	120	∞
1	4052.2	4999.5	5403.3	5624.6	5763.7	5859.0	5928.3	5981.6	6022.5	6055.8	6106.3	6157.3	6208.7	6234.6	6260.7	6286.8	6313.0	6339.4	6366.0
2	98.503	99.000	99.166	99.249	99.299	99.332	99.356	99.374	99.388	99.399	99.416	99.432	99.449	99.458	99.466	99.474	99.483	99.491	99.501
3	34.116	30.817	29.457	28.710	28.237	27.911	27.672	27.489	27.345	27.229	27.052	26.872	26.690	26.598	26.505	26.411	26.316	26.221	26.125
4	21.198	18.000	16.694	15.977	15.522	15.207	14.976	14.799	14.659	14.546	14.374	14.198	14.020	13.929	13.838	13.745	13.652	13.558	13.463
5	16.258	13.274	12.060	11.392	10.967	10.672	10.456	10.289	10.158	10.051	9.8883	9.7222	9.5527	9.4665	9.3793	9.2912	9.2020	9.1118	9.0204
6	13.745	10.925	9.7795	9.1483	8.7459	8.4661	8.2600	8.1016	7.9761	7.8741	7.7183	7.5590	7.3958	7.3127	7.2285	7.1432	7.0568	6.9690	6.8801
7	12.246	9.5466	8.4513	7.8467	7.4604	7.1914	6.9928	6.8401	6.7188	6.6201	6.4691	6.3143	6.1554	6.0743	5.9921	5.9084	5.8236	5.7372	5.6495
8	11.259	8.6491	7.5910	7.0060	6.6318	6.3707	6.1776	6.0289	5.9106	5.8143	5.6668	5.5151	5.3591	5.2793	5.1981	5.1156	5.0316	4.9460	4.8588
9	10.561	8.0215	6.9919	6.4221	6.0569	5.8018	5.6129	5.4671	5.3511	5.2565	5.1114	4.9621	4.8080	4.7290	4.6486	4.5667	4.4831	4.3978	4.3105
10	10.044	7.5594	6.5523	5.9943	5.6363	5.3858	5.2001	5.0567	4.9424	4.8492	4.7059	4.5582	4.4054	4.3269	4.2469	4.1653	4.0819	3.9965	3.9090
11	9.6460	7.2057	6.2167	5.6683	5.3160	5.0692	4.8861	4.7445	4.6315	4.5393	4.3974	4.2509	4.0990	4.0209	3.9411	3.8596	3.7761	3.6904	3.6025
12	9.3302	6.9266	5.9526	5.4119	5.0643	4.8206	4.6395	4.4994	4.3875	4.2961	4.1553	4.0096	3.8584	3.7805	3.7008	3.6192	3.5355	3.4494	3.3608
13	9.0738	6.7010	5.7394	5.2053	4.8616	4.6204	4.4410	4.3021	4.1911	4.1003	3.9603	3.8154	3.6646	3.5868	3.5070	3.4253	3.3413	3.2548	3.1654
14	8.8616	6.5149	5.5639	5.0354	4.6950	4.4558	4.2779	4.1399	4.0297	3.9394	3.8001	3.6557	3.5052	3.4274	3.3476	3.2656	3.1813	3.0942	3.0040
15	8.6831	6.3589	5.4170	4.8932	4.5556	4.3183	4.1415	4.0045	3.8948	3.8049	3.6662	3.5222	3.3719	3.2940	3.2141	3.1319	3.0471	2.9595	2.8684
16	8.5310	6.2262	5.2922	4.7726	4.4374	4.2016	4.0259	3.8896	3.7804	3.6909	3.5527	3.4089	3.2588	3.1808	3.1007	3.0182	2.9330	2.8447	2.7528
17	8.3997	6.1121	5.1850	4.6690	4.3359	4.1015	3.9267	3.7910	3.6822	3.5931	3.4552	3.3117	3.1615	3.0835	3.0032	2.9205	2.8348	2.7459	2.6530
18	8.2854	6.0129	5.0919	4.5790	4.2479	4.0146	3.8406	3.7054	3.5971	3.5082	3.3706	3.2273	3.0771	2.9990	2.9185	2.8354	2.7493	2.6597	2.5660
19	8.1850	5.9259	5.0103	4.5003	4.1708	3.9386	3.7653	3.6305	3.5225	3.4338	3.2965	3.1533	3.0031	2.9249	2.8442	2.7608	2.6742	2.5839	2.4893
20	8.0960	5.8489	4.9382	4.4307	4.1027	3.8714	3.6987	3.5644	3.4567	3.3682	3.2311	3.0880	2.9377	2.8594	2.7785	2.6947	2.6077	2.5168	2.4212
21	8.0166	5.7804	4.8740	4.3688	4.0421	3.8117	3.6396	3.5056	3.3981	3.3098	3.1729	3.0299	2.8796	2.8011	2.7200	2.6359	2.5484	2.4568	2.3603
22	7.9454	5.7190	4.8166	4.3134	3.9880	3.7583	3.5867	3.4530	3.3458	3.2576	3.1209	2.9780	2.8274	2.7488	2.6675	2.5831	2.4951	2.4029	2.3055
23	7.8811	5.6637	4.7649	4.2635	3.9392	3.7102	3.5390	3.4057	3.2986	3.2106	3.0740	2.9311	2.7805	2.7017	2.6202	2.5355	2.4471	2.3542	2.2559
24	7.8229	5.6136	4.7181	4.2184	3.8951	3.6667	3.4959	3.3629	3.2560	3.1681	3.0316	2.8887	2.7380	2.6591	2.5773	2.4923	2.4035	2.3099	2.2107
25	7.7698	5.5680	4.6755	4.1774	3.8550	3.6272	3.4568	3.3239	3.2172	3.1294	2.9931	2.8502	2.6993	2.6203	2.5383	2.4530	2.3637	2.2695	2.1694
26	7.7213	5.5263	4.6366	4.1400	3.8183	3.5911	3.4210	3.2884	3.1818	3.0941	2.9579	2.8150	2.6640	2.5848	2.5026	2.4170	2.3273	2.2325	2.1315
27	7.6767	5.4881	4.6009	4.1056	3.7848	3.5580	3.3882	3.2558	3.1494	3.0618	2.9256	2.7827	2.6316	2.5522	2.4699	2.3840	2.2938	2.1984	2.0965
28	7.6356	5.4529	4.5681	4.0740	3.7539	3.5276	3.3581	3.2259	3.1195	3.0320	2.8959	2.7530	2.6017	2.5223	2.4397	2.3535	2.2629	2.1670	2.0642
29	7.5976	5.4205	4.5378	4.0449	3.7254	3.4995	3.3302	3.1982	3.0920	3.0045	2.8685	2.7256	2.5742	2.4946	2.4118	2.3253	2.2344	2.1378	2.0342
30	7.5625	5.3904	4.5097	4.0179	3.6990	3.4735	3.3045	3.1726	3.0665	2.9791	2.8431	2.7002	2.5487	2.4689	2.3860	2.2992	2.2079	2.1107	2.0062
40	7.3141	5.1785	4.3126	3.8283	3.5138	3.2910	3.1238	2.9930	2.8876	2.8005	2.6648	2.5216	2.3689	2.2880	2.2034	2.1142	2.0194	1.9172	1.8047
60	7.0771	4.9774	4.1259	3.6491	3.3389	3.1187	2.9530	2.8233	2.7185	2.6318	2.4961	2.3523	2.1978	2.1154	2.0285	1.9360	1.8363	1.7263	1.6006
120	6.8510	4.7865	3.9493	3.4796	3.1735	2.9559	2.7918	2.6629	2.5586	2.4721	2.3363	2.1915	2.0346	1.9500	1.8600	1.7628	1.6557	1.5330	1.3805
∞	6.6349	4.6052	3.7816	3.3192	3.0173	2.8020	2.6393	2.5113	2.4073	2.3209	2.1848	2.0385	1.8783	1.7908	1.6964	1.5923	1.4730	1.3246	1.0000

Table 5.

Chi-Squared Distribution

Probability of a larger value of χ^2

D.F. \ α	.99	.98	.95	.90	.80	.70	.50	.30	.20	.10	.05	.02	.01	.001
1	$.0^3157$	$.0^3628$	.00393	.0158	.0642	.148	.455	1.074	1.642	2.706	3.841	5.412	6.635	10.827
2	.0201	.0404	.103	.211	.466	.713	1.386	2.408	3.219	4.605	5.991	7.824	9.210	13.815
3	.115	.185	.352	.584	1.005	1.424	2.366	3.665	4.642	6.251	7.815	9.837	11.345	16.268
4	.297	.429	.711	1.064	1.649	2.195	3.357	4.878	5.989	7.779	9.488	11.668	13.277	18.465
5	.544	.752	1.145	1.610	2.343	3.000	4.351	6.064	7.289	9.236	11.070	13.388	15.086	20.517
6	.872	1.134	1.635	2.204	3.070	3.828	5.348	7.231	8.558	10.645	12.592	15.033	16.812	22.457
7	1.239	1.564	2.167	2.833	3.822	4.671	6.346	8.383	9.803	12.017	14.067	16.622	18.475	24.322
8	1.646	2.032	2.733	3.490	4.594	5.527	7.344	9.524	11.030	13.362	15.507	18.168	20.090	26.125
9	2.088	2.532	3.325	4.168	5.380	6.393	8.343	10.656	12.242	14.684	16.919	19.679	21.666	27.877
10	2.558	3.059	3.940	4.865	6.179	7.267	9.342	11.781	13.442	15.987	18.307	21.161	23.209	29.588
11	3.053	3.609	4.575	5.578	6.989	8.148	10.341	12.899	14.631	17.275	19.675	22.618	24.725	31.264
12	3.571	4.178	5.226	6.304	7.807	9.034	11.340	14.011	15.812	18.549	21.026	24.054	26.217	32.909
13	4.107	4.765	5.892	7.042	8.634	9.926	12.340	15.119	16.985	19.812	22.362	25.472	27.688	34.528
14	4.660	5.368	6.571	7.790	9.467	10.821	13.339	16.222	18.151	21.064	23.685	26.873	29.141	36.123
15	5.229	5.985	7.261	8.547	10.307	11.721	14.339	17.322	19.313	22.307	24.996	28.259	30.578	37.697
16	5.812	6.614	7.962	9.312	11.152	12.624	15.338	18.418	20.465	23.542	26.296	29.633	32.000	39.252
17	6.408	7.255	8.672	10.085	12.002	13.531	16.338	19.511	21.615	24.769	27.587	30.995	33.409	40.790
18	7.015	7.906	9.390	10.865	12.857	14.440	17.338	20.601	22.760	25.989	28.869	32.346	34.805	42.312
19	7.633	8.567	10.117	11.651	13.716	15.352	18.338	21.689	23.900	27.204	30.144	33.687	36.191	43.820
20	8.260	9.237	10.851	12.443	14.578	16.266	19.337	22.775	25.038	28.412	31.410	35.020	37.566	45.315
21	8.897	9.915	11.591	13.240	15.445	17.182	20.337	23.858	26.171	29.615	32.671	36.343	38.932	46.797
22	9.542	10.600	12.338	14.041	16.314	18.101	21.337	24.939	27.301	30.813	33.924	37.659	40.289	48.268
23	10.196	11.293	13.091	14.848	17.187	19.021	22.337	26.018	28.429	32.007	35.172	38.968	41.638	49.728
24	10.856	11.992	13.848	15.659	18.062	19.943	23.337	27.096	29.553	33.196	36.145	40.270	42.980	51.179
25	11.524	12.697	14.611	16.473	18.940	20.867	24.337	28.172	30.675	34.382	37.652	41.566	44.314	52.620
26	12.198	13.409	15.379	17.292	19.820	21.792	25.336	29.246	31.795	35.563	38.885	42.856	45.642	54.052
27	12.879	14.125	16.151	18.114	20.703	22.719	26.336	30.319	32.912	36.741	40.113	44.140	46.963	55.476
28	13.565	14.847	16.928	18.939	21.588	23.647	27.336	31.391	34.027	37.916	41.337	45.419	48.278	56.893
29	14.256	15.574	17.708	19.768	22.475	24.577	28.336	32.461	35.139	39.087	42.557	46.693	49.588	58.302
30	14.953	16.306	18.493	20.599	23.364	25.508	29.336	33.530	36.250	40.256	43.773	47.962	50.892	59.703

† Reprinted from Table IV of R. A. Fisher and Frank Yates, "Statistical Tables for Biological, Agricultural and Medical Research," Oliver & Boyd, Ltd., Edinburgh and London, 1953, by permission of the authors and publishers.

Table 6.

One-Sided Tolerance Factors for Normal Distributions

Factors K such that the probability is γ that at least a proportion $(1-\alpha)$ of the distribution will be greater than $\bar{x}$-Ks (or less than $\bar{x}$ + Ks), where $\bar{x}$ and s are unbiased estimates of the population mean and standard deviation from a sample of size n.

*Columns labeled "A" & "B" are the K factors for the A & B minimum strength levels of MIL-HDBK-5.

	γ = 0.75					γ = 0.90					γ = 0.95					γ = 0.99				
n \ α	0.25	0.10	0.05	0.01	0.001	0.25	0.10	0.05	0.01	0.001	0.25	0.10 B	0.05	0.01 A	0.001	0.25	0.10	0.05	0.01	0.001
3	1.464	2.501	3.152	4.396	5.805	2.602	4.258	5.310	7.340	9.651	3.804	6.158	7.655	10.552	13.857					
4	1.256	2.134	2.680	3.726	4.910	1.972	3.187	3.957	5.437	7.128	2.619	4.163	5.145	7.042	9.215					
5	1.152	1.961	2.463	3.421	4.507	1.698	2.742	3.400	4.666	6.112	2.149	3.407	4.202	5.741	7.501					
6	1.087	1.860	2.336	3.243	4.273	1.540	2.494	3.091	4.242	5.556	1.895	3.006	3.707	5.062	6.612	2.849	4.408	5.409	7.334	9.540
7	1.043	1.791	2.250	3.126	4.118	1.435	2.333	2.894	3.972	5.201	1.732	2.755	3.399	4.641	6.061	2.490	3.856	4.739	6.411	8.348
8	1.010	1.740	2.190	3.042	4.008	1.360	2.219	2.755	3.783	4.955	1.617	2.582	3.188	4.353	5.686	2.252	3.496	4.287	5.811	7.566
9	0.984	1.702	2.141	2.977	3.924	1.302	2.133	2.649	3.641	4.772	1.532	2.454	3.031	4.143	5.414	2.085	3.242	3.971	5.389	7.014
10	0.964	1.671	2.103	2.927	3.858	1.257	2.065	2.568	3.532	4.629	1.465	2.355	2.911	3.981	5.203	1.954	3.048	3.739	5.075	6.603
11	0.947	1.646	2.073	2.885	3.804	1.219	2.012	2.503	3.444	4.515	1.411	2.275	2.815	3.852	5.036	1.854	2.897	3.557	4.828	6.284
12	0.933	1.624	2.048	2.851	3.760	1.188	1.966	2.448	3.371	4.420	1.366	2.210	2.736	3.747	4.900	1.771	2.773	3.410	4.633	6.032
13	0.919	1.606	2.026	2.822	3.722	1.162	1.928	2.403	3.310	4.341	1.329	2.155	2.670	3.659	4.787	1.702	2.677	3.290	4.472	5.826
14	0.909	1.591	2.007	2.796	3.690	1.139	1.895	2.363	3.257	4.274	1.296	2.108	2.614	3.585	4.690	1.645	2.592	3.189	4.336	5.651
15	0.899	1.577	1.991	2.776	3.661	1.119	1.866	2.329	3.212	4.215	1.268	2.068	2.566	3.520	4.607	1.596	2.521	3.102	4.224	5.507
16	0.891	1.560	1.977	2.756	3.637	1.101	1.842	2.299	3.172	4.164	1.242	2.032	2.523	3.463	4.534	1.553	2.458	3.028	4.124	5.374
17	0.883	1.554	1.964	2.739	3.615	1.085	1.820	2.272	3.136	4.118	1.220	2.001	2.486	3.415	4.471	1.514	2.405	2.962	4.038	5.268
18	0.876	1.544	1.951	2.723	3.595	1.071	1.800	2.249	3.106	4.078	1.200	1.974	2.453	3.370	4.415	1.481	2.357	2.906	3.961	5.167
19	0.870	1.536	1.942	2.710	3.577	1.058	1.781	2.228	3.078	4.041	1.183	1.949	2.423	3.331	4.364	1.450	2.315	2.855	3.893	5.078
20	0.865	1.528	1.933	2.697	3.561	1.046	1.765	2.208	3.052	4.009	1.167	1.926	2.396	3.295	4.319	1.424	2.275	2.807	3.832	5.003
21	0.859	1.520	1.923	2.686	3.545	1.035	1.750	2.190	3.028	3.979	1.152	1.905	2.371	3.262	4.276	1.397	2.241	2.768	3.776	4.932
22	0.854	1.514	1.916	2.675	3.532	1.025	1.736	2.174	3.007	3.952	1.138	1.887	2.350	3.233	4.238	1.376	2.208	2.729	3.727	4.866
23	0.849	1.508	1.907	2.665	3.520	1.016	1.724	2.159	2.987	3.927	1.126	1.869	2.329	3.206	4.204	1.355	2.179	2.693	3.680	4.806
24	0.845	1.502	1.901	2.656	3.509	1.007	1.712	2.145	2.969	3.904	1.114	1.853	2.309	3.181	4.171	1.336	2.154	2.663	3.638	4.755
25	0.842	1.496	1.895	2.647	3.497	0.999	1.702	2.132	2.952	3.882	1.103	1.838	2.292	3.158	4.143	1.319	2.129	2.632	3.601	4.706
30	0.825	1.475	1.869	2.613	3.454	0.966	1.657	2.080	2.884	3.794	1.059	1.778	2.220	3.064	4.022	1.249	2.029	2.516	3.446	4.508
35	0.812	1.458	1.849	2.588	3.421	0.942	1.623	2.041	2.833	3.730	1.025	1.732	2.166	2.994	3.934	1.195	1.957	2.431	3.334	4.364
40	0.803	1.445	1.834	2.568	3.395	0.923	1.598	2.010	2.793	3.679	0.999	1.697	2.126	2.941	3.866	1.154	1.902	2.365	3.250	4.255
45	0.795	1.435	1.821	2.552	3.375	0.908	1.577	1.986	2.762	3.638	0.978	1.669	2.092	2.897	3.811	1.122	1.857	2.313	3.181	4.168
50	0.788	1.426	1.811	2.538	3.358	0.894	1.560	1.965	2.735	3.604	0.961	1.646	2.065	2.863	3.766	1.096	1.821	2.296	3.124	4.096
75												1.570		2.748						
100												1.527		2.648						
150												1.478		2.611						
250												1.431		2.542						
500												1.385		2.475						
1000												1.354		2.430						
∞												1.282		2.326						

Reprinted with the kind permission of the publishers, Prentice-Hall, Inc., and the authors, A. H. Bowker and G. J. Lieberman, from *Engineering Statistics* (1959).

TABLE 7

RANDOM NUMBERS

24	81	06	14	98	24	93	58	63	66	58	26	24	45	65	91	42	68	67	42	61	74	77	93	46
75	55	54	29	67	02	81	01	67	54	08	81	34	00	79	62	38	52	14	88	38	66	59	41	97
49	71	80	54	37	73	34	11	74	14	91	86	82	41	02	76	12	36	71	38	43	72	84	36	27
04	19	48	35	54	98	00	41	47	44	63	13	27	50	18	75	16	72	40	90	02	45	87	82	15
66	15	52	42	22	91	22	96	38	41	03	27	15	67	26	36	81	75	11	82	94	33	62	08	94
10	80	17	67	83	05	31	23	08	07	40	00	60	44	65	70	16	31	73	05	46	41	47	64	68
40	42	27	55	76	82	88	42	76	51	58	49	58	75	38	23	57	06	64	69	46	90	09	55	68
95	57	21	21	25	12	05	41	70	28	03	59	97	37	64	48	69	48	59	60	89	76	35	83	05
57	27	64	94	98	88	93	70	86	59	46	84	08	32	31	75	61	19	49	11	28	46	76	79	28
80	56	69	49	63	83	78	78	76	36	89	51	16	47	35	86	69	96	69	88	91	22	47	24	84
44	51	75	51	08	17	43	53	31	09	60	34	34	61	93	66	01	94	37	13	24	09	75	29	21
55	42	48	76	50	13	89	69	00	05	99	45	82	01	53	86	68	81	36	50	75	20	17	94	47
80	50	67	83	01	97	76	21	64	34	62	43	02	84	38	13	60	26	32	36	81	43	17	56	41
03	64	65	44	02	75	41	33	91	28	82	97	57	38	49	27	26	97	34	44	26	12	00	68	24
14	53	75	37	91	43	95	15	13	26	33	27	45	48	33	80	80	26	69	76	04	87	83	58	32
01	64	43	36	30	71	24	75	92	73	07	81	13	35	46	88	62	80	64	69	86	25	73	92	98
39	38	79	42	17	77	99	55	32	85	13	35	48	49	80	83	59	06	34	94	06	03	61	85	02
74	96	24	94	89	54	66	29	35	88	50	46	65	50	26	62	45	80	61	95	07	99	57	10	54
21	16	54	55	77	46	38	33	88	55	21	56	18	93	32	94	24	80	97	03	78	39	73	87	70
58	51	99	53	96	73	60	77	21	06	76	59	78	55	96	99	07	53	91	95	99	60	56	61	79
46	98	27	95	19	22	29	41	56	76	83	48	49	82	79	79	20	00	26	40	22	50	14	30	73
58	46	36	76	19	18	00	60	50	28	32	44	18	35	99	28	91	50	53	62	21	61	26	46	81
43	05	50	00	20	39	25	46	84	39	27	39	92	42	59	04	64	15	09	35	07	11	25	51	17
84	07	33	83	87	14	33	79	07	66	60	43	66	57	57	57	59	01	78	80	13	77	63	58	10
93	54	23	72	70	09	36	16	24	04	74	05	65	29	64	67	37	28	13	98	01	48	29	75	89
54	46	72	02	34	52	81	38	52	96	14	54	27	32	41	74	84	83	90	01	97	59	87	66	41
43	60	84	28	32	93	91	76	70	31	50	22	09	40	89	64	85	82	76	91	16	71	99	98	70
64	80	80	16	92	46	42	46	47	22	87	16	20	65	82	01	45	21	49	80	17	39	70	74	03
78	70	39	30	06	59	65	14	84	04	82	28	46	64	05	89	81	80	09	89	56	11	27	81	44
14	88	67	03	59	32	15	83	04	01	20	82	92	25	34	88	84	80	76	69	25	10	04	86	02
69	28	06	18	56	78	97	49	14	85	01	58	31	16	20	53	74	03	27	05	80	39	15	67	49
99	68	09	96	36	54	10	77	95	88	90	84	52	16	52	58	87	51	31	71	68	53	11	85	50
01	66	22	15	54	63	83	64	15	30	21	86	48	17	11	68	92	16	17	49	36	05	17	80	24
67	85	26	91	23	14	28	01	76	47	65	12	58	24	27	61	59	43	20	15	93	47	30	56	27
13	91	16	76	91	97	85	48	99	50	40	96	30	66	97	82	66	06	90	97	65	28	44	98	08
95	82	20	95	52	65	95	03	48	75	64	25	04	13	85	80	13	37	08	18	09	28	63	07	69
44	06	82	49	28	27	34	53	42	35	44	12	40	64	35	06	28	14	37	23	97	38	07	60	80
99	22	26	64	15	71	06	96	22	93	77	46	73	57	51	22	54	82	37	99	96	27	25	87	77
08	44	26	12	87	72	42	13	57	77	61	07	94	24	62	17	76	19	45	18	98	11	47	40	31
14	96	76	06	37	32	09	72	81	22	87	70	81	93	78	93	37	22	32	25	38	45	38	03	31
27	86	41	53	58	16	49	99	19	03	62	98	79	81	98	15	03	62	32	93	68	24	14	44	50
99	67	81	61	25	52	97	87	98	15	85	99	01	86	59	00	11	39	32	53	49	18	62	51	65
89	14	37	94	03	22	32	45	42	61	97	83	04	26	30	48	49	40	99	99	69	96	13	94	21
34	13	53	15	32	42	02	58	32	14	83	73	02	82	49	25	62	91	14	94	70	72	64	50	51
72	11	79	75	79	36	07	12	92	61	89	93	77	82	08	23	74	75	67	56	37	45	35	13	44
19	72	57	61	99	08	62	02	26	82	52	90	72	51	94	84	59	79	34	19	95	76	21	49	91
96	99	76	63	90	27	60	94	15	70	17	74	92	31	85	24	47	55	64	51	91	47	13	39	69
44	15	86	76	18	15	57	29	51	62	95	84	20	83	01	11	90	66	80	81	40	43	65	87	35
33	83	94	07	50	18	89	86	16	50	09	97	04	76	51	41	20	56	50	20	33	53	70	10	22
53	07	06	16	30	84	43	40	57	32	18	09	47	16	69	41	03	38	24	02	16	41	58	39	58

TABLE 8

RANDOM NORMAL DEVIATES

$\mu = 0, \sigma = 1$

−0.670	0.518	0.387	0.523	0.641	1.243	0.322	−2.607	−1.097	−0.012
−2.912	1.448	1.343	−0.122	0.726	−0.617	0.609	2.319	−0.450	−1.197
−0.028	−0.790	0.057	1.425	1.940	1.161	−0.878	−0.716	−0.244	−1.151
−1.257	0.774	0.003	0.388	1.060	1.028	−0.236	1.172	0.442	−0.157
2.372	−1.376	−1.318	1.236	0.738	0.337	−0.534	0.090	0.886	0.676
−0.970	0.438	−0.672	−0.180	0.667	1.370	−0.481	0.329	0.842	0.449
−1.228	0.129	−0.426	−0.165	0.028	2.696	1.201	−1.351	0.724	−1.017
−0.369	0.310	0.432	0.237	0.884	−1.224	0.539	0.852	0.497	−0.283
1.161	1.219	1.615	0.336	1.100	−0.528	0.161	0.278	0.675	−1.143
−0.284	2.609	0.792	1.825	−0.249	1.654	0.621	0.979	−1.472	−1.173
−0.578	−0.789	0.106	0.832	−0.597	0.496	−0.561	−1.033	−0.578	−0.378
0.074	0.261	−0.766	−1.046	0.361	−0.043	−1.927	1.527	0.605	1.475
0.230	0.046	0.978	−1.901	1.162	−0.545	0.697	1.151	2.033	0.080
2.162	−0.562	1.190	0.925	−1.057	0.015	−1.371	1.067	−1.080	−1.129
−1.020	−1.130	−0.315	0.628	−0.140	2.050	−0.030	−0.629	0.128	−1.221
1.323	−0.836	−0.284	−0.249	−0.768	1.242	−0.879	−0.417	0.013	−0.502
2.329	1.884	0.033	0.598	−0.217	0.260	0.431	−1.914	0.205	1.155
2.761	1.800	−0.562	0.714	−0.407	0.009	−0.724	−1.168	0.247	1.166
−0.232	0.605	−0.023	−0.531	0.542	−0.155	0.697	1.037	−0.316	−0.003
−0.742	0.210	−0.741	−1.099	0.158	2.112	−0.765	−0.319	−0.247	0.345
−1.410	0.413	0.705	1.444	1.057	−0.843	0.043	−0.571	−0.001	0.203
2.272	−0.719	0.679	2.007	−0.180	0.698	−1.137	0.688	−0.571	−0.100
2.832	0.925	−1.350	1.529	−0.260	−1.007	−2.350	−1.501	0.289	1.522
−1.086	−0.558	−0.973	−1.285	−0.021	0.077	0.915	−0.241	−0.249	−0.529
0.134	1.815	0.313	1.571	−0.216	2.261	0.696	−0.130	0.393	0.017
0.783	0.600	−0.745	1.127	−0.684	−0.519	0.125	−0.499	1.543	−0.082
0.174	−0.897	0.575	−0.751	0.694	−2.959	0.529	1.587	0.339	−0.813
−1.319	0.556	2.963	1.218	1.199	−1.746	1.611	0.467	−0.490	0.202
1.298	−0.940	−1.143	−1.136	−1.516	0.548	0.629	0.250	−1.087	0.322
−0.676	−1.107	−1.483	0.278	0.493	−0.442	1.078	−0.336	−0.177	−0.057
−1.287	0.775	−1.095	1.161	−1.877	1.874	1.703	−1.619	−0.725	−1.407
0.260	−0.028	−1.982	0.811	0.999	1.662	0.908	1.476	−1.137	−0.945
0.481	1.060	1.441	0.163	0.720	1.490	−0.026	−0.502	0.427	−0.351
0.794	0.725	1.971	0.384	−0.579	−1.079	−1.440	−0.859	−0.346	0.077
0.584	−0.554	1.460	0.791	−0.426	−0.682	0.430	1.922	−2.099	0.221
−0.114	0.379	−0.698	1.570	−0.511	−0.725	0.680	−0.591	−1.091	0.357
−1.128	−1.707	0.921	−0.859	−1.566	1.523	−0.900	−0.988	0.264	0.282
0.691	0.153	0.076	1.691	0.553	0.457	−1.107	0.322	0.633	0.007
1.115	0.777	−0.738	0.868	1.484	−1.792	0.950	−0.842	−0.192	0.620
−0.389	0.559	0.670	−0.315	1.234	0.475	1.117	1.286	−0.649	−1.880
0.330	0.750	−0.642	0.148	−0.608	0.866	−1.720	0.653	−0.210	−0.959
−0.333	−0.084	1.239	−0.049	−0.095	−0.197	−0.213	−1.420	−0.491	0.102
1.718	1.111	−0.548	−0.653	1.534	−0.456	−0.395	1.614	−0.531	−0.785
−0.182	0.620	1.178	−1.071	0.444	−0.072	−1.001	1.325	−0.302	−1.119
1.260	−1.192	0.182	−0.397	−0.705	−1.085	−1.492	1.642	0.673	−0.707
−1.204	−1.725	1.695	1.473	0.665	−0.489	0.020	0.267	1.230	0.865
−0.619	0.307	−0.226	−0.096	0.987	−1.195	−1.412	0.433	2.052	0.022
−0.272	−0.096	0.137	−0.361	0.653	−0.156	1.309	−0.480	−0.397	1.302
0.245	−0.690	0.493	−1.123	1.465	0.132	0.582	−0.429	0.225	0.125
0.101	−0.855	0.782	−1.040	2.113	−1.423	−1.010	0.158	0.106	−1.232

SECTION G1 - LISTING OF SUMMARIES OF IBM COMPUTER PROGRAMS

The following pages contain a listing of computer programs which are useful in solving problems encountered by structures personnel. They are subdivided into the following categories:

The availability of additional reference material in the form of reports, memos, etc. is indicated. Information concerning some of the reference material can be found in Section A6.

Detailed information on any of the listed programs can be obtained from the Computer Technology Group (X7701).

LISTING OF SUMMARIES OF IBM COMPUTER PROGRAMS

General Title	Summary
Grumman Large Scale Matrix Package for IBM 7094	Consists of many subroutines which perform a variety of matrix operations. These operations include matrix additions, subtractions, multiplications, inversions, consolidations, row or column deletion, and partitioning. The subroutines have a common data format and communication medium. They are linked together by a program that controls the flow of data between them and also establishes the operations to be performed. Use of the large scale matrix package requires a joint effort by computer personnel and engineers. The formulation of the matrix problem, tabulation of input data and results is the responsibility of the engineer. Processing data and supplying the results to the structures engineer is the responsibility of the computer group.
Fortran Matrix Package	This program can carry out a chain of matrix operations provided row and column size does not exceed 90. Input matrix data must be in standard single word Grumman Format. These operations are controlled by a series of two digit code numbers, each number causing a matrix operation. Three storage zones designated A, B, and C are provided. As an example, the code number 06 causes the matrix multiplication of A x B and stores the result in C. Small matrix jobs can be

LISTING OF SUMMARIES OF IBM COMPUTER PROGRAMS

General Title	Summary
Fortran Matrix Package	easily coded and processed. Programs which utilize this matrix package include the following: 45135 - elastic analysis 45138A - matrix multiplication with and and without punched output, 45138B respectively. 45139 - solution of equations
Gismo Matrix Package (Ref: Bu-Docks GISMO Users Manual Contract No. NBy-33778)	Gismo performs similiar matrix operations as the Grumman Large Scale Package. It is intended primarily for the analysis of large scope structural problems. The decision as to which matrix package is preferable for a particular problem should be made jointly by the engineer and the Computer Technology Group.

LISTING OF SUMMARIES OF IBM COMPUTER PROGRAMS

Stress Distribution

Program Number	Title	Summary
45144	General Frame Analysis	Performs routine elastic analysis of following types of frames or beams: 1. One-celled frames with symmetrical or anti-symmetrical loading. 2. U-frames with symmetrical or anti-symmetrical loading. 3. Curved beams with the resisting forces or reactions at the ends of the beams. 4. Some types of curved beams with resisting shears and end reactions. The programs involved have additional capabilities which can be utilized to satisfy specific problem requirements. These capabilities include the following: 1. Shear and axial energy effects in addition to bending energy effects. 2. Pressure conditions (uniform and hydrostatic). 3. Two lines of shear flows. Frame member forces and flexibilities corresponding to the applied loads are punched out in standard Grumman format and can easily be incorporated into a fuselage analysis.
45156	General Unsymmetric Shell Analysis Program	This program is capable of performing a linear unsymmetric shell analysis and a linear or non-linear axisymmetric analysis. It can cope with any shell configuration that can be idealized into twenty-five or less shell segments and twenty-six or less node points. Each shell segment can have any one

LISTING OF SUMMARIES OF IBM COMPUTER PROGRAMS

Stress Distribution

Program Number	Title	Summary
45156	General Unsymmetric Shell Analysis Program	of the following geometric configurations: ellipsoid, ogive, parabola, cylinder, and cone. The program also has the capability of handling a "rigid" segment or kinematic linkage. Program output consists of stiffness coefficients for each shell segment. If shell segments are coupled, then final stresses, displacements, and yield stresses, are printed out along each shell segment at desired intervals.
45180	Shear Buckling - Rectangular Orthotropic Plates	Determines the shear buckling coefficients for both the symmetric and antisymmetric modes of buckling of simply supported, finite rectangular orthotropic plates from prescribed values of stiffness and geometry parameters.

LISTING OF SUMMARIES OF IBM COMPUTER PROGRAMS

Stress Distribution

Program Number	Title	Summary
45051	Flexibilities, Quadrilateral Shear Panel (Ref. GE 196)	Calculates the member flexibilities in a quadrilateral shear panel and in surrounding bar systems. This program also calculates appropriate terms to adequately consider Poisson's Ratio and sweep coupling effects.
45091	Argyris Redundants (Ref. GE 196)	Calculates redundant load distribution in an "Argyris Box" structure. Also calculates "kick" loads induced by warping of the cover panels and components of spar and rib cap strip loads. Structure is assumed to be symmetrical about a horizontal plane.
45045	Minimum Compression Buckling Load for Single and Double Corrugation Sandwich	The buckling equation for a single or double corrugation sandwich is minimized to determine the lowest buckling load for any given set of parametric values used to classify this type of structure.
45140	Axially Symmetric Shell Buckling (Non-Linear Shallow Shell Iteration)	This program calculates the non-linear deflected shape of an axi-symmetrically loaded shallow spherical shell. As a special case, non-linear arch deflections can also be determined. Internal load distributions are also provided.

LISTING OF SUMMARIES OF IBM COMPUTER PROGRAMS

Stress Distribution

Program Number	Title	Summary
45160	Variable Cross Section Column	Calculates the buckling coefficient and critical buckling load of a member with a varying EI. The member is pin connected at both ends and must be symmetric about a line through it's midpoint. Tabulated values of EI/EI max. must be provided as input data.
45132	Strength of Laminates Made of Orthotropic Materials	Computes the stress distribution in laminated plates of orthotropic materials under any combination of planer loads and edge moments. The laminates can have any orientation with respect to each other. The failure criterion used in the program is the modified Von Mises criterion recommended in MIL-HDBK 17.

LISTING OF SUMMARIES OF IBM COMPUTER PROGRAMS

Stress Distribution

Program Number	Title	Summary
45006	Cumulative Fatigue Damage	Based on Grumman Structures Manual fatigue curves, the program will calculate fatigue damage for both the pre-residual and post-residual life cycles. The theory of this program is explained in the fatigue section of the Structures Manual. For notched specimens, the accuracy of this method is greatest when the range of stresses predict more than 10,000 cycles of life.
45164	Barrel Shell Analysis (Ref: GE 209)	The ASCE Manual #31 equations are programmed for solution. Circular barrel shell stresses are computed for various normal loadings, simply supported transverse edges, and arbitrary longitudinal edge supports. Poisson's ratio is neglected. A plotting routine is incorporated into the program.
45128	Matrix Analysis Methods Inelastic Structures - Part I Elastic Plastic Solution of Shear Lag Problem (Ref. ADR 02-11- 62.2	Calculates the internal load distribution in a redundant in-plane structure considering inelastic plastic and creep effects. Material properties are isotropic or anisotropic. Input data consists of: 1) Components of Planar stress at the node points due to the applied loads and inposed strains (a maximum of 55 nodes are allowed). 2) Stress-strain table. 3) Creep coefficients. 4) Loading sequence. 5) Anisotropic params.

LISTING OF SUMMARIES OF IBM COMPUTER PROGRAMS

Stress Distribution

Program Number	Title	Summary
45174	Astral Automated Structural Analysis (Ref. ADN 02-11-65.1)	A series of linked programs for the solution of an idealized structure with only the structure geometry and material properties as input data. The programs included are: 1) Direct Stiffness Analysis - For the various options listed below the output is in form suitable for input to GISMO (G1. 01-2) for further coupling of structures. a) Large Package - For structures with a maximum of 150 joints at 3 degrees of freedom or 75 at 6 degrees of freedom. b) Small Package - For structures with a maximum of 45 joints at 2 degrees of freedom or 30 joints at 3 degrees of freedom or 15 joints at 6 degrees of freedom. For small structures this program requires much less computer time than (a) above or (c) GISMO Input - For structures which exceed the capacity of (a), this program will compute the stiffness matrix required for a solution. (d) Band Characteristic Program - For particular structures where the joints can be numbered so as to create a "banded" stiffness matrix not exceeding 270 elements in width, this option can solve structures with 300 joints at 3 degrees of freedom. 2) Automated Force Method - Solves structures composed of bars and shear panels. A maximum of 44 joints at 2 degrees of freedom are allowed. 3) Member Load Conversion - Generates a matrix to convert member loads from the stiffness

LISTING OF SUMMARIES OF IBM COMPUTER PROGRAMS

Stress Distribution

Program Number	Title	Summary
45174	Astral Automated Structural Analysis (Ref. ADN 02-11-65.1)	type to the force type. 4) Buckling - Computes critical buckling loads for structures composed of bars and beams. A maximum of 30 joints at 3 degrees of freedom, or 15 joints at 6 degrees of freedom are allowed.
45175	Structural Synthesis (Ref. ADR 02-21-65.1)	Optimizes the weight of an infinitely wide integrally stiffened panel subjected to compressive and shear loading. A realistic nonlinear failure criteria accounting for buckling and post buckling behavior of the panel elements is specified.

LISTING OF SUMMARIES OF IBM COMPUTER PROGRAMS

Dynamic Loads Under Transient Conditions

Program Number	Title	Summary
45151	Single Degree of Freedom Response (Ref. GE 90A)	Presents dynamic response of a linear, single degree of freedom system subjected to various forcing functions. The effects of viscous damping can be included.
45041	Equipment Shock Response (Ref. IOM 7/10/57 Shock Load Criteria for the Design of Electronic Equipment for the WF-2 Airplane R. Harris, A. Kelsey)	This program calculates the response of a non-linear spring-mass system with viscous damping to a half-sine wave acceleration pulse applied to the base of the system. This can represent the response of equipment (black boxes) mounted on vibration isolators when the base is subjected to the shock of MIL-E-5400 C or to a typical aircraft landing.
45172	Calculation of Normal Modes of Vibration	Obtains normal modes and frequencies of vibrations of structures idealized into lumped masses connected by weightless, flexible members. Input data requirements consist of mass, flexibility influence coefficient, and transformation matrices. Up to 144 relative degrees of freedom plus 6 degrees of freedom of a reference point can be allowed.

LISTING OF SUMMARIES OF IBM COMPUTER PROGRAMS

Dynamic Loads Under Transient Conditions

Program Number	Title	Summary
45122 45123 A,B,C,D	Response of a Wing to Transient Loading Conditions Induced by Landing and Catapulting (Ref. GE 172)	Predicts the behavior of an elastic airplane wing during catapulting, arrested or field landing. Decks 45122 A and B are used simultaneously to calculate the response of the wing to symmetric loading conditions. Decks 45123 A,B,C,D are used simultaneously to calculate the response of the wing to unsymmetric loading conditions. Both programs calculate wing net loads relative to a prescribed structural axis.
45182	A Method for Predicting the Dynamic Behavior of a Particular Type of Articulating Landing Gear (Ref. ADN 02-10-65.1)	Predicts the behavior of a landing gear which articulates in a plane parallel to the plane of symmetry during the initial landing impact. All the important parameters required to define the ground loads are considered. The program prints out all the pertinent design data.

LISTING OF SUMMARIES OF IBM COMPUTER PROGRAMS

Dynamic Loads Under Transient Conditions

Program Number	Title	Summary
45034	Metering Coefficient from Strut Dimensions	Calculates metering coefficient K, which is used to determine the viscous damping force as a function of the shock strut stroking velocity squared. Metering pin and orifice diameters and the density of the hydraulic fluid must be provided.
45023	Dynamics of Arresting Hook Due to Impact with Deck (Ref. GE 184)	Predicts behavior of arresting hook when it strikes deck structure during a carrier landing. Determines stresses in hook, path of toe, hold-down dashpot requirements, and loading on hook bumper should hook contact it.
45145	Nose Tow Catapult	Predicts structural loads and general behavior induced during the nose tow catapulting of an aircraft. The airplane is assumed to be a single rigid body except for the nose gear assembly and the two main gears.
45142	Nose Tow Catapulting Off Center Spotting Dynamics (Ref. GE 203)	Predicts nose gear lateral loads due to off-center spotting during nose tow catapulting. The effect of nose gear lateral flexibility has been included. Aerodynamic forces and structural damping are neglected. This restricts the validity of the results to the first load cycle experienced by the gear or approximately the

LISTING OF SUMMARIES OF IBM COMPUTER PROGRAMS

Dynamic Loads Under Transient Conditions

Program Number	Title	Summary
45142	Nose Tow Catapulting Off-Center Spotting Dynamics (Ref. GE 203)	first second of motion. Output of the program includes translation, rotation, velocity, and acceleration in the X, Y, and β directions.
45130	Dynamics of Unsymmetric Landing (Ref. ADR 02-10-62.1)	Predicts dynamic behavior of an airplane during an unsymmetrical landing. Six degrees of freedom are allowed at the aircraft C.G. Aerodynamic and thrust forces can be applied to the aircraft. Metering, bending flexibility, and bearing friction of the oleo struts are provided for. Flexibility of supporting gear braces and of the airplane structure at the gear attachment points are also provided. The effects of cable arrestment during carrier landings can be accounted for.

LISTING OF SUMMARIES OF IBM COMPUTER PROGRAMS

Dynamic Loads Under Transient Conditions

Program Number	Title	Summary
45036	Arrested Landing with Cable Impact (Ref. GE 176)	Determines rigid aircraft motion and landing gear load-time histories for either symmetrical shipboard arrestments or field landings. This analysis is also capable of determining loads induced when a wheel impacts and rolls over an arresting cable. Coupled aerodynamic, inertial, arrestment, and landing gear forces, excluding aerodynamic drag are fully described.
45043	Tail Bounce Analysis	Determines tail bumper loads when aircraft brakes are applied as aircraft rolls backward. Analysis can consider the fuselage as flexible. The main gear is represented by a non-linear spring assigned the flexibility properties of the tire and strut combination. The spring located at the bumper represents the local flexibility of the bumper material as well as airframe flexibility.
45067-M	Water Impact of Manned Space Craft (Ref. ADR-04-03a-61.1)	Determines the effect on spacecraft subjected to rough water impact. The theoretical NASA approach for

LISTINGS OF SUMMARIES OF IBM COMPUTER PROGRAMS

Dynamic Loads Under Transient Conditions

Program Number	Title	Summary
45067-M	Water Impact of Manned Space Craft (Ref. ADR-04-03a-61.1)	rotationally constrained, prismatic bodies impacting smooth water is expanded to account for the behavior of a pitching, non-prismatic vehicle penetrating rough water. The analysis calculates normal acceleration, rotational acceleration, attitude, and vehicle velocity.
45087	Transient Response Using Transfer Function Data (Ref. Str. Methods Note: An Introduction to Mechanical Transfer Functions, A. Kelsey - 5/61)	The transient response for a linear system is obtained by means of a modified Duhamel integral solution. The integrand is a function of experimental transfer function data.
45087 TF	Evaluation of Transfer Function (Ref. See 45087)	The theoretical transfer function is calculated based upon normal mode data for a multi-degree of freedom system. A tabulation is made of transfer function vs. frequency.

LISTING OF SUMMARIES OF IBM COMPUTER PROGRAMS

Dynamic Loads Under Transient Condtions

Program Number	Title	Summary
45103	Roving Vehicle Dynamic Analysis (Ref. ADR 06-04b-61.1)	Predicts behavior of wheeled vehicle traveling on the lunar surface. The chassis of the idealized vehicle is assumed to be a simple rigid body with its mass and inertia properties concentrated at its C.G. The wheel masses, which are asssumed concentrated at the axles, are connected to the chassis by a suspension system idealized as non-linear springs in parallel with velocity sensitive damping devices.
45500	LEM Symmetric Landing Study - Tripod Gears	Predicts the dynamic behavior of the Lunar Excursion Module during symmetrical or un-unsymmetrical landing. Principal features of the analysis are:
45501	LEM Unsymmetric Landing Study - Tripodal Gears	1. The vehicle may possess 4, 5 or 6, "tripodal" type or "cantilever" type gears.
45505	LEM Symmetric Landing Study - Cantilever Gears	2. Six degrees of freedom are allowed at the vehicle C.G. for unsymmetric motion (three degrees of freedom of the C.G. are allowed for the symmetric case).
45514	LEM Unsymmetric Landing Study - Cantilever Gears	3. Three degrees of freedom are allowed at each of the gear foot pads.
	(Ref. LED 520-6)	4. Strut load-stroke charateristics may be represented by any single valued function.

LISTING OF SUMMARIES OF IBM COMPUTER PROGRAMS

Dynamic Loads Under Transient Conditions

Program Number	Title	Summary
45514	LEM Unsymmetric Landing Study - Cantilever Gears (Ref. LED 520-6)	5. The landing surface may be inclined and may contain protuberances and depressions. 6. Each pad may impact a surface of different energy absorbing capacity. 7. Built in crushing characteristics of the foot pads are considered.

LISTING OF SUMMARIES OF IBM COMPUTER PROGRAMS

Temperature Distribution

Program Number	Title	Summary
45113-E	Ablating Slab & Sub-Structure Transient Temperature Response	Determines transient temperature response in a charring ablator and a 2-dimensional backup structure subjected to convective heat input on the outer surface ablation material. No surface recession is assumed. Depth of charring can be determined.
45060	Honeycomb Sandwich Panel Temperature Distribution	Computes transient temperature distribution in a honeycomb sandwich panel subjected to aerodynamic heating on one or both sides. The program accounts for radiant heat transfer on both inner and outer surfaces and conduction through honeycomb core.
45061	Corrugated Sandwich Panel Temperature Distribution	Computes transient temperature distribution in a corrugated sandwich panel subjected to aerodynamic heating on one or both sides. The program accounts for radiant heat transfer on both inner and outer surface and conduction through honeycomb core.
45062	Multi-slab Temperature Distribution	This program calculates the transient temperature response of a plate which is divided into "N" isothermal zones where N varies from 3 to 20. Heat input by convection, as well as a more general heat input, are permitted as a function of time. Temperature-time histories for each isothermal zone are calculated. The effects of heat loss by radiation from the heated

LISTING OF SUMMARIES OF IBM COMPUTER PROGRAMS

Temperature Distribution

Program Number	Title	Summary
45062	Multi-slab Temperature Distribution	surface are included. Variation of specific heat and thermal conductivity with temperature is permitted.
45063	Isolated Plate Temperature Response	Computes transient temperature distribution in a thin, isothermal plate subjected to aerodynamic heating on one or both sides. Program accounts for radiant heat transfer on the surfaces. Specific heat as a function of temperature can be described as part of the input data.
45177	Thermal Protection System - Composite	Program description source as program 45178 (above) except: 1. Magic subroutine is employed for forward integration. 2. Time variation in boundary layer oxygen. 3. Automatic plot routine is incorporated for temperature response & mass loss.

LISTING OF SUMMARIES OF IBM COMPUTER PROGRAMS

Temperature Distribution

Program Number	Title	Summary
45065	Thick Walled Cylinder - Transient Temperature Response	Computes transient temperature distribution through the wall of a cylindrical cross section where both inner and outer surfaces may be subjected to aerodynamic heating. Program accounts for radiant heat transfer from the surfaces. Thermal conductivity and specific heat as a function of temperature can be described as part of the input data.
45113-A	Radiant Interchange & Equilibrium Temperatures	Determines radiation interchange factors and equilibrium temperature distribution in a three dimensional system. Thermal boundary conditons can consist of: (a) convective heat input as a function of temperature, and (b) heat input by convection, conduction, and radiation from fixed temperature sources.
45113-B	Radiant Interchange & Transient Temperatures	Determines transient temperature response in a three dimensional system identical to that described for program 45113-A. Thermal boundary conditions applied to the system can consist of: (a) convective heat input which is a function of temperature and time, and (b) heat input by convection, conduction, and radiation from fixed temperature sources.

LISTING OF SUMMARIES OF IBM COMPUTER PROGRAMS

Temperature Distribution

Program Number	Title	Summary
45113-C	Configuration Factors - Axisymmetric Enclosures	Determines black body radiation configuration factors in a system consisting of surfaces of revolution. These surfaces of revolution are described around a common axis. Shadowing effects between surfaces are accounted for.
45113-D	Configuration Factors - General	Determines black body radiation configuration factors in a system consisting of surfaces of revolution and flat, rectangular plates arranged in random fashion. Shadowing effects between surfaces are accounted for.
45178	Reentry Ablation Temperature Response	Program calculates temperature response and mass loss for a one-dimensional ablation system with substructure. The ablation material is divided into two layers (representing charred and uncharred portions) whose boundaries can move with time. The boundary recession is determined by the mass losses of the two layers. Char removal can take

LISTING OF SUMMARIES OF IBM COMPUTER PROGRAMS

Temperature Distribution

Program Number	Title	Summary
45178	Reentry Ablation Temperature Response	place through oxidation and sublimination while uncharred material is thermally degraded into Char material and a gas that passes through the char layer to the front (heated) surface. Temperature response is calculated by a forward difference numerical technique. The analysis was principally developed for charring ablators subjected to reentry thermal enviornments but is applicable to impregnated ceramics, subliming ablators or any conduction problem involving up to 3 layers of material. Principal data required for use with charring ablators are: 1. Cold wall convective heating rates and radiative heating vs. time. 2. Density, specific heat vs. temperature, and thermal conductivity vs. temperature, for char layer, uncharred layer & substructure. 3. Heat of pyrolysis of virgin plastic, reaction rate factors, or ablation temperature, and specific heat of decomposition gases vs. temperature. 4. Boundary layer enthalpy pressure and oxygen concentration.

STRUCTURES MANUAL

BULLETIN # 1

HAS BEEN INTENTIONALLY OMITTED

FROM THIS EDITION:

THE MATERIAL OF THAT BULLETIN

HAS EITHER BEEN INCORPORATED INTO THE

BASIC STRUCTURES MANUAL, OR

HAS BEEN SUPERSEDED.

July 2, 1956
(Revised March 31, 1966)

STRUCTURES BULLETIN NO. 2

To: All Holders of Structures Manuals

From: J. Meirs

Subject: Fatigue Allowables for AN509 Screws, Sheet-Fastener Combinations

A method is presented here for determining the fatigue life of joints with AN509 screws machine-countersunk in R301-T6 or 75S-T6 aluminum alloy sheet, clad or bare. The method is based upon fatigue test data obtained at Grumman, which indicated no significant differences in fatigue allowables for the different sheet materials. The test data and the procedures used to extend the information beyond the range of the tests will be presented in GE-150.

John Meirs

J. Meirs
Chief of Structures

No 2

Fatigue Allowables for Joints with AN509 Screws Machine Countersunk in R301-T6 or 75S-T6 Sheet

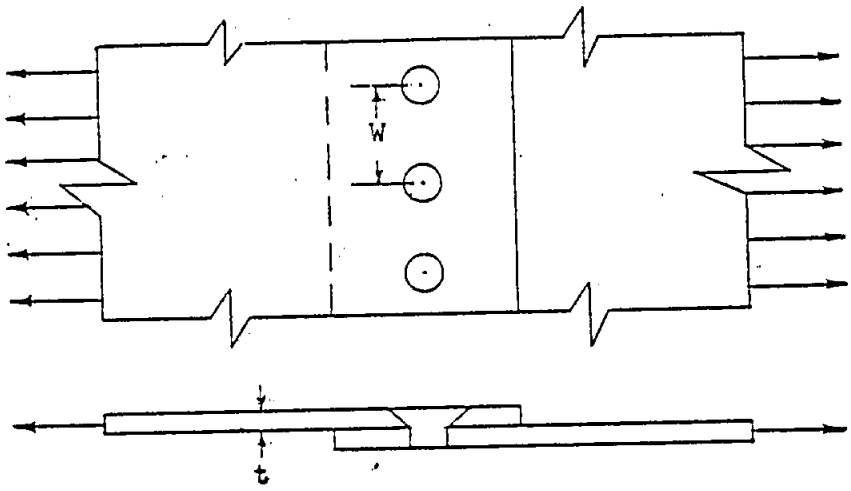

Fig. 1

Symbols:

C = Percentage increase in the fatigue strength per screw for a joint with a wide screw spacing ($\frac{W}{D}$ = 12) over a joint with a narrow screw spacing ($\frac{W}{D}$ = 3.5). (See Fig. 5.)

D = Shank diameter of screw

f_{nt} = Average tensile stress in countersunk sheet at the net section

$f_{nt_{nom.}}$ = $\frac{P}{(W-D)t}$ = nominal tensile stress in the countersunk sheet at the net section

$f_{nt\,①}$ = A reference value of net-tension fatigue stress (see Fig. 3). (In particular, it is the net-section stress causing fatigue failure in a joint with a 3/8 inch screw, with $\frac{W}{D}$ = 3.5)

$f_{nt_{diff.}}$ = Size effect correction to the reference fatigue stress, $f_{nt\,①}$, (see Fig. 4). (In particular, it is the difference in net-tension fatigue stress at a given number of cycles between a joint with some given screw diameter D, and a joint with a 3/8 inch screw, where $\frac{W}{D}$ = 3.5 in both cases.)

No. 2

Symbols (Cont.)

K = Ratio of bearing stress to tension stress, where $\frac{W}{D} = 3.5$. (See Fig. 2.)

P = Load per screw

$P_{(1)}$ = A reference value of fatigue strength per screw. (In particular, it is the load per screw causing fatigue failure in a joint with $\frac{W}{D} = 3.5$.)

R = $f_{nt_{min}}/f_{nt_{max}}$ = ratio of minimum to maximum stress in the fatigue cycle.

t = Countersunk sheet thickness

W = Screw spacing perpendicular to load line

Determination of Fatigue Strength for a Given Lifetime

The load per screw causing failure at any given number of cycles in a countersunk sheet-screw combination can be obtained by using the curves in Fig. 3 to 5. Fig. 3 can be used to determine $f_{nt_{(1)}}$, a reference value of net-tension fatigue strength at the given number of cycles. Fig. 4 gives $f_{nt_{diff.}}$, a correction to $f_{nt_{(1)}}$ that depends upon the screw size.

$P_{(1)}$, a reference value of fatigue strength per screw, can be determined by:

$$P_{(1)} = K\,(f_{nt_{(1)}} + f_{nt_{diff.}})\,Dt \qquad (1)$$

where, K is given in Fig. 2.

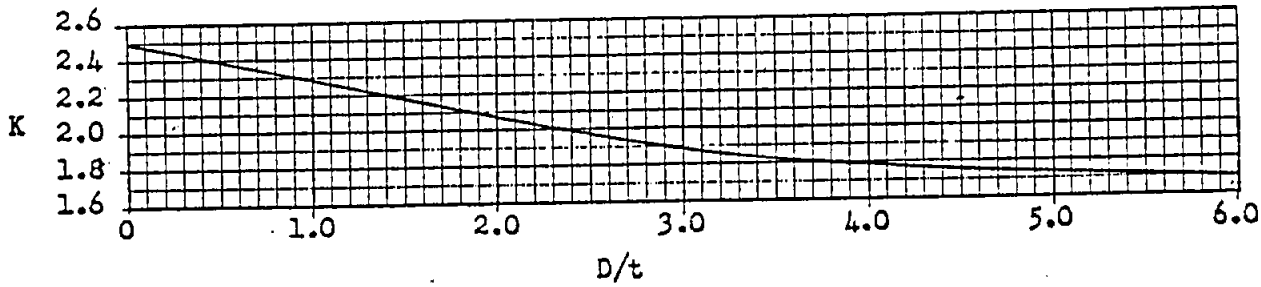

FIG. 2

P, the actual value of fatigue strength per screw at the given number of cycles, can now be determined by:

$$P = P_{(1)}\left[1 + \frac{C}{100}\left(\frac{\frac{W}{D} - 3.5}{8.5}\right)\right] \qquad (2)$$

where, C is given in Fig. 5.

No. 2

Determination of Fatigue Strength for a Given Lifetime (Cont.)

Example #1

Given a joint as shown in Fig. 1, with t = 0.102 inches, D = 3/16 inches, W = 1.0 inch. The sheet is of 75S-T6 bare aluminum alloy, machine countersunk, and the fasteners are AN509-#10 screws. Assuming that the stress ratio R is 0.20, determine the load per screw for a fatigue life of 50,000 cycles.

1. Determine $\frac{D}{t}$, Dt, and $\frac{W}{D}$;

$\frac{D}{t} = \frac{.188}{.102} = 1.84$, $Dt = (.188)(.102) = 0.0192$ in.^{2}, $\frac{W}{D} = \frac{1.0}{.188} = 5.33$

2. Determine the reference stress, $f_{nt_{①}}$, at 50,000 cycles.

From Fig. 3: $f_{nt_{①}} = 14{,}800$ psi.

3. Determine the correction stress, $f_{nt_{diff.}}$, at 50,000 cycles.

From Fig. 4: $f_{nt_{diff.}} = 7{,}000$ psi.

4. Determine the reference fatigue strength per screw, $P_{①}$.

$$P_{①} = K(f_{nt_{①}} + f_{nt_{diff.}})\, Dt \quad \text{----------(Eq. 1)}$$

K = 2.1 (Fig. 2)

$\therefore P_{①} = (2.1)(14{,}800 + 7000)\,(0.0192) = \underline{\underline{880}}$ pounds

5. Determine the actual failing load per screw, P, at 50,000 cycles.

$$P = P_{①}\left[1 + \frac{C}{100}\left(\frac{\frac{W}{D} - 3.5}{8.5}\right)\right] \quad \text{----------(Eq. 2)}$$

From Fig. 5: C = 43%

$\therefore P = (880)\left[1 + \frac{43}{100}\left(\frac{5.33 - 3.5}{8.5}\right)\right] = \underline{\underline{961}}$ pounds

Determination of Fatigue Life for a Given Load

If the problem is to find the fatigue life of a given joint, where the load per screw is known, the following procedure is recommended:

A. Determine the nominal net-tension stress in the joint. Then, as a first approximation to the fatigue life, set the reference stress, $f_{nt_{\textcircled{D}}}$, equal to the nominal net-tension stress, and determine the corresponding number of cycles to failure from Fig. 3. The actual fatigue life of the joint will, of course, be somewhat different from this.

B. Determine the load necessary to cause fatigue failure in the joint at the number of cycles calculated in Step (A) above. Use the method outlined in Example #1.

C. If the load calculated in Step (B) is less than the applied load, repeat the calculations in Step (B) at some lower number of cycles. If the load calculated in Step (B) is greater than the applied load, repeat the calculations at some higher number of cycles.

If the loads determined in Steps (B) and (C) bracket the applied load, plot them on log paper (Fig. 6) against the corresponding fatigue lives, and connect the two points with a straight line. A good approximation can then be obtained for the fatigue life corresponding to the given load.

D. If the loads determined in Steps (B) and (C) do not bracket the applied load, then Step (C) can be repeated for a different number of cycles until the applied load is bracketed. Then, the graphical solution described above can be used.

Example #2

Consider the same joint as in Example #1. Assuming that the stress ratio R is 0.20, determine the fatigue life if the maximum load per screw is 1,200 pounds.

A. (1) Determine $\frac{D}{t}$, Dt, $\frac{W}{D}$, and K.

$$\frac{D}{t} = 1.84,\ Dt = 0.0192\ in.^2,\ \frac{W}{D} = 5.33,\ K = 2.1 \quad \text{(Fig. 2)}$$

(2) Determine $f_{nt_{nom.}}$, the nominal net-tension stress at maximum load.

$$f_{nt_{nom.}} = \frac{P}{(W-D)t} = \frac{1200}{(1-.188)(.102)} = 14{,}500\ psi$$

(3) Assuming $f_{nt_{\textcircled{D}}}$ is equal to $f_{nt_{nom.}}$, determine the first approximation to the fatigue life from Fig. 3.

$$n = 53{,}000\ cycles$$

Determination of Fatigue Life for a Given Load (Cont.)

Example #2 (Cont.)

B. Determine the load per screw causing failure in the actual joint at 53,000 cycles. (See the procedure outlined in Example #1.)

(1) $f_{nt_{①}}$ = 14,500 psi. (From Fig. 3)

(2) $f_{nt_{diff.}}$ = 7,000 psi. (From Fig. 4)

(3) $P_{①} = K (f_{nt_{①}} + f_{nt_{diff.}}) Dt$

$= (2.1)(14,500 + 7,000)\ (0.0192) = 867$ pounds

(4) $P = P_{①} \left[1 + \frac{C}{100} \left(\frac{\frac{W}{D} - 3.5}{0.5} \right) \right]$ (From Eq. 2)

$= (867) \left[1 + \frac{43}{100} \left(\frac{5.33 - 3.5}{0.5} \right) \right] = 948$ pounds/screw

where, C = 43% from Fig. 5.

This value of P is less than the given loading of 1200 pounds per screw. Therefore, the fatigue life must be less than 53,000 cycles.

C. Assume the fatigue life is 10,000 cycles and determine the failing load per screw.

(1) $f_{nt_{①}}$ = 25,200 psi. (From Fig. 3)

(2) $f_{nt_{diff.}}$ = 8,300 psi. (From Fig. 4)

(3) $P_{①} = K (f_{nt_{①}} + f_{nt_{diff.}}) Dt$

$= (2.1)(25,200 + 8,300)\ (0.0192) = 1,350$ pounds

(4) $P = P_{①} \left[1 + \frac{C}{100} \left(\frac{\frac{W}{D} - 3.5}{0.5} \right) \right]$ (From Eq. 2)

$= (1350) \left[1 + \frac{20}{100} \left(\frac{5.33 - 3.5}{0.5} \right) \right] = 1,410$ pounds/screw

where, C = 20% from Fig. 5.

This value of P is greater than the given loading of 1200 pounds per screw. Therefore, at the given loading, the fatigue life will be between 10,000 cycles and 53,000 cycles.

Plotting the two failing loads obtained in (B) and (C) against the number of cycles at failure on Fig.6, and connecting the two points with a straight line, the number of cycles at failure for P = 1,200 pounds/screw is:

n = 20,000 cycles (From Fig. 6)

FIGURE 3

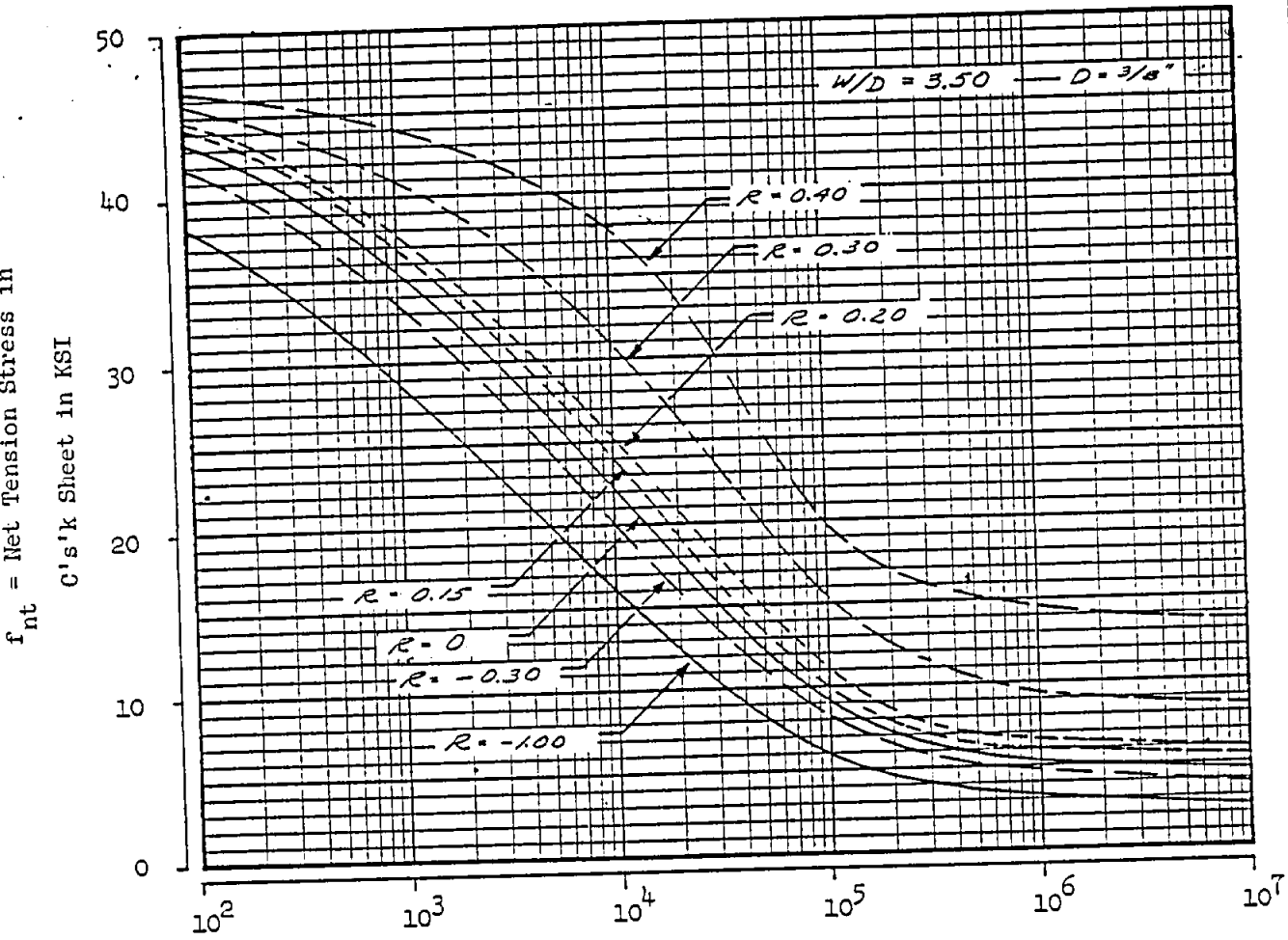

FIGURE 4

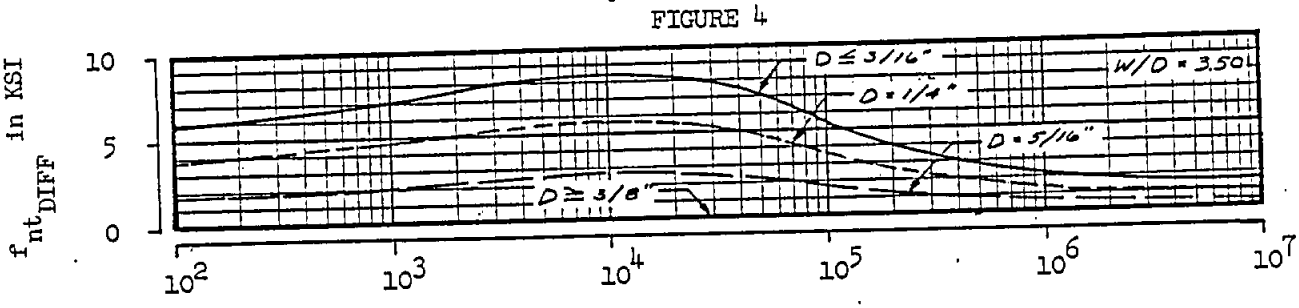

FIGURE 5

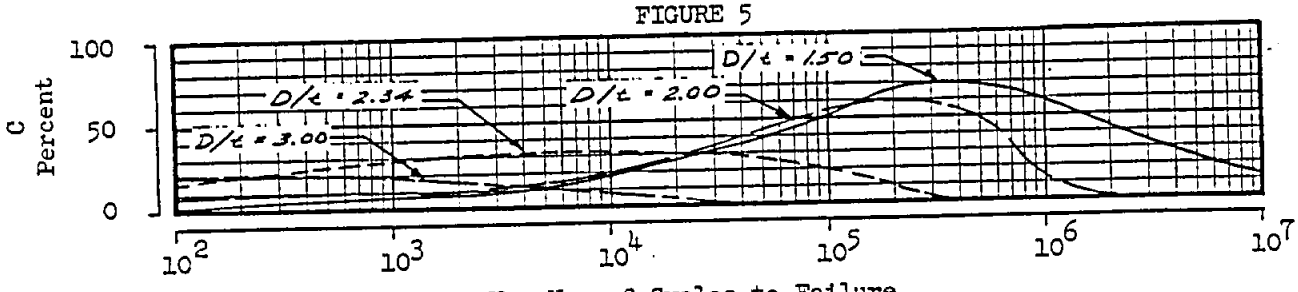

N = No. of Cycles to Failure

(Revised March 24, 1966)

Grumman

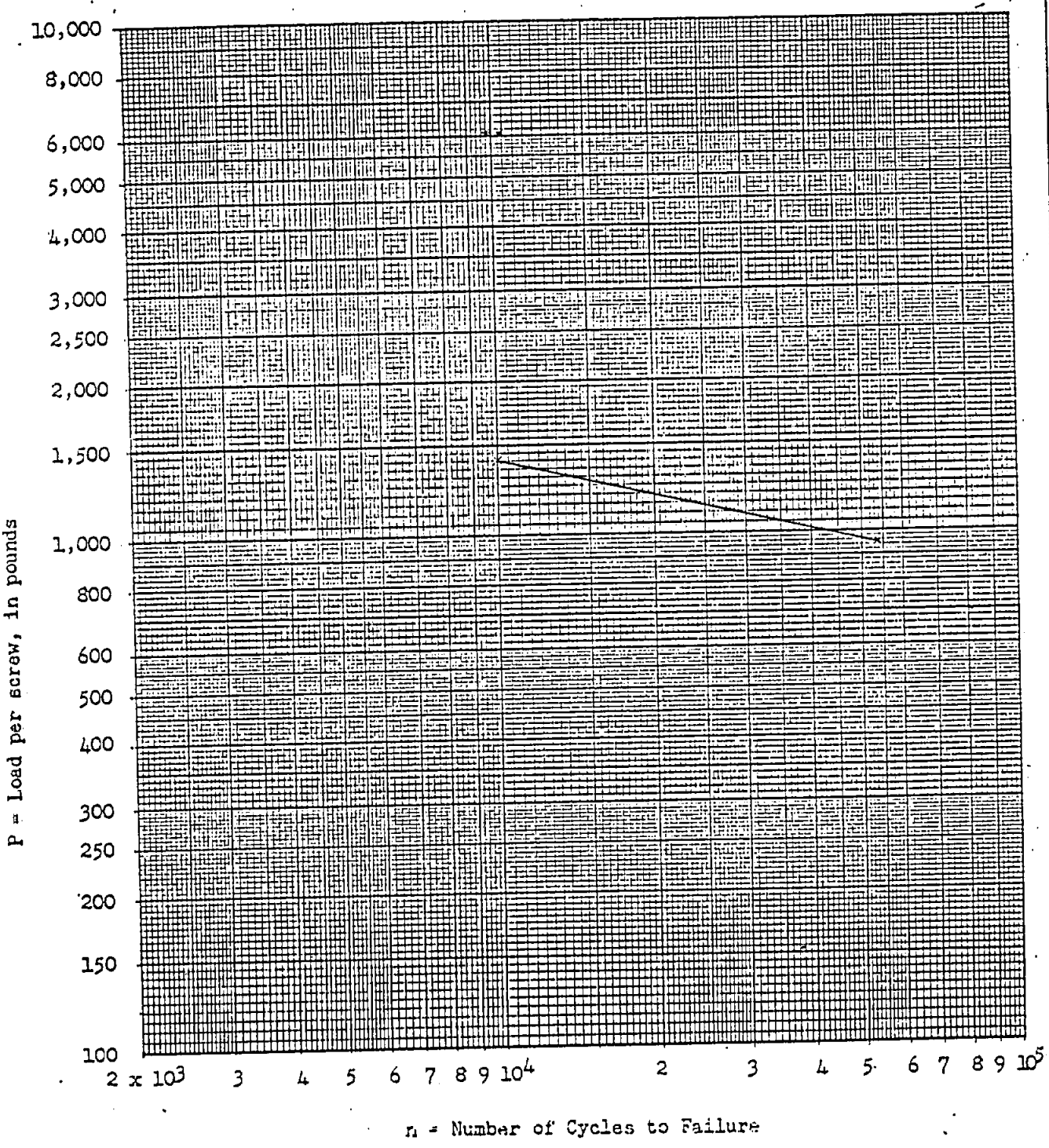

FIGURE 6

NOTE: Horizontal Scale can be adjusted to suit any particular problem.

STRUCTURES MANUAL

BULLETIN # 3

HAS BEEN INTENTIONALLY OMITTED

FROM THIS EDITION:

THE MATERIAL OF THAT BULLETIN

HAS EITHER BEEN INCORPORATED INTO THE

BASIC STRUCTURES MANUAL, OR

HAS BEEN SUPERSEDED.

February 15, 1957
(Revised March 24, 1966)

STRUCTURES BULLETIN NO. 4

To: All Holders of Structures Manuals

From: J. Meirs

Subject: Stagnation and Adiabatic Wall Temperatures for "NACA Standard Day" and "Navy Hot Day" Conditions

Nomograms for the rapid calculation of Stagnation and Adiabatic Wall Temperatures are presented.

Temperatures for either "NACA Standard Day" or "Navy Hot Day" conditions can be obtained for altitudes up to 100,000 feet and Mach Numbers up to 5.

John Meirs

J. Meirs
Chief of Structures

STRUCTURES BULLETIN NO. 4

Stagnation and Adiabatic Wall Temperatures for "NACA Standard Day" and "Navy Hot Day" Conditions

Introduction

Vehicles flying at supersonic speeds are subjected to heating of an aerodynamic nature. This heating is due to an increase in temperature in a thin layer of air around the body. The air in this layer, known as the "Boundary Layer", is slowed down by viscous forces and part or all of its kinetic energy is converted into heat.

The performance of a structure subjected to aerodynamic heating will depend on the maximum temperature and thermal gradients that result as heat is being transferred from the boundary layer air to the structure. A nomogram-type method for the determination of the temperatures in the boundary layer air has been developed and is presented in this Bulletin.

The structure in supersonic flight will be exposed to these temperatures. The temperature distribution at any time in the structure will depend, however, on other factors as well. Some of these are: the heat transfer coefficient of the boundary layer air and the temperature alleviating effects of reradiation, significant at high temperatures only, and possible surface cooling schemes.

The Stagnation and Adiabatic Wall Temperatures (defined below) can be determined from the nomogram on Page 6 for either an "NACA Standard Day" or "Navy Hot Day" condition for altitudes ranging from sea level to 100,000 feet and for speeds up to Mach 5.

The temperatures so obtained are accurate within $\pm 5^{\circ}F$ if below $300^{\circ}F$. Temperatures in excess of $300^{\circ}F$ are obtained with engineering accuracy by the joint use of the nomograms on Pages 6 and 7.

Stagnation Temperature

This is the temperature the air will attain when brought to a stop. As such, it will exist only on the leading edge of an airfoil or the nose of a cone.

Stagnation Temperatures obtained from the basic nomogram, Page 6, satisfy the relationship:

$$T_{st} = (T_o + 460)\,(1 + M^2/5) - 460 \quad \ldots\ldots\ldots\ldots\ldots\ldots \quad (1)$$

where:

T_{st} = Stagnation Temperature ($^{\circ}F$)

T_o = Free Stream or Ambient Temperature ($^{\circ}F$)

M = Mach Number

STRUCTURES BULLETIN NO. 4

Stagnation and Adiabatic Wall Temperatures (Continued)

Adiabatic Wall Temperature (Boundary Layer Temperature)

Due to the existence of a velocity gradient in the boundary layer, extending from zero at the body surface to the free stream velocity at the edge of the boundary layer, a temperature gradient is also present. The air thus loses heat to the structure as well as to the free stream.

The maximum temperature to be attained by a body, if its internal surface were perfectly insulated, and if it were exposed to the boundary layer long enough to reach an equilibrium condition*, is known as the Adiabatic Wall or Boundary Layer Temperature. As such, it is the temperature to which parts of a vehicle other than the leading edges or the nose of a cone are exposed. The Adiabatic Wall Temperature is always less than the Stagnation Temperature due to the heat losses mentioned above. The reduction in temperature from a Stagnation value is expressed by a Recovery Factor varying from 0.85 for laminar flow to 0.90 for turbulent flow. In the nomogram, the Recovery Factor is taken as 0.90.

Adiabatic Wall Temperatures obtained from the basic nomogram, Page 6, satisfy the relationship:

$$T_{aw} = (T_o + 460)(1 + M^2 r/5) - 460 \quad \ldots\ldots\ldots\ldots (2)$$

where:

$T_{aw} = T_{bl}$ = Adiabatic Wall or Boundary Layer Temperature (^oF)

T_o = Free Stream or Ambient Temperature (^oF)

r = Recovery Factor = 0.90

M = Mach Number

Correction Nomogram

The temperatures read on the basic nomogram shown on Page 6 are accurate only up to the 300°F range. For higher temperatures, equations (1) and (2), based on the room temperature value of the specific heat of air (c_p), yield values that could be in considerable error.

Temperatures of engineering accuracy can be obtained however, by the use of the correction nomogram shown on Page 7. The corrected temperatures, determined by the simultaneous use of the two nomograms, agree well with values shown elsewhere (Ref. 1).

* Reradiation not considered

STRUCTURES BULLETIN NO. 4

Stagnation and Adiabatic Wall Temperatures (Continued)

The corrections do not reflect high temperature effects such as dissociation and departures from the law of perfect gases. These variations become significant for Mach Numbers higher than 5.

Procedure for Use of Basic Nomogram (Page 6)

To use the nomogram, the following steps are necessary:

(a) Locate altitude on axis I (Right side for NACA Standard Day, left side for Navy Hot Day)

(b) Locate Mach Number on axis III (Right side when determining Adiabatic Wall Temperature, left side when determining Stagnation Temperature)

(c) Connect points selected on axis I and axis III and read temperature on axis II (Right side for Stagnation Temperature, left side for Adiabatic Wall Temperature).

Note that for altitudes between 35,300 and 100,000 feet for "NACA Standard Day" and between 43,750 and 100,000 feet for "Navy Hot Day" conditions, the values on axis I do not change.

Example No. 1:

The Adiabatic Wall Temperature is desired on the surface of a wing flying at M = 2 at 40,000 feet during an "NACA Standard Day" flight condition.

(a) Locate 40,000 feet on the right side of axis I

(b) Locate M = 2 on the right side of axis III

(c) Connect points on axis I and III, and read T_{aw} = 216°F on left side of axis II

Procedure for Use of Correction Nomogram (Page 7)

When the temperature as determined with the basic nomogram is in excess of 300°F, the use of the correction nomogram is advisable; the following steps are necessary in using it:

(a) Locate on axis A the temperature just determined by using the basic nomogram of Page 6

(b) Locate the Mach Number on axis C and connect with the point obtained above

STRUCTURES BULLETIN NO. 4

Stagnation and Adiabatic Wall Temperatures (Continued)

Procedure for Use of Correction Nomogram (Page 7) (Cont.)

(c) Read a "Corrected Mach Number" on axis B

(d) Find a corrected temperature on the basic nomogram of Page 6 following the procedure outlined previously. Note that the only change is a somewhat smaller value for the Mach Number.

(e) Repeating points (a) through (d) will improve the correction, but it will be found that in most cases, one correction is sufficient. Each new correction is made using the original Mach Number and the temperature obtained previously.

Example No. 2

The Stagnation Temperature is desired on the leading edge of a wing flying at Mach Number 4 at 70,000 feet during a "Navy Hot Day" flight condition.

1. Basic Nomogram:

   (a) Locate 70,000 feet on left side of axis I

   (b) Locate M = 4 on left side of axis III

   (c) Read T_{st} = 1200°F on right side of axis II

2. Correction Nomogram:

   (a) Locate 1200°F on axis A

   (b) Connect M = 4 on axis C with the above point and read M' = 3.85 on axis B

   (c) Repeat Basic Nomogram procedure changing in step (b) only, to M = 3.85

   (d) Read corrected temperature T_{st} = 1100°F

   (e) A second correction yields M' = 3.86 and T_{st} = 1110°F

Ref. 1:
WADC Technical Report 55-305, Part 1
Structural Design for Aerodynamic Heating
W.H. Dukes and A. Schnitt

STAGNATION AND ADIABATIC WALL TEMPERATURE

Basic Nomogram

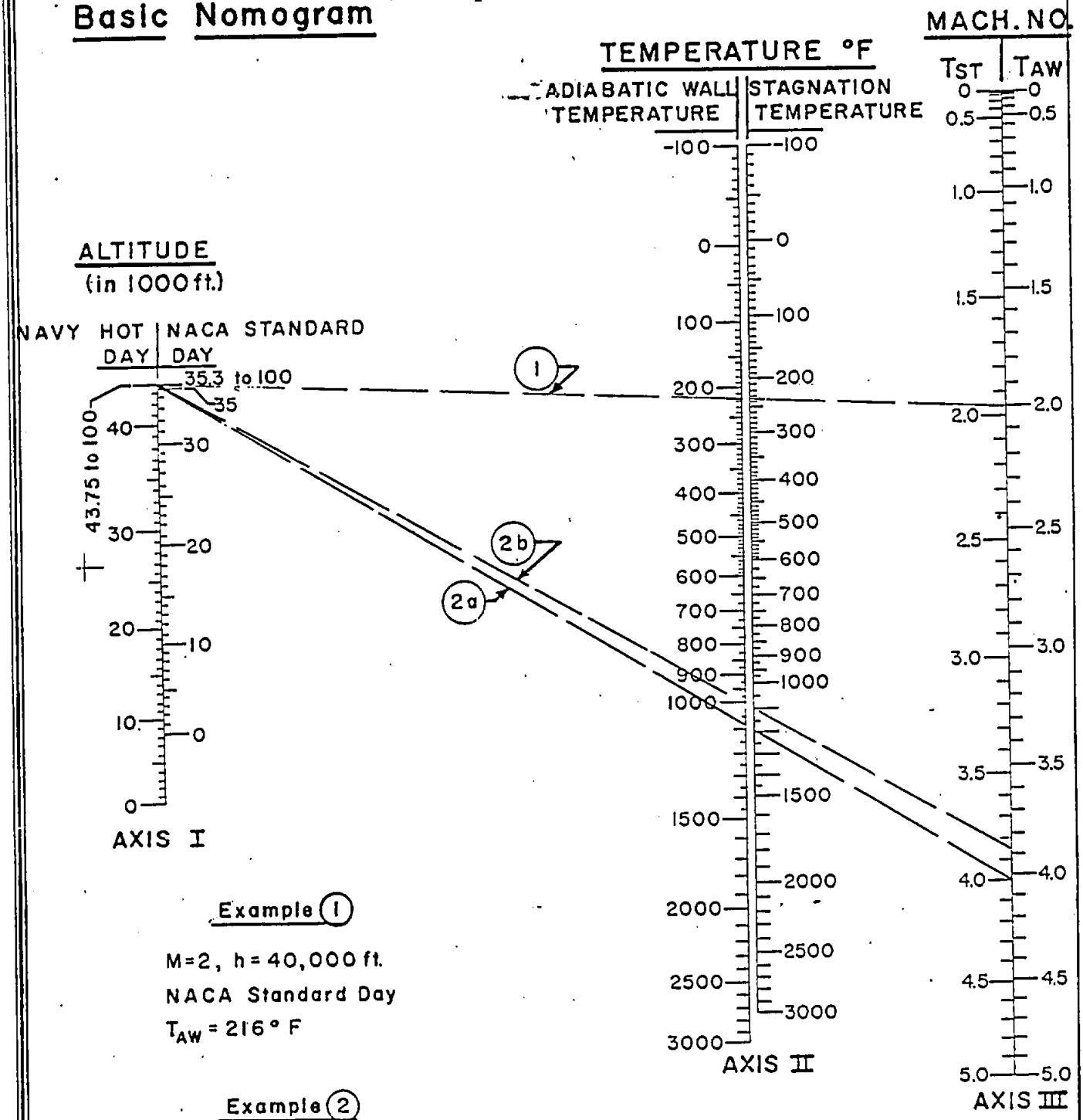

Example (1)

M=2, h=40,000 ft.

NACA Standard Day

T_{AW} = 216° F

Example (2)

M=4, h=70,000 ft.

"Navy Hot Day"

a) T_{ST} = 1200° F (uncorrected)

b) T_{ST} = 1100° F (1st correction) See page 7

c) T_{ST} = 1110° F (2nd correction, not shown)

Structures Bulletin No.4

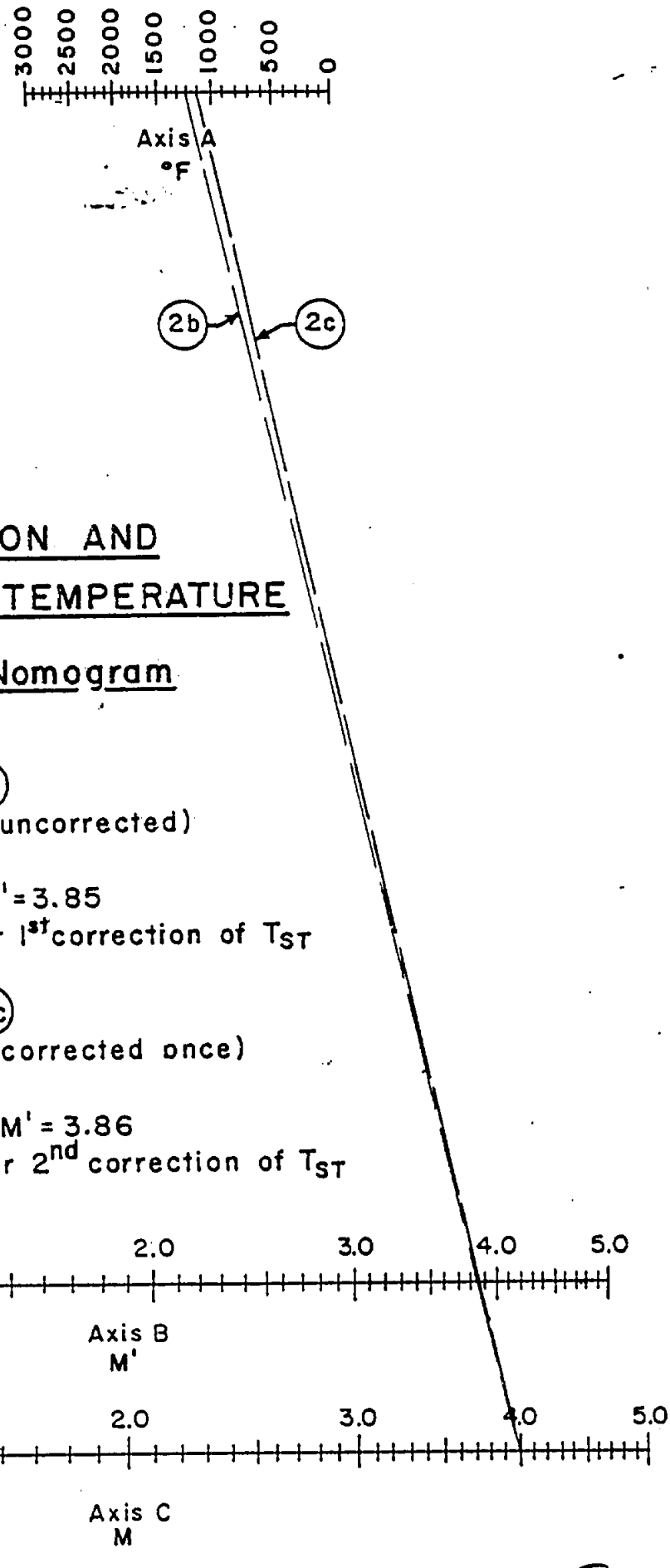

STAGNATION AND ADIABATIC WALL TEMPERATURE

Correction Nomogram

1st Correction (2b)

T_{ST} = 1200°F (uncorrected)

M = 4

M corrected = M' = 3.85

See page 6 for 1st correction of T_{ST}

2nd Correction (2c)

T_{ST} = 1100°F (corrected once)

M = 4

M corrected = M' = 3.86

See page 6 for 2nd correction of T_{ST}

Grumman

STRUCTURES MANUAL

BULLETIN # 5

HAS BEEN INTENTIONALLY OMITTED

FROM THIS EDITION:

THE MATERIAL OF THAT BULLETIN

HAS EITHER BEEN INCORPORATED INTO THE

BASIC STRUCTURES MANUAL, OR

HAS BEEN SUPERSEDED.

STRUCTURES MANUAL

BULLETIN # 60

HAS BEEN INTENTIONALLY OMITTED

FROM THIS EDITION:

THE MATERIAL OF THAT BULLETIN

HAS EITHER BEEN INCORPORATED INTO THE

BASIC STRUCTURES MANUAL, OR

HAS BEEN SUPERSEDED.

STRUCTURES MANUAL

BULLETIN # 7

HAS BEEN INTENTIONALLY OMITTED

FROM THIS EDITION:

THE MATERIAL OF THAT BULLETIN

HAS EITHER BEEN INCORPORATED INTO THE

BASIC STRUCTURES MANUAL, OR

HAS BEEN SUPERSEDED.

STRUCTURES MANUAL

BULLETIN # 8

HAS BEEN INTENTIONALLY OMITTED

FROM THIS EDITION:

BULLETIN # 8 HAS BEEN

SUPERSEDED BY BULLETIN # 16

STRUCTURES MANUAL

BULLETIN # 9

HAS BEEN INTENTIONALLY OMITTED

FROM THIS EDITION:

THE MATERIAL OF THAT BULLETIN

HAS EITHER BEEN INCORPORATED INTO THE

BASIC STRUCTURES MANUAL, OR

HAS BEEN SUPERSEDED.

March 8, 1966 (revised)

STRUCTURES BULLETIN NO. 10

TO: All Holders of Structures Manuals

FROM: T. C. Adee

SUBJECT: Static Allowable Loads for 3/8" D. Blind Bolts in Countersunk 2024-T81 Sheet and -T851 Plate.

Shear allowable ultimate static loads for FF375 JoBolts, WF375 high strength JoBolts and B 100-T12 Huck bolts machine countersunk in aluminum alloy 2024-T81 bare sheet and 2024-T851 bare plate are given in the accompanying table.

Tests which have been performed show a wide range of allowable loads for the WF375 bolts. The material specifications of the FF375 and WF375 bolts overlap throughout much of their range. It is more realistic to use common allowables for these bolts. The specified Rockwell C hardness values for the pin and nut of each are listed below.

Bolt Type	Rc Hardness
FF375	39-43
WF375	39.8-46.5

The allowables given in this bulletin are to be used in all future design.

TCA/amp

Shear Allowable Ultimate Static Loads (lbs.) for FF375 JoBolts, WF375 JoBolts, and B100-T12 Huck Bolts in Machine Countersunk 2024-T81 Bare Sheet and 2024-T851 Bare Plate(1)

Thickness of Countersunk Sheet(2), in	FF375 & WF375		B100-T12	
	ULT_Y(4) (6)	ULT_U(5) (6)	ULT_Y(4) (6)	ULT_U(5) (6)
.100	2010	3260	2580	3620
.125	3150	4980	3440	4920
.160	3330	6540	3760	6580
.190(3)	4260	7780	5260	7880
.224	5710	9240	7170	9350
.250	6420	9750(7)	8150	10500(7)
.312	7840		9630	
.375	9000		10500(7)	
.438	9750(7)			

Ref. 310 MT D-4

(1) All test specimens were single shear, single bolt lap joints.

(2) In cases where the lower sheet is thinner than the upper sheet, the shear-bearing allowable for the lower sheet-bolt combination should be computed.

(3) Use of sheet thicknesses which are less than the bolt head height are not recommended. (Head height = 0.160-0.165 in.)

(4) ULT_Y = 1.304 Average test yield load.

(5) ULT_U = Average test ultimate load/1.15.

(6) Yield is critical ($ULT_Y < ULT_U$).

(7) Minimum guaranteed single shear load.

STRUCTURES MANUAL

BULLETIN # 11

HAS BEEN INTENTIONALLY OMITTED

FROM THIS EDITION:

THE MATERIAL OF THAT BULLETIN

HAS EITHER BEEN INCORPORATED INTO THE

BASIC STRUCTURES MANUAL, OR

HAS BEEN SUPERSEDED.

STRUCTURES MANUAL

BULLETIN # 12

HAS BEEN INTENTIONALLY OMITTED

FROM THIS EDITION:

THE MATERIAL OF THAT BULLETIN

HAS EITHER BEEN INCORPORATED INTO THE

BASIC STRUCTURES MANUAL, OR

HAS BEEN SUPERSEDED.

STRUCTURES BULLETIN NO. 13

September 22, 1966

TO: All Holders of Structures Manuals

FROM: T. C. Adee TCA

SUBJECT: Fatigue Strength of Axially-Loaded Aluminum Alloy Lugs.

A method for determining the fatigue strength of 2024-T3 and 7075-T6 aluminum alloy lugs under axial loading is presented. The method is semi-empirical and is based on work by S. E. Larsson of the SAAB Aircraft Company, originally published in SAAB Technical Report No. KHU-0-2294R, April 1965. Lug fatigue test data from various sources has been utilized in the preparation of the design curves, and these data, together with a more detailed discussion of the method, will be presented in a Grumman Advanced Development Report.

References

1. Larsson, S. E., "The Development of a Calculation Method for the Fatigue Strength of Lugs, and a Study of Test Results for Lugs of Aluminum," S.A.A.B. Technical Report No. KHU-0-2294R, April 1965.

2. Smith, Clarence R., "Linear Strain Theory and the Smith Method for Predicting Fatigue Life of Structures for Spectrum Type Loading," Aerospace Research Laboratories, ARL 64-55, April 1964.

3. Schijve, J., Broek, D. and Jacobs, F. A., "Fatigue Tests on Aluminum Alloy Lugs With Special Reference to Fretting," National Aero-and Astronautical Research Institute, N.L.R.-TN M.2103, March 1962.

4. "Static and Fatigue Tests With Lugs of Steel and Dural," FAA Report HU 281 (in Swedish).

5. Hill, H. N. and Eaton, I. D., "Effect of Discontinuities on the Fatigue Strength of 7075-T6 Pin-Loaded Lugs," Alcoa Research Laboratories, Report No. 12-60-42, November 24, 1964.

6. Heath-Smith, J. R., "Fatigue Strength at Elevated Temperature of L.65 Aluminum Alloy Notched and Lug Specimens," Royal Aircraft Establishment Technical Note No. Structures 328, March 1963.

7. Heywood, R. B., "The Strength of Lugs in Fatigue," Royal Aircraft Establishment Technical Note No. Structures 182, January 1956.

8. Fatigue Tests of Aluminum Lugs for the 10-F Airplane, GAEC Unpublished Data.

- Symbols

a	distance from edge of hole to edge of lug, (see Fig. 1), in.
c	(net section width)/2, (see Fig. 1), in.
D	hole diameter of lug, in.
f_a	cyclic stress amplitude on net section of given lug, lbs/in.^{2}
f_m	mean cyclic stress on net section of given lug, lbs/in.^{2}
f_{max}	maximum cyclic stress on net section of given lug, lbs/in.^{2}
f_{min}	minimum cyclic stress on net section of given lug, lbs/in.^{2}
F_{nL}	allowable net-section tensile ultimate stress
F_{nyL}	allowable net-section tensile yield stress
k_1, k_2, k_3	fatigue parameters
N	fatigue life, number of cycles
R	stress ratio, f_{min}/f_{max}

Note: All stresses are average values across the net section of the lug.

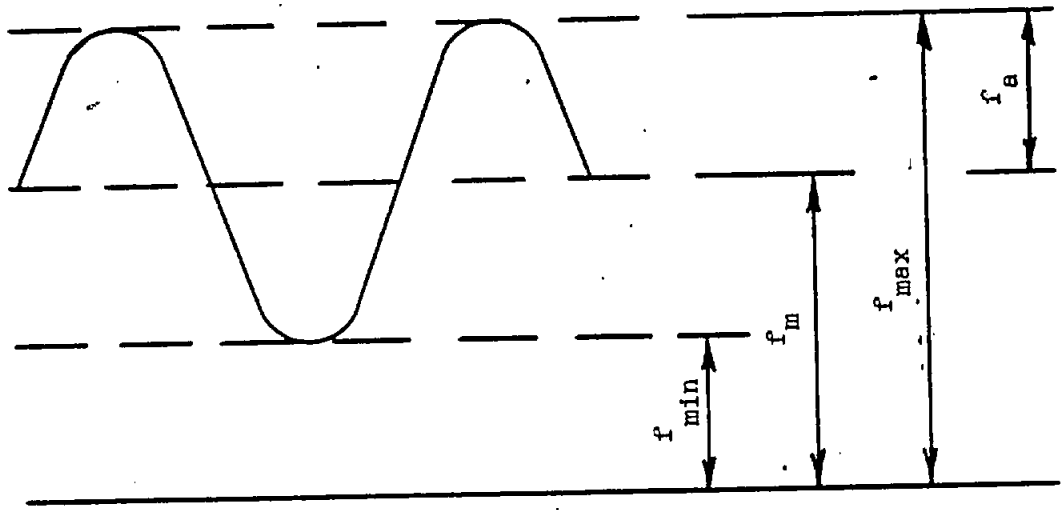

$0 < R < 1$

$$f_m = \frac{f_{max} + f_{min}}{2}$$

$$f_a = \frac{f_{max} - f_{min}}{2}$$

Method Description

Figures 1 and 2 show the lug and the range of lug geometries covered by the fatigue strength prediction method. Fatigue lives for lugs having dimensional ratios falling outside the region shown should be corroborated by tests.

In this method the important fatigue parameters are k_1, k_2 and k_3 (see Figure 3).

To find the allowable life knowing the applied stresses and lug dimensions, or the allowable stresses knowing the life, R value ($R = f_{min}/f_{max}$) and lug dimensions use the following procedure:

1) Enter Figure 2 to check that the lug dimensional ratios fall within the region covered by the method. Enter Figure 3 and read k_1, k_2 and k_3; calculate the product $k_1k_2k_3$.

2) Calculate the allowable net-tension static stress for the lug, F_{nL}, according to the method described in Section B3.13 of the Structures Manual.

3) Determine the value 0.4 F_{nL}. This is the alternating stress corresponding to a maximum stress value of 0.8 F_{nL} when $f_{min} = 0$. 0.8 F_{nL} was chosen as an average yield stress value for 2024 and 7075 aluminum alloy lugs.

4) Using the value 0.4 F_{nL} as an alternating stress, draw a straight line between the intersection or this value and the appropriate $k_1k_2k_3$ curve on Figures 4 or 5, and the point 0.5 F_{nL} at 1 cycle. This extends the $k_1k_2k_3$ curve to cover the entire life range to static failure.

5) Enter Figure 4 or 5 (lug fatigue curves for the case where R = 0) with $k_1k_2k_3$. For values of life, $N = 10^3$, 3×10^3, 10^4, etc., or any other convenient values, determine the corresponding values of f_a, the stress amplitude causing fatigue failure when R = 0.

6) Plot the values of f_a found in Step 5 along the R = 0 line in a Goodman diagram such as shown in Figure 6 ($f_m = f_a$ when R = 0). The Goodman diagram shown in Figure 6 applies to a particular 7075-T6 lug for which $k_1k_2k_3 = 1.32$ (see example problem 1), but is typical of all such diagrams.

7) Plot the allowable net tension static stress found in Step 2 as f_m at the point (f_m, 0) of the Goodman diagram. ($f_m = f_{max}$ when $f_a = 0$). For the case considered in Figure 6, this point is plotted as (f_m = 70,000 psi, $f_a = 0$).

Method Description (cont'd)

8) Connect the point plotted in Step 7 with each of the points plotted in Step 6 by straight lines. These are the constant life lines for the particular lug being analyzed. The Goodman diagram is now complete and may be used to determine a life for any given applied stresses, or to determine allowable stresses knowing the life and R value.

Example Problem 1

Given a concentric 7075-T6 aluminum lug as shown in Figure 1, with the following dimensions: a = 0.344 in; c = 0.344 in; D = 0.437 in. If the lug is subjected to a cyclic axial load such that the maximum net-section stress is 27,700 psi and the minimum net section stress is 18,470 psi, find the fatigue life.

From the lug dimensions

$$a/c = 1.0 \qquad c/D = 0.787 \qquad (D/c = 1.27)$$

1) Figure 2 indicates that the lug may be analyzed using this method. From Figure 3:

$$k_1 = 1.0,\ k_2 = 1.33,\ k_3 = 0.99,\ k_1k_2k_3 = 1.32$$

2) Calculate the allowable net-section tensile ultimate stress, F_{nL}, from equation (4) in Section B3.13 of the Structures Manual. For the given lug F_{nL} = 70,000 psi.

3) $0.4\ F_{nL} = 0.4 \times 70{,}000 = 28{,}000$ psi.

4) Draw a light pencil line on Figure 4 from the point (f_a = 28,000 psi on $k_1k_2k_3 = 1.32$) to the point (f_a = 35,000, N = 1 cycle) (This is illustrated, for clarity, on Figure 7).

5) Enter Figure 4 and read values of f_a for various values of lives on the $k_1k_2k_3 = 1.32$ line. These are:

N	10^2	10^3	3×10^3	10^4	3×10^4	10^5	10^6	10^7
f_a	30KSI	24.5	18.8	13.5	8.88	5.70	2.34	1.30

6) Plot the values of f_a along the R = 0 line of the Goodman diagram. (Refer to Figure 6).

7) Plot F_{nL} = 70,000 psi, as f_m at the point (f_m,0) of the Goodman diagram. (Refer to Figure 6).

8) Connect the points plotted in Step 6, with the point plotted in Step 7 by straight lines. The Goodman diagram is now complete.

9) Enter the Goodman diagram with values of $f_a = \frac{27,700 - 18,470}{2} = 4,615$ psi and $f_m = \frac{27,700 + 18,470}{2} = 23,085$ psi, and read the fatigue life, $N = 8 \times 10^4$ cycles by interpolation (Test results show $N = 8.6 \times 10^4$ cycles).

If the known quantities are life and R value, e.g., $N = 10^4$ cycles and $R = 0$, the allowable stresses can be obtained using the same Goodman diagram. Enter the completed Goodman diagram at $R = 0$ and $N = 10^4$ cycles and read the amplitude and mean stresses (in this case $f_a = f_m = 13,500$ psi).

Only if the lug dimensions are changed, must a new Goodman diagram be drawn.

Example Problem 2

Consider the lug in Example 1. If this were subjected to stresses of $f_{max} = 60,000$ psi and $f_{min} = 10,000$ psi the corresponding alternating and mean stresses would be: $f_a = 25,000$ psi $f_m = 35,000$ psi. Reference to the Goodman diagram, Figure 6, gives a life, $N = 140$ cycles. In this case, the stresses are in the yield range, and this illustrates the reason for the procedure described in Step 4, Page 3.

Note:

Spectrum type loading:

The method may be used in conjunction with Miner's Cumulative Damage Rule to obtain fatigue life of elements subjected to spectrum loading. The life obtained will generally be conservative, since residual stress effects are neglected, and such stresses are mainly beneficial. It is anticipated that the method will eventually be extended to include residual stress effects.

TCA/amp

LUG GEOMETRY

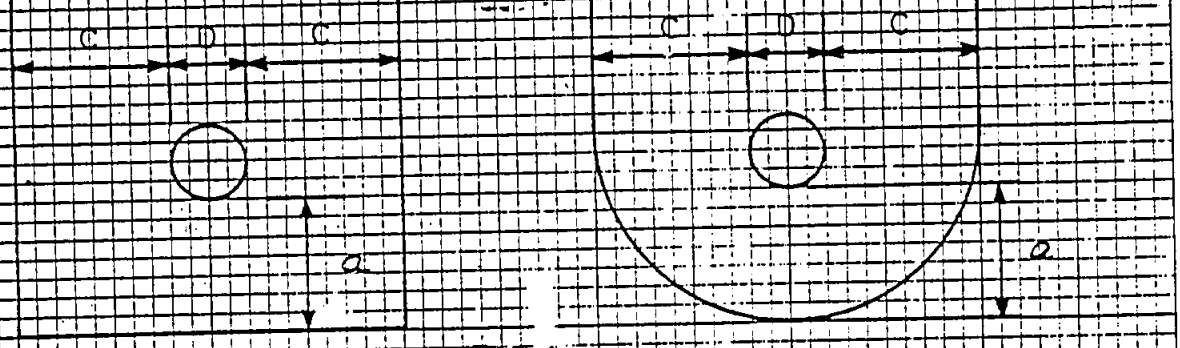

FIG. 1

REGION OF LUG GEOMETRIES COVERED BY FATIGUE PREDICTION METHOD

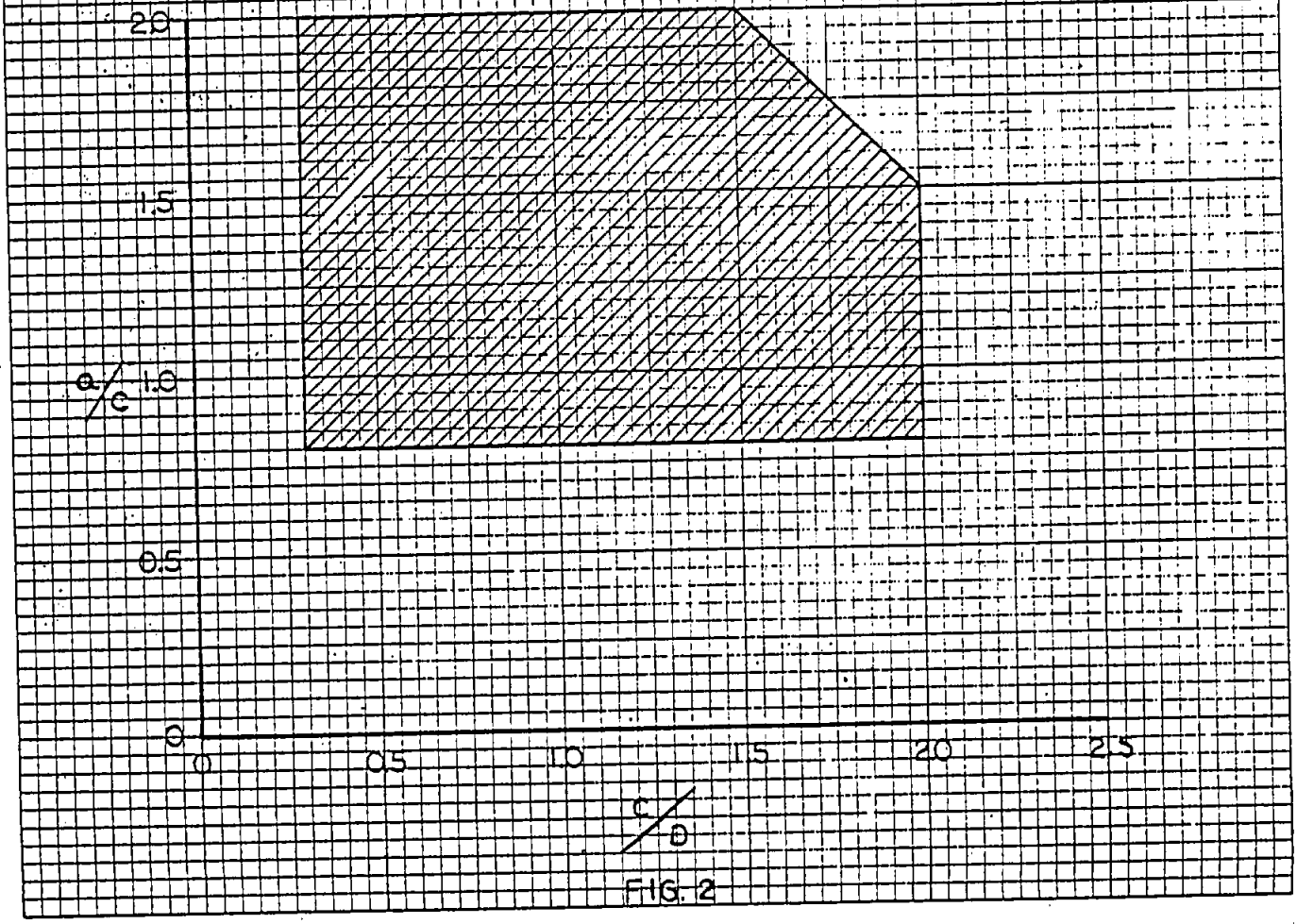

FIG. 2

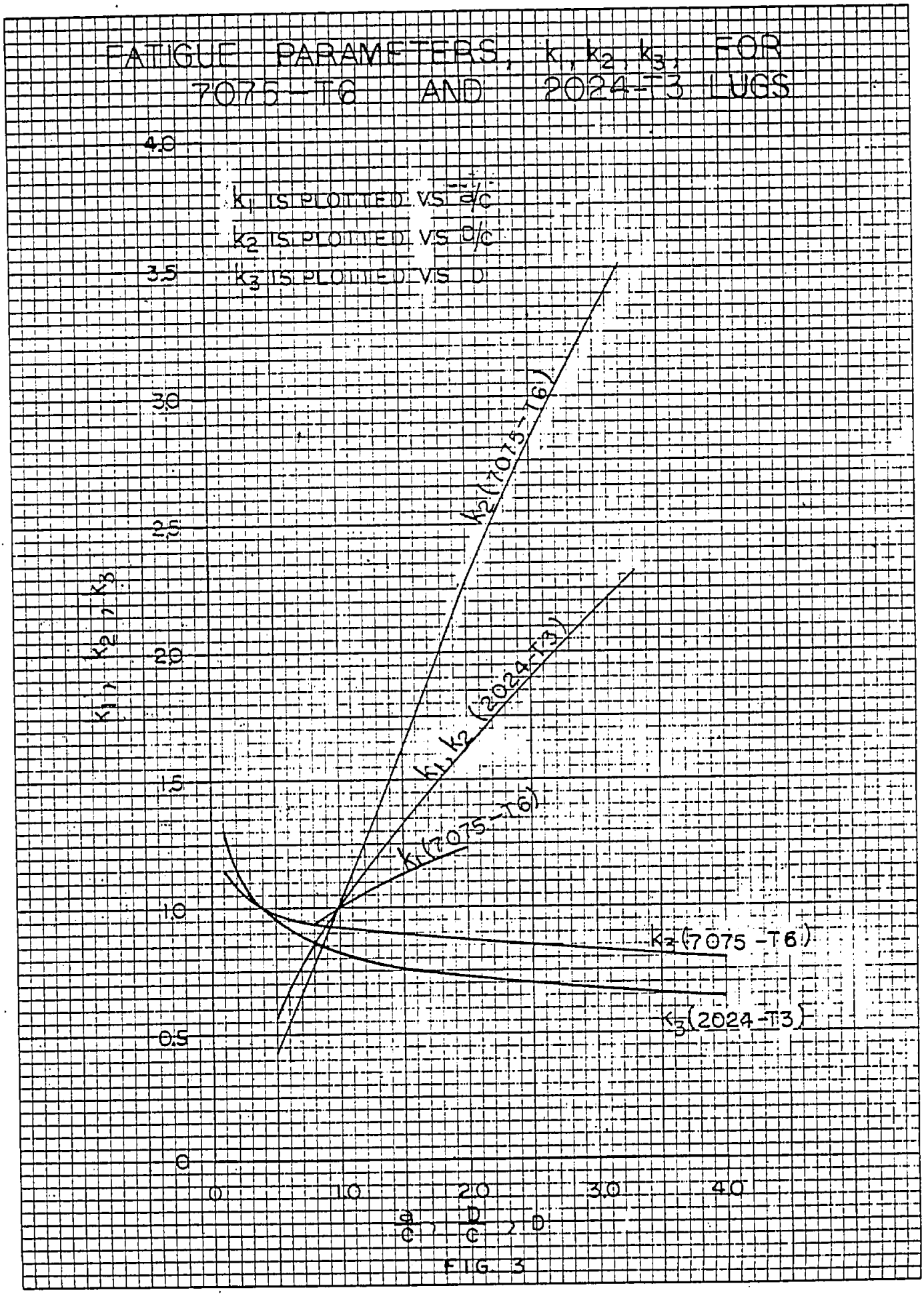
FATIGUE PARAMETERS, k_1, k_2, k_3, FOR 7075-T6 AND 2024-T3 LUGS
k_1 IS PLOTTED VS $\frac{d}{c}$
k_2 IS PLOTTED VS $\frac{D}{c}$
k_3 IS PLOTTED VS D
k_2 (7075-T6)
$k_1 k_2$ (2024-T3)
k_1 (7075-T6)
k_3 (7075-T6)
k_3 (2024-T3)
k_1, k_2, k_3
4.0
3.5
3.0
2.5
2.0
1.5
1.0
0.5
0
0
1.0
2.0
3.0
4.0
$\frac{d}{c}$, $\frac{D}{c}$, D

FIG. 3

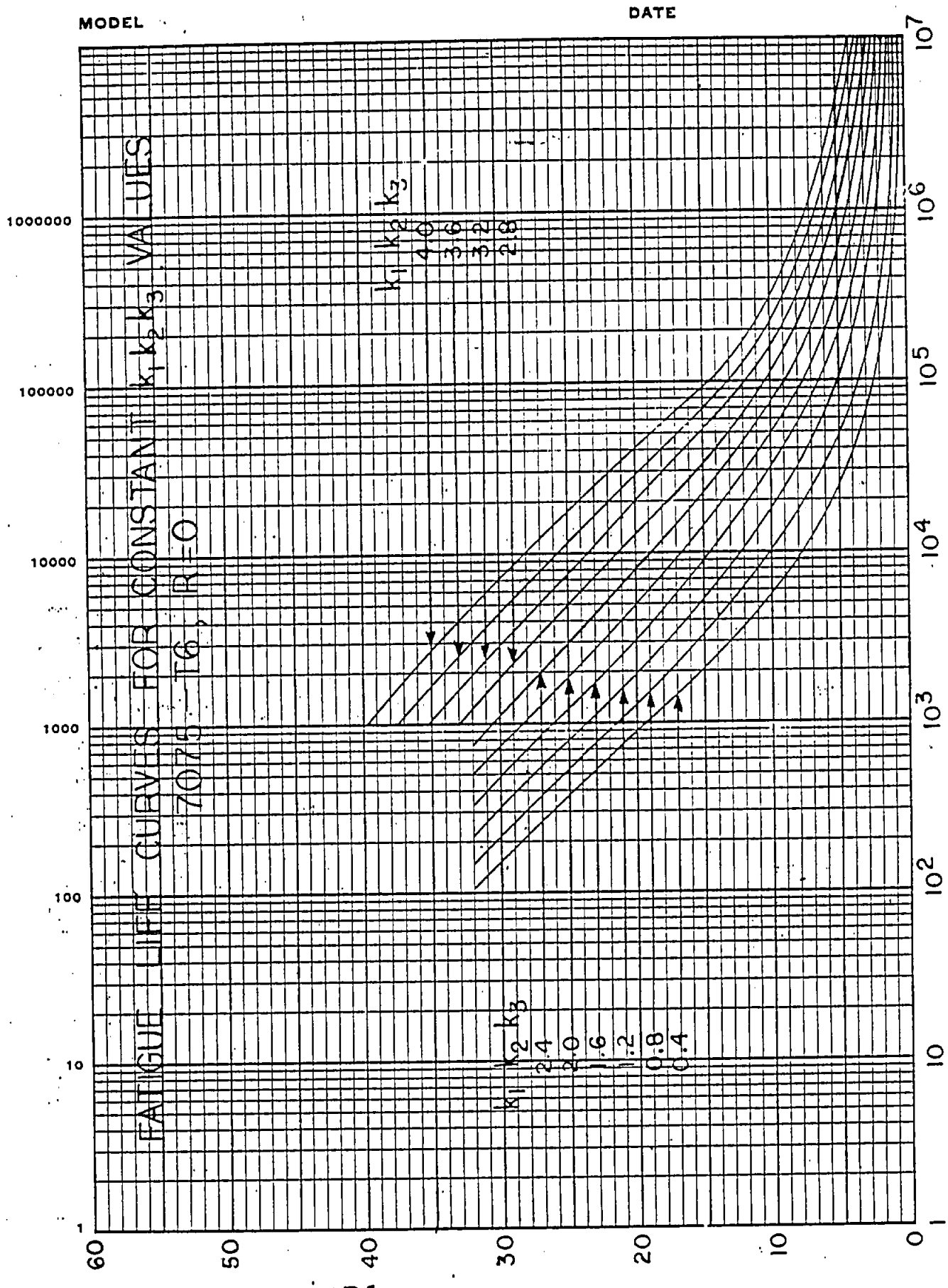
MODEL
DATE
FATIGUE LIFE CURVES FOR CONSTANT k_1, k_2, k_3 VALUES
7075-T6, R=0
k_1 k_2 k_3
4.0
3.6
3.2
2.8
k_1 k_2 k_3
2.4
2.0
1.6
1.2
0.8
0.4
1000000
100000
10000
1000
100
10
1
10^7
10^6
10^5
10^4
10^3
10^2
10
1
60
50
40
30
20
10
0
ALTERNATING STRESS, f_a, KSI
N, NO. OF CYCLES

FIG. 4

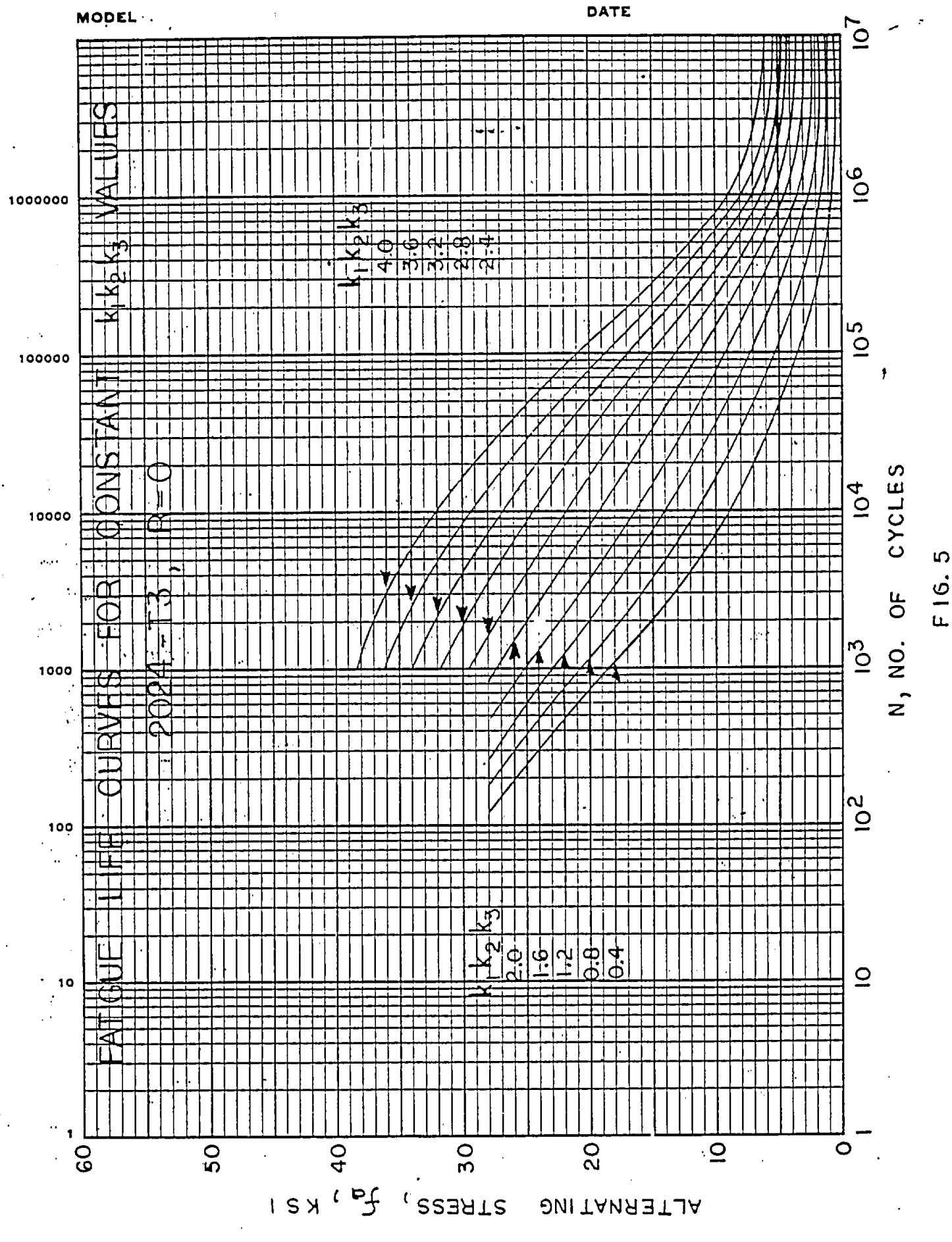
MODEL
DATE
FATIGUE LIFE CURVES FOR CONSTANT $k_1 k_2 k_3$ VALUES
2024-T3, R=0
$k_1 k_2 k_3$
4.0
3.6
3.2
2.8
2.4
$k_1 k_2 k_3$
2.0
1.6
1.2
0.8
0.4
1000000
100000
10000
1000
100
10
1
10^7
10^6
10^5
10^4
10^3
10^2
10
1
60
50
40
30
20
10
0
ALTERNATING STRESS, f_a, KSI
N, NO. OF CYCLES

FIG. 5

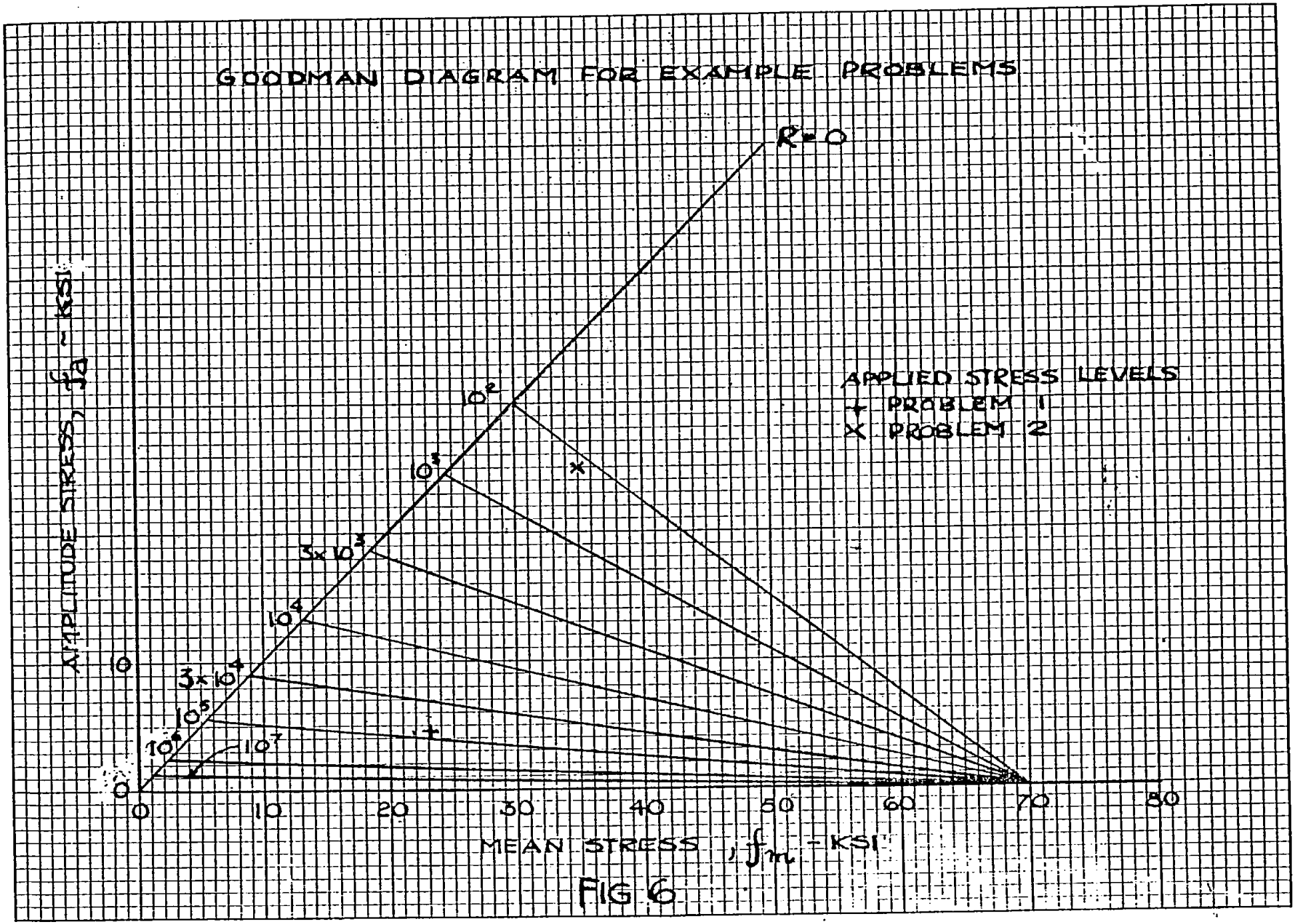
GOODMAN DIAGRAM FOR EXAMPLE PROBLEMS
R = 0
APPLIED STRESS LEVELS
+ PROBLEM 1
× PROBLEM 2
10^2
10^3
3×10^3
10^4
3×10^4
10^5
10^6
10^7
AMPLITUDE STRESS, f_a - KSI
MEAN STRESS, f_m - KSI
0
10
20
30
40
50
60
70
80

FIG 6

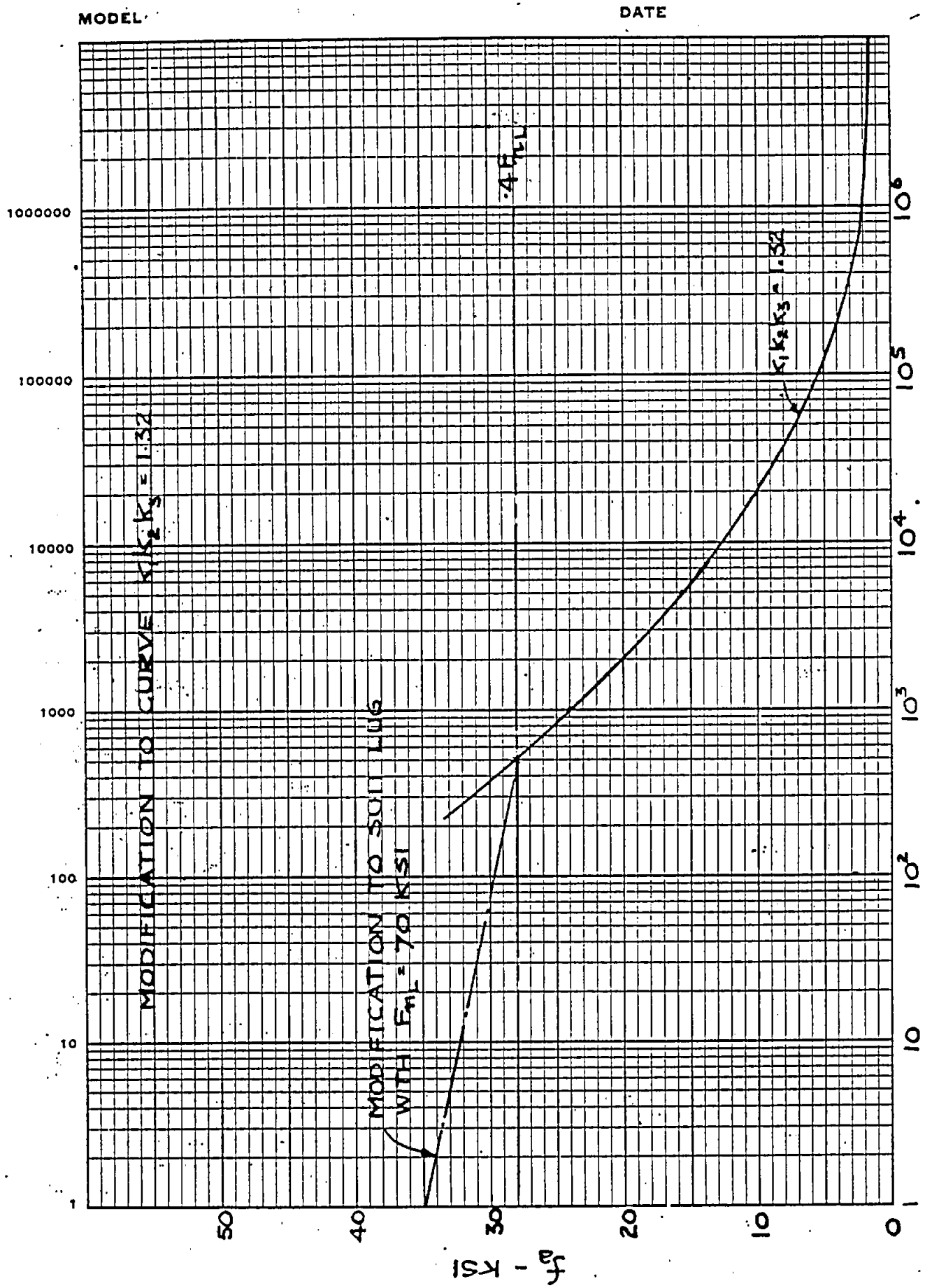
MODEL
DATE
1000000
100000
10000
1000
100
10
1
50
40
30
20
10
0
f_a - KSI
N - CYCLES
10^6
10^5
10^4
10^3
10^2
10
1
$.4F_{TL}$
$K_1K_2K_3 = 1.32$
MODIFICATION TO CURVE $K_1K_2K_3 = 1.32$
MODIFICATION TO SOLID LUG
WITH $F_{TL} = 70$ KSI

FIG. 7

STRUCTURES BULLETIN NO. 14

To: All Holders of Structures Manual

From: G. T. Raynor/D. W. Bone D.B.

Subject: USE OF GRUMMAN STANDARD GS28A

The purpose of this standard is to define an acceptable criteria of surface roughness and mismatch of aluminum alloy, titanium and steel machine parts to avoid secondary hand finishing operations as a general requirement. The net effect of using GS28A is to reduce costs in producing machine parts. This standard GS28A is to be used only where specifically called out on the engineering drawing and may be superceded by specific drawing callouts.

The Engineers use of GS28A requires a "type" callout definition on the drawing to classify the critical nature of the surface or mismatch.

Where GS28A is called out by a drawing, it will normally specify Type II and IV conditions which are defined in the attached GS28A specification. This is structurally acceptable for most structural parts including parts wherein fatigue life is a design consideration.

Where parts are extremely fatigue critical or where there is considerable fatigue life sensitivity to surface finish one or more of the following options should be specified for the local areas in question:

(1) Callout of Types I and III in GS28A

(2) Callout of symbol ◇F (see DP215A Classification of Characteristics 4 January 1971)

(3) Callout of finer finish than 125 RMS (See Engineering Manual Procedure No. C150 - Surface Roughness 30 September 1970)

The structural analyst is responsible to identify areas, if any, where these options must be specified. In case of questionable interpretation in use of GS28A or the options, refer question to the Structural Analysis Group Head or Section Head.

Designers may also specify these options for fuel sealing, aero smoothness or mechanical functional requirements.

GRUMMAN

INTER-OFFICE MEMORANDUM

FROM: G. Raynor GR Structural Analysis 35 2468 DATE June 2, 1975
NAME GROUP NO.& NAME PLANT NO. EXT.

TO: All Structures Analysts NO. EG-STAN-75-046

SUBJECT: COST SAVINGS BY USE OF GRUMMAN STANDARD GS28A

A significant cost savings to the Grumman Company can be realized by incorporation of GS28A on machine part drawings. GS28A is an engineering standard whose purpose is to avoid the costly secondary hand finishing operations as a general requirement on machined parts and as an aid in specifying and defining those surfaces and surface conditions so that the secondary operations may be limited and controlled. The standard actually expands the controls on the machined parts by defining the expected maximum mismatches and maintaining the surface roughness designated. Previously the hand finish was essentially a shop practice.

Future machined part drawings will incorporate GS28A in the initial release. An effort is presently underway to incorporate GS28A on present A6, EA6B, and F-14 parts through a drawing change.

Using the latest release of GS28A, there is an engineering identification requirement to classify the machine parts by a type callout, critical or non-critical, in terms of the cusp height, and type for surface mismatch.

The definition of cusp height is the distance from the highest to lowest point in the cutter pattern and is the resulting metal remaining between the center of cutter passes, additional material at all times. This cusp height will be included in the part thickness measurement and therefore will require a proper type callout for thin parts especially where the tolerance would be effected.

The intended use of GS28A is not to call all parts critical where there would be no help to the cost savings. The non-critical type should be used where static strength or fatigue could tolerate the "as machined" surface. Note, the existing maximum surface roughness of 125 rms will not be changed by use of GS28A. The usage of GS28A is not to change the part in any respect such as thickness in terms of adding weight or to degrade the part structurally, but to reduce the hand finishing that presently takes many hours where hand finishing is not required.

Some surface defects are not covered by the surface roughness callout or the GS28A such as nicks, dents and scratches. For surface critical for special defects, drawing notes will still be required.

cc: L. Mead, N. Spiess, N. Lewin, D. Bone AB., J. Culletin, P. Obedzinski, R. Cyphers, T. Adee, A. Barbero, J. Brennan, H. Krier

GAC 1168 REV. J
5-70 250M

Bulletin #14 Page 2 of 16

SURFACE ROUGHNESS
(ALUMINUM ALLOY, TITANIUM AND STEEL MACHINED PARTS)

APPLICATION: THIS STANDARD TO BE USED ONLY WHERE SPECIFICALLY CALLED OUT ON THE ENGINEERING DRAWING AND MAY BE SUPERSEDED BY SPECIFIC DRAWING CALLOUTS.

SCOPE: MACHINING OF ALL PARTS SUCH AS BULKHEADS, FITTINGS, LONGERONS, SKINS AND SPARS WHERE THE FOLLOWING CONDITIONS APPLY.

DEFINITIONS: CRITICAL: A CRITICAL SURFACE IS ANY SURFACE ENGINEERING IDENTIFIES AS SUCH, DUE TO FUEL SEALING REQUIREMENTS, FATIGUE OR ANY OTHER REASON.
CUSP HEIGHT: CUSP HEIGHT IS THE DISTANCE FROM THE HIGHEST TO LOWEST POINT OF THE CUTTER PATTERN INCLUDING WAVINESS.

BASIC STANDARD: THE SURFACE ROUGHNESS DATA CONTAINED HEREIN, IS BASED ON ANSI B46.1-1962 "SURFACE ROUGHNESS, WAVINESS AND LAY".

NOTE 1- ALL PROFILOMETER READINGS TO HAVE A 0.030 CUTOFF WIDTH.
NOTE 2- SURFACE ROUGHNESS VALUES AS MENTIONED IN THIS GRUMMAN STANDARD ARE DEFINED AS THE ARITHMETICAL AVERAGE ROUGHNESS HEIGHT RATING EXPRESSED IN MICRO-INCHES.
NOTE 3- VISUAL TYPE COMPARATOR GAUGES ACCEPTABLE TO GRUMMAN MAY BE USED FOR ACCEPTANCE CRITERIA OF ALL TYPES.

PURPOSE: TO AVOID SECONDARY HAND FINISHING OPERATIONS AS A GENERAL REQUIREMENT; AND AS AN AID IN SPECIFYING AND DEFINING THOSE SURFACES AND SURFACE CONDITIONS SO THAT THESE SECONDARY OPERATIONS MAY BE LIMITED AND CONTROLLED. TO ACHIEVE THIS PURPOSE THE FOLLOWING SURFACE TYPES HAVE BEEN ESTABLISHED.

TYPES: TYPE 1- CRITICAL AREAS (SEE FIGURE 1).
REQUIRES A SURFACE ROUGHNESS OF 125 WITH A MAXIMUM CUSP HEIGHT NOT TO EXCEED 0.0005. CUSP HEIGHTS EXCEEDING THIS AMOUNT REQUIRE SECONDARY HAND FINISHING IN ORDER TO OBTAIN SMOOTH AND UNIFORM CONTACT OF BEARING AREAS.

TYPE 2- NON-CRITICAL AREAS (SEE FIGURE 1)
SURFACE CONDITIONS MUST MEET EITHER OF THE FOLLOWING TWO ALTERNATES
A. AVERAGE SURFACE ROUGHNESS IS 125 WITH CUSP INCLUDED IN THE PROFILOMETER READING.
B. CUSP HEIGHTS OF .003 MAXIMUM WITH MINIMUM PEAK TO PEAK WIDTHS OF 20 TIMES THE CUSP HEIGHTS IS ALLOWED IF SURFACE ROUGHNESS IS 125.

TYPE 3- SURFACE MISMATCH-CRITICAL AREAS (SEE FIGURE 2)
OCCURING DUE TO MULTIPLE CUTTER PASSES ON A SINGLE SURFACE AS DEPICTED IN FIGURE 2 IS ALLOWED IF SURFACE ROUGHNESS IS 125 AND MISMATCH HEIGHT DOES NOT EXCEED 0.0005 WITH A MINIMUM CUTTER RADIUS OF .125.

TYPE 4- SURFACE MISMATCH-NON-CRITICAL AREAS (SEE FIGURE 2)
OCCURING DUE TO MULTIPLE CUTTER PASSES ON A SINGLE SURFACE AS DEPICTED IN FIGURE 2 IS ALLOWED IF SURFACE ROUGHNESS OF 125 AND A MISMATCH HEIGHT DOES NOT EXCEED 0.005 WITH A MINIMUM CUTTER RADIUS OF .125.

TYPE 5- MISMATCH AT INTERNAL INTERSECTING SURFACES (SEE FIGURES 3 AND 4)
A. OCCURING AS DEPICTED IN FIGURE 3 DUE TO INTERSECTING ANGULAR FLANGES WITH RIBS; OR FLANGES AND RIBS TO WEB; OR CHANGING RADII IS ALLOWED IF THEY DO NOT EXCEED MISMATCH ALLOWANCES SPECIFIED ON THE ENGINEERING DRAWING.

B. OCCURING WHEN FORM CUTTERS ARE USED, AS DEPICTED IN FIGURE 4, DUE TO INTERSECTING ANGULAR FLANGES WITH RIBS; OR FLANGES AND RIBS TO WEB; OR CHANGING RADII IS ALLOWED IF THEY DO NOT EXCEED MISMATCH ALLOWANCES SPECIFIED ON THE ENGINEERING DRAWING.

ENGINEERING INFORMATION

TYPICAL DRAWING NOTES AND FIELD CALLOUTS ARE AS FOLLOWS:

125 ✓ TYPE 1 & 3 [1]

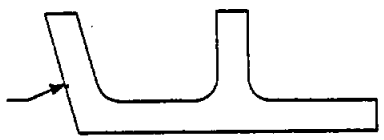

GENERAL DRAWING NOTE:

[1] INTERPRET SURFACE ROUGHNESS AND MISMATCH PER GS28A

A. INSIDE INTERSECTING CORNER MISMATCH: TYPE 5A .030 MAX TYPE 5B .060 UNLESS OTHERWISE SPECIFIED.

B. ALL OTHER SURFACES PER TYPE 2 AND 4 EXCEPT AS SPECIFIED

NOTE: THIS DRAWING INFORMATION IS SHOWN FOR REFERENCE ONLY. IN THE EVENT OF DIFFERENCES BETWEEN DRAWING PRACTICES HEREIN SHOWN AND THE LATEST PROCEDURES CONTAINED IN THE CORPORATE ENGINEERING MANUAL, THE MANUAL PROCEDURES SHALL GOVERN.

APPROVED 11-6-67 | REVISED & REDRAWN © 5-22-70 Ⓔ 9-12-74

D

SURFACE ROUGHNESS AND MISMATCH
ALUMINUM ALLOY, TITANIUM AND STEEL MACHINED PARTS

GRUMMAN DESIGN
GRUMMAN STANDARD
GRUMMAN AEROSPACE CORPORATION BETHPAGE N.Y. 11714

SHEET	NO.	1	2	3	4	5	6	7	8	9	10
STATUS	REV	C	C								

GS28A

CODE IDENT NO. 26512 | SHEET 1 OF 2

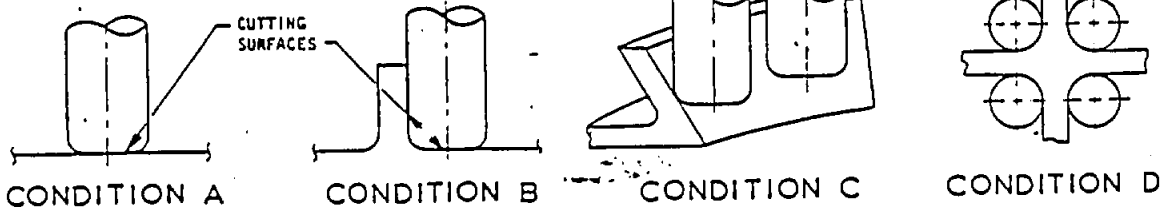

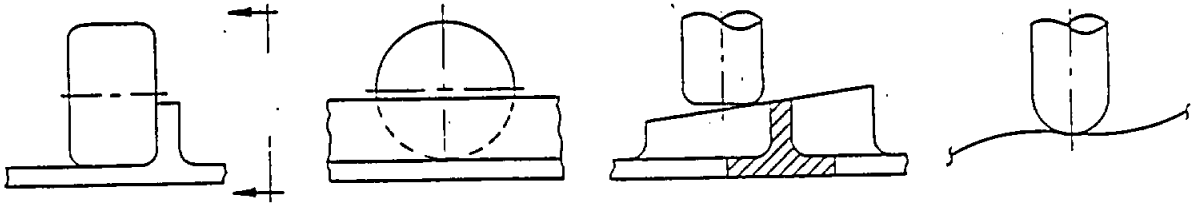

NOTE: CUTTER SHAPES SHOWN ARE FOR ILLUSTRATION ONLY. IT IS UNDERSTOOD THAT MANY CUTTER SHAPES WILL PRODUCE SIMILAR CONDITIONS.

INTERPRETATION: ROUGHNESS- MISMATCH

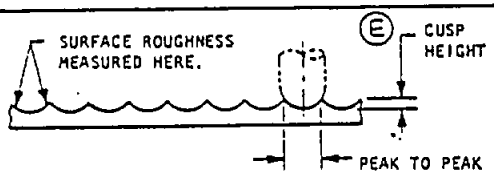

FIGURE 1

(AS MAY BE PRODUCED BY CONDITIONS B, C, F OR G)

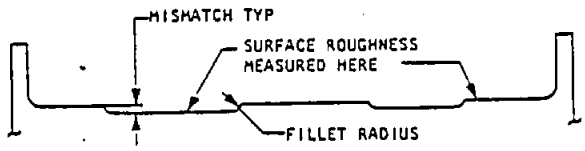

FIGURE 2

(AS MAY BE PRODUCED BY CONDITIONS A, B, OR E)

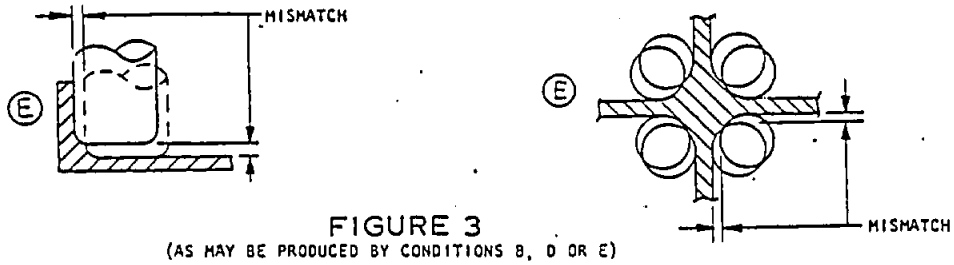

FIGURE 3

(AS MAY BE PRODUCED BY CONDITIONS B, D OR E)

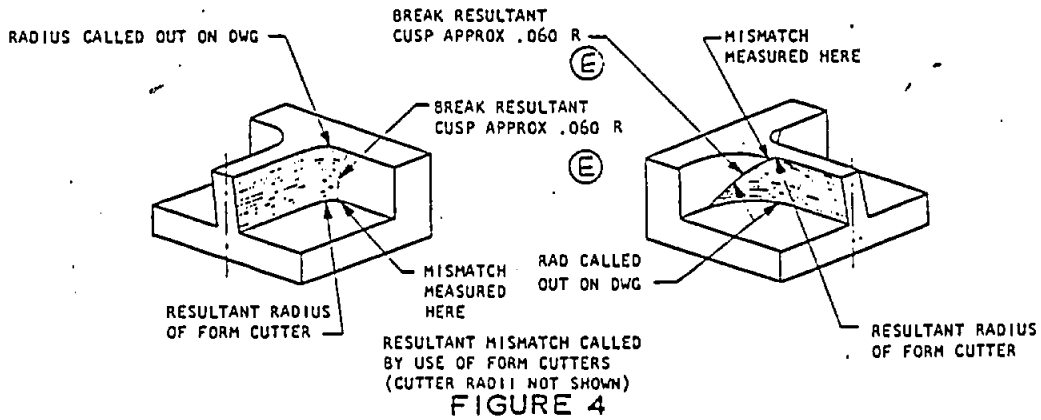

FIGURE 4

APPROVED 11-6-67 | REVISED Ⓓ 2-20-74 Ⓔ 9-12-74

GRUMMAN STANDARD

S28A

CODE IDENT NO. 26512 | SHEET 2

GRUMMAN AEROSPACE CORPORATION

ENGINEERING DEPARTMENT DRAWING PROCEDURES NOTICE

DP 215A

(Supersedes DP 215 dated 16 October 1970)

4 January 1971

To: All Engineering Personnel (Except F-111 Project)

Subject: CLASSIFICATION OF CHARACTERISTICS

NOTE: This revised DP is similar in intent and content to DP 215 dated 16 Oct. 1970, with the following differences:

a. Definitions use "vehicle" in lieu of "aircraft" to include LM program. (Paragraph 2.1)

b. Classification responsibility for critical LM characteristics added. (Paragraph 3.1)

c. "Interface" characteristics not applicable to LM program. (Paragraphs 2.1, 3.2, 6.1a diagram, sample note for "I" in 6.2)

d. "Interface" inspection level data no longer required on drawing. (Paragraph 5.2 , sample note for "I" in 6.2)

1.0 GENERAL

1.1 In order to highlight those characteristics of parts (e.g., dimensions, surfaces, areas, etc.) where special manufacturing and inspection attention is extremely important, this procedure based on Grumman Specification SP-G-022, CLASSIFICATION OF CHARACTERISTICS, is hereby established.

2.0 CLASSIFICATION AND DEFINITIONS

2.1 Those parts containing characteristics requiring classification shall have those characteristics identified on related drawings by use of a symbol. The symbol, consisting of a letter in a .38 diamond, shall be placed adjacent to the characteristic being classified.

SYMBOL	CLASSIFICATION	DEFINITION
◇C◇	CRITICAL	A critical characteristic is one, other than "fatigue critical", that if discrepant could result in a hazardous or unsafe condition for individuals using or maintaining the vehicle; or which is likely to prevent performance of the tactical function of the vehicle. Such a condition requires 100% inspection of these characteristics.
◇F◇	FATIGUE CRITICAL	A fatigue critical area is one where the stress level is sufficiently high that if a defect occurs in the area, it can result in a significant fatigue failure which may result in the loss of the vehicle and its occupants. Such a condition requires 100% inspection of the characteristics within the area with particular attention being given to surface discontinuities (mismatch).
◇I◇	INTERFACE	An interface dimension is one that if discrepant could cause a defective assembly and could have a serious impact on the schedule.
△K (NOT APPLICABLE TO IM PROGRAM)		

2.2 Proper Usage -

a. Only those parts containing characteristics which are covered by the definitions in Paragraph 2.1 shall be classified. Classification shall not be used to invoke a more rigid control of manufacturing or quality control procedures, i.e., the use of ◇C◇ and ◇F◇ classifications shall be restricted to only those parts which could jeopardize the safety of the vehicle or its occupants.

b. Tolerances - Tolerances do not necessarily establish the need for classification. It is possible that a dimension with a ±.03 tolerance may require an ◇F◇ classification while an adjacent dimension with a ±.005 tolerance may not require any classification.

c. Usage of "G" Std GS28A - Before application of classification symbol ⟨F⟩ it is important that Grumman Standard GS28A, SURFACE ROUGHNESS, be fully reviewed. The callout of this standard (which deals with the inter-relationship of surface roughness, waviness and mismatch) on a part with an ⟨F⟩ classification can assist in producing an acceptable part without requiring expensive and potentially damaging rework. This approach shall be seriously considered, since classification may increase the cost of manufacturing and inspecting the item.

3.0 CLASSIFICATION RESPONSIBILITY

3.1 Parts Containing "Critical" and "Fatigue Critical" Characteristics -

The responsibility for designating those parts and the characteristics contained therein which are to be classified as "critical" or "fatigue critical" shall be as follows:

Critical	The originating Sub-system (LM only) Design or Structural Analysis (All other projects)
Fatigue Critical	Structural Analysis (Stress)

These groups shall also designate the various detail and/or assembly drawings involved, including those higher levels of assembly at which these characteristics shall be repetitively inspected. The applicable documents (i.e., drawings, EO's, etc.) shall be approved by Production Engineering prior to release.

△R 3.2 Parts Containing "Interface" Characteristics (Not applicable to LM project) - Production Engineering shall be responsible for designating those parts and the characteristics contained therein, together with their applicable drawings, which are to be classified as "interface".

3.3 Multiple Classifications - When more than one classification is required on a drawing each classification shall be designated by the cognizant group.

4.0 LEVELS OF CLASSIFICATION

4.1 Classification of characteristics will generally be applied to dimensions, tolerances, geometric tolerances, surface finishes, hole diameters and locations, etc. of the part at its detail level. All, or some of these classifications may be further applied to the initial assembly of the part or to higher levels of assembly, as required. Classification callouts on drawings and PL's shall be as described in Paragraph 6.0.

5.0 QUALITY ASSURANCE INSPECTION PROVISIONS

5.1 Inspection Responsibility - Quality Control shall be responsible for assuring compliance with the inspection requirements of this procedure.

(R) 5.2 Drawing Callout of Inspection Requirements - All detail parts and assemblies containing "Critical" or "Fatigue Critical" characteristics shall have these characteristics inspected on all parts. This represents 100% inspection, with no sampling procedure permitted. The phrase, "100% INSPECTION REQUIRED", shall be appended to each drawing note or group of notes referencing classified characteristics in these categories. See paragraph 6.2. "Interface" parts require no inspection level indication.

6.0 DRAWING CALLOUTS

6.1 Field of Drawing Callouts -

a. Classified characteristics will be identified on the field of the drawing with the applicable symbol placed adjacent to the characteristic(s) as shown in the following typical examples.

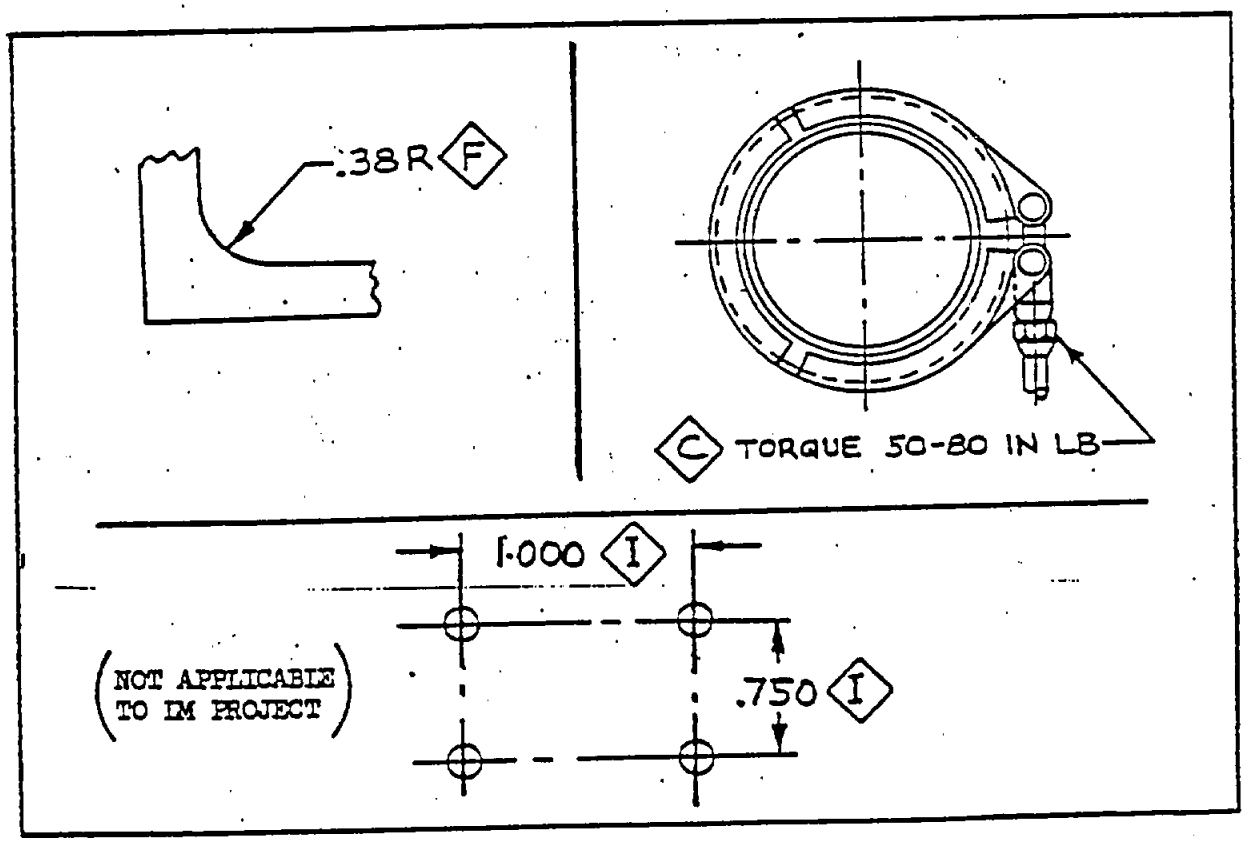

(R)

b. When it is required to inspect a general area visually, rather than measure specific dimensions, the features involved shall be identified by enclosing the area containing them with a phantom line and attaching a symbol as shown below. The associated decal, (See paragraph 6.2) shall be altered by crossing out the sentence, "DETAIL PART DIMENSIONS, PARTICULARLY RADII, MUST BE MAINTAINED". (R)

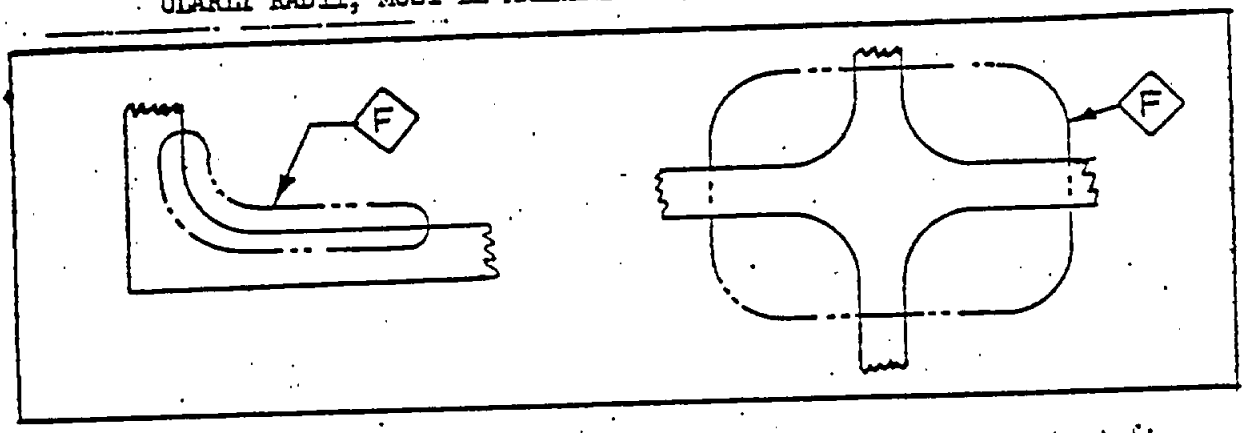

6.2 Drawing Notes - It is preferred that classification of characteristic notes be grouped beneath the Supplementary Data Decal with a heading title, "CLASSIFICATION OF CHARACTERISTICS". All notes shall begin by defining the symbol, i.e., ◇C = CRITICAL; ◇F = FATIGUE CRITICAL; ◇I = INTERFACE, and may then contain such additional clarifying information as required. The ◇F note below is suggested for general usage and is available as decal, ENG 773.12; but, the sample notes are not intended to impose any restrictions not contained in the text. Sample notes shown below pertain to examples shown in paragraph 6.1a.

CLASSIFICATION OF CHARACTERISTICS

◇F FATIGUE CRITICAL AREA. EXTRA CARE MUST BE EXERCISED TO INSURE THAT THIS AREA IS FREE OF NICKS, GOUGES, SCRATCHES, SHARP EDGES, ETC., THAT ARE VISIBLE TO THE NAKED EYE. DETAIL PART DIMENSIONS, PARTICULARLY RADII, MUST BE MAINTAINED. 100% INSPECTION REQUIRED.

◇C CRITICAL TORQUE REQUIREMENT. 100% INSPECTION REQUIRED.

◇I INTERFACE.

(R) (NOT APPLICABLE TO IM PROJECT)

WD/rf

H. K. Kreier

H. K. Kreier
Manager of Design Support

GRUMMAN AEROSPACE CORPORATION

ENGINEERING MANUAL

PROCEDURE NUMBER

C150

ADVANCE DESIGN INFORMATION

SURFACE ROUGHNESS

Prepared By:

DESIGN SUPPORT -
DRAFTING PROCEDURES GROUP
x2300

30 September 1970

SURFACE ROUGHNESS

1.0 GENERAL

1.1 Surface roughness is defined as irregularities on the surface of solid materials. The terms and ratings contained in this procedure apply to surfaces produced by such means as machining, abrading, extruding, casting, molding, forging, rolling, coating, plating, blasting, burnishing, etc.

1.2 Surface roughness ratings are derived by arithmetically averaging surface irregularities from a mean line. This average is specified in microinches. (0.000001 inch).

2.0 PRODUCTION METHODS AND COST FACTORS

2.1 A typical range of surface roughness values produced by common production methods is given in Table 1.

2.2 The finer the surface finish the greater the cost. Care should be exercised in the choice of surface roughness ratings to insure that the coarsest surface finish compatible with design requirements is used. Figure 1 illustrates a cost comparison curve which typifies the exponential rate of cost rise required to obtain increasingly fine surface finishes with turret lathe operations.

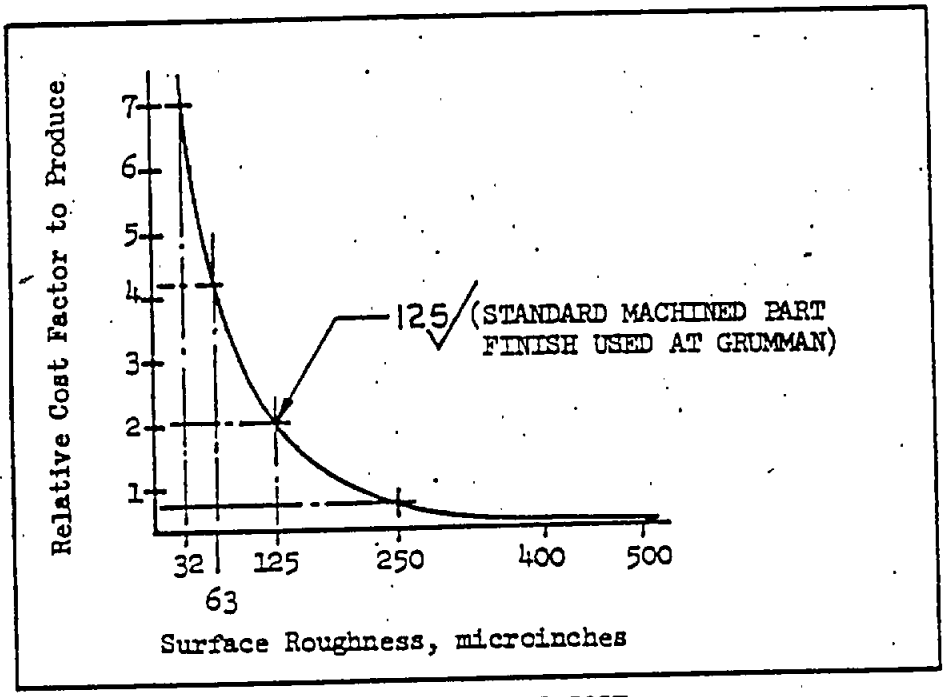

SURFACE ROUGHNESS VS COST
Figure 1

3.0 ROUGHNESS RATING SYMBOL

3.1 Basic Symbol - The basic symbol used on engineering drawings to indicate surface roughness shall be constructed as follows:

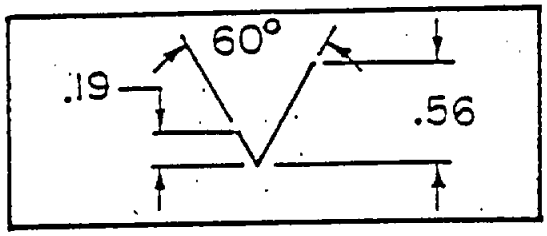

(NOTE: All dimensions are approximate)

3.2 Roughness Rating - Selection of roughness ratings should be based on the rating characteristics given in Table 2.

The desired roughness rating shall be placed above the short leg of the symbol, using .19 inch high numerals. When only one value is given, it shall be considered to be a maximum value, and any lesser value will be acceptable. When a maximum and minimum value are specified, the maximum value shall be shown above the minimum value.

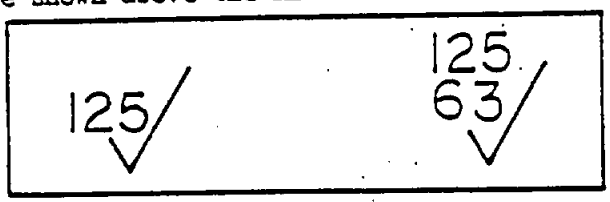

4.0 DRAWING REQUIREMENTS

4.1 Machined Parts Drawing - On machined parts drawings, the Supplementary Data decal (ENG 771.4) shall be used. This decal contains preprinted surface roughness requirements as shown in Figure 2. When a drawing contains any surface roughness requirements, the general surface roughness statement ((a) in Figure 2) shall be checked. In addition boxes (b) and/or (c) may be checked if applicable, or field callouts may be applied as described in Paragraph 4.4. The surface roughness values shown in (b) and (c) may be changed to meet the requirements of the drawing. When more than one value is required, the predominent value shall be entered in the decal and the remaining surfaces shall be identified on the field of the drawing as indicated in Paragraph 4.4.

In the case of castings, forgings, extrusions, "altered item" parts, etc where an original surface already exists; part of which will remain "as is" and only part of which will be machined, the word "MACHINED" shall be added to box "b" in Figure 2.

GRUMMAN AEROSPACE CORPORATION

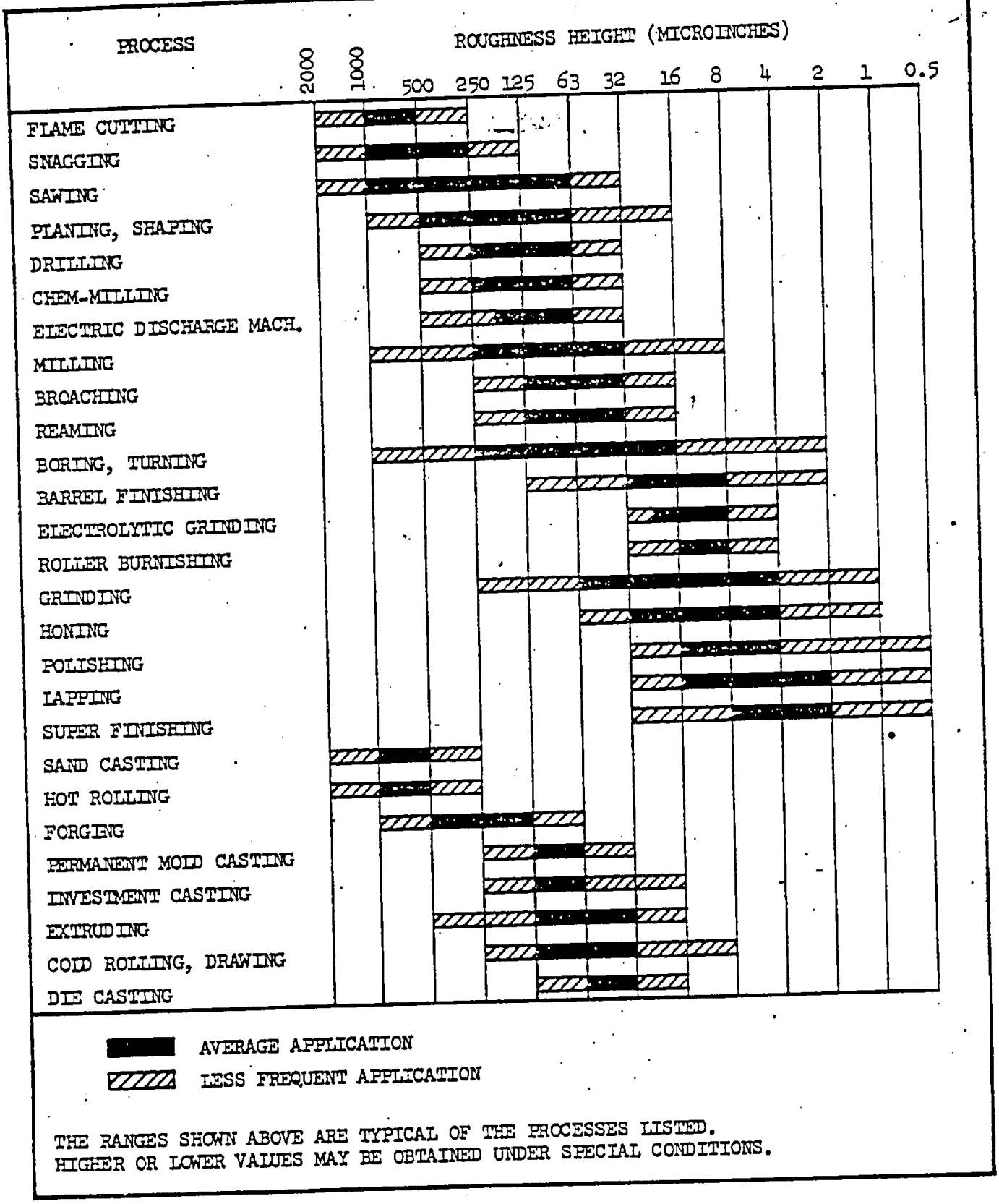

THE RANGES SHOWN ABOVE ARE TYPICAL OF THE PROCESSES LISTED.
HIGHER OR LOWER VALUES MAY BE OBTAINED UNDER SPECIAL CONDITIONS.

SURFACE ROUGHNESS PRODUCED BY COMMON PRODUCTION METHODS

Table 1

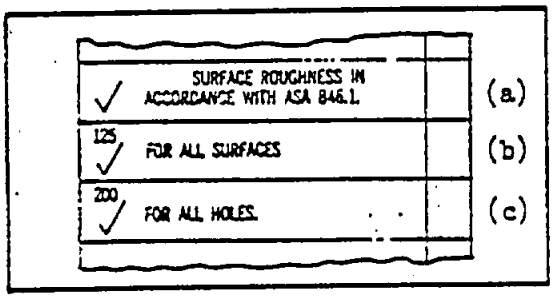

SURFACE ROUGHNESS PORTION OF SUPPLEMENTARY DATA DECAL (ENG. 771.4)

Figure 2

4.2 Casting and Forging Drawings - Where separate drawings are required for the rough casting or raw forging, surface finish requirements must be specified for the as-cast or as-forged surfaces. The decals used with these drawings contain a surface finish section which is shown below. The surface roughness box shall be checked and the applicable value entered as described in Paragraph 4.1.

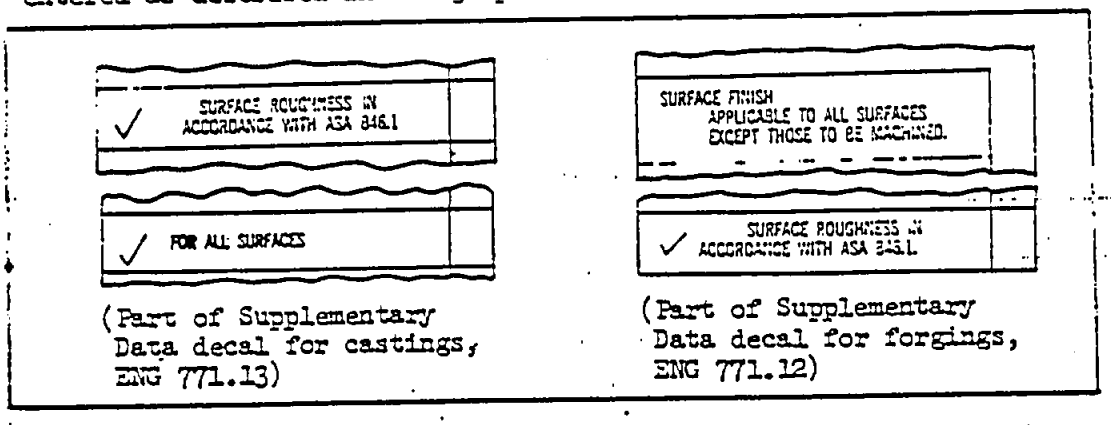

(Part of Supplementary Data decal for castings, ENG 771.13)

(Part of Supplementary Data decal for forgings, ENG 771.12)

4.3 Waviness and Mismatch - Surface roughness may be inter-related with waviness and mismatch in defining surface irregularities. Refer to Procedure C100, MACHINING PROCESSES, for general data on waviness and mismatch.

4.4 Field of Drawing Callout - When symbols are entered directly on the part in the field of the drawing, the point of the symbol shall be placed on the surface to be controlled; on an extension line; or on a leader pointing to the surface. The long leg shall slant to the right. All symbols shall be positioned so that they read from the bottom of the drawing. See Figure 3. Symbols shall appear in one location only for any affected surface. Do not repeat a symbol in another view or section.

500	Used on parts which are not critical in fatigue or stress concentration, the failure of which would not endanger safety or reliability.
250	A coarse production finish for unimportant clearance and cleanup operations. This degree of roughness is often produced on the natural surfaces of forgings, permanent mold castings, extrusions and rolled surfaces.
125	A medium commercial machine finish. This is the roughest surface recommended for parts subject to loads, vibration and high stress. Also permitted for bearing surfaces when motion is slow and the loads are light or infrequent. Do not specify for fast rotating shafts, axles or parts subject to extreme vibration or extreme tension.
63	A good machine finish. May be specified where close fits are required, and may be used for all stressed parts, except for fast rotating shafts, axles and parts subject to extreme tension. Satisfactory for bearing surfaces when motion is slow and the loads are light or infrequent.
32	A high grade machine finish. Satisfactory for bearing surfaces when motion is not continuous, and loads are light.
16	A high quality surface. Specify only where smoothness is of primary importance for proper functioning of a part, (e.g. rapidly rotating shaft bearings, heavily loaded bearings, and extreme tension members).
8	Very fine Surface. Specify where packings and rings must slide across the direction of the surface grain, maintaining or withstanding pressures; (e.g. the interior honed surfaces of hydraulic cylinders).
4	Refined surfaces produced by special finishing operations.
2	Very refined surfaces produced only by the finest super finishing equipment.

ROUGHNESS HEIGHT RATING CHARACTERISTICS

Table 2

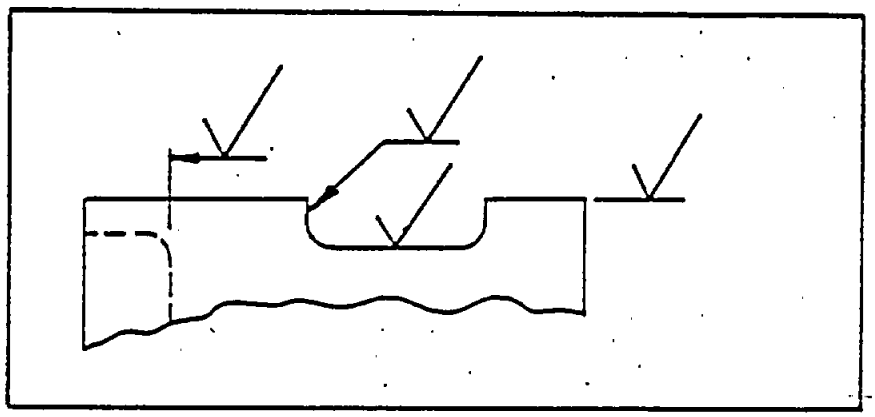

SURFACE ROUGHNESS SYMBOL USAGE
ON FIELD OF DRAWING

Figure 3

4.5 Plated and Coated Parts - On plated and coated parts it may be required to indicate whether the symbol applies before, after, or before and after plating or coating. Refer to the PLATING AND FINISHES section of this Manual for the specific process involved, its surface finish requirements and the drawing callouts to be used. —

4.6 Areas of Transition - Where the roughness symbol is used with a dimension, it affects all surfaces defined by the dimension. Areas of transition, such as chamfers and fillets, may conform to the roughest adjacent finished area unless otherwise specified.

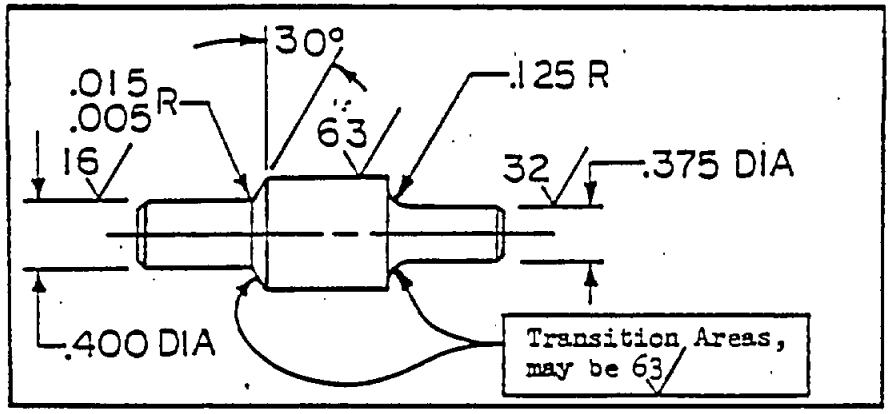

S P E C I A L N O T E S

F O R

BULLETIN NO.15

(1) THERE ARE SOME KNOWN ERRORS IN THIS BULLETIN-

(2) A CORRECTED BULLETIN WILL BE ISSUED AS SOON AS POSSIBLE

(3) FURTHER INFO:

ERNIE RANALLI X21467

Structures Bulletin No. 15

To: All Holders of Structures Manuals

From: E. Ranalli/R.E. Hooson ERR REH

Subject: Calculation of Notch and Constraining Material Stresses

Summary

Two recent problems have shown the necessity for increased understanding of the proper procedures for fatigue analysis. The first problem is concerned with determination of the proper stress relationships between the notch and the material constraining the notch. The second problem deals with the increased notch stress related to shear transfer (mostly torsional) between adjoining axially loaded members.

Problem 1 - Multiple net section structures - Crack initiation analyses are dependent upon the parts notch stress ($K_N f$) and the average stress (f) of the constraining material. The constraining material is defined as material remote from the notch but monolithically joined to the notch. Knowledge of only the peak notch stress ($K_N f$) is not sufficient since, in the plastic range, notch stresses and strains are controlled by the normally elastic constraining material remote from the notch. However in parts with several holes, multiple net sections are created which may have significantly differing individual net section stresses. One such example is illustrated in this bulletin. The calculations shown utilize data from R.E. Peterson's "Stress Concentration Factors" which, on an elastic basis, permit the calculation of net section loads and hence individual net section stresses.

The selected example represents the geometry associated with a 3/16 size miniature anchor nut with the exception that the primary attachment hole is 0.250 inches (representing an oversize condition). Additional comments and recommendations for anchor nuts are given on page 6.

Example 1 - Multiple Net Sections

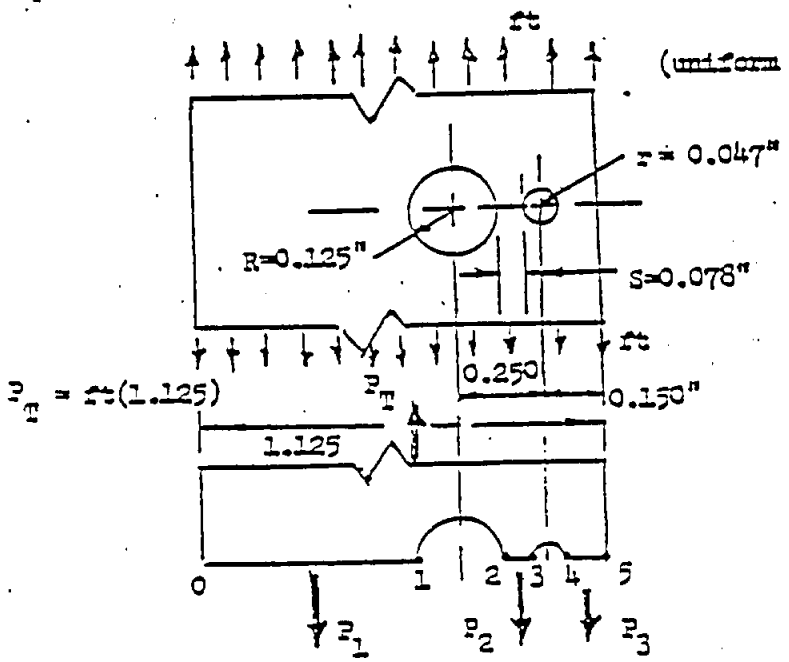

The notch stresses at points 1, 2, 3 and 4 and also the <u>average</u> net section stresses 0-1, 2-3 and 4-5 will be calculated. First a shear stress free boundary between the two holes must be established. Peterson suggests that such a shear free plane can be established by proportioning the distance between the holes according to the hole radii.

$$\text{Therefore } S_1 = S\left(\frac{R}{R+r}\right)$$

$$= 0.078\left(\frac{0.125}{0.125 + .047}\right) = 0.057"$$

$$S_2 = S\left(\frac{r}{R+r}\right) = 0.021"$$

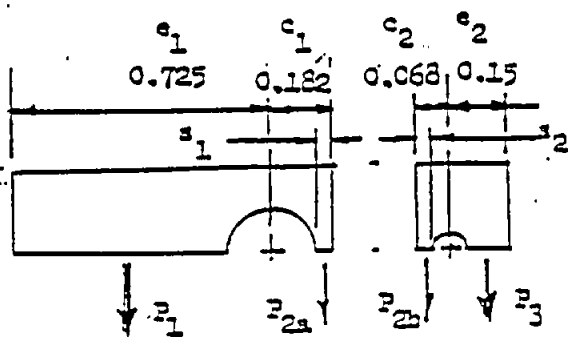

In effect, the problem is now reduced to two finite width plates with eccentric holes. Calling the smaller edge distance c and the larger edge distance e, the above picture is obtained.

From Peterson (equation 57) the net section load carried by the short edge for the example dimensions is

$$P_{2a} = ftc_1 \left[\frac{\sqrt{1-\left(\frac{R}{c_1}\right)^2}}{1-\frac{c_1}{e_1}\left(1-\sqrt{1-\left(\frac{R}{c_1}\right)^2}\right)} \right] = 0.142 \text{ ft}$$

Note that for a semi infinite plate (ie: e_1 large) the value of P_{2a} is lower (0.133 ft). This is important information from which an adjusted notch stress for finite width sheet can be obtained. Note that literature solutions for stress concentrations for multiple holes are available only for infinite width sheets.

From equilibrium of the left element

$$P_1 = (0.725 + 0.182) \text{ ft.} - 0.142 \text{ ft.} = 0.765 \text{ ft.}$$

Correspondingly

$$P_{2b} = ftc_2 \left\{ \frac{\sqrt{1-\left(\frac{r}{c_2}\right)^2}}{1-\frac{c_2}{e_2}\left(1-\sqrt{1-\left(\frac{r}{c_2}\right)^2}\right)} \right\} = 0.056 \text{ ft.}$$

and again, if e_2 were large P_{2b} would have been 0.049 ft.

Finally $P_3 = (0.150 + 0.068) \text{ ft.} - 0.056 \text{ ft.} = 0.162 \text{ ft.}$

The three net section stresses are therefore

$$f_{0-1} = \frac{P_1}{(e_1 - R)t} = \frac{0.763 \text{ ft.}}{(0.725 - 0.125)\,t} = 1.272\, f$$

$$f_{2-3} = \frac{P_{2a} + P_{2b}}{st} = \frac{(0.142 + 0.056) \text{ ft.}}{0.078} = 2.54\, f$$

$$f_{4-5} = \frac{P_3}{(e_2 - r)\,t} = \frac{0.162 \text{ ft}}{(0.150 - 0.047)\,t} = 1.573\, f$$

By way of comparison the average net section stress for the entire part is

$$f_{aver.} = \frac{P_T}{w-2R-2r} = \frac{1.125 \text{ ft.}}{1.125 - 2\,(0.125 + 0.047)} = 1.440f$$

To determine the peak notch stresses (at 1, 2, 3, 4) some requires additional engineering judgment. Notice that the net section load between holes is always larger for a finite width plate. Hence all stresses (including the notch stress) can be expected to be higher in the finite sheet case. It is hypothesized that the notch stress increase can be taken as proportional to the net section load increase.

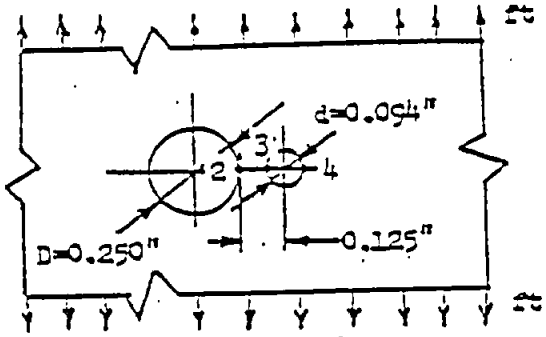

From Page 15-5

$$e/d = \frac{0.125}{0.094} = 1.33$$

$$D/d = \frac{0.250}{0.094} = 2.66$$

At point (3) $K_t = 3.8$ or $K_t f = 3.8\,f$ for the infinite case

$$K_t f = 3.80\,f \left[\frac{0.142 + 0.056}{0.133 + 0.049}\right] = 4.14\,f \text{ for the finite case}$$

therefore apparent K_t relative to the constraining net section material is

$$\text{Apparent --- } (K_t) = \frac{\sum (K_t f)_3}{f_{2-3}} = \frac{4.10f}{2.538f} = 1.615$$

$$K_N = 1 + \frac{K_T - 1}{1 + \frac{\sqrt{A}}{\sqrt{r}}} = 1 + \frac{0.615}{1 + \frac{0.14}{\sqrt{0.047}}}$$

$$\text{or } (K_N f) = 1.37 \times 2.538f = 3.48f$$

$\sqrt{A} = 0.14$, assuming an aluminum alloy with $F_{tu} \simeq 70000$ psi,

(Ref. Grumman Struct. Manual page 37,030-26)

Similarly for point (2) page 15 gives:

$K_t \simeq 3.0$ or $K_t f = 3.0f$ for the infinite sheet case

Again ratioing by the net section load increase, the finite case is obtained.

$$K_t = 3.0 \left(\frac{0.142 + 0.056}{0.133 + 0.049}\right) = 3.27$$

$$\text{Apparent } K_t = \frac{K_t f_2}{f_{2-3}} = \frac{3.24f}{2.538f} = 1.275$$

$$K_N = 1 + \frac{1.275 - 1.0}{1 + 0.14/\sqrt{0.125}} = 1.197$$

$$(K_N f)_2 = 1.197 \times 2.538\, f = 3.04\, f$$

Point (4), using Page B7.040.1-1, Grumman Structures Manual

with $d_1/d_2 = 0$ $\quad \frac{r}{e_2} = \frac{0.047}{0.150} = 0.313$

gives $K_t = 3.25$ (infinite case)

$$(K_t f)_4 = 3.25\, f \times \left(\frac{0.162}{0.142}\right) = 3.70f \quad \text{(finite case)}$$

$$\text{Apparent } K_t = \frac{K_t f}{f_{4-5}} = \frac{3.70f}{1.573f} = 2.35 \qquad K_n = 1 + \frac{2.35 - 1.0}{1.0 + \frac{0.14}{0.047}} = 1.82$$

and $\quad (K_N f)_4 = 1.82 \times 1.573\, f = 2.86\, f$

In summary:

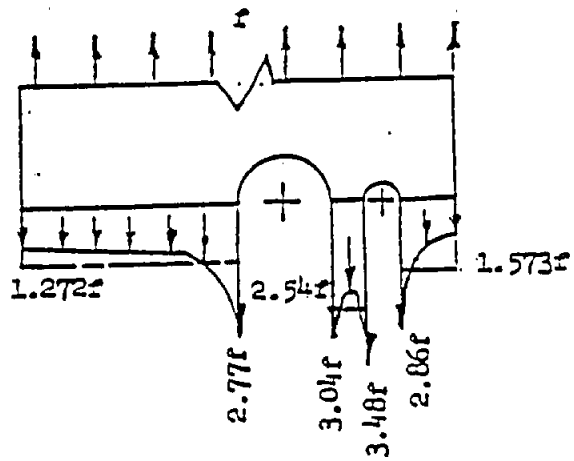

Common airframe applications of multiple holes - There are at least three commonly occurring examples of multiple holes of varying diameters. These cases are:

- o Anchor Nuts - Small attaching rivets adjoining primary removable fastener
- o Access Holes - Removable fasteners surrounding a large cutout
- o Sealed Fuel Tanks - Small injection screw holes, or preferably tapped pressed fit plugs, adjoining primary structural fasteners.

The latter two cases do not have common geometry. In addition it must be noted that for the case of multiple satellite attachments surrounding a primary access hole, stress concentration reduction due to "shadowing" is possible. "Shadowing" occurs when the holes are closely and repetitively spaced such that the presumption of uniform gross section stress remote from the critical holes is invalid. An estimate of the importance of this effect can be obtained by comparing page B7.040.1-1 (for a single central hole in a finite sheet) with page B7.040.1-5 (for repetitive centrally located holes). The anchor nut problem is of singular geometry and will be dealt with in general terms.

Anchor nuts are available in various shapes illustrated on pages 4-8 through 4-10 of the Grumman Fastener Manual (dated December 1976). The center to center hole spacing between the primary fastener and the smaller attaching rivets is either of reduced dimension (commonly referred to as miniature) or standard. For commonly used 3/16 and 1/4 attachments we have

	℄ to ℄ Spacing		Calculated e and e/d			
Fastener	3/16	1/4	e(3/16)	e/d(3/16)	e(1/4)	e/d(1/4)
Miniature	0.250 in	0.281 in	0.153 in	1.63	0.150 in	1.60
Standard	0.344 in	0.500 in	0.247 in	2.63	0.369 in	3.93

Utilizing the curve on page 15, we observe that since the primary parameter e/d is larger than 2.5 that standard anchor nuts can be considered as a single hole. However, for miniature anchor nuts e/d is only about 1.6 making orientation and potential oversize holes very important. At the small hole edge K_{td} can be as high as 3.4 x 1.11 = 3.77 (angle about 65°) but as low as 3.0 for all fasteners in line (angle about 0°). Therefore, it is recommended, in all primary structural parts, that only standard anchor nuts be used. If miniatures must be used due to

space limitations, only types with in line fastener configuration should be used. Control of the orientation on the Engineering Drawing is considered mandatory in those cases.

Problem 2 - Increased Notch Stress due to Torsional Shear

The fatigue problem of adjoining axially loaded parts with shear transfer between the parts has not been properly addressed in the past.

An example is provided by the structural free body representing a typical Gulfstream integral wing cover construction, shown below.

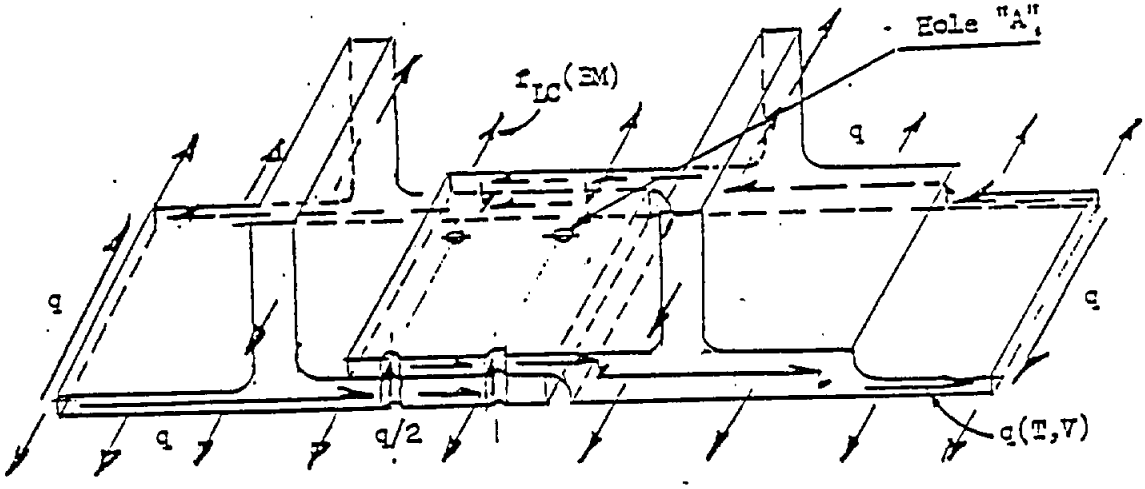

In fatigue the critical problem is at points of stress concentration. Examining the state of stress around hole A on the inner cover pictured above.

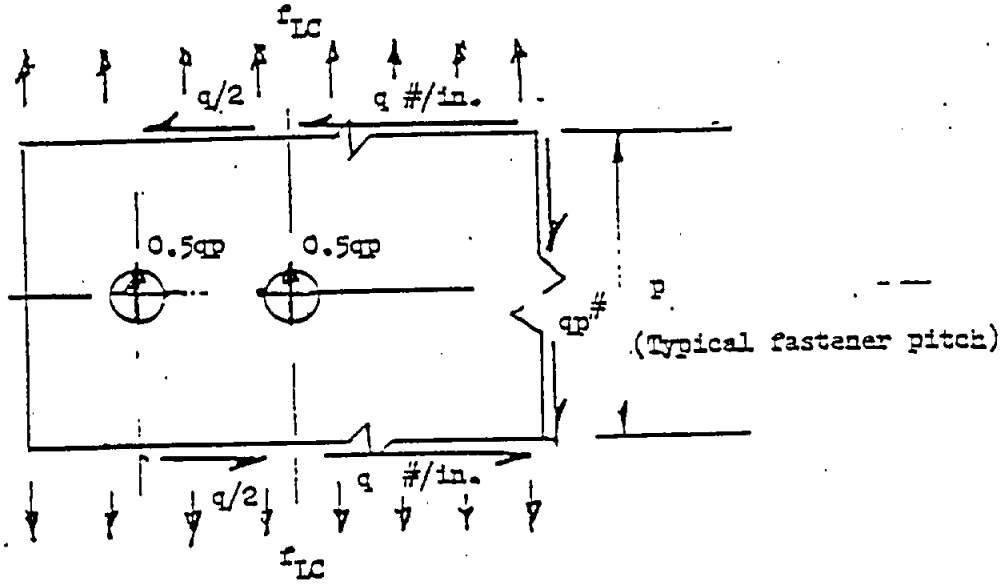

Presuming that f_{LC} will be virtually constant over a spanwise distance of one fastener pitch and the stress concentration superposition principle is valid the complex stress distribution is reducible to the addition of the following three cases.

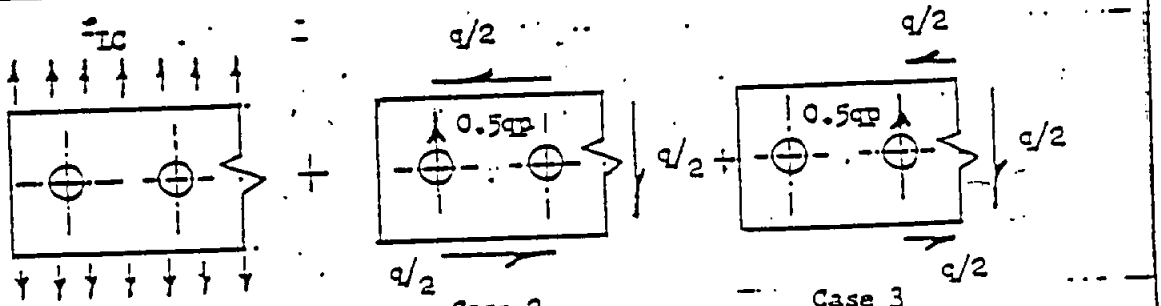

Case 1 Bypass Tension — Case 2 Remote Shear — Case 3 Pin Load Balanced by Shear

Superposition of stress concentration factors is strictly valid only for unfilled, unloaded holes. For problems in which the holes contain neat (line to line) fit pins inward radial displacements of the hole boundary are effectively eliminated. For lugs, this effect strongly influences the load distribution in the lug and reduces the stress concentration that would have occurred with an undersize pin. Experience has shown that the effect does not normally vary appreciably under complex loading and superposition is valid as a first order approximation. For important problems with unusually high oblique direction pin loads, consideration should be given to further study by either photoelastic or finite element techniques.

Cases (1) and (2) can readily be obtained from standard references like the Grumman Structures Manual or R.E. Peterson "Stress Concentration Design Factors". Case 3 can be approximated by the superposition of the three cases shown.

Case 3 - Pin Load Balanced by Shear

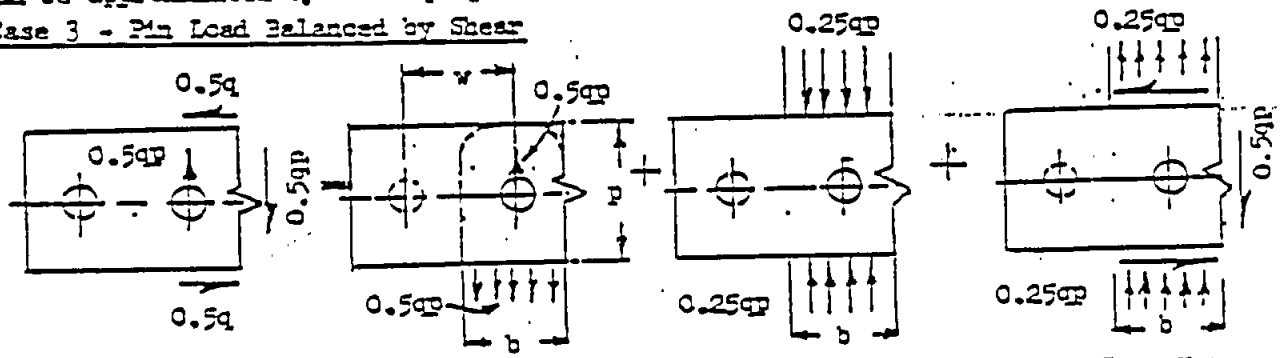

Case 3A - Pin Loaded Hole Balanced by Tension
b is lesser of p or w

3B - Relieving Bypass Compression

3C - Zero Net Shear Load

Case (3A) is a lug (or pin loaded hole effect) which has a relatively high stress concentration factor. Case (3B) is a bypass compression stress (relieves the notch stress) and Case (3C) has no net stress across the critical net section and it is therefore hypothesized that the notch stress for this case is negligible. An application of this procedure is shown in the following example.

Example 2 - Typical lower cover section of the Gulfstream III Wing

MATERIAL: Aluminum Alloy Plate, 2024-T351

F_{tu} ≈ 65000 psi

$\sqrt{A}$ = 0.15

t = plate thickness = 0.110 in. (aft plank fwd edge)

D = fastener diameter = 0.25 in.

W = distance between fastener rows = 0.75 in.

P = fastener pitch = 1.18 in. (Staggered pattern)

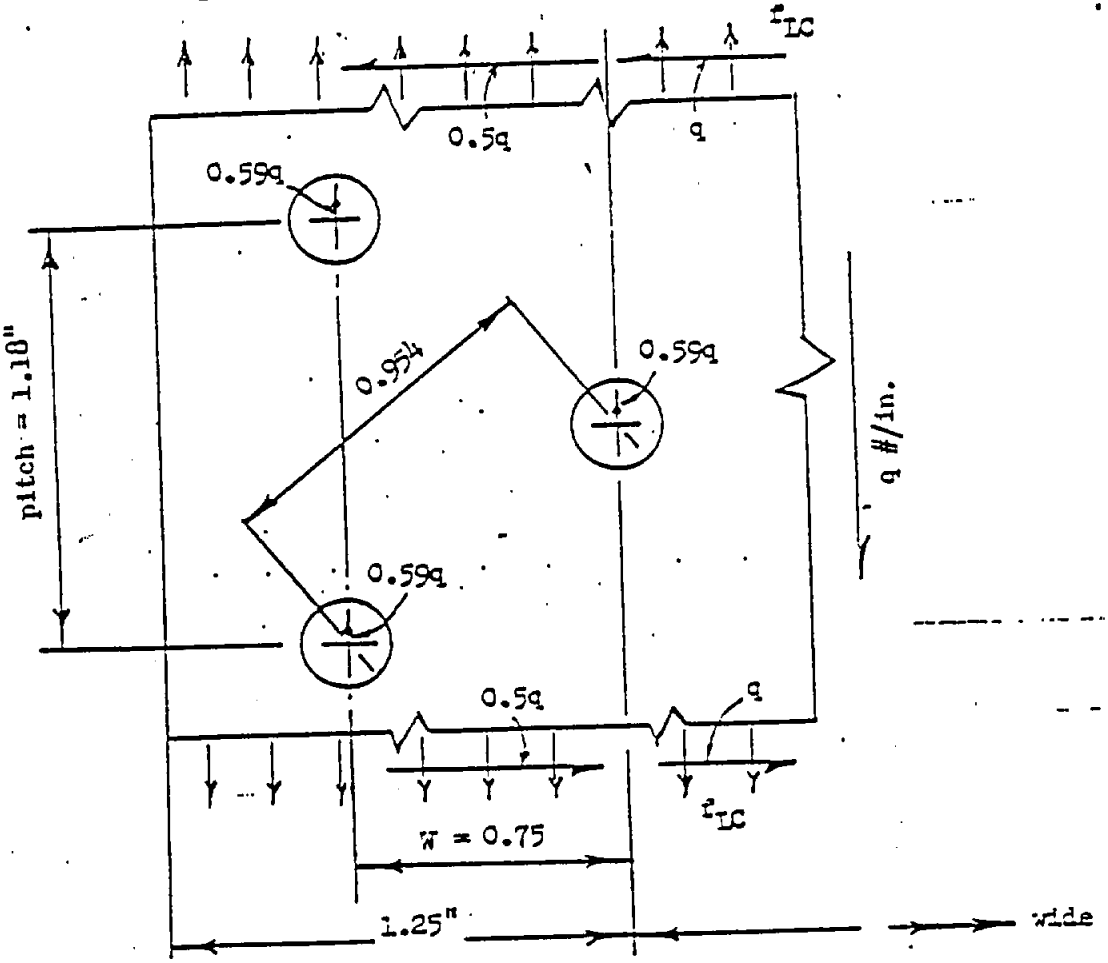

Case (1) Bypass Tension Page B7.040.1-6 GSM (Conservative Solution)

$$b/d = \frac{0.75}{0.954} = 0.786 \qquad D/b = \frac{0.25}{0.75} = 0.333 \qquad K_{t_{net}} = 2.08$$

$$K_{t\ gross} = 2.08\left(\frac{0.75}{0.75 - 0.25}\right) = 3.12$$

finally $(K_t f)_{LC} = 3.12\, f_{LC}$

which is as expected, just over 3 times the nominal gross section stress. Recall that for any hole in an infinite sheet a gross stress concentration of 3.0 exists for a tension field at a point 90° to the load.

Case (2) Remote Shear - Although a maximum axial stress of 4.0 times the nominal shear stress occurs (an infinite plate in shear) the critical point is 45° to the load. At the 90° point this stress is zero (antisymmetry load principle) and hence no additional axial stress occurs at the critical 90° point for this axial load dominated problem. Points between 45° and 90° are potentially critical for high shear stress problems.

Case (3A) - Pin loaded Hole Balanced by Tension

Ref page B7.040.3-1 Grumman Structures Manual

$e/W \gg 1$ $\qquad D/W = \frac{0.25}{0.75} = 0.333$

$$K_{t_{net}} = 3.2 \qquad \text{or} \qquad \left(K_t f_{LC}\right)_{net} = \frac{3.2 \times 0.59\, q}{(0.75-0.25)t} = 3.776\ q/t$$

Note the unusually high net stress concentration which corresponds to a gross stress concentration of 4.8. Large values like this one can occur in pin loaded hole problems.

Case (3B) - Bypass Compression

Ref page B7.040.1-1 Grumman Structures Manual

$$\frac{R}{W/2} = \frac{0.125}{0.375} = 0.333 \qquad K_{t_{net}} = 2.3$$

$$\text{or} \quad K_{t_{net}} = 2.3 \times \frac{(-0.59q)}{(0.75-0.25)t} = 1.357\ \frac{q}{t}$$

Therefore the net effect of the shear transfer is the sum of cases (3A) and (3B)

$$(K_t f) = (3.776 - 1.357)\frac{q}{t} = 2.42\frac{q}{t}$$

The total apparent raised stress (Case (1) plus Case (3)

$$\Sigma(K_t f) = 3.12\, f_{LC} + 2.42\frac{q}{t}$$

The stress on the constraining material must now be calculated. Since the holes are of equal size the shear load free boundary is midway between the holes.

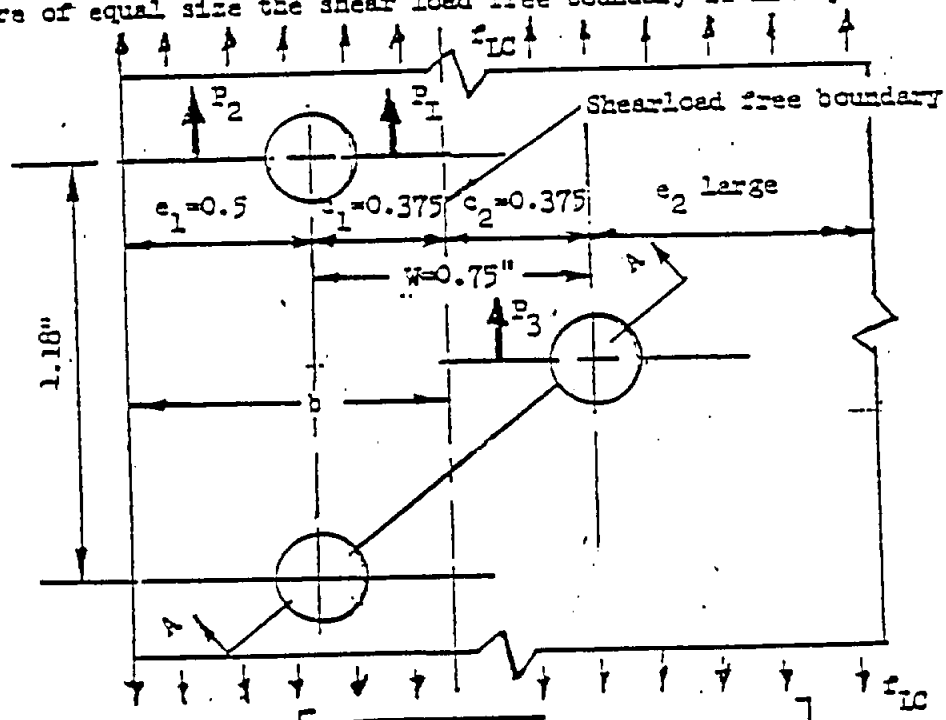

$$P_1 = f_{LC} c_1 t \left[\frac{\sqrt{1 - (r/c_1)^2}}{1 - c_1/e_1\,(1 - \sqrt{1 - (r/c_1)^2})}\right]$$

$$= 0.375\, f_{LC} t \times 0.985 = 0.369\, f_{LC} t$$

Therefore $P_2 = 0.875\, f_{LC} t - 0.369\, f_{LC} t = 0.506\, f_{LC} t$

$$P_3 = f_{LC} \times 0.375t \sqrt{1 - (r/c_2)^2} = 0.354\, f_{LC} t$$

$$P_{Net} = P_1 + P_3 = 0.369\, f_{LC} t + 0.354\, f_{LC} t = 0.723\, f_{LC} t$$

Examining Section A-A

$$(f_t)_{Net} = \frac{0.723\, f_{LC} t}{(0.954 - 0.25)\, t} \cos 38^\circ = 0.809\, f_{LC}$$

$$(f_s)_{Net} = \frac{0.723\, f_{LC} t}{(0.954 - 0.25)\, t} \sin 38^\circ = 0.632\, f_{LC}$$

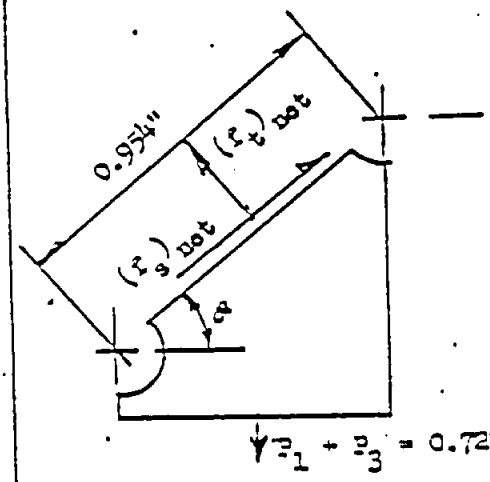

Using Octhedral Shear Stress for Combined Stresses :

$$f_{oct}^2 = f_t^2 + 3 f_s^2$$

$$= (0.809\, f_{LC})^2 + 3(0.632\, f_{LC})^2$$

$$f_{oct} = 1.36\, f_{LC}$$

Apparent Stress Concentration Factor

$$K_t = \frac{\sum K_t f_{Net}}{f \text{ constraining}} = \frac{3.12\, f_{LC} + 2.42 \quad q/t}{1.36\, f_{LC}}$$

$$K_t = 2.30 + 1.78 \frac{q/t}{f_{LC}}$$

$$K_N = 1 + \frac{1.30 + 1.78 \frac{q/t}{f_{LC}}}{1 + \frac{0.15}{\sqrt{0.125}}} = 1.93 + 1.275 \frac{q}{f_{LC} t}$$

$$\text{finally } K_N f_{\text{Net}} = \left\{1.93 + 1.275 \frac{q}{f_{LC} t}\right\} \left\{1.36 f_{LC}\right\}$$

$$K_N f_{\text{Net}} = 2.625 f_{LC} + 1.734 \frac{q}{t}$$

For the Aft Plank $t = 0.110$ (forward edge)

$$K_N f_{\text{Net}} = 2.625 f_{LC} + 15.76 q$$

To make the analysis meaningful from a design point of view, assume that it is required to determine the allowable ultimate gross lower cover stress (f_{LC}) to satisfy the Gulfstream Life Requirement. Assume, for example, that the calculated allowable limit raised notch stress ($K_N f$) for the Gulfstream III is 88000 psi for the cover material and the maximum value of sheer flow (q) for this plank is 1100 pounds per inch ultimate.

Therefore $(K_N f) = 88000 \times 1.5 = 2.625 f_{LC} + 15.76\ (1100)$

or Allowable $f_{LC} = 43680$ psi ultimate

Note, as is often the case for modern long life aircraft, this allowable ultimate stress is considerably below the material ultimate tensile strength (F_{tu} = 65000 psi, B-Basis) and a weight penalty would be incurred in order to satisfy the fatigue life requirement. For this reason interference fit fasteners and/or cold worked holes are being widely used throughout the aircraft industry, including Grumman, in fatigue critical structures.

Although it is beyond the scope of the bulletin, it can be shown that the interference fit fastener improves fatigue life by reducing the value of the raised notch stress. For example, the theoretical stress concentration factor for an infinite width sheet in tension, at low stresses, is 1.6 (rather than 3 for open holes). However, the stress concentration can increase in a very non-linear manner at high loads, if and when the initial radial compression between the hole and fastener is relieved. Cold worked holes, on the other hand, improve fatigue life by introducing tangential compressive residual stress around the hole boundary, and therefore increasing the allowable notch raised stress. Here again stress relaxation due to temperature exposure or applied compressive loads may drastically reduce this effect in certain cases. Therefore the potential weight savings of such systems must be carefully assessed including, in addition to the above consid-

erations, reliability and manufacturing costs before the decision to increase the allowable fatigue stress in design is made. Any decision of this type must be made with the concurrence of the structures project group leader and the project's engineering management (i.e. Project Engineers and the Engineering Manager).

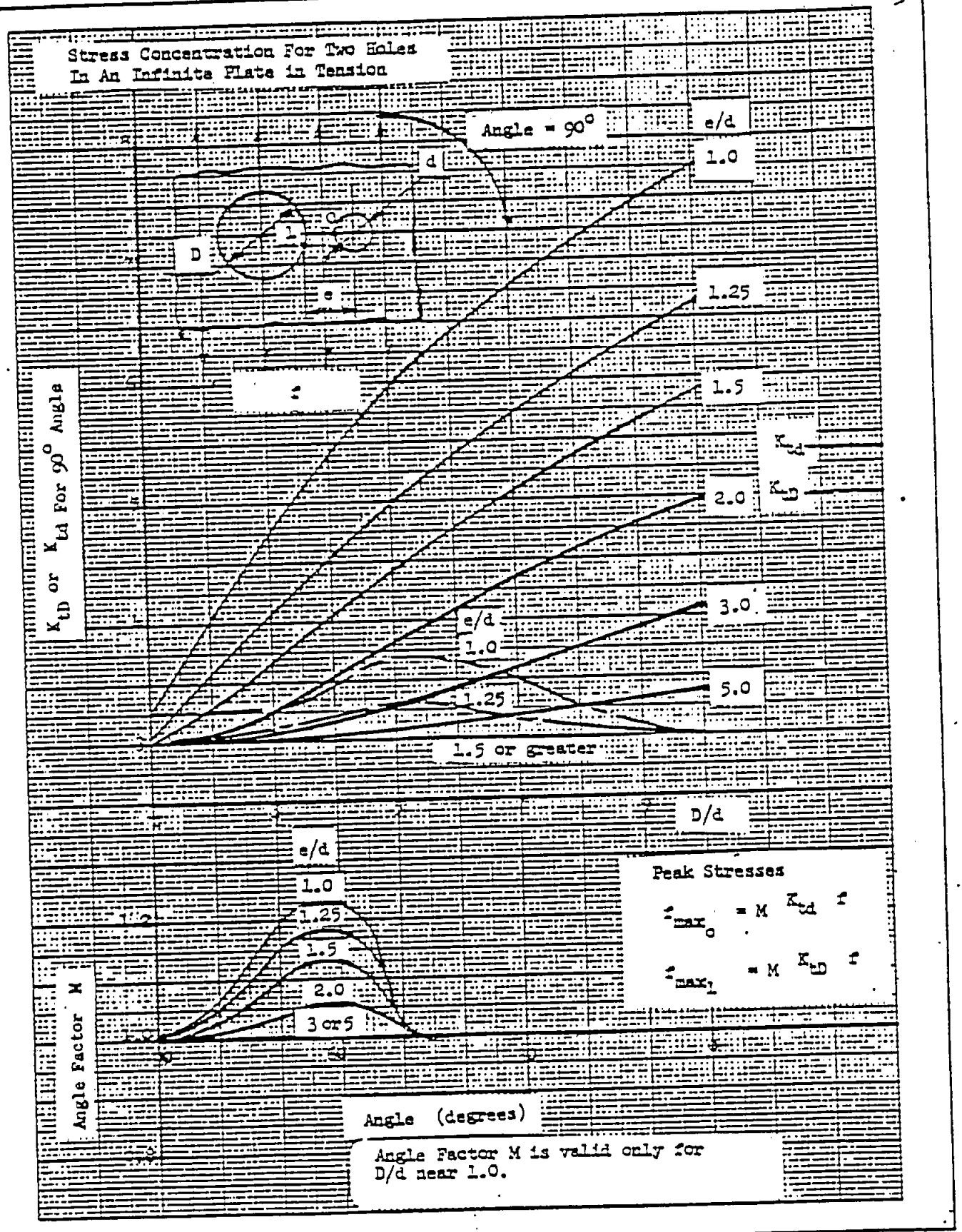
Stress Concentration For Two Holes
In An Infinite Plate in Tension
Angle = 90°
e/d
1.0
1.25
1.5
2.0
3.0
5.0
d
D
e
f
K_{td}
K_{tD}
K_{tD} or K_{td} For 90° Angle
e/d
1.0
1.25
1.5 or greater
D/d
e/d
1.0
1.25
1.5
2.0
3 or 5
Angle Factor M
Angle (degrees)
Peak Stresses
$f_{max_o} = M K_{td} f$
$f_{max_1} = M K_{tD} f$
Angle Factor M is valid only for
D/d near 1.0.

This Page
was
Intentionally
left
Blank

From: D.W.Bone Struct. Analysis B-43/35 GAC 7809 21 Sept. 1979
EG-STAN-79-056

To: All Holders of Structures Manuals

Subject: DIMENSIONAL TOLERANCES IN STRESS ANALYSIS CALCULATIONS

Enclosures: 1) Structures Bulletin No. 16
2) Grumman Standard GM15B

The Presidential Audit Committee on Product Quality has concluded that future designs shall incorporate modified analytical rules with respect to dimensional tolerances to insure greater conservatism in stress analysis.

Structures Bulletin No. 16, provides required guidelines for future design and shall be implemented immediately.

cc: T.J. Kelly
N. Lewin
W. Bischoff
A. Mead
R. Keenan

Distribution:

M/A Lists: B2 - 3A & 8A

Structures Bulletin No. 16

To: All Holders of Structures Manuals

From: D. Bone

Subject: Dimensional Tolerances in Stress Analysis Calculations

Summary

Guidelines are presented herein for the use of dimensional tolerances for all fatigue and static stress analysis calculations for future design. "Future design" includes modification of an existing design when necessitated by requirements other than tolerance requirements. It is not intended to cause a sequence of existing part changes solely as a result of implementing these tolerance guidelines. The guidelines in this Bulletin supersede Structures Bulletin No. 8 and any or all prior directions.

The guidelines are applicable to both load critical and deflection critical calculations. Deflection critical structures are defined as structures wherein the stress is primarily controlled by compatibility of deflections with adjacent structural members. The appropriate most critical high side or low side tolerance within the guidelines shall be used for load critical or deflection critical calculations.

Thickness Tolerances:

For all safety of flight structures, the nominal (average) thickness or five percent of the thickness from the extreme tolerance thickness shall be used, whichever is the more critical.

For structures other than safety of flight, nominal thickness shall be used.

Thickness tolerances to be considered shall include material stock thicknesses as purchased as well as fabrication tolerances resulting from machining, chem milling or any other material removal processing.

Grumman Standard GM15B defines tolerances for sheet and tubing material and is the standard to which GAC purchases material. Any thickness tolerance specified on the engineering drawing takes precedence over specifications.

Dimensional Tolerances Other Than Thickness:

For safety of flight structures, the most critical extreme tolerance allowed by the engineering drawing or specification shall be used for stress analysis calculations and for the derivation of stress concentration factors.

For structures other than safety of flight, nominal thickness shall be used.

"Tolerances other than thickness" include, for example, hole size tolerances, edge distance tolerances, straightness tolerances, misalignment tolerances at joints and length or width tolerances.

Special Consideration for Stress Corrosion:

In the calculation of built-in residual stresses due to press fits, clamping or any other pre-stressing process, the most critical extreme tolerances shall be used.

Definition of Safety of Flight Structures:

A Safety of Flight Structure shall be any structure, the failure of which, would cause loss of the aircraft in flight or catapulting operations or cause a catastrophic carrier landing accident affecting crew safety or other aircraft or personnel on a carrier deck.

Documentation:

All "future design" structural analyses, published or unpublished, shall reference the source of any tolerance used in the analysis. The reference must be a drawing or a specification which is used for material procurement or part or assembly fabrication and inspection.

Design Considerations:

Analysts should be alert to poor dimensioning practices or large tolerances on drawings or layouts which would cause weight increases without providing significant cost savings. Such examples should be brought to the attention of the cognizant structural designer and the structural analysis group leader.

cc: T.J. Kelly
N. Lewin
W. Bischoff
A. Mead
R. Keenan
Engineering Managers
Project Engineers

PREFERRED SHEET METAL GAGES, TUBING SIZES AND THEIR TOLERANCES

1. THE FOLLOWING TABLES CONTAIN THE PREFERRED SHEET METAL GAGES, TUBING SIZES, AND THEIR TOLERANCES CONSIDERED STANDARD AT GRUMMAN.

2. GRUMMAN STANDARD GMISA, THE PREFERRED MATERIAL LIST FOR DEPARTMENT OF DEFENSE (DOD) PROGRAMS SHALL BE USED FOR METALLIC MATERIAL SELECTION. REFER ALSO TO THE GRUMMAN PARTS LIST (GPL), THE GS30A SUBSTITUTION AND CROSS REFERENCE LIST, AND THE CORPORATE ENGINEERING MANUAL (DRAWING SYSTEM/DOCUMENTATION) FOR SPECIFIC PROGRAM APPROVAL AND THE CORRECT MATERIAL CALLOUT AND DRAWING PARTS LIST IMPLEMENTATION.

3. THE USE OF OTHER THAN THE PREFERRED STANDARD SIZES REQUIRES MATERIALS AND PROCESSES DEPARTMENT CONCURRENCE AND ENGINEERING STANDARDS APPROVAL.

4. FOR AVAILABILITY OF MATERIAL IN SIZES SPECIFIED, REFER TO THE M59012 ALLOWABLE PARTS CATALOG (CORPORATE MIN./MAX.).

5. FOR PREFERRED GAGES AND SIZES OF METALLIC MATERIAL NOT YET INCLUDED IN THIS STANDARD CONSULT MATERIALS AND PROCESSES DEPARTMENT AND ENGINEERING STANDARDS

6. AUTHORIZED MATERIAL SUBSTITUTIONS CAN BE FOUND IN THE FOLLOWING DRAWINGS.

   GS30B SUBSTITUTION LIST, MATERIALS, ALUMINUM AND ALUMINUM ALLOYS

   GS30C SUBSTITUTION LIST, MATERIALS, STEEL AND STEEL ALLOYS

   GS30D SUBSTITUTION LIST, MATERIALS, TITANIUM AND TITANIUM ALLOYS

   GS30E SUBSTITUTION LIST, MATERIALS, NON-METALLIC

7. INFORMATION CONTAINED WITHIN THIS STANDARD WAS EXTRACTED FROM GOVERNMENT, INDUSTRY, AND COMPANY STANDARDS AND SPECIFICATIONS.

SHEET METAL	
TABLE 1	ALUMINUM & ALUMINUM ALLOYS
TABLE 2	STEEL (CARBON & CARBON ALLOYS)
TABLE 3	STEEL (CORROSION RESISTANT)
TABLE 4	TITANIUM & TITANIUM ALLOYS

TABLE	TUBING (ROUND)
5	PREFERRED SIZES FOR ALUMINUM ALLOY TUBING (ROUND)
6	TOLERANCES FOR ALUMINUM ALLOY TUBING (ROUND) DRAWN
7	TOLERANCES FOR ALUMINUM ALLOY TUBING (ROUND) EXTRUDED
8	PREFERRED SIZES FOR CORROSION RESISTANT STEEL TUBING (ROUND)
9	TOLERANCES FOR CORROSION RESISTANT STEEL (ROUND) SEAMLESS TUBING
10	TOLERANCES FOR CORROSION RESISTANT STEEL (ROUND) WELDED TUBING
11	PREFERRED SIZES FOR CARBON & CARBON ALLOY STEEL (ROUND) TUBING

TABLE	TUBING (ROUND)
12	TOLERANCES FOR CARBON & CARBON ALLOY STEEL (ROUND) SEAMLESS, COLD FINISHED TUBING, AIRCRAFT TYPE
13	TOLERANCES FOR CARBON & CARBON ALLOY STEEL (ROUND) SEAMLESS, COLD FINISH TUBING, MECHANICAL TYPE
14	TOLERANCES FOR CARBON & CARBON ALLOY STEEL (ROUND) WELDED, ANNEALED, NORMALIZED, OR STRESS RELIEVED TUBING.
15	WALL THICKNESS TOLERANCES FOR CARBON & CARBON ALLOY STEEL (ROUND) WELDED TUBING, AIRCRAFT TYPE.
16	PREFERRED SIZES FOR TITANIUM 3AL-2.5V TUBING, SEAMLESS, ANNEALED
17	TOLERANCES FOR TITANIUM 3AL-2.5V ROUND TUBING, SEAMLESS, ANNEALED

REVISED (A) 1-23-76 (B) 3-12-76 APPROVED 12-5-75

MATERIAL - METALLIC
PREFERRED GAGES AND ROUND TUBING

GRUMMAN DESIGN

GRUMMAN STANDARD

GRUMMAN AEROSPACE CORPORATION, BETHPAGE, N.Y. 11714

SHEET NO.	1	2	3	4	5	6	7	8	9	10
STATUS REV	B	-	B	B	B	B	B	B	B	B

GM15B

CODE IDENT NO. 26512 | SHEET 1 OF 10

ENG 46-6 12-70

Examples of Thicknesses to be Used for Stress Calculations for Safety of Flight Structures

From Structures Bulletin 16, page SB16-1:
"For all safety of flight structures, the nominal (average) thickness or five percent of the thickness from the extreme tolerance thickness shall be used, whichever is the more critical"

Assume an aluminum part, fabricated in three different ways as follows:
(a) Sheet stock as received from the mill for width < 36 in., see GM15B
(b) Machined part with ± .010 tolerance called out on drawing
(c) Chem Milled part with + .008/-.002 tolerance called out on drawing

	Case (a) - Sheet	Case (b) - Machined	Case (c) - Chem Milled
Thickness Call-out	.100 ± .004	.100 ± .010	$.097^{+.008}_{-.002}$
Nominal (Average) Thickness	.100	.100	.100
Extreme Thickness			
Load Critical	.100 -.004 = .096	.100 - .010 = .090	.097 - .002 = .095
Deflection Critical	.100 +.004 = .104	.100 + .010 = .110	.097 + .008 = .105
5% From Extreme Thickness			
Load Critical	.096 + .05(.100)=.101	.090 + .05(.100)=.095	.095 + .05(.100)=.100
Deflection Critical	.104 - .05(.100)=.099	.110 - .05(.100)=.105 *	.105 - .05(.100)=.100
Thickness for Stress Calcs.			
Load Critical	.100 (Nominal)	.095 (5% Rule)	.100 (Nominal & 5% Rule)
Deflection Critical	.100 (Nominal)	.105 (5% Rule)	.100 (Nominal & 5% Rule)

In the above examples, a weight penalty will be incurred on the machined part because the thickness for stress calculations is more conservative than the nominal thickness. See last paragraph in Bulletin entitled "Design Considerations".

* REVISED 12/3/79

TABLE 1

ALUMINUM AND ALUMINUM ALLOYS (TOLERANCES: IN. PLUS & MINUS)					
GAGES IN.	WIDTH RANGE (INCHES)				
	UP TO 18	19-36	37-48	49-54	55-60
.016	.0015	.0020	.0025	.0035	—
.020	.0015	.0020	.0025	.0035	.004
.025	.0015	.0020	.0025	.0035	.004
.032	.0020	.0020	.0025	.0040	.005
.040	.0020	.0025	.0030	.0040	.005
.050	.0025	.0030	.0040	.0050	.006
.063	.0025	.0030	.0040	.0050	.006
.071	.0030	.0030	.0040	.0050	.006
.080	.0035	.0035	.0040	.0050	.006
.090	.0035	.0035	.0040	.0050	.006
.100	.0040	.0040	.0050	.0050	.007
.125	.0045	.0045	.0050	.0050	.007
.160	.0060	.0060	.0080	.0080	.009
.190	.0070	.0070	.0100	.0100	.011

TABLE 2

STEEL: CARBON AND CARBON ALLOYS (TOLERANCE: IN. PLUS & MINUS)			
GAGES IN.	WIDTH RANGE (INCHES)		
	12-20	21-40	41-48
.020	.003	.003	.003
.036	.004	.004	.004
.050	.005	.005	.005
.063	.006	.006	.006
.071	.006	.007	.007
.080	.006	.007	.007
.095	.006	.007	.008
.125	.008	.009	.010
.160	.008	.009	.010
.190	.008	.009	.010

TABLE 3

STEEL: CORROSION RESISTANT (TOLERANCE: IN. PLUS & MINUS)	
GAGES	CONTINUOUS MILL 48" MAX. WIDTH
.018	.0015
.025	.0015
.032	.0020
.036	.0020
.050	.0030
.063	.0030
.080	.0040
.095	.0040
.125	.0050
.160	.0070
.190	.0070

TABLE 4

TITANIUM AND TITANIUM ALLOYS (TOLERANCE: IN. PLUS & MINUS)		
GAGES IN.	GAGE RANGE IN. (1)	UP TO 48" WIDTH
.0100	.008 - .0110	.0020
.0160	.012 - .0160	.0020
.0250	.017 - .0260	.0030
.0360	.027 - .0400	.0040
.0500	.041 - .0580	.0050
.0630	.059 - .0720	.0060
.0800	.073 - .0830	.0070
.0900	.084 - .0980	.0080
.1100	.099 - .1140	.0090
.1250	.115 - .1300	.0100
.1400	.131 - .1450	.0120
.1600	.146 - .1875	.0140
.1800	.146 - .1875	.0140

(1) TITANIUM ALLOY IS NOT STOCKED IN ANY STANDARD GAGE. ALL GAGES ARE HAND ROLLED TO ORDER AND TO ANY THICKNESS THE DESIGNER REQUESTS. HOWEVER THE GAGES LISTED ABOVE ARE PREFERRED.

REVISED

APPROVED 12-5-75

GRUMMAN STANDARD

GM15B

CODE IDENT NO. 26512 | SHEET 2

ENG 48.8 12-70

TABLE 5

PREFERRED ALUMINUM ALLOY ROUND TUBING

OUTSIDE DIAMETER (NOMINAL) INCHES	WALL THICKNESS (NOMINAL) INCHES										
	..028	.035	.049	.058	.065	.083	.095	.120	.156	.188	.250
.187	5052 O	5052 O									
.250	2024 T3 5052 O 6061 T6	2024 T3 5052 O 6061 T6	2024 T3 5052 O		2024 T3						
.312	5052 O	2024 T3 5052 O 6061 T6	2024 T3 5052 O	2024 T3							
.375	2024 T3 5052 O 6061 T6	2024 T3 5052 O 6061 T6	2024 T3 5052 O 6061 T6	2024 T3	2024 T3		2024 T3				
.437	2024 T3	2024 T3 5052 O	2024 T3	2024 T3		2024 T3	2024 T3				
.500	2024 T3 5052 O 6061 T6	2024 T3 5052 O 6061 T6	2024 T3 5052 O 6061 T6	2024 T3 6061 T6	2024 T3 6061 T6		2024 T3	2024 T3			
.625	5052 O	2024 T3 5052 O 6061 T6	2024 T3 5052 O 6061 T6	2024 T3	6061 T3	2024 T3	2024 T3		2024 T3		
.750	5052 O 6061 T6	2024 T3 5052 O 6061 T6	2024 T3 5052 O 6061 T6	2024 T3 6061 T6	2024 T3 6061 T6	2024T3	6061 T6	2024 T3			
.875		2024 T3 5052 O	2024 T3	2024 T3 6061 T6	2024 T3		2024 T3				
1.00	5052 O	2024 T3 5052 O 6061 T6	2024 T3 5052 O 6061 T6	2024 T3	2024 T3 5052 O 6061 T6		2024 T3	2024 T3	2024 T3		
1.13		2024 T3	2024 T3	2024 T3	2024 T3						
1.25	5052 O	2024 T3 5052 O	2024 T3 5052 O 6061 T6		2024 T3	2024 T3		2024 T3			2024 T3
1.38		2024 T3	2024 T3	2024 T3 6061 T6	2024 T3						
1.50	5052 O	2024 T3 5052 O 6061 T6	2024 T3 5052 O		2024 T3		2024 T3			2024 T3	2024 T3
1.63		2024 T3	2024 T3	2024 T3						2024 T3	
1.75	5052 O	2024 T3 5052 O	2024 T3 5052 O	2024 T3	5052 O	2024 T3	2024 T3	2024 T3			2024 T3
2.00	5052 O	50520	2024 T3 5052 O 6061 T6	2024 T3		2024 T3				2024 T3	2024 T3
2.25	5052 O			2024 T3	2024 T3			2024 T3			
2.50	5052 O	5052 O.	2024 T3 5052 O 6061 T6		2024 T3 5052 O			2024 T3			
2.75		2219 T31	5052 O					2024 T3			2024 T3
3.00	5052 O	5052 O	2024 T3 5052 O		5052 O 6061 T6						2024 T3

TABLE 5 CONTINUES ON PAGE 4

APPROVED 1-23-76 | REVISED & REDRAWN (B) 3-12-76

GRUMMAN STANDARD

GM15B

CODE IDENT NO. 26512 | SHEET 3

CONTINUE TABLE 5

OUTSIDE DIAMETER (NOMINAL) INCHES	WALL THICKNESS (NOMINAL) INCHES										
	.028	.035	.049	.058	.065	.083	.095	.120	.156	.188	.250
3.50		5052 O	5052 O		5052 O						
3.75				2024 T3				2024 T3			
4.00		5052 O	5052 O								
4.50			5052 O								

TABLE 6

ALUMINUM ALLOY DRAWN ROUND TUBING

SPECIFIED OUTSIDE DIAMETER INCHES	TOLERANCE INCHES IN PLUS & MINUS ALLOWABLE DEVIATION OF MEAN DIAMETER (2) FROM SPECIFIED DIAMETER	SPECIFIED THICKNESS INCHES (3)(4)	TOLERANCE INCHES IN PLUS & MINUS ALLOWABLE DEVIATION OF (3) MEAN WALL THICKNESS FROM SPECIFIED WALL THICKNESS
.188 - .500	.003	.028 - .035	.002
.625 - 1.00	.004	.049	.003
1.13 - 2.00	.005	.058 - .083	.004
2.25 - 3.00	.006	.095	.005
3.25 - 4.50	.008	.120 - .188	.006
		.250	.008

TABLE 7

ALUMINUM ALLOY EXTRUDED ROUND TUBING

SPECIFIED OUTSIDE DIAMETER INCHES	TOLERANCE INCHES IN PLUS & MINUS ALLOWABLE DEVIATION OF MEAN DIAMETER FROM SPECIFIED DIAMETER (2)	SPECIFIED WALL THICKNESS INCHES (3)(4)	TOLERANCE INCHES IN PLUS & MINUS (3) ALLOWABLE DEVIATION OF MEAN WALL THICKNESS FROM SPECIFIED WALL THICKNESS		
			OD .188-1.25	OD 1.38-2.50	OD 3.00-4.50
.188 - .437	.008	.028 - .035	.006	-	-
.500 - .875	.010	.049 - .058	.007	.008	.008
1.00 - 1.75	.012	.065	.008	.008	.009
2.00 - 3.75	.015	.083 - .095	.009	.009	.010
4.00 - 4.50	.025	.120 - .188	.009	.009	.013
		.250	.011	.011	.016

(2) MEAN DIAMETER IS THE AVERAGE OF TWO DIAMETER MEASUREMENTS TAKEN AT RIGHT ANGLES TO EACH OTHER AT ANY POINT ALONG THE LENGTH.

(3) THE MEAN WALL THICKNESS OF ROUND TUBE IS THE AVERAGE OF TWO MEASUREMENTS TAKEN OPPOSITE EACH OTHER.

TOLERANCES LISTED WERE EXTRACTED FROM
FED STD 245 (MIL-T-7081, MIL-T-787 AND MIL-T-700/SERIES)

APPROVED (A) 1-13-76 | REVISED & REDRAWN (B) 3-12-76

GRUMMAN STANDARD

G M15B

CODE IDENT NO. 26512 | SHEET 4

TABLE 8

PREFERRED STEEL: CORROSION RESISTANT ROUND TUBING

OUTSIDE DIAMETER (NOMINAL) INCHES	WALL THICKNESS (NOMINAL) INCHES						
	.016	.020	.028	.035	.049	.058	.065
.187		321 1/8H	304 1/8H 321 ANN				
.250		304 1/8H 321 1/8H	304 1/8H 321 ANN	304 1/8H 321 ANN			
.312				304 1/8H 321 ANN			
.375			304 1/8H 321 ANN 321 1/8H	321 ANN	304 1/8H 321 ANN		
.500			321 ANN	304 1/8H 321 ANN	321 ANN		
.625			304 1/8H 321 ANN		321 ANN		
.750		321 ANN	321 ANN	321 ANN 321 1/8H	304 1/8H		
.875		321 ANN					
1.00		321 ANN	304 1/8H 321 ANN	321 ANN	321 ANN	304 1/8H 321 ANN	
1.25				321 ANN	321 ANN		
1.38			321 ANN		321 ANN		
1.50	321 ANN		321 ANN	321 ANN	321 ANN		321 ANN
1.75		321 ANN		321 ANN			321 ANN
2.00			321 ANN	321 ANN	321 ANN		321 ANN
2.50			321 ANN	321 ANN	321 ANN		
2.75					321 ANN		321 ANN
3.00			321 ANN				321 ANN
3.50			321 ANN				
4.00			321 ANN	321 ANN			321 ANN
4.50				321 ANN			

APPROVED 1-1-74 | REVISED & REDRAWN (B) 3-12-76

GRUMMAN STANDARD

GM15B

CODE IDENT NO. 26512 | SHEET 5

ENG 48.6 12-70

TABLE 9

STEEL: CORROSION RESISTANT SEAMLESS: COLD FINISHED			
OUTSIDE DIAMETER INCHES	TOLERANCE OUTSIDE DIAMETER INCHES		TOL. WALL THICKNESS (4) (% OF THICKNESS) INCLUDES OVALITY
.187 - 1.00	+.003	-.000	+15% -0%
1.25 - 4.50	+.006	-.000	

(4) OVALITY IS THE DIFFERENCE BETWEEN MAX AND MIN OUTSIDE DIAMETERS MEASURED AT ANY ONE CROSS SECTION. THERE IS NO ADDITIONAL TOLERANCE FRO OVALITY ON TUBES HAVING A NOMINAL WALL THICKNESS OF MORE THAN 3 PER CENT OF THE O.D. OUTSIDE DIAMETER.

TABLE 10

STEEL: CORROSION RESISTANT WELDED					
OUTSIDE DIAMETER INCHES	TOLERANCE ± OUTSIDE DIAMETER INCHES	WALL THICKNESS INCHES (5) (6)	TOLERANCE, WALL THICKNESS ±		
			OUTSIDE DIAMETER RANGE		
			.187-.375	1.00-1.75	2.00-3.00
.187 - .375	.003	.016 - .020	.002	.003	.004
.500 - .750	.004	.028	.003		
1.00 - 1.38	.005	.035 - .049		.004	-
1.50 - 1.75	.006	.058 - .065	.005	.005	.005
2.00	.007				
2.50 -- 3.00	.010				
3.50 - 4.50	.015				

(5) FOR NOMINAL OUTSIDE DIAMETER 0.625 INCH AND UNDER, WALL THICKNESS TOLERANCES OF SEAMLESS TUBING APPLY.

(6) FOR REDRAWN WELDED CORROSION RESISTANT STEEL TUBING, WALL THICKNESS TOLERANCES ARE ±.10%

TOLERANCES LISTED WERE EXTRACTED FROM MIL-T-8973. REF. MIL-T-6845 & MIL-T-8808(MS33531) FOR LOOSER TOLERANCES.

APPROVED 1-11-76 | REVISED & REDRAWN (B) 3-12-76

GRUMMAN STANDARD

GM15B

CODE IDENT NO. 26512 | SHEET 6

ENG 48.8 12-70

TABLE II

PREFERRED STEEL: CARBON & CARBON ALLOYS ROUND TUBING

OUTSIDE DIAMETER (NOMINAL) INCHES	WALL THICKNESS (NOMINAL) INCHES												
	.028	.035	.049	.058	.065	.083	.095	.120	.156	.188	.250	.312	.375
.187		4130											
.250	4130		4130		4130								
.375		4130	4130	4130									
.500		4130		1025 4130	4130	4130		4130	4130				
.625		4130	4130		4130			4130		4130			
.750		4130	4130	4130	4130	4130	4130	4130	4130	4130	4130		
.875			4130	4130	4130			4130			4130		
1.00			4130	4130	4130			1015 4130	4130	4130		4140	
1.25			4130		4130			4340	4130		4130		
1.38					4130			4130	4130				
1.50					4130 4140	4130		4130	4130	4130 4340			4340
1.63				4130	4130						4340		
1.75					4130		4130	4130			4130		
2.00			4130		4140		4140	4130 4140		4130	4130		
2.50					4130					4130	4130 4140	4330 CEVM	4130
2.75						4140	4130						4130
3.00											4130		

APPROVED (B) 3-12-76 REVISED

GRUMMAN STANDARD

GM15B

CODE IDENT NO. 26512 SHEET 7

TABLE 12

STEEL: CARBON AND CARBON ALLOYS AIRCRAFT TYPE, SEAMLESS (COLD FINISHED)			
OUTSIDE DIAMETER INCHES	TOLERANCE, OUTSIDE DIAMETER, INCHES (7)		TOLERANCE WALL THICKNESS INCHES
	ANNEALED, NORMALIZED, OR STRESS RELIEVED	QUENCHED & TEMPERED	
.187 - .500	±.005	±.010	SEE NOTE (8)
.625 - 1.50	±.005	±.015	
1.63 - 3.00	±.010	±.030	

(7) TUBES WITH WALL THICKNESS LESS THAN 3% OF THE NOMINAL OUTSIDE DIAMETER (OD) WILL BE ALLOWED AN OVALITY TOLERANCE OVER AND UNDER EQUAL TO 0.5% OF THE NOMINAL OD IN ADDITION TO THE TOLERANCE INDICATED IN THE TABLE, BUT THE MEAN OD SHALL BE WITHIN THE INDIVIDUAL MEASUREMENT TOLERANCE SPECIFIED IN THE TABLE.

(8) WALL THICKNESS OF TUBES 0.5IN. OR LARGER NOMINAL INSIDE DIAMETER (ID) SHALL NOT VARY MORE THAN ±.10%
WALL THICKNESS OF TUBES LESS THAN 0.5IN. NOMINAL INSIDE DIAMETER (ID) SHALL NOT VARY MORE THAN ± 15%

TABLE 13

STEEL: CARBON AND CARBON ALLOYS MECHANICAL TYPE, SEAMLESS (COLD FINISHED)					
OUTSIDE DIAMETER INCHES	NOMINAL WALL THICKNESS, INCHES ANNEALED, NORMALIZED, QUENCHED & TEMPERED	TOLERANCE OUTSIDE DIAMETER INCHES	NOMINAL WALL THICKNESS FINISHED OR STRESS RELEASED SEE (9), (10) & (11)	TOLERANCE - OUTSIDE DIAMETER INCHES	
				PLUS	MINUS
.187 - .500	ALL	±.010	ALL	.004 (7)	0 (7)
.625 - 1.50	3% OF OD OR MORE	±.015	ALL	.005	0
1.63 - 3.00	3% OF OD OR MORE	±.013	ALL	.010	0

WALL THICKNESS TOLERANCE

MECHANICAL TYPE, COLD FINISHED (ALL CONDITIONS)

(9) WALL THICKNESS OF ALL TUBES SHALL NOT VARY MORE THAN ±10%, EXCEPT FOR THOSE LISTED BELOW ((10) & (11))

(10) WALL THICKNESS MAY VARY ±12.5% FOR TUBES WITH LESS THAN 4.50 IN. OD HAVING A WALL THICKNESS OVER 25% OF THE NOMINAL OD.

(11) FOR TUBES LESS THAN 0.5 IN. NOMINAL ID (OR LESS THAN 0.625 INC. WHEN WALL THICKNESS IS MORE THAN 20% OF (OD), THE WALL THICKNESS MAY VARY ±15%.

TOLERANCES LISTED WERE EXTRACTED FROM AMS22530

APPROVED (B) 3-12-76 REVISED

GRUMMAN STANDARD

GM15B

CODE IDENT NO. 26512 | SHEET 8

ENG 48.8 12-70

TABLE 14

STEEL: CARBON AND CARBON ALLOYS AIRCRAFT TYPE, WELDED ANNEALED, NORMALIZED, OR STRESS RELIEVED			
OUTSIDE DIAMETER INCHES	NOMINAL WALL THICKNESS INCHES	TOLERANCE, INCHES	
		PLUS & MINUS	OVALITY ④
.187 - .500	ALL	.003	.004
.625	ALL	.004	.004
.750 - 1.00	.028 - .058	.004	.005
.750 - 1.00	.065 - .120	.004	.004
1.25 - 1.38	.028 - .120	.005	.008
1.50 - 2.00	.028 - .058	.006	.008
1.50 - 2.00	.065 - .120	.005	.006
2.50	ALL	.007	.010
2.75 - 3.00	.028 - .065	.010	.020
2.75 - 3.00	.083 - .120	.010	.015

TABLE 15

STEEL: CARBON AND CARBON ALLOYS AIRCRAFT TYPE, WELDED WALL THICKNESS TOLERANCE			
NOMINAL WALL THICKNESS INCHES	TOLERANCE, WALL THICKNESS, INCHES, PLUS & MINUS OUTSIDE DIAMETER RANGE, INCHES		
	.375-.875	1.00-2.00	2.50-3.00
.028 - .035	.004	.004	.005
.049	.004	.005	.006
.058 - .065	.004	.006	.006
.083	.004	.006	.006
.095	-	.006	.006
.120	-	.006	.008

APPROVED (.) 3-11-76 REVISED

GRUMMAN STANDARD

GM15B

CODE IDENT NO. 28512 | SHEET 9

TABLE 16

PREFERRED SIZES FOR TITANIUM 3AL-2.5V TUBING, SEAMLESS, ANNEALED

OUTSIDE DIAMETER INCHES	.028	.036	.042	.044	.054	.073
.375	X					
.500		X				
.625				X		
.750					X	
1.00						X
1.50			X			

TABLE 17

TOLERANCES FOR TITANIUM 3AL-2.5V ROUND TUBING SEAMLESS - ANNEALED			
OUTSIDE DIAMETER (NOMINAL), INCHES	TOLERANCE OUTSIDE DIAMETER INCHES	OVALITY TOLERANCE OUTSIDE DIAMETER INCHES	TOLERANCE WALL THICKNESS INCHES
.375 - .500	+.004 - .000	.004 MAX	WALL THICKNESS NOT TO EXCEED ±10% OF NOMINAL WALL THICKNESS
.625 - 1.500	+.005 - .000	.005 MAX	

TOLERANCES LISTED WERE EXTRUDED FROM GM31188

APPROVED (B) 3-12-76 REVISED

GRUMMAN STANDARD

GM15B

CODE IDENT NO. 26512 SHEET 10

ENG 48.6 12-70

STRUCTURES BULLETIN NO. 17

From: E. Ranalli/B.Whitman

To: All Holders of Structures Manuals

Subject: Determination of Fastener Load Distributions in Multiple Sheet Packups

Reference: (1) Grumman Structures Manual Section B2.50

(2) Grumman Drawing Procedure Notice DP304 (79-4)

Summary: Elastic Analyses of mechanically fastened multiple layer packups must employ parallel as well as series springs to represent the fasteners which interconnect the laminates. Two closed form equations are presented which permit the calculation of the required parallel spring flexibilities. These parallel springs must account for the additional fastener flexibility due to the gaps between the laminates. The data of reference 1 does apply to this configuration.

The use of these fastener flexibility equations requires an investigation to insure that the maximum stiffness (minimum flexibility) for the configuration is obtained. Additional equations are developed to assist this investigation.

Finally, a relatively simple symmetric double shear splice joint is analyzed to demonstrate the deficiency of the existing series spring only solution.

I. Fastener Flexibility Equations

Fastener flexibilities usually control splice joint load distributions. Analyses of these joints can give incorrect results for multiple layer packups, that is, in configurations where the load is being transferred from one part to two or more parallel parts. Situations of this type have recently occurred in understrength splice joints reinforced by local doublers. The difficulty is traceable to the use of only series springs between the elements rather than a combination of series and parallel springs to connect all laminates with each other. The springs are used to mathematically represent the fasteners.

To correct these analyses, parallel as well as series springs are required. To accomplish this, the components of the fastener flexibility must be identified and quantified insofar as possible.

The term fastener flexibility is associated with that joint deflection which cannot be attributed to the simple axial extension of the test plates. The additional deflection is associated with three effects:

(1) Fastener deflection in shear and bending.

(2) Joint motion attributable to localized bearing distortions at the fastener locations.

(3) Joint motion due to fastener rigid body rotation.

The latter effect is bounded by the two limiting cases (i.e.) single and double shear which have maximum and zero fastener rigid body rotations respectively.

The following figures show the general configurations of single and double shear joints whose fastener flexibilities must be determined prior to joint analysis.

Single Shear
Joint Configuration

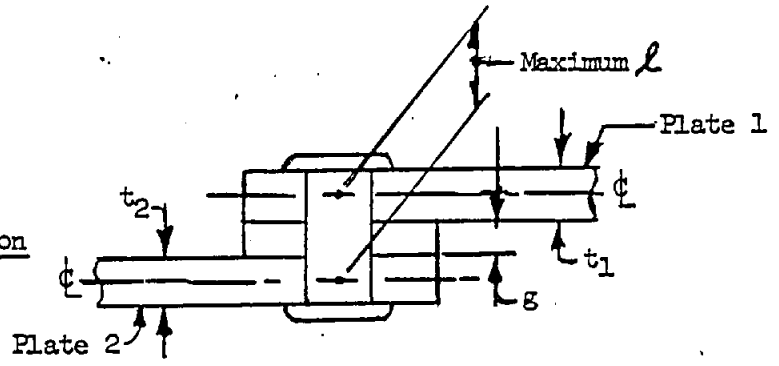

Double Shear
Joint Configuration

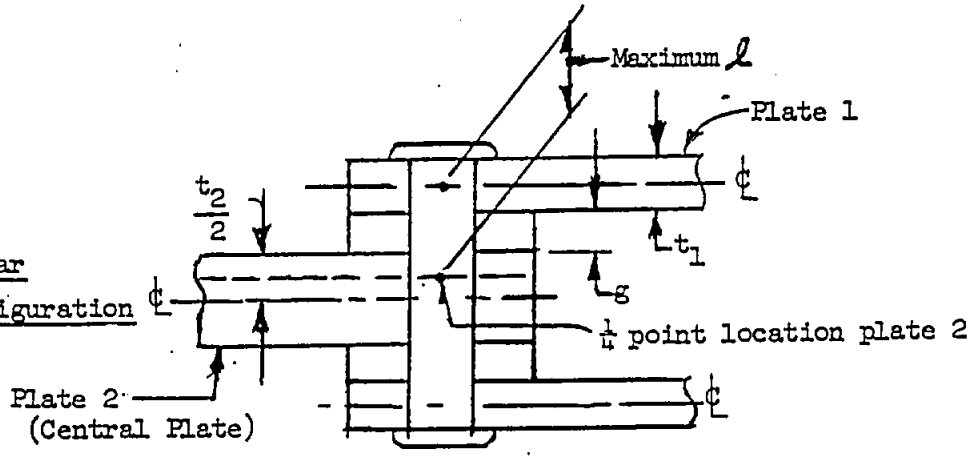

To correctly analyze multiple laminate structures, the flexibility of the parallel springs must include the effects of the gaps between the layers. Since reference (1) data does not include this effect the following two empirical equations are to be used.

Flexibility equation for single shear fasteners (Protruding Head):

$$\frac{1}{K_{SS}} = \left(\frac{\Delta}{P}\right)_{SS} = \frac{3.5\ell}{E_F d^2}\left[1 + 2\left(\frac{\ell}{d}\right)^2\right] + 0.040\left[\frac{1}{F_{bry_1} t_{e_1}} + \frac{1}{F_{bry_2} t_{e_2}}\right] \quad (1)$$

Flexibility equation for double shear fasteners (Protruding Head): (per shear face)

$$\frac{1}{K_{DS}} = \left(\frac{\Delta}{P}\right)_{DS} = \frac{3.5\ell}{E_F d^2}\left[1 + 2\left(\frac{\ell}{d}\right)^2\right] + 0.024\left[\frac{1}{F_{bry_1} t_{e_1}} + \frac{2}{F_{bry_2} t_{e_2}}\right] \quad (2)$$

The first terms in these expressions represent the fastener deflection in shear and bending (for a unit load) while the second represents the total of the local deflections of the plate (for a unit load). The nomenclature is as follows:

- ℓ = distance the load is assumed to be transferred (in) accounting for gaps as applicable.
- E_F = Modulus of Elasticity of fastener material (psi)
- d = Fastener diameter (in)
- F_{bry} = Lower of fastener or sheet bearing yield strength (psi)
- t_e = Effective thickness of the plate (in)

where $t_{ei} = t_i\left[3.9\left(\frac{t_i}{d}\right)^{0.75}\left(1-1.5\frac{t_i}{d}\right) + 1.5\frac{t_i}{d}\right]$ for $\frac{t_i}{d} \leq 0.65$ and $d > 0.156$ in (3)

i indicates the i^{th} plate.

and $t_{ei} = t_i$ for $\frac{t_i}{d} \geq 0.65$

Note t_e is only used for the sheet deflection calculation but never in determining ℓ, for reasons explained in the next paragraph.

The idea of using an effective thickness for low plate thickness to fastener diameter ratios was empirically determined. It is conjectured that in relatively thin plates (say $t/d < 0.4$), the allowable load per unit of plate thickness is limited by the allowable bearing stress (proportional to diameter times plate

thickness) while for relatively thick plates ($t/d \geq 0.65$) the load distribution is not bearing stress limited but rather determined from simple bending and axial load through-the-thickness distribution (which are proportional to thickness only).

The decision to use either the single or double shear stiffness equations in an unsymmetric joint is somewhat arbitrary and so the following rule is recommended:

If the load is being transferred to both sides of a central or nearly central plate, use the double shear equation. The maximum distance, ℓ, over which the load will be transferred, is from the quarter point of the central plate to the mid point of a side plate. If the load is being transferred from one side plate to another, use the single shear equation with ℓ having a maximum value of the distance between the plate center lines.

II. Concept of Maximum Fastener Stiffness (minimum flexibility)

The fastener flexibility equations (1) and (2) must be used with judgement. In gap free joints, the values predicted by the fastener flexibility equations will approach a minimum value and then increase as the plate thickness increases. This occurs in the predictive equations due to the rapidly increasing fastener deflections with increasing ℓ, but is not in agreement with test data.

A reasonable explanation is that once the fastener carries the load across the plate interface a sufficient distance for it to be introduced into the plate in bearing, the plate interlaminar stiffness will then move the load to the plate quarterpoint or centerline. Re-examining equations (1) and (2) and introducing a single constant C for the 0.04 and 0.024 values, we have (for equal plates of common material):

$$\left(\frac{1}{K}\right) = \frac{3.5(t_x + g)}{E_F\ d^2}\left\{1 + 2\left[\frac{t_x + g}{d}\right]^2\right\} + \frac{2C}{F_{bry}\ t_x\left(\frac{t_{xe}}{t_x}\right)}$$

where $t_x \leq t$, $\ell = (t_x + g)$ and $\frac{t_{xe}}{t_x}$ is the plate's effective (bearing) thickness to thickness ratio using equation (3).

Differentiating with respect to t_x, equating to zero, and rearranging:

$$\frac{d}{d t_x}\left(\frac{1}{K}\right) = 21\left(\frac{t_x + g}{t_x}\right)^2 \left(\frac{t_x}{d}\right)^2 + 3.5\left(\frac{t_x}{d}\right)^2 - \frac{2CE_F}{F_{bry}\left(\frac{t_{xe}}{t_x}\right)} = 0$$

finally, the value of t_x ($\leq t$) which gives the maximum fastener stiffness is

$$\frac{t}{d} \geq \left(\frac{t_x}{d}\right) = 0.154\left(\frac{t_x}{t_x+g}\right)\sqrt{-3.5 + \sqrt{3.5^2 + 168\left(\frac{t_x+g}{t_x}\right)^2 \frac{CE_F}{F_{bry}\left(\frac{t_{xe}}{t_x}\right)}}} \qquad (4)$$

Equation (4) may be iteratively solved for a family of $\frac{CE_F}{F_{bry}}$ when $g = 0$ and is plotted in Figure 1'.

III. Determination of t_x for fasteners with gap g

When an arbitrary gap g is introduced between the loaded laminates, as in the case of the parallel springs, the value of t_{x_g} is determined from t_x (gapless value) from

$$t_{x_g} \simeq t_x \sqrt{\frac{t_x + g}{t_x}} - g \qquad (5)$$

To familiarize the reader with the concepts discussed above, some examples are presented on page 7 illustrating how fastener stiffnesses can be calculated.

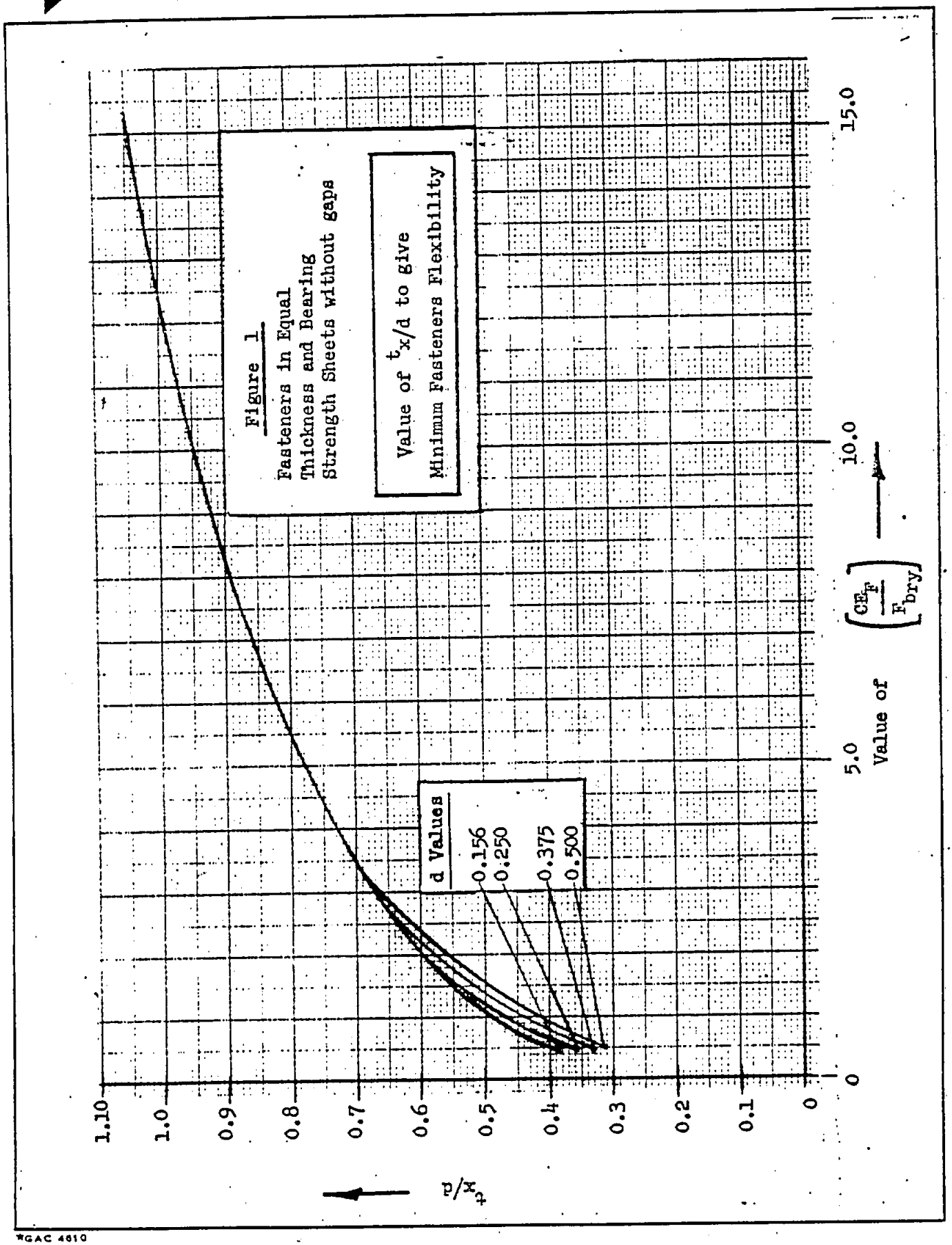
Figure 1
Fasteners in Equal
Thickness and Bearing
Strength Sheets without gaps
Value of t_x/d to give
Minimum Fasteners Flexibility
d Values
0.156
0.250
0.375
0.500
t_x/d
1.10
1.0
0.9
0.8
0.7
0.6
0.5
0.4
0.3
0.2
0.1
0
0
5.0
10.0
15.0
Value of $\left(\frac{CE_F}{F_{bry}}\right)$

IV. Example of Fastener Stiffness Determination

Find the single shear fastener stiffness for a 1/4 Steel HiLok (E_F = 29 x 10^6 psi) in 7075-T651 Aluminum Alloy Plate (F_{bry} = 115000 psi) for both gapless and 0.100 gap configurations.

$$\frac{CE_F}{F_{bry}} = \frac{0.04 \times 29 \times 10^6}{115000} = 10.$$

From Figure 1; $t_x/d \simeq 0.95$ or t_x = 0.2375 in;

Therefore, only thicknesses less than or equal to 0.2375 inch need be considered.

Table 1 - 1/4 in. Steel HiLok Fasteners in 7075-T6 (without Gaps) Comparison of Predicted Stiffnesses - Reference 1 with Equations (1) and (2).

t	t/d	t_e (1)	$\frac{1}{K_F}$	$\frac{1}{K_P}$	$\frac{1}{K_T}$	K	K_{GSM} (2)
.04	.16	.0515	8.12×10^{-8}	1.351×10^{-5}	1.36×10^{-5}	73.5×10^3	77×10^3
.08	.32	.096	1.86×10^{-7}	7.25×10^{-7}	7.436×10^{-6}	134×10^3	136×10^3
.12	.48	.133	3.385×10^{-7}	5.23×10^{-6}	5.568×10^{-6}	180×10^3	180×10^3
.16	.64	.162	5.621×10^{-7}	4.29×10^{-6}	4.852×10^{-6}	206×10^3	205×10^3
.20	.80	.200	8.806×10^{-7}	3.478×10^{-6}	4.359×10^{-6}	229×10^3	216×10^3
≥ .2375	.95	.2375	1.286×10^{-6}	2.929×10^{-6}	4.215×10^{-6}	237×10^3	220×10^3

(1) Equation 3

(2) Reference 1 Page B2.50-7

Table 2 - Predicted stiffness for 1/4 Steel HiLok Fasteners in 7075-T6; .1 gap

t	t/d	t_e	ℓ	$\frac{1}{K_F}$	$\frac{1}{K_P}$	$\frac{1}{K_T}$	K_T
.04	.16	.0515	.140	4.40×10^{-7}	1.351×10^{-5}	1.395×10^{-5}	72×10^3
.08	.32	.096	.180	7.08×10^{-6}	7.25×10^{-6}	7.958×10^{-6}	126×10^3
.12	.48	.133	.220	1.083×10^{-6}	5.23×10^{-6}	6.313×10^{-6}	158×10^3
.16	.64	.162	.260	1.588×10^{-6}	4.29×10^{-6}	5.878×10^{-6}	170×10^3
≥ .183 (3)	.732	.183	.283	1.947×10^{-6}	3.801×10^{-6}	5.748×10^{-6}	174×10^3 (4)

(3) Maximum effective fastener length for gap configuration (g = 0.100 in.)

$$t_{x_g} \simeq t_x \sqrt{\frac{t_x + g}{t_x}} - g = 0.2375 \sqrt{\frac{0.2375 + 0.100}{0.2375}} - 0.100 = 0.183 \text{ in.}$$

(4) Predicted Stiffness ratio 0.100 gap to gapless $\frac{1}{4}$ Steel HiLok = 174/220 = 0.79

From Grumman Test Report 310MTB-1 (6-4-64) Measured Ratio = 0.87 (P260 JoBolts)

V. Illustrative Problem - Two demonstrable observations of the validity of the series - parallel spring solution over the series only solution can be shown by considering the following symmetric double shear joint.

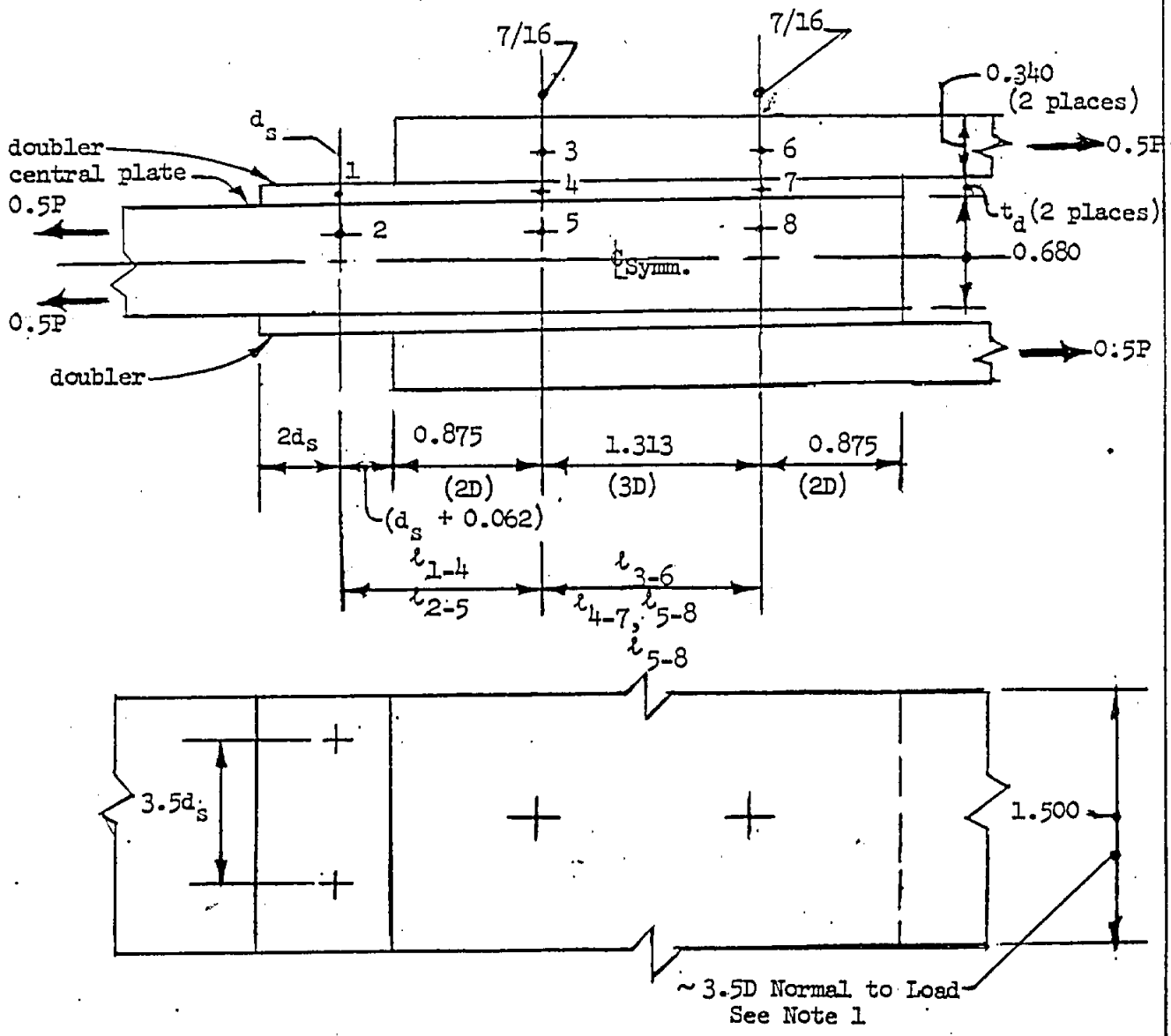

Notes: 1 - All dimensions agree with reference 2 minimums except 3.50 normal to load to allow for one oversize attachment without any significant fatigue life reduction.

2 - The edge distance of 2D and pitch distance of 3D are arbitrary and in the untapered joint shown excessive. In an actual design, fish-mouth tapers or reduced dimensions based on improved tooling should be considered.

The first observation is that for a zero doubler thickness, the problem becomes statically determinate (based on bolt and plate size symmetry) and the joint deflection parameter, $\left(\frac{E\Delta_{26}}{P}\right)$, can be independently calculated using reference 1 data. Therefore, as t_d approaches zero, the correct indeterminate solution will approach this value. Figure 2 shows how this only occurs in the five degree indeterminate series-parallel spring solution with the series only solution becoming very flexible since the load is forced to enter and exit the relatively thin doubler or shim. The second observation is that the stress in the doubler (points 1 to 4) should be lower than the stress in the central remotely loaded splice plate (points 2 to 5). This is true since the additional flexibility produced by the fastener connecting points 1 and 2 will be felt by the load path points 2-1-4 but not by the load path 2-5. Figure 3 illustrates stress results from the series only spring solution compared to the values obtained from the series-parallel spring solution.

It is concluded that the series/parallel spring approach provides a more accurate solution for problems when multiple element packups exist. In general, the series/parallel spring solution should be regarded as a state-of-the-art improvement and must be used in all future analyses where applicable.

The illustrative problem was solved in closed form to show the effect of doubler thickness variations. The analysis is presented in summary form on the next page.

To illustrate the correct use of fastener flexibility equations (1) and (2), the fastener flexibility calculations used in the illustrative example are included (see pages 14, 15, and 16). Particular attention is directed to the concept of effective bearing thickness (equation 3) for t/d ratios below 0.65 and to the length for minimum fastener flexibility for which equations (4) and (5) are of assistance. Observe however that equations (4) and (5) are for equal gage identical bearing yield strength material and must be used with judgement when this condition does not exist. This situation is illustrated by all fasteners except 3-5 and 6-8.

Illustrative Joint Problem Solution: Basic Load and Flexibility Data

Element	Node Nos.	Redundants: Series Only 1	2	3	Complete 4	5	Statically Deter. Dist. xP	Elastic Modulus times Flexibility: L/A (Bars) or E/K (Springs) Doubler Thickness .01	0.05	0.093	0.125	0.188
Bars	1.4	+1						75.0	15.0	8.1	6.3	4.7
	2.5	-1					+0.5	2.2	2.2	2.2	2.3	2.6
	3.6			+1	+1	+1		2.6	2.6	2.6	2.6	2.6
	4.7		+1	-1				76.6	17.5	9.4	7.0	4.7
	5.8		-1		-1	-1	+0.5	2.6	2.6	2.6	2.6	2.6
Springs (1) Series	1.2	+1						88.9	26.6	19.9	19.3	17.9
	3.4			+1		+1		186.2	50.9	36.0	31.2	27.7
	4.5	-1	+1			+1		112.3	31.3	22.4	19.6	17.9
	6.7			-1			+0.5	186.2	50.9	36.0	31.2	27.7
	7.8		-1				+0.5	112.3	31.3	22.4	19.6	17.9
Springs (1) Parallel	3.5				+1			18.2	19.5	20.6	21.7	22.9
	6.8				-1	-1		18.2	19.5	20.6	21.7	22.9

(1) Series Springs are those springs which connect contacting laminates. Parallel springs are those springs which connect laminates which are at least one loaded laminate remote from each other.

From minimum strain energy principle, (ie) $\sum \frac{\partial U}{\partial q_i} = 0$,

where $i = 1, 2, 3, 4, 5$, the governing equations (page 11) were determined. The first three equations without redundants 4 and 5 apply to the series only springs while the entire five equations are used for the series-parallel spring solution.

Continued: Illustrative Problem Solution:

- Redundants q_1, q_2 and q_3 pertain to series spring solution.
- Redundants q_1 thru q_5 pertain to series-parallel spring solution.

$$\left(\frac{E}{P}\right)\begin{bmatrix} \alpha_{14}+\alpha_{25} & -\alpha_{45} & & & -\alpha_{45} \\ \alpha_{12}+\alpha_{45} & & & & \\ \hline -\alpha_{45} & \alpha_{47}+\alpha_{58} & -\alpha_{47} & +\alpha_{58} & \alpha_{58} \\ & \alpha_{45}+\alpha_{78} & & & +\alpha_{45} \\ \hline & -\alpha_{47} & \alpha_{36}+\alpha_{47} & \alpha_{36} & \alpha_{36} \\ & & \alpha_{34}+\alpha_{67} & & +\alpha_{34} \\ \hline & \alpha_{58} & \alpha_{36} & \alpha_{36}+\alpha_{58} & \alpha_{36}+\alpha_{58} \\ & & & \alpha_{35}+\alpha_{68} & +\alpha_{68} \\ \hline -\alpha_{45} & \alpha_{58} & \alpha_{36} & \alpha_{36}+\alpha_{58} & \alpha_{34}+\alpha_{45} \\ & +\alpha_{45} & +\alpha_{34} & +\alpha_{68} & +\alpha_{68} \end{bmatrix} \times \begin{bmatrix} q_1 \\ \hline q_2 \\ \hline q_3 \\ \hline q_4 \\ \hline q_5 \end{bmatrix} = \begin{bmatrix} 0.5\alpha_{25} \\ \hline 0.5\alpha_{58} \\ +0.5\alpha_{78} \\ \hline 0.5\alpha_{67} \\ \hline 0.5\alpha_{58} \\ \hline 0.5\alpha_{58} \\ 0.5\alpha_{58} \end{bmatrix}.$$

NOTE:

The above equations were obtained from the minimum strain energy principle.

Identical equations are easily obtained using results of standard Force Method $[A]^T[B][A]$ matrix algebra which circumvents the requirement to determine the derivatives $\frac{\partial U}{\partial q_i}$.

Figure 2 - Illustrative Joint Problem: Joint Deflection Parameter Versus Doubler Thickness

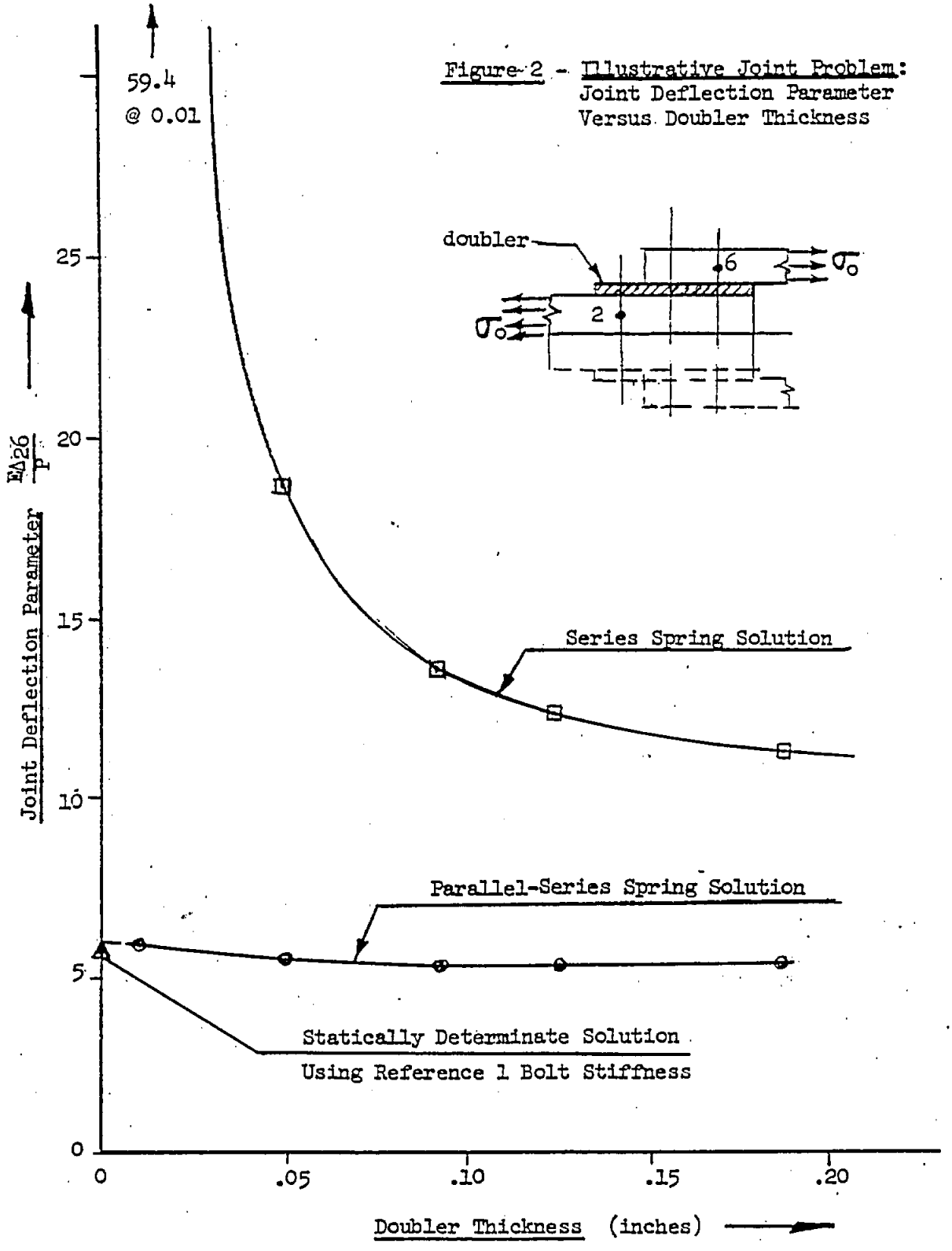

Figure 3 - Illustrative Joint Problem: Member Stress to Remote Stress σ_o Versus Doubler Thickness

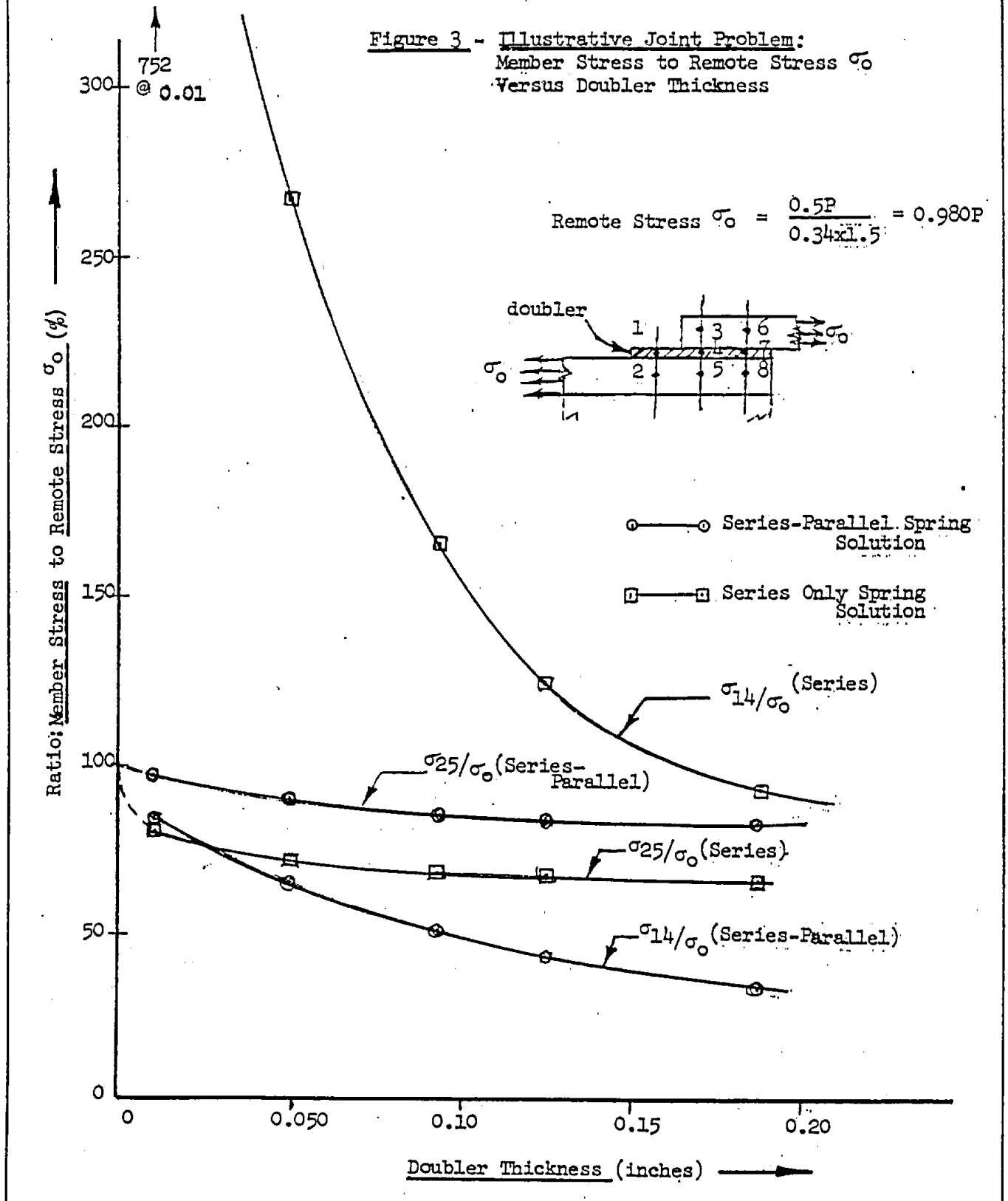

Illustrative Joint Problem:

Calculation of Fastener Flexibility 1-2 (in Double Shear). Series spring.

t_d	$t_{2/2}$	d	$t_d/_d$	t_{d_e}(1)	ℓ(2)	ℓ_m(3)	$t'_{2/2}$(4)	$\frac{t'_2}{d}$(5)	$\frac{1}{K_F}$(6)	$\frac{1}{K_P}$(7)	K_T(8)	K_T(9) GSM	$E/_{K_T}$(10)
0.010	0.340	3/16	.0533	.012	.175	0.155	0.300	1.60	1.259×10^{-6}	1.809×10^{-5}	51.7×10^{3}	86×10^{3}	88.9
0.050	↑	3/16	.2667	.056	.195	0.155	0.260	1.386	1.259×10^{-6}	4.529×10^{-6}	172.8×10^{3}	177×10^{3}	26.6
0.090		3/16	.4960	.095	.215	0.155	0.220	1.173	1.259×10^{-6}	3.078×10^{-6}	230.6×10^{3}	240×10^{3}	19.9
0.125	↓	1/4	.500	.141	.233	0.206	0.287	1.148	0.938×10^{-7}	2.207×10^{-6}	318.0×10^{3}	345×10^{3}	19.3
0.1875	0.340	3/8	.500	.236	.264	0.309	0.340	0.906	0.451×10^{-7}	1.498×15^{-6}	513.2×10^{3}	542×10^{3}	17.9

(1) Ref. equation (3)

(2) $\ell = 0.5\ (t_d + t_{2/2})$

(3) For Double Shear, C = 0.024 $\therefore$ $C_{EF}/F_{bry} = 0.024 \times 29 \times 10^6/1.15 \times 10^5 = 6.1$ Figure 1 gives $\ell_m = 0.825d$

(4) $(t'_2/2) = 2\ (\ell_m - t_d/2)$

(5) Since all values of $\frac{t'_{2/2}}{d}$ exceed 0.65 equation (3) does not apply

(6) $\frac{1}{K_F} = \frac{3.5\ell_x}{29\times10^6 d^2}\left[1 + 2\left(\frac{\ell_x}{d}\right)^2\right]$ using underlined ℓ or ℓ_m for ℓ_x

(7) $\frac{1}{K_P} = \frac{0.024}{1.15\times10^5}\left[\frac{1}{t_{d_e}} \quad \frac{1}{t'_{2/2}}\right]$

(8) $\frac{1}{K_T} = \frac{1}{K_F} + \frac{1}{K_P}$

(9) Reference 1 ~ page B2.50-7

(10) E/K_T $\underbrace{\text{per 1.50 inches}}_{\text{width}} = \frac{E \times 1.5}{K_T \times 3.5d}$

Illustrative Joint Problem:

Calculation of Fastener Flexibility 3-5 or 6-8 (in Double Shear) - These flexibilities represent the parallel series springs and hence contain gaps. It is necessary to determine the fastener length for minimum flexibility without gaps first and then with the variable gap length g.

d = 0.4375 in DS: CE_F/F_{bry} = 6.05 gives t_x = 0.825 d for g = 0

g = t_d	$t_{i=}\frac{t_2}{2}$	$\frac{t_i}{d}$ (1) or $\frac{t_{2/2}}{d}$	ℓ_1 (2)	t_{xg} (3)	ℓ_{xg} (4)	$\frac{t_x}{d}$	t'_{xe}	$\frac{1}{K_f}$	$\frac{1}{K_p}$	K_T	E/K_T
0	0.340	0.777	0.340	0.361	0.361	0.777	0.340	4.73×10^{-7}	1.23×10^{-6}	$587\times10^{+3}$ (6)	17.9
0.010	↕	↕	0.350	0.356	0.366	0.777	0.340	5.03×10^{-7}	1.23×10^{-6}	$577\times10^{+3}$	18.2
0.050			0.390	0.335	0.385	0.766	0.335	6.19×10^{-7}	1.25×10^{-6}	$535\times10^{+3}$	19.6
0.090			0.430	0.313	0.403	0.715	0.313	6.85×10^{-7}	1.33×10^{-6}	$496\times10^{+3}$	21.2
0.125			0.465	0.294	0.419	0.672	0.294	7.49×10^{-7}	1.42×10^{-6}	$461\times10^{+3}$	22.8
0.1875	0.340	0.777	0.5275	0.257	0.445	0.587	0.296	8.61×10^{-7}	1.42×10^{-6}	$438\times10^{+3}$	24.0

(1) since t_1/d and $t_{2/2d}$ > 0.65, then $t_e = t$

(2) $\ell_1 = 0.5\,(t_1 + t_{2/2}) + g$

(3) $t_{xg} = t_x \sqrt{\frac{t_x + g}{t_x}} - g$ where $t_x = 0.825 \times 0.4375 = 0.361$

(4) $l_{xg} = (t_{xg} + g)$

(5) the smaller of t_1/d or t_{xg}/d

(6) From Reference 1 (for g = 0) $K_{DS} = 1.7 \times 3.90 \times 10^3 = 663 \times 10^3$ #/in.

Illustrative Joint Problem:

Calculation of Fastener Flexibility 3-4 or 6-7 (in Single Shear). These flexibilities represent series springs as recommended on page 4.

d = .4375 in SS: CE_F/F_{bry} = 10 gives t_x = .95d for g = 0

t_d	t_d/d	t_{de}	ℓ (1)	$\frac{1}{K_F}$	$\frac{1}{K_P}$	$\frac{1}{K_T}$	K_T	K_T (2)	$\frac{E}{K_T}$
0.010	0.023	.021	0.175	1.457×10^{-7}	1.758×10^{-5}	1.77×10^{-5}	$56.4\times10^{+3}$	——	186.2
0.050	0.114	.095	0.195	1.718×10^{-7}	4.68×10^{-6}	4.85×10^{-5}	$206.2\times10^{+3}$	201×10^{3}	50.9
0.090	.206	.158	0.215	2.034×10^{-7}	3.225×10^{-6}	3.43×10^{-6}	$291.5\times10^{+3}$	286×10^{3}	36.0
0.125	0.286	.203	0.2325	2.294×10^{-7}	2.737×10^{-6}	2.97×10^{-6}	$336.7\times10^{+3}$	323×10^{3}	31.2
0.1875	0.429	.261	0.2638	2.873×10^{-7}	2.355×10^{-6}	2.64×10^{-6}	$378.8\times10^{+3}$	371×10^{3}	27.7

(1) For CE_F/F_{bry} = 10; $t_x = 0.95d = 0.4156$ which exceeds ℓ in all cases.

(2) Derived using page B2.50-7 GSM

Calculation of Fastener Flexibility 4-5 or 7-8 (in Double Shear). These flexibilities represent series springs as recommended on page 4.

d = .4375 in SS: CE_F/F_{bry} = 6.05 gives t_x = 83d for g = 0

t_d	$t_{2/2}$	t_d/d	t_{de}	ℓ	$\frac{1}{K_F}$	$\frac{1}{K_P}$	$\frac{1}{K_T}$	K_T	$\frac{E}{K_T}$	K_T (GSM)
0.01	0.340	0.023	0.021	0.175	1.457×10^{-7}	1.055×10^{-5}	1.07×10^{-5}	$93.5\times10^{+3}$	112.3	——
0.05	↑	0.114	.095	0.195	1.718×10^{-7}	2.81×10^{-6}	2.812×10^{-6}	$335.4\times10^{+3}$	31.3	340×10^{3}
0.09	↓	0.206	.158	0.215	2.010×10^{-7}	1.935×10^{-6}	2.043×10^{-6}	$468.2\times10^{+3}$	22.4	478×10^{3}
0.125		0.286	.203	0.2325	2.294×10^{-7}	1.642×10^{-6}	1.805×10^{-6}	$534.4\times10^{+3}$	19.6	549×10^{3}
0.1875	0.340	0.429	.261	0.2638	2.873×10^{-7}	1.413×10^{-6}	1.666×10^{-6}	$588.1\times10^{+3}$	17.9	631×10^{3}

In general, the results of any analysis to which this bulletin applies should be examined to establish the validity of all assumptions used. The equilibrium of shear forces on each of the fasteners can, for example, be helpful in indicating whether the single shear, double shear, or some intermediate value of flexibility is appropriate for the problem. There may be cases wherein it is also profitable to examine the deflected shape of the splice members. The overall load distribution and stresses should always be assessed.